Advances in Textile Engineering

Edited by
Rui Wang and Huawu Liu

TRANS TECH PUBLICATIONS

Advances in Textile Engineering

Edited by
Rui Wang
Huawu Liu

Advances in Textile Engineering

Selected, peer reviewed papers from the
2011 International Conference on
Textile Engineering and Materials,
(ICTEM 2011),
23-25 September, 2011, Tianjin, China

Edited by

Rui Wang and Huawu Liu

TTP

Copyright © 2011 Trans Tech Publications Ltd, Switzerland

All rights reserved. No part of the contents of this publication may be reproduced or transmitted in any form or by any means without the written permission of the publisher.

Trans Tech Publications Ltd
Kreuzstrasse 10
CH-8635Durnten-Zurich
Switzerland
http://www.ttp.net

Volumes 331 of
Advanced Materials Research
ISSN 1022-6680

Full text available online at *http://www.scientific.net*

***Distributed** worldwide by*

Trans Tech Publications Ltd
Kreuzstrasse 10
CH-8635Durnten-Zurich
Switzerland

Fax: +41 (44) 922 10 33
e-mail: sales@ttp.net

and in the Americas by

Trans Tech Publications Inc.
PO Box 699, May Street
Enfield, NH 03748
USA

Phone: +1 (603) 632-7377
Fax: +1 (603) 632-5611
e-mail: sales-usa@ttp.net

Preface

The 2011 International Conference on Textile Engineering and Materials (ICTEM 2011) took place at Tianjin, China from September 23th to September 25th, 2011. ICTEM 2011 brings together an international audience interested in this area and related topics. The objectives of ICTEM 2011 are to foster research on the textile engineering and textile materials, to promote related international cooperation among scientists and engineers and to provide means for the public dissemination of the results from these efforts.

All papers included in this book are peer reviewed internationally before accepted for publication. This book covers the subject areas of Textile Science and Technology, Textile Dyeing and Finishing, Textile Machinery and Equipment, Apparel Design and Merchandising and New Trends in Textile Industry.

We would like to acknowledge the efforts of the organizers of ICTEM 2011, as well as the contributions of all the speakers and participants. Most importantly, we thank all referees for their constructive comments.

Prof. Rui Wang
Tianjin Polytechnic University, China

Prof. Huawu Liu
Tianjin Polytechnic University, China

The 2011 International Conference on

Textile Engineering and Materials

(ICTEM 2011)

Organized by:

Tianjin Polytechnic University, China

Conference Organization

Chairman

Prof. Changfa Xiao, Tianjin Polytechnic University, China

Local Organizing Committee

Prof. Rui Wang, Tianjin Polytechnic University, China

Prof. Xiaoming Qian, Tianjin Polytechnic University, China

Prof. Huawu Liu, Tianjin Polytechnic University, China

Technical and Organizing Committee

Prof. Philippe Boisse, University of INSA-Lyon, France

Prof. Dominique Coupe, Snecma Propulsion Solide, France

Prof. Bowen Chen, Tianjin Polytechnic University, China

Prof. Li Chen, Tianjin Polytechnic University, China

Prof. Wenxing Chen, Zhejiang Sci-Tech University, China

Prof. Jianyong Chen, Zhejiang Sci-Tech University, China

Prof. Julie Chen, University of Massachusetts Lowell, USA

Prof. Brian Cox, Rockwell Scientific Co., USA

Prof. Tsu-Wei Chou, University of Delaware, USA

Prof. Li Chen, Tianjin Polytechnic University, China

Prof. Guoqiang Chen, Soochow University, China

Prof. Tilak Dias, Nottingham Trent University, UK

Prof. Qinguo Fan, University of Massachusetts, USA

Prof. Xuerong Fan, Jiangnan University, China

Prof. Tushar K. Ghosh, North Carolina State University, USA

Prof. Jack Gillespie, University of Delaware, USA

Prof. Weidong Gao, Jiangnan University, China

Prof. Frank Ko, University of British Columbia, Canada

Prof. Nandan Khokar, University of Boras; Biteam AB, Sweden

Prof. John W S Hearle, University of Manchester Institute of Sci. and Tech., UK

Prof. Hiroyuki Hamada, Kyoto Institute of Technology, Japan

Prof. Tae Jin Kang, Seoul National University, Korea

Prof. Jia-horng Lin, Feng Chia University, Taiwan

Prof. Jialu Li, Tianjin Polytechnic University, China

Prof. Andrew Long, University of Nottingham, UK

Prof. Alfred Loos, Michigan State University, USA

Prof. Huawu Liu, Tianjin Polytechnic University, China

Prof. Stepan Lomov, Katholieke University Leuven, Belgium

Prof. Asami Nakai, Kyoto Institute of Technology, Japan

Prof. Ning Pan, University of California, USA

Prof. Xiaoming Qian, Tianjin Polytechnic University, China

Prof. Yiping Qiu, Donghua University, China

Prof. Stephen J. Russell, University of Leeds, UK

Prof. Seeram Ramakrishna, National University of Singapore

Prof. Francois Robitalle, University of Ottawa, Canada

Prof. Darrell Reneker, University of Akron, USA

Prof. Xiaoming Tao, Hong Kong Polytechnic University, HK

Prof. Ignaas Verpoest, Katholieke University Leuven, Belgium

Prof. Rui Wang, Tianjin Polytechnic University, China

Prof. Xungai Wang, Deakin University, AU

Prof. Wenhao Xing, Chinese Culture University, Taiwan

Prof. Weilin Xu, Wuhan Textile University, China

Academician Prof. Mu Yao. Xi'an Polytechnic University

Prof. Xingchuan Yao, National Taipei University of Technology, Taiwan

Prof. Jianyong Yu, Donghua University

Prof. Zhiyun Wu, Inner Mongolia University of Technology, China

Table of Contents

Preface and Committees

Chapter 1: Textile Science and Technology

The Application of Folkloric Textile Decorative Art to the Regional Character of the Hotel
J. Zhu and Y.F. Chen 3

Impact of Soft Nursing Care on Drying Efficiency of Cotton Fabric
C.J. Qian, J.L. Tu, H.Y. Ge and J.Q. Liu 9

The Effect of Calcination Temperature on the Surface Evolution and Photocatalysis Activity of Co-Doped PVAc/TiO_2 Composite Nanofibers
N. Wu, Y.N. Jiao, Z.Q. Yuan, Y.X. Liang and L. Chen 14

Cell Immobilization with Textile Carriers for TA Biodegradation
H.Q. Li, J.X. Gong, Q.J. Li, Z. Li, J.F. Zhang, K.N. Chen, Z.X. Tang, G.Q. Ding and S.Y. Lin 19

Study on Spunlaced Nonwoven Fabric's Moisture Absorption and Permeability Based on BP Network
X.H. Wu, J.C. Lv and X.N. Jiao 23

Methods for Measuring the Surface Area of Nude Body
Q. Li, J. Li and M. Wang 27

A Stochastic Simulation of Cotton Combing Process
G.S. Yan, Y.H. Su and C.W. Yu 31

Research on Wearable Sensors Based on Knitted Fabrics with Silver Plating Fiber
J.F. Wang and H.U. Long 36

Comparison of the Cost Performance between Pure Cashmere Siro-Spun Yarn and Pure Rabbit Hair Ring-Spun Yarn
Y.L. Liu and B.K. Sun 40

Modelling and Simulating Textile Structures Using TexGen
H. Lin, L.P. Brown and A.C. Long 44

Effect of Fabric Construction on Water Permeability Rate of Woven Filter Cloth
C.D. Mao 48

Mechanical Properties of 2D Braided Polyester Ropes
J.Q. Zhang and L. Cheng 52

Objective Evaluation Based on Main Factors Analysis of the Wool Knitted Fabric Style
P.L. Li and L. Cheng 56

Preparation of Collagen/PVA Composite Fiber
Z.H. Sui, Y.J. Wei and X. Zhao 61

Mechanical Properties of Ramie Fiber Woven Composites under Biaxial Tensile Loadings
G. Wang, F.M. Chen, H.T. Cheng, Z.X. Yu, Z.H. Jiang, X.M. Chen and W.F. Zhang 65

Design and Research of the Foldable Decorative Screen with Ethnic Style Based on Weft-Backed Structure
A.D. Zhang and X.Q. Wang 69

The Development and Status of the Stab-Resistant Body Armor
Z.Z. Ding, Y.Q. Zhang and X.M. Qian 73

Research on the Clustering Color Separation of Fabric Based on Genetic-Fuzzy Algorithm
B.J. Luo 77

Studies on the Composite Thermochomic Energy-Storage Materials Prepared by Sol-Gel Method
Z.L. Wu and X.G. Ma 83

The Mechanical Properties of Bamboo/PLA Composites Made by Biaxial Weft Knitted Fabrics
C. Zhao, G.L. Song and H.W. Liu 89

Graphene Modified Cotton Textiles
W.L. Gu and Y.N. Zhao 93

Analysis on Green Initiative Costume Design Concept
J. Zhao 97

Study on Body Foundation of Brassiere Steel Ring Shapes
S.Z. Liang 101

Microwave Promoted Effect of Starch-g-Butyl Acrylate Sizing Copolymer Grafting
H.L. Wu and Y.Q. Shen 105

Study on the Mechanical Properties of Jute/Carbon Hybrid Composites
J.M. Wang, L. Zhao and X. Qin 110

Exploration on the Production of Natural Green Anti-Bacterial Health-Care Textiles
Y. Weng 115

Influence of Mechanical Properties of Lightweight Silk Fabrics on Seam Shrinkage
Q.Y. Wu and W.B. Zhang 119

Statistical Property of Ideal Drafting Sliver
Y.H. Su, W.L. Zou and G.S. Yan 123

Tensile Properties Study of Polyester/Cotton/Silk Tri-Component Sirofil Composite Yarn
L.B. Lv and M. Du 129

Surface Modification of Polyester Fibers by Encasing Sucrose Ester and Grafting Soybean Protein
S.H. Gao, G.X. Zhang and F.X. Zhang 133

Influences of Soft Monomers on the Application Properties of Hydrophilic Polyurethane with Mixed Polyether Segment
H. Quan and Z.Y. Gu 139

Preparation and Properties of Cationic Graft Starch Sizing Agent
H. Zhang, J.K. Wang, R. Wang and X.P. Fan 144

Evolutionary Engineering of Bacillus for Terephthalic Acid Degradation
J.X. Gong, Z. Li, Q.J. Li and J.F. Zhang 148

Correction for Classical Theory of Yarn Cross-Section Shape in Woven Fabric
L.H. Yang, Y.J. Yu and W.X. Liu 152

Analysis of Color Symbology Focused on Folk Costume Colors in Northern and Southern Regions of China during Republic Period
Y. Qi, X.R. Fan, R.R. Cui and Q. Wang 156

Preparation of Chitosan/Acacia Microcapsule Facilitating Photo-Catalytic Degradation of Polypropylene Nonwovens
X.M. Wang and C.R. Zhang 160

Surface Deposition of Chitosan on Wool Substrate by Electrospraying
S. Islam, A. Jadhav, J. Fang, L. Arnold, L.J. Wang, R.J. Padhye, X.G. Wang and T. Lin 165

Study on Numetrical Representation of Topological Architecture of 3D Woven Composites
S.L. Wang and L.H. Yang 171

The Effects of Fiber Volume Fraction on the Experiment Modal Behavior of 30°/-60° Carbon Fiber Plain Woven Fabric / Epoxy Resin Composites
X.Y. Pei and J.L. Li 175

Structure and Properties Research of Multi-Antibacterial Polyamide Fibers
W.W. Sun, H. Zhang and Y.K. Zhou 179

Thermal Comfort Properties of Knitted Fabrics Suitable for Skin Layer of Protective Clothing Worn in Extreme Hot Conditions
N. Nawaz, O. Troynikov and C. Watson 184

A New Test Method for Weft Tension in Shed on Air-Jet Looms
H.L. Ma, L.X. Leng, Z.Y. Zheng and X.H. Zhou 190

Annealing Treatment of the SnO_2 Thin Film Prepared by Sol-Gel Method
Q. Xiao, R. Wang and L. Xu 194

Weave Structures Effect on the Shear Deformation of Annular Shaped Woven Fabrics
H.C. Chen and X.F. Guo 198

Weaving 3D Fabric with a "" Shaped Cross-Section
Y.T. Chang, X.M. Qian, H.W. Liu and H.W. Liu 202

Manufacture of Composite Nanofiber Mats with Fiber Diameters Grads by Electrospinning for Filtration Use
S.S. Guo, X.Y. Jin, H. Wang and Q.F. Ke 206

Study on the Tensile Properties of the High-Performance Cored Rope
Q.J. Zhao and Y.N. Jiao 210

The Application Study of the Fabric Reconstruction in the Design of Home Textiles
M. Su 214

Predicting Yarn Unevenness Using Improved BP Neural Network
H.J. Li and X.H. Wang 219

Chapter 2: Textile Dyeing and Finishing

The Printing Technology of New Pigment Used on Cashmere Products
M.Z. Li, H. Yin and Y. Cheng 225

Research Progress of Fluoride-Containing Acrylate Derivatives and their Application on Textile
H.H. Ye, Z.X. Li, G.Q. Chen, S.Q. Zhou and J.H. Cai 229

Effect of a Hydrophobic Finishing on Moisture Management Performance of Cotton Fabric
T.H. He, J.B. Yao and S.Y. Chen 237

Combination Technology of Spunbond & Spunlace
Z.M. Lu and X.M. Qian 241

Synthesis of Chelating Surfactant and its Application in Silk Degumming
Y. Zhang, X.T. Sun and X.R. Wang 245

Characterization of Cotton Fabric Treated with a Si/P Flame Retardant
R. Wang, Y.J. Bai, X.C. Wang and Y.Q. Wang 249

Application of Ionic Liquid in Silk Dyeing
D.H. Cheng 253

Stability of *Salvia miltiorrhiza* Bge Extract and its Application on Silk
S.S. Sun, J.J. Wang and R.C. Tang 257

Study on the Enzyme Desizing Process for Cotton Fabric Using Ultrasonication
Q.M. Zhao and S.Y. Zhang 261

Synthesis and Application of Isothiazolinone as Durable Antibacterial
D.J. Kong, Z.D. Liu and Y.L. Li 265

TiO_2 and ZnO Water Sol Preparation by Sol–Gel Method and Application on Polyester Fabric of Antistatic Finishing
Y.Y. Chu, Q. Wang and S.Z. Cui 270

Sorghum Red Pigment Dyeing Properties of Tencel Loose Fibre
Z.P. He, Z.M. Wu and X.L. Zhou 275

Investigation of Ultraviolet Protection Properties of Cotton Fabric via Azoic Dyeing with Green Tea Extract
N. Punrattanasin 279

Application of Chitosan on Anti-Shrinkage of Wool Fabric
Q.F. Zhang, W.F. Yang, Y.L. Qiao and X.X. Shen 283

Dyeing of Silk and Nylon 6 Fibers with Baicalin
X.C. Li and J.L. Cao 287

Adsorption Kinetic Study of Reactive Dyes on Silk with Octyl Trimethyl Ammonium Bromide as Accelerant
L. Zhong, G.X. Zhang, F.X. Zhang and X.T. Xue 291

Dyeing Analysis of Jade Polyester Fiber Knitted Fabric
H.X. Hu 298

Dyeing of Natural Dyestuff Extracted from Henna to Silk Fabric
H. Li, D.F. Zhao and R. Liu 302

Preparation of Jasmine Microcapsules and Aroma Finishing of Cotton Fabrics by UV-Curing
N. Xu, D. Yu and W. Wang 306

Research of Wool-Like Modification of Polyester with Sodium Alginate
L. Min, J.Y. Tian and M.Y. Liu 310

Research on the Application of G7 in the Gravure Printing Products
L.H. Guo, M.Y. Zhang and X.H. Guo 314

Study on Polyester Fabric Anti-Static Treated by Polyaniline
L.P. Guan 318

Effect of Preparation Parameters of Titania Sol on Textile UV-Resistance
R. Wang, Y. Chen, J. Wang and Y. Yang 322

Shrinkage Properties of Wool Treated with Ionic Liquid and Chitosan Biopolymer
H.F. Wang, H.N. Lv and X.L. Zhang 326

Anti-Bacterial Property of Tussah Silk Fabric by Nano-Titanium Dioxide and Chitosan Modification
Y.H. Lu and Z.M. Liu 330

Study on the Dyeing of PET Fiber with Disperse Dyes in D5 Media
S.Z. Li, J.Q. Liu, Y.Q. Li and L.M. Li 334

Research on Improving the Properties of Wool Fabric with Low-Temperature Plasma
Y.L. Qiao, W.F. Yang, Q.F. Zhang and X.X. Shen 338

Preparation of Temperature-Sensitive PET Fabrics by Plasma-Induced Grafting
Y.Q. Li, J.Q. Liu, C.J. Qian and T.T. Liu 342

Moderate Hydrolysis of Nylon 6 Fabric with Different Acids
X.C. Wang, P.Y. Wang, L.F. Ren and T.T. Qiang 347

Dyeing Properties of Tussah Silk Fabric with Indigo Naturalis and Turmeric
X. Hao and Y.H. Lu 352

Uniformity and Penetration of Surface Modification Effects of Atmospheric Pressure Plasma Jet into Textile Materials
C.X. Wang, M. Du and Y.P. Qiu 356

The Practice of the Printing and Dyeing Wastewater Treated by the Process of the First Coagulation Sedimentation/Hydrolysis Acidification/Anoxic/Oxic System/Secondary Coagulation Sedimentation
Z.W. Lei, G.Y. Yang and C.L. Xi 360

Dyeing Research of Aramid Fiber-Nomex
Y.J. Tan and Y.E. Yu 364

The Treatment of Printing and Dyeing Wastewater by Using Coagulation and Fenton Reagent Oxidation Combined Process
L.P. Wang, Y.C. Guo, Y.Z. Chen, E.D. Du and Y.J. Mao 368

Comparison of Dye Adsorption Behaviors of Sodium Polyacrylates Freely Dissolved in Water and Grafted onto Poly(*Ethylene Terephthalate*) Fiber
X.L. Shi, H. Song, X.S. Zhu and Z.J. Pan 372

Dyeing Properties of Chitosan-Sulfamic Acid Solution Treated Wool with Silane Coupling Agent
X.M. He and K.L. Xie 377

Wrinkle-Resistant Property of Cotton Fabric Treated by Chitosan and Epoxy-Silicon Micro-Emulsion
H. Wang, C. Huang and N. Liu 382

Deepening Effect of Superfine Dyed Polyester by Escaping Electron-Beam Atmospheric Pressure Glow Discharge Plasma
T.T. Liu, Y.Q. Li, J.Q. Liu and L.J. Meng 386

The Synthesis Characterization and Application of Amino-Modified Polymethylhydrosiloxane Softener
X. Zhao and W.Y. Zhu 390

Anti-Hairfalling Finishing of Rabbit Hair Knitted Fabrics
J. Liu, R.Y. Zhu and Y. Zhang 394

Effects of the Cotton Fabric Pretreatment on Application Properties of Digital Inkjet Printing with Reactive Dyes
Q. Zhu, J.D. Cao, W. Wei, J.C. Zhong, J. Yao, Y. Ye and X.X. Yang 398

Preparation and Application of VE Microcapsules with Polyurethane Shell for Skin-Care Textiles
G.P. Yao, J.H. Zheng and H.F. Chen 402

Preliminary Study on the Green Anti-Counterfeiting Printing Materials
Y. Yang, X.H. Zhou, G. Zhao and X.P. Lu 407

Morphology and Properties of PET Fabric Finished by β-Cyclodextrin and Citric Acid
Y.L. Wang, W.L. Xu, Y. Wang, Y.M. Wu and S. Cheng 412

Study on Reuse of Dyes from Wastewater
M.Z. Li and J. An 416

The Manufacture and Dyeing of Cationic Dyes Dyeable Linen Fibers
S.Z. Gao, Q. Liu and Q.J. Liu 420

Structure and Properties of Modifier for Heat Transfer Printing on Cotton Fabric
Y. Mu, L. Wang, M.H. Wu and J.X. Lin 426

Chapter 3: Textile Machinery and Equipment

The Application of Motion Control Technology to Textile Production
M. Han, C.Y. Miao and J.M. Chang 433

Affect of Application of Hairiness Reduction Equipment on Winding Quality
J.P. Lin and H.J. Cui 437

Optimal Geometry Design of the Coat-Hanger Die Used for Melt Blown Nonwoven Processing
W.L. Han and X.H. Wang 444

Prediction of Yarn Quality Based on BP Neural Network
J. Yuan, Y.L. Li and S.Y. Chen 449

The Impact of Weft Quality on Air-Jet Loom Weaving Efficiency
H.J. Cui, J.P. Lin and L.J. Li 454

Comparative Study on Vibratory Stress Relief (*VSR*) and Thermal Stress Relief (*TSR)* of Cylinder Wallboard
X.W. Dong, X.P. Zhao, S.Q. Yu, X.W. Zhou, D. Ren and Y.F. Zhai 460

Study on New Drafting Form of Comber
X.R. Li, X.M. Jiang and J.C. Yang 465

Research on Mechanism of Magnetic Suspended Knitting Needles
X.G. Wu, W.B. Zhu, C. Zhang and C.J. Zhang 472

Circular Nets Printing Machine Synchronicity System Based on Intelligent PI Controller
X.D. Gao, G. Wang and Z.M. Nie 476

Fabric Defects Detection Using Multi-Scale Wavelet and Locating
J.F. Jing, H. Li and P.F. Li 481

Curve Matching Algorithm Applied to Fabric Automatic Register Detection
J.F. Jing, G.Y. Li and P.F. Li 485

The Research of Two-for-One Twisting Spinning Frame
X.Q. Ren, W.Y. Li and X.F. Shen 489

Reducing Yarn Hairiness in a Modified Ring Spinning Yarn Path by Various Offsets
X.Z. Su, W.D. Gao, T.T. Wu, X.J. Liu and Y. Zhang 493

Quasistatic Model for the Symmetrical Ring Spinning Triangle
X.J. Liu, X.Z. Su and T.T. Wu 498

Effect of Siro-Spun Processing Parameters on Properties of 55/45 Flax/Cotton Blended Yarn
S.Q. Liu, J.M. Dai, H.S. Jia, X.G. Liu and B.S. Xu 502

Research on the Manufacture of Tapered Artificial Vascular
X.Q. Dong, Y.L. Li, X. Ding and L. Wang 512

Test Reliability of Impurity Parameters of Uster AFIS
P.Z. Sun and J.P. Cao 516

Heart Move with Color - Color Psychology and Textile Color Aesthetic
X. Yi 528

Effects of Enzyme and Softener Treatment on Properties of Ramie Fabrics
L.H. Bai and H.Q. Yu 532

The Study on 3D Weaving Method for Tubular Fabric
Z.H. Sun, S.H. Zhou, F.F. Tang, C. Liu, D. Ran, J.R. Yuan and Z.Y. Li 536

Chapter 4: Apparel Design and Merchandising

The Researchment of Knitted Antifouling Fabrics and the Splicing Design on Leather Garment
H.T. Deng 543

Research on Children's Functional Clothing of Keeping Safety in the Car
L. Shen, X.H. Jiang and Y.Y. Chen 547

The Functional Requirements Analysis of A/W High Altitude Cleaning Overall Materials
W.W. Huang and B. Guo 551

Study on Improvement of Manufacturing Cycle Effectiveness of Apparel Vendor - Case Study of Order Scheduling and Batch Feeding manegement and Control
C. Yang, Y.X. Yang and W.N. Qi 555

Application of Pattern Recognition System in the Automatic Generation Pattern Technology
L. Qiu and X.D. Chen 561

Research on Bra Constitute and Performance Evaluation
H. Shi, J.P. Wang, Z.Y. Wu and X.N. Chen 566

Research on Consumer Motivation for Luxury Products in China
Z. Zheng 570

Comparative Analyses between Consumers' Actual and Targeted Transaction of Menswear Based on Taobao E-Business
X.Q. Wang, M.H. Chen and A.D. Zhang 574

Women's Suit Pattern Parameterized Intelligent Design
Y.Z. Wang, J.P. Wang, S. Sun and Y.M. Li 578

The Application of Chinese Element in Fashion Design
G.H. Li, R. Shi and G.L. Liu 582

Study on the Innovative Design of Fur Clothing
T. Xu, M. Fang and G.D. Li 586

Application of Typology Method in Chinese-Style Clothing Pattern Design
S.G. Wu 590

Regression Analysis on Influences of Hem Parameters on Flare Sagging of Semi-Circular Skirt
H. Ni 594

The Analysis of Structural Mathematical Model of Suitable Female Jacket Design Based on Waist and Hip
P. Zou and S.G. Wu 599

Redesigning the Apparel Product Development Process Based on the No-Interval Coherently Phased Product Development Model
C.S. Wu and Q.Y. Wu 603

An Analysis of Marketing Function of Fashion Show
Y. Xu and M. Zhang 607

Mathematical Model of Attaching Sleeve Based on the Change of Underarm Point
Y.M. Liu, L. Zhang and G.H. Feng 611

Research on Clothing Styles Classification Model Based on the MDS and K-Means Method
H.J. Xu, F.Y. Zou, J. Wei and Y. Zhang 616

Research on the Development Situation of Transmutability Clothing
H.E. Liang and L.M. Jin 620

BWH Reshaped Made Use of Reshape Underwear Based on the Model of Female Physical Beauty
W. Jiang, X.M. Qian and L.L. Zhai 624

Aerobics Clothing Consumption Behavior of College Students in Hangzhou
Y.X. Yan, W.J. He, L.J. Lou, J.W. Tao and M.B. Lin 628

Research on Dynamic Clothing Show of Virtual Character during the Online Shopping
Z.Y. Wu and Y. Zhang 632

Simulation of Efficiency of Liquid Cooling Garments
M.W. Tian, S.K. Zhu and N. Pan 636

Evolution Law of the Traditional Baina Textile and its Application Style in the Clothing
H.E. Liang and L. Xing 640

Research on the Influence of the Fabric Organization to Wind-Resistant Property of Sportswear
Y.X. Yan, X. Yi, J.W. Tao, M.B. Lin and R.Q. Li 646

Establishment and Application of Evaluation Model for College Students' Perceived Quality of Clothing
Z. Li 650

Relationship between Special Body Variable and Figure of Women's Trousers Pattern
X. Lu 654

Study on the Fashionable and Preferable Emotion of Men's T-Shirt between Males and Females
X.X. Zhang, S.S. Wang and G.L. Liu 658

Research on the Relationship between Special Dart and Fabric of Women's Wear
L. Wang 662

Zen View of Nature in the Performance of Modern Fashion Design
N. Qiao, L.J. Liu and Y.Y. Lv 666

The Application of Geometric Form in Clothing Design
C.M. Lin, C.H. Lin, P.C. Hsiao and Y.C. Yang 670

The Drapability Effects Test Method of Lining and Shell Fabric
F. Yu 675

Design and Development of Chinese Primary and Secondary New Type School Uniform
M. Yu and X. He 679

Chapter 5: New Trends in Textile Industry

Predictive Modeling and Empirical Analyses of Regional Silk Fabrics Price Index Based on BP Neural Network
H. Liu, B.D. Liu and X. Yang 685

Influence of Color and Style on Clothing Identification
X.F. Jiang, X.X. Zhang and G.L. Liu 689

Rising Labor Cost and the Comparative Advantage of Chinese Textile Industry Analysis
J. Wang 694

The Molding Technology of Manufacturing Waste Blend Fiber Composites by Mixed Hotpressing
L.H. Lv, G.J. Wan and Y.L. Yu 699

Study on Water-Based Highly Reflectivity Insulation Coating
Y.F. Luo, Z.Q. Du and W.D. Yu 703

The Influence on Hydrophilic after the Surface Treatment of the Singed Gray Fabric by the Low Temperature Plasma
P. Li, S.J. Zhang and S.G. Wang 708

Comparison of Plasma-Aided Desizing with Conventional Desizing of Polyacrylate on PET Fabrics
X.M. Li and Y.P. Qiu 713

Influence of Atmospheric Pressure Plasma Pre-Treatment on Sodium Bicarbonate Desizing of Polyacrylate on PET Fabrics
X.M. Li and Y.P. Qiu 718

An Analysis of Shaoxing Textile Industry's International Competitiveness: The Perspective of the Export Evaluation Indexes
A.Q. Jiang and R. Zhang 722

Strategies for Textiles and Apparel Enterprises in Jilin Province "Going Global"
Y. Liu and F.Y. Wang 726

Design Driven Innovation for Textile Industry
A. Lottersberger 730

The Analysis of Fashion Buyers' Development in Clothing Industry of China
L.J. Liu, N. Qiao, X.P. Li and M. Feng 735

The Apparel Industry as an Example of Industry Development Trend of China – Segmentation Module within the Industry, Strengthening of Cooperation between Industry
A.Y. Yun, M. Fang and D.M. Wang 740

CHAPTER 1:

Textile Science and Technology

© (2011) Trans Tech Publications, Switzerland
doi:10.4028/www.scientific.net/AMR.331.3

The Application of Folkloric Textile Decorative Art to the Regional Character of the Hotel

Jin Zhu [1, a], Yi Fan Chen [2, b]

[1] Fashion · Art Design Institute, Donghua University, 1882, West Yan An Road, 200051, Shanghai, P.R.China

[2] Fashion · Art Design Institute, Donghua University, 1882, West Yan An Road, 200051,Shanghai, P.R.China

[a] zhujin_dhu@yahoo.com.cn, [b] yifan2867@sina.com

Keywords: Textile, Folkloric decoration, Regionalism, Hotel interior space

Abstract. The construction of the regionalism is not only affected the architecture space pattern, but also is closely related to the soft decoration art. This paper has analyzed the elements of the folkloric textile decorative art from the level of decoration pattern, color, material and technology. Taking decorative arts with regional characteristics as an example, the paper discusses how folkloric textile decorative art express the theme of the hotel and implicate the regional characteristics in symbolic elements and stylized language combined with the cultural history and folk custom in different areas. Meanwhile this paper summarizes approaches of creating regional character of modern hotel space. The adornment style should be determined according to the hotel orientation. The folkloric features should be strengthened in serialized designs to create the non-material artistic conception combined with other soft adornment.

Introduction

The conception and type of the folkloric textile decorative art. The conception of the folkloric textile decorative art is refer to the modeling way and aesthetic tendency in the textile to represent the traditional region culture, human custom, local technology and any other natural or cultural traces or element characteristics left over by history.

The soft adornments in the hotel space include textiles, furnitures, plants and the other redisplay articles that their position can be changed and they can move freely. Within these soft furnishings，folkloric textile decorative art is one of direct and concrete visual media that reflects the hotel regional characteristics.

The textile features of folkloric decoration art are widely used in hotel interior space. Judging from the structure of product category, it can be divided into two broad categories. They are interior decoration products (including carpets, tapestries, sofa & chair covers, curtains, towels, tea towels, tablecloth etc.) and beddings (including sheets, bedding bags, bedspreads, blankets, pillow cores, pillowcases etc.).

The conception of regionality. Regionality is a comprehensive conception. It contains not only the geographical and meteorological and other natural features, but also the tradition created by local cultural factors. People always require a sense of belonging and identity. Therefore, when technology began to dissolve social cohesion, people questioned on the effectiveness of technology and put forward to the requirements for regionality and nationality [1].

The Elements of the Folkloric Textile decorative art

The forms of folkloric adornment have the characteristics of aesthetic generalization and plebification. Most of them were manufactured by hand. Decoration pattern is regarded as relatively concrete. Majority of the adornment color and the method of collocation are derived from folk practice. Second, the adornment of folkloric forms are usually rooted in the mainland where is rich in

cultural content generated under the background of special region and time. These decoration forms have abiogenetic character which could not be replicated. However its uniqueness determines the regional authenticity.

The folkloric decorative pattern in textiles. There is a wide range of folkloric decoration pattern and subject used in textile design. It could be divided into animal patterns, figure patterns, plant patterns, flower patterns, landscape patterns, auspicious patterns, totemic patterns and so on. The root-causes are the emotion of humanbeing which expresses invocation for auspicious welfare or evasion of the evil. For example, "Tang Cao Wen" Pattern signifies the meaning of exuberance and permanence.

As the distinction of various subjective and objective factors like climate environment, religious beliefs and natural worship in different regions, there are different folkloric decoration patterns among different countries and regions. For example, in Tibet the "eight lucky patterns" symbolizes the power of Buddhism and the "Wan Zi Wen" pattern implicates the meaning of endless blessing.

The folkloric decorative color in textiles. In China confucians matched the five elements with five virtues which were expressed by five colors: gold for white, wood for green, water for black, fire for red, soil for yellow [2]. Because our country was influenced by the traditional feudal etiquette for long time, it had set up a strict color level system according to the statement of noble and humble. Yellow and red were the highest level of color. Generally, only the royal buildings, color paintings and adornment implements were qualified to use such splendid color. Green, blue and purple taken the second place. Black, gray taken the lowest level and were used for commoner civilians.

Because the consciousness of traditional colors which made a deep recessive influence to public aesthetic has already solidified, colors in different regions have specific symbol connotation and emotion orientation. For example, the Burj Al Arab Hotel located in Dubai has win high admiration of luxurious hotel in the world. Each corner in interior space shows its high temperament. Hotel lobby, the atrium, suites, even the door handles and water faucets in the bathroom are painted with golden vela. Soft adornment and fabric ornament are also used gold and red series. The colors of carpets, wall pictures and beddings are all in high lightness and hue. Although in the harmonic color system, that still challenges the guests' visual limitation.

The folkloric decorative materials in textiles. The folkloric decorative materials in textiles mainly include natural fibers and chemical fibers two categories. The folk textiles usually adopt natural fibers including cotton, hemp, silk, wool etc. Currently the folk textiles also use chemical fibers including synthetic fiber (polyamide, polyester and acrylic, vinylon, polypropylene fiber, chloro fiber, spandex etc) and recyclable fiber (Also called artificial fiber) two types.

The materials also possess affluent languages to express emotion due to their special touch sensation such as texture and qualia structure. Silk was known as "the queen" in textiles which have the bright color and luster, exquisite texture. The silk not only reveals its beauty of femininity, but also the symbol of quality. Soft and comfortable cotton material has the civilian affinity; Linen material with the coarse texture shows up its inherent nature of economic and environmental.

Different areas were rich in different materials. Specific characteristics of materials implant the iconic symbol of regionalism into the textile handicrafts. Most of the traditional handicrafts tend to use local materials. Normally they have unvarnished selection consciousness of resources optimization. Wujiang located in China's famous Tai lake where abounded in silk production. Since Ming dynasty, following the development of handicraft silk Chengze and Shengze became the professional silk towns. The silk economy played an extremely important role in this location. Silkworm raisers, machine households, businessmen were all made their living from silk [3]. Regional materials provided villagers with livelihoods, meanwhile it became the most adopted materials in regional textiles.

The folkloric manufacturing crafts in textiles. Traditional textile technology was breed in different environment and cultural context, which has its manufacture technique and manual process. Taking our country's textile embroidery technology for example, from south to north, town to countryside, there are totally different production processes. Suzhou Embroidery ranks the first in the four most

famous embroideries. It includes not only the flat embroidery and double-sided embroidery, but also crewel works in Changzhou, Dan Yang, Baoying, Nantong's simulation embroidery, Yangzhou's archaize embroidery and Chetai's hair embroidery. Changsha in Hunan province is the center of Xiang Embroidery. Yue Embroidery takes Guangdong as the center. Shu Embroidery in Sichuan takes soft satin and color silk as the main raw materials. Sophisticated materials are used in Beijing Embroidery. Shandong area's mainly bases on Lu Embroidery . Whatever the technology types of the embroidery were, all had their technological processes that could not be duplicated.

Technology and process also affect the subtle changes in adornment gradation, they even play the key role in the final adornment effects. Manual works, selection of the mould types, the orders of the process were the direct factors which affect the final forms of textile handicrafts. For example, the principles of wax printing were basically similar to tie dyeing. However slight difference between the techniques would cause the otherness in visual forms. The first step of wax printing is pouring wax on the materials for hot melt and dyeing in indigo. The next step is removed wax layers. The final form of the batik article will be white flowers on the blue background or blue flowers on the white background. The process of tie dyeing is tying the textiles and dipping it into the color paste to dyeing. Compared with wax printing, the technological process of tie dyeing is more casual and the final effect of the finished products is also more natural, which is always carried with a sort of vivid occasional texture.

The Channels of the Folkloric Textile Decorative Art Conveying to the Regional Character of the Hotel

Symbolic translation. The value of traditional decoration symbols lies in the information and meaning. It is easier for people to get information from graphics. Graphics built symbols and symbols built information. Significance could be generated through the interaction between communication and reception and make people understand and receive traditional culture [4]. Before words to be created, people materialized their experiences and emotions as graphics. These patterns acted as translating function which was responsible for communicating subjective and objective world. Initially these natural and geometric patterns with symbolic significance were just concrete images. However, once they were classified and be given spirit connotation, they had established specific corresponding associations between signified and signifier of semiotics.

The translating ways which the folkloric textile decorative art convey the regional character of hotel could not only adopt typical pattern symbols but also use folk events as symbols. For example, there are "dragon beds" in the guest room of Wangfu Hotel in Beijing. It is a symbol of the identity of emperors in ancient times. Dragon pillows and dragon quilts are the symbols materialized by folkloric textiles. Another example, the textile adornment on the subject of wayang kulit and the painting of farmers in Hu county frequently make people have association of folk customs in northwest with a strong local flavor. The reason is because these northwest "events" had been symbolized to be the pronoun of northwest.

The local popular language."Word" and "grammar" in adornment languages constituted different "language". "Word" in adornment languages is different adornment elements mentioned above, and "grammar" is the composition pattern and logical relation. There is a set of stylization system and inheritance mode that belongs to certain nation customs about tools, materials, modeling rules. The stylized rules must get approval over time and through the test of practice. It came down as the "dialect" from generation to generation.

Once the "dialect" gets involved in hotel interior space, the "paronomasia" should be subjected to the overall control of the regional design principles. Actually, the design principles are "grammar" which be depended to finish many rich sentences. In different regional hotels, textiles and supporting art had rules for modeling that could be caught easily. Stylized color matching principles and display methods state the local conditions and customs in skilled visual "dialects". In some hotels in Southeast Asia the chair cushions and pillows are densely laid out. That is different from the elegant

and homogeneous modes like in other countries, but it corresponds with the aesthetic orientations in Mahayana Buddhism that beauty acts usually full of ornaments. Basing on the value system of recognizing common customs and appreciating on simple art forms, folk art adornment generated. Despite the lack of rhetoric, the localizable ways are more straightforward and bold. The impression given to tourists is brighter. The expression for regional character is clearer compared with the metaphysical expressions like White Snow in Early Spring.

Thematic interpretation. In textile decoration design, a kind of method is to convey the themes through some widely known folk stories. The embroidery "Riverside Scene of Pure Brightness" reappeares the natural scenery and people's livelihood bustling scene in capital Bianjing in northern Song dynasty by different embroider line and delicate stitches.

Another method is to make "hidden" cultural heritage as space clues to express the core content in manifest language like reel off the raw silk fiber from the cocoons. For instance, the Guibin Hotel in Beijing uses Beijing Opera as the textile design theme to match the furniture and display in Chinese classical style. The recessive characters of folk imaginations from Beijing Opera culture and the exaggerated expressions to good and evil would come out naturally by means of typical color, graphic and brushwork.

Design Methods of Folkloric Textile Decorative Art to Regional Character of the Hotel

Determining adornment style according to the hotel orientation. Textile decorative art localization should belong to the hotel orientation about consumption levels and the whole functions. For the types of holiday hotel, textiles decoration art should bases on natural, totem or other freehand style. In the timeshare vacation hotel and apartment hotel which are booming in recent years should decorate certain of leisurely and place easy hugging pillow, curtain, bedding products according to the residential space scale and atmosphere. The pattern should be simple, the tone should not be too gaudy. Commercial convention hotel is relatively serious and rational, the folk adornment art of the textiles could take geometric figure primarily.

Strengthening regional characteristic by series design. In order to highlight the central theme of folkloric textile decorative art in the series design, it could carry out a series of repetitious and specific elements design for different textiles interfaces to strengthening the regional characteristics.It can work through the following ways. First, the various classification of textiles should be clarified. Each type or the division should have the unified typicality modeling motif and each part should certain continuity. Second, different composition methods could be used such as homogeneity in color but diversity in structure, homogeneity in form but diversity in structure or diversity both in shap and composition. Finally, the Interfaces and carriers could be both two-dimensional surface and three-dimension spaces or cubic.

Cooperating with other soft decoration to create immaterial artistic conception. Folk textiles should also match other soft adornments to keep all components in line with the overall environmental atmosphere. In Jiangsu Fhoenix Palace Hotel in Nanjing,there is not luxurious interior space, carved beams or painted pillars. But it uses the partition which cooperated with the antique furniture to create an artistic conception full of romantic and nostalgic. Meanwhile, it combines with the overlapped silk curtains and folk textiles with fine broidering to make a peaceful atmosphere.

In addition to respecting the aesthetic law at the level of materialization and coordinate unified form, immaterial aesthetic artistic conception to be the purpose still need to be created [5]. For instance, the textile decoration of bamboo could create an artistic conception of peaceful, serene, sublime and reclusive. In present era the folkloric decoration form should keep the non-material style and content to arouse people's reflection to the prospect of decoration art and to evoke people's attachment to their national culture rather than to be assimilated into the aesthetic cognition of globalization.

The Inheritance and Updating of the Folkloric Textile Decorative Art to the Regional Character of the Hotel

Recovery of the concrete form. Recovery of the concrete form is point to maintain the folk textile configuration of traditional art completely and then translated it to the new environment space. In a sense, this is a kind of " ready-made art" and there is no need to redesign this decoration pattern. For example, in some hotels in Yunnan minority areas, wedding dresses and handmade embroideries from the Miao, Yi and other minority nationalities are mounted and framed. They are exhibited as interior decoration directly. This soft adornment design is economical and feasible. Although as a sort of concrete reduction, it causes audiences' imagy of the daily life, work and rest, ceremony etiquette in minority areas.

In addition, it could give traditional design vitality via modern technology or the replacement with the new materials. It should be considered that the adaptive relationship between the hotel environmental space and the decoration pattern after transposition or conversion. Folkloric decoration pattern mostly appeared heavy, complicated and delicate. The interior space and interface where the patterns be placed should be concise in modeling, simple in material and solid in quality, symphonious in tone. On such cases, the subtle and sensual features of textiles can be set off. Then they can effectively communicate information and let audience focus on vision central point.

Summarizing the elements of the original decoration and unit reproduction. Facing various adornment forms, we should analyze and abstract them. Meanwhile with the aid of decorative pattern composition method, the concrete pattern should be transformed into abstract symbol and motif elements which will be used as original conception. It is considered that any forms are perceptual integration with highly organization level in Gestalt Psychology. People are more vulnerable to transform the complicated and irregular shape into simple forms or the correct combination in the visual activity. Basing on this theory, if we extracted and purified the folk pattern unit as well as the rule of organization, and then made a repeated breeding to this simplified unit, the new created pattern could not only reserve original characteristics but also be simple and clear while easier to grasped by vision. Our country's traditional folk patternes usually include separate pattern, fit pattern, corner pattern, edge pattern, scatterplot pattern, continuous pattern and so on. They could be extracted and generalized as some geometric or natural organic symbol. Meanwhile, following some traditional composition rules such as symmetry, center radiation, two directions and four directions continuous composition, the abstract new pattern could be designed.

In hotel space, the display way of the textiles also can refer to pattern organization and composition rules, it can be even intensive layout. The contemporary design does not repel to use other modern compositions such as pop art to piece many concrete units together as a giant concrete pattern prototype again.

Transformation and variation of decorative vocabulary. In order to collapse prototype and generate new form, we can take a bold attempt to the prototype with rotation, extrusion, stretching during the process of redesign to the folk decoration pattern. Topological transformation is one of specific ways. It points that under continuous transformation the geometric figure the would not changed its basic nature. If we drawn the folk pattern in rubber membrane, when rubber membrane was deformed by external forces but would not broken or enfold, some graphic attributes such as closed curve, intersection, overlap, centrality etc. still remain the same. All these features provide us an open approach to create imagies.

Compared the new form with prototype, the distorted pattern is more irrational. It also inclined to regain prototype. Transformation is just like the "variation" in music movement, but its usage should belong to hotel's integral style. For example, through central extrusion the circle folk pattern can produce optical illusion about three-dimensional sphere. Designers wants to use this exaggerated transformation symbols to express the emotion of irony, teasing and ridicule. Such textile setting style wouldn’t be incompatible in post-modern hotel space.

Decomposition and restruction of decorative vocabulary. In terms of the creation of the decoration pattern, we can decompose, scatter and eliminate the original prototype's linear structure. Meanwhile using computer parametric design and make it involve in the process of pattern formation, we can adopt nested loop or nonlinear structure to experience the essence of decoration pattern formation with the way of natural organization.

The hotel space can also show up like "fragment" or "ongoing outlook". Decoration pattern clips could distribute in certain part of the textiles. Sometimes they appear in the corner, on the roof, sometimes on the pillar. That looks like the center picture is disintegrate casually into pieces, and melt into every corner in the space. Pattern integrity of the monomer component in traditional sense is eliminated. Each component get rid of the bondage of latitude, the new continuity between textile accessories and space interface is being built. The way of amplifying and blurring the interface of textile decoration pattern liberates modeling methods. The folk regional features in hotel also generate a surprisingly aesthetic explosive force by means of the technique of diverse, random, open and dynamic.

Conclusion

Basing on the situation that our country is a developing country, we should use the immaterial cultural resources to make up for the lack of material resources. Using the means of "immateriality" to emphasizes spirituality of "artistic conception" while brush over the "luxury" as creation standards, that could be regarded as the positive response to face the poor conditions in our country design field [6]. It is a kind of economically mean using textiles and other soft adornment arts nimbly to deal with different hotel space. It also reflects the flexibility to adapt to sustainable development design that the textile with folkloric characteristics can be changed according to space, seasons and festival ceremonies.

In addition to the expression of symbolic, intuitive and labels type, we still need to analyze the deep regional culture and philosophy background, rather than following the "symbol consumption". The re-design of folkloric decorative art is not the simply restoration or just to satisfy the curiosity about cultural differences. Through the extraction and summarization from original adornment elements we can update and recreate them in the new context. Therefore the expression of the regionality and nationality will not confine to the level of pattern restoring.

Folk custom is not the same thing as tasteless or raffish custom. During use popular language moderately in textile arts, we should start from the practical way of life and the habit of aesthetic, rather than base on one-sided understanding of folk-custom or under the pathological understanding. We should take the analysis for folk adornment color, readjust tone and the component of constitution to meet the aesthetic needs of the contemporary audiences.

References

[1] Qinnan Zhang: *Characteristics to Win-Architectural Theory Discussion*. (China Machine Press, Beijing,2005). 33-35.

[2] Zhilin Zhan: *Chinese folk arts*. (The First Edition. China Intercontinenal Press, Beijing,2004).8:99-100. In chinese.

[3] Dehua Zhou: The Wujiang Sericulture Folk Custon. CNKI:SUN:ZJSG.0.1993-03-006. In chinese.

[4] Zhiliang Zheng, Yanfeng Jia: The unique performance of multimedia art means for the traditional art [J]. (2006)In chinese.

[5] Citing Editorial Committee. (*Citing·Compact Edition[K]*.Shanghai, 1979). 680. In chinese.

[6] Qinnan Zhang: *Characteristics to Win-Architectural Theory Discussion*. (China Machine Press, Beijing ,2005).Postscript. In chinese.

© (2011) Trans Tech Publications, Switzerland
doi:10.4028/www.scientific.net/AMR.331.9

Impact of Soft Nursing Care on Drying Efficiency of Cotton Fabric

Chunjie Qian[1,a], Jili Tu[1,b], Huayun Ge[2,c] and Jinqiang Liu [1,2,d]

[1]Engeneering Research Center for Eco-Dyeing & Finishing of Textiles, Ministry of Education, Zhejiang Sci–Tech University, Hangzhou 310018, China.

[2]Key Laboratory of Advanced Textile Materials & Manufacturing Technology, Ministry of Education, Zhejiang Sci–Tech University, Hangzhou 310018, China.

[a]qianchunjie_1986@126.com, [b]Tu579@126.com, [c]guy_654321@163.com,

[d]jqliu@zstu.edu.cn(corresponding author)

Keywords：home laundry，softening agent，wicking，heat transfer coefficient，drying efficiency

Abstract. The performance of heat transfer coefficient, wicking and water vapour permeability (WVP) of cotton fabric were tested after adding amino-functional silicone softening agent in simulating process of home laundry. Meanwhile, the experiment of line drying of fabric soaked in water after spinning was designed to study the impact of soft nursing care on drying efficiency of fabric. The result showed that with the amino-functional silicone softening agent added, handle was improved obviously. With the concentration of softening agent increasing, WVP of fabric increased, while heat transfer coefficient had the opposite result. Wicking effect increased slowly at the beginning and decreased sharply later. It was found that soft nursing care improved the drying efficiency.

Introduction

Household clothing care contains two aspects--dehydration and drying. The two processes are time-consuming and energy consumption, as well as the main reason for the unreasonable energy consumption, as it is the case in textile industry. In the textile industry, drying of fabric is a necessary process in the textile finishing, hence how to develop a energy-saving and time-saving method should be paid more attention to. Many researches were carried out to improve the drying efficiency, for example, Liqiu Chen [1] designed new mangle bowls to lower the pick-up of fabric to improve the drying efficiency. Drying rate of fabric depending on the fiber moisture regain and speed of capillary migration were investigated [2]. JinQiang Liu [3] found the water can drip from fabric quickly due to reducing the water surface tension. LiMing Zhou [4] studied that dehydration efficiency could increase greatly after repellent finishes on fabric.

Softening finishes is one of the most common treatments on fabric finishing. With chemical softeners, textiles can achieve an agreeable soft hand (supple, pliant, sleek and fluffy), some smoothness, more flexibility and better drape and pliability [5,6]. With fabric absorbing softening agent, the surface energy decreases, which resulting in easily expansion surface and extension length of fiber, followed by becoming fluffy and improving the feeling of added fullness. The fluffiness has an effect on the performance of fabric, such as, air permeability, water vapour permeability (WVP), heat transfer and moisture conductivity. Jianhui Yang [7] proved that softening finishes could improve the moisture conductivity of fabric. Therefore, the good performance of fabric mentioned above, may be obtained via depending on fluffiness of the fabric with softening agents.

Based on the above viewpoints, in this work, the amino-functional silicone softening agent was used for soft nursing care to make cotton fabric fluffy. And then, the effects of softening agent W on performances of fabric were focused on, such as heat transfer coefficient, wicking and WVP. Finally, line drying of fabric soaked in water after spinning was discussed the impact of soft nursing care on drying efficiency of fabric.

Experimental

Materials and instruments. The fabric used in this work is 100% cotton woven fabric. HangZhou ZhuoLi Chemical Co., LTD supplied the softening agent W. The instruments are Guard heated plate instrument (YG(B)606D, WenZhou DaRong Instrument Co., LTD), Moisture Permeability testing instrument (YG601-Ⅰ/Ⅱ, NingBo Textile Instrument Co.), Washer (EWS 850, Electrolux) and cloth rack (man-made).

Methods. Simulating process of home laundry. Different solutions with concentrations of 1g/L, 2g/L, 3g/L and 4g/L were prepared using softening agent W. And then the examples were soaked in the solutions, and put into water bath to simulate process of home laundry. Followed by centrifugal dehydrated in washer, the samples were dried at 60℃ for 1h in oven, and then put in laboratory with constant temperature and constant humidity for use.

Determination of heat transmitting of fabric. The warmth retention rate and coefficient of heat transfer of fabric were determined based on "Testing method for warmth retention property" (GB/T11048-1989), using Guard heated plate instrument (YG(B)606D). The warmth retention rate was calculated as follows:

$$Q=(Q_1-Q_2)/Q_1\times 100\%. \quad (1)$$

In the equation, Q_1 is heat dissipating capacity without sample and Q_2 is heat dissipating capacity with sample.

The coefficient of heat transfer was calculated as follows:

$$U_2=U_{bp}\times U_1/(U_{bp}-U_1). \quad (2)$$

Where U_2 is referred to heat transfer coefficient. U_{bp} is the coefficient of heat transfer of test board without sample and U_1 is the coefficient of heat transfer of test board with sample.

Determination of moisture permeability of fabric. By using Moisture Permeability testing instrument (YG601-Ⅰ/Ⅱ), the WVP of fabric was tested, based on "Determination of water vapour transmission rate－Dish method" (GB/T12704-91). The WVP was calculated as follows:

$$WVP=24\times(W_1-W_2)/(s\times t). \quad (3)$$

WVP is referred to water vapour permeability. W_1 in the equation above is the weight of test dish in experimental environment conditions for 1h, while W_2 is the one for 2h. S is the experimental area of sample fabric, and t is the experimental time.

Determination of fabric height of wicking of fabric. The performance of wicking of fabric was measured by employing the standard "Test method for capillary effect"(ZBW04 019-90).

Line drying experiment. The samples were soaked in pure water for 30 min, centrifugal dehydrated, and line dried on a lab-made equipment till the balance. With the initial water retention of the fabric setted as 75%, the wet weight of sample was recorded per 5 min, Ambient Temperature 20℃±1℃, RH 60%±1%. And then the relation curves between water retention and time could be drawn. The water retention was calculated as follows:

$$M\%=(m_1-m_2)/m_2\times 100\%. \quad (4)$$

In the equation, M is the water retention, and m_1 is wet weight of fabric, while m_2 is dry weight of fabric.

Results and discussions

Heat transmitting of fabric. Table 1 gives the warmth retention rate and heat transfer coefficient of fabric after soft nursing care. With the concentration of softening agent increasing, the warmth retention rate increases, while the heat transfer coefficient of fabric decreases. Amino-functional silicone softening agent orient themselves with their positively charged ends toward the partially negatively charged fiber, creating a new surface of hydrophobic carbon chains that provide the characteristic excellent softening and lubricity seen with cationic softeners. The improving warmth retention rate and decreasing heat transfer coefficient are assigned to increasing distance between fibers which result in more static air.

Table 1 Warmth retention rate and Heat transfer coefficient of fabric after soft nursing care

Concentration of softening agent [/L]	Warmth retention rate [%]	Heat transfer coefficient [/m^2 • ℃]
0	33.6	33.43
1	36.2	29.81
2	37.1	28.71
3	37.5	28.15
4	37.7	27.94

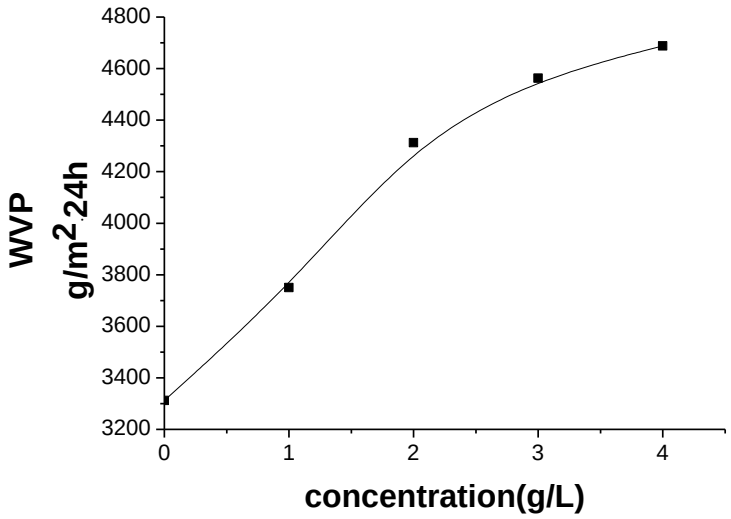


Figure 1 WVP of fabric done with soft nursing care with different concentrations

Moisture penetrability of fabric. As shown in Figure 1, the values of WVP increase rapidly till a value after which the tendency increases slowly, according to the higher concentration of softening agent. WVP is referred to the transfer rate of water vapour in fabric, which is connected with transferring rate of water vapour in apertures between fibers and fiber interior. The bigger distance, the more moisture penetrability.

Wicking of fabric. Figure 2 shows the distance travelled by water in fabric done with soft nursing care in 30 min. The distance of water in fabric could be calculated as:

$$h=\gamma\times\cos\theta\times r\times t/\rho. \quad (5)$$

Where h is the height of the liquid rise in time t, γ is liquid surface tension, θ is contact angle, r is radius of capillary of fiber, t is time and ρ is fiber viscosity [8]. From Figure 2, wicking effect increases slowly at the beginning, while decreases sharply later. The soft nursing care enlarges the radius of capillary, which is favor for wicking. However, with concentration of soften agents increasing, the water repellency of fabric become dominated, followed by is the contact angle being larger. All these are unfavorable for wicking.

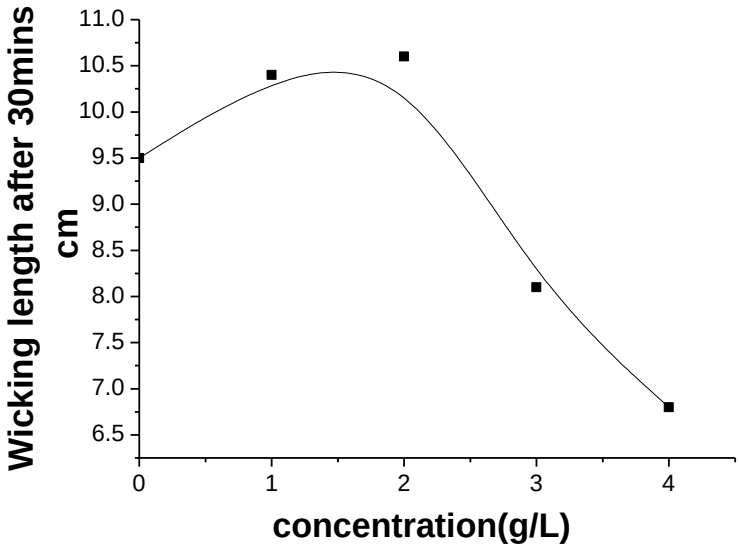


Figure 2 Wicking of fabric done with soft nursing care with different concentrations

Line drying of fabric. Figure 3 shows the relation between water retention of fabric and time with line drying after soft nursing care. As shown in Figure 3, to reach the same water retention, it is required less time for fabric done with soft nursing care than the ones not. Since drying process is a process with simultaneous heat and mass transfer, the drying rate in the initial period is invariable, which is entirely controlled by the fluid dynamic state of the drying air. However, the drying rate is limited as water can pass through the fabric to the free surface [9,10]. Moreover, the soft nursing care improves the ability of fabric to pass water, as well as give better water repellency. Combination with the two factors could account for improving the drying efficiency of fabric.

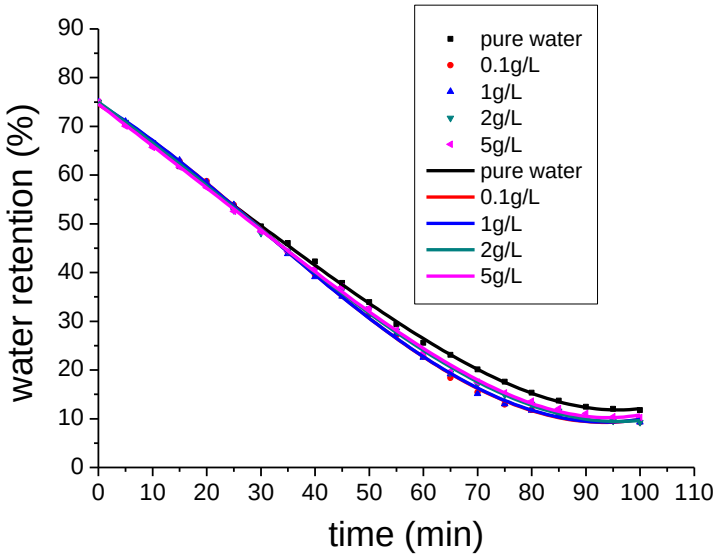


Figure 3 Instant water retention of fabric with drying time

Conclusions

The soft nursing care in home laundry, could increase the distance between fibers and fiber interior, which is favor for water to pass among fiber. Consequently, WVP of fabric is improved, and more static air improves warmth retention rates and decreases heat transfer coefficients simultaneously.

The higher concentration of softening agent, the more softening agent on fabric, and the above lead to water repellency of fabric increase, which is to the disadvantage of wicking.

By line drying, the fabric done with soft nursing care contain less water than original sample after the same time, indicating soft nursing care on fabric have an good effects on fabric drying.

References

[1] Liqiu Chen, To reduce drying energy consumption by decreasing free water in fabric, Technology of energy-saving, 1997,4: 36-39. (In Chinese)

[2] A.K.Haghi, Journal of Thermal Analysis and Calorimetry, 2004,76:1035-1055.

[3] Jili TU, Chunjie Qian, Huayun Ge and Jinqiang Liu, The Impact of Liquid Surface Tension on Fabric Drying Efficiency, International conference on Eco-Dyeing/Finishing & Green Chemistry 2011. (accepted).

[4] Liming Zhou and Yugao Zhang, Cotton Woven Fabric with less Energy Consumption during Home Laundry, International conference on Eco-Dyeing/Finishing & Green Chemistry 2011. (accepted).

[5] W.D.Schindler, P.J.Hauser, Chemical finishing of textiles, Textile Institute (Manchester, England), 2004: p29-41.

[6] P. Bajaj, J Appl Polym Sci, 2002, 83: 631–659.

[7] Jianhui Yang, Analysis of air and moisture permeability of P/C fabric done with softening finishes, Shanghai Textile Science&Technology, 2010,38(12): 3-5. (In Chinese)

[8] A. Patnaik, R. S. Rengasamy, V. K. Kothari and A. Ghosh, Wetting and Wicking in Fibrous Materials, Textile Progress, 2006, 38: 1, 1-105.

[9] A.B. Etemoglu, Y. Ulcay, M. Can, and A. Avci, Fibers and Polymers, 2009, 10:252-259.

[10] T. K. Sherwood. Int. Eng, Chem., 21, 12 (1929).

© (2011) Trans Tech Publications, Switzerland
doi:10.4028/www.scientific.net/AMR.331.14

The effect of calcination temperature on the surface evolution and photocatalysis activity of co-doped PVAc/TiO_2 composite nanofibers

Ning Wu[1,a], Yanan Jiao[1,b], Zhiqing Yuan[2,c], Yunxing Liang[1,d] and Li Chen[1,f]

[1]Tianjin and Ministry of Education Key Laboratory of Advanced Textile Composite Materials, Institute of Textile Composite, Tianjin Polytechnic University , Tianjin 300160

[2] Hebei entry-exit inspection and quarantine bureau, Shijiazhuang 050051

[a]wuning@tjpu.edu.cn,[b]jiaoyn@tjpu.edu.cn,[c]yuanzhiqing@126.com,[d]chaoyueziwo569@126.com,

[e]chenli@tjpu.edu.cn

Keywords: calcination tempreture, Fe^{3+},La^{3+} co-doped, PVAc/TiO_2 nanofiber, surface evolution, photocatalysis activity.

Abstract. The Fe^{3+},La^{3+} co-doped polyvinyl acetate(PVAc)/titanium dioxide(TiO_2) composite nanofibers were firstly prepared by combining sol-gel method and electrospinning process, and then calcined under 300℃and 600℃ separately. The effect of calcination temperature on structures, surface morphologies, crystalline state, elemental composition and photocatalysis activity were characterized by scanning electron microscope (SEM), atomic force microscope (AFM), X-ray Diffraction (XRD) , energy dispersive X-ray spectroscopy (EDX) and ultraviolet-visible spectrophotometer(UV-Vis) respectively. The SEM and AFM images showed that the nanofibers were randomly distributed to form the fibrous web, the diameters and surface roughness of nanofibers were obviously changed as the calcination tempreture increasing. The EDX analysis and XRD spectra indicated the percentage of C,O,Ti elements varied as the increase of tempreture and the formation of anatase crystal form TiO_2 nanofibers under 600℃.The UV-Vis curves revealed strong adsorption to methylene blue under 600℃ calcination.

Introduction

Titanium dioxide (TiO_2) has been recognized as a promising photocatalysis material due to its low cost, low energy consumption, stability and unique photoelectric performance. But the wide forbidden band (3.2 ev), light producted electronic and cavities easily compound result in the low photocatalytic and light quantum efficiency. In order to improve the utilization efficiency of the visible light, researchers are trying to use the precious metal deposition, metal ion doping, nonmetal ion doping, semiconductor compound, surface photosensitive change wait for method to modified TiO_2 light catalyst [1-5]. It uses transition metal ions and rare metal ions in expanding the light of doping can also reduce response range of electronic and cavities compound, thus it can effectively improve the TiO_2 photocatalytic activity [6].Because of the porous structure of TiO_2 light catalyst has more reactive spot, which favor the surface adsorption of the reactants in optical catalyst and the desorption of degradation products [7],in recent years, researchers investigated various doping modified methods for improving the photocatalysis of TiO_2 nanofibers[8,9]. Comparing to the evolution process from doped composite nanofiber to inorganic nanofiber in different calcination tempreture, these research works focused on discussing the surface and photocatalysis properties of ultimate doping TiO_2 nanofiber products.

In this work, Fe^{3+},La^{3+} co-doped PVAc/TiO_2 nanofibers are prepared by combining sol-gel method and electrospinning. The porous structure co-doped nanofibers are prepared after 300℃and 600℃ calcination respectively. The effect of calcination tempreture on the surface morphology, crystal, elements and catalysis activities of co-doped nanofiber in the evolution process of organic/inorganic composite nanofibers, carbonization nanofibers and inorganic nanofibers are investigated and discussed.

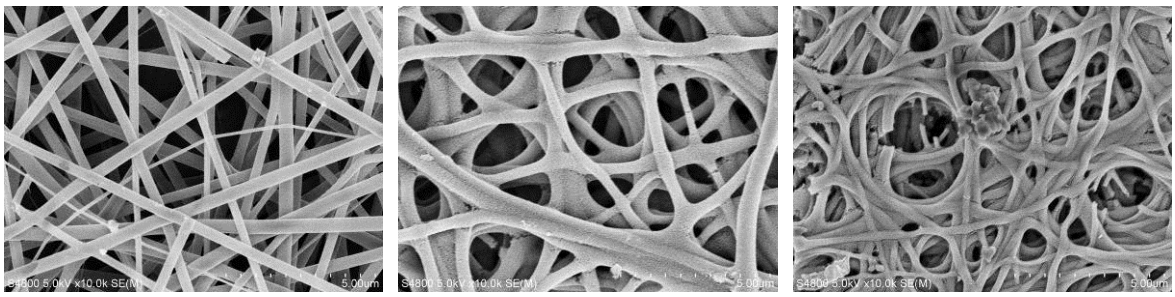
Experimental

PVAc solution with a concentration of 15wt % (Solution A) was prepared by dissolving the PVAc particles in acetone. The ratio of acetylacetone:$Ti(OC_4H_9)_4$:anhydrous ethanol in 1:1:2 with stirring (Solution B). The preparation of Solution C is by adding a given amount of $Fe(NO_3)_3 \bullet 9H_2O$ and $La(NO_3)_3 \bullet 6(H_2O)$ into the mixture solution of deionized water and ethanol. Then, Solution C was added dropwise into Solution B with vigorous stirring for 5h at room temperature, solution D prepared. Solution D was mixed with Solution A in a 1:1 ratio by stirring for 8 h, to obtain the composite solution.

The composite solution is placed in a syringe for electrospinning. A high voltage (20KV) was applied to the spinning solution via an alligator clip attached to the syringe needle. The solution was delivered to a blunt needle (the nozzle diameter was about 0.7mm) via a microinfusion pump (WZ-50C2, Zhejiang, China) to control the solution flow rate at 1.0ml/h. The electrospun fibers were collected on a sheet glass. The as-prepared composite fibers were subjected to 300℃ and 600℃ calcination for 2h respectively, to obtain carbonized and inorganic Fe^{3+}, La^{3+} co-doped TiO_2 nanofibers.

The fibrous structures and element variation of the nanofibers were investigated by SEM (HITACHI S-4800). XRD patterns were employed to analyze the crystal form of nanofibers, which were obtained at room temperature with a BRUKER D8 diffractometer (Cu Kα radiation, λ = 1.5406 A°) with the scanning rate of 5°/min. The surface morphologies of single nanofiber were characterized by AFM(CSPM4000 ,Benyuan, China).Irradiation was provided by a 150W tungsten halogen lamp and an 8W UV lamp, located in the center of the quartz jacket. The amount of nanofibers chosen was 0.3g/L methylene blue solution was used for each photocatalytic degradation study. A certain amount of reactive solution was withdrawn at 30min intervals. \The degradation ration can be calculated using the formula: $w = (c_0 - c_t) / c_0 \times 100\ \%$, c_0 is the initial concentration of methylene blue; c_t is the t moment concentration of methylene blue .

Results and discussion

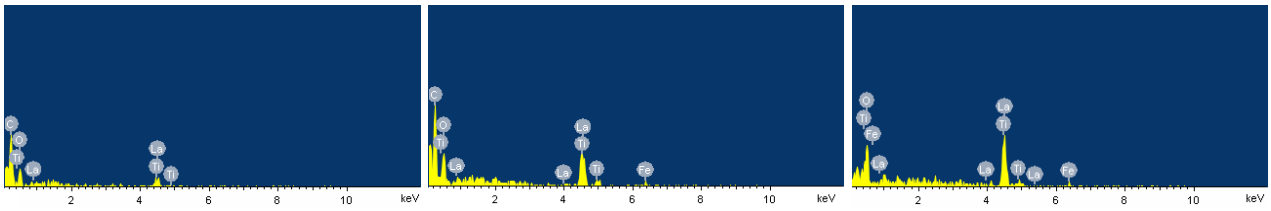


(a) (b) (c)

Fig. 1 The SEM images of Fe^{3+},La^{3+} co-doped TiO_2 nanofibers calcined at different temperatures,

(a) 0℃,(b)300℃,(c)600℃

The fibrous structure of Fe^{3+},La^{3+} co-doped TiO_2 nanofibers at different calcinate tempretures are illustrated in Fig. 1. As shown in Fig.1, the fibrous structure is clear and straight, some threadlet structure and punctiform protuberance are appeared on the surface, this characteristic have not been found in our previous research for un-doped PVAc/TiO_2 nanofibers[10]. The doping of Fe^{3+} and La^{3+} induced the electron uneven distributed in the jet, some intensive parts produced branch, the punctiform protuberance may caused by the oxidation of metal ion. When the calcination tempreture up to 300℃, the threadlet structure is disappeared, fibers become curved and thicker, some fibers adhered together. After 600℃ calcined, the porous structure is obvious and the diameters of fibers become thinner.



(a) (b) (c)

Fig. 2 The EDX spectra of Fe^{3+},La^{3+} co-doped TiO_2 nanofibers calcined at different temperatures.

(a) 0℃,(b)300℃,(c)600℃

Table1 The elements atom percentage of Fe^{3+},La^{3+} co-doped TiO_2 nanofibers with different calcination tempreture

Ratio (%) / T (℃)	C	O	Ti	Fe	La
0	49.90	46.04	3.75	—	0.31
300	52.17	32.66	13.56	0.47	1.14
600	—	67.45	27.68	2.24	2.63

The EDX spectrogram and chemical element contents are revealed in Fig.2 and Table 1. Before calcination, C, O, Ti, La elements are detected, the atomic percentage content of C is close to O, occupy 49.90% and 46.04% respectively. After 300℃calcined, the atomic percentage content of C element is increased, while the O element is obvious decreased. It is due in the thermal high tempreture condition, the active sidegroup in PVAc molecular chains appear elimination reaction, which caused some molecular chains carbonized and exhibited some linear chain and crosslinking structures. The atomic percentage content of Ti,La are also increased compare with the nanofibers before calcination. When the calcination tempreture up to 600℃, C element is oxided totally , the nanofibers are constituted by O, Ti, Fe, La elements.

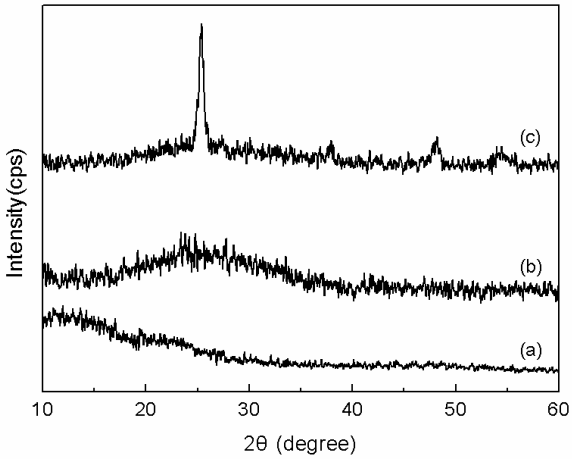
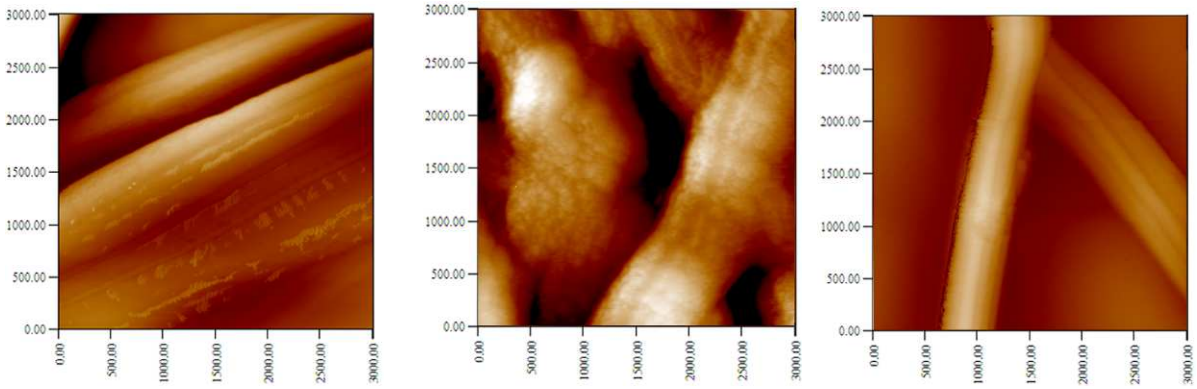


Fig. 3 The XRD pattern of Fe^{3+},La^{3+} co-doped TiO_2 nanofibers calcined at different temperatures

(a) 0℃,(b)300℃,(c)600℃

The XRD pattern of Fe^{3+},La^{3+} co-doped TiO_2 nanofibers calcined at 300℃and 600℃ are illustrated in Fig. 3.As can be seen from Fig. 3(b), the broad peak is appeared after 300℃ calcination, the TiO_2 are existed in amorphous state. Some features diffraction peak have initial formed, which corresponding to the 2 θ =25.3° ,37.8° ,48.0° and 55.1° , the product is Fe^{3+},La^{3+} co-doped TiO_2 nanofiber with anatase crystal form.



(a) (b) (c)

Fig. 4 The AFM images of Fe^{3+},La^{3+} co-doped TiO_2 nanofibers calcined at different temperatures (a) 0℃,(b)300℃,(c)600℃

Fig. 4 reveals the surface morphology of Fe^{3+},La^{3+} co-doped TiO_2 nanofiber in AFM image. Fig. 4(a) shows some intermittently particle aggregate, which corresponding to the observed punctiform protuberance structure in Fig.1(a).After 300℃ calcination, the nanofiber is undergone the carbonized process, the surface appears very coarse ,which may caused by the elimination reaction products on the nanofiber surface. The coarse structures are disappeared, the Fe^{3+},La^{3+} co-doped TiO_2 nanofibers reveal the evenly stripe structure.

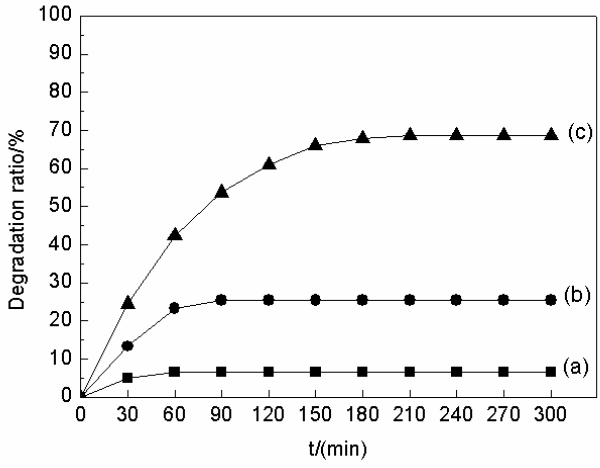


Fig.5 The photocatalysis activity of Fe^{3+},La^{3+} co-doped TiO_2 nanofibers calcined at different temperatures (a) 0℃,(b)300℃,(c)600℃

The photocatalysis curve of Fe^{3+},La^{3+} co-doped TiO_2 nanofibers are illustrated in Fig. 5. The curve (a) presented weak absorption of methylene blue in the first hour, which may caused by the interfacial adsorption between porous nanofiber structure and solution. It can be observed from curve(b) that after 300℃calcination, the co-doped TiO_2 nanofiber reveals better degradation ratio, which may give rise to the big amount of C element created and enlarged specific surface of nanofibers. These two factors are accelerated the adsorption and catalysis degradation process. As shown in curve c, the

degradation ration of anatase Fe^{3+},La^{3+} co-doped TiO_2 nanofiber up to 68.64%, the atom radii of Fe^{3+},Ti^{4+} and La^{3+} are 69,74.5 and 115pm, respectively. So the Fe^{3+} are readily to enter into the TiO_2 lattice and replace the lattice point, then some electrons and holes be caught by Fe3+, which restrained the combination of electrons and holes. The doping of La^{3+} induced the lattice distortion and expansion in the crystal matrix, which enforced the unbalance of the electron system, further declined the combination of electrons and holes, leading to the improve of photocatalysis activity [11].

Conclusions

The Fe^{3+},La^{3+} co-doped TiO_2 nanofibers are prepared by combining electrospinning and high tempreture calcination. The porous fibrous structure is formed by calcinating the Fe^{3+},La^{3+} co-doped PVAc/TiO_2 nanofiber. In 300℃ calcination, Fe^{3+},La^{3+} co-doped TiO_2 nanofibers in amorphous state, the content of C element reach to peak value, the surface of fibers are very coarse. Up to 600℃ calcination, the Fe^{3+},La^{3+} co-doped TiO_2 nanofibers reveal anatase crystal form, the surface of single fiber appears stripe shape. In the process of photocatalzed reaction, the Fe^{3+}, La^{3+} co-doping exhibited legible promoting actions in the crystalline system. In the evolution process from organic/inorganic composite, amorous to crystalline, the increasing calcination tempreture resulted in a significant variation on structure and photocatalysis property of Fe^{3+},La^{3+} co-doped TiO_2 nanofibers.

Acknowledgement

The research work was financial supported by the National Natural Science Foundation of China (NO.11072175)

References

[1] C. H. He and J. Gong : Polym. Degrad. Stab. Vol. 81(2003), p. 117
[2] J. Xu, Y. Ao and D.Fu: Appl. Surf. Sci.Vol. 254(2008), p. 3033
[3] Z. H. Yuan, J. H. Jia and L. D. Zhang: Mater. Chem. Phys. Vol. 73 (2002), p. 323
[4] W.W.So, K.J. Kim and S.J. Moon:Int. J. Hydrogen Energy Vol.29(2004), p.229
[5] A. Fujishima, X. Zhang and D. A. Tryk: Surf. Sci. Rep.Vol.63(2008),p.515
[6] J.W. Shi, J. T. Zheng and Y. Hub: Mater. Chem. Phys. Vol .106(2007),p.247
[7] X. Wang, J. C. Yu and C. Ho: Langmuir Vol.21(2005), p.2552
[8] Y. Ding, P.Zhang, Z. Long, Y. Jiang, F. Xu and J. Lei: J. Sol-Gel Sci. Technol.Vol.46(2008),p.176
[9] H. Tang, F.Yan , Q. Tai and H. L.W. Chana: Biosens. Bioelectron.Vol.25(2010),p.1646
[10] N. Wu, A. Wei and Q. Wei: J. Ind. Texti. Vol.39(2010), p.293
[11] H.Xia, H. Zhuang and D. Xiao: J. Alloys Compd. Vol. 465(2008),p.328

© (2011) Trans Tech Publications, Switzerland
doi:10.4028/www.scientific.net/AMR.331.19

Cell immobilization with textile carriers for TA biodegradation

Huiqin Li [1.2.a], Jixian Gong [1.2.b], Qiujin Li[1.2], Zheng Li [1.2], Jianfei Zhang[1.2], Kening Chen[3], Zhuxian Tang[3], Guoqiang Ding[3], Shengyuan Lin[3]

[1.] School of Textiles, Tianjin Polytechnic University, Tianjin, 300160, China;

[2.] Key Laboratory of Advanced Textile Composites (Tianjin Polytechnic University), Ministry of Education, Tianjin 300160, China

[3.] Quanzhou textile garment vocational institute, Quanzhou, Fujian,362700, China

[a]e-mail: zhxlihuiqin@163.com; [b]e-mail: gongjixian@126.com

Keywords: Cell immobilization; Carrier; weave structure; Absorption; Fabrics

Abstract. Fabrics provide an attractive alternative for cell immobilization carrier. In this study, the relationship of weave structure of fabrics and the effects of cell immobilization was investigated. Several kinds of fabrics with different weave structure were designed and produced acting as cell immobilization carrier. Adsorptive capacity of the textile carriers with different weave structure was measured and the biodegradation rate of TA by cells absorbed on textile carriers was also investigated. It is showed that adsorptive capacity and stability was significantly affected by weave structure of fabric carriers. The result also indicated that the ability to TA degradation was also improved by cell immobilization.

Introduction

Currently, cell immobilization technology has rapidly developed into one of the focus approach in biological engineering. The immobilized whole cell system is an alternative to enzyme immobilization. Unlike enzyme immobilization, where the enzyme is attached to a substrate, in immobilized whole cell systems the target cell is immobilized on carriers. Such methods may be implemented when the enzymes required are difficult or expensive to extract, an example being intracellular enzymes. Also, if a series of enzymes are required in the reaction; whole cell immobilization may be used for convenience.

Carrier selection plays an important role in cell immobilization. The materials used for cell carrier must have controlled porosity and a specific area. They must also be inert to biological attack, insoluble in the growth media and non-toxic to microbial cells. Textiles have an attractive potential in acting as carrier for cell immobilization due to the large specific surface area, good mass transfer performance, easy to processing and low-cost. So the fabrics can be used as ideal biosupports. However, there are few studies for cell immobilization with textiles [1-3]. Thus, the application of textiles in cell carrier is still need to investigate and development.

Terephthalic acid (TA) is the most important starting material for making synthetic products, especially polyester fiber and plastics. In textiles manufacturing, alkali de-weighting finishing of polyester fabrics was a main resource for producing waster water containing TA. Both TA and its manufacturing wastewater show acute, chronic and molecular toxicity to organisms. Although the technology for TA recycling from waste water have been studied, it is necessary to develop new innovative methods of depredating the residual TA in wastewater effectively.

In this investigation, several kinds of fabrics with different weave structure were designed and produced acting as cell immobilization carrier. Cells of TA depredating strain were immobilized through adhesion on polyester fabrics with different weave texture. Adsorptive capacity of the textile carriers with different weave structure was measured and the biodegradation rate of TA by cells absorbed on textile carriers was also investigated.

Materials and methods

Strains and medium. The initial Bacillus strain, *comamonas testosteroni* F4, was isolated from waste water of chemical fiber factory and stored in our laboratory. Culture medium (beef extract 3 g/L, peptone 5 g/L, sodium chloride 5 g/L) was prepared and sterilized, then TA was added into the medium.

Culture conditions. Bacillus strain cell inoculum was grown in 50 ml of YM medium in a 250-ml Erlenmeyer flask under constant temperature of 30°C, stirrer speed of 120 rpm, for 24 h. Fresh medium was inoculated with the seed culture at 10% volume.

Estimation of cell growth and TA degradation. The growth of *comamonas testosteroni* was examined with spectrophotometer at the absorbency of 600 nm marking as OD_{600}. The concentration of TA in the medium was measured with ultraviolet spectrophotometer at 240 nm.

Results and discussion

Adsorption performance. Adsorption performance is a key property for cell immobilization carrier. In this study, eight kinds of polyester fabrics with different weave structure were designed and produced to act as cell immobilization carrier. Adsorptive capacity of the textile carriers with different texture was measured and the relationship of weave structure of fabrics and adsorptive capacity was investigated. The fabrics were dyed with methylene blue, a kind of direct colourant, and the K/S value was measured as an indicator of colour yield (Fig 1).

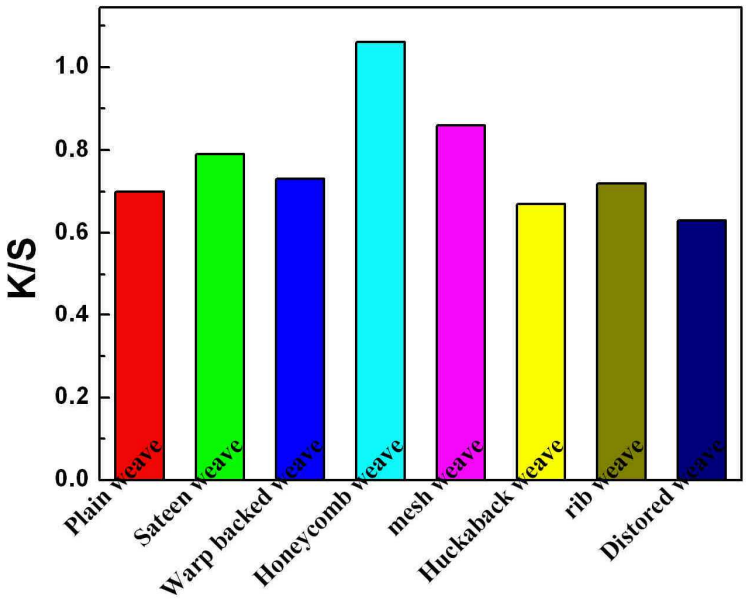


Fig.1 K/S value of the fabrics with different texture dyed with methylene blue

The absorption of fabrics to methylene blue molecule was conformed to monolayer adsorption. So the molecules of methylene blue absorbed on the surface of fabric can be reflected by colour yield. The result showed that the fabrics with different texture have different absorption capability.

Cell adsorption. Cell adsorption is a main symbol parameter for carrier in cell immobilization. In this investigation, microbe cells were immobilized on fabric carriers through adsorption. In this case, surface properties of fabrics play an important role in controlling the adsorption and adhesion of the textile carriers. In order to estimate the effect of fabric carrier, cells adsorbed on the textiles were measured through calculating the weight increase of fabric after cell absorption (Fig. 2).

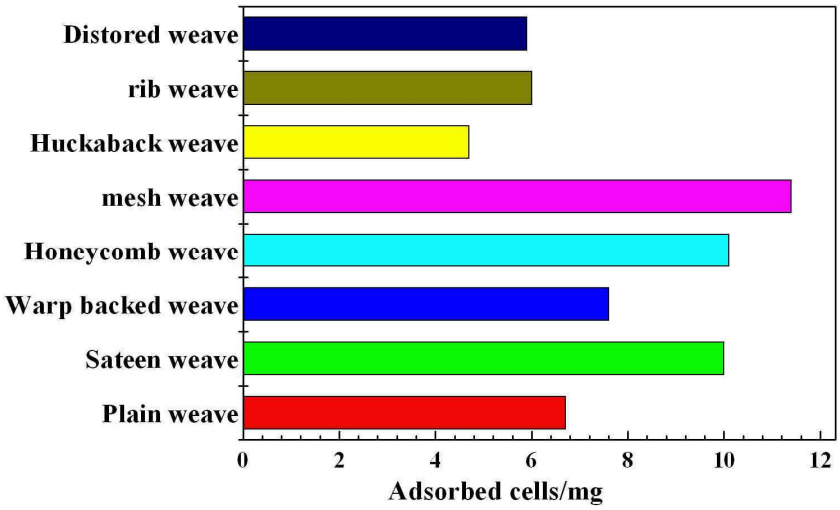


Fig.2 Cell adsorption of fabric carriers with different texture

The result showed that there is the highest cell adsorption on the fabrics with mesh weave texture. The result also demonstrated that the weave structure of fabrics did have effect on cell adsorption ability. The weave structure of textiles may impact the adsorption and diffusion of cells on/in fabrics. Recently, the control of the adsorption and adhesion of biomolecules and cells on material surfaces has attracted considerable attention in the fields of biosensors, biomaterials, and tissue engineering. The design of fabric structure provides an important approach for changing the adsorption capacity of textile materials.

Biodegradation of TA. In this study, the immobilized cells were employed to remove TA from the liquid medium. The TA degradation ability of cells adsorbed on fabrics of mesh weave and honeycomb weave structure was evaluated and the biodegradation rate of TA with adsorbed cells was compared with that of the free cells (Fig.3).

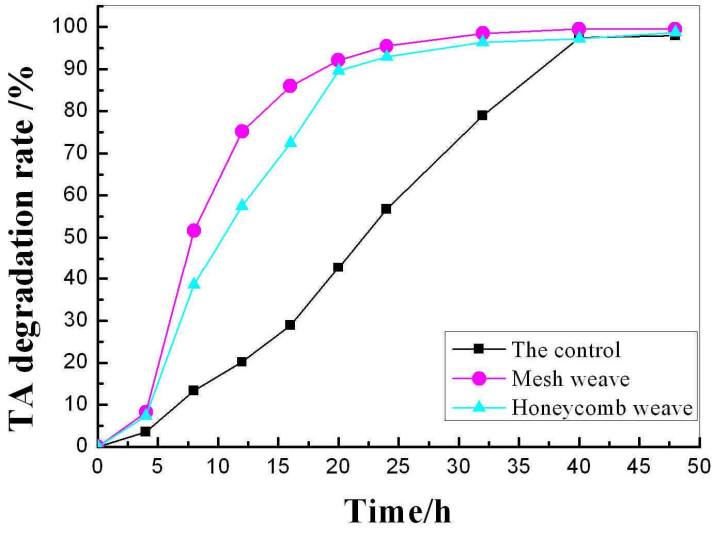


Fig.3 TA biodegradation of adsorbed cells and the free cells

It can be seen from the result that the degradation rate of TA with adsorbed cells was higher than that of the control. TA degradation rate in cell immobilization system can reach 90% within 24 h, while the control one was only 45%. The result demonstrated that the immobilizing cells in faith have some advantage than free cells.

Acknowledgements

This work was financially supported by National Natural Science Foundation of China (NSFC-20875068, NSFC-21006072), Natural Science Foundation of Tianjin (No.09JCZDJC26400) and Shishi Science and Technology Foundation (No. 2010SF07).

References

[1] P. Kilonzo, A. Margaritis, M. Bergougnou, Journal of biotechnology Vol.143 (2009), p. 60.

[2] Y. F. Chu, C. H. Hsu, P. K. Soma, Y. M. Lo, Bioresource technology Vol.100 (2009), p.3167.

[3] S. F. D'Souza, J. S. Melo, Process Biochemistry Vol.36 (2001), p. 677.

© (2011) Trans Tech Publications, Switzerland
doi:10.4028/www.scientific.net/AMR.331.23

Study on Spunlaced Nonwoven Fabric's Moisture Absorption and Permeability based on BP Network

Xionghua Wu [1], Jianchi Lv[1,2], Xiaoning Jiao [1,3]

[1] School of Science, Tianjin Polytechnic University, Tianjin 300160, China

[2] School of Electronics and Information engineering, Tianjin Polytechnic University, Tianjin 300160, China

[3] School of Textiles, Tianjin Polytechnic University ,Tianjin 300160, China

[a]wuxionghua2003@163.com, [b] lvjianchi @163.com, [c]xiaoningj@tjpu.edu.cn

Keywords: spunlaced nonwoven fabric, moisture absorption and permeability, BP network, computer simulation; optimal technological parameters , PCA

Abstract. Using BP neural network, a predictive model has been set up between the parameters of spunlaced nonwoven fabric and its two important performances which were the moisture permeability and absorption. The results showed the model was very ideal. Based on this, various parameters corresponding to the optimal values were obtained through computer simulation, that while the viscose content was 80% and the surface density was 58g/m^2, the maximum permeability was 6627.3 g/m^2. d and the horizontal moisture absorption also reached the maximum of 22.41cm. While the viscose content was100% and the surface density was 68g/m^2, the vertical moisture absorption reached the maximum of 19.1429cm. In the end, the PCA was used to integrate the three properties into one target and the optimal parameters were also obtained, which viscose content was 80 % and surface density was 58g/m^2 .Besides, according to the method of the computer simulation, a variety of different spunlaced nonwovens also can be obtained to meet different needs, which could be a reference in the future production and experiments.

Introduction

Spunlaced nonwoven fabric is the preferred one-time materials in medical service domain and has been taken great attention all over the world. In isolation, served under the hot and humid environment in the close, the one-time underwear made from spunlaced nonwoven fabric can rise to sufficient moisture absorption, air permeability and moisture transmission that made the skin keep relatively dry and comfortable[1]. At the same time, because in spunlaced nonwovens' processing, any binder and pulp had not been added, it had no stimulation to skin when it directly contacted with the skin and the secondary infection chance can be greatly reduced, and the safety was improved for medical personnel by using one-time underwear[2].

In this paper, firstly the BP neural network predictive model was established between the two parameters which were the proportion of the raw material and surface density and the two properties. Then, according to this model, using computer simulation, the optimal parameters were determined while the properties were best. In the end the principal component analysis(PCA) was used to integrate the properties into one index and put forward a optimal designing scheme which could be a reference to the design and experiment in future.

BP neural network model

In the actual production of spunlaced nonwoven fabric, generally by experience or tests to finally determine the quantitative ratio of raw materials and the surface density .Empirical method was too subjective and the test method required a lot of time, human and material resources[3]. When these two parameters function together, the interaction between them led it to be complex between the process parameters and the final product[4,5]. Although the relationship between the various process parameters and the product's properties can been obtained by the method of mathematical statistics to some extent[6,7], from the simplicity and dynamic adaptability to solve this problem in manufacturing processes, the neural network model has more obvious advantages[8]. In this paper, BP neural network predictive model had been established using part of experiment data as training samples and others as testing samples to check the model. Because the optimal process parameters

can't been directly obtained from the BP neural network, computer simulation has been made to determine the optimal process parameters which can save a significant amount of time and human resources required for the actual tests. So it has high value in practice[9].

The first two columns in table 1 and table 2 were experiment conditions called process parameters, and the columns "EV" (experimental value) were the results corresponding to each condition in experiment, the columns "PV" were the values predicted by BP network, and the "RE" were the relative errors between the experiment results and prediction ones. Table 1 was training samples and table 2 was testing ones.

Experimental products: a different mix of viscose and polyester fibers and a number of different surface density spunlaced nonvevens of parallel-laid web (X-series) and vertical-laid web (Y-series). XTS30 type Microscope, Beijing Tech Instrument .Co., Ltd..

Test method: moisture penetrability was conducted according to GB/T 12704-91, moisture absorbability was conducted according to ZB W 04019-90.

Note: viscose for 10 means viscose content is 100% namely pure viscose, for 7 is 70%, and so on.

Table 1 was training samples selected randomly from experiment data and table 2 was the test ones which were the rest of experiment data. BP neural network has 7 neurons in hidden layer, and the transfer function from hidden layer to output was "*tansig*", and the one of output layer transfer was "*logsig*". Corresponding predictive results of BP neural network in training samples shown in the columns "PV" in table 1 and the same results of test samples in table 2 (to save space, the lists only show X-series' results, the same following).

Table 1 The results of experiment and prediction for training samples

X-series		moisture permeability($g/m^2 \cdot d$)			horizontal moisture absorption（cm）			vertical moisture absorption (cm)		
Content Of Viscose	surface density (g/m2）	EV	PV	RE (%)	EV	PV	RE (%)	EV	PV	RE (%)
10	50	5625.3	5612.7	-0.22	20.11	20.81	3.48	16.00	15.47	-3.31
10	55	5448.4	5487.6	0.72	22.32	22.18	-0.63	16.03	16.03	0.00
10	60	5652.3	5643.7	-0.15	24.16	23.65	-2.12	18.22	18.34	0.66
10	65	5863.2	5854.6	-0.17	23.94	23.92	-0.08	19.87	19.16	-3.57
7	40	5926.3	5911.3	-0.25	8.83	9.07	2.72	5.17	5.21	0.77
7	50	6048.4	6047.2	-0.02	16.54	16.41	-0.76	11.37	11.70	2.90
7	65	6098.5	6067.4	-0.51	13.52	14.08	4.17	10.87	11.19	2.89
7	70	6044.2	6034.8	-0.16	17.78	17.49	-1.63	14.43	13.71	-4.99
0	40	5496.9	5465.3	-0.58	0	0.41	—	0	0.20	—
0	50	5433.2	5414.2	-0.35	0	0.31	—	0	0.14	—
0	55	5395.8	5401.3	0.10	0.03	0.31	933.3	0	0.14	—
0	70	5408.2	5401.1	-0.13	0.56	0.49	-12.50	0.09	0.30	233.3
0	75	5412.6	5403.4	-0.17	0.77	0.65	-15.58	0.13	0.41	215.3
10	55	5448.4	5487.6	0.72	22.31	22.17	-0.63	16.03	16.02	-0.06
8	55	6717.9	6621.2	-1.44	20	20.13	0.65	15.03	14.97	-0.40
7	55	6138.9	6179.6	0.66	18.69	17.87	-4.39	14.47	13.91	-3.87
6	55	6161.9	6081.3	-1.31	16.54	16.78	1.45	13.1	12.81	-2.21
5	55	5867.3	5880.0	0.22	14.29	14.33	0.28	11.3	10.89	-3.62
0	55	5395.8	5401.3	0.10	0.03	0.31	933.3	0	0.14	—

Table 2 The results of experiment and prediction for testing samples

X-series		moisture permeability(g/m2 • d)			horizontal moisture absorption（cm）			vertical moisture absorption (cm)		
Content Of Viscose	surface density (g/m2）	EV	PV	RE (%)	EV	PV	RE (%)	EV	PV	RE (%)
10	70	5539.4	5635.7	1.74	22.94	22.91	-0.18	18.17	18.27	0.55
10	40	6234.4	6143.7	-1.45	16.08	16.16	0.53	13.28	12.72	4.20
7	60	6102.3	6111.2	0.15	15.72	15.71	-0.11	12.40	12.39	-0.01
0	60	5396.6	5408.4	0.22	0.04	0.48	90.82	0.03	0.36	986.23
4	55	5625.1	5568.5	-1.01	8.16	8.03	-1.57	6.55	5.86	-10.53
7	55	6153.1	6182.8	0.48	18.20	17.49	-4.03	14.26	13.96	-2.10
0	65	5399.4	5401.3	0.04	0.11	0.59	81.86	0.06	0.32	473.21

From the results above of BP neural network prediction model, for both the training samples and test ones, the absolute values of relative error in moisture permeability were below 2% and the ones in moisture absorption below 5% when the sample experiment value was more than 8cm. And in practice, often high value in moisture absorption was payed attention to. So the BP prediction model was very ideal.

Numerical experiment and analysis

As well known, the values of dependent variable corresponding to the largest independent variables could not be obtained by mathematical deduction. So the approach to obtain process parameters was using by numerical simulation in this paper[10,11]. The ideas was as follows: the content of viscose was from 100% to 90% ,followed by decreasing to 0, and the surface density was from 40 to 41 , gradually increased to 80 g/m^2 .it iwas equivalent to 451 experiment conditions. Inputting these conditions to the trained BP neural network model above, which was equivalent that 451 experiments had been made, then from all the results, the best experiment conditions were selected as the optimal parameters.In the end, principal component analysis was used to integrate the three properties(moisture permeability , horizontal and vertical absorption) into one target named "integrated variables" below. The model was also established and tested, and the numerical simulation was done too.

Using the method described above, selected and sorted the optimum results, the optimal conditions for moisture permeability ,horizontal and vertical absorption shown in Table 3.

Table 3 Some optimal conditions and the predictive values

Content of viscose	Surface density (g/m^2)	PV of moisture permeability ($g/m^2 \cdot d$)	PV of horizontal absorption (cm)	Content of viscose	Surface density (g/m^2)	PV of vertical absorption (cm)
8	58	6627.3	22.41	10	68	19.1400
8	59	6625.4	22.38	10	67	19.1440
8	57	6617.8	22.24	10	69	19.1159
8	60	6609.6	22.09	10	66	19.1093
8	56	6599.7	21.91	10	70	19.0628
8	61	6580.0	21.55	10	65	19.0403

For the moisture permeability, horizontal and vertical absorption, 3 eigenvalues were 2.366,0.628 and 0.005 in PCA. The corresponded contribution rates (%) were 78.875, 20.949 and 0.176. That was, taking the first principal component could maintain 78.875% information of the original data. So the first eigenvector could be used as the weight to integrate the three properties into one target named "integrated variable" in follows. The weight vector was $w = (0.4624,0.6263,0.6277)^T$. The results of numerical experiment showed as table 4. These results also could be said by contour map image shown as figure 1 and figure 2.

Table 4 Some optimal conditions and the predictive values for integrated variable

Content of viscose(%)	Surface density(g/m^2)	PV of integrated variable
8	58	4748.4
8	59	4747.3
8	57	4741.4
8	60	4735.5
8	56	4728.1
8	61	4713.8

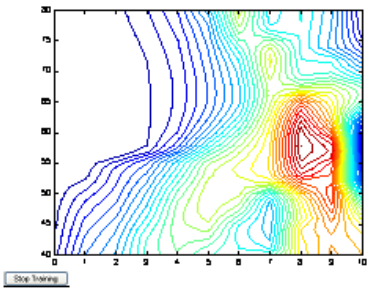


Fig.1 2-D contour for integrated variable

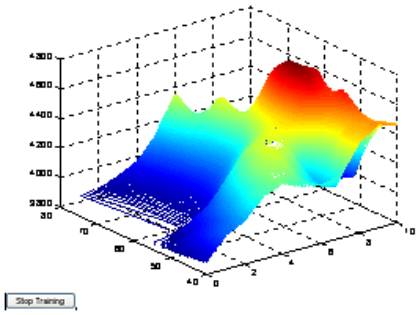


Fig.2 3-D contour for integrated variable

In the end, if considering the three variales at the same time and let moisture permeability greater than 5800 g/m^2·d, horizontal and vertical absorption greater than 8cm, results obtained from computer simulation shown as Table 5. Of course, by this way, any result could be obtained to meet any requirement of different customers.

Table 5 Some optimal conditions and the predictive values considering the three variables

Content of viscose (%)	Surface density (g/m^2)	PV of moisture permeability (g/m2·d)	PV of horizontal absorption (cm)	PV of vertical absorption (cm)
5	49	6115.2	13.09	9.21
5	48	6114.2	13.07	8.85
5	50	6111.2	13.02	9.51
5	47	6107.1	12.94	8.43
5	51	6102.2	12.85	9.76
5	52	6087.0	12.58	9.98

Conclusions

In this paper, using BP network, a predictive model between the parameters of spunlaced nonwovens and its two important performances, the moisture permeability and absorption, was established. And the model was tested ideal. Based on this, various parameters corresponding to the optimal values were obtained through the computer simulation. Besides, according to the method of the numerical simulation, a variety of different spunlaced nonwovens could be obtained to meet different needs, which could be a reference in the future production and experiments.

References

[1] Yongmei Ma,Yuan Sun:Nonwovens Vol.19(2001),P.20,in Chinese
[2] Fubing Peng,Xiaoning Jiao, Xiaofang Ye: Journal of Anhui University of Technology and Science Vol.20(2005),P.61,in Chinese.
[3] Shancai Hu: Nonwovens Vol.9(2001),P.21,in Chinese
[4] Qian Cheng: Journal of Textile Research Vol.29 (2008), P. 46, in Chinese.
[5] Ya Liu, Bowen Chen, Wei Zhuang, et al: Journal of Textile Research Vol.30 (2009), P. 55, in Chinese.
[6] Fengxia Hu,Zhao fang Du,Chunyan Gao et al: Journal of Textile Research Vol.25 (2007), P. 51, in Chinese.
[7] Jingfeng Zhang,Xiangyu Jin,Jianhui Rao: Journal of Textile Research Vol.26 (200), P. 55, in Chinese.
[8] Xionghua Wu, Ya Liu: Journal of Textile Research Vol.32(2011),P.51,in Chinese.
[9] Xilin Zhu,Boda Wu,Xingxing Wu, et al: Computer Integrated Manufacturing Systems Vol.10(2004),P.1139,in Chinese.
[10] Hong Ni, Yonghui Pan: Journal of Textile Research Vol.30 (2009), P. 41, in Chinese.
[11] Haitao Cao, Weijie Zhang:China Science and Technology Information Vol.6(2009),P.279,in Chinese.

© (2011) Trans Tech Publications, Switzerland
doi:10.4028/www.scientific.net/AMR.331.27

Methods for Measuring the Surface Area of Nude Body

Qing Li [1, a], Jun Li[1,2,b], Min Wang[1,2 c]

[1]Protective Clothing Centre of Fashion Institute, Donghua University, 1882 West Yan'an road, Shanghai 200051, Shanghai, P. R. China

[2]Key Laboratory of Clothing Design & Technology, Ministry of Education, Donghua University, 1882 West Yan'an Road, Shanghai 200051, P. R. China

[a]lqqqq@mail.dhu.edu.cn, [b]lijun@dhu.edu.cn, [c]minmin1202@dhu.edu.cn

Keywords: Clothing area factor, Body surface area, Sector, Method comparison

Abstract. 3 Dimension scanning for measuring surface area of nude body is practiced and is compared to the empirical formula method and paste method. The surface area of every body sector is collected by the regional classification standard: *ISO9920*. The results indicate that the area value collected by 3D scanning is lower than the others. The combination of 3D scanning and matched software is the most efficient method espacially to the trunk and limbs.

Introduction

There are several standards for measuring clothing insulation, such as *ASTMF1291*, *ENV342*, *ISO/FDIS15831*, *ISO9920*. While the heated manikin is needed in clothing insulation measurement, the surface area of a clothed body is larger than nude body, the increased surface will increase the dry heat transfer from the surface to the surrounding environment[1]. Therefore, a correction by using clothing area factor is introduced. Clothing area factor (f_{cl}), which appears in various equations as a term or dimensionless index, is the ratio of the outer surface area of the clothed body to the surface area of the nude body.

$$f_{cl} = A_{cl}/A_{du} \quad (1)$$

In order to study the method for measuring the f_{cl}, the methods for measuring A_{du} are first summarized and a new method with the combination of 3D scanning and matched software is introduced. The methods for measuring A_{du} include direct and indirect ways. The direct way always use tools directly, such as empirical formula, 3 Dimension scanning and paper pasting. The indirect way is measuring A_{du} through collecting pixel value, gram weight, or other elements instead of area. All these methods always have different results in measuring a certain individual. The article compared the methods existed and studied the regularity of human surface area more accurate by introducing the advanced software technology combined with 3 Dimension scanning.

Experiment

Subjects . The information of four female subjects is shown in Table 1.

Table 1 Subject's information

Subject	Height/cm	Weight/kg	Bust/cm	Waist/cm	Hips/cm
S1	155.00	46.00	81.00	69.20	88.00
S2	160.00	46.50	76.00	61.80	90.50
S3	160.00	52.00	86.20	67.70	90.20
S4	166.50	51.80	84.30	63.30	89.30

Methods. Three methods are used in the study, shown in Table 2.

Table 2 Three methods for measuring surface area

Type	A	B	C
Name	Empirical formula	Paste method	3D scanner and software

Method A. Stevenson formula (S-formula), DuBois formula (D-formula) and HU-yong mei correction formula (HU- formula) are introduced, based on the test results of four subjects.

S-formula, which is deduced on the survey of surface body area of Chinese, is a linear formula suitable for Chinese above 6 years old.

$$S(\text{S formula}) = 0.0061 \times H + 0.0128 \times H - 0.1529. \quad (2)$$

D-formula is commonly deduced on the survey of surface body area of European human body. *W* refers to weight, *H* refers to height, *K* is constant (Western 0.007184, Japanese 0.007246) [2].

$$S = W^{0.425} \times H^{0.725} \times K. \quad (3)$$

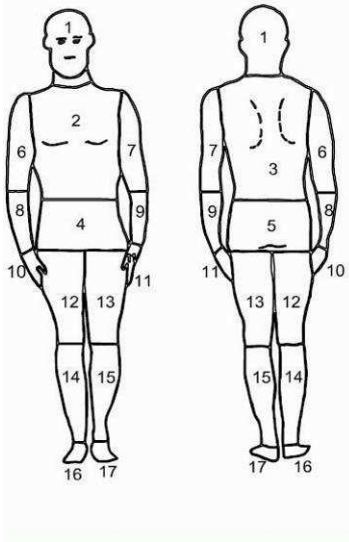
HU-formula is corrected in 2005, which uses paper pasting. It includes male and female formula and a uniform formula for Chinese without considering gender [3].

$$S_{(male)} = 0.0057 \times H + 0.0121 \times W + 0.0882.$$

$$S_{(female)} = 0.0073 \times H + 0.0127 \times W - 0.2106.$$

$$S_{(HU\text{-}formula)} = 0.0061 \times H + 0.0124 \times W - 0.0099. \quad (4)$$

Method B. Four subjects only wear corsets, with their hair covered in a bath cap. According to *ISO9920: 2007 Annex H*, the nude body surface areas is divided into 17 sectors, which is shown in Fig.1. The trunk is further divided into two symmetrical parts by the midline. Then the subjects' right side is bond with clear plastic (stretch resistant and stick less, width about 4.5cm). The plastic should be perfectly attached onto skin. The excess or overlap are marked and cut off. The area of body surface is substituted by clear plastic: 1) using the method of counting squares, 2) weighing them (the unit area of clear plastic is $4.622 \times 10^{-3} g$).



	Segment	% total area
1	Head + neck	8,7
2	Chest	10,2
3	Back	9,2
4	Abdomen	6,1
5	Buttocks	6,6
6	Right upper arm	5,0
7	Left upper arm	5,0
8	Right lower arm	3,1
9	Left lower arm	3,1
10	Right hand	2,5
11	Left hand	2,5
12	Right thigh	9,2
13	Left thigh	9,2
14	Right calf	6,1
15	Left calf	6,1
16	Right foot	3,7
17	Left foot	3,7
Total		100

Fig.1 Schematic diagram of template for body division

Method C. A 3D body scanning system (BMS provided by American [TC] [2] companies) was used. It scans the whole body with white light in seconds and rapidly produces a true-to-scale 3D body model which collected (30~50) $\times 10^4$ pixel points from 180 tailor's measurements [4]. Limited by scanning positionit, it was difficult to capture reflections of white light from the sides and some

details about head, foot, hands.After scanning; the point clouds can be repaired and fitted into curved surface using reverse engineering software, such as *Rapidform 2006*. The areas of nude body surface can also be quickly calculated by this software.

Results and Discussion

The results of Method A, B and C are shown in Table 3.

Table 3 The results of three methods(cm^2)

Subject	Method A			Method B		Method C
	S formula	D formula	HU formula	Counting squares	Weighing	3D scanning
S1	13814.00	14125.83	15051.00	13637.00	12922.61	11860.45
S2	14183.00	14521.31	15479.50	12617.91	13510.53	11759.36
S3	14887.00	15227.89	16178.00	14473.88	13605.98	12711.34
S4	15257.90	15648.29	16627.10	15158.05	14968.74	12852.62

Method A is generalized through paste methods. The surface area of nude body measured by HU-formula is the largest, and by S-formula is the smallest among Method A. The surface area increases with the increase of body's height and weight is further confirmed.

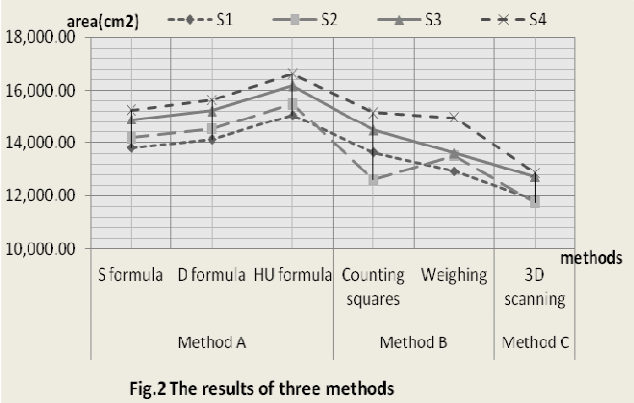


Fig.2 The results of three methods

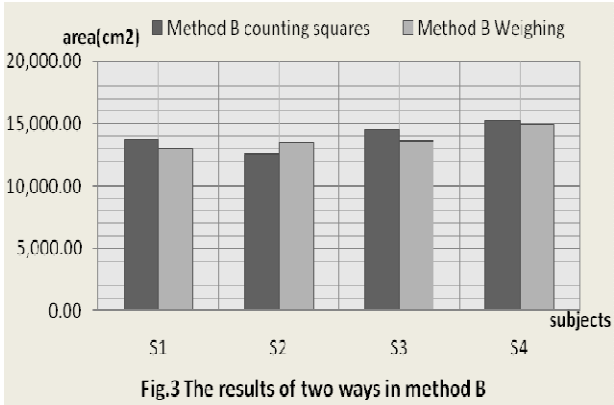


Fig.3 The results of two ways in method B

Method B always costs 2.5h/p on pasting the clear plastic, and another 1h counting squares. The results of two ways are shown in Fig. 3. Data collected form square counting way is, however, lower than weighing way, thus S2 against whole tendency. Two reasons cause difference in paste pasting process, and calculating process. However, Paired Samples Test ($p=0.62>0.01$) indicates no statistical difference between the two ways ($p<0.01$).

Table 4 Paired Samples Test (cm^2)

b1 - b2	Paired Differences					t	df	Sig. (2-tailed)
	Mean	Std. Deviation	Std. Error Mean	99% Confidence Interval of the Difference				
				Lower	Upper			
	219.75	796.46	398.23	-2106.29	2545.78	0.55	3.00	0.62

3D scanning can more quickly reflect the subjects in shape, collect surrounded degree information (bust and waist, hips, etc). Method C is fast in scanning, but costs time on repairing images with software. The areas by method C are the smallest, as shown in Fig. 2. Due to the limitation of the scanning fixed position, some point cloud cannot be collected, when optimization with *Rapidform 2006*, the human body surface morphology was changed to a certain extent, such as body side curve will turn slightly flat after repair thus that causes smaller total area of body surface.

As shown in Fig.4, method A and B are compared, the result indicates the value of the paste method are lower than formula method, more close to S-formula method. T-text showed no significant differences among three methods of measuring three subjects($p<0.01$). Take S1 as an example, the

average area value of the six measurement methods is 13568.48cm2. The average value of method C is 11860.45cm2. The mean difference of both is 1708.03cm2, t=3.849, tail test value p=0.012 > 0.01, as shown in Table 5. while p=0.017 for S2, 0.015 for S3,both greater than 0.01,but for S4, p=0.007<0.01, it has significant differences,so the number of subjects should be increased.

Table 5 One-Sample Test (cm^2)

	N	Mean	Std. Deviation	Std. Error Mean	Test Value = 11860.45 t	df	Sig. (2-tailed)	Mean Difference	99% Confidence Interval of the Difference Lower	Upper
s1	6	13568.48	1087.01	443.77	3.85	5.00	0.01	1708.03	-81.31	3497.38

Surface area of every body sector are shown in Fig.5. They present the same rule as the whole body surface area, i.e.A>B>C.

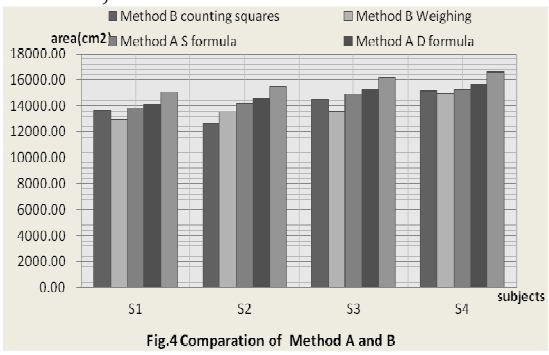


Fig.4 Comparation of Method A and B

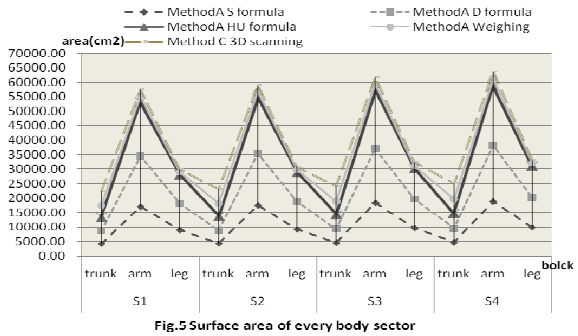


Fig.5 Surface area of every body sector

Conclusions

The surface area of nude body differs on different subjects as well as diffident methods. T-text shows nearly no significant differences among three methods of measuring the nude area (p<0.01).The empirical formula method on the subjects is fast and easy, height and weight are the only precondition. The area value by empirical formula method is generally higher than the other methods. Paste method is time consuming, with some error in plastic pasting and counting. But Paired Samples Test indicated no statistical difference between the two ways (p<0.01). 3D scanning method is the most convinent, which can collect body surface area through approriate image reparing with software. Three methods can all collect surface area of every body sector, which presents the same rule as the whole body surface area, i.e.A>B>C.

Acknowledgements

This work is financially supported by the Fundamental Research Funds for the Central Universities (No.11D10701).

References

[1] ChuansiGao, K. Kuklane, I. Holmer: Using 3D Whole Body Scanning to Determine Clothing Area Factor. Publication/Series Proceedings of the 11th International Conference on Environmental Ergonomics (2005)

[2] S.Y. LI, L.B. ZHANG, Q.ZHU, S.H. LU: A study on body surface area of students. Acta Anthropologica Sinica, Vol.22 (2003), p. 51-55

[3] Y. M. HU, L. M, Z. H. HU, et al: Studies on the application of a new formula for calculating body surface area of the Chinese adults. Basic Medical Sci. and Clinics, Vol. 23(2003), p. 444-446

[4] Y. ZHANG, J. LI. Application of 3 Dimensional Body Measurement System Developed by [TC]2. J. Donghua University, Vol. 30 (2004), p.93-96

© (2011) Trans Tech Publications, Switzerland
doi:10.4028/www.scientific.net/AMR.331.31

A Stochastic Simulation of Cotton Combing Process

Guangsong Yan[1,2, a] Yuheng Su[2,b] Chongwen Yu[1,c]

[1] College of Textiles, Donghua University, Shanghai 201620, China;

[2] Department of Textile Engineering, Henan Institute of Engineering, Zhengzhou 450007, China

[a]gsyan_2005@163.com, [b]fzsyhsyh@126.com, [c]yucw@dhu.edu.cn

Key words: random distribution, fiber length distribution, stochastic simulation, cotton combing

Abstract: The properties of plain fiber assembly are discussed, and the fiber alignment in the assembly is investigated. Some theories in yarn irregularity research are applied to the study of the random and parallel fibers in fiber assembly and a stochastic method is used to generate the fiber assembly. For a given fiber length distribution, the combing process is simulated on the basis of the plain fiber assembly. If the main parameters in cotton combing are known, the simulation can be conducted, yielding the fiber length distributions in combed cotton slivers and in waste cotton that is combed down. With the variation of combing parameters, the influence of combing parameters on the combing results can be discussed from the simulation.

Introduction

Cotton combing is an important operation in the production of high quality yarns. After the cotton fibers being processed in carding and doubling, they are produced into a cotton screen which has a width and thickness with fibers being straight and parallel and evenly distributed in the screen. In the cotton combing process, the cotton screen is input the comber and is combed by the combing process. The fiber length distribution of the cotton screen is changed through the combing process. Shorter fibers are combed down and longer fibers are remained and turned into combed slivers. An ideal combing process should comb down longer fibers as little as possible, and at the same time the combed slivers should contain shorter fibers as little as possible. If the combing process is not in normal state, some errors may occur. The fibers that are combed down may contain large amount of longer fibers, causing the waste of cotton fibers. Sometimes, the error may cause a larger amount of shorter fibers in combed cotton slivers. Thus the quality of slivers may be influenced.

The decisive factors in cotton combing are the fiber length distribution in cotton screen and the feed length of the screen for each step. And the combed length in cotton screen is another factor influencing the combing process. In the past, most of the research relies on the experiment. In those studies, some parameters are set and the resulting slivers are tested. But these methods can not include all the cases. So the result is not a universal solution. If the combing process can be simulated, the combing mechanics can be investigated, the result can be helpful in the design and manufacture of combing machines.

To simulate the cotton combing process, the most important step is to generate an evenly aligned plain fiber assembly which refers to the cotton screen. In the cotton screen, fibers are aligned randomly. Such a fiber assembly has a dramatic similarity to the ideal yarns that has been studied by a lot of researchers for a long time. So many results in yarn studies can be applied to the simulation of cotton screen, because when a cotton screen is projected to a line along it length, the situation is just like a yarn with fibers being straight and parallel. Fifty years ago, Rao[1] gave a mathematical expression of ideal yarns with identical fiber length. And a little earlier year, Martindale discussed the measurement of the yarn unevenness and gave the limit of the lower

bound for yarn unevenness[2]. Some simulation work about yarns has been done by Realff in recent years[3]. Suh discussed the fibers in yarn by means of geometric-probabilistic method[4]. Brown investigated the probabilistic expression of yarns with different fiber length distributions, combining the yarn unevenness and the constituent fiber length distribution[5]. Zeidman at el studied the factors influencing yarn irregularity and discussed the control methods[6]. Yan constructed a binomial model for the yarn unevenness and gave the relation between yarn unevenness and the number of fibers in yarn cross section, making a new result for the limit yarn unevenness[7]. All the research above can serve as an important reference for the study and simulation of cotton screen. The cotton plain assembly can be generated by a proper model and can be programmed and analyzed.

At first, we develop a generation of the cotton screen with random method. And the simulation of cotton combing process is simulated in terms of the change of fiber length distributions. Some parameters are set and the two parts of cotton fiber length distributions are obtained.

The Plain Fiber Assembly

The fed cotton in a comber is a cotton screen produced in the later process by carding and doubling. The cotton screen can be viewed as a plain fiber assembly in which fibers are straight and parallel and evenly arranged. To describe such an assembly mathematically, we make the following assumptions: (1) Fibers in the cotton screen has a specific fiber length distribution, and fibers in the assembly are straight and parallel; (2) Fibers in the screen are evenly assigned, that is, the per unit area of the screen has a almost same fiber amount in any place within the screen; (3) The fiber assignment in the screen is similar to the assignment of an ideal yarn when it is projected to its length direction.

The assignment of fibers in cotton screen can be see in Figure 1 as follows.

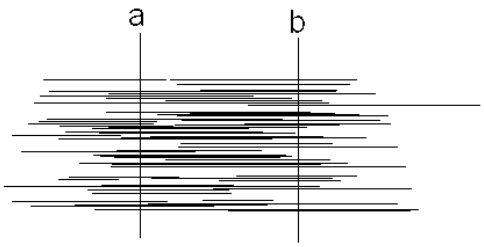


Fig 1. The fiber assignment in cotton screen

In order to generate a plain fiber assembly, we can regard the assembly as a rectangle area. And the rectangle can be divided identically into some little rectangles with width δ. We assume that for each little rectangle there are the same numbers of fiber left ends, e.g. n. And we assume that the location of the fiber left ends in each little rectangle follows uniform distribution. When the fiber left ends are generated according to the rules above, there will be some fibers going through the line on the right the large rectangle. We denote the number of fibers going through the right line of the rectangle as N. Obviously, N has a relation with n and δ, and is also related to $f(x)$, the fiber length distribution.

For a given fiber length distribution, the probabilistic density function is $f(x)$, we can generate the fiber plain assembly as follows.

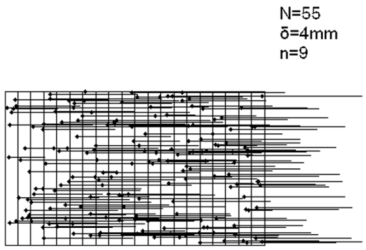


Fig 2. Generated plain fiber assembly

From figure 2 we can see that if the large rectangle is divided into some small rectangles, and when the fiber left ends are generated randomly, the plain fiber assembly can be obtained. Over the right line of the large rectangle is the protruding part of the fiber assembly, which is similar to the combed part of cotton screen in cotton combing process.

Simulation of the Cotton Combing Process

After the cotton screen is generated, the combing process can be simulated according to the combing principle. In combing process, there are usually two forms of feeding of cotton, one is forward feed, and another is backward feed. Here we only take forward feed as a example to simulate the combing process. Figure 3 shows the forward feed process in combing. Ⅰ - Ⅰ is the line when tong plate is in back position. Ⅱ - Ⅱ is the line when tong plate is in front position. Ⅲ - Ⅲ is the line of detaching roller, and R is the detaching distance, F is the feed length in a period in combing process. a is the feed coefficient, that is, the ratio of the feed length before the combing and the total length of the cotton feed.

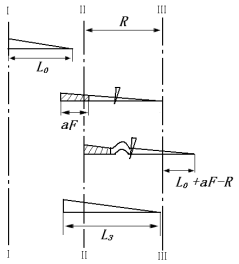


Fig 3. The process of forward feeding of cotton combing

For the cotton screen generated above, it is obvious that the generated part is only a segment of the real cotton screen. But the simulation is done randomly, and the results are the fiber length distributions. So the scale or size of the generated part has noting to do with the results. The concrete simulation can be shown in Figure 4.

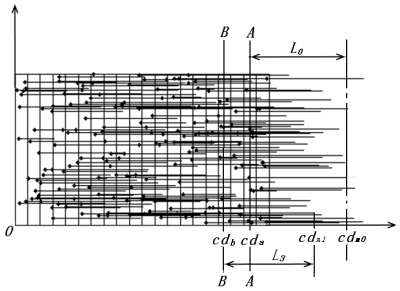


Fig 4. The combing process of the cotton screen

Figure 4 is the simulation process of the cotton combing. The left line of the rectangle is taken as 0 in axial and the right line of the rectangle is taken as the working line of the combing. When the combing starts, the nip line $A-A$ is taken as the arbitrary line in the small rectangle next to the right line of the rectangle (the working line). In combing, when the fiber ends are in the right place of $A-A$, the fibers will combed down into waste cotton.

When the first combing is conducted, the rest screen has a maximum protruding length, that is the difference of cd_{m0} and the cd_a for $A-A$. This deference is denoted by L_0. The first combing will have a different fiber length distribution than the normal combing. It is usually longer than the normal ones. So the first combing in the simulation can not be added to the simulation result.

Because of the forward weeding, the machine sends a cotton screen of the length aF, so the fiber beard has the length of $L_0 + aF$. The detaching nip length is $L_1 = L_0 + aF - R$. The first detaching is not added to the simulation result.

When the normal combing begins, the new nip line is $B-B$.

Simulation Results of Cotton Combing

At first the fiber length distribution of the constituent fibers in the cotton screen should be given. Figure 5 is the fiber length distribution of the screen.

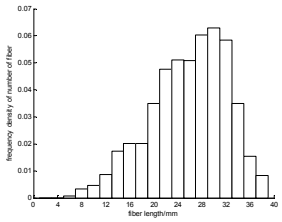


Fig 5. Fiber length distribution density in the cotton screen

We then simulate the combing process with the given fiber length distribution. We tried several parameters and obtained the fiber length distributions in cotton droppings and combed cotton slivers.

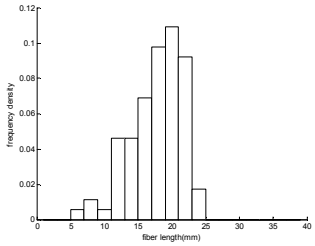


Fig 6. Fiber length distribution in dropping ($a = 0.6, F = 5.2mm, R = 22mm$)

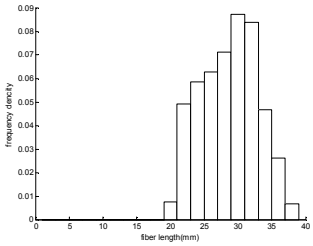


Fig 7. Fiber length distribution in combed slivers ($a = 0.6, F = 5.2mm, R = 22mm$)

Figure 6 and Figure 7 are simulation results at the same parameter levels. In this case, the simulated droppings rate is 10.06%. We change the parameters and have a new result in Figure 8and Figure 9.

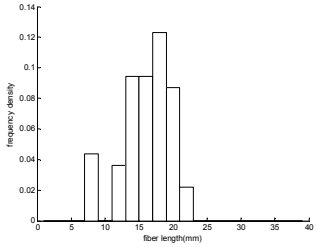


Fig 8. Fiber length distribution in dropping ($a = 0.6, F = 5.2mm, R = 20mm$)

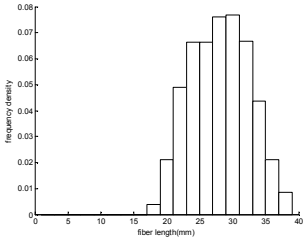


Fig 9. Fiber length distribution in combed slivers ($a = 0.6, F = 5.2mm, R = 20mm$)

Figure 7 and 8 gives another case in which the dropping rate yields in 4.95%, much smaller than the first case.

In the third case, we adopt a new set of parameters. The results are seen in Figure 9 and 10.

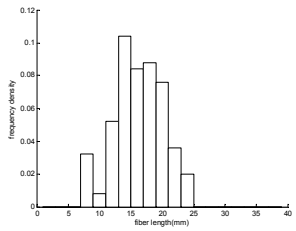


Fig 9. Fiber length distribution in dropping ($a = 0.6, F = 7mm, R = 22mm$)

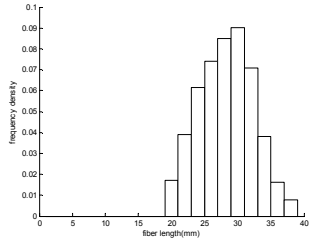


Fig 10. Fiber length distribution in combed slivers ($a = 0.6, F = 7mm, R = 22mm$)

In the third case the dropping rate is 10.11%. In all the three cases we can see that the parameter a, F, R all have influence on the dropping rate, in which R has an impact pn dropping rate dramatically.

Conclusions

Cotton combing process can be simulated from a randomly generated cotton screen. And various parameters can be set in the simulation process. Then different results can be obtained from the simulation. The fiber length distributions in cotton dropping and combed silvers can be simulated. Comparing those fiber length distributions, we can analyze the influence of the parameters on the combing result and optimize the combing process.

Experimental data indicated that the simulated results have a difference from the experiments. That is because that the simulation has been done under an ideal assumption. This difference can be reduced in the modified simulation that a series of new assumptions can be added to the simulation process. This work is to be done in the future research.

Acknowledgement

The financial support of the Shuguang Project of Shanghai Education Commission is gratefully acknowledged.

Reference

[1] Rao J Sudarsana: J Text Inst Vol.52(1961), P.570
[2] J.G. Martindale: J Text Inst. Vol.36(1945), P. 35
[3] M.L.Realff: Textile Res. J. Vol.70(2000), P. 415
[4] M.W Suh: Textile Res. J. Vol. 45(1976), P. 291
[5] G. H.Brown, G. N Ly: Textile Res. J. Vol.55(1985), P. 206
[6] M. Zeidman, M. W.Suh, S. K. A Batra: Textile Res. J. Vol.56(1998), P.1
[7] Guangsong Yan, Jinzhong Zhu, Chongwen.Yu : J. Text Inst. Vol.101(2010), P.753

© (2011) Trans Tech Publications, Switzerland
doi:10.4028/www.scientific.net/AMR.331.36

Research on Wearable Sensors Based on Knitted Fabrics with Silver Plating Fiber

Jinfeng Wang[1, a], Hairu Long[1, b]

[1] College of Textiles, Donghua University, Shanghai, 201620, China

[a]wangjinfengwjs@mail.dhu.edu.cn, [b] hrlong@dhu.edu.cn,

Keywords: Silver Plating Fiber, Weft Knitted Fabric, Wearable Sensor, Conductivity, Sensitivity

Abstract. Two kinds of plain fabrics, made of silver plating yarn, were tested on conductivity under weft extension to investigate the relationships between tensile property and resistance. The results are following: the resistances of two kinds of fabrics have a linear relationship with strain within a definite range; the strain sensitivity of the inelastic plain fabric is smaller than that of the elastic plain fabric; the changes of contact resistance of the overlapped yarns cause the inelastic plain fabric sensitive to strain; when two kinds of fabrics were stretched repeatedly to simulate heartbeat signals, their resistance remained stable at a value. So they satisfy stability requirement.

Introduction

Sensors can measure the accelerations of objects in motion along reference axes [1]. The results in Accelerometers have been widely accepted as useful and practical sensors for wearable devices to measure and assess Physical activity (PA) in either clinical/laboratory settings or free-living environments [2].Recently, wearable sensors measure not only PA monitoring signs, but also kinds of health indicator signs. It is obvious that we use cardiorespiratory signs, such as heartbeat and respiratory cycle, to estimate person's health condition [3]. Now, the application of wearable activity monitors should be integrated to so-called 'health smart home' monitoring systems [4]. The Internet can provide a sufficient network anywhere to connect ambulatory devices together or to a specialist center to support this system. For example, Vivometric's Lifeshirt uses this strategy to provide services to the patients, especially old patients. All Lifeshirts are connected to a specialist monitoring station where vital parameters are analyzed.

Hence, the purpose of this research is to develop a novel wearable cardiorespiratory sensor, which can sense person's cardiorespiratory signs for long time, especially in sleep condition.

Experimental

Sliver plated yarn At 20℃ 65% R.H., silver plated yarn was extended by YG061-1500 single-yarn strength tester at clamping gauge 500mm, to measure the relationship between breaking strength and elongation. It can be seen from Fig.1 that breaking strength of sliver plated yarn is 409.93CN and elongation at break is 28.181%.

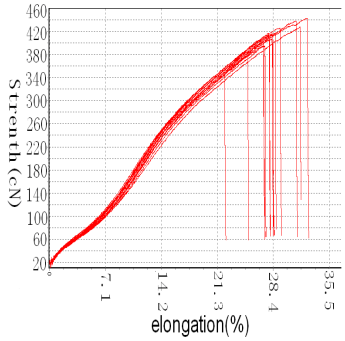
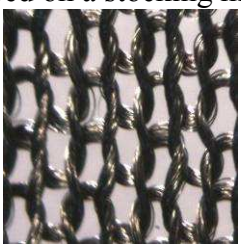


Fig.1 The relationship between breaking strength and elongation

Specimen preparation This paper adopted two kinds of weft knitted fabrics, made of sliver plated yarn (516Ω/m conductivity and 110dtex fineness), to investigate the relationship between tensile property and resistance. Fabrics is shown in Fig.2 ('A' is the inelastic plain fabric made of silver plated yarn, while 'B' is the elastic plain fabric made of silver plated yarn and spandex). Two kinds of fabrics were produced on a stocking machine, which works very well in knitting processing.


A


B

Fig.2 Two kinds of plain knitted fabrics

Tests and results

The resistance of two kinds of fabrics was tested by VC9805A + digital multimeter under weft extension to explore the relationship between tensile property and resistance, and calculate sensitivity of wearable sensor. Sensor sensitivity refers to the ratio of output steady state variations and input change amounts. Static sensitivity K is the slope of a linear sensor calibration curve. It goes without saying that the higher sensitivity of a sensor, the better its performance. Eq.1 is the calculation method of static sensitivity.

$$K = \frac{\Delta R}{\Delta L}. \tag{1}$$

Where ΔR is resistance variation; ΔL is stretching length variation of the fabric.

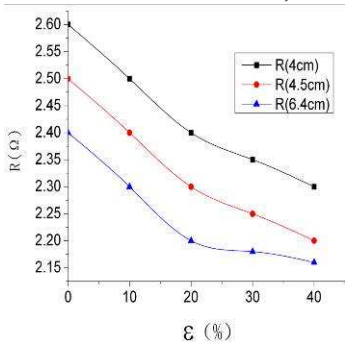


Fig.3 Resistance variations of plain fabrics

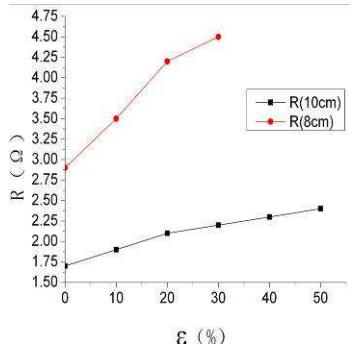


Fig.4 Resistance variations of elastic plain fabrics

Fig. 3 shows the relationship between resistance and strain of the inelastic plain fabrics, which are all 10cm long, but 4cm, 4.5 cm and 6.4 cm wide respectively. It is clear that the resistance of the inelastic plain fabrics decreases with increase of width; the resistance has a linear relationship with strain within a definite range; while the resistance changes are not obvious in large strain.

According to measurements, we can get $K = 10\Omega / m$. That is to say K values of three fabrics with different widths are all $10\Omega / m$. Thus the sensor sensitivity of the inelastic fabric does not depend on fabric width, but on material and structure. It is deduced from $R_4 > R_{4.5} > R_{6.4}$ that, the smaller width the knitted fabric, the larger the resistance. Therefore, it makes a small part of fabric as the wearable sensor for signal acquisition possible that it only need to be considered whether it meets the size of human body.

The elastic plain fabrics, made of silver plated yarn and spandex, are all 3cm wide. In Fig.4, square line displays the relationship between resistance and strain of the 10cm long single-layer elastic fabric; while dot line shows that of an 8cm long double-layer elastic fabric. Judging from these fabrics, the resistance has a linear relationship with strain within a definite range. The elastic plain fabric is different from the inelastic plain fabric in density and loop figuration because of spandex.

In order to achieve the same strain, the sliver plated yarn of the elastic fabric elongates and tapers, thus the resistances of yarn segments become larger. When the elastic plain fabric is extended within small stress, the resistances of needle loops and sinker loops get larger with strain than those of the inelasticity fabric. Therefore, its equivalent circuit is different from inelastic plain fabric. When it is extended, the resistance rises with elongation. According to measurements, we can get; $K_{s1}=20\Omega/m$; $K_{s2}=10\Omega/m$; $K_{r1}=60\Omega/m$; $K_{r2}=30\Omega/m$. Where K_{s1} and K_{s2} are the sensitivities of the single-layer elastic fabric at strain 0~20% and 20~30% respectively; K_{r1} and K_{r2} mean the sensitivities of the double-layer elastic fabric at strain 0~20% and 20~30%. The sensitivity of the double-layer elastic fabric is 3 times as large as the single-layer's. The sensitivity of the single-layer elastic fabric can reach $20\Omega/m$ within a definite range; while beyond elastic range, the sensitivity is the same as that of the inelastic plain fabric. Because there is spandex in close-fitting underwear, which can raise the sensitivity of fabric within smaller strain, the underwear is technically feasible as a flexible sensor.

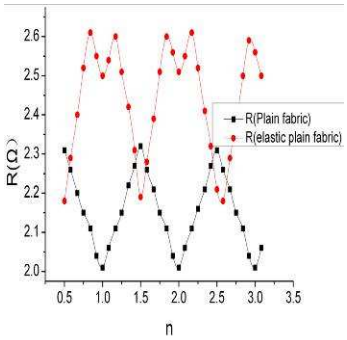


Fig.5 Resistance repeatability of two kinds of plain fabrics

When the heart pumps out or receives blood, it makes pulses, thus beats happen. Heart rate (HR) is heartbeats in unit of time (usually a minute) (HBM). Because pulses are the result of heartbeats, heart rate can be monitored through flexible sensors. Therefore, when two kinds of plain fabrics were extended repeatedly from 10cm to 13cm to simulate heartbeat signals, the changes of resistance were measured to observe repeatability about sensors. Fig.5 shows that, the resistance can recover to the original level and satisfy reproducibility and stability requirement. So they can be used to measure heartbeat and breathing signals.

Analysis of influence factors of inelastic plain fabric resistance

The effects of plain fabrics on resistance include yarn resistance, the transfer of loop yarn segments and the contact resistance of the overlapped yarns.

Yarn resistance rises with tensile strain, which fits metal conductor resistance law as fellow.

$$R=\rho\frac{l}{A}. \tag{2}$$

Yarn length and yarn cross section are all functions of tensile strain. When strain increases, yarn length augments; and yarn cross section becomes small, so resistance correspondingly grows.

Fig.6 shows the resistance variations caused by loop transfer. The left and the right are loop shape of the inelastic plain fabric after lateral stretching and the equivalent circuit respectively. A unit loop comprises two contact resistances (RC) and three yarn segment resistances (RL). The circuit of the inelastic conductive fiber plain fabric can be seen as a complex network formed with serial-parallel resistances caused by each yarn segment resistance and contact resistance. The effects of loop transfer and contact resistance shall be respectively discussed in the following passages.

The effect of loop transfer on the fabric resistance regardless of *RC* is represented in fig.7. Because needle loops and sinker loops are nearly same, we measure them all by *Rla* in the figure. If the fabric is lateral extended, the leg yarn segments will divert to needle loops and sinker loops, therefore *Rla* will grow but *Rlb* will decrease. The resistance of silver plated yarn is 0.516 Ω/mm, but the length of leg, needle loop and sinker loop are very short, so the changes of yarn length caused by loop transfer are very small. After complex series-parallel circuit on the fabric, the influence of resistance changes is not clear.

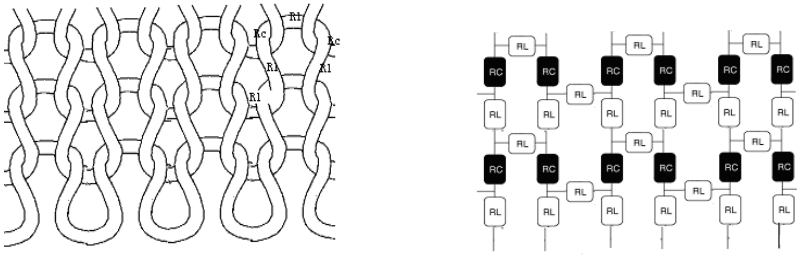


Fig.6 The equivalent circuit of an inelastic plain fabric

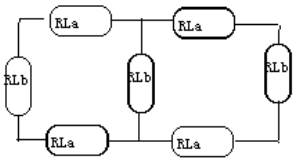


Fig.7 Resistance variations caused by loop transfer

When the fabric is suffered from weft extension, contact area between yarns gets smaller, thus contact pressure becomes larger. According to the theory of contact resistance, influence factors of contact resistance can be expressed by the formula as given below.

$$R_c = \frac{\rho}{2}\sqrt{\frac{\pi H}{nP}}\ [5]. \tag{3}$$

Where ρ is the resistivity of the material, n is the number of contact points, P is the contact pressure, H is the hardness of contact materials.

Subjected to an extended force, the resistivity ρ and hardness H of materials can be regarded as constant, the number of contact points n and the contact pressure P rise. So the contact resistance R_c will decrease with the increase of strain. It can be used to deduce that the fabric sensing mechanism is mainly because yarn contact resistance changes in tensile process.

Conclusions

Comparing two kinds of plain fabrics with silver plated yarn, we can see the conductive sensitivity of the inelastic fabric is smaller than that of the elasticity fabric. For the elastic fabric, the resistance grows with elongation within tiny strain, but beyond the elastic range, the sensitivity is the same as that of the inelastic plain fabric. Investigating the resistance repeatability of two kinds of plain fabrics, the resistance of all fabrics can recover to the original level and satisfy reproducibility and stability requirement. So they can sense person's cardiorespiratory signs for long time, especially in sleep condition.

Reference

[1]K Chen and D Bassett: Med. Sci. Sports. Exerc. Vol. 37 (2005), p. 490.
[2]M Mathie, A Coster and Lovell: Physiol. Meas. Vol. 25 (2004), p. 1.
[3]M Hazinksi, D Markenson. Circulation. Vol. 109 (2004), p. 278–291.
[4]C Scanaill, S Carew and P Barralon:. Ann. Biomed. Eng. Vol. 34 (2006), p. 547.
[5] Xianshu Liu. The Study and Application on Electric Contact Material[M]. Beijing: National Defense Industry Press, 1979: 1.

© (2011) Trans Tech Publications, Switzerland
doi:10.4028/www.scientific.net/AMR.331.40

Comparison of the Cost Performance between Pure Cashmere Siro-spun Yarn and Pure Rabbit Hair Ring-spun Yarn

Yueling Liu[a],Bukun Sun[b]

Taiyuan University of Technology, jinzhong, shanxi, 030600, China

[a]szl_ly@126.com,[b]sunbukun6310@sina.com

Keywords: Cost performance ratio;Cashmere; Rabbit hair; Analytic hierarchy process (AHP); Siro-spun yarn; Ring-spun yarn; Yarn evenness;Yarn strength; Yarn hairiness; Wearing resistance

Abstract: This paper systematically analysied and measured the main properties of the pure cashmere siro-spun yarn and pure rabbit hair ring-spun yarn, including the yarn evenness, thin and thick , neps, raw material nature, yarn strength, yarn hairiness, twist level, wearing resistance and etc. And the market price of yarn was also investigated. The model of the cost performance ratio was established to analyse the yarn properties scientifically. The results indicated that the pure rabbit hair yarn is better than the pure cashmere yarn. It provided the guidance suggestions and scientific basis for the manufacturers to improve the performance and reduce the cost price of the yarn.

Introduction

With the gradual perfection of the high-grade textile market, 20.8 tex×2 pure cashmere yarn and pure rabbit hair yarn are more requested in the textile market. Cost performance ratio is an important index of evaluating the commodities, However , there is few research on the cost performance of the textiles. This article deals with value engineering theory to build the cost performance model of textiles. The model provides quantitative measurement and references for consumers and manufacturers.

Establishment of the cost performance model of yarn

The cost performance model of yarn is based on the value engineering theory. The model can be described as ARP=A/P. Then the cost performance ratio index (APRI) can be defined as a/p where a stand for the performance index and p stand for the price index.

1.Definition of performance index

Table1 showed that A_1,A_2, … ,A8 represented the evaluating indicators including yarn evenness, thin and thick , neps, raw material nature, yarn strength, yarn hairiness, twist level, wearing resistance. In accordance with the use of the yarn (knitted yarn), they were analysed and compared pairwise, then the judging matrix A can be obtained from Table 1.

Table1 The judging matrix A

	A_1	A_2	A_3	A_4	A_5	A_6	A_7	A_8
A_1	1	2	2	6	3	5	6	4
A_2	1/2	1	1	4	2	4	5	3
A_3	1/2	1	1	4	2	4	5	3
A_4	1/6	1/4	1/4	1	1/3	1/2	2	1/3
A_5	1/3	1/2	1/2	3	1	1/3	3	2
A_6	1/5	1/4	1/4	2	3	1	2	1/2
A_7	1/6	1/5	1/5	1/2	1/3	1/2	1	1/3
A_8	1/4	1/3	1/3	3	1/2	2	3	1

(1) Calculating the geometric means of the elements aij in each row of the judging matrix.

$$\beta_i = \sqrt[n]{\prod_{j=1}^{n} \alpha_{ij}} \quad (i = 1,2,\ldots,8)$$

(2)Normalizing the vector $\beta = (\beta_1, \beta_2, \ldots, \beta_8)^T$, then obtain the eigenvector

$$W = (W_1, W_2, \ldots, W_8)^T$$

$$W_i = \beta_i \Big/ \sum_{k=1}^{n} \beta_k \quad (i = 1,2,\ldots,8)$$

(3)Calculating the maximum latent root λ_{max}

$$\lambda_{\max} = \frac{1}{n}\sum_{k=1}^{n}\frac{(A\times W)_i}{W_i} = \frac{1}{n}\sum_{k=1}^{n}\frac{\sum_{i=1}^{n}\alpha_{ij}W_j}{W_i} \quad (i=1,2,\ldots,8)$$

(4)Consistency check

$$CR = \frac{CI}{RI} = \frac{\lambda_{max}-n}{(n-1)RI} = \frac{\lambda_{max}-8}{7\times 1.41}$$

The values were substituted into the formula to get the weight coefficient

$$W = (W_1, W_2, \ldots, W_8)^T = (0.206, 0.165, 0.165, 0.076, 0.112, 0.099, 0.070, 0.107)^T$$

According to the expert system assistant decision-making comprehensive evaluation,the performance index (by 100 score system counting) could be obtained based on Uster Statistics. Then all the scores given by experts were comprehensive analysed and eight evaluation index scores of the yarn could be obtained. K_1,K_2,.....,K_8 representrd eight evaluation index scores of the yarn. Performance index of the yarn could be expressed as:

$$A = \sum_{i=1}^{8} K_i W_i \,/\, \sum_{i=1}^{8} W_i$$

2.Definition of price index

The price index is a dimensionless number, hypothesize the yarn price is P_0 when its performance reach to the perfect score (perfect yarn), the price index P_0 can be $P_K \times 100/P_0$. P_0 was obtained by the expert system assistant decision-making comprehensive evaluation as well. [1]

3.Explanation of cost performance ratio index

The two-dimensional evaluation map (see as Fig.1) was illustrated according to the performance index as abscissa and the price index as coordinate. Point A on the abscissa located the level of 75% of the Uster Statistics. [2]

When the point that represented the performance index and the price index fell in zone A (see as Fig.1), the cost performance index ratio is greater than 1 and it illustrated that the performance value was greater than the sale price while the performance of the yarn was not ideal. When it fell in zone B, the cost performance index ratio was greater than 1 and it indicated that the performance value was greater than the sale price. The cost performance index ratio was less than 1 and the performance was fine when it was in zone C. The cost performance index ratio was less than 1 and the sale price was greater than the performance value when it was in zone D.

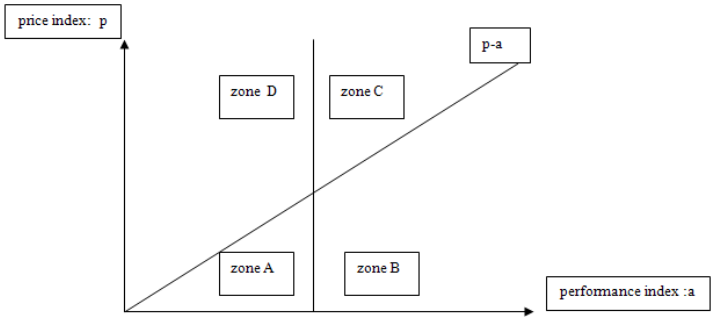


Fig.1: The two-dimensional evaluation map

Comparison with the factors and analysis

Performance index analysis

1.1Raw material nature

The quality of the rabbit hair can be evaluated by the level of length, looseness, whiteness and cleanliness. The average length of the top grade rabbit hair is 55.1mm or above, the one of the first grade is 45.1mm or above, the one of the second grade is 35.1mm or above and the one of the third grade is 25.1mm or above. In this experiment the length of the pure rabbit hair for ring-spun yarn was 42mm.

Cashmere is a kind of high-grade textile material which has a lot of advantages such as fineness, evenness, softness, good elasticity, subdued luster and high strength. In this experiment the fineness of the pure cashmere for siro-spun yarn is 15.20μm and the length is 28mm. [3]

The raw material nature indices are: pure cashmere: 70; pure rabbit hair: 90

1.2 Hairiness

Table 2 Hairiness test results

Yarn species[unit of hairness]	3mm	4mm	5mm	6mm	7mm	8mm	9mm
Pure cashmere siro-spun yarn[Number / 10m]	109.66	29.00	3.66	2.00	0.66	0.00	0.00
Pure rabbit hair ring-spun yarn[Number / 10m]	207.66	103.33	33.00	20.33	7.33	4.00	2.33

The hairiness of the pure cashmere siro-spun yarn was obviously less than that of the pure rabbit hair ring-spun yarn according to the result in Table 2. The two reasons of raw material and spinning technology could explain the result. On one hand, the rabbit hair fibers had surface smooth and fiber friction was small, so yarn hairiness was more. On the other hand, two roving that kept certain interval were parallelly fed in the siro-spinning, after drawing, the front set of rollers output the two single yarn, and because the twist can be transferred to each single yarn with small amounts of twist, to combine two single yarn with twist into similar plied yarn, so hairiness are less in yarn.

The hairiness indices are: pure cashmere siro-spun yarn: 100, pure rabbit hair ring-spun yarn: 80.

1.3 Yarn strength

Table3 Strength test results

Yarn species	Breaking strength [cN]	Stretching quantity [mm]	Elongation [%]	Breaking time [s]	Breaking work [N.m]	Breaking tenacity [cN/dtex]
Pure cashmere siro-spun yarn	250.9	42.49	8.46	18.24	0.080	0.601
Pure rabbit hair ring-spun yarn	340.7	96.58	19.28	21.09	0.243	0.816

The strength of the pure cashmere siro-spun yarn was obviously less than the pure rabbit hair ring-spun yarn according to Table 3. First, in view of the fiber surface, the rabbit hair fibers were smoother and fiber friction was smaller than those of cashmere. Second, in view of the fiber fineness, the rabbit hair was finer considerably than that of cashmere. So the number of fibers in cross-section of rabbit hair yarns was larger than that of cashmere yarn. Third, in view of the fiber length which decided the cohesiveness, the rabbit hair fibers were longer than that of cashmere. At last, siro-spinning technical increased the yam strength. By comprehensive analysis, it was known that influence of the previous three factors is greater than the effect of technical aspects. So the strength of the pure cashmere siro-spun yarn was obviously less than that of the pure rabbit hair ring-spun yarn.

The yarn strength indices are: pure cashmere siro-spun yarn: 70,pure rabbit hair ring-spun yarn: 90.

1.4 Yarn evenness

Table4 Evenness test results

Yarn species	Coefficient of variation{CV[%]}	-30%Thin [number/200m]	+35%Thick [number/200m]	+140%Neps [number/200m]
Pure cashmere siro-spun yarn	10.54	79	14	47
Pure rabbit hair ring-spun yarn	9.62	14	10	50

Table 4 showed that the evenness coefficient of variability and nips and slubs of the pure cashmere siro-spun yarn were more than that of the pure rabbit hair ring-spun yarn. This was mainly caused by longer rabbit hair fibers and the obvious effect of process control. However the neps of the pure rabbit hair ring-spun yarn were more than the pure cashmere siro-spun yarn, The reason was that rabbit hair fibers were longer and tended to snarl into neps during the combing process. However, in general, the both the two kinds of yarn have more neps than other kind..

According to the Uster Statistics and experiences, the yarn evenness indices were:

Pure cashmere siro-spun yarn: 90

Pure rabbit hair ring-spun yarn: 90

The thin and thick indices were:

Pure cashmere siro-spun yarn: 90

Pure rabbit hair ring-spun yarn: 90

The neps indices were:
Pure cashmere siro-spun yarn: 50
Pure rabbit hair ring-spun yarn: 50
1.5 Wearing resistance

Table5 Wearing resistance test results

Yarn species	Average times[times]	CV[%]
Pure cashmere siro-spun yarn	209.1	11.17
Pure rabbit hair ring-spun yarn	181.7	10.44

The result inTable 5 indicated that the wearing resistance of the pure cashmere siro-spun yarn was better than that of the pure rabbit hair ring-spun yarn. This was because cashmere fibers were thicker and heavier and the siro-spun processing enhanced the wearing resistance.

According to the Uster Statistics and experiences, the wearing resistance indices were:
Pure cashmere siro-spun yarn: 80
Pure rabbit hair ring-spun yarn: 80
1.6 Twist level

Table6 Twist level test results

Yarn species	Average twist [twist /25cm]	CV[%]
Pure cashmere siro-spun yarn	99.6	8.51
Pure rabbit hair ring-spun yarn	102.8	7.42

In view of the fact that the yarn species are both knitted yarn, the twist levels of the yarn are basically identical (see as Table6). The twist irregularity is mainly caused by the performance variance of the machines.

According to the Uster Statistics and experiences, the twist level indices are:
Pure cashmere siro-spun yarn: 80
Pure rabbit hair ring-spun yarn: 80
2. Analysis of the price index
According to the expert analysis and market research, the market price of the perfect pure cashmere siro-spun yarn was 700 yuan per kilogram, while the one of the perfect pure rabbit hair ring-spun yarn was 300 yuan per kilogram. The market price of the pure cashmere yarn was 650 yuan per kilogram and the pure rabbit hair yarn was 240 yuan per kilogram in the experiment.
3. Cost performance ratio

cashmere siro-spun yarn: $APRI = \frac{a}{p} = 0.8495$

rabbit hair ring-spun yarn: $APRI = \frac{a}{p} = 1.0080$

Conclusions

According to the cost performance ratio of the yarn, the point of the pure cashmere siro-spun yarn fell in the zone C in Fig.1, while the point of the rabbit hair ring-spun yarn fell in the zone B. It indicated that the cost performance of cashmere siro-spun yarn is less than that of the rabbit hair ring-spun yarn. Therefore the rabbit hair ring-spun yarn is more worthy to buy for the consumers. For the manufacturers, it is necessary to modify their technologies and reduce the cost price of the cashmere siro-spun yarn to improve its cost performance.

References

[1] Suozhang Cai, Hongbin Zhang, Youwen Li, in The principle and method of mathematical modeling , published by China ocean press(2000) in chinese
[2] Chongwen Yu, in Spinning process design and quality control, published by China textile press(2005) in chinese
[3] Mu Yao, in Textile material science, by China textile press(2009) in chinese

© (2011) Trans Tech Publications, Switzerland
doi:10.4028/www.scientific.net/AMR.331.44

Modelling and Simulating Textile Structures using TexGen

Hua Lin*, Louise P Brown and Andrew C Long

Faculty of Engineering, University of Nottingham, NG7 2RD, UK

hua.lin@nottingham.ac.uk

louise.brown@nottingham.ac.uk, andrew.long@nottingham.ac.uk
*Corresponding author: Hua Lin (hua.lin@nottingham.ac.uk)

yarn path and the tangent should vary smoothly. Splines are used to address this criterion and in TexGen three spline interpolation functions are available: cubic Bezier, natural cubic and periodic cubic.

Keywords: TexGen software, 3D geometric textile modelling.

Abstract. This paper provides an overview of TexGen, the open source software package for 3D modelling of textiles and their composites developed at the University of Nottingham. The underlying modelling theory is briefly discussed followed by descriptions of applications utilising TexGen in the fields of textile mechanics, textile composite mechanics and permeability. The limitations and further development of the approach are also considered.

Introduction

Realistic geometric representation of fabrics is essential for modelling of mechanical and physical properties of textiles and textile composites. If this can be achieved then a reduction in expensive physical iterations required during a textile design are possible. TexGen [1,2] is open source software developed by the Polymer Composites Group at the University of Nottingham as a modelling pre-processor for textiles for a variety of applications including solid mechanics [3-4], fluid dynamics [5-6] and thermodynamics. The objective of this paper is to demonstrate the modelling techniques and concepts implemented in TexGen and show the multi-functionality of the software when applied to commercial fabrics.

Modelling theory

The core of the TexGen program has been written to give maximum flexibility to the textile model that can be produced, thus allowing accurate modelling of a wide range of textiles. The geometry of any textile fabric is generated in a generic way by independent specification of yarn path and yarn cross-sections. This approach allows easy modelling of any textile fabric structure, e.g. woven, knitted, braided and non-crimp (Fig1). For a comprehensive description the reader is referred to Sherburn [1].

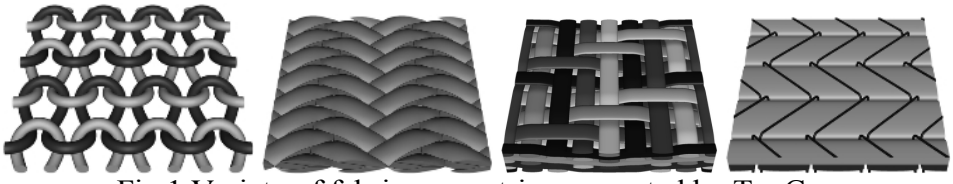


Fig 1 Variety of fabric geometries generated by TexGen

Yarn path. The yarn path is modelled by specifying its centreline, defined by a position in three dimensional space as a function of the distance along the yarn. The smallest repeatable section of the yarn is specified by means of a series of points along its length, known as master nodes, and an interpolation function to give the exact path between those nodes. The interpolation function must give at least C^1 continuity. That is there should be no gaps in the

Yarn cross-section. The yarn cross-section is defined as the 2D shape of the yarn when cut by a plane perpendicular to the yarn path tangent. Yarns are treated as solid volumes and the cross-section is approximated to be the smallest region that encompasses all of the fibres within the yarn. There are five options available to describe cross-sections: Ellipse, power ellipse, lenticular, hybrid and polygon. The last two of these give the most flexibility to the shape, particularly useful where

yarns are in contact at cross-sections causing the yarn shape to be deformed and necessitating modifications to the cross-section to avoid intersections between yarns in the model. The hybrid section utilises any combination of the ellipse, power ellipse and lenticular sections. As shown in Fig 2a different cross-sections can be assigned to a selected sector of the cross-section. The polygon cross-section gives a high degree of flexibility allowing individual points to be specified around the outline of the section. It is used in the "refine section" option where the points around the sections are moved in order to reduce the yarn interference as shown in Fig 2b.

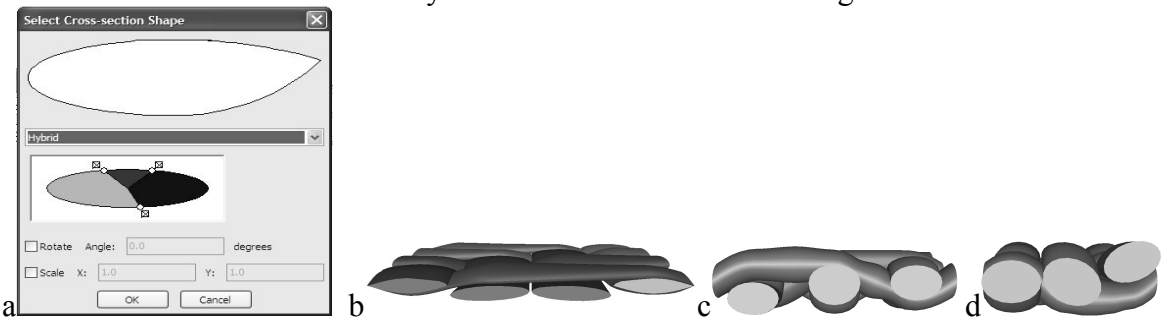


Fig. 2 Examples different cross-sections (a-b); A twill weave with varying yarn cross-section (c) and rotated yarns in the twill weave (d)

Interpolation between yarn sections. Yarns are easily deformed even under low loads and, typically, woven yarns will be compacted at crossover points. The ability to model a yarn with uneven cross-sections and create smooth transitions between the cross-sections at different points on the yarn is therefore essential. An interpolation function, either smooth or polar, is imbedded in TexGen, describing the way in which the cross-section varies along the length of the yarn. Fig 2c shows an example of a modelled polyester/cotton twill weave with varying yarn cross-section. Further flexibility can be achieved by utilising functions which allow cross-sections to be scaled and rotated. Rotation is particularly useful to create realistic models for non-symmetric fabric structures such as twill weaves as can be seen in Fig.2d.

Intersections. The method of modelling textiles used in TexGen can lead to yarn intersections (ie. part of one yarn volume intersecting with/ penetrating either a crossing or parallel yarn volume). The problem can be addressed in two stages: firstly identification of where the intersections occur and secondly modifying the textile in order to eliminate or reduce the intersections to an acceptable level.

Several strategies have been implemented to address the issue of yarn intersections and this may depend on the size of the intersections and also how far the textile is along the modelling and output process. Sherburn [1] describes a method for refining a yarn mesh by first adjusting the yarn width and then rotating yarn sections at crossovers in the weave. Subsequent adjustment of the yarn cross-section by taking advantage of the flexibility of the polygon cross-section gives further refinements which minimise the intersections. This model was validated for a tightly packed nylon filament plain weave fabric for vehicle airbags. Fig 3a shows a comparison of the final refined model with the actual textile.

There are some cases where small intersections in the model may be acceptable. If the model is to be discretised directly within TexGen, it may be exported as either a tetrahedral or voxel mesh. In both of these cases the mesh is adapted to eliminate intersections as it is generated. This does lead to some loss in yarn volume, which may affect the accuracy of (for example) Computational Fluid Dynamics (CFD) simulations to predict fabric permeability. To address this, a method has been developed which is suitable for making fine adjustments to the dry fibre volume mesh. The method is based on interference depth and an iterative method is used to adjust the node position in the volume mesh until the intersection is reduced to a given tolerance. The local fibre volume fraction of the yarn is recalculated at the adjusted points to take into account the local change in cross-section. Fig 3b and 3c show solid and mesh views of a small section of intersecting yarns with Fig 3c showing the rendered intersection points. The fine adjustments made to the final volume mesh are shown in Fig 3d.

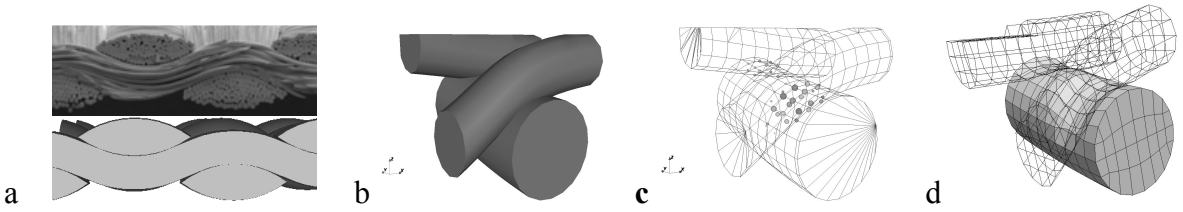


Fig 3 Comparison of actual densely packed fabric and TexGen model (a); Volume mesh adjusted for small intersections (b-d)

Yarn properties. Properties can be assigned to each yarn as follows: yarn linear density, fibre density, fibre diameter, fibres per yarn, Young's modulus and Poisson's ratio. These are currently used in the calculation of fibre volume fraction and within the export functions to calculate yarn or composite properties as required for the relevant model.

Rendering and export of model

Once a model has been specified as described above it can be meshed to visualise the textile and enable it to be output in various formats as required for further processing. Dry fibre volume meshes can be created in TexGen using hexahedral and wedge elements as illustrated in Fig 4a. This mesh may be exported to external packages for further processing to predict textile mechanical behaviour. When the volume mesh is exported as an Abaqus input file the textile is interrogated to find the yarn tangent and fibre volume fraction at the centre point of each element. Material properties will also be set, taken either from master yarn properties or from those set for individual yarns within the textile. Where both the yarns and resin matrix are required to be meshed a tetrahedral mesh is created. Views of the resulting yarn and combined yarn/matrix meshes are shown in Figs 4b-c. Generation of conformal meshes can be challenging for textile geometries. In particular, close to yarn crossovers it is often difficult or impossible to generate elements of acceptable quality that conform to the local yarn surfaces. Here a voxel mesh may be preferred, which is formed by dividing the domain area into cuboids or rectangular bricks. By interrogating the model at the centre point of each voxel the fibre volume fraction and yarn direction can be obtained for each element and output with the position information to an input file for subsequent analysis, selecting yarn, matrix or both to be output. Fig 4d shows an example of a voxel mesh.

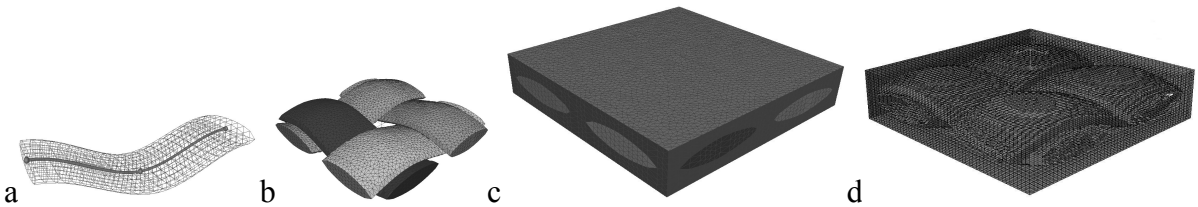


Fig 4 Volume mesh for single yarn (a); Triangulated yarn areas for plain weave (b); Tetrahedral yarn/matrix mesh for plain weave (c); Example voxel mesh for plain weave (d)

Applications

TexGen has been used in a variety of different applications some of which are outlined in the following sections.

Textile mechanics. The application of the TexGen model to mechanical modelling of a commercial polyester/cotton plain weave fabric is described by Lin et al [7], in which the textile was meshed and exported to the Abaqus finite element analysis (FEA) package. Deformations were predicted for the plain weave unit cell in tension, compression, shear and bending, utilising their measured equivalents for individual yarns as input data. The predictions were then validated against experimental data for fabric samples which showed that the model was able to represent the fabric behaviour very accurately, particularly during tensile and shear loading.

Textile composite mechanics. Voxel meshes generated from TexGen models have been used as input for FE analysis to predict mechanical properties of textile composites, including elastic and failure behaviour. Smitheman et al [8] describe a voxel-based homogenization technique for predicting warpage of a textile reinforced composite during manufacture. TexGen is used to provide the geometric model of the representative volume element (RVE) which is then divided into voxels.

The composite is modelled as being homogeneous in each voxel. Subdivision into subcuboids and interrogation by TexGen gives the local fibre volume fraction, from which effective thermomechanical properties are determined using micromechanics. The thermomechanical properties of the bulk composite are then obtained using FEA based on the RVE. On application of appropriate periodic boundary conditions, the method was shown to give good agreement with experimental data for a carbon/epoxy composite.

Textile permeability. TexGen has been used to generate models to predict fabric and reinforcement permeability using a variety of techniques. Broadly these aim to predict in-plane and/or through-thickness permeability as input data for macro-scale models of resin infusion during composites manufacture or water permeability for clothing fabrics. For example, a voxel mesh approach has been taken for flow simulation of 3D textile fabrics using Ansys CFX CFD software [6]. Using the average values for width and height of warp, weft and binder yarns gives reasonably close agreement with experimental data. Predictions based on the lower bounds from measured dimensions of all yarns (corresponding to a reduction in around 10% in yarn width and height) lead to a doubling in the predicted permeabilities. This illustrates the sensitivity of permeability predictions to small changes in the geometric model, indicating the importance of accuracy in geometric parameters for flow simulation.

Summary

The paper has presented the overview of TexGen. One particular feature of this software is to give maximum flexibility to the textile model that can be produced, thus allowing accurate modelling of as wide a range of textiles as possible. It ensures a realistic contact surface between yarns with minimal interpenetration. In addition, TexGen has automated functions to discretise the model, assign material orientations and properties to elements, and export the model to external analysis software in several data formats. All this functionality provides a solid foundation for a priori prediction of physical properties of textiles and textile composites as demonstrated by a variety of applications. However, the software is still in development. One of the key areas for current and future development of TexGen is further improvement of model accuracy. Broadly speaking models generated automatically by TexGen are very accurate for 2D weaves, whereas accurate modelling for 3D weaves requires fairly extensive experimental characterisation of the textile geometry. The ultimate goal is to be able to predict the textile geometry with sufficient accuracy based on simple geometric parameters easily determined by the fabric manufacturer.

References

[1] M.Sherburn: Geometric and Mechanical Modelling of Textiles. PhD thesis, University of Nottingham,(2007).

[2] TexGen, Available from: http://www.texgen.sourceforge.net [Accessed 23 October 2010]

[3] H. Lin, M. Sherburn, J. Crookston, A.C. Long, M.J. Clifford and I.A. Jones: Finite Element Modelling of Fabric Compression. *Modelling Simulation Mater Sci Eng* (2008); **16** 035010 (16pp).

[4] H. Lin, M.J. Clifford, A.C. Long and M. Sherburn: Finite element modelling of fabric shear. *Modelling Simulation Mater Sci Eng* (2009); **17** 015008 (16pp).

[5] C. C. Wong, A. C. Long, M. Sherburn, F. Robitaille, P. Harrison and C. D. Rudd: Comparisons of novel and efficient approaches for permeability prediction based on the fabric architecture, Composites Part A(2006), **37** (6), 847-857.

[6] X. S. Zeng, A. Endruweit, A. C. Long and M. J. Clifford: CFD flow simulation for impregnation of 3D woven reinforcements, Proceedings of the 10th International Conference on Textile Composites (TexComp 10), Lille, October 2010.

[7] H. Lin, M. Sherburn, A. C. Long, M. J. Clifford, I. A. Jones and C.D. Rudd: Modelling and simulations of fabrics using TexGen, Proc. Fibre Society's Spring 2009 conference, Shanghai.

[8] S. A. Smitheman, I. A. Jones, A. C. Long and W. Ruijter: A voxel-based homogenization technique for the unit cell elastic and thermoelastic analysis of woven composites, Proc. 17th Int. Conf. On Composite Materials (ICCM-17), Edinburgh, July 2009.

© (2011) Trans Tech Publications, Switzerland
doi:10.4028/www.scientific.net/AMR.331.48

Effect of Fabric Construction on Water Permeability Rate of Woven Filter Cloth

Chengdong Mao[1, a]

[1] Eastern Liaoning University, 325 Wenhua Road, Dandong, Liaoning, 118003, China

[a]ddmcd@126.com

Keywords: Water Permeability Rate, Fabric Tightness, Twist, Textile Weave

Abstract. In order to explore the filtration performance of woven filter cloth to provide a design basis for filter cloth, the relationship of water permeability of filter cloth and fabric structural parameters is analyzed and studied by measuring the mass of water through the filter cloth within a specified time. The results show that water permeability rate of filter cloth decreases with the increase of fabric tightness, and the two assume the exponential function relationship. The relationship between yarn twist and water permeability rate assumes the linear positive correlation. The increase of yarn twist makes water permeability rate of filter cloth increase. The effect of textile weave on water permeability of filter cloth is that the water permeability rate of plain weave is the smallest and that of twill weave is the biggest.

Introduction

The water permeability of woven filter cloth is an important characteristic to express filter speed of filter cloth. For the liquid-solid separation, the water permeability resistance can more directly reflect the filter speed of filter cloth than the air permeability resistance. The water permeability rate can be used to indicate the water permeability of filter cloth. Water permeability rate means the volume of water through unit area of filter cloth per unit time under prescriptive water pressure difference between both sides of filter cloth. Water permeability rate, to a certain extent, reflects the filtration performance of filter materials, and is a basic index of filter cloth [1,2].

The filtration performance of filter cloth can be influenced by many factors, mainly including fabric construction of filter cloth, fiber cross-sectional shape, surface characteristics of filter cloth and finishing processing and so on [3]. The water permeability of filter cloth is influenced by these factors and the filtration conditions, thus exhibiting the corresponding filtration performance. In these factors, the effect of fabric construction on water permeability of filter cloth is most remarkable [4]. This paper studies the effect of fabric tightness, yarn twist and textile weave on water permeability of woven polyester filament filter cloth under the condition of a certain pressure difference.

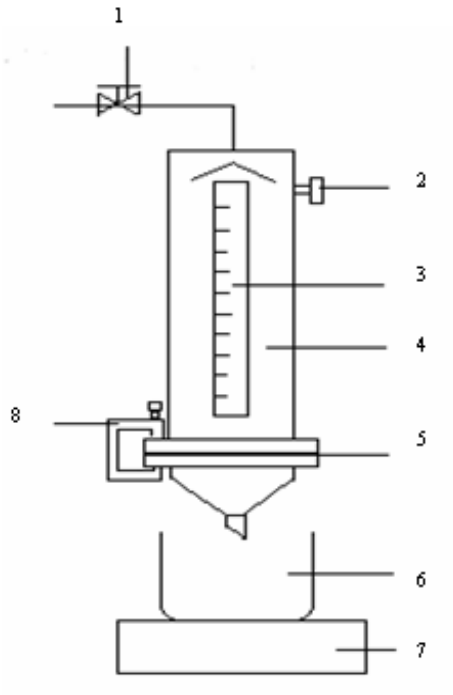
Experimental

Experimental Principle. Forming a certain pressure difference between both sides of filter cloth, the corresponding water permeability rate can be calculated by measuring the mass of water through filter cloth during a certain time. The formula is:

$$Q = \frac{W}{TA\rho}. \tag{1}$$

In equation (1), Q is for water permeability rate of a sample at certain pressure difference point [$m^3/(m^2 \cdot s)$]; A is for water permeability area of a filter cloth (m^2); W is for water permeability mass of a sample at certain pressure difference point (kg); T is for the time used to permeate water through a sample at certain pressure difference point (s); ρ is for the density of water under the measuring temperature (kg/m^3) [5].

Experimental Device. Due to the different use occasions, the measure of water permeability of woven filter cloth differs from that of general wearing fabrics, so according to the test principle [5], self-restraint testing device, shown in Fig. 1, is used to test the sample of filter cloth.



1-water inlet valve 2-level control valve 3-pressure difference scale division ruler
4-pressure difference cylinder 5-filter cloth 6-beaker 7-electronic balance 8-flange clip

Fig.1 Schematic diagram of water permeability of filter cloth testing device

Sample Preparation. Select a representative filter cloth, and cut five samples (each 130mm in diameter) uniformly along the width direction of filter cloth in the point of 1 / 10 width away from each side of filter cloth. Electric iron is required to trim the sample edge to ensure the sample edge neat, flat, not curled or wrinkle, not thread-off; the sample is not be pressed. Place the single sample on the surface of the distilled water, until it goes down due to weight; if the overlapping samples are needed to soaked, dip in the distilled water for 24 hours. When testing, the ambient temperature is 20 ± 2℃ and the relative humidity is 65 ± 2%; the determination water uses the distilled water or the ionic exchange water.

The Samples are from Liaoning Tianze Industrial Textiles Co. Ltd. Five pieces are taken for each sample and the water temperature is 18℃ when testing. The arithmetic mean of five samples is used to express water permeability rate.

Experimental Method. Clip the sample in the centre of the high and low flange surface of the testing device and fasten tightly with a flange clip 8; the water permeability area of the sample is 5.0 × $10^{-3}m^2$. Turn the level control valve 2 and the overfall mouth aims at the selected pressure difference scale division line. Turn on the water inlet valve 1 and start the water pump; pour water into the pressure difference cylinder 4; make the height of water column stabilize on the pressure difference scale division line through the regulation of level control valve 2; put the beaker 6 on the electronic balance 7 and clear zero, then receive the water sample through filter cloth; at the same time, press the stopwatch to start to time.

Selected principles of pressure difference is that both make the water through the filter cloth have a certain flow velocity and the water can not flow too fast, thus reducing the effect of onflow on the testing and be convenient for measuring water permeability time and mass. If the water permeability pressure difference is less than 2.0kPa, the plywood is needed to change the water permeability area of the sample; the water permeability area is $2.5\times10^{-3}m^2$. In the ordinary course of events, do not install the plywood and the water permeability area is 5.0 × $10^{-3}m^2$. In this experiment, the pressure difference scale division line is 204mm (about 2kPa) and the stopwatch time is 20s.

Results and Discussion

Effect of Fabric Tightness on Water Permeability Rate. Take 2/2 twill polyester filament woven filter cloth； the twist of warp and weft is 217 t/m and 177 t/m respectively; the warp linear density and the weft linear density are all 167dtex × 9. The same setting process of filter cloth is used; the fabric count of filter cloth is 171.5 × 123.0/10cm, 182.0 × 124.5 /10cm, 190.5 × 130.5/10cm, 216.0 × 132.5 /10cm, 232.5 × 137.0/10cm respectively. The relationship of water permeability rate Q and total fabric tightness E is shown in Fig. 2.

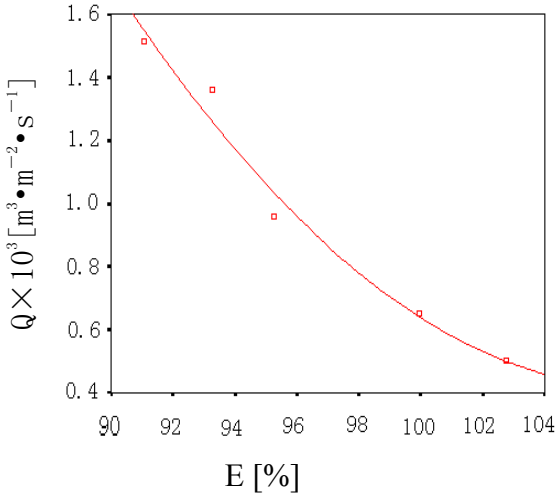


Fig.2 Effect of total fabric tightness on water permeability rate

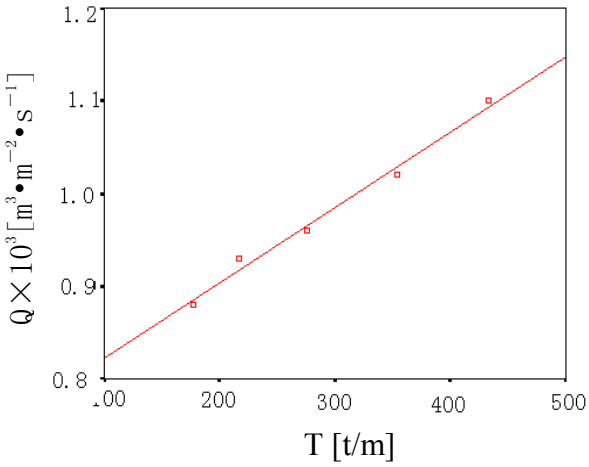


Fig.3 Effect of weft twiston water permeability rate

The exponential function fitting equation of water permeability rate Q and total fabric tightness E is $Q = 11002.0209e^{-0.09739E}$; the correlation coefficient is 0.986. It can be seen from the test results, when textile weave and twist of warp and weft are constant, the relationship between water permeability rate Q and fabric tightness is descending, that is, the bubbling aperture of filter cloth decreases along with the increase of fabric count. This can be explained by the tightness of filter cloth, because when textile weave and linear density of warp and weft are the same, fabric tightness also increases along with the increase of fabric count, and the gap between the yarns in the fabric is reduced, thus water permeability rate Q is also reduced.

Effect of Twist on Water Permeability Rate. Take 2/2 twill polyester filament woven filter cloth ； the fabric count is 190.5 × 130.5/10cm; the warp linear density and the weft linear density are all 167dtex × 9; the warp twist is 217 t/m. The same setting process of filter cloth is used; the weft twist is 177 t/m, 217 t/m, 275.8 t/m, 354.3 t/m, 433.1 t/m respectively. The relationship of water permeability rate Q and weft twist T is shown in Fig. 3.

The linear function fitting equation of water permeability rate Q and weft twist is Q=0.7403+0.0008T; the correlation coefficient is 0.988. It can be seen from the test results, when fabric count and warp twist are constant, the water permeability rate Q increases along with the increase of weft twist. This is mainly because the yarns can be packed tightly when the yarn twist is big under the same fabric count, and in a certain range, the bigger the yarn twist, the smaller the yarn diameter, thus the gap between the yarns in filter cloth is increasing and water permeability rate Q is also increasing.

Effect of Textile Weave on Water Permeability Rate. Take the polyester filament filter cloth; the fabric count is190.5 × 130.5/10cm; the twist of warp and weft is 217×177 t/m. The same setting process of filter cloth is used; compare the water permeability rate Q of 2/2 twill,2/2 basket and 1/1 Plain weave. The results are shown in Table 1.

Table 1 Relationship between fabric water permeability rate Q and textile weave

Textile weave	2/2 Twill weave	2/2 Basket weave	1/1Plain weave
Water permeability rate $Q\times10^3$ $[m^3\bullet m^{-2}\bullet s^{-1}]$	0.960	0.956	0.885

As shown in Table 1, when fabric count and yarn twist are the same, water permeability rate Q of plain weave is the smallest; 2/2 basket is next; 2/2 twill is the biggest, and the difference between plain weave and twill weave is also bigger; this reflects the weave structure characteristics of filter cloth, which can be explained by the interlacing time of warp and weft in the fabric and the different loom tension in the weaving process. In the view of weave structure, the tightness of 1/1 plain weave is bigger than that of 2/2 basket and 2/2 twill, thus the plain weave is the tightest under the same fabric count, linear density of warp and weft, and twist of warp and weft. 2/2 basket and 2/2 twill have same interlacing points, but considering unique style with the certain concave-convex degree needed to diagonal line, excessive loom tension is not used in the weaving process, so the tightness is smaller than that of hopsack[6].

Conclusions

Under certain kinds of raw materials, twist of warp and weft and setting methods, fabric tightness has obvious influence on water permeability rate; water permeability rate decreases with the increase of fabric tightness, and the two assume the exponential function relationship.

When warp twist and fabric count are constant, the increase of weft twist makes water permeability rate of filter cloth increase, and the two assume linear positive correlation relationship.

Water permeability of filter cloth has the close relation to textile weave; interwoven structure is the important factor affecting this relation. Plain weave has smaller water permeability rate than other weaves due to its tight structure.

References

[1] Renhui Guo, Jianshe Zhang: *Performance Determination and Selection of solid-liquid separation filter cloth* (China Machine Press, China 1998). In Chinese.

[2] KULICHENKO A V，LANGENHOYE V L: Journal Texttile Institute Vol. 83 (1992), p.127.

[3] Hua Yu, Chun Li: Technical Textiles Vol. 14 (1996), p.20. In Chinese.

[4] A. Rushtouu, Qixin Zhu, Li Xu: *Solid-liquid filtration and separation technology* (China Chemical Industry Press, China 2005). In Chinese.

[5] FZ/T 64015-2009. Woven Filter Cloth . In Chinese.

[6] Zhejiang Institute of Silk Textiles: *Textile Weave and Jacquard Weaving* (Volume One) (China Textile& Apparel Press, China 1998). In Chinese.

© (2011) Trans Tech Publications, Switzerland
doi:10.4028/www.scientific.net/AMR.331.52

Mechanical Properties of 2D Braided Polyester Ropes

Jinqiu Zhang[1, a], Ling Cheng[1, b]

[1]Key Lab of Advanced Textile Composites, School of Textiles, Tianjin Polytechnic University, Tianjin 300160, China

[a]zhangjinqiu1987@126.com, [b]chengling@tjpu.edu.cn

Keywords: 2D Braided, Polyester, Ropes, Mechanical Properties.

Abstract. The relationship between the structure parameters and the mechanical properties of two-dimensional braided polyester ropes were studied. 22 times of polyester ropes were braided with different pitch length and different yarns, and their tensile properties were tested, then the relationship between the mechanical properties of the rope and braiding pitch was obtained. The results showed that the breaking strength of 2D braided ropes increased with the increase of pitch length, but after achieving certain length, the strength began to decline, and the breaking elongation decreased along with the increase of unit length.

Introduction

The rope plied by multi-yarn or thread is a special variety of textile industry, it has large diameter and can be divided into rope, ropes and cables according to the weaving method and the diameter size. The property of rope is determined by its raw materials and the processing method. The rope can be basically divided into three series: braiding, coil buckling and twist [1]. Rope can be made from natural fibres or synthetic fibres. With the development of chemical fibre industry, chemical fibre rope with its light weight, high strength, wear resistance and other advantages, gradually replaces the natural fiber rope. At present, the common chemical fibers used in rope are nylon, polypropylene, polyethylene, polyvinyl alcohol and polyester at home and abroad. There is a great demand for rope, it is widely used in modern industry, national defense and military industry, agriculture and other area such as people's daily life. Especially in recent years, more and more attention was paid to the correct usage and performance of lifeline in fire environments. However, the processing method of these ropes is mostly twisting. The method of 2D braided is relatively few. Chen, et al. tested the relationship between the rope's elongation and a series of processing parameters [2], East China Sea Fisheries Research Institute studied on properties of high-performance 8-strand polyethylene Ropes [3], Fontenot and Stenvers did a research on the aramid-fibre rope used in high-temperature or fire environments [4], etc. The structure of these types of rope are mostly three strands, 8-strand twisted rope and multi-strand braided rope, the method of 2D braiding as its simple structure, uncomplicated process, high production efficiency and mass production, was adopted in this paper.

The mechanical properties of ropes involved many factors, but the relevant research are seldom. The pitch length has close connection with strength, the main question is that how to meet the mechanical and portable requirements in security, but also use less material, etc. Research in this area is still not sufficient. Polyester was used as the material because of its high strength, low elongation, abrasion resistance, corrosion resistance and other characteristics. How the processing parameters on the internal structure affect the mechanical properties of the rope was discussed. With further study on process, we hope to provide the reference for future research and the determination of the optimum parameters in actual production.

Experimental

Experiment Procedures. The experiments were finished on the vertical 2D braided machine with 16 spindles which was made in China. 2D braid rope has simple body structure, easy operation, low energy consumable, small investment and high production efficiency. 2D braided machine consists of yarn carrier, braided mechanism and extraction mechanism. According to fabric molding ways, the machine can be divided into vertical and horizontal, and the former is widely used because the machine occupies small area. When braiding, the yarns are divided into two groups, they both move in the "8" track at the same time. Yarns in the same group running along the same direction, clockwise or counterclockwise, while other yarns running in the opposite direction. To ensure the two groups interlaced, the machine provide such a movement, that is, yarns in each group, some move towards the center of pipe, and the rest of yarns move towards the outer of pipe. At the same time, yarns move not only along the direction of the radius, but also along the pipe's circumference direction. Through observing the final structure of the fabric, the angle between yarn and the direction of fabric forming is same but in the opposite direction, and yarn will not be crossed with other yarns in the same group. The structure of 2D braided fabric is classified into diamond, regular and Hercules braided structure. Regular braided structure is also known as 2/2 interwoven structure, that is to say the yarn continuously pass through the above of two yarns in other group, and followed by the same step so as to complete the braid [5,6]. The method was adopted in this paper.

8-strand rope and 16 stands rope made of polyester filament were braided, and then compare with combination yarn. Pitch length refers to the length generated by a cycle machine movement. The length is tied to braided angle, cloth-fell, forming points, braiding speed, elevating speed, etc. It not only reflects the state of the fabric of the extrusion, but also is a direct physical quantity that represents the internal structure of the fabric. The rope performance was mainly influenced by pitch length, so we selected pitch length as variable.

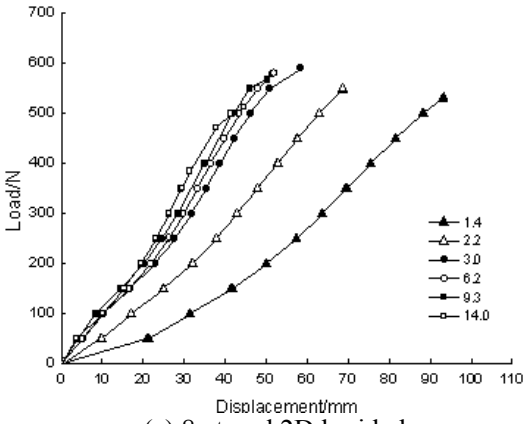
Experiment Materials. Raw materials are untwisted and twisted polyester multifilament that is composed of 200 monofilaments. The linear-density of multifilament is 167tex, breaking strength is 6.11cN/dtex, the twist of polyester filament is 8.2 T/10CM and breaking strength is 4.37cN/dtex.

Test Conditions. Tests were finished on AG-250KNE type universal tester of Shimadzu in standard laboratory environment, lab temperature (20 ± 2)℃, relative humidity (65 ± 5)%, the samples were balanced over 24 h, their length were all 500mm.The loading speed of tensile is 50mm/min.

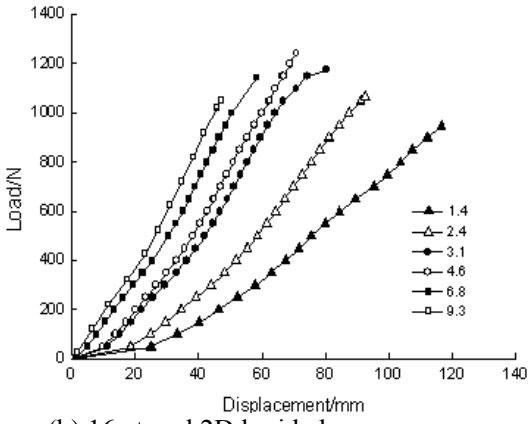
Results and Discussion

Load-Displacement Curves of 2D Braided Rope. Fig. 1(a) represents the tensile curves of 8-strand twisted polyester ropes, pitch length are 1.4 mm, 2.2 mm, 3.0 mm, 6.8 mm, 9.3 mm, and 14.0mm respectively. Fig. 1(b) is the tensile curves of 16-strand twisted polyester ropes, pitch length are 4 mm, 2.4 mm, 3.1 mm, 4.2 mm, 6.2 mm and 9.2 mm respectively. The tensile curves of 8-strand untwisted polyester ropes are shown in Fig. 2(a), pitch length are 0.9 mm, 1.4 mm and 2.4 mm respectively. As shown in Fig. 2(b), the tensile curves of 16-strand untwisted polyester ropes are described, pitch length are 0.7 mm, 1.4 mm and 2.8 mm respectively.

The tensile displacement-load curves of 8-strand and 16-strand braided polyester ropes are given in Fig. 1 and Fig. 2. We can find that load may increase with the increase of displacement until the rope was fractured, no matter which rope it is, and the curve is nonlinear. In the initial stage of tensile, the rope overcame the friction caused by bending change between the yarn and fibre, and stretched slowly by pull force. The load increased slowly, the curve was comparatively flat and this stage was very short. Next, most of the yarns extended and bore the load, as the displacement increased. The load increased quickly, the slop of the curve increased, and the curve is nearly straight line. Finally, the rope fractured and in the weak binding area, the fibre was pulled out, the load achieved its maximum. We also see that the breaking strength of untwisted rope is slightly larger than the twisted, comparing the Fig. 1 (a) (b) and Fig. 2 (a) (b) under the same condition. It may be due to uneven stress distribution when fibre together bear external tension, causing the strength declined.

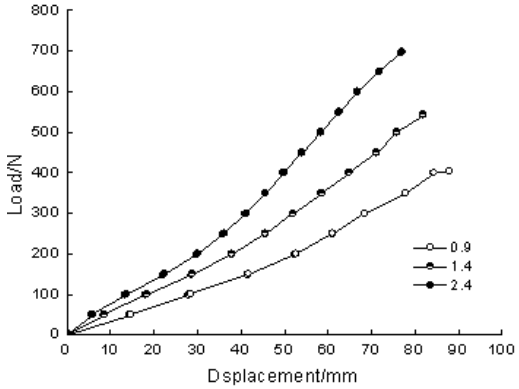


(a) 8-strand 2D braided ropes

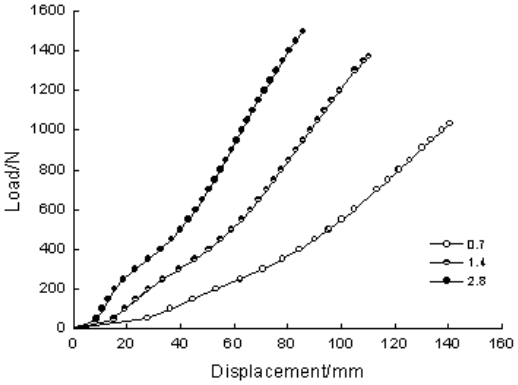


(b) 16-strand 2D braided ropes

Fig. 1 Tensile load-displacement curves of twisted polyester ropes



(a) 8-strand 2D braided ropes



(b) 16-strand 2D braided ropes

Fig. 2 Tensile load-displacement curves of untwisted polyester ropes

The Influence of 2D Braided Ropes Structure on Its Breaking Strength. Fig. 3 represents the relation of braiding pitch and breaking strength curves of 8-strand and 16-strand twisted polyester ropes, 8 strands ropes' pitch length are 0 mm, 1.4 mm, 2.2 mm, 3.0 mm, 4.2 mm, 5.1 mm, 6.2 mm, 8.2 mm, and 9.2 mm respectively; 16 strands ropes' pitch length are 0 mm, 1.4 mm, 2.4 mm, 3.0 mm, 4.6 mm, 6.8 mm and 9.3 mm. As shown in Fig. 2(a), 8 strands untwisted ropes' pitch length are 0.9 mm, 1.4 mm and 2.4 mm, the corresponding breaking strength are 402.50 N, 543.75 N and 697.50 N; 16 strands untwisted ropes' pitch length are 0.7 mm, 1.4 mm, and 2.8 mm, the corresponding breaking strength are 1033.75 N, 1370.00 N and 1496.25 N.

Fig. 3 shows that the breaking strength increases with the increase of knot length, when unit length is less than 5mm. It is due to the strength along the axis decline with smaller unit length, more obvious obliquity between yarn and rope axis, larger twist angle, tension and elongation. The trend is obviously reflected in Fig. 2 (a), (b). However, for more than 5mm of the knot length, breaking strength decreases, and is gradually close to the strength of non-woven fibres. It is probably because the yarn of axial unit length is fewer, braid coverage and cohesion is lower, structure is not close and the evenness in the length is poor, then weak link emerges easily, directly resulting shear fracture. Therefore, for ropes in this paper, the most suitable pitch length is 3-5 cm. It is also seen from Fig. 3 that trend of breaking strength about 8-strand twisted rope is small.

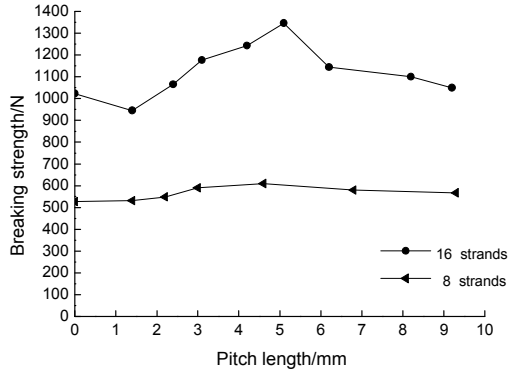


Fig. 3 Relation of unit length and breaking strength

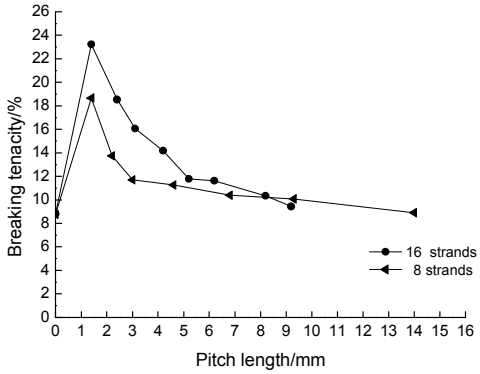


Fig. 4 Relation of unit length and breaking elongation

The Influence of 2D Braided Rope Structure Parameter on Its Breaking Elongation. Fig. 4 shows that the relation of braiding pitch and breaking elongation curves of 8-strand and 16-strand twisted polyester ropes, 8 strands ropes' pitch length are 0 mm, 1.4 mm, 2.2 mm, 3.0 mm, 4.2 mm, 5.1 mm, 6.2 mm, 8.2 mm, and 9.2 mm respectively; 16 strands ropes' pitch length are 0 mm, 1.4 mm, 2.4 mm, 3.0 mm, 4.6 mm, 6.8 mm and 9.3 mm. As shown in Fig. 2(a), 8 strands untwisted ropes' pitch length are 0.9 mm, 1.4 mm and 2.4 mm, the corresponding breaking elongation are 17.60%, 16.53% and 15.01%; 16 strands untwisted ropes' pitch length are 0.7 mm, 1.4 mm, and 2.8 mm, the corresponding breaking elongation are 28.15%, 22.10% and 17.15%.

The breaking elongation was mainly influenced by pitch length as illustrated in Fig. 4. It is obviously seen that the breaking elongation decreases with the increase of knot length. The breaking elongation is close to the non-woven fibre bundle finally. When the pitch length grows, the braid coverage and cohesion become smaller, fibre straightness is good, causing the breaking elongation decline, and so it is for untwisted polyester rope.

Conclusions

The breaking strength of 2D braided ropes increased with the increase of pitch length, but after achieving certain length, the strength began to decline, and the breaking elongation decreased along with the increase of unit length.

The breaking elongation was mainly influenced by pitch length to 16-strand, but not obviously to 8-strand polyester rope.

The suitable pitch length is 3-5mm for this work.

The strength of untwisted polyester rope is larger than twisted with the identical pitch length.

Acknowledgements

The authors would like to acknowledge the support of the National Natural Science Foundation of China through grant No. 11072175.

References

[1] Editing Committee of the Corpus of Textiles: China Textile & Apparel Press, 898, (2005)

[2] L. Chen, J. Yu and S. Wang: Journal of China Textile University, 20(1):45-53 (1994)

[3] J. Shi and L. Wang: Journal of Modern Fisheries Information, 25(11): 17-20 (2010)

[4] N. Fontenot, D. Stenvers and J. Gilmore: Proceedings of IEEE/MTS Oceans, 1-6 (2009)

[5] R. Bi and Y. Jiang: China Textile Leader, 22(2): 56-58 (2006)

[6] Y. Jiao and D. Wang: Journal of Textile Research, 30(8): 56-58 (2009)

© (2011) Trans Tech Publications, Switzerland
doi:10.4028/www.scientific.net/AMR.331.56

Objective Evaluation based on Main Factors Analysis of the Wool knitted Fabric style

Peilong Li[1, a], Ling Cheng[1, b]

[1]School of Textiles，Tianjin Polytechnic University，Tianjin 300160

[a]lipeilongqdu@163.com，[b]chengling@tjpu.edu.cn

Keywords: Wool knitted fabric, Fabric styles, KES fabric style testing instrument, Main factor analysis.

Abstract. In this paper, an objective evaluation method based on main factor analysis of the wool knitted fabric was researched. Because 17 parameters for expressing fabric style were simplified into several main factors in the method, the evaluation system for fabric style was simplified into four index: stiffness, glutinous degree, rebound elasticity and fullness softness, which provides a theoretical reference between fabric mechanical properties and wool knitted fabric style research.

Introduction

Since the 1990s, Fabric style research based on the KES-F fabric style testing instrument developed by Kawabata and FAST system developed by Australia tend to internationalization and mature. Today, fabric style research has gradually connected with garment production, High-grade Wool knitted fabrics are popular to consumers, and the fabric style has also been put forward new requirements, but the KES-F system and the fast system is expensive and the stylistic analysis of the knitted fabric has deviation. Therefore, the prediction of the wool fabric style based on the basic physical and mechanical properties of the wool knitted target test are taking seriously. In this paper, 17 physical and mechanical properties of 11 samples of wool knitwear were tested and the basic fabric style was evaluated by the main factors analysis [1]. This provides a theoretical reference between fabric mechanical properties and wool knitted fabric style research.

Experimental

Sample preparation. In this paper, the sample yarn adopted (26/2s) of acrylic yarn, wool yarn, yak yarn, and different blending ratio of yak hair/cashmere yarn. The fabric was knitted by stoll flat knitting machine of Germany, by changing the depth of weaving yarn bending, and finally got 7 different knit loop lengths of acrylic wool knitwear and 4same knit loop length of different blending ratio of yak hair/cashmere knitted fabric. All sample using weft plain stitch. The basic parameters of the finished fabric was shown in table 1

The Basic physical and mechanical properties tests of the fabric. In this paper, the mechanical index of the samples were tested by KES-FB-A fabric style instrument, which including tensile and shear test instrument(FB1), bending test instrument(FB2),compression test instrument(FB3)and surface properties test instrument(FB4).16 mechanical quantities used for assessment of the fabric style were measured. The sample were placed under the conditions that temperature was 20±2.C and the relative humidity was 65%±2% for 24 hours before testing. The testing results was shown in table 2

Table 1 Basic parameters of the sample

Number	Raw materials	Loop length(mm)	Pick density （longitudinal/10cm)	End spacing （weft/10cm）
1	100% Yak	6.667	60	88
2	80/20yak/cashmere	6.732	60	82
3	75/25 yak/cashmere	6.780	60	82
4	100%cashmere	6.710	58	82
5	Acrylic	5.6	66	98
6	Acrylic	6.173	62	84
7	Acrylic	6.568	58	82
8	Acrylic	7.184	52	78
9	Acrylic	7.782	48	70
10	Acrylic	8.379	44	64
11	Acrylic	9.174	42	60

Table 2 Testing results of the fabric mechanical index

KES index	Sample1	Sample 2	Sample 3	Sample 4	Sample 5	Sample 6	Sample 7	Sample 8	Sample 9	Sample 10	Sample 11
LT	0.183	0.171	0.159	0.171	0.212	0.191	0.198	0.188	0.176	0.172	0.176
WT	4.45	5.4	5.12	5.22	2.23	2.24	1.9	4.16	3.38	3.95	3.82
RT	47.54	48.67	47.01	42.56	42.12	41.9	39.47	38.26	38.27	37.55	33.88
EMT	24.45	31.6	32.25	30.6	10.51	11.64	9.61	22.58	19.3	23.05	22.07
G	0.48	0.42	0.26	0.28	0.73	0.5	0.46	0.35	0.31	0.27	0.26
2HG	1.82	1.4	0.9	1	2.17	1.67	1.69	1.45	1.24	1.1	1.13
2HG5	1.74	1.34	0.91	1.02	2.76	2.05	1.98	1.55	1.3	1.1	1.16
B	0.0538	0.038	0.0403	0.0413	0.0896	0.0739	0.0761	0.0623	0.0512	0.0455	0.0543
2HB	0.0646	0.0592	0.0504	0.0551	0.0779	0.06	0.068	0.0583	0.0416	0.0388	0.0545
LC	0.899	0.884	0.85	0.895	0.827	0.818	0.908	0.941	0.939	1.061	0.979
WC	0.558	0.579	0.648	0.544	0.462	0.39	0.486	0.517	0.472	0.608	0.746
RC	48.84	46.85	45.49	47.32	49.09	50.73	45.92	44.89	49.26	47.88	43.41
T	0.9853	0.782	1.001	1.3873	1.223	0.6047	1.552	0.932	1.3747	1.012	1.0303
W	24.993	26.973	24.025	21.665	24.87	22.033	20.323	19.685	17.143	16.05	16.263
MIU	0.211	0.21	0.264	0.213	0.265	0.239	0.247	0.248	0.231	0.252	0.27
MMD	0.009	0.008	0.0085	0.0084	0.0096	0.0112	0.0098	0.0099	0.0097	0.01	0.0091
SMD	7.722	7.808	7.713	8.852	5.682	7.363	9.177	6.733	7.326	6.147	5.811

Notes[1]:LI is the tensile linearity, no units; WT is drawing power, unit:cN.cm; RT means the response rate of stretching power, unit:%; B is bending stiffness, unit: $cN.cm^2$;2HB is hysterics of bending distance, unit: cN/cm; G is the shear stiffness, unit: cN/cm; LC is compression linearity, no units; WC means compression work, unit: cN.cm; RC is recovery rate of the compression work, unit:%; MIU is average friction coefficient, no units; MMD means the average deviation of friction coefficient, no units; SMD is surface roughness, no units; T is thickness of the light load, unit:mm; W means mass per unit area; unit: mg/cm^2.

Main factor analysis of the wool knitted fabric style

Main Factor analysis method. Main factor analysis method is classifying several correlation variables in the same class, each class variable classified as a factor to reflect most of the information of the original date by a fewer number of factors[2][3]. There are two main aspects of the main factor analysis application: one is searching for the basic structure and simplify the observation system; anther is classifying the samples.

The Correlation Analysis and the Principal Factor Selection. The normalized date of correlation matrix can be calculated by the correlation formula [4],and obtained of the initial eigenvalue by the correlation coefficient matrix. In the main factor analysis, the main factors were selected by the principle that the maximum ratio of common factor variance of the total variance. Factor number k(k <m) identified by the cumulative total percentage of common factors corresponding to the figenvalues in eigenvalue was greater than 85%.that is:

$$(\lambda_1 + \lambda_2 + \cdots + \lambda_k) \setminus \sum_{i=1}^{k} \lambda_k \geq 85\% \quad . \qquad (1)$$

The data in table 2 was processed by using SPSS 17.0 software in this article, and got four main factors; the eigenvalues from large to small were 8.260, 3.850, 1.906, 1.538 and the cumulative variance contribution rate reached 91.942. Where, the first factor eigenvalue was 8.260 and the variance contribution rate is 45.575.the second factor eigenvalue was 3.850 and the variance contribution rate is 21.975. The first two variance contribution rate of the factor eigenvalue was 67.548, which mean the first two eigenvalues were considerable representatives for all eigenvalues.

Factor analysis of objective wool knitted style Assessment. Using SPSS software, the public factor loading matrix was obtained by using the model based on principal component. The factor loading table was obtained by using the varimax rotation method, as table 4 shown.

Table 3 Rotation matrix elements

	Component 1	Component 2	Component 3	Component 4
LT	0.975	-0.023	0.099	0.023
WT	-0.865	0.34	-0.263	-0.022
RT	-0.2	0.93	0.146	0.036
EM	-0.891	0.324	-0.265	-0.018
G	0.871	0.395	0.172	-0.108
2HGΦ=0.5	0.931	0.208	0.17	-0.083
2HG5 Φ=5°	0.958	0.178	0.181	-0.086
B	0.984	-0.082	0.095	-0.059
2HB	0.811	0.489	-0.21	0.096
LC	-0.399	-0.764	-0.194	-0.028
WC	-0.544	-0.16	-0.768	-0.189
RC	0.255	0.131	0.869	-0.084
T	0.199	-0.274	-0.216	0.831
W	0.153	0.984	0.018	-0.014
MIU	0.396	-0.38	-0.526	-0.443
MMD	0.516	-0.507	0.551	-0.287
SMD	-0.204	0.316	0.228	0.799

As we can saw form table 3, the first factor had a strong relationship with shear lag, shear rigidity, bending rigidity and had weak ties with other physical parameters. Therefore, the first factor is defined as fabric stiffness. The second factor had a strong relationship with tensile elasticity, weight per unit area and compression linearity, but had weak ties with other physical parameters, so the second factor is defined as the degree of smooth waxy. The third factor mainly contacted with recompressions resilient, compression work, the average deviation of the friction coefficient, was defined as the elasticity. The fourth factor mainly related to the fabric thickness, defined as fullness. The objective evaluation fabric style factor of wool knitted fabric was identified as Y1: stiffness, Y2: smooth waxy degrees, Y3: elasticity Y4: fullness.

According the basic style calculation formula, four directly calculated basic style values was obtained by calculating 12 wool knitted fabric samples. To facilitate the evaluation of the data file and analysis, the value of each basic style was divided into 1-5 five levels artificially. The basic style values was made linear interpolation transformation, and the mapping interval is (1,5). Through access to information, interpolation transformation formula as follow:

$$Yij' = 1 + (5-1)\frac{Yij - \min j}{\max j - \min j} \qquad (2)$$

Table5 Main component value of sample

No.	Calculated directly				Interpolation transform to the interval（1,5）			
	Y_1	Y_2	Y_3	Y_4	Y_1`	Y_2`	Y_3`	Y_4`
1	-16.7542	86.84783	43.73844	3.137654	1.39848	4.279397	3.346454	2.727952
2	-25.2996	92.1345	39.95975	3.141004	1.068549	5	2.074126	2.731825
3	-27.0751	87.28378	38.05093	3.395642	1	4.338819	1.431403	3.026151
4	-24.6006	80.86816	39.67478	4.395104	1.095539	3.464333	1.978172	4.18139
5	0.876765	76.14386	47.27388	1.642705	2.0792	3.954771	4.536879	1
6	-1.93978	74.13139	48.64931	2.496545	1.970455	4.397243	5	1.98692
7	-1.17416	68.9921	44.80711	5.103331	2.000015	2.857978	3.706287	5
8	-15.2203	71.26893	39.10067	2.465238	1.457704	3.539911	1.784861	1.950733
9	-11.4202	67.99138	43.92503	3.110179	1.604422	2.558252	3.409279	2.696195
10	-15.944	66.99717	41.06067	1.886615	1.429763	2.260475	2.444816	1.281926
11	-15.1932	62.7887	36.76971	1.857252	1.45875	1	1	1.247986

Evaluation of the basic style wool knitwear . In the result of factor analysis, Fabric stiffness had a strong correlation with 2HG5 shear lag(Φ=5°),shear rigidity, bending rigidity, their correlation coefficients were 0.958、0.984、0.871. With bending stiffness for horizontal, and fabric stiffness for vertical coordinates, the curve of the stiffness and bending stiffness was obtained, as shown in figure 1.

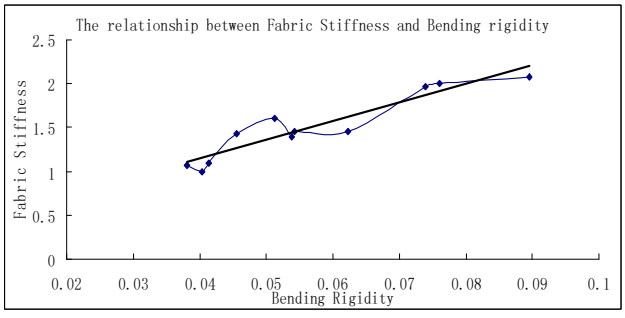


Figure 1 The relationship between Fabric stiffness and bending rigidity

As the figure 1 shows, the fabric stiffness was tender to larger with the increase of fabric bending rigidity. This result was consistent with the results of factor analysis, so that the fabric stiffness obtained by calculating was reasonable and effective. In the result of factor analysis, Fabric smooth waxy degree had a strong correlation with resilience tensile and fabric weight; their correlation coefficients were 0.930 and 0.984. With resilience tensile for horizontal, and fabric smooth waxy degree for vertical coordinates, the curve of the smooth waxy degree, resilience tensile was obtained, as shown in figure 2.

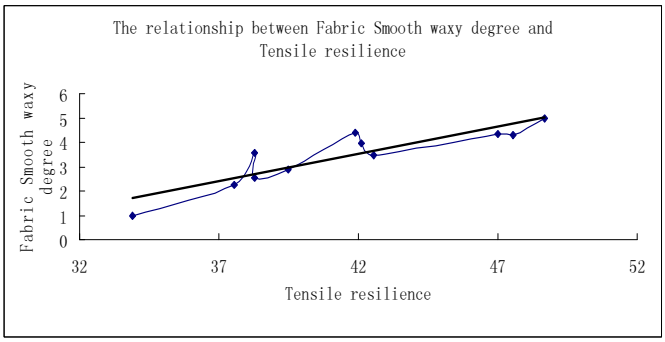


Figure2 The relationship between Fabric Smooth waxy degree and Tensile resilience

As the figure 2 shows, the Fabric smooth waxy degree was tender to larger with the increase of resilience tensile. This result was consistent with the results of factor analysis, so that the Fabric smooth waxy degree obtained by calculating was reasonable and effective.

Similarly, the relationship between the third factor (the fabric elasticity), the fourth factor (the fabric fullness) and the relevance physical index of each factor could well reflected the accuracy of the factor analysis results.

Conclusions

The 17 Mechanical and physical indicators of expressing the knitted wool fabric style can be made into four main factors by the main factor analysis method. They were stiffness, smooth waxy degrees, elasticity and fullness. The cumulative contribution rate of 4 factors was up to 91.492, which was represented a high level of information contained in fabric style. The purpose of factor analysis was achieved and greatly simplified the analysis of experimental data. The result can comprehensively and objectively expressed the basic fabric style, and made full use of mechanical and physical indicators that tested, which provides a theoretical reference between fabric mechanical properties and wool knitted fabric style research.

References:

[1] J Zhou and S Chen: the modern textile technology, (6):37-40. 2005
[2] Z Yuan and J Zhou. Science press, 2008.
[3] X Ni: tsinghua university press, 2010(3)
[4] J Sun, L Cheng, D Zhang: Tianjin Polytechnic University, (8):40-43. 2010
[5] H Qi and Y Shen: Modern Textile Technology, (4): 49-52. 2010

© (2011) Trans Tech Publications, Switzerland
doi:10.4028/www.scientific.net/AMR.331.61

Preparation of collagen/PVA composite fiber

Zhihui Sui[a], Yujiao Wei[b] and Xin Zhao[c]

School of Light Industry and Textile Engineering, Qiqihar University, Qiqihar 161006, China

[a]email: szh2736@163.com, [b]email: weiyujiao00000@126.com, [c]email: zhaox2738@sina.com

Keywords: collagen; polyvinyl alcohol; chrome shavings; grafting modification; composite fiber

Abstract. Alkali was used to extract collagen from chrome shavings. Grafting modification of collagen was carried out with acrylic ester as grafting monomers. The structure of the product was characterized using infrared spectroscopy. Spinning liquid was prepared with collagen and PVA(polyvinyl alcohol). Collagen /PVA composite fiber could be produced by wet spinning. The results showed that the optimal conditions of collagen grafting reaction were as follows: the dosage of modified monomers was 30% of collagen (mass fraction), the addition of emulsifier was 10% of butyl acrylate (mass fraction), reaction time was 2h and reaction temperature was 70℃. The collagen composite fiber had a strength of 3.65 cN/dtex and a elongation of 19%. The composite fiber had certain spinnability.

Introduction

China possesses the largest volume of production with leather-making and leather goods processing industry in the world and produces more than 300,000 t chrome shavings. Chrome shavings contain collagen at 90% above (mass fraction)as well as Cr_2O_3 at 3.5%~4.0%(mass fraction). At present, only a few chrome shavings are used to produce regenerated leather and animal protein feed which have a low value-added. And the rest of chrome shavings can only be disposed by burning and landfill, which not only cause tremendous waste of valuable resources (collagen and chromium)， but also pollute environment seriously (mainly chromium pollution). It is a effective way to resolve environmental pollution and to achieve high value conversion by the method which extracts collagen from chrome shavings then make full use of it[1]. Collagen may apply directly to produce fiber[2-3]. As a result of difficult spinning and poor fiber performance, the application of pure collagen spinning is restricted[4]. Collagen /PVA composite fiber belongs to regenerated fiber that could be produced by wet spinning with the mixed liquor of collagen which is extracted from peltry and vionl under certain conditions[5]. More and more people pay attention to this fiber which not only possess the characteristics of natural protein, but also owns excellent film forming and fiber forming performances[6-9].

Alkali (CaO) was used to extract collagen from chrome shavings in this paper. By using acrylic ester as monomer grafting and modifying collagen, their mixed ability and blended spinning ability were promoted and improved. The formation and performance of modified collagen and PVA composite fiber were reported.

Experimental

Main materials and Reagents. Chrome shavings, Qiqihar tannery; calcium oxide, AR, Jiangsu Menghe Chemical Reagent Factory; ammonium sulfate, AR, Tianjin Binhai Cody Chemical Reagent Co., Ltd; absolute ethylalcohol, AR, Tianjin Kaitong Chemical Reagent Co., Ltd; potassium persulfate, AR, Shanghai Aijian Reagent CO., Ltd; emulsifier OP, AR, Tianjin Quartz Clock Factory and Bazhou Chemical Branch; Butyl acrylate, AR, Tianjin Bodi Chemical Co., Ltd; lauryl sodium sulfate, CP, Tianjin Beichenfangzheng Reagent Factory; polyvinyl alcohol (PVA, 2099), industrial grade, Anhui Wanwei Upated High-Tech Material Industry Comany Limited.

Main instruments. PHS-3E acidity, Chengdu Ark Technology Development Company; HZS-H water bath oscillator, Harbin Donglian Electronic Technology Company; RG2000-10 universal sample unit, Shenzhen Ruiger Company; KXS-4 thermostatic waterbath, Shanghai Kexi Experimental Instrument Factory; BS223S electronic scales, Beijing Sartorius Instrument Systems Inc.; Spectrum One Fourier transform infrared spectrometer, PE Company; wet spinning device, home-made.

Method

The modification of collagen. Firstly, alkali (CaO) was used to extract collagen from chrome shavings, which could make the collagen extraction rate reach 70% above (mass fraction).

Secondly, the certain quality collagen which prepared by alkali treatment method was put into a 250mL beaker. Joined the amount of deionized water in the above beaker then heated it to dissolve collagen. Put certain quality carbamide into beaker in order to dissolve. Added some preparation emulsifier aqueous and stirred to mix well .Put the above blended solution into one 500mL round bottom flask. Then took this flask into the constant temperature water-bath pot which was heated. When the solution was heated to a certain level temperature, dropping acrylic ester monomers and initiator respectively. Kept the above intermixture reacting for a while. Then the product was cooled down and took out.

The infrared spectrometry of grafting collagen. The sample should be ground into powder. KBr presser was used to determine Fourier transform infrared spectrometer whose scanning range was beween 600 cm^{-1} and 4000 cm^{-1}.

Preparation of collagen composite fiber. Took PVA to deionized water and heated to dissolve it. Cooled to 60℃ after 3h. Put the solution of modified collagen into reactor. Stirring and keeping the temperature of 60℃ for 2h. The process ended with filtering, deaeration and spinning.

The test of mechanical performance of collagen composite fiber. Universal testing machine was used to test the mechanical properties of composite fiber under tensile speed for 100 mm/min.

Results and discussion

The effect of butyl acrylate monomer dosage on collagen grafting rate. Under certain conditions, such as the dosage of emulsifying agent, reaction temperature, reaction time and the dosage of initiator, the effect of the dosage of butyl acrylate monomer on collagen grafting rate is showed in Fig. 1.

Fig. 1 shows, the influence of the dosage of butyl acrylate monomer on collagen grafting rate is remarkable, with the increase of monomer, the grafting rate increases rapidly. This is because, under experimental conditions, collagen produces large amounts of free radicals grafted to the collagen molecules. However, the increase of monomer dosage will raise costs and produce a certain amount of homopolymer. When the dosage of butyl acrylate reaches 30%, the grafting rate can reach 20%.

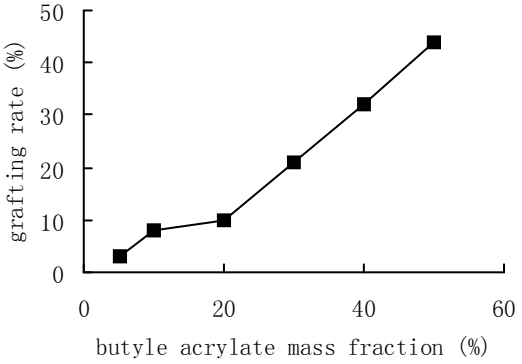


Fig. 1 The effect of butyl acrylate dosage on grafting rate

The effect of the dosage of emulsifier on collagen grafting rate. Under certain conditions, such as grafting monomer dosage, reaction temperature and reaction time, the effect of the dosage of emulsifier (accounted for butyl acrylate monomers of quality score) on collagen grafting rate is showed in Fig. 2.

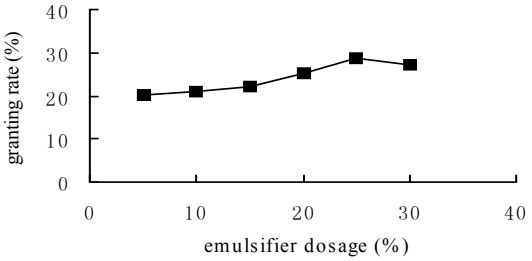


Fig. 2 The effect of the dosage of emulsifier on grafting rate

From Fig. 2, we can see, with the dosage of emulsifying agent increasing, the grafting rate increases slowly, then the last varying tend is gentle. This is due to the appearance of emulsifying agent, which forms micelle in solution, then wraps monomer up, which is beneficial for grafting reaction. But, with the dosage of emulsifying agent increasing, the micelle tends to saturation, the effect of the emulsifying agent dosage on the reaction starts to decrease. In addition, the increase of emulsifier dosage will significantly increase the production cost. This experiment do not just need high grafting rate, the effects of modification of collagen to benefit its spinning are the key aims. Comprehensive considerated, the optimal dosage of emulsifier is 10%.

The effect of reaction time on the collagen grafting rate. Under certain conditions, such as the dosage of grafting monomer and emulsifying agent and reaction temperature, the effect of reaction time on the collagen grafting rate is showed in Fig. 3.

Fig. 3 shows, with the extension of reaction time, grafting rate increases. But, when time is more than 2h, the increasing tendency of grafting rate starts to become slowly gradually. Because graft copolymerization reaction proceeds with the passage of time, when the reaction reachs a certain degree, with free radical gradual disappearence, reaction stops at last. After that, continuing reaction, the grafting rate is not remarkably increased. Therefore, the experiment chooses 2h as the optimum reaction time.

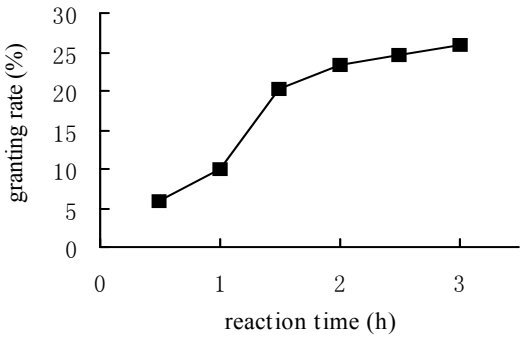


Fig. 3 The effect of reaction time on grafting rate

The effect of reaction temperature on collagen grafting rate. Under certain conditions, such as the dosage of grafting monomer, emulsifying agent and initiator, the effect of reaction time on the collagen grafting rate is showed in Fig. 4.

Fig. 4 shows, the grafting rate varies with reaction temperature rising up slowly, when temperature exceeds 65℃, the grafting rate ranges from 25% to 30%. The rise of temperature will improve the reaction rate and promote the initiator to convert into free radicals, eventually increase the grafting rate. However, higher temperature will not only require much more exacting terms for equipment, but also will consume more energy. Therefore, the optimum reaction temperature is 70℃.

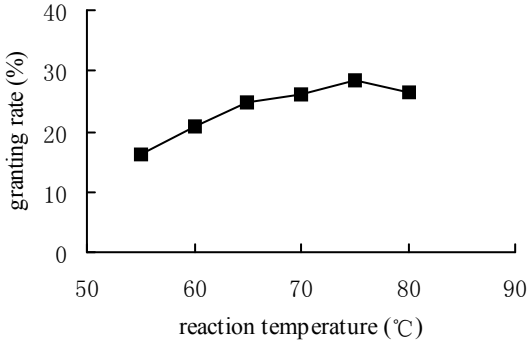


Fig. 4 The effect of reaction temperature on grafting rate

The infrared spectrum analysis for collagen grafting polymer. In order to determine the structure of collagen grafting polymer, the infrared spectrum analysis was conducted for collagen grafting polymer. The infrared spectrum analysis for butyl acrylate modifying collagen is showed in Fig. 5.

From Fig. 5, we can see that there is a strong absorption peaks of the product of butyl acrylate modifying collagen at 1737cm^{-1}, which is caused by ester group (C = O) stretching vibration; At 1163cm^{-1} and

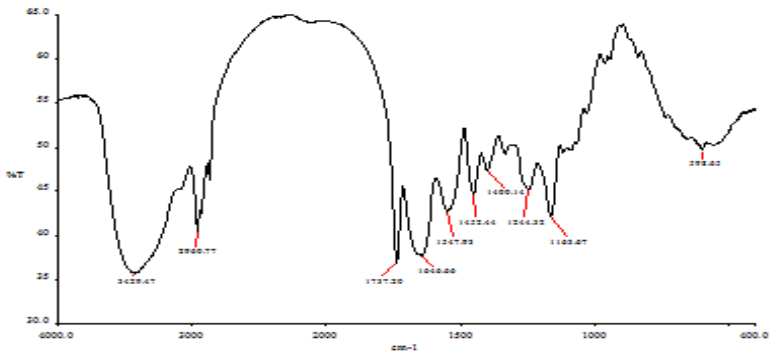


Fig. 5 FT-IR spectra of the product of butyl acrylate modifying collagen

1244cm^{-1}, there are respectively symmetric and antisymmetry telescopic vibration absorption peaks with moderate intensity characteristics for the group of C-O-C; Absorption peaks produced by antisymmetric stretching vibration of methyl and methylene group is at 2960 cm^{-1}. In brief , we can draw a conclusion that butyl acrylate has successfully grafted in the collagen molecules.

The mechanical performance for collagen/PVA composite fiber. According to the determination, the strength of collagen/PVA composite fiber prepared by this research reachs for 3.65 cN/dtex and the elongation of composite fiber at break is 19%.

Acknowledgment

The authors are supported by the Key Project of Chinese Ministy of Education (No 211052). We thank Chinese Ministy of Education for supporting this work.

Conclusions

Alkali was used to extract collagen from chrome shavings in this paper. Grafting reaction of collagen was carried out with acrylic ester as grafting monomers. To get the optimal conditions, the influence of various factors on collagen grafting reaction was investigated. The optimal process parameters were that, the dosage of modified monomers was 30% of collagen (mass fraction), the addition of emulsifier was 10% of butyl acrylate (mass fraction), reaction time was 2h and reaction temperature was 70℃.

Fourier transform infrared spectroscopy analysis proved that acrylic monomers successfully grafted in collagen molecules.

The collagen composite fiber prepared by the experiment had a strength of 3.65 cN/dtex and a elongation of 19%. And the composite fiber had certain spinnability.

References

[1] J. Cao, X.J. Chen and S. Zeng: China leather Vol. 32 (2003), p. 12

[2] K. Takaku, T. Kuriyama and I. Narisawa: Journal of Application Polymer Science Vol. 61(1996), p. 2437

[3] S. Hirane, M. Zhang and M. Nakagawa: Biomaterials Vol. 21 (2000), p. 997

[4] X.J. Wang, Y. Tang and W.Y. Wu: Journal of Textile Research Vol. 28 (2007), p. 13

[5] L.M. Yang, Y. Tang and W.Y.Chen: Leather Science and Engineering Vol. 17 (2007), p. 8

[6] L.M.Yang, Y. Li and X.Y. Zhang: Leather Science and Engineering Vol. 17 (2007), p. 31

[7] L.M. Yang, Y. Tang and W.Y.Chen: Leather Science and Engineering Vol. 16 (2006), p. 17

[8] L.R. Yao, H. Lin and Y.Y. Chen: Journal of Textile Research Vol. 27 (2006), p. 105

[9] Y.Z. Lin, L.M. Yang and W.Y. Chen: Leather Science and Engineering Vol. 16 (2006), p. 8

© (2011) Trans Tech Publications, Switzerland
doi:10.4028/www.scientific.net/AMR.331.65

Mechanical Properties of Ramie Fiber Woven Composites under Biaxial Tensile Loadings

Ge Wang[1,a],Fuming Chen*[1,b] , Haitao Cheng[1,c] , Zixuan Yu[1,d] , Zehui Jiang, Xiaomeng Chen[1,e] and Wenfu Zhang[1,f]

[1]International Center for Bamboo and Rattan, Beijing, 100102, China

[a]wangge@icbr.ac.cn, [b]chenfuming1985@126.com, [c]zd_cht@sina.com, [d]zixuan1118@126.com, [e]xiaomenglinxi@163.com, [f]zhangwenfu542697@163.com

Keywords: Ramie, Natural Fiber Fabric Composite, Biaxial tension, Digital Spackle Correlation Method, Strain Filed

Abstract. The objective of this work was to use a novel 3-D test analysis system for evaluating the mechanical properties of the natural fiber fabric composites under biaxial loads. Composites with three resin matrices (water-based epoxy resin, isocyanate resin, phenolic resin) were investigated, and strain-filed were characterized by using the digital speckle correlation. The water-based epoxy resin plate and isocyanate resin plate demonstrated a characteristic of orthotropy and elastoplasticity, while the phenolic resin board revealed linear elastic and brittle-fracture simultaneously at X,Y-axial. Dissimilarities of biaxial load value were related to the orthotropy of composite structure, and load changes in fracture direction had a negative effect on the other directions at breaking moment. The degrees of dropping presented a positive correlation with the load values at rift direction. Under the linear elastic stage, the value of load and average strain at Y-direction were larger than that under X-direction within the same testing area. The strain-filed at X/Y-direction provided by isocyanate and phenolic resin plates illustrated a more smooth change than that of the water-based epoxy resin plate.

Introduction

Natural fibers, offered a renewable resource and a lower cost feedstock, have been extensively used for composite manufacturing. In addition, the fibers' high specific strength and stiffness, damage tolerance, and eco-friendly characteristics make them desirable for utilization [1]. These composite products suffer from uniaxial stress in practical engineering applications, but they also develop biaxial or even multi-axial stress states, in many situations, such as wind or seismic effects [2, 3]. This brings about considerable difficulty to evaluate its mechanical properties objectively. Investigating and simulating the non-liner response characteristics of stress-strain due to the complex stress state and material anisotropy have became a key part for structural design successfully or not. Experimental techniques and different kinds of material cruciform-specimens have been used to produce biaxial stress states, such as soft textile composites, notched composite and sheet molding laminates as well as fiber reinforced laminates [4-9].

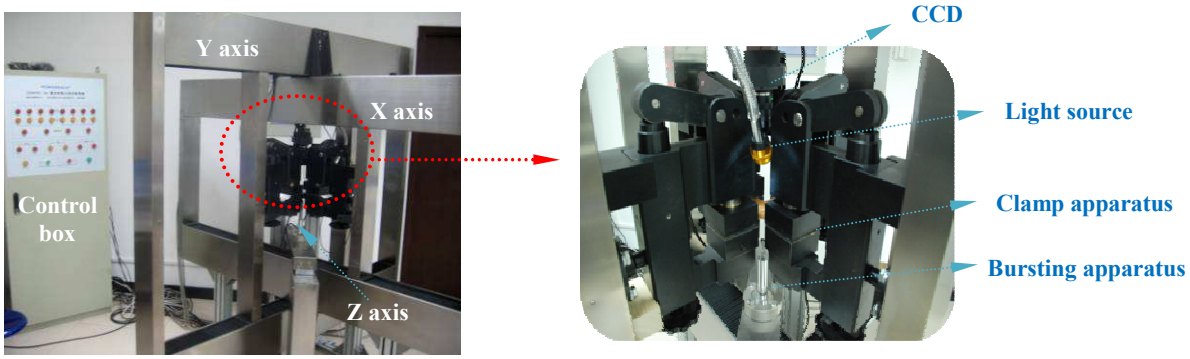


Fig. 1 3-D loading test device for composite material analysis system

In order to successfully model and simulate the behavior of materials for optimal use in structural applications, a novel testing device, the 3-D Composite Material Analysis System (Fig. 1) was developed at the International Center for Bamboo and Rattan (ICBR) in Beijing, China.The overall objective of this research was to investigate the mechanical properties of natural fiber woven composites based on three thermosetting resins under biaxial tensile loading. Meanwhile, the strain-fields were characterized by digital speckle correlation method (DSCM) during the stretching process.

Sample preparation

Balanced plain woven ramie fabrics were supplied by the company Hua Sheng. The basic parameters were: surface density- 244.8 g/m2, yarn linear density- 74.1 tex, thickness- 0.4 mm, warp density 184 roots/10 cm, and weft density- 137 roots/10 cm. Resin types: water-based epoxy resin (epoxide equivalent: 1,200-1,850g/eq), phenolic resin(Solids content: 47%) and isocyanate resin (supplied by Huntsman Corporation). Firstly, ramie woven is soaked in water-based epoxy resin, phenolic resin and isocyanate resin respectively. Then, putting them in an oven (65°,3-hours) can reserve for compressing composites. Molding technological conditions: hot-pressing pressure, time and temperature are 2MPa,5min and 120°,and paving way：$[(0/90)]_5$.

Equipment

The 3-D Composite Material Analysis System (Fig.1) can evaluate materials not only for tension or compression in the X and Y axial directions, but also bursting at the Z axis simultaneously.There are two sensors for measuring the forces in x, y direction and each direction has two clamps. Sensor accuracy is 1.0 N,maximum load value is 5.0 kN,and drawing speed is 0.013-1.066 mm/s. The system is equipped with Digital Speckle Correlation Method Analysis System software**(DSCM)**.

Biaxial Testing and Digital Speckle Correlation Methods

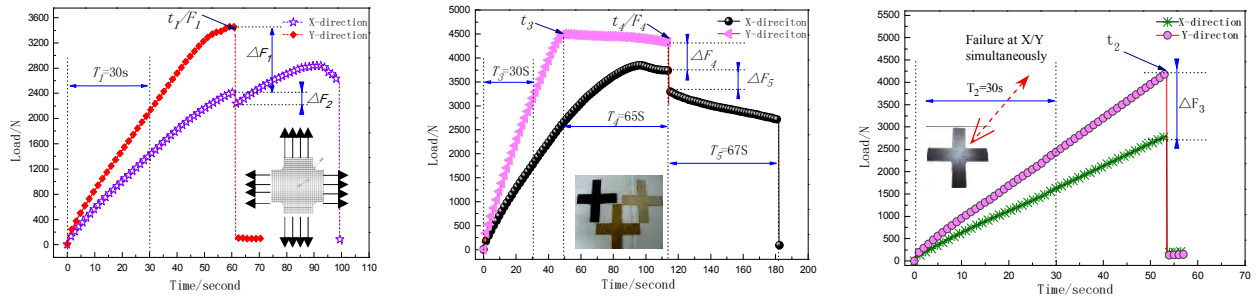
Fillet cruciform specimens were cut to shape with a laser to a total length of 300.0 mm with each arm measuring 50.0 mm wide. In order to form a uniform and randomly distributed speckle image, the surface of each cruciform specimen was sprayed with a layer of black glass bead paint layer for image enhancement. Biaxial tensile tests were conducted at stretching rates of 0.033 mm/s in each direction. The biaxial tensile test was conducted with the modulated speckle image captured by a high speed charge-coupled device (CCD) camera for description of the microscopic changes occurring on the surface. The pictures were saved in a file for analysis of the strain field. The observed speckle pattern included information on the object's surface height with the different degrees of gray reflecting the different stress-strain states of the specimens. The data were smoothed 3 pixels in both the X and Y directions. Ten samples were tested. The size of measured surface area of fabric was: 60 x 60 pixle, and the accuracy of measurement is about 0.01pixel theoretically.

Results and Discussion

Biaxial tension experiment.

Fig.2 illustrates: (1)mechanical properties at X-direction are different from Y-direction for all three types composites,namely X-direction fracture load value are smaller at than Y. This dissimilarity are linked with fiber volume fraction in X/Y-direction. Under the paving way of $[(0/90)]_5$, there are two warp-layers and three weft-layers in X-direction, while Y-direction has three warp-layers and two weft-layers. Warp yarns are fabricated to a higher density than those for weft（Y-direction）as yarns in the warp direction（X-direction）, resulting fiber volume fraction in X are less than Y-direction.

(2)Composites demonstrated variable characteristics of stress-strain behavior under biaxial tensile loads. Orthotropy and elastoplasticity were showed by water-based epoxy resin plate and isocyanate resin plate (Fig.2a,b), while phenolic resin board revealed a high-quality linear elastic in Load-Time curve and simultaneous brittle-fracture properties in X,Y-direction(Fig.2c) .



(a) (b) (c)

Fig.2 Time-load curves under biaxial loads for composites:（a）water-based epoxy resin plate; （b）isocyanate resin plate;（c）phenolic resin plate.

(3) Water-based epoxy resin composites'Y-directional failure occurred firstly at the moment of t_1, load difference value bet ween X and Y-direction was $\triangle F_1$=875.92N. As Y-direction load became disappearance suddenly, stress state transformed from biaxial loadings (both X and Y tensile) into a unaixal (only X-axial tension). The instant change of suffering loading way has a decreasing effect on the value of load in X-direction, and the X-load dropping value was $\triangle F_2$=210.12N(Fig.2a) .

Ahead of t_3, isocyanate resin plate showed a generally linear variation curve of load-time under biaxial tension. However, plastic deformation began at t_3 and formed necking down gradually after the moment of t_3,the lasting time was T_4=65S,the loading value reduced to F_4= 4322 N, $F_4 > F_1$. At the moment of t_4, Y-direction failure happened and load difference value between X and Y-direction was $\triangle F_4$=588.59 N,with $\triangle F_1 > \triangle F_4$; the X-load dropping value was $\triangle F_5$=309.48 N (Fig.2b) .

These analysis above indicates that the load instant variation at breaking-direction has a negative effect on the other directions' load values, and the dropping degrees were linked with breaking load as well as load difference value between X and Y-direction.

Strain-filed by DSCM. We can see in Fig .2 the curves of time-load represent a high quality linear during 0-30seconds in biaxial tensile process, so their linear variation stage are correctly selected for investigating information of strain-filed(Fig. 3) by using DSCM.

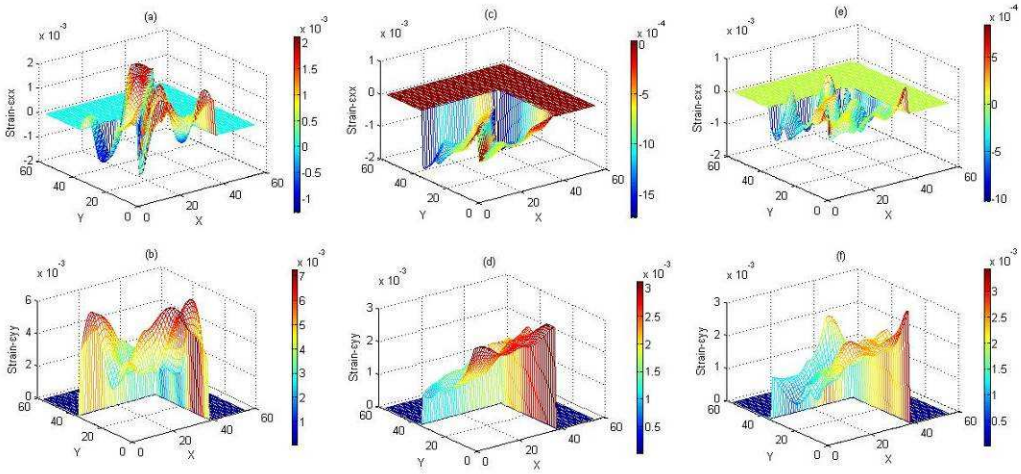


Fig. 3 Strain-fields for composites during 0-30seconds under biaxial tensile loads: a),b) for X ,Y-direction of water-based epoxy resin plate; c),d) for X ,Y- direction of isocyanate resin plate; e),f) for X and Y- direction of phenolic resin plate.

Values of field-strains revealed for Figure 3 shows: ε yy> ε xx ,and X,Y-directions' strain mean value of water-based epoxy resin plate, phenolic resin and isocyanate resin plate are respectively e_{xx}=0.67,-0.86,-0.15, and e_{yy}=4.42,2.08,1.82(unit-10-3) during T1,T2,T3.The loads for 0-30seconds are within the limit in the elastic proportion and the value of loads in Y-direction are larger than X-direction, therefore the strain in Y-direction are larger than X-direction for elastic modulus unchanged and the same testing cross sectional area.

Fig. 3a and 3b show that the values of water-based epoxy resin plate' strain has a larger fluctuating range with a distribution range of -1.38 to -2.03 in X-direction and 0 to 7.13 in Y-direction, while strain-filed for phenolic resin plate and isocyanate resin plate are comparatively gently, with a distribution range of -1.81～0.01 and 0～3.21 in X-direction, and -1.01～0.92,0～3.52 in Y-direction respectively,Figures 3c,d,e,f. Analysis of the strain-field accounted for characteristics of orthogonal anisotropy of water-based epoxy resin plate.

Results and Discussion

1) Under thebiaxial tensile loads, the mechanical behavior for the composites from three resin matrices have different properties. The water-based epoxy resin plate and isocyanate resin plate represented orthogonal anisotropy and elastoplasticity, while phenolic resin board revealed a high-quality linear elastic and simultaneous brittle-fracture properties at X,Y-direction. Instant load change at the breaking-direction had a negative effect on the other direction. The dropping degrees were positively related to breaking load as well as load difference value between X and Y-direction.

2) Within the limit in the elastic proportion of biaxial tension, the mean value of strain-field are larger in Y-direction than X because of material anisotropy. Variation of strain-filed for phenolic resin plate and isocyanate resin plate are moderately gently and smoothly, while water-based epoxy resin plate' strain fluctuation are comparatively large.

Acknowledgement

We are grateful to the National High Technology Research and Development Program of China (863 Program,2010AA101701) financially supporting this project, Dr. Sheldon Q.Shi kindly assisted with preparing this manuscript.

References

[1] X. Xu , K. Jayaraman, C. Morin, and N. Pecqueux: Journal of Materials Processing Technology. Vol. 198(2008), p.168

[2] H.Kong, A.P. Mouritz and R. Paton:J. Composite Structures. Vol.66(2004),p.249

[3] Y.X. Luo, H. Hu and R. Fangueiro: J. India Journal of Fiber & Textile Research. Vol. 33 (2008), p.146.

[4] Q.Virginio , C.Carola and P.Carlo: J. Composites Part A: Applied Science and Manufacturing. Vol.39 (2008), p.1331

[5] D.Bigaud , C.Szostkiewicz and P.Hamelin: J. Composite Structures. Vol. 62 (2003), p.129

[6] W. S. Arnold, M. D. Robb and I. H. Marshall: J. Composites. Vol.26(1995), p.739

[7] A. Smits, D.V. Hemelrijck, T.P. Philippidis, and A.Cardon: J. Composites Science and Technology. Vol.66(2006), p.964

[8] T. Foecke, M. A. Iadicola, A. Lin and S. W.Banovic : J. Metallurgical and Materials Transactions A. Vol.38(2007) , p.306

[9] D. E. Green , K. W. Neale , S. R. MacEwen , A. Makinde and R. Perrin: International Journal of Plasticity. Vol.20,(2004) , P.667

© (2011) Trans Tech Publications, Switzerland
doi:10.4028/www.scientific.net/AMR.331.69

Design and Research of the Foldable Decorative Screen with Ethnic Style Based on Weft-backed Structure

Aidan ZHANG [1, a], Xueqin WANG[2, b]

[1,2]Key Laboratory of Advanced Textile Materials and Manufacturing Technology of MOE，

Zhejiang Science and Technology University, Hangzhou, Zhejiang, China.

[a]zad.andan@163. COM, [b]WXQ780@163.COM

Keywords: decorative screen; double-faced jacquard; weft-backed structure; the ethnic brocade style; design.

Abstract On the basis of typical weft-backed structure, a double-faced jacquard fabric with specially ethnical and cultural brocade styles on both sides is produced. This fabric is supposed to be used for some Chinese foldable decorative screen. A crucial premise is to create an integrated pattern with transparent effect by superimposing two pieces of patterns for both sides of the fabric. In this case, two layers of wefts interweaving with a mono-layer warp can achieve the double-faced effect. The product will be a type of high-graded and Chinese-featured souvenir. Some significant design elements have been considered in detail, including the fabric appearance design, the fabric technical specification design, the weave design, and so on.

Introduction

Among the woven jacquard textiles, double-face fabrics usually adopt double-layered structures, on which the front and the back sides of the each fabric are two independent layers and become a full whole by using a stitching weave. With the application of the digital design and more advanced manufacturing techniques, the new design method provides some innovative opportunity for the double-faced jacquard fabric. The method in this paper can integrate processes of two independent designs for the double-face jacquard. Without any stitching weave structure, this approach can reduce the difficulty of textile weave designs. This type of design has improved the design of traditional weft-backed jacquard and broken through the confine that the figured double-face jacquard fabric must to be double-layer fabric structures.

Design Intention and Pattern Design

For a high-graded and featured souvenir that can be used as a decorative screen, the appearance of the produce which including the patterns and colors is very important, and the double-faced effect also should be considered as its essential character. The double-faced effect reflects the design trend of the jacquard fabric, because of a perfect aesthetic effect from the both ornamental sides.

The pattern designs for both sides of the product were inspired by ethnic brocades of Guangxi province in China. The whole patterns of both sides consist of three separate parts to meet the need that the decorative screen can be the folded. The main figures on the face side are the “chrysanthemum”, the Chinese characters ‘Shou’(means long live), and arch-shaped patterns. By contrast its background frame is rhombus, which composes the continuous pattern for four different directions. For the color design, black is the background color, and the color of other figures is blue, green, yellow and the mutual combination of the three colors, as shown in the Figure 1.

The back side pattern is neat and compact, but its sense of the level is rich. It also includes three separated parts for matching with the face side. The irregular shape is the active frame of the picture plane, in which figures of the plum blossom and the aniseed with different size were arranged, and the contrast of the dark and light colors help to highlight the intense form sentiment, as shown in the Figure 2.

All those objects and graphic elements of the minority brocade have been applied to make the fabric having the ethnic characteristics. Segmentation and reconstruction of the design elements has endowed the final design with the modern sense. Derived from the tradition but not constrained by tradition, the redesigned traditional figure elements have expressed the modern design ideas.



Fig.1 The front pattern of the fabric

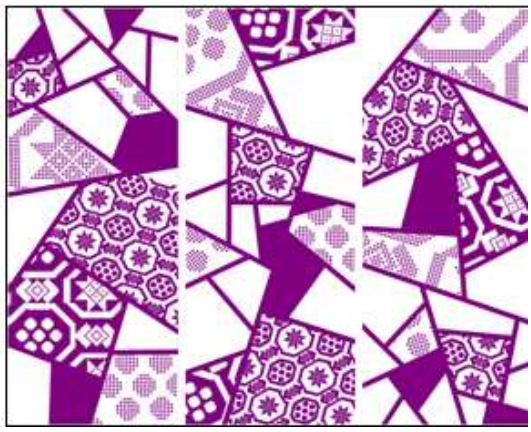


Fig.2 The back pattern of the fabric

Design Approach and Principle

Superimposing the face and the back patterns to become a piece of transparent picture is the essential premise of producing the double-faced jacquard fabric based on the weft-backed structure. All of figures should be unbroken, and none of them is be covered by others, as shown in the Figure 3. The structurally technical treatments will be carried out for the face and the back sides of the jacquard fabric in the synchronous step. The common process of the double-faced fabric weave design is to design the face and the back weave individually at first, and then to plan the ideal stitching weave according to the finished face and back weave. By this way, the weave structure design of the figured double-face jacquard fabric is completed finally. Relative to the general method, the new way in this article can integrate the two independent design programs for both sides respectively. In other words, the front and the back fabric have been treated as a whole at the same time.



Fig 3. Transparent figure of the front and back pattern（part）

The new weaves only consist of the face and the back weave, and there is no stitching weaves. Because of having just one set of warp in the new product, attentions need to be paid to the designs of both of the back weaves and the face weaves at exactly same time. Meanwhile, both patterns of the fabric should be seen at once. There are no any back weave points be laid barely, which should not be exposed when the front and back weaves are designed and coordinated, as shown in Fig.4. For example, the (a) and (b) are the weaves used for the face fabric, and (c) and (d) are the back weaves. There are four kinds of combinations of weft-backed structure, and the amount is the number of the front color multiplied by that of the back. The (e) is the combination of the (a) and (c); (f) is the combination of (b) and (c); (g) is the combination of the (a) and (d); and (o) is the combination of the (b) and (d).

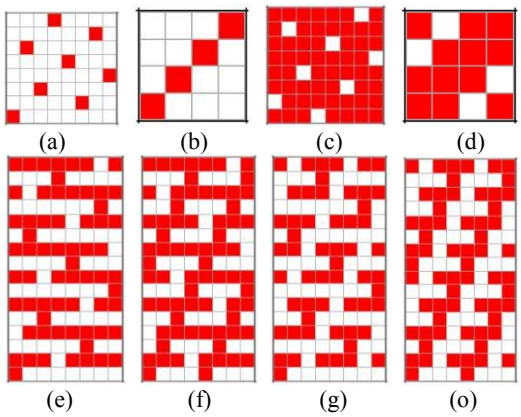


Fig 4. Design principle of weave structure for the double-faced jacquard fabric via weft-backed structures
(a) eight-end sateen weave; (b)1/3 twill weave; (c) eight-end satin weave; (d)3/1 twill weave

In the pattern design of the foldable decoratibe screen, the color amount of the face side is five, and he back side is two. According to the above design principle, there will be ten different kinds colors after being superimposed. This means there are ten diferrent kinds weave combinations for the related each color one by one.

Technical Specification and Weave Design

The warp density is 115 yarns per centimeters, that of the weft is 27 yarns per centimeters.The warp combination: [22.2/24.4dtex×1silk 8T/S×2]6.8T/Z . The weft combination: 133.3 dtex×1 bright rayon.The arrangement of the weft is A:B:C:D:E=1:1:1:1:1. The black, blue, yellow, rose red, and white are the colors of wefts. The cloth width is 208CM,and consist of two repeats of the pattern. Three parts are involved in this design, and their total length is 100CM, and each part is 40 CM widths. The spacing distance between each part is 5 CM.

This jacquard fabric is interwoven with five sets of wefts and single set of warp. The warp interweaves with the A, B, and C wefts, and produces the face patterns. Colors are developed by not only the each of the three wefts, but also combinations of any two of them for the abundant effect of the figure on the fabric. The back side of the fabric is produced by the same warp and the D and F wefts. For the back face, there are two kinds of colors that produced respectively by each of the two wefts. All wefts that are not shown on the face of back surface should be hided between the other wefts.

The basic weave of the fabric is twenty-four ends, and five of them are used in the fabric totally, as shown in the figure 5. Among them, (a), (b) and (e) are three kinds of surface weaves for the face of the jacquard fabric, while (b) and (d) are two surface weaves for the back side.

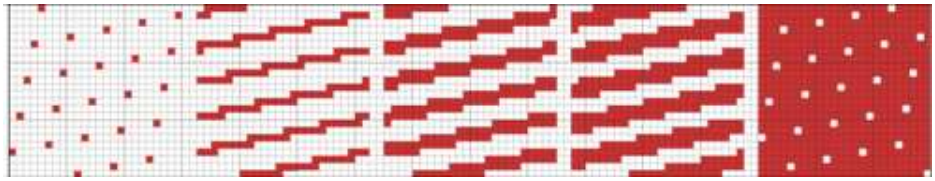


Fig. 5 The basic weaves

For the perfect decorative effects, the weave of two sides are the same type. Namely the face weaves are twenty-four ends satin, and the back one is twenty-four ends satin too. In this way, we could ensure the absolutely match of the weaves for the both sides, and the weave points could be evenly spread. It also can be understood that the relation of the weave cycle numbers for both sides are multiple. The initial point should be at the same place in order to maintain the texture and the color are same. The real fabric effect of the face and the back is shown in Figure 6. The double-faced jacquard fabric with ethnic brocade style has not only special appearance but also original internal weave structures.

Conclusion

The treatments of superimposing the face and the back patterns is the essential premise of producing the double face jacquard fabric based on the double-layer fabric structure. Only when the face and the back patterns are seen at the same time, all figures should be unbroken, and none of them is covered by others. In this way both sides can be considered synchronously.



Fig 6. The effect of the real product

Regarding to the perfect decorative effects, the weaves of two sides are the same type. Because the face weave is 24-ends sateen, the best choice for the back one is 24-end satin too. In this way, we could ensure the absolutely match of the weaves for the both sides, and the weave points could be spreaded evenly. It also can be applied that the relation of the weave numbers for both sides are multiple. In this case, the initial point of weaves should be at the same place in order to maintain the textures and the colors are unified.

Designing and developing the double-faced jacquard fabric with the ethnic brocade style needs not only the equipment and technique conditions but also the outstanding design of the patterns and the material combination designs of the warp and weft. In terms of decorative pattern, it expresses specific style of ethnic and cultural brocade, and that echos with the development trends of cultural recreation and interaction in the current world. Moreover, it reflectes the design innovation of the double-faced jacquard fabric on the woven structure, which breakes the limitation that the double-faced jacquard fabric must be double-layered structure.

Acknowledgements

This work was financially supported by the Key Lab of Advanced Textile Materials and Manufacturing Technology of MOE, Zhe Jiang Sci-tech University （2010QN08）.

References

[1] Jiu ZHOU, Frankie NG: Journal of Dong Hua University (Natural Science) Vol.34-1(2008), p44-47.

[2] Jiu ZHOU, Frankie NG: Journal of Textile Research Vol. 28-5 (2007), p 47-50.

[3] Lingxiang CAO, Zimin JIN, Liyu MA: Silk Monthly, 4(2008), p 10-12.

[4] Rong HAN, Senlin ZHANG: Journal of Textile Research, 8（2006), p 90.

[5] Gan SHEN: Modern Textile Technology Vol. 12-5(2004), p 41-42.

[6] Chunjun LIU, China. Patent 200,920,123,149 (2010).

[7] Zimin JIN, Xinglong RU, Liyu MA etc., China. Patent 200,810,162,430 (2009).

© (2011) Trans Tech Publications, Switzerland
doi:10.4028/www.scientific.net/AMR.331.73

The development and status of the stab-resistant body armor

Zhizhong Ding[1,2] Yueqing Zhang[1] Xiaoming Qian[1*]

[1]School of textile, Tianjin Polytechnic University, Tianjin, 300160, China

[2]Key Laboratory of Advanced Textile Composites, Ministry of Education of China, Tianjin 300160, China

[1*]Corresponding Author: qianxiaoming@tjpu.edu.cn

Keywords: body armor, stab-resistant, high performance fiber, status

Abstract. This paper summarized the state of the stab-resistant body armor, and summed up the main developing trends and important study ports of the area. Then, we discussed the frequently-used fibers, structures, performance tests and numerical simulation. Predictably, the future trends of the stab-resistant body armor is the balance of functionality and comfort

Introduction

As is known to all, even in times of peace, terrorism and violence sometimes appear in the world. In some countries, dagger and knife become the main threats people faced as guns under strict controls. It is against this backdrop that stab-resistant body armor gets rapid development in many military and civilian areas. Today, stab-resistant products have entered into the standardized stage. Stab resistant body armor is now a standard item of equipments for police officers in the United Kingdom, and it is usually required to PSDB standard [1].

The concept of stab-resistant body armor is simple. First, it should prevent weapons penetrating the protective layer and reaching a wearer's body. Second, it should spread or expend the most energy of weapon to reduce the damage.

According to the hardness, stab-resistant body armor can be classified as hard, half hard and soft. The stab-resistant layer is usually composed of lapped high-performance fiber fabrics or flexible unidirectional composite materials. Relative to hard and half hard armor, soft one can daily wear because of good flexibility and high concealment performance.

Research status

Although metal body armor has good stab-resistant ability, heaviness and inflexibility limits its use. Besides the stab-resistant ability and wearability, high performance fibers like aramid and ultra-high molecular weight polyethylene fiber (UHMMPE) with its excellent shearing capacity and breaking strength become legitimate contenders of body armor materials.

At present, great progress has been made in studying of stab resistant body armor at home and abroad. The stab resistant fiber Kevlar® Correctional™, which invented by Du Pont Company, can be closely intertwined. When encountered suddenly strong energy, the fiber can consume and absorb energy to prevent the separation. In addition, it has the advantage of light weight, flexibility and strong occult. Stab vest made by this fiber past all the levels of NIJ0115.00 standard in America. Warwick Mills company produced TurtleSkin MFA material which combines high-performance fiber textiles and metal stab resistant panel with thickness of 3.5mm. The textile component makes it comfortable for daily use. The hard armor component provides the required puncture protection. TurtleSkin MFA material achieves outstanding protection against knives, spikes, and hypodermic needles. TurtleSkin MFA material is shown in Fig. 1. Criminology company in America applies for a patent of light-weight knitted stab vest [2].This vest knitted by aramid or high-strength glass fiber, and all layers are sticking or thermal bonding together. It has very good stab resistant effect.

In home, there are also some enterprises researching the stab-resistant body armor like BEIJING JUNANTAI company, Chongqing King Shield company etc. JUNANTAI company developed soft stab-resistant vest with chopped aramid and UHMWPE fibers, which blocks cutting and stabbing

attack effectively. The vest, 0.3square meters of protection area, is only 1.15 kilograms. Semi-rigid stab-resistant vest, made by Chongqing King Shield company, consists of various new techniques. It can effectively block the invasion of general explosives and fragments. Meanwhile it provided good resistance to water, acids, alkalis. This kind of products is very suitable for court polices, financial outlets defends, enterprises cashiers.

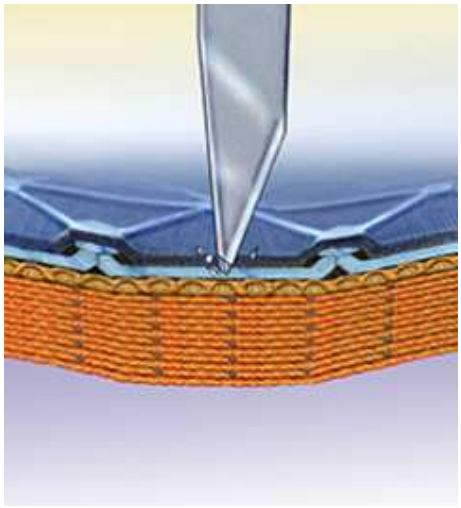


Fig.1 TurtleSkin MFA material

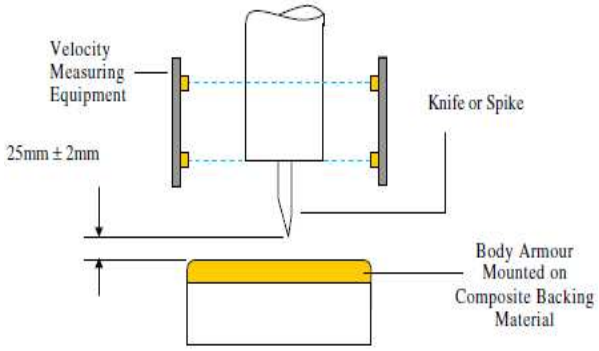


Fig.2 Test Apparatus for Knife and Spike Testing

Research Fields

High performance fibers. As one of the body armor materials, the fiber of the fabric should have high properties of strength, modulus, impact resistance. The common fibers which are used extensively for the armor products are aramids, ultrahigh molecular weight polyethylene (UHMWPE) and polybenzoxazole (PBO), ceramic fiber and carbon fiber etc. PBO yarns have been discontinued in body armors since 2005 because of degrading by hydrolysis in humid conditions. Unlike other fibers, PBO is unsuitable to be exposed to warm and moist environment [3]. The properties of the main fiber types used in personal body armor are summarized in Table 1.

Table 1. Comparison of fiber properties

	Tenacity		Modulus		Breaking	Density	Moisture		Heat
	cN/dtex	GPa	cN/dtex	GPa	extension%	g/cm³	regain%	LOI	resistance℃
PBO(Zylon®)	37	5.8	1150	180	3.5	1.54	2.0	68	650
UHMWPE (Spectra®/ Dyneema®)	35	3.5	1300	110	3.5	0.97	0	16.5	150
Aramid (Kevla®)	19	2.8	850	109	2.4	1.44	4.5	29	550

Shear thickening fluid (STF). The U.S. Army Research Laboratory is developing a new material called STF to make the body armor more light and flexible. Shear thickening fluid (STF), which is a non-Newtonian flow behavior, composes of hard particles suspended in a liquid. It is observed as an increase in viscosity with increasing shear rate or applied stress [4].

In the ordinary conditions, STF is a flowable and deformable material. It turns into a rigid material suddenly once a strong impact was applied to the STF. The reason is that the formation and percolation of shear induced transient aggregates dramatically increase the viscosity of the fluid [5,6,7]. When the force of impact disappears, the impact point restores to liquid state, and the materials become soft again. This tells us the transition exhibits reversible process.

The main method of enhancing the stab-resistant ability of the fabric is impregnation with a colloidal shear thickening fluid. STFs were generated by dispersing colloidal silica particles in polyethylene glycol at a volume fraction of approximately. M.J. Decker et al. [8] dispersed colloidal silica particles (average diameter 450nm) in 200 Mw polyethylene glycol(volume fraction 52%)to get STF. The comparison test shows that STF–Kevlar fabric (treated by STF) exhibits significantly better stab resistance as compared with the common Kevlar target. For the spike impactor, Kevlar target penetrates five layers, at an energy of only 4 J. In contrast, STF–Kevlar target only penetrates through three layers even at the highest energy level of 17 J. Furthermore, the spike impactor was plastically bent then.

Structures. In order to achieve excellent stab-resistant ability, structures and aggregations of fiber must be considered. The body armor structures contain woven, knitted, UD ,non-woven fabric and so on. To enhance the stab proof ability, stab-resistant layer always lined with high-performance fiber woven fabric.

Zhaowen Gu [9] analysis stab proof ability of different structures of UHMWPE by defining quasi-static stab-resistant performance as the ratio of quasi-static maximum force and areal density. The experimental results demonstrate that plain weave fabric is better than UD, and nonwoven fabric is worst of all. However, Zhongjia Yang[10]tests the stabbing ability dynamically, the result shows that there is little difference to protection effect of knives with three edges between UHMWPE plain weave fabric and nonwoven fabric. And a bigger difference of single-edged knife, nonwoven fabric is better, whereas to spike, nonwoven fabric's advantage is obviously. The main reason is that plain weave consists of filament bundles, which have better shearing. Bur the friction coefficient between fiber bundles is small which leads to exclusion resistance weak. In contrast, nonwoven fabric has a balance of shearing and exclusion, the entanglement of chopped yarn improves the resistance to exclude. Tuba Alpyildiz et al. [11] developed the double-sided knitting structure which has a very good stab resistance through introducing the mosaic yarn.

Test methods. The tests of stab resistance have entered the standardized stage. Criteria required by the HOSDB of UK and Standard 0115.000 set up by NIJ of America are authoritative. These standards set rules for test equipment, testing tool, backing materials, etc. In HOSDB (2007), the test shall be performed using the guided rail drop tube assembly, which will enable the knife/spike missile to fall under the influence of gravity and strike the armor sample at a pre-determined point of impact. The engineered test implements used in this standard are P1/B for the knife and SP/B for the spike [12].The typical test apparatus for knife and spike testing is shown in Fig.2.

As people understand the mechanism of stabbing further, present standards have some disadvantages to give a more realistic picture of stab attack. In order to make the experiments more accurate, some researchers develop new test methods. C A Walker et al. [13] consider that HOSDB standard still exists some obvious flaws, and detailed characterization of real human stabbing actions is needed. They developed a multi-component dynamic system, which reflects the dynamic constitution of the attacking person and the knife. It is a basis for designing of new, lightweight armor.

In addition, the comfort tests of body armor also are indispensable. The two main aspects are hot-wet comfort and flexibility. I. Horsfall et al. [14] developed a mechanical flexibility test which was used to assess multi layer body armor systems. The results show that the flexibility ranking from test machine concurs with the subjective assessments.

Numerical simulation. Due to the complexity of stabbing process, analytical approaches cannot be directly used and one has to resort to numerical simulation models.

Zhaowen Gu [15] simulates fabric impact test under dynamic and quasi-static applying FEA (Finite element analysis). The result shows that shear failure and tensile failure of fiber occur meanwhile when knife penetrates the body armor. Shearing plays the leading role in this process. Yves Termonia [16] developed a model for the study of the factors against needle puncture. It describes the resistance of fiber structures under large projectile impact. Four different stages were revealed: (1) contact pressure of the tip of the needle increase (2) slippage of the tip resulting in puncture (3) friction of the fabric against the needle (4) the tip slippage through the fabric.

Conclusions

With the fast development of stab-resistant body armor, the research on stab proof materials attracts more attention these years. Soft stab resistant material has good performances, and wears comfortable, flexible, undoubtedly, it is the key point in this field. Liquid body armor becomes the new study hot with STF developed. In addition, comfort is indispensable besides stab resistant to body armor. The balance of functionality and comfort directly affects its market promotion. Meanwhile, although stab proof and bulletproof standards are independent at home and abroad, it will be a trend to develop the soft materials which combine two excellences.

References

[1] Ian Horsfall, Celia Watson, Steve Champion, Philip Prosser, Trevor Ringrose: J. Applied Ergonomics.Vol. 36 (2005), p. 505

[2] Goerz D J Jr, Smith H R Jr, Miguel-Bettencourt K C, U.S. Patent 5,472,769(1995)

[3] K. Kanchi Govarthanam, S. C. Anand, S. Rajendran: J. Journal of Industrial Textiles. Vol. 40, (2010), p.145

[4] Tae Jin Kang, Kyung Hwa Hong, and Mi Ran Yoo: J. Fibers and Polymers. Vol. 11(2010), p.719

[5] Bender JW, Wagner NJ: J.Colloid Interf Sci. Vol. 172(1995), p.171

[6] Maranzano BJ, Wagner NJ: J. Chem Phys . Vol. 117(2002),p.10291

[7] Catherall AA, Melrose JR, Ball RC: J. Rheol . Vol.44(2000),p.1

[8] M.J. Decker, C.J. Halbach, C.H.Nam, N.J.Wagner, E.D.Wetzel: J. Composites Science and Technology. Vol. 67(2007), p.565

[9] Zhaowen Gu: J. Journal of Textile Research. Vol. 27(2006), p.83.

[10] Zhongjia Yang: J. COMPOSITES . Vol. 1(2010), p.43

[11] Tuba Alpyildiz, Maryline Rochery, Arif Kurbak and Xavier Flambard: J. Textile Research Journal. Vol. 81(2011), p.214

[12] John Croft, Daniel Longhurst, 2007. HOSDB Body Armour Standards for UK Police (2007), Part 3: Knife and Spike Resistance Publication No. 39/07/C

[13] C A Walker, T G F Gray, A C Nicol, E K J Chadwick: Proc. Instn Mech. Engrs. Vol. 218 Part L: Journal of Materials Design and Applications

[14] I. Horsfall, S.M. Champion, C.H. Watson: J. Applied Ergonomics. Vol. 36 (2005), p.283

[15] Zhaowen Gu: J. Journal of Textile Research. Vol. 27(2006), p.82

[16] Yves Termonia: J. International Journal of Impact Engineering. Vol. 32 (2006), p.1520

© (2011) Trans Tech Publications, Switzerland
doi:10.4028/www.scientific.net/AMR.331.77

Research on the Clustering Color Separation of Fabric Based on Genetic-Fuzzy Algorithm

Bingjin luo[1,a]

[1] Zhejiang textile-fashion college, 495#Fenghua road, Ningbo,zhejiang province, 315211, China

[a]luobing191210@sina.com

Keywords: Color separation, Clustering analysis, Genetic-Fuzzy Algorithm,Fabric

Abstract. An improved fabric color separation method is put forward based on genetic fuzzy clustering algorithm.At first, adopt six basic primary colors are used to carry on color separation to images of fabric including C(blue), M(magenta), Y(yellow), G(green), K(black) and W(white),and the data set of fuzzy cluster is formed , consequently, the division of fuzzy cluster can be completed, at last Genetic-fuzzy cluster algorithm is applied to color separation of decorated Jacquard fabric. The experimental results show that the fidelity of fabric patterns after color separation using this improved method is superior to that after color separation using traditional color separation method.

Introduction

The color separation technology of fabric is one of key technologies of digital textile design, the quality of color separation will affect the decoration of surface of fabric directly. The colors and layers of patterns decorating the fabric are formed by the organizational structures of fabric and mutual cooperation of warp and weft yarn; the color number of decorated Jacquard fabric after being separated must accord with the organizational and technical requirements of fabric.

The traditional color separation methods include autonomic color separation of fabric CAD, color separation with self-selected primary colors, and color separation combining special colors based on primary colors. We improved the method based on traditional color separation methods and applied the clustering analysis method to deal with image by color separation, then used K-means clustering algorithm, chose initial representative points by applying the method of combing the largest frequency with the smallest distance in cluster; divided pixel color space, and selected the center color according to the frequency in each sub-space, then set the threshold by using the distance of chromatic difference and frequency of each sub-space to guarantee the reserved color total [1],In the clustering analysis, determining the threshold is the key of color separation, while after the threshold has been determined, we can carry on the comparison between threshold and pixel value, and division of pixel by each pixel in parallel, the result of division can be embodied in the area of image directly.Comparing with traditional autonomic color separation method, the clustering color separation method can obtain satisfied quantized effect, and make the distortion between the real thing and image very small, so this kind of color separation method can get better effect to enable fabric to keep the style of manuscript.

However, this color separation method based on clustering analysis is very sensitive to the selection of initial cluster center, especially, the color separation effect of image with uneven color distribution is still not perfect, and the result of cluster and the efficiency of algorithm are closely related to the selection of initial conditions; when carry on color separation to image, the contradiction between whole layers and local detail hasn't been solved well, because the cluster algorithm often regard the smallest distance as cluster rule, and analogous colors will be

consolidated and lost the color layers of image, if keep the rich color layers of image, then some important details in the image will be lost; on the contrary, if the details of image are kept completely, then the color layers of whole image will be lost [2].

The applications of genetic algorithm

The genetic algorithm is a global optimization search method using natural selection of biology and natural genetic mechanism for reference, takes all individuals in a group as objects, and searches a coded parameter space efficiently with random technology instruction. Here, the genetic operation of genetic algorithm is consisted of selection, crossing and variation; the core of genetic algorithm is consisted of parameter coding, setting of initial group, fitness function design, genetic operation design and setting of control parameters. The genetic algorithm is an efficient and parallel global search method to solve the problem in natural, and introducing it into multi-threshold color separation processing of image will reduce the calculation time.

When we carry on color separation to image with genetic algorithm, the pixels with similar attribution are dealt with fuzzy clustering, and then demarcated according to their species; consequently, the image segmentation will be realized. We consider the pixel points of image as sample points of data set,and the characteristics of pixel point namely gray for gray image as those of sample points, and then the segmentation of image is converted to optimization of data set function[3]. Then, we search the optimized clustering center globally with genetic algorithm and carry on optimization search calculation; this will avoid the problem of falling into local optimal solution resulting from directly using clustering algorithm effectively.

Selection of color model

People divide all colors into four basic primary color weights including C, M, Y, K by four-color separation method in the colored printing industry, and all kinds of colors can be formed by the overlay of these four weights.

The colors and pattern outlines of fabric are formed by colors of warp and weft yarn and blending of fabric, in the color separation of fabric, in order to make the pattern edge of fabric with many colors and patterns such as colorful images to have clear outline and colors with rich layers, we adopt six basic primary colors to carry on color separation to images of fabric including C(blue), M(magenta), Y(yellow), G(green), K(black) and W(white); then there are two kinds of assemblies of warp and weft yarn, the first is warp assembly: M, Y, C, G, K (or W), and weft assembly: K and W form warp jacquard of multi-color warp backed weave; the second is weft assembly: W(or K), and weft assembly: C, M Y and K form multiply weft jacquard of multi-color weft[4].

If we adopt the second method, choose W and K as warp yarn, these two kinds of yarn will show the shading color of whole fabric on the surface of fabric; choose yarns with four kinds of colors including C, M, Y and K as weft yarn, enable this two quadruple weft yarn to present different floats. The result of four color separation is four gray images in nature, if we deal with warp and weft yarn of each layer respectively, we will obtain organization maps of C, M, Y and K separately.

Classification of fuzzy clustering data set

Setting the data set $X = \{X_1, X_2 \ldots X_K \quad \ldots X_n\} \subset R$ is a finitely data set of clustering analysis with n samples, and each object x_K of X can be described with finitely parameters, and each parameter will describe certain feature of x_K, and the division C ($2 \leq C < n$) of X will be produced according to the close or distant relationship between samples, Dividing data set X will obtain C subset X_1, $X_2 \ldots X_K \ldots X_C$, if they meet following conditions, they can be called hard C division of X set[5].

$X_1 \cup X_2 \cup X_K \cup X_C = X$ （1）

$X_I \cap X_J = \varphi$， $1 \le I \ne J \le C$ （2）

$X_J = \varphi$， $X_I \ne X$， $1 \le I \le C$ （3）

If U_i represents membership function, then we define membership function as formulation (4).

$$u_i = \frac{\sum_{k=1}^{n} [u_i(x_k)]^b x_i}{\sum_{k=1}^{n} [v_i(x_k)]^b} \quad (4)$$

U_i represents that samples X_K（$1 \le k \le n$） belong to X_i（$1 \le i \le c$）, namely U_i is characteristic function of subset X_j, and $U_i \in \{0, 1\}$. When they converge according to the algorithm in formulation (4), we can get the membership degree of clustering center to each category, and that of each sample to each category.

The object function of clustering algorithm can be defined as formulation (5):

$$J(v,u) = \sum_{i=1}^{c} \sum_{k=1}^{n} [v_i(x_k)]^b \| x_k - u_i \|^2 \quad (5)$$

In the formulation (5), C represents the number of categories; b>1 is a constant that can control the fuzzy degree of results of clustering; x_k is P dimension vector; u_i is the cluster center of i category; $v_i(x_k)$ is the membership function of K sample to I category.

Bezdek proposed the necessary condition of optimizing object function as followed:

$$u_{ik} = \frac{(1/d_{ik})^{1/(m-1)}}{\sum_{j=1}^{c} (1/d_{jk})^{1/(m-1)}} \quad (6)$$

$$v_i = \frac{\sum_{k=1}^{n} (u_{ik})^m x^k}{\sum_{k=1}^{n} (u_{ik})^m} \qquad d_{ik} = \| x^k - v^i \| \quad (7)$$

So the membership function can be calculated with formulation (6), and then cluster center of each category can be calculated with formulation (7), when the algorithm is convergent, the cluster center of each category and membership function of each sample to each category can be obtained, and consequently, the division of fuzzy cluster can be completed.

Application of genetic-fuzzy cluster algorithm

In the genetic algorithm, variation ratio P_m and crossing rate P_c will affect the performance of genetic algorithm greatly, and they need many experiments to determine aiming at different optimizing objects. Here, we adopt a kind of adaptation method P_c and Pm, and measure the convergence of algorithm with fitness function， the expressions are formulation (8) and (9), here, f_{max} is the largest fitness value in group; fmin is the smallest fitness value; fa is average fitness value of each generation group; f_c is the bigger fitness value of two individuals that will be crossed; f is the fitness value of individual that will vary; $(f_{max} - f_a)$show the convergence degree of group[5] [6].

While the variation rate should be adjusted properly according to the evolution process, we determine the initial variation rate is 0.103, and the adjusting strategy is that when (f_{max} - f_{min}) /f_{max}≤20%, the variation rate is changed to 0.1045, and the termination condition is (f_{max}-f_{min}) /f_{max}≤8%.

$$p_m = \begin{cases} \dfrac{(f_{max} - f)^2}{(f_{max} - f_{min})(f_{max} - f_a)}, & f \geq f_a \\ \dfrac{f_{max} - f}{f_{max} - f_{min}}, & f < f_a \end{cases} \qquad p_c = \begin{cases} \dfrac{(f_{max} - f)^2}{(f_{max} - f_{min})(f_{max} - f_a)}, & f \geq f_a \\ \dfrac{f_{max} - f}{f_{max} - f_{min}}, & f < f_a \end{cases} \tag{8}$$

The process of genetic algorithm used in cluster algorithm is shown as followed:

(1) Input the R, G and B value of each pixel of scanning image, utilize the human-computer interaction to determine the standard value of four color CMYK and the number of cluster n, consequently, establish the data set of fuzzy cluster X =$\{ x_1, x_2, \cdots x_K \cdots x_n \}$, and carry on hard C division to data set X, and utilize formulation (4) to produce membership degree function U_i.

(2) Optimize object function with formulation (5), (6) and (7), calculate the membership degree of each pixel in color image; classify the pixel points according to the rule of maximum membership degree. (3) Initialize group: produce initial group containing P individuals by the method of random, and set the genetic generation as GEN=0. Each individual represents the center of each category of n categories$\{ u_1 \ u_2 \ ... \ u_v \}$; u_v is P dimension vector.

(4) Crossing: set the crossing probability as Pc, and for each individual, we produce a random m that is from 0 to 1, if m<Pc, then carry on crossing operation. Randomly select an individual in P, and produce an integer j from 1 to n, and carry on crossing operation at the position of j according to following method, and that is center exchange of j category namely[7]:

$\{ u_1 \ u_2 \ ... \ u_v \} \rightarrow \{ u_1 \ u_2 \ ... \ u_j \ u_{j+1} \ ... u_v \}$

(5) Variation: setting the variation probability as Pm, and carry on variation operation to u_j for each selected individual at any randomly selected position j of$\{ u_1 \ u_2 \cdots \ u_v \}$; and produced a new u_j randomly.

(6) Calculate the fitness value

The fitness degree H of individual can be calculated by formulation H=$\dfrac{1}{1+J(v,u)}$, compare the new individuals produced from crossing and variation with individuals in the group, and the individuals with bigger fitness value will be selected and enter into group.

(7) Produce next generation group according to the strategies of selection, crossing and variation. GEN = GEN + 1, calculate (f_{max} - f_{min})/f_{max}, if it don't meet the termination condition of algorithm, then return to (2) and continue to iterate; otherwise, the algorithm end.

Namely, after initializing group, apply genetic algorithm to each individual of group to enable it to converge to local optimization, then carry on crossing and variation operation; in addition, new individuals produced by crossing and variation operation of each generation in genetic algorithm can converge to local optimization before it is added into group. That is shown in figure 1.

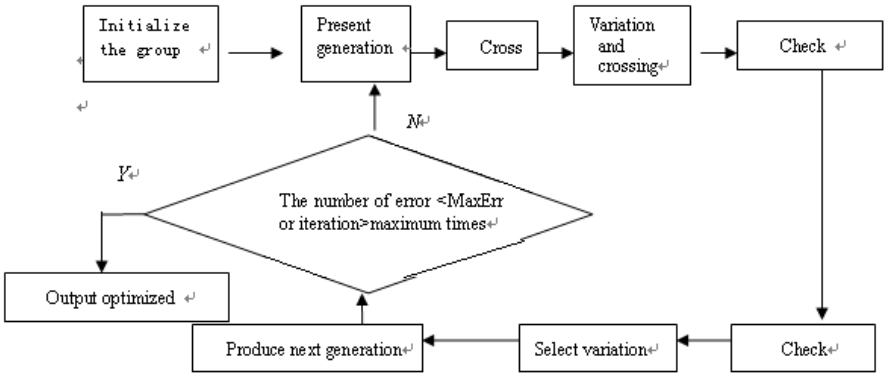


Figure 1 The process of genetic algorithm

Conclusions and discussions

We apply genetic method to fuzzy clustering algorithm, adjust variation rate according to the process of evolution, at the preliminary stage of evolution, the smaller variation rate can accelerate the speed of evolution; while at the later stage of evolution, if we increase variation rate, we could expand the variety of solution and guarantee the algorithm could search optimization globally. This genetic and fuzzy clustering algorithm is applied in color separation of colorful fabric with 40×50 image, run in XPsp2 , is realized by matlab 7.0, the scale of group is 70, N=4(four basic primary colors including C, M, Y and K), the times of circle is 12, crossing probability is *P*c=0.8, variation probability is *P*m=0.08.

This algorithm depends on selection of initial cluster center little, has strong adaptive, and usually can find cluster center after cycling only more than ten times, the running speed is perfect too, the image has rich color layers after color separation without too much distortion comparing with original image, and achieve the effect similar with original manuscript. The pattern of fabric is shown in figure 2, fabric simulation drawing separated into two colors warp and four colors weft is shown in figure 3.



Figure 2 The pattern of fabric



Figure 3 The fabric simulation with two colors warp and four colors weft

References

[1] MaLingzhou. Research&Implementation of the System for Computer Aided Innovative Fabric Design and Manuafature. Dissertation Submitted to Zhejiang University for the Degree of Doctor Philosophy. Feb,2005.

[2] Liang Daolei, Huang Guoxing and Jin Jian, The Application of ClusteringAnalysis

in Color Separation of the Color Woven Photograph, *Computer Science*, 2006

[3] Zhou Ming and Sun Shudong. *Genetic Algorithms: Theories and Applications* [M]. Beijing: National Defence Industrial Press, 2002

[4] Zhou, J.*The Principles and Framework of Research on Digital Jacquard Fabric*, J. Textile Res. 24(3), 17–19 (2003).

[5] Xiedong cao. *Fuzzy Information Processing and Application* [M]. Beijing: Science Press, 2003

[6] Wenxiu zhang. *Mathematical Foundation of Genetic Algorithms* [M]. Xian: Xian Jiaotong University Press, 2001

[7] Xuguo zhou. *Topographic Map Segmentation based on Genetic Fuzzy C - Means*

© (2011) Trans Tech Publications, Switzerland
doi:10.4028/www.scientific.net/AMR.331.83

Studies on the Composite Thermochomic Energy-Storage Materials Prepared by Sol-Gel Method

WU Zhi-lei [1,2], MA Xiao-guang[1,2]

1. School of Textile, Tianjin Polytechnic University, Tianjin 300160，China;

2. Key Laboratory of Advanced Textile Composites (Tianjin Polytechnic University), Ministry of Education, Tianjin, 300160, China
Correspondence to xgma@tjpu.edu.cn

Key words: thermochomic; energy-storage; sol-gel; composite materials

Abstract: Composite thermochromic energy-storage materials (CTEM)were prepared by sol-gel method, Factors exerting influence on thermochomic and thermal properties of composite materials were discussed, such as the molar ratio of ester to water, the dosage of thermochomic materials, pH value were optimized via 3 factors and 3 levels of L_9 (3^3) orthogonal design. Based on the research,when the molar ratio of ester to water was 1:7, dosage of thermochomic materials was 14g, pH value was 3, the optimal chromatic aberration and cooling time of the composite thermochromic energy-storage materials was successfully acquired. Results showed that the thermochomic materials were firmly enwrapped in silica of three-dimensional network structure, solving the problem of liquid release in the process of phase change and increasing its applications in textile, meanwhile it also had excellent thermochomic and thermal performance.

Introduction

Thermochromic materials were a kind of intelligent materials, whose color can change into another with temperature. It was usually composed by chromophoric reagent, delomorphic reagent and solvent [1], of which chromophoric reagent decided the properties such as the color and stability of the reversible thermochomic materials, delomorphic reagent decided the color shade and the solvent decided the temperature to change color. Due to the thermal property of the solvent during the phase change, it endued the thermochomic materials with energy-storage function. When the temperature changed, the electrons transferred between the chromophoric reagent (so called electron donor) and delomorphic reagent (so called electron acceptor) during the phase transformation of the solvent. This kind of thermochromic materials had become a major direction of development in the field of thermochomic materials, which could be widely used in industrial, medical, security, clothing and daily decorations [2-5], however, the thermochromic materials presented liquid solvents at a high temperature [6], which greatly limited its application. In this paper, using TEOS as precursor, CTEM were prepared by sol- gel method. Owing to the three-dimensional network structure and high thermal conductivity of SiO_2 [7], the color sensitivity of composite thermochomic energy-storage materials was improved substantially. Various factors that influence the thermochromic and thermal properties of the CTEM were carefully discussed, such as the molar ratio of ester to water, the dosage of thermochomic materials, pH value and so on, the optimum formulation was successfully acquired at last, subsequently broadening the use of the organic phase change materials and laying the foundation for the development of intelligent textiles.

Experimental

1.1 Materials

Aliphatic alcohol CR-1(made by myself), Chemical agents included tetraethoxysilane(TEOS), ethanol, hydrochloric acid, boric acid and bromocresolpurple (all provided by Tianjin Kermel Chemical Reagent Factory. Tianjin, China), Deionized water.

1.2 Methods

1.2.1 Sol - Gel method mechanism

In this experiment, under constant mechanical stirring, TEOS as precursor, was mixed in ethanol solvent to form a homogeneous solution. After numerous hydrolysis and condensation reactions in the presence of catalysis of hydrochloric acid, the colloidal particles or sol were obtained in the form of Si-O-Si bond; and then after the aging process, a desirable three-dimensional network structure in the gel was got. The hydrolysis and condensation reactions took place as follows [8]:
Hydrolysis reaction:

$Si(OC_2H_5)_4+4H_2O \rightarrow Si(OH)_4+ C_2H_5OH$

Condensation reactions:

$\sim Si—OH+C_2H_5O—Si\sim \rightarrow \sim Si—O—Si—O—Si\sim\cdots\cdots OC_2H_5+ C_2H_5OH$

$\sim Si—OH+HO—Si\sim \rightarrow \sim Si—O—Si—O—Si\sim\cdots\cdots OH+H_2O$

During the process of hydrolysis and condensation reactions, Silicon alkoxide formed polymer particles gradually, sol particles grew as the chain connected to form three-dimensional network structure, serving a cage to hold CTEM. Instead of overflowing, liquid-state CTEM could be firmly enwrapped in the three-dimensional network and embedded in the cage [9], overcoming the liquid leakage problem of high alcohol solvent existing in the CTEM at a hot environment. Simultaneously the three-dimensional network structure SiO_2, having high thermal conductivity, enhanced the CTEM thermal conductivity and color sensitivity effectively.

1.2.2 Principles of thermochromism and energy-storage

In this experiment, thermochromic materials were prepared with bromocresol purple as leuco, boric acid as developer, and phase change material CR-1 as solvent. Due to the fact that bromocresol purple had lactone structure, with the phase transition of CR-1 at high temperature, electronics given by bromocresol purple combined with developer, bromocresol purple changed its structure from lactone to quinone, thus the growth of the conjugated system gave rise to the color change from light red to yellow, in another word, the color changed with temperature[10], meanwhile the process of phase transition was accompanied by energy absorption and release, it endued the thermochromic materials with dual function of thermochromism and energy-storage. The thermochromism temperature of the material was near the melting point [11].

1.2.3 The preparation of thermochomic energy-storage materials

To prepare the thermochomic energy-storage materials, a certain proportion of bromocresol purple, boric acid were weighed in the beaker, and some amount of aliphatic alcohol CR-1 as a solvent were added into the magnetism msier for uniform mixing with the temperature 95 ℃, time 60min, thermochomic energy-storage materials were got after cooling.

1.2.4 The preparation of composite thermochomic energy-storage materials

A certain qualities of TEOS, deionized water and ethanol were weighed into beaker according to certain proportion, and the beaker was placed into the magnetism msier and mixed for some time, after that the catalyst hydrochloric acid was added, a desirable transparent sol was obtained after reaction for 150min. The sol was put into the oven to age for a certain time and the aging time was recorded at the same time.

The thermochomic energy-storage materials were wrapped based on the optimal sol-gel method. The specific process: TEOS, distilled water, ethanol→ heating and stirring→ adding catalyst→ adding thermochomic energy-storage materials →heating and stirring →aging → CTEM.

1.3 Performance Test

1.3.1 Measurement of the aging time

To record the aging time, the sol was put into oven and the change of the sol was observed at intervals of 5 minutes until all the system became gel, this time is the gel time.

1.3.2 Measurement of thermochromism

The color change of the samples was tested by using SF-600 spectrophotometer color measurement instrument, read the total color difference△E and reflectivity curve respectively.

1.3.3 Measurement of thermochomic time

The melting thermochomic material was coated on the glass slide and put into the thermostat, whose temperature was adjusted before measurement, then the thermochomic material was cooled completely. Starting point for the thermochromic time was subject to local thermochromism of the material and completed with total thermochromism. Measurement should be repeated three times to minimize experimental error. Above all, thermochromism should be completed by the same observer lest cause error.

1.3.4 Step-cool curve and cooling time

The thermal probe of thermometer was immersed into 1g CTEM, which was put into a test tube, then the tube was removed into 60 ℃ water bath until 50 ℃, followed by a natural cooling process at room temperature until 25 ℃, synchronously, the stopwatch was started and the temperature of the sample was recorded at intervals of 10s, the cooling time M was written down at last.

1.3.5 Infrared spectrum

The sample was mixed with KBr and pressed to measure the infrared spectrum by TENSOR37IR spectrometer (made by BRUKER Company, Germany).

1.3.6 TG / DTG Testing

The sample was analyzed to measure TG and DTG spectra by integrated thermal analyzer (made by NETSCH Company, Germany).

Results and Discussion

2.1 The orthogonal design

For the purpose of studying the effect of the process parameter on the preparation of CTEM, as well as processing conditions on the phase change material quality, the molar ratio of ester to water, the dosage of thermochomic materials, pH value were optimized via 3 factors and 3 levels of L_9 (3^3) orthogonal experiment. The total color difference of △E before and after heated and the cooling time of M were chosen for experiment indexes. The orthogonal experiment design table and results were showed in Table 1:

Table 1 L_9 (3^3) orthogonal experiment design

Number	A	B	C	△E	M
1	1:6	13	2.5	8.131	186
2	1:6	14	3.0	9.872	514
3	1:6	15	3.5	10.198	522
4	1:7	13	3.0	10.235	512
5	1:7	14	3.5	11.062	603
6	1:7	15	2.5	11.790	715
7	1:8	13	3.5	9.376	423
8	1:8	14	2.5	9.957	556
9	1:8	15	3.0	10.878	707

Table 2 Extreme difference analysis of orthogonal experiment

	△E			M		
	A	B	C	A	B	C
K1	28.201	27.924	29.878	1222	1121	1457
K2	33.087	30.891	30.985	1830	1673	1733
K3	30.211	32.866	30.636	1686	1944	1548
k1	9.400	9.308	9.959	407	374	486
k2	11.029	10.297	10.328	610	558	578
k3	10.070	10.955	10.212	562	648	516
R	1.629	1.647	0.369	203	274	92

According to the R value in Table2, the influence weight of the influencing factors on two indexes were got as follows: the amount of thermochomic materials> molar ratio of ester to water > pH value, which indicated the amount of thermochomic materials had a significantest impact. This was because the thermochomic material itself had the dual function of temperature adjustment and thermochromism , the more the amount of thermochomic materials, the more obvious the performance of temperature adjustment and thermochromism. However, adding too many thermochomic materials would exceed the capacity of the network structure. The impact of ester water ratio were also significant, because the sol-gel was a process of ester hydrolysis and condensation, too small amount of water would lead to incomplete hydrolysis of ester, even brought changes to the capacity of the gel, and vice versa. pH value also had a significant impact in this experiment, under acidic conditions, H^+ attacked-OR first, causing the electron cloud to shift to -OR，and increased the gap between the silicon surface and electron cloud, meanwhile the strong negative charge Cl^- attacked Si^{2+}, accelerating the hydrolysis of TEOS, the hydrolysis of TEOS affected the capacity of the gel directly, so pH value was an important factor.

2.2 The performance of the composite thermochomic energy-storage materials

2.2.1 Thermochomic performance

Reflectivity of the CTEM before and after thermochromism was measured by spectrophotometer color measurement instrument, the results were showed in Fig 1:

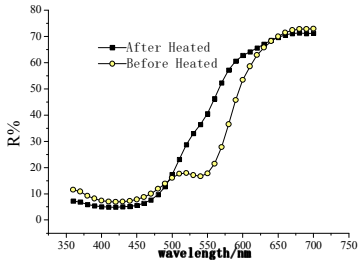


Fig 1: Reflectivity curves of the CTEM before and after heated

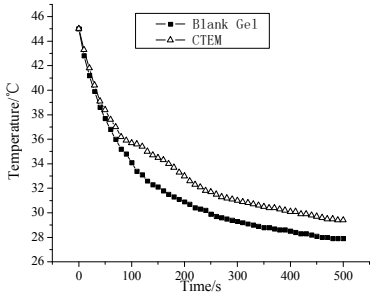


Fig 2: The step-cool curves of CTEM and blank gel

It was obviously indicated that the reflectivity of the CTEM had undergone a tremendous change before and after heated, reflectivity increased greatly after heated, especially at the wavelength 525-600nm. Two curves could not fully overlap, The CTEM could change color from orange red to yellow by the naked eyes, hence it was evident that the CTEM was an ideal thermochromic material.

2.2.2 The thermal performance

Phase change material was used as solvent of thermochromic materials, which had an excellent energy-storage performance. In order to compare its thermal performance with the blank gel (without thermochromic materials), the CTEM and blank gel were placed in a simulated environment to measure their step-cool curves in cooling process. The results were showed in Fig 2:

Fig 2 presented that the CTEM had good thermo-regulated performance compared with blank gel, the temperature of bland gel and CTEM both declined with temperature, yet the temperature of CTEM declined slightly with the increase of cooling time and could keep a relative invariableness due to the occurrence of "phase-change" course, in addition, along with extending of time, the temperature difference between CTEM and blank gel continued to increase, the maximum temperature difference reached up to 4 ℃. From this point of the view, a prominent effect of thermoregulation was exhibited.

2.2.3 Analysis of infrared spectra

The bromocresol purple / boric acid / CR-1constituents were studied by infrared spectrometry before and after composite, the results were showed in Fig 3 and Fig 4:

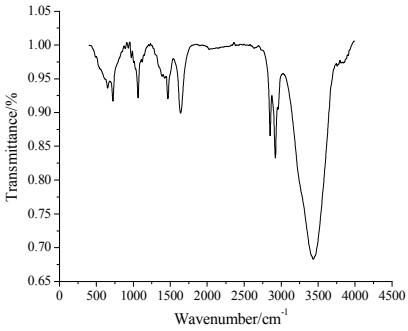


Fig 3: The infrared spectra of thermochromic material

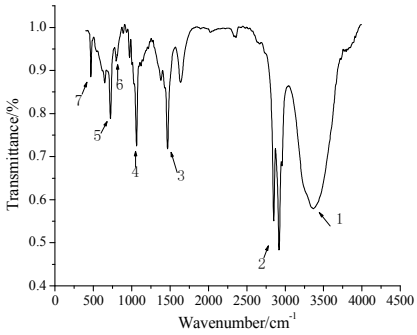


Fig 4: The infrared spectra of the CTEM

By comparing Fig 3 and Fig 4, there were same characteristic peaks which were derived from the solvent of CR-1, such as absorption peak of-OH at 3298cm^{-1}, stretching vibrational absorption of saturated hydrocarbons at 2980 cm-^{1} and 2850 cm^{-1}, 1467 cm^{-1} corresponding to the asymmetric bending vibrational absorption of CH_3 and scissors vibrational absorption of CH_2, it indicated that the two substances had the same functional group and the phase change material had entered into the CTEM. In addition, A weak bending vibrational absorption peak of H—O—H from water, due to capillary and hydrophilic effect in the structure of gel, was found at 1643cm^{-1}, the stretching vibrational peak and bending vibrational peak from Si-O at 797 cm^{-1} and 453 cm^{-1} respectively account for the fact that the phase change material was enwrapped in the three-dimensional network of SiO_2 gel. Furthermore, there was no new absorption peak in the curves, indicating that no other substances formed, it can be proved that thermochromic material combined with SiO_2 in a chimeric way.

2.2.4 TG / DTG characterization of composite thermochomic energy-storage materials

Thermal stability was a key parameter to the thermochomic energy-storage materials to be applied on textiles, consequently it was necessary to measure its thermal property, the TG / DTG testing chart was showed in Fig 5:

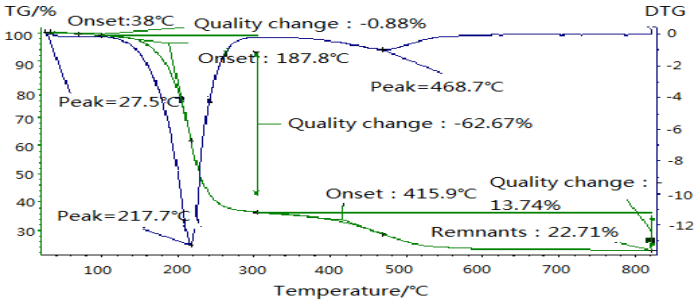


Fig5: TG / DTG spectra of CTEM

Judging from the TG testing chart, the whole process can be divided into three phases: a very slight weight loss rate was 0.88% as a result of residual solvent evaporation from the product (ethanol and some adsorbed water) before 50℃. Since then, the weight loss rate was significantly increased up to 62.67% from 187.8 ℃, due to the evaporation of thermochromic materials in the three-dimensional network of SiO_2 gel. The weight loss rate reached 13.74% in that the gel hydrolysis and condensation reactions were incomplete, producing a lot of residual reactants. It could be seen from the DTG, there were two weight loss peaks. A lower weight loss rate happened before 150 ℃, after that, the weight loss rate increased significantly with temperature, reaching its maximum at 217.7 ℃. In brief, composite thermochromic energy-storage materials were stable within 187.8 ℃, showing it was feasible to be treated on the fabric and could satisfy the need of people in our daily life.

Conclusions

(1) Composite thermochromic energy-storage materials were successfully prepared by sol-gel method, the optimum process conditions were determined through the orthogonal experiment: the molar ratio of ester to water is 1:7,dosage of thermochomic materials is 14g, pH value is 3.
(2) The thermochromic energy-storage materials prepared through appropriate formula were tested for reflectivity and thermal properties, the results showed that it had excellent chromogenic and thermal performance.
(3) The thermochromic energy-storage materials were analyzed by infrared spectrometry and TG / DTG tests, the results indicated that the thermochromic material combined with SiO_2 in a chimeric way and it had excellent thermal stability to satisfy our daily needs.

Reference

[1] Wang Kaijun. Preparation of Thermochromatic Material and Its Microcapsulization〔D〕. Jiang Su：Su Zhou University,2008. In Chinese

[2] Liu Weijin,HuQian,Li Suzhi, et al: submitted to Applied Chemical Industry(2008) In Chinese

[3] Zhang Shusheng: submitted to DYESTUFF INDUSTRY (2002) In Chinese

[4] Huang Huihua, Liu Jishi: submitted to Chemical Fiber& Textile Technology (2006) In Chinese

[5] Liang Xiaorui, Zhang Yong, Zhang Lichun: submitted to Chemical Engineer (2009) In Chinese

[6] Yi Shi-xiong, MA Xiaoguang, Li Hua: submitted to Journal of Tianjin Polytechnic University (2009) In Chinese

[7] Li Xiqi,Yao Xueliang,Wang Haifeng: submitted to Materials Review(2010) In Chinese

[8] Huang Jianfeng, in: The Principle and Technology of Sol-Gel BeiJing:Chemical Industial Press(2005) In Chinese

[9] Lin Kunping, ZhangYinping, Xu Xu, et al: submitted to Building and Environment (2004) In Chinese

[10] Wang Fang, Du Jiang yan, Zhou Zhi hua: submitted to Chemical World (2001) In Chinese

[11] Ren Huiping.The Study on Thermochromism of Bromocresolpurple Materials〔D〕.Shan Xi: Zhong Bei University (2008) In Chinese

© (2011) Trans Tech Publications, Switzerland
doi:10.4028/www.scientific.net/AMR.331.89

The Mechanical Properties of Bamboo/ PLA Composites Made by Biaxial Weft Knitted Fabrics

Cang Zhao[1,a],Guangli Song[1],and Huawu Liu[1]

[1]Key Laboratory of Advanced Textile Composites, School of Textiles, Tianjin Polytechnic University, Tianjin 300160, China

[a]cangzhao_tj@163.com

Keywords: Composites, Bamboo fiber, Polylactic Acid, Biaxial weft knitted fabrics.

Abstract. Bamboo fiber reinforced polylactic acid composite is a kind of green composite materials with excellent performance, which is environmental safe and degradable in natural environment. Literature regarding the characteristics of reinforcement and matrix, pretreatment methods, preparation technology and biodegradable nature of the bamboo/ polylactic acid composite was reviewed and a particular bamoo/ polylactic acid composite made by biaxial weft knitted fabrics was developed. The composite demonstrated excellent tensile and flexural performance. In addition, the influence of the linear density of the binder yarns on the mechanical properties of this composite was insignificant.

Introduction

In recent years, natural fiber reinforced thermosetting and thermoplastic composites have been widely applied since 1980s, due to their attribute of environment safe. Since late 1990s, biodegradable resins, such as polylactic acid (PLA), polycaprolactone (PCL) and polyhydroxybutyrate (PHB), have been used as a replacement of previously non-degradable matrix, to develop completely degradable green composites. In China, the compositing mechanism and mechanical properties of bamboo fiber reinforced composites have been first explored by Xi et al. [1]. In the early 1980s, Ginsbusy and Shin in Canada investigated the manufacturing method of bamboo-plastic composites. Fujii, Goda and Takagi et al., have promoted the studies regarding bamboo fiber reinforced biodegradable composites after millennium [2-7]. In the last decade, bamboo fiber reinforced biodegradable composites have already been well developed in Japan and Europe, many products have gradually commercialized. This study characterizes the bamboo fiber reinforced PLA composites made by biaxial weft knitted fabrics and the relevant prospects.

The reinforcing bamboo fiber

Bamboo is a natural herbaceous plant, rich in cellulose and lignin, with the characteristics of low price, extensive resources. Bamboo as a engineering material has been widely used in daily necessities and building constructions [8]. Bamboo fiber can be classified into bamboo fiber and bamboo pulp fiber. The bamboo fiber is known by its high strength and low elongation, thus is used for reinforcement [9].

The mechanical properties of bamboo fiber are compared with glass fiber and other plant fibers, as shown in Table 1 [10].The tensile strength and elastic modulus of bamboo fiber are between these of hemp fibers, but lower than glass fiber. However, the specific strength of bamboo fiber is far better than the other comparison fibers, since the density of bamboo is far smaller than the rest fibers.

Table 1. The mechanical properties of bamboo, glass, kenaf and ramie fibers.

Kinds of fiber	Specific gravity	Average diameter /mm	Tensile strength /MPa	Specific strength	Young's modulus /GPa	Specific modulus
Bamboo	0.80	0.187	465	581.3	18.0-55.0	22.5-68.8
Kenaf	1.04	0.078	448	430.8	24.6	23.7
Ramie	1.16	0.034	560	482.8	24.5	21.1
E-glass	2.56	0.008-0.014	1400-2500	546.9-976.6	55.8-99.6	21.8-38.9

The polylactic acid matrix

Polylactic acid (PLA) is one of the most widely used biodegradable resins. Firstly, starch is extracted from corn or other starch crops. Then lactic acid is obtained through starch fermentation. Finally, polylactic acid is obtained by direct condensation polymerization, or azeotropic dehydrogenation condensation, or dimer open-looppolymerization [11,12]. PLA is the commonly used commercial biodegrable resin, because of its advantages of low density (1.21 ~ 1.25 g / cm^3), moderate degradation time (1~2 a), glass transition temperature (45 ~ 60 ^oC) and melting point (170 ^oC or so) [13]. The physical properties of the material is between the polyester and polypropylene under normal temperature, as shown in Table 2 [14].

Table 2. The physical properties of Polylactic acid

Kinds	Elastic modulus /GPa	Stress /MPa	Fracture strength /MPa	Elongation/%	Melting point/ ^oC
PGA	3.33	77.3	77.3	3.9	225-235
Poly D, l-lactic acid	2.16	46	46	2.6	Unknown
L - polylactide	2.17	59	57	3.3	170-175

The bamboo/ PLA composites made by biaxial weft knitted fabrics

Bamboo fiber and PLA resin are hydrophilic and hydrophobic materials, thus incompatible. Graft copolymerization and the interface coupling are normally adopted before compositing. Hot pressing is applied to make the composites, more frequently than extruding, pulling, blending knead legal, impregnation and laminating methods, since hot pressing is simple, easy to control, and the low cost of required facilities.

In this study, bamboo fiber reinforced PLA composite samples were made by compression molding. The 28 tex bamboo yarns and 16.7 tex PLA filaments were knitted into biaxial weft structure. The optimal ratio of bamoo over PLA was around 1:1 in weight, for ultimate mechanical properties as recommended [15]. After carefully calculation, it was found that the mass ratio of bamboo and PLA would reach 45.6:54.4 when the ratio of bamboo yarns and polylactic acid filaments was 1:2. Three layers of bamboo/PLA biaxial weft knitted fabrics were hot pressed, at 168 ^oC for 20 minutes under external load of 8MPa.

The two groups of biaxial weft knitted fabrics comprised 6 or 12 binder yarns, respectively. The mean longitudinal tensile strength, longitudinal bending strength, transverse tensile strength and transverse bending strengths of the fabrics with 6 warp yarns were 25.11, 52.20, 18.66 and 38.87 MPa, progressively. While the corrsponding strengths of the fabrics with 12 warp yarns were 26.27, 49.37, 20.06 and 25.88 MPa, respectively. This reveals that the composites made by bamboo / PLA biaxial weft knitted fabrics have excellent tensile and flexural performance. In addition, the influence of the linear density of the binder yarns on the mechanical properties was insignificant.

The degradation of bamboo / PLA composites

In the early stage of biological degradation, the decomposition mainly occured in polylactic acid resin and the interface between the resin and bamboo fiber. With the development of degradation, the gap between the polylactic acid resin and the bamboo fiber gradually increased. The bamboo fibers were exposed to air and the rate of degradation was getting accelerated until the resin falling off.

This observation was confirmed by Wang [16]. She stated that the degradation initiated in the material interfaces; the developed checks in the resin led the fiber to be exposed and decomposed. The higher the fiber content, the faster the degradation speed. The longer the time of degradation, the higher the loss of mass.

Discussions

Biodegradable composites are mainly used for automobile parts, interior decoration, and packaging. Regarding biodegradable plant fiber reinforced composites, the previous studies mainly focused on the manufacturing processes, such as preparation, molding, fiber modification etc., rather than the understanding of the phenomena to underpin the future improvement.

In addition, researches regarding the reliability of the biodegradable materials in service have been rather limited, which may lead to the biomass products fail before the expected time frame.

The cutting-edge research is polymer nano-compositing technology to develop fully biodegradable polymer nano-composites, which is significant to extend the application scope of biodegradable materials.

Referances

[1] X. Xian, D. Xian,W. Zheng: Acta Materiae Compositae Sinica, 5(3):7-16 (1988).

[2] T. Fujii: J. Soc. Mat. Sci. JP, 50(5):556 (2001).

[3] J. Jiang, T. Fujii: Reinforced Plastic, 45: 365 (1999).

[4] K. Goda, Y. Kitamura: Men. Fac. Eng. , Yamaguchiuniv, 53(1): 61 (2002).

[5] K. Goda, Y. Kitamura, J. Ohgi: in:Proc. of 32th FRP Symposium, Soc. Mat. Sci., JP. p29. (2003).

[6] H. Takagi, R. Takara and Y. Ichihara: J. Soc. Mat. Sci. JP, 52(4): 353 (2003).

[7] H. Takagi, R. Takara: J. Soc. Mat. Sci. JP, 52(4):357 (2003).

[8] Y. Cao, et al. : J. Acta Materiae Compositae Sinica, 21(2):119-125 (2007).

[9] L. Tao, Y. Jiang, M. Wang:J. Advanced Textile Technology, 14(3): 14 (2006).

[10] J .Ge: Chemical Industry Press, Beijing (2002).

[11] D. L. Kaplan: M. Springer-Verlag Berlin Heidelberg. Germany (1998).

[12] D. Garlotta: J. Journal of Polymers and the Environment, 9(2): 63-68 (2001).

[13] K.V. De Velde, P.Kiekens, J. Polymer Testing, (21): 433 - 439 (2002).

[14] Y. Qian: J. China Textile Leader, (4):38- 42 (2004).

[15] X.Wang, G. Wang: Soochow University, Master's Thesis (2009).

[16] C. Wang, R. Wang, etal: J. Engineering Plastics Application, 36(1): 8-11 (2008).

© (2011) Trans Tech Publications, Switzerland
doi:10.4028/www.scientific.net/AMR.331.93

Graphene modified cotton textiles

Wenlong Gu, Yongnan Zhao

Institute of Nanostructured Materials, School of Material Science and Engineering and Tianjin Key Laboratory of Fiber Modification and Functional Fiber, Tianjin Polytechnic University, Tianjin 300160, China

zhaoyn@263.net

Keywords: Graphene, Electric conduction, Cotton textiles, Modified

Abstract: The graphene oxides are abundant in hydroxyl and carboxyl groups that are close to the reactive dyes. These structural features gave a possibility to modify textiles to enhance the conductivity by using the dyeing and finishing method. Herein, graphene modified cotton textiles are fabricated by soaking cotton cloth in graphene oxide colloid. After reduction, the modified textiles exhibit an improved conductivity. The present work contributed a facile strategy for graphene modified textiles.

Introduction

Graphene is an ideal two-dimensional (2D) honeycomb lattice of single layer carbon atoms [1]. Due to the unique structure and physical [2] and electrical [3] performance, graphene is presently the most eye-catching materials with wide applications. Cotton textiles were considered as the most comfortable garment materials. The poor conductivity limited the future applications. Recently, conductive textiles have been developed to exploit functional garment that can monitor the heart rate and breathing to protect people from the emergency, analyze the sweat and temperature to control the temperature, and provide power for electronic devises from the solar energy [4, 5]. Herein, a facile method was developed for fabricating conductive cotton textiles with graphene.

Experimental

Preparation of graphene oxide (GO): GO was prepared by the conventional Hummers method [6]. 10 g graphite powder and 5g of $NaNO_3$ were added into 230 mL concentrated sulfuric acid under vigorous stirring. The mixtures were then cooled to 0°C in an ice-bath. 30 g $KMnO_4$ were added to the reactants. For safety concerns, the addition rate must be slowly to keep the temperature of the reactants below 20°C. The low-temperature stage was kept for 2 hours [7]. Afterward, the temperature of the reactants was elevated to 35 °C and maintained at the intermediate temperature stage for 30 minutes. Finally, 460 mL distillated water were poured into the mixtures. To control the reaction temperature around 98˚C and prevent from local overheating, the water was added in a slow rate. This high temperature reaction stage [7] was kept for 15 minutes. The suspension was then diluted with distilled water to 1.4 L. The residual $KMnO_4$ and MnO_2 were reduced into soluble $MnSO_4$ by using 100 mL 50% H_2O_2. The mixture was filtered and treated with HCl pickling until no precipitation appeared in the filtrate when the barium chloride was added. The product was dried in a vacuum at 50°C in the presence of phosphorus pentoxides.

Preparation of GO colloid: 0.5 g GO were dispersed in 100 mL distilled water under ultrasonication for 1 hour. The mixtures were then centrifuged for 30 minutes to separate the un-exfoliated graphite powders and other impurities. GO colloid was collected in a matrass carefully [8].

Modification of the cotton textiles: The modification of cotton textiles was completed by soaking the cotton cloth in GO colloid. Typically, the cotton textiles were merged into the GO colloid for 30 minutes with or without ultrasonication. The detailed experiment conditions were listed in Table 1. The treated cotton textiles were dried at 60°C. the GO modified textiles were denoted as GMCT−n. Reducing the GO modified textiles were achieved by refluxing the modified samples in 300 mL 27 wt% hydrazine solutions at 100°C for 24 hours. The reduced samples were correspondingly denoted as GMCT−nR.

Table 1 The different conditions of modification

Sample code	Concentration	Soaking time	Conditions
GMCT−1	4 $g \cdot L^{-1}$	30 mins	Static
GMCT−2	4 $g \cdot L^{-1}$	30 mins	Ultrasonication
GMCT−3	3.2 $g \cdot L^{-1}$	30 mins	Ultrasonication
GMCT−4	1.6 $g \cdot L^{-1}$	30 mins	Ultrasonication
GMCT−5	0.8 $g \cdot L^{-1}$	30 mins	Ultrasonication

Characterization: Transmission Electron Microscope (Hitachi H-7650) was used to observe the morphology of GO. The surface topography of the modified cotton textiles were observed by using scanning Electron Microscope (Hitachi S-4800). Electric resistance of the textiles was tested by using an electrochemical workstation (LK−3200).

Results and discussion

The morphology of the graphene oxides was characterized by TEM observations (Fig. 1a). The as-prepared GO comprises a lot of very thin lamella with many wrinkles. No impurity was detected.

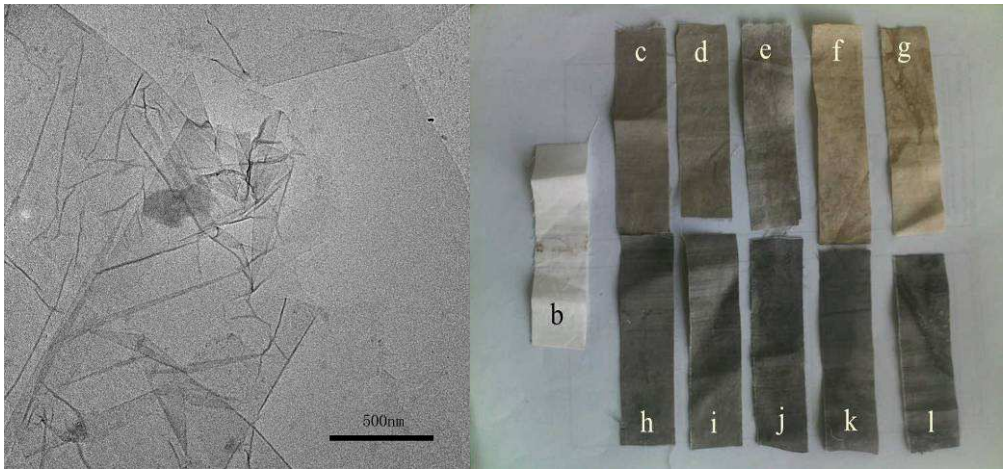


Fig. 1 The TEM image of the as-prepared GO (a) and the pictures of the original cotton textiles (b), GMCT−5 (c), GMCT−4 (d), GMCT−3 (e), GMCT−2(f), GMCT−1 (g), GMCT−5R(h), GMCT−4R(i), GMCT−3R(j), GMCT−2R(k) GMCT−1R(l).

As shown in Fig.1 (c− l), the color of the textiles was changed from yellow to gray that depended on the modification conditions after modification. Further reduction changed the color of the cotton cloth to dark grey.

SEM observations revealed the presence of coatings on the fibers of the original cotton textile after modification (Fig. 2a and 2b). The enlarged image of the raw textile showed the presence of many grooves and rough surfaces of the fibers (Fig.2c). After modification, the surface changed smoother than that of the original textiles. The fiber was obviously coated by a layer of lamellae with some wrinkles on the surface (Fig.2d). These results proved the successful coating GO onto

the cotton fiber. Sonication also affected the coating effect as shown in Fig. 2e and Fig. 2f. Without ultrasonication, the cotton fiber could not be thoroughly coated with some pendant lamella. The sample modified under sonication showed a smooth surface. The ultrasonication possibly promoted the curling of the GO to spread out on the surface of the cotton fibers.

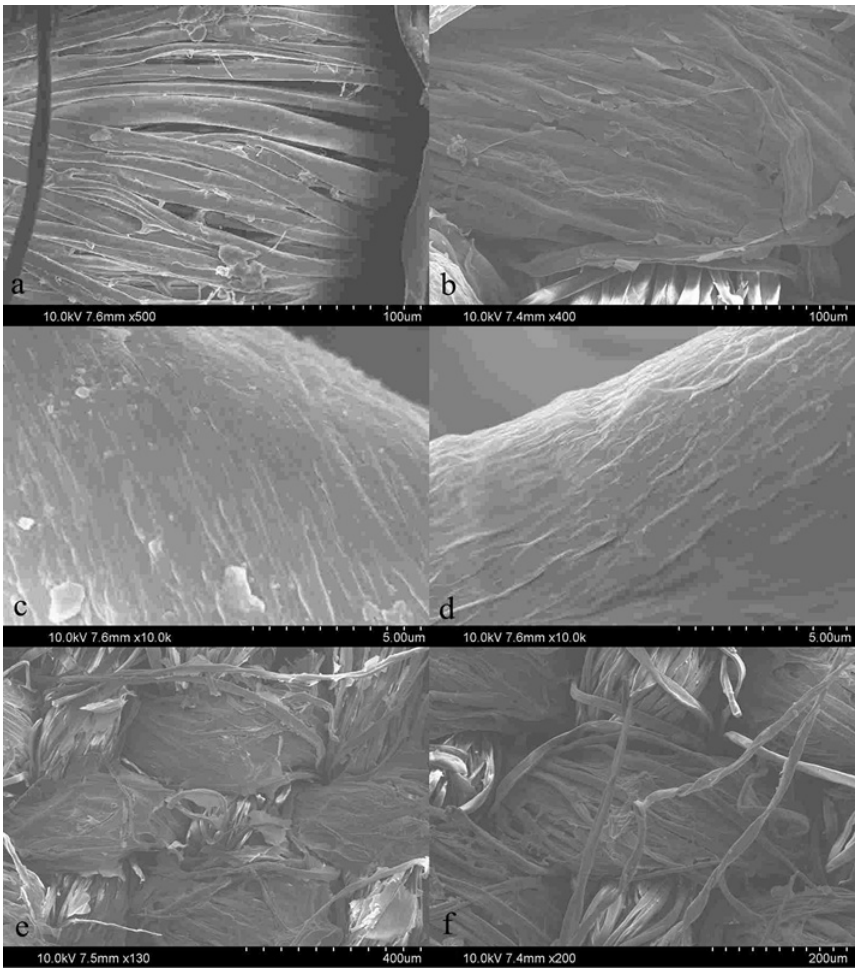


Fig. 2 SEM images of modified cotton textiles: original cotton cloth (a, c), GMCT−1 (b, e), and GMCT−2 (d, f).

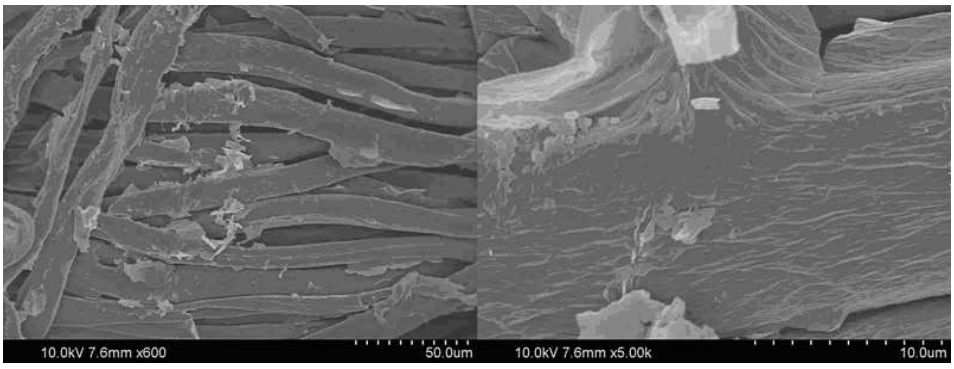


Fig. 3 S
EM image of GMCT−2 after sonication.

The GO coatings exhibited a strength adhesion to the cotton fibers and were hard to be peeled off (Fig. 3). After sonicated for half hour, the SEM image indicated the existence of the GO coatings. As is well-known, GO is abundant in hydroxyl and carboxyl groups. The cotton fibers contain a lot of hydroxyl groups. These groups possibly interact to each other through complex H-bonds. The presence of H-bonds also promotes the spreading of GO on the fiber surfaces.

Graphene is conductive 2-D nanosheet. Graphene coating may improve the conductivity of cotton textiles. The original cotton cloth is insulating with a huge resistance of 4.1050×10^{15} Ω (Fig. 4a). The resistance of the GO modified sample decreased to 8.4501×10^{10} Ω. Chemical reduction further improves the conductivity of the cotton textiles with a smaller resistance. The resistance was related to the concentration of GO colloid. The concentrated colloid directed to a better conductivity. The resistances of different modified textiles are listed in Table 2.

Table 2 Resistances of different modified textiles

Sample	GMCT−5R	GMCT−4R	GMCT−3R	GMCT−2R	GMCT−1R
Resistance	1.9129×108 Ω	4.0253×107 Ω	3.5944×107 Ω	2.0132×107 Ω	2.7483×107 Ω

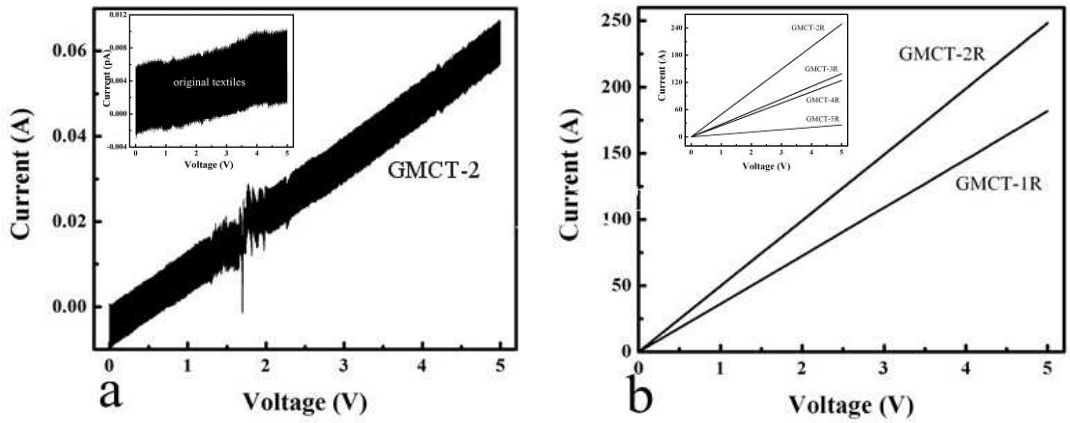


Fig. 4 CV curves of different textiles.

Conclusions

By using the dyeing and finishing method, graphene modified cotton textiles are fabricated. After reduction, the modified cloth exhibited a greatly improved conductivity. High concentration of GO colloid and sonication are benefit to reduce the resistance.

Acknowledgement

The authors are grateful to the financial support by the NSF of Tianjin (10JCZDJC21500) and TJPU.

Reference

[1] K. S. Novoselov, A. K. Geim, S. V. Morozov, J. Y. Zhang, S. V. Dubonos, I. V. Grigorieva, A. A. Firsov: Science, Vol. 206 (2004), p. 666

[2] S. V. Morozov, K. S. Novoselov, M. I. Katsnelson, F. Schedin, D. C. Elias, J. A. Jaszczak, A. K. Geim: Phys. Rev. Lett., Vol. 100 (2008), p. 016602

[3] C. Lee, X. Wei, J. W. Kysar, J. Hone: Science, Vol. 321 (2008), p. 385

[4] A.G. Avila, J.P.Hinestroza: Nature Nanotech., Vol. 3 (2008), p. 458

[5] P. Gould: Mater. Today, Vol. 6 (2003), p. 38

[6] S. William, Jr. Hummers, R. E. Offenman: J. Am. Chem. Soc., Vol. 80 (1958), p. 1339

[7] L. Fu, H. Li, Y. Zou, B. Li: Carbon, Vol. 4 (2005), p. 10

[8] Y. Xu, K. Sheng, C. Li, G. Shi: ACS Nano, Vol. 4 (2010), p. 4324

© (2011) Trans Tech Publications, Switzerland
doi:10.4028/www.scientific.net/AMR.331.97

Analysis on Green Initiative Costume Design Concept

Jian Zhao [1, a]

[1]Shaoxing university, Huanchengxi road508, Shaoxing city, Zhejiang province,312000,China

[a]happy2002lady@hotmail.coml

Keywords: Environmental Protection; Nature; Costume; Exploration

Abstract. Through the analysis of the three design performance of green Initiative costume design concept, the thesis interpreted the environmental protection theme, costume's "ecological cycle" as well as the green Initiative costume show respectively, and accordingly proceeded the future prospect, believing that the new design approach, new material selection and the new aesthetic concept of green clothing will have a significant impact on the green costume design concept which will then generally influence the consumers and provide some reference and guidance to the development of future design of green costume in the meanwhile.

Introduction

The green initiative costume design concept was bought in the costume date from the 1980s; in February 1997 in the Germany Dusseldorf latest clothing exhibitions, it firstly concentrated exhibited the green costume and awarded the environmental prize which promoted the green concept to a new height, the environmental protected and healthy costume language then start to be a global hot spot.

Designers spared no effort and designed various green clothing in accordance with the rhyme of environmental protection, exhibited them in varied topic fashion shows like: eco-fashion show, underwater world fashion show, protection of the global village, etc. Designers devoted their own pursuit of environmental protection in their fashion design themes [1] and tried to find the law of green clothing design by means of the environmental protection rhyme.

It should utilize the high-tech materials to reduce ozone's damage to human skin, alleviate atmospheric temperature's impact on the human body environment, lessen acid rain's damage to clothing and fibrous tissue, etc. Designer used the natural polymer materials, green fiber and the environment fiber that manufactured by micro-organisms to design costumes through synthetic approach. [2]

From an environmental point of view, re-transform the discarded bottles and applied it to the clothing decoration (see in Figure 1) can not only show the personality of costume design but also can express the theme of environmental protection. The material of decoration is no longer limited to gold and silver ornaments jewelry, the spring of environmentally friendly materials give clothing more profound meanings.



Fig1 Decoration made by discarded bottles

2. Design performance of green costume

2.1 The thyme of environmental protection

TV Medias has done many public services advertising appealing people to protect the environment, slogans were written on the walls, and various posters and flyers fled all round the world. The clothing is essential for people's lives; people can wear costumes which can reflect the healthy and green theme of the environmentally friendly costume.[3]

2.2 Costume's "ecological cycle"

Recycling use of resources is one important way of environmental protection. Now there's a new environmentally friendly fabric called "eco-cycle fabric". It is cut into ordinary fashions the same as the fabric; however, they are old clothes, waste paper, and even Coke bottles before recycling. When this kind of clothe is dirty or becoming old, wearer can put it back to the designated locations, re-crushed it and made into clothing once again, such unlimited circles endow a piece of clothing an eternal life.

2.3 Costume exhibition in the show

Green dress is usually a fashion show that can inspire and enlighten people by the theme. In the T stage, there exist various styles green costumes. Paint playful marine live in the costumes can lively perform the vast of oceans. Creative paper fashions are very impressive (As shown in Fig2).



Fig2 Creative Paper Fashion

3. The tendency of the green costume

3.1 New forms of expression

In the future, this simplified form of the green dress design will be replaced by more humane and technical forms. Due to people's increasingly enhanced awareness of environmental protection and their constantly looking for new design elements, they will form new manifestations through the extraction and re-combination of existing design elements to coordinate with users' psychological needs of clothing and their environmental awareness. For instance, the none-accessories fashion design adopted the Chinese-style plate buttons instead of plastic buttons and metal zipper.

3.2 New environmental friendly materials

In addition to that costumes can be made by discarded cans, plastic rope, optical disk, etc, green costume also has its specialty in the utilization of materials, new materials that can be repeatedly used like edible fiber, adsorption material that can rapidly degrade poison have been widely adopted. The role of environmental friendly costume performed in many ways, for instance, the productive process of the shell fabric can avoid letting out toxic sulfur gases and waste to the environment; dissolvent used in the spinning production can be fully recycled; rationally and scientifically select chemicals and pigment that has no harm to human body and the effective control of harmful substance can realize the harmful substance among nature, human beings and technology; etc.[4]

3.3 New aesthetic concept of green clothing

With the industrialization of modern society, environmental protection activities have also affected people's daily clothing selection and thereby emerges several of environmental friendly colors; in the mean while, people's pursuit of clothing styles tends to be simple, the choice of fabric also tends to the pursuit of natural fiber so as to manifest the significant natural character. This unique way of thinking and style then formed a new aesthetic concept of green clothing.

Costume design philosophy now emphasizes more on the return to nature, the protection of the environment as well as the harmony between human and nature beauty. Human being's living space is an organic whole whose organic development constitutes the human ecosystem that is a natural system interacted by the Biological communities and the geographical environment. Human's dependence on natural ecosystems is very large. Therefore, it must emphasize more on the green costume design philosophy.

Conclusions

In the future, people will pursuit more on the environmental friendly costume that full of environmental protection concept not only in the design styles and colors, clothing production and processing but also in consumers' using and handling of waste clothing. Today's clothing market is booming, so it should pay enough attention to environmental protective issues. The urgent affair to develop and manufacture green costumes is to enhance the environmental awareness of designers, consumers as well as the garment enterprises, try to find relative design rules, and ultimately make efforts to design, research and development the environmentally friendly clothing. Jointly promote the overall development of China's garment industry with the premise of the physical environment protection.

References

[1]. Mei Hua, Clothing Art, [M]. Beijing: People's Publishing House, 2008

[2]. Gongkai Pan, Fusheng Lu, Textile and Fashion Design, [M]. Shanghai: Shanghai Calligraphy and Painting Press, 2000

[3] Fred Kruup. New Environmentalism Factors in Economic Needs .Wall Street Journal. 1986

[4] Thoreau, quoted from Roderick Nash, The Rights of Nature. A History of Environmental Ethics .Wisconsin: The University of Wisconsin Press, 1989:37 .

© (2011) Trans Tech Publications, Switzerland
doi:10.4028/www.scientific.net/AMR.331.101

Study on Body Foundation of Brassiere Steel Ring Shapes

Su-Zhen Liang[1, a]

1 Fashion and Art Engineering Department, Min Jiang University, Fuzhou Fujian, China

[a] lsz520351@sina.com

Keywords: Brassiere, Breast Root Girth, Steel Ring Girth of Breast, Steel Ring.

Abstract. The pattern design of brassieres is the core technology for the design and manufacture of brassieres, while the female breast shape and part dimensions are the foundations for pattern design of brassieres. Based upon 3D body scanning, this paper studied the relationship between the breast root shape and the steel ring by considering the features of the pattern design of the brassiere. It concludes that the breast root girth is a complicated three-dimensional curve; it's inappropriate for the neighboring size's brassieres to adopt the steel ring with the same specification; the material design of the steel ring should be moderate. The purpose is to provide human body basis for pattern design of brassieres and achieve more standard and scientific pattern design of the brassiere by the underwear enterprises.

Introduction

The pattern design of brassieres is the core technology for the design and manufacture of brassieres, while the female breast shape and part dimensions are the foundations for pattern design of brassieres. The steel ring is an important component of brassiere shaping. Whether or not its shape matches the breast shape has a direct impact on the plastic and comfort of the brassiere. The breast shapes are different among people in different regions, different bodies and different cup sizes. However the steel ring shapes of brassieres are limited, and therefore we need to study the relationship between the steel ring shape and breast root shape. Based upon 3D body scanning, this paper studied the relationship between the breast root shape and steel ring shape to lay a foundation for the pattern design of brassieres.

Methods

(1) Slice up, select points and calculate 10 key parts of breast related to the basic breast shape of 254 female undergraduates of West China by ScanWor digital interactive scanning software of Tecmath non-contact laser 3D body scanner [1].

(2) Taking the aesthetic standard of breasts by modern people as the basis, the basic breast shapes are divided into 9 types, including the inward-high shape, inward-medium shape, inward-sagging shape, external expansion-high shape, external expansion-medium shape, external expansion-sagging shape, medium-high shape, medium-sagging shape and standard shape, while including 102 samples of standard breasts [1].

(3) As required by the study, we firstly confirmed measurements of detailed features and dimensions of the breast, mainly including the arc length of front cup, straight-line distance of front cup, vertical distance of front cup, arc length of side cup, straight-line distance of side cup, vertical distance of side cup, distance between bust points, bust depth, breast root girth and steel ring girth of breast (as shown in Figure 2(c)); slice up, select points and calculate samples of standard breasts. Specific measurements referred to reference 2 [2].

(4) 102 samples of standard breasts were divided into several types according to classification standard of brassiere's size, as shown in Figure 1 [2].

(5) By the aid of CorelDraw, we fit the curve drawing of the steel ring girth of breast in Figure 2(b) into the vector drawing and maintained its dimension and shape during the fitting process.

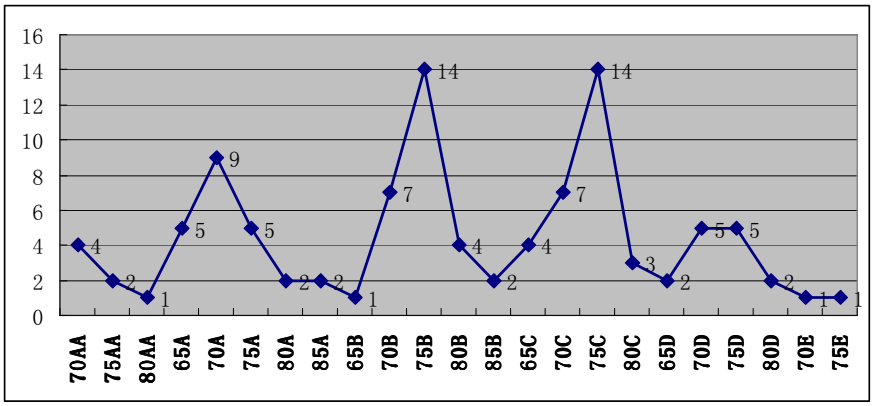
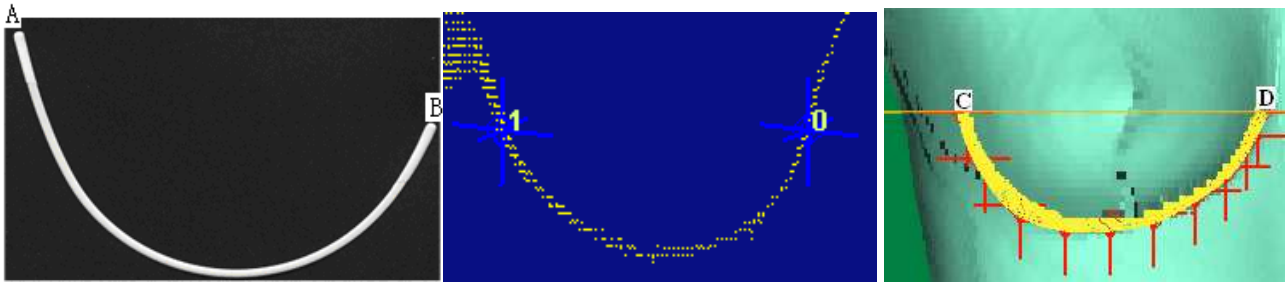


Fig.1 Distribution map of bra sizes for Standard breasts

Data Analysis

Definition of Steel Ring, Steel Ring Girth of Breast and Breast Root Girth. As shown in Figure 2, the steel ring is used for the underside of brassiere cup, as the important component to maintain the brassiere shape [3]. The steel ring girth of breast refers to a certain concept defined in this paper according to the study, namely the curve section of inward point, outward point and lower point of the breast, between the steel ring and breast root girth. The breast root girth refers to root curve under the bust girth.



（a）Steel ring curve of 75B （b）Steel ring girth of breast （c）Breast root girth

Fig. 2 Diagram of steel ring, steel ring girth of breast and breast root girth

Difference between Steel Ring and Breast Root Girth. From several major measurements of detailed features and dimensions of the breast, including the arc length of front cup, straight-line distance of front cup, vertical distance of front cup, arc length of side cup, straight-line distance of side cup, vertical distance of side cup, distance between bust points, bust depth, it indicates that the left and right bust points are not within the same coronal plane. The arc CD of breast root girth in Figure 2 is a complicated three-dimensional space curve [2]. However, the steel ring of the brassiere can not produce the three-dimensional space curve totally fitting with the breast root girth, but only the smooth two-dimensional plane curve (as the steel ring curve in Figure 2). There are two reasons: one is that it can not be done technically; the other one is that the steel ring will lose the function to modify the body and build the shape. Therefore, it will be difficult to study whether the shape and size fit each other between the steel ring curve and breast root girth curve. On this point, to study the relationship between the steel ring curve and breast root girth curve, we introduce an intermediate variable, steel ring girth of breast, as shown in Figure 2(c).

Relationship between Steel Ring Girth of Breast and Breast Root Girth. From the definition of steel ring girth of breast, we know that it is actually the result of approximate conversion of complicated three-dimensional space curve of the breast root girth into the two-dimensional plane curve. As the results of measurements of detailed features and dimensions of the breast in this paper indicate, the size difference between the breast root girth curve and steel ring girth of breast curve is because of the different shapes of breast roots: when the breast root girth curve is relatively round and

smooth, both values are basically equal; when the front and back shapes of breast root girth curve are greatly different, both values will be accordingly different, or the value of breast root girth is larger, or the value of steel ring girth of breast is larger. But from the role of the steel ring, the steel ring girth of breast and the steel ring adopted in the brassiere are relatively close with each other in shape. The opening of the steel ring girth of breast (line-segment"01" in Figure 2(c), straight-line distance between front and back points of the breast) and the opening of the steel ring (line-segment AB in Figure 2(a)), the steel ring girth of breast (arc "01" in Figure 2(c)) and the girth of steel ring (arc AB in Figure 2(a)) are similar with each other. Therefore, this paper considers that comparing with the breast root girth, the steel ring girth of breast is more likely to provide the body foundation for the shape and value of the steel ring.

Relationship between Steel Ring and Steel Ring Girth of Breast. To understand the differences of shapes and amounts between the steel ring and steel ring girth of breast, this paper adopted two groups of 75B brassiere and 70C brassiere, the intermediate values that are adopted by most people, according to the results of samples classification, with 7 persons of each group respectively (sample size of 70C). According to the above grading principle of brassiere and the practical production of underwear manufacturers [3], the brassiere steel ring of these two groups is the same, namely 75B of steel ring. Therefore, this paper took comparison between 75B common steel ring and the steel ring girth of breast of these two groups.

- **Comparison between Steel Ring Girths of Breast of Two Groups.**

Figure3 is the comparison diagram of curves (fitting curves) of steel ring girth of breast for 75B and 70C samples, where A refers to the front point of the breast, B the side point of the breast, C the lower point of the breast, BP the bust point, red curve the curve of steel ring girth of breast for 75B samples, and blue curve the curve of steel ring girth of breast for 70C samples.

From the overall curves in the figure, except two curves above and below, most curves are distributed closely, taking the straight line BP-C as the symmetrical axis. But the front and back sides of the curve of steel ring girth of breast are not symmetrical, which indicates that the front and back sides of the breast are not symmetrical: the curvature (arc AC) of the front side is larger than the one of the back side (arc CB); from the single sample, the shape and size of steel ring girth of breast is different with each other; from the total sample with the same type, the opening and circumstance of steel ring girth of breast of 70C samples is smaller than the one of 75B, but the height (distance between BP point and C point) is larger. Consequently, theoretically speaking, when selecting the steel ring, the opening and circumstance of 70C steel ring should be smaller than the ones of 75B and it should not be generally in common. However, during the practical application of the underwear enterprises, considering the quantity of space of the brassiere and the strong plasticity of the breast, they always ignore the existence of this difference and design the size of 75B and 70C as the same, in order to reduce the sample size and enhance the work efficiency. In this way, for the individual consumer, the opening of some steel ring of brassiere may be too large, without the function of breast shaping; but the opening of some steel ring may be too small, which may oppress the breast and cause various breast diseases. It indicates that it may be inappropriate for the neighboring brassieres to adopt the steel ring with the same specification.

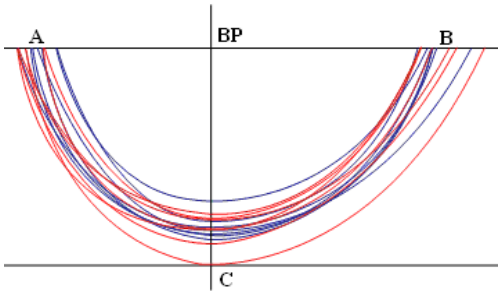


Fig3. Comparison of steel ring girths of breast between 75and 70C

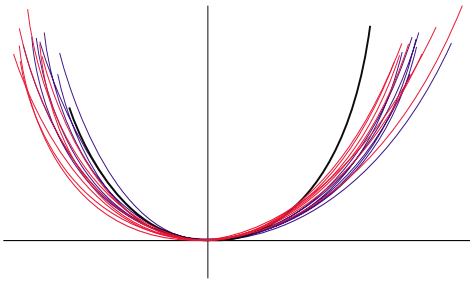


Fig4.Comparison between steel ring and steel ring girth of breast of two groups

- **Comparison between 75B Common Steel Ring and Steel Ring Girths of Breast of Two Groups.**

Figure 4 is the comparison diagram between the steel ring curve (black) and the steel ring girth of breasts of two groups. As the figure indicates, the fitting degree between the steel ring curve and the button of steel ring girth of breast is highest, following by the one between the steel ring curve and the front side of steel ring girth of breast. But there is a large deviation with the shape backside and the opening of the steel ring curve is too smaller than the actual steel ring girth of breast, especially for the back side of the steel ring. The steel ring is designed to make the female use the function steel ring to gather the breast after wearing the brassiere, which will push the back fat of the breast forwards to reduce the distance between the bust points and make the breast look like a ball and more bosomy. Meanwhile, due to the difference between the back shape of the steel ring girth of breast and the one of the steel ring, when designing the lower line of the brassiere, the front shape of the steel ring is remained as the same, while for the back side, the opening of the steel ring will always be widened 1cm according to the changes of the breast arc [4]. When people wear the brassiere, the back-pulling force of the brassiere will make the steel ring arc fit the breast arc. Understanding the difference between the shape of the steel ring and the one of steel ring girth of breast, we have to adopt the steel ring with the moderate hardness during the manufacture of the brassiere: too soft, the steel ring will be deformed easily, without any function to rectify the breast; too hard, the steel ring will be hard to be deformed and hard to be fit with the breast arc. It will closely lock the back fat of the breast, bringing along the uncomfortable experience.

Conclusion

Based upon three-dimensional body scanning, this paper measured the detailed features and dimensions of the breast for 102 western young women with the relatively perfect breasts, and studied the relationship between the breast root shape and the steel ring by considering the features of the pattern design of the brassiere. It concludes that the breast root girth is a complicated three-dimensional curve; it's inappropriate for the neighboring brassieres to adopt the steel ring with the same specification. The material design of the steel ring should be moderate: too soft, the steel ring will be deformed easily, without any function to rectify the breast; too hard, the steel ring will be hard to be deformed and hard to be fit with the breast arc, bringing along the uncomfortable experience.

Acknowledgements

The authors would like to thank Shaanxi Research Center of Clothing Engineering & Technology for providing experiment conditions and the technical guidance of Professor Xin Zhang.

References

[1] Suzhen Liang, Xin Zhang, Jie Zhou. Basic breast shapes of female undergraduate in the westof China based on 32D body scanning [J]. Journal of Textile Research, 2007, 28(8):75-78.(In Chinese)

[2] Suzhen Liang, Xin Zhang, Dong Sheng Chen. Body foundation of major part-dimensions in the bra pattern-design on the basic of 3-D body scanning [J]. Journal of Textile Research, 2008, 29(12):73-77. (In Chinese)

[3] Suzhen Liang, Xin Zhang. Inquisition and analysis of bra design in undergarment factories [J]. Journal of Xi'an University of Engineering Science and Technology, 2006, 20(5):555-559. (In Chinese)

[4] Jianrong Ying, Jianliang Chang. Underwear pattern design principle and techniques [M]. Shanghai: Shanghai science and technology publishing house, 2004, 6:31-55. (In Chinese)

© (2011) Trans Tech Publications, Switzerland
doi:10.4028/www.scientific.net/AMR.331.105

Microwave Promoted Effect of Starch-g- Butyl Acrylate Sizing Copolymer Grafting

Hai-liang WU[1,a], Yan-qin SHEN[1,b]

[1]Xi'an Polytechnic University, Xi'an 710048, China

[a]whl@xpu.edu.cn, [b]shenyanqin1208@126.com

Keywords: micro-wave. starch. butyl acrylate. grafted copolymerization

Abstract. Grafted Copolymers of Starch-g-Butyl acrylate were prepared under conditions of micro-wave field and the normal heat resource, the ammonium peroxysulfate (APS) was used as initiator and the reagent was in sub-solid state. The structures of the grafted copolymers were characterized by FT-IR, and the copolymer graft ratio, molecular weight of grafted chain and grafting frequency were tested. The results showed that the micro-wave not only had heat effect but also had non-heat effect during Starch-g-Butyl acrylate copolymerization.

Introduction

Characterized by high efficiency and energy conservation, microwave has been applied in chemical industry and a new subject-Microwave Chemistry has been formed. As a subject which studies the promoted and changed effects of microwave field on chemical reaction, microwave chemistry has become a fast developing front subject-MORE Chemistry(Microwave-include Organic Reaction Enhancement Chemistry)[1,2]. Microwave technology shows many advantages in chemical reaction, chemical analysis, environmental protection and other fields, for example, it can save energy and time, simplify operating procedure, decrease the usage of organic solvent, raise reaction rates and significantly reduce the damage to environment caused by the waste of chemical reaction. Under such a background, researchers began to study the graft copolymerization process of graft starch polymer in microwave field[3-5]. CAI Xi-mei etc. have studied the synthesis of One-pot Multicomponent Condensation of Aldehydes with Cyclic Ketones with microwave radiation, and yielded good results[6]; ZHAO Xue etc. have used microwave to treat wool fabrics, the result indicated that the breaking strength and tear strength of microwave irradiated wool fabrics with different water-retention value both showed a general trend of increasing[7]. All the researches demonstrated that the application of microwave have a good future in textile field.But the researchers didn't separately study the heat effect and non-heat effect of microwave during reaction, and thus they can't really master the mechanism of microwave's promoted effect during starch-g-butyl grafting. The study of the mechanism of microwave promoted effect is a major focus of current research. In this paper, starch-g-butyl acrylate copolymers were prepared under the conditions of microwave and normal heat source. The structures of copolymers was characterized by FT-IR, the grafting ratio, molecular weight of grafted chain and grafting frequency of starch-g-butyl acrylate graft copolymer were tested as well, in this way we will observe the microwave promoted effect during starch-g-butyl acrylate grafting.

1 Experimental

1.1 Chemical agents and apparatus

Butyl acrylate (chemically pure, purity≥98%), Acetone (analytically pure, purity≥98%), Interface agent DMSO (chemically pure Tianjin Jindong Tianzheng Precision Chemical Reagent Factory), Ammonium peroxysulfate (APS: analytically pure); Concentrated HCL(analytically pure); Corn starch, Dongguan DongMei Food Co.Ltd.

PERKIN2ELMER Infrared spectrometer, Soxhlet extractor, constant temperature oven (YHW-1102Yuyao Changjiang Temperature Instrument and Meters Factory), Raytex PM Plus Infrared thermometer.

1.2 Preparation of graft polymer

1.2.1 Graft polymerization process in microwave field

A certain amount of APS was dissolved in de-ionized water and stirred, and mixed uniformly with DMSO, butyl acrylate monomer and starch. Because the mixture contained very little water, it appeared a sub-solid state. Then the mixture was put under microwave field with 110W power and 2450MHz frequency. The mixture was radiated at different time intervals and crude starch graft copolymer was obtained. Fig. 1 is the scheme of homemade microwave reaction device.

The influences of initiator quantity, radiation time, interface agent and monomer quantity on grafted ratio, molecular weight of grafted chain and grafted frequency of the graft copolymerization was studied, and the optimal reaction condition was acquired as following: reaction time is 9-15 min, initiator quality is 3.99% of starch, adequate amount of interface and monomer quality is 33.33% of starch.

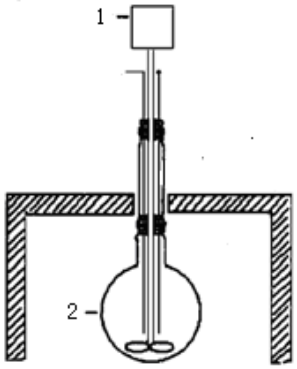


Fig.1 Microwave reaction device
1-Stirring motor, 2-Three-necked flask

1.2.2 Graft polymerization process in normal heat source

A certain amount of APS was dissolved in de-ionized water and stirred, and mixed uniformly with starch, butyl acrylate, APS and interface agent. Because the mixture contained very little water, it appeared a sub-solid state. Mixture was put into a three-necked flask and heated with water bathe heat, thus we obtained the graft copolymer.

The influences of initiator quantity, heating time, interface agent and monomer quantity on grafting ratio molecular weight of grafted chain and grafting frequency of the graft copolymerization was studied, and the optimal reaction condition was obtained: reaction time of graft copolymerization is 60 min, initiator quality is 3.99% of starch, adequate amount of interface agent and monomer quality is 33.33% of starch.

1.3 Separation of graft polymerisate and grafted chain[8]

The crude product prepared under the forehead conditions is the mixture of corn-starch-g-butyl acrylate graft polymer, butyl acrylate homopolymer(PBA) as well as unreacted corn-starch and butyl acrylate. Corn-starch and corn-starch-g-butyl acrylate graft polymer can't be dissolved in acetone, however, butyl acrylate homopolymer (PBA) and butyl acrylate can be dissolved in acetone. According to this principle, the pure graft copolymer can be obtained from extracting for more than 48 hours in Soxhlet extractor.

The pure graft copolymer was put into 1 mol/L HCI, and then reflowed and hydrolyzed for 10 hours. Starch was completely hydrolyzed and degree of hydrolysis was examined by I_2-KI solution, so the grafted chain can be obtained. Hydrolysis solution was filtered by 3# core funnel and then the core funnel was washed by acetone. Distilled the acetone solution and grafted chain was acquired.

1.4 IR spectrum characterizations for grafts

Purified graft copolymers, and PBA were tested by PERKIN2ELMER infrared spectrometer.

1.5 Estimation of grafting ratio[7]

Grafting ratio *G* was calculated from Equation 1:

$$G = \frac{M}{M_0} \times 100\%, \quad (1)$$

where *G* is grafting percentage(%), *M* is the quality of hydrolysis sediment(g) and M_0 is the quality of separated hydrolysis sample(g).

1.6 Test of average molecular weight of grafted chian

Intrinsic viscosity of grafted chain was tested by Ubbelohde Viscometer Capillary and viscosity-average molecular weight of grafted chain was calculated from Mark-Houwink Equation:

$$[\eta] = K \cdot M^{\alpha}, \quad (2)$$

where *M* is the viscosity-average molecular weight, $[\eta]$ is intrinsic viscosity, *K* and α are empirical constants. For butyl acrylate monomer and acetone, $K=14.9\times10^{-2}$， $\alpha=0.52$[8].

1.7 Test of grafting frequency[8]

Grafting frequency, F_g,, is the quantity of average interval glucose units(AGU between two adjacent polymer chain which is grafted onto starch molecular chain and its unit is AUG/branch. Grafting efficiency was calculated from Equation 3:

$$F_g = \frac{(1-G)/162}{G/M_g} \quad (3)$$

where 162 is the molar mass of glucose, g/mol; *G* is grafting ratio, %; M_g is relative molecular weight of grafts.

2 Results and discussion

2.1 Infrared spectrogram analysis of grafted copolymers

MW(PBA-g-S), H(PBA-g-S) and PBA were shown in Fig.2, and they respectively reflected Fourier infrared spectrogram of two kinds of graft copolymer compounded in both microwave field and normal heat source and PBA. As can be seen in Fig.2, graft polymerization and PBA have the same absorption peak near the 1735cm^{-1} which is the feature of $-\overset{O}{\overset{\|}{C}}-$. Because graft copolymer was extracted in acetone and butyl acrylate monomer and its copolymer were completely removed, we can conclude that butyl acrylate had been grafted onto starch and starch-g-butyl acrylate grafted copolymer had been produced.

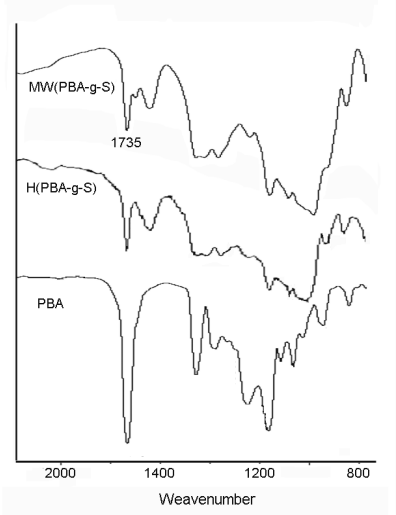


Fig.2 FT-IR spectrogram of starch-g-butyl acrylate and poly *n*-butyl acrylate

Infrared spectrogram shows that grafted copolymerization reaction for starch-g-butyl acrylate can be realized in both microwave and normal heat source.

2.2 Measurement of reaction's temperature

Temperature of reaction system in microwave field was tested by Raytex PM Plus Infrared Thermometer and it was 78.3℃ and the temperature in normal heat source was 95℃.

2.3 Grafted ratio contrast

Two kinds of pure graft copolymer prepared in two different heat sources were weighed separately. Weight of grafted chain can be acquired with the same method stated in section 1.3 and grafted ratio can be calculated from Equation 1. The results showed in table 1.

Table 1 Grafted ratio contrast

Test conditions	Weight of graft edcopolymer [g]	Weight of grafted chain[g]	Graftedratio[%]
Microwave heat source	16.785	3.665	21.83
Water bathe heat source	9.587	0.912	9.51

As can be seen in table 1, grafted copolymerization reaction for starch-g-butyl acrylate can be realized in both microwave and normal heat source. But when initiator category, initiator amount and monomer amount were the same, speed of graft copolymerization reaction and grafted ratio were both higher. Although graft copolymerization reaction can be realized in normal heat source, its reaction time was longer and grafted ratio was lower.

2.4 Molecular weight of grafted chain contrast

Viscosity-average molecular weight of grafted chain prepared in two different heat sources were measured with the same method stated in section 1.6 and results were shown in table 2.

Table 2 Viscosity-average molecular weight of grafted chain contrast

Test conditions	Viscosity-average molecular weight
Microwave heat source	1.160×10^5
Water bathe heat source	1.398×10^5

Table 2 shows that viscosity-average molecular weight of grafted chain produced in microwave field was smaller than that produced in normal heat source, which indicated that microwave can promote butyl acrylate to be grafted faster onto starch.

2.5 Grafted frequency contrast

Grafted frequency of grafted starch was calculated with the same method stated in section 1.7 and results were shown in table 3.

Table 3 Grafting frequency contrast

Test conditions	Grafting frequency[AGU/branch]
Microwave heat source	2564
Water bathe heat source	8211

Table 3 shows that the number of butyl acrylate's grafted sites on starch macro-chain in microwave heat source was far more than that in water bathe heat source.

The above experimental results show that graft copolymerization reaction for starch-g-butyl acrylate can be realized in both microwave and normal heat source. However, under the same conditions, reaction speed and grafted ratio of graft copolymerization reaction were both higher. Although graft copolymerization reaction can be realized in normal heat source, its reaction time was longer and grafted ratio was lower, and grafted ratio can't be increased even if reaction temperature and reaction time are increased. This was mainly because free radicals can be generated by both initiator and butyl acrylate monomer under the condition of water bathe heat. Because there was much difference in hydrophility between starch and monomer, there wasn't enough affinity between them and they repelled each other. Besides, because when ammonium peroxysulfate dissolved in water, it can easily permeate starch's amorphous region, free radicals generated by initiator would firstly oxidize starch and graft copolymerization reaction would happen if radicals meet monomer. Free radicals generated by thermal cracking of butyl acrylate would preferentially combine with butyl acrylate monomer to produce homopolymer, which leaded to low grafted ratio. In microwave induced

reaction, microwave selectively heated polar material, as a result of which initiator promoted starch to generate macromolecular radicals. Because kinetic energy of these macromolecular radicals was very small, both radicals termination can't happen easily and these radicals can only graft onto monomer, as a result of which grafted ratio was higher.

Analysis and experimental results above show that in microwave inducing reaction there were not only more grafted sites on starch long-chains, but also less reaction time needed and higher grafted ratio gained for the graft copolymers. This conclusion can also be demonstrated by the lower grafted frequency under the condition of microwave.

3 Conclusions

(1) Graft copolymerization reaction for starch-g-butyl acrylate can be realized in both microwave and normal heat source. Under the condition of microwave heat source, graft copolymerization reaction for starch-g-butyl acrylate can be realized more easily and we can acquire starch-g-butyl acrylate graft copolymer whose grafting ratio was as high as more than 20%. However, under the condition of non-microwave heat source, grafted ratio was less than 10%.

(2) In microwave inducing reaction, molecular weight of grafted chain was relatively small and this was mainly because microwave can make graft copolymerization reaction for starch-g-butyl acrylate quicker.

(3) In microwave inducing reaction, there were more grafting sites on starch's molecular chain, which was also demonstrated by test results of grafted frequency.

Overall, under the condition of microwave, time of graft copolymerization reaction for starch-g-butyl acrylate was shorter and grafted ratio was higher.

Acknowledgements

This work was financially supported by the The Ministry of Science and Technology of the People's Republic of China Foundation (2009GJG00030) and Shaanxi Bureau of Science and technology(2010ZKC05-03). The project was also suported by Special Foundation Item of the Key Academic Subjects Development of Shaanxi Province[Shaanxi Education Supporting(2008)169].

References

[1]Fan Xingjun, Yu Jinmao, Tan Ganzu, Yu Xianda etc. Progress in Microwave Organic Reaction Enhancement Chemistry. Progress in Chemistry, 1998, Vol. 10(3):285-294,In Chinese.

[2]Sha Yaowu, Han Tao, Shen Lian, Chen Rui. Microwave Promoted Organic Reactions. Specialty Petrochemicals, 2000, 6:21-24,In Chinese.

[3]Wu Hailiang, Li Dongmei, Wu Changchun. Synthesis of Grafted Starch Copolymerization Size for Wool Yarn Sizing in the Microwave Field, 2006 China International Wool Conference and IWTO Wool Forum, China Textile Press, 654-659.

[4]ZHENG Xiao-xia，LUO Yan-bin，CHEN Ze-fang，ZHENG Chang-yi. Grafting of Butyl Acrylate onto Core Starch by Microwave Radiation, Petrochemical Technology, 2000，29（1）：19-22,In Chinese.

[5]ZHNG Hong-mei，CHEN Ling，LI Lin. The Application of Microwave in Starch Modifying, Modern Chemical Industry, 2001，21（5）：60-62,In Chinese.

[6]CAI Xi-mei, WANG Qi-fang, YAN Chao-guo. Efficient Synthesis of Dicycloalkenopyridines：One-pot Multicomponent Condensation of Aldehydes with Cyclic Ketones. Chemical Research in Chinese Universities, 2009, Vol. 25(5), 657-661,In Chinese.

[7]ZHAO Xue, HE Jin-xin, ZHAN Yi-zhen. Study on the Structure and Properties of Wool Fabrics Treated by Microwave. Textile Auxiliaries, 2009, Vol. 26(11): 36-38,In Chinese.

[8]Fan Xuerong, Rong Ruiping, Ji Huijun. Test Technology of Textile Sizing Agents [M], 2007, 2, Beijing: 82-89,In Chinese.

© (2011) Trans Tech Publications, Switzerland
doi:10.4028/www.scientific.net/AMR.331.110

Study on the Mechanical Properties of Jute/Carbon Hybrid Composites

Jianming Wang [1, a], Lei Zhao [1, b],Xiao Qin[1,c]

[1] Yancheng Textile Vocational Technology College, Yancheng, 224005, china

[a]ycfywjm@163.com,[b]zhaolei7365@163.com,[c]qinxiao1980@126.com

Key words: jute fiber, carbon fiber, needled mat, hybrid, mechanical properties, prediction

Abstract: Carbon fibers were used to lay lengthways into three lays in jute fiber needled mat and the same fiber volume content of jute fiber needled mat were fabricated. Those two mats and the lengthways carbon fibers reinforced vinyl resin composites were made by VARTM. We made a comparison of the hybrid reinforced composites between the test value and the theoretical value which was predicted by establishing tensile and bending math-model and their mechanical properties were analyzed. The results show that there was a certain line between the theoretical value and the test value of the hybrid composites, so we can establish the mixing ratio between jute fiber and carbon fiber during the engineering application. Although the use of carbon fibers had greatly enhanced the tensile properties of hybrid composite, whose tensile strength and tensile modulus increased by 85.94% and 30.99% respectively than that without carbons, the bending model can't be changed a lot.

Introduction

As an excellent representative of a large composite family, the hybrid composites not only have the characteristics of the conventional composites, but have many other advantages, i.e., flexible performances design, lower cost, lighter product weigh. The hybrid composites can be widely applied not only in the aerospace industry, automobile industry, and other fields, but as the fine building materials, medical and health materials [1-3]. Jute fiber is a kind of high-performance natural fiber which has high specific strength and specific modulus, so it attract much attraction in the natural fiber reinforced composites.[4]. As a new low-viscosity thermosetting resin, Atlac580 vinyl ester resin has the advantages of unsaturated polyester resin and epoxy resin [1].

N.M.Mehta,etc[5] studied the mechanical properties of jute and biological resources-rice shell, husk, sugar cane and bark reinforced staple hybrid composites. Deng Zong[6] summed up the latest research results of the hybrid effect of FRP at home and abroad and analyzed the theoretical model. In this paper, the mechanical properties of jute/carbon hybrid composites were predicted theoretically. Carbon fibers were used to lay lengthways into three-storey in jute fiber needled mat and the same fiber volume content of jute fiber needled mat were fabricated. Those two mats and lengthways carbon fibers reinforced vinyl resin composites were made by VARTM(the vacuum assisted resin transfer molding method). We made a comparison of the hybrid reinforced composites between the test value and the theoretical value. Meanwhile, those two composites were analyzed about their mechanical properties.

Experimental

1.1 Materials and equipments.

Raw jute fibers provided by Jiangsu Redbud Dyeing Technology Co., Ltd. Jute fiber needled felt prepared by Yixing City, Fei-tech Materials Co., Ltd.; Atlac580 vinyl ester resin provided by JDR; NaOH provided by Shanghai Reagent Factory; H_2SO_4(AR) from Zhejiang Pinghu Chemical Reagent factory ; H_20_2 provided by Shanghai Baorui Chemical Co., Ltd. Mechanical properties tested by WDW-100 microcomputer controlled universal testing machine; SEM tested by Japanese electronics JSM-5600 LV scanning electron microscope.

1.2 Pretreatment of jute fiber

The pretreatment process of jute fiber is as follows[7]: raw jute fiber→soaking water→soaking acid→alkali treatment→H_20_2 treatment→Pickling→washing→dry. The specific parameters of those processes are shown in table.1.

Table.1 The process parameters of pretreatment about jute fibers

Soaking acid(H_2SO_4)			Alkali treatment(NaOH)			H_2O_2 treatment		
concentration/ (g/l)	temperature/℃	time/h	concentration/(g/l)	temperature/℃	time/h	concentration/(g/l)	temperature/℃	time/h
1	55	1.5	20	100	1	20	100	1

1.3 The preparation of jute/carbon hybrid needled mat

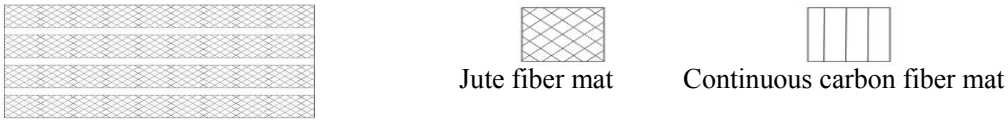


Figure.1 The structure of jute/carbon hybrid needled mat

The structure of jute/carbon hybrid needled mat is shown in Figure.1.Three thin layers of unidirectional carbon lay evenly between jute fibers, carbon fibers lay along longitudinal direction of needled machine.

1.4 The preparation of composites

The one layer jute fiber needled mat, one layer of continuous carbon fiber needled mat and hybrid needled mat reinforced Vinyl ester resin composites were prepared by VARTM [8]. The ratio of vinyl ester resin, methyl ethyl ketone peroxide accelerator and epoxy cobalt initiator is 100:1.5:1.0.

1.5 Testing of composites

Testing of tensile properties of composite is in accordance with GB/T 1447-2005 test; Testing of flexural properties of composite is in accordance with GB/T 1447-2005 test. The fracture surface of composite was tested by SEM.

The establish of mechanical model

2.1 The tensile model of jute/carbon reinforced hybrid composite [2, 6, 9]

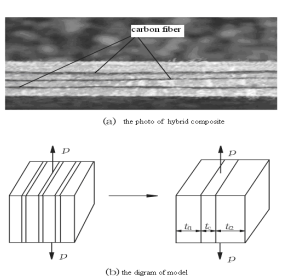
This experiment is a tension test along the plate surface of sandwich structure. We let the three unidirectional carbon fiber concentrated into a layer in the, as shown in Figure.2. Tensile strength (σ) and tensile modulus (E) is calculated as follows:

$$\sigma = \sigma_f \times A_f + \sigma_c \times A_c \tag{1}$$

$$\varepsilon_L = \varepsilon_f = \varepsilon_c \tag{2}$$

$$E = E_f A_f + E_c(1 - A_f) \tag{3}$$

Where σ_f and σ_c represent respectively the strength of panel and core; E_f and E_c represent respectively the modulus of panel and core; ε_L, ε_f and ε_c; represent respectively the deformation of sandwich, panel and core; A_f and A_c represent respectively the percentage of area about panel and core at the cross-sectional area.



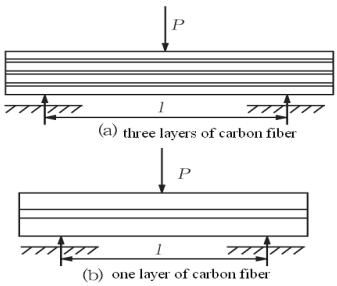


Figure.2 The tensile model diagram of sandwich plate (Left)

Figure.3 The bending model diagram of sandwich plate under concentrated load (Right)

Because of the same deformation condition, the relationship of the load distribution between the panel and core is as follows:

$$\frac{P_f}{P_c} = \frac{t_f \times E_f}{t_c \times E_c} \tag{4}$$

Where P_f and P_c represent respectively the load of panel and core; where t_f and t_c represent respectively the thickness of panel and core.

2.2 The bending model of jute/carbon reinforced hybrid composite [2, 6]

This bending experiment isn't pure plane bending under concentrated load and free shear. We concentrate three layers of carbon fiber into one layer as shown in Figure.3.

According to the normal stress formula of beam, we find the inertia moment of solid rectangular beam, then we solved the inertia moment of panels and of core (J_f and J_c).

$$J_f = \frac{t_f}{4}(t_c + \frac{t_f}{2})^2 \tag{5}$$

$$J_c = 2 \times \int_0^{\frac{t_C}{2}} z^3 dz = 2 \times \frac{z^3}{3}\Big|_0^{\frac{t_C}{2}} = \frac{t_c^3}{12} \tag{6}$$

By mathematical treatment and substituting into the maximum bending moment, we can solve the bending strength(σ_F) under the concentrated load.

$$\sigma_F = \frac{Pl/4}{t_f(t_c + \frac{t_f}{2})} = \frac{Pl}{t_f(2t_c + t_f)} \le [\sigma_{Fb}] \tag{7}$$

The calculation formula of flexural bending modulus about the sandwich plane which isn't pure bending is as follows:

$$E_F = \frac{E_f(t^3 - t_c)^3 \times E_c t_c^3}{\left[E_f(t^3 - t_c^3) + E_c t_c^3\right] \times t^3} \le [E_{Fb}] \tag{8}$$

Where z represent integral variable; l represent the testing span of bending strength; $[\sigma_{Fb}]$ and $[E_{Fb}]$ represent respectively ultimate bending strength and ultimate bending modulus of elasticity

Results and Discussion

3.1 The theoretical value and test value of mechanical properties about the hybrid composite

Table.2 The parameters of the tensile model and the bending model

	A_f/%	A_c%	σ_f /MPa	σ_c /MPa	E_f/GPa	E_c/GPa
Tensile model	84	16	51.43	287.56	1.71	7.44
	p/N	l/mm	t_c/mm	t_f/mm	E_f/GPa	E_c/GPa
Bending model	305	110	1.05	5.46	4.59	0.01

After testing, the required parameters of the tensile model and bending model are shown in table.2.The theoretical value of jute/carbon hybrid composite which was derived by formula (1), (3), (7) and (8) was compared with the measured values; the above results are shown in Table.3. As can be seen from Table 3, there was a certain line between the theoretical value and the test value of the hybrid composites. There exist the situation that the theoretical value is greater than the actual value, i.e., the theoretical value of bending strength of 81.28Mpa is close to the actual measured value of 80.33Mpa. This is mainly because the formula neglects the bending capacity of core during the derivation of the bending strength. The theoretical value of bending modulus is smaller than the test value, because the design of model need sufficient thickness of core, but the three layers of carbon fiber lay in the middle of the jute fiber needled mat, and the model is conversed, as a result, there exists some errors. There is no big difference between theoretical value and actual value of tensile strength and tensile modulus, but the actual value is slightly larger, from Figure.1 we can see that there must exist six layers of interfacial bond strength between jute fiber layers and the carbon fiber

layers when hybrid composites is tested, but it neglect the shear force between jute fiber layers and directional carbon fiber layers during the transformation of the mathematical model, so the theoretical value is small relatively.

Table.3 The theoretical value and test value of jute/carbon hybrid composite

	tensile		bending	
	Theoretical value	Test value	Theoretical value	Test value
strength/MPa	89.21	95.63	81.28	80.33
modulus/GPa	2.17	2.24	4.39	4.63

3.2 Analysis on the mechanical properties of jute/carbon reinforced hybrid composites

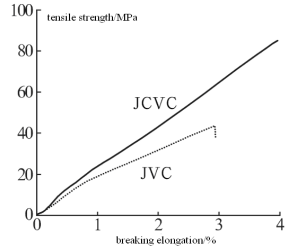
The jute fiber reinforced composites and hybrid reinforced composites recorded JVC and JCVC separately, the mechanical properties of those composites are shown in Table.4; The tensile stress-strain curves and the bending stress-deflection curve of those composites are shown respectively in Figure.4 and Figure 5 .

It can be seen from Figure 4 that JVC and JCVC have two different breaking states.The tensile strength of JVC doesn't increase with the increase of the deformation when the tensile strength reach the maximum but abruptly reduce to the minimum value, then the composite was broken. While the tensile strength of JCVC increases with the increase of the deformation, and JCVC is broken directly when the tensile strength reach the maximum. Moreover, the area of JCVC under stress-strain curve is larger relatively, which indicate that hybrid composites need to absorb more energy when they are subject to the tensile test. From Figure.4 we also can see that the tensile modulus of the composite is enhanced because of the addition of carbon fiber. They are because the reinforced unidirectional carbon fiber in JCVC can endure tensile stress well [6]. From table.4 we can find that tensile strength of increased by 85.94%from 51.43MPa to 95.63MPa, while the tensile modulus of JCVC increased by 30.99% from 1.71GPa to 2.24GPa.

It can be seen from Figure.5 that the initial slope of bending-deflection curve about JCVC is same to that of JVC, which indicate that the addition of carbon fiber doesn't affect the modulus of composites significantly, because the force mainly concentrate on the outer layer when the JCVC is subject to bending performance testing, so the bending modulus of JCVC close to that of JVC .Moreover, JVC has more larger bending deflection, while JCVC have higher bending breaking strength and the area under bending stress-strain of JCVC is larger relatively, this indicate that the addition of carbon fiber has effectively improved the flexural toughness of the composite.

Table.4 The mechanical properties of composites

	Tensile		Bending	
	strength/MPa	modulus/GPa	strength/MPa	modulus/GPa
JVC	41.39	1.71	77.07	4.67
JCVC	95.63	2.24	80.33	4.63



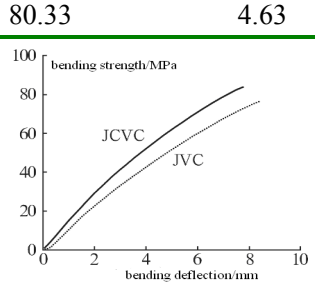
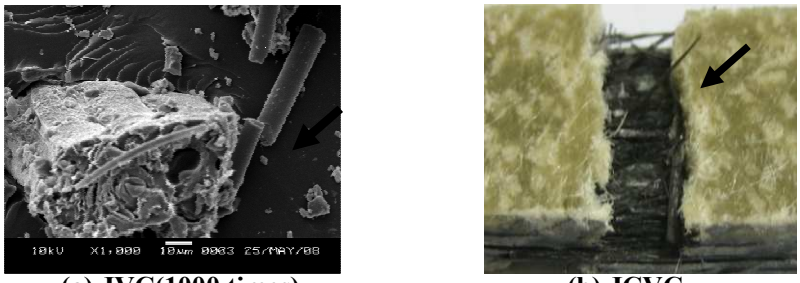


Figure.4 The tensile stress-strain curve of the composites(Left)

Figure.5 The bending stress-deflection curve of those composites(Right)

3.3 Analysis on the interface morphology of jute/ carbon Hybrid Composites



(a) JVC(1000 times) (b) JCVC

Figure.6 The cross-section and the morphology of tensile breaking about composites

The SEM of tensile cross-section about JVC and the morphology of tensile breaking about JCVC are shown in Figure.6.It can be seen from Figure.6 (a) that there exist much resin on the surface of fiber which is pulled off. This is mainly because the interfacial compatibility between the treated fibers and resin is improved. From Figure.6 (b) we can find that the jute/carbon reinforced composite has been broken into two splits, but there still exist some connection because of the adhesion and the carbon fibers isn't completely pull off.

Conclusions

There was a certain line between the theoretical value and the test value of the hybrid composites, so we can establish the mix ratio of fiber during the engineering application. But there is a minor error between the theoretical value and the test value, because it neglects the shear force and other factors between the interfaces when we design the mathematical model, so the model needs to be studied further. There are two different breaking modes about jute fiber reinforced composite and hybrid reinforced composites, and there is great change of the initial slope about the two composites. These results indicate that the addition of the unidirectional carbon fibers improve the modulus of composites greatly. The tensile strength and tensile modulus of the hybrid composite increased by 85.94% and 30.99% respectively than that without carbons, the bending model can’t be changed a lot.

Acknowledgements

The authors want to thank Yancheng Textile Vocational Technology College for financial support of this investigation.

References

[1] Zhao L,Yu Jiany, Surface treatment of jute fiber and the mechanical properties of jute fiber mat reinforced composites. Technical Textiles, 2009, 10, 10–15.

[2] Song Huanc,Hybrid fiber composites, Beijing university of Aeronautics and Astronautics Press, Beijing ,1988.

[3] Lu Bo, Natural Fiber Composites.Beijing, Chemical Industry Press, Beijing, 2005.

[4] Huang Gu, Modern Textile Composites, China Textile Press, Beijing, 2002.

[5] N. M. Mehta，P. H. Parsania,Fabrication and evaluation of some mechanical and electrical properties of Jute-Biomass based hybrid composites, Journal of Applied Polymer Science,2006,100:1754–1758.

[6] Deng Zongc, Li Jianh, Rsearch and Developmeny of Hybrid Effect of Hybrid FRP Composites,Fiber Reinforced Plastic/Composites, 2008,1: 9–13.

[7] Jin Jiayan,Cheng, A Study on Jute Fiber Reifining Methods, China Textile Leader, 2006,4,60–64.

[8] Diao Yan,Chen Yimin,The Application of Vacuum Assisted RTM and its Favourable Resin System, Chinese Polymer Bulletin, 2006, 12: 84–88.

[9] RAY D, The mechanical properties of vinyl ester resin matrix composites reinforced with alkali-treated jute fibers, composites (part A), 2001,32: 119–127.

© (2011) Trans Tech Publications, Switzerland
doi:10.4028/www.scientific.net/AMR.331.115

Exploration on the Production of Natural Green Anti-bacterial Health-care Textiles

Yi Weng[1,a]

[1]Zhejiang Textile Fashion College, Ningbo, Zhejiang Province, China

[a]wengyi8839@126.com

Key Words: anti-bacterial, textiles, production

Abstract. Chitosan has the function of anti-bacterial, and it can produce natural green anti-bacterial health-care textiles. However, after the finishing process, the fabrics properties are influenced as well. With the experiments, we study the impaction of chitosan on the fabrics properties. The results indicate: the anti-bacterial performance is good after the finishing process, and the shrinkage has been greatly improved.

Introduction

The textiles provide a good medium for the microbial adhesion and spread, as a result, with the development of science technology and improvement of living standard, the textiles require for more and higher demands on the antibacterial antifungal treatment world-widely. Since we have entered the WTO, to make our country transform from big textiles country to strong textiles country, upgrade the additional textiles value is one of the very important means. Therefore, our country should follow the development trend of world textiles, and participate in the international market competition with products that yields high added value and produced with advanced technology.

Chitosan is a natural polycation polysaccharide, and the product of chitin deacetylation. Chitin consists in shell of crustaceans, insects and other invertebrates, cell wall of algae and fungi. The structure of chitosan is similar to cellulose, and hydroxy is substituted by a more lively Amino. Chitin is rich in resources, which is the second largest biological resources only after cellulose on the earth. The bio-synthesis is amount to 10 billion tons per year, which appears to be inexhaustible [1,2].Meanwhile, since it is natural, and has good biocompatibility, application study is active world-widely. The application field has been penetrated into industry, agriculture, environmental protection, national defense, and other aspects of living. In the textile field, people pay more attention to the chitosan application, and make researches on its excellent performance. As a member of Chitin Application Team, we utilize its excellent antibacterial property, and explore on the natural anti-bacterial health-care textiles. After a series of tests, we successfully developed the industrialized pilot testing products. This article mainly discuss about this.

The Antibacterial Mechanism of Chitosan

Basically, the chitosan has two antibacterial mechanisms: The mutual attraction between amino cation of chitosan and anions of sialic acid phospholipid in microorganism cell wall constraints the microbial freedom, impedes the metabolism and reproduction[3];The chitosan molecules of quite low molecular weight invade the microbial cells, and impede the genetic code of microbes replication from DNA to RNA, thus impede the propagation of microorganisms [4].

The development of the anti-bacterial health-care textiles is mainly proceed from the textile finishing application of chitosan. In the small scale experiments, on the premise of maintaining the antimicrobial properties of textile fabrics, we successfully solve the technical problems such as the stiff feeling and yellow discolouration after chitosan dispose, and make some progress in textiles wrinkle-free, shrink-proof performance. And we finally successfully develop the pilot testing products.

Test Portion

Raw material. Chitosan, acetic acid for industrial use, medical gauze, raschel blanket, knitted fabrics and gripper jacquard and so on.

Solution preparation. Chitosan powder down → water → acetate → stirring →quiescence defoaming

Treatment craft. Conditioning fluid **p**adding infiltration →$NaHCO_3$ treatment →washing →softing→drying → finishing

Craft prescription. Acetic acid: 1%; Chitosan: a variety of concentrations

Test results. To enable the textile finished by chitosan has the antibacterial effect, without affecting its original physical properties, we conducted a number of comparison tests with various chitosan concentrations. The representative 14.6tex × 27.8tex 551 × 295 cotton waffle shrinkage test is shown in Table 1 and Figure 1. JC 27.8 tex×2 250g·m^{-2} knitted fabrics shrinkage test is shown in Table 2 and Figure 2. And 9.7tex × 14.6tex 677 × 465 cotton jacquard WRA test is shown in Table 3 and Figure 3.

Table 1 The Shrinkage of Cotton Waffle Comparison Test

Washing times	Shrinkage of different concentrations of chitosan（%）				
	0.0%(Original Sample)	0.1%	0.3%	0.5%	1.0%
1	-2.9%	-2.0%	-1.7%	-1.2%	-1.4%
2	-3.4%	-2.7%	-2.1%	-1.8%	-1.5%
3	-4.0%	-2.9%	-2.6%	-2.0%	-1.9%

(①equipment in use: YG701N automatic shrinkage testing machine; ② Test Standard: GB / T 8629-2001 Textiles Trial domestic washing and drying process)

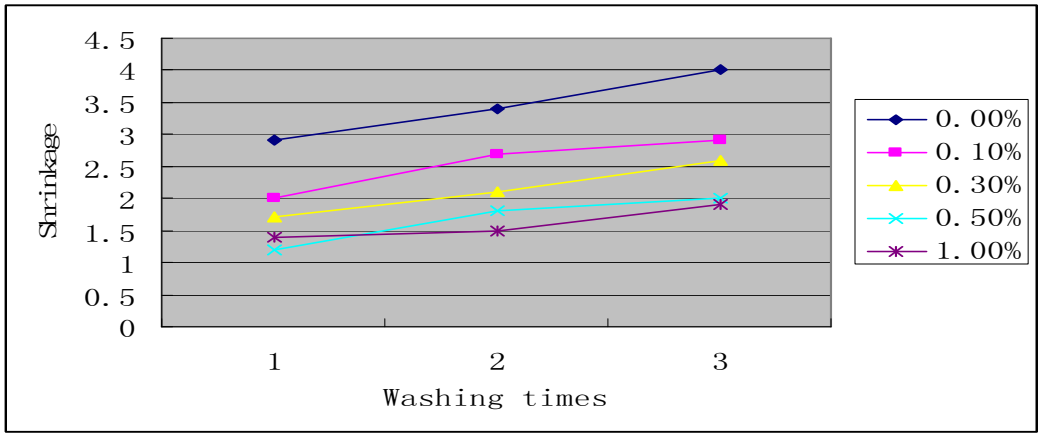


Fig.1 The Shrinkage of Cotton Waffle

Table 2 The Shrinkage of Cotton Combing Knitted Fabric Comparison Test

Washing times	Shrinkage of different concentrations of chitosan（%）				
	0.0%(Original Sample)	0.1%	0.3%	0.5%	1.0%
1	-4.6%	-3.5%	-2.9%	-2.5%	-2.4%
2	-5.1%	-4.1%	-3.2%	-2.7%	-2.5%
3	-5.5%	-4.4%	-3.5%	-3.0%	-2.8%

(①equipment in use: YG701N automatic shrinkage testing machine; ② Test Standard: GB / T 8629-2001 Textiles Trial domestic washing and drying process)

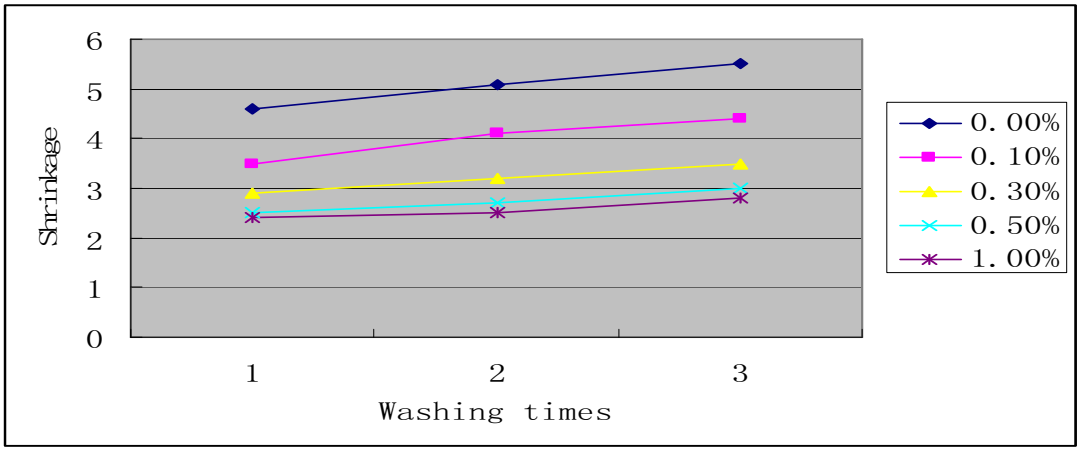


Fig.2 The Shrinkage of Cotton Combing Knitted Fabric

Table 3 Cotton Jacquard WRA Comparison Test

Recovery angle	chitosan concentration（%）				
	0.0%(Original Sample)	0.1%	0.3%	0.5%	1.0%
warp (°)	58.2	58.3	59.6	58.7	51.3
weft (°)	64.7	67.1	68.3	61.5	58.9
warp+weft(°)	122.9	125.4	127.9	120.2	110.2

(①equipment in use: M003A wrinkle recovery angle tester; ② test standard: GB/T3819-1997 textile fabrics Determination of fabric crease resilience recovery angle method)

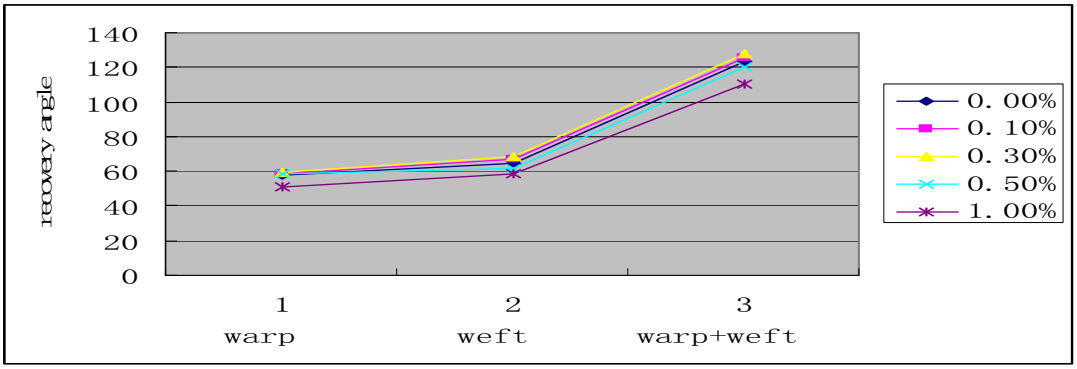


Fig.3 The Recovery Angle of Cotton Jacquard WRA

The overall results show that the anti-shrinkage increase by 25% on average, rebound resilience recovery rate is about 60-70%. The flexibility is increased, and other physical parameters are similar to the ordinary textiles, while with the increase of chitosan concentration, there is a trend that hand feeling become worse. When the concentration is more than 0.3%, the fabric elasticity will cause adverse effects.

Antibacterial properties. We test the chitosan treated fabric with SBZ 1036-96 non-leaching antibacterial hygienic products effect test method. The results show that when the chitosan concentration is above 0.3%, it has excellent antibiotic property of Escherichia coli and Staphylococcus aureus; the antibiotic property is still good after soap 50 times. The comparison between antimicrobial agents treated textiles and chitosan treated textiles is shown in Table 4.

Table 4 The Comparison Between Two Textiles with Different Treatment

Comparison Items	Chitin /Chitosan Textiles	Textiles Treated with Antibacterial Agents
Antibacterial Effect	good	good
Antibacterial Perdurability	long	ordinary
Antibacterial Effect washability	washable	not washable
Impact on human body	no sensitization	side effects
Impact on Physical properties	improve the elasticity and shrink resistant property	none

Taking all factors into account, 0.3% -0.5% chitosan concentration is more appropriate.

Conclusions

From the test, the fabric treated with chitosan, after washing 50 times, the cross-link between the chitosan and the fabric is relatively stable and solid.

After treated with chitosan, the fabric shrinkage improved significantly, which provided conditions for the chitosan to substitute resin finishing.

This project has simple craft, high function and added value, meanwhile, it is easy to operate. According to the preliminary estimate, textiles treated with chitosan, the additional cost increased by 3%, while the price increased by more than 10%, the economic benefits is remarkable. At the present time, the chitin raw material is expensive, this craft is of great practical significance and promotional value.

Chitosan has broad-spectrum antibacterial effect, and it can inhibit various bacteria and fungi.

The craft technology of chitosan development in the textile industry is feasible and correspondence with the contemporary health care and environmental protection trend, it can also increase the technical contents of textiles, and improve the textile products quality.

References

[1] Ying X, JY Chen. Research on the combination of chitosan and cellulose and its Antibacterial Properties [J], Dyeing & Finishing, 2002, 28(2):p.1.

[2] FX Hu, KY Dong. Advances in Development and application of functional textiles (Part 1). China Textile Leader, 2003, (3):p.40

[3] BW Chen, F Zhou, JM Guo, etc. Research on the antibacterial property of Chitosan and its derivatives finishing fabrics [J], Journal of Textile Research, 2003, 24(4):p.55.

[4] P Zhu, HN Lv, B Wang, etc. Research on the cotton fabrics multi-functional finishing of Chitosan and BTCA [J], Dyeing & Finishing, 2004, 30(11), p.10.

© (2011) Trans Tech Publications, Switzerland
doi:10.4028/www.scientific.net/AMR.331.119

Influence of Mechanical Properties of Lightweight Silk Fabrics on Seam Shrinkage

Qiao-Ying Wu [1,2 a], Wen-Bing Zhang [1,b]

[1] Fashion College, Dong Hua University, West Yan-An Road, Shanghai, P.R.China

[2] School of Fashion, Zhejiang Sci-Tech University, Hangzhou, Zhejiang, P.R.China

[a]bettywu2000@126.com, [b]zhangwen@dhu.edu.cn

Keywords: seam shrinkage, seam pucker, lightweight silk fabric, mechanical properties.

Abstract. The purpose of this article is to study the effects of mechanical properties on seam shrinkage of lightweight silk fabrics. Thirty five silk fabrics are used for experiment. Mechanical properties of the fabrics on warp and weft directions were tested by FAST instrument. Seam shrinkage rate were tested. Curve regressions were used to analyze the influence of mechanical properties on seam shrinkage. The results showed that the bending rigidity and extensibility were closely correlated with the seam shrinkage rate, while the formability and rigidity were not the main factor of affecting the seam shrinkage of the light-weight silk fabric. The regression equations of bending rigidity and seam shrinkage rate, extensibility and seam shrinkage rate were obtained.

Introduction

Seam pucker problems in lightweight silk fabric are serious in garment manufacturing plant, reducing the aesthetic value and degrading quality of garment. With the increasing demand for quality products from market, it's an absolutely emergency to solve this problem and to improve the sewing quality of silk garments. For several decades, much research has been conducted to solve the problem in garment manufacturing. In 1997, De Boos AG summarized influences of wool fabric properties on tailoring performance and proposed that fabric weight and mechanical properties under low stress influenced tailorability of wool fabric [1]. In 1998, Tasaki K et al. reported that seam pucker level was relative with fabric properties such as fabric weight, thickness, extensibility, and bending rigidity, however, the relationships between fabric properties and seam pucker were difficult to describe quantitatively by multiple regression equation [2]. In 1998, Kawabata S et al. considered seam shrinkage as the cause of seam pucker level and derived equation to express the relationship between seam shrinkage and pucker level [3]. Many researchers have been working on seam pucker problems in lightweight fabrics [4-13]. However, researches on influences of fabric properties on seam pucker were not sufficient since fewer amounts of experimental fabric samples involved.

In this paper, thirty five common used lightweight silk fabrics were chosen to conduct experiment and the curve regression were used to find out the effect of mechanical properties on seam shrinkage.

Experimental

35 lightweight silk and silk type fabrics were tested, including pure silk fabrics, silk/cotton blended fabrics, and polyester fabrics sold on market. Fabric thickness was tested by FAST instructment under pressure of 2cN/ cm^2. Basic properties of experimental fabrics were as follow: warp density 30~120 warp/cm, weft density 27~80 weft/cm, warp yarn count 1.67~9.33tex, weft yarn count 3~15tex, thickness 0.064~0.374mm, and weight 23~95 g/m^2.

Fabric mechanical properties were tested and calculated by FAST instrument under standard conditions [14]. Implications and contents of the mechanical properties were described in table 1.

To prepare the specimens for seam pucker study, the fabrics' stripes of 350×6mm dimensions were cut in warp and weft directions. The sewing conditions were as follows: stitch type, 301; stitch length, 2mm; needle, DB×1(ball point type), no.7 size (Organ Co.); sewing threads, polyester thread with 9.8×2tex; sewing machine, DDL-8500-7 (Brother Co.).

Table 1 Implications and contents of the mechanical properties

Symbols	Characteristic value	Unit	Symbols	Characteristic value	Unit
E5	Extension at 5 cN/cm	%	B	The bending rigidity	μN.m
E20	Extension at 20 cN/cm	%	F	Formability	mm^2
E100	Extension at 100 cN/cm	%	G	Shear rigidity	N/m

Two stripes at same directions (θ + θ) were sewn together across the center line in longitudinal direction without external tension added at the edge of the fabric sample to avoid influence of operator. Three specimens of same directions were sewn. The sewing experiments were done in silk garment manufacturing factory by the same experienced sewer. The seam shrinkage rate (SS) was used for objective evaluation of seam appearance level. We can calculate SS from equation (1) [4]:

$$SS=（L0- L1）/ L0\times 100\%. \quad (1)$$

Where, L0 is the length of specimen before sewing and L1 is the length of specimen after sewing.

Results and Discussion

Influence of bending rigidity on seam shrinkage. To exam the relationship between the bending rigidity and the seam shrinkage rate, the bending rigidity versus seam shrinkage rate of warp-wise samples and weft-wise samples are shown in figs. 1 and 2, respectively. By fitting the above data using power function, the regression models of bending rigidity (B) with seam shrinkage rate (SS) were obtained as Eqs. (1) and (2).

$$SS1=2.67(B1^{0.48}), \quad r=0.85 \quad (1)$$

$$SS2=1.23(B2^{0.35}), \quad r=0.51 \quad (2)$$

Where, r is the correlation coefficient. It can be seen that with the increasing of bending rigidity, the seam shrinkage rate show the similar variation trends for warp-wise and weft-wise samples, that is, the seam shrinkage rate has decreased much faster at the beginning, and then gradually level off, which indicates that bending rigidity is closely correlated with the seam shrinkage rate.

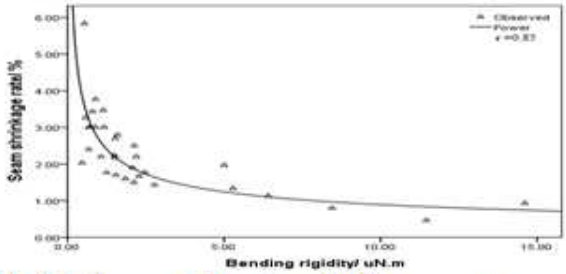


Fig.1 Influence of bending rigidity on seam shrinkage rate of warp-wise samples

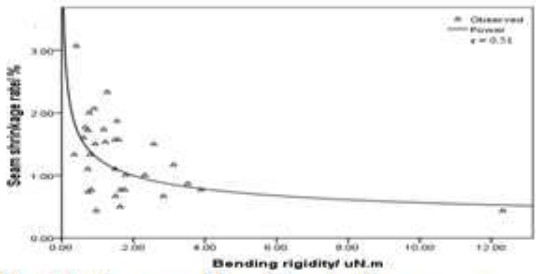


Fig.2 Influence of bending rigidity on seam shrinkage rate of weft-wise samples

To probe into the influence of yarn direction of fabric on seam shrinkage rate, using linear relation to fit the data, the regression model of bending rigidity (B) and yarn direction (warp-wise: direction=1; weft-wise: direction=0) with seam shrinkage rate (SS) were obtained as Table 2.

Table 2 Regression model of bending rigidity and yarn direction with seam shrinkage rate

Model	Understandard coefficients	Standardized coefficients	t	Sig.	r
(Constant)	0.27		4.10	0.000	0.79
Yarn Direction	0.71	0.61	7.76	0.000	
ln(B)	-0.43	-0.60	-7.60	0.000	

a. Dependent Variable: ln(SS)

It can be seen that yarn direction and bending rigidity have significant impact on seam shrinkage rate. Furthermore, fabric in warp-wise direction (direction=1) shows larger seam shrinkage than fabric in weft-wise direction, while increasing bending rigidity could result in decreasing rate of seam shrinkage.

Influence of extensibility on seam shrinkage. To exam the influence of extensibility on seam shrinkage, the extensibility under constant load of 100 $cN.cm^{-1}$ and the seam shrinkage rate of warp-wise samples and weft-wise samples were investigated. The results are shown in figs.3 and 4,

respectively. The data of warp-wise samples are fitted by using quadratic function, while the data of weft-warp samples are fitted by using cubic function. The regression models of extensibility (E) with seam shrinkage rate (SS) were obtained as Eqs. (3), (4).

$$SS_1 = 0.66 + 1.15 \times E_1 - 0.12 \times E_1^2, \quad r = 0.71 \tag{3}$$

$$SS_2 = 0.08 + 1.37 \times E_2 - 0.32 \times E_2^2 + 0.02 \times E_2^3, \quad r = 0.83 \tag{4}$$

It can be seen that for warp-wise samples, the seam shrinkage rate increases with extensibility increasing from 0 to approximately 5%, and then decreases. On the other hand, for weft-wise samples, the seam shrinkage rate increases with extensibility increasing from 0 to approximately 3%, and then decreases. The extensibility shows significant impact on the seam shrinkage rate.

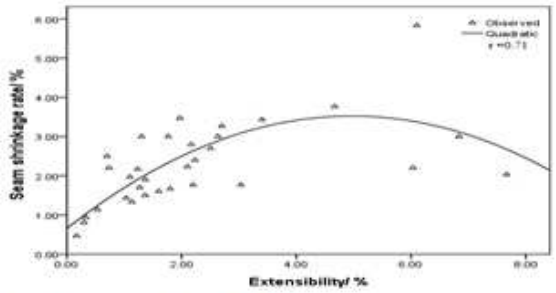


Fig.3 Influence of extensibility on seam shrinkage rate of warp-wise samples

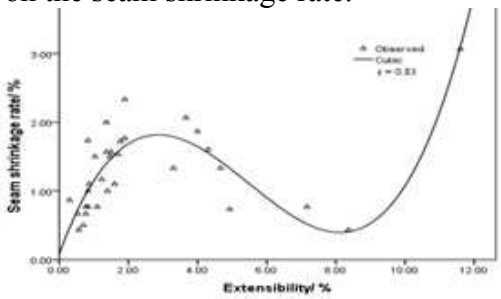


Fig.4 Influence of extensibility on seam shrinkage rate of weft-wise samples

Influence of formability and shearing rigidity on seam shrinkage. Figs. 5 and 6 demonstrate the relationship between formability and seam shrinkage. As can be seen, the formability, most of which is smaller than 0.1mm^2, is very weakly correlated with the seam shrinkage rate. Thus we may conclude that since the variation of formability among lightweight silk fabric is very small, the formability is not the main factor of affecting the seam shrinkage of the light-weight silk fabric. Figs. 7 and 8 demonstrate the relationship between shearing rigidity and seam shrinkage. As can be seen, the shearing rigidity is very weakly correlated with the seam shrinkage rate.

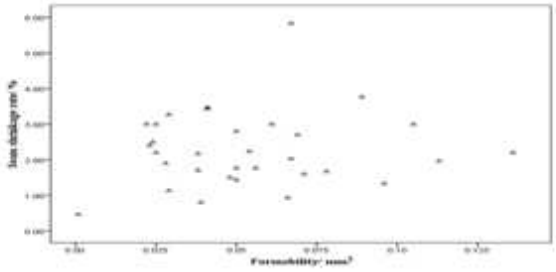


Fig.5 Influence of formability on seam shrinkage rate of warp-wise samples

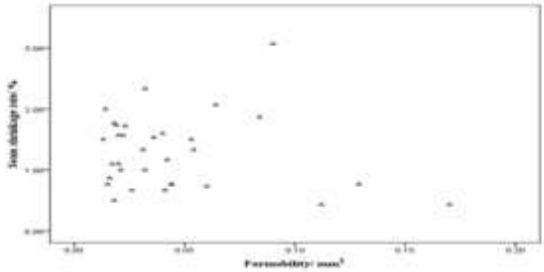


Fig.6 Influence of formability on seam shrinkage rate of weft-wise samples

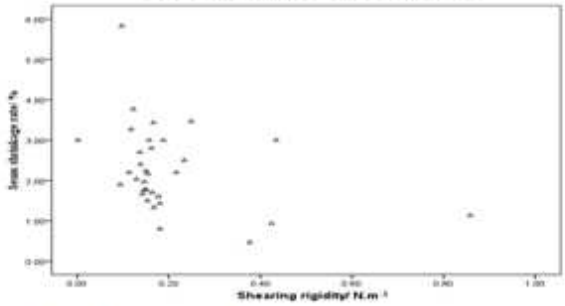


Fig.7 Influence of shearing rigidity on seam shrinkage rate of warp-wise samples

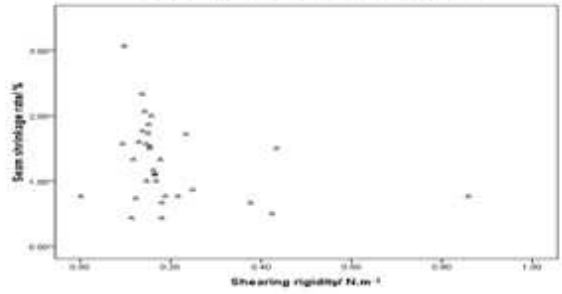


Fig.8 Influence of shearing rigidity on seam shrinkage rate of weft-wise samples

Conclusions

The formability and rigidity are not the main factor of affecting the seam shrinkage of the light-weight silk fabric. The bending rigidity and extensibility have significant impact on the seam shrinkage rate. Increasing bending rigidity could result in decreasing rate of seam shrinkage, meanwhile, with increasing bending rigidity, the seam shrinkage rate has decreased much faster at the beginning, and then gradually level off. For warp-wise fabrics, the seam shrinkage rate increases with extensibility increasing from 0 to approximately 5%, and then decreases, while for weft-wise fabrics, the seam shrinkage rate increases with extensibility increasing from 0 to approximately 3%, and then decreases. The results also show yarn direction has significant impact on seam shrinkage rate. Fabric in warp-wise direction has larger seam shrinkage than fabric in weft-wise direction.

References

[1] A.G. De Boos. The Objective Measurement of Finished Fabric. In: Brady PR, editor. Finishing and Wool Fabric Properties. A Guide to the Theary and Practice of Finishing Woven Wool Fabrics. CSIRO: IWS, 1997, pp.44.

[2] K.Tasaki and T. Kanamitsu. Seam Pucker Prediction from Fabric Properties and its Preventive Method. J Text Mach Soc Jap, 1998, Issue 1, pp.107-112.

[3] S. Kawabata and M. Niwa, Clothing Engineering Based on Objective Measurement Technology. Int J Clo Sci Tech, 1998, Issue 10, pp.263-272.

[4] Qiaoying Wu, Wenbin Zhang, Chunsheng Wu, et al. Investigation of Seam Pucker in Lightweight Silk Fabric (Part1): Relationship between Seam Appearance and Properties of Lightweight Silk Fabric along Diagonal Directions. Proc. TBIS 2010, pp. 620-660.

[5] G. Stylios and J.O. Sotomi, Investigation of Seam Pucker in Lightweight Synthetic Fabric as an Aesthetic Property (Parts I, II). J Text Inst, 1993, Issue 4, pp. 593-607.

[6] Y. Yamada , M. Mori, M. Niwa, A Study of Seam Puckering. Prediction of Seam Puckering of Ladies' Thin Dress Fabrics Based on Mechanical Properties. Journal of the Japan Research Association for Textile End-Uses, 1995, Issue 36, PP.45-53.

[7] S. Kawabata and M. Niwa. Objective Evaluation of the Quality of Ladies' Garment. Int J Clo Sci Tech, 1992, Issue 4, PP. 34-39.

[8] M. Niwa and Y. Yamada, Prediction of Seam Pucker of Shingosen Fabrics Woven with Micro Denier Fibers. Int J Clo Sci Tech, 1991, Issue 3, PP.7-18.

[9] C.S. Park. A Study of Seam Puckering in Thin Fabrics. Kor Soc Clo Textiles, 1997, Issue 1, pp. 23-28.

[10] V.Dobilaitė and A. Petrauskas, The Effect of Fabric Structure and Mechanical Properties on Seam Pucker. Material Sience 2002, Issue 8, pp.495-499.

[11] JianzhongYang, Shanyuan. Study on the Relationship between Seam Appearance and Mechanical Properties of the Lightweight Fabric along the Bias Direction (In Chinese). J NW Inst Text Sci Tech 2001, Issue 15, pp.16-19.

[12] Hong Tang, Study on Properties of Silk Chiffon and its Seam Puckering Directions (In Chinese), J Tex Res , 2008, Issue 26, pp.87-91.

[13] Xuelian Gao, Qiaoying Wu , Lili Wu. Research on the Relationship between Properties of Structure, Physics, and Mechanics and Seam Puckers of Thin Silk Fabrics (In Chinese). Silk, 2011, Issue 3, pp. 22-25.

[14] D. Tester, Application of FAST to Fabric and Garment Manufacture. CSIRD press, 1988, pp.25.

© (2011) Trans Tech Publications, Switzerland
doi:10.4028/www.scientific.net/AMR.331.123

Statistical Property of Ideal Drafting Sliver

Yu-Heng Su[a], Win-Lin Zou[b], Guang-Song Yan[c]

Henan Institute of Engineering, TongBai Road, ZhengZhou, Henan Province, 450007, China

[a]fzsyhsyh@126.com, [b]wenlinzou@163.com, [c]gsyan_2005@163.com

Keywords: Ideal Drafting, Sliver, Statistical Property, Simulation

Abstract: Given the fiber length distribution, the strand in back roller nip is generated by the stochastic method and the virtual ideal drafting process is achieved by computer program. Two different ideal slivers are simulated according to the ideal drafting virtual process, and the statistical properties of the ideal sliver are discussed. The hypothesis test method is used to judge the distribution of the number of fiber in the cross section of silver. The result indicates that the CV of the ideal drafting slivers are near the value of Martindale's limit evenness, the number of fibers in the silver cross section follows the Poisson distribution when all fibers are identical in length and the variant of that number in fiber sliver follows the Normal distribution, where the second point puts forward the challenge to the traditional theory.

Introduction

In the spinning process of staple yarns, because the fiber could not be precisely controlled, there are less or more unevenness in the resulting sliver. So the studying of the ideal sliver plays the important role in the research of evaluation and test of yarn unevenness. The ideas of ideal sliver were pointed out first by Martindale in 1945. In that research, the ideal sliver is defined as the sliver in which the fibers are arranged in the sliver as random as possible and the opportunity of any fiber appearing in any position of the sliver is equal. According to these ideas, it is assumed that the number of fibers in sliver cross section follows Poisson distribution, the formula of limit of the lower bound for yarn unevenness is established. This formula is the basis of the theory of sliver unevenness [1]. In 1961, Rao made the strict mathematical definition about the ideal sliver, and pointed out four base cases, established the mathematical model and analyzed the statistical property and power spectrum of the ideal silver, and firstly suggested the method to describe the character of the fiber alignment in a sliver using the distribution of fiber ends(right or left)[2]. Qiu introduced the stationary processes and the time windows to the fibers, weakened the Rao's cases and made a new mathematical model. Based on this model， more complicated statistical properties of the ideal sliver are discussed. But with no precise fiber distribution, all application and validation of the model were made in the case of identical fibers in length, therefore the results don't totally satisfy the actual situation[3,4].

Along with the development of the modern testing technology, such as HVI, AFIS and Premier aQura, large capacity fiber samples can be tested accurately in a short time, and the length-number or length-heavy distribution histogram can be easily obtained. Lin and Yan fitted the fiber length distribution by using the nonparametric kernel estimation method, promoting the spinning basic research of the structure of fiber alignment in fiber assembly, and the sliver irregularity and the moving law of fiber in drafting zone [5]. Simulating the random event by using computer is an important method to solve the complex scientific problems, it could weaken many assumption, and simplify the complex calculation, and solve the difficult equations [6].

There are many strict assumptions in the study of ideal slivers, for example, the number of fiber in the sliver cross section follows the Poisson distribution and the linear density of fiber must be a strong stationary random process etc., in fact, the sliver is completed by using the roller drafting to rearrange the fibers, so under the virtual ideal drafting situation, a drafting sliver can be simulated using the method called ideal drafting sliver, and then the difference or consistency between tow ideal slivers can be discussed.

In this subject, we assume that all fibers in the sliver are straight, parallel to the axis, and accelerated at the same position in the roller drafting zone, for the given the fiber length distribution. The strand in back roller nip is generated by the stochastic method, and the virtual ideal drafting process is achieved by computer program. Two different ideal slivers are simulated according to the ideal drafting virtual process, and thus the statistical properties of the ideal sliver are discussed.

Simulation of Ideal Drafting Sliver

The Fiber Length Distribution at One Side of the Back Roller Nip. For variant fiber in length, Hertel presented the theory of fibrogram, it says that when we hold fibers randomly by comber, measures the one side fibers length and volume out of the holding line[7], there is a certain relationship between the value measured and the distribution of fiber length, and it is shown that:

$$R(l) = \int_{l}^{w}\int_{l}^{w} f_n(l)dldl \tag{1}$$

Where $f_n(x)$ is the fiber length distribution density function; w is the maximum fiber length(mm); $R(l)$ is the fiber length distribution curve twice integrals.

Su etc. got the fiber length distribution density function of the fiber out of the roller holding line, when they simulate the motion of fibers in the drafting zone[8,9], it is shown that:

$$v(l) = \frac{\int_{l}^{w} f_n(l)dl}{\int_{0}^{w}\int_{l}^{w} f_n(l)dldl} \tag{2}$$

For equal length fiber distribution, the length out of the holding line of equal length fibers follows the uniform distribution at $0-l$, the density function is shown that:

$$v(l) = \frac{1}{l} \tag{3}$$

Simulation of the Ideal Drafting Process

According to the traditional drafting theory, ideal drafting process is defined as all fibers in the strand that are completely straight, parallel and identical in length, every fiber is accelerated on the same position in the drafting process, namely, all the fiber heads complete the movement at back roller surface speed and are accelerated on the front roller nip or a fixed position in drafting zone, so the relative displacement between fibers would not be influenced by the shifting deviation, therefore the ideal drafting slivers are obtained.

Assuming the back roller nip as coordinate point and the X axis pointing front roller in single area simple roller drafting zone, a coordinate system is established. For a given fiber distribution, the number of fibers and the fiber length of one side can be randomly generated by Monte Carlo method, then these fibrous head coordinates can be fixed. The distribution histogram of variant fibers can be got by drawing out cotton samples and testing on the Premier Large capacity cotton detector made in India, and the distribution function can be fitted by using nonparametric kernel estimation method, these curves are shown as figure 1.

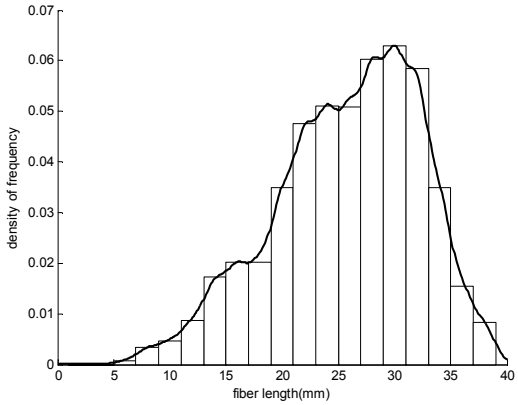


Fig 1. The histogram and density function curve of fiber length

Suppose T is the total time of the fiber bundle passing through the whole drafting zone, the value of T would be guarantee all fibers in back roller nip moving away the front roller nip, and the known linear velocity of the back roller as v_1 and that of the front roller as v_2, then the position coordinate of all fibers can be calculated after T. The distance between the Max coordinate of fiber heads and the Min coordinate of fiber tails is the resulting sliver length, counts the number of fiber in various cross section of this end sliver, the distribution curves of the number of fibers in cross section can be got, the curves of the variant fibers and identical fibers are shown as figure 2 and 3. Here the total fibers are 50000, the distance of drafting zone is 40mm, the drafting ratio is 1000, the identical fiber length is 38mm, and the variant fiber mean length is 25.6mm.

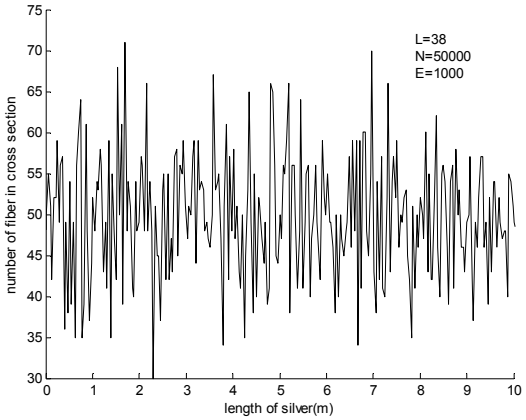


Fig 2. The ideal drafting sliver for equaling length fibers

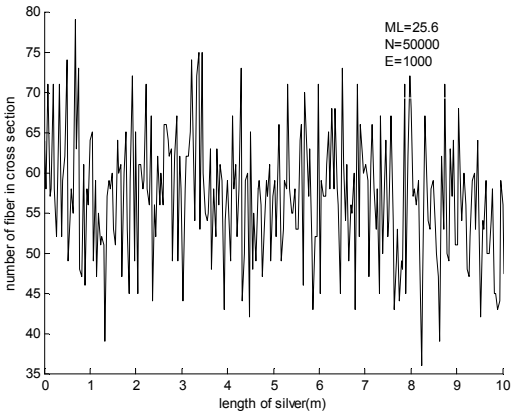


Fig 3. The ideal drafting sliver for variant length fibers

Statistical Properties of Ideal Drafting Sliver

Characteristics. Selecting the valid part of the sliver simulated, the values of mean, variant and coefficient variance are calculated, and listed with the limit of the lower bound for yarn unevenness values in table 1.

Table 1. The characteristics of ideal drafting slivers

Distribution of fibers	MEAN	STD	VAR	CV%	Martindale's CV%
equaling	50.0	7.48	55.98	14.96	14.14
variant	57.4	7.84	61.52	13.65	13.2

Probability Distribution. Many researchers consider that the distribution of the number of fibers in the ideal sliver cross section follows Poisson distribution. To verify the distribution feature of ideal drafting sliver, we test the validation of the Poisson hypothesis of the distribution of the number of fiber in the cross sections of sliver.

Poisson Distribution Test. For identical length fiber sliver, the data of number of fiber in cross section is the same value with figure 2, these data are divided into 39 groups evenly before test.

The null hypothesis is $H_0 : \xi \sim P(\lambda)$, $\lambda > 0$ and the alternative is $H_1 : \xi$ does not follow $P(\lambda)$, where λ is the maximum likelihood estimation of the number of fiber in cross section. $\hat{\lambda}$ is calculated as 50.103, namely, $H_0 : \xi \sim P(50.103)$. χ^2 statistic is calculated as 44.76, and $\chi^2_{1-\alpha}(k-r-1) = \chi^2_{1-0.05}(39-1-1)$=52.192>44.76.

So we accept the null hypothesis. That is to say, the number of fiber in cross section of the ideal drafting sliver follows a Poisson distribution.

Then we can test the ideal drafting sliver with variant length fibers in the same method, its data are divided into 43 groups evenly before test. The null hypothesis is $H_0 : \xi \sim P(\lambda)$, $\lambda > 0$ and the alternative is $H_1 : \xi$ does not following $P(\lambda)$, where $\hat{\lambda}$ is calculated as 57.11, χ^2 statistic is calculated as 90.93, and $\chi^2_{1-\alpha}(k-r-1) = \chi^2_{1-0.05}(43-1-1)$=56.942<90.93.

So we reject the null hypothesis. That is to say, the number of fiber in cross section of the ideal drafting sliver does not follow a Poisson distribution.

Normality Test. For variant length fiber ideal drafting sliver, we reject the Poisson distribution, so we try to test the validation of normal hypothesis. There are many methods for normality test, here we select the skewness-kurtosis testing method.

The null hypothesis $H_0 : \xi \sim N(\mu,\sigma^2)$, $-\infty < \mu < +\infty, \sigma^2 > 0$, and the alternative is $H_1 : \xi$ does not follow $N(\mu,\sigma^2)$. Calculate the following statistics:

$$n = 263 \tag{4}$$

$$\bar{x} = \frac{1}{n}\sum_{i=1}^{43} x_i v_i = 57.011 \tag{5}$$

$$s^2 = \frac{1}{n}\sum_{i=1}^{43}\left(x_i - \bar{x}\right)^2 v_i = 7.829^2 \tag{6}$$

$$s^2 = \frac{1}{n}\sum_{i=1}^{43}\left(x_i - \bar{x}\right)^2 v_i = 7.829^2 \tag{7}$$

$$\mu_4 = \frac{1}{n}\sum_{i=1}^{43}\left(x_i - \bar{x}\right)^4 v_i = 1475.732 \tag{8}$$

The skewness is：

$$b_s = \frac{\mu_3}{s^3} = \frac{52.758}{7.829^3} = 0.11 \tag{9}$$

The kurtosis is：

$$b_k = \frac{\mu_4}{s^4} = \frac{1475.732}{7.829^4} = 2.83 \tag{10}$$

Check the point (0.11, 2.82) in the boundary curves figure of the skewness-kurtosis testing critical region ($\alpha = 0.05$) , this point locates inside the isoheight line ring for $n = 43$, and near the central, so we accept the null hypothesis. That is to say, the number of fiber in cross section follows a normal distribution.

Conclusions

From the characteristics of ideal drafting sliver, the CV is near the Martindale's limit CV, and the MEAN of variant length fiber is more than identical length fiber, but the CV is less, these indicate that this sliver simulated is a very closed result of ideal sliver, and the efficiency of drafting to variant length fiber is lower than identical length fibers. The simulation of ideal drafting sliver bases on the ideal drafting theory, and the model of fibrogram distribution and the density function of variant fiber length distribution are introduced, the assumption of Poisson distribution to number of fiber in the sliver cross section is discarded. If enough fiber volume and enough drafting radio are given, a longer sliver would be gotten.

An unprecedented result we got by the hypothesis testing is that the number of fiber in the cross section of the identical length fiber sliver follows Poisson distribution, but it is not in the variant length fiber sliver, it follows normal distribution observably, although this is a result for only one fiber length distribution, that would have indicated that the Poisson distribution could not be as assumption to describe the structure and evenness of the staple fiber sliver uniquely.

Acknowledgements

This work was financially supported by the Henan Ministry of Education Natural Science Foundation (2009B540002), Project New Cotton-type Production Engineering and Technology Center of Henan Colleges and Universities (2009).

References

[1] J.G.Martindale: J. Textile Inst Vol.36(1945),P.35

[2] Rao J Sudarsana: J Text Inst Vol.52 (1961), P.570

[3] YW Qiu: J. China Text Uni Vol.25(1999),P.6

[4] YW Qiu: J. China Text Uni Vol. 25(1999),P.68

[5] Q Lin, GS Yan, CW Yu: J. of Tex. Res Vol.29(2008),P.22

[6] N.A.G. Johnson: J. Textile Inst Vol.72(1981),P. 69

[7] K.L. Hertel: Textile Research Journal Vol.12 (1940), P.510

[8]YH Su, GS YAN,JZ Ren: J. Tex. Res Vol 32(2011),P.30

[9]YH Su, LN Chen: J. Tex. Res Vol.31(2000),P.39

© (2011) Trans Tech Publications, Switzerland
doi:10.4028/www.scientific.net/AMR.331.129

Tensile Properties study of Polyester /Cotton/Silk Tri-component Sirofil Composite Yarn

Libin Lv[1, a], Mei Du[2,b]

[1]Yancheng Institute of Technology , Yancheng, Jiangsu, 224051, China

[2]Yancheng Textile Vocational Technology College , Yancheng, Jiangsu, 224005, China

[a]llb@ycit.cn, [b]dumplum@126.com

Keywords: Composite Yarn, Tensile Properties, Multinomial Regression, Mathematical Modal

Abstract. The tensile properties of tri-component Sirofil composite yarn is analyzed. To characterize the stretchability of the composite yarn, a three-element model with little distortion has been established. It is concluded that the elasticity modulus can be improved when three single yarns with different modulus of elasticity are composited. Under this condition, the modulus of elasticity of the composite yarn is among the three. Furthermore, in order to describe the elongation of the composite yarn at break, a four-component dynamic model of drawing with large distortion is developed. And the results obtained are verified by non-linear regression analysis. It is demonstrated that the properties of non-linear visco-elasticity of sirofil composite yarn can be characterized by using multinomial and the curve plotted according to the experimental result is basically in agreement with that deduced by the theoretical model.

Introduction

The tensile property is one of the most important properties of yarn. Most research has been focused on looking for differences among Sirofil composite yarn, traditional ring spinning yarn, plied strand and Sirospun composite yarn. However, little has been reported about the mechanism and tensile strength of Sirofil composite yarn.In this paper, the polyester/cotton/silktri-component Sirofil composite yarn is selected. In the cross section, the silk and polyester/cotton is paralleland cotton fiber is located around polyester. Since the tri-component Sirofil composite yarn has polyester and silk, the tensile curve could be explained through studying breaking mechanism and tensile strength of the tri-component yarn.

Mechanical model of composite yarn under small deformation

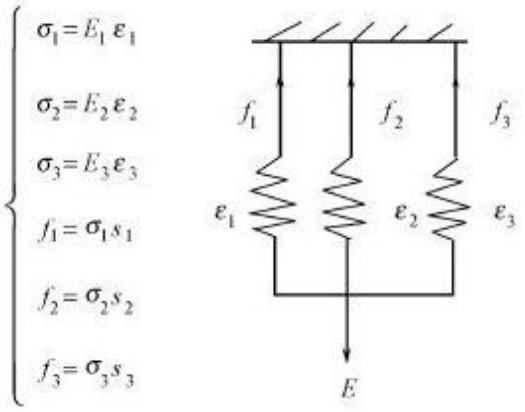


Fig.1 Mechanical model of weak deformation

Usually, the composite yarn is under small load in the weaving and drawing process, which means the deformation is within the limit of elasticity. Therefore the mechanical model was established in Fig.1. Suppose E_1, E_2, and E_3 are tensile modulus of elasticity of three materials. s_1, s_2, and s_3 are areas of cross section. ε_1, ε_2, andε_3 are strain. σ_1, σ_2, and σ_3 are stress. The elongations of three components are the same under tensile strength, so $\varepsilon_1=\varepsilon_2=\varepsilon_3=\varepsilon$.

$F=f_1+f_2+f_3=(E_1s_1+E_2s_2+E_3s_3)\varepsilon$ (1)

$\sigma=F/(s_1+s_2+s_3)$

$=(E_1s_1+E_2s_2+E_3s_3)\ \varepsilon/(s_1+s_2+s_3)$ (2)

$E=(E_1s_1+E_{2s2}+E_3s_3)/\ (s1+s2+s3)$ (3)

$E_1>E_2>E_3$, and E_2 is close to E_3, so E is smaller than E_1 and larger than E_3. This means when the components of tri-component yarn have different elastic modulus, the tensile modulus of elasticity is improved significantly, and the value is among the modulus of three materials.

Mechanical model of composite yarn under large deformation

A new mechanical model should be established if we want to study the process from strething to breaking of componentyarn. the polyeset/cotton/silk tri-component Sirofil composite yarn showed significant non-linear viscoelastic property. The stress-strain curve of cotton yarn could be considered as elastic deformation because there was no obvious yield point. However, the polyester filament and raw silk have obvious yield point, and there is a viscoelastic area in the curve. Therefore it is necessary to include linear spring that reflects mechanical properties, viscoelastic element that reflects viscoelasticity, and non-linear element reflecting non-linear mechanical properties [1-2]. In the model, E_1 is elastic constant of spring. E_2 is elastic constant of linear spring. The relationship between stress and strain is consistent with Hook's Law. η is damping factor of Newtonian damping. The relationship between stress and strain of non-linear spring was quadratic, and the coefficient was b. When the model was under stress σ, the corresponding strain was ε. Suppose yarn elongation was under the same speed $\varepsilon=Kt$. K is a constant and t is time. The initial condition is $\sigma(0)=0$. So the mechanical model was obtained as in Fig.2.

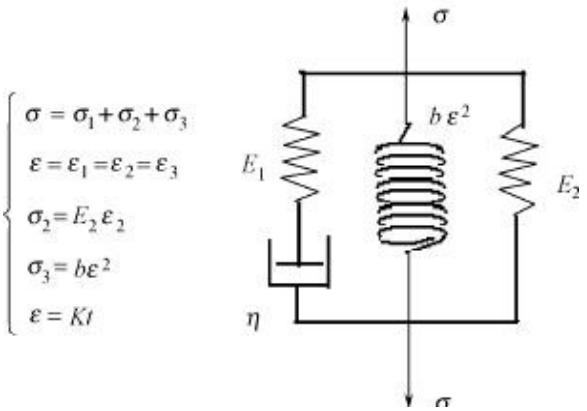


Fig. 2 Model of tensile fracture

Due to $\sigma_2=E_2\varepsilon_2$ and $\sigma_3=b\varepsilon_2$, $\varepsilon=Kt$, we only need to infer the relationship between σ1 and t, instead of between σ_2, σ_3 and t.

According to Maxwell model [1], it canobtain as followings:

$\varepsilon_1=\sigma_1/E_1+(\sigma_1/\eta)t$

$d\varepsilon_1/dt=(1/E_1)(d\sigma_1/dt)+\sigma_1/\eta$ (4)

Due to $\varepsilon=Kt$, $d\varepsilon_1/dt=K$, it can obtain:

$\sigma_1=Ce^{-(E1/\eta)}+K\eta$ (5)

Due to $\sigma_1(0)=0$，it can obtain as followings:

$\sigma_1=\eta K(1-e-(E_1/\eta K)\delta)$ (6)

So the stress strain curve of component yarn is [1]:

$\sigma=\sigma_1+\sigma_2+\sigma_3$

$=b\varepsilon_2+E_2\varepsilon+\eta K(1-e^{-E1\cdot\delta/\eta K})$ (7)

Accoring to ISO 2062, the pre-tension of yarn tensile is 0.05cN/tex. Considering the influence of pre-tension onyarn, the equation should be amended.

$\sigma=\sigma_0+A\varepsilon+B\varepsilon^2+C(1-e^{-D\delta})$ (8)

$A=E_2$; $B=b$; $C=\eta K$; $D=E_1/\eta K$.

The regression analysis is difficult due to the index in Eq.(8). Therefore, it is expanded with naturalogarithm and the general form is obtainded[3].

$\sigma=\sigma_0+\alpha_1\varepsilon+\alpha_2\varepsilon_2+\alpha_3\varepsilon_3+\alpha_4\varepsilon_4+\ldots$ (9)

Verification of mechanical model under large deformation

In order to verify the mechanical model under the large deformation, the 40 tex polyester/cotton/silk tri-component Sirofil composite yarn was used in this experiment. The tensile strength of polyester filament was 25cN. The distance between raw silk andfilament is 8 mm. The tensile strength of raw silk is 15cN. The spindle speed ofspinning machine was 10500 r/min. The twist added was 73.6/10 cm. The type of steel wire loop was 6903 with 1/0 size. The tri-component compositeyarn was tested for 60 times under the same experiment conditions. The average strength, elongate ratio and average stress-strain curve were obtained in the experiment[3]. The α1 α_2, α_3, α_4 were calculated by multinomial regression between breaking strength and elongate ratio.The strain and stress is shown in Tab.1. The polynomial and variance analysis is shown in Tab.2 and Tab.3.

Tab.1 Strain and stress

Strain/%	2	4	6	8	10	12	14
Stress/(cN/tex)	2.00	3.90	6.20	8.50	11.40	14.10	15.70

$\sigma=\sigma_0+\alpha_1\varepsilon+\alpha_2\varepsilon^2+\alpha_3\varepsilon^3+\alpha_4\varepsilon^4$

$x=(\varepsilon-2)/2+1=\varepsilon/2$

$x_1=1$, $x_2=2$, $x_3=3,\ldots$, $x_7=7$

$y\hat{}=\sigma_0+\alpha_1\varphi_1(x)+\alpha_2\varphi_2(x)+\alpha_3\varphi_3(x)+\alpha_4\varphi_4(x)$

$Lyy=\sum y^2_k-ny^2$

$=705.16-7\times 8.8286^2=159.551$

$U=\sum b_i l_{iy}=159.22$

$Q=Lyy-U=159.551-159.522=0.029$

Tab.2 Calculation of polynomial regression

x	$\varphi_1(x)$	$\varphi_2(x)$	$\varphi_3(x)$	$\varphi_4(x)$	$\sum y$	$\sum y^2$
L_{iy}	66.7	1.7	-1.7	-4.3	61.8	705.16
S_i	28	84	6	154	n=7	
b_i	2.3821	0.0202	-0.2833	-0.0279	$y\hat{}$=8.8286	
$b_i\times L_{iy}$	158.886	0.034	0.482	0.120		
λ_i	1	1	1/6	7/12		

Tab.3 Variance analysis table

Source	Square sum	Freedom degreee	Average square sum	F	Significance
One	158.866	1	158.886	10957.66	**
Two	0.034	1	0.034	2.34	
Three	0.482	1	0.482	33.24	*
Four	0.120	1	0.120	8.28	
Residual	0.029	2			
Sum	59.551	6			

The regression equation is obtained as followings by calculating.

$y\hat{}^{(1)}= 1.1911\varepsilon-0\cdot 6998$

$y\hat{}^{(2)}= 0.0051\varepsilon^2+1.1103\varepsilon-0\cdot 4574$

$y\hat{}^{(3)}=-0.0059\varepsilon^3+0.1468\varepsilon^2+0.1406\varepsilon+1.2424$

$y\hat{}^{(4)}=-00010\varepsilon^4+0\cdot 0267\varepsilon^3-0.2048\varepsilon^2+1.6007\varepsilon-0.5099$

The experimental and theoretical curvesare shown in Fig.3.

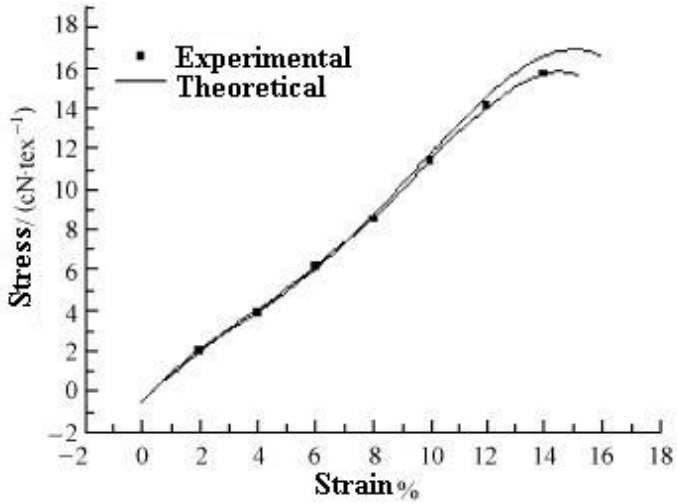


Fig.3 Curve comparison

From Fig.3, the results from experiment are consistent with the theory. The non-linear viscoelastic property of Sirofil composite yarn could be described by multinomial. When the elastic deformation was small, the shape of stress-strain curve of Sirofil composite yarn was similar to the initial curve of polyester filament and raw silk, which verified that in the initial stage, the rawsilk and polyester filament have a main effect on the deformation. Along with the increase of deformation, the cotton fiber was elongated from curving state, which had a main effect on the formation of composite yarn gradually. Therefore, the shape of stress-strain curve of Sirofil composite yarn was similar to that of cotton yarn under large deformation.

Conclusions

The breaking mechanism of polyester/cotton/silk tri-component Sirfil composite yarn was ananlyzed. Under large deformation, a four-element tensile mechanical model was established to describe elongation and breaking of tri-component yarn. A non-linear regression analysis was used to verify the result. It was proved that the non-linear viscoelasticity could be described by multinomial. The experimental results were consistent with theoretical model.

Reference

[1] Shizhong, Cui. Journal of Textile Research, 2003, 24(4): 324-326.

[2] Weidong Yu. Textile Material Science, 2006:110-112.

[3] Xufen Yu. Textile Material Science Experimental Technology, 2003: 167-169.

© (2011) Trans Tech Publications, Switzerland
doi:10.4028/www.scientific.net/AMR.331.133

Surface Modification of Polyester Fibers by Encasing Sucrose Ester and Grafting Soybean Protein

Suhua Gao[1,a], Guangxian Zhang[1,b]*, Fengxiu Zhang[2,c]

[1] College of textiles and garments, Southwest University, China

[2] School of chemistry and chemical engineering, Southwest University, China

[a]3965536@qq.com,[b]zgx656472@sina.com, [c]zhangfx656472@sina.com

* Corresponding author Tel.:+0 86 02368251681; fax:+086 02368251228

.*E-mail address:* zgx656472@sina.com.

Key words: polyester, encase, graft, protein

Abstract: Polyester has many superior characteristics such as high strength, durability, and good wash-and-wear properties. But it is not comfortable to wear. Modifying polyester fiber with animal and plant protein was seldom reported, and the fastness of protein was not good enough because there are only few hydroxyl groups on the surface of polyester fibers. In this study, sugar ester(SE) which had both hydrophobic aliphatic chain and hydrophilic hydroxyl groups were encased into surface layer of polyester fiber at high temperature and pressure. The hydrophobic part of sugar ester could be inserted into the polyester fiber, and the reactive hydroxyl groups would stay on the surface of polyester fiber. Then soybean proteins could be grafted on the surface of polyester fiber with sugar ester glycidyl ether (SEGE) as crosslinking compound. Surface morphology and structure of the fabric were studied by SEM,FT-IR,XRD,DSC. The results showed that the surface of polyester fiber was covered by SE and soybean protein overlay film, the encased sugar ester and grafted soybean protein fiber had little change on structure, and the proper grafting temperature was 100˚C, time 30min. Encasing and grafting technology is a promising method for modification of polyester fiber.

Introduction

Polyester which is the largest output and the most widely used synthetic varieties in the world is characterized by its high strength, excellent abrasion resistance, wash-and-wear and so on. However, polyester fabric is not comfortable to wear for its hydrophobic characteristic. So, modification is necessary to improve the wearability of polyester fiber.

Many proteins were used to modify polyester fiber. For instance, the soybean protein was added into the schmelze of polyester. And blends of soybean protein concentrate and polyester were prepared by using glycerol as a compatibilizing agent, and good miscibility was obtained when the soybean protein was initially combined with glycerol under high shear and at elevated temperatures in an extruder. Soybean protein/polyester blends had a lower degree of crystallinity, which improved the dyeability of the fiber, but the clothing cosiness was not improved greatly [1,2].

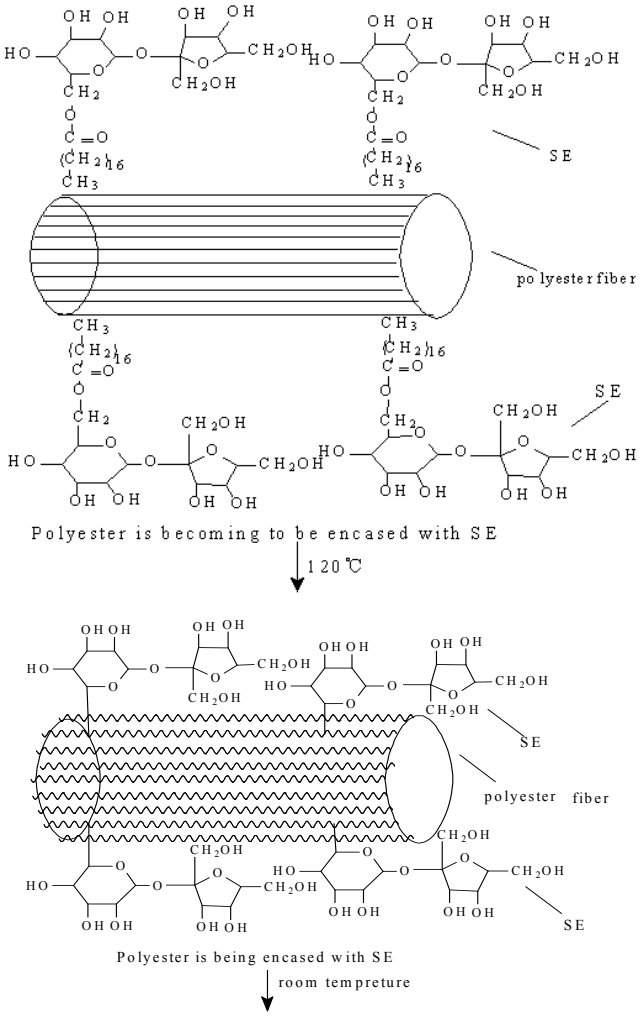
Proteins such as fibroin, sericin were applied onto the polyester fibers along with glutaraldehyde as a crosslinking agent with a pad-dry-cure method. But the fastness of which was not satisfied because there are only two hydroxies at the ends of macromolecule of polyester [3-5]. Therefore, many studies treated polyester fiber with NaOH to increase –OH and –COOH, the grafting fastness more or less enhanced [6-8]. But the alkali deweighting finish of polyester fibers still did not graft protein firmly with crosslinkage, meanwhile, the fiber strength decreased because of some of macromolecule broke.

In this study, we invent a high temperature and pressure method to encase SE to endue polyester fiber lots of –OH. Then encased polyester fiber could be grafted soybean protein firmly to improve its characteristics.

Materials and methods

Materials Polyester fiber provided by Oriental Knitting Factory was used without further treatment. SE was obtained from Liuzhou Foodstuff Co.Ltd. Soybeans bought from Chongqing Surpermarket were soaked for 24 h, and were smashed by juice extrator. The soybean proteins were gotton after centrifugation.

Encasing theory. Polyester is thermoplastic fiber, when the temperature is higher than the glass transition temperature Tg of polyester fiber, the movement of macromolecular chain is very violent. Then the gaps among molecular chains become greater. The sugar ester has hydrophobic aliphatic chain and hydrophilic hydroxyl groups. Then the hydrophobic part can easily insert into the gaps between polyester molecules chains at high temperature, and the -OH will be on the surface of polyester fibers. When the temperature decreases, the movement of macromolecular chain stops, and the hydrophobic part of SE is left in the surface layer of fiber, so there are lots of hydrophilic hydroxyl groups on the surface of polyester. The procedure was shown in Fig.1.



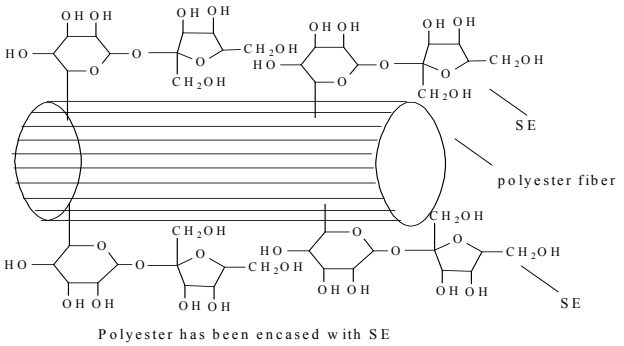


Fig. 1 The procedure of polyester encased with sugar esters（SE）

Synthesis of sugar ester glycidyl ether (SEGE) The crosslinking agent is SEGE. It was synthesized with sugar ester and epichlorohydrin. The synthesis was performed in the solution of epichlorohydrin and tetrabutylammonium, and the concentration of sugar ester was 20g/L, epichlorohydrin 2%, tetrabutylammonium 0.5g/L, 40℃, after 24h, sugar ester glycidyl ether was gotton. The reaction equation is shown in Fig.2.

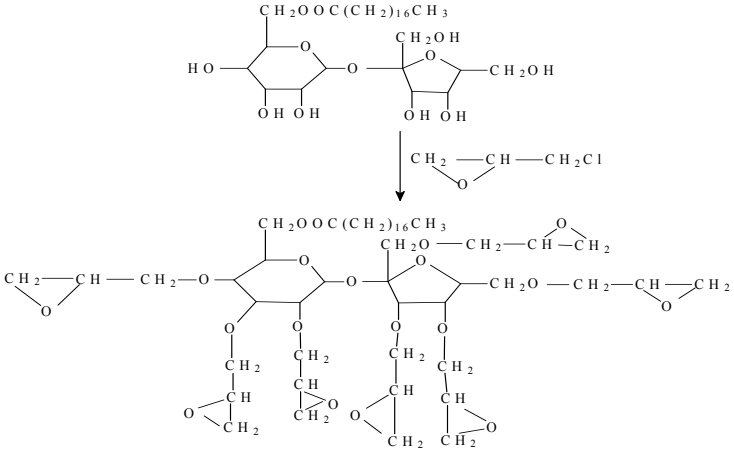


Fig. 2 The synthesis of sugar ester glycidyl ether(SEGE)

Grafting theory. The crosslinking agent has many epoxide groups, which can react with he hydroxyl groups of encased polyester and hydroxyl, carboxyl and amino groups of soybean protein, so soybean protein could be firmly grafted on the surface of polyester fiber. The grafting procedure was shown in Fig.3.

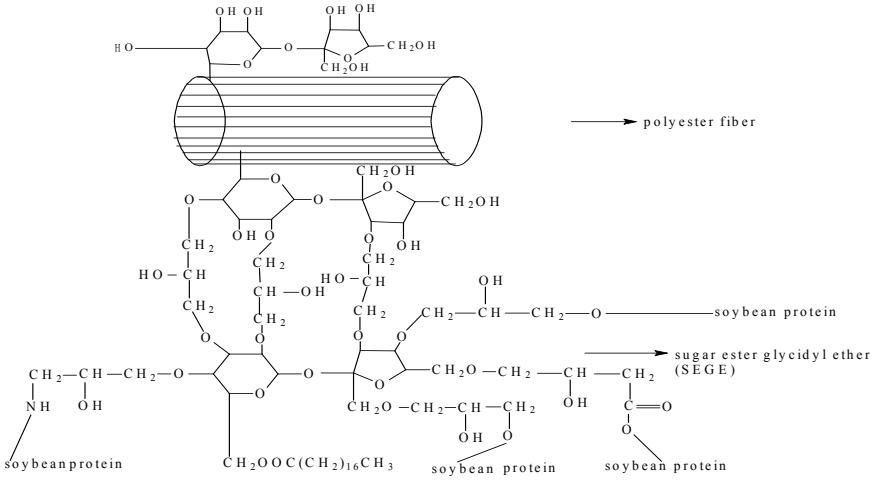


Fig. 3 Schematic diagram of encased polyester fiber grafted with soybean protein

Encasing sugar ester and grafting soybean protein on polyester fiber. Encasing sugar ester on polyester fiber surface layer was carried out for 1 h at 120 ˚C, and concentration of sugar ester was 20g/L, and followed by extensive washing with water. Then the encased sugar ester fibers were soaked in the solution of soybean protein and sugar ester glycidyl for 10 min at 60˚C, and the concentration of soybean protein was 50g/L, the concentration of SEGE was 6.4g/L. Then the fibers were put in the oven and dried at 60˚C. The grafting process was carried out in the oven at temperature (70-120˚C) for (0-50min). After grafting the fibers were washed with water.

The grafting fastness to laundering. The grafted polyester fibers were washed at 60˚C with the solution of sodium carbonate (0.2%) and soap (0.1%) at a liquor of 1:100, and then dried.

Characterization. IR analyses were carried out using an FT-IR spectrometer(Brucher Co. Ltd.,EQUINOX55). About 2 mg of fiber was mixed with 200 mg of spectroscopic grade KBr. XRD was measured by a D/Max2000PC Rigaku wide angle X-ray diffractometer at a scan speed of 5°min^{-1}. For SEM analysis, fiber was shadowed with gold and then examined with Philips-FEIModel Quanta 2000 field emission scanning electron microscopy, which was operated at 20 kV. Differential scanning calorimetry (DSC) measurements were performed using a Thermoanalyzer System, model Q600SDT(TA Co.Ltd.). About 5 mg of samples, placed in a DSC pan, were heated from -10 to 550˚C at a scanning rate of 10˚C min^{-1} under nitrogen atmosphere.

Results and Discussion

Grafting soybean protein on polyester fibers. Fig.4 showed the effect of temperature on grafting soybean protein onto the polyester fibers encased sugar ester From Fig.4, the grafting rate increased with the increase of temperature until the temperature to 100˚C. However, the grafting rate decreased when the temperature was above 100˚C. This may be due to that the overlay film of soybean protein was destroyed at high temperature and be washed down.

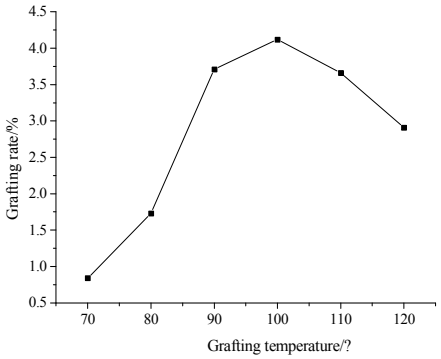


Fig.4.the Relationship Between grafting Temperature and Grafting Rate

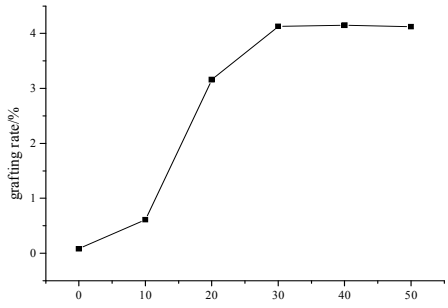


Fig.5.the Relationship Between Grafting Time and Grafting Rate

Fig. 5 showed **t**he relation between grafting time and grafting rate. Grafting temperature was 100 ˚C. As shown in Fig.5, The grafting rate increased with the increase of time within 30 min. After 30 min, the grafting rate kept a constant value.

Residual rate of grafted soybean protein on polyester fiber after washing. From Fig.6, it can be known that the residual rate of grafting was very high. The resudial rate kept above 91% after many times of washing. This was because the encased sugar ester polyester fibers had lots of reacting hydroxyl groups, which provided many reacting position for SEGE. And SEGE had many epoxy groups, which could react with hydroxyl groups encased on polyester fibers and amido, carboxyl and hydroxyl groups of soybean protein. So the soybean protein could be grafted firmly onto the surface of polyesters, and could not be washed down.

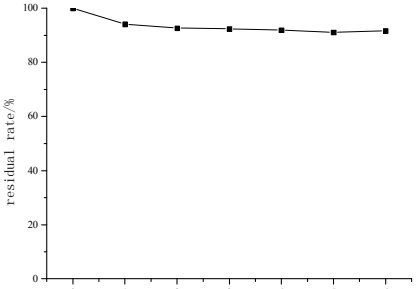
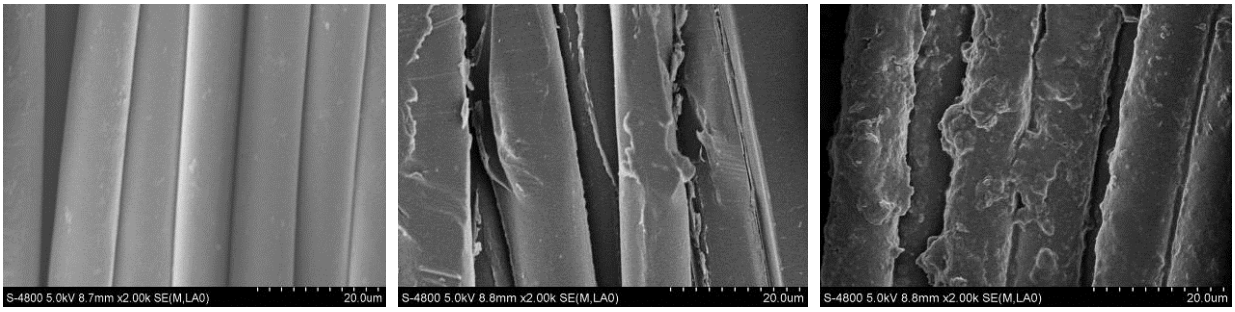


Fig.6 the residual rete after washing

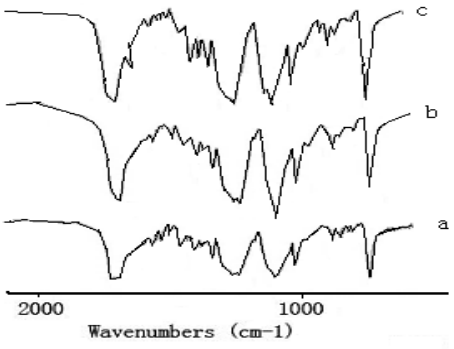
Structure analyses. The surface morphology of the polyester fiber, encased sugar ester polyester fiber and grafted soybean protein polyester fiber are shown in Fig.7. The polyester fibers had a very smooth and compact surface (Fig.7a). After encased SE, some materials can be seen on the surface of the polyester fibers. The surface of grafted soybean protein fibers were quit different from raw polyester fiber and an overlay film was coated on the surface of grafted polyester.



(a) (b) (c)

Fig.7 SEM images of (Magnification, 2000×): (a) polyester, (b) encased polyester, (c) grafted polyester

The IR spectra of the polyester fiber, encased sugar ester polyester fiber and grafted soybean protein polyester fiber are shown in Fig.8. The spectrum of encased sugar ester fiber is almost the same as the raw polyester except the peak at 1096 cm^{-1}, where the peak intensity increased obviously as a result of large quantity of hydroxies of tertiary alcohol. For the grafted polyester fiber, The spectrum exhibited $–NH_2$ out-of-plane bending vibration absorption around 900 cm^{-1}, and the peak intensity at 1633 cm^{-1} is the β-sheet of protein.



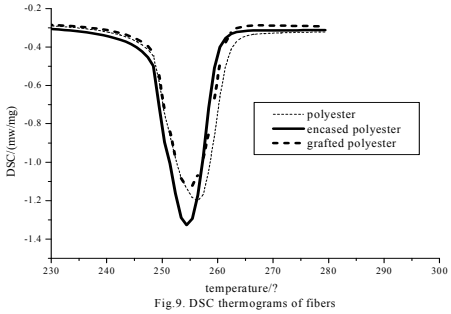


Fig.9. DSC thermograms of fibers

Fig.8. FT-IR spectra of (a) polyester, (b) encased sugar ester polyester,(c) grafted soybean protein polyester

The DSC results of polyester fiber, encased sugar ester polyester fiber and grafted soybean protein polyester fiber are shown in Fig.9. The melting point of raw polyester is 256.8˚C, and after encasing, declined to 254.5˚C, because the hydrophobic part of SE encased into polyester fiber, which made that the macromolecules at the surface layer of polyester fiber do not interact very well, and the

orientation of fiber only changed a little. After grafting with soybean protein, the soybean protein molecules and the hydroxides on polyester fiber surface were connected by SEGE. Then the melting point increased to 255.0˚C. The melting points of the three kinds polyester fibers actually are similar, the thermal stability do not change after encasing and grafting.

The XRD patterns of polyester, encased sugar ester polyester fiber and grafted soybean protein polyester fiber are shown in Fig.10. The curves of three kinds of polyester fibers are quite similar. This showed the structures of the three kind polyester fibers didn't change.

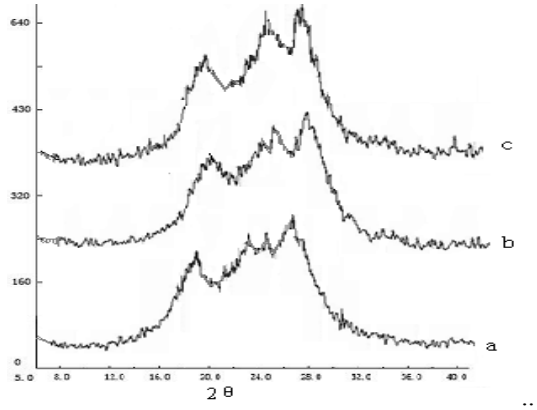


Fig.10. XRD patterns of (a) polyester, (b) encased polyester, (c) grafted polyester

Conclusions

Encasing sugar ester on surface layer of polyester fiber is an efficient method to endue surface of polyester fibers a lot of hydroxyl groups. Then the polyester fibers have enough hydroxyl groups to connect soybean protein through crosslinks. Sugar ester glycidyl ether is a high efficient crosslink, which can graft soybean protein firmly on surface of polyester fiber encased sugar ester. Then through the encasing and grafting technologies, the polyester fibers can be firmly grafted a layer of protein

Acknowledgments

This study was supported by Chongqing science fund (CSTC,2010AA1002, CSTC,2008BB4250).

References

[1] Graiver.D, Waikul.LH, Berger. C, Narayan. R (2004) Journal of applied polymer science 92: 3231-3239

[2] Mungara.P, Chang.T, Zhu.J, Jane J (2002) Journal of polymers and environment 10:31-37

[3] Yang Ruxin,Yang Baichun (1992) Journal of Suzhou institute of silk textile technology12:25-35

[4]Ji Peizhen (1994) Journal of Zhejiang institute of silk textiles11:23-26

[5]Pan Fukui, Pan Tingsong,Xie Liqiang (2005) Joumal of Qingdao university (E&T) 20:61-63

[6]Kongdee A, Okubabayashi S, Tabata I (2007) Journal of applied polymer science105:2091-2097

[7]Du Mengfang, Min Sijia, Zhang Haiping, Feng Qiang, Zhu Liangjun (2007) CANYE KEXUE33:427-432

[8]Gulrajani ML, Brahma KP, Kumar PS, Purwar R, Purwar R (2008) Journal of applied polymer science109:314-321

© (2011) Trans Tech Publications, Switzerland
doi:10.4028/www.scientific.net/AMR.331.139

Influences of Soft Monomers on the Application Properties of Hydrophilic Polyurethane with Mixed Polyether Segment

Heng Quan[1,a], Zhenya Gu[2,b]

[1]Faculty of Chemical Engineering, Wuhan Textile University, 430073 Wuhan, PR China

[2]School of Textiles, Tianjin Polytechnic University, 300160 Tianjin, PR China

[a]quanheng2002@163.com, [b]guzhenya@gmail.com

Key words: Hydrophilic polyurethane, Polyether, Soft segment, Structure, Property

Abstract. A series of hydrophilic polyether polyurethanes were prepared with two-steps technique from 4,4'- diphenylmethane diisocyanate (MDI), polytetramethylene glycol 1000 (PTMG1000) and polyethylene glycol 1000 (PEG1000) with 1,4-butanediol (BDO) as the chain extender. Further more, the relationships between structure and moisture permeability, water resistance, hydrophility and phase inversion temperature (PIT) of the polyurethanes was investigated. For polyether polyurethanes with nicer micro phase separation structure, the studies show that the hydrophilic ether bond content and mobility of soft segment chains have decisive effect on their water resistance, moisture permeability and hydrophility without reference to the soft segment content on the whole.

Introduction

Polyurethane has aroused broad interest and found its applications in various fields because of its outstanding intensity, abrasion resistance, adhesion performance, controllable properties and their technologically significance etc[1].

The macroscopical properties of hydrophilic polyurethane not only lie on its chemical structure but also multi-micro-phase separate morphologies[2-4]. In application of hydrophilic polyurethane, the structure dependency of water resistance and moisture permeability is an important factor should be considered for effective utilization of the materials[5,6].

In our former study, polyester and polyether with different molecular weight are employed as mixed soft segments of polyurethanes for their influences on structure and properties of samples[7]. In this study, we prepared another 4 groups of polyurethanes with mixed polyether whose hydropility are dissimilar for the relationships between structure and properties.

Experimental

Preparation of the polyurethane. In the experiment, both PEG1000 and PTMG1000 were employed as mixed hydrophilic soft monomers of polyurethanes. Dimethyl formamide (DMF) as solvent. The two-steps procedure described in references [6] and [7] was followed to synthesize polyurethanes, which gives less random and more block polymer.

Preparation of specimens. Concerning preparation of the film of polyurethanes and the pure Dacron fabric coated with samples, refer to reference [6] please.

Analytical methods. Phase inverse temperature (PIT) of polyurethane samples is detected with modulated differential scanning calorimeter, DSC (Du Pont DSC-2000). The specimens (about 10mg) were heated from -50˚C to 150˚C at the heating rate of 20˚C/min. Moisture permeability (Water vapor transmission, WVT), water resistance and hydrophility, are described in detail in references [6] and [7].

Structure of hydrophilic polyurethane and its properties

Tab.1 Structure parameters of segmented hydrophilic polyurethanes with mixed polyether

Items / Serial number	Group D					Group E				
Soft segment content %	75.9	70.4	65.7	61.6	56.8	75.9	70.4	65.7	61.6	56.8
Ether bond content %	16.8	15.6	14.6	13.7	12.6	20.1	18.6	17.4	16.3	15.0
Hard segment mol. wt	317.5	420.4	522.1	623.4	760.6	317.5	420.4	522.1	623.4	760.6
Soft monomers charge ratio	PEG1000:PTMG1000 = 0:10					PEG1000:PTMG1000 = 3:7				

Tab.2 Structure parameters of segmented hydrophilic polyurethanes with mixed polyether (continuation)

Items / Serial number	Group F					Group G				
Soft segment content %	75.9	70.4	65.7	61.6	56.8	75.9	70.4	65.7	61.6	56.8
Ether bond content %	22.2	20.6	19.2	18.0	16.6	24.4	22.6	21.1	19.8	18.2
Hard segment mol. wt	317.5	420.4	522.1	623.4	760.6	317.5	420.4	522.1	623.4	760.
Soft monomers charge ratio	PEG1000:PTMG1000 = 5:5					PEG1000:PTMG1000 = 7:3				

Structure and water resistance & moisture permeability. Obviously, the more PEG1000 and the higher hydrophilic soft monomer dosage (lesser hard segment content) in polyurethane, the better moisture permeable it will be (Fig.1). It's well known that the solubility and "diffusing ladder" of water vapor in nonporous hydrophilic polyurethane membrane play an important role for the WVT[7,8]. Higher hydrophilic soft monomer content will certainly result in a 'molecular/ether bond ladder for moisture transmission' with the shorter steps and more expedite diffusing channels in swelled polymer. Accordingly, the water vapor could transfer more smoothly in the membrane.

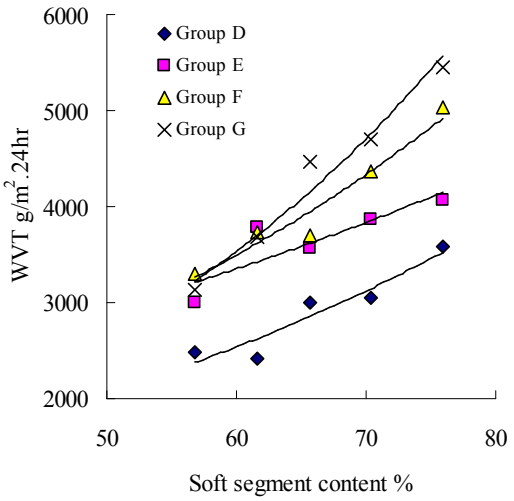


Fig.1 Soft segment content and WVT

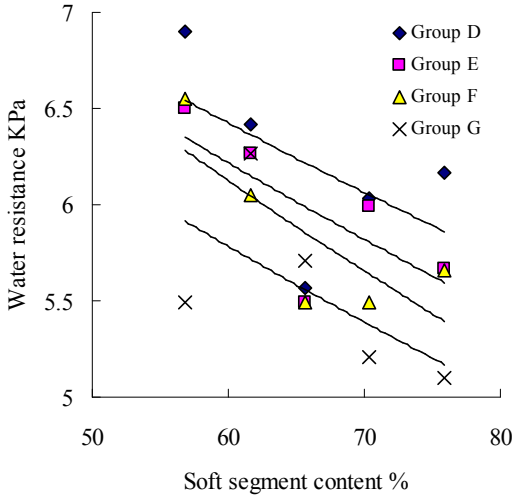


Fig.2 Soft segment content and water resistance

Of course, the better hydrophility of polyurethane consequentially goes with the decrement of its water resistance. The improvement of moisture permeability of the hydrophilic polyurethane is also enslaved to its water resistance (Fig.2).

In spite of the fact that the better water resistance and worse moisture permeability of coated fabric are derived from decreasing hydrophilic soft segment content, but we can not ignore another causation that the dissolution of hard segment into the soft segment domains is also enhanced as the soft segment content in polymers is decreased, which leads the mobility of breathable hydrophilic soft chains being confined by hard segments. The guess can be testified by the change of PIT with soft segment content of samples (Fig.5).

The interesting is that the spaces between the 4 curves are not equidistant and beeline (Figs.1 and 2). So, the change in WVT with respect to PEG1000/PTMG1000 ratio and soft segment content in samples should not be linear relationship, but perhaps exponential. With the increasing of PEG or soft segments content, moisture permeability is better and better. It is believed that water vapor will dramatically enhance the polarity of PEG domains and force them to phase separate from PTMG domains, which resulting in the important significance of ether bond for the waterproof and breathable properties of hydrophilic polyurethane.

In conclusion, the WVT and water resistance of hydrophilic polyurethane with mixed soft segments not only depend on the micro phase separation between hard and soft segment domains, but also the micro phase separation between PEG and PTMG domains.

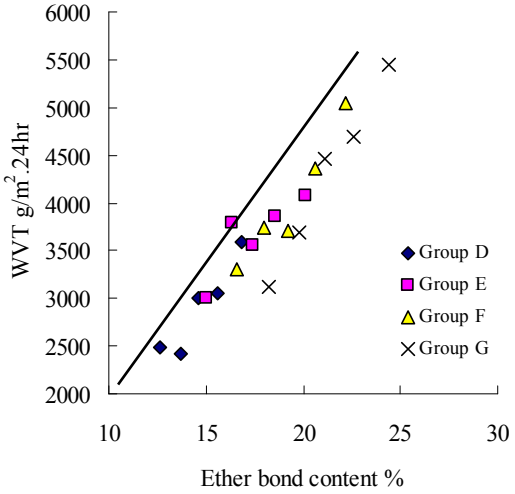


Fig.3 Ether bond content and WVT

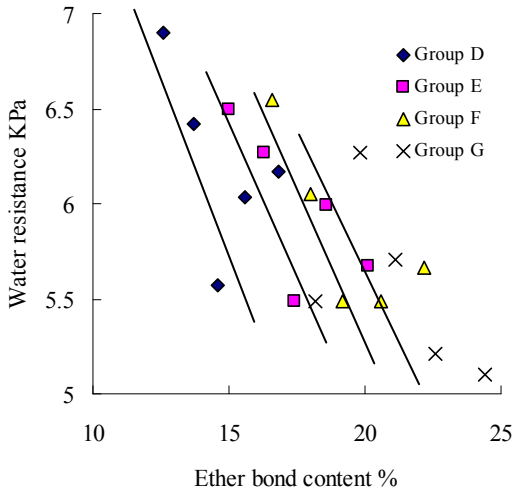


Fig.4 Ether bond content and water resistance

According to Tab.1, Fig.1 and Fig.2, the samples of Group D, E, F and G take on different properties in WVT and water resistance markedly, notwithstanding their soft segment content, hard and soft segment average mean mol. wt are accordant. Actually, the WVT and water resistance of hydrophilic polyurethanes almost respectively takes on linear increasing or decreasing relationship with ether bond content without reference to their content, average mean mol. wt of soft or hard segment and soft monomers charge ratio (Figs.3 and 4).

This phenomenon shows that the effects of hydrophilic ether bond in soft domains on the water resistance and moisture permeability of hydrophilic polyurethane membrane is decisive and explicit.

The noticeable is that the WVT of coated fabric puts up a better correlativity to ether bond content than its water resistance (Figs.3 and 4). In order to compensate the worse membrane-forming ability of PEG, the samples with higher charge ratio of PEG to PTMG are supposed to hold lesser soft segments (more hard segments) than those whose soft charge ratio is lower to carry through a same water resistance (Fig.4).

Structure and phase inverse temperature (PIT). Within a group, the PIT of sample moves to higher temperature with the decrease of its soft segment content (Fig.5), which can be attributed to the decrease in the purity of soft segment domains and hence the increase of molecular hindrance experienced by the soft segments in the vicinity of the hard segment domains derived from better compatibility of the two phases[9,10].

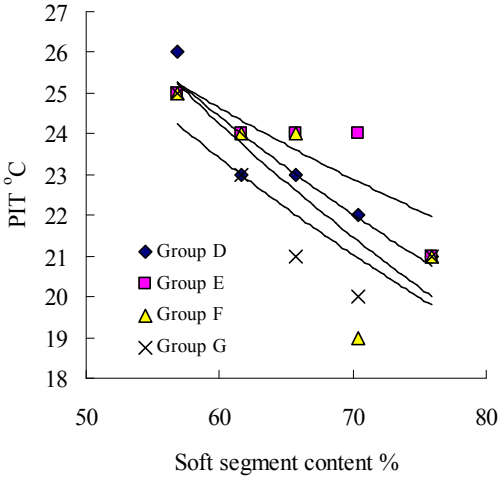


Fig.5 Soft segment content and PIT

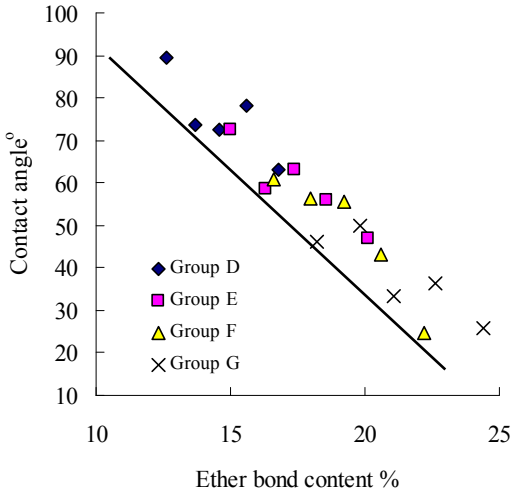


Fig.6 Ether bond content and contact angle

In addition, the PIT of samples becomes lower and lower with the increase of the charge ratio of PEG1000 to PTMG1000, which can be attributed to the better flexibility and the lower PIT of PEG than PTMG.

Structure and surface property. The hydrophility of polyurethane film shows a linear direct proportion relationship with its ether bond content (Fig.6). Since the flexible ether bond can form numerous hydrogen bonds with moisture molecule, the contact angle with water of samples has been continuously declined.

Domains structure and properties. According to Fig.5, the PIT of samples becomes lower and lower with the increase of the soft segment content and the charge ratio of PEG1000 to PTMG1000, but the change is not so conspicuous, which implies their similar domain structure.

In fact, the weaker polarity of PEG1000 and PTMG1000 as well as contrary polarity between polyether soft segments and urethane segment (hard segment) result in sufficient separation between hard and soft domains along with almost homogeneous soft domains, which cause the PIT of soft segments almost only lies on the PIT of the “soft segments mixture”. Clearly, the hard (or soft) segment content is inessential to the PIT of soft segment for polyether polyurethane with sufficient micro phase separation structure. The perfect micro phase separation structure of polyether polyurethane can also be employed to explain that why the various properties of polyether polyurethane clearly depend on its hydrophilic groups (ether bond) in soft domains much more (Fig.3, 4 and 6).

Furthermore, an interesting phenomenon detected in our former studies is that the effects of ether bond of hydrophilic polyurethane on its WVT, water resistance and hydrophility is not strictly selfsame when the ether bond content is changed within a Group or between Group A, B and C for the polyurethane with mixed soft segments of PEG1000 and PBA2000. That is because the indistinct domains structure and different soft chain mobility of Group A, B and C deriving from the stronger polarity of PBA2000 and different average mean molecular weight of mixed soft segment respectively[7]. Surely, the “strange” phenomenon can not be observed among the Group D, E, F and G owing to their perfect, similar micro phase separation structure and lesser hindrance experienced by soft segments (Fig.3, 4 and 6).

Conclusions

1 Hydrophility and concentration of polyether monomers have important effects to the waterproof and breathable of hydrophilic polyurethane with mixed polyether. Especially, the ether bond content is more important to the properties. The pivotal factor deciding the diffusion behavior of moisture in the polyurethane membrane is the mobility of hydrophilic soft chains, which is definitely not only rated to the micro phase separation structure between hard and soft domains but also between different soft segments.

2 Ether bond content or the hydrophility of polyether in hydrophilic polyurethane acts on more important effects than the soft segment content on the waterproof and breathable properties, which takes on direct proportion relationship with the WVT or hydrophility and inverse proportion relationship with the water resistance of polyether polyurethane in the rough without reference to their soft segment content.

3 Polyurethanes with different domains structure will show an obvious difference on their macroscopical properties even if their chemical structure is the same.

Acknowledgements

This work was financially supported by the Key Natural Science Foundation of Shaanxi Province Education Department, China (No.04JK-181) and the Direction Program of China Textile Industry Association (No.2007-049).

References

[1] H. Quan, J.W. Xing, Z.L. Fan: Textile transaction (in Chinese) Vol. 28 (2007,11), p. 60-64

[2] Yang J H, Chun B C, Chung Y C, et al: Polymer Vol. 44 (2003), p. 3251-3258

[3] Ashish A, G L Wilkes: Polymer Vol. 45 (2004), p. 927-935

[4] D.J. Hourston, G. Williams and R. Satguru et al: Journal of Applied Polymer Science Vol. 67 (1998), p. 1437-1448

[5] X.M. Ding, J.L. Hu, X.M. Tao, et al: Textile Research Journal Vol. 76 (2006), p. 383-387

[6] H. Quan, J.W. Xing, Z.L. Fan: Proceedings of 2006 China international wool textile conference & IWTO wool forum (2007), p. 466-470

[7] H. Quan, Z.Y. Gu, S.S. Wu. Journal of Donghua University Vol. 26 (2009), p. 408-412

[8] Lin J.R., Chen L.M: Journal of Applied Science Vol. 69 (1998), p. 1563-1574

[9] Tsonos C., Viras K., Stepanenko L., et al: Journal of Macromolecular Science Vol. 39 (2000), p. 155-174

[10] Bradley F, Peter Halley, Kevin Jack, et al: Journal of Applied Polymer Science Vol. 102 (2006), p. 128-139

© (2011) Trans Tech Publications, Switzerland
doi:10.4028/www.scientific.net/AMR.331.144

Preparation and properties of cationic graft starch sizing agent

Hao Zhang [1,a], Jiankun Wang [1,b], Rui Wang [1,c], Jimei Zhang [2,d]

[1] School of Textiles, Tianjin Polytechnic University, China 300160
[2] School of Environmental and Chemical Engineering, Tianjin Polytechnic University, China 300160
[a]zhanghaoyangyong@yahoo.cn, [b]jiankunwang@tjpu.edu.cn, [c]wangrui@tjpu.edu.cn, [d]zjimei@gmail.com

Keywords: cationic graft starch, textile, sizing agent, sizing performance.

Abstract. In this article, a new kind of starch sizing agent, cationic graft starch [CS-g-P(AM-co-HEMA-co-BA)] was synthesized. Its structure was identified by Fourier transform infrared spectroscopy (FTIR). The results of sizing experiment show that polyester/cotton blended yarn (T/C 55/45) sized with cationic graft starch exhibits better tensile strength, abrasion resistance and lower hairiness counts than cationic starch and PVA. This new starch sizing agent can be an ideal substitute for PVA.

Introduction

Quaternary ammonium cationic starch，as an important ether derivative of starch, has many advantages like good water dispersion and solubility, low pasting temperature, high size stabilization and biodegradability, and has been widely used in paper industry, wastewater treatment and synthetic detergent industry [1]. The positive charge on its nitrogen atoms gives cationic starch good compatibility to synthetic fibers, which gives it great potential as a warp sizing agent [2]. But in fact, the application of cationic starch in textile industry develops very slowly and still in primary stage. This is partly due to its excessive high viscosity limits its use, and what more importantly, cationic starch itself lacks hydrophobic groups that structural similar to synthetic fibers, so it lakes enough affinity to this kind of yarn. Grafting polymerization is the most important means to improve hydrophobicity of starch. There have been many studies on grafting polymerization of native starch, but few is about cationic starch [3-6].

In this work, a new kind of cationic graft starch [CS-g-P(AM-co-HEMA-co-BA)] was synthesized. Cationic starch was taken as raw material, after acid-modified, acrylic amide (AM), 2-hydroxyethyl methacrylate (HEMA) and butyl acrylate (BA) were grafted onto it. The sizing performances of this new modified starch size have also been tested.

Approach

Materials and reagents: Cationic starch: substitution degree 0.03, industrial grade (Tai An City Jin Shan modified starch Company); hydrochloric acid, anhydrous sodium sulfate, anhydrous sodium carbonate, acrylamide (AM), 2-hydroxyethyl methacrylate (HEMA), butyl acrylate (BA), dimethyl sulfoxide (DMSO), ammonium persulphate (APS), sodium acid sulfite, anhydrous ethanol, acetone, all reagents are analytically pure (Tianjin Kermel Chemical Reagent Company); distilled water, deionized water, native starch (Zhao Xian Qing Yang starch Company), acetate starch (self-made), sizing assistant including: antifriction agent, smooth agent, emulsifying oil and poly-acrylic size were provided by Tianjin textile Group Co. Ltd, 13.3 tex polyester/cotton blended yarn (T/C 55/45), polyester/cotton blended roving (T/C 55/45).

Instruments: DF-101S constant temperature magnetic stirrer, SHB-Ⅲ circulating water vacuum pump, D-8401WZ multifunctional mechanical stirrer, HHS electric-heated thermostatic water bath, electric blowing oven, Soxhlet apparatus, Buchner funnel, Gang Dong FTIR-650 Fourier transform infrared spectrometer, HD026N electronic fabric strength tester, YG061F electronic single yarn strength tester, YG172 yarn hairiness testing instrument, A-2071.TM cohesion testing machine.

Acid hydrolysis of cationic starch: 1000g of dry cationic starch was dispersed in 1500ml of distilled water, 50g of Na_2SO_4 was added, the emulsion was transferred into 3000ml boiling flask-3-neck with mechanical stirring, thermometer and condenser tube, heated by constant temperature water, then a volume of 2mol/L HCl solution was added. The acidification reaction was carried on at 55°C for 5 hours. After that, the emulsion was neutralized with 5% Na_2CO_3 solution and filtered. The filter cake was washed with distilled water for several times, then dried at 60°C, crushed and sieved to pass through 100 mesh-sieve.

Synthesis and purification of cationic graft starch [CS-g-P(AM-co-HEMA-co-BA)]: 15g of acidized cationic starch was dispersed in deionized water, and transferred into 250ml boiling flask-3-neck with thermometer and condenser tube, heated in constant temperature water and stirred with nitrogen incoming for 20 minutes. After that, when the system reached reaction temperature, interfacial agent DMSO, grafting monomer AM, HEMA, BA and initiator APS, sodium acid sulfite was added, the grafting copolymerization was carried on with continuous magnetic stirring and nitrogen incoming. After grafting reaction, the product was filtered, washed with 50% ethanol solution then with 100% anhydrous ethanol for several times, dried at 60°C. Then the raw grafting product was put into Soxhlet apparatus to remove the non-grafted homo-polymer firstly with water then with acetone as extraction solvent, for 10 hours, respectively.

Structure identification of cationic graft starch: The structure of cationic graft starch was confirmed by Gang Dong FTIR-650 Fourier transform infrared spectrometer.

Measurement of grafting effect of cationic graft starch: The grafting effect including grafting ratio (GR), grafting efficiency (GE) and total monomer conversion (TC) of cationic graft starch was measured under FZ/T 15001-2008 [7].

Adhesive performance test of cationic graft starch: The adhesive performance of cationic graft starch was tested using roving gum dipping method under FZ/T 15001-2008 [7]. The strength of roving was tested by HD026N electronic fabric strength tester.

Sizing experiment of cationic graft starch and the sizing performance tests: Sizing experiment was carried on with 13.3 tex polyester/cotton blended yarn by self-made singly-end sizing instrument. The size formulas was given in Table 1.The sizing performances including: single yarn strength, hairiness and abrasion resistance were tested by YG061F electronic single yarn strength tester, YG172 yarn hairiness testing instrument and A-2071.TM cohesion testing machine, respectively, under the instructions of Textile size measurement technology [8].

Table 1. Sizing formulas for 13.3 tex polyester/cotton blended yarn (T/C 55/45)

Sizing formula / Composition [%]	1	2	3
cationic starch	100	---	---
PVA	---	100	---
cationic graft starch	---	---	100
acetate starch	100	100	100
native starch	80	80	80
antifriction agent	9.5	9.5	9.5
smooth agent	9.5	9.5	9.5
emulsifying oil	10	10	10
poly-acrylic size	12.5	12.5	12.5
solid content	16	16	16

Results and Discussion

Structure identification of cationic graft starch:

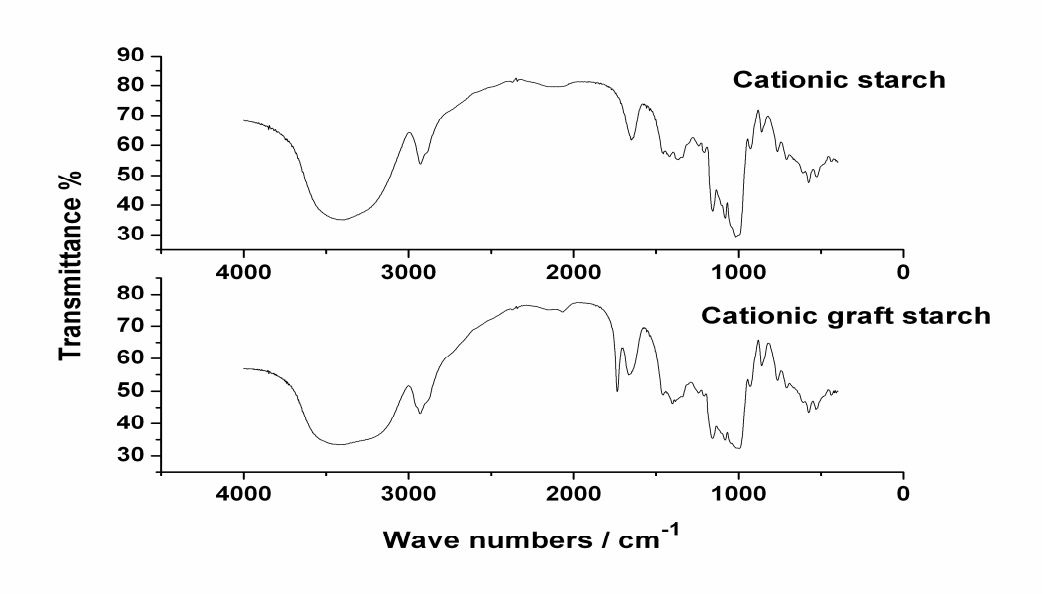


Fig.1. Infrared spectrum of cationic starch and cationic graft starch

As seen in Fig.1, bands at 3411cm^{-1} (O-H) , 2927 cm^{-1} (-CH_2-), 1077 cm^{-1}(six membered ring ether), 859cm^{-1} (O-H) and 571cm^{-1} are the characteristic peaks of starch, the bands at 1205 cm^{-1} (C-N) and 1017 cm^{-1} (open chain ether C-O-C) are the absorption peaks of quaternary ammonium cationic groups. Cationic graft starch has absorption peaks of carbonyl groups (C=O) at 1736 cm^{-1} and C-N bond of amide groups at 1402 cm^{-1}, which not found in the infrared spectrum of cationic starch, this can prove that monomer AM, HEMA and BA were successfully grafted on to cationic starch [9].

Grafting effect of cationic graft starch:

Table 2. Grafting effect of cationic graft starch

	GR [%]	GE [%]	TC [%]
Cationic graft starch	19.06	88.87	41.89

In Table 2 we can see the synthesized cationic graft starch has good grafting effect, its grafting ratio and grafting efficiency are both far higher than most of graft starches sell on market [10], its total monomer conversion is also ideal.

Adhesive performance test of cationic graft starch:

Table 3. Adhesive performance of cationic graft starch and other sizing agents

	Braking strength [N]	Breaking elongation [%]
Native starch	48.85	7.11
Cationic starch	53.61	7.56
PVA	61.80	10.08
Cationic graft starch	72.91	10.59

Results were shown in Table 3, native starch has worst adhesion to polyester/cotton roving yarn, cationic starch has some improvement, but still weak. Cationic graft starch has the strongest adhesion than other three kinds of sizing agent, including PVA. This is because the side chains of cationic graft

starch have massive ester groups that in structural accordance with polyester fibers, which can help to enhance van der Waals force between polyester fiber molecular and cationic graft starch molecular chain, as a result its adhesion to polyester fibers greatly reinforced.

Sizing performance of cationic graft starch:

Table 4. Sizing performance of cationic graft starch and other sizing agents

Index [%] / Sizing formula	Breaking strength reinforce ratio	Elongation reduce ratio	Abrasion resistance reinforce ratio	Hairiness reduce ratio (⩾3mm)
1	22.67	39.33	98.59	99.24
2	25.23	37.74	159.52	99.39
3	27.58	34.98	247.32	99.51

Tensile strength and extension, abrasion resistance and hairiness count are critically important for weavability in fabric manufacturing. As shown in Table 4, polyester/cotton blended yarn sized by cationic graft starch exhibits the best sizing performances in each respect, especially in abrasion resistance. This is because cationic graft starch has better compatibility to synthetic fibers and lower viscosity, which gives it better film forming ability, coating ability and permeability than other two kinds of sizing agent.

Conclusions

In this work a new kind of cationic graft starch has been synthesized, its grafting ratio reaches 19.05%, that far higher than similar products sell on market. This newly synthesized starch size combines advantages of cationic starch and graft starch for the first time, and it also has other advantages including low cost, pollution-free and easy for production. Sizing experiments prove that this new starch size has good sizing performances and can completely replace PVA.

References

[1] Y.Y. Zhou: *Textile Size* (China Textile & Apparel Press, China 2004).

[2] G.D. Wang, L.M. Guo: Cotton Textile Technology. Vol. 34 (2006), p. 134-137.

[3] A. Hebeish, M.K. Beliakova, A. Bayazeed: Journal of Applied Polymer Science. Vol. 68 (1998), p. 1709-1715.

[4] K.M. Mostafa, A.A. El-Sanabary: Journal of Applied Polymer Science. Vol. 88 (2003), p. 959-965.

[5] M.K. Beliakova, A.A. Aly, F.A. Abdel-Mohdy: Starch-Starke. Vol. 56 (2004), p. 407-412.

[6] J. Liang, L.M. Guo: Cotton Textile Technology. Vol. 36 (2008), p. 14-16.

[7] FZ/T 15001-2008. *Commonly used modified starch in textile warp sizing*, Edited by National Development and Reform Commission, (Standards press of China, China 2008).

[8] X.R. Fan, R.P. Rong, H.J. Ji: *Textile size measurement technology* (China Textile & Apparel Press, China 2007).

[9] Hang Zhou university chemistry department Analytical chemistry teaching and research section: *Analytical chemistry book* (Chemical Industry Press, China 1983).

[10] B. Zhang, Y.Y. Zhou: Journal of Dong Hua University. Vol. 31 (2005), p. 86-89.

© (2011) Trans Tech Publications, Switzerland
doi:10.4028/www.scientific.net/AMR.331.148

Evolutionary Engineering of Bacillus for Terephthalic Acid Degradation

Jixian Gong [1.2.a], Zheng Li[1.2],Qiujin Li[1.2], Jianfei Zhang[1.2]

[1.] School of Textiles, Tianjin Polytechnic University, Tianjin, 300160, China;

[2.] Key Laboratory of Advanced Textile Composites (Tianjin Polytechnic University), Ministry of Education, Tianjin 300160, China

[a]e-mail: gongjixian@126.com

Keywords: Evolutionary engineering, Biodegradation, Terephthalic Acid (TA)

Abstract. Evolutionary engineering is a novel whole-genome wide engineering strategy inspired by natural evolution for strain improvement. Terephthalic acid (TA) is the most important starting material for making synthetic products, especially polyester fiber and plastics. Both TA and its manufacturing wastewater show acute, chronic and molecular toxicity to organisms. In textiles manufacturing, alkali de-weighting finishing of polyester fabrics was a main resource for producing waster water containing TA. Microorganisms can hardly adapt to the high pH caused by the alkali in wastewater of alkali de-weighting process. Although the strain for TA biodegradation already have been isolated, it is necessary to develop new innovative methods of treating TA in alkali de-weighting wastewater effectively. In this investigation, evolutionary engineering was applied to improve the characterization of Bacillus strain and the high pH resistance phenotypes were obtained. The approach of selection procedure presented in this investigation may provide an attractive promising alternative for improvement of pH resistance strain.

Introduction

Evolutionary engineering is a novel whole-genome wide engineering strategy inspired by natural evolution for strain improvement. This method exploits natural design principles and can be vary effective in phenotype improvement. There have been many recent examples in which satisfactory performance of rationally designed strains was achieved only through evolutionary engineering [1-13].

Terephthalic acid (TA) is the most important starting material for making synthetic products, especially polyester fiber and plastics. Both TA and its manufacturing wastewater show acute, chronic and molecular toxicity to organisms [14, 15]. In textiles manufacturing, alkali de-weighting finishing of polyester fabrics was a main resource for producing waster water containing TA. Microorganisms can hardly adapt to the high pH caused by the alkali in wastewater of alkali de-weighting process. Although the strain for TA biodegradation already have been isolated, it is necessary to develop new innovative methods of treating TA in alkali de-weighting wastewater effectively.

In this investigation, evolutionary engineering was applied to improve the characterization of Bacillus strain and the high pH resistance phenotypes were obtained.

Materials and methods

Strains and medium. The initial Bacillus strain, *comamonas testosteroni* F4, was isolated from waste water of chemical fiber factory and stored in our laboratory. Culture medium (beef extract 3 g/L, peptone 5 g/L, sodium chloride 5 g/L) was prepared and sterilized, then TA was added into the medium.

Culture conditions. Bacillus strain cell inoculum was grown in 50 ml of YM medium in a 250-ml Erlenmeyer flask under constant temperature of 30°C, stirrer speed of 120 rpm, for 24 h. Fresh medium was inoculated with the seed culture at 10% volume.

Construction of initial population. To increase genetic variability, cultures were randomly mutagenized with UV light. And the UV-mutagenized population was used as initial population. UV mutagenesis was done with cells grown in YM medium to an optical density of 0.3 to 0.4 at 600 nm. Cells were aseptically poured into a Petri dish in a sterile inoculating hood equipped with a UV light and exposed to >90% kill (15 to 30 min depending on the strain). Cells were grown for 18 h in the dark and then plated on selective agar or YM agar.

Estimation of cell growth and TA degradation. The growth of *comamonas testosteroni* was examined with spectrophotometer at the absorbency of 600 nm marking as OD_{600}. The concentration of TA in the medium was measured with ultraviolet spectrophotometer at 240 nm.

Results and discussion

Determination of selective pressure. Although the technology of evolutionary engineering was an attractive potential approach for strain improvement, the applications were restricted to only a few phenotypic improvements, such as substrate spectrum extension or acquirement of resistant strains. The challenging task in application of this combinatorial cell optimization method was due to the difficulty to design a suitable selection strategy.

In this study, high pH was employed as selective pressure. First of all, resistance of wild-type strain to high pH condition induced by alkali in environmental niches was estimated by growing cells in shake flask for 32 h (Fig.1).

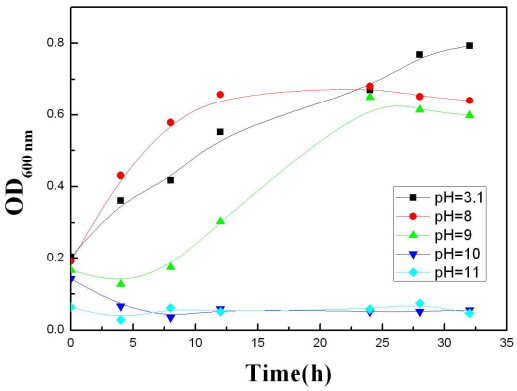


Fig.1 Growth characterization of initial strain in different pH condition.

The result showed that the initial Bacillus strain cannot adapt to high pH medium and the biomass became lower in the medium with high pH. It indicated that the growth of cells was inhibited by the adversity. It can be seen that the pH value of 10 was sufficient to reduce the cell density. So the medium with pH 10 was acted as selection stress in this study.

Evolution of high pH resistant strain in long-term continuous culture. To increase genetic diversity, the initial Bacillus strain, *comamonas testosteroni* F4, was mutagenesised and this mutagenized population was used to inoculate selection preparations. Then five initial populations were cultivated for 265 h at selective pressure and the culture was transferred every 24 h (Fig 2).

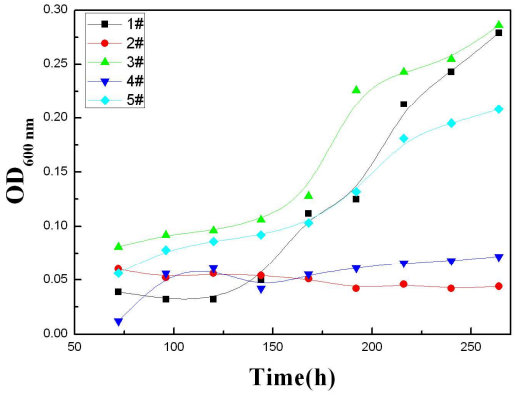


Fig. 2 Evolution of Bacillus strain under high pH stress

Evolution of Bacillus strain was carried out by sequentially subculturing under high pH stress environmental niches. Within the first 150 h, the cell density was very small. During the following 100 h, the cell density of three populations (1#, 3# and 5#) increased distinctly, while the biomass of the two populations (2# and 4#) remained at the low level. This indicated that the cells in the three populations can adapt to the environmental stress during the long-term continuous culture under selection pressure.

Quantification of the evolved strains. After 11 round of transfer, the strains were subjected to 265 h continuous culture and three adaptive populations were obtained. Then six evolved strain was isolated from the three adaptive populations through streaking on Petri dish cultures at pH of 10. The ability of biodegradation of TA at comparative higher pH conditions was measured and evaluated (Fig 3).

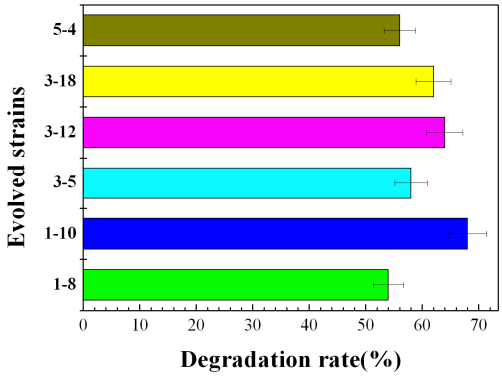


Fig. 3 TA biodegradation rate of evolved strains

The result showed that degradation rate of TA can be above 60% with the evolved strains at pH of 10. This indicated that the high pH resistant strains were obtained through evolutionary engineering. The approach of selection procedure presented in this investigation may provide an attractive promising alternative for environmental resistant strain.

Acknowledgements

This work was financially supported by National Natural Science Foundation of China (NSFC-20875068, NSFC-21006072), Natural Science Foundation of Tianjin (No.09JCZDJC26400).

References

[1] O. Selifonova, F. Valle, V. Schellenberger, Applied and Environmental Microbiology Vol.67 (2001), p.3645.
[2] M. Sonderegger, U. Sauer, Applied and Environmental Microbiology Vol.69 (2003), p.1990.
[3] Steiner P, Sauer U, Biotechnology and Bioengineering Vol.84 (2003), p.40.
[4] A. J. A. van Maris, J. M. A. Geertman, A. Vermeulen, M. K. Groothuizen, A. A. Winkler, M. D. W. Piper, J. P. van Dijken, J. T. Pronk, Applied and Environmental Microbiology Vol.70 (2004), p.159.
[5] Z. P. Cakar, U. O. S. Seker, C. Tamerler, M. Sonderegger, U. Sauer, FEMS Yeast Research Vol.5 (2005), p.569.
[6] M. Kuyper, M. J. Toirkens, J. A. Diderich, A. A. Winkler, J. P. van Dijken, J. T. Pronk, FEMS Yeast Research Vol.5 (2005), p.925.
[7] H. W. Wisselink, M. J. Toirkens, M. D. F. Berriel, A. A. Winkler, J. P. van Dijken, J. T. Pronk, A. J. A. van Maris, Applied and Environmental Microbiology Vol.73 (2007), p.4881.
[8] P. M. R. Guimaraes, J. Francois, J. L. Parrou, J. A. Teixeira, L. Domingues, Applied and Environmental Microbiology Vol.74 (2008), p.1748.
[9] K. Jantama, M. J. Haupt, S. A. Svoronos, X. L. Zhang, J. C. Moore, K. T. Shanmugam, L. O. Ingram, Biotechnology and Bioengineering Vol.99 (2008), p.1140.
[10] J. P. Meijnen, J. H. de Winde, H. J. Ruijssenaars, Applied and Environmental Microbiology Vol.74 (2008), p.5031.
[11] Z. P. Cakar, C. AlkIm, B. TuranlI, N. Tokman, S. Akman, M. SarIkaya, C. Tamerler, L. Benbadis, J. M. Francois, Journal of Biotechnology Vol.143 (2009), p.130.
[12] A. Gilbert, D. P. Sangurdekar, F. Srienc, Biotechnology and Bioengineering Vol.103 (2009), p.500-512.
[13] H. W. Wisselink, M. J. Toirkens, Q. Wu, J. T. Pronk, A. J. A. v. Maris, Applied and Environmental Microblology Vol.75 (2009), p. 907.
[14] N. Scholz, Chemosphere Vol.53 (2003), p.921.
[15] S. Qi, X. Wang, X. Xu, Q. Xiang, Wei sheng yan jiu, Journal of hygiene research Vol.31 (2002), p.10.

© (2011) Trans Tech Publications, Switzerland
doi:10.4028/www.scientific.net/AMR.331.152

Correction for Classical Theory of Yarn Cross-section Shape in Woven Fabric

Lianhe Yang[1, a], Yajuan Yu[1,b], Weixin Liu[1,c]

[1] School of Computer Science and Software, Tianjin Polytechnic University, Tianjin 300160, China

[a]yanglh@tjpu.edu.cn, [b]yyjprincess@yahoo.cn, [c]liuweixin1979@126.com

Keywords: Woven Fabric, Yarn Cross-section Shape, Visualization Technology, Volume Cutting.

Abstract. The cross-section of yarn in plain woven fabric has always been viewed as an invariable shape by academe. However, with visualization technology, problems in the classical model are exposed based on traditional convex model, and when solving the problems with calculus, the rule of yarn cross-section deformation is found. The results show the diversity of yarn cross-section shape in both one-layer and multi-layer woven fabric, instead of unitarity, especially for warps weaving multi-layer wefts, whose convex cross-section alternates with concave one periodically in length. The results take exception to "invariant cross-section assumption" and have theoretical value and guidance for the real shape of yarns and the simulation of fabric appearance.

Introduction

There have been a variety of discussions about the shape of yarn cross-section in plain woven fabric for decades. Some scholars claimed to describe with round or oval shape, another advocated to describe with runway shape, and still another scholars advocated with convex lens shape (double convex) [1,2]. In contrast, convex lens shape seems more reasonable, more classical, and much closer to the physical situation. It seems no one has argued it over the years and this "invariable cross-section theory" has also been extended to multi-layer woven fabrics as well as three-dimensional woven composites preform[3-7]. In other words, people think that yarn cross-section of multi-layer woven fabric still shows a changeless form. Recently, some scholars have pointed out that there exists difference between the external and internal yarn cross-sections in a three-dimensional orthogonal architecture [8].

With the development of computer graphics, visualization technology has been applied gradually[9]. After the spacing data field of fabric solid model has been generated, we can observe the shape of yarn through visualization technology. i.e., a woven fabric's three-dimensional graphics can be displayed vividly on screen for one to observe the shape of a yarn in any proportion, from any angle, and select any profile to cut the unit cell (representative volume cell). Simulation result shows that there has been erroneous understanding in the description of yarn cross-section shape in a fabric.

Start from the classical cross-section theory of plain woven fabric, by using calculus idea and visualization techniques, we found that the cross-section of yarn in plain fabric was not invariable, but changed periodically, and this result applied to multi-fabric in particular, therefore classical theory of yarn cross-section shape in woven fabric was amend, expanded and generalized.

Problems Existed in Classical Model

According to the classical theory, the axis shape of a yarn in a plain woven fabric could be assumed to be a sine shape[1]. As for the cross-section shape, although it was assumed to be a double-convex lens pattern, the classical theory did not state how to use a function to describe the top and bottom contours exactly. However, according to the simple idea that warp and weft "imitate each other", it is not difficult to imagine that a warp's sine shape makes the contour lines of cross-section of the interwoven weft take the same shape, and vice versa.

To exclude the interference of other factors, based on the traditional assumptions—— "sine axis, double-convex cross-section", following constraints are added in this paper:

(1) The same untwisted tows are used for warp and weft;

(2) Warp and weft have the same tension;

(3) Warp and weft have the same count and interweave closely.

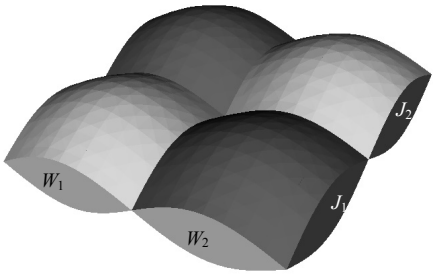
The above assumptions can guarantee the same flexion degree for warp and weft so as to make the unit cell of plain woven fabric be square in the horizontal direction. If the side length of the square is L, and the thickness of the unit cell is T, then the width of the yarn is $L/2$, and its thickness is $T/2$. Set the coordinate system used here is right-handed, and x, y, z are warp, weft and fabric thickness direction respectively. Thus, the top and bottom surfaces of warp can be described by the surface function Eq. 1.

$$\begin{cases} z_t = \dfrac{T}{2} + \dfrac{T}{4}\sin(\dfrac{2\pi}{L}x) + \dfrac{T}{4}\sin(\dfrac{2\pi}{L}y) \\ z_b = \dfrac{T}{2} + \dfrac{T}{4}\sin(\dfrac{2\pi}{L}x) - \dfrac{T}{4}\sin(\dfrac{2\pi}{L}y) \end{cases} \tag{1}$$

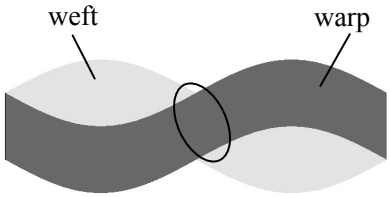
Weft function can be described similarly, with x and y exchanged.

With functions of a yarn, the coordinates of the sampling points in a unit cell can be calculated directly, and the spacing data field can be constructed. By using visualization tool-kit(VTK)[10], the three-dimensional graphics generated can be observed, as shown in Fig. 1 (a).

At first glance, the unit cell seems impeccant, but we find that the yarn thickness become thinner in the midpoint of the peak and trough after volume cutting (the vertical distance between the top and bottom is still $\Delta Z = T/2$), as shown in Fig. 1 (b) . The problem is particularly prominent when multi-layer woven fabric is described by a similar surface function.



(a) 3D appearance



(b) Internal cross-section

Fig.1 Plain-weave model from equation

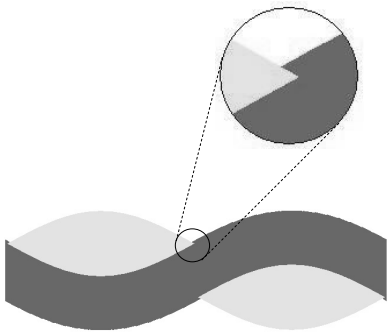


Fig.2 Overlapped warp and weft

To make yarn's thickness "uniform", the angle of orientation, θ_i, for each yarn segment (micro-element) can be calculated, and then the Z coordinates of both top and bottom of the segment can be extended, making $\Delta Z = T/2/\cos\theta_i$. Although the expansion of Z coordinates solves the problem of yarn's uniform thickness, after volume cutting it can be found that there exists some overlap region between warp and weft, as shown in Fig. 2.

And this means that, according to the traditional "sine axis, double-convex cross-section" assumption, the warp and weft constructed will *overlap*! The same simulations show that any other invariable cross-section assumptions will lead to the same results. Thus, the classical cross-section theory is not flawless.

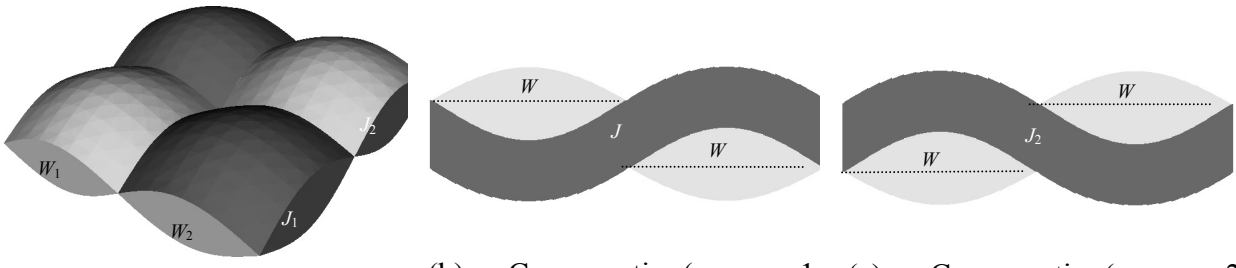
Use calculus to solve the problem of overlapping

Calculus provides a way to solve the problem above, making the overlapping problem be resolved.

First, "differential": divide the unit cell into n equal portions along x, y direction (n is even). Thus when viewed from x-y plane, the unit cell is divided into n^2 square columns, with each column having both warp element and weft one, which may overlap in the contacted area. In accordance with "moving each tow back halfway" and "smoothing" algorithm, the problem of overlapped warp and weft elements can be solved.

Second, "integral": all the micro-elements are "integrated", the entire unit cell can be regenerated, and the spacing data field will be obtained.

Finally, "reconstruction": with the data field obtained, visualization technology can be used to reconstruct three-dimensional graphics, as shown in Fig. 3(a).



(a) 3D appearance (b) Cross-section(warp 1 (c) Cross-section(warp 2

Fig.3 Unit cell and section without overlap internal

Comparing Fig. 1(a) with Fig. 3(a), no difference can be seen. But after the implementation of volume cutting, it is found that the warp peak becomes flatten, and the top and bottom contour lines in weft cross-section are no longer symmetrical, as shown in Fig. 3(b). Comparing Fig. 3(b) with Fig. 3(c), it can be found that one weft has different cross-sections in different locations.

Theoretically, the top and bottom warp contour lines in Fig. 1(b) are composed of two "parallel" sine curves (moving one parallelly obtain another); Fig. 3(b) are composed of two "isometric" curves. It is clear that the former could not have been isometric curves, and the later could not have been sine curves. Accordingly, the weft cross-section contour lines imitating the curve are not the sine curves. Obviously, It is hard to use a mathematical expression to describe a physical yarn axis and cross-section precisely.

Now, the key question is: under the assumption mentioned above, how to prove that the simulation cross-section shape shown in Fig. 3(b) and (c) is the physical shape of a yarn cross-section?

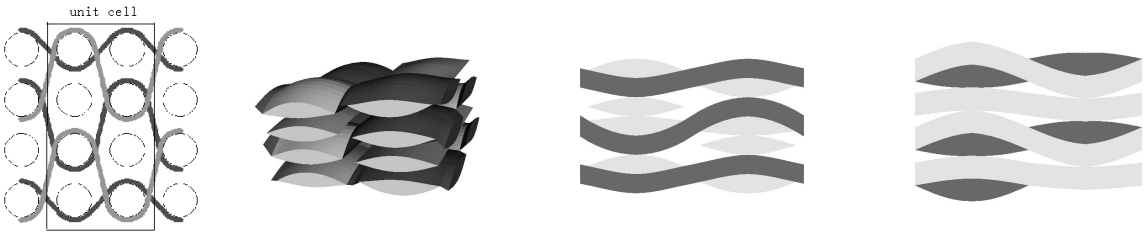
In accordance with the ideas of calculus, a circle's area and circumference can be approximated by a polygon. i.e., as long as the number of sides of a regular polygon is sufficient, its area can approximate a circle's aera, and its circumference can approximate a circle's circumference. Similarly, in the issue above, as long as the selected n is large enough, we justifiably believe that the section pattern in simulation is the physical shape of yarn cross-section.

By the way, we have assumed that warp and weft have the same material, tension and count, because only in this way can warp and weft have the same deformation in plane woven fabric, and the "moving each tow back halfway" algorithm has its practical significance.

In fact, when simulating a two-dimensional plain woven fabric, it is difficult to tell whether the axis is a standard sine curve with the naked eye. So is the symmetry of a cross-section. But when the same analysis is put on the multi-layer fabric as shown in Fig. 4(a) and (b), the cross-section asymmetry issue is much more significant, and so is the flattening of an axis at the peak, as shown in Fig. 4(c) and (d).

The simulation also shows that when the number of fabric layer increases further, especially when a warp interweaves more layers of weft, the warp's cross-section will change from convex to concavo, as shown in Fig. 5.

It can be seen that no matter how many layers the woven fabric have, a yarn cross-section shape is not an invariable pattern that the traditional literature talks about, instead, it is diversified.



(a) Topology (b) Geometry model (c) Weft section (d) Warp section

Fig.4 Topology, geometry and sections of 4-layer woven fabric

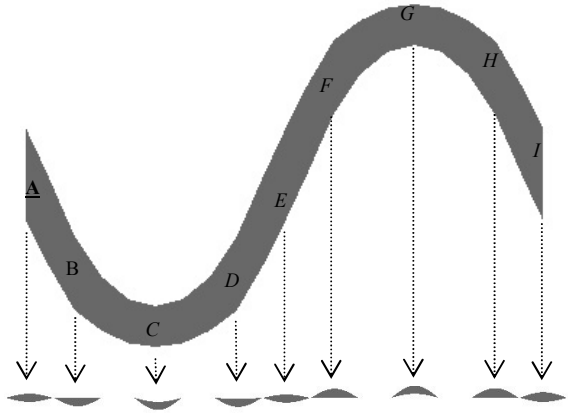


Fig.5 Variation of warp cross-section in length

Conclusions

In this study, volume cutting function and local reconstruction one in visualization technology make it possible to observe the shape of an internal yarn of a fabric. With this technology, the yarn patterns of plain and multi-layer woven fabrics were studied. From the above study we can arrive at the following conclusions:

(1) The shape of internal yarn cross-section along its length is not invariable even though the woven fabric has a plain weave.

(2) The classical yarn cross-section pattern in plane woven fabric cannot be extended to multi-layer fabric directly.

(3) The yarn cross-section pattern in multi-layer woven fabric is diversiform and changes along its length periodically.

References

[1] B.X. Cai. *Fabric structure and design*, *3rd Edition*(China Textile Press, Beijing,2004).(In Chinese)
[2] Q.W. Guo, X.Q. Wu: Journal of Textile Research, Vol. 29(2008),p.42-45. (In Chinese)
[3] X.F.Wang, X.W.Wang, G.M. Zhou:Journal of Composite Materials, Vol. 41(2007),p.1773-1788.
[4] W. Sun, F. Lin, X. Hu:Composites Science and Technology,Vol.61(2001),p.289-299.
[5] G. Hivet,P. Boisse:Finite Elements in Analysis and Design,Vol.42(2005),p. 25-49.
[6] H.J. Kim, C.C. Swan: International Journal for Numerical Methods in Engineering, Vol.58(2003),p. 1683-1711.
[7] S.V. Lomov,G. Huysmans:Composites Part A,Vol.32(2001),p.1379-1394.
[8] X.F.Guo: Journal of Textile Research, Vol.29(2008),p.62-65. (In Chinese)
[9] J.G.YAO:High performance calculation development and application, Vol.21(2007),p.27-31.
[10] Y.G.REN, G.Yu:Computer Science, Vol.31(2004),p.92-96. (In Chinese)

© (2011) Trans Tech Publications, Switzerland
doi:10.4028/www.scientific.net/AMR.331.156

Analysis of Color Symbology Focused on Folk Costume Colors in Northern and Southern Regions of China during Republic Period

QI Yan[1, a], FAN Xuerong[1, b], CUI Rongrong[1, c], Qiang Wang[1, d]

[1]School of Textiles and Clothing, Jiangnan University, Wuxi, Jiangsu 214122, China
[a]qiyan830@126.com, [b]wxfxr@163.com, [c]cuirong3369@sina.com, [d]qiang_wang@163.com

Keywords: costume color, color symbology, cultural code, costume geography, Q-Model

Abstract. Costume color samples from the rural areas in northern and southern regions of China during the Republic Period were collected, measured with a spectrophotometer, and the symbolization of colors as cultural codes were analyzed by the Q-model. The results show that red, blue and black which are included in the traditional five colors system are more frequently-used colors in the northern region, and dark grayish blue and black are more significant colors of high frequency in the southern region. These colors all acted as cultural codes with cultural significance. This paper furthers understanding of color symbology from perspective of cultural semiotics focused on folk costume colors.

Introduction

Costume is not only daily consumer goods but also a symbol system of folk-custom culture. As an important visual element of costume, costume color reflects the collective thinking and aesthetic concepts of the times. The formation, development and evolution of costume colors are results of long-term effects of nature, human geography and other factors. The analysis of costume colors as cultural codes is one tool language to understand a specific nation's culture [1]. Despite some studies for the costume colors, there have been little literatures to investigate their role as cultural codes. In this study, we have made a comparative analysis of costume colors from the perspective of cultural semiotics and interpreted them as cultural codes.

Method and Terms

The range of this study focused on costume colors in the rural areas during the Republic Period. The formation of the Republic Period puts an end to over two thousand years of imperial rule [2]. The colors representative of each region during this times were interpreted as cultural codes to understand Chinese culture. Furthermore, costume colors in the southern region and the northern region were analyzed. The northern region mainly focuses on Beijing, Tianjin, Shandong and their surrounding areas, and the southern region mainly focuses on Jiangsu, Zhejiang, Shanghai and their surrounding areas.

In this paper, the costumes from each region were limited to the women's everyday dress, and costumes of the proletariat women in the rural areas were taken as main research objects. Many folk costume collections in the northern region and southern regions were selected, and other costume samples were collected from relics, digital images of books and fashion magazines. Each sample was measured and photographed to give a more detailed description about the colors. Then the colors were converted by computer graphics manipulation with the use of Adobe Photoshop. 803 color samples were collected from digital images of costumes and each sample was measured with a spectrophotometer. Then the colors were analyzed by 10 hues with the Munsell Color system and 12 tones with Practical Color-ordinate System.

To analyze the significance of costume colors as cultural codes, we used a 'Q-model' (Quillian-Model [3]) based on the semantic system of Greimas [4] (Fig.1). The model is a hierarchical analyzing method for analyzing the cognition system in semiotics. With the Q-model, the signification of a code can be separated into 'underlying meanings' and 'additional meanings' [5]. With the semantic system of Greimas, a process of unlimited semiosis can be expanded into various fields of meaning. The Q-model can be applied to the nonverbal signs such as costume colors.

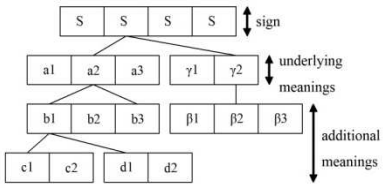
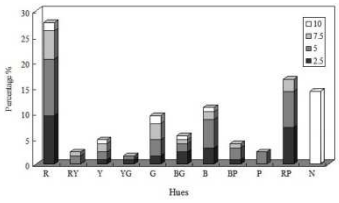
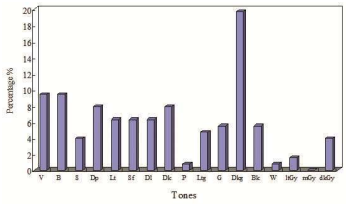


Fig. 1 Semantic structure



(a) Hue

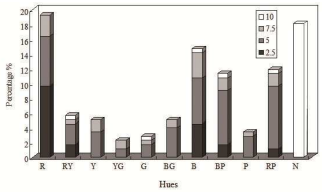


(b) Tone

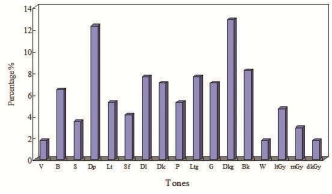
Fig. 2 Hue (a) and tone (b) charts of main colors of the northern region.

Results

For the study of the costumes in the northern region, 450 costume colors were collected. These colors were divided into main colors and decoration colors. The main colors refer to the colors that have the largest area in the hues and tones of costume colors. The decoration colors are the costume colors except the main colors. Comparing the two groups of colors, we found that hue frequency of main colors of the northern region was as follows (Fig.2-a): red (27.8%), red-purple (16.7%), neutral colors (14.3%), blue (11.1%), green (9.5%), green-blue (5.7%) and yellow (4.8%). In the tone analysis, dark grayish (19.7%) tone showed the highest frequency of main colors and the next orders from the northern region were as follows (Fig.2-b): vivid (9.5%), bright (9.5%), deep (7.9%), dark (7.9%), light (6.3%), soft (6.3%), dull (6.3%), black (5.6%) and grayish (5.6%). Hue frequency of decoration colors was as follows (Fig.3-a): red (19.3%), neutral colors (18.1%), blue (14.8%), purple-blue (11.4%), yellow-red (5.7%), yellow (5.1%) and green-blue (5.1%). In the tone analysis, dark grayish (12.9%) tone showed the highest frequency in decoration colors and the next orders were as follows (Fig.3-b): deep (12.3%), black (8.2%), dull (7.6%), light grayish (7.6%), dark (7.0%) and grayish (7.0%).



(a) Hue

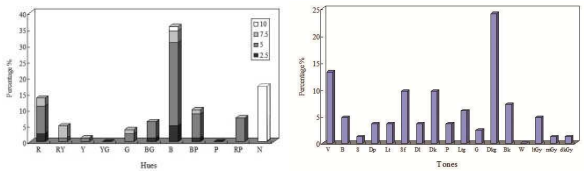


(b) Tone

Fig. 3 Hue (a) and tone (b) charts of decoration colors of the northern region.

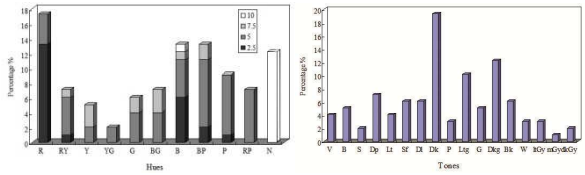
To analyze the color characteristics of the costumes in the southern region, 353 costume colors were collected. A hue analysis of samples from the southern region showed that frequency of main colors was as follows (Fig.4-a): blue (35.8%), red (13.6%), neutral colors (17.3%), purple-blue (9.9%), red-purple (7.4%) and green-blue (7.4%). Tone frequency of main colors of the costume samples was as follows (Fig.4-b): dark grayish (24.1%), vivid (13.3%), soft (9.6%), dark (9.6%) and black (7.2%). Meanwhile, hue frequency of decoration colors of the costume samples was as follows (Fig.5-a): red (17.4%), blue (13.3%), purple-blue (13.3%), neutral colors (12.2%), purple

(9.2%), red-purple (7.1%) and green-blue (7.1%). Tone frequency of decoration colors of the costume samples was as follows (Fig.5-b): dark (19.4%), dark grayish (12.2%), light grayish (10.2%), deep (7.1%), black (6.1%), dull (6.1%) and soft (6.1%).



(a) Hue (b) Tone

Fig. 4 Hue (a) and tone (b) charts of main colors of the southern region.



(a) Hue (b) Tone

Fig. 5 Hue (a) and (b) tone charts of decoration colors of the southern region.

Discussion

In the process of understanding the changes in folk costumes of rural areas according to the diachronic stages of culture as well as the changeless geographical location, we found that the colors that changed the most in their symbolic meanings were red, blue, black, gray and green.

Red included in the traditional 'Five-element theory' was understood to represent the 'Yang' segment in the theory of 'Yin-yang Wu-hsing', a positive force signifying strength, passion, absolute power and life. As such, red was frequently used in costume colors of both lower and higher class in China during the Republic Period.

Blue was also included in the traditional 'Five-Element theory', it was commonly used to decorate the costumes and it represent trees. The reason why it was widely used in the costumes of rural areas was that it was an economic color to use on clothing, as it faded slowly, was less likely to be damaged by hugs, and could be dyed using various methods with inexpensive dyes. In the southern region, dark grayish blue showed the highest frequency in main colors while light red showed the highest frequency in decoration colors. The use of this chromatic contrast shows that the costume colors in the southern region expressed their aesthetic perception of forms in the same contrast method as the costume colors in the northern region. However, the proportion of blue was greater than red in main colors but was less than red in decoration colors, which was different from the characteristic of the costume colors in the northern region that the proportion of red was always greater than blue both in main colors and decoration colors. It was because that the southern costume colors in the rural areas were closely related to the local geographical and natural environment.

In ancient China, gray was considered to be a low-class color and it was banned from all formal uses. It was generally not even considered a color. Black which was used as a code for sadness and winter was also rarely used for women's costumes. However, during the Republic Period of China, black signified practicality, the beginning of western-style education, the accommodation of new cultures, and the social acclimatization of women. Li ever mentioned in his paper, "it thought that Women liked black dress in that time was because they had tired of blue robe and red dress and turned to like the quiet black" [6]. In that time, gray was also becoming the representative color, it was associated with domains related to metals, buildings and cutting-edge technologies, and its underlying meaning had changed from a grave, devout image to a modern, futuristic image. The higher use frequency of gray and black brought about a great change to color esthetic relative to high pure color and low secondary color in Chinese traditional theory [7].

Meanwhile, the frequency of gray and black accounts for the obviously regional distinction of costume. There were large differences between large city, middle-size and small cities, coastal city and inland city, and the same between city and village. Some costumes which had outmoded in

large cities began to be fashionable in middle-size and small cities, and possibly had not appeared in some rural and remote areas. In China, the southern region tends to be radical and revolutionary, while the northern region is stolid and conservative. The southern costume colors were easily influenced by foreign cultures. Black and gray (mGy, dkGy), therefore, tended to be used with higher frequency in the southern region than the northern region (FIG.6).

In some cultures, green symbolizes hope and growth, while in others, it is associated with death, sickness, envy or the devil. Green is also associated with regeneration, fertility and rebirth for its connections to nature. Women in the rural areas had more chances to know or wear military uniforms under the advantageous condition of revolutionary. Therefore, green showed higher frequency in main colors of the northern region than the southern region. However, the frequency of green in decoration colors of the northern region had far exceeded the one in the northern region (FIG.7), it was because these colors most came from the patterns of embroidery costumes which was unique to the southern region.

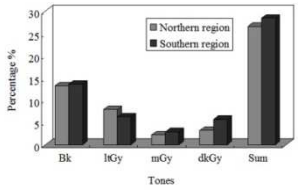


Fig. 6 Tone chart of noncolors based on the two different regions of China

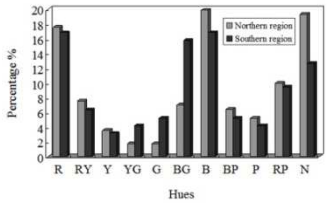


Fig. 7 Hue chart of decoration colors based on the two regions

Conclusion

With the analysis of the Q-model, these colors functioned as cultural codes. The formation of costume colors in the northern region, on one hand, was influenced by the traditional five colors system; on the other hand, it can form contrast with the wintery environment of the northern region. However, the formation of the costume colors in the southern region was more closely influenced by the foreign cultures because the cities in this region are more open than the cities in the northern region, although it was also influenced by the traditional five colors system. From the perspective of environment, the costume colors in the northern region adapted to local farming culture while it was more relevant to local Watertown culture in the southern region. In conclusion, colors have been used as cultural codes with cultural symbolisms, and could be used as a tool to analyze the peculiarities of a nation's culture.

References

[1] J.H. Lee and Kim Y.I.: Analysis of color symbology from the perspective of cultural semiotics focused on Korean costume colors according to the cultural changes. *Color Research and Application*, Vol.32 (2007), pp.71-79.

[2] X.Y. Bian: Shanghai' fashion during Republic Period. *Journal of Donghua University (Eng. ed.)*, Vol. 2 (2004), pp. 6-17.

[3] M.R. Quillian: Semantic memory. In: Minsky M, editor. Semantic Information Processing. (Cambridge, Massachusetts: MIT Press, 1968).

[4] A.J. Greimas: Semantique Structurale. (Paris: Larousse; 1996).

[5] U. Eco: A Theory of Semiotics. (Seoul: Moonhak & Jisung Sa, 1985).

[6] Y.Y. Li: The judgment of clothes' beauty. *Women Magazine,* Vol. 14(3) (1928), pp. 23-26.

[7] J.Q. Zhang: From Monism to Dualism: Inheritance Meridians of Modern Chinese clothing. (Beijing: China Textile & Apparel Press, 2009). (in Chinese)

© (2011) Trans Tech Publications, Switzerland
doi:10.4028/www.scientific.net/AMR.331.160

Preparation of Chitosan/Acacia Microcapsule Facilitating Photo-catalytic Degradation of Polypropylene Nonwovens

Xiaomei Wang[1,a], Chengrong Zhang[2,b]

[1,2] School of Textile and Clothing, Wuyi University, Middle Yingbin road 99, Jiangmen, Guangdong, 529020, China

[a] wxm@wyu.cn, [b]zincring@163.com

Keywords: photo-catalytic degradation, nanometer titanium dioxide, complex coacervation, chitosan, acacia, polypropylene nonwovens

Abstract. Since the "plastic limit order" was released, shopping bags made of polypropylene spun-bonded nonwovens have been wildly used in daily life for their portability and recyclability. However, polypropylene materials are difficult to be degraded in natural conditions, thus they are not the "real" environmental protection bags. Many studies demonstrate that TiO_2 has obvious effects on raising nonwovens' photo-catalytic degradation rate. In this study, the microcapsules were prepared with complex coacervation method using chitosan and acacia as wall and TiO_2 as core material. In addition, the main process parameters including the concentration of chitosan, PH of the coacervation solution and stirring speed, which have effects on the microcapsule formation behavior were discussed specially. The results show that the good microcapsules were produced at the condition of the chitosan concentration of 0.4%, the PH valued about 3.18, stirring speed of 300r/min, temperature of the coacervation 60℃and the condensation reaction time for 15 minutes.

Introduction

In order to avoid the environment pollution of disposable plastic bags, nonwovens shopping bags come out at the historic moment, and gradually replace the plastic shopping bags [1].

Presently, the photo-catalytic degradation on disposed polypropylene spun-boned nonwovens materials has been the focus. For example, Yaoming Zhao [2] produced the polypropylene spun-bonded nonwovens containing 0.0%~1.2% TiO_2 photosensitizer. We have prepared titania sol by using $Ti(OC_4H_9)_4$ as a precursor with the sol-get method, and the prepared titania sol was used to finish the polypropylene spun-bonded nonwovens with the dip padding process. The tested break strength of the nonwovens sample showed that the finished polypropylenes nonwovens with the titania sol photodegraded faster [3].

The microcapsules were prepared with complex coacervation method using chitosan and acacia as wall material and TiO_2 as core material in this paper. They can be adhered to the nonwovens and once the microcapsules fracture and the nano-TiO_2 is released, hence the photo-degradation of the polypropylene material happens.

Experimental

Materials. Chitosan (degree of deacetylation 87.2, viscosity 69, Shandong AK biotech Ltd, China). Acacia (Gum arabic) was obtained from Damao chemical company (Guangdong, China). Anatase nanon-TiO_2 was purchased from Jianghu titanium white product Co. Ltd. (Shanghai, China).All other reagents and chemicals used were of analytical grade.

Equipments. The main equipments used in the preparation of the microcapsules include JH-2/60 stirrer, PH-3G PH meter and XSP-16A electrical microscope, JA5003A electronic balance.

Experiment. The microcapsules can be prepared with several methods [4] such as physical method, chemical method and physical-chemical method. The complex coacervation method is generally used in laboratory, and it also was used to prepare chitosan/acacia titanium dioxide microcapsu- le in this paper. The procedures of microencapsulation are as follows.

Firstly, adequate amount of acacia, titanium dioxide and distilled water were mixed in a dry mortar and grinded to be solution A. Amount of chitosan and anhydrous calcium chloride dissolved in 1% of acetic acid were prepared as solution B which were reserved in water-bath at 60℃.

Secondly, the two solutions were mixed and stirred at 60℃.The PH was adjusted by addition of acetic acid or NaoH (10% w/w) to induce coacervation. And then the acidified distilled water (60℃) was added into the mixed solution.

Thirdly, the temperature of the whole system was lowed to 10℃ and stirring was continued. After formaldehyde (37%, w/w) was added, the solution should be stirred for 15 minutes. And then the sodium hydroxide (20%, w/w) was added to adjust the PH of whole system to 8.0~9.0.

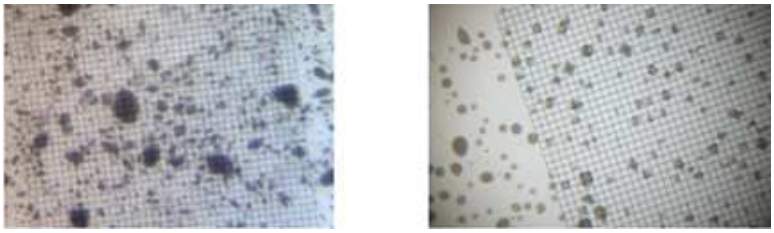
Finally, the upper clear liquid was decanted and the lower precipitate was washed with the distilled water until the odour of formaldehyde disappeared.

Particle size analysis. The microcapsule size and size distribution are mainly focused on, so the microcapsules sampled directly from the coacervation mixture system were analyzed. The optical microscope was used to observed the images of the microcapsules (10×10 magnification) and the particle sizes were scaled by the eyepiece micrometer.

Results and Discussion

As the particle size distribution of microcapsules [5] is one of the important indexes, many factors should be studied in the experiment. So the factors such as the concentration of the chitosan, PH of the mixture system and the stirring speed, temperature of the coacervation and so on were studied in this paper.

Effect of grinding process. The images of the obtained microcapsules are shown in Fig.1.

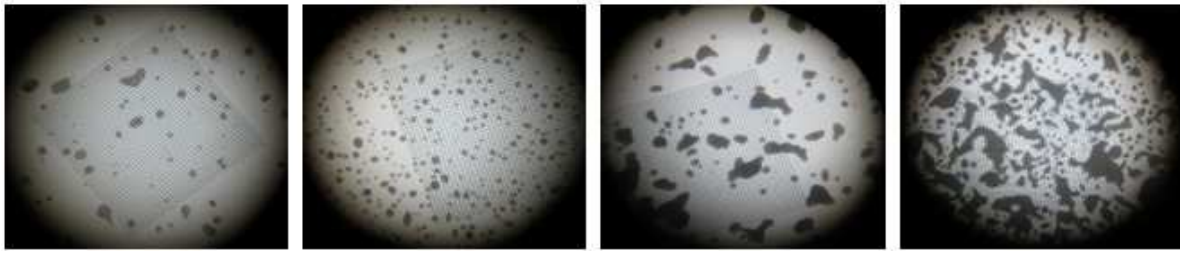


(a) (b)

Fig.1 Photomicrographs obtained without grinding (a) and with grinding (b)

It can be seen from Fig.1 that the microcapsules obtained without grinding were obviously different in size and shape, while the microcapsules obtained with grinding were more uniform, rounder and smaller in particle size. Through calculation, the CV% value of the former was10.81%, while the later was only 3.64%. Because in the grinding process, the TiO_2 particle were distributed more uniform in the emulsion, which facilitate the acacia coacervate with chitosan, leading the good microcapsules.

Effect of chitosan concentration. Produce the microcapsules with the chitosan concentration of 0.2%, 0.4%, 0.6%, 0.8% respectively, the produced microcapsules are shown in Fig.2.

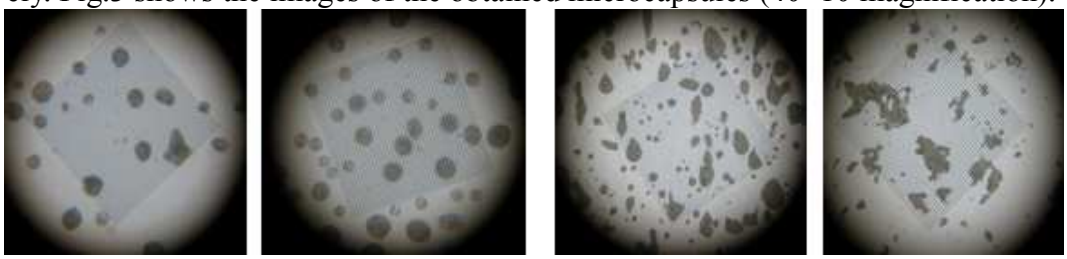


(a) (b) (c) (d)

Fig.2 Photomicrographs of microcapsules obtained with chitosan concentration: (a)0.2%, (b)0.4%, (c)0.6%, (d)0.8%

Fig.2 shows that when the chitosan concentration was 0.2%, the particle size distribution was relatively scattered, but when the concentration was 0.4%, the chitosan-acacia system produced large quantity of microcapsules with round surface, small and uniform particle size. When the concentration was 0.6%, the system could produce less microcapsules without uniform shape and even some adhered together. As for the concentration of 0.8%，the microcapsules with extremely irregular shape and particle adhesion were observed. This is because the chitosan is positively charged while the acacia is negatively charged, and the coacervation occurs due to the interaction of the two oppositely charged colloids. However, when chitosan concentration is improved, the positive charges of chitosan increase but the number of negatively charges keeps constant, so the extra chitosan can't work with acacia.

Effect of PH value. The PH value during the coacervation was adjusted to 3.0, 3.18, 4.0 and 5.0 respectively. Fig.3 shows the images of the obtained microcapsules (40×10 magnification).



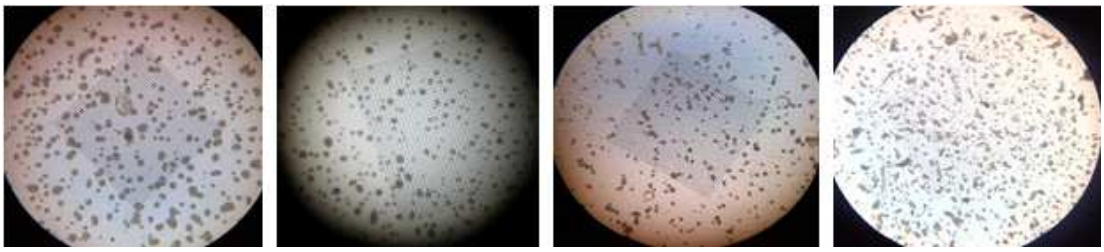
（a） (b) (c) (d)

Fig.3 Photomicrographs of microcapsules obtained at various PH (a) PH=3, (b)PH=3.18, (c)PH=4, (d)PH=5

According to the observed phenomena during the microcapsulation and Fig.3, it can be known that when PH was 3.0, the particle sizes were not uniform and also the curdy precipitate was observed. When PH was 3.18, the microcapsuls have round and uniform small particle size. Also when PH was 4.0, irregular shapes，bad uniformity and the flocky precipitate were observed. When PH was 5.0, there were no microcapsules but adhesion observed.

In conclusion, when PH was between 3 and 4, the coacervation was better, at this time, the chitosan positively charged is equal to the acacia negatively charged, which benefits for coacervation.

Effect of stirring speed. The stirring speed during the microcapsules formation was set to 200, 300, 400, 500r/min respectively. The images of the produced microcapsules are shown in Fig.4.

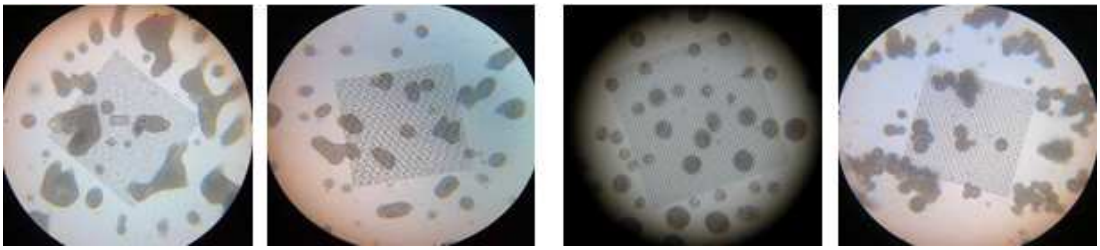


(a) (b) (c) (d)

Fig.4 Photomicrographs of microcapsules obtained with different stirring speed:
(a)r=200r/min, (b)r=300r/min, (c)r=400r/min, (d)r=500r/min

From Fig.4, it can be seen that when the speed was 200r/m, the round surface and good distribution but slight adhesion phenomenon of the microcapsules were obtained. The same but a little smaller size microcapsules were got when the speed was 300r/m. Furthermore, when the speed was 400r/m, the particle size obviously decreased but the wall became a little fragile. As the speed went up to 500r/m, the particle size turned to be much smaller while the shape was not round, and some microcapsules got broken. Therefore, the improvement of the stirring speed makes the shear rate accelerate in the solution, which is good for decreasing the microcapsules size. But too high stirring speed tends to lead the microcapsules rupture.

Effect of the temperature of the coacervation. Keep the other parameters constant, and set the temperature of the coacervation at 40, 50, 60 and 70℃ (the other parameters as stated in the Experiment part). The photomicrographs of the produced microcapsules are shown in Fig.5(40×10 magnification).

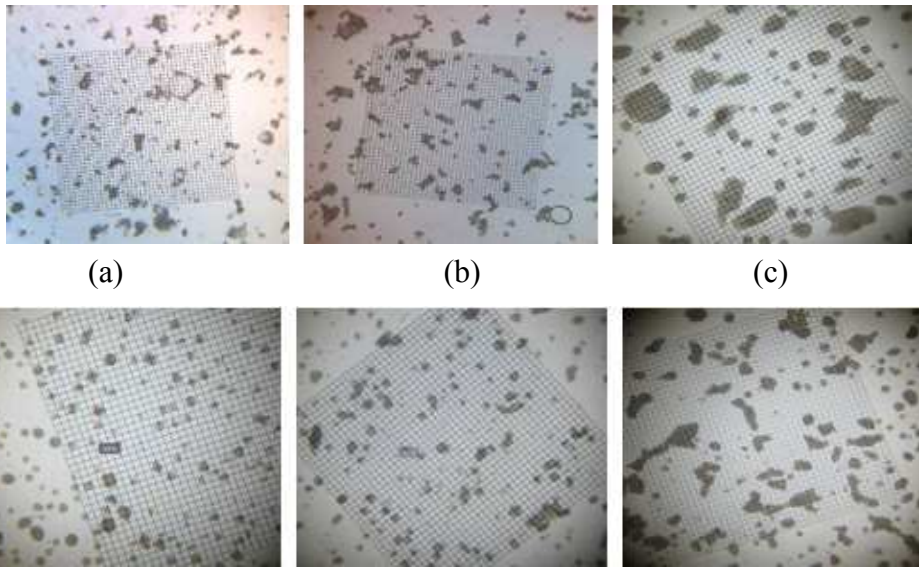


(a) (b) (c) (d)

Fig 5. Photomicrographs of microcapsules obtained at different coacervation temperature:
(a)T=40℃, (b)T=50℃, (c)T=60℃, (d)T=70℃

According to the Fig.5, it can be known that the temperature has an evident effect on microcapsules formation. When the temperature was 40℃, small numbers of microcapsules were observed and even some microcapsules adhered together. When the coacervation temperature was 50℃, the shape of the microcapsules was not round and still some microcapsules adhered together. However, when the temperature was 60℃, the produced microcapsules were round, small and uniform. As the temperature was up to 70℃, the microcapsules adhered together seriously without being well distributed. Theoretically, the low coacervation temperature leads to poor soluble property for the wall materials, which limits the polymer move, and hence affects the formation of the microcapsule. When the coacervation temperature is increased, the viscosity of the chitosan and acacia decreases. So the coacervation reaction is facilitated by the fluidity of the electrolyte improved. However, too high temperature will lead the wall of the microcapsules intenerate and microcapsules adhere together. Thus, the coacervation temperature of 60℃ is the best in the research extent.

Effects of complex coacervation time. According to the method mentioned in the Experiment part, the samples were taken from the solution every 5 minutes. The photomicrographs of the produced microcapsules are shown in Fig.6.



(a) (b) (c)

(d) (e) (f)

Fig.6 Photomicrographs of microcapsules obtained with different complex coacervation time : (a)t=0min, (b)t=5min, (c)t=10min, (d)t=15min, (e)t=20min, (f) t=25min

From Fig.6, it can be seen that within the complex coacerxation time of 5 minutes, there were no obvious microcaopsules but the flocky precipitate. After 10 minutes, the formed microcapsules appeared rounder while the curdy precipitate still existed. As the reaction lasted for 15 minutes, the produced microcapsules had a rapid increasing in number and the particle sizes are small and uniform. Until 20 minutes, lots of microcapsules but slight adhesion phenomena were observed. Unfortunately，after 25 minutes, the microcapsules adhered together seriously. Therefore, the complex coacervation time should be 15 minutes.

Conclusions

During the preparation of chitosan-acacia microcapsules, the grinding, chitosan concentration, PH, stirring speed, and the coacervation time have effects on the microcapsules formation. The grinding process can produce a good microcapsule shape, and when the chitosan concentration is 0.4%, PH value is of 3.18, the stirring speed is 300r/m, the complex coacerxation temperature is 60℃and the microcapsules formation time is 15minutes, at this condition the morphology of the resultant microcapsules are good.

References

[1] Bingxuan Ni, Xiaoning Jiao:Technical Textiles Vol. 27(2009),p. 29, in Chinese

[2] Qingshan Liu, Siyuan Zhou and Yaoming Zhao: Technical Textiles Vol. 24(2006), p. 8, in Chinese

[3] Xiao-mei WANG, Sun-hui LI: Journal of TianJin Polytechnic University Vol. 29(2010), p. 36, in Chinese

[4] Hong Hao, Guozheng Liang: Modern Chemical Industry Vol. 22(2002), p. 60, in Chinese

[5] Wei-yan Han, You-xi Zhao, Ping Gong: China Biotechnology Vol. 30(2010),p. 104, in Chinese

© (2011) Trans Tech Publications, Switzerland
doi:10.4028/www.scientific.net/AMR.331.165

Surface deposition of chitosan on wool substrate by electrospraying

Saniyat Islam[1,a], Amit Jadhav[2,b] , Jian Fang[3,c],Lyndon Arnold[4,d],
Lijing Wang[5,e],Rajiv Padhye[6,f], Xungai Wang[7,g], Tong Lin[8,h]

[1,2,4,5,6] School of Fashion and Textiles, RMIT University, Melbourne, Australia

[3,7,8] Centre for Material and Fibre Innovation, Deakin University, Geelong, Australia
[a]saniyat.islam@rmit.edu.au , [b]amit.jadhav@gmail.com , [c]jian.fang@deakin.edu.au,
[d]lyndon.arnold@rmit.edu.au, [e]lijing.wang@rmit.edu.au, [f]rajiv.padhye@rmit.edu.au,
[g]xungai.wang@deakin.edu.au, [h]tong.lin@deakin.edu.au

Keywords: Chitosan, wool, electrospraying, antibacterial, coating, deposition

Abstract. Electrospraying or electrohydrodynamic spraying is a technique of liquid atomisation by utilising electrical forces. In the electrospraying technique, the liquid at the outlet of a nozzle is subjected to an electrical shear stress by maintaining the nozzle at high electric potential. This produces a fine mist of extremely small and in some cases down to nanometer size droplets. The charge and size of the droplets can be controlled by adjusting the flow rate and voltage applied to the nozzle. Extending the scope of electrospraying, textile substrates can be coated with suitable polymer solution to enhance the surface functionalisation. This paper highlights the deposition of chitosan on wool subtrates using elctrospraying and its potential application in medical textiles.

Introduction

Electrospraying is a method of generating a fine mist or aerosol of intended specific precursor material using electrostatic charging. When this precursor material (in dissolved form or a liquid of particular viscosity) passes through a needle, fine droplets are generated by electrically charging the liquid to a very high voltage. Because of the identical electrical charge, these droplets repel each other very strongly. At the tip of the needle, the liquid becomes unstable as it is forced to hold more and more charge. When the liquid can hold no more electrical charge, it disperses into numerous, micron-sized, highly charged droplets at the tip of the needle as shown in Fig.1. In general, these tiny droplets fly about searching for a potential surface in which to land. This surface has an opposite charge to the droplets of the material. As the droplets fly about, they shrink rapidly as solvent molecules evaporate from their surface.

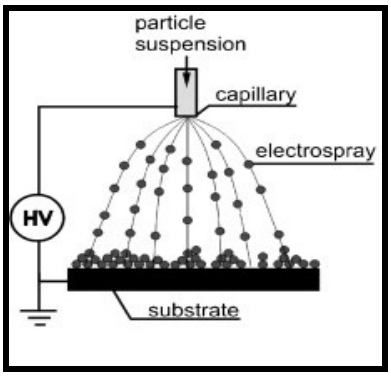


Figure 1: Schematic diagram of electrospraying [1]

Chitosan, a biopolymer is well-known for its applications in medical textiles [2-9]. An electrospraying technique was applied to generate nano spheres of chitosan for drug delivery purposes [10]. A study [11] reported that a combination of controlled electrospraying and subsequent freeze drying can produce a fibrous chitosan 3D network structure from low concentration chitosan solutions. Nanoparticle suspensions of chitosan were first fabricated by electrospraying and then freeze drying assembled the nanoparticles into fibrous networks. Porous

chitosan nano-particles and cross-linked chitosan capsules for drug delivery were also reported [12, 13]. Solid micro-and nanoparticles were prepared from chitosan/acetic acid solution in one-step by the electrospraying method [14]. Production of thin films of $LiMn_2O_4$ was reported using electrospraying techniques [15]. To date no study has been conducted to evaluate the coating technique utilising electrospraying onto textile substrates. The current study reports the electrospraying of chitosan to coat a wool substrates and evaluates the antimicrobial properties of the coated substrates.

Experimental

Preparation of wool substrate: The wool Nonwoven substrate was prepared using an integrated card-crosslapper with subsequent needlepunching. A SCG-600-60 model integrated card-crosslapper from SHIN CHIANG Machinery Co. Ltd. was used to prepare laps of 100% wool. Parameters were optimised for uniform lap preparation. The prepared lap was subsequently needle punched using a SNP-50M-6, make SHOOU SHYNG MACHINERY CO., LTD., Down-stroke needle punching machine with a working area of 500 mm×296 mm. The needles used were 15× 18 ×36#×3 ½″ R222G3027 type with 11 mm needle penetration and 400 strokes/minute. Feed rate move step was 1.80 mm/stroke. The resulting needlepunched wool substrate had a mass per unit area of 400 g/m^2.

Preparation of Chitosan solution: Chitosan from crab shells (Brookfield viscosity 200 Cps, degree of de-acetylation > 80%) was sourced from Sigma-Aldrich Pty. Ltd. Australia, and used as received for the experiments. Chitosan was dissolved in 1% (w/w) acetic acid until a clear solution was achieved. Freshly prepared solutions were used for all the experiments.

Surface Characterisation: To characterise the deposition of chitosan and to observe the morphological nature of coated wool substrates a FEI Quanta 200 environmental scanning electron microscope (ESEM) was used.

Electrospraying of chitosan: The chitosan solution was placed into a 5 ml syringe with a metal syringe needle (23 Gauge) which was connected to a syringe pump (KDS 100, KDS scientific) as shown in Fig.2. Wool needle punched fabric was mounted on a metal plate at a distance of 15 cm from the needle. The electrospraying was performed under an applied voltage of 15~25 kV with a solution flow rate of 4.0 ml/h.

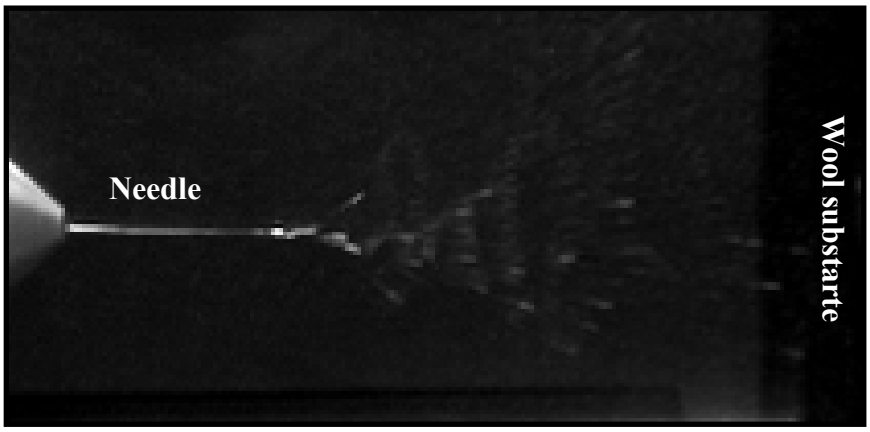


Figure 2: Spray formation of chitosan during electrospraying on wool

During electrospraying, the chitosan particles were coated onto the wool fabric mounted on the collector.

Antibacterial Testing: Escherichia *coli* (E. coli) – ATCC 11229 a gram negative bacteria, was used as the test specimen organisms. Bacterial inoculums were prepared to obtain a suspension in an exponential growth of 10^8 colony forming units (CFU) mL^{-1} in a 5 mL of nutrient broth which was a modified trypton soya broth from Oxoids. A tryptone soya agar (from Oxoids) was used as the nutrient agar for agar plates. Antibacterial test was carried out with both the batches of coated and

uncoated wool. The uncoated wool fabric was used as a control sample against the coated one. Fabric swatches of 4 cm diameters were cut and then sterilised using UV light. Each fabric swatch was placed in a conical flask. AATCC 100-2004 (clause 10.2) test standard was followed to perform the antibacterial test. A series of diluted solutions were prepared as 10^0, 10^1, 10^2 and 10^3 times with sterile distilled water and they were plated in triplicates and subsequently incubated for 18 h at 37°C. After incubation, the 10^2 dilution was taken to compare the coated and uncoated swatches. The plates corresponding to 10^0 and 10^1 times had uncountable colonies and that for 10^3 times had too few colonies for the control swatch.
The percentage reduction of the bacteria by the fabric specimen treatment was calculated with the following formula [16]:

$$\text{Reduction in CFU \%} = \frac{(B-A)}{B} \times 100\% \qquad \text{(Eq. 1)}$$

Where, B = average number of bacterial colony in uncoated wool fabric
A = average number of bacterial colony in wool fabric coated with chitosan

Results and Discussion

Surface morphology: Scanning electron micrographs were used to characterise the coating of chitosan on wool substrates. Fig. 3 shows the untreated sample of wool substrate. The scales of the wool are less pronounced.

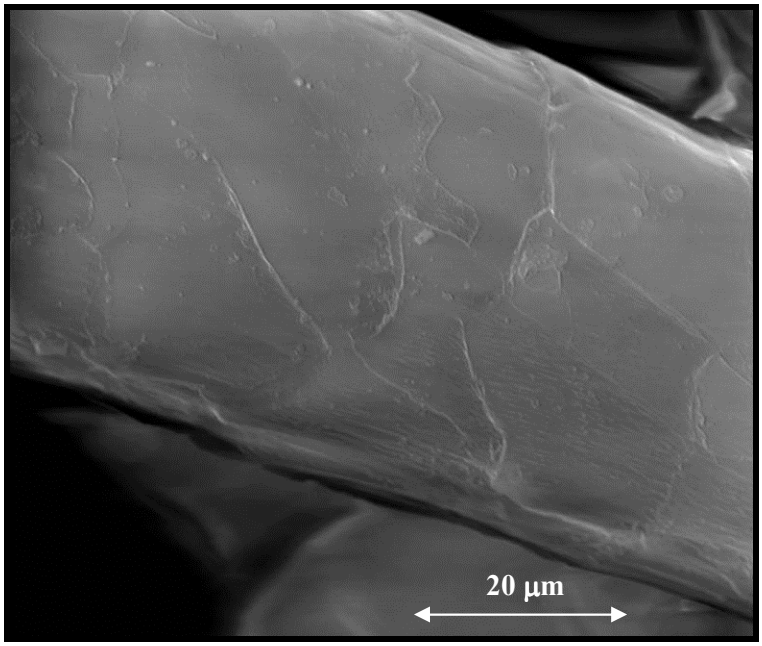


Figure 3: Untreated wool substrate

Figures 4 and 5 illustrate the chitosan coated samples in different magnifications. It is clearly visible from the figures that individual fibres are coated and the presence of chitosan has made the scales on wool more pronounced. Fig. 5 shows the surface deposition and coating of chitosan on the individual fibres.

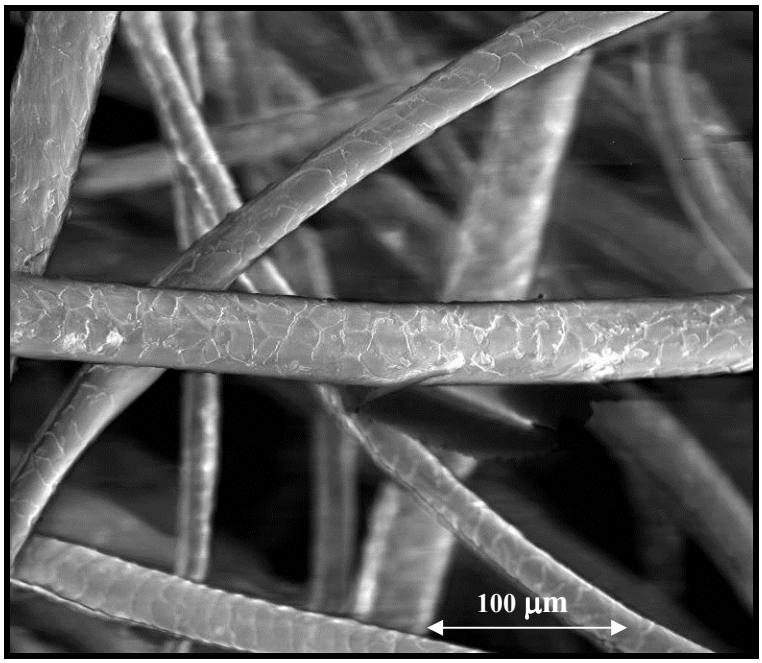


Figure 4: Coated wool substrate

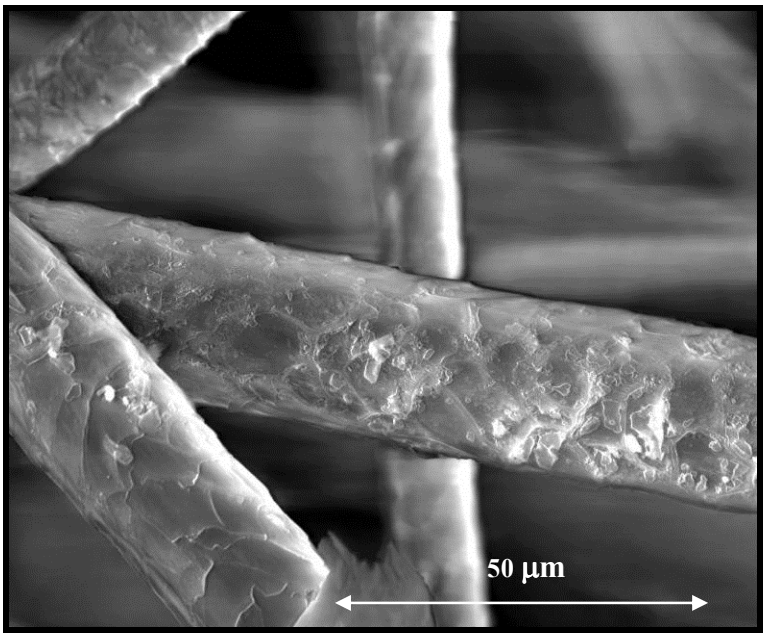


Figure 5: Coated wool substrate

In some cases, as shown in Figures 6 and 7, chitosan formed a loose film on the wool fibres. This was due to the random fibre structure of the needled nonwoven. The applied voltage, needle to collector distance and the viscosity of chitosan play an important role for successful coating. The effect of viscosity and concentration of chitosan on electrospraying on wool (woven, knitted and nonwoven) will be discussed elsewhere.

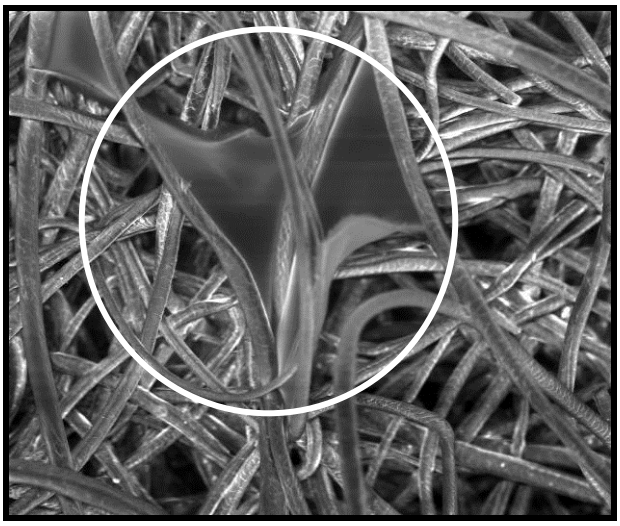


Figure 6: Loose film formation of chitosan

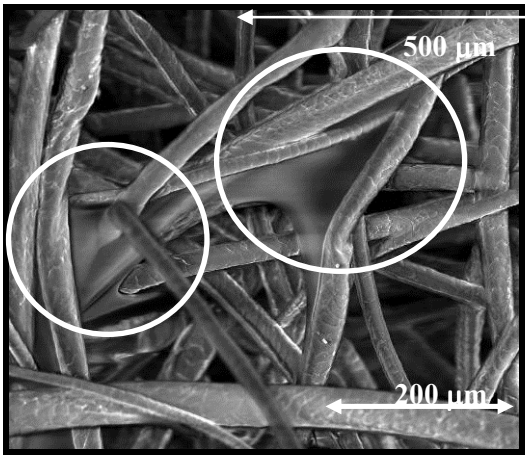
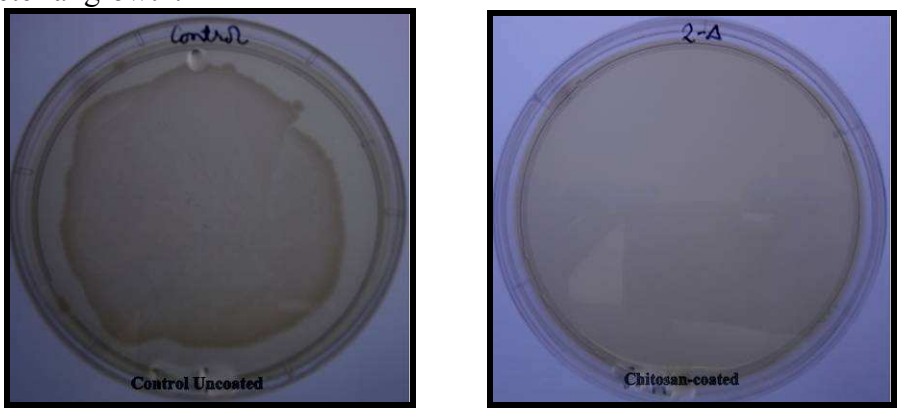


Figure 7: Failures in coating individual fibres

Applied voltage, solution flow rate and nozzle collector distance on different manmade and natural fibres has been extensively studied and optimised for this application and will be the scope of another paper.

Antibacterial testing: The coated and uncoated substrates were tested for their antimicrobial efficacy. Fig. 8 (a) shows the full bacterial growth on the agar plate for the control sample which is the uncoated wool substrate. Fig. 8 (b) shows the agar plate containing the chitosan coated sample with no bacterial growth.



(a) **(b)**

Figure 8: Agar plates showing (a) growth of bacteria with the control sample and (b) zero-growth of bacteria from the chitosan-coated sample

All the coated samples showed similar results i.e., the bacterial reduction percentage was found to be 100%. The excellent antimicrobial efficacy against the gram negative bacteria shows this has potential application in medical textiles such as wound dressings.

Conclusion

A novel coating technique was proposed in this study utilising the electrospraying method. Resultant fabric substrate showed successful coating on individual fibres and excellent antimicrobial properties. As such, these developed fabrics have potential use in medical textiles specifically in wound dressing materials.

Acknowledgements

This work was financially supported by the Australian Wool Education Trust (AWET). Wool fibre was kindly contributed by Mr. Jack Roosenboom, RMIT University.

References

[1] A. Jaworek and A. Sobczyk, "Electrospraying route to nanotechnology: An overview," *Journal of Electrostatics,* vol. 66, pp. 197-219, 2008.

[2] A. Niekraszewicz, "Chitosan medical dressings," *Fibres & Textiles in Eastern Europe,* vol. 13, p. 54, 2005.

[3] D. Ciecha ska, "Multifunctional bacterial cellulose/chitosan composite materials for medical applications," *Fibres & Textiles in Eastern Europe,* vol. 12, p. 48, 2004.

[4] C. Knill, J. Kennedy, J. Mistry, M. Miraftab, G. Smart, M. Groocock, and H. Williams, "Alginate fibres modified with unhydrolysed and hydrolysed chitosans for wound dressings," *Carbohydrate Polymers,* vol. 55, pp. 65-76, 2004.

[5] Q. Cheng and D. Shuqin, "Chitosan Fiber Nonwovens and the Prospects for Medical Dressings [J]," *Technical Textiles,* vol. 1, 2004.

[6] Q. Cheng, "Production and application of chitosan fiber medical dressings [J]," *Journal of Textile Research,* vol. 11, 2006.

[7] K. H. Jung, M. W. Huh, W. Meng, J. Yuan, S. H. Hyun, J. S. Bae, S. M. Hudson, and I. K. Kang, "Preparation and antibacterial activity of PET/chitosan nanofibrous mats using an electrospinning technique," *Journal of applied polymer science,* vol. 105, pp. 2816-2823, 2007.

[8] A. Rigby, S. Anand, and A. Horrocks, "Textile materials for medical and healthcare applications," *Journal of the Textile Institute,* vol. 88, pp. 83-93, 1997.

[9] S. Petrulyte, "Advanced textile materials and biopolymers in wound management," *Danish medical bulletin,* vol. 55, p. 72, 2008.

[10] N. Arya, S. Chakraborty, N. Dube, and D. S. Katti, "Electrospraying: A facile technique for synthesis of chitosan based micro/nanospheres for drug delivery applications," *Journal of Biomedical Materials Research Part B: Applied Biomaterials,* vol. 88, pp. 17-31, 2009.

[11] M. Y. Kim and J. Lee, "Chitosan fibrous 3D networks prepared by freeze drying," *Carbohydrate Polymers*.

[12] K. Pancholi, N. Ahras, E. Stride, and M. Edirisinghe, "Novel electrohydrodynamic preparation of porous chitosan particles for drug delivery," *Journal of Materials Science: Materials in Medicine,* vol. 20, pp. 917-923, 2009.

[13] Y. Xu and M. A. Hanna, "Electrosprayed bovine serum albumin-loaded tripolyphosphate cross-linked chitosan capsules: Synthesis and characterization," *Journal of microencapsulation,* vol. 24, pp. 143-151, 2007.

[14] S. Zhang and K. Kawakami, "One-step preparation of chitosan solid nanoparticles by electrospray deposition," *International journal of pharmaceutics*.

[15] A. Van Zomeren, E. Kelder, J. Marijnissen, and J. Schoonman, "The production of thin films of LiMn2O4 by electrospraying," *Journal of aerosol science,* vol. 25, pp. 1229-1235, 1994.

[16] D. Z. Feng Zhang, Yuyue Chen,Hong Lin, "The antimicrobial activity of the cotton fabric grafted with an amino-terminated hyperbranched polymer," *Cellulose,* vol. 16, pp. 281-288, 2009.

© (2011) Trans Tech Publications, Switzerland
doi:10.4028/www.scientific.net/AMR.331.171

Study on numetrical representation of topological architecture of 3D woven composites

Shanli Wang [1,a] , Lianhe Yang[2,b]

[1]Information center ,Tianjin Polytechnic University, Tianjin, China, 300160

[2]school of computer, Tianjin Polytechnic University, Tianjin, China, 300160

[a]wangshanli@tjpu.edu.cn , [b]yanglh@tjpu.edu.cn

Key words: 3D woven composite; yarn structure; numetrical representation; key control point

Abstract. The numetrical representation of yarn structure of reinforcing material has become a precondition in designing architecture and predicting properties of 3D woven composites. The numetrical representation of topological architecture of woven is discussed in this paper. Yarns are sub-classified and according to the warp yarns fabric directions. A key control point method was proposed to solve the descriptive issue of arbitrary 3D woven composite architecture . In the end, the contrastive tests are done to verify the method.

About the Architecture of 3D Woven Composites

Textile composite, which is solidified by reinforcing material and matrix material, is one of the most important trends of composites. According to different technologies of reinforcing materials, textile composites can be sub-classified as braided , woven and knitted composites. 3D woven composite which has much superiority is an important branch of composites.

As 3D woven composite is a kind of materials whose structure and mechanical properties can be designed, it plays a dominant role to make a precise forecast about their mechanical properties before production, and this is the premise of an effective utilization which makes contributions to a higher quality and a lower aimless manufacture as well as a higher utilization ratio. The investigation of topological architecture of reinforcing materials from micro-structure viewing angle is one of the basic researches of forecasting mechanical properties. Some studies have indicated that the topological architecture of reinforcing material of 3D woven composites plays a dominant role for the mechanical properties of composites under a invariable circumstance. Generally speaking, computer systems is necessary when designing an architecture or predicting mechanical properties of reinforcing material, as these materials commonly have a complex architecture and need a vast of calculation. For this reason, the numetrical representation of yarn structure of reinforcing material has become a precondition in designing structure and predicting properties of 3D woven composites. Thus, it is a precondition of designing and forecasting the mechanical properties of 3D composites to finding a proper method to describe various kinds of topological architecture of yarn structures, especially to adapt all the reinforcing structures.

The Yarn Micro-structure in 3D Woven Composites

The micro-structure of 3D woven composites mainly includes the topological pattern of woven, the topological shape of yarn' s axis, and the shape of yarn’s cross-section as well as the density of resin and fiber. The numetrical representation of topological architecture of woven is discussed in this paper, whereas other micro-structure will be the further investigation in other papers.

According respective directions, yarns can be sub-classified as warp, weft, binder warp and filling warps. Warp, weft and filling warps make up a 2 dimensional structure without through any plane, while binder warps usually link such a 2D structure in a thickness direction. Different link ways lead to a different architecture. Totally speaking, wrap, binders and filling are all follow a warp direction, but binders usually through different *X*-*Y* planes which looks like a sine wave curve, going up and down between different lines of weft. Warp also follows a sine wave curve only have certain obvious differences in frequency and amplitude. Different from warps, fillings usually neither twine with the weft nor through them. Their function is to isolate weft of every layer. Some documents have showed that the ordered weft commonly follow *Y* direction without initiatively curve. By adding marked yarns into woven composite , for example, Reference [1] have indicated that the path of weft is near to a line.

By this token, we can make a conclusion that the design of warping direction will not only be the key of 3D woven composites designing ,but also the main factor that determining the mechanical properties. And the binder ways , which show characteristics of topological pattern of 3D woven structure, usually make a dominant contribution to mechanical properties. In order to describe various type of yarn structures, different kind of numetrical representations of wrap have been discussed here with the weft as a datum mark of discussion and as a control point of warp.

Numetrical Representation of Yarn Structure

As numetrical representation of yarn structure is the precondition of computer designing and mechanical properties prediction, to find a general purpose numetrical representation method has been the hot of composites investigations. And this method should not only be easily represent by computer, but also be able to describe all kinds structures of woven composites, besides ,its parameter should be convenience to calculate other micro-structures and to be a foundation of a prediction of mechanical properties.

Typical space structure of 3D yarn

The observation and analyis of 3D woven composites structure illustrates that the analysing of binders yarns is the key problem. Some definitions concerned have been made as follows with the purpose of having a more convenient analysis and discussion.

3D coordinate system as Fig. 1：*X, Y, Z* respectively indicates three directions .As the picture shows: to X from left to right means positive , to Y goes into the principal plane means positive, to Z from down to up means positive. Investigation of binder' path has been discussed here with the orthogonal architecture as an example. The turning point of binder in a unit cell, which means the place to change the number of plies and the number of columns to cross, plays a key role in this problem.

Wrap : follows X direction, also the length of yarns, form left to right.

Weft: follows Y direction , also the breadth of yarns , going into or out of the principal plane vertically.

Binders: follows Z direction, also the yarns that follows thickness directions.

Row: parallel to the principal plane，growing goes inside with the principal plane and the principal Plane means 0.

column: means the rank pattern of weft, following Z direction and parallel to it.

line:means warp ranked as X and parallel with it .

+: means up the yarn according Z and have a touch point.

-: means under the yarn according Z and have a touch point.

Weft coordinate: (line , column) for instance, (3,2) means the weft that in the third line and the second column.

Control point: means the weft that leads a binder becoming curve and changing its direction into Z. For example, (+5, 6)means the binder has changed its direction on the point of fifth line and the sixth column.

Setting parameter

The description of control point of every weft is made when designing a 3D woven composite structure. The unit of 3D woven composite structure was named as a cell , for it has a repetitive organizational architecture. Usually, five parameters (row, line, column, up and down) which can be used to describe the location and direction of the whole yarns, should be given before a designing. For example, the following parameters make the design and description of 3D woven composites available: the row of wrap, the line of weft, the column of weft, the control point of wraping yarn and the location of filling ratio.

Parameter representation

Parameter representation with the fig.2 is as following:

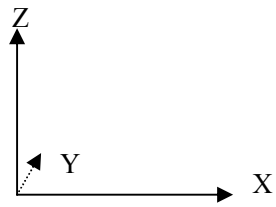


Fig. 1 The 3D coordinate system

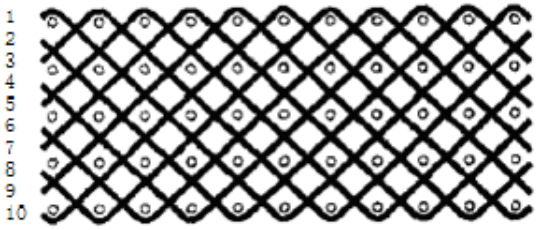


Fig. 2 Angle interlock and through thickness structure

1:0,[+1,1],[-6,5],[+1,11]
2:1,[+2,1],[-5,5],[+1,10]
3:2,[+2,1],[+1,2],[-5,7]
4:3,[+3,1],[-5,4],[+1,9]
5:4,[+3,1],[+1,3],[-5,8]
6:5,[+4,1],[-5,3],[+1,8]
7:6,[+4,1],[+1,4],[-5,9]
8:7,[+5,1],[-5,2],[+1,7]
9:8,[+5,1],[+1,5],[-5,10]
10:9,[-5,1],[+1,6],[-5,11]

We can gave a detailed explain for "1:0,[+1,1],[-6,5],[+1,11]" . 1 means the NO. 1 binder yarn. 0：means this binder yarn locates the first row. [+1，1] means it going into the cell from the first line and the first column weft and up the point. The point [-6，5] in this place is the control point of binder that bindered under the 5^{th} line and 6^{th} column. The point [+1，11] is the second control point by which the binder directly goes up to the 1^{th} line and the 11^{th} column.

And " 9：8，[+5，1]，[+1，5]，[-5，10]" also means the 9^{th} binder which located 8^{th} row goes up into the cell from the 5^{th} line and the 1th column and then connects up on the weft that on the 1^{th} line , the 5^{th} column .Besides, with a direction changing , the binder go directly under to the weft that located in 5^{th} line and 10^{th} column. For the same idea , other representations are leave out here.

The general representational methods are as following:

ID number of wraping yarn: row, [the point of line, the point of column],[1^{th} control point of line, 1^{th} control point of column],[2^{th} control point of line, 2^{th} control point of column],[3^{th} control point of line, 3^{th} control point of column].For convenience, the up or down direction of control point usually marked up on the line. In addition, in this method, the sign "+ "and "-" respectively indicates up or down place of the yarn for which reason the sign "–N" and "+N+1" has been defined as the same meaning in a cell.

General testing and other parameter calculation

Usually, there are mainly three standards to measure the reasonable of a representational method. (1) Whether it can adapt all kinds of woven architecture .(2)Whether it can be input easily.(3) whether it can be easily transformed into a 3D woven architecture by computer and can be well stored.

Taking the architecture of (c) and (d) of the Fig. 3 for test , we have defined the cell at a dotted line as a unit, hence the wraping yarn of this unit were numbered as Fig.3.

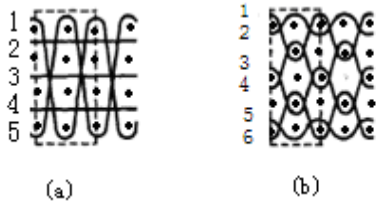


Fig. 3 Typical unit cell of 3D woven architecture

Fig. 3 (a), for example , has been numbered as following:

1:0,[+1,1],[-4,2],[+1,3] 2:1,[+2,1],[+2,2] ,[+2,3] 3:1,[+3,1],[+3,2],[+3,3]

4:1,[+4,1] ,[+4,2] ,[+4,3] 5:2,[-5,1] ,[+1,2] ,[+4,3]

The architecture in Fig. 3（b）has been numbered as following:

1:0,[+1,1],[-2,2],[+1,3] 2:1,[-1,1],[+1,2],[-1,3] 3:0,[+2,1],[-4,2],[+3,3]

4:1,[-3,1],[-2,2],[-3,3] 5:0,[+5,1],[-5,2],[+5,3] 6:1,[-5,1],[+4,2],[-53]

What's more , this method can also be applied to those woven fabrics whose yarns are not straight. Thus, this numetrical describe pattern can not only be easy to describe various structure of woven ,but also be easy to be entered by computers. In addition, since the pattern can be stored as structured data into 2D database in computer, it is available to automatically create a woven fabric with a special architecture by computer programs.

Conclusion

The numetrical representation of yarn structure plays a key role in designing, modeling and predicting of mechanical properties. A general purpose numetrical representation model has been discussed in this paper. With the wide applicability, this model is capable to model a woven architecture as well as to calculate other micro-structures of 3D woven composites under a tight conditions of yarn which will be good for concerned mechanical investigations such as the angle of yarn, counting volume fraction of fiber, density, hole ratio, binder depth, binder distance as well as the proportion of various kinds of yarn.

Reference

[1] TANG Xun,etc:Yarn Observing and Meso Geometry Modeling of 3-D Woven Composites, Journal of Nanjing University of Aeronautics & Astronautics, 2008(6).

[2] MIAO Xinyun, GU Bohong, ZHENG Tianyong, topological and Mathematical Characterization of 3D Orthogonal Woven Fabric Architecture, Fiber Composites,2009.12.

[3] YI HongLei, Study on the Structural Design and Mechanical Properties of 3D Woven Composites, DongHua University, 2000,7

[4]DING Xin,YI Hong-lei ,Representation of Geometric Architecture of Three-dimensional Woven Structures by Numerical Method, Journal of DongHua University ,2003,6

[5] YANG Lianhe, LI Jiang ,CHEN Li , Architecture description and solid modeling of 3D woven composite, Acta Materiael Compositae Sinica , 2009,8.

© (2011) Trans Tech Publications, Switzerland
doi:10.4028/www.scientific.net/AMR.331.175

The Effects of Fiber Volume Fraction on the Experiment Modal Behavior of 30°/-60° Carbon Fiber Plain Woven Fabric / Epoxy Resin Composites

Xiaoyuan Pei[1, a], Jialu Li[1, b]

[1]Composites Research Institute of Tianjin Polytechnic University & Tianjin and Education Ministry Key Laboratory of Advanced Composite Materials, Tianjin 300160, China

[a]woshipeixiaoyuan@126.com, [b]lijialu@tjpu.edu.cn

Keywords: experimental mode analysis, 30°/-60° carbon fiber plain woven fabric /epoxy resin composites, transfer curves, attenuation curve of acceleration

Abstract. A study on dynamic mechanical properties of carbon fiber plain woven fabric (with fiber orientation of 30°/-60°) / epoxy resin laminated composites with different fiber volume fraction was carried out. The test method is single input single output free vibration of cantilever beam hammering modal analysis method. The effect of different fiber volume fraction on the modal parameters of laminated composites was analyzed. The experimental results show that with the fiber volume fraction increasing, the natural frequency of laminated composites becomes larger and damping ratio becomes smaller. The fiber volume fraction is greater, the peak value of natural frequency becomes higher and the attenuating degree of acceleration' amplitude becomes slower.

Introduction

Compared with traditional metal materials, such as steel, aluminum and titanium, composite materials are used extensively in marine and aerospace structures due to their higher specific strength and specific stiffness, lower density and flexibility in design. At present, laminated composite materials are the main practical application of composite structure. It puts two or more layers bonded together to form a whole structure. Each ply material of the composite could be same or different. In addition, the different order of layer angle and fiber laminated make the material have different strength and stiffness in different direction which can meet the load requirements of the structure. Therefore, it will have evident significance to study its dynamic mechanical properties which are helpful to its structural optimization design, performance evaluation, strength check, life prediction and expand its high-tech industrialization.

For the dynamic characteristics of the laminated composites, natural frequency and damping ratio are important kinetic parameters. They are mainly dependent on the reinforcing fiber and matrix dynamic performance, fiber volume fraction, the interaction of fiber and matrix and so on. Vaidya [1] studied the vibration characteristics of the E-glass fiber woven three-dimensional hollow structure. Berthelot [2] used the vibration method of cantilever beam to analyze the dynamic characteristics of glass fiber and Kevlar fiber composite. Simply supported beam test method was adopted for analyzing stiffness and modal of 3 layer laminated composites which has 2 different layers by Hao [3]. Song xiang [4] and others used the n-order shear deformation theory to analyze the vibration of laminated composite plates.

In this paper, the influence of different fiber volume fraction (FVF) on the dynamic mechanical properties of 30°/-60° carbon fiber plain woven fabric /epoxy resin laminated composites was researched. Firstly, the specimens of 30°/-60° carbon fiber plain woven fabric /epoxy resin laminated composites were produced. Secondly, the testing program was designed with the reference of ASTM E756-2005 Standard Test Method for measuring vibration-damping properties of materials. Finally, the dynamic characteristics of 30°/-60° carbon fiber plain woven fabric /epoxy resin laminated composites was investigated by means of experimental modal analysis method. Whit the same fiber orientation angle, the influence of FVF on laminated composite modal parameters (such as damping ratio, natural frequency) has been defined.

Preparation of the Specimen

In the experiment, the carbon fiber plain woven fabric (T700-12K) was used for the reinforcement of the specimen and the weight is 500g/m^2. The angle between the warp direction of plain woven fabric and the length direction of specimen is 30° . So the angle between the weft direction of plain woven fabric and the length direction of specimen is -60° . The matrix is TDE-86 epoxy resin. The formation process of specimen is resin transfer molding (RTM) process. The strengthening plate was affixed to the one end of the specimen (Fig. 1). The groups of specimens were named as L-A, L-B and L-C with the FVF of 45%, 55% and 65%, respectively.

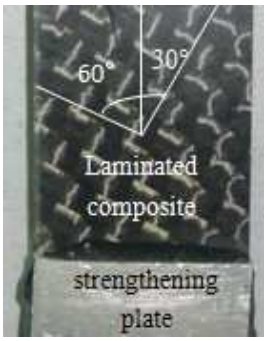


Figure 1 Specimen

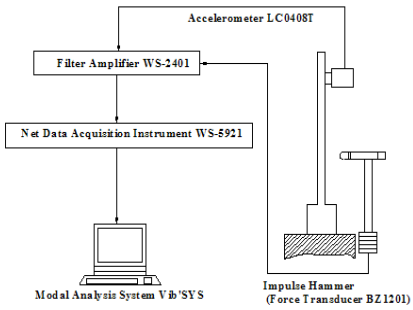


Figure 2 The block diagram of modal testing device

Test Equipment and Test Method

The block diagram of modal testing is showed in Figure 2. The test process is: at first, the specimen was fixed (Figure 3). Then, along the perpendicular direction of specimen, the specimen was blown by a hammer. The distance between fixed end (A) and hammering point (B) is 20mm (Figure 4). The hammering force should be uniform for the different specimen in order to ensure the specimen has a same testing condition. During hammering, the force signal and the vibrating signal of specimen were received and were input to net data acquisition instrument WS-5921. Subsequently, the frequency response function was obtained by using analysis calculation of the modal analysis system. And the force signal was also obtained. Finally frequency and damping ratio were obtained. Three specimens with same FVF were tested.



Figure 3 Specimen clamped

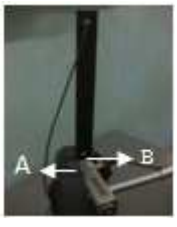


Figure 4 Hammering point

Results and Discussions

Frequency and Damping Ratio

The modal parameters of laminated composite specimens with different FVF are list in Table 1.

Table 1Modal parameters of laminated composite specimens with different FVF

Specimen	FVF %	frequency /Hz			damping ratio /%		
		1st-Order	2nd-Order	3rd-Order	1st-Order	2nd-Order	3rd-Order
L-A	45	37.483	255.668	742.309	4.362	1.193	1.302
L-B	55	44.115	287.095	831.9847	4.162	1.147	1.294
L-C	65	44.176	294.483	853.421	3.651	0.926	1.161

From table 1, it can be seen that the FVF of laminated composite materials has a major impact on the natural frequency and damping ratio.

The first natural frequency of L-C is 0.061Hz larger than that of L-B and 6.693Hz larger than that of L-A. The second frequency of L-C is 7.388Hz larger than that of L-B and 38.815Hz larger than that of L-A. The third frequency of L-C is 21.436Hz larger than that of L-B and 111.112Hz larger than that of L-A. The natural frequency of laminated composite is larger; the ability of resisting deformation is higher. That is to say, flexural stiffness of it is strong; coefficient of stiffness distortion may be small; the performance of it will be relatively stable. Higher natural frequency of each mode will make the structure of laminated composites easer to avoid resonance effect in practical application.

During vibration and deformation, the ability of transforming the mechanical vibration energy into heat energy in the material is called damping. The physical meaning of damping ratio is that the ratio of the energy loss to energy input in the system. From Table 1, it can seen that the first order damping ratio of L-C is 0.511 smaller than that of L-B and 0.711 smaller than that of L-A. The second order damping ratio of L-C is 0.221 smaller than that of L-B and 0.267 smaller than that of L-A. The third order damping ratio of L-C is 0.133 smaller than that of L-B and 0.141 smaller than that of L-A. Different materials have different loss factor, so that how to make the kinetic energy of oscillation converting to other forms of energy (for instance, heat energy, deformation energy), and how to make the system restore pre-stimulated state are the considerations during the design of laminated composite materials structural. During the design of material structure, choosing the relatively low fiber volume fraction of the structure can improve the damping property of laminated composite materials.

Transfer Function

The amplitude-frequency maps of the laminated composite material at measuring point were obtained by transforming the signals of acceleration response from time domain into frequency domain using FFT (Fast Fourier Transform) method. The amplitude-frequency curves of specimens with different FVF are showed in figure 5.

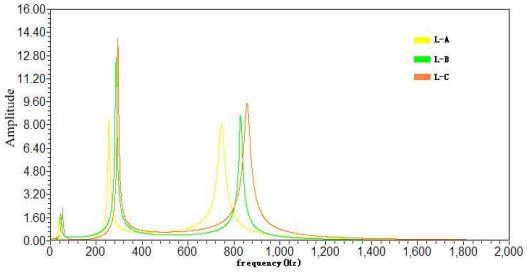


Figure 5 Transfer function

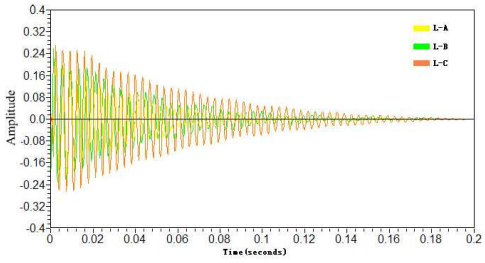


Figure 6 Attenuation curve of acceleration.

In Figure 5, the abscissa is the frequencies and the ordinate expresses the value of vibration amplitude. Through analyzing the amplitude-frequency diagram of laminates with different FVF, it can be also seen that, at instantaneous load, with the increase of fiber volume fraction, natural frequency becomes larger, the resonance peak become higher, and the width between neighboring peaks becomes wider.

Damping Characteristics

Figure 6 is the attenuation curve of acceleration of laminated composite specimens with different FVF. The vibration model can be simplified to a single mode of damping vibration when only considering the vibration of laminated composite specimens perpendicular to the exciting force in the plane at the transient impact force. Due to exist the damping of the structural, the response curve shows an exponential decay and is a non-periodic oscillation curve. However, because of the different FVF, the varying degrees of the response curves of the laminated composite specimens are different. The FVF is lower, the damping is larger, the initial amplitude is smaller, the decay time is shorter, and the process of damping is quicker. The FVF of specimens is higher, the initial amplitude is larger, the attenuation is lower, and the trend of attenuation is not obvious. These indicate that the laminated structure with low FVF have better performance to absorb and consume the elastic strain energy at the transient loads of the excitation pulse, which reflects that the vibration damping decreases quicker of the laminated composite specimens at the shock pulses.

Conclusions

By studying the experimental performance mode of 30°/-60°carbon fiber plain woven fabric /epoxy resin laminated composites with different FVF, the modal parameters and transfer functions are derived, and the dynamic response characteristics under the impulse loads have been analyzed. Under transient load, with the increase of FVF of laminated composites, the natural frequency of laminated composites is larger and the height of resonance peak increases, the damping decreases; the initial amplitude at the acceleration attenuation curves becomes big, the decay time is longer, and the process is slower. When the FVF of laminated composites is less, the damping is larger, the performance of amplitude reduction, vibration absorption, and energy dissipation are all better. These mean that when the FVF of laminated composites is low, the damping characteristics of laminated composites are excellent, but the frequency and stiffness will reduce. Therefore considering the relationship of mutual restrictions, various factors must be taken into account in the structure design process. It is very important to select the appropriate value of FVF of laminated composites, in order to make the materials to achieve the best vibration performance and meet the actual application requirements.

Acknowledgement

The authors acknowledge the Tianjin Municipal Science and Technology Commission, China, for sponsorship of this research under the contract, No. 10SYSYJC27800 and No. 11ZCKFSF00500.

References

[1] A.S. Vaidya, U.K. Vaidya, N. Uddin: Materials Science and Engineering A, 472 (2008), p.52
[2] Jean-Marie Berthelot, Youssef Sefrani：Composites Science and Technology, 64(2004), p.1261
[3] HAO Min, RAO Mohan D：Journal of Composite Materials, 2005, 39(18), p. 1621
[4] Song Xiang, Shao-xi Jiang, Ze-yang Bi, Yao-xing Jin: Composite Structures, 93 (2011), p. 299

© (2011) Trans Tech Publications, Switzerland
doi:10.4028/www.scientific.net/AMR.331.179

Structure and Properties Research of Multi-antibacterial Polyamide Fibers

Weiwei Sun[1,a], Hua Zhang[2,b], Yongkai Zhou[1,c]

[1]Beijing Institute of Fashion Technology, Beijing 100029, China;

[2]The Quartermaster Research Institute of General Logistics Department of the CPLA, Beijing 100088, China;

[a]violetsunweiwei@163.com; [b]st.hua@263.net; [c]zykbta@yahoo.com.cn

Keywords: Polyamide fibers; Multifunction; Bacterial; Far-infrared; Negative oxygen ions.

Abstract: To explore the effect of multi-antibacterial powders on the polyamide fibers, we analyzed the structure and properties of the polyamide fibers in this paper, which have features of antibacterial, far-infrared emission and negative oxygen ions emission. The effects of adding multi-antibacterial power were tested by Scanning Electron Microscopy and spectrum tests, X-ray diffraction, thermal analysis and infrared spectroscopy. Our data indicated that multi-antibacterial polyamide fibers have excellent antibacterial effect, good far-infrared emission and the negative oxygen ions emission features, while have little affect on polyamide fibers' structure properties.

Introduction

In daily life, people are inevitably exposed to various types of bacteria, fungi and other microorganisms. Under proper external conditions, these microorganisms will rapidly grow and proliferate and transmit diseases to human in various pathways, affecting people's health. Unfortunately the most existing fiber products tend to provide a suitable environment for microorganisms such as bacteria [1-2]. As the social developing and people's living standard improving, people demand high environmental health, and self-health awareness is also growing. As for textiles, besides colorful, beautiful and practical, environmental health, it is especially important to be bacterial [3].

This article has studied the effect of multi-bacterial powders to polyamide fibers, which have the function of antibacterial, far-infrared emission and negative oxygen ions emission feature, and analysis the structure and properties.

Materials and methods

Materials. The different addition multi-bacterial polyamide fibers were obtained by blending melt spinning. In spinning process, first of all, put the Ag^+, TiO_2, the nanometer tourmaline powders and silane coupling agent together at high speed mixing and in 140~160℃, in the mixing process added oxygen-resistant agents, obtained multi-antibacterial powders. Then put the powders in polyamide vehicle sections at low speed, stirred at high speed, at the same time added organic dispersing agent, extruded strips by twin screw machine, cooled in water bath, after dried and pelletized, obtained multi-bacterial master batch. In spinning process, added different proportions of multi-bacterial master batch with actual needs, first spun pre-orientation multi-bacterial spun fibers, taking the heat drawing false twist texturing method to make the original filament POY to elastic fibers DTY, and then added water, oil, got the multi-bacterial polyamide elastic fibers. The multi-bacterial polyamide fibers studied in this article are no addition multi-bacterial powders and 1%, 1.5% and 2% addition proportions.

Morphology Observation. Morphology analysis of the fiber cross-section was by scanning electron microscope JSM-7100F of Japanese Electronics Company. Fiber cross-section samples were prepared with resin embedded method. First put the propped fibers in the molds, put epoxy resin and oxidant in ratio of 1:1 to reconcile, then poured into the mold and completely surround the fiber, waiting until the resin samples cured, grooved around the resin samples, and break them in liquid nitrogen, obtained the fibers' cross-sections. The samples were glued to the sticky conductive gel stage, and then put them into a vacuum coating machine to coat carbon, to prepare for observation.

X-ray Diffraction Test. The fiber samples were cut to powders, compacted them to glass containing sets. Experimental apparatus was dmax-b X-ray diffraction of Rigaku Electric Co. Experimental conditions were as follows: tube voltage 40kV, tube current 50mA, using Cu tube, continuous scanning, scanning speed 6°/min, scanning rage 6°~36°.

Thermal Analysis. Cut the fiber samples to powders, to prepare for observation. Experimental apparatus was EXSTAR DSC 6200 of Seiko Instruments Inc. Experimental conditions were as follows: heating temperature from room temperature to 300℃, in 10℃/min, N_2 flowing was 20mL/min.

Infrared Spectroscopy. Experimental apparatus was infrared Raman spectroscopy Nexus 670 of American Nicolet Company. Spectral range was from 500 to 4000cm^{-1}.

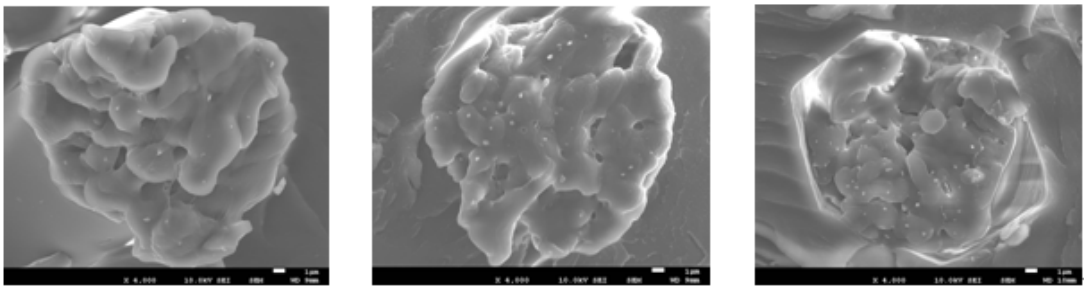
Antibacterial Functional Test. Antibacterial properties were evaluated against S. aureus strains ATCC 6538, Escherichia coli 8099, Candida albicans ATCC10231, according to GB/T 20944.3-2008 oscillation, taking 100% cotton fabric as control. We need sterilize the samples for 15min in high-pressure steam121℃. The inhibitory rate was calculated using the following equation: Y=(Wt－Qt)/Wt×100%, which Y is the reduction rate, Wt is the viable cells concentration(CFU/ml) of control, Qt is the number of multi-bacterial fiber samples.

Far-infrared Emission Function Test. According to FZ/T 64010-2000 Far-infrared Textile, testing the fibers' wear emissivity. Far-infrared emission of ordinary polyamide fibers is 70%, when the increased number of functional polyamide fibers is more than8.0%, the functional fibers have far-infrared emission features.

Negative Oxygen Ions Emission Functional Test. Negative oxygen ions emission functional was tested according to CTTC.F024-2007. World Health Organization suggests that when the number of negative oxygen ions' concentration in air is greater than 1500/m^3, then considered it as clean air [4].

Results and Discussion

Morphology Observation Analysis. To observe the distribution of multi-bacterial powders in fiber, we did electron microscopy experiments (Figure 1). Polyamide as macromolecular polymer, has different toughness with resins, therefore has a certain tensile deformation. It can be seen from the figures there are particulate matters on the cross-section of polyamide fibers, and particulate matters disperse very uniform in fibers. We also can see with the increase of addition proportions, particulate matters increase significantly, so we analysis particulate matters what we see in fibers are multi-antibacterial powders. But we also see the presentation of particulate matter in no addition multi-antibacterial polyamide fiber.



(a) No addition multi-antibacterial powder polyamide fiber

(b) 1.5% addition multi-antibacterial powder polyamide fiber

(c) 2% addition multi-antibacterial powder polyamide fiber

Fig.1 Polyamide fibers' cross section of different multi-antibacterial powder's addition: 0 (a), 1.5% (b) and 2% (c)

To further analysis the composition of particulate matters in no addition multi-antibacterial powders polyamide fiber, energy spectrum tests were took (Figure 2). The results show that the main components of the particulate is Ti, no other antibacterial ingredients, so the particulate matters are matting agent added in the spinning process in order to prevent the aurora phenomenon of synthetic fibers.

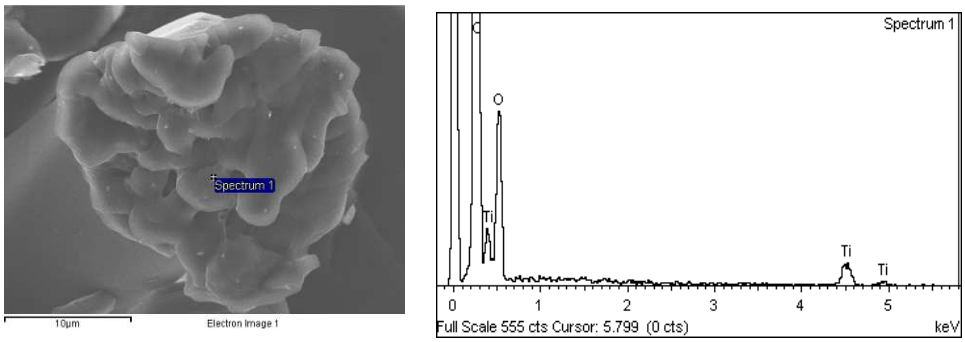


Fig.2 Energy spectrum of the particulate in the no addition polyamide fiber

We can see clearly in Figure 3 the existing of Ag, Zr, P and so on, indicates that the particulates in the multi-antibacterial fibers are indeed the multi-bacterial powders.

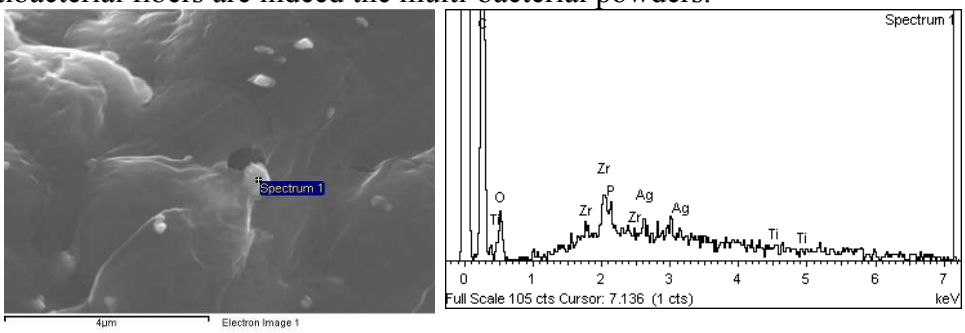


Fig.3 Energy spectrum of the particulate in the 2% addition polyamide fiber

X-ray Diffraction Analysis. We did X-ray diffraction experimentals to analysis the effect to crystallization (Figure 4 and Table 1). As we can see from the chart, with the increase of the addition proportions, the crystal of fibers decrease first and then increase. Because when the addition proportions are less than 1.5%, a small amount of powders play the role of impurities disturbing crystallization, but when the addition proportion is 1.5% and more than 1.5%, the crystallinity is increases, as the powders play the role of inducing crystallization in the other hand. So the crystallinity of polyamide fibers is not always reduced [5].

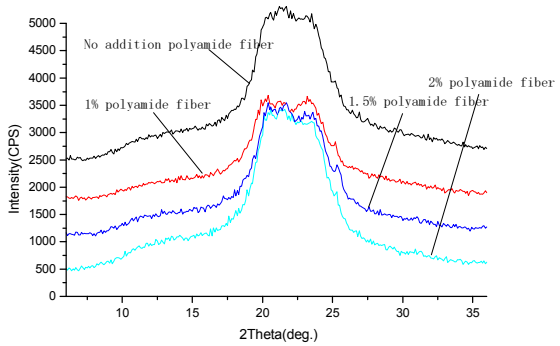


Fig.4 X-ray diffraction curses of polyamide fibers

Tab.1 X-ray diffraction data of polyamide fibers

Samples	Crystallinity/%
No addition polyamide fiber	45.3
1% polyamide fiber	44.6
1.5% polyamide fiber	52.7
2% polyamide fiber	53.2

Thermal Analysis. To analysis the effect to thermal properties, we did DSC experimentals (Figure 5 and Table 2). We can see from the data that adding multi-bacterial master batch makes little change to polyamide fibers' melting temperature, just a little wave. However, with the increase of addition multi-bacterial master batch, the melting enthalpy Delta H declines first, but when the addition ratio is 2%, the data increases significantly. The reason is that a small amount of multi-bacterial agents disrupt the crystallization, but when the ratio is greater than 1.5%, they can play the role of perfect crystal, basically consistent with the crystallization results [6].

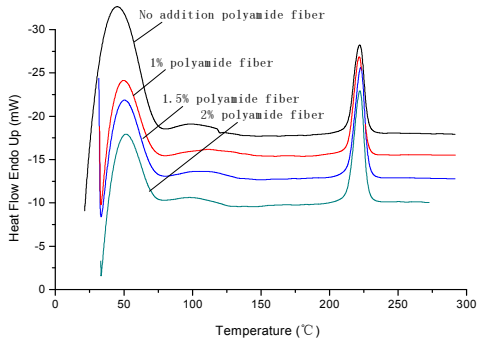


Fig.5 DSC curses of polyamide fibers

Tab.2 DSC data of polyamide fibers

Samples	Tm/℃	Area/mJ	Delta H /(J/g)
No addition polyamide fiber	222.03	306.115	64.8550
1% polyamide fiber	221.68	306.929	64.6167
1.5% polyamide fiber	222.74	363.366	63.7484
2% polyamide fiber	222.14	375.133	68.3302

Infrared Spectroscopy Analysis. As we can see from Figure 6, comparison with no addition multi-bacterial powders polyamide fiber, the IR curses of multi-bacterial polyamide fibers are basically no change, so is the characteristic absorption peak. Therefore, multi-bacterial powder is not connected with the fiber macromolecules, but just only embed in the fiber, so the main properties of the fibers are not significantly affected [7].

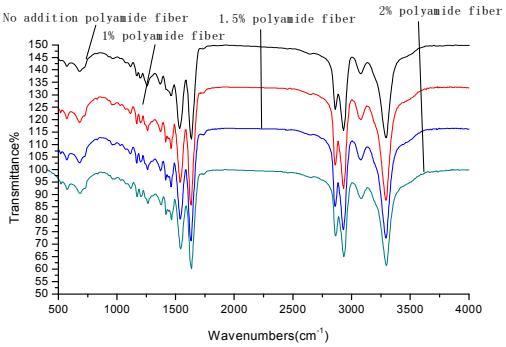


Fig.6 IR curses of polyamide fibers

Antibacterial Functional Analysis. The testing results according to GB/T 209944.3-2008 oscillation are shown in Table 3, the selected species are Gram-positive bacteria Staphylococcus aureus, Gram-negative bacteria E. coli and Candida albicans. When the inhibition rate on Staphylococcus aureus and E. coli are higher than 70%, and the inhibition rate on Candida albicans is higher than 60%, confine samples be antibacterial. It can be seen in Table 3 that 1% addition fibers have a certain antibacterial properties, with the increase of the addition proportions, when up to 2%, the inhibition rate has reached more than 99%, and the fibers have a very good antibacterial effect.

Tab.3 The inhibition rate of polyamide fiber samples

Samples	Inhibition rate/%		
	Staphylococcus aureus	E. coli	Candida albicans
No addition polyamide fiber	0	0	0
1% polyamide fiber	70	70	40
1.5% polyamide fiber	90	90	60
2% polyamide fiber	＞99	＞99	＞99

Far-infrared Emission and Negative Oxygen Ions Emission Functional Analysis. Taking in the important indicator of multi-antibacterial polyamide fibers is antibacterial property, far infrared emission and negative oxygen ions emission function are based on antibacterial function. Therefore, we just take 2% addition polyamide fiber to analysis the multi-function (Table 4). The results were from the National Textile Center for Quality Supervision, far-infrared emission properties was tested according to FZ/T64010-2000, negative oxygen ions emission performance was tested according to CTTC.F024-2007. We can see obviously from the testing results that the far-infrared normal emissivity is 78%, compared to no addition polyamide fibers 70%, increases by 8%, reaches the standards, fibers have far-infrared emission features, to achieve good insulation effect. The negative oxygen ions concentration is 4170 /m^3, far exceeding the World Health Organization provisions clean air is 1500/m^3, then the fibers have good negative oxygen ions generation function, to be good at people's health care.

Tab.4 Far-infrared and negative oxygen ion function test of the 2% addition polyamide fiber

Test items	Measured data	Reference standards
Far-infrared emittance of law /%	78	FZ/T64010-2000
Negative oxygen ions concentration /(/m^3)	4170	CTTC.F024-2007

Conclusions

Put multi-antibacterial master batch in polyamide fibers by melt spinning, got multi-bacterial polyamide fibers, multi-antibacterial powders have a good dispersion in fibers.

Polyamide fibers' structure and properties have an impact when add multi-antibacterial powders. As the addition proportions increase, the crystallinity of the fibers first decline and then increase; the results shown in DSC testing, adding multi-bacterial master batch made little change to polyamide fibers' melting temperature, the effects to melting enthalpy Delta H are basically consistent to the crystallization results; the results shown in IR testing, multi-bacterial powders are not connected with polyamide fibers macromolecules, and affect the characteristic absorption peak.

Polyamide fibers with adding multi-bacterial master batch have good antibacterial, far-infrared and negative oxygen ions emission features. 2% addition proportion fibers' inhibition rate to Staphylococcus aureus, Escherichia coli and Candida albicans are more than 99%, fibers have a very good antibacterial effect. Moreover, the far-infrared normal emissivity increase by 8% compared to no addition polyamide fibers, have good thermal insulation effect; negative oxygen ions concentration is up to 4173/m^3, be good at people's health.

References

[1] In Chinese Juan Sun, Chen Yao, Xinsong Li: Polymer Bulletin, 2010,8(8):27-33.
[2] In Chinese Jinming Dai, Ruiping Zhang: Chemical Fiber & Textile Technology, 2005,3(1):31-34.
[3] In Chinese Daojiang Chen, Zhengsheng Ma: Guangxi Textile Science, 2006,35(1):43-47.
[4] In Chinese Jianhua Qian, Fu Sun, Ronggen Ling: Journal of Textile Research, 2007,28(4):16-18.
[5] Sang Young Yeo etc: Journal of Materials Science,2003,V38:2143-2147.
[6] In Chinese Xianhong Chen, Hailiang Zhang, Xiayu Wang, et al: China Plastics Industry, 2001,7(4):44-46.
[7] In Chinese Xinzhao Huang, Zhongyi Zhang, Xiaodong Zhang: Journal of Qingdao University, 2008,23(1):21-24.

© (2011) Trans Tech Publications, Switzerland
doi:10.4028/www.scientific.net/AMR.331.184

Thermal comfort properties of knitted fabrics suitable for skin layer of protective clothing worn in extreme hot conditions

Nazia Nawaz[1a], Olga Troynikov[1b], Chris Watson[1c]

[1]School of Fashion and Textiles, RMIT University, 25 Dawson St., Brunswick 3056, Melbourne, Australia

Email[a]: nazia.nawaz@student.rmit.edu.au, Email[b]: Olga.troynikov@rmit.edu.au,

Email[c]: chris .watson@rmit.edu.au

Key words: Physiological comfort, knitted fabrics, protective clothing

Abstract. Thermal comfort of clothing is associated with the thermal balance between human body and the environment, and also a balance between the body heat production and the heat loss. During work activities performed in extreme hot conditions, the body produces substantial amount of heat energy which leads to raised body temperature. As a result the body perspires in liquid and vapour form to reduce the increased temperature. When this perspiration is transmitted to the atmosphere, the body temperature reduces. Thus the garments worn next to skin should allow the perspiration and heat to easily pass through them; otherwise the result will be a significant discomfort of the persons working in extreme hot conditions. Therefore, thermal properties and water vapour permeability of the fabrics used for the next-to-skin layer of protective clothing are very important for the maintenance of physiological comfort of workers. In the present study physical parameters, air permeability, porosity, thermal and water vapour permeability of six commercially available knitted fabrics of different fibre blends, different and knitted structures suitable for skin layer garments of protective clothing worn in extreme hot conditions were evaluated. The influences of fabric physical parameters, and optical porosity on thermal conductivity and water vapour permeability of fabrics were determined and correlation coefficients were calculated between these variables.

Introduction

Thermal comfort of clothing concerns the heat and moisture transport properties of clothing. Clothing should ensure appropriate heat transfer between the human body and its environment in order to maintain the physiological thermal balance of the wearer. Working in extreme hot environment results in considerable elevation of body core temperature. To reduce this elevated temperature to normal, the body perspires in liquid and vapour form. To keep body temperature at normal level, the evaporation of perspiration is necessary. Evaporation is an endothermic process which allows the lowering of the temperature providing a physiological comfort to the human body [1]. Therefore, to provide thermophysiological comfort the garment next to the skin must have the following important characteristics: ability to absorb heat, vapour and liquid perspiration from skin and then transfer these to the outside of the garment [2]. These garment attributes depend in turn on thermal and moisture management properties, porosity and air permeability of the fabrics, yarns and fibres used [3]. The thermal comfort properties of textile fabrics are influenced by the type of fibre, yarn spinning method, count, twist and hairiness, fabric thickness cover factor, porosity and finish applied [4]. Milenkovic et al. demonstrated that fabric thickness, amount of still air enclosed within the fabric and external air movement are the major factors that affect the heat transfer through fabric [5]. Similarly, Havenith found that heat and water vapour resistance increases incrementally with the incremental increase of material thickness and the amount of air entrapped in the fabric [6].

In addition, Majumdar studied knitted fabrics made from 100% cotton, 100% regenerated bamboo cellulosic fibres and cotton/bamboo fibre blends using different yarn counts in plain, rib and interlock structures for their thermal properties. He concluded that thermal conductivity of knitted fabrics

reduced with the increase of the proportion of bamboo fibre in the yarn. The water vapour permeability showed simultaneous increase as the proportion of bamboo fibre increased with cotton fibre [7-9].

The present research is focused on investigation of the possible relationship between fabric thermal comfort properties, its physical parameters and *Fabric optical porosity*, of six commercially available knitted fabrics of different fibre blends and knitted structures suitable for skin layer protective clothing worn in extreme hot conditions.

Experimental

In the present study thermal comfort properties six commercially available different knitted fabrics (Table 1) were investigated. The influence of fabric physical parameters on thermal comfort properties of these fabrics were discussed and analysed. The Pearson correlation coefficients were calculated for different fabric's physical parameters and their thermal comfort properties.

Materials

Six commercially available knitted fabrics SJ1-IM2 (Table 1) of different constructions and fibre blends were studied.

Test methods

Fabric physical properties

Fabric mass per unit area: Five specimens of 100mm×100mm from the fabric samples were prepared and each of the specimens was weighed by measuring balance. The mass per unit area was calculated as the mean mass per unit area [10]. *Fabric thickness* :The thickness of fabric samples was measured as the distance between the reference plate and parallel presser foot of the thickness tester [11]. *Fabric density:* The number of courses and wales in an accurately measured length of fabric were counted along a line at right angles to the warp or weft being considered [12]. *Fabric optical porosity, %:* Total optical porosity of the fabric *OP* , defined as the portion of all air spaces in knitted fabric both between yarns and inside them, was determined using Motic Image Tool 3.0 software:

$$\textit{Fabric optical porosity (\%)} = \textit{Black pixels/ Black pixels + White pixels} * (100) \quad (1)$$

Fabric thermal conductivity and water vapour resistance properties

Fabric thermal conductivity

Thermal conductivity of the fabrics was calculated using Tog meter with units $Wm^{-1}K^{-1}$ [13].

Fabric vapour resistance

Fabric vapour resistance was tested using Sweating Guarded Hot Plate [14] at the following conditions: the air temperature is at 35 °C, the relative humidity is at 40%, air speed is at 1 m/s. The total thermal resistance of the fabric is calculated after the system reached a steady state:

The total water vapour resistance of the fabric is calculated as:

$$\mathrm{Re}t = A(Ps - Pa)/H \quad (2)$$

Where,

Ret is the total vapour resistance resulted from the liquid barrier between hot plate and the membrane used for vapour testing, the fabric and the boundary air layer, *A* is the area of specimen test section in m^2, *Ps* is the water vapour pressure at plate surface in Pa, *Pa* is the water vapour pressure of the air in Pa, *H i*s the electrical power in Watts used by the instrument.

Pearson correlation analysis was carried out to find the relation between fabric thermal properties and physical properties. The Pearson correlation coefficients were calculated between fabric thickness and thermal conductivity and vapour resistance. These were also calculated between *Fabric optical porosity and* thermal conductivity and vapour resistance.

Results and discussion

Physical properties of sample fabrics

Table 1. Physical and structural properties of sample fabrics

Fabric code	Fibre composition	Construction	Fabric mass/unit area [g/m^2]	Fabric thickness [mm]	No. of Wales/cm	No. of courses/cm
SJ1	100% Merino wool	Single Jersey	139	0.35	18	18
SJ2	60% Merino Wool/ 40% Bamboo	Single Jersey	156	0.34	18	18
SJ3	100%Cotton	Single Jersey	149	0.47	16	20
SJ4	94% Merino wool/ 6% Elastane	Single Jersey	185	0.55	18	20
IM1	100%Polyester	Interlock based mock mesh	168	0.61	16	16
IM2	52% Merino wool / 48% Biophyl	Interlock based mock mesh	216	0.97	12	16

Physical properties of fabrics demonstrate that fabrics SJ1 and SJ2 have similar thickness and stitch density to each other. SJ2 is 12% heavier than SJ1 which is most likely due to the higher density of SJ2 being a blend of wool and bamboo fibres. SJ3 is 100% cotton fabric and it has more open structure in comparison to SJ1 and SJ2 due to their different stitch density. SJ4 is heavier and thicker than SJ1, SJ2 and SJ3 with similar stitch density to SJ1, SJ2 and SJ3; its higher thickness and mass/unit area is greater due to blending of wool with continuous filament elastomeric fibres. IM1 and IM2 have similar fabric structure to each other but, being double-jersey fabrics, they are different in construction to other sample fabrics of the study. IM2 is the heaviest and thickest fabric among all the sample fabrics of this study, and has different wales/courses stitch densities which is all due to the use of coarser yarns and coarser knitting machine gauge.

Thermal properties

Table 2. Properties of sample fabrics relevant to their thermal comfort

Fabric code	Thermal conductivity [W/(m.K)]	Water vapour resistance [m^{2}Pa/W]	*Fabric optical porosity* (%)
SJ1	0.0492	2.093	8.19
SJ2	0.0520	1.994	5.84
SJ3	0.0961	2.123	9.94
SJ4	0.0661	2.440	8.05
IM1	0.0576	2.861	8.23
IM2	0.0485	4.955	14.76

In Figure 1 mean values *Fabric optical porosity*, thickness and thermal conductivity for all the sample fabrics are shown.

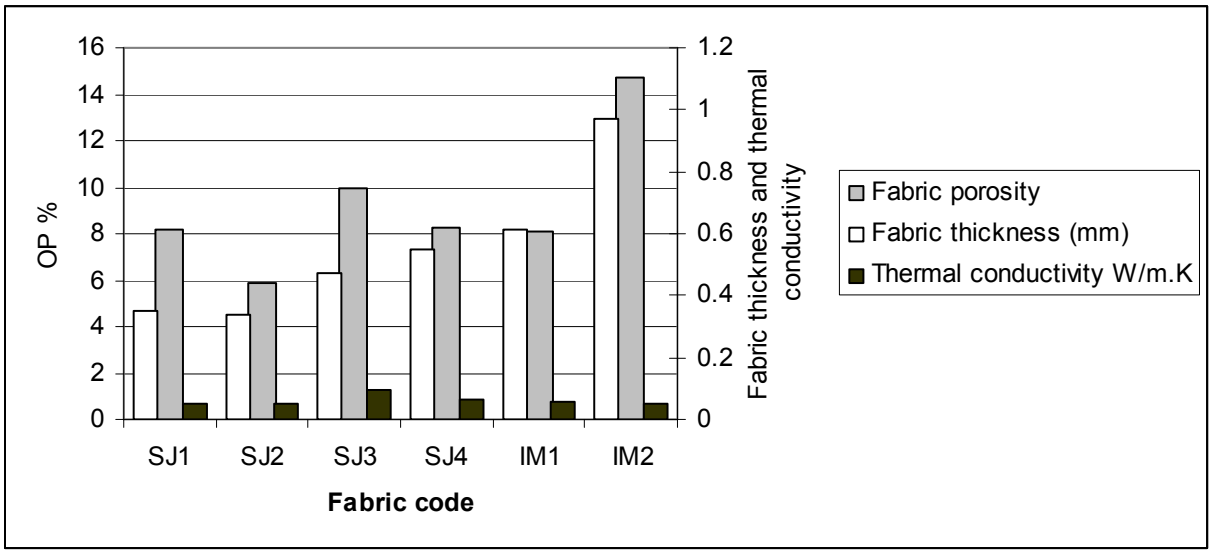


Figure 1. OP %, thickness and thermal conductivity of sample fabrics

SJ1 and SJ2 have similar thickness to each other and OP % of SJ2 is 28% lower than SJ1. Thermal conductivity of SJ1 and SJ2 is approximately similar to each as both fabrics have similar fabric structure, thickness and stitch density (Fig. 1, Table 1).

SJ3 is showing highest thermal conductivity demonstrating higher heat transferability than any other sample fabrics of the study. SJ3 is 100% cotton fabric having single jersey structure. *Fabric optical porosity* of SJ3 is greater than SJ1, SJ2 and SJ4. SJ4 and IM1 have similar *Fabric optical porosity* to each other. IM1 is 10% thicker than SJ4. SJ4 has single jersey structure and IM1 has interlock mockmesh fabric structure which can trap more air than single jersey structure and air is a poor conductor of heat. Hence, thermal conductivity of SJ4 is 12 % higher than IM1. IM2 has the lowest thermal conductivity among all the sample fabrics. IM2 has interlock mockmesh fabric structure with non-uniform stitch density creating larger air gaps. IM2 has highest OP % and thickness as compared to other fabrics of the study.

Wool fibre has convolutions on its surface which contribute to trap air enhancing the insulation of the fabric resulting lower thermal conductivity. In case of cotton it cannot trap air like wool fibre and inherently have better thermal conductivity as compared to wool, and wool blends. That could be a possible reason for SJ3 showing highest thermal conductivity among all the sample fabrics of the study. Therefore for fabric thermal conductivity fibre type, fabric thickness and fabric structure are the most critical factors.

In Figure 2 mean values of water vapour resistance and fabric thickness through all the sample fabrics are shown.

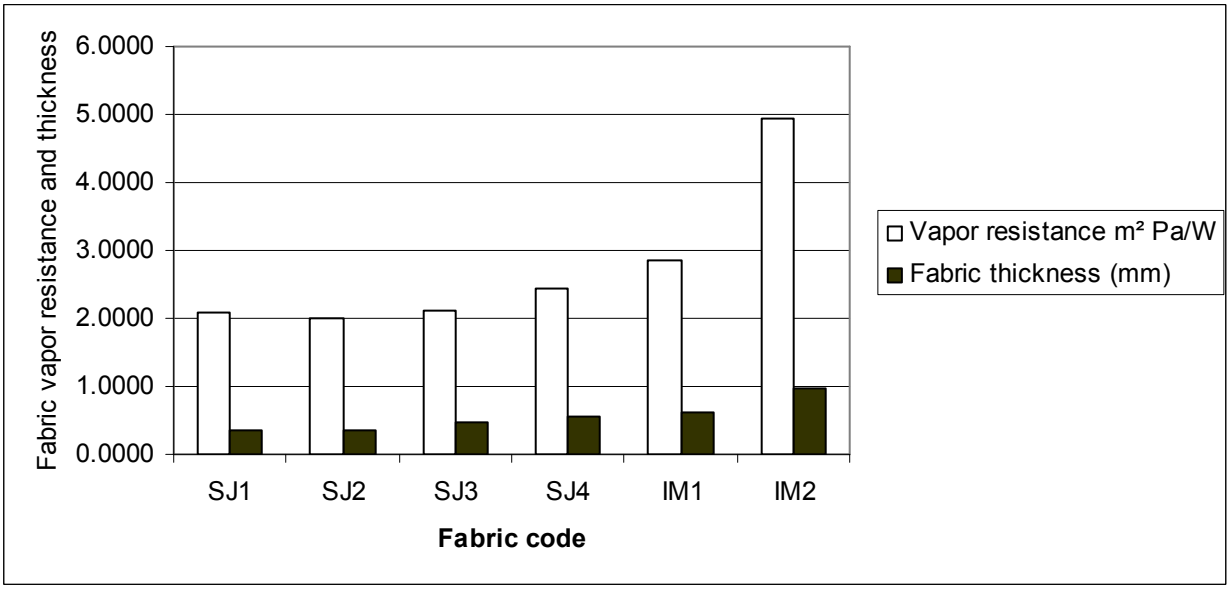


Figure 2. Water vapour resistance and fabric thickness of sample fabrics

SJ1, SJ2, SJ3 and SJ4 are in single jersey form and showing lower water vapour resistance than IM1 and IM2. SJ4 has slightly higher water vapour resistance than SJ1, SJ2 and SJ3 and it can be due to its higher thickness than SJ1, SJ2 and SJ3. But in case of vapour resistance, SJ3 is not showing the least vapour resistance as it has the highest thermal conductivity. For vapour resistance SJ2 which is a wool/bamboo fibre is demonstrating the least resistance indicating the highest ability to transfer skin moisture vapour to outer atmosphere. This might be due to the blending of wool with bamboo fibre. Because bamboo fibre has unique micro structure having micro pores on its surface which increase it absorption capacity, and allow the water vapour molecules to pass through [15]. IM1 and IM2 are comparatively thicker fabrics than all other sample fabrics of the study. Both of these two fabrics have higher vapour resistance as compared to other single jersey sample fabrics of the study. Therefore, from the results it is clear that water vapour resistance of the fabrics is also influenced by the type of the fibre, the thickness of the fabric and also its structure.

Calculated Pearson coefficient of correlation between fabric thickness and vapour resistance was 0.970 indicating a strong positive linear relationship between fabric thickness and vapour resistance. For fabric thickness and thermal conductivity, coefficient of correlation was negative – 0.0189 indicating no linear relationship between these two variables. It means that increasing fabric thickness will decrease the thermal conductivity.

For fabric porosity similar correlation was observed for thermal properties as in case of fabric thickness. Coefficient of correlation between *Fabric optical porosity* and vapour resistance was 0.886 which indicates that a strong positive linear relationship exists between *Fabric optical porosity* and vapour resistance. Correlation coefficient between OP % and thermal conductivity was negative -0.008 indicating no linear relationship between *Fabric optical porosity* and thermal conductivity,

Conclusion

The main objective of the study was to investigate the thermal comfort properties of different knitted fabrics used for skin layers of protective clothing worn under extreme hot environments. In this study 100% wool, wool blends, 100% cotton and 100% polyester were studied. The results and discussions demonstrate that 100% cotton is a good choice for transferring heat but in hot conditions where body sweats heavily it might not be preferable. Cotton has the ability to hold water but unable to transfer moisture to outer atmosphere. For vapour resistance both wool and wool/bamboo blend

fabrics in single jersey construction demonstrated the best result among all the sample fabrics of the study. 100% wool fabric can also be used with acceptable results. Correlation analyses show that thermal conductivity and water vapour resistance are strongly influenced by fabric porosity *Fabric optical porosity* and fabric thickness. Therefore it can be concluded that the fibre content, fabric construction and fabric thickness significantly influence, thermal comfort properties of knitted fabrics suitable for skin layer of protective garments and have to be taken into consideration at the design and engineering stage for the protective ensembles. Furthermore the single jersey construction is the preferable one for the fabric to be used next to the skin in these garments.

Acknowledgements

We would like thank Charles Parsons & Co for supplying us with suitable sample fabrics and their support through this research.

References

[1] M. J. Pac, M.A.B., M. Renner, *Warm-cool feeling relative to tribological properties of fabrics.* Textile Research Journal, 2001. 71: p. 806-812.

[2] Das, B., Das, A., Kothari, V.K., Fanguiero, R., Araújo, M., *Moisture Transmission Through Textiles Part I: Processes involved in moisture transmission and the factors at play* AUTEX Research Journal, 2007. 7(2): p. 100-110.

[3] Cotton Incorporated, C.N.C., *100% Cotton Moisture Management.* Journal of Textile And Apparel, Technology and Management, 2002. 2(3).

[4] Li, Y., ed. *The Science of Clothing Comfort*. Textile Progress. 2001. 1-135.

[5] Milenkovic, L., Skundric, P., Sokolovic, R., Nikolic, T., *comfort Properties of Defence Protective clothing.* The scientific Journal Facta Universities, 1999. 1(4): p. 101-106.

[6] Havenith, G., *The Interaction of Clothing and Thermoregulation.* Exogenous Dermotology, 2002. 1(5): p. 221-230.

[7] Abhijit Majumdar, S.M., Ravindra Yadav, *Thermal Properties of knitted fabrics made from cotton and regenerated bamboo cellulosic fibres.* International Journal of Thermal Sciences, 2010. 49: p. 2042-2048.

[8] Troynikov, O., Wardiningsih, W., ed. *Comfort properties of fabrics for winter sportswear*. 1st ed. 2010, Saarbrucken, Germany : VDM Verlag Dr Mueller, 2010.

[9] Troynikov, O., Wardiningsih, W., *Moisture management properties of wool/polyester and wool/bamboo knitted fabrics for sportswear base layer.* Textile Research Journal, 2011. 81(6): p. 621-632.

[10] AS, *Determination of fabric mass per unit area.* 2001. 2001.2.13-1987.

[11] AS, *Determination of fabric thickness.* 2001. 2001.2.15-1989.

[12] AS, *Determination of No. of ends per cm and No. of picks per cm.* 2001. 2001.2.5-2001.

[13] *BS 4745 Thermal Resistance Measurement*. 1979.

[14] ISO, *Textiles - Physiological effects- Measurements of thermal and vapour resistance under steady-state conditions (Sweating Guarded Hot Plate)*. 1993.

[15] Erdumlu, N. and B. Ozipek, *Investigation of regenerated bamboo fibre and yarn charcteristics.* Fibres and Textiles in Eastern Europe, 2008. 16(4): p. 43-47.

© (2011) Trans Tech Publications, Switzerland
doi:10.4028/www.scientific.net/AMR.331.190

A New Test Method for Weft Tension in Shed on Air-jet Looms

Hongli Ma[1, a], Lixia Leng[1, b], Zhiyu Zheng[1, c] and Xiaohong Zhou[1, d]

[1]The Key Lab of Advanced Textile Materials &Manufacturing Technology Ministry of Education China, Zhejiang Sci-Tech University, Hangzhou 310018, China

[a]michelle_hongli@163.com, [b]lenglixia@163.com, [c]zzytex@163.com,

[d]zhouxh314@163.com

Keywords: weft tension, air-jet loom, high-speed camera, weft insertion.

Abstract. During weaving, broken picks and irregular pick always lead to loom stop and cloth defect. Weft tension is one of the important factors. This paper introduces a kind of method that can be used to measure weft tension when the weft is in the shed on the loom. The weft tension in shed of 296.5 dtex + 70 D spandex covering combed cotton yarn was be measured on the TaiTan TT-800 air-jet loom, and the results we got is sound. It is seen that the method we used effectively solves testing weft tension in shed on air-jet looms.

Introduction

Air-jet loom is one of the fastest growing shuttleless looms with its high speed, high efficiency and high quality [1], but its weaving efficiency is still to be improved. In the process of weaving, one of the most important factors for loom stop and cloth defect in fill-wise is weft tension [2]. So far, there are two methods that can be used to test weft tension: the one is the dynamic resistance strain gauge. In this method, light oscilloscope or tape recorder is employed to record the fluctuations of the weft tension [3]. The other system consists of the sensor, the data acquisition card, computer and the corresponding software. The signal of weft tension can be acquired and transformed. Finally the curve of weft tension with the loom main shaft angle was shown on the computer [4]. The two kinds of methods only can be used to measure the weft tension between weft accumulator and main nozzle.

High-speed camera is also called digital industry camera. It is a professional camera that can continuous acquired pictures at a high rate of speed. For its high stability, high transmission capacity and high anti-interference ability, high-speed camera is used in instant physical phenomenon, microscopic high-speed image and traffic control, etc [5]. In this paper, a kind of method that can be used to test weft tension while the weft yarn is in the shed on the air-jet loom was introduced. The high-speed camera plays an important role in the method.

Principle and Method of the Test

When the yarn along the lengthways has the tension force, the blending of fibers in the yarn will reduce, which means the straightness of fiber in the yarn will be improved. It also results that the cross of the yarn shrinks, the loads applied in inner layer fibers from out layer fibers will increase, and the yarn will come into elongation.

At first we marked certain length on the yarn and wound it onto the bobbin. Then while the yarn was inserted into the shed on air-jet loom, the yarn tensile buckling pictures was recorded by high-speed camera. Finally extension rate of the weft yarn was acquired and the weft tension in shed can be calculated on the basis of the yarn strength elongation curves.

Fig. 1 is the schematic of measuring the weft tension in the shed on air-jet loom. TaiTan TT-800 air-jet loom was employed in this experiment. The marked weft yarn is unwind from the bobbin, passes through weft accumulator (a) and main nozzle (b), then be brought into weft aisle which composed by special-shaped reed (c) , weft yarn is inserted into shed by relay nozzles (d). The CooKe PRO.1200s high-speed camera (f) is fixed over against the shed along width-ways and acquired the yarn tensile buckling pictures.

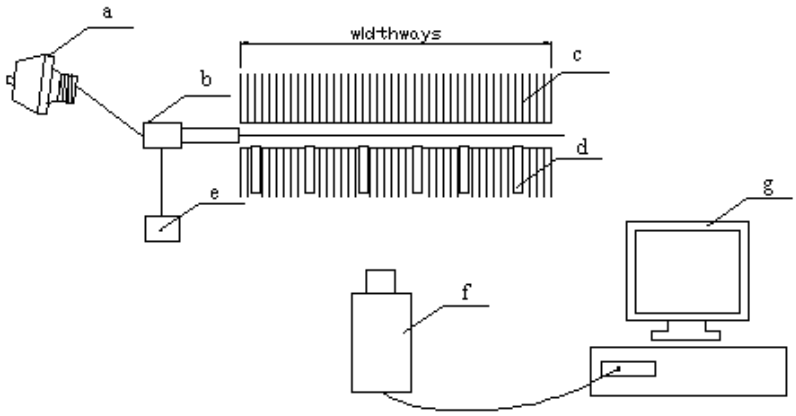


Fig. 1 The schematic of measuring the weft tension in the shed on air-jet loom: (a) weft accumulator; (b) main nozzle; (c) special-shaped reed; (d) relay nozzles; (e) air works; (f) high-speed camera; (g) computer.

The TaiTan TT-800 air-jet loom is developed by Zhejiang TaiTan Co., Ltd. It can be widely used in weaving of the garment fabrics, decorative cloth and industrial-purpose cloth with cotton, filament yarn and wool as the raw materials.

The PCO.1200s high-speed camera is manufactured by CooKe Corporation. This high performance with digital CMOS camera system is perfectly suited for life science and machine vision applications, where an excellent image quality and high offset stability is required. The camera features excellent resolution is (1280 x 1024 pixel), exposure times is from 1 μsec to 5 sec, spectral range is from 290 to 1100 nm, superior frame speed is from 500 to 32023 frame per second, internal frame buffer for continuous image capture is (4 G max.) and standard interface IEEE is 1394 .

Results and Discussion

The weaving parameters of TaiTan TT-800 air-jet loom described as follows: The speed of main shaft was 500 rpm. The supplied air pressure of main nozzle was 0.25 Mpa. The start angle of weft insertion was 80° of the main shaft rotation angle. The distance between main nozzle and the first relay nozzle was 80 mm. Relay nozzles was divided into six groups. The front three groups included 5 relay nozzles per group and the supplied air pressure to them was 0.2 Mpa. The later three groups include relay nozzles were 4, 3 and 3 and the supplied air pressure was 0.25 Mpa. The time of main nozzle was started at 80° and closed at 180° of the main shaft rotation angle. The time of every group of relay nozzle was started at 80, 100, 120, 140, 160 and 180 °and closed at 160, 180, 200, 220, 240 and 260° of the main shaft rotation angle.

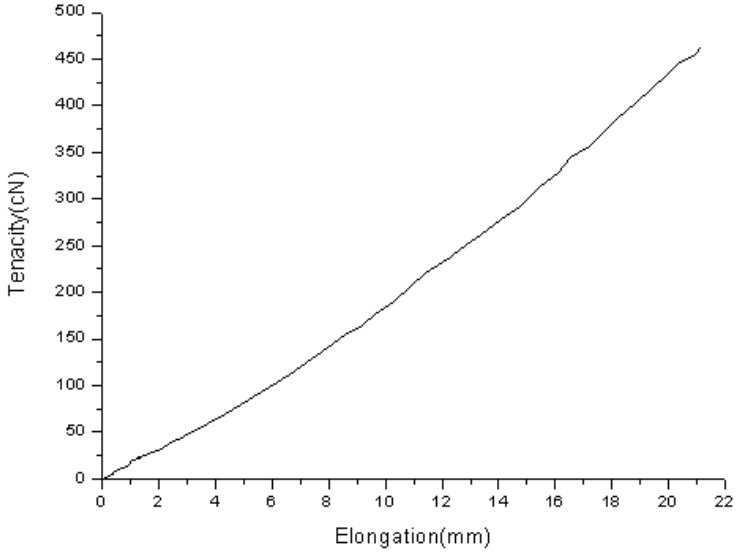


Fig.2 The strength elongation curve

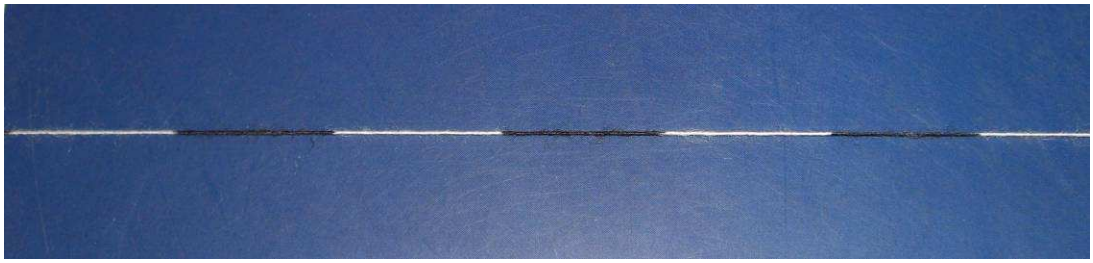


Fig. 3 The marked weft yarn

The yarn of 296.5 dtex + 70 D spandex covering combed cotton is usually used for weft in casual fabrics. We uses 296.5 dtex + 70 D spandex covering combed cotton as weft yarn in this experiment, its strength elongation curve obtained from yarn tension tester is described in fig. 2. The marks which were made in 0.5 cN/tex pre-tension on the weft yarn are shown in fig. 3. All of the mark distances are 2 cm.

In this experiment, the PCO.1200s high-speed camera was used to take the weft tensile pictures in shed. The exposure time was controlled at 445 μs. The delay time was controlled at 0μs. The size of the picture was regulated at 1280*378 pixels. The frame speed was 1342.26 frames per second. The positions of the high-speed camera were 30, 60, 90 and 120 cm from the shed left. The pictures of the tensiled weft yarn were acquired while weft yarn was inserted into the shed on TaiTan TT-800 air-jet loom.

The tensile weft yarn inserted the shed on TaiTan TT-800 air-jet loom is showed in fig.4. The background of the tensile weft yarn is the special-shaped reed. The distances among the dents are absolutely equal. The reed number of 19 dents/cm was employed in this experiment. The marked weft yarn covered a certain number of dents of reed. According to Eq. 1 the extension rate of weft yarn in the shed can be calculated.

$$\varepsilon = \frac{\frac{N}{P} - L_0}{L_0} \tag{1}$$

Where, ε is the extension of weft yarn in shed (%), N is the number of dents of reed that the tensile weft yarn covered in shed, P is the reed number (dent/cm), L_0 is the length of the marked weft yarn (cm).

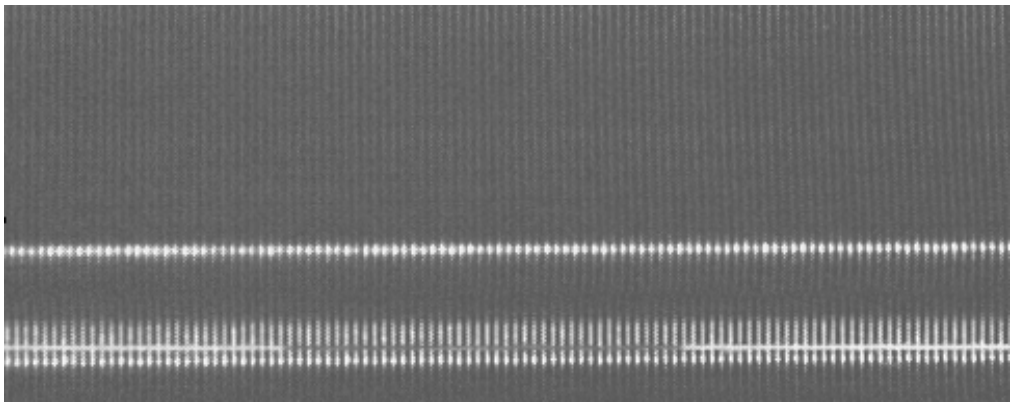


Fig.4 The tensile weft yarn inserted the shed on TaiTan TT-800 air-jet loom

The experimental data are listed in table 1. The dents covered by the marked weft yarn were counted in the pictures acquired by the PCO.1200s high-speed camera. Base on the Eq. 1 and the strength elongation curve, the average tension of the yarn of 296.5 dtex + 70 D spandex covering combed cotton in the shed on the air-jet loom is 36 cN and their discrete data CV% is equal to 3.06%.

Table 1 The data of weft yarn during weft insertion

Length from the left end shed (cm)	30	60	90	120
Dents that marked weft yarn coverd	41.0	42.0	41.0	42.5
Extension of weft yarn in shed (%)	7.89	10.53	7.89	11.84
Tension (cN)	29.78	41.43	29.76	41.67
Discrete CV%	2.30%	1.48%	3.08%	5.39%

Conclusion

It is a breakthrough for measuring the tension of weft in shed to use the high-speed camera. The high-speed camera can be used to not only observe the tensile of weft yarn in shed, but also calculate the tension of the weft yarn in shed based on the yarn tensile properties. The average tension of the yarn of 296.5 dtex + 70 D spandex covering combed cotton in the shed on the TaiTan TT-800 air-jet loom is 36 cN and their discrete data CV% is equal to 3.06%. It will be helpful to decrease loom stop and cloth defect and improve the weaving efficiency and fabric quality.

References

[1] Yang Xu, Xueping Wu, Qiang Zhang: China Textile Leader No.2, 58-60 (2007), p.58 (In Chinese)

[2] Haoyi Xu: Silk Monthly No.8, 29-32 (2010), p.29 (In Chinese)

[3] Xingfeng Guo: Cotton Textile Technology Vol 25, 102-104 (1997), p.102 (In Chinese)

[4] Weibing Xiao: Instrument Technique and Sensor No.11, 45-47 (2007), p.45 (In Chinese)

[5] Information on http://www.baidu.com

© (2011) Trans Tech Publications, Switzerland
doi:10.4028/www.scientific.net/AMR.331.194

Annealing Treatment of the SnO_2 Thin Film Prepared by Sol-gel Method

Qi Xiao[1,a], Rui Wang[1,2,b], Lei Xu [1,2]

1, Key Lab of Advanced Textile Composites

2, School of Textiles, Tianjin Polytechnic University, Tianjin 300160, China

[b]wangrui@tjpu.edu.cn, [a]Xiaoqi223638@yahoo.com.cn

Keywords: Chloride; Sol-gel; Annealing; Transmittance; Resistivity

Abstract: SnO_2 thin film on the glass fiber was prepared by the ethanol solvent and crystalline tin chloride based Sol-gel method, including the process of solution preparation, fiber dip-immersing, gel reaction and annealing. The sol was prepared by alcoholysis reaction of 0.9mol/l chloride- ethanol solvent under 80˚C. A thin film of sol was prepared by dip-immersing process, then a post annealing process with various temperatures and time was adopted to form a stable crystallized film on the surface of the glass fiber. X-ray diffraction, scanning electron microscope (SEM) and fiber electric resistance measurement were utilized to characterize the transmittance and resistivity of the thin film With the rising of annealing temperature, the transmittance of the thin film was firstly increased and then decreased while the resistivity changed adversely. At last, an optimized annealing process with 550˚C and 3h was chosen.

Introduction

With the energy crisis and global warming appearing, governments have engaged in the development of renewable energy, and solar energy holds an important position. In recent years, many reports focused their interests in the nano-technique based thin films for solar cells [1-4]. Among them, Tin oxide transparent conductive film is an essential material for solar cells, for its high conductivity, high transparency and chemical stability. There are many reports about the preparation of Tin oxide transparent conductive films, such as magnetron sputtering [5,6], chemical vapor deposition [7], physical vapor deposition [8], spray pyrolysis [9], RF reactive sputtering [10], etc.

However, there are many shortages of these methods, especially the expensive equipment and complex operation. Sol-gel method is low-cost in equipment, simple in operation and easy in control. Organic solvent especially ethanol are mostly used as the solvents in the Sol-gel process. For ethanol solvent have many advantages, including the low surface tension, the stable Sol and the gel process without the interference of chloride ions.

Pan Qingyi et.al [11] carried out the research on the coated glass plates by Sol-gel, but the coated glass fiber was rarely studied. In this paper, SnO_2 thin film on the glass fiber was prepared by Sol-gel with solvent of ethanol and crystalline tin chloride. Furthermore, the effect of the different annealing temperature and time on the grain size of thin film, transmittance and resistivity of thin film were discussed.

Experimental

The preparation of sample

Sol Reaction. The Sol was prepared by dissolving moderate quality of $SnCl_4 \cdot 5H_2O$ in the ethanol to yield a 0.9mol/L solution. After stirring for 15 minutes at the room temperature, it was placed and stirred in the oil path pot at a constant temperature of 80˚C for half an hour to yield a transparent Sol.

The Preparation of the Glass Fiber. The glass fiber was cleaned in the acetone solution by ultrasonic wave scouring for three times, then in the demonized water by ultrasonic wave for twice, finally in the ethanol by ultrasonic wave for three times. After the scouring, the glass fiber was placed in the dry and clean environment for 12 hours.

Filming. The filming of the glass fiber was executed by a dip-coating method. Dry glass fiber was impregnated in the $SnCl_4$- ethanol Sol and then was dropped out from the Sol at a steady drawing rate of 4cm/min.

The Gel Process. After it dried, the surface of the glass fiber reacted to yield the tan gel at the environment of 130˚C. Then it was aged for 30min.

Annealing. The fiber was placed in an electric tube furnace, and the temperature was set as 350˚C, 450˚C, 550˚C and 650˚C, respectively, and the annealing time was set as 2h, 3h, 4h and 5h, respectively. And finally the SnO_2 thin film was obtained.

The fiber was placed in the tube furnace, and the temperature was set as 350˚C, 450˚C, 550˚C and 650˚C, respectively; and the annealing time was set as 2h, 3h, 4h and 5h respectively. Finally the SnO_2 thin film was obtained.

Tests

X-ray diffraction (XRD). The structure and morphology of SnO_2 thin film was characterized by using a Rigaku D/max-2500 X-ray diffractometer with Cu Kα radiation (λ=1.5418 Å, Tokyo, Japan).

Morphology Observation of the film on the fiber. Field emission scanning electron microscopy (FE-SEM) images were taken on a JEOL JEM-6700F microscope (Tokyo, Japan) equipped with energy dispersive X-ray (EDX) spectroscopy.

The test of conducting performance of the thin film. The resistivity of the thin film was analyzed voltammeter. A four-electrode based volt-ammeter method was adopted to test the electric resistance of a single glass fiber.

The test of the transmittance of the thin film. The transmittance was measured by spectrophotometer.When the incident light hits the fiber,the transmitted light is detected. So the transmittance equals the transmitted light intensity divided by the incident light intensity.

Results and Discussion

Reaction principle

(1) Alcoholysis reaction

$$SnCl_4 + 4C_2H_5OH \rightarrow \mathrm{Sn(OC_2H_5)_4} + 4HCl, Sn(C_2H_5)_4 + xH_2O \rightarrow n(OH)_xO(C_2H_5)_{nx} + xC_2H_5OH$$

(2) Poly-condensation reaction

$$2(C_2H_5)_3SnOH \rightarrow (C_2H_5)_3SnOSn(O(C_2H_5)_3) + H_2O, m(C_2H_5O)_2Sn(OH)_2 \rightarrow [M(OC_2H_5)_2O]_m + mH_2O$$

$$m(C_2H_5O)Sn(OH)_3 \rightarrow [O\text{-}M(OC_2H_5)_2O]_m + mH_2O + 4H^+$$

From the reaction equations above, it can be seen that the impurity in the outcome in the Sol-gel with organic solvent is very limited because of the continuous evaporation of water, ethanol and hydrogen chloride, which yield during the reaction as the temperature rises. Moreover, ethanol acts as a complex agent (the polymer network structure was formed) and release agent during the reaction (the reunion among the metal oxide was hindered during the gel process). So the good performance of the film can be obtained.

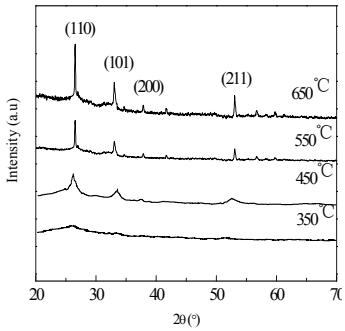
The phase of the thin film

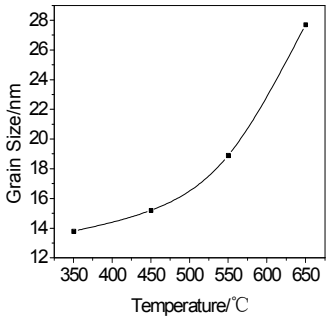
The XRD pattern of SnO_2 thin film is shown in Fig.1, where includes the films obtained by using the concentration of 0.9mol/L the solution annealed at 350˚C, 450˚C, 550˚C and 650˚C respectively for 3h. It can be seen from the Fig.1 that the diffraction peaks of SnO_2 which was yielded by annealing at 550˚C is smaller than that of other annealing temperatures, and the FWHM broadens. So the grain size produced in this case is relatively small. This can be inferred from the Fig.2. And the relationship between the annealing temperature and the grain size and FWHM was shown in the Fig.3.

The morphology of the thin film

It can be inferred from the SEM that the grain size grows continually as the increasing of the annealing time. When the time is longer than 4h, the grain trends to agglomerate, which lead to destruct the structure of the film to form the black spots on the glass fiber, as follows in the Fig. 4.

It can be seen from Fig.4 that the morphology of the thin film is the best. And the detailed observation of the film is shown in the Fig.5.





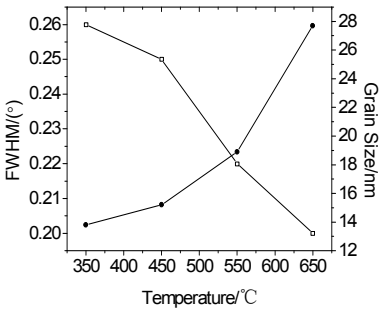


Fig.1 Fig.2 Fig.3

Fig.1 XRD patterns of the thin films annealed at different temperatures for 3h
Fig.2 Grain size versus annealing temperature of the thin films
Fig.3 FWHM of the XRD and grain size of the film annealed at various temperatures

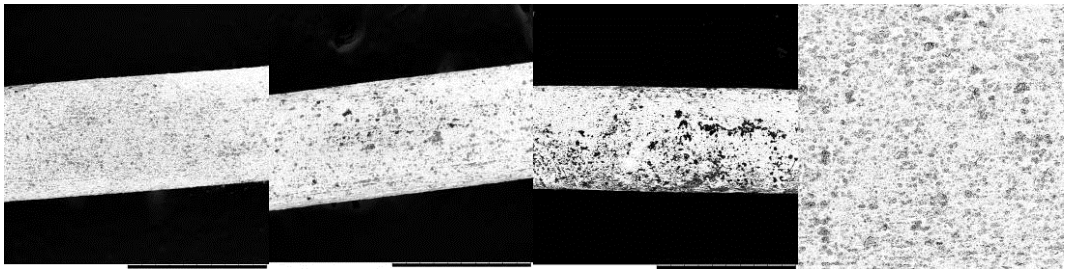
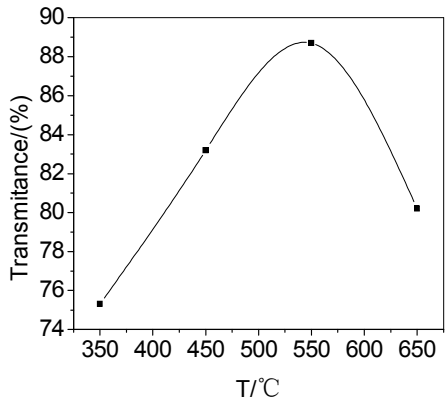


Fig.4(a) Fig.4(b) Fig.4(c) Fig.5

Fig.4 SEM of the thin film annealed at (a) 550˚C for 3h; (b) 550˚C for 4h; and (c) 550˚C for 5h
Fig.5 SEM image of the thin film annealed at 550˚C for 3h

The Relationship of the Transmittance and Annealing Temperature of the Thin Film

It can be seen from Fig.6 that the transmittance of the thin film trend to increase firstly and then reduce as the increasing of the annealing temperature. The reason is mainly that in the initial stage, as the annealing temperature arises, the dense of the film increases, the thickness becomes thinner and the surface roughness decrease, so the transmittance enhanced. However, when the temperature is too high, the surface roughness becomes reverse bigger to make light scattering strengthen, leading to the reducing transmittance.



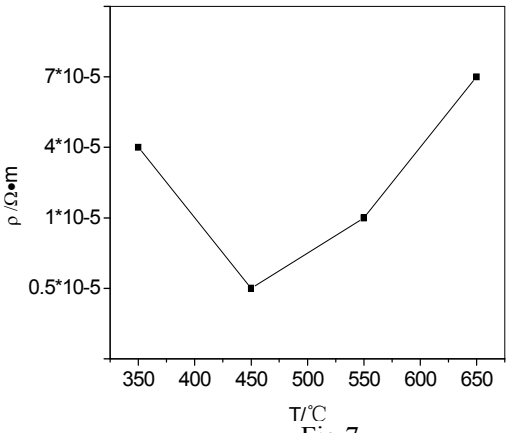


Fig.6 Fig.7

Fig.6 The transmittance versus the annealing temperature of the thin film
Fig.7 The relationship between resistivity versus annealing temperature of the thin film

The Relationship Between Resistivity and the Annealing Temperature of the Thin Film

It can be seen from Fig.7 that the resistivity trend to firstly drop and then increase as the increasing of the annealing temperature. This may be the effect of the grain size of the film. The resistivity of the thin film depends on the grain size. The bigger the grain size is, the larger the resistivity is. However, the two high temperatures will promote the more intense lattice vibrations, which will form the defects of the lattice to finally make the resistivity increase.

Conclusion

The stability of the Sol prepared by Sol-gel with solvent and material of $SnCl_4 \cdot 5H_2O$ is very well. Moreover, the operation and the equipment are both simple, at the same time the same time .The parameters are easy to control.

The factors of the performance of the SnO_2 thin film is complicated, including the initial concentration, the rate of the stirring, the temperature of the reaction, the aged time, the time of the drying and the temperature and time of the annealing etc. In this paper, the effect of the different annealing temperature and time on the grain size, transmittance and resistivity of the thin film were studied.

The effects of the different annealing temperature and time on the grain size of the thin film are analyzed by using the technology of XRD and SEM. At the same time, the effects of the annealing temperature on the transmittance and resistivity of the thin time are also discussed. The results showed that: the grain size of the thin film can increase as the rising of the annealing temperature. So do the temperature time. But when the time is too long, the structure of the thin film will be destructed to make the black spots formed on the surface of the thin film. The best annealing temperature and time are 550˚Cand 3h respectively. The transmittance of the thin film trends to firstly increase and then decrease as the rising of the annealing temperature, while the resistivity trends to firstly drop and then increase.

References

[1] Nakada T., Kume T., Mise T., Kunioka A: Japan Journal of Applied Physics, 1998.
[2] Ramanathan K., Contreras MA., Perkins CL., Asher S, Hasoon FS, Keane J, Young D, Romero M, Metzger W., Noufi R.,Ward J., Duda A:Progress in Photovoltaics Research and Applications, 2003, 11: 225-230.
[3] Xu, L., Wang, R., Liu, Y., Dong, L. A. Chinese Physics Letters, 28.
[4] Mathew X., Thompson GW., Singh VP., McClure JC., Velumani S., Mathews NR., Sebastian PJ:Solar Energy Materials and Solar Cells, 2003, 76(3): 293-303.
[5] X.Lin.,W.Zheng.,Y.Lin: Journal of functional materials, 1993, 24(5): 412-415.
[6] Xu, L., R. Wang., Y. Liu., et al:Chinese Science Bulletin 56(15): 1535-1538.
[7] Javier F., Michael L.,Sarkis H.J.Mater:Chem., 1997, 7(8): 1421-1427.
[8] Ansari SG., Gosavi SW., Gaugal SA:Materials in Electronics,1997,8: 23-27.
[9] Cricenti A.,Generosi R.,Scarselli MA:J.Vac.Sci.Technol.,B, 1996, 14(2): 1527-1530.
[10] Lehan P., Appl.Opt.,1996,35: 5048.
[11] Q.Pan., J.Zhang., X.Dong., Z.Cheng., L.Shi:Bulletin of the Chinese Ceramic Society, 2001, 1: 6-9.

© (2011) Trans Tech Publications, Switzerland
doi:10.4028/www.scientific.net/AMR.331.198

Weave Structures Effect on the Shear Deformation of Annular Shaped Woven Fabrics

Hechun Chen[1, a], Xingfeng Guo[2,b]

[1] Nantong Textile Vocational Technology College, Nantong, 226007,

[2] Tianjin Polytechnic University, Tianjin, 300160

[a]yacht_103@163.com, [b]xfguo@tjpu.edu.cn

Keywords: Shear Deformation, Annular Shaped Woven Fabrics, Weave Structures.

Abstract. The annular woven shaped fabrics are woven on ordinary weaving frames, and equally distributed long and short wefts in the fabric, which can make the whole fabric has equal weft density. Though the fabric is woven on ordinary weaving frame, the batch roller is cone frustum, not cylinder. When batching the annular shaped woven fabric, the share deformation happens. In this paper, adopted plain weave and twill weave to weave the shaped fabric, and contrast the shear deformation between the two weaves. The result shows that the woven fabric with twill weave is softer, and easy to reach deformation balance in the process of weaving, so the woven fabrics with twill weave have more equal weft density and more flatten.

Introduction

The shape weaving process is the development of the traditional weaving technology [1]. It can manufacture the monolayer fabric according to preform contour shape and using abnormity batch roller**.** The produced fabrics are curve or annular structure in accordance with the shape requirement of composite products [2]. The preform is interlaced by two sets of yarns, that is, weft and warp yarns at different length. When used in composite manufacturing, the preform can be wound or laminated to form the composite shape just by needed layers of preform fabric, which makes the composite forming process much easier.

In the weaving process, there are longer warps at big radius of pick-up roll and shorter warps at the small radius, because of the non-cylinder pick-up roll (such as taper). In another word, the warps velocity at big radius is faster than at small radius. Therefore, the interweaving of warps and wefts will be no longer vertical, but will appear different degree shear deformation along with take-up.

Plain and twill structure are chosen, and taper pick-up roll is adopted to weave annular preform. Record the weft shear deformation angle in the weaving process and contrast the shear deformation between the plain and twill.

Materials and Methods

A. The weaving principle of preform

The preform is interlaced by two sets of yarns, that is, weft and warps, the weaving principle sketch as shown in Fig.1[3]. Warps should be drawn from special yarn shelf, and be rounded guide roller, then entered traditional cloth fell. Each warp matched along with individual cone to meet the different needed warp length. The shape of the batch roller determines the curved fabric's 3D shape.

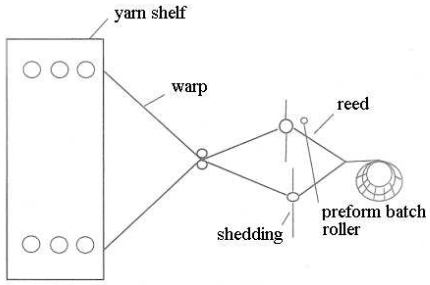


Fig.1 The sketch of shape weaving process

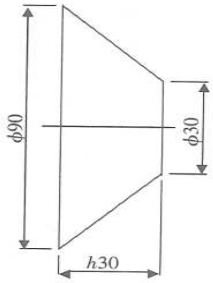


Fig.2 The structure sketch of preform's batch roller (taper)

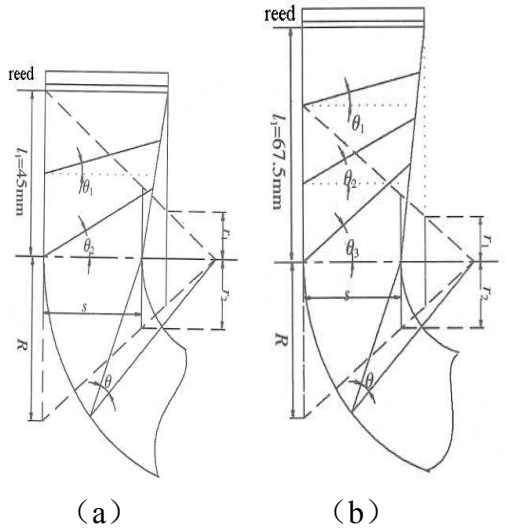
The annular preform's btach roller is a cone frustum when weaving the perform shaped fabric, as shown in Fig.2. (A unit is mm) The parameters of the cone frustum are: $R = 45mm, r_1 = 15mm, \beta = 45°$. Where R is the bottom radius, r_1 is the top radius, and β is the basilar angle of the cone frustum.

B. The weaving parameters of annular shaped fabric

The width of fabric should be equal to generatrix length of batch roller, that is, the fabric width is 42.4mm. Fabric's warp number is 22, and reed width is 44mm, the warp density is 50 ends/10cm. Two weaving structure were selected to weave annular fabric, one is plain, the other is twill.

C. The shear deformation of annular fabric

l_1 is supposed the distance between fell and pick-up start line. The pick-up start line is weft position which weft was completely involved in batch roller. In this experiment, there are two weaving situation, the first is $l_1 = R = 45mm$, the second is $l_1 = 3R/2 = 67.5mm$. Meanwhile, the plain and twill were selected to weave fabric at different l_1.



（a） （b）

Fig 3 (a) Fabric weaving sketch and when $l_1 = 45mm$, (b) Fabric weaving sketch and when $l_1 = 67.5mm$.

In Fig 3(a), θ_1 is shear angle when first point of weft away to the reed is 22.5mm, θ_2 is shear angle when first point of weft away to the reed is 45mm, θ is shear angle when wefts were completely picked-up into batch roller, S is the fabric width of the shape woven on weaving looms.

In Fig 3(b), θ_1 is shear angle when first point of weft away to the reed is 22.5mm, θ_2 is shear angle when first point of weft away to the reed is 45mm, θ_3 is shear angle when first point of weft away to the reed is 67.5mm, θ is shear angle when wefts were completely picked-up into batch roller, s is the fabric width of the shape woven on weaving looms.

RESULTS AND DISCUSSION

TABLE 1, The summary statement of the perform fabric on weaving loom

Values / Content		Plain Weave		Twill Weave	
		Avg. of 15 measurement	CV%	Avg. of 15 measurement	CV%
45*mm*	θ_1(°)	16.6	3.05	19.4	6.69
	θ_2(°)	27.3	4.52	30.7	3.79
	θ(°)	34.2	4.31	33.7	2.90
	$S(mm)$	37.1	4.49	36.3	2.25
67.5*mm*	θ_1(°)	13.5	9.64	15.5	8.75
	θ_2(°)	22.0	9.25	23.5	7.35
	θ_3(°)	30.4	6.19	31.4	4.63
	θ(°)	40.3	3.34	39.6	2.99
	$S(mm)$	32.9	1.95	33.7	2.37

From the table 1, when $l_1 = 45mm$, and take plain weave, $\theta_{1p,45mm}$ is 16.6 degree, $\theta_{2p,45mm}$ is 27.3 degree, $\theta_{p,45mm}$ is 34.2 degree, $s_{p,45mm}$ is 37.1mm($\theta_{1p,45mm}$, $\theta_{2p,45mm}$, $\theta_{p,45mm}$, $s_{p,45mm}$ respectively indicate $\theta_1, \theta_2, \theta, S$ when take Plain weave and at $l_1 = 45mm$); when adopt twill, $\theta_{1t,45mm}$ is 19.4°, $\theta_{2t,45mm}$ is 30.7°, $\theta_{t,45mm}$ is 34.2°, $S_{t,45mm}$ is 36.3mm($\theta_{1t,45mm}$, $\theta_{2t,45mm}$, $\theta_{t,45mm}$, $S_{t,45mm}$ respectively indicate θ_1, θ_2, θ, S when take Twill weave and $l_1 = 45mm$); the results are $\theta_{1p,45mm} < \theta_{1t,45mm}, \theta_{2p,45mm} < \theta_{2t,45mm}$, and $\theta_{p,45mm} \approx \theta_{t,45mm}$.

When $l_1 = 3R/2 = 67.5mm$ and take plain weave, $\theta_{1p,67.5mm}$ is 13.5°, $\theta_{2p,67.5mm}$ is 22.0°, $\theta_{3p,67.5mm}$ is 30.4°, $\theta_{p,67.5mm}$ is 40.3°, $S_{p,67.5mm}$ is 32.9mm($\theta_{1p,67.5mm}$, $\theta_{2p,67.5mm}$, $\theta_{3p,67.5mm}$, $\theta_{p,67.5mm}$, $S_{p,67.5mm}$ respectively indicate θ_1, θ_2, θ_3, θ, S when take Plain weave and at $l_1 = 3R/2 = 67.5mm$); When $l_1 = 3R/2 = 67.5mm$ and take twill weave, $\theta_{1t,67.5mm}$ is 15.5°, $\theta_{2t,67.5mm}$ is 23.5°, $\theta_{3t,67.5mm}$ is 31.4°, $\theta_{t,67.5mm}$ is 39.6°, $S_{t,67.5mm}$ is 33.7mm ($\theta_{1t,67.5mm}$, $\theta_{2t,67.5mm}$, $\theta_{3t,67.5mm}$, $\theta_{t,67.5mm}$, $S_{t,67.5mm}$ respectively indicate θ_1, θ_2, θ_3, θ, S when take Twill weave and at $l_1 = 3R/2 = 67.5mm$); the results are $\theta_{1p,67.5mm} < \theta_{1t,67.5mm}$, $\theta_{2p,67.5mm} < \theta_{2t,67.5mm}$, $\theta_{3p,67.5mm} < \theta_{3t,67.5mm}$, $\theta_{p,67.5mm} \approx \theta_{t,67.5mm}$, and $\theta_{1t,67.5mm} - \theta_{1p,67.5mm} = 2.0 > \theta_{2t,67.5mm} - \theta_{2p,67.5mm} = 1.5 > \theta_{3t,67.5mm} - \theta_{3p,67.5mm} = 1.0 > \left|\theta_{t,67.5mm} - \theta_{p,67.5mm}\right| = 0.7$

CONCLUSIONS

Seen form the table 1, if take plain weave, the degree of weft deformation is less than twill at initial stage. But when weft is closed to pick-up start line, the difference of deformation angle is less and less. That means, the weft of plain fabric is constrained by weave structure, there is little weft deformation at first, but finally, it will reach equilibrium deformation since shear force grow. The weft of twill fabric is liable to deform when subjected shear force. Because twill fabric structure is loose, and there is little resistance among wefts. Twill fabric surface evenness and uniformity of the weft density is better than plain fabric, meanwhile, there is better mould effect. So when weaving annular shaped fabrics, twill is the better choice.

REFERENCES

[1] Huang g., "Modern Textile Composites[M]", China Textile & Apparel Press, 2001, 90-91.

[2] Guo X.F., Liu C.Y, Wang R., "Weaving Principle and Design of Annular Shaped Woven Fabrics [J]", *Textile Journal*, 2006.27(1), 12-15.

[3] Peng S.J., Guo X.F., Chen H.C., "Design and Weaving of Annular Cloth[J]", *Journal of Tianjin Polytechnic University*, 2005,22(4),18-20.

© (2011) Trans Tech Publications, Switzerland
doi:10.4028/www.scientific.net/AMR.331.202

Weaving 3D Fabric With a "中" Shaped Cross-Section

Yutao Chang[1,a] , Xiaoming Qian[1,b], Haiwen Liu[2] , Huawu Liu[1]

[1]Key Laboratory of Advanced Textile Composites, School of Textiles, Tianjin Polytechnic University, Tianjin, 300160, China

[2] School of Textiles ,Hebei Science and Technolgy University, Shijiazhuang,,China

[a]icerainzz@163.com, [b]qxm@tjpu.edu.cn

Keywords: 3D woven fabrics, weaving methods, "中" shaped cross section.

Abstract: 3D woven fabric significantly improves the mechanical properties, especially the strength resulting from the between layers connections of yarns Hence, 3D woven fabrics have been widely used as reinforcing material in prefabricated composites, A particular 3D woven fabric with "中" shaped cross section was developed in this study .The fabric was made in a plane loom weaving machine. The designing procedure and processing methods are given in details.

Introduction

Prefabricated composite enhanced by 3D woven fabrics is a cutting-edge material , for high performance components[1]. The composites reinforced by 2D fabrics is weak when subjected to shear stresses from many directions. In such cases, 3D fabrics are ideal replacements to overcome these shear stresses, because the planar layers are interlaced by the yarns and hard to be torn apart.

3D fabrics could be made by weaving, knitting, nonwoven and braiding methods. Among these methods, 3D woven fabric is distinguished by its high structural strength, pattern stability, and versatility of structural organizations[2]. In this study, a particular 3D fabric with "中" shaped cross section was developed using weaving method and the processing methods are described in details.

Weaving 3D fabric with a "中" Shaped Cross Section

The method for weaving the 3D fabric with " 中 " shaped cross section is called flattening-unfolding[3]. Firstly, we flatted the 3D structure into a planar organization, in order to weave it in a loom for 2D fabrics. Secondly, we divided fabric into several regions according to the flatten structure. Then, a suitable picking route was chosen to ensure that these layers could be integrated into one piece afterwards. At last, a looming draft was designed following the picking route. In this way, a thin fabric was made with interlaced layers, which may be unfolded into 3D fabric[4].

The design of looming draft for the 3D fabric with a "中" shaped cross section

Firstly, we flatted the "中" shaped cross section and divided it into five zones, including a1, a2, a3, a4, a5 (Fig.1). In a1, a2, a3, a4, a5, there were one, three, three, three and one layers of the fabric, respectively the line-segments in Fig.1 from left to right were denoted by S1, S2….S11, progressively. In this draft, we may find that S2, S5 and S8 represent the upper layers, S3, S6, S9 represent the middle layers, S4, S7, S10 represent the lower layers. On the basis of Fig.1, we drawn the picking route shown in Fig.2, under the condition that two weft yarns should be inserted in each layer. In Fig.2, P1, P2, P3, P4, P5 and P6 denote the 1^{st}, 2^{nd},3^{rd}, 4^{th},5^{th} and 6^{th} inserted weft yarn. Similarly, P6 denoted the sixth inserted weft yarns, progressively. The arrows in Fig.2 denote the direction of picking. Every six pickings makes a recurrent. During weaving, the picking route

followed the design shown in Fig.2. The first picking P1 passes through five zones, the second picking P2 passes through four zones, including a2, a3, a4 and a5， the P3, P4, P5 pass through a2, a3 and a4, P6 passes through a1, a2, a3 and a4.

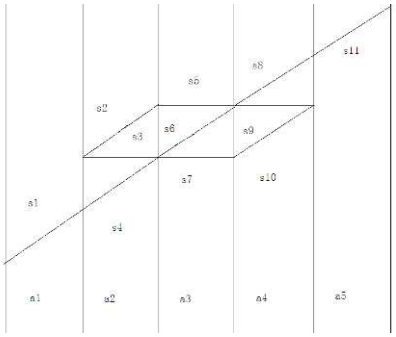


Fig. 1. The flatted structure.

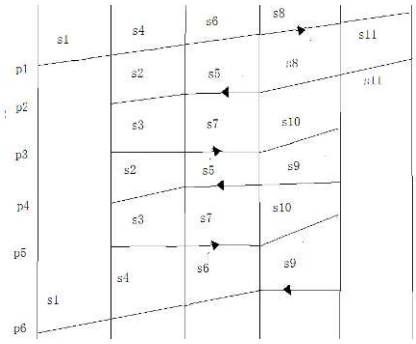


Fig. 2. The design of picking route.

As shown in figure 1 and figure 2, there are 5 zones and 11 layers in the looming draft. Using plain weaving method, each layer needs two warp yarns and 22 warp yarns in each recurring are required for 11 layers. As stated above, the first picking passes through five zones, including S1, S4, S6, S8 and S11.

There is only one layer S1 in a1 zone, so no specific attention is required. In a2 zone, the warp yarns of the first and second layers must be lifted up to ensure that only the warp yarns in the third layer interlace with the inserted weft yarns. S6 is in the middle layer of a3 zone ,thus the upper and lower layers should be pushed apart to ensure the inserted weft yarns only interlace with warp yarns in the middle layer. In a4 zone, we needed to weave S8 which was in the surface, so we must press the second and third layers down to make sure only first layer of warps interlaced with inserted weft, in a5 zone, there was only one layer-S11, just like a1 zone. Following the discussion above, we could draw a weave diagram shown in Fig.3, Figure 4 is the corresponding intersection chart in cross-section.

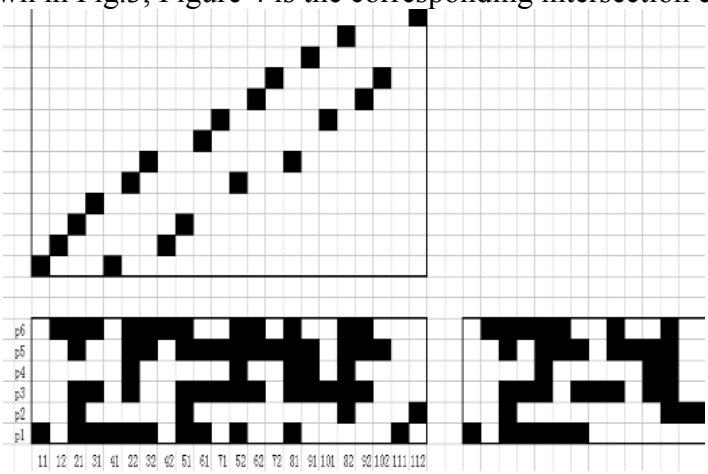


Fig. 3. Looming draft of the 3D fabric.

The organization of this fabric is fairly complex and part of the warp yarns move through the same path. The warp yarns moving in the same path were healded in the same harness eye, following the harness draft shown in Fig.3. In the harness draft shown in the upper side of Fig.3, the first and fifth warp yarns were designed to enter the first heddle, the second and the eighth warp yarns were expected to enter the second heddle and so on. Totally, thirteen heddles are required for weaving this fabric.

The right part of Fig.3 is called chain draft. We match each yarn with one reed, since the yarns used in this study were coarse yarns with large diameter. In a1, a2, a3, a4, a5, the reeds ratio was 1:3:3:3:1, determined by the corresponding fabric layer in these zones.

Weaving process

There were four steps to weave this 3D fabric in conventional loom including warping, threading heddle, reeding, and weaving [5].

In warping step ,the number of warp yarns were determined by the fabric width , incorporating the damage of yarns during processing .In this warping process ,400 warp yarns were taken ,around 30-yarn each in eleven layers .

In threading heddle step, six heddle sheets were needed according to the looming draft shown in Fig. 3. In a1 zone, we needed two heddles, donated as 1 and 2. In a2 zone, the six heddles were named as 3, 4, 1, 5, 6 and 2. In a3 zone, the six heddles were 3, 7, 8, 5, 9 and 10. In a4 zone, we also used six pieces of heddles, including 5, 11, 8, 12, 9 and 10. In a5 zone, the heddles were 1 and 13. There were 15 repeats in each zone.

In reeding step, 40 reeds were used in this study. The number of reeds in each zone should be proportional to the number of fabric layers within the zone. Therefore, the reeds used in a1, a2 ,a3 , a4 and a5 zones were 1, 3, 3, 3 and 1, progressively.

In weaving step, the flat fabric was completed and unfolded into 3D form as shown in Fig.5.

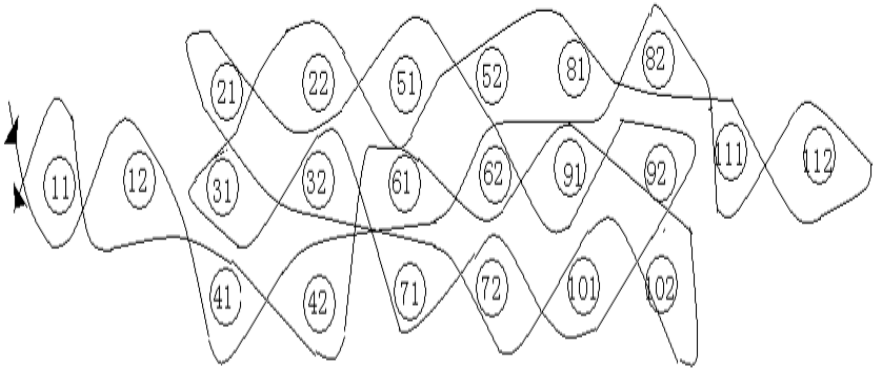


Fig. 4 The cross section chart

Conclusion

Compared with other methods for 3D fabrics, the flattening-unfolding method adopted in this study has great advantages in terms of high structural strength, pattern stability, and versatility of structural

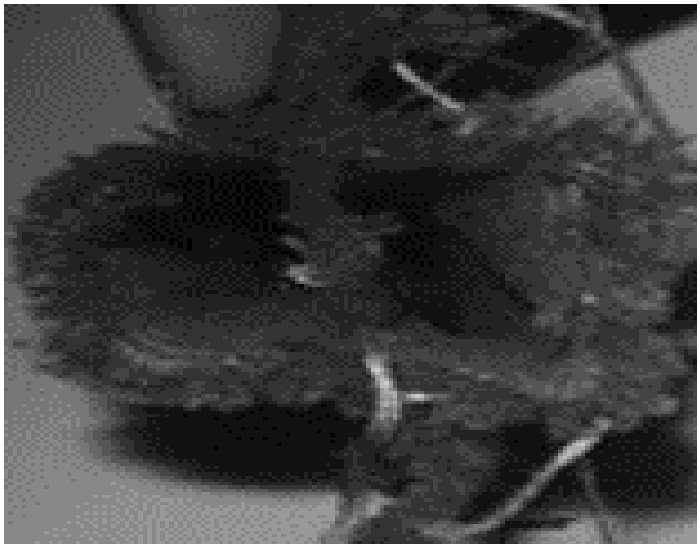


Fig. 5 A sample fabric with “中” shaped cross section.

organizations. A 3D fabric with “中” shaped cross section was developed in this study, which may provide strong reinforcement for prefabricated composites [6].

Acknowledgements

I am grateful to school of textile in Tianjin Polytechnic University and thank for my teachers' support in Hebei Science and Technology University

References

[1] X. Chen: Textile Research J., 73(5): 375-380. (2003)

[2] J. A. Soden and B. J. Hill: Elsevier Science Ltd J., 29(8): 757-762. (1998）

[3] H. Liu and J. Gu: Technical Textiles J., 29(2): 5-7. (2011)

[4] H. Liu and J. Guo: Cotton Textile Technology J., 33(2): 15-17. (2005)

[5] P. Gu: Journal of Textile Research J., 23(5): 24-26. (2002)

[6] X.Yan: Technical Textiles J., 9(2): 8-12. (2003)

© (2011) Trans Tech Publications, Switzerland
doi:10.4028/www.scientific.net/AMR.331.206

Manufacture of Composite Nanofiber Mats with Fiber Diameters Grads by Electrospinning for Filtration Use

Shasha Guo [1, a], XiangYu Jin[1, b], Hong Wang [1], Qinfei Ke [1*, c]

[1]College of Textiles, Donghua University, Shanghai, 201620, P.R.China

[a]guoss1986@163.com;[b] nwcen@dhu.edu.cn;[c] kqf@dhu.edu.cn

Keywords: Electrospinning; Meltblown; Nanofiber; PET

Abstract: The objective of this study is to prepare a filtration material with fiber diameter grade by electrospinning technique using meltblown nonwovens as collecting materials. The average fiber diameter of PET electrospinning in the top layer was 309.60nm and PET meltblown nonwoven in the bottom layer was 1.82um respectively. And this structure leads to the average pore size of electrospinning-meltblown composite material was 0.73um while it is up to 5.36um for the PET meltblown nonwoven. This design is especially good for high accurate filtration such as cells filtration, hydronium filtration.

Introduction

In decades, electrospinning technique has received considerable interest due to its ability to produce nanofibrous mats which is much thinner than meltblown nonwovens[1-3]. It has been proved that nanofiber material has many advantages for filtration such as low-flux and high filtration efficiency due to its highly interconnected pore structure and high surface area to volume ratio. At the same time, it is well-known that electrospinning mats have a lot of disadvantages such as lower output, lower strength which reduce the chance of its application. In addition, meltblown nonwovens are wildly used as filtration material which has mature manufacture technique and equipments; its fiber diameter is only 1-10 um. Consider the above situation, a composite with both electrospinning and meltblowm material can make full use of their good properties and solve the problems of electrospinning material in practical application. The aim of this study was to prepare a composite material by electrospinning using meltblown nonwovens as collecting materials.

The material in this study is PET. PET is widely used as fibers, films etc. for its excellent characteristics such as outstanding processability, nice mechanical properties and low cost.

Materials and methods

2.1 Materials

PET pellets used to produce electrospinning nanofiber mat were purchased from Sinopec Yizheng Chemical Fibre Company Limited. Trifluoracetic acid (TFA) and dichioromethane (DCM) of analytical grade from Sinopharm Chemical Reagent CO., LTD were used as solvents.

2.2 Electrospinning of nanofiber mats

The research of PET electrospinning has been reported [4-6]. In this research, PET was dissolved in a 50/50 v/v mixture of TFA and DCM. The experimental conditions were: flow rate 0.8 ml/h, voltage 15-30KV, distance between the tip and collector 13cm, the concentration of polymer solution 20-30% w/v. The nanofibers were deposited on PET meltblown nonwoven mats. The electrospinning-melt composite samples were dried under a vacuum 20℃ for 24h.

2.3 Characterization

The morphology of nanofibrous electrospinning-melt composite mats were observed by the Scanning Electron Microscope (JSM-5600, JEOL Co.,Ltd, Japan), the obtained SEM picture has consequently used for the fiber diameter analysis.

The pore sizes and their distribution were tested by the method of Bubble-Point using Capillary Flow Porometer (CFP-1100-Al, PMI, USA). The method was based on the measurement of pressure necessary to blow air through a liquid-filled material. The relationship between pore size and the corresponding pressure is shown as follow [7]:

$$D = \frac{4\gamma \cos\theta}{\Delta P} \quad (1)$$

Where D is the diameter of pore; γ is the surface tension of the wetting agent and θis the contact angle; ΔP is the differential pressure.

Results and discussion

In this study, PET electrospinning were successfully obtained onto PET meltblown. The spinnable range of PET solution concentration for electrospinning is about 20-30 wt%. According to the experiments, the optimal condition for electrospinning was: flow rate 0.8 ml/h, voltage 25 kV, distance between the tip and collector 13cm, the concentration of polymer solution 25% w/v, and its SEM image can be seen in Fig.1 (a). Fig.1 (b) was the SEM image of PET meltblown used as collecting materials. From Fig.1(a) it can be seen clearly the fiber in the top layer is much thiner than that in the bottom layer which is PET meltblown nonwovens.

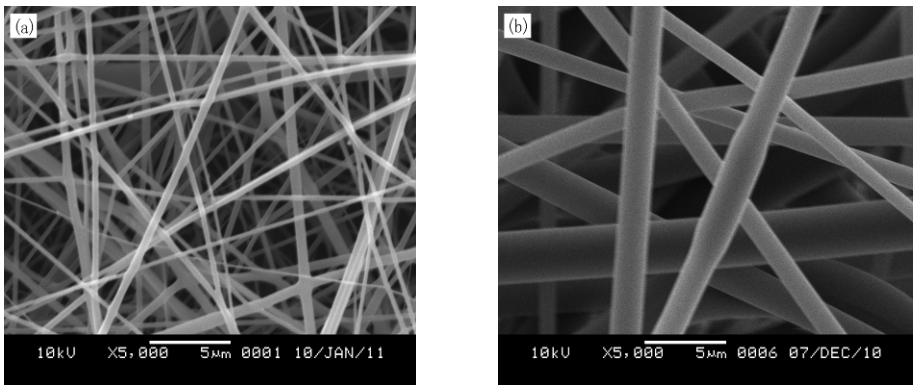


Fig.1 SEM images: (a) PET electropinning-meltblown composite material; (b) PET meltblown

3.1 Fiber diameter

The average fiber diameter and distribution of fiber diameter can be obtained using Image J which is a software for image analysis. The average fiber diameter of 25wt % PET electrospinning was 309.6nm while it was 1.822um for PET meltblown materials. The distribution of fiber diameters was shown in Fig.2 (a) and Fig 2(b) respectively. It was clear that the fiber of PET electrospinning was much thinner than that made by meltblown technology which made the material possess with great properties for filter such as high surface area to volume ratio, high porosity. The smaller the fiber diameter was, the stronger of filtration and adhesive functions were, due to the increasing of the surface tension of fiber in filtration material.

In this way, the combination of fibers in nanometer grade and micron grade formed a material with grads in fiber diameter which was especially good for filtration to get high filtration efficiency.

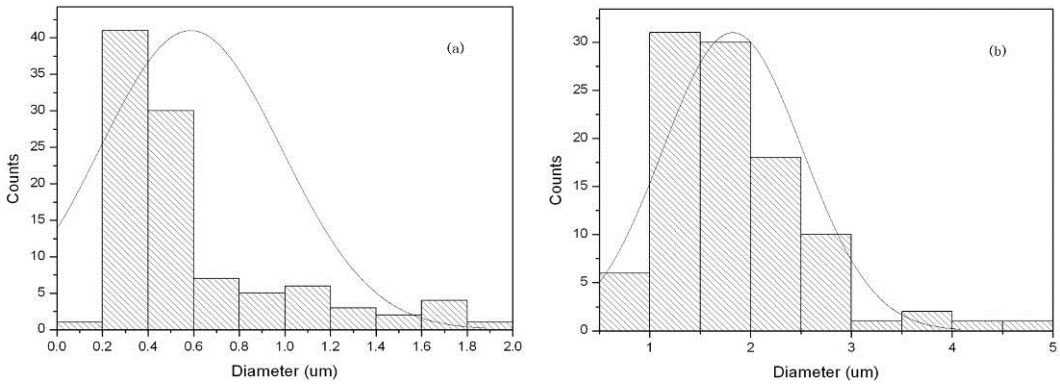


Fig.2 The distribution of fiber diameters: (a) PET electropinning; (b) PET meltblown

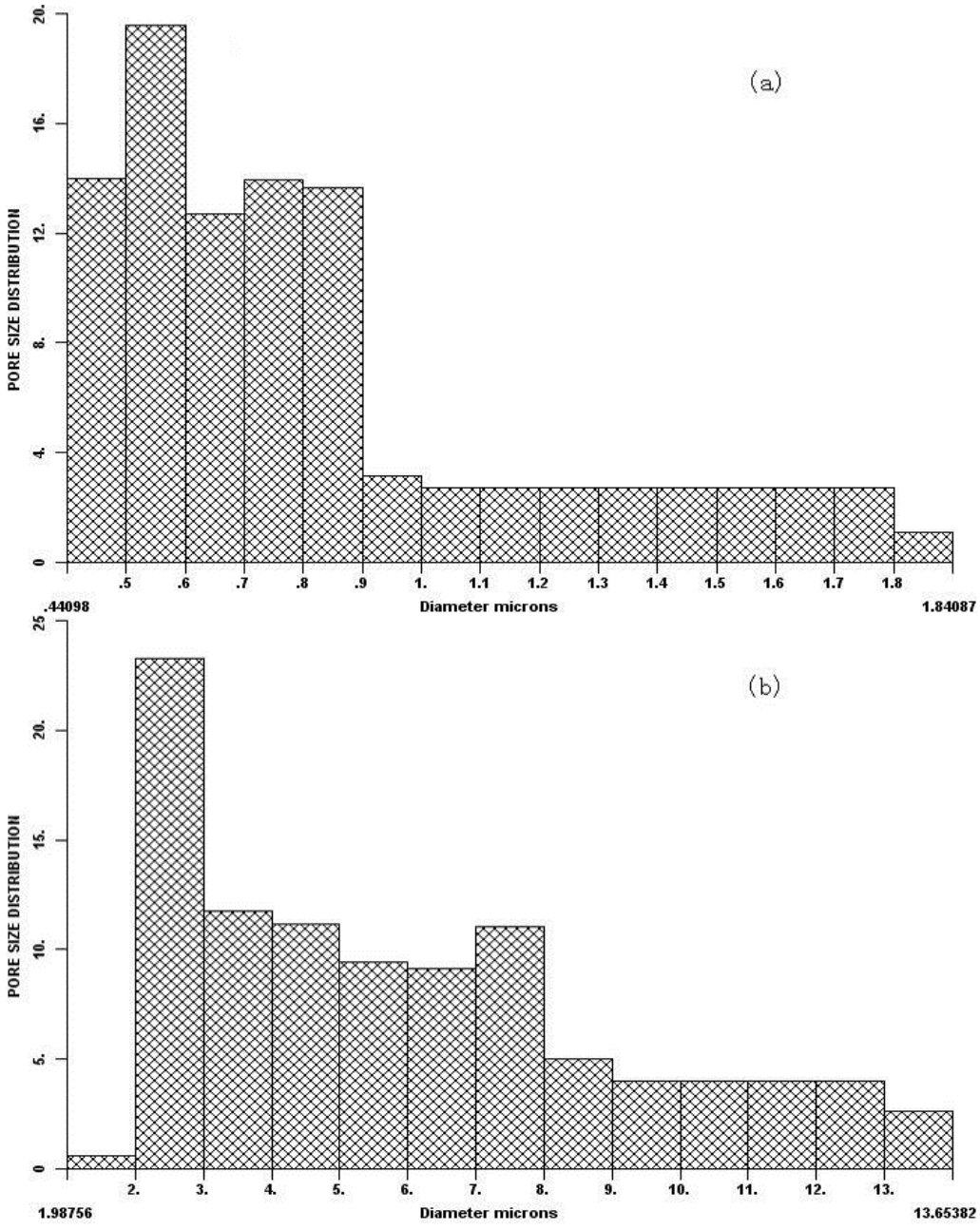


Fig.3 The pore distribution histogram & diameters: (a) PET meltblown-electropinning composite material; (b) PET meltblown

3.2 Pore size of filtration materials

It is known that pore size is the key parameter of filtration material. The smaller the pore size is the bigger of sieving function is. In Fig.3, the pore distribution histogram & diameters of PET electrospinning-meltblown composite material and meltblown material were shown in (a) and (b) respectively. The conclusion could be got that the pore size of PET electrospinng-meltblown was mainly below 0.90um. But the pore size of PET meltblown was mostly around 2.00um-8.00um. The mean pore size and bubble pore size can be seen in table 1.

Table 1 The mean pore size and bubble pore size of two kinds of filtration materials

Num	Mean pore size [um]	Bubble pore size[um]
PET meltblown	5.361	13.654
PET electrospinning-meltblown	0.726	1.841

As the development of filtration industry, it is hoped that some smaller particles or even bacteria can be removed by filtration method. But it is difficult to achieve by only using meltblown nonwovens for its pore size is mainly about 1-10 um. This design greatly reduces the pore size of nonwoven filtration materials which made it possible for the removal of the above particles.

Conclusions

The electrospinning-meltblown composite nanofibrous mats were got by electrospinning PET using PET meltblown nonwovens as collection material. The combine of them formed a material with different fiber diameter which was especially good for filtration. PET meltblown nonwovens make sure that the flux went through the filtration material with low resistant and PET electrospinning material with nanograde fibers can capture the smaller size of particles further which passed PET meltblown. All in all, electrospinning-meltblown composite nanofibrous mats means significant for the development of filtration materials.

Acknowledgment

Financial support of this study was supported by the Government of P. R. China, 111 Project B07024 “Biomedical Textile Materials Science and Technology”.

References

[1]. Xiao-Hong Qin, Shan-Yuan Wang. Filtration Properties of Electrospinning Nanofibers. Journal of Applied Polymer Science. 2006:102(2): 1285-1290.

[2]. Kitai Kim, Changhwan Lee, Won Kim, et al. Performance modification of a melt-blown filter medium via an additional nano-web layer prepared by electrospinning.2009:10(1):60-64.

[3]. Yimin Sang, Fasheng Li, Qingbao Gu ,et al. Heavy metal-contaminated groundwater treatment by a novel nanofiber membrane. Desalination. 2008: 223: 349-360.

[4]. Renuga Gopal, Satinderpal Kaur, Zuwei Ma, et al. Electrospun nanofibrous filtration membrane. Journal of Membrane Science. 2006.281:581-586

[5]. Beatriz Veleirinho, Manuel F. REI, J. A. Lopes-Da-Silval. Solvent and Concentration Effects on the Properties of Electrospun Poly(ethylene terephthalate) Nanofiber Mats. Journal of Polymer Science: Part B: Polymer Physics, 2008,10:460-471

[6]. Kwan Woo Kim, Keun Hyung Lee1, Myung Seob Khil.et al. The Effect of Molecular Weight and the Linear Velocity of Drum Surface on the Properties of Electrospun Poly(ethylene terephthalate) Nonwovens, Fibers and Polymers,2004,5(2):122-127.

[7]. Beatriz Veleirinho, J.A.Lopes-da-Silva. Application of electrospun poly(ethylene terephthalate) nanofiber mat to apple juice clarification. Process Biochemistry. 2009.44:353-356.

© (2011) Trans Tech Publications, Switzerland
doi:10.4028/www.scientific.net/AMR.331.210

Study on the Tensile Properties of the High-performance Cored Rope

Qianjuan Zhao[1,2,a] and Ya'nan Jiao[1,2,b]

[1]Composite Materials Research Institute, Tianjin Polytechnic University, Tianjin, 300160, China

[2]Tianjin and Ministry of Education Key Laboratory of Advanced Composites, Tianjin polytechnic University, Tianjin, 300160, China

[a]zhaoqianjuan@126.com, [b]jiaoyn@tjpu.edu.cn

Keywords: 2-D Braiding, Cored Rope, Kevlar-49, Tensile Property.

Abstract. The tensile property of two-dimensional (2-D) braided cored ropes with high-performance is investigated and found that braiding angle has an evident fluence on the tensile characteristic. In the skin-core structure, the core yarns are straight and parallel with each other, and have a larger percentage than those in other style of cored rope. The tensile strength and breaking elongation of the samples with different braiding angle is tested by Shimadzu universal testing machine. The load-displacement curves of the rope are drawn and analyzed. It shows that of the tensile fracture mechanism is different from the other structural ropes, and the straight state of the core yarns leads to higher utilization of fiber strength. The results also indicate that braiding angle has a great influence on the strength and breaking elongation of cored rope. In the five samples, the sample with 30°has the both ideal tensile strength and ideal elongation. Beyond the angle, the greater braiding angle is, the much more closely the core yarns are wrapped. The greater friction between fibers of core yarn decreased motion of the fiber in core yarn, some of them was fractured before all the yarns were straighten. The utilization of the braiding yarn fiber strength decreased.

Introduction

In recent years, the ropes with high-strength, high-modulus, light-weight and flexible has been widely used in engineering filed. Case where synthetic-fiber ropes have replaced steel wire ropes are used of ropes for supporting cable, lifting equipment and materials at construction sites, ship assist lines, anti-collision and protective nets and mountaineering ropes [1]. The nylon and polyester fiber ropes have a small intensity, low modulus and poor resist vermicular degeneration. When the nylon and polyester fiber ropes suffer a tension, the rope diameter varies greatly. Under a particular application, the high-performance rope is also required deformation resistance. In order to ensure the precision of reflective surface, spatial antenna cable must not deform under a continued tension for a long time [2]. The aramid fiber with high performance, low density and excellent abrasion resistance is used to braid all kinds of rope and suture, such as the fixed rope used in the space antenna [3].

2-D braided cored ropes were composed of braiding yarns and core yarns. Core yarns were straight and parallel with each other. The volume fraction of core yarns can achieve 80%, braiding yarns wrapped core yarns tightly, firmly and evenly [4]. Fiber axial of core yarn is in a line along external force direction, fiber strength utilization improved. Yarn interwoven rule of conventional rope was twisted and braided. When it sustain tension, rope's deformation is great. After fiber was twisted, fiber axial and force direction weren't in one straight line, fiber strength cannot be effectively used.

There are many reports on the braiding parameters while the research on the mechanical properties of 2-D braided core rope is few. M. Sakaguchi et al. presented the method of using 2-D braided skin-core structure to manufacture unidirectional fiber-reinforced thermoplastic composites. Non-braiding yarns can be inserted in the braiding yarns to manufacture glass-fiber/PA 6-Nylon composites [5]. P. Potluri et al has simulated geometrical modeling of a braided structure, and the braiding angles, cover factors and yarn volume fractions can be calculated form modeling [6]. Todd M. Mower has studied on the influence of cyclic loading upon the residual strength of aramid-fiber strength members [7]. Rui Bi et al introduce the working principle of 2-D braiding machine and detail

the 2-D braided core yarn principle [8]. JIAO Ya'nan et al study that 2-D braided glass fiber thread had better breaking tenacity and elongation than the glass tow. The knot performance was mainly influenced by pitch length [9]. Braiding angle is important braiding parameter [10], are directly related wrapped density, braiding tightness, the fiber ratio between braiding yarns and core yarns, braiding efficiency. This paper adopts 2-D braided technology made the Kevlar fiber cored ropes, research on braiding angle impede on tensile properties of rope.

Experimental

Tensile Strength of Kevlar-49 Fiber. The linear density of Kevlar-49 fiber tow from DuPont is 158tex. The tensile property of Kevlar-49 fiber was measured in preparation for the tensile test of ropes. Experimental results were the mean tensile load of Kevlar-49 fiber is set to 212 N, the average of elongation at break is 2.3%.

Specimen Preparation. Sample is made on a 8-carrier braiding machine. The braided samples consisted of two sets of braiding yarns; one was in the clockwise direction and the other in the counterclockwise direction. In the braiding process these two sets of braiding yarns interlaced with each other. The internal core yarns is not interlaced,under a certain tension the core yarns is parallel along the direction of shaping, core yarns was wrapped tightly by braiding yarns, as illustrated in Fig1.

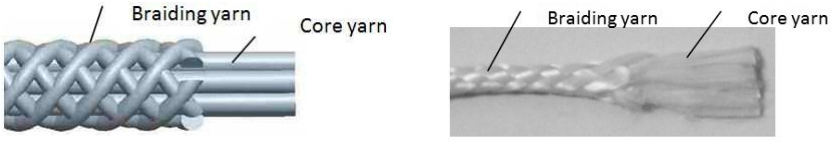


Fig.1 Core rope structure and the photo of sample

In the internal structure of braided cored rope, braiding yarns and core yarns are contacted but not connected. So damage to ropes is a complicated process that could depend on a variety of factors. To study the relationship between braiding angle and axial tensile properties, compare the tensile properties of different braiding angle samples. When other parameters keep constant, the fracture load generally is increased with the increase of linear density of the rope. So this paper presents the different braiding angle samples with the same linear density, parameters show in table 1.Sample 1# and sample 2# is parallel fiber bundles, as compared specimens.

Tab.1 2-D braided cored rope parameters

sample	braiding angle (°)	braiding yarn （tex）	corn yarn （tex）
1#	0	/	3160
2#	0	/	1896
3#	20	1264	1896
4#	30	1264	1896
5#	40	1264	1896

Tensile Test. Tensile tests were conducted on Shimadzu AG-250 KN test machine with GB/T 8834-2006. Sample gap is 500 mm, and tensile speed is set 30 mm/min. Before tensile test starts, exert certain pretension on the sample to ensure core yarn fiber stretched.

Results and Discussion

Fracture Load and Breaking Elongation. Fig 2 showed braiding angles and fracture load curve. The braiding angle of parallel fiber bundles were defined 0°. As shown in the Fig 2, braiding angle has a great influence on the fracture load, and the tensile load of parallel fiber bundles is higher than the braiding specimens. The data indicates that, compare with other sample, the fracture load is slightly higher for the 3# sample with 30° braiding angle.

The results show that parallel fiber bundles is straight and parallel along the axis, and have the maximum utilization of fiber strength. Therefore, the proportion of one-way straight fibers should be increase in the braided structure of high-strength rope, but we must ensure the structure of the rope

stability at first. It has been found that braiding angle becomes larger, the core yarn is wrapped much more tightly and core yarn fiber can be stretched better. But the greater the angle between the braiding yarn and tensile axial is, the worse utilization of the braiding yarn fiber strength is. And braiding angles influence on the softness of the rope. In contrast, when the braiding angle is smaller, the core yarn is wrapped not close enough, the core yarn fibers inside cannot keep well straight, and the core yarn fiber is prone to expose, and structure becomes uneven. Taken together, when braiding angle is 30°, tensile strength is better, structure is uniform, braiding yarn coated the core yarn better.

As shown in Fig 3 the relationship braiding angle and breaking elongation. From the Fig 3, the influence of braiding on elongation is great, the elongation of sample 1# is approximately 2.2%; braiding angle change between 20° - 40°, the elongation at break change little at about 2.4%.Parallel fiber bundles suffer tension at the same time, so the elongation of fiber is shorter.

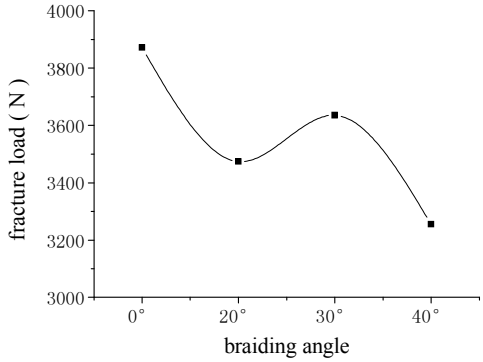


Fig.2 Relationship between braiding angle and fracture load

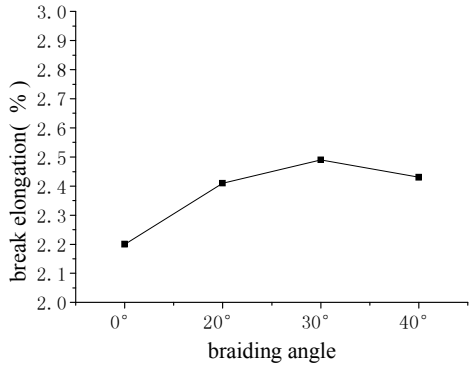


Fig.3 Relationship between braiding angle and breaking elongation

Tensile Processes. From Fig 4, breaking elongation of Kevlar rope is small, the load-displacement curve is a straight line until the break no yield point, so Kevlar rope can be repeatedly used, and there is not residual strain phenomenon. The load-displacement curve of Kevlar rope remained linear, basically load increases with displacement increasing. When the displacement is 6 mm, the fracture load of braiding ropes and 16 fiber bundles is practically the same, but is smaller than 20 fiber bundles. The reason of difference tension between Point A and point C is the tension of braiding yarns consumes. When the tension is 1500 N, the elongation of braiding ropes is much bigger, Due to internal friction between the core yarns fibers and interwoven structure of braiding yarns, the elongation of cored ropes become bigger. The composition of the yarn from a single filament, its property is a superposition of a single filament, but not simple mathematical superposition. The composition also depends on the arrangement of monofilament yarn layers and structure, so to choose 2-D braided cored rope structure; it can significantly increase the fiber strength utilization. During the whole process fiber go through tension - extension - by force - the fracture process, accord with the flexible fabric tensile failure rules.

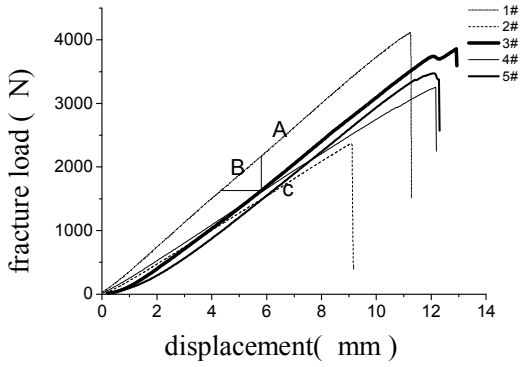
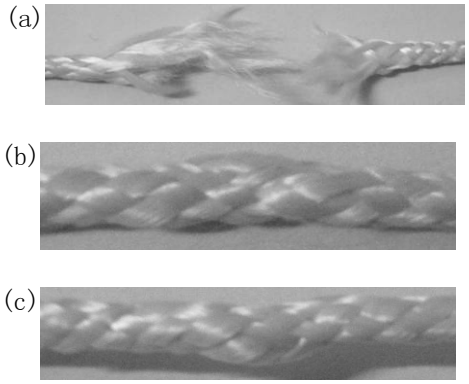


Fig 4 Load - displacement curve

Tensile Failure Modes. Figure 5 shows photos of sample through the axial tensile. From the figure shows, the sample with braiding angle 20° completely broken, the sample with braided angle 30° and 40° is not damaged from the outside. In theory, Core yarns stretched parallel, and bear the tension in the first. The core yarns break; braiding yarns elongated but not severely injured. This conjecture can be verified, mechanical properties of 2-D braided rope depends on the properties of core yarn fiber bundles. Smaller braiding angle is, less friction between the fibers, core yarns is easy to straight, fibers of core yarn can suffer tension at the same time. 2-D braided core rope has good tensile properties along the axial direction.Through the correct choice of braiding parameters, the mechanical properties of fibers can give full play, so the axial tensile properties of yarn increased significantly.



（a）Sample 2#（b）Sample 3#（c）Sample 4#

Fig5 photos of failure pattern

Conclusions

(1) The advantages of 2-D braiding machines are ideally suited for low-cost and high-efficiency producing. And braiders are inexpensive, easily available, and flexible.
(2) Utilization of fiber strength of cored yarns is high in 2-D braided cored rope structure, comparing with the other structure. And damage for the fiber is smaller in the braiding production process.
(3) Braiding angle of cored rope impact on strength greatly, reasonable choice of parameters can improve the cored rope mechanical properties and surface structure.
(4) The mechanical properties of cored rope performance depend mainly on fiber, Kevlar cored rope is a light weight, high strength and modulus than stable performance of flexible rope.

References

[1] LIU Shenghua, WANG Jieliang:Applied Engineering Plastics Vol.6 (2003), p.33.

[2] YU Yan'e, TAN Yanjun:Hi-Tech Fiber&Application Vol.59 (2004), p.37.

[3] CHEN Yifen:Jiangsu Textile Vol.8 (2007), p.40.

[4] LIUJianjun,WANG Yanxiang.WANG Chengguo:Chemical Technology Vol.4 (2002), p.6.

[5] M.Sakaguchi, A.Nakaib,H.Hamada, N.Takeda:Composites Science and Technology Vol.60 (2000), p.717.

[6] P. Potluri,A.Rawal, M.Rivaldi,I.Porat:Composites:Part A Vol.34 (2003), p.481.

[7] Todd M. Mower:International Journal of Fatigue Vol.22 (2000), p.121.

[8] BI Rui, JIANG Yaming, LIU Liangsen:China Textile Leader Vol.2 (2006), p.56.

[9] JIAO Ya'nan , WANG Dongning:Journal of Textile Research Vol.8 (2009), p.21.

[10] DONG Weiguo, HUANG Gu:Journal of Textile Research Vol.2 (2004), p.66.

© (2011) Trans Tech Publications, Switzerland
doi:10.4028/www.scientific.net/AMR.331.214

The Application Study of the Fabric Reconstruction in the Design of Home Textiles

Miao Su

College of Materials and Textiles, Zhejiang Sci-tech University

No.5 Street Two, Xiasha University Town, Hangzhou, Zhejiang Province, China, 3100018

sumiao611@sina.com

Keywords: fabric reconstruction; home textile design; artistic creativity; application

Abstract. Fabric reconstruction is to redesign the artistic effect of fabrics. The paper centers on the materials and design technique of fabric reconstruction in the home textile design, and explores the diversity and artistic effect of fabric reconstruction using the related design practice as evidence in order to provide the reference to the creative design and study of home textiles.

Introduction

As the material of the home textiles, fabric is the basis of the home textile design. Fabric reconstruction is able to display the personality of home textile design and it has become one important standard of creativity capacity in home textile design. It is not simply an adornment. It can embody the level of the technology of the modern home textiles. As the customers are more and more willing to accept the fabric reconstruction, it is of great operation significance and profound influence to explore how to better apply the fabric reconstruction in the home textile design.

The concept of fabric reconstruction in the home textile design

Compared with the once-through design, fabric reconstruction is to apply all kinds of methods to implement the secondary designing on the basis of the attained fabric according to the design need and esthetic need. It can produce more rich visual effect and tactual effect so that give play to the visual beauty of the works to the fullest degree. Fabric reconstruction of home textile design is the secondary designing of the shapes of the fabrics. The application of fabric reconstruction in the home textile design enables the home textiles to display personalities and differences, to cater to the demand of modern customers, to help increase the added value of home textiles and to multiply the brand value [1].

The home textile fabric reconstruction discussed in the paper refers to the action to change the plane fabrics creatively by hand. It changes the features or shapes of fabrics, changes the two-dimensional space into the one that is between two-dimensional space and three-dimensional space, making it have richer visual and textural effect.

The common materials used in the home textile fabric reconstruction

Since textile fabric reconstruction is kind of art of materials, materials carries great meaning to us [2]. At present the common materials in the fabric reconstruction can be classified into dotted materials, linear materials and plane materials according to their shapes.

Dotted materials. The dotted materials in the home textile fabric reconstruction are mainly buttons, paillettes, pearls, small shells, stones, glass and so on. Other kinds of materials in dot shape such as yarn ball, and cloth ball are also included.

Linear materials. The linear materials in the home textile fabric reconstruction mainly are all sorts of common yarns, woolen yarns, fancy yarns, braided cords and so on. Other kinds of materials in linear shape such as a string a beads, cloth and so on are also included.

The plane materials. The plane materials in the home textile fabric reconstruction mainly are all sorts of fabrics, leather, big shell, papers, feathers and so on.

What should be emphasized is that if we want to use the dotted, linear and plane material freely, we should not only design based on the texture of the materials but also transform the materials into different shapes by design and process regardless of their original shapes. For example, the plane

materials can be transformed into dotted materials or linear materials, the linear materials into dotted materials or plane materials, the dotted materials into linear materials or plane materials, the plane materials into new ones and so on.

The design technique in the home textile fabric reconstruction

What we study is the secondary fabric processing technique that is more three-dimensional and has more visual impact. It is different from the traditional technique that centers on the plane processing. It brings the new life to the textiles [3]. There are a considerable number of fabric reconstruction design techniques. According to the processing methods and the achieved artistic effect, the techniques can be classified into transform design technique, plus design technique, and minus design technique.

Transform Design technique in the Home Textile fabric reconstruction

The transform design technique the paper discusses is a process that changes the surfaces of the fabrics. It changes the plane features of the fabrics without destroying the surface of the single kind of the fabric, forming the artistic effect of 2.5-demensional space or 3-demensional space. The common transform design techniques in the home textile fabric reconstruction include pleat, quilting, remodeling treatment and so on.

Pleat. Pleat is the most typical home textile fabric transform technique. No matter in the traditional regular order or in the modern free order, it applies different stitch methods to create a large quantity of compressions, bends and transitions, making the fabrics produce various half there-dimensional effects. It is often applied in the design of cushions and hugged pillows as well as the edge adornment of pillowcases, bed covers, curtains and table cloths. In the Fig. 1 and Fig. 2, the regular pleating is applied in the design of the hugged pillow, and in Fig. 3, the irregular pleating is shown.

Quilting. Quilting is to add some stuffing into the space between two fabrics, and to embody the 2.5-dimensional relief sculpture effect by stitches. The stuffing has certain thickness and elasticity, so the place stitched will sink, and the other places will protrude, thus the fabrics produce the relief sculpture effect that is unique and has a strong sense of three-dimensional space [1]. Quilting is often applied in the design of bedding set and the decoration of cushions. In Fig. 4, the cushion applies the rhombus quilting, and in Fig. 5, the free centripetal treatment is shown.



Fig. 1. Regular pleat



Fig. 2. Regular pleat



Fig. 3. Irregular pleat



Fig. 4. Rhombus quilting

The remodeling technique. The remodeling technique refers to the process which makes the plane fabrics has the three-dimensional effect by ways of stitching and stuffing. It gives people strong visual impact and endless space for imagination. In the Fig. 6, the cushion with the shape of beasts is formed by the way of the transitional stitching and stuffing. In the Fig. 7, the carpet with the solid shape is formed by the way of slicing and stitching the leathers. In the Fig. 8, by way of stuffing and stitching, the special surface of the sofa is formed. All these works have strong sense of fashion and personality



Fig.5. Centripetal quilting



Fig.6. Cushion in the shape of beast face



Fig.7. Individualistic carpet



Fig.8. Creative sofa design

The plus design technique of home textile fabric reconstruction

The plus design technique of home textile fabric reconstruction refers to the process which uses the single or multiple fabrics to paint, embroider, combine and add in order to form the, multilayer, half solid or solid effect. The specific design techniques are shown as follows:

The painted home textile fabric reconstruction. Designers paint directly on the surfaces of all kinds of home textile fabrics to realize the art recreation, which is free and easy and isn't be restricted by the technology. As to the composition, the designers can paint the whole picture or only part of the picture on the tailored fabrics according to the designing need.

The designers can choose flowers, animals, sceneries, traditional patterns as subjects according to the whole matching style of home textiles. The painting skills such as watercolor painting, Ink Painting, oil painting, elaborate-style painting can be applied to create the crude or refined artistic effect. Fig. 9 shows the home textile design with a Jiangnan flavor created by Xie-Yi freehand brushwork style. In Fig.10 and 11, the home textiles with the tropical flavor are shown.



Fig.9. Home textile with Jiangnan style



Fig.10. Decoration with tropical style



Fig.11. Chairs with tropical style

Embroidered home textile fabric reconstruction. In the design of home textile fabric reconstruction, the application of embroidery is common. Both the machine embroidering and hand embroidering can be used. The materials are not like traditional ones. They can be fancy yarns, woolen yarns, paillettes and so on. The stitches include straight needle, Rob needle, trochar, disorderly needle, cross-stitch embroidery. The aim is to create the bold and eye-catching decorative effect. Fig. 12 shows the embroidered cushion with traditional style. Fig. 13 shows the embroidered Tibetan cushion with modern style.



Fig.12. Traditional embroidery style



Fig.13. Modern embroidery style

The remodeling design in home textile fabric reconstruction. By overlapping, seaming, braiding one kind or multiple kinds of home textile materials, we get the fabrics with multiple layers that have visual effect of being concave-convex, interlock, consecutive and contrast.

Overlap design. By tacking or stitching one kind or multiple kinds of home textile materials, the half solid forms such as overlapping and piling up are achieved. Overlap design emphasizes combining the fabrics with different colours, patterns, textures to create visual impact. The technique is often applied in the design of home textiles such as curtains and hugged pillows. The overlap design of cotton fabrics in the same colour is shown in the Fig. 14, and the overlapping of the materials in different colours is shown in the Fig. 15.

Seaming design. By tailoring fabrics in different colours and patterns or different material qualities into the same size or different sizes and seaming them together, we get the mashup of the materials. Just as the Fig. 16 shows, this technique can be applied in the design of bed covers, single coverlets, cushions, chair cushions and so on. It can help to create a lively and rich artistic atmosphere.

Braiding design. The braiding design in the home textile fabric refers to the process that folds the fabrics or cuts them into cloth or binds them into strings, and then create the new fabrics or directly makes the textiles by means of braiding. Since the processing methods applied in the fabrics are different, the braiding forms are also different. So textures of fabrics are different in spacing, width. They are either concave or convex, consecutive or inconsecutive [4]. The materials of braiding can be fabrics, leather, plastics, papers or strings and so on. The home textiles applying the braiding methods can have special texture and details. In the Fig. 17, in the case of cushion, the same kind of fabrics is made into strings. After being braided, a strong sense of beauty of form is shown.



Fig.14. Overlap of same colour and texture



Fig.15. Overlap of different colours and textures



Fig.16. Table mat with seaming design



Fig.17. Cushion with braiding design

The added decorative design of special materials. It has been very popular these years to add the special materials into the design of home textiles. It means adding the paillettes, laces, embroidered squares, buttons, rhinestones and other materials into the surfaces of the fabrics by the means of tacking, stitching, embroidering, tangling, pasting, thermal bonding and so on. It can make the fabrics have rich visual effects. The decoration of shells and feathers is shown in the Fig. 18, the decoration of spangles is shown in the Fig. 19, the decoration of stones and gauzes is shown in the Fig. 20 and the decoration of coconut shells is shown in the Fig. 21. In the process of designing, we should take full advantage of the luster, texture and other features of materials to match them properly to achieve different artistic effects.



Fig.18. Shell, feather decoration



Fig.19. Spangle decoration



Fig.20. Stone, gauze decoration



Fig.21. Coconut shell decoration

The minus design technique in the home textile fabric reconstruction

The minus design technique in the home textile fabrics refers to the process that destroys the plane fabrics and forms the multilayer solid effect and special texture effect that combines virtual with reality. The common minus design techniques include fagoting, hollowing out, tearing and so on.

Fagoting. The ways of fagoting are various. The common method is to reel off warp yarns and weft yarns. As the Fig. 22 shows, this method can make the products look elegant, achieving the effect of being between the virtual and reality. This technique is generally applied in the design of napkins, table cloths, curtains and hugged pillows.

Hollowing out. Hollowing out means destroying the fabrics by means of scooping and cutting and making the fabrics possess the beauty of being incomplete and intangible. In the design of home textiles, the fabrics being hollowing out will serve as a foil to other fabrics, being in contrast to them in colour, texture and tactile impression. In the Fig. 23, the change of colour of the background fabrics makes the intangibility of the butterfly pattern more manifest.

Other destroying design techniques. The patching in the Fig. 24, the threading, sanding and tearing shown in the Fig. 25 are also common home textile fabric reconstruction techniques. The rough style is favored by the young people.



Fig.22. Fagoting



Fig.23. Hollow out



Fig.24. Patching



Fig.25. Sanding, threading

The comprehensive design of home textile fabric reconstruction

The means of home textile fabric reconstruction is bountiful. When designing the fabrics, we often comprehensively apply multiple processing methods since in doing so richer visual beauty can be achieved and the charm of home textiles is enhanced. In the Fig. 26, the upper part of the curtain applies the method of hollowing out, and the bottom part of it applies the method of braiding different fabrics. In the Fig. 27, the cushion applies the methods of remodeling, seaming and so on. The whole set of home textiles shown in the Fig. 28 comprehensively painting, embroidery, and seaming. We should utilize the various methods flexibly to enrich the expressions of fabrics and create stunning visual effect.



Fig.26.Curtain design



Fig.27. Cushion design



Fig.28. Comprehensive home textile design

Conclusions

The design determines the style and the market of the products, and it will become the home textile enterprises' strongest weapon used to compete for the market. The reform and creative change of home textile fabrics will provide the home textile industry with sustainable vitality. Home textile designer should attach importance to the fabric reconstruction skills, follow the law of the beauty of forms and reorder the visual focuses of the fabric, in order to guide the customers to appreciate the characteristics of home textile design and understand the meaning of fabric reconstruction. Nowadays, as more and more people pursue the home environment with a sense of fashion and personality, the application of fabric reconstruction in the home textile design will promote the development of home textile industry in China, make for the diversity of the home textile design and stylization of home textile products. It facilitates the promotion of home textile brand and caters to the demand of the customers.

PS: The works in all the pictures in this paper were made by the author and the students of Zhejiang Sci-tech University.

References

[1] Xuan Zhong and Zhirong Zheng: Zhejiang Textiles and Clothing Vocational and Technical College Journal. Vol. 2008. 12. (4),p19,p20. (In Chinese)

[2] Qingzhen Wang: *Fabric Re-creation of Textile Design.* The Southwest Normal University Publisher.(2007)p9. (In Chinese)

[3] Miao Su: The Silk. Vol.2006.7,p17. (In Chinese)

[4] Yueting Ma: The Fabric Reconstruction of textiles from the perspective of the trend of 2009-2010. master degree paper of Suzhou University. 2010.3, p35. (In Chinese)

© (2011) Trans Tech Publications, Switzerland
doi:10.4028/www.scientific.net/AMR.331.219

Predicting yarn unevenness using improved BP Neural Network

Li Huijun, Wang Xinhou

College of Textiles, Donghua University, Shanghai 201620, China.

Li Huijun，lihuijun@xju.edu.cn

Corresponding author: Wang Xinhou, xhwang@dhu.edu.cn

Keywords: Improved BP; CV value; knots; NEPS

Abstract: The objective of this research is to predict yarn unevenness. The model of predicting yarn unevenness is built based on improved BP neural network. The improved BP neural networks are trained with HVI test results of cotton and USTER TENSOJET 5-S400 test results of yarn. The results show prediction models based on improved BP neural network are very precise and efficient.

Introduction

CV value, knots, NEPS of yarn are indexes of yarn unevenness and they affect yarn strength, strength CV, weaving preparation, weaving efficiency and cloth smoothing. It has a very great practice significance to predict precisely yarn CV value, knots and NEPS in controlling production. In recent years evaluating cotton and yarn quality are more precise and comprehensive with the improvement and development of textile test technique [1, 2, 3]. It makes that it is possible to improve precision of predicting yarn CV value, knots and NEPS. Predicting of cotton yarn quality by neural network has some better results [4, 5]. A nonlinear model of cotton count-strength products and yarn CV value, knots, NEPS is built by artificial neural network in this paper, and the prediction effect is ideal.

Artificial neural network and improved BP algorithms

Artificial Neural Network is a network system of simulating the data processing unit in human brain, which develops based on research's newest achievement of the modern neurobiology. Using multilayer perceptron of BP algorithm is the most widely used neural network by far. BP neural network, which constituted by the input layer, the hidden layer and output layer, is a feedforward neural network. Each layer is contacted by weights and thresholds. 3-layer BP neural network (including input layer) can approximate any nonlinear function with arbitrary precision, the network adjust the weights and thresholds constantly through learning training. Learning process is conducted by the signal of propagation and error back propagation. It can be used to predict after the neural network is trained [6,7,8]. The BP algorithm is a forward multi-layer network, which uses error's back propagation algorithm to train the network. The standard BP algorithm is a simple static optimization of the steepest descent algorithm, there are some deficiencies such as slow convergence and easy to fall into the local minimum points. Therefore, this paper uses an improved BP algorithm, with algorithm of adaptive learning rate with momentum, through increasing the momentum term, the appropriate momentum factor will accelerate the improvement of network convergence, adaptive learning rate is adjusted according to learning error, and then improve the prediction capacity [9] .

Experiment

3.1 Data collection and preparation

In our research, 45 sets of data of combed cotton yarn were collected. All results of 50s yarn came from the history database of a cotton mill. From these 45 sets of data, 36 lots were selected at random to serve as the learning set for the neural network, and 9 sets of data recorded were used as test sets. Fiber properties were measured using the high volume instrument (HVI) testing system manufactured by User Technologies. Micronaire (MIC),upper half mean length (Len), Uniformity(UNF), Strength (STR), reflectance degree(Rd), yellowness(+b) and NEPS(NEPS) are included. In this network, they are adopted as input nodes. Yarn unevenness (CV), knots (+50%), NEPS (+140%), NEPS (+200%) are tested by User TESTER 5-S400 Evenness Tester. Four of them are served as output nodes. It is necessary for data normalization before training and testing sets are input into neural network to eliminate the effect of original index unit. Original indexes are converted using maximum-minimum normalization as shown in equation 1.

$$x_i = \frac{x - x_{\min}}{x_{\max} - x_{\min}} \qquad (1)$$

Where xi is the data processed, the range of its value is from -1 to 1, x is the data unprocessed, Xmax and Xmin are the maximum and minimum of the data unprocessed respectively.

3.2 MATLAB programming

In the MATLAB simulation program used in the main function is newff, train and sim function, newff function is used to create the BP network model, train function is used for training models, and sim function used the trained model to simulate. Set the parameters of the network in the program: The network layers were 3, the tansig is the transfer function of hidden layer, output layer's transfer function is logsig, while traingdx is its training algorithm and the MSE is the performance function. Hidden layer and output layer transfer function selected the sigmoid function, the network algorithm takes the improved BP algorithm, the maximum number of training is 30,000 times, and the prediction accuracy is 0.01. The main part of the programming code is as follows:

```
P＝[a1,a2,a3,a4,…,an]；％Output vector;
T＝[b1,b2,b3,b4,…,bm]；％Target vector;
[Pn, minp, maxp, Tn, mint, maxt ]=premnmx(p, t) ; ％Data normalization;
[pn,ps] = mapminmax (p);
[tn,ts] = mapminmax (t);
net= newff (P,T,[S1]) (‘tansig’ ,’ logsig’,’ traingdx’) ; ％The Improved BP Network;
net = traingdx(net,pn,tn ); ％Training Network;
a=sim(net,pn) ; ％prediction;
[y]=postmnmx(a,mint,maxt); ％Anti-normalization;
```

3.3 Establishing and Training of Network Model

Established by the three neural Network, The unit number of the hidden layer directly affect the Network accuracy. If the unit number of the hidden layer is too small, the network accuracy and fault tolerance will be poor; if the unit number of the hidden layer is too large, more learning time will increase, and cause over-fitting problems. The unit number of the hidden layer is decided by equation (2).

$$n_1 = \sqrt{(n+m)} + a \qquad (2)$$

Where n_1 is the unit numbers of the hidden layers, n is the number of neurons of input layer, m is the number of output layer neuron, a is a constant between 1 and 10. In this study, to improve the prediction results, the 7 - n_1-1 of the network model is established, so m is 7, n is 1. Can be obtained by calculation, the range of n1 is from 4 to 13, after training through the network, according to the prediction results to finalize.

3.4 Experimental results and discussion

Table I Prediction results of neural network with improved BP algorithms

Yarn index	Mean error	Maxim-um error	Mean relative error	Maximum relative error	Correlation coefficient
Yarn evenness	0.16	0.21	4	7.6	0.97968
Knots (+50%)	6.2	14.6	6	6	0.96077
NEPS (+140%)	0.62	1.07	3	5	0.94247
NEPS (+200%)	0.72	2.08	7	8	0.93763

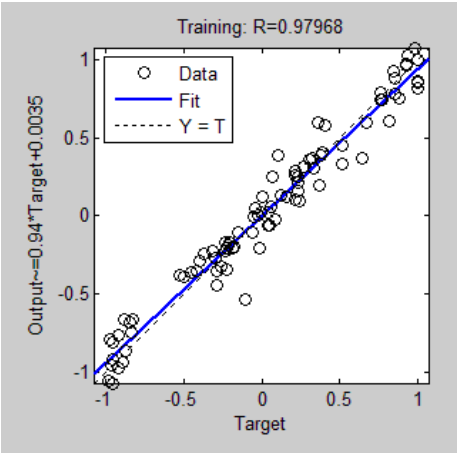


Figure1 Correlation Analysis of Yarn evenness

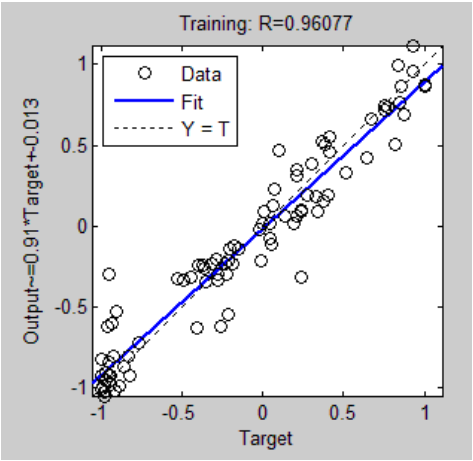


Figure2 Correlation Analysis of Knots

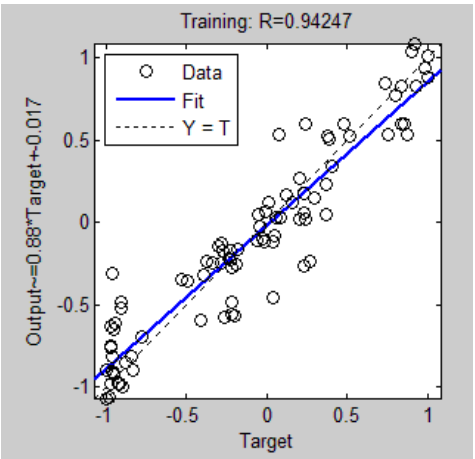


Figure 3 Correlation Analysis of NEPS (+140%)

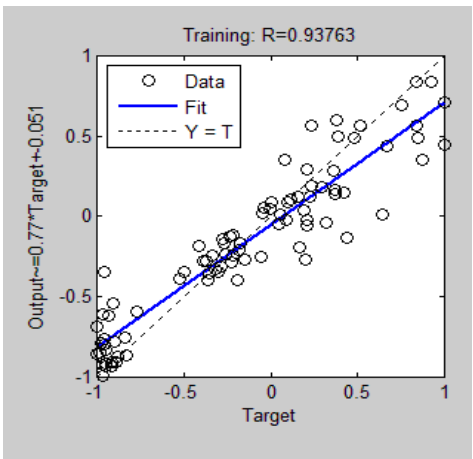


Figure 4 Correlation Analysis of NEPS (+200%)

Figure 1 to Figure 4 shows the correlation coefficient (R is the correlation coefficient) between the predicted and test value. Specifically, the correlation coefficients between the predicted and test values were 0.97968 (yarn unevenness), 0.96077(Knots+50%) 0.94247(NEPS +140%), 0.93763 (NEPS +200%), It could be seen the network system was able to predict steadily with a good coefficient of determination, and the average error is small.

Table II shows correlation analysis of the predicted and measured values for indexes of yarn. As can be seen from the prediction results of above four indexes, predicted correlation coefficient is greater than 0.93763, and predicted correlation coefficient of both yarn evenness and knots (+50%), NEPS (+140%) is greater than 0.94247.

For four indexes of yarn unevenness, knots (+50%), NEPS (+140%) and NEPS (+200%), their values of mean relative error are within 7%. However, maximum prediction error of yarn evenness and NEPS (+200%) are large and the error value of yarn knots (+50%) and NEPS (+140%) are small for maximum prediction error.

Conclusion

Predicting CV value of yarn evenness, NEPS and knots using improved BP neural network, the values of relative error of the predicted and test value are small. So the improved BP neural network can realize prediction of yarn evenness.

For maximum relative error, maximum prediction error of yarn unevenness and NEPS (+200%) are large and the error value of knots (+50%) and NEPS (+140%) are small.

All the predicted correlation coefficient are greater than 0.93763, and predicted correlation coefficient of both yarn evenness and knots (+50%) are greater than 0.94247.

Acknowledgement

The authors would like to acknowledge the financial support from the National Natural Science Foundation（60965003）for this work.

References:

[1] A. Babay, M. Cheikhrouhou, B.Vermeulen., J Text Inst, 2005, 96(3), 185-192.

[2] A. Majumdar, P. K. Majumdar, B. Sarkar. J Text Inst,2005, 96(1), 55-60.

[3] C. Luo, D.L Adams., Textile Res J, 1995, 65(9), 495-500.

[4] R.Beltran, L.Wang, X.Wang, J Text Inst, 2006, 97(1), 11-16.

[5] P .K Majumdar, A. Majumdar., Textile Res J, 2004, 74(7), 652-655.

[6] L.Jain, Srivastava and S.N.Singh, IEEE Trans. PowerSyst, vol.18, no.4, pp.1359–1366, Nov.2003.

[7] L. Jain, Srivastava, S.N.Singh and J.Sharma, Electr. Power Syst. Res, vol.53, pp.187–195, 2000.

[8] N.B.Karayiannis and G.W.Mi, IEEE Trans. NeuralNetw, vol.8, no.6, pp.1492–1506, Nov. 1997.

[9] Zulfiqar Khan and K. Allan E, Textile Research Journal, 2009, 79(8), 714-720

CHAPTER 2:

Textile Dyeing and Finishing

© (2011) Trans Tech Publications, Switzerland
doi:10.4028/www.scientific.net/AMR.331.225

The Printing Technology of New Pigment Used on Cashmere Products

Mei Zhen LI [1,a], Hui YIN [1], Yan CHENG [2]

[1.] Institute of Light Industry and Textile, Inner Mongolia University of Technology, Hohhot 010051, Inner Mongolia, China

[2.] Inner Mongolia Erdos Group, Erdos 017000, Inner Mongolia, China

[a]lmz2909@126.com

Keywords: Printofix Pigment, Color Rubbing Fastness, Handfeel.

Abstract. In this paper, we selected printofix pigment produced by Clariant to print the Cashmere fabric. The effect factors of rubbing fastness and handfeel in the printed fabric, such as baking temperature, baking time and the dosage of binder, thickener and fixing agent etc, were deeply analyzed by extensive experiments. Experiments show that this series of coatings and related agents can get better color rubbing fastness and handlefeel. Finally, we optimized the printing technology to achieve the desired color rubbing fastness and handfeel.

Introduction

The coating printing process is energy-saving，water -saving and small environmental pollution. Comparing with the dye printing, coating printing is suitable for various kinds of fiber fabrics. But this process used to cashmere products is innovative.

Printofix pigment produced by Clariant Company has good water-disperse, superior quality, environmental protection reliability. Cooperating with the additives printofix series, the printing and dyeing process is stable. In this article, the various coating printing properties and the purposes of various additives were analyzed by experiments in order to improve the fastness and handle problems.

Experimental

Materials and Apparatus. Materials including Printofix YellowT-G，Printofix Red TN01，Printofix BlueT-K，Printofix GreenT-X，Printofix VioletT-L，Printofix NavyT-V, binder SDP, thickener DS, softener SFT, fixing agent ZF, glycerin and urea are all provided by Clariant. Chemcials(China)Ltd .And pure Chasmere knitted fabrics were also used in the experiment.

Experimental apparatus containing motor stirrer, dyeing friction fastness apparatus (the electronic instrument Co., LTD, Laizhou, China), electronic balance (Asia-pacific electron balance Company), constant timing and temperature oven, printing screen and printing scraper were all applied in the printing.

Coating Printing Process. The coating process presents as follows: printing→baked (105℃~110℃for1.5 min) →baking →washing→drying.

Printing Paste Preparation. To shorten mixing time, the mixing sequence shows as follows: softener →adhesives→ pigment →thickener. And the paste formulas compositions are shown in Table 1.

Table 1 Paste Formulas Composition

Paste Composition	Pigment	Binder	Thickener	Fixing Agent	Softener	Glycerin and Urea	Water
Relative Mass Fraction (%)	X	Y	4%	1%	1%	moderation	100g

Characterizations

Rubbing Fastness. According to GB/T3920-2008 *test for colour fastness to rubbing of textiles,* the friction colour fastness was tested. And it was rated based on GB/T 251-2008 *gray scale to colour staining for test evaluation of textile fastness*.

Handfeel. Handle is mainly characterized by subjective evaluation methods namely kneading, touch, catch, seeing to assess smooth, soft, plump, elastic and loose features of the fabric. To compare more intuitively, 5 levels representation are used. Of all the levels, level 1 stands for the worst and level 5 represents the best [3].

Results and discussion

Dosages of Pigment and Adhesive. The dosages of pigment and adhesive in printing paste are the main factor to affect color fastness and handfeel of pigment printing fabric. According to formulas as shown in Table 1, the influence of Printofix Dosage on printing effect is presented in Table 2 under four chromaticity requirements (taking neutral colour Printofix Red TN 01 in condition of specified amount of adhesive for example).

Table 2 Influence of Printofix Dosage on Printing Effect

Printofix Red TN01(%)		0.5	1.0	1.5	2.0
Rubbing Fastness	Dry	4-5	4-5	4	3-4
	Wet	4	4	4	3-4
Handle		3-4	4	4-5	3-4

According to Table 2, it is known that painting paste affects the handfeel. Therefore, coating dosage should not be too much nor too less. Because if Printofix dosage is too low, the adhesive dosage would be relatively too much, thus influences handle. But when Printofix dosage is used too much, the coatings will heap up on the surface of fabric immediately causing lower rubbing fastness. According to the experimental, it is shown that the optimal Printofix dosage is 1.5%. Moreover, the types of coatings have less impact on rubbing fastness and handle of fabric, but just have some effect on its color saturation.

Table 3 shows reference for adhesive requirements under different chromaticties. It can be seen that with the increase of coating, the adhesive dosage is increasing. Thus, the printing fabric handle will gradually become harder [4].Furthermore, we can determine the amount of coating and adhesive on basis of color samples.

Table 3 Reference for Adhesive Amount under Different Chromaticity

Name	Light Color	Neutral Color	Deep Color	Special Dark Color
Coating (%)	<0.5	0.5-2	2-4.5	4.5-7
Adhesive SDP (%)	8	10-12	12-15	16-19

The coating printing depends on chemical physics function from binder polymer in order to form macromolecular film, so that coating is mechanically fixed on the fabric. In this way, it makes coating that has a certain friction resistance and scrub resistance [5]. Table 4 demonstrates the influences of adhesive content (%) on the rubbing fastness and handle of fabric coating with neutral colour BlueT - K .

Table 4 Influence of Adhesive Amount on Printing Effect

Adhesive SDP (%)		5	10	15	20
Rubbing Fastness	Dry	4	4-5	4-5	4
	Wet	4	4-5	4	3-4
Handle		4-5	4-5	4	3-4

From Table 4, binder amount directly affectes the handfeel and fastness of BlueT - K coating fabric. But when binder exceeds a certain amount, rubbing fastness of coating printing does not improve but fall. This is because more coating accumulated on the surface, resulting in too thick film, increase of friction coefficient and also bad hand-feel. Besides, plug nets phenomenon obviously happens [6]. The result shows that 10% adhesive dosage has the best effect. By Experiments, it is proved that printings effects of the other three colors are also affected by the dosage of adhesive, but they are minor related to the dosage of Printofix adhesives.

The Thickener Dosage. The same amount of coatings pulp and adhesive and different dosage of the thickener were combined into pigment printing paste. And then it was undertaken printing, drying and baking processing. Experimental result shows in Table 5.

Table 5 Effect of Thickener Dosage to Printing

Thickener (%)		2	3	4	5	6
Rubbing	Dry	4	4	4-5	3-4	3
Fastness	Wet	3-4	4	4-5	4	3-4
Handle		4-5	4-5	4	3-4	3

As shown in Table 5, handfeel of printed fabric is better when thickener dosage is 2-3%. But with less dosage of thickener and low viscosity of printing paste, dry and wet rubbing fastness both could not achieve ideal effect. With further increase of thickener dosage, the rubbing fastness and handle are both better. But when dosage is continued increasing, the printed fabric feels hard by hand because higher viscosity of printing paste makes more printing paste accumulated on the surface fabric. Comprehensively considering, the dosage of thickener would be chosen for 4%.

Fixing Agent Dosage. Adding to fixing agent ZF can improve the fabric washing fastness and wet rubbing fastness. That is because the fixing agent belongs to nonionic, so it can not react with the viscosity change. In Table 6, it is shown that fixing agent dosage should not be too large , and small dosage can achieve good rubbing fastness and printing handle effect. Therefore, 1% fixing agent dosage is appropriate.

Table 6 Effect of Fixing Agent Dosage to Printing

Fixing Agent Dosage (%)	0.5	1	1.5	2
Dry Rubbing Fastness	4	4-5	4-5	4
Wet Rubbing Fastness	3-4	4	4-5	4-5
Handle	4-5	4	4	3-4

Softener Dosage. Non-ionic SFT softener is especially suitable for pigment printing of knitted fabrics, which makes printing position softer and better durability. It can improve dry rubbing fastness, wet rubbing fastness of fabric, and has not impact on wet rubbing fastness. So, the dosage of softener is typically chosen for1-1.5%.

Glycerin and Urea Dosages. Joining urea into printing paste can reduce moisture evaporating, so it is helpful for printing paste dissolving, scraping, and not easy to plug nets. Just right amount is used in the experimental [7].Because Glycerin has characteristics of excellent smooth, it can make coating grain in paste well-distributed and also make the viscosity of paste more suitable for printing. Its effect is very apparent especially when printing the fabric with high-precision pattern. And appropriate amount is all right.

Pre-drying Process. Fabrics Dried after printing has important influence on printing patterns outline and color uniformity [8]. Fabrics after scraping were usually dried at about 110 ˚C for 1.5 min.

Baking Temperature. After pre-drying, baking treatment can make some cross-linking between adhesives and fabric. Moreover, coating will be adherent on the fabric. Table 7 presents the influence of different baking temperature on printing effect for 2min.

Table 7 Effect of Baking Temperature to Printing for 2min

Baking Temperature(˚C)		110	120	130	140
Rubbing Fastness	Dry	3-4	4	5	5
	Wet	3	3-4	4-5	5
Handle			4-5	4	3-4

From Table7, it is shown that lower baking temperature makes poorer fastness, and too higher baking temperature brings harder handfeel. This is because low baking temperature makes binder not fully crosslinking. And when temperature is too high, the fabric changes yellow and handfeel becomes stiff. By comprehensive consideration, 130˚C temperature is more appropriate for baking.

Baking Time. Baking time is also an important influencing factor to fastness and handfeel of the fabric. At130 ˚C baking temperature, effect of baking time to printing is shown in Table 8. It is found that the same as baking temperature, baking time cannot be too long or too short. It can be seen that baking for 2min could obtain ideal handfeel and fastness.

Table 8 Effect of Baking Time to Printing at 130 ˚C

Buring Time(min)		1	2	3	4
Rubbing Fastness	Dry	3-4	4	4-5	4-5
	Wet	3	3-4	4	4-5
Handle			4	3-4	3

Conclusions

1．In condition of Printofix coating cooperating with relevant additives series, the printing process can be easily controlled. Adhesives for 10% (relatively little) made cashmere knitted fabric handle improved. In the experimental, we got a group of formulas and conditions which were suitable for printing coating process of Printofix as follows: coating was 1.5%, adhesives was 10%, thickener was 4%, fixing agent was 1%, softener was 1%; Pre-baking temperature was 105˚C ~ 110˚C and time was for1. 5 min; baking temperature was 130 ~ 140˚Cand time was for 2min.

2．The fabric washing fastness and wet rubbing fastness can be improved by a little color fixing addition. And the right amount of urea addition is in favor of printing paste dissolving and scraping. Glycerin addition makes paint more evenly distributed due to its excellent smooth characteristic. And softener makes printing parts softer.

3．Coating printing process is simple, and also it leaves out washing process and reduces wastewater discharges. Meanwhile, this process reduces wastewater cost and brings considerable economic benefits. Coating printing can be applied for all kind of fibers, so it has very promising prospect.

References

[1] J. Zhang: Textile Information Weekly Vol.17 (2005) ,p.14.

[2]S. L.Wang: *Textile Printing Practical Technology*(China Textile University Press,Shanghai2002).

[3] H.B. Liang, H.J. Zou: Journal of Printing and Dyeing Vol.20 (2009), p. 23.

[4] Y. M. J. Ge, Q. Zhu, J.J. Pan, B. Lv: Journal of Printing and Dyeing Vol.17 (2009), p.23.

[5] Y.E.Yu: *Coating Printing and Dyeing Technology* (China Textile Press, Bejing2003).

[6] H.Y. Shang: Journal of Screen Printing Vol.1 (2008), p. 13.

[7] Y.E.Yu: Printing and Dyeing Assistant Vol.8 (2002), p.5.

[8] L.P. Wang, Z. Y. Wu, J.Y. Gao, X.P. Gao: Woollen TechnologyVol.7 (2007), p.14.

© (2011) Trans Tech Publications, Switzerland
doi:10.4028/www.scientific.net/AMR.331.229

Research Progress of Fluoride-containing Acrylate Derivatives and their Application on Textile

Haohua Ye[1,2,a], Zhanxiong Li[1,2,b], Guoqiang Chen*[,1,2,c], Shaoqiang Zhou [3,d] and Jianhe Cai [3,e]

[1]National Engineering Laboratory for Modern Silk, Suzhou, Jiangsu, 215123,China; [2]College of Textile and Clothing Engineering Soochow University, Suzhou, Jiangsu, 215006,China; [3]Industrial Products Inspection Center of Jiangsu Exit-Entry Inspection & Quarantine Bureau of P.R.C, Nanjing, Jiangsu,210000, China

[a]yehaohua2007@163.com, [b]lizhanxiong@163.com,[c]chenguojiang@suda.edu.cn,

[d]rainzheu@gmail.com, [e]caijh@jsciq.gov.cn.

Keywords: Fluoride-containing Acrylate, Synthesis, Research Progress.

Abstract. The research progress of fluorine-containing acrylate monomers and their polymers has been discussed. These monomers were classified systematically according to chemical structure, such as perfluoroalkylinyl esters monomers, methyl trifluoroacrylate monomers, and so on. The synthesis of fluorinate acrylate and their polymerization were introduced. In addition, the features of these fluoride-containing chemicals were discussed as well as their applications on fabrics and research trend.

Introduction

Fluorine is the strongest electronegative of all the elements, with small atomic radius, short and strong Carbon-Fluorine bond. The intermolecular cohesion of organic fluorine compound is low, as well as the surface free energy and surface friction coefficient, and its molecular force between air and polymeric interface is weak, what contributes to the unique water resistance, oil resistance and wear resistance. Because of the "three high and two abhor" behavior-high surface activity, high heat resistance, high chemical stability, hydrophobic and oleophobic, the fluorine contained compound is superior to silicone and acrylic ester in such respects as hydrophobic, oleo phobic, antifouling, good fastness to wash, wear resistance, and corrosion resistance[1].

Acrylic ester possesses good film forming property. Its film has the property of water resistance, light resistance, acid and alkali resistance, aging resistance and color retention. Fluorine-containing acrylate is a kind of organic fluorine compound with double bond, and is one of the most important fluorine monomer. The introduction of fluorine-containing groups into acrylic ester polymer could change the structure of the polymer, without change the film forming property, and could effectively improve the aging resistance and water resistance of polymer film. Due to fluorine's electronegativity, C-F bond could hardly be polarized, fluorine-containing acrylate has excellent chemical stability, low toxicity and low friction coefficient. This enables the extensive use of fluorine-containing acrylate in textile, coating, architecture, optical fiber and national defense material[2].

As it was mentioned above, fluorine-containing acrylates have excellent property. Researching and developing of fluorine-containing acrylates has been a research hot spot in 21 century. Molecular design, synthesis and biological activity and application of these compounds have attracted vast attention of researchers in chemistry and biological field. It has been extensively used in textile, coating, architecture, optical fiber and national defense materials. Developing fluorine-contained acrylic ester polymer has high technology and economic value, it is also significant for the development of material industry in our country[3].

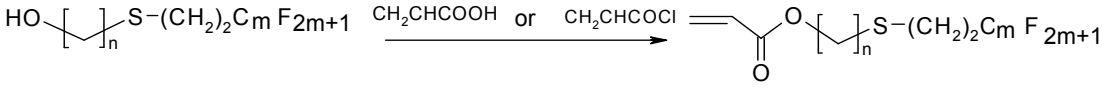
Synthesis of fluorinate esters monomers

Synthesis of perfluoroalkylinyl esters monomers. 1,3-HFAB was first reacted with dimethylsulfate in the presence of aqueous sodium hydroxide to yield 1-(hexafluoro-2-hydroxy-2-propyl)-3-(hexafluoro-2- methoxy-2-propyl)benzene which was reacted with acryloyl or methacryloyl chloride to give the corresponding fluorinated acrylate or Methacrylate monomers[4]. A series of novel silicon-containing fluoroacrylate polymers and copolymers (with methyl acrylate) has been prepared, starting from 1,3-bis(hexaftuoro-2-hydroxy- 2-propyl)benzene (1,3-HFAB)[5].

Industrial synthesis of fluorine s perfluoroalkylinyl methacrylate is obtained by the esterification of fluoride alcohol and methacrylate, and the preparation of fluorine substituted alcohols is the crucial technology. The current feasible approaches to synthesis fluorine-contained alcohols are stated as bellow: (1) reduced from carbonyl compounds, such as reduced from perfluoroalkyl ketone, perfluoroalkyl carboxylic acid and acryl chloride; (2) prepared by telomerization of perfluoride iodide; (3) by the telomeric reaction of methanol-tetrafluoroethylene[6].

For fluorine substituted alcohols, perfluoride alcohol does not exist actually. There are at least two-commonly four H atoms in a fluorine contained alcohol molecular. Owing to the acidic property of fluorine contained alcohols, esterification of such alcohols with acrylic acid directly is difficult. Acryl chloride is usually used to react with fluorine contained alcohols to prepare fluoride contained acrylic esters. Fluoride contained acrylic ester could also be obtained by reaction of methacrylate and fluorine contained alcohols with oleum as dehydrant or by transesterification.In the1950s, 1H,1H-Heptafluorobutyl had been obtained in American and Soviet by reacting CF3CF2CF2CH2OH with CH2=CHCOCl[7].

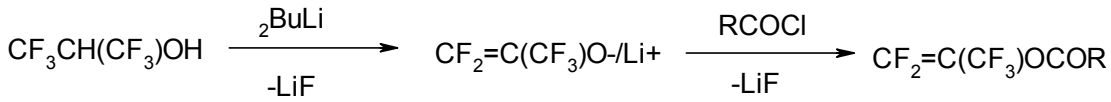
In the year of 2001, a wide range of original ω-hydroxy monomers bearing a thioether bridge and a perfluorinated end-group have been synthesized [8], he reaction was expressed as scheme.1:



Scheme.1 Synthesis of novel fluorinated acrylates

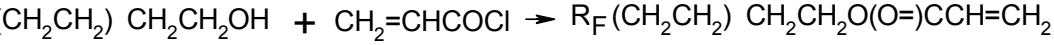
2003, perfluoroalkylethyl acrylate had been synthesized by Zhou et al[9]. The target product was obtained through the reaction of fluorine-contained alcohol and acrylic acid in the present of p-Toluene Sulfonic Acid in nitrogen environment.

More recently, Nakai et al. described the synthesis of CF2=C(CF3)-OCOR by dehydrofluorination of hexafluoroisopropanol (HFIP),followed by the addition of acid chloride according to the following scheme. 2[10]:



Scheme. 2 Synthesis of CF2=C(CF3)-OCOR

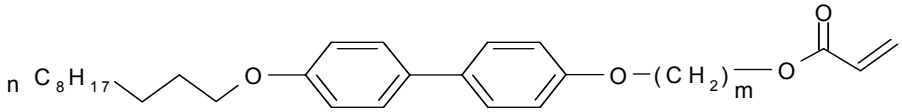
Wang Yun-fang et al[11], had prepared an F-containing acrylate-AFSN by low temperature reaction of duPoud's commercial surfactant Zonyl FSN with acryloyl chloride(AC) at the presence of proper reagents. The reaction equation was expressed as scheme.3.



Scheme.3 Synthesis of the AFSN (where, $R_F=(CF_2CF_2)_y$, x=1~25.)

Tetrafluoropropyl acrylate could be synthesized by using acrylic acid and tetrafluoro-propanol in the catalysis of sulfuric acid [12].

At the same time, Patrice C.Hartmann, Andre Collet,Michel Viguier etal synthesized the monomers (a) and (b) in five steps and the monomer (c) (without spacer) in six steps[13]. The structure was expressed as scheme.4:

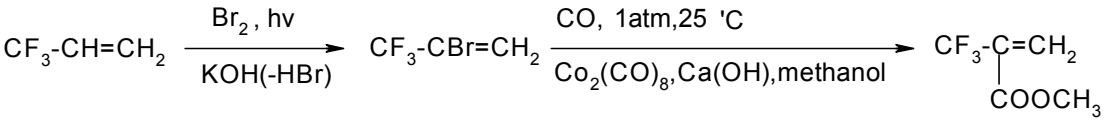


a: m=6; b: m=11; c: m=0

Scheme.4 The structure of acrylic monomers (a), (b) and (c)

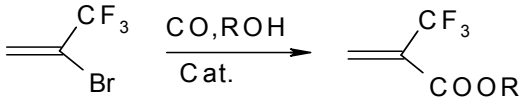
Radical addition of 2-benzoxypentafluoropropene [CF2=C(CF3)OCOC6H5] (BPFP) with alcohols such as ethanol and 2-propanol was investigated to afford fluorinated alcohols. Radical addition of BPFP with cyclic ethers such as tetrahydrofuran, 1,3-dioxolane and tetrahydropyran was also achieved to afford addition products, followed by hydrolysis to yield fluorinated alcohols possessing cyclic structures. Novel fluoroalkyl acrylates and methacrylates were synthesized from the fluorinated alcohols with (meth)acryloyl chlorides[14].

Synthesis of methyl trifluoroacrylate monomers. It is known that vinyl-and other alkenyl chlorides or bromides undergo the carbonylation reaction only in the presence of a stoichiometric amount of alkyl cobalt carbonyl complexes at atmospheric CO pressure in alcoholic solvent and at room temperature, affording the corresponding esters[15]. The reaction equation was expressed as scheme.5:



Scheme. 5 Synthesis of CF3CCH2COOCH3

Esters of 2- trifluoromethyl acrylic acid (TFMAA) have been synthesized by two different routes involving CO-chemistry. The alkoxy carbonylation of 2-bromo-3, 3.3-trifluoropropene was carried out in the presence of PdCl2 (PPh3)2.High substrate conversions were obtained[16]. The reaction equation was expressed as scheme 6:



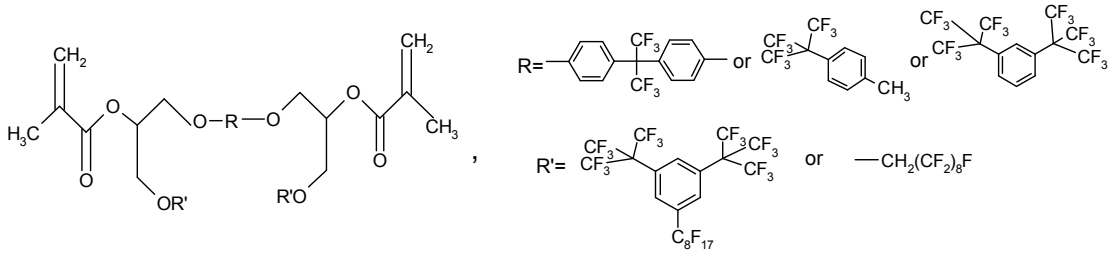
Scheme.6 Synthesis of esters of 2- trifluoromethyl acrylic acid (TFMAA)

For many researchers in our country[17], pentadecafluorooctanoic acid was used as starting material to synthesize N-(perfluorooctanoyl)aminoethyl methacrylate, then by homopolymerization its polymer was obtained.

Shi Hong-xin of Zhejiang University of Technology[18], reacted p-Perfluorononenoxy benzamide with formaldehyde, then esterified it with acrylic acid to produce p-perfluorononenoxy benzamidomethyl acrylate.

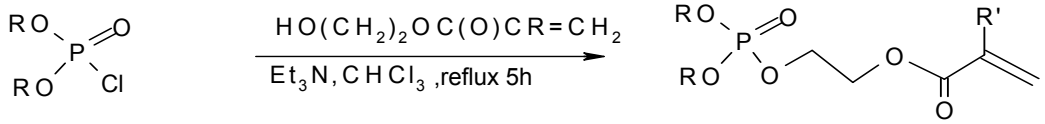
Synthesis of Other Types of Fluoric-Containing Acrylate Monomers. Perfluorooctanoyl chloride was prepared by reaction of perfluorooctanoic acid and SOCl2, then it was treated with ethanolamine to give N-hydroxyethyl- perfluorooctanamide. Under the catalysis of dibutyltin dilaurate and the protection of N2, N-hydroxyethyl-perfluorooctanamide was firstly treated with 2, 4-tolylene diisocyanate, then the reaction mixture was further treated with β-hydroxyethyl methylacrylate to give the perfluoro acrylate monomer [19] .

A series of fluorinated dimethacrylate monomers were prepared by reaction of aromatic diepoxides with fluoroalcohols and subsequent conversion of the resulting diols to the methacrylates [20].The structures of the monomers is expressed as schem.7.



Scheme.7 Fluorinated monomers synthesized by ring opening of diepoxides with fluoroalcohols and conversion of the diol intermediates to the dimethacrylates

The bis(fluoroalkyl)acrylic and methacrylic phosphate monomers were prepared by reaction of the chloridates with 2-hydroxyethyl acrylate or 2-hydroxyethyl Methacrylate[21]. The reaction equation was expressed as scheme.8:



R=CF_3CH_2 or C_2F_5 CH_2 or C_3F_7 CH_2, R'=H or Me
Scheme.8 Synthesis of halogenated monomers

In 2005, epoxy group contained poly-acrylic ester was synthesized in South China University of Technology[22].

In 2007, Zhou et al[23]. had designed and synthesized Ethyl 2-cyano-3-methylthio-3-(N-2-fluorophenethylamino) acrylate. Ethyl 2-cyano-3, 3-dimethythioacrylate was prepared from the reaction of ethyl cyanoacetate and dimethyl sulfate, then it was reacted with 2-fluorophenethylamine, yielded ethyl 2-cyano-3-(N-2-fluoro-phenethylamino) -3-methythioacrylate.

As for Chen's reseach [24], methylacryloylamidoethyl perfluorooctanoate was successfully obtained by the reaction of N-(2-Hydroxyethyl) methacrylamide and perfluoroacyl chloride at room temperature.

A new type of fluorinated (meth) acrylates was successfully synthesized through a simple reaction of 2-hydroxyethyl (meth) acrylate (EMA or EA) with the di- or trimer of hexafluoropropylene oxide (HFPO) n (n= 2, 3) in a yield of 82%~ 86% [25].

Copolymer of fluorinate ester monomers

As we all known, bulk polymerization, solution polymerization, suspension polymerization and emulsion polymerization are commonly used polymerization methods. Solution polymerization, emulsion polymerization and bulk polymerization are usually adopted to obtain fluoric-containing acrylate monomers. Fluoric-containing acrylate polymerizations applied on the textiles mainly adopt emulsion polymerization. AIBN, persulfate and BPO could be selected as the initiator, also there was reported UV as a initiator[26-28].

Water and oil proofing polymer was synthesized by Shimokawa through conventional emulsion polymerization with acrylate, acrylic acid and fluorine contained acrylate as monomer. In Suzuki's experiment, fluorine contained surfactant/fluorine free composite emulsifier was used to substitute conventional emulsifier. Acrylate, N-hydroxymethyl acrylamide and fluorine contained acrylate were polymerized into stable thermosetting acrylic emulsion[29].

Fluorinated latexes in the size range of 100-250 nm were obtained by the polymerization of miniemulsions with fluoroalkyl acrylates as fluorinated monomers under employment of rather low doses of protonated surfactants. In addition, it is shown that miniemulsifaction of mixed monomer species allows efficient copolymerization reactions to be performed with standard hydrophobic and hydrophilic monomers in a joint heterophase situation, resulting either in core-shell latexes or in statistical copolymers. Contrary to the pure fluorinated polymers, copolymers could dissolve in organic solvents but still show the profitable interface properties of the fluorinated species[30].

Fluorinated polyacrylate latices with core-shell structure were synthesized by semi-continuousemulsion polymerization[31], using a mixed emulsifier system composed of a reactive emulsifier and a small amount of anionic emulsifier, Compared with the core-shell structure with a fluorinated core，the core-shell structure with a fluorinated shell was more effective for modifying theproperties of the latex films. After then, Core-shell fluorine-containing polyacrylate latex particles with fluorine-containing polymer rich in shell were successfully prepared by emulsifier free seeded emulsion polymerization of fluorine-containing acrylate and fluorine-free acrylate monomers in water with PMMA particles as seeds.Transmission electron microscopy (TEM), scanning electron microscopy (SEM) and dynamic light scattering (DLS) analysis indicated that the core-shell particles were uniform and possessed narrow size distributions. X-ray photoelectron spectroscopy (XPS) analysis revealed that a gradient concentration of fluorine excited in the structure of the core-shell fluorine-containing latex film from the film-air interface to the film-glass interface[32], the phenomenon was also observed in other researches, such as the waterborne cationic perfluorinated acrylate soap-free emulsion prepared from perflu-orinated alkylethyl acrylate (FM) and other acrylate monomers[33].

A cationic water and oil repellent finishing agent were prepared by emulsion polymerization using six F-n-butyl methacrylate (FMA), methyl methacrylate (MMA) and butyl methacrylate(BMA) as monomers,FK-300B and cetyl trimethylammonium bromide as emulsifier, and APS as initiator[34].

Applications of fluorinate ester polymers on fabrics

Latex based fluorinated acrylates such as perfluorooctylethyl methacrylate (FMA) and perfluorooctylethyl acrylate (FA) and fluorine-free acrylates such as n-butyl methacrylate (BMA)was prepared by means of emulsion polymerization in the presence of octadecyltrimethylammonium bromide (C18TAB) and 2,2'-azobis(2-amidinopropane) dihydrochloride (V50) as water-soluble azo initiator. Stable poly- (perfluorooctylethyl methacrylate)/poly(n-butyl methacrylate) (PFMA/PBMA) latex blends were formed with average particle sizes varying between 50 and 300 nm. Such latex blends are of interest in water-, oil-, and soil-repellent coatings[35].

Dae-Hwan Jung[36] et al had reported the preparation of water- and oil-repellent surfaces using surface-attached monolayers of perfluorinated polymer molecules. A covalent attachment of the polymer molecules to the substrate surfaces is achieved by generation of the polymer chains through starting a surface-initiated radical-chain polymerization of a fluorinated monomer. It is shown that perfluorinated polymer films can be grown with controlled thicknesses on flat and even on porous silica surfaces, essentially without changing the surface roughness. The combination of the low surface energy coating and the surface porosity allows generation of materials which are both water and oil repellent.

Two series of semifluorinated fluorocarbon diblock copolymer poly(butyl methacrylate-co-perfluoroalkyl acrylate)have been synthesized by atom transfer radical polymerization(ATRP) [37]. Contact angle measurements on the thin polymer films showed low critical surface tension and low dispersion force contributions to the surface energy, which indicated the presence of the fluorinated block at the surface. The results showed that the water- and oil-repellency increased with the fluorine content in the diblock copolymers. After annealing at different temperatures or different times, the water- and oil-repellent properties of diblock copolymer were increased to approach maximum values. This phenomenon proved the propensity of polymer for fluorine enrichment at air-polymer surface.

Various rough surfaces coated with titanium oxide nanoparticles and perfluoroalkyl methacrylic copolymer were conducted to explore the influence of surface roughness on the performance of water-repellence and oil-repellence. Due to the surface nanocoating, the maximum contact angles of water and ethylene glycol (EG) droplets increased up to 56% and 48%. The excellent water- and oil-repellence of the prepared surfaces was ascribed to this increase of surface roughness and fluorinated-contained surface[38].

Latex based on fluoroacrylate (TAN) and other comonomers was prepared via miniemulsion polymerization in the presence of stearyl trimethyl ammonium chloride (STAC) and 2,2'-azobis (2-amidinopropane) dihydrochloride(ABAP) as a water soluble initiator. Given suitable reaction temperature and quantities of TAN, STAC, DPM, and DM, a copolymer emulsion of fluoroacylate with a particle size of 50 nm was produced. The water repellency tested on polyester fabrics displayed greater effectiveness than that of commercial products with higher fluorine content[39].

In 2006, Cao Xue qin[40] etal studied the fluomacrylate which was copolymerized in emulsion in the presence of a composite emulsifying agent. Textile finished by the fluorocopolymer emulsion were provided with good oil repellency but no water repellency.

By some researchers in Donghua University[41], the hexafluorobutyl acrylate monomer and other acrylic monomers were used to copolymerize, and a stable emulsion was obtained. Fabrics finished with the emulsion had a water contact angle of 142°.

A superhydrophobic complex coating for cotton fabrics based on silica nanoparticles and perfluorooctylated quaternary ammonium silane coupling agent (PFSC) was reported[42]. The complex thin film was prepared through a sol-gel process using cotton fabrics as a substrate. Silica nanoparticles in the coating made the textile surface much rougher, and perfluorooctylated quaternary ammonium silane coupling agent on the top layer of the surface had lowered the surface free energy. Textiles coated with this coating showed better water and oil repellent property than that treated with pure PFSC.

In 2008, Stuart A. Brewer and Colin R.Willis[43] provided data on how certain plant structures can be used to develop surfaces that provide repellency towards both polar and non-polar, low surface tension fluids. Combining fluoropolymer coatings with 'hairy' fibres was particularly beneficial for providing liquid-repellent textiles. None of these surfaces can however be regarded as super-repellent to low surface tension liquids.

A series of polyhedral oligomeric silsesquioxane (POSS) based hybrid terpolymers P(POSS-MMA-(HFPO)3MA) were synthesized. The cotton fabrics coated with these polymers possessed excellent water and oil repellency. Compared with P(MMA-(HFPO)3MA) copolymercoated cotton fabrics, POSS-based polymer coated cotton fabrics showed better oil repellency with a tendency of first increasing and then decreasing with an increase of the POSS content[44].

Zhou et al. had synthesized the waterborne cationic perfluorinated acrylate soap-free emulsion, and found the contact angle of water and liquid paraffin on the fabric treated by the emulsion was138°and 125°, respectively. The surface free energy of themembrane was 19. 01m J/m2 when ω (FM)= 50%. The structure of the fluorinated membrane surface appeared the lotus-effect[33].

In addition, Yamaguchi, Shen Yiding and Cao Tongyu et al.[45-47] had researched the application of fluorinate ester polymers on textiles, and found the fluorinate ester polymers exhibited a good oil and water repellent on cotton fabrics.

Maekawa [48]and other researchers[49-51] had studied a series of fluoric-containing polymers with excellent characteristic in the durability of the water and oil repellency against washing or abrasion, it was found the fluoric-containing polymers is lower fluoride containing and high effect finishing agent and with excellent oil- and water- repellent in textiles industry, and showed a good prospect in their application.

Developing Trend

Since the appearance fluorine-containing acrylate monomers and polymers, for its outstanding performance, its application developed rapidly in various fields, the market size and the market prospect were unanimously widespread promising, and it has attracted the attention over the world from the late former century, synthesis and application of fluorine-containing acrylate monomer and polymer have never stopped.

The research showed that if the fluorine-containing acrylate monomer and polymer connects with substituting group , such as P(Ⅲ), N, Si, S, it would made a catalytic activity, so as to realize flame retardant, water-repellent, oil-repellent, herbicidal, sterilization, anti-cancer and other important bioactivity. On the other hand, for design and synthesis of fluorine-containing acrylate monomer and polymer, there will be a new research hotspot of fluorine-containing acrylate monomer and polymer with flame retardant, water-repellent, oil-repellent, herbicidal, sterilization, anti-cancer and other important bioactivity.

Acknowledgements

This work was supported by Quality Supervision public industry research special funds for projects（200910013）.

References

[1] Shungen Zhu: Organo-Fluorine Industry.Vol.4(1997), pp.21-43(in Chinese).

[2] Ping Zhong, Dajian Qiu, Dingyi Zhao, et a1: Journal of Materials Protection,Vol.37(2004),pp.11-15(in Chinese).

[3] Jun Tian, Jinfen Xu, Guangming Peng, et al: Journal of functional polymers,Vol.8 (1995), pp.504-509(in Chinese).

[4] V. Sreenivasulu Reddy, W.J.Weikel, J.Arbaugh:Polymer, Vol. 37(1996), pp.4653-4656.

[5] V. Sreenivasulu Reddy,B. D. Lunceford,P. E. Cassidyt: Polymer, Vol. 38(1997),pp.703-706.

[6] Zhengyu Long, Qingyun Chen: Acta chimical sinica, Vol.58(2000),pp.713-716(in Chinese).

[7] Guohong Lu, Zhengguo Chen, Shiyuan Cheng,et al: Chinese Journal of Colloid & Polymer,Vol.18(2000),pp.31-34(in Chinese).

[8] B.pees, A.Cahuzac, M.Sindt, et al:Journal of Fluorine Chemistry, Vol. 108 (2001)pp.133-142.

[9] Yuming Zhou, Jingyan Huang: Chemical world, Vol.44(2003),pp.263-265(in Chinese).

[10] J.Guiot, B.Ameduri,B.Boutevin, et al:European Polymer Journal, Vol.39(2003),pp.887-896.

[11] Yunfang Wang, Ying Kong, Jinrong Yang, et al: oilfield chemistry, Vol.21(2004),pp.333-335(in Chinese).

[12] Zili Yu, Long Zhang, Yi Lin, et al: Chemical research and application, Vol.16(2004),pp.671-672(in Chinese).

[13] Patrice C.Hartmann,Andre Collet,Michel Viguier, et al: Journal of fluorine chemistry, Vol.125(2004)pp.1909-1918.

[14] Tadashi Narita,Yoshiomi Sakuragi,Hiroaki Yabata.: Journal of Fluorine Chemistry, Vol.128 (2007),pp.965-970.

[15] Carlo Botteghi, Claudia Lando, Ugo Matteoli, et al: Journal of Fluorine Chemistry, Vol.83(1997),pp. 67-71.

[16] Ugo Matteoli,Carlo Botteghi,Federico Sbrogio, et al: Journal of Molecular Catalysis A: Chemical,Vol.143(1999),pp.287-295.

[17] Yuming Zhou, Jingyan Huang, Xuejia Xue: Fine chemicals, Vol.19(2002),pp.77-79.

[18] Hongxin Shi, Fei Qiu, Juping Xiang. Synthesis of a Acrylate Containing Perfluorononenyl[J]. Fine Chemical, 2010,27(2):190-194(in Chinese).

[19] Weihua Li, Xiaodong Zhou, Zhengshui Hu. Fine Chemical, Vol.19(2002),pp.661-663(in Chinese).

[20] J.W.Stansbury ,J.M.Antonucci: dental materials, Vol.15(1999),pp.166-173.

[21] Christopher M. Timperley, Robert E. Arbon, Michael Bird et al: Journal of Fluorine Chemistry, Vol.121(2003),pp. 23–31.

[22] Fang Liu, Fanghua Wang, Rui-yan Lin,etal. Journal of south china university of technology(natural science edition),Vol.33(2005),pp.52-55(in Chinese).

[23] Jinkang Zhou, Deyu Hu, Linhong Jin, et al: Journal of Guizhou education institute(natural science),Vol.18(2007),pp.49-51(in Chinese).

[24] Yaobo Chen, Wenjuan Li, Zhonggang Wang: Fine Chemical, Vol.26(2009),pp.395-398,407(in Chinese).

[25] Cong Li, Jiacai Li, Guangxuan Liu: Polymer materials science and engineering, Vol.26(2010),pp.1-3(in Chinese).

[26] Bin Li, Wenguang Chen, Xiaogong Wang, Qixiang Zhou. ACTA polymerica sinica,Vol.6(2002),pp.786-790(in Chinese).

[27] Peizhi Chen, in Annual meeting of fluorine & silicon coating industry fluorine resin and fluorocarbon coatings technology seminar, Ningbo university press, Ningbo(2007),pp.78-85(in Chinese).

[28] Junfeng Han, Shuang Lu, Zhengping Wang: Applied Science and Technology, Vol.33(2006),pp.57-59(in Chinese).

[29] Tingting Yang, Shimin Wang, ZuShun Xu,et al: Polymer bulletin, Vol.6(2003),pp.13-18.

[30] Katharina Landfester, Regina Rothe, Markus Antonietti: Macromolecules, Vol.35(2002), pp.1658-1662.

[31] Chaocan Zhang, Yanjun Chen:Polymer International,Vol.54(2005),pp.1027-1033.

[32]Xuejun Cui, Shuangling Zhong, Hongyan Wang: Colloids and Surfaces A: Physicochem. Eng. Aspects, Vol.303(2007),pp.173-178.

[33] Wenmin Zhou, Xiaorui Li, Peizhi Li.et al: Fine Chemicals, Vol.27(2010), pp.913-917(in Chinese).

[34] Mingjun Zhang, Hongmin Zhu, Shaohai Fu: Journal of textile researchVol.30(2009),pp.61-65(in Chinese).

[35]Reinhard F. LinemannThomas , E. Malner, Rainer Brandsch: Macromolecules, Vol.32(1999),pp.1715-1720.

[36] Dae-Hwan Jung, In Jun Park, Young Kook Choi: Langmuir, Vol.18(2002),pp.6133-6139.

[37] Kun Li, Ping ping Wu, Zhewen Han: Polymer, Vol. 43(2002),pp.4079-4086.

[38] Chien Te hsieh, JinMing Chen, Rongrong Kuo. et al: Applied Surface Science,Vol.240(2005),pp.318-326.

[39] Pei Yuan Huang, YuChou Chao, Yih Tyan Liao: Journal of Applied Polymer Science, Vol.94(2004),pp.1466-1472.

[40] Xueqin Cao, Zhanxiong Li, Guoqiang Chen: Fine Chemical, Vol.23(2006),pp.1194-1197(in Chinese).

[41] Wenjuan Zhou, Wanchao Jiang, Zhengrong Li.et al: Textile Auxiliaries, Vol.24(2007),pp.31-33(in Chinese).

[42]Minghua Yu, Guotuan Gu,WeiDong Meng: Applied Surface Science,Vol. 253(2007),pp.3669-3673.

[43] Stuart A. Brewer and Colin R.Willis: Applied Surface Science, Vol.254 (2008),pp.6450-6454.

[44] Yu Gao, Chuanglong He, Yangen Huang. et al:Polymer, Vol.51(2010),pp.5997-6004.

[45] Yamaguchi, Hiromasa, Yamaguchi, Kochi.JP:09,296,134.1998.

[46] Yiding Shen, Xiaorui Li. The Preparation and Appl ication of N2Hydroxyethyl Perfluorooctamide Acrylate Copolymers for Leather Soilproof ing[J].Fine Chemicals,1997,5:11-14(in Chinese).

[47] Tongyu Cao, Qingpu Liu, Jinsheng Hu.Synthesis Mechanism and applycation of polymer emulsion. Beijing: Chemical Industry press, 1997:568(in Chinese).

[48] Maekawa T , Shimada M , Seki R, U.S.Patent 6,872,324(2005).

[49] Tanaka H, Kuwamura S, Yoshino F, JP. Patent 0,656,944. (1999).

[50] Akira O , Ibaraki H, Inukai S, U.S.Patent449,442.(1989).

[51] M asahiro M, Tsukasa A, M asak i F, et al, EP.Patent1,195,420. (2002).

© (2011) Trans Tech Publications, Switzerland
doi:10.4028/www.scientific.net/AMR.331.237

Effect of a Hydrophobic Finishing on Moisture Management Performance of Cotton Fabric

Tianhong He [1,a] , Jinbo Yao[2,b], Suying Chen[3,c]

[1]College of Art Design and Fashion, Tianjin Polytechnic University, Tianjin, China

[2] College of Textile, Tianjin Polytechnic University, Tianjin, China

[3]College of Textile & Clothing, Qingdao University, Qingdao, China

[a]tianhonghe@yahoo.com.cn, [b] yao-yaojinbo@tjpu.edu.cn, [c]chensyhk@sina.com

Keywords: cotton fabric; single-printing finishing; moisture management, One-way moisture transport; MMT

Abstract. Moisture transfer properties in fabric are critical to determine the thermal and sensorial comfort. Cotton fabric possesses many desirable characteristics that contribute to clothing comfort. However, in hot and wet environment or during some activities that human perspiration occurs, high absorbency of cotton makes its use undesirable. In this study, a chemical finishing method is developed to increase liquid moisture transfer properties on cotton fabric or clothing. The moisture management properties of the finished fabric or clothing were evaluated by using moisture management tester. Further wear trials were conducted to verify the comfort feeling toward finished area and unfinished area, which showed that this technique can effectively improve the overall comfort sensation especially during prolonged perspiration.

Introduction

Moisture management is defined as the engineered or inherent transport of moisture vapor or liquid moisture such as perspiration through fabric, which involves the transport of both water vapor and aqueous liquid. It has been reported the moisture vapor transmission through fabrics is predominately controlled by fabric thickness and porosity rather than by the type of fiber materials, since fabric thickness determines the passage distance of vapor moisture transform.[1] However liquid perspiration is transferred through fabric from the skin to outer surroundings by wicking or capillary effect, different from water vapor transport. Fabrics with the most effective moisture management properties move liquid moisture (sweat) quickly from inside surface/layer to outside surface/layer, keep the skin dry. So a comfortable fabric should transmit moisture during the period the bodyUse *italic* for emphasizing a word or phrase. sweats actively, and when the body has stopped sweating, the fabric should release the moisture held in the space to the atmosphere rapidly to reduce the humidity at the skin. In hot and humid environment, people wearing high hygroscopic materials would have higher skin temperature and sweat generation than wearing low hygroscopic ones, where intense perspiration occured.[2] In hot and high humid environment or during some activities when intense human perspiration occurs, high absorbency of cotton makes its use undesirable because it creates a wet discomfort. A good moisture management material requires performance well in absorbing, transporting and releasing moisture simultaneously. This paper presents a chemical finishing method which was developed to increase liquid moisture transfer properties on cotton fabric. The moisture management properties of the finished fabric were evaluated.

Materials

The fabric used was a twill fabric of 100% cotton, with a fabric weight of 173g/m2. A half sleeve T-shirt used was knitting fabric of 100% cotton. The fabric and T-shirt were prewashed, dried and ironed. The fluoric finishing agent was well blended with thickeners in advance. The printing grid was made by particular pattern. The procedures for finishing process and the test of moisture management performance, and wear trial are briefly described below.

Approach

A hydrophobic chemical finish is applied to the inner side (next to skin) of the cotton fabric in a discontinuous pattern by using single-side print finishing technique. A hybrid pattern with hydrophobic and hydrophilic areas on fabric surface is created. Through this method, one side (worn next to skin) of the fabric will be hydrophobic and the other side of the fabric will be hydrophilic. Therefore the surface worn next to skin of the fabric is discontinuously hydrophobic, while the opposite is continuously hydrophilic, wicking windows are formed between the two surfaces that allow the passage of liquid moisture.

The similar hybrid of finished knitting T-shirt is illustrated in Figure 1.

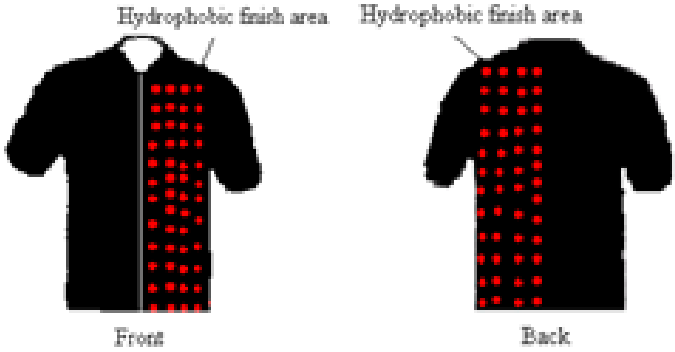


FIGURE1. The model of finished knitting T-shirt

Moisture Management Measurements

The moisture management tester (MMT) was used to evaluate the moisture management properties of fabric 3. Unlike traditional steady-state testing methods 4 (such as upright cup, the sweating guarded hot plate), the MMT can measure the dynamic liquid transport properties of fabric in three dimensions at one time 5.

Wear Trail Test

The participants gave informed consent to take part in this study. The participants are 4 healthy male students, 25-28 years of age, and 170-175cm height. Table Ⅰ. describes the test protocol. This test is aimed at eliciting wearer response to any tiny differences produced by finishing. An evaluation form was designed to record subjective sensations of comfort and sticky feelings, listed in Table Ⅱ.

Table Ⅰ. Test protocol for the wear trial test.

Rating Period	Time (min.)	Activity	Temperature (℃)	Relative humidity (%)
0	10	Preconditioning	28	75
1	10	Sitting and Reading	28	75
2	10	Ordinary activity indoors	28	75
3	30	Walking outdoors	25	67
4	30	Playing table tennis	28	75

Table Ⅱ. Comfort rating terms

Overall comfort	Stickiness sensation
Comfortable	No sticky
Slightly uncomfortable	Slightly sticky
Uncomfortable	Sticky

Results and Discussions

The results of MMT revealed that the finished fabric has an improved moisture management performance, and the finished fabric with the ratio of 70% exhibits the highest liquid moisture management capacity (OMMC=0.83) and one way transfer capacity (OWTC=542.84), indicating that the liquid sweat can be transferred from inner surface to the outer surface of fabric efficiently, keeping the skin dry. The spreading speed or drying rate (SSb) of 70% finished fabric, however, is not significantly changed comparing with the other finished fabrics. The fabric with 50% finishing area showed higher drying rate. The results of subjective evaluation were shown in Table IV and Table Ⅴ. It demonstrated that wearers have different sensations toward finished areas and unfinished areas when wearing this partly finished T-shirt next to skin: the overall comfort was improved and sticky feeling was reduced in finished area. But it also showed that this finished fabric was more suitable for wearing during summer, under medium or slightly activities.

Fabric (pure cotton)		WT_t	WT_b	MAR_t	MAR_b	MWR_t	MWR_b	SS_t	SS_b	OWTC	OMMC
Unfinished fabric	Mean	2.46	2.49	55.18	58.10	30	30	6.37	6.26	102.30	0.55
	SD	0.09	0.11	2.84	2.91	0	0	0.07	0.04	15.89	0.02
30% finished fabric	Mean	2.46	2.44	49.27	59.65	30	30	6.13	6.30	135.60	0.59
	SD	0.11	0.16	13.82	3.95	0	0	0.25	0.24	27.94	0.02
50% finished fabric	Mean	2.60	2.52	57.08	66.98	30	30	6.67	6.85	198.82	0.68
	SD	0.11	0.11	2.45	0.21	0	0	0.40	0.40	14.04	0.02
70% finished fabric	Mean	2.92	3.18	40.38	38.41	25	30	5.04	5.62	542.84	0.83
	SD	0.44	0.12	21.64	12.52	0	0	0.51	0.36	70.60	0.03

Talbe IV.Comfort Comparison of T-shirt on finished area and unfinished area

Wearers	Sitting and Reading	Slightly activity indoors	Walking outdoors	Playing table tennis
A	Comfortable within finished area	Comfortable within finished area	Comfortable within finished area	Comfortable within finished area at the beginning of activity
B	Comfortable within finished area	Comfortable within finished area	Comfortable within finished area	Comfortable within finished area at the beginning of activity
C	Comfortable within finished area	Comfortable within finished area	Comfortable within finished area	Slightly Uncomfortable
D	Comfortable within finished area	Comfortable within finished area	Comfortable within finished area	Uncomfortable

TABLE V. Sticky Comparison of T-shirt on finished area and unfinished area

Wearers	Sitting and Reading	Slightly activity indoors	Walking outdoors	Playing table tennis
A	No sticky on both areas	Sticky on unfinished area and no sticky on finished area	Sticky on unfinished area and no sticky on finished area	Sticky on both areas after several minutes
B	No sticky on both areas	Sticky on unfinished area and no sticky on finished area	Sticky on unfinished area and no sticky on finished area	Sticky on both areas after several minutes
C	No sticky on both areas	Sticky on unfinished area and no sticky on finished area	Sticky on unfinished area and no sticky on finished area	Sticky on both areas after several minutes
D	Slightly sticky on unfinished area and no sticky on finished area	Sticky on unfinished area and no sticky on finished area	Sticky on unfinished area and slightly sticky on finished area	Sticky on both areas after several minutes

Conclusions

A chemical finishing method was introduced to improve moisture management property. Using single-side print finishing technique to obtain a hybrid fabric with discontinuous hydrophobicity on inner surface and continuous hydrophilicity on outer surface. A new moisture management tester (MMT) was used to evaluate the moisture management capacity of fabric. The results demonstrate a significant difference in moisture management property in the finished fabric. The fabric of 70% finished area shows the highest liquid moisture management capacity and one-way transfer capacity. The results of subjective evaluation are consistent with the rules of MMT, showing this single finishing method can effectively improve the overall comfort performance of pure cotton fabric.

References

[1] Ching-luan Su., Jun-Xian Fang., & Xin-Hong Chen., Moisture absorption and release of profiled polyester and cotton composite knitted fabrics, Textile Research Journal, 77(10), 2007, 764-769.

[2] Q. Zhang ., S.C. Harlock., & D.B. Brook., Transfer wicking mechanisms of knitted fabrics used as undergarments for outdoor activities, Textile Research Journal, 72(8), 2002, 727-734

[3] Junyan Hu., Yi Li., Kwok-wing Yeung., Anthony S.W. Wong., & Weilin Xu, Moisture management tester: A method to characterize fabric liquid moisture management properties, Textile Research Journal, 75(1), 2005, 57-62.

[4] C. Parahsarn, R.L. Barker., & B.S. Gupta, Moisture vapor transport behavior of polyester knit fabrics, Textile Research Journal, 75(4), 2005, 346-351.

[5] Bao-guo Yao,Yi Li., Jun-yan Hu, Yi-lin Kwok, Kwok-wing Yeung., An improved test method for characterizing the dynamic liquid moisture transfer in porous polymeric materials, Polymer Testing, 25, 2006, 677-689

© (2011) Trans Tech Publications, Switzerland
doi:10.4028/www.scientific.net/AMR.331.241

Combination technology of spunbond & spunlace

Zhimin Lu[1, a], Xiaoming Qian[1, 2, b]

[1] School of textile, Tianjin Polytechnic University, Tianjin, 300160, China

[2] Key Laboratory of Advanced Textile Composites, Ministry of Education of China, Tianjin 300160, China

[a]13920501677@139.com, [b]qianxiaoming@tjpu.edu.cn

Keywords: Combination technology, Spunbond, Spunlace, Nonwoven, Application.

Abstract. The combination technology of spunbond & spunlace were introduced briefly. The advantages of spunbond-spunlace process were emphasized particularly. Composite technology is a effective method to develop new nonwoven product. Advantages of spunbond and spunlace technique with strong union could be utilized to produce high-grade nonwoven products which have excellent performances and high additional value. Their superior performances and broad applications determined that it would have a very wide market prospect.

Introduction

Since the reform and opening up, China's nonwoven industry has been expanding dramatically. Based on the relevant statistical data, the total output of nonwoven materials in China was 1.87 million tones last year. It accounts for 65.19% of the total output in Asia. Output of nonwoven of main Asia countries is shown in the Fig. 1.

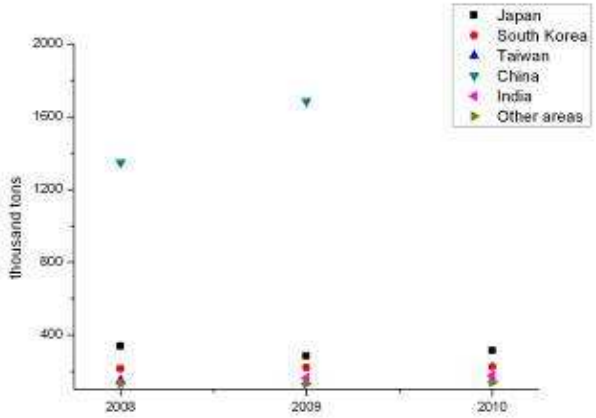


Fig. 1 Output of nonwoven of main Asia countries

Compared to the rapid growth of output, the nonwoven industry's profits of China are plummeting. Especially in the recent ten years, with equipment costs greatly reduced, the threshold into the non-woven industry is rapidly declining. There are thousands of nonwoven fabric production lines in China today, but most of them are repetitive constructed. The structure of products is too single that adds the competition in the market. So enterprises that want to struggle for the greater space of survival must develop functional and differential nonwovens.

New concepts

The nonwovens industries have worked with proven web forming, bonding and finishing technologies for a long time. Lately, there has been considerable movement in spunbond markets. Today's spunbond market is dominated mainly by calendered spunbonds for the health care fields and mechanically needled spunbonds for geotextiles, filters and roofing applications [1, 2].

Spunlace is the fastest growing web bonding technology in recent years. Spunlaced nonwovens have already replaced and superceded many other nonwoven products that were produced by other bonding methods. However, spunlace was not used to bond spunlaid webs in the past. A combination

of spunbonding and spunlacing was not economical because of the differences in speed. The spunbonding technology had already reached high speeds, while spunlacing was still operating at moderated speeds because of limited water pressures resulting from the line design.

But now the state of development reach for spunbonding and spunlacing lines makes a combination of both useful, allowing to create new product qualities. With this process, weights from under 10 to more than 600 g/m2 can be bonded [3].

Both the spunlace technology and the spunbond process already have maximum growth rates today. In the future, new bonding methods such as spunlace technology will be used more and more for the production of new generations of spunbonds.

Advantages of spunbond-spunlace process

Hydroentanglement offers advantages for many spunbond nonwoven products with respect to more softness, higher strength, higher speeds, higher line capacities and development of new products with superior characteristics mainly also in the sector of multi-layer composites.
Advantages speaking for spunbond-spunlace technology:

- High operation speeds for web forming. The speeds of spunlaid are more than 500 m/min while carding speeds are usually under 100m/min.
- No need or reduced use of chemical binder, which is especially advantageous for medical and hygienic applications.
- No reinforced points or zones by calendering and therefore the products are more soft and permeable than conventional spunbond nonwovens.
- Water entanglement involves no risk of fiber damage, consequently higher strength is achieved and product cost is reduced because of fiber costs saving.
- Spunlace technology can be used to bond and condenses several layers to get a multi-layer composite with engineered performance of the products.

Often lightweight webs that have been calendered do not offer the desired softness for applications in the hygiene sector. ANDRITZ Perfojet's expertise in the spunlace industry has lead to development of the spunjet process for spunlaid nonwovens. This new technology is particularly suitable for technical applications, such as geotextiles, roofing, synthetic leather and many more. The process comprises in line hydroentanglement of continuous spunlaid filaments, thus creating a new generation of nonwovens with superior fabric properties as regards bulk, softness, drape, and tensile strength. Spunjet fabrics unite the strength of spunbond and the softness of spunlace [4].

Bonding by the spunlace technology makes it possible to operate at higher production speeds which increase line efficiency. At the same time, the improvement of tensile strength can reduce fiber costs by the reduction of web weights. This considerably increases the economic efficiency of the process.

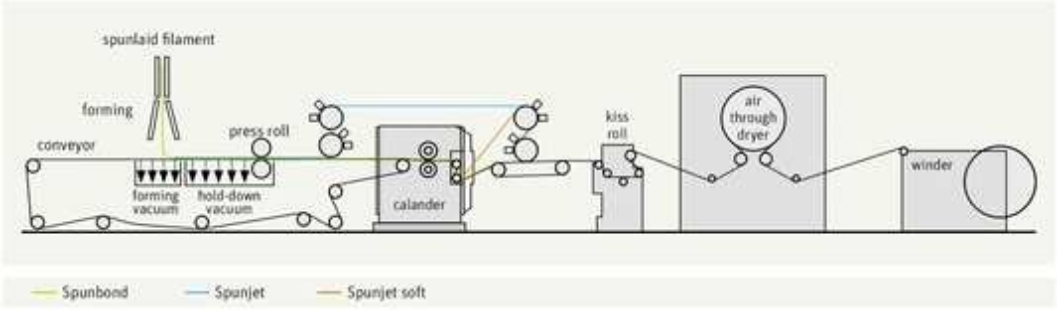


Fig. 2 The process of thermal bonding, spunjet soft and spunjet technology

ANDRITZ's customers now have the opportunity to combine two first-class bonding technologies in one line. Depending on the requirement of the final product, the process can apply either thermal bonding and / or spunjet technology as showed in Fig. 2. At INDEX 2011, held in Switzerland,

Andritz Nonwovens announced that it had entered into a contract with BG Filter in China for a 6.6 meterwide spunjet machine [5]. This line, which has a total capacity of 19,000 tons per year, is dedicated to the filtration and geotextile markets.

A new micro-fibrous nonwoven

Microfiber commonly refers to any fiber with strand less than 1 denier. Microfiber use in textile industry consecutively expanded, as it has lots of advantages, including greater surface area and flexibility, that can't get from conventional fibers. Microfiber can be processed into very lightweight fabrics with excellent draping qualities, good handing and luxurious appearance. When microfiber is made into nonwovens, they have even more properties: good isolation, impermeability, breathing ability, wrinkle-resistance, stain-resistance, easy washability. Their potentially greater comfort and functionality offer many applications in areas.

Conventional spunbond nonwovens have a considerable higher tensile strength than other nonwovens as their filaments' structure. But they are lacking the properties of softness, drapability, and loftiness because of the uncrimped filaments. That is why conventional spunbond nonwovens did not have a chance to be used for example in garment industry. Only crimping or the use of very fine filaments for spunbonded endless filaments makes it possible for nonwoven webs to be successful use for high-quality applications.

We can't get microfilaments through conventional spunbond technology. When we combine segmented pie bicomponent spunbond and spunlace, we can get a new method of forming micro-fibrous nonwoven by the splitting of bicomponent filament [6].

The said filaments having, in cross section, a configuration in the form of segments of an orange with a central orifice is showed in Fig. 3. The said segments or sectors being composed alternately of one of the two aforementioned polymeric materials and in direct contact with the adjacent segments or sectors, each composite filament being formed from several elementary filaments made one polymer and several elementary filaments made of the other polymer.

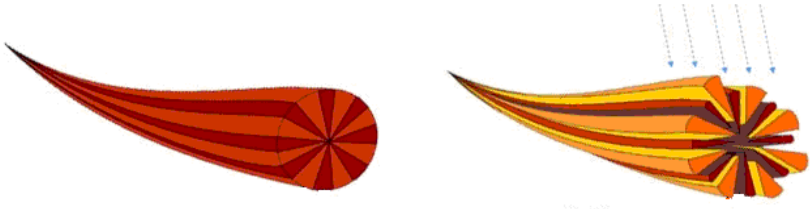


Fig. 3 The configuration of segmented pie filament before and after splitting

After web formation, the aforementioned nonwoven web is subjected to the action of jets of pressurized fluid for the purpose of separating the composite filaments into elementary filaments and to entangle and bond the latter. Commonly used polymers for this new nonwoven are PET and PA6. The production flow of PA6/PET segmented pie spunbond-spunlace is shown in Fig.4.

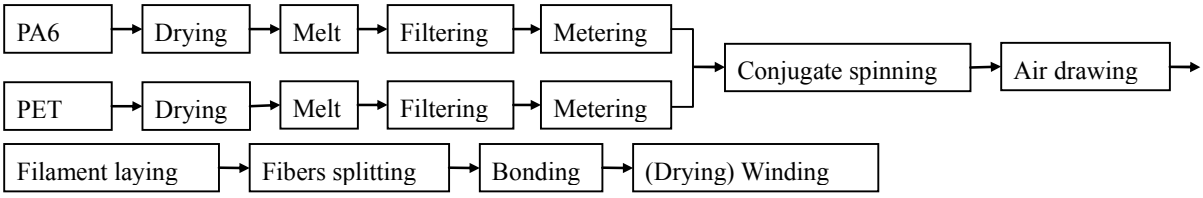


Fig. 4 The production flow of PA6/PET segmented pie spunbond

The fabric means comfort and ease of use, comforting performance and customer satisfaction, because it is lightweight, soft, breathable, drapable and no fiber release. Furthermore, the fabric is a perfect protective layer against dust mite allergens. Its filtration ability is due to the dense, compact structure of tightly entangled microfilaments. The very small dust mite allergen parts are retained under the layer, and cannot get in contact with the allergy sufferer. No "plastic" coating, no additional chemical treatment is needed to achieve this protection. So the micro-fabrics are suitable for a

diversified range of applications: anti–mite bedding, printing media for signs and advertising, cleaning cloths, sound absorption, technical packaging, sun protection and window treatment, coating and synthetic leather, and many others [7].

Conclusion

Spunbond and spunlace are the two fastest growing nonwoven technologies in recent years. When the two leading technologies with high capacities potentials come together, then the production of spunbond-spunlace nonwovens will become new generations of high-quality nonwovens. Combination technology of spunbond and spunlace represents the future direction of development of the nonwoven industry. With the further development of new products, I trust that spunbond-spunlace nonwovens will hold more and more important position in the near future.

References

[1] J. Srinivasan and S. Kathirvelu: Synthetic Fibres. Vol. 35 (2006), p. 27

[2] H.G. Geus and S. Sommer: International Fiber Journal. Vol. 22 (2007), p. 28

[3] A. Watzl: Technische Textilien. Vol. 44 (2001), p. 230

[4] Information on http://www.andritz.com/ANONID3C32FB70462ED37/index

[5] F. Patricia: Nonwovens Industry. Vol. 42 (2011), p. 14

[6] O. Bittner: Textilveredlung. Vol. 36 (2001), p. 35

[7] Information on http://www.evolon.com/

© (2011) Trans Tech Publications, Switzerland
doi:10.4028/www.scientific.net/AMR.331.245

Synthesis of Chelating Surfactant and Its Application in Silk Degumming

Yun Zhang[1,a], Xitao Sun[2,b], Xiangrong Wang [1,2,c]

[1]National Engineering Laboratory for Modern Silk, Soochow University, Suzhou 215123, China

[2]College of Textile and Clothing Engineering, Soochow University, Suzhou 215021, China

[a] zhangyun0222@163.com, [b] xitaosun@163.com

[c] Corresponding author, wangxiangrong@suda.edu.cn

Keywords: chelating surfactant; Ethanediyl-N-hexadecyl-tri(sodium α-glycinate); surface activity; silk; degumming.

Abstract: Ethanediyl-N-hexadecyl-tri(sodium α-glycinate) (N-hexadecyl ED3A), which belongs to the chelating surfactants, was synthesized by three-step reactions in this study. The structure of the product was characterized by IR. The surface activity and the properties of N-hexadecyl ED3A as degumming agent were investigated. The IR spectra showed the characteristic bands corresponding to the stretching vibration of C-N, -COONa, and C-H groups. The critical micelle concentration (cmc) of N-hexadecyl ED3A was 0.249mmol·L^{-1}, and the surface tension at the cmc (γ_{cmc}) of it was 33.03mN·m^{-1}. This revealed that the surfactant had fairly low cmc and excellent surface activity. Lower dosage of N-hexadecyl ED3A showed as good result as the conventional soap in silk degumming process, and the degumming result was also excellent without adding the chelating dispersant.

Introduction

Chelating surfactant, which was named by Toshio Takeshita et al from Kagoshima university (Japan), was first seen in 1956. It was invented in order to synthesize metal surfactant at that time. What's more, this kind of surfactant, like some transition metal ion hydrates, has special adsorption properties in aqueous and organic solvents, such as the easy absorption on the surface of fiber, polyvinyl alcohol and other polymers owing to its central metal ion isn't completely coordinated[1-2].

This kind of surfactant has both chelating capacity and surface activities, which is a new functional surfactant developed on the purpose of solving the increasing serious environmental problems in recent years [3-5]. The original intention of its research is to solve the environmental problem caused by the detergent of sodium tripolyphosphate. Its superior performances have been widely paid attention to by far. Moreover, the surfactant has been applied to industrial detergents, personal skin care products, municipal waste disposal and many other fields. There are many kinds of chelating surfactants, and the industrial synthesis of ethylenediamine triacetate derivatives has been achieved abroad, whose applications are more widely at present, however, there are no reports in the textile dyeing and finishing auxiliaries [6-8].

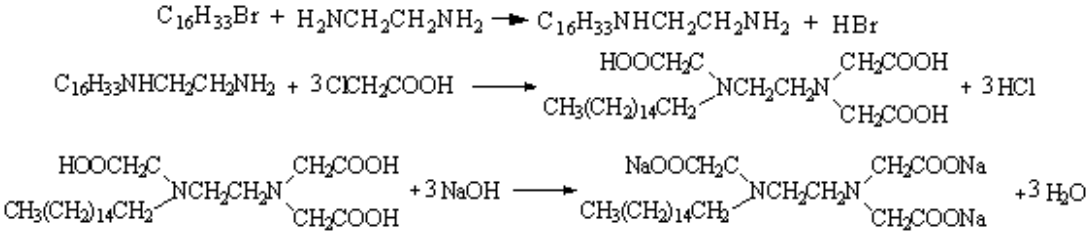
Chelating surfactant N-hexadecyl ED3A was synthesized in this study. Figure 1 shows the reaction route of the synthesis. The surface activity and basic application performances of the product were tested. The application of N-hexadecyl ED3A in silk degumming was investigated, which provided a theoretical basis on the application of chelating surfactants in textile dyeing and finishing processing.

Experiment

Materials. Natural color silk (undegummed) was supplied by Xinyuan Cocoon Silk Group Stock Co. Ltd. Chelating dispersant was purchased from Tongde Chemical Co. Ltd. (Jiangsu, Changzhou), without purification. All other chemicals were analytical grade.

Methods.

Synthesis of N-hexadecyl ED3A. Scheme 1 shows the three-step reaction route for the synthesis of N-hexadecyl ED3A.



Scheme 1

Application of N-hexadecyl ED3A in silk degumming. The natural color silk was degummed by alkali soap method. The process consisted of four steps: pretreatment，first degumming，second degumming and after-treatment. The formula was shown in Table 1.

Table 1 The formula of silk degumming

Reagent		Na_2CO_3 /g.L^{-1}	Soap /g.L^{-1}	N-hexadecyl ED3A /g.L^{-1}	Chelating dispersant /g.L^{-1}
Pretreatment		1	0	0	0
First degumming	Process 1	1	5	0	3
	Process 2	1	0	2	3
	Process 3	1	0	2	0
Second degumming	Process 1	0.5	0	0	1
	Process 2	0.5	0	0	1
	Process 3	0.5	0	0	0

Pretreatment temperature: 80-85℃; first degumming temperature and second degumming temperature were 95℃; time of each step was 40min; liquor ratio was 1:50.

The natural color silk was washed in hot water (70-80℃), warm water and cold water for 10min in sequence, and then dried.

Infrared spectroscopy (IR). The surfactant structure was characterized and analyzed with Nicolet-5700 infrared spectrometer by KBr tablet method.

Surface tension. The surface tensions of surfactant solutions were measured with a BZY-1 surface tensiometer by the Wilhelmy plate technique. The cmc and surface tension at the cmc were determined from the breakpoint of the surface tension and logarithm of concentration curve.

Calcium chelating ability. The calcium chelating value was measured by titration of EDTA standard solution.

Degumming rate. The undegummed and degummed silk fabrics were dried in the oven at 105℃ for 2h. Then they were kept in the silica gel drier for 24 h. The degumming rate was calculated by Eq.(1):

$$\text{Degumming rate}(\%) = \frac{w_1 \quad w_2}{w_1} \times 100\% \qquad (1)$$

w_1: weight of silk fabric undegummed; w_2: weight of silk fabric degummed.

Capillary effect. Samples were hung vertically and its end was immersed into deionized water for 30min. Then the capillary effect of the sample was determined by measuring the length of the water sorption part.

Tensile strength. The tensile strength of the silk fabric was measured by the YG206 fabric strength tester.

Results and discussion

Infrared spectroscopy. The IR spectrum of the surfactant is showed in Fig.1, which could characterize the structure of the surfactant synthesized. As can be seen from Fig.1, the absorption peaks at 2848cm^{-1} and 2918cm^{-1} are attributed to the C-H stretching vibration; the spectral peak at 724cm^{-1} belongs to the -CH_2- in-plane wagging and bending vibration of the cetyl in the synthesized surfactant. Besides, it is well known that the characteristic peak at 1609 cm^{-1} corresponds to the stretching vibration of -COONa, and the peak at 1453 cm^{-1} is caused by C-N stretching vibration.

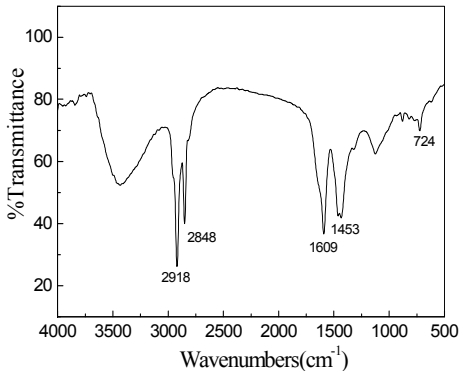


Fig.1. IR spectra of N-hexadecyl ED3A

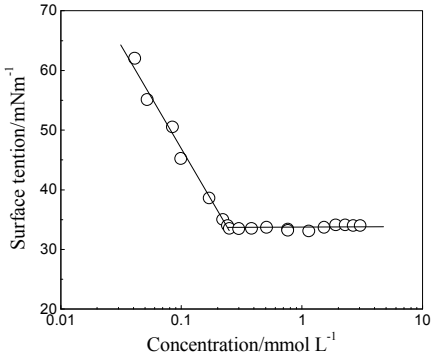


Fig.2. Variation of the surface tension with the surfactant concentration at 25℃

Surface tension. As can be seen in Fig.2, the surface tension of N-hexadecyl ED3A decreased with concentration increasing and then reached a clear breakpoint, which was taken as cmc. When the concentration continued to increase after cmc, the surface tension stayed the same. The cmc of the synthesized surfactant was 0.249mmol·L^{-1}, and its corresponding surface tension (γ_{cmc}) was 33.03mN·m^{-1}. Therefore, N-hexadecyl ED3A had not only fairly low cmc, but also great efficiency in lowering the surface tension of solution.

Calcium chelating value (CV). The chelating ability of traditional chelating agent, such as EDTA, is 260mg$CaCO_3$·g^{-1} EDTA, no matter what the concentration varies [9]. On the contrary, the chelating ability of chelating surfactant, which is relevant to its mass concentration, can rise with the concentration increasing. From table 2, we can see that N-hexadecyl ED3A had a pretty strong calcium chelating ability, and its CV was significant high when the concentration exceeded cmc. Consequently, the excellent chelating ability of N-hexadecyl ED3A can provide the foundation for its wide application prospect.

Table 2 Effect of N-hexadecyl ED3A concentration on the CV

Concentration/mmol·L^{-1}	1.0	2.5	4.0	5.0
CV/mg $CaCO_3$·g^{-1}	120	280	290	292

Measurement condition: pH=10； 25 ℃.

Properties of N-hexadecyl ED3A in silk degumming. Table 3 shows the properties of the degummed silk fabric with different degumming formulas. From process 1 and process 2, we can see that 2 $g \cdot L^{-1}$ N-hexadecyl ED3A gave the same degumming rate as 5 $g \cdot L^{-1}$ soap with other conditions unchanged, and the capillary effect of process 2 was better, which indicated that the property of 2 $g \cdot L^{-1}$ N-hexadecyl ED3A was better than 5 $g \cdot L^{-1}$ soap. As can be seen from process 2 and process 3, the excellent degumming result was obtained whether the chelating dispersant was added or not. Furthermore, the tensile strength of all the degummed silk fabric decreased almost the same but not much. All the above suggested that the properties of the synthesized surfactant used as silk degumming agent was considerably exceptional. Besides, the excellent chelating ability of N-hexadecyl ED3A could save the cost and reduce pollution emission in industrial production, which showed that N-hexadecyl ED3A had a very wide application prospect.

Table 3 Properties of the degummed silk fabric

	Degumming rate/%	Capillary effect/cm	Tensile strength /N	
			Warp	Weft
Undegummed	-	-	521.8	447.6
Process1	24.40	6.5	481.6	423.4
Process2	24.38	8.5	473.3	352.5
Process3	24.29	8.6	441.6	357.5

Summary

The critical micelle concentration (cmc) and the γ_{cmc} of surfactant synthesized in this study were 0.249mmol$\cdot L^{-1}$, 33.03mN$\cdot m^{-1}$, respectively. These showed that N-hexadecyl ED3A had fairly low cmc and high efficiency in lowering surface tension. The properties of the surfactant used as silk degumming agent were pretty good with the dosage of it significantly lower than that of the traditional soap, and the excellent chelating ability of N-hexadecyl ED3A could take the place of the chelating dispersant in silk degumming process.

Acknowledgements

This work was financially supported by the Priority Academic Program Development of Jiangsu Higher Education Institutions and the Open Foundation of National Engineering Laboratory for Modern Silk

References

[1] H. M. Zhang and J. P. Niu: China surfactant detergent & cosmetics, vol. 37(2007), No.4, p258-263. (In Chinese)
[2] J. Wang: Synthesis and Application of Functional Surfactants, Beijing: Chemical Industry Press, 2009. (In Chinese)
[3] J. Wang, Y. Y. Shi and G. S. Li: China Cleaning Industry, vol. 2(2007). (In Chinese)
[4] Z. Y. Liang, Z. W. Ye and C. X. Lu: Fine and Specialty Chemicals, vol. 12(2004), No.2, p18-19. (In Chinese)
[5] J. P. Niu and Y. M. Han: China Surfactant Detergent & Cosmetics, vol. 30(2008), No.1, p58-61. (In Chinese)
[6] M. M. R. Khan, M. Tsukada, Y. Gotoh, H. Morikawa, G. Freddi, and H. Shiozaki : Bioresource Technology, vol. 101 (2010) , p8439–8445.
[7] N. Ferlin, D. Grassi, C. Ojeda, J.L. Castro, and E. Grand: Carbohydrate Research, vol. 345 (2010), p598–606.
[8]] G. Mitra, S. K. Bhaltacharya, P. K. Mazumdar and M. A. Moon: Colourage, vol. 56(2009), p48-52.
[9] C. Z. Liao, Z. W. Ye and Z. Y. Liang: Jiangsu Chemistry, vol. 33(2005), p189-192. (In Chinese)

© (2011) Trans Tech Publications, Switzerland
doi:10.4028/www.scientific.net/AMR.331.249

Characterization of Cotton Fabric Treated with a Si/P Flame Retardant

Ran Wang[1,2,a], Yijin Bai[1,b], Xiaochun Wang[1,2,c], Yanqiu Wang[3,d]

[1]School of Material Science and Engineering, Beijing Institute of Fashion Technology, Beijing 100029, China

[2]Beijing Key Laboratory of Clothing Materials R&D and Assessment, Beijing 100029, China

[3]School of Science, Hebei University of Science & Technology, Shijiazhuang 050018, China

[a]clywr@bift.edu.cn, [b]byj512@163.com, [c]clywxch@bift.edu.cn, [d]wangyanqiu288@163.com

Keywords: flame retardant agent, cotton fabric, SEM/EDS, FT-IR.

Abstract. A Si/P flame retardant was prepared using tetraethyl orthosilicate (TEOS) and phosphoric acid (H_3PO_4). Original cotton fabric, treated fabric and its charcoal were examined by FT-IR, SEM, and EDS. Results showed that the TEOS/H_3PO_4 flame retardant has little affect on the cotton chemical structure and the surface morphology of cotton fiber. Main absorption peaks of the charcoal in the FT-IR are attributed to the P-O-C and the Si-O-Si bonds. And the surface of the charcoal was covered with white particles. EDS illustrates Si-O-Si bonds form on the surface and exhibit white particles in the SEM image.

Introduction

The demand for textile flame retardancy is growing rapidly [1]. In recent years, traditional halogen-containing flame retardants have been gradually phased out because of their toxicological and harmful environmental consequences [1, 2]. As an alternative to the use of halogenated flame retardants, the organosilicon-containing flame retardant, a type of halogen-free agent, has been accorded considerable attention [3-5].

In our previous reprot, a novel Si/P flame retardant was prepared using tetraethyl orthosilicate (TEOS) and phosphoric acid (H_3PO_4). Cotton fabric treated with it exhibits excellent flame retardant and possesses smoke suppression properties. In this report, cotton fabric and its charcoal were examined by FT-IR and SEM. And flame retardant mechanism of TEOS/H_3PO_4 was further investigated.

Experimental

Materials. Cotton fabric (100%; weight, 165 g/m^2) was desized, scoured, and bleached. Tetraethyl orthosilicate TEOS, $Si(OC_2H_5)_4$ and H_3PO_4 were purchased from Shanghai Fucheng Reagent Co., Ltd (Shanghai, China). All reagents were used without purification.

Preparation of TEOS/H_3PO_4 Flame Retardant. The mixture of H_2O/TEOS was stirred under acidic conditions. Thereafter, H_3PO_4 was added into the mixture while stirring. The mixture was agitated until a homogeneous solution was obtained. The molar ratio of the reactants was TEOS:H_3PO_4:H_2O = 1:0.5:10.

Treatment. The fabric was dipped and nipped twice in the flame retardant to obtain an 80% pickup. Then, the treated fabric was dried at 80 °C for 3 min and cured at 120 °C for another 3 min.

Analytical Method. In order to compare permances between fabric and its charcoal, fabric was placed in a cone calorimeter (Dual Analysis Calorimeter 2000, Fire Testing Technology Ltd., UK) under an air atmosphere and free convective air flow conditions, in accordance with ISO 5660. A pre-set heat flux of 25 kW/m^2 was used in this study. After the burning, the charcoal was collected.

FT-IR spectra of fabric and its charcoal were recorded with a NEXUS-670 spectrometer (Nicolet, U.S.) over the range of 4000- 400 cm^{-1} at room temperature. The absorption spectra of samples were recorded as KBr pellets.

Photomicrographs of fabric surfaces were examined with a JSM-6360LV scanning electron microscopy (JEOL, Japan). Fabric samples were glued to aluminum specimen stubs and coated with a layer of gold by means of thermal evaporation in a vacuum-coating unit. Samples were then examined in the SEM with an accelerating voltage of 10keV.

EX-54175 energy dispersive X-ray analyzer equipped in the SEM was operated in EDAX mode for analysis of characteristic X-ray spectra.

Results and Discussion

FT-IR spectra of the original cotton fabric, the treated fabric, and charcoal of the treated fabric were shown in the Fig. 1. The absorption spectrum of the treated fabric was very close to that of the original one. It implies that the TEOS/H_3PO_4 flame retardant has little affect on the cotton chemical structure. However, the FT-IR spectra of the treated fabric charcoal is quite different from them. The absorption peak at 1573 cm^{-1} is attributed to the P-O-C in the charcoal. The bands at 1089 and 995 cm^{-1} correspond to the asymmetric stretch of Si-O-Si. The 789 cm^{-1} band is ascribed to the bending of the linear Si-O-Si. The 440 cm^{-1} band is assigned to its symmetric stretch. No other peaks are observed at the range 4000-400 cm^{-1}, indicating that the sample is completely combusted.

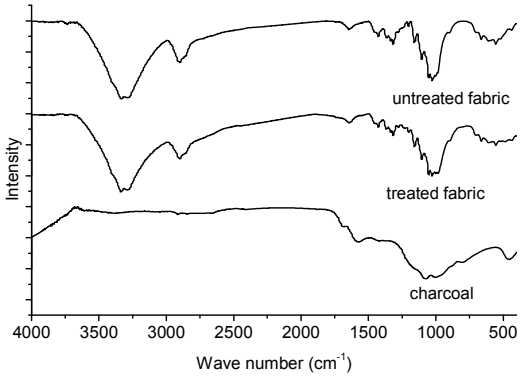


Fig. 1 FT-IR spectra of original fabric, the treated fabric and its charcoal

The surface morphology of the treated fabric and its charcoal are illustrated in the Fig. 2 and 3. There are significant difference between them when samples are magnified 2000 and 5000 times. The grooves and fibrils of treated cotton fiber can be observed clearly, whereas the surface of the charcoal is covered with white particles.

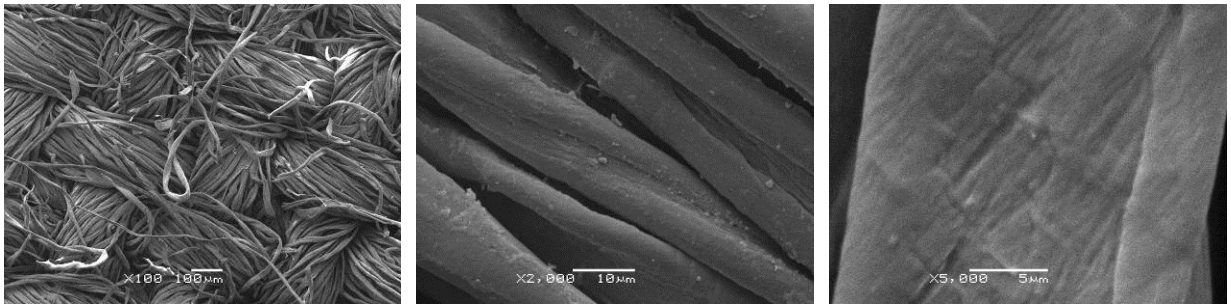


Fig.2 Surface morphology of the treated fabric

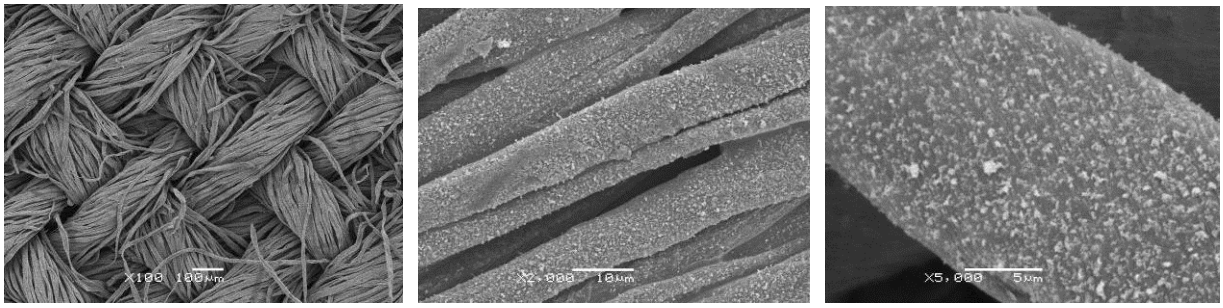
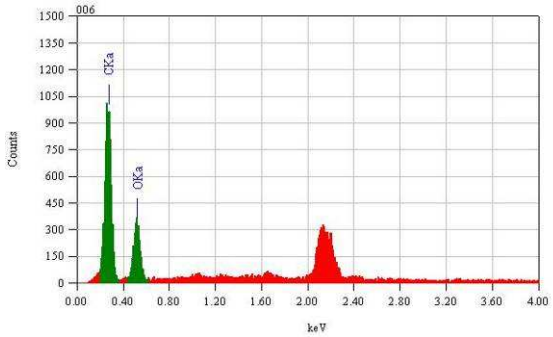
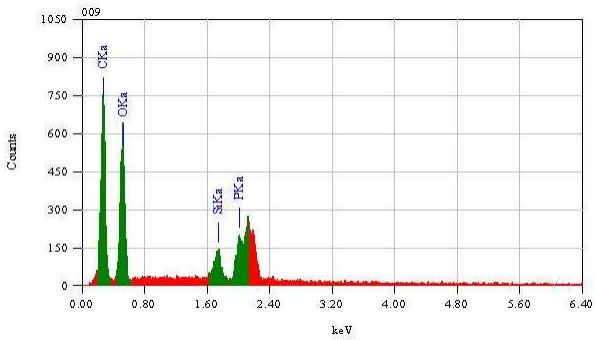


Fig. 3 Surface morphology of the charcoal

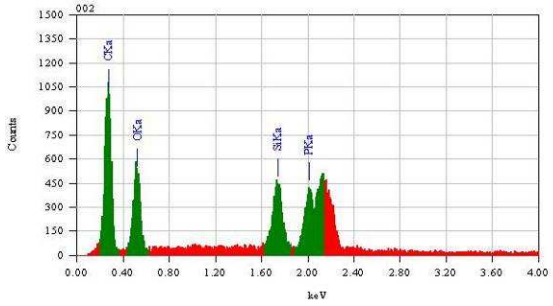
With the purpose of investigate the chemical composition, the element analysis of treated fabric and its charcoal were also investigated, as shown in Fig. 4. No Si element and no P element are found in the untreated fabric. Si and P contents notably increase in the treated fabric, and reaching their maximum levels in the charcoal.



(A)



(B)



(C)

Fig. 4 Element analysis of original fabric, the treated fabric and its charcoal

In accordance with flame retardant mechanism of cotton fabric treated phosphoric acid, phosphoric acid reacts with cellulose and induces the dehydration of cellulose. After the reaction P is observed in the charcoal in the form of P-O-C bonds. That will not result in white particles on the charcoal surface.

On the other hand, hydrolysis of tetraethyl orthosilicate to produce hydroxides, followed by poly-condensation of the resulting hydroxyl groups to form the Si-O-Si bonds. During the combusition, the condensation reaction is made progress and the Si-O-Si bonds increase. Consequently, the Si-O-Si bonds form on the surface and exhibit white particles in the SEM image. The Si-O-Si bonds generated from the heated silicate enhances the density and stability of the charcoal. The dense charcoal prevents the fabric from reacting with oxygen, thereby reducing the flammability of the fabric, retarding the thermal decomposition, and suppressing smoke yield. Those explain the good flame retardant and excellent smoke suppression propertise of the TEOS/H_3PO_4 treated fabric.

Conclusion

The TEOS/H_3PO_4 flame retardant has little affect on the cotton chemical structure and the surface morphology of cotton fiber. Main absorption peaks of the charcoal in the FT-IR are attributed to the P-O-C and the Si-O-Si bonds. And the surface of the charcoal is covered with white particles. The element analysis illustrates Si-O-Si bonds form on the surface and exhibit white particles in the SEM image. The Si-O-Si bonds generated from the heated silicate enhances the density and stability of the charcoal.

Acknowledgements

This work was financially supported by the Beijing Institute of Fashion Technology Research Program, No. 2009A-28.

References

[1] D. E. Weil, V. S. Levchik: Journal of Fire Sciences Vol. 26 (2008), p. 243

[2] A. R. Horrocks, B. K. Kandola, P. J. Davies, S. Zhang, S. A. Padbury: Polymer Degradation and Stability Vol. 88 (2005), p. 3

[3] A. Cireli, N. Onar, M. F. Ebeoglugil, I. Kayatekin, B. Kutlu, O. Culha: Journal of Applied Polymer Science Vol. 105 (2007), p. 3747

[4] S. Hribernik, M. S. Smole, K. S. Kleinschek: Polymer Degradation and Stability Vol. 92 (2007), p. 1957

[5] T. Kashiwagi, J. W. Gilman, K. M. Butler, R. H. Harris, J. R. Shields, A. Asano: Fire and materials Vol. 24 (2000), p. 277

© (2011) Trans Tech Publications, Switzerland
doi:10.4028/www.scientific.net/AMR.331.253

Application of Ionic Liquid in Silk Dyeing

Dehong Cheng*

Eastern Liaoning University, Dandong, Liaoning, 118000, China

14113200@qq.com

Keywords: Ionic liquid, dyeing, silk, dyeing performance, accelerating agent

Abstract. In this paper ionic liquid 1-butyl-3-methylimidazolium chloride (BmimCl) as accelerating agent was applied in silk dyeing and the dyeing performances of silk with ionic liquid were determined under different dyeing conditions. The obtained results indicated that the rate of dye uptake was about 85.4%, the K/S value was 11.2, breaking strength was 426 when 2 g silk was immersed in 60 ml dye solution, the concentration of ionic liquid was 2.0%, dyeing temperature was 50 ℃ and bath ratio was 1:30. Investigation on dyeing mechanism of silk with ionic liquid indicated that ionic liquid BmimCl interacted with amino acid in surface of silk and dyes through the electrostatic interaction between cation $Bmim^+$ and the CO_2^- group of amino acid and SO_3^- group of dye in dyeing process.

Introduction

Ionic liquids (ILs) are organic salts composed entirely of ions and have been termed as "designable solvent" for the feasibility of obtaining an IL of desired property by proper choice of the cationic and anionic components [1, 2]. The distinct physicochemical features of ILs, i.e., negligible vapor pressure, nonflammability, high chemical/thermal stability, low toxicity, favourable conductivity and controllable hydrophobicity/hydrophilicity has made it attractive and green alternative to the conventional volatile organic solvents [3].

Because of the poor dyeing performance of silk sodium chloride was applied as accelerating agent in silk dyeing to enhance the rate of dye uptake. Ionic liquid was the same as sodium chloride composed entirely of ions. In this paper the hydrophilic ionic liquid BmimCl was applied to substitute for sodium chloride in silk dyeing. The dyeing performance of silk with ionic liquid was investigated and a superior rate of dyeing uptake was obtained. The ionic liquid BmimCl interacted with amino acid in surface of silk and dyes through the electrostatic interaction between cation $Bmim^+$ and the CO_2^- group of amino acid and SO_3^- group of dye, which reduced the charge repulsion between amino acid of silk and dye molecules.

Experimental process

Silk dyeing with ionic liquid as accelerating agent. The dyeing technology of silk was obtained via a documented pathway by modification [4]. 2 g silk was immersed in 60 ml dyeing solution including 2% Reactive red B_2BF and a amount of ionic liquid BmimCl and then vibrated for 30 min in XW-ZDR-25*12 Vibrating Dye Prototype at 50 ℃. 0.6 g sodium carbonate was added into dyeing for fixation and then dyed for 30 min. after dyeing silk was washed, soaped and then dried in vacuum drying chamber at 100 ℃.

Results and discussion

Application of ionic liquid as accelerating agent in silk dyeing. The neutral salt such as sodium chloride was added to the dyeing solution to enhance the rate of dye uptake [5]. Ionic liquid was the same as sodium chloride to ionize in liquid solution and in this paper ionic liquid was introduced to

substitute sodium chloride in silk dyeing. After dyeing the rate of dye uptake, colour depth value and breaking strength of silk were determined and showed in Table1. The obtained results showed that rate of dye uptake was more than 85 %, colour depth value was more than 11 and breaking strength of silk was enhanced to 440 N when ionic liquid BmimCl or sodium chloride was added to the dyeing solution. This result indicated that ionic liquid as accelerating agent could enhance the dyeing performances of silk.

Table 1 The dyeing performances of silk with BmimCl

Samples	Rate of dye Uptake (%)	K/S Value (Colour Depth)	Breaking strength (N)
0 %	46.1	5.8	392
2.0 % NaCl	86.5	11.1	454
2.0 % BmimCl	86.9	11.6	445

Effect of BmimCl concentration on the dyeing performances of silk. In order to obtain the best dyeing performances of silk an amount (0.2-1.8 g) of ionic liquid BmimCl were added to 60 ml dyeing solution. The dyeing performances of silk under different concentrations of ionic liquid were investigated and shown in Fig. 1 and 2. Fig. 1 showed the rate of dye uptake increased with the increment of BmimCl concentration and the rate of dye uptake was more than 85 % when the concentration of BmimCl was 2.0 %. Fig. 2 showed that colour depth value of silk. The results indicated that dyeing performances of silk was best when the concentration of BmimCl was 2.0 %. When the concentration of BmimCl was more than 2.0 % the dyeing performances of silk decreased and the reason may be that ionic liquid BmimCl interacted with dye, which reduced the concentration of dyes in dyeing solution.

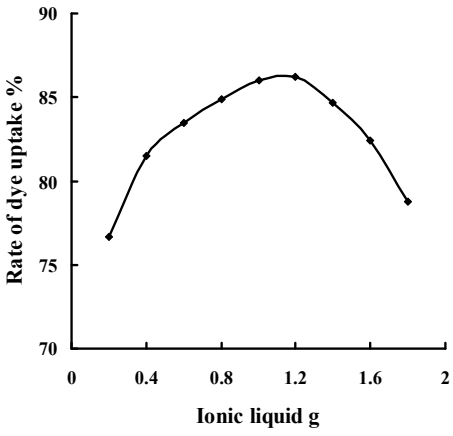


Fig. 1 Effect of ionic liquid concentration on the rate of dye uptake of silk

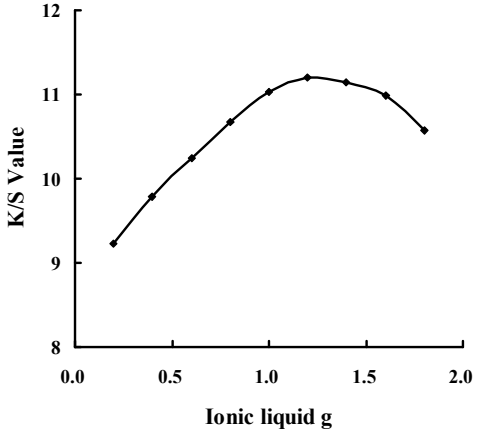


Fig. 2 K/S values of silk under different ionic liquid concentrations

Effect of dyeing temperature on the dyeing performances of silk. For Reactive red B_2BF the conventional dyeing temperature was about 60℃. Table 2 showed the dyeing performances of silk with different dyeing temperature and the results indicated that when the dyeing temperature was 50 ℃ the rate of dye uptake was more than 85%, K/S value was more than 11 and breaking strength was more 440 N. When the concentration of ionic liquid was 2.0% and the dyeing temperature was 50 ℃ the best dyeing performances of silk was obtained.

Table 2 The dyeing performances of silk under different dyeing temperature

Temperature ℃	40	50	60	70
Rate of dye uptake (%)	78.8	85.4	86.9	84.7
K/S value	9.9	11.7	11.6	10.8
Breaking strength (N)	456	445	399	339

The best dyeing performances of silk with ionic liquid. The best dyeing performances of silk was determined and shown in Table 3.When 2 g silk was immersed in 60 ml dye solution, the concentration of ionic liquid was 2.0%, dyeing temperature was 50 ℃ and bath ratio was 1:30 the rate of dye uptake was about 85.4%, the K/S value was 11.2, breaking strength was 426.

Table 3 The best dyeing performances of silk with ionic liquid

Samples	1	2	3	4	5	Average value
Rate of dye uptake (%)	85.3	86.4	84.9	86.3	82.3	85.4
K/S value	10.9	11.2	11.1	11.3	11.2	11.2
Breaking strength (N)	423	447	435	403	420	426

Dyeing mechanism of silk with ionic liquid The obtained results showed that ionic liquid as accelerating agent could enhance the dyeing performances of silk; however when the concentration of ionic liquid was more than 2.0 % the dyeing performance of silk decreased, which indicated the ionic liquid BmimCl maybe interact with amino acid in surface of silk and dyes through the electrostatic interaction between cation $Bmim^+$ and the CO_2^- group of amino acid and SO_3^- group of dye. In order to investigate and testify dyeing mechanism of silk with ionic liquid two projects was actualized and shown in Fig. 3. Fig. 3 (A) showed that silk was immersed in 20% ionic liquid BmimCl aqueous solution and then to dye and Fig. 3 (B) showed that ionic liquid and dyes was at the same time added to the dyeing solution and then silk was dyed in this solution.

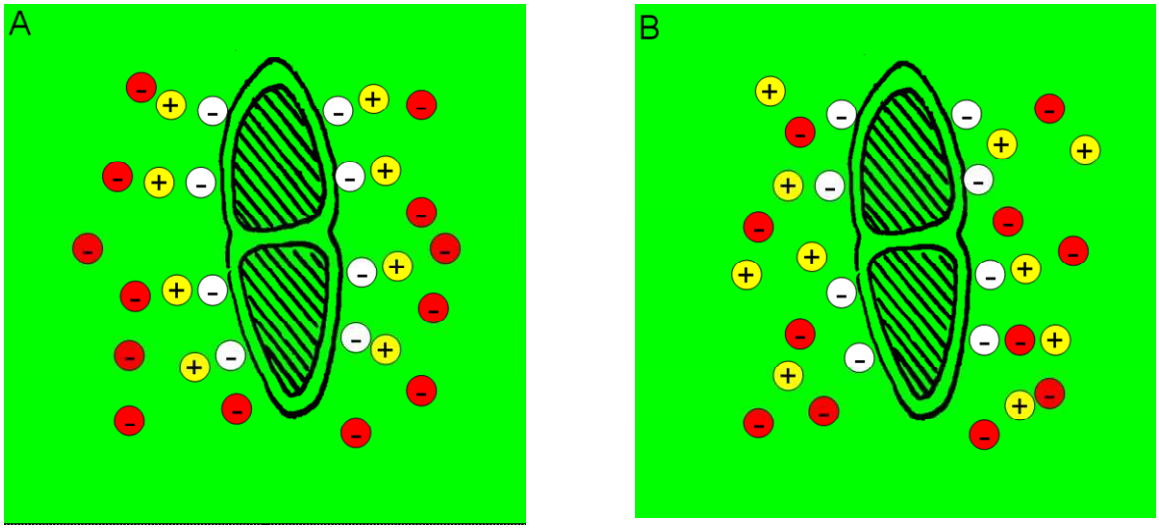


Fig. 3 Two projects for silk dyeing
(A: ionic liquid was first added; B: ionic liquid and dye was synchronously added)

The dyeing performance of silk for two projects was shown in Table 4. For projects A the rate of dye uptake was less than that of project B, however the K/S value for project A was more than that of project B, which indicated that cation $Bmim^+$ maybe absorb in surface of silk through the electrostatic interaction between cation $Bmim^+$ and the CO_2^- group of amino acid. After interaction the dyes molecule could not directly absorb in surface of silk, which resulted in the decrement of rate of dye

uptake. The K/S value for project A was enhanced and the reason for this may be that the electrostatic interaction between cation $Bmim^+$ and SO_3^- group of dye was stronger than that between CO_2^- group of silk and SO_3^- group of dye.

Table 4 The dyeing performances of silk for two projects

Project	A	B
Rate of dye uptake （%）	63.4%	85
K/S value	17.3	11
Breaking strength （N）	383	420

Ionic liquid BmimCl also was applied to dye silk using other dyes such as cationic brilliant blue RL and weak acid blue 6B and the obtained results shown in Table 5. For cationic brilliant blue RL the rate of dye uptake was only 49.4% and obvious less than 88.6% of weak acid blue 6B and 85 % of Reactive red B_2BF. Cationic brilliant blue RL ionized cation and then interacted with silk in dyeing solution, however cation $Bmim^+$ also interacted with silk, which resulted in decrement of rate of dye uptake.

The FT-IR spectra also was applied to investigate the surface of silk, however the amount of ionic liquid in surface of silk was too little to determine. in spite of the more detailed investigation was not carried out, however the obtained results also indicate that the dye mechanism of silk with ionic liquid BmimCl was that ionic liquid absorbed in the surface of silk and the cation $Bmim^+$ could interact with silk and dye through electrostatic interaction.

Table 5 The dyeing performances of silk with other dyes

Samples	cationic brilliant blue RL	Weak acid blue 6B
Rate of dye uptake （%）	49.4	88.6
K/S value	18.329	22.304
Breaking strength （N）	421.82	388.52

Conclusions

Ionic liquid BmimCl was for the first time applied in silk dyeing and the superior dyeing performances of silk was obtained. Ionic liquid not only played as accelerating agent but also interacted with silk and dyeing. In spite of more application of ionic liquid on silk dyeing was not investigated this research showed us an attractive expectation.

Acknowledgements

This work is financially supported by the Science and Technology Foundation of Liaoning (20091030) and the Natural Science Foundation of Eastern Liaoning University.

References

[1] J.S. Wilkes, M.J. Zaworotko: Journal of Chemical Society, Chemical Communications Vol. 13 (1992), p. 965

[2] S. Carda–Broch, A. Berthod, D.W. Armstrong: Anal. Bioanal. Chem. Vol. 375 (2003), p. 191

[3] D.H. Cheng, X.W. Chen, Y. Shu, J.H. Wang: Talanta Vol. 75 (2008), p. 1270

[4] Y.Z. Zhang, W.F. Hou, Y.P. Tan: Dyes and Pigments Vol. 34 (1997), p. 25

[5] D. mausezahl, Biel-Benken, P. locw, munchenstcin, U.S. Patent 4,917, 705. (1990)

© (2011) Trans Tech Publications, Switzerland
doi:10.4028/www.scientific.net/AMR.331.257

Stability of *Salvia miltiorrhiza* Bge Extract and Its Application on Silk

Sha-Sha Sun[1, a], Jie-Jie Wang[2] and Ren-Cheng Tang[1, b]

[1]National Engineering Laboratory for Modern Silk, College of Textile and Clothing Engineering, Soochow University, Suzhou 215123, China

[2]College of Textile and Clothing Engineering, Soochow University, Suzhou 215021, China

[a]sunsha_1117@163.com, [b]tangrencheng@suda.edu.cn

Keywords: *Salvia miltiorrhiza* Bge; natural extract; dyeing; mordant dyeing; Ultraviolet protective property; silk.

Abstract. The stability of *Salvia miltiorrhiza* Bge (SMB) extract and its dyeing and ultraviolet protective properties on silk were investigated. The results indicated that SMB extract was stable at acidic conditions and stable to heat and ultraviolet light. The building-up and UV-protective properties of SMB extract for silk were good and can be enhanced by mordanting with ferrous and ferric sulfate and copper sulfate. The light fastness rating was improved using ferric sulfate, while the washing and light fastness properties were worsen using ferrous sulfate.

Introduction

An interest in the use of natural dyes and natural agents in textile dyeing and finishing has been grown throughout the world because natural dyes/colorants are non-toxic, non-carcinogenic and biodegradable [1-3]. This is an inexorable trend in a response to the stringent environmental standards and the toxic and allergic reactions associated with synthetic dyes. However, only a limited number of studies on other functions of natural dyes such as UV-protection properties have been performed [4]. *Salvia miltiorrhiza* Bge (SMB) is a commonly used traditional Chinese medicine, the antibacterial as well as antispasmodic, antitoxic properties attributes to the present of water soluble components which are phenol acids containing a lot of hydroxyl groups and carboxyl groups. In this study, we investigated the stability of water extract from SMB, the possible use of SMB extract as natural dye and its UV-protective property without and with post-mordanting. The color fastnesses were also measured.

Experimental

Materials. The silk fabric of crepe de Chine was purchased from Wujiang Zhiyuan Textile Co. Ltd, China. Dry SMB was purchased from Suzhou Tianling Chinese Herbal Pieces Co. Ltd., China. Sodium hydroxide, phosphoric acid, boric acid, acetic acid sodium acetate, copper sulfate, ferrous sulfate, ferric sulfate, aluminum sulfate, and zinc chloride were of analytical reagent grade.

Extraction of natural dyes. Dry SMB was extracted with water at 90 ℃for 60 min in an oscillated dyeing machine, using a 25:1 liquor ratio. After extraction, the insoluble residues were separated by sedimentation and filtration. The resulting extract was used for the subsequent experiments and its concentration was defined by the mass of dye SMB in the solution.

Stability of SMB solution. The stability of SMB solution against pH was measured at 3.29, 5.02, 7.00, 8.95 and 10.88 by means of Britton-Robinson buffer. The heat stability was measured after heating at 50, 60, 70, 80, 90 and 100 ^{o}C for 30min. In order to evaluate the ultraviolet light resistance of SMB extract, the solution was exposed for 0, 24, 48 and 72h in a WFH-203B UV analyzer at 365nm.

Dyeing and post-mordant. The silk fabric was dyed with SMB extract in pH 4.0 buffer (HAc/NaAc) in a XW-ZDR oscillated dyeing machine, using a 50:1 liquor ratio. The dyeing was performed as follows: the dye-bath was raised from 40 to 80 °C over 20 minutes, and held for 60 minutes. The samples were then washed in tap water and dried in the open air. To study the effect of mordanting, the pre-dyed samples with 10g/L SMB extract were treated with 4% (owf) of mordant in a 80°C bath for 30 min, applying a liquor ratio of 50:1. Ferrous sulfate, ferric sulfate, aluminum sulfate, copper sulfate, and zinc chloride were used as mordants. Furthermore, ferrous sulfate, ferric sulfate and copper sulfate were used to post-mordant at 2%, 4%, 6%, 8% and 10% owf.

Measurements. The absorbance of SMB extract was measured with a Shimadzu 1800 UV-Vis spectrophotometer. The color depth (*K/S*), the CIE *Lab* color co-ordinates of dyed silk fabric were evaluated in a HunterLab UltraScan PRO reflectance spectrophotometer (illuminant D65; 10° standard observer). The ultraviolet protection factor (*UPF*) values of dyed silk were determined in a Labsphere UV-1000F ultraviolet transmittance analyzer. Wash fastness tests were conducted according to the standard ISO 105-CO1. Light fastness was tested according to ISO 105-BO2 method. The dyeings were exposed to xenon arc lamp for 10 h at standard testing conditions.

Results and Discussion

Stability of SMB extract. Fig.1a describes the stability of SMB extract at different pH values. Under acidic and neutral conditions, the spectra of SMB extract coincided with that of control sample, showing an excellent stability; whereas those under alkaline conditions changed obviously and a new absorption peak was observed at 366 nm, which may be the result of the reaction of hydroxyl groups and carboxyl groups with alkali and the oxidation of coloring component. In the case of heat and ultraviolet light, SMB extract showed a good stability with a little change in absorbance (Fig.1b). The above facts reveal that SMB extract is suitable for the application to textile dyeing under acidic conditions.

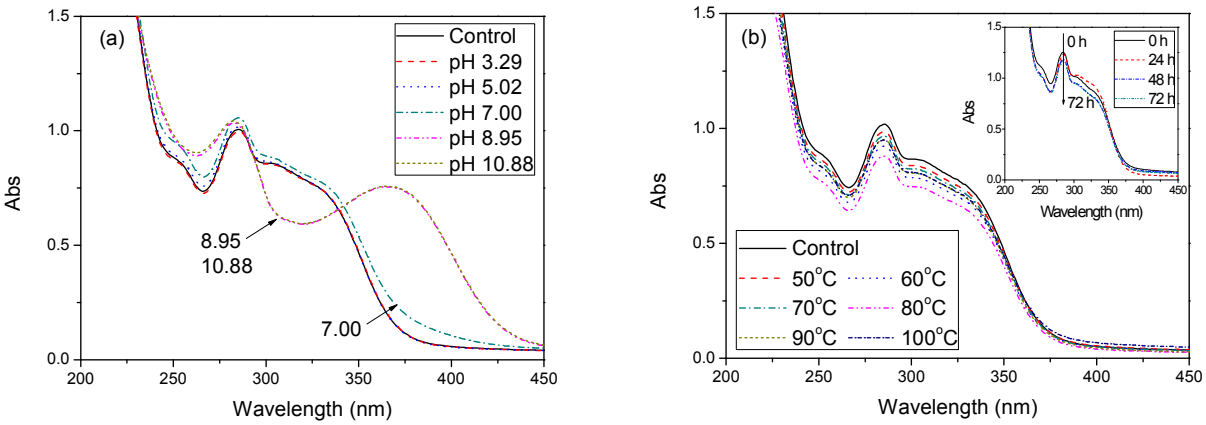


Fig.1 Stability of SMB extract against (a) pH, and (b) heat and ultraviolet light.

Dyeing and UV-protective properties. The building-up properties were studied. The *K/S* values of silk dyed with SMB extract at 2, 4, 6, 8, 10 and 12g/L were 0.90, 1.31, 1.66, 2.07, 2.50 and 2.65, respectively. The color depth linearly increased as the concentration of SMB extract increased. It is demonstrated that the SMB extract shows good building-up properties on silk fabric. It is worth noting that the corresponding *UPF* values at different SMB extract concentration were 16.66, 20.75, 25.84, 28.70, 34.03 and 34.71, showing an increasing trend with the increasing SMB extract concentration and finally reaching the "very good" range of UV protection [5]. In comparison, the *UPF* value of the undyed silk fabric was only 6.58.

Mordant types. In order to study the effect of different mordants on the color and the *UPF* values of the silk dyed with SMB extract, five common mordants were applied to treat the dyed silk fabric. Table 1 lists the *UPF* values and color coordinates of silk fabric treated with SMB extract by post-mordanting dyeing method. It is clearly seen that the fabrics mordanted with ferrous and ferric sulfate and copper sulfate exhibited lower L* values compared with that without mordant, indicating their dull color characteristics. And the enhanced *K/S* values offer the evidence in support of this fact. Moreover, the change of color coordinates of silk fabric mordanted with ferrous and ferric sulfate and copper sulfate indicates that the corresponding silk fabric develop a new color, exhibiting grey, dark brown and yellowish brown colors, respectively. Post-mordant with aluminum sulfate and zinc chloride did not result in any color change in hue but zinc chloride led to an apparent decrease in *K/S*. Hence, the different hues and depth of dyeings can be obtained by means of post-mordanting and selective mordants.

In case of *UPF* values, the trend was the same with the change of *K/S*. The *UPF* values increased with the increasing *K/S*. The decrease in *UPF* and *K/S* of silk mordanted with zinc chloride attributed to the poor complexing property of zinc chloride with SMB extract and the desorption of SMB extract.

Table 1 CIE Lab values and UPFs of silk dyed with SMB extract without and with post-mordanting.

Type of mordants	*L**	*a**	*b**	*K/S (at 365nm)*	*UPF*	*Color obtained*
Without mordant	85.62	3.33	14.78	2.14	28.17	Pale yellow
Ferrous sulfate	55.15	-1.21	0.41	3.41	34.80	Grey
Ferric sulfate	60.79	2.27	12.85	4.53	40.94	Dark brown
Aluminum sulfate	84.09	3.14	15.15	2.19	27.08	Pale yellow
Copper sulfate	64.06	3.89	16.90	3.76	31.82	Yellowish brown
Zinc chloride	85.32	3.53	14.73	1.60	23.36	Pale yellow

To investigate the UV-protective properties of SMB extract clearly, the ultraviolet transmittance spectra of silk post-mordanted with different mordants were depicted in Fig.2. As can be seen, there was a significant difference between the dyed and undyed silk fabrics, indicating the absorbing capacity of SMB extract to UVB (280-315nm). Compared with the silk fabrics without mordanted and mordanted with aluminum sulfate and zinc chloride, the transmittance of those mordanted with ferrous sulfate, ferric sulfate and copper sulfate decreased remarkably over the ultraviolet light range of 280-450 nm. It indicates that the complex compounds of ferrous and ferric sulfate and copper sulfate with SBM extract can absorb UVB and UVA efficiently.

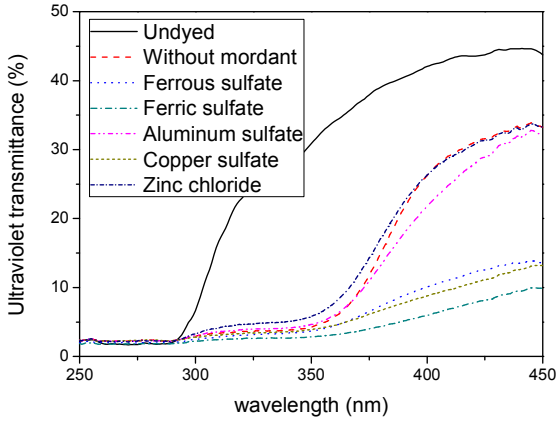


Fig. 2 Ultraviolet spectral transmittance of silk post-mordanted with different mordants.

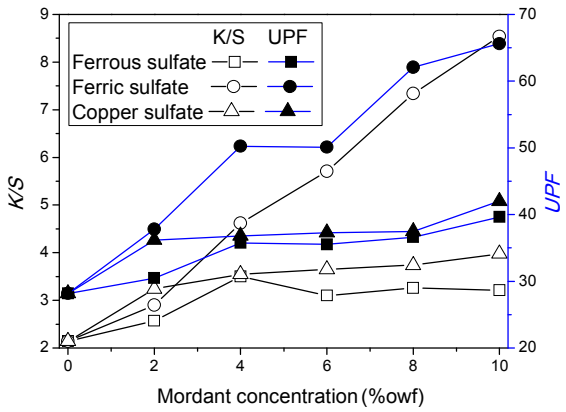


Fig.3 *K/S* and *UPF* values of silk post-mordanted with different mordants and concentrations

Mordant concentration. As shown in Fig.3, both the *K/S* and *UPF* values increased with the increasing mordant concentration. An increase in ferric sulfate concentration caused a dramatic increase in *K/S* and *UPF* values. While a slight increase occurred with the further increase of ferrous sulfate concentration. The same phenomenon has also been observed in copper sulfate. This may be due to the different complexing properties of mordants with SMB extract. In the production practice, the *K/S* and *UPF* values of silk fabric mordanted by ferrous sulfate can be enhanced by increasing mordant concentration.

Color fastness. Table 2 displays the fastness properties of silk fabric dyed with SMB extract without mordant and with post-mordanting at 4%owf mordants. All samples gave excellent rating washing fastness of staining and good to very good rating washing fastness in shade change. As an exception, there is an improvement in light fastness in case of postmordanting with ferric sulfate. In most cases, washing and light fastness properties had no improvement. In some cases, the fastness showed deterioration in the case of mordanting. Ferrous sulfate mordanting resulted in poor color fastness, it can be attributed to the catalytic effect of mordant for SMB extract [3].

Table 2 Fastness of silk dyed with SMB extract without and with post-mordanting.

Type of mordants	*Light fastness*	*Washing fastness*						
		Shade Change	*Staining*					
			WO	PAN	PES	PA	CO	AC
Without mordant	4	4	5	5	5	5	5	5
Ferrous sulfate	3	3	5	5	5	5	5	5
Ferric sulfate	5	4	5	5	5	5	5	5
Aluminum sulfate	4	3	5	5	5	5	5	5
Copper sulfate	4	4	5	5	5	5	5	5
Zinc chloride	4	4	5	5	5	5	5	5

Notes: WO-wool, PAN-acrylic, PES-polyester, PA-nylon 66, CO-cotton, AC-diacetate.

Conclusions

SMB extract was stable at acidic conditions and stable to heat and ultraviolet light. The building-up and UV-protective properties of SMB extract for silk fabric proved to be good. The color yield and UV-protective property of silk fabric were enhanced by mordanting dyeing, but mordanting did not result in significant improvement in fastness properties. Ferrous sulfate, ferric sulfate and copper sulfate as mordants can broaden the range of dyeing shades. In summary, SMB may be developed as a multifunctional natural agent for silk with colorant and UV-protective properties.

Acknowledgements

This work was funded by the Priority Academic Program Development of Jiangsu Higher Education Institution, and by the Technology Innovation Foundation of National Engineering Laboratory for Modern Silk.

References

[1] R.C. Tang, H. Tang and C. Yang. *Ind. Eng. Chem. Res*. Vol. 49 (2010), p. 8894.
[2] S.S. Sun and R.C. Tang. *Ind. Eng. Chem. Res.* Vol. 50 (2011), p. 4217.
[3] S. Ali, T. Hussain and R. Nawaz. *J. Clean. Prod*. Vol. 17 (2009), p. 61.
[4] X.X. Feng, L.L. Zhang, J.Y. Chen and J.C. Zhang. *J. Clean. Prod*. Vol. 15 (2007), p. 366.
[5] Sun protective clothing - Evaluation and classification; AS/NZS 4399:1996.

© (2011) Trans Tech Publications, Switzerland
doi:10.4028/www.scientific.net/AMR.331.261

Study on the Enzyme Desizing Process for Cotton Fabric Using Ultrasonication

Qiming Zhao[1,a], Shanyan Zhang[1,b]

[1]School of Textile and Clothing, Wuyi University, Middle Yingbin road 99, Jiangmen, Guangdong, 529020, China

[a]zhqm@wyu.cn, [b]ap0511240@163.com

Keywords: cotton fabric, Ultrasonication, desizing enzyme, auxiliary devices, orthogonal experiment.

Abstract. The auxiliary devices of ultrasonic treatment was designed and manufactured. The cotton fabric was desized using 2000L desizing enzyme with the conventional enzyme desizing process and ultrasonic enzyme desizing process respectively. Through the orthogonal experiment, the optimum process conditions of conventional enzyme desizing process and ultrasonic enzyme desizing process were determined. For the conventional enzyme desizing process, the optimized desizing conditions of cotton fabrics were: desizing enzyme dosage was 1.5g/l, temperature was 80℃, PH value was 6, and time was 60mins. The optimum process conditions of ultrasonic enzyme desizing process were: desizing enzyme dosage was 1.5g/l, temperature was 50℃, PH value was 6 and time was 45minutes. The research result indicates that, under the same desizing condition, ultrasonication can improve the desizing percentage and whiteness of cotton fabric, but the fabric strength loss increases slightly. And for the same required desizing percentage, the ultrasonic enzyme desizing process saved time and reduced the temperature of experiments compared with traditional enzyme desizing process.

Introduction

With the development of the ultrasonic technology, using of ultrasonic in wet processing of textile materials have been paid more and more attention. For the ultrasonic technology, the powerful wallop is developed by the cavitation effect coming from the ultrasound oscillation, which can strengthen the mass and heat transfer, and improve the activity of reactant molecules and increase the chance of colliding. Ultrasonic technology can be applied in the desizing, boiling, bleaching and other short-processes pretreatment process[1-5]. Specially, using of ultrasonic technology in enzyme desizing process can improve the activity and the diffusion rate of enzyme molecular, enhance the accessibility of the solution to the fiber and increase the treatment efficiency[6,7]. Moreover, it can realize time and energy saving at the same required desizing percentage.

The sample should be rotated, so as everywhere of which can get the same ultrasonic energy during the ultrasonic enzyme treatment process. Due to the fact that the ultrasonic generator applied in this research has no the fuction of temperature controlling and sample rotating, the auxiliary devices was first manufacture to realize the functions above. And then, through the orthogonal experiment, the best processes of the normal enzyme desizing technology and ultrasonic enzyme desizeing on the cotton woven are studied.

Experimental

Materials. Purified plain cotton(commercial).Iodine(AR). Potassium Iodide (AR). Dextrin (AR). Soluble starch (AR). Disodium hydrogen phosphate (AR). Citric acid (AR).Enzyme(2000L, Nonozymes Company). JFC(nonionic infiltrator, Sida textile chemical Co., LTD). Washing powder (commercial)

Equipments. L-1200 Ultrasonic cleaner with single slot, JA5003 Electronic analytical balance, Y802N Basket conditioning oven, AHYQ501 The Thermostatic Water Bath, YG(B)026D-250 Electronic fabric strength machine, WSB-V Intelligent whiteness Measuring Instrument, Self-made auxiliary device.

The self-made auxiliary device mainly includes the two parts of temperature controller and sample rotator. The temperature controlling part consists of a cylinder, as shown in Fig.1, and AHYQ501 super constant temperature water-bathing. The rotating part consists of a stirrer and self-made stirring rod head, as shown in Fig.2. The cylinder is placed in ultrasonic cleaning trough, and the stirring rod drives the cloth sample rotate in the solution of the cylinder. Moreover, stirring rod head has also a stirring effect, which can make the test solution evenly

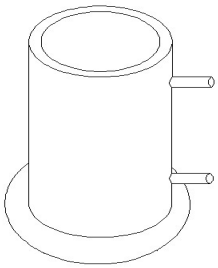


Fig. 1 Diagram of the cylinder

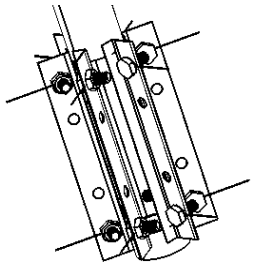


Fig. 2 Diagram of the stirring head

In Fig.1, the cylinder consists of two stainless steel tube with the thickness of 1mm and the diameter of 150 mm and 160 mm respectively, and the water can circulating flow in the slot between these two tubes. In Fig.2, six stainless sheet of 80mm×8mm×0.2mm are welded in the bottom of the stirring rod at intervals of 60°. Another six stainless steel sheets were fast to each stainless steel sheet above with two bolts, and spacing adjustable two fine-needles are placed in the gap of each pair sheets. The needles can pitch cloth sample when enwound on the stirring head.

Treatment processes. Conventional enzyme desizing process is as follow: grey cloth→ dipping (5 min in hot water) → squeezing→ dipping again(enzyme desizing treating fluid) → washing (washing twice at 85~95˚C for 20min) → cold water wash → dry. In the ultrasonic enzyme desizing process, ultrasonication is added in the second dipping stage of the conventional enzyme desizing process and the power density is of 0.5 W/cm^2.

Experimental design. Orthogonal experimental method was used in choosing the optimum process of conventional enzyme desizing process and ultrasonic enzyme desizing process respectively. Four factors in orthogonal test are : desizing enzyme dosage (A), Desizing Temperature (B), PH value (C) and Desizing time (D) . Table 1 and Table 2 show the orthogonal experimental factors and their levels for conventional enzyme desizin process as well as ultrasonic enzyme desizing process respectivelly.

Tab.1 Orthogonal conventional experiment

Level	A(g/L)	B(˚C)	C	D(min)
1	0.5	40	5	20
2	1.0	60	6	40
3	1.5	80	7	60

Tab.2 Orthogonal ultrasonic experiment

Level	A(g/L)	B(˚C)	C	D(min)
1	0.5	40	5	15
2	1.0	50	6	30
3	1.5	60	7	45

Measurements. The warps of cotton fabric were sized with starches. The iodin volume method was used to determine the desizing percentage[8]. The Intelligent Whiteness Measuring Instrument WSB-V was used to measure the whiteness of cotton fabric which is dried and moisture equilibrium equilibrated. The breaking strength of cotton fabric was measured by YG026pc-250 Electronict strength tester.

Results and discussion

Discussion of the optimum process conditions of conventional enzyme desizing treatment. The results and analysis of orthogonal experiment are given in Table 3. Desizing percentage (E),Whiteness(F), and Breaking strength (G) are target value of orthogonal experimental.

Tab. 3 The experiment data and result analysis

NO		A	B	C	D	E(%)	F(%)	G(cN)
1		1	1	1	1	51.851	52.1	973.3
2		1	2	2	2	66.543	52.8	923.2
3		1	3	3	3	77.932	53.4	874.1
4		2	1	2	3	81.781	53.9	854.5
5		2	2	3	1	59.520	53.1	943.6
6		2	3	1	2	72.625	53.3	901.4
7		3	1	3	2	73.179	52.1	903.5
8		3	2	1	3	83.559	54.3	844.7
9		3	3	2	1	68.625	53.7	914.8
E(%)	k_1	65.442	68.937	69.345	59.999			
	k_2	71.309	69.874	72.316	70.782			
	k_3	75.121	73.061	70.210	81.091			
	R_1	9.679	4.124	2.971	21.092			
F(%)	k_1	52.8	52.7	52.9	53.0			
	k_2	53.4	53.4	53.5	52.7			
	k_3	53.4	53.5	52.9	53.9			
	R_2	0.6	0.8	0.6	1.2			
G(cN)	k_1	923.5	910.4	906.5	943.9			
	k_2	899.8	903.8	897.5	909.4			
	k_3	887.7	896.8	907.1	857.8			
	R_3	35.8	13.6	9.6	86.1			

For the desizing percentage, the extreme difference order of the for factor is: D>A>B >C, and the best experiment program is $A_3B_3C_2D_3$. As for the whiteness, the extreme difference order is: D>B>C > A, the best best experiment program is $A_2B_3C_2D_3$ or $A_3B_3C_2D_3$. For the breaking strength, the extreme difference order is: D>A>B>C, the best experiment program is $A_1B_1C_3D_1$. Of the three indexes, desizing percentage is the most important index, considering all these three indexes synthetically, and the production cost item, the final optimum process scheme is: enzyme dosage 1.5g/l, desizing temperature 80℃, PH value 6, and desizing time 60min.

Discussion of the optimum process conditions of Ultrasonic enzyme desizing treatment. The results of orthogonal experiment and analysis are given in Table 4.

Tab. 4 The experiment data and result analysis

NO		A	B	C	D	E(%)	F(%)	G(cN)
1		1	1	1	1	63.214	53.9	924.7
2		1	2	2	2	77.953	54.6	878.2
3		1	3	3	3	79.226	55.5	830.4
4		2	1	2	3	85.006	55.9	812.1
5		2	2	3	1	71.715	55	896.4
6		2	3	1	2	80.448	55	857.3
7		3	1	3	2	84.241	53.9	859.3
8		3	2	1	3	93.014	56.3	802.6
9		3	3	2	1	75.148	55.6	870.1
E(%)	k_1	73.464	77.487	78.892	70.026			
	k_2	79.057	80.894	79.369	66.230			
	k_3	84.134	78.274	78.394	85.749			
	R_1	10.670	3.407	0.975	19.519			
F(%)	k_1	54.7	54.6	55.1	54.8			
	k_2	55.3	55.3	55.4	54.5			
	k_3	55.3	55.4	54.8	55.9			
	R_2	0.6	0.8	0.6	1.4			
G(cN)	k_1	877.8	865.4	861.5	897.1			
	k_2	855.3	859.1	853.5	864.9			
	k_3	844.0	852.6	862.0	815.0			
	R_3	33.8	12.8	2.5	82.1			

For the desizing percentage, the extreme difference order is: D>A>B >C, the best experiment program is $A_3B_2C_2D_3$. As for the whiteness, the extreme difference order is: D>B>A >C, the best experiment program is $A_2B_3C_2D_3$. For the breaking strength, the extreme difference order is: D>A>B >C, the best experiment program is $A_1B_1C_3D_1$. Of the three indexes, desizing percentage is the most important index, considering all these indexes synthetically, and the cost item, the optimum process scheme is: desizing enzyme dosage 1.5g/l, desizing temperature 50℃, PH value 6, and desizing time 45min.

Effect of Ultrasonic on the enzyme desizing. From Table 3 and Table 4, it can be seen that ultrasonic enzyme desizing treatment improves the desizing percentage and whiteness by 11.7% and 3.6% respestively, but decreases the breaking strength by 5.2% as compared with conventional enzyme desizing treatment. Ultrasonic have the function of washing and emulsificationare, which are the reasons for the enhancement in whiteness of cotton fabric. The breaking strength of cotton fabric declines, which is because the cavitated action of Ultrasonic will increase the weaknesses of fiber. But it is not enough to affect the wearability of cotton fabric.

Under the same required desizing percentage condition. Ultrasonic applying can reducing treatment temperature and save treatment time. Comparing the test result of numbere 3 in table 3 with that numbere 2 in table 4, it can be found that with the same desizing percentage and the quantity of desizing enzyme, the Ultrasonication can decrease the treat temperature 30℃and time about 30 min.

CONCLUSIONS

By using self-made auxiliary devices in the experiment, the optimum process conditions of the convensional enzyme desizing and Ultrasonic enzyme desizing through orthogonal test are studied in this paper. Furthermore, the effect of ultasonication on enzyme desizing process of cotton fabric is analyzed. The main conclusions are as follows.

The optimum process conditions of the conventional enzyme desizing of cotton fabric is desizing enzyme dosage 1.5g/l, temperature 80˚C, PH value 6, and time 60min.

The optimum process conditions of Ultrasonic enzyme desizing of cotton fabric is desizing enzyme dosage 1.5g/l, temperature 50˚C, PH value 6, and time 45min.Ultrasonication increases the whiteness and desizing percentage of cotton fabric, but decreases the breaking strength damage slightly.

Under the same desizing percentage condition, Ultrasonication saves treatment time or reduce the treatment temperature.

References

[1] G. Portenlänger and H. Heusinger: Ultrasonic-sonochemistry Vol. 4(1997), p.127-130

[2] J. Moses: Colourage Vol. 43(1996), p.19-25

[3] Yunling Gao: Textile Dyeing and Finishing Journal (2000), p. 27-28, in chinese

[4] K. A. Thakore : Textile Technology Overseas (1991), p.28-33, in chinese

[5] Jiamin Yin,Juping Wang,Feng Zhang and Yuyue Chen: Vol. 27(2006), p. 31-34, in chinese

[6] Lan Wang and Jun Yan: Journal of Textile Research Vol. 27(2006), p. 77-79, in chinese

[7] Aimin Tang, Hongwei Zhang and Gang Chen: Journal of Cellulose Science and Technology Vol.13(2005), p. 26-33, in Chinese

[8] Suying Cai, in: Dyeing and Finishing Technological Experiment, edtied by China's Textile Industry Publising, Beijing, NY(2002), in press.

© (2011) Trans Tech Publications, Switzerland
doi:10.4028/www.scientific.net/AMR.331.265

Synthesis and Application of Isothiazolinone as Durable Antibacterial

Dejia Kong[1,a], Zhendong Liu[1,2,b] and Yanli Li[1,c]

[1]School of materials science & engineering, Beijing institute of fashion technology, Beijing, 100029, China

[2]Beijing key laboratory of clothing materials R&D and assessment, Beijing, 100029, China

[a]kdj06@163.com, [b]bictlzd@tom.com,[c]liyanli0523@163.com

Keywords: Reactive, Antibacterial, Cotton Fabric, Finishing

Abstract. A new antibacterial with two reactive groups was synthesized from isothiazolin-3-one and characterized by ^{1}H-NMR and ESI-MS. Through the orthogonal experiments the optimal finishing process was got, that was bath ratio 1:20, Na_2SO_4 20 g/L, $NaHCO_3$15 g/L, T_1:60˚C, T_2:70˚C, t_1:10 min, t_2:20 min, t_3:30 min (as shown in fig.1). The antibacterial evaluations of treated cotton fabrics showed that the antibacterial rates for Escherichia coli and Staphyloccocus aureus were 95.64% and 97.83% respectively, and 88.13% and 90.05% respectively after 30 washing cycles. The results indicated that the treated fabric had excellent antibacterial performance and washing durability.

Introduction

The growth of micro-organisms, in particular bacteria, on textiles leads to a number of undesirable outcomes, including unpleasant odor, discoloration of the fabric, reduction in fabric strength, and even harm to the health of human. All of these can be prevented or diminished through the antimicrobial finishing of the textiles. Therefore, safe extermination of microbe is very important to human health care. The intensive research on antimicrobial textiles have been reviewed in a number of recent articles [1~3]. The antimicrobial materials have the potential to reduce the transmission of infectious diseases and have recently become highly popular in certain products, such as medical textiles and plastics. Cotton is one of the most popular textiles, especially for underwears, and antibacterial textiles are gradually becoming consumers' favorite. At present, antibacterial treatment of cotton fabric are mainly through finishing[4-5]. For improving the wash-bearability and durability of antibacterial textiles, the only way is to enhance the binding force between the antibacterial and fiber. Various small organic antibacterials with different reactive groups have attracted wide attention. Another method makes use of a regenerable antibacterial precursor[6-7].

The 3-isothiazolone derivatives have shown antibacterial, antifungal, pesticidal and algaecidal activities and have shown to be useful as preservatives for the control of living organisms in cosmetics, paints, soaps, fabrics, leather, swimming pools and etc. However, the poor binding ability to fiber restricted its use in textiles[8-10]. Therefore, it is of great significance to change it into a reactive antimicrobial which can form covalent bond with fiber by chemical modification. The isothiazolin-3-one with a reactive siloxane coupling group had been synthesized before, but due to its poor water-solubility, it wasn't easy to manipulate the finishing process[11]. As continue to this work, we had redesigned and synthesized a new reactive antibacterial agent.

2. Experimental

2.1 Materials and instruments

Cotton fabrics; cyanuric chloride; sulfuryl chloride; thionyl chloride; enthanolamine; enthanol; phthalic anhydride; hydrazine; acetone; N,N-dimethylformamide; sodium hydride; dichloromethane; am monia; agar; pancreatic protein jelly; soybean protein jelly; beef extract; sodium chloride.

Avance II 500MHz NMR (Bruker, Germany); RCMS-2010 mass spectrometer (Shimadzu, Japan); MIR-153 thermostatic incubator (SANYO Electric Biomedical CO. Ltd, Japan); Milliq Academic water purification system (Millipore, US); J-2 colony counter (Jiangyan Kangtai Medical Equipment, China); YX- 280 steam disinfection pot (Jiangyin Binjiang Medical Equipment, China).

2.2 Preparation of the reactive antibacterial

Sodium 2-(p-aminophenylsulfonyl)ethyl sulfate (8.08 g, 28.8 mmol) was dissolved in 50mL ice water in a 100mL flask and the pH was adjusted to 7 with sodium carbonate. While stirring and control temperature between 0˚C and 5˚C cyanuric chloride (5.05 g, 27.4 mmol) was added. The reaction process was monitered with TLC while the pH was kept at about 6 with 15% aqueous solution of sodium carbonate. When the reaction was over, N-(2-aminoethyl)-isothiazolin-3-one (3.95 g, 27.4 mmol) was added dropwise to this solution through a drop funnel. The suspension was heated slowly to 50˚C. At this stage the pH was controlled in the range of 7-8 till the reaction was finished. The reaction mixture was salted out with a 20% sodium chloride solution. Collect the solid by filtration and wash the solid with 10% sodium chloride solution to give light brown solid 13.2 g, yield 86.4%.

2.3 Technology of finishing

Bleached cotton fabric in this work were washed in hot water with NaOH (1 mol/L) and air-dried at RT before use. The complete process was depicted in figure 1. T_1 was the temperature of absorption stage. T_2 was the temperature for fixation. And t_1, $t_2$and t_3 were the times for different stages. Cotton fabrics were treated with 5% owf antibacterial aqueous solution in 1:20 bath ratio. The fabrics were first treated at T_1 temperature for t_1 and then sodium sulfate was added to about 20 g/L, and then for t_2. Then the solution was heated to 70˚C and sodium bicarbonate was added to 15 g/L. The bath was kept at 70˚C for additional t_3 min. The treated fabrics were pre-dried at 80 ˚C for 10 min and baked at 160˚C for 2 min. Then the fabrics were washed according to a standard program.

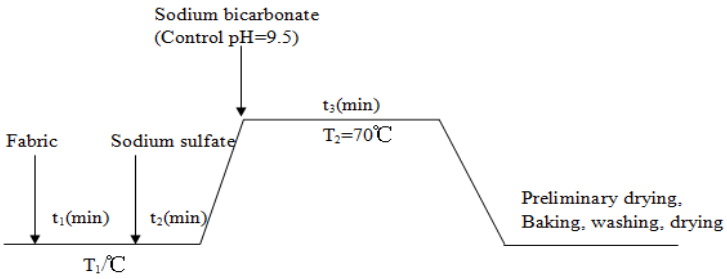


Figure 1 Route of finishing

2.4 Tests antibacterial performance

Gram-negative Escherichia coli and gram-positive Staphyloccocus aureus strains were used for antibacterial evaluation.

Tests were conducted according to the Chinese national standard GB/T20944.3-2008.

3. Results and discussion

The route of synthesis is depicted as below

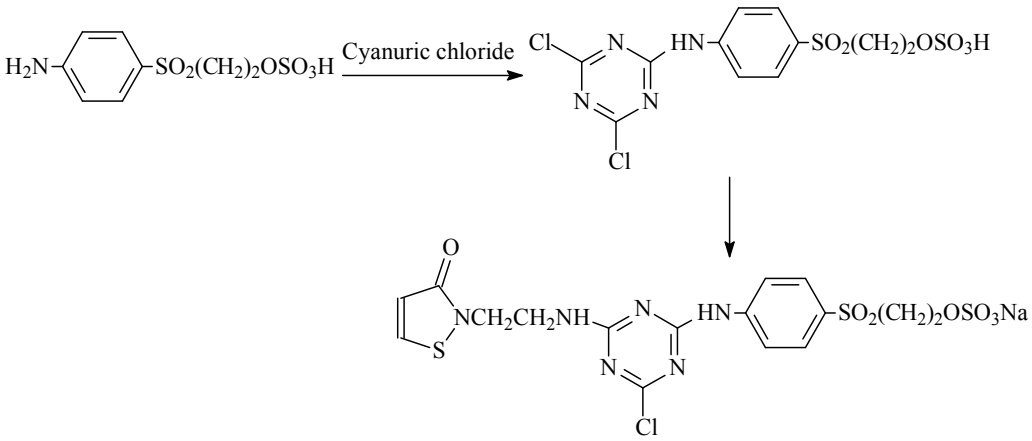


Figure 2 Route of synthesis

3.1 Synthesis and structure characterization

N-(2-aminoethyl)-isothiazolin-3-one was prepared before use. In our previous work, a reactive isothiazolinone with a siloxane coupling group was synthesized. Since there was no ionic group present, the water solubility was poor. In order to improve the aqueous solubility, sodium 2-[(p-aminophenyl)sulfonyl]ethyl sulfate was incorporated into the molecule. The advantage of this moiety is that it can not only contribute to solubility but also function as a reactive group. Therefore, the two reactive groups are similar to some common reactive dyestuffs. This feature is more favorable to form a covalent linkage between antibacterial and fiber. Thus, more efficient finishing process and more wash-bearable and durable antibacterial property should be anticipated.

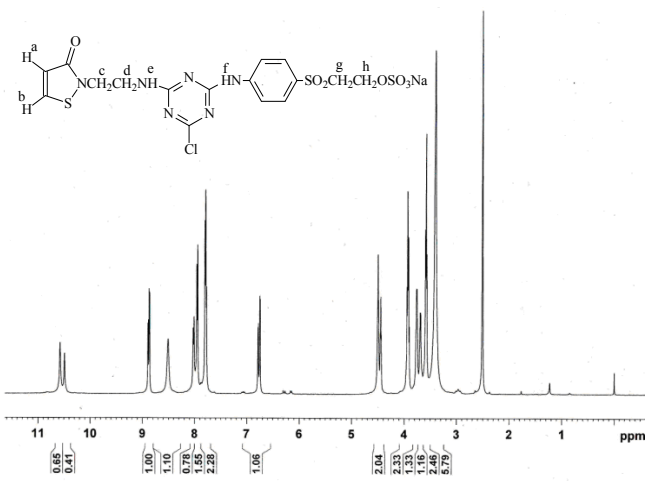


Figure 3 ^{1}H NMR of target molecule

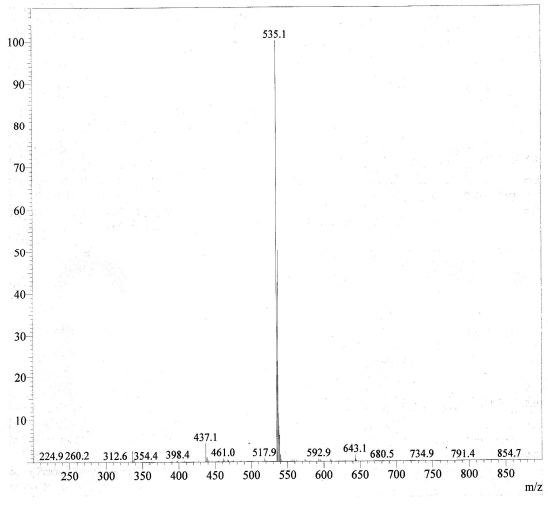


Figure4 ESI-MS spectrum of TM

Table 3 ^{1}H-NMR analysis of TM

δ(ppm)	Splitting	Number of H	Belonging
3.5	T	2	d
3.6~3.7	Q	2	e
3.9	Q	2	i
4.4	Q	2	j
6.7	Q	1	a
7.7	T	2	g
7.9	D	2	h
8.0	D	1	e
8.5	S	1	f
8.8	Q	1	b

The results shown in fig. 3 and table 3 were consistent with the molecule of the antibacterial. The final product was also proved with ESI-MS. The molecular weight of this salt final product is 558. Thus, the highest peak with m/z 535 in fig. 4 gives the clear evidence that the peak is M−Na.

3.2 Finishing and Antibacterial evaluation

The reactive antibacterial possesses two reactive groups, the triazine ring chlorine and the vinylsulfone precursor. When applied for the finishing of cotton fabrics, both of the reactive groups could form covalent bonds with the hydroxyl group on cellulosic fiber. There are many factors that may have influence on the outcome of finishing, we think T_1, t_1, t_2, t_3 are the major ones. In order to get an optimal finishing process, 4 factors and 3 levels orthogonal experiments were designed as table 4.

From the antibacterial data, it was obvious that the treating temperature and time were the most prominent factors attributing to the antibacterial performance. Higher temperature and prolonged time were more beneficial to inhibition rate. This implied that higher temperature could accelerate the coupling between antibacterial and fiber macromolecule and prolonged time could help this process be closer to completion. Thus, more antibacterial should be immobilized to fiber and form a covalent bond. That's why 5% owf could give the same results as 20% owf[11].

Table 4 Orthogonal results on the inhibition rate of S. aureus

Levels	T_1(˚C) A	t_1(min) B	t_2(min) C	t_3(min) D	Inhibition rate for S. aureus(%)
1	40	10	10	20	89.49
2	40	15	15	25	90.67
3	40	20	25	30	92.97
4	50	10	15	30	95.67
5	50	15	20	20	92.03
6	50	20	10	25	93.60
7	60	10	20	25	96.69
8	60	15	10	30	94.30
9	60	20	15	20	91.23

Table 5 Range analysis of inhibition rate of S. aureus(%)

$\overline{K}$	A	B	C	D
$\overline{K}_1$	90.94	93.95	92.46	90.92
$\overline{K}_2$	93.77	92.33	92.53	93.65
$\overline{K}_3$	94.07	92.60	93.90	94.31
R	3.31	1.35	1.44	3.39

K: Arithmetic mean of each factor, R: range

Table 6 Inhibition tests and washing durability

	Washing cycles	Inhibition of E. coli(%)	Inhibition of S. aureus(%)
sample	0	95.64	97.83
	10	93.18	94.54
	20	92.57	92.57
	30	88.13	90.05

It was seen that $R_D > R_A > R_C > R_B$, the most prominent factor was t_3 and the least was t_2 from table 5. The optimal technology was $A_3B_1C_3D_3$. A further experiment was conducted to confirm this. The cotton fabric treated by this process gave the inhibition rate of S. aureus 97.83%. Hence, the optimum finishing process was T_1:60˚C, t_1:10min, t_2:20min, t_3:30min. From table 6, it was clear that the finished fabrics had outstanding antibacterial performance and prominent washing durability both for gram negative and gram positive bacteria[5].

Conclusions

A reactive antibacterial agent with two reactive groups was synthesized. The immobilization was fulfilled through a normal finishing process in water. The finishing process was more efficient than the former siloxane antibacterial and the usage was greatly reduced. Through the orthogonal experiments, the optimal finishing process was T_1:60˚C, t_1:10min, t_2:20min, t_3:30min. The treated cotton fabrics showed excellent broad band antibacterial property. Even after 30 washing cycles, the fabrics could still reserve more than 88% inhibition which meant exceptional washing durability.

Acknowledgement

The research was financially supported by Beijing Educational Committee (KM200810012006) and Beijing key laboratory of clothing materials R&D and assessment (2010ZK-02).

References:

[1] Y. Gao, R. Cranston, An Effective Antimicrobial Treatment for Wool Using Polyhexamethylene Biguanide as the Biocide, Part 1:Biocide Uptake and Antimicrobial Activity. http://onlinelibra ry.wiley.com/doi/10.1002/app.32088/full(accessed April 2010)
[2] Y.Gao, R.Cranston: J.Text. Res. Vol. 78 (2008), p. 60-72
[3] G.Q. Lu, D. C. Wu, R. W. Fu: React. Funct. Polymers. Vol. 67 (2007), p. 355–366
[4] N. Hashemi and G. Sun: J. Ind. Eng. Chem. Res. Vol. 49 (2010), p. 8347–8352
[5] G.Q. Lu, W. M. Dong, H.J. Zuo: Ion Exch. Adsorp. (In Chinese). Vol. 26 (2010), p. 289-299
[6] Z.J. Yin, Y.L. Guo, Y. Jin, et al: China Text. Leader (In Chinese). Vol. 11 (2007), p. 79-83
[7] J.X. He, Q. Zhu, J.S. Wang: J. Chin. Text. Univer (Eng. Ed). Vol. 15 (1998), p, 1-5
[8] A. Khalaj, N. Adibpour, A. R. Shahvedi, et al: Eur. J. Med. Chem. Vol. 39 (2004), p. 699-705
[9] J.O. Morley, A. J. Olive, M. H. Charlton: J. Mol. Struct. Vol. 429 (1998), p. 103-110
[10] S.F. Heng, X. Liu, Y. Yang, et al: J. Text. Res. (In Chinese). Vol. 30 (2009), p. 87-92
[11] Z.D. Liu, X. Liu, X.B. Chen, Synthesis of a Reactive Antibacterial Agent and Preliminary Evaluation on Antibacterial Efficiency, C. The 4th Textile Bioengineering and Informatica Symposium Proceedings, Beijing, 2011. p. 225-229

© (2011) Trans Tech Publications, Switzerland
doi:10.4028/www.scientific.net/AMR.331.270

TiO_2 and ZnO Water Sol preparation by Sol –Gel Method and Application on Polyester fabric of Antistatic Finishing

Yanyan Chu[a], Qing Wang[b] and Shizhong Cui[c]

[1]ZhongYuan University of Technology, Zhengzhou, Henan, 450000, China

[a]yychu@126.com, [b]wangq_6588@163.com, [c]szcui@zzti.edu.cn

Keywords: Polyester Fabric, Water sol, TiO_2, ZnO, Antistatic Finishing, Washing Fastness

Abstract: Pure TiO_2 water sol, pure ZnO water sol and three compound TiO_2/ZnO water sols are prepared under low temperature. Then the padding and baking process is used to put the functional sol liquid on the fabric. SEM is use to analyzed the change of surface feature and the result show that all of the water sol except pure ZnO water sol liquid formed a thin film on the fiber The stability of pure ZnO water sol is the best one and the pure TiO_2 water sol is the worst one at temperature of 15˚C. The compound water sols stabilities are between these two water sols and with the more amount of ZnO, the stability last longer. Both mole of TiO_2 and ZnO with the rate of 5 to 5 and 7 to 3 display the best antistatic behavior, but the washing fastnesses are not good. After treatment, the moisture regain displays most dramatically changes; the next one is whiteness of fabric, but the other physical and mechanical properties have a little change.

Introduction

The polyester fiber is widely used in apparel and decoration fields, but the main drawback of it is prone to generate electrostatic, which restrict it to apply to more areas. The electrostatic not only make the clothing likely to attach to limbs and trunks and adsorb dust, which make people feel uncomfortable and look unbeautiful, but also have harm to the health of people ,such as reduce calcium concentration in the blood and increase the calcium content in urine. Therefore， it become a focus to strength the antistatic of polyester fabric[1-3]. It is a convenient method to treat the fabric and make it get antistatic property. The common material used to do antistatic finishing are usually clarified to two types, one is organic materials including quaternary ammonium salts, polyoxyethylene, phosphonate and polyether and the other one is inorganic substances, such as titanium dioxide[4-5], tin peroxide and antimonic oxide. Nowadays, the inorganic material get more attention to treatment for antistatic of polyester because of its higher chemical stability, heat stabtility non-toxic and nonirritant.

The inorganic materials are usually made nano size to treat on fabric. There are two measures. One is to dissolve nano oxide particles in some solvent and then treat it to the fabric, but it has been found that there are many problems using this way of process, such as self-oxidation and aggregation of nano grain. The other is to make sol by sol-gel which is one of measure to make nano material and treat the sol to fabric, which is under investigation by more scholars [6-10]. This method can be controlled at the early preparation period and the material is even to nano grade or goes so far as to molecular size. It requires lower synthetic temperature and process conditions for reaction. The product is evener and purer. When it is used to textile treatment, it is usually put on the fabric at the stage of sol liquid and use the padding and baking process. It is a novel method to finish fabric with nano material and avoid the process to anneal the gel under high temperature to form oxide material particles and the nano particles aggregation in dissolving process before treatment.In this study, the water sol containing pure TiO_2 water sol, pure ZnO water sol and compound TiO_2/ZnO water sol are prepared under low temperature. Then the padding and baking process is used to put the functional sol liquid on the fabric. Then the antistatic property and wearability are evaluated in further analysis.

Experiment

Precursor solutions for TiO_2 /ZnO compound sol were prepared using tetrabutylorthotitanate, zinc acetate hydrated, dehydrated alcohol, ethanolamine, acetic acid glacial, and distilled water. Zinc acetate dehydrate and 1/3 dehydrated alcohol were dissolved in distilled water. After stirring vigorously for about 15min at room temperature, zinc acetate dehydrate was dissolved completely, then ethanolamine was dripped to it and the solution viscosity increased gradually. In the end, it became white sedimentation which was $Zn(OH)_2$. At this time propriety acetic acid glacial was added to it in order to dissolve the white sedimentation. Until the white sedimentation dissolved and the solution became transparency, tetrabutylorthotitanate and 1/3 dehydrated alcohol and acetic acid glacial were mixed together and added to the solution. After stirring vigorously for 1.5h, transparent and colorless compound water sol had been gained. According to the rate of mole of tetrabutylorthotitanate and zinc acetate hydrated，three compound water sol with mole rate of 3:7, 5:5 and 7:3 were obtained.The ZnO water sol was prepared in the following step. Zinc acetate dehydrate and dehydrated alcohol were mixed and dissolved in distilled water. After about 10min, ethanolamine was added into the mixture and a white sedimentation appeared which was $Zn(OH)_2$. Followed by propriety acetic acid glacial was added to it and a transparent and colorless turned up and then stirred it vigorously for 1.5h and came into being ZnO water sol.The TiO_2 water sol was got through the following procedure: Tetrabutylorthotitanate mixed uniformly with dehydrated alcohol and acetic acid glacial together and be added to water with 1/3 dehydrated alcohol, and then stirred the mixture for 1.5h, thus TiO_2 water sol was obtained.

The warp count and weft count of pure polyester fabric was 630 radix/10cm and 310 radix/10cm.The fabric was dipped and rolled two times respectively with 0.2Mpa stress. Then dried at 80˚C for 3min and later baked it at 150˚C for 4min. After that, put the fabric baked in a scour prepared and washed it at 95 ˚C for 3min and At last dried it at 80˚C for 3min.The fabric finished was kept in a hermetic bag.

The stability of water sol was measured by the time of duration when the clear and transparent sol began to become muddy at temperature of 15˚C. Scanning electron microscope(SEM)(JSM-6360LV, Japan) was used for the morphological observations of all samples. The surface compare toresistance were observed from the ZC36 model of 1017ultra-high resistance and 10-14 Micro-current Measurement at temperature of 20˚C and relative moisture degree of 50%. The strength and elongation of fabric was tested on Instrong and the whiterness obtained from the Datacolour. The rigidity got from LLY-01B stiffness instrument controlled by computer and the gas permeability was gained on 461D fabric gas permeability instrument. The moisture regain get under the condition of temperature of 20˚C and relative moisture degree of 60%.

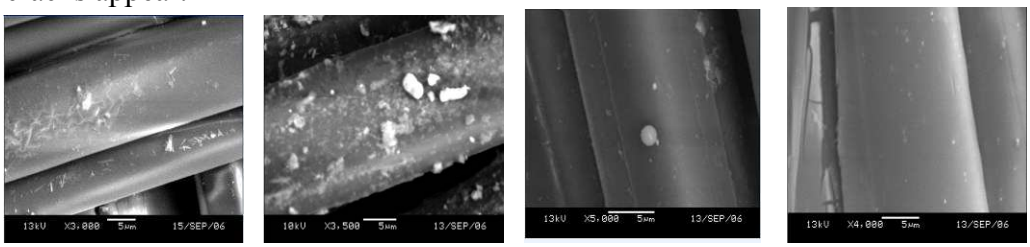
Results and Discussions

It can be seen clearly from table 1 that all of the five sorts of water sol don’t become muddy after three month when they are stored in the refrigerator with temperature of 5˚C and all of them behave differently on the condition of temperature of 15˚C. The pure ZnO water sol keeps clear and transparent both under condition of 15˚C and 5˚C, which means the temperature doesn’t have any effect on the stability of it. The pure TiO_2 water sol only lasts for 4days at the temperature of 15˚C. The other three compound water sol stabilities on the condition of 15˚C are decreasing with the higher mole rate of TiO_2. This maybe because ZnO water sol is prone to constitute line polymer but TiO_2 is likely to form three dimensional polymers, which is namely gel. Therefore, the more rate of TiO_2, the less stability the compound water sol will be.

Table 1 Stability of all water sol

Water sol	rate of mole between TiO_2 and ZnO	time of duration(days) (15˚C)	stored in refrigerator at temperature of 5˚C for three month
Pure ZnO water sol	0:10	Don't become muddy	
TiO_2 /ZnO compound sol	3:7	60	
TiO_2 /ZnO compound sol	5:5	40	Don't become muddy
TiO_2 /ZnO compound sol	7:3	15	
Pure TiO_2 water sol	10:0	4	

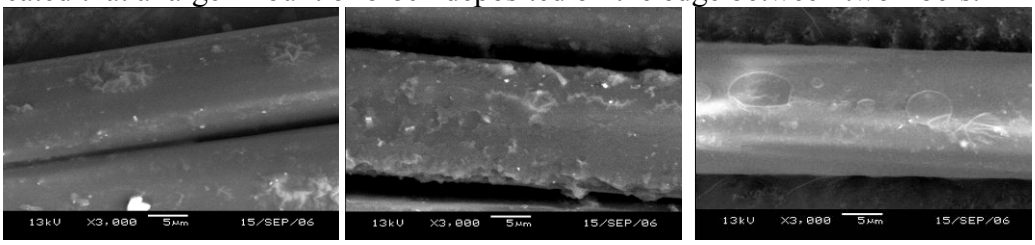
Fig.1(a) shows images of polyester fiber without sol treat. The image clearly indicates that it is smooth on its surface. The image of polyester fiber treated with pure ZnO water sol shows that a great deal of particles on the surface of fiber and not form a thin and consecutive film on it. The ZnO gel is deposited on the fiber and it is not even and regular. From the Fig.1(c), it is clearly clarified that a thin and consecutive gel film is formed on the fiber and it is tightly attach to the fiber. The film is a little more transparent and thinner than that formed with pure TiO_2 sol on polyester fiber, which is shown in Fig.1(d). Both of the film on the Fig (c) and (d) are even and uniform and there are not any particles on them. However, the edge of film between the two fibers treated with TiO_2 does not continue, in which the cracks appear.



(a) (b) (c) (d)

Fig.1 (a) SEM image of original fiber and SEM image of polyester fiber treated (b) with pure ZnO water sol (c)with compound ZnO/TiO_2 water sol at rate of 5 to 5(d) with pure TiO_2 water sol

Fig2.(b') shows the appearance of fiber treated with pure ZnO water sol after 50 times washing. Compared with that correspondent fiber without washing, the surface image is different. It is shown that some films appear on the fiber but not attach the fiber firmly. Some area of the film is filled out and other area is hollowed. The particles are substituted by the film. Fig2.(c') shows the image of fiber treated with compound ZnO/TiO_2 water sol at rate of 5 to 5 after washing with 50 times varies greatly from the one not washing, on which the even and regular film disappeared, instead with rougher and thicker block. The continue film is destroyed by the washing process. The surface of sample (Fig2.(d')) treated with pure TiO_2 water sol become smoother after 50 times washing, but it is also clearly indicated that a larger mount of block deposited on the edge between two fibers.



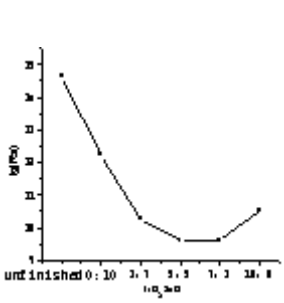
(b') (c') (d')

Fig.2 SEM image of polyester fiber treated after 50 times washing(b')with pure ZnO water sol (c')with compound ZnO/TiO_2 water sol at rate of 5 to 5 (d') with pure TiO_2 water sol

The changes of surface compare toresistance of samples treated with different water sol are shown in Fig.3. Y-axis is expressed in terms of a designated power of 10, the base of logarithms and Rs represents surface compare toresistance. The original polyester fabric's surface compare toresistance is high to 10^{15} and it is decrease greatly to 10^{12} after treated with pure ZnO water sol. The Rs of polyester with compound water sol of rate 3 to 7 is approximately 10^{10}, which is same to that of fabric treated with pure TiO_2 water sol. The antistatic performance of fabric treated with compound water

sol of rate 5:5 and 7:3 are the best, which the Rs decline close to 10^9, which is nearly equate to the surface compare toresistance of cotton fabric. It is indicated that synergistic effect is contained in TiO_2/ZnO blends and the mole rate of this two inorganic materials between 5 to 5 and 7 to 3 display the best antistatic behavior.

Fig.4(a) shows the duration of antistatic property of polyester fabric treated with pure ZnO water sol after several times washing. It is clearly showed that with the increase of washing time, the antistatic property of polyester fabric treated by pure ZnO water sol decreases a little and the surface compare toresistance changes from 10^{12} to nearly 10^{13}. The surface compare toresistances almost stay at the same level and do not change with the increase of washing time. The Fig.4(b) illustrate antistatic finshing durationfor polyester fiber treated with compound water sol TiO_2/ZnO at rate of 5 to 5. The surface compare toresistance dramatically goes almost up to 10^{13}, however, it display little changes with increase of washing time. From the comparison of SEM image of polyester fiber between corresponding samples, the morphology varies differently caused by washing. Maybe because the consecutive and even film is destroyed by washing process, which has contribution to increase of antistatic property, the surface compare toresistances rebound more after washing. The Fig.4(c) shows that the washing time has great effect to the polyester fabric finished by pure TiO_2 water sol. The figure greatly rises to 10^{13} after 10 times washing and the figure after 20 times washing almost keeps the same level. Then it lower to 10^{11} and maintain that value at 40 times washing. However, it again has a little increase at 50 times washing.



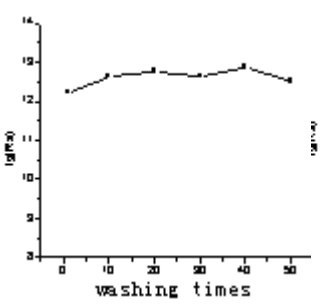






Fig.3 Fig4.(a) Fig4. (b) Fig4. (c)

Fig.3 Surface compare toresistance of samples with different water sol

Fig.4 Duration of antistatic property of polyester fabric (a) with pure ZnO water sol(b)with compound TiO_2/ ZnO water sol at rate of 5 to 5 (c) with pure TiO_2 water sol

The table 2 showed that physical and mechanical properties of the polyester fabric have different changes after treatment. It was observed that the warp and weft of the tensile strength and elongation after the finish process almost hold the same level compared with that of the unfinished and the largest increase rate is 3.92% and the largest decrease rate is 3.11%. It is indicated that the sol treatment has not much effect on the tensile strength of polyester fabric. The reasonable probability might be owing to the polyester fiber has better resistance to acid liquid. However, the tensile elongation changes more than tensile strength after treatment. It is showed in the table that the warp tensile elongation decreases much more largely after treatment by TiO_2/ZnO at the rate of 7 to 3 (11.93%) and the lowest decline rate is 5.59% after finished by TiO_2/ZnO of rate 5 to 5. However, all of weft tensile elongations after the five kinds of treatment yet increase. The figure of the least increase rate is 5.21% obtained from pure ZnO water sol treatment and the maximum figure is 8.77%, which result in treating with pure TiO_2 water sol.

All of he moisture regain rise according to figure in table2 except the figure from the fabric finished by TiO_2/ZnO water sol with rate of 3 to 7， which decrease 35.14%. The largest increase figure belong to fabric treated by pure TiO_2 water sol(178.38%). With the increase of ZnO amount on compound water sol, the moisture regain begin to fall off. However, the moisture regain of fabric finished by pure ZnO water sol increases 167.57%. Compared with the figure in Fig.3, the surface compare toresistance of fabric treated with TiO_2/ZnO water sol with rate of 5 to5 and 7 to3 is minimum, but the moisture regain of corresponding fabric is not the largest, therefore, the increase in moisture regain is not the main cause for improving in antistatic property.

The fabric finished by compound TiO_2/ZnO has largest decrease in gas permeability, approximately from 15% to 18% while the fabric treated by pure water sol has lowest decrease in gas permeability, 6.27% for pure ZnO water sol and 2.6% for TiO_2 water sol, respectively.The rigidity of polyester fabric finished by pure TiO_2 water sol increases a little with the figure of 2.75%, but that of polyester fabrics finished by the other water sols go down. The largest decrease rate is 14.77%, from the fabric treated by pure ZnO water sol. The fabric treated by TiO_2/ZnO of rate of 3 to 7 and 7to 3 has lower decrease in rigidity, with figure of 8.07% and 9.93%, respectively. The rigidity of fabric treated by TiO_2/ZnO water sol at the rate of 5 to5 just drops 3.30%.The CIE whiteness changes differently with different water sol treatment. The whiteness of fabric treated by TiO_2/ZnO water sol at the rate of 3 to7 increase 11.48% while the fabrics finished by the other water sols descend. The largest decrease rate is 34.05%, which is own to fabric treated by TiO_2/ZnO water sol at the rate of 7 to3. The fabric finished by pure TiO_2water sol fall off 20.05% and fabric finished by TiO_2/ZnO water sol at the rate of 5 to5 has lower decrease (10.47%) and the lowest decrease belong to pure ZnO water sol, which is 6.43%.

Table 2 Physical and mechanical property of polyester fabric finished

Fabric treated with		Pure ZnO water sol	TiO_2/ZnO (3:7)	TiO_2/ZnO (5:5)	TiO_2/ZnO (7::3)	Pure TiO_2 water sol
				changing percentage		
tensile strength	warp	-0.90%	-0.17%	-1.45%	-2.16%	-3.11%
	weft	-0.94%	3.92%	-0.78%	0.91%	0.89%
tensile elongation	warp	-7.25%	-7.13%	-5.59%	-11.93%	-7.85%
	weft	5.21%	7.78%	8.07%	5.92%	8.77%
Moisture regain		167.57%	-35.14%	59.46%	94.59%	178.38%
Gas permeability		-6.27%	-18.07%	-18.56%	-15.23%	-2.60%
Rigidity		-14.77%	-8.07%	-3.30%	-9.93%	2.75%
CIE whiteness		-6.43%	11.48%	-10.47%	-34.05%	-20.05%

Conclusion

(1) The stability of pure ZnO water sol is the best one and the pure TiO_2 water sol is worst. For the compound water sol stability, with the more amount of ZnO, the stability last longer.
(2) All of the water sol except pure ZnO water sol form a film on the fabric finished, but the films are destroyed after washing.
(3) Both mole of TiO_2 and ZnO with the rate of 5 to 5 and 7 to 3 display the best antistatic behavior, but the washing fastnesses are not good.
(4) After treatment, the moisture regain display most dramatically changes; the next one is whiteness of fabric, but the other physical and mechanical properties have a little change.

References

[1]Tadanaga K, Kitamuro K, Matsuda A.. Journal of Sol-Gel and Technology. 2003 (26): 705-408.

[2]Xu peng, Wangwei, Chen shuilin. Melliand International,2005, 11(1): 56-59.

[3]Qing,Wang, Shizhong Cui,Yanyan Chu, China. Patent ZL200610048570.3. (2009)

[4]Q. Li, Y.C Li and S.L Chen: Textile Auxiliaries,Vol21(2004) ,p.23-25

[5] T.Textor, T. h.. Bahners and E. Schollmeyer: Melliand Textilberichte Vol 80 (1999),p.847～848.

[6]Helmut Schmidt. J.Non-Cryst.,Solids 1994,178:303-312.

[7]C Z Zhao,et al. Chemical Journal of Chinese University, 1999,20(5):171-174.

[8]Straweridge I; James P. J.Non-Cryst., Solids,1986,82:366～372.

[9]Guglielmi M; Zenezini S. J.Non-Cryst.,Solids 1990,121:303～309.

[10]Jones W M; Fischbach D B. J.Non-Cryst.Solids,1988,101:123～126.

© (2011) Trans Tech Publications, Switzerland
doi:10.4028/www.scientific.net/AMR.331.275

Sorghum Red Pigment Dyeing Properties of Tencel Loose Fibre

He Zhipeng[a], Wu Zanmin[b], Zhou Xiaoli

College of Textiles Tianjin Polytechnic University

Key Laboratory of Advanced Textile Composites (TJPU), Ministry of Education

Tianjin 300160, P. R. China.

[a]penpen966922@163.com, [b]wuzanmin54@163.com

Keywords: Sorghum red pigment, Tencel loose fibre, Dyeing properties, Fastness.

Abstract: Dyeing of tencel loose fibre with sorghum red pigment as natural dyes has been studied. The values of dye uptake and fixation ratio have been calculated and disscussed. The effect of dyeing time, dyeing temperature, dye concentration and salt concentration were studied. Dye uptake and fixation ratio were high, and the fastness of dyed fibre were good.

Introduction

Commercial use of natural dyes shall definitely minimize the environmental pollution as the production and consumption of synthetic dye-stuff release carcinogen gases and other toxins[1]. The natural pigment sorghum red is extracted from sorghum shell[2]. And the main ingredient of sorhum red pigment is isoflavone galactose glucoside, with good thermal and light stability[3]. It has widespread use on food, cosmetic and medicine industries for its wide resource, low cost, simple extraction process and non-toxic features[4]. But it is still at the laboratory research stage in the textile profession.

As a regenerated cellulose fibre, tencel has high dry/wet force, good hygroscopicity, soft and smooth hand and excellent dyeing property[5].Tencel product can compete with other chemical fibres for its good wearability. The paper studies the sorghum red pigment dying properties of tencel loose fibre in order to extend the application of the natural pigment.

Experiment

2.1 Materials and Instruments

Tencel loose fibre (1.25D*38), sorghum red pigment (Fuyang city, Tiancheng pigment Co. Ltd.), sodium chloride (AR); heated thermostatic water bath (Tianjin central experiment electric stove Co. Ltd.), 723-type visible spectrophotometer VIS—723(Shanghai precision &scientific instrument Co. Ltd.).

2.2 Dyeing

A x mL dyebath, suitable for y g tencel loose fibre (liquor ratio 1:25), was prepared. The dyed fibre was rinsed with hot and cold water before and after, then dried at the room temperature.

The tencel loose fibre was dyed at various dyebath conditions (dyeing time, dyeing temperature, sodium chloride concentration and dye concentration) in order to investigate their effects on the dyeing properties of sorghum red pigment.

The dye uptake and fixation ratio were calculated using Equation (1) and Equation (2), respectively by the absorbance spectroscopic analysis of the dyebath before and after dyeing:

$$\text{Dye-uptake (\%)} = \left(1 - \frac{A * C}{B * D}\right) \times 100\% \quad \text{Equation (1)}$$

$$\text{Fixation (\%)} = \left(1 - \frac{E * F}{B * D}\right) \times 100\% \quad \text{Equation (2)}$$

Where A: absorbance of dyebath after dyeing,
B: absorbance of dyebath before dyeing,
C: dilution factor of dyebath after dyeing,
D: dilution factor of dyebath before dyeing,
E: absorbance of mixed liquid of dyebath after dyeing and rinse water,
F: dilution factor of mixed liquid of dyebath after dyeing and rinse water.

2.3 Fastness

The color fastness was determined according to GB/T 3921-2008 (color fastness to washing) and GB/T 3922-1995(color fastness to rubbing). Staining and change in color were assessed using grey scales.

Results and discussion

3.1 Effect of dyeing time and temperature

The effect of dyeing time and temperature on the dyeability of tencel loose fibre with sorghum red pigment was conducted at owf 2%, pH 5-6. The dyeing time were 30min, 40min and 50min, under each time dying at temperature of 303.15K, 313.15K, 323.15K, 333.15K, 343.15K and 353.15K, respectively. Figs.1-2 shows the dye uptake and fixation ratio, respectively.

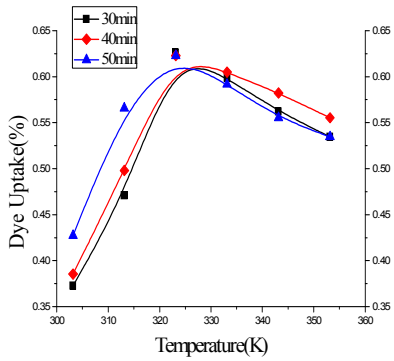


Fig. 1 Dye uptake under different dyeing time and temperature

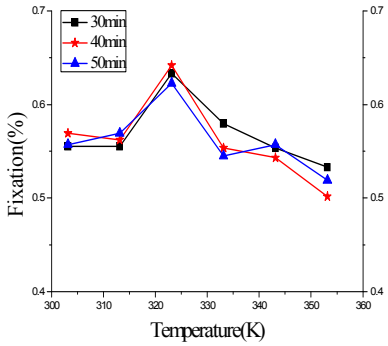


Fig. 2 Fixation ratio under different dyeing time and temperature

Figs. 1-2 demonstrates that an increase in the dye uptake and fixation ratio of sorghum red pigment on tencel loose fibre are obtained as the dyeing temperature increased from 303.15K to 323.15K. However, increasing the temperature from 323.15K to 353.15K is accompanied by a significant decrease in the dye uptake and fixation ratio. The results show that the temperature 323.15K is the optimum dyeing temperature. As is know that with the increasing of temperature, followed by the swelling of fibre which leads to a higher dye uptake. But highter temperature allows to much dye redissolve in the bath which have adhered to the fibre, and make the dye uptake and fixation ratio decrease. So the results can be explained as follows. The former plays a main role at low temperature, and the latter plays the leading role when the temperature higher than 323.25K. Figs. 1-2 also shows that the dye uptake and fixation ratio are similar under different dyeing time. The optimum dyeing time is 30min.

3.2 Effect of dye concentration

Dye uptake and fixation ratio at differdent dye comcentration (1-5%, owf) were investigated. Which was conducted at pH 5-6, dyeing time 50min. The results are shown in Figs. 3-4.

Figs. 3-4 demonstrates that an decrease in the dye uptake and fixation ratio of sorghum red pigment on tencel loose fibre are obtained as the dye conc. increased from 1% to 5% when dyeing temperature was 303.15K. The results observed are lower than the others. And the results of dye uptake and fixation ratio are resemble when dyeing temperature were 323.15K and 343.15K, respectively. At low dyeing temperature (303.15K) the swelling of fibre is low, and the energy of dye is low. As the dye conc. increase, among dye may happen aggregation especial at low temperature. Which make the dye attaching to fibre decline. Tencel fibre has high degree of polymerization and orientation, and the cristallinity is also higher than other cellulose fibre[5]. Which make the dye uptake and fixation ratio decline as well.

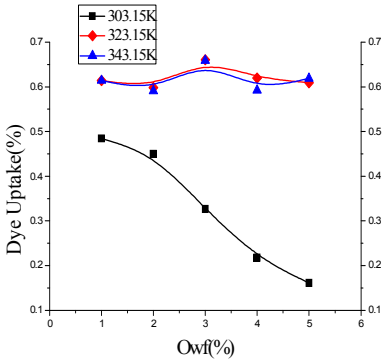


Fig. 3 Dye uptake under different dye conc.

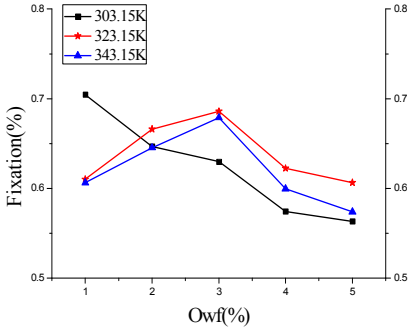


Fig. 4 Fiation ratio under different dye conc.

3.3 Effect of salt concentration

Figs. 5 shows the effect of salt concentration on the dye uptake and fixation ratio of sorghum red pigment on tencel loose fibre, which was conducted at owf 2%, pH 5-6, dyeing time 50min and salt conc. 0-25g/L.

Fig. 5 demonstrates that as the increase of salt conc., the dye uptake is increasing, and the fixation ratio has little increase. However, when salt conc. exceeding by 15g/L the dye uptake is tend to flat. Add-on salt plays a accelerating effect to dye adherence. The optimum salt conc. is 15g/L.

3.4 Dyeing rate curve

Fig. 6 shows the dyeing rate curve of tencel loose fibre with sorghum red pigment, which was conducted at owf 2% and pH 5-6. Fig. 6 demonstrates that as the increase of dyeing time, the dyeing uptake is increasing. However, when dyeing time exceed 20min(dyeing temperature 303.15K) or 30min(dyeing temperature 323.15K and 343.15K), the curve is tend to plat. When dye dyes fibre, which accompanies with adsorption and resolving process simultaneously. Adsorption occupies the main status at the beginning. The dyeing ability reduces unceasingly with the prolongation of dyeing time.But the speed of resolving is increasing ceasingly, until achieves a balance between adsorption and resolving process[6].

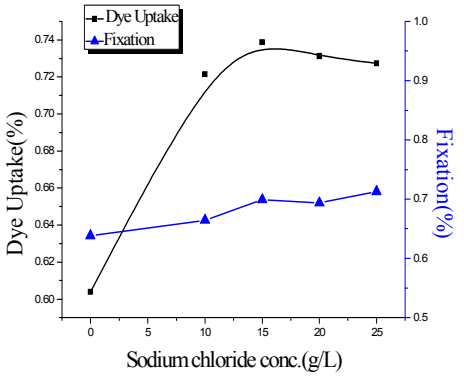


Fig. 5 Dye uptake and fixation ratio underdifferent salt conc.

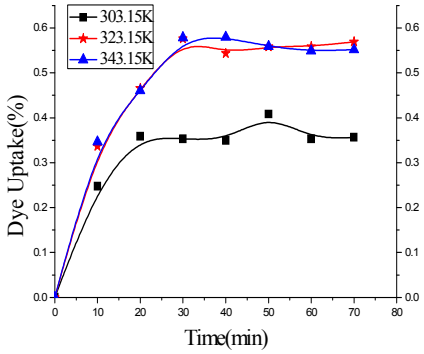


Fig. 6 Dyeing rate curve

3.5 Fastness

Table 1 shows that the washing fastness and acid perspiration fastness are according with the wearability requirement. The results could be attributed to excellent affinity to fibre of sorghum red pigment.

Table 1 Fastness

	Washing fastness			Acid perspiration		
	Staining[a]	Staining[b]	Change	Staining[a]	Staining[b]	Change
333.15K	3-4	4	3-4	4	4	3
343.15K	4	4-5	3	4	4-5	3
353.15K	3-4	4-5	4	4-5	4-5	3-4

Staining[a]: stain on tencel fabric;
Staining[b]: stain on wool fabric.

Conclusion

Dyeing tencel loose fibre with sorghum red pigment with high dye uptake and fixation ratio. Color fastness tests also show satisfactory results. The study shows that sorghum red pigment can serve as a noteworthy source of dye. Natural dyes are the essential alternatives in textile industry.

References:

[1] A. V. Shivaprakash: Man-made Textiles in India J., 53(5): 174-179. (2010)
[2] M. Gui Zhen, P. Shi Quan: Rain Fed Crops J., 4: 51-51, 54. (1994)
[3] Z. Hong Yu, L. Yu Zhang: Modern Food Science and Technology J. 26(3): 300-302. (2010)
[4] L. Zhi Mei, L. Jie: Journal of Liaodong University(Natural Sciences) J. 14(1): 10-12. (2007)
[5] S. Hui Fang, S. Bo: Shanxi Textiles J. 4: 29-31. (2008)
[6] M. Jin, Z. Jian Bo: Textile Dyeing and Finishing Journal J. 31(5): 1-7. (2009)

© (2011) Trans Tech Publications, Switzerland
doi:10.4028/www.scientific.net/AMR.331.279

Investigation of Ultraviolet Protection Properties of Cotton Fabric via Azoic Dyeing with Green Tea Extract

N. Punrattanasin

Department of Textile Science and Technology, Faculty of Science and Technology,

Thammasat University, Rangsit Center, Pathum Thani 12121, Thailand

pnattaya@tu.ac.th

Keywords: Ultraviolet protection, natural dye, green tea, azoic dyeing, cotton

Abstract. Green tea dyeing of cotton fabric via azoic combination method was investigated in order to improve ultraviolet protection properties without the application of polutting metal mordants. Three types of diazonium salts were prepared from three different primary aromatic amines (aniline, *p*-nitroaniline and 2,4 dichoroaniline) and subsequently, reacted with pretreated cotton fabric with coupling component or polyphenolic compounds found in green tea extract to form an azo dye inside the cellulose matrix. The result showed that as the strength of electron withdrawing groups of the substituents in the primary aromatic amines increase, both color strength and ultraviolet protection factor (UPF) of dyed fabrics dramically increased.

Introduction

Natural dyes are more environmental friendly and less risk to human health than synthetic dyes. However, in order to obtain high color strength and reasonable fastness properties, heavy metal mordants (alum, iron, tin, chrome and copper) are usually utilized [1-3] which gives negatively impact to environmental and must be treated before release into the environment. Nowadays, biomordants such as chitosan [4-7], tannic acid [8-13], tartaric acid [14-16] are an alternative approach for textile coloration using natural dyes. However, the dyed fabrics still displayed lower dye uptake and moderate-poor fastness properties.

One third of cancers worldwide are skin related. Although, there are several factors involved in development of skin cancers but the use of proper apparel and sunscreen are the most recommended methods. Cotton is the most preferable textile material worn during summer but its UV protection ability is quite low [17]. Therefore, it is required a proper treatment to enhance UPF values.

In this study, mordant-free dyeing of cotton fabrics via azoic combination method with green tea extract as natural colorant was investigated. Firstly, cotton fabrics were pretreated with green tea extract as a coupling component and finally, treated with diazotized arylamines to form an azo dye inside cotton fibers. Green tea extract contained an active polyphenol moiety called “catechin” and was found to have ability to exert proper UV protection properties [18]. From extensive study, it was found that UV protection properties of green tea dyeing of cotton fabrics can be achieved using chitosan mordanting process but the color strength of dyed fabric is still low (K/S less than 2.5) [18]. Therefore, the objective of this study was to investigate UV protection properties as well as to improve color strength of dyed cotton fabrics via azoic combination process.

Experimental

Materials

Green tea leaves was obtained from Doi-kham, Royal Project Foundation, Thailand. Bleached and mercerized 100% cotton fabric (80.74 g/m^2, plain weave) was purchased from Thai Num Choke Textile Co. Ltd, Thailand. Reagent grade sodium nitrite, aniline, *p*-nitroaniline and 2,4 dichloroaniline were purchased from Sigma-Aldrich Chemical. All other chemicals were reagent grade obtained from Asia Pacific Specialty Chemical Ltd., Thailand.

Extract preparation

Extracts of green tea were achieved by mixing 5 grams of tea leaves to 500 ml distilled water and boiled for 1 hour, allowed to stand for 20 min and then filtered. The filtrate was then used for pretreatment of cotton fabrics.

Pretreatment of cotton with green tea extract

Pretreatment of cotton fabric (10 grams) with green tea extract was carried out in an Infrared dyeing machine (Ugolini, S.R.L., Italy) at 100°C, at a liquor ratio of 1:25 for 1 hour.

Azoic dyeing

The diazonium salt was prepared by suspended primary aromatic amines (aniline, *p*-nitroaniline and 2,4 dichloroaniline; 0.5, 2 and 5% owf) in water (5 ml) and hot concentrated H_2SO_4 (1 ml). The reaction mixture was cooled down to 0-5°C using an ice bath and then $NaNO_2$ (a slight excess moles of diazo component) dissolved in distilled water (2.0 ml) was slowly added. The solution was stirred for 30 min and then sulfamic acid was added to destroy excess HNO_2.

The pretreated cotton fabric with green tea extract from previous process was immersed in the diazonium salt solution for 20 min to ensure complete coupling reaction and soaped in warm detergent using AATCC detergent (2.0 g/l) at 50°C for 10 min. The fabrics were rinsed again in tap water and dried.

Measurement

To evaluate performance of azoic dyeing with green tea extract, color strength (K/S) was evaluated using a Gretag Macbeth i5 spectrophotometer with illuminant D_{65} and 10° observer.

The transmittances and UPF values of original and dyed fabric with green tea extract were measured using UV Visible Spectrometer (Lambda 650, Perkin Elmer Instruments) in the range of 280-400 nm. The Ultraviolet Protection Factor (UPF) and percent blocking in UV-A (315-400 nm) and UV-B (280-315 nm) were calculated from the following equations [19];

$$UPF = \frac{\sum_{\lambda=280\ nm}^{400\ nm} E_\lambda \times S_\lambda \times \Delta\lambda}{\sum_{\lambda=280\ nm}^{400\ nm} E_\lambda \times S_\lambda \times \Delta\lambda \times T_\lambda}. \quad (1)$$

Where E_λ = relative erythema spectral effectiveness, S_λ= solar spectral irradiance, T_λ = average spectral transmittance of the specimen (measured) and $\Delta\lambda$ = measured wavelength interval (2 nm)

$$T\ (UV\text{-}A)_{AV} = \frac{\sum_{315\ nm}^{400\ nm} T_\lambda \times \Delta\lambda}{\sum_{315\ nm}^{400\ nm} \Delta\lambda}. \quad (2)$$

$$T\ (UV\text{-}B)_{AV} = \frac{\sum_{280\ nm}^{315\ nm} T_\lambda \times \Delta\lambda}{\sum_{280\ nm}^{315\ nm} \Delta\lambda}. \quad (3)$$

$$UV\text{-}A\ Blocking\ (\%) = 100\% - T(UV\text{-}A). \quad (4)$$

$$UV\text{-}B\ Blocking\ (\%) = 100\% - T(UV\text{-}B). \quad (5)$$

Results and discussion

Mordant-free dyeing of cotton fabrics via azoic combination method with green tea as natural colorant is a two-step method involving pretreatment of cotton fabric with green tea extract containing a major species of catechins or polyphenols as the coupling components in an aqueous medium, while the second step was developed by diazotization of diazo components or primary aromatic amines and finally, azoic dye was developed inside fiber (Fig 1) [20]. Bathochromic shift of the shade of dyed fabrics showed colors ranging from pale yellow to dark orange depending on the strength of electron withdrawing groups of the substituents in the diazo component. The influence of substituent effect on the color depth of dyed fabrics are in the order of 2,4 dichloroaniline > *p*-nitroaniline > aniline.

From Table 1, it can be observed that at the same diazo component concentration, color depth of dyed fabric also dramatically increased with increasing electron withdrawing substituent into diazo component. In addition, the K/S values increased with an increase of arylamine concentrations (0.5-5 % owf). A significant improvement in UPF value between the undyed and dyed fabrics was observed. It was found that all dyed fabrics showed a significantly higher UPF values than the undyed reference sample (UPF = 2.88). In addition, it was observed that the higher color strength of dyed fabrics, the greater UV protection. For example, in case of azoic green tea dyeing cotton fabric with *p*-nitroaniline, the K/S increased form 9.33 to 15.30 and the UPF value rose from 17.15 to 25.49. Therefore, these results correlated with previous studies investigated by Sarkar [21] and Mongkholrattanasit *et al.* [22] who show that a pale color give less UV protection. The influence order of primary aromatic amines for UV protection is 2,4 dichloroaniline > *p*-nitroaniline > aniline.

From the corresponding UPF values, the undyed fabric and dyed fabrics with aniline as primary aromatic amine cannot be rated as offering any degree of protection because the UPF values are less than 15. The degree of UV protections are noticed in case of using *p*-nitroaniline and 2,4 dichloroaniline. The rating of those dyed fabrics are ranging from "Good UV protection (UPF values between 15-24) and "Very good UV protection" (UPF values between 25-39).

From the % blocking values, it can be clearly observed that all dyed samples had a significantly higher % blocking values than undyed reference in both UV-A and UV-B regions. In addition, over 90% blocking in UV-A and UV-B was shown in all concentrations of dyed fabrics diazotized with *p*-nitroaniline and 2,4 dichloroaniline (0.5-5 % owf) but in case of dyed fabrics diazotized with aniline, show lower UV-A protection properties due to lower K/S values and paler shade.

Table 1 K/S, UPF, protection class and % blocking of azoic dyeing with green tea extract

Primary aromatic amines	% owf	K/S	UPF	UPF Protection class	% Blocking UV-A	% Blocking UV-B
undyed	-	-	2.88	No class	63.06	33.26
	0.5	0.82	9.14	No class	85.91	90.06
aniline	2	1.21	9.32	No class	87.35	90.18
	5	1.41	9.74	No class	87.39	90.63
	0.5	4.53	15.83	Good	93.61	94.05
p-nitroaniline	2	9.33	17.15	Good	94.43	94.37
	5	15.30	25.49	Very good	96.44	96.16
	0.5	8.09	18.15	Good	94.62	94.80
2,4 dichloroaniline	2	18.39	35.74	Very good	97.55	97.29
	5	20.11	38.83	Very good	97.67	97.54

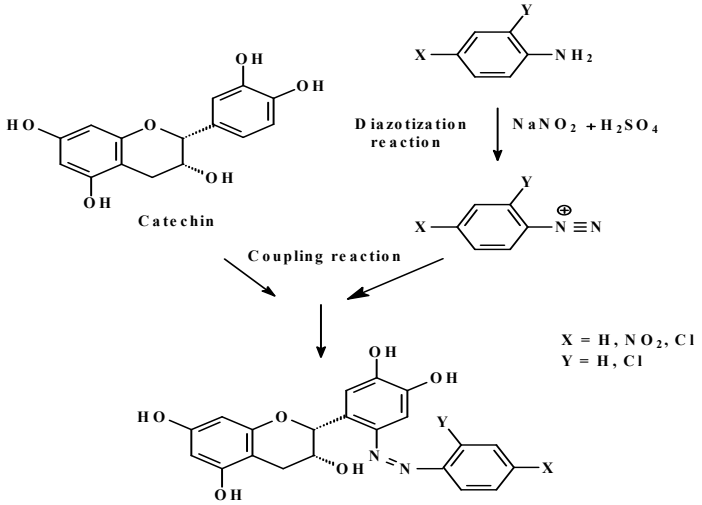


Fig. 1 Suggested mechanism of green tea azoic dyeing.

Summary

It is concluded that mordant-free dyeing of cotton fabric with green tea extract using an azoic combination technique was successfully established. Dyed fabrics exhibited high color strength. UV protection properties and % blocking in both UV-A and UV-B of dyed fabrics were increased with increasing of both concentrations and the strength of electron withdrawing groups of the substituents in the diazo component.

Acknowledgements

This work was financially supported by a New Researcher Scholarship of Coordinating Center for Thai Government Science and Technology Scholarship Students (CSTS), National Science and Technology Development Agency, Thailand.

References

[1] M. H. Han: J. Korean Soc. Dyers and Finishers Vol. 12 (2) (2000), p. 51.
[2] S. Y. Park, Y. J. Nam, and D. H. Kim: J. Korean Sococitey of Dyers and Finishers Vol. 14 (1) (2002), p. 1.
[3] J. E. Lee, H. J. Kim and M. C. Lee: J. Korean Soc. Dyers and Finishers Vol. 13 (3) (2001), p. 11.
[4] S. H. Kim: Fibers and Polymers Vol. 7 (3) (2006)2, p.55-261.
[5] A. Abou-Okeil and O. A. Hakeim: Coloration Technology Vol. 121 (1) (2005), p. 41.
[6] T. Kako and A. Katayama: J. of Sericultural Science of Japan Vol. 66 (5) (1997), p. 330.
[7] S. Saxena, V. Iyer, A. I. Shaikh and V. A. Shenai: Colourage Vol. 44 (11) (1997), p. 23.
[8] N. N. Fathima, S. Saravanabhavan, J. R. Rao and B. U. Nair: J. of the American Leather Chemists Association Vol. 99 (2) (2004), p.73.
[9] S. M. Burkinshaw and B. Bahojb-Allafan: Dyes and Pigments Vol. 60 (2) (2004) p. 91.
[10] S. K. Bhattacharya, S. M. Chatterjee and C. Dutta: Man-Made Textiles in India Vol. 47 (3) (2004), p. 85.
[11] L. Yu, B. Yu, and S. Chen: International Dyer Vol.189 (8) (2004), p. 12.
[12] R. Sudhakar and K. N. N. Gowda: Man-Made Textiles in India Vol. 48 (7) (2005), p.255.
[13] S. R. Maulik and S. C. Pradhan: Man-Made Textiles in India Vol. 48 (10) (2005), p. 396.
[14] N. H. El-Sayed, A. A. Haroun, and M. Stoll: J. of the Society of Leather Technologies and Chemists Vol. 87 (4) 92003), p. 138.
[15] H. T. Deo and R. Paul: International Dyer Vol. 188 (11) (2003), p. 49.
[16] H. T., Deo and R. Paul: International Textile Bulletin Vol. 50 (5) (2004), p. 66.
[17] I. Algaba, A.Riva and P. C. Crews: AATCC Review Vol. 4 (2) (2004), p. 26.
[18] S. H. Kim: Fibers and Polymers Vol. 7 (3) Z2006), p. 255.
[19] American Association of Textile and Chemists and Colorists: AATCC Test Method 183 (2004).
[20] N. Punrattanasin: Proceedings of International conference on Technology and Innovation for Sustainable Development 28-29 January 2008, Khon Kean, Thailand, (2008), p.624.
[21] A. K. Sarkar: BNC Dermatology Vol. 4 (15) (2004), p. 1.
[22] R. Mongkholrattanasit, J. Krystufek, J. Wiener and M. Vikova: The Journal of The Textile Institute Vol 102 (3) (2011), p. 272.

© (2011) Trans Tech Publications, Switzerland
doi:10.4028/www.scientific.net/AMR.331.283

Application of chitosan on anti-shrinkage of wool fabric

Qingfu Zhang[1, 2, a], Wenfang Yang[1, 2, b] ,Yanli Qiao[1, 2, c] , Xiaoxing Shen[1, 2, d]

1 School of Textiles, Tianjin Polytechnic University; Tianjin 300160, China

2 Key Laboratory of Advanced Textile Composite, Ministry of Education of China; Tianjin 300160, China

[a]keep433@126.com, [b]yangwf2@126.com, [c]qiaoyanli87@126.com, [d]shenxiao_xing@126.com

Key word: wool, anti-shrinkage, chitosan, finishing

Abstract: As the problem of shrinkage on wool fabric, the chitosan was applied to solve it in this paper. The volume of retraction bulb and strength were considered to describe the results of anti-shrinkage after the finishing. It shows that great anti-shrinkage is got in this experiment, and the best treatment process is defined as follow: the concentration of chitosan 6g/l, pH 5, 80min, 90˚C and bath ratio 1:50.

Introduction

Wool is used to make various of clothing as its good characters, however, its directional friction effect which is brought by the scale of wool is disadvantageous to textile. Currently, many treatments have been applied widely to resolve this problem of wool fabric, but any others problems are brought about by the treatments, such as waste of water, environmental pollution and insufficient treatment [1].

Chitosan is rich in the nature and it has many excellent properties [2]. In wool textile industry, the chitosan is applied to the anti-shrinkage of wool based on principles of addition anti-shrinkage [9]. It can fill the uneven surface of wool to reduce the directional friction effect, so as to achieve the purpose of anti-shrinkage [6].

Experimental

2.1 Test methods

2.1.1 Test method for shrinkage:

1.5g wool yarns was placed into the beaker and 5 steel balls, 40ml distilled water were added into the beaker. The beaker was put into the fastness to washing tester at 40 ˚C for 20 minutes, and then dried. The diameter (2R) of the sample was measured in five different directions. To calculate the volume of retraction bulb, the Eq. 1 was used.

$$V = \frac{4}{3} \times \pi \times R^3 \quad (1)$$

The volume of retraction bulb was used to describe the effect of anti-shrinkage. The effect was better as the increasing of the volume [7].

2.1.2 Test method for the strength of wool yarn

The strength was measured by the standards GB/T 13835.5-1992.

2.2 Experimental methods and contents

2.2.1 Preparation of chitosan solution

The solution of chitosan: A certain amount of chitosan was dissolved in 4% acetic acid solution at room temperature which shredded before wetting, and then the solution was filtered after 48 hours [9]. Solution of chitosan was confected as the solid content was 2.63%.

2.2.2 Effect of different finishing factors on anti-shrinkage

Process: finishing of chitosan → baking (130 ˚C, 3 minutes) → washing → drying → test.

Basic technology: chitosan 4g/l, cross linker 1g/l, bath ratio 1:50. pH = 4, 90 ˚C, 60min

Table 1 Factors and levels for finishing

Factors and levels considered for anti-shrinkage finishing					
Concentration (g/l)	1	2	3	4	5
pH value	3	4	5	6	7
Temperature (˚C)	25	55	70	90	100
Time (min)	20	40	60	80	100

Other conditions were the same as the basic technology when each factor was considered.

2.2.3 Determine the optimum finishing by orthogonal design

The optimum finishing was determined by orthogonal design L_9 (3^4).

Results and Discussions

3.1 Effect of chitosan concentration on anti-shrinkage

It was known from Fig.1 that the volume of retraction bulb was getting larger with the adding of the concentration. However, when the concentration was high, too much chitosan would affect the handle and the style of the textile.

We can see from Fig.1, the fracture strength of the treated fabrics increased slightly with increasing the concentration of chitosan. It was ascribed that chitosan not only formed films, also glued the fibers.

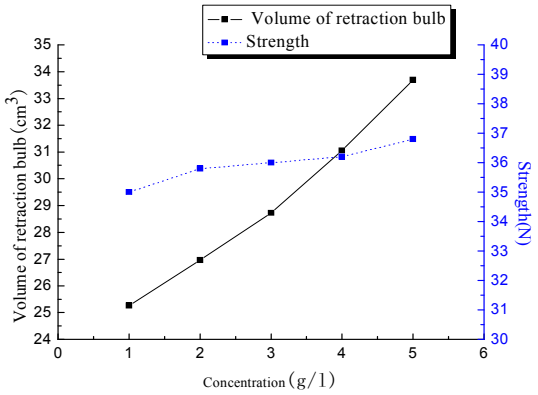


Fig. 1 Effect of concentration on anti-shrinkage and strength

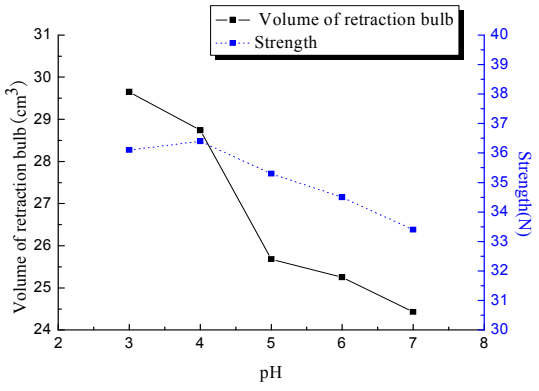


Fig. 2 Effect of pH on anti-shrinkage and strength

3.2 Effect of pH on anti-shrinkage

What we can see in Fig. 2 is that the volume of retraction bulb decreased significantly with rising pH value. With low pH value, the macromolecules dissolved sufficiently and stretched out which was beneficial for the adsorption of chitosan on protein. Conversely, it made against the adsorption of chitosan, so the volume of retraction bulb decreased along with the raise of pH value [11].

It can be known from Fig. 2 that the strength of wool fibers descended slightly when the pH value rose. The optimal pH value was 5 considering the influence of chitosan on t anti-shrinkage.

3.3 Effect of treatment temperature on anti-shrinkage

As shown in Fig. 3, the volume of retraction bulb began to increase and then decreased with increasing temperature. However, the chitosan molecules were destroyed when the temperature was too high. So, the best anti-shrinkage properties can be got when the temperature was 90 ˚C.

It can be seen in Fig. 3 that the strength was not affected obviously by the temperature and increased a little with rising of the temperature.

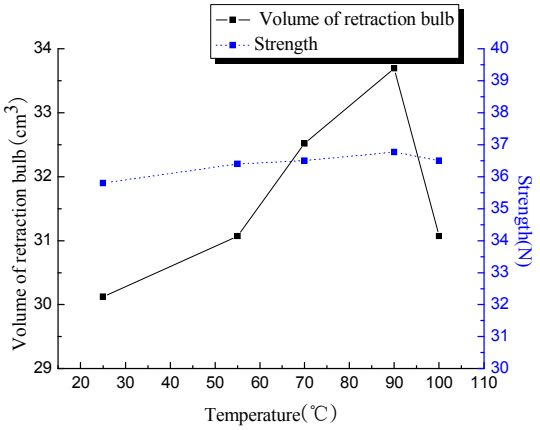


Fig. 3 Effect of treatment temperature on anti-shrinkage and strength

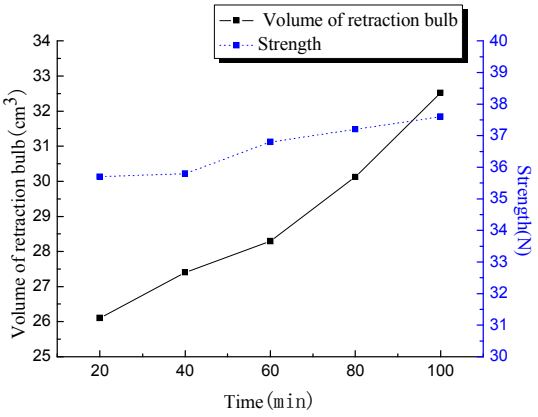


Fig. 4 Effect of processing time on anti-shrinkage and strength

3.4 Effect of the processing time on anti-shrinking

What we can see from Fig. 4 is that the performance of anti-shrinkage and the strength of wool both improved with the extension of treatment time. Although more chitosan molecules can be adsorbed to wool, the structure of l, 4 - glycosidic bond in chitosan would be hydrolyzed with the extension of treatment time. In summary, the optimum treatment time was considered to be 60min.

3.5 Determine the optimum finishing by orthogonal design

pH (A), density (B), temperature (C) and time (D) were considered by the single factor experiments to screen the best technology of chitosan processing.

Table 2 Programs and results of orthogonal design L_9 (3^4)

Factors / Number	A	B(g/l)	C(˚C)	D(min)	The volume of retraction bulb (cm^3)
1#	4	2	60	40	26.53
2#	4	4	90	60	30.59
3#	4	6	100	80	31.07
4#	5	2	90	80	32.52
5#	5	4	100	40	26.53
6#	5	6	60	60	33.52
7#	6	2	100	60	25.86
8#	6	4	60	80	26.96
9#	6	6	90	40	26.10
Average 1	29.397	28.303	29.003	26.387	———
Average 2	30.857	28.027	29.737	28.990	———
Average 3	26.307	30.230	27.820	30.183	———
Graduation	4.550	2.203	1.917	3.796	———

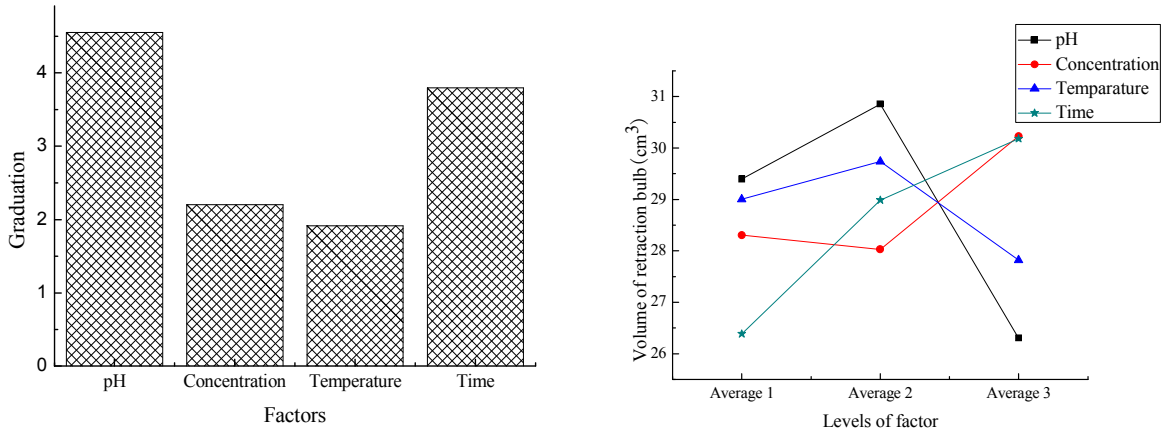


Fig.5 Analysis of the graduation

It showed in Table 2 and Fig. 5 that the influence degree of each factor from high to low was pH, time, temperature and then chitosan concentration. $A_2B_3C_2D_3$ was considered to be the optimum finishing conditions by calculation and analysis.

Conclusions

Good effects of anti-shrinkage and strength can be achieved by the finishing of wool based on principles of addition anti-shrinkage.

The optimum finishing conditions on anti-shrinkage was described as follow: chitosan concentration of 6g / l, pH value 5,80 min, 90˚C, cross linker agent for the 0.5g / l, bath ratio 1:50.

References

[1] B. Li, F.Q. Jiang, B.Z. Tong. Wool Textile Journal, Vol. 3(2003), p. 28-30.
[2] L.P. Guan etc. Wool Textile Journal, Vol. 1(1999), p. 41-42.
[3] J.S. Wang, K. Sun. *Principle and Technology of Textile Dyeing and Finishing*, edited by China Textile & Apparel Press, Bei Jing (1983).
[4] J.B. Yao. *New Finishing Technology of Wool Fiber*, edited by China Textile & Apparel Press, Bei Jing (2000).
[5] Baird. K. Textile Res.J. Vol. 33 (1963), p. 973-984.
[6] Y.L. Huang. Dyeing and Finishing, Vol. 24(1998), p. 12-16.
[7] X.J. He. Wool Textile Journal, Vol. 2(2000), p. 34-36.
[8] L.F. Peng. Chemical World, Vol. 6(2000), p. 176-179.
[9] X.J. He. Wool Textile Journal, Vol. 6(2000), p. 20-22.
[10] L. Ji, Y.D. Shi, Y.Y. Ren. Sichuan Textile Technology, Vol. 5(2004), p. 27-28.
[11] L.H. Liang, H.Y. Huang. Shandong Textile Science & Technology, Vol. 5(2005), p. 1-3.
[12] Y.G. Wang, Y.Z. Whang. Ready-Mixed Concrete, Vol. 4(2010), p. 47-49.

© (2011) Trans Tech Publications, Switzerland
doi:10.4028/www.scientific.net/AMR.331.287

Dyeing of silk and nylon 6 fibers with baicalin

Xiaochun LI[1, a], Jiliang CAO[1, b]

[1]Department of Materials and Chemical Engineering; Henan Institute of Engineering, Zhengzhou 450007, China

[a]lxc888@163.com, [b]caojiliang301@163.com

Keywords: baicalin, silk, nylon 6, dyeing, natural dyes

Abstract: Natural dye baicalin was applied to dye silk and nylon 6 fibers. The effects of dyeing temperature, time, pH and dosages of sodium chloride and baicalin on dyeing properties of silk and nylon 6 fibers were analyzed, the color fastness of dyed fabrics also investigated. It was found that, the optimal process conditions were as follows: dyeing at 90°C(silk) or 80°C(Nylon 6), with pH 4, for about 60min. The built-up properties of baicalin on silk and nylon 6 fabrics were good, the color fastness of dyed fabrics were above 3-4 grade.

Introduction

Pollution may be considered to be one of the most important problems in the recent years. Therefore, a great concern with this problem has appeared all over the world to find suitable and acceptable solutions for reducing pollution of environment. One of the most important and effective ways for reducing pollution is the replacement of polluting materials and chemicals by eco-friendly natural materials[1-5].

For realizing this aim and to prevent or minimize the toxicity and allergic reaction of synthetic dyes, a new trial for dyeing silk and nylon 6 fibers with natural dye baicalin were made. Baicalin, a natural anionic colorant, is the major component of Scutellaria baicalensis Georgi extract[6-7]. Thus, the aim of this work was to examine the feasibility of using baicalin for dyeing of silk and nylon 6. The structure of baicalin is shown in Fig. 1.

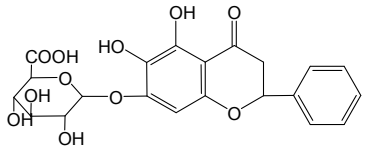


Fig. 1. Chemical structure of baicalin

Materials and Methods

Materials

Pretreated 100 % silk fabric, weight 40 g/m^2 was obtained from the First Silk Wave Factory. (Wuxi, China). 230T nylon 6 woven fabric, weight 80 g/m^2 was kindly supplied by Zhengzhou Yuxing Textile Printing and Dyeing Co., Ltd. (Henan, China). Baicalin（95%）were kindly supplied by Shaanxi Huike Botanical Development Co., Ltd. (Shaanxi, China); sodium hydroxide, sodium chloride, acetic acid, boric acid and phosphoric acid were of analytical reagent grade.

Dyeing process

The dyeing of baicalin on nylon was performed in 2%omf of baicalin and conical flasks in a universal dyeing machine at pH 4 using a 50:1 liquor ratio. The fabrics were immersed into the baicalin solutions at 40°C, and subsequently the treatment solutions were heated to the required temperature at a rate of 1 °C/min and the treatment continued for 60 min. At the end of dyeing, the dyed samples were removed, rinsed thoroughly in tap water and were allowed to dry in the open air.

Color measurement

Colorimetric of dyeings were determined using an X-rite CE7000A spectrophotometer interfaced to a PC. Measurements were taken with specular component of the light excluded and the UV component included, using illuminant D65 and 10° standard observer.

Color fastness

The washing fastness of the dyeing was tested using method of GB/T3921.5-1997; the rubbing fastness of the dyeing was tested using method of GB/T3920-1997.

Results and discussion

Effects of pH on dyeability

Silk and nylon were dyed with 2%omf baicalin at various levels of pH at 95 °C for 60 min using a 50:1 liquor ratio to determine their effects on the K/S and the results are shown in Fig. 2, from which it may be concluded that the stronger acidic conditions(pH 2 to 3) yielded very good K/S for nylon fabrics, but yielded very poor K/S for silk fabrics. This could be explained that the solubility of baicalin was very poor under pH 2 to 3, so the uptake of baicalin on silk and nylon occurred primarily by H-bonding and ion-dipole forces. Under slightly acidic, neutral and alkali conditions(pH 4 to 12), as used in this work, the K/S of dyed fabrics decreased with the increasing of pH. This could be explained that the uptake of baicalin occurred primarily by electrostatic interaction between the anionic groups($-COO^-$) in the baicalin and the protonated amino groups($-NH_3^+$) in the silk and nylon, although the solubility and anionic groups of baicalin were increased from pH 4 to 12, the protonated amino groups of silk and nylon decreased with increasing of pH. In addition, the H-bonding interaction between baicalin and nylon also played an important part from pH 4 to 12.

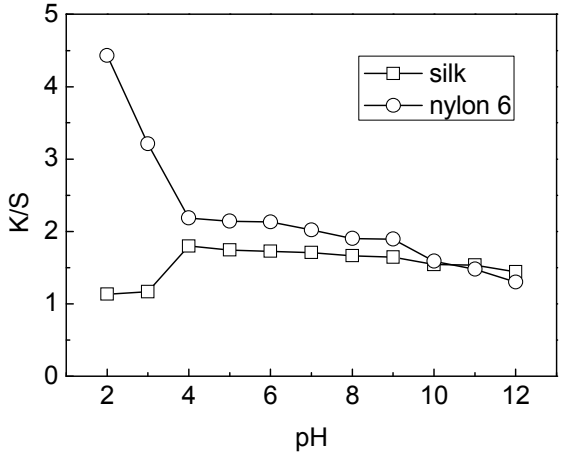


Fig. 2. Effects of pH on K/S of silk and nylon

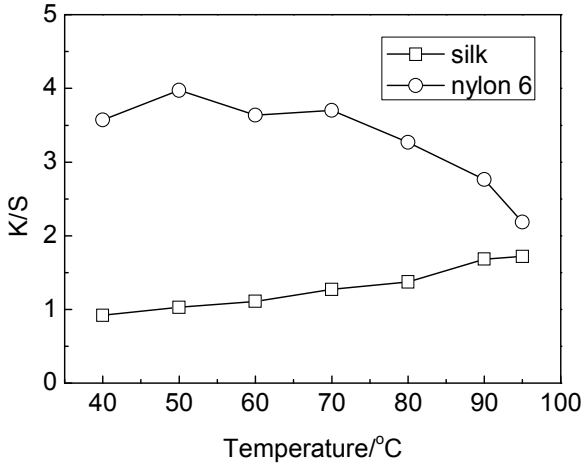


Fig. 3. Effects of dyeing temperature on K/S of silk and nylon

The influence of dyeing temperature on dyeability

Silk and nylon fabrics were dyed with 2%omf baicalin at different temperatures (40 °C, 50 °C, 60 °C, 70 °C, 80 °C, 90 °C and 95°C) using a pH of 4 for 60 min with a 50:1 liquor ratio. The influence of dyeing temperature on K/S value of silk and nylon fabrics were shown in Fig. 3. The data of silk shows that the good K/S was achieved by the range of the temperature from 40 to 95°C, and the K/S of dyed silk fabrics increased with the increasing of dyeing temperature, this may be attributed to the higher kinetic energy of the baicalin molecules and their consequent greater diffusional rate within the substrate, together with higher fibre swelling that accompanied an increase in application temperature. The data of nylon shows that the good K/S was achieved by the range of the

temperature from 40 to 70°C, but the K/S of dyed nylon decreased with increasing of temperature from 70 to 95°C. This could be explained that the solubility of baicalin was increased with the increasing of dyeing temperature, the H-bonding of baicalin and nylon was decreased with the increasing of dyeing temperature. For the sake of the level-dyeing and permeability, the fabric was optimally dyed at 80 °C for nylon and 90 °C for silk.

The influence of sodium chloride on dyeability

Silk and nylon fabrics were dyed with 2%omf baicalin at different amount of sodium chloride (0, 5, 10, 20, 30, 40g/L) using a pH of 4 at 90°C (silk) or 80°C (nylon) for 60 min with a 50:1 liquor ratio. The effects of sodium chloride addition were studied. The effects of the addition of sodium chloride on the K/S of dyed fabrics are shown in Fig. 4. Fig. 4 represents that the K/S of dyed silk fabrics were increased with the increasing concentration of NaCl. However, the K/S values of dyed nylon fabrics were increased slightly with the increasing concentration of NaCl. This could be explained that the interaction between baicalin and nylon was primarily by H-bonding, the interaction between baicalin and silk was primarily by electrostatic interaction.

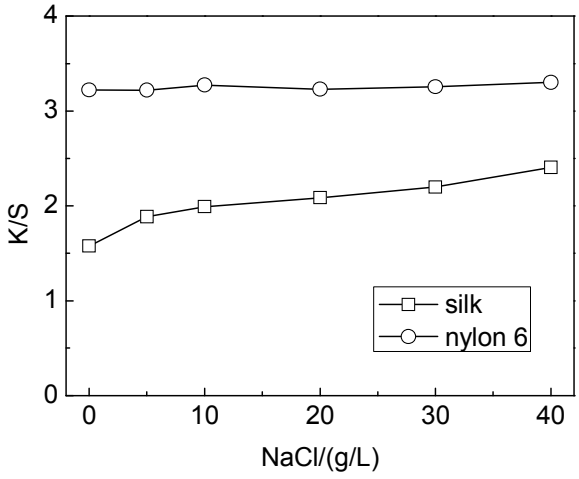


Fig. 4. Effects of sodium chloride on K/S of silk and nylon

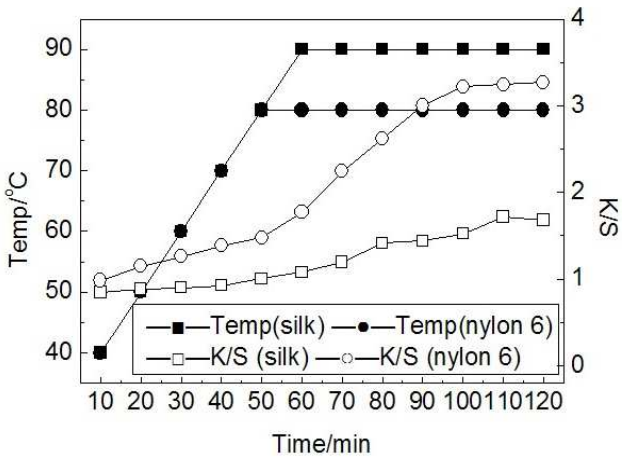


Fig. 5. Effects of dyeing time on K/S of silk and nylon

The influence of dyeing time on dyeability

Silk and nylon fabrics were dyed with 2%omf baicalin at different time using a pH of 4 with a 50:1 liquor ratio. The influence of dyeing time on K/S value of silk and nylon fabrics dyed with baicalin were shown in Fig. 5. As can be seen in Fig. 5, with the increasing of the dyeing time, K/S values of the dyed fabric considerably rose. When the dyeing time hit 50min under 80 °C for nylon, and 90 °C for silk, the K/S values increased slightly. For the sake of the level-dyeing and permeability, the fabric was optimally dyed at 80 °C(nylon) or 90 °C(silk) for about 60min.

The built-up properties of baicalin on silk and nylon 6 fabrics

Silk and nylon fabrics were dyed with different amount of baicalin (0.5, 1, 2, 4, 6, 8, 10% omf) using a pH of 4 at 90°C (silk) or 80°C (nylon) for 60 min with a 50:1 liquor ratio. Fig. 6 shows the K/S of silk and nylon dyed with different amount of baicalin. It is found that the K/S of dyed fabrics increased with increasing the amount of baicalin, the equilibrium K/S of dyed fabrics was achieved when the sample was dyed with a concentration of 8%omf baicalin.

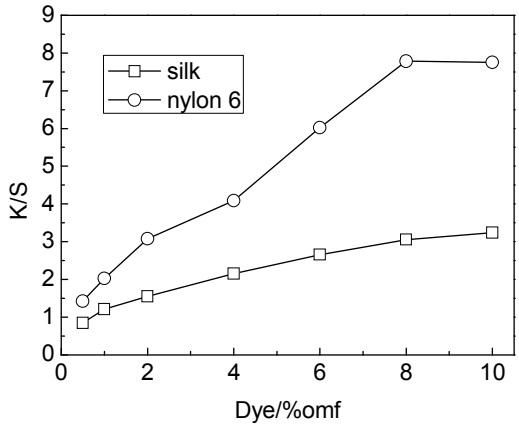


Fig. 6. The built-up properties of baicalin on silk and nylon

Color fastness properties

The fastness ratings of dyed fabrics are presented in Table 1. Table 1 indicates that the washing and rubbing fastness ratings of silk and nylon 6 fabrics dyed with baicalin were good.

Table. 1 Color fastness of the dyed fabrics

Dyed fabrics	Washing fastness							Rubbing fastness	
	Change in color	Staining						Dry	Wet
		Wool	Acrylic	Polyester	Nylon	Cotton	Acetate		
Silk	4-5	4	4	4	4	5	5	4-5	4
Nylon 6	4	3-4	4	4-5	4	4-5	4-5	4-5	4

Conclusions

1-Silk and nylon fabric were successfully dyed with natural dye baicalin, and the dyeing conditions were optimized.

2-Temperature broke down the aggregate of dyes and increased their solubility as well as opened up the fibre structure and thus accelerated the diffusion of dye molecules inside the fibre, but high temperature also decreased the H-bonding between baicalin and nylon.

3-The pH of dyeing was found to play a great role since maximum colour strength was achieved at strong acidic medium for nylon, which may be attributed to the high H-bonding interaction between baicalin and nylon.

4-The K/S of dyed silk fabrics were increased with the increasing concentration of NaCl, but had little effect on nylon.

References

[1] R Shanker, P.S. Vankar: Dyes and pigments, Vol.74(2007), p.464
[2] F.A. Nagia, R.S.R. EL-Mohamedy: Dyes and pigments, Vol.75(2007), p.550
[3] M.M. Kamel, M.M. El Zawahry, N.S.E. Ahmed, F. Abdelghaffar: Ultrasonics Sonochemistry, Vol.16 (2009), p.243
[4] R Paul, C Solans, P Erra: Colloids and Surfaces A: Physicochem. Eng, Vol.253 (2005), p.175
[5] E. Tsatsaroni, M. Liakopoulou-Kyriakides: Dyes and pigments, Vol.29(1995), p.203
[6] X.J. Li, Y.P. Zhang, Z.B. Yuan: Chromatographia, Vol.55(2002), p.453
[7] Y. K. Zhao, Q. E. Cao, H. T. Liu, K. T. Wang, A. X. Yan, Z. D. Hu: Chromatographia, Vol.51 (2000), p.483

© (2011) Trans Tech Publications, Switzerland
doi:10.4028/www.scientific.net/AMR.331.291

Adsorption Kinetic Study of Reactive Dyes on Silk with Octyl Trimethyl Ammonium Bromide as Accelerant

Ling Zhong[1,a], Guangxian Zhang[1,b,*], Fengxiu Zhang[2,c], Xuting Xue[1,d]

[1] College of textiles and garments, Southwest university, China

[2] School of chemistry and chemical engineering, Southwest university, China

[a]395146401@qq..com, [b]zgx656472@sina.com, [c]zhangfx656472@sina.com, [d]xtxue@swu.edu.cn

[*] Corresponding author, tel.:+0 86 02368251681; fax: +086 02368251228

Keywords: Adsorption; kinetics; Silk; Reactive dyes; dyeing

Abstract. The dyeing accelerating effect of octyl trimethyl ammonium bromide (OTAB) on dyeing silk with reactive red dye B-3BF, reactive yellow dye B-4RFN and reactive dark blue dye B-2GLN was studied in this paper. The dye-uptake rates increased with increasing concentration of OTAB, and the highest dye-uptake rates of three reactive dyes were 91~98%. The adsorption kinetics of dyeing process at different temperatures was also investigated by using pseudo first- and second-order kinetic models. The results showed that adsorption rates increased with increasing temperature. The adsorption kinetics of three reactive dyes on silk with OTAB as accelerant was found to follow the pseudo second-order sorption kinetics equation. The activation energy of reactive red dye B-3BF, reactive yellow dye B-4RFN and reactive dark blue dye B-2GLN dyeing on silk with OTAB as accelerant were found to be 26.91, 17.31, 6.99 kJ/mol, respectively.

Introduction

Reactive dyes react chemically with the fabric by forming covalent bond together in the dyeing process. That is a strong interaction, so the fabric does not fade in the washing process. However, silk has a large number of negative charges at alkaline solution, and reactive dyes also have negatively charges, so that directly-uptake rates of reactive dyes on silk are very low in general [1]. Then, the utilization rate of reactive dyes on silk is low, and wastewater is generated with dyeing. Many people have been working on improving these drawbacks of dyeing on silk with reactive dyes. For example, micro-suspension dyeing method and reverse micellar dyeing method are developed recently [2]. Yingling Li [3] and Bingtao Tang [4] synthesized several novel dyes in the original basis of reactive dyes to improve the dyeability of reactive dyes, respectively. Other workers grafted silk with cationic compounds to improve the dyeability of silk [1]. The dyeing acceleration effect of octyl trimethyl ammonium bromide on dyeing silk with reactive dyes and adsorption kinetics were studied in this paper.

Experimental

Materials and chemicals. Crepedechine 12101 was obtained from Chongqing Jinfeng silk company. Three reactive dyes (reactive red dye B-3BF, reactive yellow dye B-4RFN and reactive dark blue dye B-2GLN) were obtained from Zhengjiang province Wenling dyeing chemical plant. Octyl trimethyl ammonium bromide(AR) was obtained from Aladdin.

Dyeing. The silk fabrics were dyed in a bathing constant temperature vibrator(SHA-B), the liquor ratio being 1:20. All dyeing were carried out using 2% (o.m.f) dye. Accelerating agent octyl trimethyl ammonium bromide was varied in the ranges of 0-8 g/L. Fabric was immersed in the dye

bath (20 mL) at 80˚C and the dyeing continued for further 60 min. Then sodium carbonate (2 g/L) was added into dye-bath at 60˚C lasting for 30 min. After dyeing, all the dyed samples rinsed with water and air-dried.

Measurement of dye exhaustion(*E*). The absorbance of the diluted dye solution was measured at the wavelength of maximum absorption (λ_{max}) of the dye using a UV-Visible spectrophotometer (TU-1810). The exhaustion *E* of the dye on the silk was calculated according to Eq. 1:

$$E(\%)=(1-A_1/A_0)\times 100. \quad (1)$$

where A_0 and A_1 are the absorbance values of the dye-bath before and after the dyeing process, respectively.

Fixation (*F*). The fabric was soaped-off at a goods -to- liquor ratio of 1:50 using DSASS (1 g/l) and sodium carbonate (2 g/l) at 90˚C for 30 min. After soaping, all the dyed samples rinsed with water and air-dried. The overall fixation efficiency *F* were calculated according to Eq. 2:

$$F(\%)=(K/S)_1/(K/S)_0\times E\%\times 100. \quad (2)$$

Where $(K/S)_0$ and $(K/S)_1$ are the K/S values of the fabrics before and after the soaping process, respectively.

Batch kinetic experiments. All dyeing were carried out using 0.4 g/L dye liquor and 7 g/L octyl trimethyl ammonium bromide. The dyeing of reactive dyes was carried out in water using silk fabric (1g) at a liquor ratio of 1:50. The silk fabric was immersed in the dye solution (50 mL). Then put it in a thermostatted shaker bath operated at 80 rpm shaking at 60, 70, 80˚C, respectively. The silk samples were rapidly withdrawn after different immersion times. Dye concentrations were determined at subsequent times using a calibration curve based on absorbance at λ_{max} versus dye concentration in standard reactive dye solutions. The amount of dye adsorbed per gram of silk (q_t) (mg/g silk) at any time was calculated by a mass-balance relationship (Eq. 3) as follow:

$$q_t=(C_0-C_t)\times V/W. \quad (3)$$

Where C_0 and C_t are the initial and dye concentrations (mg/L) after dyeing time *t*, respectively. V is the volume of dye solutions (mL) and W is the weight of silk fabric (g) used.

Results and discussion

The effect of the concentration of octyl trimethyl ammonium bromide (OTAB) on reactive dyes onto silk. The OTAB is an organic cationic compound. It was designed to be accelerant in dyeing process of reactive dyes on silk instead of sodium sulphide. Fig. 1 showed the acceleration effect of different concentration of OTAB on dyeing silk with reactive dyes. It was found that with the increase of concentration of OTAB, the dye-uptake rate increased monotonously like salt as accelerant. The highest dye-uptake rates were 91~98%. The acceleration theory of OTAB is that: The molecule weight of OTAB is higher than Na^+, which results in the effect of thermal movement on OTAB is smaller than on Na^+. Meanwhile, OTAB has hydrophobic hydrocarbon chain which can make the electric double layer thinner than Na^+. What is more, because of the hydrophobic reaction, OTAB and dyes can compose an ion pair. These make the dyes molecular weight become higher, the solubility decreases. So the dyes can be absorbed on fabric more easily.

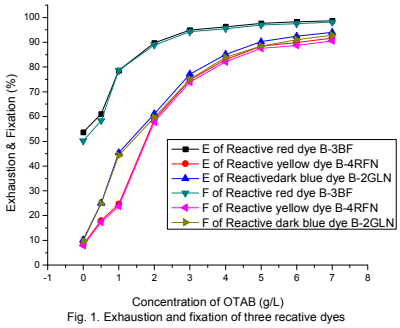


Fig. 1. Exhaustion and fixation of three recative dyes

The effect of temperature on the adsorption of three reactive dyes on silk with OTAB as accelerant. A series of experiments were undertaken to study effect of temperature by performing experiments at 60, 70 and 80˚C. The influences of temperature on the sorption of three reactive dyes

on silk with OTAB were shown in Fig. 2, Fig. 3 and Fig. 4. The rate of sorption increased with increasing temperature, indicating an endothermic process. The dyeing condition was that: initial dye concentration was 400 mg/L , OTAB concentration 7 g/L and MLR 1:50.

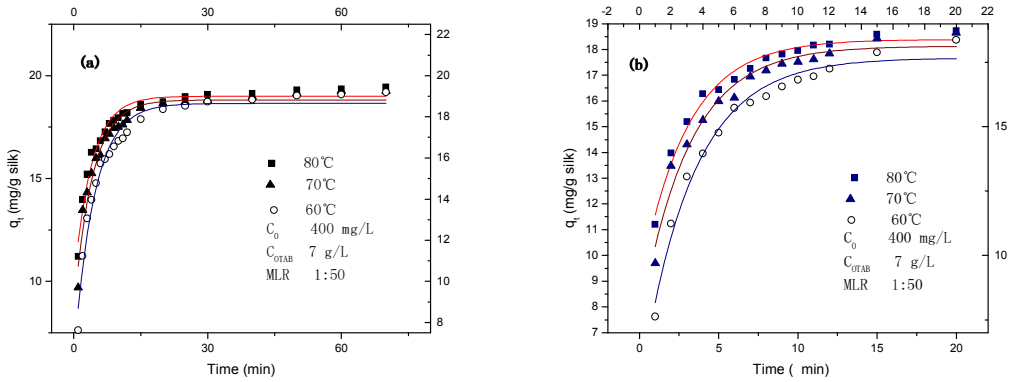


Fig. 2. The effect of contact time and temperature of reactive red dye B-3BF on silk with OTAB as accelerant. (a) The effect of contact time and temperature over a period of 0-70 min. (b) The effect of contact time and temperature over a period of 0-20 min.

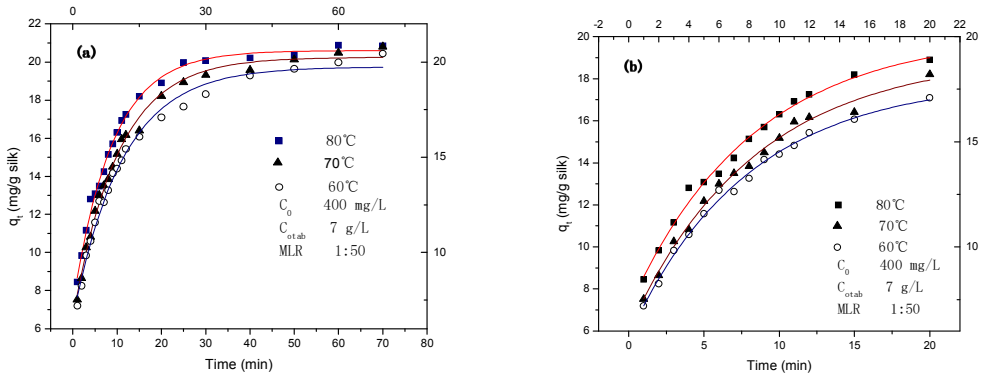


Fig. 3. The effect of contact time and temperature of reactive yellow dye B-4RFN on silk with OTAB as accelerant. (a) The effect of contact time and temperature over a period of 0-70 min. (b) The effect of contact time and temperature over a period of 0-20 min.

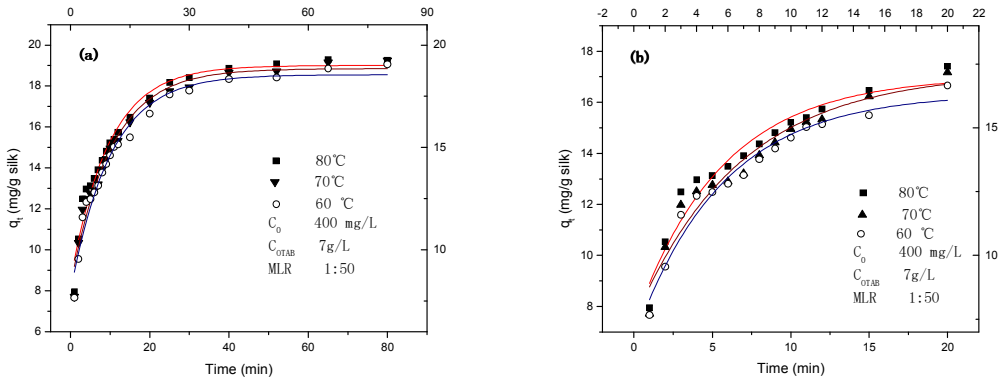


Fig. 4. The effect of contact time and temperature of reactive dark blue dye B-2GLN on silk with OTAB as accelerant. (a) The effect of contact time and temperature over a period of 0-80 min. (b) The effect of contact time and temperature over a period of 0-20 min.

Kinetics of adsorption. In order to analyze the controlling mechanism of the adsorption process, pseudo first-order and pseudo second-order equations were used to test the experimental data.

The Lagergren [5] rate equation is one of the most widely used sorption rate equations for the sorption of a solute from a liquid solution [6]. The pseudo first- and second-order kinetic models were used to analyze the adsorption kinetics of reactive dye with OTAB as accelerant on silk.

The Lagergren equation, a pseudo first-order equation, is a simple kinetic analysis of adsorption. It may be represented:

$$\frac{dq_t}{dt} = k_1(q_e - q_t) \tag{4}$$

where k_1 is the rate constant of pseudo first-order adsorption (s^{-1}), and q_e and q_t are the amounts of dye adsorbed per gram of silk (mg/g silk) at equilibrium and at time t. Integrating Eq. 4 for the boundary conditions $q_t = 0$ at $t = 0$ and $q_t = q_t$ at $t = t$, the equation becomes:

$$\ln(q_e - q_t) = \ln q_e - k_1 t \tag{5}$$

Eq. 5 is a linear form by plotting the $\ln(q_e - q_t)$ against t. The first-order rate constant k_1 and equilibrium adsorption density q_e were calculated from the slope and intercept of this line.

Ho's [7] differential equation of the pseudo second-order adsorptive rate equation can be expressed as:

$$\frac{dq_t}{dt} = k_2(q_2 - q_t)^2 \tag{6}$$

where k_2 (g silk/mg min) is the constant for pseudo second-order adsorption. When the boundary conditions are defined $q_t = 0$ at $t = 0$ and $q_t = q_t$ at $t = t$, integrating and rearranging Eq. 6, gives:

$$\frac{t}{q_t} = \frac{1}{k_2 q_e^2} + \frac{1}{q_e} t \tag{7}$$

and the initial dye adsorption rate h_i (mg/g silk min) is expressed as:

$$h_i = k_2 q_e^2 \tag{8}$$

The slope and intercept of the linear relationship (t/q_t) versus t were used to calculate the pseudo second-order rate constant k_2 and q_e.

Kinetic data of three reactive dyes on silk with OTAB in the study were analyzed using the pseudo first-order kinetic equation Eq. 5. The results are listed in Table 1. The correlation coefficients are all above 0.9, but there are great differences between the equilibrium adsorption of pseudo first-order equation ($q_{e,cal}$) and q_e. So the adsorption of three reactive dyes on silk with OTAB is not likely to be a first-order reaction.

Table 1 The pseudo first-order adsorption rate constants of three reactive dyes onto silk with OTAB at an initial dye concentration 400 mg/L and OTAB concentration 7 g/L, MLR 1:50 and contact time 70 min

Dye	Temperature [°C]	q_e [mg/g silk]	$q_{e1,cal}$ [mg/g silk]	k_1 [min^{-1}]	R^2
Reactive red dye B-3BF	60	19.19	10.18	1.48×10^{-1}	0.9477
	70	19.27	8.19	1.58×10^{-1}	0.9456
	80	19.44	7.27	1.62×10^{-1}	0.9541
Reactive yellow dye B-4RFN	60	20.44	13.09	7.39×10^{-2}	0.9772
	70	20.8	13.58	8.43×10^{-2}	0.9817
	80	20.84	12.94	1.01×10^{-1}	0.9878
Reactive dark blue dye B-2GLN	60	19.05	10.08	7.63×10^{-2}	0.9738
	70	19.25	10.09	7.92×10^{-2}	0.9804
	80	19.25	9.93	8.75×10^{-2}	0.9824

Table 2 The pseudo second-order adsorption rate constants of three reactive dyes onto silk with OTAB at an initial dye concentration 400 mg/L and OTAB concentration 7 g/L, MLR 1:50 and contact time 70 min

Dye	Temperature [°C]	q_e [mg/g silk]	$q_{e2,cal}$ [mg/g silk]	k_2 [min^{-1}]	h_i [mg/g silk min]	R^2
Reactive red dye B-3BF	60	19.19	19.6	3.24×10^{-2}	12.45	1
	70	19.27	19.57	4.62×10^{-2}	17.7	1
	80	19.44	19.64	5.61×10^{-2}	21.64	1
Reactive yellow dye B-4RFN	60	20.44	21.36	1.09×10^{-2}	4.99	0.998
	70	20.8	21.74	1.18×10^{-2}	5.58	0.999
	80	20.84	21.79	1.53×10^{-2}	7.24	0.999
Reactive dark blue dye B-2GLN	60	19.05	19.64	1.69×10^{-2}	6.54	0.999
	70	19.25	19.88	1.73×10^{-2}	6.85	0.999
	80	19.25	19.92	1.92×10^{-2}	7.62	0.999

The experimental data were also test by using the pseudo second-order adsorption kinetic equation Eq. 7, and plots of (t/q_t) against t for the adsorption of three reactive dyes on silk with OTAB as accelerant are given in Fig. 5, Fig. 6 and Fig. 7. The equilibrium adsorption of pseudo second-order equation ($q_{e2,cal}$) and the rate constant (k_2) was calculated by using the slopes and intercepts of these plots. The results calculated with linear fitting method are listed in Table 2. The experimental data showed the correlation coefficients for the linear plots were all higher than 0.998, even the correlation coefficients of reactive red dye B-3BF were 1. Also, there was a tiny discrepancy between the calculated ($q_{e2,cal}$) values and the experimental data (q_e). These suggested that the pseudo second-order adsorption kinetic equation could be well represented the adsorption kinetic process of three reactive dyes on silk with OTAB as accelerant. Similar kinetics were also observed in lac dyeing on cotton and silk [8,9].

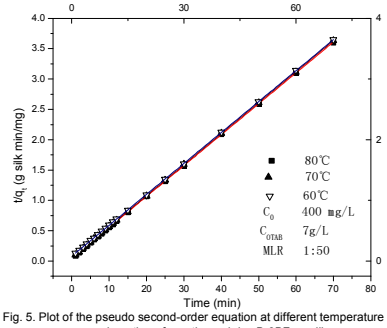


Fig. 5. Plot of the pseudo second-order equation at different temperature for the adsorption of reactive red dye B-3BF on silk.

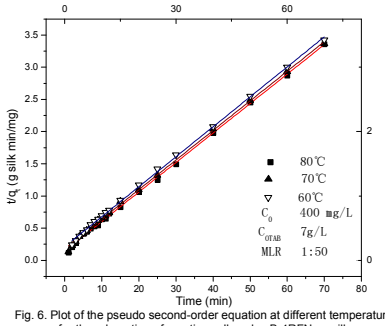


Fig. 6. Plot of the pseudo second-order equation at different temperature for the adsorption of reactive yellow dye B-4RFN on silk.

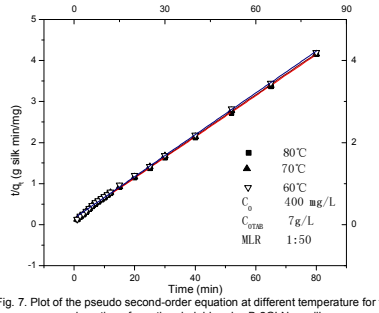


Fig. 7. Plot of the pseudo second-order equation at different temperature for the adsorption of reactive dark blue dye B-2GLN on silk.

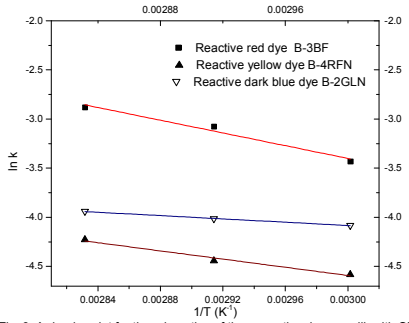


Fig. 8. Arrhenius plot for the adsorption of three reactive dyes on silk with OTAB

Activation parameters. The activation energy (E_a) for the adsorption of three reactive dyes on silk with OTAB was determined using the Arrhenius Eq. 9 [10]:

$$\ln k = \ln A - \frac{E_a}{RT} \tag{9}$$

where E_a, R and A refer to the Arrhenius activation energy, the gas constant (8.314 J/mol K) and the Arrhenius factor, respectively.

The Arrhenius plot of $\ln k$ against $1/T$ for the adsorption of three reactive dyes on silk with OTAB is shown in Fig. 8 and the activation energy value is listed in Table 3.

Table 3 Activation parameters for the adsorption of three reactive dyes on silk with OTAB at an initial dye concentration 400 mg/L and OTAB concentration 7 g/L, MLR 1:50 and contact time 70 min

Dye	Temperature[°C]	k_2 [g silk/mg min]	E_a [kJ/mol]	R^2	ΔH [kJ/mol]	ΔS [J/mol K]	ΔG [kJ/mol]	R^2
Reactive red dye B-3BF	60	3.2×10^{-2}	26.912	0.977	24.06	-201.92	91.33	0.971
	70	4.6×10^{-2}					93.35	
	80	5.6×10^{-2}					95.37	
Reactive yellow dye B-4RFN	60	1.0×10^{-2}	17.31	0.963	11.1	-250.24	94.66	0.948
	70	1.1×10^{-2}					96.97	
	80	1.5×10^{-2}					99.47	
Reactive dark blue dye B-2GLN	60	1.7×10^{-2}	6.999	0.999	4.15	-267.34	89.07	0.999
	70	1.8×10^{-2}					91.74	
	80	1.9×10^{-2}					94.42	

The enthalpy (ΔH), entropy (ΔS) and free energy (ΔG) of activation were also calculated using the Eyring Eq. 10 [10] as follows:

$$\ln(\frac{k}{T}) = \ln(\frac{k_b}{h}) + \frac{\Delta S}{R} - \frac{\Delta H}{RT} \quad (10)$$

where k_b and h refer to Boltzmann's constant and Planck's constant, respectively. The enthalpy (ΔH) and entropy (ΔS) of activation were calculated from the slope and intercept of a plot of $\ln k/T$ versus $1/T$. Reactive red dye B-3BF was y=-0.5274-2894; R^2=0.9712; Reactive yellow dye B-4RFN was y=-5.1828-173.92x; R^2=0.9478; Reactive dark blue dye B-2GLN was y=-8.39579-498.9x; R^2=0.999. While the free energy of activation (ΔG) was obtained from Eq. 11:

$$\Delta G = \Delta H - T\Delta S \quad (11)$$

The calculated values are listed in Table 3. The negative value of the activation entropy (ΔS) was supportive of an interaction between reactive dyes and silk.

Conclusions

This article studied silk dyeing with reactive red dye B-3BF, reactive yellow dye B-4RFN and reactive dark blue dye B-2GLN by using octyl trimethyl ammonium bromide(OTAB) as dyeing acceleration. The results suggested OTAB was an effective accelerant for reactive dyes dyeing on silk. Reactive red dye B-3BF, reactive yellow dye B-4RFN and reactive dark blue dye B-2GLN had high dye-uptake rates. The rate of adsorption increased with increasing temperature. The adsorption kinetics of three reactive dyes on silk with OTAB was found to follow the pseudo second-order model. The activation energy of reactive red dye B-3BF, reactive yellow dye B-4RFN and reactive dark blue dye B-2GLN dyeing on silk with OTAB as accelerant were found to be 26.91, 17.31, 6.99 kJ/mol respectively.

Acknowledgements

This study was supported by Southwest university doctor fund(swu.109053).

References

[1] Guangxian Zhang, Cheng Lu. Effect of silk fabric grafted with cation compound on it's characteristics of dyeing rate and fastness[J]. Science of Sericulture. 2008, 34(4): 701-705, in Chinese.

[2] K. Sawadaa, M. Uedab. Dyeing of protein fiber in a reverse micellar system[J]. Dyes and Pigments, 2003, 5(8),199-203.

[3] Yingling Li, Shufen Zhang. Synthesis and application of novel crosslinking polyamine dyes with good dyeing performance[J]. Dyes and Pigments. 2008, 76:508-514.

[4] Bingtao Tang, Shufen Zhang, Jinzong Yang, Feng Liu. Synthesis of a novel water-soluble crosslinking polymeric dye with good dyeing properties[J]. Dyes and Pigments, 2006, 68: 69~73.

[5] S. Lagergren. About the theory of so-called adsorption of soluble substances[J]. Kungliga Svenska Vetenskapsakademiens Handlingar Band, 1898, 24(4): 1-39.

[6] Y. S. HO, G. MCKAY. The sorption of lead (Ⅱ) ions on peat [J]. Water Res, 1998, 33(2): 578-584.

[7] HO Y S. Adsorption of heavy metals from waste streams by peat [D]. UK Binrmingham: University of Birmingham, 1995.

[8] Saowanee Rattanaphani, Montra Chairat, John B Bremner. An adsorption and thermodynamic study of lac dyeing on cotton pretreated with chitosan[J]. Dyes and Pigments. 2007, 72: 88-96.

[9] Montra Chairat, Saowanee Rattanaphani, John B Bremner. An adsorption and kinetic study of lac dyeing on silk[J]. Dyes and Pigments. 2005,64:231-241.

[10] M. D ogan and M. Alkan. Adsorption kinetics of methyl violet onto perlite[J]. chemosphere. 2003, 50: 517-528.

© (2011) Trans Tech Publications, Switzerland
doi:10.4028/www.scientific.net/AMR.331.298

Dyeing analysis of Jade polyester fiber knitted fabric

Haixia Hu

Zhe Jiang Industry Polytechnic College, ShaoXing 312000, P.R.China

Email-huhaixia1982@sohu.com

Keywords: Jade polyester fiber, dyeing, analysis

Abstract: This study analyzes the principle of dispersal dyeing on jade polyester fiber knitted fabric, and confirms the suitable dyeing technology on jade polyester fiber knitted fabric. By testing the color fastness to washing, color fastness to rubbing and color fastness to perspiration, the results show good. So it indicates that this dyeing process is very suit for the jade polyester fiber knitted fabric.

Introduction

Jade polyester fiber is a new type of functional fiber. It made the jade into jade powder to particle size below 0.5μm at first，then put the jade powder treated by silicon surfactant into polyester spinning at a high temperature to get the new type of fiber through traditional system [1]. The general percentage composition of jade powder is between 2% and 3%.

Jade polyester fiber has cool and health protection specialties because it contains rich minerals and trace elements. When the fabric of jade polyester fiber was attached to human skin, the good effect of jade will be released. It will improve people's blood circulation and promote metabolism. So it can prevent disease and eliminate fatigue for people [2]. In addition, Jade polyester fiber has cooling and natural antimicrobial function characteristics, so it very suits to produce knitting fabric products (such as T-shirt, underwear and so on) in summer [3]. In addition, research and production is good for human ecology and the health of functional textile products, has become the development trend in today's world. So the jade polyester fiber knitted fabric meet the consumer trend of health care and fashionable and it will enjoy a promising market．But now this fiber is a new material and research about jade polyester fiber is rarely, especially about dyeing process of jade polyester fiber knitted fabric. So it is necessary to analysis and research the dyeing with it to improve the class and increase its added value of the product.

2. Experiment

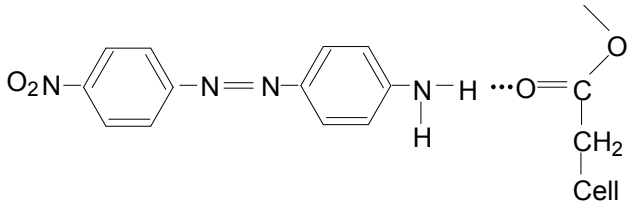
2.1 Materials and apparatus

Fabrics: 100% pure jade polyester fiber knitted fabric of bleaching.

Apparatus: Infrared dyeing machine, PH tester, color fastness to washing tester SW-12M, colorfastness to rubbing tester Y571M, color fastness to perspiration tester YG631.

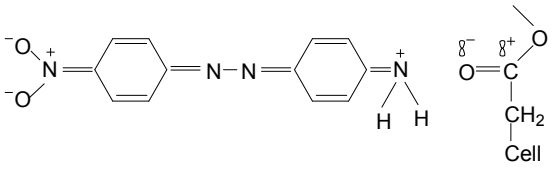
2.2 Dying principle

Dispersal dye to jade fiber mainly rely on the van der Waals force between the molecules attract each other. It because some of the molecular structure of dye polar groups (such as-OH,-NH2, -NHR and so on)can supply protons, which can bond with  of polyester base to formed molecules of hydrogen bond. Response equation is shown as equation(1):



(1)

For electronic group dipole polarization of the dye molecules, it with fiber's  to form the dipole moment. Response equation is shown as equation (2):



(2)

In the dying process, the dye transference to reduce off color has a significant effect. When choosing low transference of dyes, we can join the assistant so as to promote the dye migration. Disperse dye not only has simple structure, but also does not contain the ionization group. It will appear the sublimation phenomenon when there is a steam pressure. The higher the temperature is, the more rapid sublimation [4]-[6]. Generally speaking, the poor sublimation with high temperature type and good mobility dye, which will have levelling property dye on jade polyester fiber knitted fabric. In practice, in order to have good dyeing effect that should choose dyeing methods similar properties according to dyeing process.

2.3 Technological formulation

Dye	2%(o.w.f)
pH Value	6.0
Bath ratio	1：50
Dyeing temperature	130℃
Dyeing time	35min

Control the pH value by acetic acid and sodium acetate

2.4 Dyeing process route

The dyeing process route figure of jade polyester fiber knitted fabric is shown in Fig.1.

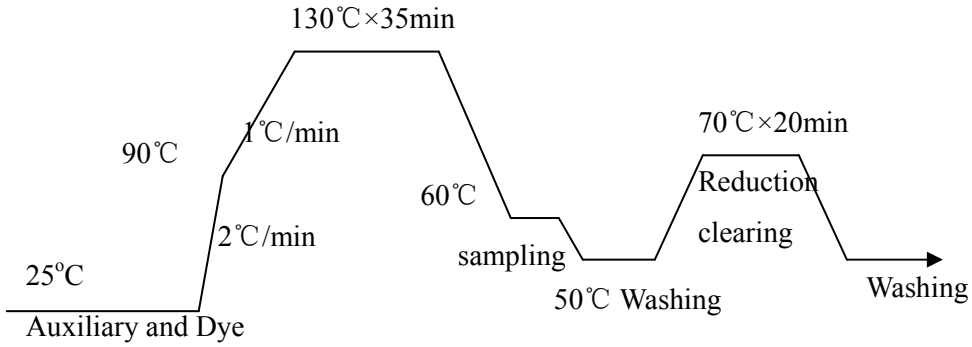


Fig.1 Dyeing process route figure of jade polyester fiber knitted fabric

3. Results and discussion

3.1 Testing and analysis of color fastness to washing

Fabric soaping fastness is the firm degree of colour and lustre of fabric dyeing and printing resistance of soaping. It accord to the Chinese national standard GB/T3921-1997 to test. The results as is shown in table 1.

Table 1 The results of color fastness to washing

Fabric number			1	2	3	4	5
The grades of color fastness to washing	Discoloration		4~5	4~5	4~5	4~5	4~5
	Staining	Wool fabric	4~5	4~5	4~5	4~5	4~5
		Cotton fabric	4~5	4~5	4~5	4~5	4~5

Note: 5th grade is the best and first grade is worst about color fastness to washing.

From Table 1, it can be found that this dyeing jade polyester fiber knitted fabric has good color fastness to washing.

3.2Testing and analysis of color fastness to rubbing

The color fastness to rubbing is the firm degree of fabric dyeing and printing the colour and lustre of tolerance of friction. It includes wet and dry friction. It accords to the Chinese national standard GB/T3920-1997 testing. The results as is shown in table 2.

Table2 The results of color fastness to rubbing

Fabric numeber			1	2	3	4	5
The grades of color fastness to rubbing	Dry friction	Warp	4~5	4~5	4~5	4~5	4~5
		Weft	4~5	4~5	4~5	4~5	4~5
	Wet friction	Warp	4~5	4~5	4~5	4~5	4~5
		Weft	4~5	4~5	4~5	4~5	4~5

Note: 5th grade is the best and first grade is worst about color fastness to rubbing.

Table 2 shows that this dyeing jade polyester fiber knitted fabric has good color fastness to rubbing.

3.3 Testing and analysis of color fastness to perspiration

The color fastness to perspiration is the firm degree of fabric dyeing and printing the colour and lustre of sweat dipping. It accords to the Chinese national standard GB/T3992-1995 testing. The results as is shown in table 3.

Table3 The results of color fastness to perspiration

Fabric numeber			1	2	3	4	5
the grades of color fastness to perspiration	Discoloration		4	4	4	4	4
	Staining	Wool fabric	4	4	4	4	4
		Cotton fabric	4	4	4	4	4

Note: 5th grade is the best and first grade is worst about fastness to perspiration.

We can see from Table 3, the dyeing jade polyester fiber knitted fabric has good color fastness to perspiration.

Conclusions

Though research and analysis of principle of dispersal dyeing on jade polyester fiber knitted fabric, the study adopt the dyeing processing formulation is: disperse dyes with 2%(o.w.f), pH value with 6.0, liquor ratio with 1:50, dyeing temperature at 130℃ and dyeing time with 35min. And then develop and confirm a dyeing process route to dye on the jade polyester fiber knitted fabric. By testing about fabric's color fastness to washing, color fastness to rubbing and color fastness to perspiration, all of color fastness is more than 4th grade. So it indicates that the dyeing process is very suit for the jade polyester fiber knitted fabric and has reference value to enterprise for actual production.

References

[1] Liu Weiwei, Shan Xiaohong, Du Zhaofang. Shanghai textile science & technology. 2010(8) :14.(In Chinese)

[2] PanRan. Textile Information Weekly.2006(24)：31. (In Chinese)

[3]Ren Cailing, Wang Jiguo, Meng JiaGuang. Knitting industry.2010(10):11. (In Chinese)

[4]Kong Fanchao. Polyester knitted fabric dyeing. Textile industry press.1982(8):107. (In Chinese)

[5]Cui Hao ran. Dyeing and Finishing .2003(10) :13-17. (In Chinese)

[6]Chen Yin, The dyeing and finishing experiments tutorial, China's textile press，2004(10)：41-43. (In Chinese)

© (2011) Trans Tech Publications, Switzerland
doi:10.4028/www.scientific.net/AMR.331.302

Dyeing of Natural Dyestuff Extracted from Henna to Silk Fabric

Hong Li[1,2 a], Defeng Zhao[1], Rui liu[2,b]

1 Faculty of Chemical ,Environmental and Biological Science and Technology of Dalian Technology University, Dalian,Liaoning 116024, China

2 School of Textile and Material Engineering of Dalian Polytechnic University, Dalian ,Liaoning,116034, China

[a]lihong@dlpu.edu.cn , [b]woliurui@126.com

Key words : henna ; natural dyestuff ; dyeing ; mordant dyeing ; silk fabric

Abstract. A natural dye was isolated from the leaves of Henna . The extracted dye was applied to silk fabric, The dyeing effects of fabric without and with different mordants were investigated . The results showed that the dyeing of silk using the post-mordanting method with ferrous sulfate, copper sulfate and alum, rare earth not only provided better depth of shade but also provided better wash fastness and rub fastness than without mordant. In addition, green and orange silk can obtained selecting rare earth as mordant.

Introduction

Lawsonia inermis Linn, a tropical shrub, belonging to family Lythraceae is widely distributed in Bangladesh as well as tropical Asiatic zone . It is harmless and causes no irritation to skin. It is also a good medicinal plant[1-3]. It is used in many countries for dyeing hair, eyebrows, palms, soles of feet, finger nails and other body parts[4]. So far there is little known about Henna dyeing on textiles except dyeing of wool and nylon 6,6[5-6] .In this investigation, the dye was extracted, isolated, identified.The extracted dye was applied to silk fibre and its color fastness was studied.

Materials

The Silk fabric used was purchased from market of Dalian. Leaves of henna was picked from Benxin City of Liaoning province in June. Leaves were sliced and dried at room temperature for 30 days, then crushed The leaves were extracted with distilled water at 80 ℃ for 1 hour. The dye solution was centrifugally filtered and distilled to give a trick paste of pigment. It was kept cold at 5℃ for further use. All other chemicals used were laboratory grade reagents purchased from Chemical and Instruments, Dalian, including copper sulphate, Ferrous sulphate, aluminum potassium sulphate , rare earth, acetic acid, and soda ash.

Experiment methods

Direct dyeing： A dye bath is prepared with 3% (o.w.f) and 1:30 bath ratio. The pre-mordanted fabric was treated in the solution of 60 ℃ at the beginning of dyeing, and then raise the temperature until 90 ℃ at the rate of 1℃ / min. Kept this temperature for 30 minutes. After that, take it out, clean and dry it under shades.

Pre-mordantinging Method：the silk fabric was soaked in mordant solution (10% o.w.f., ratio 1:30) for 30min. After pre-mordanting, the silk was squeezed to remove excess liquor and then air dried at room temperature. A dye bath is prepared with 3% (o.w.f) and 1:30 bath ratio. Dyeing was carried out at 60 ℃ , and then raise the temperature until 90℃ at the rate of 1℃ / min. Keep this temperature for 30 minutes. After that, take it out, clean and dry it under shades.

Simultaneous mordanting Method： A dye bath is prepared with 5% (o.w.f.) and 1:30 bath ratio for study. Dyeing was carried out with dye solution containing different mordants(10% o.w.f, ratio 1:30) at 60 ℃ at the beginning of dyeing, and then raise the temperature until 90℃ at the rate of 1℃ / min. Kept this temperature for 30 minutes. After that, take it out, clean and dry it under shades.

Post-mordanting Method： A dye bath is prepared with 5% (o.w.f) and 1:30 bath ratio for study. Dyeing was carried out at 60 ℃ at pH 3 at the beginning of dyeing, and then raise the temperature until it reaches 90℃ at the rate of 1℃ / min. Kept this temperature for about 30 minutes. After that, put the sample into the solution within mordant (10% o.w.f., ratio 1:30) for 30 minutes at 90℃.Then take it out, clean and dry it under shades.

Measurements

Fastness measurements： The dyed samples were tested according to Chinese standard methods. The specific tests were: color fastness for rubbing , GB 3920-1997, color fastness washing; GB3921-1997. Washing fastness instrument (Roaches,ShangHai) and Rubbing fastness instrument(Atlas CM-5,ShangHai) were used in the experiment.

Color measurements： The relative color strength of dyed fabrics expressed as K/S was calculated from the reflectance measured by Computer Color Measurement Meter(Datacolor 600 Japan) using the Kubelka-Munk equation， as is follows.

$$K/S = (1-R)2/2R. \quad (1)$$

Where R is the decimal fraction of the reflectance of dyed fabric under the max wavelength .L is correspond to the brightness (100 = white, 0 = black), a to the red-green coordinate (positive sign = red, negative sign = green) and b to the yellow-blue coordinate (positive sign = yellow, negative sign = blue).Chroma (C) is a measure of intensity or saturation of color and Hue angle (H) is derived from the two coordinates a and b. They are measured by Color Difference Meter (lolowrSF300, Germany).

Results and discussions

Silk fabric were dyed without mordant and with various mordants and mordanting method is pre-mordanting,post-mordanting and simultaneous mordanting. the dying depth of shade were assessed after dyeing of silk fabric with different dyeing methods. The results were shown in figure 2.The figure shows that K/S values increase from no-mordanting, simultaneous mordanting|and pre-mordanting to post-mordanting. The reason why mordant dyeing is better than dyeing without mordant is that rare earths ion in the mordant react with henna natural dye, and generate complex ,which can enhance the dyeing rate and deepen the color. There are two reasons why post-mordanting is better than pre-mordanting and simultaneous mordanting.On the one hand, the dye react with protein, and then coordinate with mordant. This fact increases fixation rate heavily. On the other hand ,during dyeing process, dye molecule which is fixed to surface of protein react with metallic ion and generate insoluble complex fixed on the fiber. During the process of pre-mordant, the mordant drop from sample into dye bath, react with dye and get insoluble complex. This reaction

can lower dye bath concentration. During simultaneous-mordanting process, mordant complex with dye, so dye which is to be fixed on the sample is lower. In a word , post-mordanting is better to dye silk fabric.

Table1 Comparison of the K/S values of silk dyed with henna dyestuff using different mordanting methods

Mordant	Pre-mordanting K/S	Simultaneous mordanting K/S	Post-mordanting K/S
No mordant	1.31	1.31	1.31
FeSO7H O	3.12	3.38	4.22
CuSO4*5H2O	2.98	3.45	5.09
AlK(SO4)2*12H2O	4.06	3.21	5.60
Rare earth	1.97	2.67	5.76

Different mordants effect not only the sample's color hue but also color light. In this experiment, dyeing results are indicated by K/S, L, a, b and c value . K/S value shows the depth of fabric surface color, L value shows the lightness. L value is bigger means that lightness is higher. A value shows important red factor, which is bigger means that red light of fabric is more. B value must be positive number that is bigger means yellow light is more. C value shows Chroma index. That the index is bigger means the dyed product is more colorful . The table 2 shows that using the same natural dye with different mordants can get different color on silk fabric, and dyeing with alum mordant and rare earth mordant can get bright orange silk fabric. The table 3 shows that when dyeing with different mordants, L value ,a value and c value of dyed fabric with alumina mordant and rare earth are bigger than that with others, and so dyeing with them can get bright orange silk fabric. Mordant of rare earth can solve environmental pollution that traditional heavy metal mordants caused. So rare earth is selected.

Table 2 Color of dyed fabrics with various mordants

Mordant	Rare earth	KAl(SO4) 2 ·12H2O	FeSO4·7H2O	CuSO4·5H2O	No-mordant
Color	Orange	orange	Black-gray	Gray-green	Light orange

Table 3 Impact of mordant on color characteristic of sample

Mordant agent	K/S	L	a	b	c
Without dyeing	0.445	5.71	2.11	3.01	1.45
Iron mordant	8.457	3.11	9.42	13.24	3.26
Copper mordant	5.874	3.38	4.74	5.62	5.79
Alumina mordant	5.246	4.06	12.13	16.52	6.29
Rare earth	7.324	4.13	13.91	19.78	7.21

The fastness of dyed silk fabrics is shown in table 4. Generally, the color fastness of silk fabrics with and without mordants by henna natural dyestuff reached 3 grade, This showed that henna natural dyestuff was applied to silk fabric dyeing could get a better fastness. When using mordant dyeing, the color fastness of dyed samples had a certain degree of increase. As the metallic irons can multi-complex with coordination group in natural dyes and the protein fiber to form a stable multi-complex, play a certain role in fixing the color to gain the improvement of fastness. Rub fastness and wash fastness of the dyeing samples reach over 3 grade, which satisfy clothing fastness.

Table 4 Impact of mordant on Dyeing fastness

Mordant agent	Dry rub fastness		Wet rub fastness		Wash fastness	
	Discoloration	staining	Discoloration	staining	Discoloration	staining
no mordant	3	3	3	3	3	3
iron mordant	3-4	3	3-4	3	3-4	3
Alumina dant	3-4	3	3	3	3-4	4
copper ordant	4	3-4	3-4	3-4	3	3
rare earth	4-5	4	4	3-4	3-4	4

Conclusions

Natural dyestuff extracted from the leaves of henna serves as a useful alternative natural dye for the dyeing of silk. Different shades of color were obtained by using different mordants. It was found that post-mordanted samples obtain higher K/S values than other dyeing methods. Good fastness properties were also obtained using post-mordanting with various mordants, Therefore, the extracted from the leaves of henna can be used as alternative source of natural dye for dyeing of silk. In addition, green and orange silk can obtained selecting rare earth as mordant.

References

[1] Hu SG, Zhou AJ and Yan KL: Dye and dyeing Vol.12 (2009),P. 265

[2] HAN XJ: Knitting Industries Vol.46 (2007),P.5

[3] Yu Jing and Jia LX: Knitting Industries Vol.26(2005),p.42

[4] M,K Yakubu: Foreign Textile Technology Vol.5 (2001),P.5

[5] Gulrajani ML, Srivastava RC and Goel M: Coloration Technology Vol. 22(2001), p. 225

[6] Mathur J and Gupta N: Textile Research Vol. 28(2003), p. 90

© (2011) Trans Tech Publications, Switzerland
doi:10.4028/www.scientific.net/AMR.331.306

Preparation of Jasmine Microcapsules and Aroma Finishing of Cotton Fabrics by UV-curing

Ning Xu[1, 2, a], Dan Yu[1,2,b] and Wei Wang[1,2 *, c]

[1]College of Chemistry, Chemical Engineering and Biotechnology, Donghua University, Shanghai , P. R. China 201620

[2]Key Laboratory of Textile Science & Technology, Ministry of Education,Donghua University, Shanghai, P. R. China 201620

[a]P222333x@mail.dhu.edu.cn, [b]yudan@dhu.edu.cn, [c]wangv@dhu.edu.cn.

Key words: jasmine microcapsules, UV-curing, aroma finishing, cotton fabrics

Abstract: In this paper, jasmine microcapsule was synthesized by in-situ polymerization and was applied on cotton fabric with UV curing method. The jasmine microcapsule was verified by Fourier transform infrared spectroscopy. Size distribution was evaluated using particle size analysis. The finishing durability was studied by human olfactory sensations and an optimal finishing process was determined. The results suggest that UV curing will be promising for use in aroma finishing.

Introduction

Encapsulation is an effective way to protect functional agents from reactions with moisture, light and oxygen in fragrance finishing [1]. However, during the fragrance finishing of the fabric, traditional thermal curing may cause the core component in the capsule to volatilize or possibly break the capsules and consumes large amounts of energy [2]. In this study, we apply the microcapsules on the fabrics through UV curing method which applied functional capsules onto the fabric with a UV-curable resin. The fabric was then exposed to UV light to polymerize the resin components into a continuous film that can tightly fix the capsules. In addition, the effects of reaction conditions on fragrance durability were investigated.

Materials and methods

Materials. Trimethylol melamine prepolymer (75 wt% aqueous solution), hexamethylol melamine prepolymer (55 wt% aqueous solution) and PDA (sodium styrene-maleic anhydride copolymer, 9 wt% aqueous solution) were obtained from Hansi Chemical Reagent. Acetic acid (A.R.), ammonia (C.R.) were purchased from Sinopharm Chemical Reagent. Jasmine perfume compound (Shanghai Yajia Essence Perfume Co.Ltd.) was used as the core material in the microcapsules. A bleached and mercerized 100% cotton plain woven fabric (Saintyear Holding) and an UV resin were used in the aroma finishing. The UV resin included unsaturated polyurethane (35% solid/water emulsion) as oligomer and initiators. Runtecure 1265 were used as radical photoinitiators from Changzhou Runtec Chemical Co. Ltd.

Preparation of microcapsules. Jasmine oil, PDA and distilled water were mixed and emulsified mechanically at a rate of 16000 rpm for 10 min. The emulsion was adjusted to pH 4.5 with acetic acid. The ratio of core to wall of microcapsule was 1:1 in this experiment. The trimethylol melamine prepolymer solution was added. After that, it was continuously stirred for 90 min at 65 ˚C. Next, the hexamethylol melamine prepolymer solution was droped slowly to the emulsion. After that, it was continuously stirred for 120 min at the temperature of 75 ˚C. The pH of emulsion was adjusted to 9 with ammonia solution, which terminated the reaction. At last, 1.0 g urea was added to remove the remnant formaldehyde. The obtained microcapsules were filtered and washed with 30 wt% ethanol-water solution and distilled water. The final microcapsules were stored in an aqueous solution containing an emulsifier (Disponer W-18) to prevent the formation of agglomerates and increase microcpsules water compatibilty.

Preparation of the coating pastes, coating and fixation process. The microcapsules pastes for UV-curing were prepared from demineralised water, 3 g kg^{-1} of PTF synthetic thickner, 200 g kg^{-1} of oligomer, 100 g kg^{-1} of jasmin microcapsules, 30 g $kg^{-1}$of photoinitiator. The prepared and well homogenized pastes were applied to the cotton fabric using laboratory coating machine. The surface-coated fabrics were dried at 60 ˚C for 3 min and then exposed to the UV radiation with an electrode medium pressure mercury arc continuous UV light with linear power 300 W/inch in a small box equipped with a quartz window. The distance between UV lamps and fabrics was 50 mm.

FTIR, Particle distribution. FTIR spectra were collected on a FTIR Varian (model 640-IR) in transmittance mode using KBr pellets .The particle size distribution of the produced microcapsules was analyzed by laser dispersion using Coulter LS1332.

Durability of aroma finishing. The washing conditions were in accordance with the norm of GB/T8629-2001. Abrasion test was carried out in a MARTINDALE apparatus according to the norm ISO 12947-2. In the washing test the odor evaluation method was based on Lewis's procedure [3]. In the abrasion test, the sensorial evaluation results was performed by a group of ten well-trained subjects, fabrics were smelt every five days in order to feel the scents [4].

Results and discussions

FTIR analysis. Spectrum of jasmine perfume, shell material and the formed microcapsules were all measured.

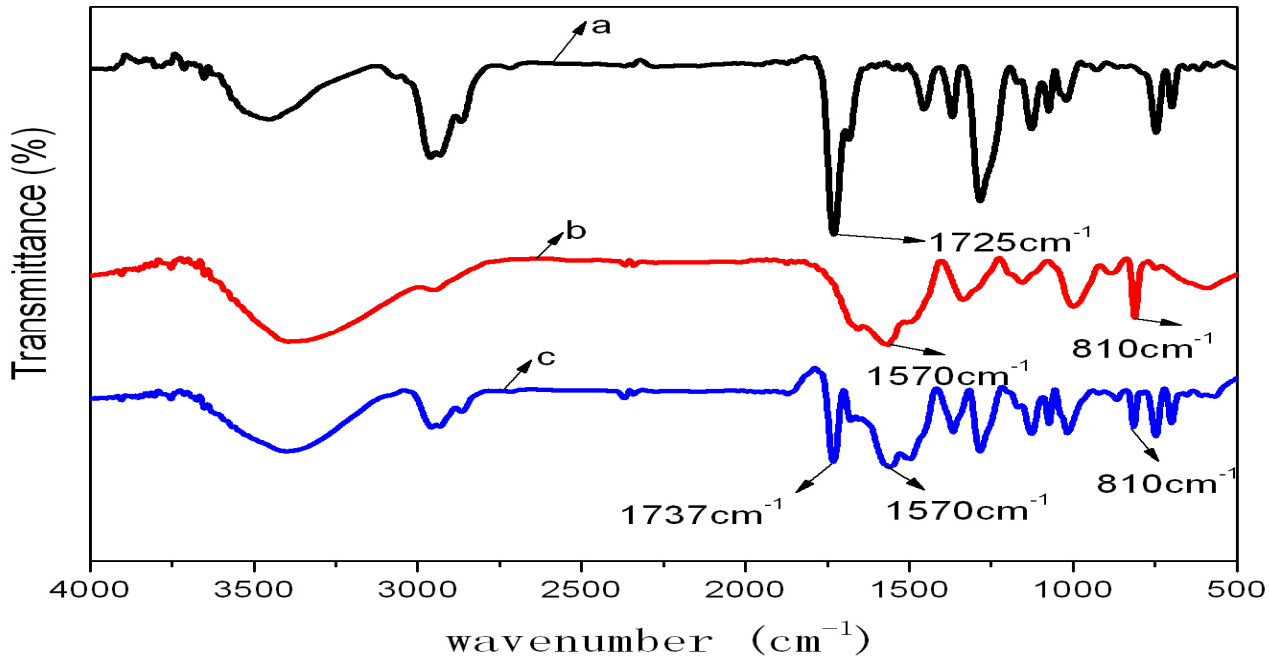


Fig.1 FTIR spectrum of the jasmine perfume, shell material and microcapsules, a: jasmine oil; b: shell material; c: microsapsules

As shown in Fig. 1, jasmine oil has carbonyl group due to the strong vibration at 1725 cm^{-1}. It is seen clearly in the spectrum of shell material the characteristic peaks of C=N stretching vibrations at 1570 cm^{-1} and triazine ring characteristic stretching vibration at 810 cm^{-1}. There's no absorption peak around 1700 cm^{-1} compared to jasmine oil which means there's no carbonyl group in the shell material. Fig. 1 also shows that the microcapsules contains C=N (presence of 1570 cm^{-1}) and triazine ring (presence of 810 cm^{-1}) just like shell material. Moreover, just like jasmine oil there appears strong absorption peak at 1729 cm^{-1}which is the stretching vibration of carbonyl group. This observation is the conformity for the formation of jasmine microcapsules.

Particle size distribution. After production of perfume microcapsules, the particle size distribution was measured by laser dispersion as shown in Fig. 2.

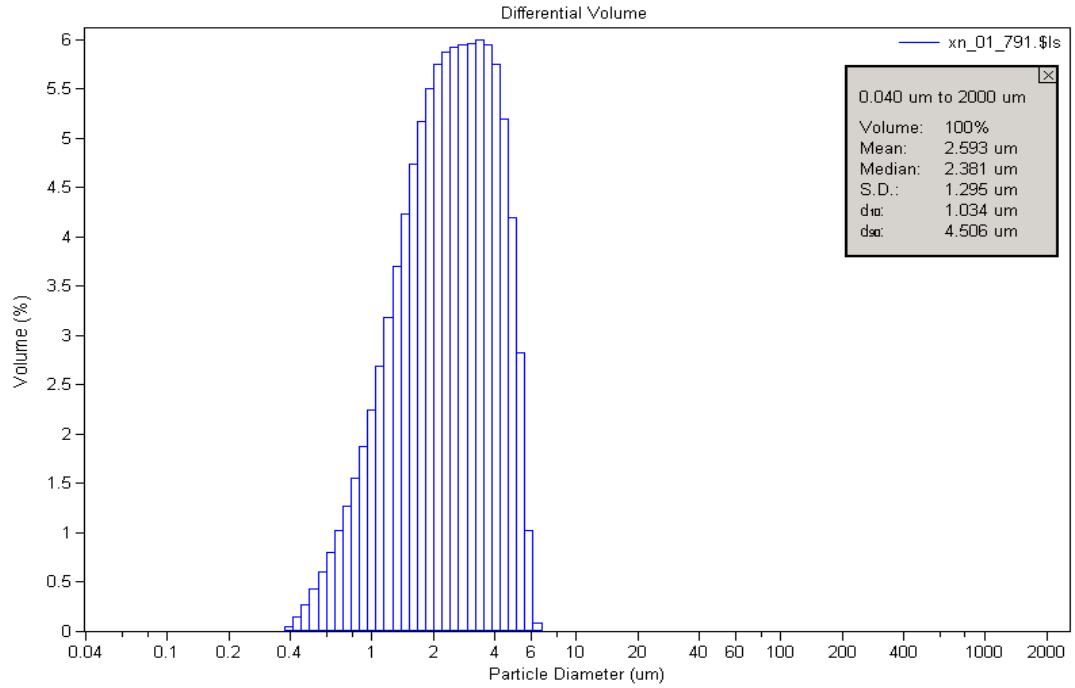


Fig. 2 Particle size distribution in volume of microcapsules with perfume

As shown in Fig. 2, the microcapsules mean size(based on volume distribution) is 2.6 μm and the diameter distribution is narrow. Since the size of the microcapsule is small, it is expected that the microcapsules could be anchored by the binder on the textile substrate.

Washing durability of fragrant fabric by UV-curing. In the finish process, the curing time can have an important influence on the UV curing. The longer the curing time, the more energy delivered to the sample. a sample cured under mercury light could bear 30 washing cycles if cured for 4 min or 5 min. However, further increasing the curing time means no adding of the wash durability. It seemed 4 min was proper for UV-curing in the aroma finishing.

Abrasion test of fragrant finish by UV curing. As can be seen in Table 1, after 10,000 abrasion cycles, the scent of aroma fabric still existed although it was not as strong as before. The results of scent evaluation of the aroma finishing by UV-curing indicated the fragrance on the fabrics had good durability.

Table 1. Sensorial evaluation of scent intensity of aroma finishing fabric after abrasion test[a]

Number of abrasion cycles	Scent intensity
0	+++++
3,000	++++
6,000	++++
10,000	++

[a]+++++ express very strong; ++++ express strong; +++ express common; ++ express weak; + express very weak.

Conclusions

The results of present investigation show that it is possible to achieve durable fragrant finishing on cotton fabrics by UV-curing.

Jasmine microcapsules with average diameter 2.6 μm have smooth globular surface.

The UV-curing method appears to be an effective technique in aroma finishing on cotton fabrics. Our research showed promising results on the condition of initiator runtecure 1265 under mercury light for 4 min.

After 10,000 abrasion cycles, the scent of aroma fabric still existed when the fabric was treated with UV resin containing Runtecure 1265 under mercury light for 4 min.

Acknowledgements

This research was financially supported by Key Laboratory of Textile Science & Technology, Ministry of Education,Donghua University, as well as sponsored by Cytec and Runtec Chemical companies.

References

[1] N. Gordon: Int. J. Pharm Vol. 31(2001), p. 57-64

[2] Shiqi Li, Lewis, Neil M. Steward, Lei Qian and Henry Boyter: Journal of the Textile Institute Vol. 99 (2008), p. 177-183

[3] S. Li, H. Boyter Jr. and L. Qian: Journal of the Textile Institute Vol. 96 (2005), p. 407-411

[4] C. X. Wang: Journal of Industrial Textiles Vol. 34 (2005), p. 157-166

© (2011) Trans Tech Publications, Switzerland
doi:10.4028/www.scientific.net/AMR.331.310

Research of wool-like modification of polyester with Sodium alginate

Min Liu[1,a], Junying Tian[2],Meiyan Liu[2]

[1]Chifeng Institute of Industry Technology , Chifeng, 024000,China

[2]Textile institute, Tianjin Polytechnic University, Tianjin, 300160, China
[a]ykslm567@163.com

Key Words: Sodium alginate, Alkali deweighting, Polyester, Wool-like

Abstract. This paper mainly discusses the influence of sodium alginate to polyester fabric in the process of wool-like. Polyester is pre-treated by sodium alginate solution firstly, and then modified by caustic soda, at last, the sample is steamed in the saturated vapor. Wool-like effect changes along with the concentration of sodium alginate and caustic soda, steaming time are analyzed. The results show that wettability, warmth retention and fullness of wool-like fabric are improved obviously. So treated with sodium alginate and then caustic soda can give polyester fabric ideal wool-like effect.

Introduction

Wool fabric has been favored by people because of it's comfortable handle and excellent elasticity. But wool raw materials can not meet the demand of textile industry, wool fiber production is influenced by many factors such as geographic conditions. However, development of synthetic fiber industry provides opportunities for wool-like products.

Polyester is impregnated into sodium alginate paste, slapped with glass rod to make sodium alginate paste distribute unevenly，and then treated with caustic soda solution, steamed with saturated steam. The purpose is to form uneven groove on the surface of polyester fiber, to imitate scale structure of wool fiber. On the other hand, sodium alginate is a polymer with high hydrophilic, polyester fabric can feel smooth, soft, warmth to achieve wool-like effect when treated by sodium alginate。

Materials and test

Polyester plain fabric. Sodium alginate produced by Shanghai cognis chemical Co., LTD

Warmth retention test

Warmth retention is tested according to GB/T11048-89《Testing method for warmth retention property》with ASTM plate-type fabric warm apparatus.

Fabric style test

KES-FB is used to test wool-like and common polyester fabric. Fabric size is 150mm×150mm，the same specimen test 3 times the average check, to achieve WOMEN'S THIN KN-201-MDY fullness.

Results and Discussion

The relation of warmth retention, full sensitivity of wool-like fabric to the concentration of Sodium alginate

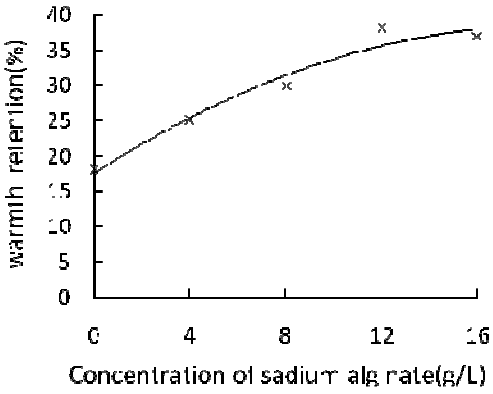


Fig.1 The relation of warmth retention of fabric to the concentration of sadium alginate

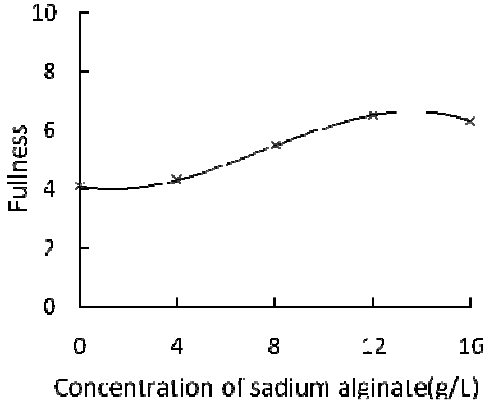


Fig.2 The relation of fullness to the concentration of sadium alginate

The warmth retention of fabric related to air content in fabric, the looser the fabric is, the better the warmth retention is. The fiber surface became more coarser after treated with sodium alginate and caustic soda，the compactness of yarns reduced, air content in fabric increased，so the warmth retention increased also.

The fullness sensitivity of fabric improved when the concentration of sodium alginate increases. The results show that sodium alginate pretreatment can influence fabric surface coarse and fullness. Fabric fullness gets maximum value when the concentration of sodium alginate is 2g/L.

The relation of warmth retention, full sensitivity of wool-like fabric to the concentration of caustic soda

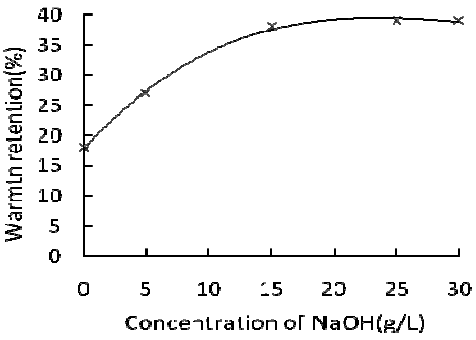


Fig.3 The relation of warmth retention to the concentration of caustic soda

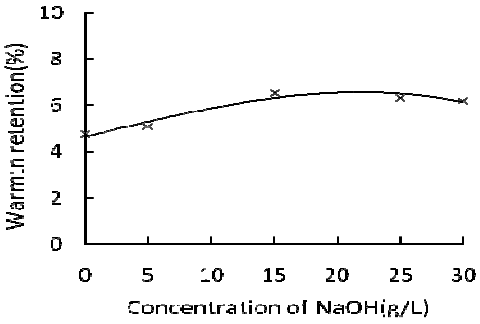


Fig.4The relation of fullness to the concentration of caustic soda

Fig.3 and Fig.4 show that warmth and full sensitivity of wool-like fabric improved as the concentration of caustic soda go up, because there are more groove on the surface of fiber, fabric became more loose and contain more air. Warmth retention achieves the maximum value when the concentration of caustic soda get 15g/L.

The relation of warmth retention, full sensitivity of wool-like fabric to the steaming time

Fig5. The relation of warmth to steaming time

Fig5. The relation of warmth to steaming time

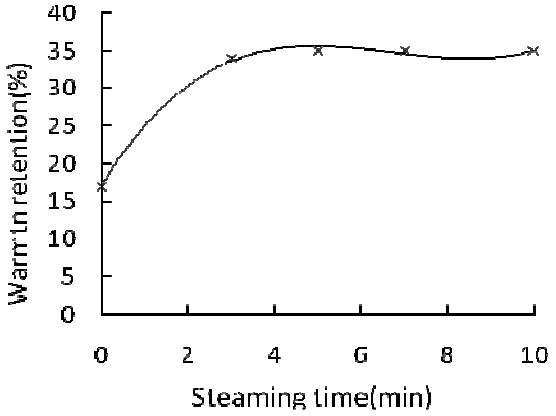


Fig5. The relation of warmth to steaming time

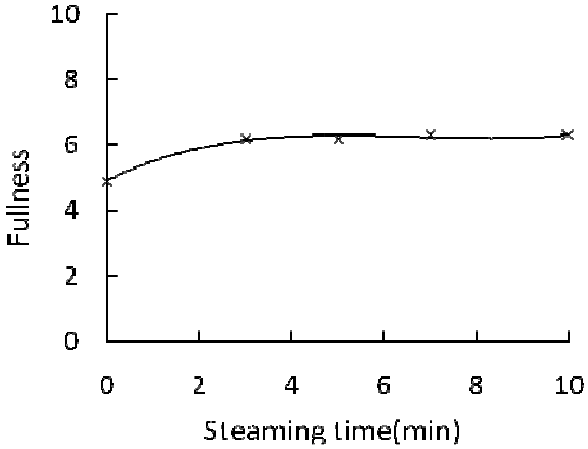


Fig6. The relation of fullness to steaming time

Fig5 shows that warmth retention of wool-like fabric increased as the steaming time prolong，if steaming time exceeds 3min, warmth retention will remain constant. Fig6 shows that the influence of steaming time on fullness sensitivity of wool-like fabric is insignificant. Steaming time can determined as 3min.

Wrinkle recovery angle, stiffness, drape and smooth sensitivity of wool-like polyester fabric

Tab.1 compared wrinkle recovery angle, stiffness, drape and smooth sensitivity of treated polyester with common polyester fabric. Data in tab.1 show that wool-like process make wrinkle recovery angle, drape and smooth degree of polyester fabric increase, and stiffness decrease, so wrinkle resistance, drape improved and fabric feels soft and smooth.

Tab.1 Performance of wool-like and common polyester fabric

Fabric	Wrinkle recovery angle(°)		Stiffness	Drape	Smooth
	warp	filling			
Polyester fabric	144	140.2	5.89	3.62	4.05
Wool-like fabric	153.7	144.5	5.31	5.43	4.18

Color fastness and K/S

Tab.2 Color fastness and K/S

Fabric	Crocking color fastness		Water washing			K/S
	Dry	Wet	Staining		Fade	
			cotton	Polyester		
Polyester fabric	4～5	4～5	4～5	4～5	4～5	20.81
Wool-like fabric	5	5	4～5	4～5	4～5	17.78

Compare to common polyester fabric, K/S of wool-like fabric decreased obviously dyeing under the same conditions. The reason of apparent color of wool-like fabric being pale is larger surface area of wool-like fabric, when incident light irradiates wool-like fabric, diffuse reflection light escalates and K/S reduces. Color fastness in tab.2 shows that color fastness to crocking of wool-like fabric is superior to common polyester fabric, because fiber surface of wool-like fabric are found to exist many small grooves, fabric surface area is increased. it is beneficial for dyes adsorbing onto fibers and diffusing into fibers，so color fastness to crocking of wool-like fabric improved.

Conclusions

By a series of experiments, optimal process conditions are sodium alginate concentration 12g/L, NaOH concentration 15g/L，steaming time7min. Common polyester fabric treated under above conditions can achieves superior performance include hydrophilic, warmth retention, full sensitivity and so on. Dyeing properties of wool-like fabric improved also.

References

[1] Lawrence E.Blackmon,Foley,Ala,John R.Dee,Wayne T.METHOD FOR PRODUCING

[2] Xianghong Zhou. Production technology of polyester wool-like fabric[J].Shanghai textile science and technology，1993 (2 ：50—53．

[3] HOWARD L, NEEDLES, DAVID B. BROOK, JOHN H, KEIGHLEY. How Alkali Treatments Affect Selected Properties Of Polyester, Cotton and Polyester/Cotton Fabrics. Treated vs. Nontreated,1985,17(9):23~26

[4] Zhiping Shen，Liangxia He. alkali reduction processing of polyester woven. China Textile Leader.2009，(1)：77～80

[5] Matsudaira Mitsuo,Matsui Masao,Changes in the Mechanical Properties and Fabric Handle of Polyester-fibre Fabrics Through the Finishing Stages[J],Journal of the Textile Institute,1992,83(1):144-155

[6] Sheth Geeta N., Musale Aparna A.,Changes in Characteristics of Polyester and Polyester/Cotton Blended Fabrics during Weight Reduction[J], AATCC Review, 2005,5(10):39-43

© (2011) Trans Tech Publications, Switzerland
doi:10.4028/www.scientific.net/AMR.331.314

Research on the Application of G7 in the gravure printing products

Linghua Guo [1, 2,a], Meiyun Zhang [1,2, b], and Xinhua Guo [3, c]

[1]Shaanxi university of science &Technology, [2]Shaanxi provincal key laboratories of papermaking technology and specialty paper development, Xian 710021, China

3Jinan University, Zhuhai 519070, China

[a] guolinghua318@126.com, [b] myzhang@sust.edu.cn, [c] xinhua008@sina.com

Key words: heat transfer printing; gravure printing; G7 technology; textile

Abstract. The heat transfer printing is a new application in the textile industry. Gravure printing is the most common method in the heat transfer printing. The Gravure printing qualities of the paper play a decisive role in the textiles. GRACoL7 breaks with tradition by raising gray balance to a more important status to realize the different printing materials with the same appearance. GRACoL 7 process is accorded with human observation rule .In this paper, We introduce the process, the principle and the parameters of G7 .The purpose was to provide reference for printing industry.

Introduction

The advent of the heat transfer printing has brought the Technology revolution on the Printing and dyeing industry. Along with the continuous improvement of people's living standards, Family adornment is taken on the diversification and personalized. The products of the heat transfer printing are met the demand of the people.

The most important factor that affects the printing quality is the way of printing. The screen printing, offset printing, flexography printing and digital printing are the common printing methods. But the Gravure printing is the most common method in the heat transfer printing. The digital printing is the trend of the textile printing in the future.

Spectrophotometric method is introduced in the printing process based on G7 [1].The most important parameters gray balance of print products explain human observing effect with the Value L,A,B. Thus, we Completed the more accurate and scientific copy. In this paper, we discussed the Application feasibility and the expected effect about the G7 which is used in the gravure printing process. In this paper, we discussed the feasibility and expected effect about the G7 process which is control the process of the gravure printing to print heat transfer paper.

The process of printing the heat transfer paper

Heat transfer printing is a new industry which is used in textile. The process of the heat transfer printing is: firstly, The copy is separated by computer and scanner.. Secondly, The gravure cylinder is engraved by engraving machine. At last, the products are finished by Intaglio printing. The image and message on the heat transfer paper are transferred on the fabrics under the certain time, temperature and pressure by heat transfer machine. It is different from the traditional printing and dyeing. The heat transfer printing is indirect method. The qualities of the fabrics are decided by heat transfer printing products. So it is important to control the color of the transfer printing paper.

The principle of G7

G7 is a new calibration method developed to support by the IDE Alliance(International Digital Enter-prise Alliance).The G7 method is applicable to almost any CMYK printing process, and has been successfully tested on a wide range of processes, including lithography, newsprint, gravure, flexography, heat-transfer printing, ink-jet, and so on, as well as a wide range of FM and AM screening methods. The purpose of the G7 is in the printing process to realize "shared appearance" between the different printing methods or different materials [2].A good method to define print 'appearance' is with a characterization data set containing colorimetric (CIE or spectral reflectance) values from a standard characterization target like the IT8 is shown fig1. So, the printing quality is expressed more scientific precise. The G7 refers to calibrating Gray values, while the 7 refers to the seven primary color values; Cyan, Magenta, Yellow, Black, Red, Green and Blue.

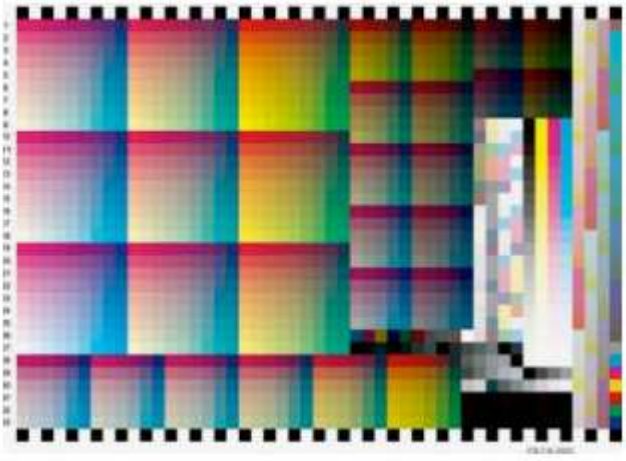


Fig.1 The IT8 Visual characterization target

The parameters of GRACoL 7

Neutral Print Density Curve (NPDC). In traditional printing, We use the dot gain curve to control the printing quality. But in the process of G7, A new concept introduced with G7 is the definition of a Neutral Print Density Curve (NPDC), which is the relationship between original halftone percentages on a printed gray scale and measured neutral density [3].. Because neutral density is an absolute value. NPDC ensures a density match and better contrast between multiple devices and materials. Two NPDC curves are specified, one for a black-ink gray scale and one for a combined CMY gray scale. According to the G7, the NPDC is got, the calibration compares printed gray scale which act as a reference scale and calculates RIP correction values of dot percentage terms Curve correction values are calculated either by plotting graphs on special graph paper or manually.

Gray balance was traditionally defined as the CMY percentages which are all the same 50% needed to match the color of a 50% black ink tint, or the color of paper, In previous gray balance was an arbitrarily constant of 0 a*, -2 b* throughout the whole CMY gray scale, regardless of paper color. but these definitions are too vague for today's ICC workflows. To avoid these ambiguities, G7 pre-defined a* and b* values for each triplet and pre-defines an arbitrary table of CMY percentage triplets based on the generic 50c, 40m, 40y ratio, G7 breaks with tradition by raising gray balance to a more important status. Grey balance is now calculated by a paper-dependent formula based on ideas from several public forums.

Highlight Range (HR).
HR is a single measurement that quickly tests the mid-tone [4]. density of a previously-calibrated device during production. For convenience, HR is expressed in neutral density (ND), which can be measured with a densitometer set to the black channel, or Visual density. HR is the middle of grey areas(50c、40m、40y), The value is 0.54 and is constant which Minus the density of the paper. The chromaticity value is: a*=0±0.5,b*=-2.0±1.0.The value is perfectly with the neutral density in traditional printing. As mentioned above, at the range of HR 0～0.54,the single K is 0.5.It is the key part of controlling the images. HR acts as the primary measure of overall print darkness and gray balance, HR is computed twice, once for CMY and again for black. Just two measurements are required for each, or just one each in absolute mode, compared to three measurements each for C, M, Y and K, HR gives a more reliable indication of pictorial darkness and contrast because HR is absolute.

Shadow Contrast (SC). A new variable introduced in G7 is Shadow Contrast (SC). In G7，SC replaces traditional printing relative contrast. In the printing process or the completion of the printing, SC is a quick way of checking the NPDC [5]. in neutral shadow tones during production. SC is computed twice, once for the grey balance of CMY and again for black. The combination of 75c, 66m, 66y ratio got the grey balance in G7. The dot percentage of single black is 75%.

Highlight Contrast (HC). HC is a quick way of checking the NPDC in neutral highlight ones during productio [6].n. Another new G7 variable introduced is Highlight Contrast. HC is computed twice, once for CMY, HC_{cmy} is computed by measuring the neutral density of a combined CMY grey patch(25c,19m,19y)and subtracting the neutral density of the paper. The formula is

$$HCcmy=ND_{(25c,19m,19y)}-ND_{(paper)} \quad (1)$$

Where HCcmy is the combined grey value; ND(25c,19m,19y) is the combined value of neutral grey; ND(paper) is the paper value of neutral grey

The other once is for black. HC_k is computed by measuring the ND of a 25% Black patch and subtracting the neutral density of the paper.

$$HCk = ND(25k) - ND(paper). \quad (2)$$

Where HCk is the K grey value; ND(25k) is the single K value of neutral grey; ND(paper) is the paper value of neutral grey

By adding the paper density to HC, the 'Absolute' HC density for that particular paper is got. SO, it can be realized the 'shared appearance'. HC is a virtual constant for dynamic ranges above about 0.8 ND.A single Lab can be used to measure gray balance and lightness simultaneously .The Absolute L* HC values for a standard paper lightness of L* 95 Absolute HCcmy = L* 75.7, Absolute HCk = L* 77.7.

HR, SC and HC aim values of dynamic range. HR and HC are effectively constants for normal printing density ranges, but SC varies values of high dynamic range.

Application of G7 in the gravure printing process

Status. G7 is applied to all the printing mode .G7 has been pushed out in the process to control the offset printing quality at home and abroad. But At present G7 certification is not exceed dozen.G7 is not applied to the gravure printing process. In the transfer printing, the common printing method is intaglio printing. In the process of intaglio printing, the printing pressure is heavier, the dot gain is larger and the small dot is easy lost. The ink film thickness is thicker than the other printing [7]. methods. There is difference on the color tone between gravure and offset printing. In the prepress

of gravure, characterization curve is adjusted to compensate the dot gain. We should control the printing pressure to meet the demand .Application of G7 in the gravure printing process , one way is that the testing image should be data interpreted by the pre-set RIP curve. It ensures the highlight points to get the minimum limited value. Another way is that the testing image on the testing plate should be adjusted to maximum limited value by the pre-set RIP curve.

Developing. The general G7 profiles have been got through continuous testing by SWOP and GRACL [8].. Owing to the gravure printing, the plate-making is engraving, the materials are newsprint paper and Kraft paper which basis weigh is 35~70g/m^2.The ink viscosity is low. On the basis of the general G7 profiles, We should set up the personalized profiles for the gravure printing. At last, the graving machines are made color management. Thus G7 can be used the heat transfer printing.

Conclusion

G7 is an advanced controlling method. In the general printing ,the tolerances of grey balance and chromaticity error is ± 1~2. The tolerances of color management and characterization is ± 0.5~1.Today.The research about G7 is just at the beginning. We first introduced the G7 into the heat transfer printing process. We recommend the new concept to the transfer print industry.

Acknowledgements

This work was financially supported by the Shaanxi provincial key laboratories of papermaking technology and special paper development and Shaanxi provincial Education Department Special Science Foundation (2010JK424). We also thank the ShaanXi University of Science & Technology and JiNan University for their experimental equipments. We thank cooperators for their technical Support.

References

[1] Kai Li.China Printing and Pzckaging Study (in Chinese) Vo2. (2010), p. 79-82

[2] Shaowu Chen and Jinlin Xu. Printing Field (in Chinese) Vo6(2007), p. 42-44

[3] Shaowu Chen and Jinlin Xu. Packing and Engineering (in Chinese) Vol. 29 (2008), p. 52~55

[4] Tao Meng,WanZhang, Hao-xue Lliu and Xu-dong Wang (in Chinese). Journal of Beijing Institute of Graphic Communication Vol.16 (2008),p. 38~40

[5] Chang- xian Cheng. packing engineer (in Chinese) Vol.16 No.29 No.7 2008 :189~191

[6] Copyright © International Digital Enterprise Alliance, Inc. [IDEAlliance] (2006)

[7] Liu Haoxue , LV Yuxiang , XU Yanfang , LIANG Jiong. in: Subjective Evaluation for Printing Image' s Colour Difference edtied by Shanghai Publishing and Printing College, (in Chinese) (2005) , in press.

[8] Information on http://www.cnki.net/

© (2011) Trans Tech Publications, Switzerland
doi:10.4028/www.scientific.net/AMR.331.318

Study on polyester fabric anti-static treated by polyaniline

Liping Guan[1, a]

[1]Advanced Textile Technology &Fashion CAD Key Laboratory, Zhejiang Textile & Fashion College, 495 Fenghua Road, Ningbo 315211, P. R. China.

[a]lpguan2002@yahoo.com.cn

Keywords: polyaniline, PAn, anti-static, polyester fabric, fabric treating.

Abstract. The utilized field of polyester fabric was limited because the static can be produced easily when it was used. In this paper, the anti-static treating crafts of polyester staple fabric treated by polyaniline were probed. The raw fabric material was weaved with polyester staple yarn and the aniline was selected as anti-static reagent. The process of aniline polymerizing was analyzed and discussed. The anti-static characteristic of the finished fabric was analyzed. With systemic experimental and data analysis, the integrate process of the fabric anti-static finished by polyaniline was achieved. The result shows that the property of anti-static can be obtained if the polyester staple fabric was treated by polyaniline at the advisable processes. And the polyester fabric can be sued in widely field.

Introduction

Polyaniline (PAn) is one of the electric polymer materials which have the most value and the most attention [1]. It is an intrinsic conduction which the raw materials obtained easily and it can be synthesized simply [2]. The electric conductivity is high. And the environmental stability is good [3]. Polyaniline is the polymer which polymerized by aniline (An) at a stated condition. The mainly synthesizing method is chemical oxide polymerizing, electrochemistry polymerizing, latex polymerizing and micro-latex polymerizing [4]. In this paper, the anti-static finishing crafts of polyester staple fabric treated by polyaniline were probed. The fabric was finished in aniline solution. And the aniline on the polyester fiber was polymerized to the intrinsic state polyaniline which have good electric conduction. So the fabric has good and lasting anti-static property.

Experimental

The sample fabric made from thin denier staple polyester yarn. The warp is 6.5 tex and the weft is 13tex. The fabric density is 620×270 per 10 centimeters.

All of the chemical agents are analyzed purity. And the aniline have distiled at 185℃ before it was used in the experimental.

The mainly process of the polyester fabric treated by aniline was showed in fig. 1. The time of the sample treated by aniline soultion is 30 min. The washing process is the that: acid washing → anhydrous alcohol washing → water washing.

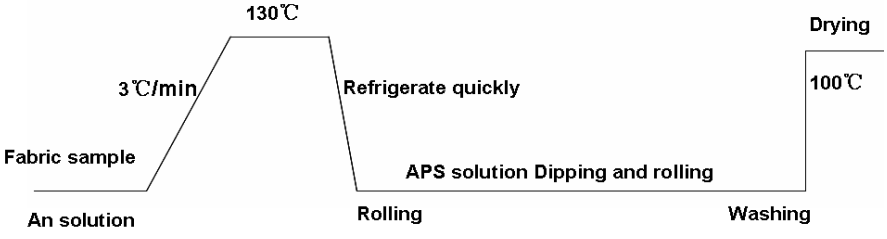


Fig. 1, Sketch of polyester fabric finishing process

The electric property of the sample fabric was tested on ZC236 micro-current testing instrument, YG2341 handle static testing equipment and BD2-II digital static pressure meter. And the testing method was conformed to GB 12014-2009 standard.

Results and Discussion

Influence of the rudimental aniline solution to the anti-static properties of the polyester fabric. The anti-static properties of the finished fabric at different rudimental aniline solution were showed in table 1. In the experiment, the HCl concentration is 1mol/l, the aniline concentration is 30% (w.o.f.), the concentration of the ammonium peroxydisulfate (APS) is 20 g/l, and the pH of it is 4.5. The reactive time is 10 min, and the temperature is 20 ℃.

Table 1, The anti-static properties of the finished fabric at different rudimental aniline solution.

The rudimental aniline solution [%]	30	50	70	90	120
The fabric colour	yellow	yellow green	dark green	blue green	black
The area density of attrition charge [$\mu C/m^2$]	6.31	0.53	0.26	0.21	7.84
The resistance of surface ratio [Ω•cm]	4.2×10^5	7.3×10^4	9.8×10^3	4.1×10^2	9.2×10^{14}
The frictional static pressure [V]	80	52	34	31	632

In table 1, we can find that, the risistance of surface ratio of the fabric decreased following the rudimental aniline solution increased. And the fabric colour would change into more dark. When the percentage of the rudimental aniline solution is 120%, the fabric is black. And the conductivity of the fabric increased remarkably. It implied that the anti-static property of the finished polyester fabric changed as the PAn colour changed. The conductivity is the best when the colour is blue green, but it is the lest when the colour is black. It is because that the oxiding polymerazing degree of the PAn effects the conductivity directly. The colour will be darker if the polymerazing degree is larger.

Also, We can find that all of the area density of attrition charge, the resistance of surface ratio and the frictional static pressure are lower if the rudimental aniline solution was controlled in the area form 70% to 90%, and the data have not notable different. So we can say that the area form 70% to 90% of the rudimental aniline solution is the best craft data for the polyester fabric anti-static treated by PAn. The anti-static property of the fabric is the best and steady.

Aniline solution concentration. The relational curve between the resistance of surface ratio of the fabric and the aniline solution concentration was showed in fig. 2. Other crafts data are confirmed. The resistance of surface ratio of the fabric decreased following the aniline solution concentration increased. But it could decrease sharply after the percentage concentration to the fabric weight (w.o.f.) exceeded 50%. It is that the polyester fiber could absorb too aniline to make the aniline polymerize to a good degree if the aniline solution concentration is too higher. The state of PAn on or in the fabric is not continuous. So the electric conductivity of the fabric could decrease contrarily. We can obtain the anti-static polyester fabric with steady and good anti-static property if the aniline solution concentration is from 20% (w.o.f.) to 50% (w.o.f.).

. **APS solution Thickness.** The resistance of surface ratio of the finished polyester fabric treated by different APS solution thickness was showed in Fig. 3, the aniline solution concentration is 30% (w.o.f.) and the other crafts data are confirmed. The data of the surface ratio resistance decreased with the APS solution thickness increased if it is lower than 30 g/l. It indicates that the anti-static property of the finished fabric increased following the dosage of APS increased. If the APS was used excessively, the reactive center would be overfull and it is disadvantageous for the forming of high molecular weight PAn. The surplus oxidant would make the high molecular weight chain oxide to lower molecular weight polymer. So the product conductivity would decline and the resistance of

surface ratio of the fabric would be fortified evidently. Fig. 3 shows that the resistance of surface ratio is low and did not changed evidently as the APS solution thickness changed if the APS solution thickness was controlled in the area from 15 g/l to 25 g/l.

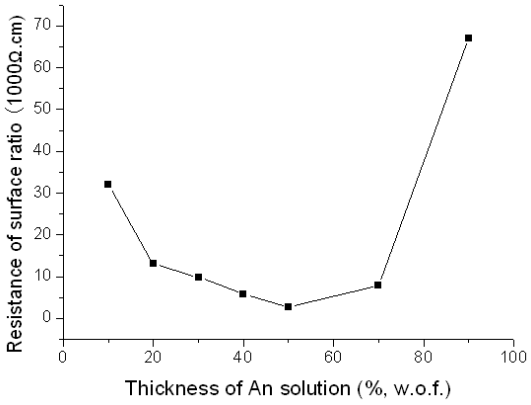


Fig. 2, The resistance of surface ratio treated by different aniline solution concentration

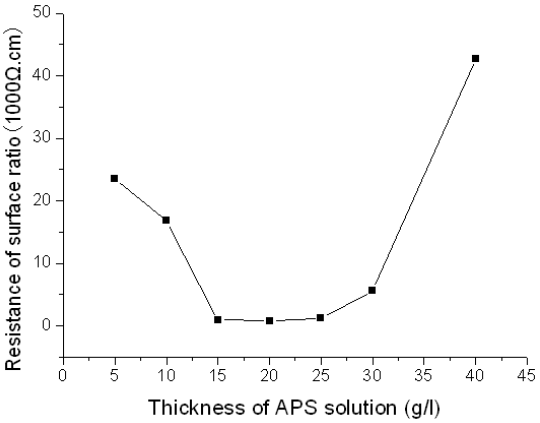


Fig. 3, The resistance of surface ratio treated by different APS solution Thickness

pH value of Polymerizing. The testing data of the surface ratio resistance of the polyester fabric treated by PAn at different pH value were displayed in table 2. The aniline solution concentration is 30% (w.o.f.), the APS solution thickness is 20 g/l and other crafts data are confirmed.

Table 2, The anti-static property of the polyester fabric treated by different polymerizing pH value

pH value	1	3	5	7	9	11	13
The resistance of surface ratio [Ω•cm]	7.2×10^{2}	2.8×10^{3}	6.3×10^{3}	3.9×10^{10}	9.2×10^{10}	1.2×10^{11}	4.2×10^{11}

The data explained that the surface ratio resistance of the finished fabric is higher if the pH value of the oxide solution is higher. Good conductivity of the fabric can be obtained just only in the condition of the aniline polymerized in acid oxide solution. If it reactive in neutral or alkaline oxide solution, the treated fabric could not meet the requirment of anti-static fabric. So it is necessary that the oxide solution is acid in the treating processes of the polyester fabric anti-static treatment to achieve good conductivity. And the acid of oxide solution is stronger, the better anti-static property of the finished fabric is. But the resistance of surface ratio have not notable changing when the pH value changed less than 5. So the pH value of the APS solution was controlled in the area from 3.5 to 4.5. Because the stronger acid can make more harmful for the polyester fabric.

Reactive time. The anti-static property of the polyester fabric treated with different time showed in table 3. The pH of APS solution is 4.0, and the other crafts are confirmed. Following the reactive time extended, the resistance of surface ratio increased at first and decreased if the reactive time exceeded 20min. The time is needed that the aniline was evocated by APS. In a short time, the polymerizing degree of the aniline is small, and the fabric have not good conductive effect. In the process, the colour of the fabric turn into darker and darker because all of the aniline molecular were polymerized into PAn and the molecular weight went larger and larger following the reactive time delayed. If the reactive time exceeded 30min, the molecular weight of PAn would be too larger to have good electric conductivity. The anti-static property would reduced sharply.

Table 3, The anti-static property of the polyester fabric treated with different time.

Reactive time [min]	0	5	10	15	20	25	30
The fabric colour	white	yellow	yellow green	yellow green	dark green	blue	dark blue
The surface ratio resistance [Ω•cm]	2.2×10^{11}	6.8×10^{6}	4.3×10^{3}	1.9×10^{3}	9.2×10^{2}	6.2×10^{3}	4.2×10^{4}

Polymerizing temperature. The lower temperature is advantageous for the polymerizing reactive because the reactive of aniline polymerizing is an exothermic reaction. High molecular weight PAn can be created easier if the aniline was polymerized at lower temperture. The PAn production decreased following the reactive temperature rose, and the peroxide reactive increased. So the electric conductivity of the finished fabric decreased. The relative curve between the fabric electric conductivity and reactive temperature was showed in fig. 4. As the reactive increased, the electric conductivity increased at first and decreased if the reactive temperature exceeded 20℃.

It is disadvatageous that the head to trial ordered joint PAn created because the derivational phase is longer if the reactive temperature is lower. And the electric conductivity of the finished fabric is lower. At the phase of chain growth, the reactive heat was released to make the reactive self-accelerate. The velocity of the chain growth enhanced. And then, the polymerizing reactive went into the phrase of chain cessation. So polymerizing at lower temperature is advantagous to leave the time of chain cessation. The PAn with higher molecular weight and longer molecular chain would be obtained. The longer molecular chain conjugate system is helpful to the current carrier transmitting because it had extended the inner channels of electron. So the finished fabric have good electic conductivity.

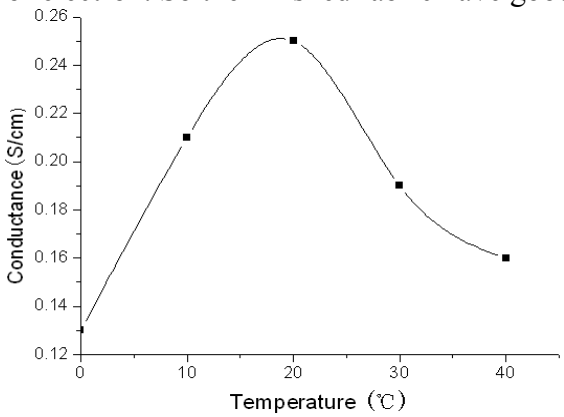


Fig. 4, The relative curve between the fabric electric conductivity and reactive temperature.

Summary

The anti-static treating crafts of polyester staple fabric treated by polyaniline were examined and analyzed. The influence of each detail craft to the fabric electric conductivity was discussed. The results shows that the anti-static property can be enhanced obviously if it was treated by PAn, and the finished fabric have arrived the standard of anti-static cloth. The main crafts influencing the anti-static property of the finished polyester fiber are **t**he rudimental aniline solution, the **A**niline solution concentration, the APS solution thickness, the polymerizing pH value, the reactive temperature and reactive time. The best treating process is that **t**he rudimental aniline solution is from 70% to 90%, the **a**niline solution concentration is from 20% to 50%, the polymerizing pH value is from 3.5 to 4.5 the reactive temperature is about 20 ℃ and the polymerizing time is about 20 min.

Acknowledgements

This work was financially supported by the Scientific Research Fund of Zhejiang Provincial Education Department (Y200908870) and the Ningbo Natural Science Foundation (2011A610112).

References

[1] T. Muthianh: J. Mac. Sci. Vol. 40 (2003), p. 1347-1355.
[2] A.G. Macdiarmid, S.L. Mu, W.Q. Wu: Mol. Cryst. Liq. Cryst. Vol. 121 (1985), p. 187-190.
[3] F. Lux: Polymer. Vol. 35 (1994), p. 2915-2936..
[4] D. Bhavana, I.S. Yu, F. Michael: J. Amer. Chem Soci. Vol. 126 (2004), p. 52-53.

© (2011) Trans Tech Publications, Switzerland
doi:10.4028/www.scientific.net/AMR.331.322

Effect of Preparation Parameters of Titania Sol on Textile UV-resistance

Ran Wang[1,2,a], Ying Chen[1,2,b], Jia Wang[1,c], Yue Yang[1,d]

[1]School of Material Science and Engineering, Beijing Institute of Fashion Technology, Beijing 100029, China;

[2]Beijing Key Laboratory of Clothing Materials R&D and Assessment, Beijing 100029, China

[a]clywr@bift.edu.cn, [b]clychenying@bift.edu.cn,
[c]wangjia4121306@163.com,[d]yangyue628@yahoo.cn

Keywords: titania nano-sol, cotton fabric, ultraviolet protection, preparation.

Abstract. Titania nanosols were prepared by a sol-gel method using tetrabutyl titanate (TTB) as precursors. Effects of the content of chelator, water, catalyst, and reaction time on the ultraviolet -resistant property of textile were investigated. An orthogonal experiment was conducted for the optimization preparation. The ultraviolet protection factor (UPF) value of fabrics increased with the enhancement of the TTB content; however, reaction time had limited influence on the UPF. When chelator, water, and catalyst contents were 5.5, 90, and 5.5% (w/w) (in solution B), respectively, the preparation was optimal, and the UPF value of fabric reached 60.

Introduction

Ultraviolet (UV) radiation reaches the surface of the earth and causes serious health problems, such as sunburn, photo-aging, and skin cancer [1]. Thus, UV-resistant finishing has received increasing attention owing to its growing demand in the marketplace [2]. In recent years, great interest in the absorptivity of titanium dioxide in nanoscale has been growing, and the application of titanium dioxide nanoparticle on the textile to enhance the UV-resistant property has been reported [1-5]. The sol-gel process and dip-coating technique are commonly used in the application. However, the influence of the preparation condition of the process on the UV-resistant property of textile has not been reported much. The sol-gel process is complex, and each factor strongly affects the resultant nanoparticle [6, 7]. Therefore, particular attention is given to the corresponding relationship between the process condition and UV-resistant property of textile.

In the present study, titania nanosols were prepared by a two-step sol-gel method using tetrabutyl titanate (TTB) as precursors. Effects of chelator, water, catalyst, and reaction time on the UV-resistant property of textile were investigated. An orthogonal experiment was also conducted to obtain the optimization preparation process.

Experimental

Materials. The desized and scoured T/C fabric (2/1 twill weave; weight, 202.7 g/m^2) was used in the present study. Ultraviolet protection factor (UPF) of the original fabric is 13. TTB was purchased from Fuchen Chemical Reagent Works, Tianjin, China. Acetic acid was obtained from Beijing Chemical Reagent Factory. All chemical reagents were used as received.

Titania Sol Preparation. TTB was dissolved in acetic acid, and the solution was stirred until homogeneous (solution A). Solution B was a diluted acetic acid solution of different strengths. Solution A was added dropwise to solution B with vigorous stirring over a certain time at ambient temperature. Thus, titanium hydrosol was obtained and diluted to 40% for the treatment. The process was performed at room temperature. The reaction is represented by

$$Ti(OC_4H_9)_4 + 4H_2O \xrightarrow{H^+} Ti(OH)_4 + 4C_4H_9OH \quad (1)$$

$$\equiv Ti-OH + HO-Ti\equiv \longrightarrow \equiv Ti-O-Ti\equiv \quad (2)$$

Sol-gel Treatment. The fabric samples were dip-and-nipped twice in TiO_2 sol with a pickup of 70%. The treated samples were dried at 80 °C for 3 min and then cured at 140 °C for 3 min.

Characterization. The UV-transmittance spectra of the fabric were measured before and after the treatment by a Lambda 750 UV/VIS spectrometer (PerkinElmer Ltd, UK). UPF values were calculated according to the *GB/T 18830-2009 Textiles–Evaluation for solar ultraviolet radiation protective properties*.

Results and Discussion

Effect of chelator content on UPF. If TTB directly dissolves in the water, it will decompose quickly and produce precipitate, making it impossible to obtain titania hydrosol. To reduce the hydrolysis rate of TTB, chelator has to be introduced. Acetic acid and acetylacetone are generally used as chelators. Acetic acid was adopted in the current work because of its colorless property. The reactions are represented by

$$Ti(OC_4H_9)_4 + 4CH_3COOH \xrightarrow{H^+} Ti(OOCH_3)_4 + 4C_4H_9OH \quad (3)$$

$$Ti(OOCH_3)_4 + 4H_2O \xrightarrow{H^+} Ti(OH)_4 + 4CH_3COOH \quad (4)$$

Theoretically, the minimum molar ratio between acetic acid and TTB is 4 if the reaction is complete. However, when the ratio of the acetic acid and TTB is lesser than 5, a clear and uniform sol cannot be obtained because there is insufficient chelator reacting with TTB, and the rate of reaction between unreacted TTB and acetic acid is too quick. Therefore, the ratio used in the current research ranged from 5−15. The other parameters in the preparation are as follows: molar ratio between water and TTB was 95; content of acetic acid in solution B was 5.5% (w/w); and reaction time was 1 h. As shown in Fig. 1, the UPF value of fabrics treated with titania hydrosols increased as the chelator content decreased. This reaction is caused by the enhancement of the proportion of TTB in the reaction system as the amount of acetic acid decreases, and the titania content in the sol increases. When the molar ratio of the acetic acid and TTB was 6, the UPF value reached the maximum.

Effect of water content on UPF. When the molar ratio between water and TTB is 4, the hydrolysis of TTB is complete according to Eq. (1). However, when the ratio of water and TTB is equal or less than 4, TTB hydrolysis is insufficient, consequently failing to obtain a uniform sol. Thus, the molar ratio was selected as 5−100. The other parameters in the preparation are as follows: molar ratio between acetic acid and TTB in the solution was 5.5, and reaction time was 1 h. The UPF values of fabrics treated with sols prepared with various water contents are shown in Fig. 2. UPF values are clearly observed to have gradually increased with the diminution of water because of the rise of titania content in the sol as water is reduced. However, diminution of water also weakens the stability of the sol. In practice, the stability of the sol reaches its best when the molar ratio of water and TTB is 95, as in the current research.

Effect of catalyst content on UPF. To decrease the types of matter in the sols, acetic acid was also chosen as a catalyst in solution B. The UPF values of fabrics treated with sols and prepared with various catalyst contents are shown in Fig. 3. Other parameters in the preparation are as follows: molar ratio between water and TTB was 95; molar ratio between acetic acid and TTB in the solution was 5.5; and reaction time was 1 h. The figure implies that UPF values of fabrics were gradually enhanced with the reduction of acetic acid caused by the increase in titania in the sols and the decrease in acetic acid content.

Effect of reaction time on UPF. The UPF values of fabrics treated with sols with different reaction times are shown in Fig. 4. The other parameters in the preparation are as follows: molar ratio between water and TTB was 95; molar ratio between acetic acid and TTB in the solution was 5.5; and content of acetic acid in solution B was 5.5% (w/w). Reaction time had limited influence on the UPF values of the treated fabric, which only slightly contracted with the prolongation of time. Therefore, 0.5 h was chosen as the optimized reaction time.

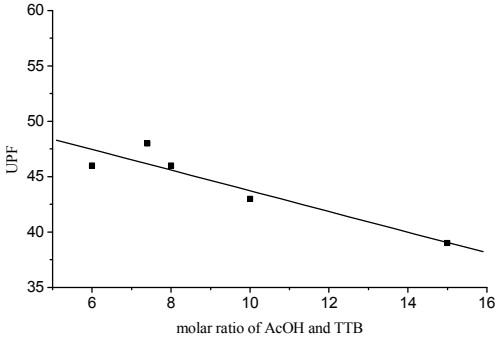


Fig. 1 Effect of chelator content on UPF

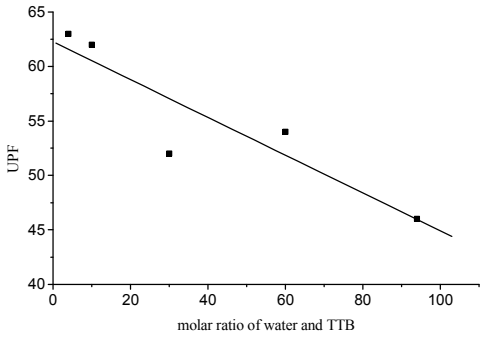


Fig. 2 Effect of water content on UPF

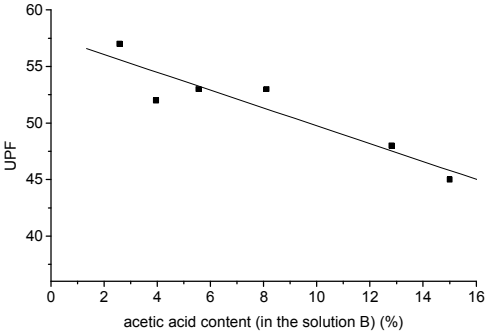


Fig. 3 Effect of catalyst content on UPF

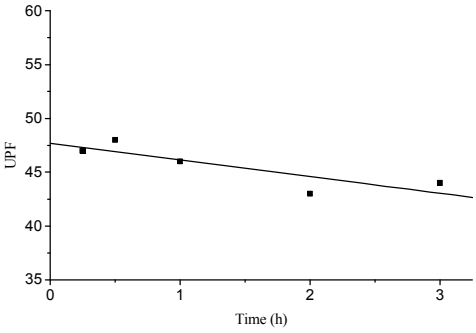


Fig. 4 Effect of reaction time on UPF

Orthogonal optimization. An orthogonal experiment was conducted to optimize the TiO_2 sol preparation. The chelator, water, and catalyst contents were selected as test factors. Their values were selected based on the above results. Result of the orthogonal experiment is shown in Table 1. In accordance with the optimal level combination, the optimization preparation parameters are as follows: molar ratio between acetic acid and TTB was 5.5; molar ratio between water and TTB was 90; content of acetic acid in solution B was 5.5% (w/w); and reaction time was 0.5 h. The UPF value of the cotton fabric treated with the sol reached 60.

Conclusion

Based on the results, the role of TTB content is suggested to be crucial with respect to the UV-resistance property of the fabric. The UPF values of treated fabrics always increased with the enhancement of the TTB content. Hydrolysis time had limited influence on the UPF values. Optimized hydrolysis time was 0.5 h. When chelator, water, and catalyst contents were 5.5, 90, and 5.5% (w/w) (in the solution B), respectively, the preparation was optimal, and the UPF value of fabric reached 60.

Table 1 Orthogonal experiment results

	molar ratio of acetic acid and TTB	molar ratio of water and TTB	catalyst content	UPF
1	1：5.5	1:90	1.5	57.20
2	1：5.5	1:95	2	58.63
3	1：5.5	1:100	2.5	54.34
4	1：6.5	1:90	2	55.77
5	1：6.5	1:95	2.5	51.48
6	1：6.5	1:100	1.5	54.34
7	1：7.5	1:90	2.5	52.91
8	1：7.5	1:95	1.5	51.48
9	1：7.5	1:100	2	52.91
K_{1j}	170.17	165.88	163.02	
K_{2j}	161.59	161.59	167.31	
K_{3j}	157.3	161.59	158.73	
R_j	12.87	4.29	8.58	

Acknowledgements

This work was financially supported by the China National Key Technology R&D Program, No. 2009BAE75B03.

References

[1] P. Xu, W. Wang, S. L. Chen: AATCC Review Vol. 5 (2005), p. 28

[2] N. Abidi, E. Hequet, S. Tarimala, L. L. Dai: Journal of Applied Polymer Science Vol. 104 (2007), p. 111

[3] K. Qi, X. Chen, Y. Liu, J. H. Xin, C. L. Makb, W. A. Daoud. Journal of Materials Chemistry Vol. 17 (2007), p. 3504

[4] Y. Xing, X. Ding: Journal of Applied Polymer Science Vol. 103 (2007), p. 3113

[5] P. Xu, X. Liu, W. Wang, S. L. Chen: Journal of Applied Polymer Science Vol. 102 (2006), p. 1478

[6] C. J. Brinker, G. W. Scherer. *Sol-Gel Science: The physics and chemistry of sol-gel processing* (Academic press, INC., San Diego 1990).

[7] J. Livage, C. Sanchez. Journal of Non-Crystalline Solids Vol. 145 (1992), p. 11

© (2011) Trans Tech Publications, Switzerland
doi:10.4028/www.scientific.net/AMR.331.326

Shrinkage Properties of Wool Treated with Ionic Liquid and Chitosan Biopolymer

Huaifang Wang[1, a], Haining Lv[2,b] and Xiaoli Zhang[1,c]

[1] Dept. of Light Chemistry Engineering, College of textile, Zhongyuan University of Technology, Zhengzhou, China

[2] Dept. of Light Chemistry Engineering, College of Material and Textile engineering, Jiaxing University, Jiaxing City, Zhejiang Province, China

[a] hfwang1980@163.com, [b] haining8047@163.com, [c]allyzxl@163.com

Keywords: Ionic Liquid, Shrinkage, wool, chitosan

Abstract. In order to improve the shrinkage resistance of wool fabrics, a new method that combine ionic liquid and chitosan was researched in this paper. Wool fabric was first pretreated with 1 - butyl - 3 - methyl bromination imidazole([Bmim]Br), and subsequently was treated with chitosan. Pretreatment temperature and time, and chitosan concentration of post-treatment were studied in this paper. Results showed that wool fabrics treated with [Bmim]Br at 80℃ for 2 hours and post-treated in 1.0% chitosan acetic acid solution exhibit good shrinkage resistance. In addition, SEM images of ionic liquid treated wool fiber indicates that the scales have been destroyed, and the surface is covered with a layer of film after post-treated with chitosan.

Introduction

Shrinkage resistant finishes is essential to minimize the natural propensity of wool which shrinks when treated in an aqueous or moist environment. In the past decades, Chlorination-resin technique was widely used for enhancing the shrinking-resist property of wool fabrics. But the chlorination is well known for producing absorbable organo halogens (AOX) in wastewater [1]. Therefore, the chlorinating agents have to be substituted by environmental agents.

Ionic liquids are organic salts that usually melt below 100℃. They have many attractive properties, such as chemical and thermal stability, non-flammability and immeasurably low vapor pressure. And what makes ionic liquids so attractive is their solubility [2] as "green" solvents for cellulose. The ionic liquids have been used to dissolving natural polymers such as cellulose [2-4], silk fibroin [5] and wool keratin [6]. And modification of wool fabrics with ionic liquids also has been investigated to improve their dyeability and hydrophilcity [7, 8].

Chitosan, poly (l, 4)-2-amino-2-deoxy-β-D-glucan, usually is obtained by deacetylation of chitin, which is the main component of the shells of crustaceans such as shrimps, crabs and lobsters [9]. It has unusual chemical and biological properties such as biocompatibility, biodegradability, nontoxicity and bioadhesive property. And it has long been proposed as a substitute for synthetic resin to improve anti-felting properties of wool fabrics [10, 11]. However, the shrink-resist properties obtained with the chitosan treatment can not meet the machine-washable requirement, and a combination with hydrogen peroxide [12], low temperature plasma [13] and enzyme [14, 15] is necessary.

This paper proposed the use of ionic liquid as a pretreatment agent and chitosan treatment as a substitute of resin for post-treatment to reduce shrinkage properties of wool fabrics.

Experimental

Materials and agent. Worsted wool fabric with specification of 80S/2*54S/1 was supplied by Shandong Ruyi Group. Ionic liquids, 1 - butyl - 3 - methyl bromination imidazole ([Bmim]Br) with a purity of 99% were purchased from Lihua Henan. Ethanol and acetic acid of analytical reagent grade was used as purchased. Chitosan (deacetylation degree 90.2%) of low viscosity, 75cps, with 8.3% water and 0.6% ash was used without further treatment.

Pretreatment. Wool fabric was added into the ionic liquid and stirred at a predetermined temperature for a given time, and then the treated fabric was washed with ethanol thoroughly.

Post-treatment with chitosan. For the chitosan treatments, chitosan solutions were freshly prepared by dissolving the the desired amount in distilled water containing acetic acid(1%,wt). Treatments were done by the exhaustion method at a liquor ratios of 20:1 at the desired temperature for some time. After the treatment, the samples were squeezed and steamed for 5 min, and then dried at room temperature.

Determination of shrinkage. Shrinkage was measured according to GB/T 3921-2008.Alternative washing in a Fastness to Washing Tester (Shandong Laizhou electronic instrument cooperation Ltd.) was conducted at 40℃ for 15min. The dimensional stability of the treated fabrics was calculated according to Eq. 1. Area shrinkage (%) $=100\times (A_a-A_b)/A_a$ (1)

where A_a is the area of fabrics after the treatment without being washed, and A_b is the area of those fabric treated, and washed according to the standard

Mechanical Properties. The strength values of the treated fabrics were measured according to GB/T 3923-1997, on an YG062B Electronic fabric strength tester using 10cm gauge length, and tensile speed was 200mm/min.

SEM Analysis. The morphological changes of the cuticle scale surface structure of wool fiber was observed with a JSM - 6360LV scanning electron microscope(JEOL)

Wetability Analysis. Wetability was analyzed according to the literature [7]. A medical syringe was used to squeeze a drop of distilled water onto the treated fabrics from a height of 10cm. Wetting time was measured as the time for the droplets to be completely absorbed into the fabrics. For each sample, five measurements were taken at different areas and the average time was recorded as the wetting time.

Results and Discussion

Effects of Pretreatment with Ionic Liquid

Ionic liquid treatment reduces the shrinkage performance of wool fabrics, and the shrinkage resistant property of treated fabric excels with the treatment temperature and treatment time increasing[16], but strength loss arise along with that.

Effects of Pretreatment Temperature and Time on Wool Strength. In this paper, influences of treatment time and treatment temperature on tensile strength of treated fabric were investigated. The values of strength of the treated fabrics were shown in Fig.1 and Fig.2.

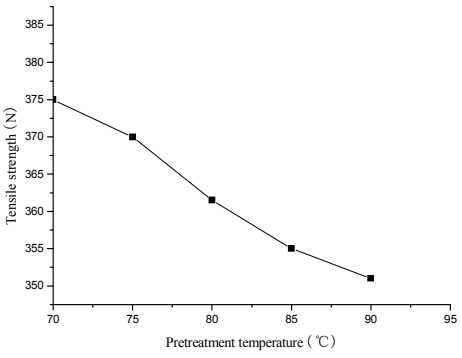


Fig.1. Effects of pretreatment time on strength (Pretreatment temperature: 80℃)

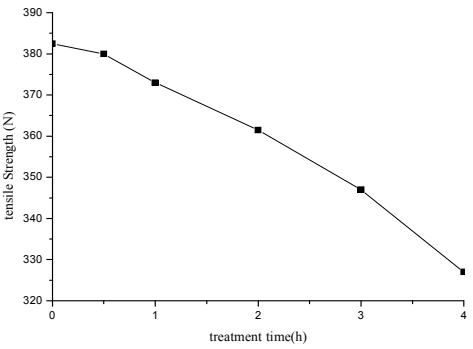
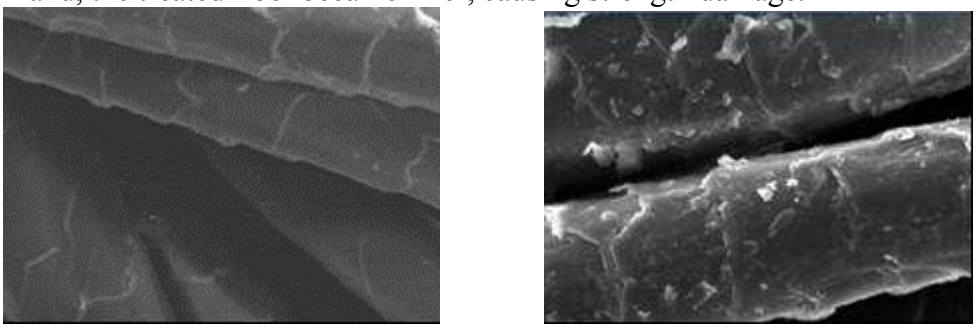


Fig.2. Effects of pretreatment temperature on strength (pretreatment time: 2h)

From Fig.1 and Fig. 2, it can be seen that strength of treated fabric decreases with treatment time and treatment temperature. That may due to the fact that fiber surface scales even inner part were dissolved along with the increasing time and temperature, causing fiber thinning or possible damage to inner microfiber and thus leading to strength loss, which was verified in the following SEM observation.

Taking shrinkage resisting and strength loss in consideration, 80℃ and 2 hours was chosen as the pretreatment condition.

SEM of Change of Surface Structure. Fig. 3 shows the SEM images of the control and the treated wool fiber surface. It can be seen that the scales covering the surface of the untreated fiber were intact. And the scales on the treated fiber had been destroyed obviously. Therefore, the Directional friction effect caused by scales was reduced, and a shrink resistant property was enhanced. On the other hand, the treated fiber became finer, causing strength damage.



（a）Original wool fiber （b）Pretreated wool fiber with ionic liquid

Figure 3 SEM images of the wool fabrics

Post-treatment of Chitosan. In attempt to provide better shrink-resistant property with less strength loss, we conducted a subsequent treatment with chitosan. Figure 4 shows the area shrinkage, wetability and strength of ionic liquid treated wool fabric post-treated with chitosan for 60min at different concentrations (0.6%, 0.8%, 1.0%, 1.2%, 1.4% wt %).

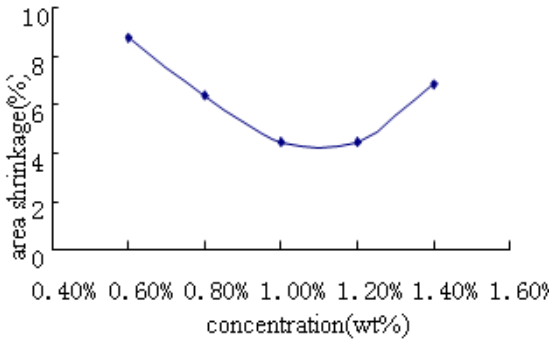


Fig.5. Effects of chitosan concentration on shrink resistant property of treated fabric

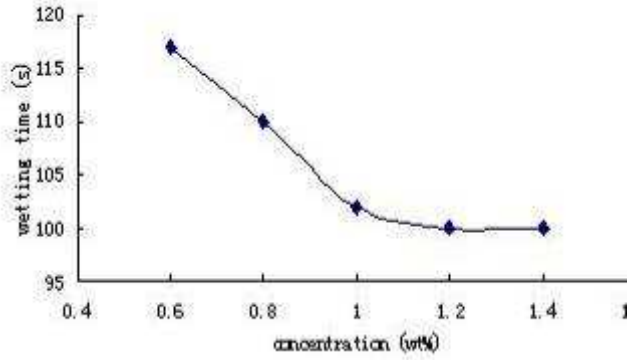


Fig.6. Effects of chitosan concentration on wetability of treated fabric

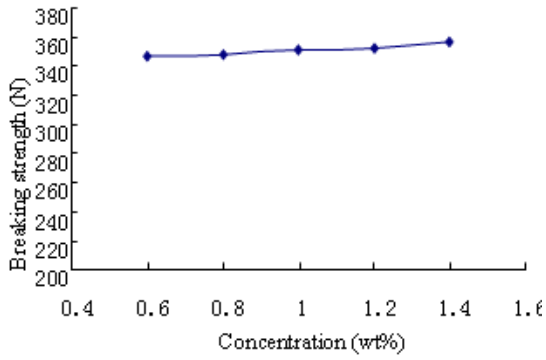


Fig.7. Effects of chitosan concentration on strength of treated fabrics

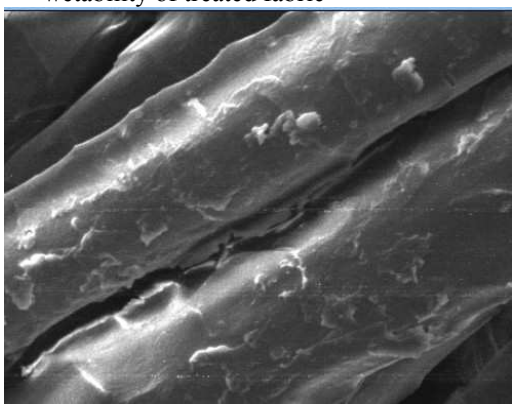


Fig.8. SEM image of wool fiber treated with ionic liquid and post-treated with 1.0% chitosan solution

Fig. 5, 6, 7 shows the influence of concentration of chitosan on area shrinkage, wetting time and tensile strength. With the increase of concentration, area shrinkage first went down and then up, that may be due to the fact that more chitosan was adsorbed on wool fibers with increasing concentration and an excess of adsorption form a thicker and rough film on treated fibers causing increasing area shrinkage. Figure 6 shows the wetability values of chitosan treated fabric, it is can be seen that wetting

time decreases with increasing concentration, that may be explained as follows: more and more chitosan was adsorbed onto the wool fiber, until concentration=1.0%, all wool fibers were coated with a film of chitosan, so the wetting time of treated fabric no longer change. These results are in accordance with the findings of M. R.Julia [12].

Fig. 7 shows the influence of concentration of chitosan on strength of chitosan treated fabrics, with the increasing of chitosan concentration, the breaking strength of chitosan treated fabric increase slightly, which could be attributed to the fact that chitosan formed a film on wool fibers, and increased the strength of treated fabric.

In order to assess the adsorption film of chitosan on the post-treated wool fiber, we mad SEM observations of chitosan treated wool fiber (Fig. 8). It is can be seen that combination of ionic liquid and chitosan treatment endowed the wool fabrics with good shrinkage resistance, wetability and acceptable strength loss.

Conclusion

A new ecological shrink-resistant treatment process was introduced by coating natural polymer chitosan to wool fabrics pretreated with ionic liquids. Higher temperature and longer time of ionic liquid pretreatment could improve the shrinkage resistance, but yet cause significant strength loss of treated fabric. In order to enhance the shrink resistance and avoid an excess of strength loss，a chitosan treatment was conducted subsequently. Results showed that chitosan treatment confer shrink resistance, wetability and acceptable strength loss to the treated fabrics.

Reference

[1] K. Yan. *Principle and Technology of Textile Dyeing and Finishing (the first part)* (China Textile Press.2005).p269

[2] R. P. Swatloski，S. K. Spear，J. D. Holbrey，et al. J.Am.Chem.Soc. Vol. 124(2002), p. 4974

[3]G. Laus, G. Bentivoglio, H. Schottenberger, et al. Lenzinger. Ber.Vol. 84(2005), p.71

[4] G. B. Diller, R. D. Rogers, R. P. Swatloski. *Investigation of Organic Liquids for Fiber Extrusion*. National Textile Center Annual Report: November 2006

[5] D.M. Philips, L. F. Drummy, D. G. Conrady, et al. J. Am. Chem. Soc. Vol. 126(2004), p.1350.

[6] H. Xie, S. Li, S. Zhang. Green Chem.(2005), 7, p. 606

[7] J. Yuan, Q. Wang, X. Fan, et al. Journal OF Textile Research. Vol.30 (2010), p. 83(in Chinese)

[8] J. Yuan, X. Fan, Q. Wang, Journal OF Textile Research. Vol.29 (2008), p. 60(in Chinese)

[9] M. Rinaudo. Polymer Sci., Vol.31 (2006), p.603

[10] E. Pascual, M. R. Julia, J. Biotechnol. Vol.89 (2001), p.289

[11] G.A.F. Roberts, F. A Wood. J. Biotechnol. Vol. 89(2001), p. 297

[12] M. R .Julia, M. R. Col, P. Erra., et al. T. C. C, Vol.30 (1998), p.7,

[13] P. Erra. Te. Re. J. Vol.69 (1999), p. 81

[14] Y. Huang, Sh. Wang, X. Wang. Journal of Beijing Union University. (2000).10, p.16 (in Chinese)

[15] P. Jovancic, D. Jocic, R.Molina, et al. Te. Re., (2001), p.11

[16]H. Wang, Q. Wang, M. Wang. Textile Bioengineering and Informatics Symposium: Advanced Textiles, Fashionable Industry, May 26-27, 2011[C]. Beijing: 646-648

© (2011) Trans Tech Publications, Switzerland
doi:10.4028/www.scientific.net/AMR.331.330

Anti-bacterial Property of Tussah Silk Fabric by Nano-titanium Dioxide and Chitosan Modification

Yanhua Lu[a], Zhimei Liu[b]

Eastern Liaoning University, Dandong, Liaoning, 118000, China

[a]email: yanhualuln@yahoo.com.cn, [b]email: liuzhimei2@126.com

Keywords: tussah silk, chitosan, nano-titanium dioxide, anti-bacterial property

Abstract. In order to increase the anti-bacterail property of tussah silk fabric, a nano-material dispersion system contained titanium dioxide nano-particles, chitosan, 1,2,3,4-butane tetracarboxylic acid, sodium monophosphate and surfactants was prepared. The particles in the dispersion solution have a narrow particle size distribution with average particle diameter of approximately 40 nm. Tussah silk fabric was then modified with the dispersion system using a conventional pad-dry-cure method. The structure of the modified tussah silk was characterized by X-ray photoelectron spectroscopy (XPS). The anti-bacterial efficiency of the treated tussah silk fabric with the dispersion system at a concentration of 0.2% nano-titanium dioxide and 0.5% chitosan showed over 99% of bacterial reduction against the *Staphylococcus aureus*（*S. aureus*） and gram-negative bacterium *Escherichia Coli* (*E. Coli*). In addition, the anti-bacterial reduction was maintained over 90% even after being exposed to 20 consecutive launderings.

Introduction

Tussah silk, as a natural fibers, is often considered to be vulnerable to microbe attack compared to those man-made fibers for its hydrophilic porous structure and moisture transport characteristics[1]. Thus, the application of antibacterial reagents to prevent or retard the growth of bacteria is becoming a promising finishing for natural textiles. However, there is an increasing concern over the possible effects of antibacterial finishing on environmental and biological systems since some antibacterial agents are toxic chemicals. And as a result, an ideal textile antibacterial finishing should be safe and environmentally benign besides killing undesirable bacteria[2]. As for chitosan, a number of investigations have focused on the anti-bacterial properties for its applications in textile finishing[3]. However, the antibacterial property of chitosan itself is limited. To overcome the problem, approaches have been performed to chemically modify the chitosan. For instance, introduction of functional groups into the chitosan backbone improved its antibacterial activity[4]. On the other hand, as it is well-known that nano-TiO_2 particles also performs the anti-bacteria properties under daylight irradiation by the photo-catalysis action when coating it on some textiles[5,6].

In this study, chitsoan and titanium dioxide nano-particles were combined to finished tussah silk fabric in the presence of 1,2,3,4-butane tetracarboxylic acid, sodium monophosphate, Span-80 and OP-10 as well. Then the antimicrobial activity of treated tussah fabrics was studied.

Experimental

Materials. Tussah silk fabric (Type 5023), Chitosan (viscosity-average molecular weight is 21000, degree of deacetylation is 92%), 1,2,3,4-Butane tetracarboxylic acid (BTCA), sodium hypophosphite(SHP), sorbitan monooleate (Span-80) and nonyl phenol polyethyleneoxy ether (OP-10) used in this experiment were chemical pure agents. Gram-positive *S. aureus* (ATCC 6538) and Gram-negative *E. Coli* (ATCC 8099) were used as the test microorganisms.

Titanium DioxideNano-particles and chitosan dispersed solution preparation. 10.0 mL and 1.0 mL acetate acid were added to 100mL anhydrous alcohol with stirring (solution A). 0.5mL HCl in 2.0 mL deionized water was added to another 20mL anhydrous alcohol (solution B). Then solution B was added dropwise to solution A with vigorous stirring for 2 h at room temperature, and transparent

and flaxen titanium dioxide sol was obtained. A definite store of chitosan was added in the solution of 2% BTCA and 2% SHP to prepare chitosan solution while Span-80 and OP-10 as dispersants. Then titanium dioxide sol was added dropwise to the above solution. Finally, nano-titanium dioxide and chitosan dispersed solution was prepared [7]. Concentration of sol TiO_2 in the chitosan solution was 0.2 % and the concentration of chitosan 0.5% so that the nano-particles disperse well.

Tussah silk fabric treatment. Silk samples were immersed in solution containing titanium dioxide and chitosan nano-particles for 30 min at 30°C, then using a laboratory padder at 90% wet pick-up. The padded samples were dried at 80°C for 5 min and then cured in a laboratory oven for 3 min at 160°C. The treated filament or fabric samples were washed with tap water until neutral to pH paper. Then the fabric samples were dried at 80°C.

Size of nano-particles in treatment solution measurement. The size of nano-TiO2 particles was measured with HPPS particle size analyzer at 30°C because the temperature of treating silk was 30°C.

XPS analysis of tussah silk fabric. XPS spectra were recorded with an XSAM800 electron spectrometer (Kratos, U. K.). The samples were irradiated with monochromatic Al Kα X-rays (1486.6 eV) using a X-ray spot size with a diameter of 100μm and a power of 25W. The standard take-off angle used for analysis was 45°, producing a maximum analysis depth in the range of 3–5 nm. Surface compositions were obtained, using manufacturer-supplied software, from both survey scans and individual spectra of each element, C1s, N1s, O1s, and Ti2p. Spectra from elements of interest were curve-fit with Gaussian peaks using manufacturer-supplied software, giving full-width at half maximum peak height, peak energy, and peak area.

Antimicrobial activity of tussah silk fabric. The antimicrobial properties of the titanium dioxide and chitosan treated fabrics were evaluated according to the shake flask method [6]. The percentage reduction was calculated using the following equation:

$$R = \frac{B - A}{B} \times 100\%$$

Where R is the percentage bacterial reduction, A and B are the surviving cells (CFU/ml) for the flasks containing test samples and the control (blank tussah silk), respectively, after 1 h contact time.

Results and discussion

Particles distribution in the nano-titanium dioxide and chitosan dispersed solution. Being dispersed homogeneously for the nano-particles in its dispersion solution is the prerequisite of making full use of the nano-particles properties. To investigate the dispersion of nano-particles in the nano-titanium dioxide and chitosan dispersed solution, the size and its distribution in the solution was characteristic by HPPS measurement. The particles' sizes in the titanium dioxide sol and in the nano-titanium dioxide and chitosan dispersed solution are shown in Fig.1 and Fig. 2.

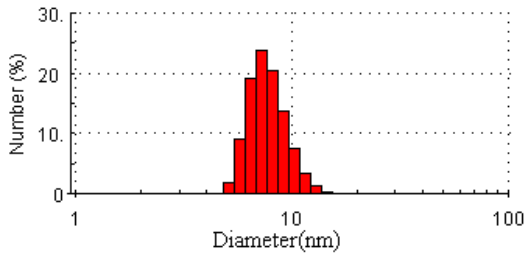


Fig. 1 Size distribution of sol-TiO_2

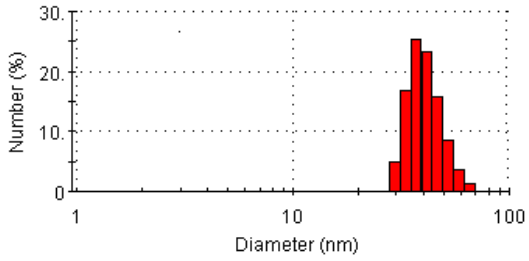
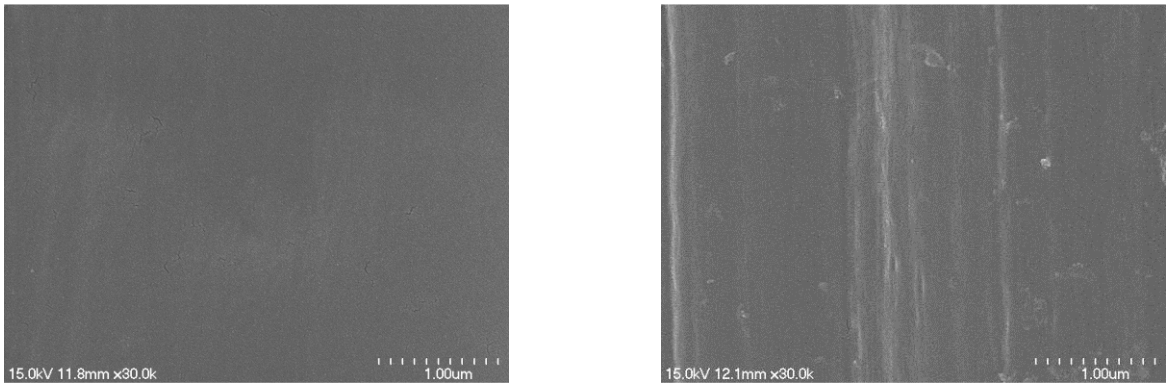


Fig. 2 Size distribution of the nano-particles in treatment solution

It was found from Fig. 1 that the particles in the titanium dioxide sol and in the nano-titanium dioxide and chitosan dispersed solution dispersed perfectly and the distribution of the nano-particles is relatively narrow. The sizes of the particles in the titanium dioxide sol were from 5 to 15 nm and the

average diameter and polydispersity index of the particles was 7.56 nm and 0.54, respectively. Fig. 2 showed that the sizes of the majority particles in the nano-titanium dioxide and chitosan dispersed solution were from 20 to 60 nm. And the average diameter and polydispersity index of the particles was 39.8 nm and 0.45, respectively.

Morphology of tussah silk fiber. Fig. 3 shows the SEM images of tussah silk fiber before and after treatment with the nano-titanium dioxide and chitosan dispersed solution.

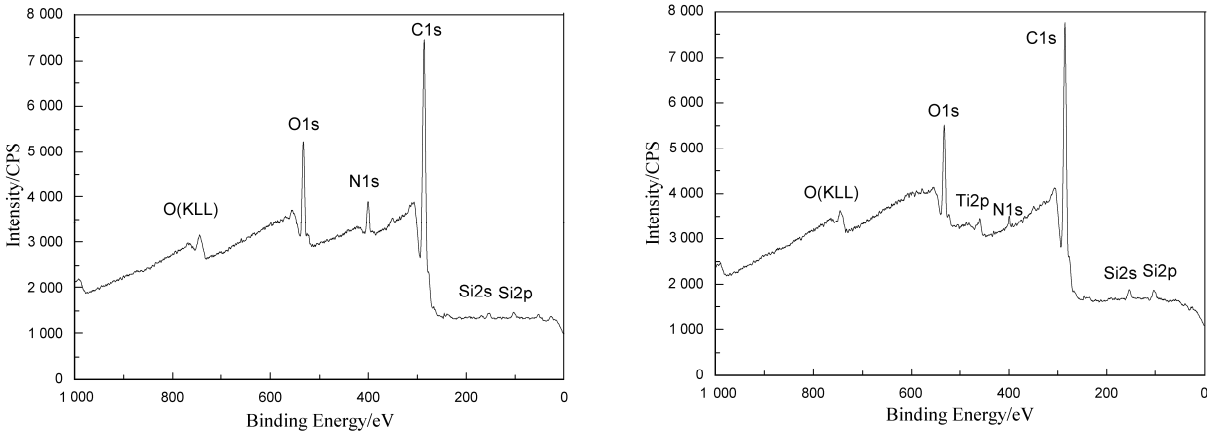


(a) untreated tussah silk fiber (b) treated tussah silk fiber

Fig. 3 SEM micrographs of tussah silk surface morphologies (30 000 times)

SEM images showed that there was a little difference in the fiber surface between before and after treatment. And individual particles are not observed on the fiber surface. However, there were some tiny longitudinal striations on the surface of treated fiber while the surface of untreated silk fiber was smooth. The striated surface on the surface of the treated silk fiber was attributed to dissolving by the action of BTCA solution [6].

XPS analysis of tussah silk fiber. As a high sensitivity analysis method, XPS can be used to study the surface property, structure, and the finishing agent state on fiber surface. The samples were washing with an ultrasound cleaner in order to remove the substance without participating in the modification and any other foreign matters.



(a) unreated tussah silk fiber (b) treated tussah silk fiber

Fig. 4 XPS spectra of tussah silk fiber

Fig. 4 shows three obvious peaks on the untreated silk fiber, 286.0eV(C1s), 400.8eV(N1s), and 532.8e(O1s). While there are four obvous peaks on the treated silk fiber, 285.2eV (C1s), 401.6eV (N1s), 533.2eV (O1s), and 459.2eV (4 valencies Ti2p). In comparison to untreated tussah silk fiber, The binding energy of N1s and O1s peaks in untreated tussah silk fiber increased 0.8eV and 0.4eV, respectively, and C1s decreased 0.4eV[8]. The result indicated that the surrounding state of those elements including C, N, O changed and TiO_2 appeared.

Anti-bacterial activity analysis of tussah silk fabrics. Nano-titanium dioxide and chitosan dispersion solution was applied to finish the tussah silk fabric, and the anti-bacterial activity of the fabric before and after treatment against *S. aureus* and *E. colis* was shown in Fig. 5.

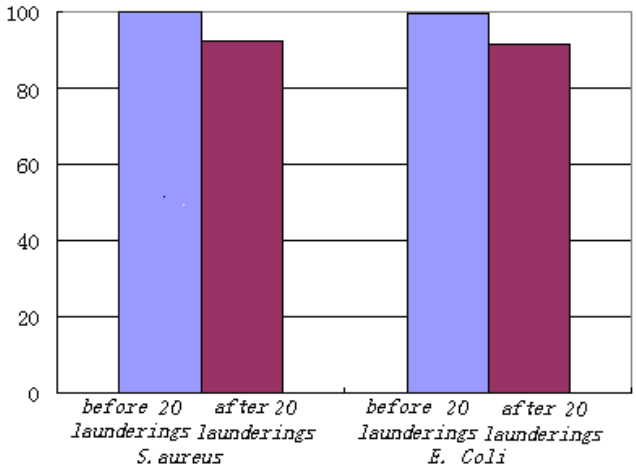


Fig. 5 Bacterial reduction of the tussah silk fabrics before and after launderings

It was indicated that the bacterial reduction of the treated silk samples before 20 launderings approximates to 100%, and decreased to about 90% even after 20 launderings. The anti-bacteria mechanism was that the protonated chitosan in acid condition and nano-titanium ioxide might contact with the bacterial cell surface and prevented the leakage of intracellular components. In addition, there was more specific surface on the treated tussah silk fiber than that of the untreated one. The good anti-bacterial property can be attributed to the combination of chitosan and TiO_2 nano-particles.

Conclusions

Nano-TiO_2 and chitosan dispersion solution was prepared has been prepared via a sol-gel method as a novel antibacterial coating for tussah silk fabric. The average diameter and polydispersity index of the particles in the nano-titanium and chitosan dispersion solution was 39.8 nm and 0.45 respectively.

The results of XPS indicate that the surrounding state of the elements including C, N, O changed and TiO_2 appeared in the modified in tussah silk fiber.

The treatment with nano-TiO_2 and chitosan dispersion solution confers tussah silk fabric with nearly 100% before 20 launderings and with over 90% bacterial reduction even after 20 launderings.

Acknowledgements

The authors gratefully acknowledge the financial support in this research from the Education Department Funds of Liaoning Province P. R. China (Proj. No. L2010144).

References

[1] Y. Kawahara, M. Shioya. J Appl Polym Sci Vol. 6(1999), p. 363

[2] M. Orhan, D. Kut, C. Gunesoglu. J Appl Polym Sci Vol. 11(2009), p. 1344

[3] V. R. G. Dev, J. Venugopal, S. Sudha. Carbohyd Polym Vol. 75(2009), p. 646

[4] S. H. Lim and S.M. Hudson. J Macromol Sci Polym Rev Vol. 43(2003), p. 223

[5] T. Yuranova, R. Mosteo, J. Bandara. J Mol Catal A: Chem Vol. 244(2006), p. 160

[6] A. Bozzi, T. Yuranova and J. Kiwi. J Photoch Photobio A: Chem Vol. 172 (2005), p.27

[7] Y. H. Lu, H. Lin, Y. Y. Chen. Fibers Polym Vol. 18(2007), p.1-6

[8] K. C.Yung, D.W. Zeng, T. M. Yue. Appl Surf Sci Vol. 173(2001), p.193-202

© (2011) Trans Tech Publications, Switzerland
doi:10.4028/www.scientific.net/AMR.331.334

Study on the dyeing of PET fiber with disperse dyes in D5 media

Shenzheng Li[1, 2,a], Jinqiang Liu[1,2,b*], Yongqiang Li[1,2,c] and Liming Li[1,2,d]

[1]Key Laboratory of Advanced Textile Materials and Manufacturing Technology, Ministry of Education, Zhejiang Sci-Tech University, Hangzhou 310018, P. R. China

[2]Engineering Research Center for Eco-Dyeing & Finishing of Textiles, Ministry of Education, Zhejiang Sci-Tech University, Hangzhou 310018, P. R. China

[a]lishenzheng.162@163.com, [b*] jqliu@zstu.edu.cn, [c]yqli@zstu.edu.cn, [d]790241857@qq.com

Keywords: D5, Disperse dye, Non-aqueous dyeing.

Abstract. This experiment selected a new kind of environmental media (D5) instead of using water on the dyeing of PET, this work provided a new method for non-aqueous dyeing. The effects of the water addition, temperature, dyeing time and reagents on adsorption amount of disperse dye were studied, one good dyeing process is, adding 0.5mL water and 0.3mL ethanol into 20mL D5 system, the temperature of dyeing was 130˚C, the preservation time of dyeing was 60min.

Introduction

Decamethylecyclopentasiloxane (D5) is an odorless, colorless, non-oily cyclic siloxane fluid, is soluble in most of organic reagents such as alcohols and benzenes, can be used as compound or carrier [1, 2, 3]. A scientific research shows that is a safe chemical products, D5 has been used in plenty of healthy and personal care products [4, 5, 6]. The chemical structure of D5 is shown in Fig. 1.

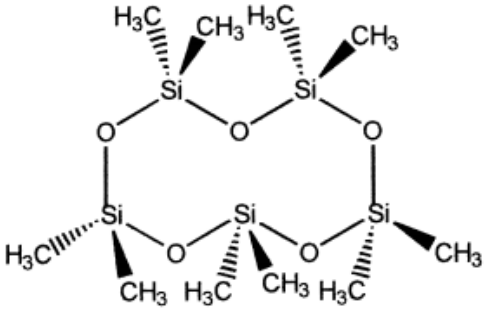


Fig. 1 Chemical structure of D5

But the research on D5 as dyeing media has not been reported. The dyeing of PET usually used high temperature and high pressure dyeing method in water media, due to disperse dye has low dissolvability in water, so commercial disperse dye need added a large amount of dispersant, thus produce large quantities of waste water after dyeing [7]. Previous studies suggested that pure disperse dye has better solubility and dispersion ability in D5 than water, and easily recycled, a good dyeing effect can be obtained on the dyeing of PET fiber with disperse dyes in D5 media. As a result, D5 has a great potential instead of using water on the dyeing of PET. In this paper, we study on the dyeing properties of PET fiber with disperse dyes in D5 media.

Experimental

Materials. D5 used was pure grade (>99.9%) and was purchased from GE Toshiba Silicones (Thailand).Ltd, and was used without further purification. Dyes used was disperse dye (C.I. disperse blue 183) and contains no dispersant, and obtained from Hangzhou Jihua Group Co., Ltd. All other chemicals were analytical reagents and purchased from Hangzhou Mike Chemical Instrument Co., Ltd.

Dyeing procedure. The process of dyeing is shown in Fig. 2.

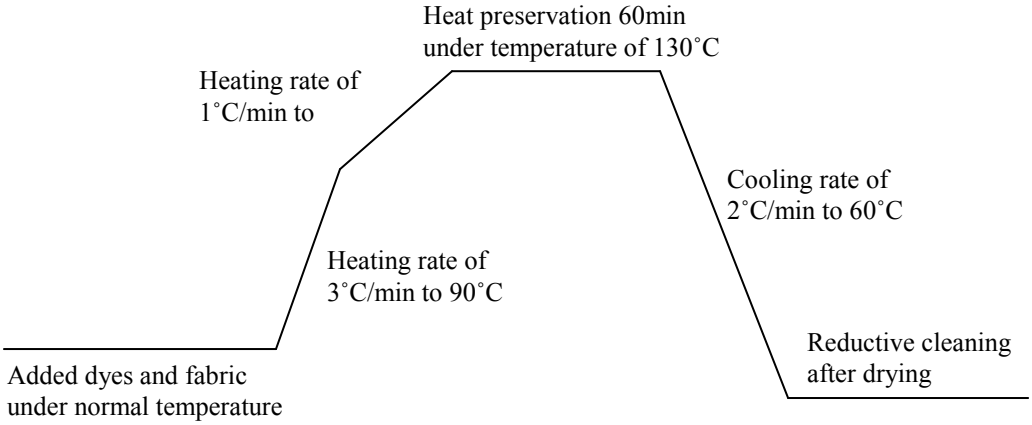


Fig. 2 Process of dyeing

Technological formulation: fabric weight: 1g; dye concentration: 0.8% (o. w. f); temperature: 130˚C; preservation time: 60min; bath ratio: 1:20; water addition: 0.5mL.

The dyeing effect of water addition in D5 media

In a preliminary experiment, we have found that added a small quantity of water have a good effect on the dyeing of PET with disperse dyes, so we conduct three experiments as fallow: Ⅰ.dyeing of PET in D5 media and not added water; Ⅱ added 1mL water into D5 media then dyeing of PET; Ⅲ padding 1mL water to PET fabric and dyeing (not added water into D5media). The effect of water addition on the dyeing is shown in Fig. 3 and Fig, 4.

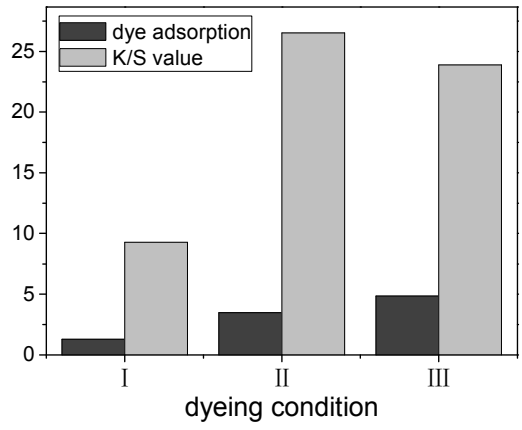


Fig. 3 The effect of water addition on the dyeing

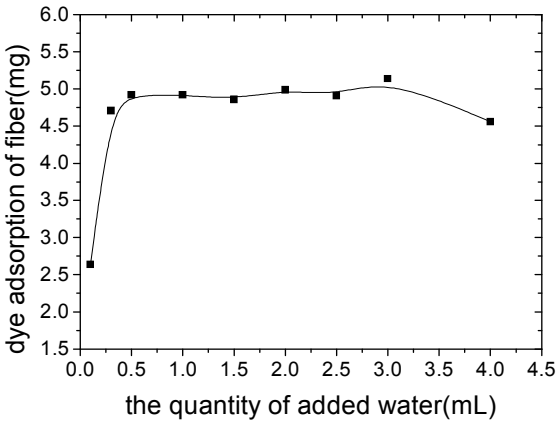


Fig.4 the effect of quantity of added water on the dyeing

As Fig. 3 shows, whether from dye adsorption of PET fibers or K/S value of PET fibers, add water can greatly improve the effect of dyeing, and different method of water addition have different effect. Compares Ⅱ with Ⅲ, Ⅱ has higher dye adsorption than Ⅲ, but Ⅲ has higher K/S value than Ⅱ. What is the cause of the phenomenon? Because disperse dyes are a series hydrophobic dyes, the internal water of fibers can prevent dyes into the fibers and dyes adsorbed on the surface of fibers when padding water to fabrics, so Ⅲ has higher K/S value but low dye adsorption. When added water into D5 system, because of synergistic action of D5 and water, it can raise the swelling effect of fibers and dyes molecular can easily into the internal of fibers, so the fabrics has high dyes adsorption and K/S value. Considering the result, we chosen Ⅲ for further study.

Fig. 4 shows the quantity of added water on the dyeing of PET. The results show that the dye adsorption of fiber increase while the water volume increased, and when added to 0.5mL water, the dye adsorption of fibers equilibrium was reached, and then increase the amount of water, fiber will not significantly increase the adsorption of dye. The figure also shows that, when added to 4mL water, the dyes adsorption of fibers decreased, the reason is to add water too much in D5 system, too much water will gather around the fiber and have a certain resistance to dyes into fibers, the dyed fabric surface has a small amount of light blue spots, which also proved too much water will prevent the dye into the fiber interior. Therefore, to determine the amount of water was 0.5mL.

The dyeing effect of preservation time in D5 media

Dyeing time is a important factor of dyeing, it determines the dye absorbing rate. The effect of preservation time on the dyeing is shown in Fig. 5.

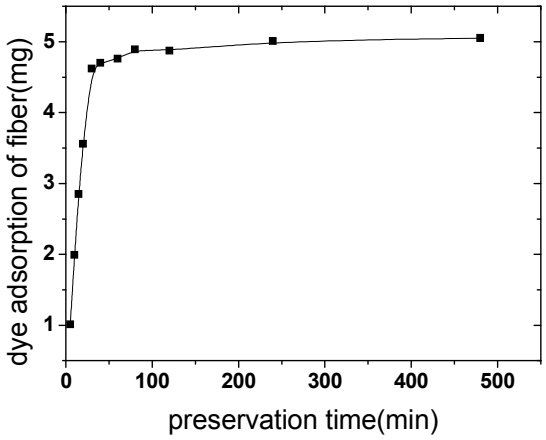


Fig. 5 The effect of preservation time on the dyeing

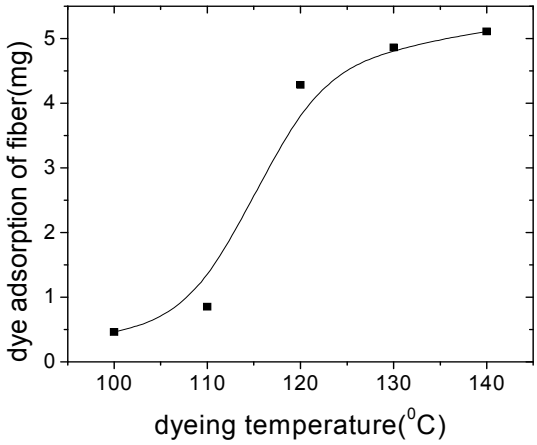


Fig. 6 The effect of dyeing temperature on the dyeing

Fig. 5 shows, as time goes on, the dye adsorption of fibers increased sharply, the in increased trend became weaker at time of 30min,its reaches equilibrium when the time of 60min. These result shows that disperse dye has high dye adsorbing rate in D5 media, this could be due to an association with D5 to PET fibers has great affinity and pure disperse dye has better solubility and dispersion ability in D5 media. Therefore, we chosen the preservation time was 60min.

The dyeing effect of temperature in D5 media

Temperature is particularly important in traditional dyeing process. The effect of temperature on the dyeing in D5 media is shown in Fig. 6.

As Fig. 6 shows, its have poor dye adsorption of fibers when dyeing temperature below 110˚C, as temperature goes on, the dye adsorption of fibers increased sharply, its has high dye adsorption of fibers at temperature of 120˚C, With the temperature increase after 120˚C the dye adsorption increased more slowly. The reason for the dyeing temperature above 120 ˚C, fiber and dye molecules are more violent activities, polyester fiber molecules gap increases, the dye molecules into the fibers of the interior quickly, prompting sharp increase of dyes on fibers. When the temperature reaches 130˚C, the adsorption of dyes on fibers basically reached. Therefore, we selected dyeing temperature of 130˚C.

The dyeing effect of reagents on dyeing in D5 media

In determining the above parameters, add a certain amount of reagents (addition 0.3mL), in order to further improve the dyeing properties of disperse dyes in D5 system. The effect of reagents on dyeing is shown in Fig. 7.

As Fig. 7 shows, the addition of non-ionic surfactant S-85 of the dyeing properties is the worst, because the S-85 has low cloud point, and dyeing temperature in the S-85 above the cloud point, lead surfactant to loss effect, a large concentration of disperse dyes flocculation and sedimentation, resulting in very low dye adsorption of fiber. The ionic surfactants oleic acid and dyeing carrier of methyl salicylate have lower dye adsorption than blank experiment, because the oleic acid and D5, D5 and methyl salicylate can be dissolved with each other, while the oleic acid and methyl salicylate has a high solubility of disperse dyes, resulting in dye solubility in the D5 system is too high, thus adsorption of the dye in the fiber below normal. The experiment of added ethanol, acetone has the highest dye adsorption, Ethanol, acetone has a lower molecular weight and easy access to the internal fiber, so there is some swelling effect on PET fibers, thus more accessible to dye molecules within the fiber. But acetone was toxic, we chosen ethanol as the best reagent in the D5 media.

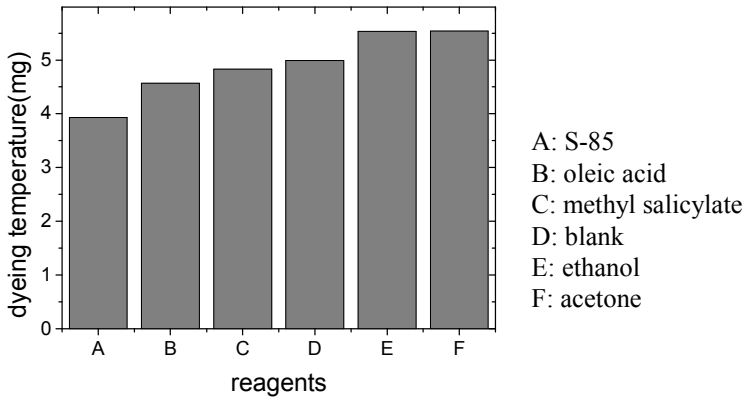


Fig. 7 The effect of reagents on the dyeing

Conclusions

The experiment studied the dyeing properties of disperse dye in D5 system, the suitable dyeing process were obtained: adding 0.5mL water and 0.3mL ethanol into 20mL D5 system, the temperature of dyeing was 130˚C, the time of dyeing was 60min.

Acknowledgements

This work was financially supported by the Esquel Group, Engineering Research Center for Eco-Dyeing & Finishing of Textiles, Ministry of Education, Zhejiang Sci-Tech University, Zhejiang Provincial Key Innovation Team (2010R50038), Zhejiang Provincial Top Academic Discipline of Applied Chemistry and Eco-Dyeing & Finishing Engineering (ZYG2010017).

References

[1] Bharadwaj C, Kames R. M: atmospheric Emviroment. Vol. 35 (2001), p. 87
[2] Brown S L, Silverman B G, Berg W A: Lancet. Vol. 350 (1997), p. 1531
[3] Charles N, Falany, GeLi: J Biochem molecular toxicology. Vol. 2 (2002), p. 129
[4] Leigh A B, Richard W M, Paal C K: Toxicological Sciences. Vol. 43 (1998), p. 28
[5] D. M. Naylor, V. T. Stannett , A. Deffieux, P. Sigwalt: Reactivities and Interpretation. Vol. 35 (1994), p. 1964
[6] Leigh A B, Richard W M, Robert G M: Toxicological Sciences. Vol. 43 (1998), p. 230
[7] Tao Zhao: Dyeing-and-Finishing Technology of Textiles (In Chinese). China Textile Press (2005).

© (2011) Trans Tech Publications, Switzerland
doi:10.4028/www.scientific.net/AMR.331.338

Research on improving the properties of wool fabric with low-temperature plasma

Yanli Qiao[1,2,a] , Wenfang Yang[1,2,b] , Qingfu Zhang[1,2,c] , Xiaoxing Shen[1,2,d]

[1] School of Textiles, Tianjin Polytechnic University; Tianjin 300160, China

[2]Key Laboratory of Advanced Textile Composite, Ministry of Education of China; Tianjin 300160, China

[a]qiaoyanli87@126.com,[b]yangwf2@126.com,[c]keep433@126.com,[d]shenxiao_xing@126.com

Key words: low-temperature plasma; wool fiber; dyeing properties; surface modification

Abstract: This paper discussed the influences of plasma processing time and power on wool fibers, the results showed that: after plasma treatment, the surface of the wool fibers occurred varying degrees of physical and chemical etching phenomenon, the wetting property was increased significantly, anti-shrinkage performance was improved. Breaking strength and elongation at fracture were increased; the beginning of dyeing properties and the balance rate were increased.

Introduction

Wool fabric, as the high-grade product of the textile, has many excellent qualities, but the existence of the surface scale has affected its dyeing performance and anti-shrinkage performance partly. Therefore, people did a lot of work in order to destroy or completely strip flakes to reduce the dyeing temperature or to improve the felt shrinkage performance [1-4].

Low-temperature plasma treatment can modify the surface properties of wool fiber without much change in the original bulk properties. Low-temperature plasma technology processing on wool fiber made its surface macromolecules chain or disulfide bond fracture, produced ions or free radicals, and improved hydrophilic of fiber. To a certain extent, it also improved its dyeing performance [5-6]. The main advantages of plasma technology are as followed: the effect is relatively uniform; it produces only rarely decomposition products (CO_2 and H_2O); plasma requires low energy, almost no water, it is an energy-saving and water conservation new technology [7-10].

Experimental

2.1 Experiment contents

The effect of different parameters:

Power 800W, processing time (min): 0.5, 1, 2, 3, 4, 5, 6, 7, 8, 9, 10.

Time 1min, processing power (W): 800, 1200, 1500, 1800, 2000, 2200.

2.2 Test methods

(1) Wettability

Wool fiber wetting property was characterized by the wetting time. The time was recorded from the moment that the ball was just dipped the surface of the distilled water to the time that the wool ball was on the surface completely immersed in water.

(2) The volume of retraction bulb

The volume of retraction bulb was used to characterize the anti-felting properties. The specimens were treated at 40 ˚C for 20 minutes, dried at 80 ˚C. Then the diameter was measured in 8 different directions, according to Eq.1 to calculate the volume of retraction bulb.

$$V = \frac{4}{3}\pi R^3 \quad (1)$$

(3) The friction coefficient and directional friction coefficient

Wool fiber was measured both on obedient and inverse directions on torsion balance and the friction coefficient was calculated respectively:

$$\mu = 0.7329 \times [1g300 - lg(300 - T)] \quad (2)$$

Where T was the torsion balance reading, substituted the measured T values into the above formula to calculate the friction factor, μ-obedient and μ- inverse, the value of directional friction effect was:

$$D.F.E\% = [(\mu_{-in} - \mu_{-ob}) / (\mu_{-in} + \mu_{-ob})] \times 100 \quad (3)$$

The value of directional friction effect was calculated according to Eq.3.

(4) Fiber breaking strength: the breaking strength was measured according to GB/T 3916-1997.

(5) Dyeing rate [11]

Results and discussion

3.1 The effects of low temperature plasma treating time for wool fiber properties

3.1.1 Wettability

Experiments showed that wool fiber treated with plasma rapidly submerged into water in less than 1s; while untreated wool fiber floated on distilled water surface, 10min or more didn't sink.

3.1.2 The influence of wool fiber surface



a. crude wool b.1min c.4min

Fig.1 Photos for different plasma treating time on the wool fiber

Fig. 1 shown that the flake structure of untreated wool fiber was clearly visible, with edges and corners obviously; 1min, the surface scale layer was partly divested or inactivated, made the surface smooth; while for a long time, the surface occurred concave-convex due to sculpture.

3.1.3 Directional friction effect and mechanical properties

Table 1 The influence of mechanical properties with different plasma treating time

Time/min	DFE/%	Breaking Strength/cN	Elongation at Break/%
0	16.69	20.58	3.49
0.5	9.36	21.63	3.82
1	8.19	22.81	3.90
2	7.28	24.07	3.93
3	7.00	24.53	4.08
4	6.50	25.28	4.20
5	5.67	24.12	3.96

6	7.92	22.90	3.91
7	6.22	22.54	3.81
8	6.67	21.60	3.58
9	6.89	21.31	3.33
10	6.54	19.52	3.27

As shown in Tab. 1, with the extension of plasma time, the directional friction effect for wool fiber was reduced. The breaking strength and elongation at break had a rising and falling process.

3.1.4 Felt shrinkage performance

As shown in Fig. 2, optimal anti-shrinkage performance was obtained at treating time for 8min and the volume of retraction bulb reached the largest. With the increase of plasma processing time, the volume of retraction bulb of wool fiber had experienced a process of rise and fall.

3.1.5 Dyeing property

As shown in Fig.3, untreated wool dyeing rate was very low, while after plasma treating, the dyeing rate and the initial uptake rate improved greatly, the same as the dyeing speed. It also showed that different plasma treating time of wool, dyeing property had certain differences, but the difference was not significant.

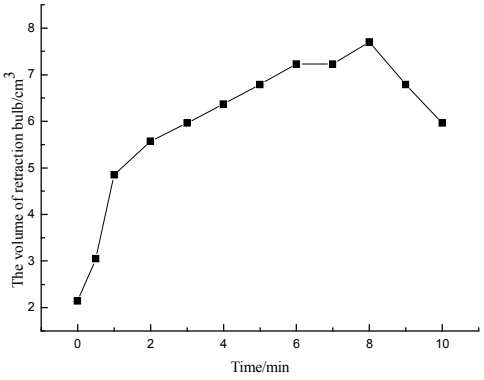


Fig.2 The volume of retraction bulb of different plasma treating time

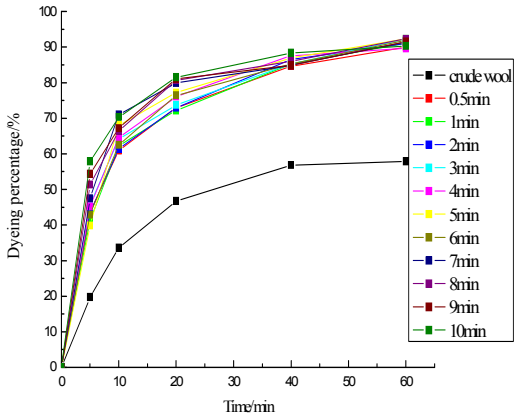


Fig.3 Staining with LANASET Blue

3.2 Low temperature plasma processing power for wool fiber properties

3.2.1 Directional friction effect and mechanical properties

Table 2 The influence of mechanical properties with different power plasma treated on wool fiber

Power/W	DFE/%	Breaking Strength/cN	Elongation at Break/%
0	16.69	20.58	3.49
800	8.19	22.81	3.90
1200	5.77	23.66	4.15
1500	4.75	25.25	4.26
1800	4.29	25.58	4.36
2000	4.74	22.35	4.11
2200	4.72	20.43	3.49

As shown in Tab. 2, with the plasma power increase, the directional friction effect of wool fiber was reduced significantly; the breaking strength of wool fiber presented to rising first and falling followed; the variation trend of breaking strength and elongation was similar.

3.2.2 Felt shrinkage properties.

As shown in Fig.4, optimal anti-shrinkage performance was obtained at treating power for 1800W and the volume of retraction bulb reached the largest.

3.2.3 Dyeing property

Fig.5 showed that the dyeing rate was improved obviously with different plasma processing power, but the dyeing rate didn't change significantly, and the impact was similar to treat-time.

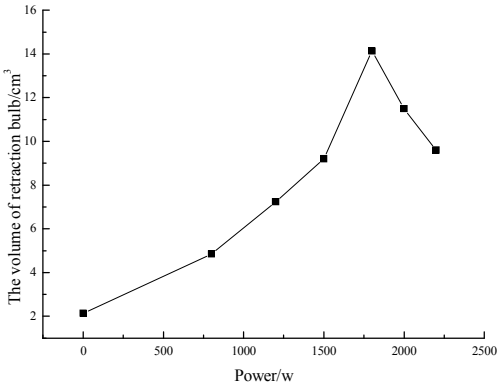


Fig.4 The volume of retraction bulb of different plasma treating power

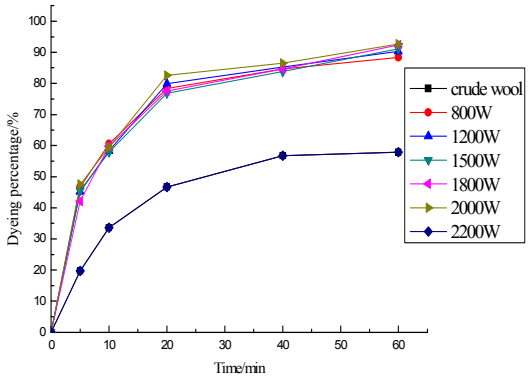


Fig. 5 Staining with LANASET Blue

Conclusions

The properties of wool fibers had improved after low-temperature plasma treatment which was as followed:

(1) The surface of the wool fibers occurred varying degrees of physical and chemical etching phenomenon, the wetting property of wool fibers was increased significantly;
(2) The anti-shrinkage performance, breaking strength and elongation at fracture were improved;
(3) The beginning of dyeing properties and the balance rate were increased.

References

[1] X.Y. Jin, B.Q. Liu. Dyeing and Finishing. Vol. 1 (2003), p. 1-3.

[2] Ryu J M, Wakida T, etal. TRJ, Vol. 61(1991), p. 595-601.

[3] Kan Chi-wai, Chan Kwong and Marcus Yuen Chun-wah. Autex Research Journal, March, Vol. 4(2004), p. 37-44.

[4] Q. Tang. Wool Textile Journal, Vol. 9(2009), p. 22-24.

[5] D.J. Liu. Silk Textile Technology Overseas. Vol. 5 (2003), p. 20-23.

[6] Y.Z. Zhan, X. Zhao, W. Wang. Textile Dyeing and Finishing Journal. Vol. 29 (2007), p. 1-3.

[7] J. Lv. Silk Monthly. Vol. 12 (2001), p. 19-21.

[8] S.Y. Xing. Wool Textile Journal, Vol. 1 (2004), p. 21-26.

[9] W.F. Yang, Z.Y. Gu. Knitting Industries, Vol. 6 (2005), p. 53-55.

[10] J.C. Jin. Dyeing and Finishing, Vol. 11 (2005), p. 39-42.

[11] Y. Chen: *Dyeing and Finishing Processing Course Books*, edited by China Textile Publishing, Beijing, (2004).

© (2011) Trans Tech Publications, Switzerland
doi:10.4028/www.scientific.net/AMR.331.342

Preparation of Temperature-sensitive PET Fabrics by Plasma-induced Grafting

Yongqiang Li [1, 2, a], Jinqiang Liu [*1, 2, b], Chunjie Qian [1, c] and Tingting Liu [1, d]

[1] Engineering Research Center for Dyeing and Finishing of Textiles (zhejiang Sci-Tech University), Ministry of Education，Hangzhou 310018, China;

[2] Key laboratory of Advanced Textile Materials and Manufacturing Technology (zhejiang Sci-Tech University), Ministry of Education，Hangzhou 310018, China

[a]yqli@zstu.edu.cn, [b]jqliu@zstu.edu.cn, [c]xiaomaojljl@126.com, [d]liutinghome@163.com
[*] Corresponding author: Jinqiang Liu .E-mail: jqliu @zstu.edu.cn .

Keywords: Low temperature plasma; Grafting; Temperature-sensitivity; PET fabric; Poly (N-isopropylacrylamide).

Abstract. In this paper, temperature-sensitive PET fabrics were prepared by Ar-plasma-induced simultaneous grafting Ploy-N-isopropylacrylamide (PNIPAAm) onto PET fabric. Fourier transform infrared spectroscopy (FTIR) was used to identify the structure of the grafted fabric. Then the surface morphology of the grafted fabric was observed from scanning electron microscopy (SEM) and AFM. The results show that the PNIPAAm was grafted onto PET fabrics, respectively. The grafted PET fabrics are characterized by differential scanning calorimetric analysis (DSC). The DSC analysis results indicated that LCST value of the grafted fabric was around 32˚C. And the water permeability of the grafted sample showed a sharp change around 32˚C. It was proved that grafted fabric was sensitive to temperature.

Introduction

The volume phase transitions of polymer gels have attracted a great deal of attentions in recent years [1]. Most of studies have been focused on Poly (N-isopropylacrylamide) (PNIPAAm) and its copolymers [2, 3]. PNIPAAm exhibits a well-defined lower critical solution temperature (LCST) in water at around 32˚C.Below the LCST the hydrophilic PNIPAAm chains do interaction with water. Above the LCST the hydrophobic PNIPAAm chains collapse and such interactions do not occur anymore. And this leads to great volume change [4]. The special thermal-sensitivity has been widely used in drug controlled-releasing, curing the enzyme, tissue engineering and other fields [5]. Likewise, we can by means of grafting to introduce PNIPAAm onto the PET fabrics and endow them with relevant thermal-sensitivity. There are many grafting methods to graft PNIPAAm onto PET fabrics, such as irradiation grafting, photochemical grafting, plasma treatment and chemical method [6]. Among these methods, the plasma treatment technique provides approach for alteration of material surfaces without alteration of their bulk properties [7].

In this paper, a novel thermo-sensitive switching fabric has been prepared by Ar-plasma-induced simultaneous grafting Ploy-N-isopropylacrylamide (PNIPAAm) onto PET fabric. Fourier transform infrared spectroscopy (FTIR) was used to identify the structure of the grafted fabric. Then the surface morphology of the grafted fabric was observed from scanning electron microscopy (SEM). And phase transition temperature of the grafted PET fabric was determined by differential scanning calorimetry (DSC).

Experimental

Materials and chemicals. Commercial sample of PET fabrics cleaned by acetone.N-isopropylacrylamide (NIPAAm) was purchased from Wako Pure Chemicals (Osaka, Japan) and purified by recrystallization from n-hexane before use. Ar gas (99.99%, Dianhua gas co., Ltd, Hang Zhou).

Procedure for modification of PET fabrics.

The plasma was produced by an inductively coupled RF discharge at 13.56 MHz. The multicusp plasma chamber, which is made from stainless steel, is surrounded by permanent magnet buttons. The diameter of the chamber is 23 cm and the length is 25 cm. The operating gas, Ar, was fed directly into the chamber. The base pressure of the system was 2Pa. The gas flow was regulated by unit mass flow controllers. The operating power varies between 50 and 200 W. The treatment time varies between 1 and 20 min.

A typical grafting procedure was carried out as follows（Fig.1）:

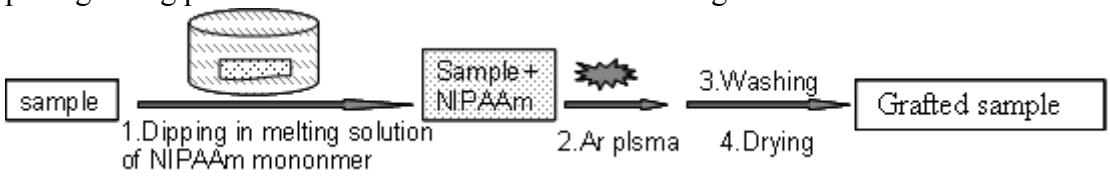


Fig.1 Procedure of preparation of sample modification.

Plasma treatment procedure: preparing samples →to vacuumize plasma apparatus (<3Pa) → to set Ar and to adjust pressure →discharging.

Pieces of PET fabrics after pretreatment were immersed in a 100 %(o.w.f) monomer (NIPAAm) solution at 75˚C for 30 min, then dried in vacuum oven.

These impregnated fabrics were placed into the plasma chamber and submitted to argon plasma. After plasma treatment, the samples were washed for 1h in a solution of 1% 209 agent to remove the monomers and non-grafted-homopolymer, then washed in deionized water at room temperature, and finally dried for 1 h at 100 °C then weighted(W_1).

In this work, the weight increase obtained after plasma treatment was calculated according to the formula (1).

$$G(\%) = [(W_1\text{-}W_0) / W_0] \times 100\ \%\ . \quad (1)$$

Where W_1 and W_0 represent the weights of the sample after and before graft, respectively.

Water permeation flux measurement. Water permeation flux, which can be simply defined as J=L/(s·㎡), is the volume (L) of water flowing through the unit area of fabric per unite time. In this work, all samples were replicated twice in same condition and the average values were plotted. The water permeation flux was expressed as formula (2).

$$J(L\cdot s^{-1}\cdot m^{-2})=Vw/(t\times F_S). \quad (2)$$

J means the value of water flux, Vw means the volume of water flowing through the fabric, t means the time of water flowing and Fs mean the area of the test fabric.

Water permeation flux of fabrics were investigated according to Chinese national patent “A method and device for testing the temperature-sensitivity of thermal-smart textiles” [8]. Water permeation flux was measured at 20˚C, 25˚C, 32˚C, 35˚C, 40˚C and 55˚C.

Apparatus. IR spectra analysis was carried out with Nicolet 5700 System FT-IR analyzer. The macroscopic morphology of grafted sample was observed using JSM-5610LV SEM (JEOL company’s products, Japan). The surface morphology of fiber was observed with atomic force microscope (AFM). TA Q200 DSC (TA, USA) was used for DSC analysis in N_2 with heating rate at 2˚C/min from 15˚C to 45˚C. Before DSC analysis, the grafted PET fabrics should be immersed in D-H_2O for 24 h to ensure the grafting polymer swell fully and then removed the surface-absorbed water by filtered paper.

Results and discussion

FT-IR analysis of grafted PET fabrics.

Fig.2 shows the FT-IR spectra of PET fabrics before and after grafting. By comparison with the virgin PET, the grafted PET exhibited signals at 1385 and 1458 cm^{-1} due to symmetrical and asymmetrical bending vibration of CH_3 groups respectively. Furthermore, PET-g-NIPAAm exhibited

peaks around 1716.7 cm^{-1} (C=O from PET) and 1663 cm^{-1} (C=O from NIPAAm), stretching vibrations due to N-H at 3309 cm^{-1} and a characteristic absorption for secondary amides at 1536 cm^{-1} corresponding to bending vibrations of N-H groups. These bands confirmed the NIPAAm was introduced to PTE fabrics surfaces.

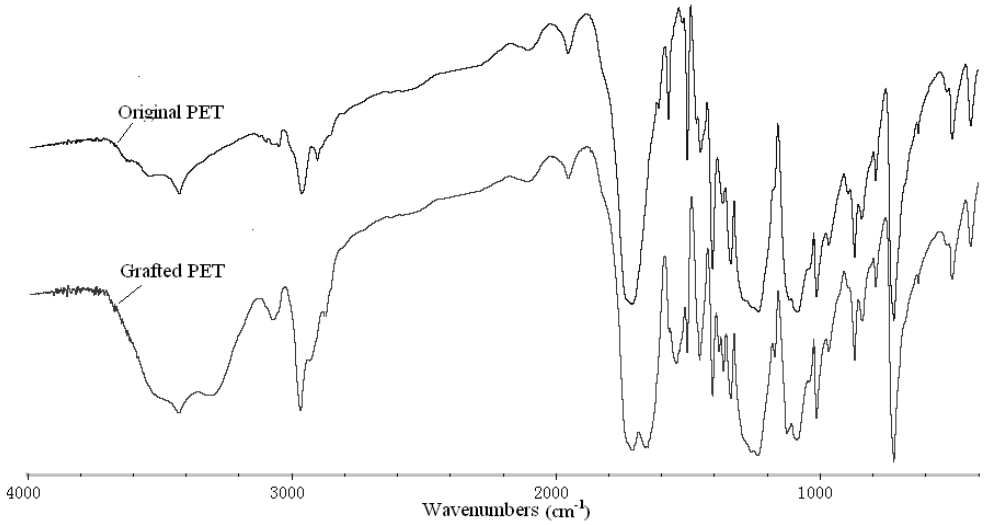


Fig.2 FTIR-KBr spectra of grafted PET and original PET.

Thermal-sensitivity test of grafted PET fabric.

The water permeation time of the virgin PET fabric as Table 1 and Fig.3 shows, the water permeation time decrease while temperature increase, the whole process of change was roughly linear trend. This is because the higher the water temperature, the more expansion of the pores between yarns, that leads to the faster of water permeation. The grafted PET fabric (G=16.4%) as Fig.3 shows, the water permeation time decrease while temperature increase as well, and increased sharply around 32˚C not similar to linear growth trend anymore. The change temperature close to the LCST of PNIPAAm, at which it undergoes a reversible volume phase transition caused by the hydrophilic-to-hydrophobic states alternation. When the temperature is above 32˚C, the PNIPAAm polymer became hydrophobic, and the network shrank. As a result, the water permeation time of the grafted PET fabric decreased with the rise of temperature. When the temperature is lower than 32˚C, the network swelled and inflated sharply, the pores between yarns blocked and even closed, a sharply increase in the water permeation time occurred as a result. This process is so-called “switching effect”.

Table 1 The water permeation time of grafted and control PET under different temperature

Samples	**Water permeation time /s**					
	20˚C	25˚C	32˚C	35˚C	40˚C	**55˚C**
Control PET fabric	5.5	5.2	4.6	4.5	4.0	**3.2**
Grafted PET fabric	**152.7**	**98.8**	**48.1**	**11.8**	**10**	**9.5**

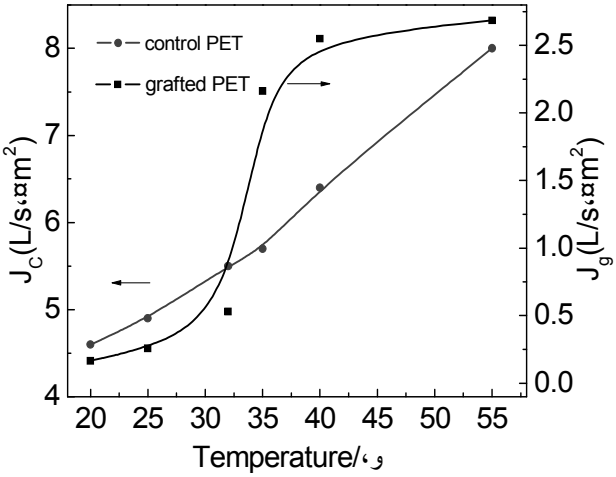


Fig.3 The water permeation flux of grafted and control PET under different temperature.

DSC analysis.DSC curve of the different grafting yields samples in wet conditions are shown in Fig.4.Comparing the DSC thermogram of original PET, there was an obvious endothermic peak during 32～33˚C on grafted fabrics, which indicated the phase transition temperature of grafted PET is about 32～33˚C. With increasing of G%, the endothermic enthalpy increased partly and the phase transition temperature didn't change nearly.

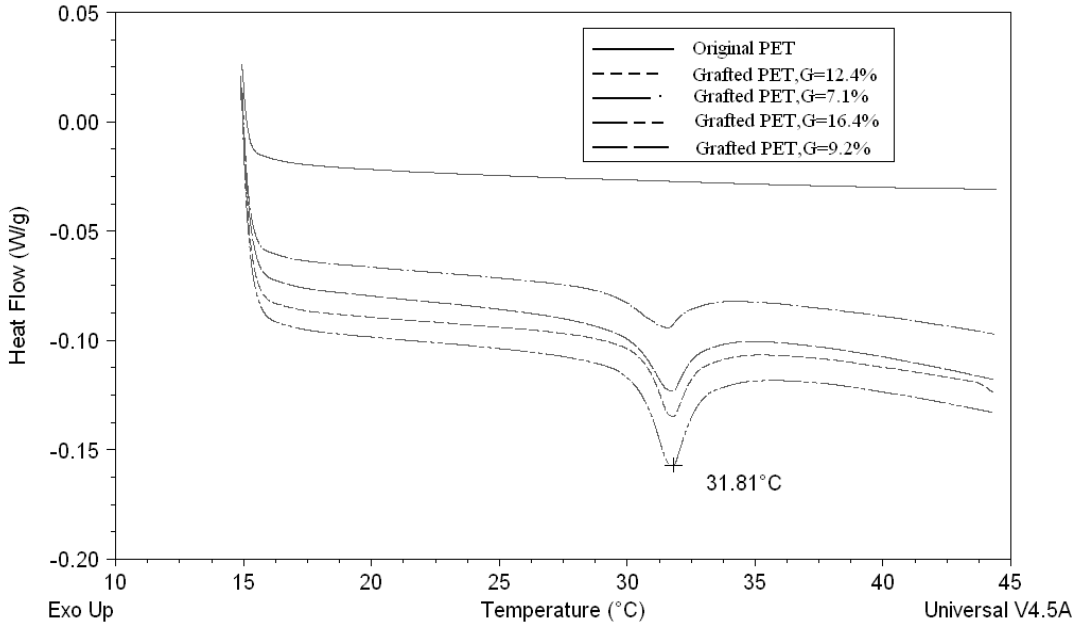


Fig.4 DSC curves of the different grafting yields samples in wet conditions.

Morphology analysis.

The cross sectional [Fig.5 (a, b)] and longitudinal [Fig.5(c, d)] SEM images of original PET and grafted PET fabrics were observed to investigate their morphological features. Comparing the cross sectional SEM image of original PET fabric [Fig.5 (a)], we can see these has been a uniform formation of a corrugated polymer layer over the surface of PET yarn [Fig.5 (b)]. From Fig.5 (d), the longitudinal SEM image, we can see these have been some binding between PET yarns. The AFM observation was performed.Fig.6 A and B showed the AFM surface morphology images of PET fiber before and after grafting. From Fig.6 A, surface of original PET fiber is very smooth, while surface roughness of grafted PET fiber (Fig.6 B) is slightly increased. This observation helps in confirming the grafting reaction having taken place between the PNIPAAm and the PET fabric again.

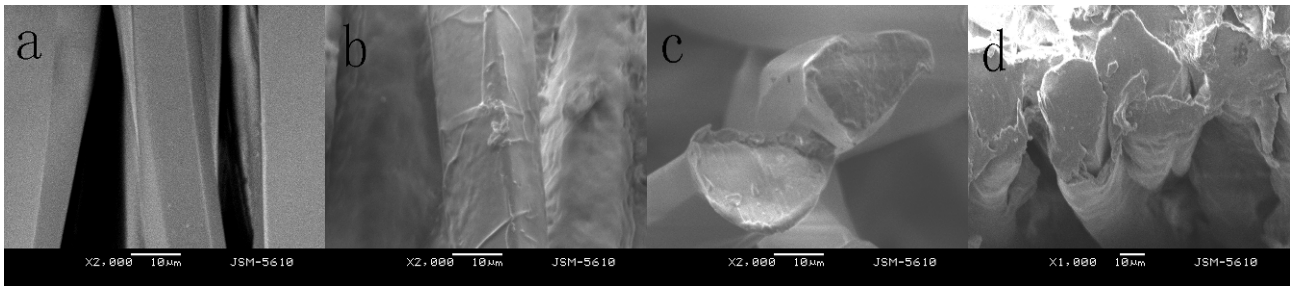


Fig.5 SEM images of original and grafted PET fabrics: a-across sectional image of original PET; b-cross sectional image of grafted PET; c- longitudinal image of original PET; d- longitudinal image of grafted PET.

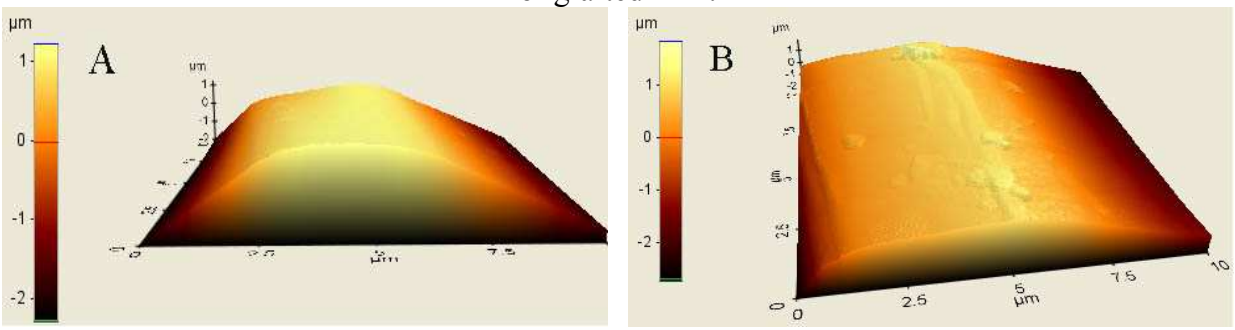


Fig.6 AFM images of original and grafted PET fiber: A- original PET; B- grafted PET.

Conclusions

In this paper, a novel thermo-sensitive switching fabric has been prepared by Ar-plasma-induced simultaneous grafting Ploy-N-isopropylacrylamide (PNIPAAm) onto PET fabric. The IR spectra, SEM and AFM results showed that the PNIPAAm was grafted onto PET fabric, respectively. The DSC analysis results indicated that LCST value of grafted sample was about 32～33˚C.The water permeation flux from 20˚C to 55˚C was used to express the thermo-sensitive property. The results showed a slight change in temperature around the LCST comparing to the control sample, which proved that the grafted fabrics were sensitive to temperature.

Acknowledgments

This research was funded by Zhejiang Provincial Top Academic Discipline of Applied Chemistry and Eco-Dyeing & Finishing Engineering (ZYG2010017 and 111125A4X05016).

References

[1] Gao J., Wu C.: Macromolecules.Vol.30 (1997), p.6873
[2] Chen Zh., Chen M., Liu X., Yang Ch., Zhu X.: Journal of Functional Polymers. Vol.17 (2004), p.46-50
[3] Wang Z., Xu X., Chen Ch., Wang G., Wang B., Zhang X., Zhuo R.: Colloid and Surfaces B:Biointerfaces. Vol. 67(2008), p.245-252
[4] C Wu, S Zhou: Macromolecules.Vol. 28(1995), p.5388-5390
[5] Zhao C., Wang Q.: Current Appl Phys. Vol.5(2005), p.497-500
[6] L.Q. Chu, X.N. Zou, Wolfgang Knoll, Renate Forch: Surface & Coatings Technology. Vol.202 (2008), p.2047-2051
[7] M.J. Tsafack, J. Levalois: Surface & Coatings Technology. Vol. 201(2007), p.5789-5795
[8] Yu Jianlei, Liu Jinqiang, Shao Jianzhong, Li Yongqiang, Wang Feng. China patent 200710068356.9. (2009) (In Chinese)
[9] Pan Tieying, Zhang Yulan, SU Keman. Spectra Analysis. 2nd ed., Shanghai, 2005(In Chinese)

© (2011) Trans Tech Publications, Switzerland
doi:10.4028/www.scientific.net/AMR.331.347

Moderate hydrolysis of nylon 6 fabric with different acids

Xuechuan Wang [1, a], Peiyi Wang [1,b], Longfang Ren [1,c] and Taotao Qiang [1,d]

[1] College of Resource and Environment,Shaanxi University of Science and Technology, Xi'an 710021, China

[a]wangxc@sust.edu.cn, [b]peiyi029@gmail.com, [c]renlf1010@163.com, [d]qiangtaotao@sust.edu.cn

Keywords: Nylon 6 fabric, Acid treatment, Dyeability, Effect.

Abstract. The aim of this work was to investigate the changes induced on nylon 6 fibers after moderate treated with formic acid and sulfuric acid. The dyeing properties of nylon 6 fibers after moderate acid treatment with reactive dye were measured. The content of amino groups, moisture absorption and contact angle of non-treated and moderate acid treated nylon 6 fabrics were determined and the effects of acid treatment on the structure, thermo-stability and morphology of nylon 6 fibers were investigated by FT-IR, SEM and DSC. The results indicate that the content of amino groups, moisture absorption and hydrophilicity of the fabrics enhanced and the dyeability improved after moderate acid treatment.

Introduction

Nylon is a widely used synthetic polymer because it has a combination of strength, flexibility, toughness, and abrasion resistance, however, shortcomings including the low light resistance and heat resistance, the moisture regain is lower than natural fibers and viscose rayon fibers cannot be ignored [1]. Modification methods of polyamide fiber refer to blend spinning, surface grafting under the radiation with electron-beam and surface modification using plasmas, enzyme and supercritical CO_2 fluid are developed to improve those properties [2-6].

Nylon 6 is an aliphatic polyamide characterized by recurring amide groups (–CONH–) in the polymeric chain and amino and carboxylic end groups. It is medium moisture absorption because those groups are kind of hydrophilic. The quantity of the amino group in nylon 6 macromolecular is 0.098 mmol/g fiber. The polyamide fibers are prone to hydrolysis due to the amide groups in the chain compared with carbon chain fibers, the hydrolysis reaction is not obvious below 100℃, and it became intense when the temperature exceeds 100℃. Polyamide fibers are unstable to acids because acids can catalyze the hydrolysis reaction. They are very sensitive to the strong inorganic acid, and can hydrolyze rapidly then dissolve in the concentrated nitric acid, hydrochloric acid or sulfuric acid even at room temperature [1]. This study treated polyamide fabric with different acids at the temperature lower than 100℃ to obtain a moderate hydrolysis of the fibers in order to improve the hydrophilicity and other related properties.

Materials and methods

Main Materials. Standard plain weave nylon 6 fabric from Wu Jiang Jinrun Textile Co., Ltd. was used, Nonionic detergent was used for scouring the nylon 6 fabric. The acids used were formic acid and sulfuric acid from Beijing Chemical Plant. The reactive dye Scarlet E-2GA provided by DyStar Company.

Moderate acid treatment of nylon 6 fabric. Fabric samples were scoured with 5% nonionic detergent. The moderate acid treatment was carried out in SH2-C water bath oscillator under the condition that optimized before. The optimum conditions are formic acid concentration of 8% o.w.f. were used and the liquor ratio was 70:1 for 30min at 55℃, sulfuric acid concentration of 6% o.w.f. were used and the liquor ratio was 70:1 for 90min at 25℃, which were optimized by the dyeing properties and the rate of decline in breaking strength of the treated nylon 6 fabric.

Reactive dyeing of different samples. The reactive dyeing process of nylon 6 fabric before and after acids treatment was started at 40℃and the temperature was raised to 80℃ over 20 min and then held at that temperature for 30 min using Reactive Scarlet E-2GA dye. The dyeability of different samples was characterized by the CIELAB color co-ordinates (L*, a*, b*, C*and h°) of the dyed samples using a Datacolor sf600 color detective instrument for 10° observer and illuminant D_{65}.

Determination of the content of amino groups, moisture absorption and contact angle. Primary amine reacts with salicylaldehyde is imine, it is an appropriate method to determine the content of amino groups of the fabric before and after acid treatment using salicylaldehyde; The fabric before and after acid treatment were placed in 100℃ oven drying to constant weight, weighed, then placed in the temperature is 25 ℃, humidity is 65% of the constant temperature and humidity environment for 24h, weighed the samples again then calculated the moisture absorption; The contact angles of the fabric before and after acid treatment were determined using the OCA 20 contact angle measuring instrument integrated with an IBM personal computer to characterize the hydrophilicity of the samples. All measurements above were repeated five times.

Instruments characterization of samples. FT-IR infrared spectra: The effect of the moderate acid treatment on the chemical structure of nylon 6 fabric was examined by the FTIR spectroscopy; Microscopic characterization: The surface of fabrics was investigated using a Scanning Electron Microscope (TM-1000, Hitachi). The surface of samples was first coated with a thin layer of gold by Physical Vapor Deposition method (PVD) using a sputter coater; Differential scanning calorimetry of the samples was carried out using a STA409PC Synchronous thermal analyzer integrated with an IBM personal computer. The samples were heated from 20℃ to 600℃ on a rate of 10 per minute, under nitrogen atmosphere.

Results and discussion

The dyeability of different samples. The L*, a*, b*, C* and h° values of acid treated reactive dyed nylon 6 fabrics and non-treated one, are given in Table 1. The color values were evaluated in CIELAB color space, the three axes namely as L*, a* and b*. The L* is the color coordinate which represents the lightness of samples and can be measured independently of color hue. Any decrease in the lightness of samples could be concluded as the more color absorption into the fibers. The a* stands for the horizontal red–green color axis. The b* represents the vertical yellow–blue axis. The C* represents brightness or dullness of the samples. Any increase in the C* of samples could be concluded as more brightness of the fibers. According to the results, the lightness (L*) value of the acid treated sample decreased compared with the non-treated one, and the lightness of sample treated with sulfuric acid decreased more. Decrease in L* values could be due to more reactive dye penetrate into the acid treated samples which may confirms the increasment of free amino groups on the surface of treated samples. The C* values of the acid treated sample increased compare with the non-treated one, which contributes to increase in brightness of the samples. The dyeability of nylon 6 treated with acid improved, which is in agreement to the result shown in Fig. 1.

Table 1. The dyeability of different samples

Samples	L*	a*	b*	C*	h°
Non-treated sample	65.485	49.209	28.539	56.885	30.112
Formic acid treated sample	62.251	54.03	33.265	63.449	31.619
Sulfuric acid treated sample	56.856	57.662	38.098	69.111	33.453

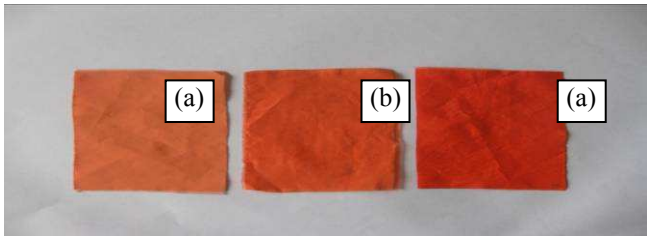


Fig. 1. The dyeing properties of different samples: (a) non-treated nylon 6 fabric, (b) nylon 6 treated with formic acid, (c) nylon 6 treated with sulfuric acid

Content of amino groups, moisture absorption and contact angle. Table 2 shows the content of amino groups, moisture absorption and contact angle of non-treated and moderate acid treated nylon 6 fabrics. Moisture absorption is important to the comfort and wear properties of textiles where body contact or extreme humidity levels are encountered. It is indicated that considerable enhancement, in the content of amino groups, moisture absorption has been attained after moderate acid treatment, the content of amino groups of samples treated with formic acid and sulfuric acid are 4.68 times and 5.16 times to the non-treated sample, the moisture absorption of samples treated with formic acid and sulfuric acid are increased by 13.1% and 23.45% to the non-treated sample. This confirms that acid catalyses the hydrolysis occurred in the amorphous regions of the polyamide chains producing more free functional groups on the surface which in turn, improve the moisture absorption of fabrics. The content of amino groups and moisture absorption of sample treated with sulfuric acid enhanced more than the sample treated with formic acid, which indicates that the catalytic effect of sulfuric is stronger than formic acid. The contact angle photo of different samples is shown in Fig. 2, it can be seen that the hydrophilicity of the fabrics treated with acids have been improved compared with non-treated sample, which is in agreement to the contact angle values given in Table 2.

Table 2. Content of amino groups, moisture absorption and contact angle of non-treated and moderate acid treated nylon 6 samples

Samples	Non-treated sample	Formic acid treated sample	Sulfuric acid treated sample
Content of amino groups/mmol/g	0.126	0.59	0.65
Moisture absorption /%	1.45	1.64	1.79
Contact angle /°	117.3	108.1	103.5

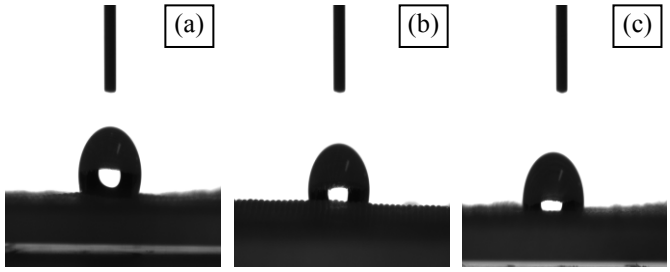


Fig. 2. The contact angle photo of different samples: (a) non-treated nylon 6 fabric, (b) nylon 6 treated with formic acid, (c) nylon 6 treated with sulfuric acid

Structural information of different samples. The infrared spectra of non-treated and moderate acid treated nylon 6 fabrics were shown in Fig. 3. The presence of amide groups in nylon 6 is well reflected as a strong band at about 1637 $cm^{-1}$and the band at 3294 cm^{-1}, respectively related to C=O stretching and N–H bending vibrations. The presence of the band at 1534 cm^{-1} along with the peak 1637 cm^{-1} is assigned to N-mono substituted amide groups in solid form of polyamide chain. The strong C–H stretching and bending vibrations of CH_2 groups, vibration of CH_3 groups relative to polyamide terminal chains and C–N stretching are appeared at 2854, 2925, 1460, 1365 and 1000–1300 cm^{-1} , respectively[5]. As can be seen in Fig. 2, after moderate acid treatment of nylon 6 with formic acid and sulfuric acid, the intensity of band at 3294 cm^{-1} were changed and the bands at

1534 and 1637 cm^{-1} relative to N–H bending and C=O stretching vibrations were shifted compared to non-treated fabric which is due to breakage of some peptide groups. The band appeared at about 1730 cm^{-1} in Fig. 3(b) and (c) which is not exist in (a) and the intensified and shifted bands at 1458cm^{-1} suggest the incresement of carboxyl groups. The presence of intensified and shifted bands at 1297 cm^{-1} relative to C–N stretching vibration clearly confirmed the polyamide chains hydrolysis. As it is evident in Fig. 3, the shape and intensity of bands at 3294cm^{-1} and finger-print area for the sample treated with acids were also changed. The assignments of FTIR spectra of non-treated and treated nylon 6 with acids clearly suggest that the fibers have undergone severe chemical hydrolysis especially at amide (–CONH–) functional groups.

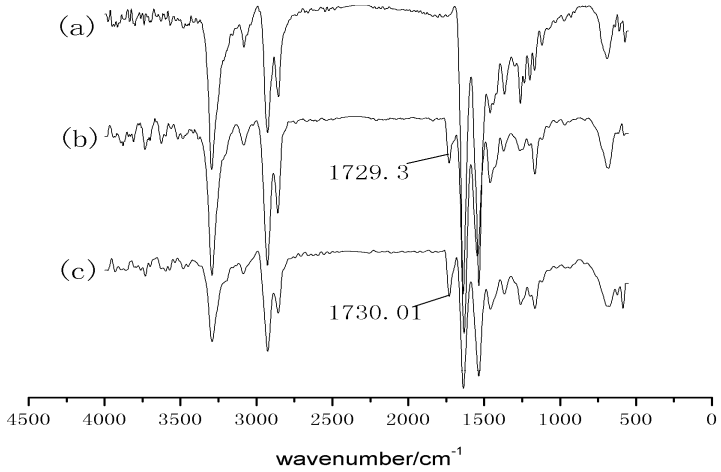


Fig. 3. FTIR spectra: a) non-treated nylon 6 fabric, b) nylon 6 treated with formic acid, (c) nylon 6 treated with sulfuric acid

Microscopic characterization of different samples. The SEM images of non-treated nylon 6 fibers and samples treated with acids are shown in Fig. 4. It can be seen that the non-treated fibers has relatively smooth surface. The SEM images of the nylon 6 fibers treated with acids show etched surfaces which indicate the surface hydrolysis of the fibers in comparison with non-treated fibers. Furthermore, the hydrolysis of nylon 6 surface can be highly responsible for the improvement of wettability and dyeability of fabrics.

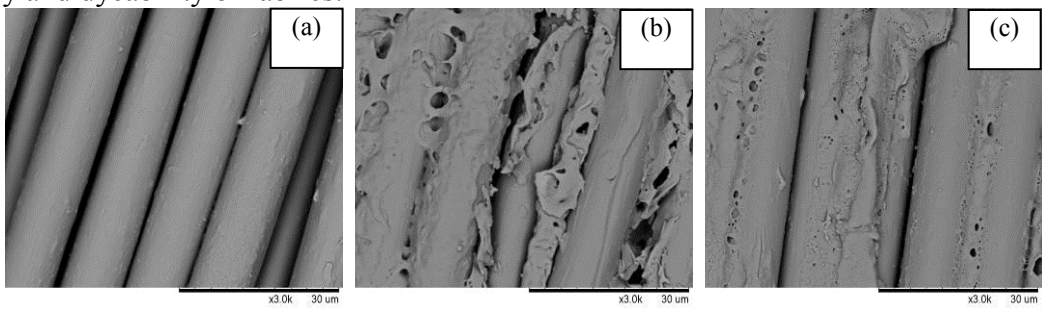


Fig. 4. SEM images of nylon 6 fibers at 3.00 K: (a) non-treated, (b) nylon 6 fibers treated with formic acid, (c) nylon 6 fibers treated with sulfuric acid

Thermal studies of different samples. Nylon 6 fiber is a semi-crystalline thermoplastic fiber [6], The degree of crystallinity is 65 – 85%. Fig. 5 shows DSC curves of the non-treated and nylon 6 treated with acids. The melting transition temperature of non-treated sample is rang from 211.9℃ to 219.6℃, the specific heat change is 8.347J / (g * K), while the melting transition temperature of sample treated with sulfuric acid is rang from 212.2℃ to 221.0℃, the specific heat change is 9.393J / (g * K). At the higher-temperature region, about 400 – 500℃, two peaks at 408.4℃ and 469.8℃ respectively are observed for the non-treated sample, which corresponds to degradation of the crystals formed during the heating process. After sulfuric acid treatment, there are two small peaks at 408.0 ℃ and 426.7℃ and a bigger peak at 478℃.

The results obtained from DSC curves suggested that the physical structure of the fabric has a significant effect on the thermal properties of nylon 6 fibers treated with acids. Acids can attack preferentially the amorphous or less-ordered (paracrystalline) regions rather than the crystalline or more-ordered regions because of the acids can migrate into these less-ordered regions compared to the more-ordered ones, hence, it accelerates the thermal degradation of nylon 6 samples. This result was consistent with those obtained from FTIR and SEM.

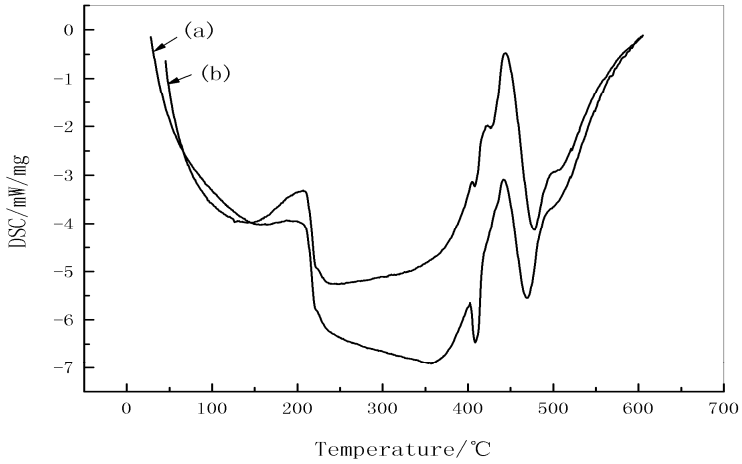


Fig. 5. DSC curves: (a) non-treated nylon 6fabric, (b) nylon 6 fibers treated with sulfuric acid

Conclusion

The content of amino groups, moisture absorption and hydrophilicity of nylon 6 treated with formic acid and sulfuric acid obtained a considerable enhancement compared with the non-treated sample because of the hydrolysis of polyamide chains. The dyeability also improved after moderate acid treatment. The SEM images of the nylon 6 fibers treated with acids show etched surfaces which indicate the surface hydrolysis of the fibers in comparison with non-treated fibers. The moderate acid treatment affected the structural information and the thermal properties of nylon 6 fibers, acid catalyzed the hydrolysis of the amide functional groups in nylon 6 macromolecular.

Acknowledgements

This work was financially supported by the National Natural Foundation of China (21076120), the Project of Science and Technology Plan in Shaanxi Province (2011JQ2012) and Shaanxi Science and Technology University Graduate Innovation Fund.

References

[1] V.T. Stannett, Radiat. Phys. Chem. 35 (1990) 82.

[2] X. Q. Jia, M Herrera-Alonso. Poly. Vol. 47 (2006) 4916–4924.

[3] Mervat S. Ibrahim, Kariman M. El Salmawi. Appl. Surf. Sci. Vol 241 (2005) 309–320.

[4] D Pappas, A Bujanda. Surf. Coat. Technol. Vol 201 (2006) 4384–4388.

[5] M Parvinzadeh, R Assefipour. Polym. Degrad. Stab. Vol 94 (2009) 1197–1205.

[6] Y.Q. Ma, J.J Long. Silk. Vol. 9 (2010) 4-10.(in chinese)

© (2011) Trans Tech Publications, Switzerland
doi:10.4028/www.scientific.net/AMR.331.352

Dyeing Properties of Tussah Silk Fabric with Indigo Naturalis and Turmeric

Xu Hao[a], Yanhua Lu[b]

Eastern Liaoning University, Dandong, Liaoning, 118000, China

[a]email: cnlnhx@163.com, [b]email: yanhualuln@yahoo.com.cn

Keywords: natural dye; indigo naturalis; turmeric; combination dyeing; dyeing property

Abstract. Two vegetable dyes of indigo naturalis and turmeric were combined on dyeing tussah silk fabric with two steps. The first step is dyeing the silk fabric with indigo naturalis by reduction process, and then dyed with turmeric by direct dyeing process. The results of single factor experiment on the indigo naturalis dyed tussah silk fabric dyeing with turmeric indicated that the relative concentration, pH value, dyeing temperature, and dyeing time had effect to a certain extent on the over dyeing. The dyeing conditions were determined by the above single factor experiment. The rubbing fastness and washing resistance of the dyed silk fabric could achieve to grade 3 more than grade 3.

Introduction

Vegetable dyes have the characteristics of non-toxicity, harmlessness and non-pollution. Natural silk fabrics dyed with vegetable dyes not only have more added values, but also have realized natural clothing. This offers a good approach to the development of ecological and green textiles with the requirements of textile green consumerism of people at present [1-3]. Indigo naturalis and turmeric are more ecological interesting source of pigments, since they are Chinese herbs. Indigo dye is very effective in clearing off the heat, detoxifying the blood, dissolve ecchymoses and cools down blood. In addition, it has the functions to treat the problem of Psoriasis on human skin [4]. Turmeric contains a mixture of powerful antioxidant phytonutrients known as curcuminoids, and has been described to have anti-inflammatory and anti-bacteria properties. It is also known to be good for the liver [5]. The two kinds of vegetable dyes have been used in the dyeing of textiles such as wool, cotton fabrics and so on [6, 7].

In this study, we combined indigo naturalis and turmeric vegetable dyestuffs on dyeing of tussah silk fabric. Dyeing process of tussah silk fabric included two steps: the first step is dyed with indigo naturalis and then with turmeric dyestuff. The purpose of the study is to achieve a series of color spectra that are different from indigo naturalis and turmeric dyestuffs.

Experimental

Materials. Tussah silk fabric, indigo naturalis, turmeric, 209 detergent and neutral soap flakes were purchased in market, China. Sodium thiosulfate, sodium hydroxide, acetic acid and anhydrous ethyl alcohol were all chemical pure reagents.

Methods

Extraction of Turmeric Pigment. Turmeric was first crash to powder, then 20g turmeric powder dipped in 500ml boiled distilled water for 60min. The exaction process repeated 3 times, the exaction solution was then filtered and settled to the volume of 2000 ml (named original extraction solution in this experiment) to be used dyeing tussah silk fabric.

Dyeing Procedure. Reduction method was used to dye tussah silk fabric with indigo naturalis. The procedure is as follows: indigo naturalis was first to prepare the solution of sodium thiosulfate in a bath of liquor ratio 50:1, tussah silk fabric sample was dipped into the above solution at 40 ℃ for 30 min, followed by the oxidation process with 0.8% hydrogen peroxide at 20℃and pH 7 for 30 min[8].

Tussah silk fabric samples dyed with indigo naturalis were then dyed with the extraction solution of turmeric with liquor ratio 50:1. The pH values were recorded with PHS pH meter and adjusted with dilute solutions of sodium carbonate and acetic acid, and the dyeing procedure was shown in Fig. 1.

Finally, the dyed tussah silk samples were rinsed with cold water, with 2 % (owf) detergent in a bath of liquor ratio 50:1 at 80℃ for 5 min. Then rinsed and finally dried at ambient temperature.

Color Strength Measurement. K/S values that meant relative color strengths were measured using by a spectrophotometer of Color-Eye 7000A (U.S.). The reflectance values at maximum absorption wavelength were converted into K/S values.

$$K/S = \frac{(1-R)^2}{2R}$$

Where R is the light reflectance at the maximum wavelength, K/S is the color shade depth on the sample surface.

Fastness Testing. Washing fastness tests were performed according to AATCC61-2003（3A）with the SW-12A washing fastness tester (Wuxi Textile Instrument Factory, China). Rubbing fastness tests were performed according to AATCC8-2004 with the LFY- 304 rubbing fastness tester (Shandong Textile Research Institute, China).

Results and Discussion

Effect of Indigo Naturalis Concerntration. As reported, indigo naturalis mainly consists of indigo (see Fig.1), and it belongs to vat dyes. According to the dyeing technology of tussah silk fabric with indigo naturalis and turmeric (see Dyeing Procedure), the concerntrations of indigo naturalis were selected from 0 to 30g/l. The effects of indigo naturalis concentrations on the color strength and color style value were shown in Fig. 1.

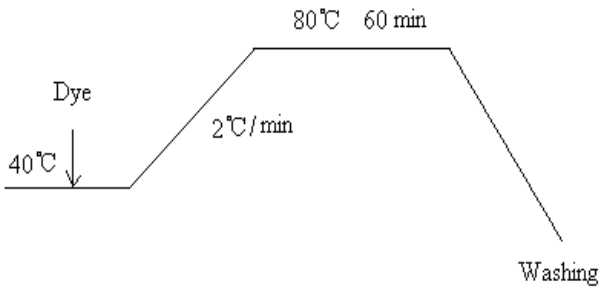


Fig. 1 Dyeing procedure of indigo naturalis dyed tussah silk fabric with the extraction solution of turmeric

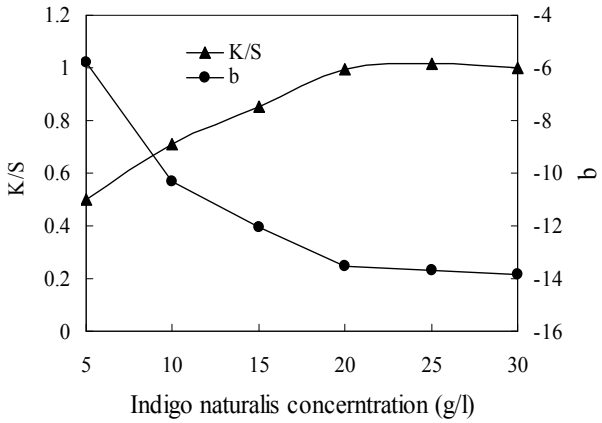


Fig. 2 Effect of indigo naturalis concentration on the color strength and color style value of dyed tussah silk fabric

Fig. 2 showed that the color strength of tussah silk fabric increased when the indigo naturalis concentration ranged from 5 to 20g/l, increased slightly when the indigo naturalis concentrations were from 20 g/l to 30 g/l. The reason was that the adsorption of indigo naturalis has reached saturated state when the concentration was greater than 20 g/l. The b values varied from about -6 to -14 when the indigo naturalis concentration ranged from 5g/l to 30g/l. In this experiment, the concentration of indigo naturalis was selected 20 g/l according to K/S value.

Effect of Turmeric Extraction Solution Amount. The dyed tussah silk fabric with 20 g/l indigo naturalis was dyed with turmeric according to the dyeing technology of tussah silk fabric (see Dyeing Procedure). The pH value was selected 4 according to the reference [9]. Fig. 3 showed that the color strength of K/S values increased and a values decreased when the turmeric relative concentration

ranged from 20% to 60%. The color strength and a values changed slightly when the relative concentration of turmeric extraction solution was more than 60%. The reason was that the adsorption of turmeric dyestuff has reached the optimum adsorption amount when the concentration was greater than 60%. The a values varied from about -9 to -14 when the turmeric relative concentration ranged from 20% to 80%. Consideration the effects of concentration of turmeric on color strength and color style tussah silk fabric, the turmeric relative concentration was selected 60%.

Effect of pH Values in the Dyeing Process with Turmeric. As reported, turmeric is chiefly made of haematoxylin. It is light yellow in acidic condition, becomes rose-red in neutral condition, and is reddish-brown or brown in basic conditions. In this experiment, indigo naturalis is blue, and turmeric is yellow in acidic solutions. According to the color mixing theory, green color can be obtained by mixing indigo naturalis and turmeric in acidic solutions. The effects of the pH value of turmeric dyeing solution on color strength and color style value were shown in Fig. 4. It was found from Fig. 4 that the color strength changed a little when pH value ranged from 3 to 5. When pH value was more than 5, the color strength decreased greatly. Consideration of the acid damage on tussah silk, pH value was selected 5. When pH=5, a value reached to the lowest and the color tone focus on the depth green.

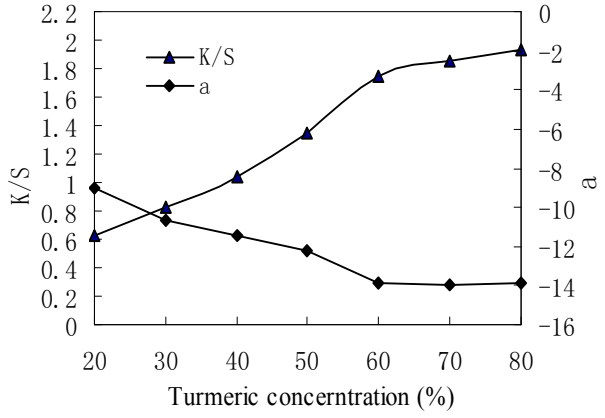


Fig. 3 Effect of turmeric relative concentration on the color strength and style values of indigo naturalis dyed tussah silk fabric

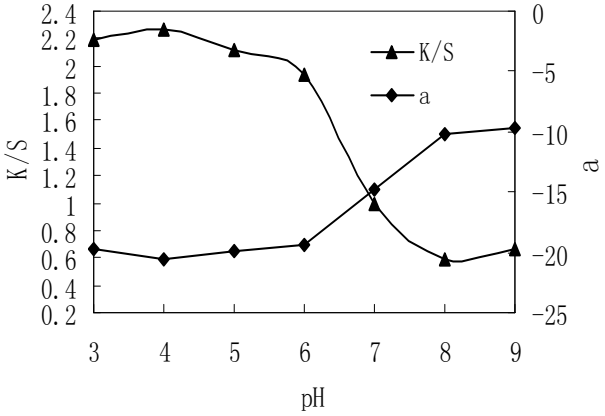


Fig.4 Effect of pH value on the color strength and color style values of indigo naturalis dyed tussah silk fabric

Effect of Temperature in the Dyeing Process with Turmeric. The dyed silk fabric dyed with 20 g/L indigo naturalis, 60% turmeric extraction solution at pH 4 according to the dyeing technology of tussah silk fabric (see Dyeing Procedure). It was found from Fig.5. that the color strength and a value increased when the temperature from 30℃ to 70℃. The color strength and a value changed slightly when the temperature was more than 70℃. The a values varied from about -10 to -14 when the dyeing temperature from 30℃ to 90℃. So the dyeing temperature was selected 70℃.

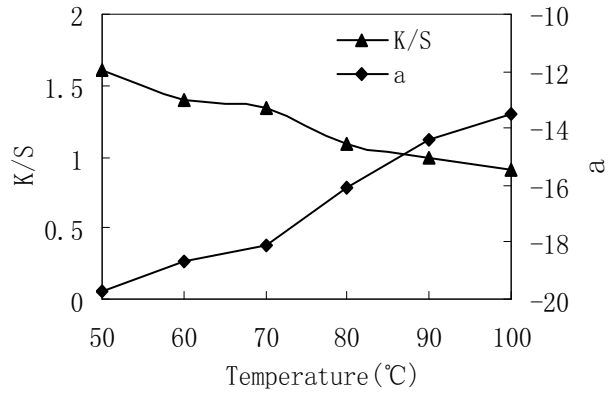


Fig.5 Effect of temperature on the color strength and color style value of indigo naturalis dyed tussah silk fabric

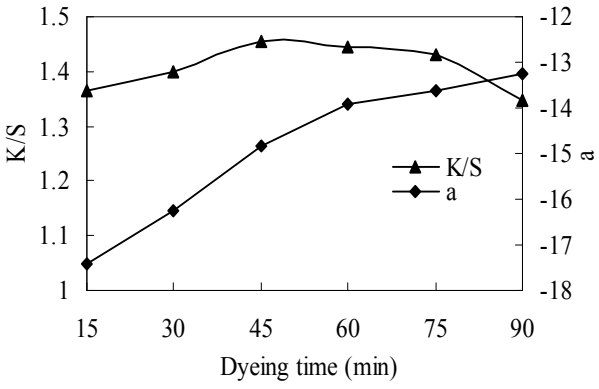


Fig.6 Effect of dyeing time on the color strength and color style value of indigo naturalis dyed tussah silk fabric

Effect of Dyeing Time in the Dyeing Process with Turmeric. The dyed tussah silk fabric dyed with 20 g/L indigo naturalis, 60% turmeric extraction solution at pH 5 and 70℃. The dyeing time ranged from 15 to 90 min. The effects of turmeric dyeing time on color strength and color style value were shown in Fig.6. Fig.6 showed that the color strength and a value increased greatly when and changed a little when the dyeing time was more than 45 min. The color strength decreased when the temperature was more than 45 min. The a values varied from about -13 to -17 when the dyeing time from 15 to 90 min. In this experiment, the dyeing time was selected 45 min considering the effects of turmeric dyeing time on color strength and color style value.

Color Fastness Measurement. The tussah silk fabric dyed with the optimum technology and then the rubbing fastness and washing fastness of the complex dyed samples were tested according to color fastness test methods. The color fastness results were as Table 1.

Table 1 Fastness properties of the complex dyed tussah silk fabrics

Rubbing fastness (Dry)	Rubbing fastness(Wet)	Washing fastness (Fading)	Washing fastness (Staining)
4	3～4	3	3～4

It could be found from Table 1 that the rubbing color fastness and washing color fastness were all reached to 3 or more. The results of the fastness properties of the complex dyed tussah silk fabrics meet the requirement of dyeing technology.

Conclusion

The concentration of indigo naturalis in the first stage is selected 20 g/l according to K/S value, and the b values varied from about -6 to -14.

A series green color spectra could be obtained when the indigo naturalis dyed tussah silk fabric dyed again with turmeric. And the optimum technology was as follows: 20 g/l indigo naturalis, 60% turmeric extraction solution at pH 5 and 70℃.

The rubbing color fastness and washing color fastness were all reached to 3 or more and meet the requirement of dyeing technology.

Acknowledgements

The authors would like to express their sincere appreciation to the financial support in this research from the Research Funds of Eastern Liaoning University P. R. China (Proj. No. 2008Z03).

References

[1] S. P. Vankar, S. Rakhi and V. Avani. J Clean. Prod Vol. 15 (2007), p.1441

[2] V. Tiwari, P. S. Vankar. Colourage Vol. 48 (2001), p. 25

[3] D. Gupta, S. Kumari, M. Gulrajani. Color Technol Vol. 117 (2001), p.333

[4] R. S. Blackburn, T. Bechtold and P. John. Color Technol Vol. 125 (2009), p. 193-207

[5] P. Anand, S. G. Thomas, A. B. Kunnumakkara. Biochem Pharmacol Vol. 76 (2008), p. 1590

[6] I. A. Bhatti, S. Adeel, M. A. Jamal, M. Safdar. Radiat Phys Chem Vol. 79 (2010), p. 622-625

[7] I. A. Bhatti, S. Adeel, M. A. Jamal, M. afdar and M. Abbas. J Cult Herit Vol.10 (2009), p. 447-457

[8] W. L. Cheng, Y. Deng and J. C. Huang. Silk Vol.12 (2000), p.16-18. In Chinise

[9] H. H.Wu, X. L.Hou, X. L. Zhang, W. D. Gao and H. Y. Gao. Wool Text. J. Vol. 37(2009), 1-5. In Chinise

© (2011) Trans Tech Publications, Switzerland
doi:10.4028/www.scientific.net/AMR.331.356

Uniformity and Penetration of Surface Modification Effects of Atmospheric Pressure Plasma Jet into Textile Materials

Chunxia Wang[1, a], Mei Du[2,b] and Yiping Qiu[3,c]

[1]College of Textiles and Clothing, Yancheng Institute of Technology, Jiangsu 224003, P. R. China

[2]Department of Textiles, Yancheng College of Textile Technology, Jiangsu 224000, P. R. China

[3]College of Textiles, Donghua University, Shanghai 201620, P. R. China.

[a]cxwang@mail.dhu.edu, [b]llb@ycit.edu.cn, [c]ypqiu@dhu,edu.cn

Keywords: Atmospheric pressure plasma jet; Uniformity; Penetration; Textile Materials; Technological parameters; Structure parameter

Abstract. The objective of this study was to investigate the uniformity and penetration of surface modification into textile materials including fiber, yarn and fabric treated by atmospheric pressure plasma jet (APPJ). Exposure to helium/oxygen plasma at atmospheric pressure made improvement in the wettability, dyeability, adhesion of single fiber, yarn and woven fabric. The results showed that such a plasma jet was possible and effective in penetration of surface modification into textile structure. It can treat the whole surfaces of a single fiber, yarn filament in the treated parallel filament tow uniformly. For porous fabrics, rapid and efficient treatment on both sides of the treated samples was found to be ensured. And the degree and depth of penetration depended on the penetration of active species in plasma jet, which was affected by plasma parameters and materials structure. The former included treatment time, power, gas temperature, jet-to-substrate distance. The latter included number of twisting and fabric pore size. These findings would have important effects on industrialization of textiles treated by atmospheric pressure plasma jet.

Introduction

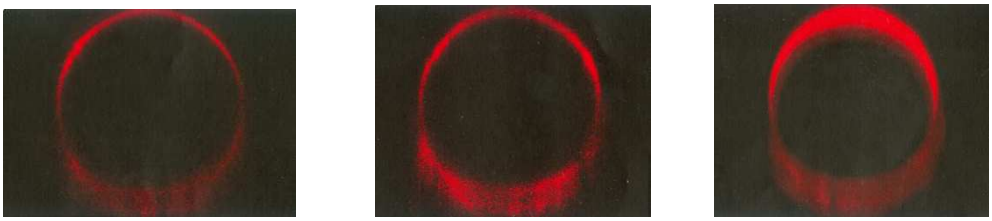
On a flat and nonporous substrate, it is believed that plasma surface modifications is only limited on the top surface that is several nanometers thick. However for porous materials, the picture gets more complicated. The different regions of a porous structure that can be visualized are outer surfaces, interior surfaces and the bulk phase [1]. For porous structure textiles, there is a difference between the visible surface and actual inner surface to be modified compared with film or foils. The fabric is made of a complex structure of single fibers and yarns, which are distributed over the total fabric thickness up to several millimeters and need to be treated homogenously throughout the entire thickness [2]. The permeation of plasma effects into porous materials would be an important area to address in this age of complex structures [3]. To ensure the plasma effects on the surfaces of all single fiber within the whole volume of textile materials, the chemically active species must be able to move through the textile structure in an acceptable time without loosing their modifying ability [3]. Therefore the penetration of plasma effects into textile structures turns out to be a crucial point for plasma modification of textile materials [4].

Previously most plasma treatments were done at low pressure, which can not realize on-line process due to expensive vacuum system. However, the recently developed non-equilibrium low temperature surface treatment at atmospheric pressure can be directly added into process line. For porous textiles, the plasma treatment effects not only limit on outer surface of substrate but also the active species in plasma can penetrate through pores in materials to modify other inner surface. There is difference in interaction of plasma and textiles between low and atmospheric pressure because of special structure and processing specialty of textiles. At low pressure or vacuum, plasma can be generated in two parallel polar plates or loops and is full of the whole vessel. All the surfaces of treated substrates are directly contacted with plasma and treated. However, at atmospheric pressure, especially for atmospheric pressure plasma jet, plasma is generated in noddle and then ejects to form

plasma jet. Only some surfaces of the treated substrate are directly contacted with plasma jet and modified. Whether the inner surfaces can be treated depends on the permeability of active species in plasma jet through pores and interaction with the inner surface of textiles.

Uniformity of Atmospheric pressure plasma jet treated single fiber

Figure 1 showed dye spatial distribution in fiber cross section. A significant difference was observed in diffusion profile between the control and the treated fibers. It could be seen that the fluorescent intensities of the treated fibers was higher than that of the control. Moreover the dyeing penetration depth of treated fibers was greater than that of control. In addition, the dyeing intensity and penetration depth increased as the treatment time increased, indicating a higher dye diffusion rate for longer treatment time. With the increase of plasma treatment time, a greater degree of etching is achieved and more polar groups such as hydroxyl and carboxyl groups are produced on the surface of the nylon 6 fibers, leading to better wettability and thus better dyeability of the fiber [5, 6]. It was concluded that atmospheric pressure plasma jet could uniformly modify whole surface of a single fiber.



(a) (b) (c)

Figure 1 Dye spatial distribution: (a) Control; (b) Treated for 1.33s; (c) Treated for 2.67s

Uniformity and penetration of Atmospheric pressure plasma jet treated filaments

The twist of filament tow was an important factor affecting the uniformity of APPJ modification effects. For the filament tow without twist, all the single filaments were parallel, so the surface area of fibers direct contact with the plasma jet was larger. The distances among fibers were large enough for active species in plasma jet to penetrate through space to react with each fiber surface. Therefore, surface properties of each fiber in filament tow would be well and uniformly modified. However, for the twisted filament tow, the single fiber turned down and up in axis direction of filament tow, which indicated that the whole surface of the single fiber could impossibly fully contact with the plasma jet. With the increasing twist of filament tow, the fibers in filament tow compacted more and more tightly. And the distances among the fibers were decreased, so the decreasing active species in plasma jet penetrated into the filament bundles and the fibers inside the filament tow may not be treated resulting in the more uneven APPJ effects of the filament tow with more twists [7].

Influence of processing parameters on APPJ Penetration into woven fabric

The wool fabric was treated under various treatment conditions such as different output power, different nozzle to substrate distance, different substrate moving speed, different gas temperature and different treatment time to see how these processing parameters influenced the penetration of plasma through the fabric [8].

Table 1 Water-absorption time (s) of two sides of fabric treated with different time (s)

Sample	0s	0.67s	1.34s	2.01s	2.68s
Top side	>1200	217	89	17	11
Bottom side	>1200	570	217	66	5

Table 2 Water-absorption time (s) of two sides of fabric treated with different power (w)

Sample	0	5	10	30	40
Top side	>1200	800	220	112	5
Bottom side	>1200	1200	572	225	10

Table 3 Water-absorption time (s) of two sides of fabric treated with different substrate moving speed (mm/s)

Sample	0	1.5	3	6	7.5
Top side	>1200	218	215	220	219
Bottom side	>1200	565	565	550	551

Table 4 Water-absorption time (s) of two sides of fabric treated with different substrate distance (mm)

Sample	0	1	2	3	6
Top side	>1200	1145	220	313	>1200
Bottom side	>1200	1123.6	572	505	>1200

The water-absorption time of the two sides of fabric was shown in Table 1 to 4. As the increase of the treatment time, the concentration of active species in plasma jet accumulating on the top side increased. Once the concentration of the active species increased to a critical level, they would have enough time to diffuse through the fabric before being neutralized [9]. This could happen when the treatment time exceeded 1.33s. In general, higher output power increased the number and activity of active species in plasma jet because at a higher output power the deterioration of the epicuticle layer could occur more rapidly than at a low output power. In addition, as the output power increased, the number of ions and free radicals reactive to wool fiber surface increased, leading to the formation of more polar groups [10]. When the distance between the plasma jet nozzle and the fabric surface was too small, the flow of the gas from the nozzle was almost blocked by the fabric and the gas could only be bounced off the surface and flow out in a more parallel to the fabric surface direction, which greatly reduced the effectiveness of the treatment. On the other hand, when the distance reached 6 mm, the velocity and the activity of the active species in the plasma jet greatly decreased when reaching the top side of the fabric and thus was not effective [11]. It can be seen that water-absorption times of the two sides of the treated fabric were smaller than that of the control but it did not depend on substrate speed within the tested range.

Influence of pore size on APPJ penetration into woven fabric

Polyester fibers pasted on the outer and inner surfaces of woven polyester fabrics with different pore size were used as the model system.

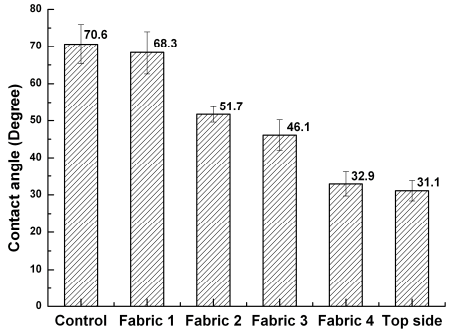


Figure 2 Contact angles of the control and the treated polyester fibers.

Figure 2 showed the contact angles for polyester fibers before and after treatment with APPJ. Changes in the contact angle on the top side reflected the effect of plasma on hydrophilicity improvement, while contact angle changes on the bottom sides implied the penetration of plasma effect through the pores. APPJ treatment caused the contact angle of the fiber to decrease since the APPJ treatment conferred a hydrophilic layer to the fiber surface as reported in literatures [12]. A

large difference between changes on the bottom sides indicated the pore size plays an important role in the plasma penetration of microporous woven fabrics. For the fabric with the bigger pores, the active species in plasma jet were not hindered and reached the bottom side, resulting in no difference in the hydrophilicity between the top and bottom sides for fabric with the pore size of 200μm. However, for the fabric with the smaller pores, more active species became less active in the interior structure, leading to significant difference in the hydrophilicity between the top and bottom sides for Fabric with the pore size of 10 μm. This is attributed to the more number of active species in plasma jet diffusing through the bigger pores in fabric. Those species can get to the inner surface without losing their modifying ability during the movement process. Therefore the pore size seems to be a more important factor affecting penetration of active species in plasma jet.

Conclusions

The uniformity and penetration of surface modification into textile materials including fiber, yarn and fabric treated by atmospheric pressure plasma jet (APPJ) was investigated. The following were the findings:

1. APPJ could uniformly modify the whole surface of a single fiber and the uniformity of fiber surface modification was increased with the increment of treatment time.
2. APPJ could homogenously treat each single fiber in filament tow without twist. The twist of filament tow influenced the surface modification of filament tows treated with APPJ. The addition of a twist had a negative effect on APPJ surface modification.
3. The effectiveness of the plasma treatment as well as plasma penetration through the fabric were positively associated to the plasma output power and the treatment time but had no relation with the substrate moving speed. When the jet-to-substrate distance was too small (<1 mm) or too large (> 6 mm) the effect of the plasma treatment diminished.
4. It is demonstrated that the degree of penetration of active species in plasma jet is increased with the increasing pore size. Complete penetration is realized in fabric with pore size bigger than 200 μm and nearly no penetration is found in fabric with the pore size smaller than 10 μm.

Acknowledgements

This work was financially supported by Jiangsu University Natural Science Research Program (09KJB54004), Yancheng Institute of Technology Research Program (XKY2009025) and Program of National Science Foundation for Post-doctoral Scientists of China (20100470664).

References

[1] J. Johansson and T. Masuoka: Macromol. Rapid Commun. Vol. 20 (1999), p. 12.
[2] N.De. Geyter, R. Morent and C. Leys: Plasma Sources Sci. Techonol. Vol. 15 (2006), p. 78.
[3] S.M. Mukhopadhyay, P. Joshi and S. Datta: Appl. Surf. Sci. Vol. 201 (2002), p. 219.
[4] H.U. Poll, U. Schladitz and S. Schreiter: Surf. Coat. Technol. Vol. 142-144 (2001), p. 489.
[5] T.Wakida, M. Lee, Y. Sato, S. Ogasawara, Y. Ge and S. Niu. J. Soc. Dyers. Colour Vol. 112 (1996), p. 233.
[6] T. Wakida, M. Lee, S. Niu, S. Kobayashi and S. Ogasawara: Sen'i Gakkaishi Vol. 50 (1994), p. 421.
[7] C.X. Wang, H.L. Xu, Y. Liu and Y.P. Qiu: Surf. Coat. Technol. Vol. 202 (2008), p. 2775.
[8] C.X. Wang and Y.P. Qiu: Surf. Coat. Technol. Vol. 201 (2007), p. 6273.
[9] S. M. Mukhopadhyay, P. Joshi and S. Datta: Appl. Surf. Sci. Vol. 201 (2002), p. 219.
[10] N. D. Geyter, R. Morent and C. Leys: Surf. Coat. Technol. Vol. 10 (2006), p. 220.
[11] Rakowski: J. Soc. Dyes Colorists. Vol. 113 (1997), p. 289.
[12] Oh.J. Kwon: Surf. Coat. Technol. Vol. 192 (2005), p. 1.

© (2011) Trans Tech Publications, Switzerland
doi:10.4028/www.scientific.net/AMR.331.360

The Practice of the Printing and Dyeing Wastewater Treated by the Process of the First Coagulation Sedimentation/Hydrolysis Acidification/ Anoxic/Oxic System/ Secondary Coagulation Sedimentation

Zhaowu LEI [1, a], Gaoying Yang [2,b] and Changlin XI [3,c]

[1] Environmental Management College of China, Qinhuangdao Hebei, 066004, China

[2] Hebei ProfessionalTechnology Institute of Construction and Material, Qinhuangdao, Hebei, 066004, China

[3] Jiujiang Huafu Fiber Limited Company, Jiujiang, Jiangxi,330300,China

[a] leizhaowu2004@163.com, [b]yanggaoying@126.com, [c] xicl19850914@163.com

Keywords: Printing and Deying Wastwater, the Technical Process, Practice.

Abstract. Printing and deying wastwater was one of the wastewater of difficulty biological treatment. the process of the coagulation sedimentation/hydrolysis acidification/Anoxic/Oxic System/coagulation sedimentation was adopted to treat the printing and dyeing wastewater, the wastewater after disposal had reached the first discharge standard of the discharge standard of water pollutants for dyeing and finishing of textile industry (GB 4287 -92).

Introduction

Textile Industry was one of important economic industry in China, quantity of printing and dyeing wastewater discharged into enviroment was about 6~7 billion tons every year. Printing and dyeing wastewater had the following characteristics: 1)large water quantity, higher concentration of organic pollutants, great variation of alkalinity and pH value, and great variation of wastewater quality; 2) bad biodegradability, the value of BOD_5/ COD_{Cr} was usually about 20 percent;3) high colority, it's values was sometime above 4000 times[1]. Now the method of treating printing and dyeing wasterwater mainly included physicochemical method, biological method, adsorption method, and ultrafiltration method etc home and abroad[2].

Printing and dyeing wastewater from producing process in one fiber limited company was treated by the process of the first coagulation sedimentation/hydrolysis acidification/Anoxic/Oxic System/ secondary coagulation sedimentation, operation results of the process showed that the wastewater after disposal had reached the first discharge standard of the discharge standard of water pollutants for dyeing and fini shing of textile industry (GB 4287 -92).

Wastewater origin and characteristics

One fiber limited company did dyeing and finishing through scouring, dyeing, washing, fixation, softness, dewatering, drying, etc working operation with raw material of white cotton and reactive dyes, and auxiliary material of glauber's salt, hydrogen peroxide, soda and acetic acid, the annual production reached 10000 tons. The reactive dyes and auxiliary retained in wastewater came into being pollutants, so the printing and dyeing wastewater was the wastewater of difficulty biological treatment.

Now wastewater quantity from the company was 4000m^3/d, representative wastewater quality index included colority, SS, COD_{Cr}, PH, etc, the wastewater after disposal should reach the first discharge standard of theDischarge Standard of wate rpollutants for dyeing and finishing of textile industry (GB 4287 -92). wastewater quality index and the values of discharge standard was as table 1.

Table 1 Wastewater quality

items	SS/mg/L	COD_{Cr}/mg/L	BOD_5/mg/L	pH	colority /time
raw water	200	1000	220	6～11	1200
discharge standard	70	100	25	6～9	40

The process and runing of wastewater treatment

The process of wastewater treatment. the process of the first coagulation sedimentation/hydrolysis acidification/Anoxic/Oxic System/ secondary coagulation sedimentation was adopted to treat the printing and dyeing wastewater, the process chart was as fig 1.

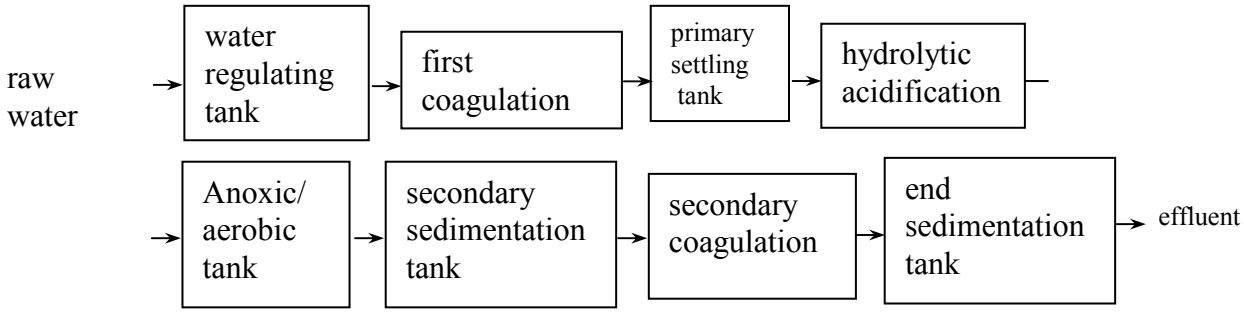


fig1 The process chart of wastewater treatment

Main structure size of the wastewater treatment process was as table 2.

Table 2 Main structure size

number	name of structure		structure size	quantity
1	water regulating tank		22.6m×15.6m×4.5m	1
2	primary settling tank		Φ20.6m×3.5m	1
3	hydrolytic acidification tank		25.6 m×15.6 m×4.0 m	1
4	anoxic / aerobic tank	anoxic basin	5.35 m×5.70 m×5.2 m	2
5		aerobic tank	40.7 m×11.5 m×5.2 m	2
6	secondary sedimentation tank		Φ20.6 m×3.5 m	1
7	end sedimentation tank		Φ22.6 m×3.3 m	1
8	sludge thickening tank		Φ12.6 m×4.5 m	1

Φ150mm filler of elastic tridimensional middle density was filled in hydrolytic acidification tank. 3300 sets microporous aerator was installed in aerobic tank.

The runing of of wastewater treatment. Wastewater from water regulating tank entered into the first coagulation reactor where wastewater pH value was adjusted to 7.5~8.5, poly aluminium chloride(PAC) and decolorant was added. after first coagulation and primary settling tank, Wastewater entered into hydrolytic acidification tank where HRT was 1.7h in anoxic basin, HRT was 24h in aerobic tank. Effluent of secondary sedimentation tank entered into secondary coagulation reactor and end sedimentation tank, further to decreas colority and COD_{Cr} in wastewater and effluent. sludge from primary settling tank, secondary sedimentation tank, and end sedimentation tank was squeezed mud cake by belt filter press after sludge thickening tank.

According to the characteristics of high concentration of organic pollutants, high colority, bad biodegradability, etc, the method of the coagulation sedimentation was adopted to decrease a great deal of organic pollutants of difficulty biological treatment, and largely decreased the organic pollutants concentration and colority, and to reduce the system load of biological treatment[3]. The secondary coagulation sedimentation could make the effluent target of colority and COD_{Cr} meet to wastewater index of discharge standard. The effluent index of Parts of the process was as table 3.

Table3 The effluent index of parts of the process

	Effluent of water regulating tank	Effluent of primary settling tank	Effluent of hydrolytic acidification tank	Effluent of secondary sedimentation tank	Effluent of end sedimentation tank
PH	9.5	8.3	8.1	7.8	7.7
COD_{Cr} /mg/L	600	400	350	120	85
colority /time	1200	600	500	200	30

The table 3 showed that removal rate of COD_{Cr}, colority was 33 percent and 50 percent in first coagulation sedimentation unit, removal rate of COD_{Cr}, colority was 70 percent and 66 percent in hydrolytic acidification/ Anoxic/ aerobic unit, removal rate of COD_{Cr}, colority was 29 percent and 85 percent in secondary coagulation sedimentation unit. So the COD_{Cr} removal was in hydrolytic acidification/ Anoxic/ aerobic unit, the colority removal was in first coagulation sedimentation unit, hydrolytic acidification/ Anoxic/ aerobic unit and secondary coagulation sedimentation unit.
The part of monitoring dataes of the system of wastewater treatment on september 2010 was as table 4.

Table 4 The part of monitoring dataes of the system of wastewater treatment on september 2010

number	Water regulating tank			primary ettling tank		secondary sedimentation tank		end sedimentation tank		
	COD_{Cr} /mg/L	pH	colority /time	COD_{Cr} /mg/L	pH	COD_{Cr} /mg/L	pH	COD_{Cr}/ mg/L	pH	colority /time
1	680	9.1	1200	430	8.7	130	8.21	78	8.02	29
2	660	9.58	1200	448	8.3	148	8.2	92	8.01	34
3	658	9.12	1200	430	7.94	150	8.1	90	8.03	33
4	688	8.95	1200	400	7.41	138	8.17	95	8.15	35
5	665	8.06	1200	500	7.49	142	8.12	82	7.93	30
6	656	9.91	1200	460	8.68	131	8.22	77	7.8	29
7	672	9.35	1200	429	8.92	130	8.2	72	8.02	28

The result of table 4 showed that effluent index after disposal with the process could reached the first discharge standard of theDischarge Standard of Water Pollutants for Dyeing and Finishing o f Textile Industry (GB 4287 -92), so the system of wastewater treatment adapted to the puality of printing and dyeing wastewater, and had good treatment effect to the printing and dyeing wastewater in the fiber limited company.

Technical and economic analysis of the wastewater treatment system

removal rate of colority was about 97 percent, removal rate of COD_{Cr} was about 86 percent with the system of wastewater treatment. Main reagents used in treatment were as table 5.

Table 5 Reagents amount in the wastewater treatment system

	poly aluminium chloride （PAC）/ mg/l	decolorizing agent / mg/l	H_2SO_4/ mg/l
first coagulation	150	180	130
secondary coagulation	80	100	

Total power consumption of the process was 0.8 degrees of electricity/m^3 wastewater, total operation cost of the process was 2.2 yuan RMP/ m^3 wastewater.

Conclusion

The process of the first coagulation sedimentation/hydrolysis acidification/Anoxic/Oxic System/ secondary coagulation sedimentation had good effect in treating printing and dyeing wastwater. The wastewater after disposal had reached the first discharge standard of the discharge standard of water pollutants for dyeing and finishing of textile industry (GB 4287 -92).

The process had good technical and economic index, removal rate of colority was about 97 percent, removal rate of COD_{Cr} was about 86 percent, total power consumption was 0.8 degrees of electricity/m^3 wastewater, total operation cost was 2.2 yuan RMP/ m^3 wastewater.

References

[1] GAO Meng ,CHEN Yucheng , XIE Qian，etc，Research on the Effects of Coagulation Treatment on Printing and Dyeing Wastewater, Journal of Southw est U niversity (Natural Science Edition), 2010, Vol 32 No 7, P.88～92,in Chinese.

[2] HE Zhenbao, Characterization of dyeing effluents and their treatment techniques, printing and dyeing，2007 No. 17,P.41~44,in Chinese.

[3] HUANG Jihua, JI Biyan, WANG Xiangtu, WANG Pixin,etc, High Density Clarification /Biochemical Treatment/Coagulation Process for Treatment of Printing and Dyeing Wastewater,CHINA WATER & WASTEWATER, 2010, Vo.l 26 No. 14,P.102~105,in Chinese.

© (2011) Trans Tech Publications, Switzerland
doi:10.4028/www.scientific.net/AMR.331.364

Dyeing research of aramid fiber-Nomex

Tan Yanjun[1 a] ,Yu Yan'e[2 b]

[1]Xi'an Polytechnic University, China

[2]Xi'an Polytechnic University, China

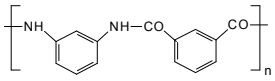
[a]lcntyj@tom.com, [b]yuyane@xpu.edu.cn

Keywords: Nomex, chemistry method dye, dyeing

Abstract. Nomex has very high crystallization degree, the mindset degrees and chemical stability, which makes its dyeing highly difficult. In the presented investigation special auxiliaries were employed to enlarge Nomex molecular gaps in order to lower the Van der Waals forces between the members and make it much easier for the dyestuffs to penetrate the fiber. The dyeing rate was also promoted significantly.

Introduction

Nomex is the trade name for aramid fibers and a kind of functional fiber and has got application in a variety of fields. Its molecule backbone consists of amide group and benzene group and this chemical structure results in its chemical stability, heat stability, high density and high modulus. The dyeing of aramid fibers has been the biggest problem for its application. In the presented investigation the special auxiliaries were used in order to promote the dyeing and the related details were disclosed.

The chemical structure of Nomex (m) is shown below:  [1]. According to the chemical structure it can be seen that Nomex consists of long linear molecule, which is made up of amide groups linked with m-benzene groups. Benzene groups in its backbone make the molecule chain harder than that of the normal polyamide compounds.

Because of very high crystallization and tropism, the glass transition temperatures and the heat resistance are improved outstandingly. It is difficulty for dyeing. And to some extent, its applications are limited [2,3,4].

This text find out a new dyeing process and solve the problem of aramid fiber dyeing during researching dyeing performance and dyeing mechanism on aramid fiber.

Textile pretreatments

On the process of making aramid fiber, we often add a little oil to it and in itself there is some oil. And so we need to wash pretreatment before dyeing. The condition is that Sodium hydroxide 3-5g/L, oil removers DO 2g/L, which is in the boiling water, boils for 15 minutes and then clean up by water.

Dyeing recipe

Dyestuff X% , Dyeing assistants Y%, pH (Formic adjust) 4-5.

Analyzing dyeing performance

Aramid fiber molecular array tightly, there is little gap in the fiber. When temperature is low the extent of molecular heat-moving changes its position hardly, in the water it is hardly swell and dyestuffs are hard to penetrate to fiber inner.

As to these results the text depends on auxiliaries chemicals to change fiber dyeing performance and improve the dyeing rate. There are two functions in the dyeing .one is that Nomex is bonded with disperse dyes and combine and form unstable compounds and so this is easily to dye. The other is dyeing assistant molecular which have strong affinity to fiber is small, which makes the edges of amorphous regions and crystallization array out of order. The volume of fiber swell, and its length reduce, its gaps increase, Tg reduce which are available to dye. Auxiliaries chemicals have affinities to fibers and can come into Nomex, destroy the hydrogen bonds between fiber molecular, at same time the hydrogen bonds of Nomex and fiber instead the hydrogen bonds of Nomex and Nomex and enlarge the gaps between aramid molecular, reduce the van der Waals forces between members, are useful to dyestuffs get into aramid fiber inners and so outstandingly improve the dyeing rate.

Effect of dyeing assistant to Nomex fiber physical performance

Textiles require pretreatments by dyeing assistants 20g/L and time 20min, then test its Tg. Results are shown in Fig. 1, Fig. 2.

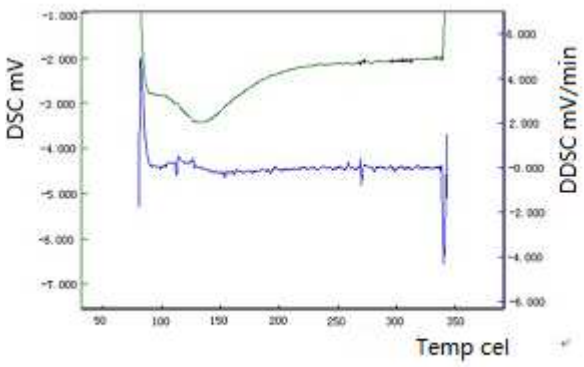


Fig. 1 Nomex DSC curve

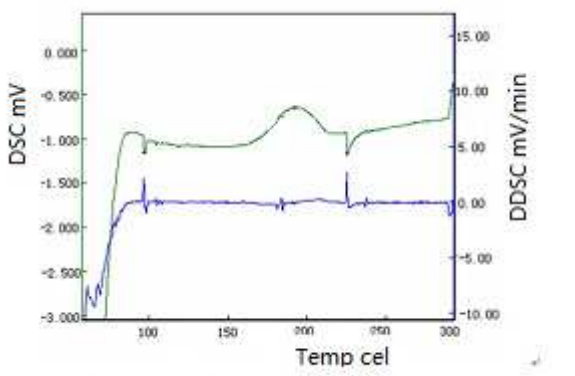


Fig. 2 Nomex pretreating by dyeing assistants DSC curve

Nomex's Tg changes largely whether require pretreatment with dyeing assistants or not Tg of the one which isn't pretreated is 273℃ and the opposite other is 97℃.

Conclusion and Discussing

Effect of agent to dyeing. Choosing four difference agents and dyeing fabric separately. From Table 1, *Lab* and Δ*E* show the playoff agents enough, the result consists with *K/S* essentially. After adding agent D, dyed textiles light-value (*L* value) is lest, which means lightness is small, color is the deepest, but color difference Δ*E* explains that the differences between sample and standard. The more differences are, the more samples are deep.

Table 1 Dyeing result of different agents

agent	*K/S*	*L*	*a*	*b*	Δ*E*
no auxiliary	3.35	50.012	24.491	-5.725	/
auxiliary A	5.51	50.592	32.295	-2.635	3.031
built-up agent S	8.12	39.437	28.497	-7.686	13.897
auxiliary D	15.56	35.857	33.103	-7.200	16.014
bulked agent P	11.47	45.483	28.168	-8.082	7.960

Note: Δ*E* is on the standard of no auxiliary, others are samples, according to color difference formula.

Effect of the dosage of agents.

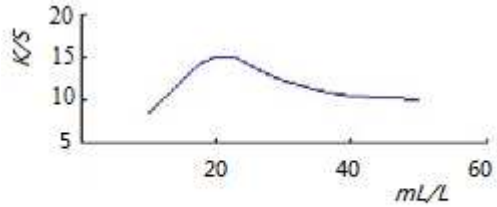


Fig. 3 effect of dosage of agents

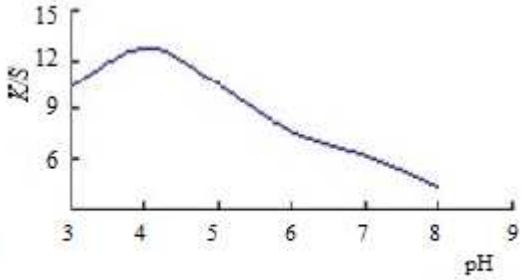


Fig. 4 effect of pH to dyeing

From figure 3, we know that the dosages of agent are not the more. If the dosage is excessive the dyeing rate is low oppositely. The reason is that dyeing assistants can accelerate dyestuff to disperse fiber inner and get more color, and can accelerate dyestuff to migration and level. The excessive dosage makes dispersion rate in contrast.

Effect of pH to dyeing.

pH plays an important function in dyeing and is shown in Fig.4. The pH of dye-liquor can destroy dyestuff sand result *K/S* into reduce.

Effect of temperature to dyeing.

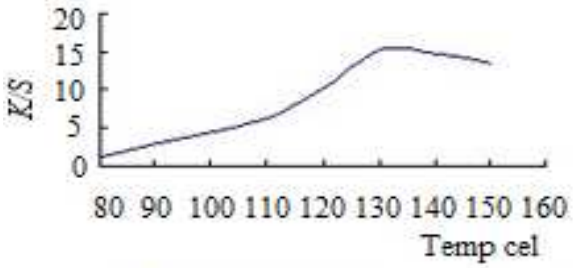


Fig. 5 effect of temperature to dyeing

FromFig.5. When the temperature is up to about 110℃ the dynamic balance of dye-liquor inner changes quickly, dyeing rate accelerates. Which easily produce to dyestuffs bump each other at this time, which the temperature is up to 130℃ dyestuffs disperse levelly into fiber inner, dyeing rate come up to the highest ,at this time, get into state balance.

Strength of dyed aramid fabrics.

Strength of dyed aramid fabrics are shown in Table 2, Table3.

Table 2 Fastness to soaping and fastness to rubbing

	Fastness to washing	fastness to dry crocking	fastness to wet crocking
grade	4	4	3

Table 3 Tests of tensile and tear strength

/	/		latitude
Tensile strength(N)	Before dyeing	1164	538
Tensile strength(N)	After dyeing	1239	570
Tearing strength(N)	Before dyeing	206	99
Tearing strength(N)	After dyeing	224	105

We know that after aramid fiber are dyed, its fastness to soaping and fastness to rubbing are all good, its tensile and tear strength are good.

Conclusions

1. Aramid fabric is difficult to dye by conventional dyeing method and only get very shallow color.
2. By chemical agent dyeing, agents can accelerate to dye and get deep color.
3. After dyeing, fabric's hue doesn't change and value is better, fastness to soaping and fastness to rubbing are good.
4. Changing different dyeing process conditions are available to improve dyeing effect.

References

[1] Xueming Ding, xiongying wu:J. Hi-Tech Fiber＆Application. Vol. Z5(1996), p. 32

[2]Zhongzhi Xu, Xiang Zhou, Tianmin Tu, Min Zhao: J. Dyeing and Finishing.Vol. 12(2003),p.4

[3] Huan Wang, Shaoping Li, Jianchun Zhang: J. Journal of Textile Research Vol. 23(2002), p.15

[4] Jinghong Feng, Q ing Zhang, Yujiao Wu: J. Dyeing and Finishing.Vol. 19(2006), p.8-9

© (2011) Trans Tech Publications, Switzerland
doi:10.4028/www.scientific.net/AMR.331.368

The Treatment of Printing and Dyeing Wastewater by using Coagulation and Fenton Reagent Oxidation combined process

Liping Wang[1,a], Yuchuan Guo[1,b],Yizhong Chen[1,c],Erdeng Du[1,d] and Yongjing Mao[1,f]

[1] School of Environmental and Safety Engineering,Changzhou University,Changzhou,China, 213164

[a]wlp@cczu.edu.cn,
[b]448788490@qq.com,[c]yzc@jpu.edu.cn,[d]duerdeng@gmail.com,[f]815993583@qq.com

Keywords: Printing and dyeing wastewater,Flocculation,Fenton reagent

Abstract. It is difficult to treat printing and dyeing wastewater, for printing and dying wastewater features complex composition, high chromaticity and many toxic substances.The paper studied the effect of the compound of inorganic and organic coagulant with Fenton reagent on the treatment of printing and dyeing wastewater. The effect of other factors were also investigated, including pH value, flocculants, Fenton reagent and reaction time. The results showed that, under the conditions of room temperature, pH 9, PAFCS dosage 100mg/L, PAMC 4mg/L, pH 4, H_2O_2 dosage 1.0mL/L, $FeSO_4 \cdot 7H_2O$ dosage 150 mg/L, the reaction time 60 min, the COD_{Cr} removal was high over 91%, and the color was also significantly removed.

Introduction

The comprehensive treatment of printing and dyeing wastewater has become a public issue, which is closely related with the economy and environment. The pre-treatment plays an important role during the treatment of printing and dyeing wastewater. Yafeng Li [1] adopted the coagulation-Fenton process to treat the printing and dyeing wastewater and achieved good results. What's more, Genlin Zhang [2] combined microwave radiation-Fenton process for the treatment of dyeing wastewater and the effluent reach level Ⅰ of discharge standard. The printing and dyeing industry is prosperous in Wujin district of Changzhou city. and the treatment of the wastewater has been an important issue. After the outbreak of cyanobacteria in Taihu Lake, the government improved the wastewater discharge standard to grade A. However, the existing facilities were insufficient and cannot meet the treatment process requirements. Due to the characteristics of dyeing wastewater, it is difficult to reach emission standard only with the traditional biological processes. The paper adopted coagulation[3] and senior oxidation method (Fenton reagent) [4,5,6] to treat the printing and dyeing wastewater from the industrial park. The experimental parameters were also optimized to achieve better drainage.

Test Methods

Coagulation. At room temperature, measured 100 ml wastewater with the pH value adjusted to the requirement. And then stirred (stirred fast for 1 min first and then slow for 2 min) at the same time put in the flocculation agent. And then put it aside for 30 min, observing the experimental phenomena at the same time, and got the supernatant (if necessary, could be filtered quickly with filter papers) to determine COD_{Cr}.

Fenton catalytic oxidation. At room temperature, measured 100 ml supernatant of the test sample that after coagulation. Stirred it (stirred fast for 1 h), at the same time put in the reagents. And then adjusted the pH value to the requirement. Put the test sample aside for 30 min, and observed the experimental phenomena. Got the supernatant (if necessary, filtered it quickly with filter papers) to determine COD_{Cr}.

Results and Discussion

Coagulation test Compared to other inorganic flocculants, the polymer structure of PAFCS produces the strong effect of adsorption and bridging, which would give fully play to the role of PAFCS. In the experiment, the paper chose PAFCS as the coagulant. Experimental results showed that, PAFCS had a wide applied range of the pH value. With the pH value in the range of 8-13, COD_{Cr} removal rate reached up to 50%. When pH was equal to 9, the removal of COD_{Cr} was 54.9.The broad applicability of pH value would avoid adding regents to adjust the pH value of the wastewater, thereby reduced the operating costs.

Fig. 1 shows that the removal rate of COD_{Cr} increases with the adding dosage of PAFCS, and later decreases when the dosage of PAFCS exceeds the critical value. Exceeding a critical value during the experiment, there were still a lot of floc sediments to form, but the settlement was slow. Overall, PAFCS removed COD_{Cr} well, and the optimum dosage was 150 mg/L.

Fig. 2 shows that the removal rate of $COD_{Cr}$by PAFCS was better than the removal by PAFCS. The max COD_{Cr} removal by PAMC could reach up to 71.3%. In the experiment, floc particles increased, and the structure of floc particles was more compact, so that the time of settlement was shorter.

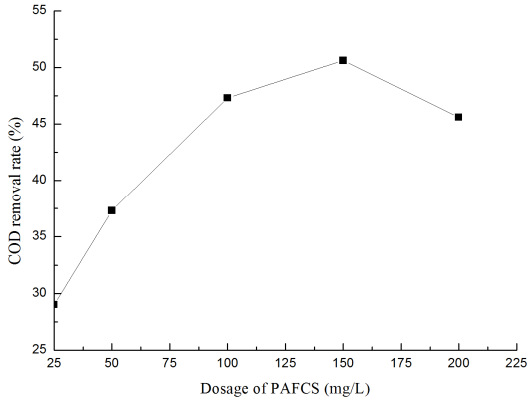


Fig.1:The impact of the dosage of PAFCS on the removal of COD_{Cr}

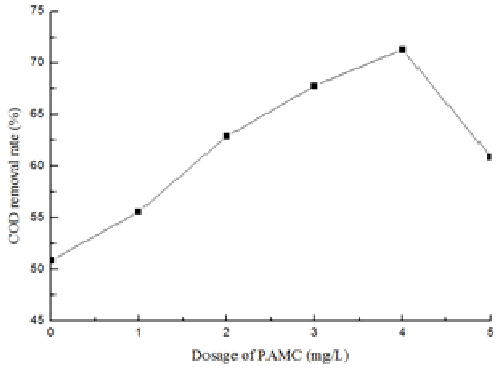


Fig2:The impact of PAMC mixed with PAFCS on the removal of COD_{Cr}

Fenton experiments. Fenton process is an advanced oxidation process usually used in the degradation of organic compounds, and can effectively remove phenols, aromatic amines, aromatic hydrocarbons, pesticides from wastewater and other organic wastewater biodegradable uneasily. Compared with other advanced oxidation processes, Fenton process is more practical for its simplicity, rapidetc. The color of printing and dyeing wastewater is caused by the system of conjugation in the molecules of dye. Fe^{2+} and H_2O_2 in Fenton reagent can generate hydroxyl radicals in acidic conditions, which can break the conjugated system, decolor the wastewater, and then mineralize the pollutants in wastewater [7]. During the process of printing and dying wastewater

treatment, Fenton reagent, in addition to its advanced oxidation (oxidation potential up to 2.8V), also played an important role in the coagulation. So the decolorization and the removal of COD_{Cr} of the wastewater were both remarkable.

The pH value was adjusted with H_2SO_4/NaOH. The results of the experiment were shown in Fig.3. The removal of COD_{Cr} is better with Fenton reagent with the pH value between 3 and 5.When pH was equal to 4, the removal rate of COD_{Cr} reached to the highest of over 70%. With higher pH value, H_2O_2 would generate invalid decomposition, which would reduce the catalytic efficiency. The optimized pH value of Fenton reagent oxidation was determined to be around 4 .

The Fenton reagent degrades pollutants by •OH generated by H_2O_2 under the catalytic oxidation of Fe^{2+}. Therefore, the effect of oxidation is directly determined by the amount of H_2O_2. The results of the experiments were shown in Fig.4. With the increase of the dosage of H_2O_2, COD_{Cr} removal first increased and then decreased with the dosage over 1.0 ml/L. The removal rate reach the peak when H_2O_2 dosgage was 1.0 mL/L.

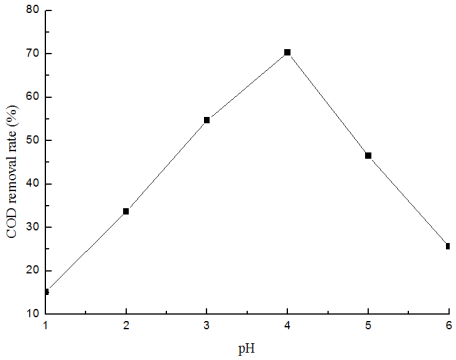


Fig.3:The impact of the pH value on the removal of COD_{Cr} with Fenton reagent

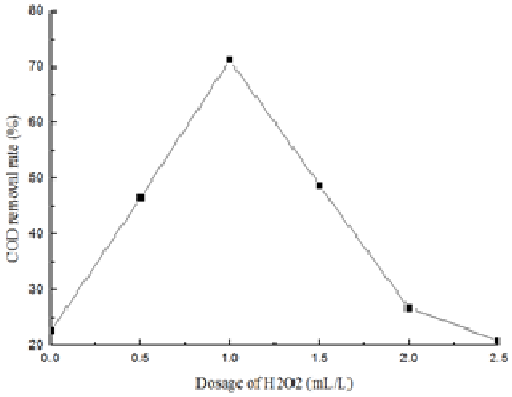


Fig.4:The impact of the dosage of H_2O_2 on the removal of COD_{Cr}

As shown in Fig. 5, with the increase of Fe^{2+} concentration, COD_{Cr} removal rate increased. When the dosage of $FeSO_4$•$7H_2O$ was equal to150 mg/L, the result reached the best. However, when continuing to add $FeSO_4$•$7H_2O$, COD_{Cr} removal rate decreased. The catalytic effect is due to the concentration of Fe^{2+}: Fe^{2+}, as the catalyst of Fenton reaction, when its concentration is low, with its increase, the amount of •OH increases. However, when Fe^{2+} concentration is in excess, it would restore H_2O_2 and Fe^{2+} is oxidized toFe^{3+}, which would result in the increase of color and the decrease of COD_{Cr} removal rate of the drain [8].

In Fig.6, COD_{Cr} removal rate rised with the increasing reaction time at first. When the reaction time was 60 min, COD_{Cr} removal rate reached 71.3%, and then the COD_{Cr} removal curve became flat. As the time went on, COD_{Cr} removal rate increased slightly. Fenton reaction is fast, and as the reaction goes on, Fenton reagent is gradually consumed, resulting in the reduction of the amount and generating speed of • OH , which causes the removal rate of COD_{Cr} to be constant at last[9].Considering the operating and investment costs, the reaction time was optimzed to be 60 min.

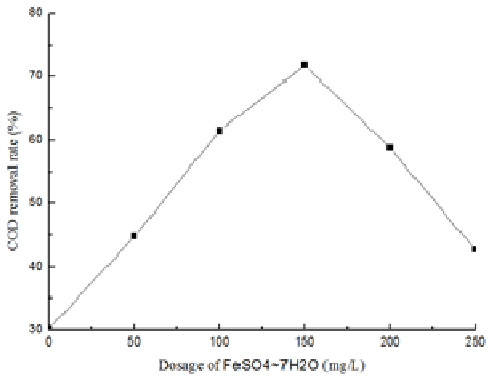


Fig.5: The impact of the dosage of $FeSO_4 \cdot 7H_2O$ removal on the removal of COD_{Cr}

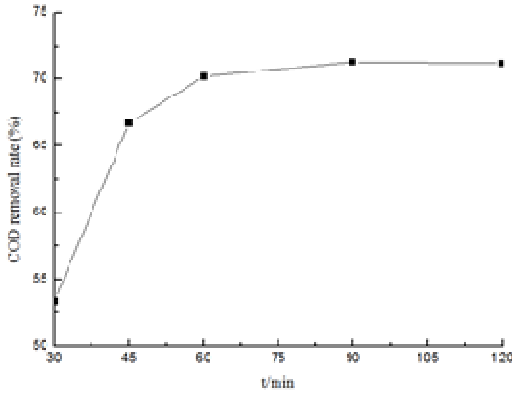


Fig.6: The impact of the reaction time on the of COD_{Cr} with Fenton reagent

Conclusions

The pH value is one of the major factors related to the treatment of wastewater. Under the conditions of room temperature, pH 9, PAFCS dosage 100 mg/L, PAMC dosage 4 mg/L; pH=4, H_2O_2 dosage of 1.0 ml/L, $FeSO_4 \cdot 7H_2O$ dosage of 150 mg/L, reaction time of 60 min, COD_{Cr} removal rate of the printing and dyeing wastewater was above 91%, and the decoloration of wastewater was notable, too.

References

[1] Y.F.Li, L.L.Zhang, X.D.Yuan: Jianzhu University (Natural Science)(In Chinese). Vol,22 (1) (2006),p.138

[2] G.L.Zhang, X.J.Xu, Y.Z.Lan: Chemical Engineering (In Chinese), vol.35 (10) (2007) ,p.57.

[3] J.Li, L.Huang: Dyeing & Finishing(In Chinese), vol.16(2008), p. 43

[4] X.D.Xue, Q.T.Jin: Environmental Protection, (In Chinese) vol. 11(6) (2001), p.13

[5] J.H.Sun, S.P.Sun, H.L.Wang: Industrial Water Treatment(In Chinese), vol. 26 (12) (2006),p. 9

[6] H.X.Shi, X.M,Hu: Liaoning Chemical Industry, (In Chinese) vol. 35(4) (2006) , p.202

[7] S.L.Ding, Z.K.Li, R.Wang: Water Resources Protection(In Chinese), vol. 26(3) (2010),P.73

[8] C.H.Chen, B.Xie, Y.Ren et al: Chinese Journal of Environmental Science(In Chinese), vol. 21 (3) (2000) , p.93

[9] S.Zhou, D.Y,Du: Environmental Science and Technology, vol. 27(2) (2004) , p.69

© (2011) Trans Tech Publications, Switzerland
doi:10.4028/www.scientific.net/AMR.331.372

Comparison of Dye Adsorption Behaviors of Sodium Polyacrylates Freely Dissolved in Water and Grafted onto Poly(ethylene terephthalate) Fiber

Xiaoli Shi[1,3,a], Huan Song[1,b], Xinsheng Zhu[1,2,c*], Zhijuan Pan[1,2,d*]

([1] Faculty of Textiles and Clothing Engineering, Soochow University, 178 Eastern Ganjiang Road, Suzhou, Jiangsu 215021, PR China

[2] National Engineering Laboratory for Modern Silk, Soochow University, 199 Ren'ai Road, Suzhou, Jiangsu 215123, PR China

[3] College of Chemistry, Chemical Engineering and Materials Science, Soochow University, 199 Ren'ai Road, Suzhou, Jiangsu 215123, PR China)

[a]shixiaoli@suda.edu.cn, [b]fengyuyanran@163.com, [c]zhuxinsheng@suda.edu.cn, [d]zhjpan@suda.edu.cn, * Corresponding author

Keywords: Sodium polyacrylate; dyes; Adsorption

Abstract. Dyes containing wastewater lead to severe environmental pollution. Polyacrylates both dissolved in water and bonded to polyester fabrics were used to remove dye molecules from simulated wastewater. The Fourier transform infrared spectra, scanning electron microscopy and UV spectrophotometry were applied to characterize the grafting and the adsorption behavior of polyacrylates. The adsorption behaviors were described by the Lagergren's pseudo second kinetic equation with physical interaction mechanism. The adsorption rate and equilibrium value were almost independent of adsorption temperature. The chemical bonding substantially suppressed the polymer chain mobility and thus weakened the removal efficiency.

Introduction

It was reported that there was 2% loss drained with water during the dye manufacturing process, whereas up to 10% dyestuff was lost in the dyeing process. Dye wastewater often contains high concentrations of a variety of organic and inorganic matters. The biologically toxic organic compounds are thought to cause cancer, teratogenic and mutagenic diseases. Dye wastewater has become an urgently tackled problem nationally wide in China.

Dye wastewater treatment methods can be divided into chemical, physical, biochemical and electrochemical methods. The dye molecules are often destroyed, and decolorization occurs in chemical methods. Among the physical methods, activated carbon, an excellent adsorbent and renewable but with high recycling cost, is used for treating less concentrated dye wastewater. Membrane separation technology, due to the presences of concentration polarization and membrane fouling, together with high cost, hasn't found a large scale industrial application yet. Low operating costs of biological techniques are highly effective for the biodegradable dyeing wastewater, especially for BOD removal, but the color removal was often not very satisfied. Electrochemical method, simple and compact, known as the cleaning technique, is reluctantly found few applications since the dye decomposition mechanism, treatment efficiency and operation cost along with expensive facility are all not fully resolved.

Several ion exchange fibers (IEF) have gradually received much attention in the removal of the dyes from textile wastewater [1]. Compared with granular ion exchange resins, IEF has an effective specific surface area, high adsorption and desorption rates. Besides, its specific textile feature

makes it much convenient to be used in practice [2]. In this study, the adsorption and separation of the sodium polyacrylates both dissolved in water and bonded to poly(ethylene terephthalate) fabric were investigated and compared. The results implied that the chemical bonding significantly weakened adsorption, although the removal of free polyacrylates bonded with dye molecules from water might be difficult.

Experimental

Raw Materials and grafting. ly(ethylene terephtthalate) fabric (area density 100g/m^2) and sodium polyacrylate (PAA), a white powder, and cationic red X-5GN were all commercial products. The grafted fabric with acrylic acid was prepared with inverse emulsion polymerization after low temperature plasma pre-irradiation and the detailed grafting process was referred to our previous work [3].

Plot of reference curve of absorbance. ationic red aqueous solutions with the concentrations 0, 20, 40, 60 and 80mg/L were made to get the reference curve on dye concentration versus adsorption with U-3010 HITACHI ultraviolet spectrophotometry. The absorbance at 513nm was recorded for the mapping of the working curve.

Adsorption with PAA dissolved in water. The cationic red aqueous solution at 1000mg/L and PAA aqueous solution at 1000mg/L were prepared respectively. Equal volumes of dye solution and PAA solution were sampled and mixed well by shaking at a temperature of 30 ˚C, 40 ˚C and 50 ˚C respectively, the few milliliters of upper clear solutions were taken at the given times 5, 10, 15, 30 and 60min and further analyzed for the absorbance at 513nm.

Adsorption with PAA grafted PET fabrics. Ca. 2.5g PAA grafted PET fabrics, the graft rates 33% and 18%, were placed in 200ml, 500mg/L cationic red aqueous solution at temperature 40˚C respectively. The upper clear solution was acquired at the times 5, 10, 15, 30, and 60min, and analyzed with spectrophotometer. In addition, ca. 2.5g ungrafted polyester fabric after pretreatment with boiling water was used as reference.

Infrared analysis. FTIR characterization was performed at ambient temperature with a Nicolet 5700 spectrometer (Thermo Electron, Madison, WI, USA) in reflection mode. The samples were analyzed with 64 scans and the resolution 4 cm^{-1} in the range of 700-4000 cm^{-1}.

Morphological observation. The surface characteristic of the grafted fiber was studied using Hitachi FE-SEM model S-4700, scanning electron microscope. The samples were gold coated prior to image sampling.

Results and discussion

Grafting of the fabrics. Fig. 1 displays the fiber morphology of pristine and grafted fabrics made by scanning electron microscopy. There were some speckles on the fiber surface and strips along the fiber for pristine fiber, while there were a lot of particles with their sizes ranged from a few micrometers to a dozen of micrometers for the modified. Fig 2 presents the infrared spectra for the ungrafted and grafted fabrics with different grafting rate. There some new adsorption peaks appeared at the bands 1640cm^{-1}, 1550cm^{-1} and 1360cm^{-1}. Among them, the peaks 1360 cm^{-1} and 1550cm^{-1} were attributed to symmetric and asymmetric stretching vibrations of carboxyl group (COO-) due to partial neutralization prior to polymerization. The band 1640cm^{-1} tended to assign the absorption of water molecules owing to the deformation vibration of O-H bond. Thus, the surface of polyester fabrics is grafted with polyacrylic acid (sodium).

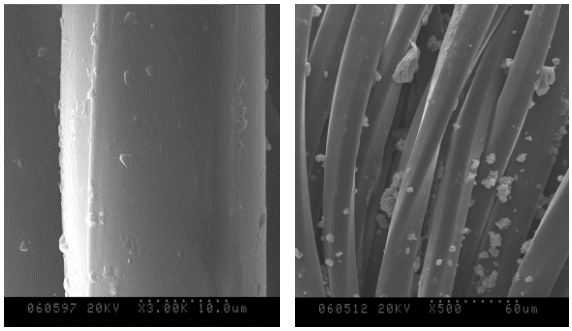


Fig 1 SEM image of grafted and ungrafted polyester fabrics

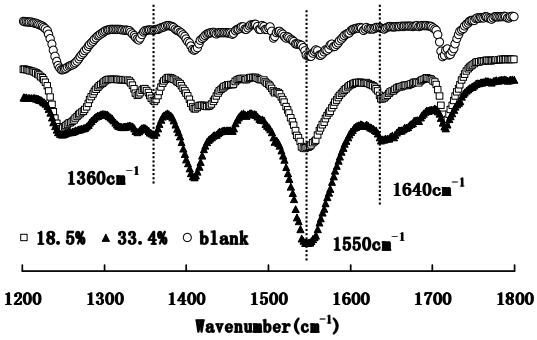


Fig. 2 Infrared spectra of the samples in the reflection mode

Adsorption of PAA dissolved in water. The reference curve for the dye adsorption isotherm is given in Fig 3. It was found that, the linear relationship between dye content and absorbance is shown in Fig 3 and a much satisfied working curve was obtained.

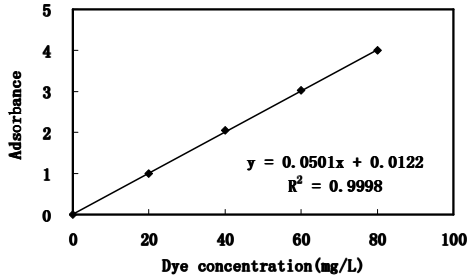


Fig 3 Reference curve of dye concentration

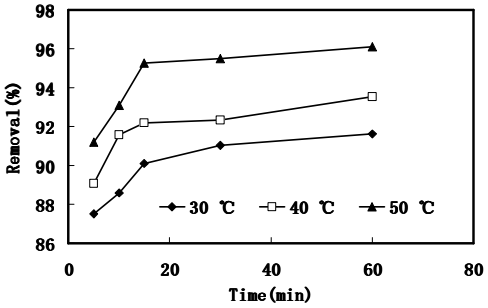


Fig 4 Dye removal of at different adsorption temperature

Fig 4 displays the dye removal at three different temperatures. The removals were generally increased with adsorption time. When the adsorption time was 5min, the removals were ca. 87%, 89%, and 91% at the adsorption temperatures of 30˚C, 40˚Cand 50˚C respectively. The removal rate was slightly lifted up with the increase of the adsorption temperature.

A dynamic process model, Lagergren's pseudo second kinetic equation, can be adopted to describe the adsorption kinetics of dye adsorption onto the PAA main chain. That is,

$$\frac{dQ}{dt} = k_2(Q_e - Q)^2$$

Where, k_2 is the adsorption rate constant. After the integral transformation, then,

$$\frac{t}{Q} = \frac{1}{k_2 Q_e^2} + \frac{t}{Q_e}$$

According to the equation, the adsorption processes are all demonstrated in Fig 5 at different temperature. The constant one of regression coefficients implied the verity of Lagergren's pseudo second kinetic equation for the system. The equilibrium adsorption values were 921, 939 and 966 mg/g respectively at the temperatures of 30, 40 and 50˚C respectively. The adsorption temperature didn't show strong influence on the values. The very large equilibrium values implied highly efficient removal for cationic red dye. The adsorption rates (k_2), 3.25, 3.47 and 3.42 min^{-1} at the three temperatures of 30, 40 and 50˚C respectively, strongly suggested the non-temperature dependence. It will be temped to be concluded that they may exist physical interaction between carboxylic group and cationic dye rather than chemical complex reaction.

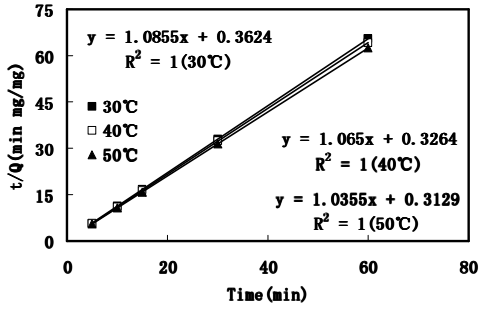


Fig 5 Isothermal adsorption kinetics at the different temperature

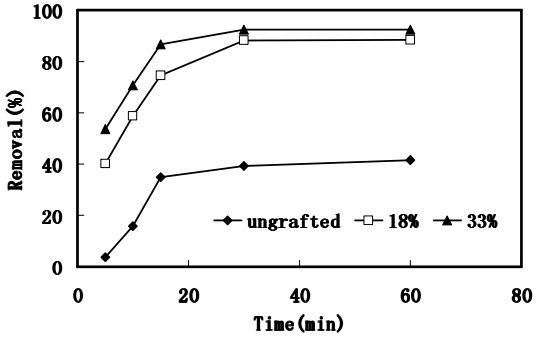


Fig 6 Dye removal with adsorption time for PAA grafted fabrics

Adsorption of PAA and PAM bonded to polyester fabrics. Fig 6 presents the relationship between the removal rate and adsorption time for the grafting rates at 40˚C. The pristine polyester fabric showed much less removal than the grafted ones. With the increases of adsorption time and the grafting rate, the removal degree of dye increased correspondingly. However, compared with the case of PAA dissolved in water, the removal efficiency of dye significantly reduced since the calculated grafting PAAs were 4.5 and 8.25 times as much as that of dissolved in water for grafting rates 18% and 33% respectively. The isothermal adsorption kinetics for the grafted fabrics is shown Fig 7. The adsorption rates of 0.76 and 2.6min^{-1} for the grafting rates 18% and 33% respectively were dropped in comparison with that of PAA dissolved in water, and this was attributed the remarkable reduction of PAA chain mobility after being grafted onto polyester fabrics. The regressed equilibrium adsorption values, 220 and 119mg/g for the grafting rates 18% and 33% respectively, implies the relatively large adsorption and separation capacity and accurately

quantitative relationship since the difference of equilibrium ones exactly corresponds to that of grafting rates. If the products of regressed equilibrium one and grafting rate are considered, 990 and 980mg/g are obtained for the grafting rates 18% and 33% respectively. These two values are very close to the equilibrium one of freely dissolved PAA mentioned above. The results indicate some quantitative physical interaction between carboxylic group and cationic dye, for instance, the molar ratio of 2, namely two molar carboxylic groups with one molar cationic dye.

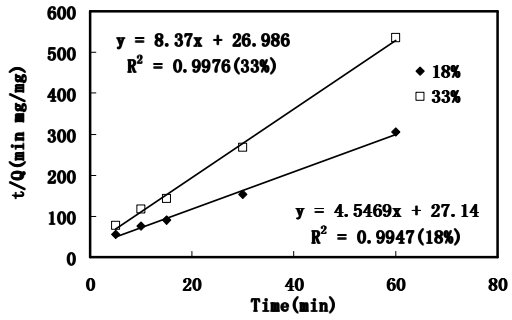


Fig 7 Isothermal adsorption kinetics for different fabrics

Conclusions

Sodium polyacrylate was successfully grafted onto polyester fabric surface via aqueous solution polymerization. Polyacrylate dissolved in water shows very strong adsorption propensity to cationic red dye via physical interaction mechanism. The adsorption rate of dye molecules is almost independent of the adsorption temperature. The PAA bonded to polyester fabric surface displays slow adsorption rate in comparison with PAA freely dissolved in water, although the equilibrium adsorption value may be same for each group.

Acknowledgement

The part of work was financially supported by the priority academic program development of Jiangsu higher education institutions.

Reference

1. J-M Huang, C-H Wang, I-J Wang:J Polym Res vol 8 (2001), p.267.
2. VS Soldatov, AA Shunkevich, IS Elinson, et al: Desalination vol 124 (1999), p.181.
3. X-L Shi, X-S Zhu, Z-J Pan, Microstructure and properties of poly(ethylene terephthalate) fabric grafted by polyacrylic acid in inverse microemulsion under low pressure plasma pre-irradiation, submitted to Journal of Donghua University (English Edition).

© (2011) Trans Tech Publications, Switzerland
doi:10.4028/www.scientific.net/AMR.331.377

Dyeing Properties of Chitosan-Sulfamic Acid Solution Treated Wool with Silane Coupling Agent

Xuemei He [1, a], Kongliang Xie [1,b]

[1] Modern Textile Institute, Donghua University, Donghua University, Shanghai, 20620, P.R.China

[a] hexuemei@ycit.cn, [b] klxie@dhu.edu.cn

Keywords: Chitosan, wool, Sulfamic acid, Silane coupling agent, dyeing.

Abstract. In this study, wool fabrics were treated with different concentration of chitosan sulfamic acid solution under using 3-glycidyloxypropyltrimethoxysilane (GPTMS) as a crosslinking agent. The structure of treated wool fabrics was investigated by SEM, DSC-TG. Treated wool fibers had a irregular surface appearance, showed the presence of amounts of Nano SiO_2 and their aggregates deposited onto surface of wool fibers. The thermal properties were obviously enhanced. Treated wool fabrics is more stable in higher temperature than that of untreatment. Treated wool fabrics were dyed with weak acid red B, and dyeing behaviour were studied by means of by light reflectance measurements. The color strength *(K/S* value) of treated wool fabrics obviously increased from 5.33 to 31.68 by comparison with the untreatment. As a result, it can be concluded that the chitosan sulfamic acid solution with GPTMS treatment could improve the weak acid red B low temperature dyeing on wool. Further, low temperature dyeing of wool fabrics with chitosan-sulfamic acid is safe, so the results obtained are quite promising as a basis for possible future industrial application.

Introduction

It is known that wool dyeing is a degradative process involving high temperature for long periods in acidic to neutral pH medium to achieve good penetration, optimum fastness, and dye bath exhaustion[1-2]. But, the results can be harsh handle, discomfort, and a deterioration of properties that impact consumer wear, care, and aesthetic appreciation[3-5]. Low temperature dyeing at temperatures below 100℃enables to get a good shade, minmize the damage of wool fiber during dyeing and consequently to avoid deterioration of its physical properties. So, it has been the subject of many investigations[6-7]. With the awareness of environment, ecology, and pollution control increasing, the application of biopolymers on textile materials is gaining popularity all over the world. Chitosan and its derivatives are useful agent in low temperature dyeing of wool. The effect of chitosan, a polysaccharide-based cationic biopolymer, on the dyeability of wool fibres has also been investigated over the last few years[8]. A method for improving the dyeability of wool fabric with reactive dyes, proposed by Julia [9-10], involves pretreating the fabric with an oxidising agent, applying chitosan to the fabric. Other authors reported that the dyeability of wool fabrics pre-treated with a chitosan/nonionic surfactant mixture improved, and their colour strength with reactive dye increased [11].

In order to improve the low temperature dyeability of wool fabric without causing any significant change to the nature of the wool fibre, in this research, the modified wool fabrics were prepared by a general padding method with the diluted chitosan sulfamic acid solution under using 3-glycidyloxypropyltrimethoxysilane (GPTMS) as a crosslinking agent. The stucture of treated wool fabrics were characterized by SEM, DSC-TG techniques. The weak acid red B was used to dye treated wool fabrics. Thus, a environmentally friendly wool fabric processes will be achieved and diminish the wastewater charge from a wool plant.

Experimental and methods

Materials. Bleached Wool fabric, Chitosan (CS) was purchased from zhejiang Jinke bio.Co. Ltd. 3-glycidoxypropyltrimethoxysilane (GPTMS) were received from yancheng Renbo Chemical Co. Sulfamic acid (AS) was of analytical grade and purchased from the Chemical Reagent Company of Guoyao.

Preparation and dyeing of suface treated wool fabrics. Suface modified wool were prepared in the non-homogeneous chitosan-sulfamic solution with GPTMS as crosslinking agent. A portion (5g) of the wool fibers was treated with pad-batch technique in 100ml of 2% chitosan sulfamic acid aqueous, and then, 3g/LGPTMS was added. The mixture was stirred for 30min to remove air bubbles on the surface of these fibers and then shaken at 40℃, After 4 h, the treated fibers were washed several times with alcohol aqueous, then the treated fabrics were washed in warm water, and air-dried at room temperature. Portions of the treated fabric and control samples were dyed with weak acid red B. The treated wool samples were steeped in the dye bath with liquor ratio (L: G) of 50:1 that prepared by 6% (o.w.f) weak acid pink B concentration and pH=4.5-5.5 (adjusted by acetic acid). Dyeing of sample was started at room temperature and the temperature was increased with the rate of 2°C/min to 70℃and heated for 60 min. The sample were rinsed with water and dried at room temperature.

Measurement of Color Strength and dye up-take. A set of experiments were designed by taking *K/S* value as a unique evaluation target and four vary parameters, e.g. time, temperature, pH and concentration of reagent. The color yield of both dyed samples were evaluated by spectrophotometrically (Macbeth Color-Eye 7000A, standard illuminant D65, 10°standard observer, and specular component included). All measured sample show the greatest λmax value at 520 nm.The color strength (*K/S* value) was assessed using the Kubelka-Munk equation[7,8]:

$$K/S = (1-R)^2/2R \quad (1)$$

Where *R* is the decimal fraction of the reflectance of dyed wool fabrics.

Results and discussion

Surface morphology and therm analysis. The surface of pure wool and treated wool were observed by the with FEI Quanta 200 scanning electron microscopy(SEM). The scale structure of the wool fiber was obviously affected after the chitosan-sulfamic solution treatment with GPTMS as crosslinking agent. In contrast to the smooth surface of pure wool (shown in Fig.1a)，Fig.1b show treated Wool yielded more irregular surface, resulting in the complete stripping of some of cuticular scales and the amounts of nano SiO_2 and their aggregates deposited onto the surface of wool fibers. Clearly, the fiber surface is covered a thin continuous film of chitosan nano silica material after treatment.

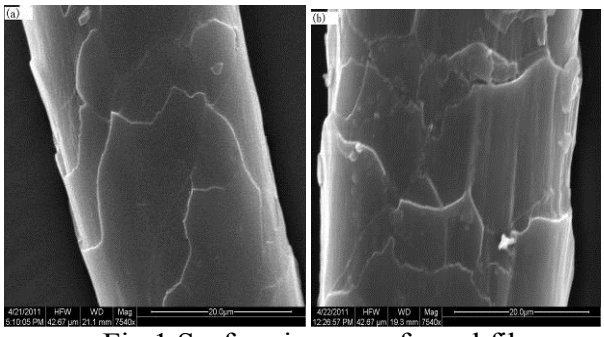


Fig.1 Surface images of wool fiber
(a)pure wool ,(b) treated wool

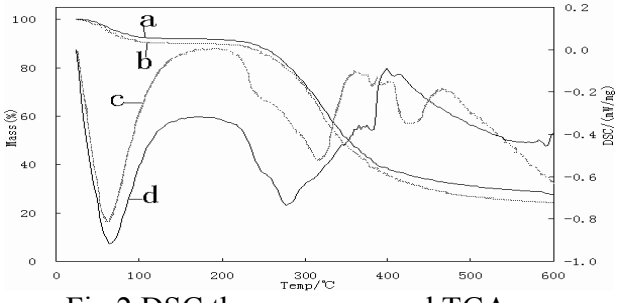
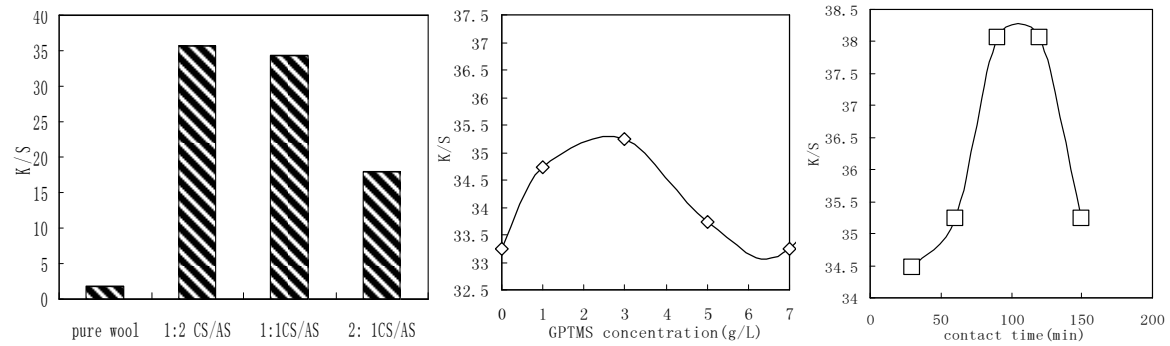


Fig.2 DSC thermograms and TGA curve
(a) treated woolTGA (b) pure wool TGA
(c) pure wool DSC (d) treated wool DSC

According to Fig.2a,b DSC thermograms of pure wool and treated wool, the main thermal events for pure wool are an endotherm at 315.4℃resulting from the melting of helices of intermediate filaments keratins. For the treated wool, an endotherm at about 279 ℃ corresponding to the melting/decomposition of highly cross-linked (disulphide bonds) inter-macrofibrillar matrix keratins, and above 381.4℃ there is extensive thermal degradation (burning). The thermal decomposition behavior of the pure wool and treated wool was performed in Fig.2c,d. The maxmium decomposition temperatures of plain pure wool and treated wool are 387.4 and 398.6℃, respectively. Clearly, the

treated wool show higher decomposition temperature (Td) than the pure wool. Thus considerable improvement on thermal stability of wool can be attained through the chitosan-sulfamic solution treatment with GPTMS as crosslinking agent.

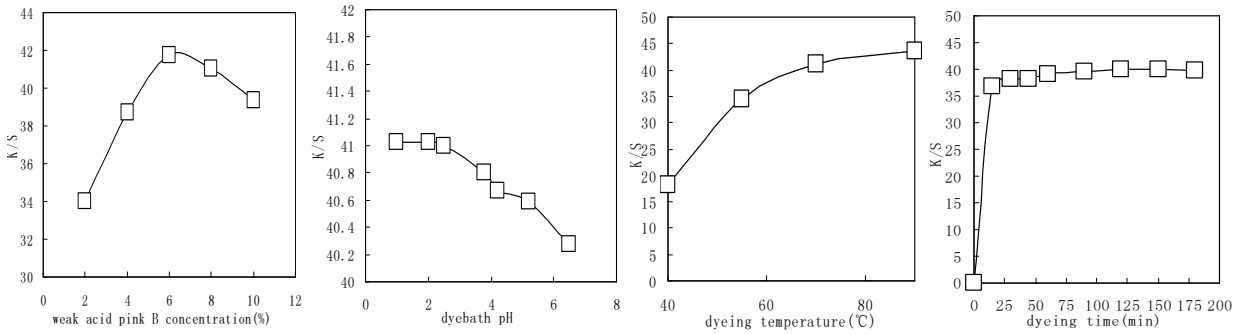
Effect of pretreatment conditions on dyeing properties of treated wool. The colour yield *K/S* values for fabrics dyed with different mass ratio of CS/AS and without treatment are shown in Fig.3a. Obviousily, compared to untreat wool, *K/S* value of treated wool fabrics increased from 5.33 to 31.68. However, *K/S* values are significantly lower with the increase of CS/AS mass ratio. It is possible that too high concentration sulfamic solution could cause more electrostatic interaction between anion dye and treated wool in strong acid condition. Fig.3b shows that curve presented a unique peak and the peaks corresponding to a critical GPTMS concentration of about 3g/L, it is in reasonable to consider that this critical concentration was better for using silanes coupling agents to cross-link with active groups on surface of treated wool. Fig.3c shows the effect of various treat time from 30 to 150min on the *K/S* values for treated wool fiber on exposure to at 20℃, 3g/L GPTMS concentration. There was a significant increase in the *K/S* values from 30 to 100min, and reached the highest at 100min. It is because electrostatic interaction strengthened between the anion dye and cationic group of the surface layer on treated wool with the treat time increasing. But, further increase intreat time (>100min) would cause a decrease in *K/S* values because of the degree of crosslinking of GPTMS increasing. Thus, we suggest that optimization treatment conditions is facilitated by 1:2 mass ratio of CS/AS, 3g/LGPTMS concentration and 100 min treatment time.



(a) (b) (c)

Fig.3 Effect of different pretreatment conditions on *K/S* value of treated wool（2% dye concentration）
(a) Effect of mass ratio of CS/AS (b) Effect of GPTMS concentration (c) Effect of contact time

Optimization of the dyeing Process for treated wool· The *K/S* values were measured for treated wool fabrics at various dye conditions as shown in Fig.4. It can be observed that the *K/S* values increased with an increase of from2% to 6%(owf) and reach maximum *K/S* values at 6% dye concentration (shown in Fig.4a). Further increase of dye concentration caused a decrease in *K/S* value.



(a) (b) (c) (d)

Fig.4 Effect of different dyeing processes on *K/S* of treated wool (a) Effect of dye concentration (b) Effect of dyebath pH value (c) Effect of dyeing temperature (d) Effect of dye time

The relationship between *K/S* values and dyebath pH (range of pH from 1 to 6.5) is shown in Fig.4b. As the pH of the dyebath is lowered to 2.0, *K/S* values increases to 41.2 while there is a lower *K/S* values around neutral pH. It is because the electrostatic interactions between weak acid red B and treated wool with positively charged surface increased in acidic solution and contributed to the increased adsorption efficiency.

Fig.4c shows an increase in *K/S* value on treated wool fabrics as the dyeing temperature increased from 40 to 85℃with dye concentration 6%, dyebath pH value 2.0. It is known that increasing the temperature allows the swelling of the blend fibers, which leads to a higher dye uptake. The results indicate that 70℃ is the suitable temperature for dyeing, at which temperature a proper reaction between the dye and amino groups on the surface of treated wool is performed. On the other hand, increasing the dyeing temperature was attributed to the de-aggregating of weak acid red B , and enhanced the uptake of acid milling dye. Considering that the final *K/S* values, cost savings and less damage for all investigated systems, we suggest that sutibale dyeing temperature is 70℃.

The *K/S* values of treated wool at different time intervals from 15 to 180 min are shown in Fig.4d with the dyeing conditions of 6% dye concentration, dye bath pH value 2.0 and dyeing temperature70 ℃. In case of treated wool dyeing process, the *K/S* value increased quickly in intial 30min of the dyeing time. It seems that equilibrium is reached after 120 min of dyeing process treated wool. We examined the acidic dyeing characteristics of treatment wool where the formed positive film barrier had been acculated dye sorption and the induced changes in wool structure led to lower temperatures for the dyeing process and shorter times to reach exhaustion to treat wool-woven fabric. Thus, optimum dyeing parameters of treated wool can be summarized as follows: 6% weak acid pink B concentration at 70℃, the dyebath pH 2 , dyeing time120min for the dyeing process.

Conclusions

Wool dyeing has benefits such as lower energy conservation and wool fibers protection by either decreasing the temperature or shortening the processing time at high temperature during dyeing. The dyeing of treated wool in chitosan-sulfamic acid solution with GPTMS as a crosslinking agent is more economic than untreatment, and also color strength (*K/S*) in case of using chitosan-sulfamic acid solution treatment leads to better results. It can be concluded that, chitosan-sulfamic acid solution treatment can be a promising method to dye wool fabrics at low temperature with weak acid dyes.

References

[1] S. Chatterjee, S. Chatterjee, B.P. Chatterjee, A.K. Guha, Colloids Surf. A.Vol. 299(2007), p.146.

[2] Mittal, J. Mittal, A. Malviya, D. Kaur, V.K. Gupta, J. Colloid Interface Sci. Vol.343(2010), p.463.

[3] H. K. Rouette, "Encyclopedia of Textile Finishing",Springer-Verlag, Berlin Heidelberg(2001).

[4] Woolmark Test Method 31, Washing of Wool TextileProducts, The Woolmark Co., May (2000).

[5] W. Rakowski, Proc., 9th Int. Wool Text. Res. Conf., IV, 359(1995).

[6] S.J. McNeil , R.A. McCall:Ultrasonics Sonochemistry. Vol.18 (2011) , p. 401.

[7] M. Naebe, P.G. Cookson, J.A. Rippon, X.G. Wang: Text. Res. J. Vol. 80(2010) , p.611.

[8] S. Vìchez, A.M. Manich, P. Jovancic, P. Erra: Carbohydrate Polymers.Vol. 71 (2008) , p.515.

[9] M.R. Julià, E. Pascual and P. Erra: Journal of the Society of Dyers and Colourists.Vol.116(2000), p.62

[10] J. A. Maclaren and B. Milligan,"Wool Science. The Chemical Reactivity of the Wool Fiber", p.89-107,Science Press, Marrickville, 1981.

[11] S. Vílchez, P. Jovan i, and P. Erra: Fibers and Polymers Vol.11(2010),P.28.

© (2011) Trans Tech Publications, Switzerland
doi:10.4028/www.scientific.net/AMR.331.382

Wrinkle-resistant Property of Cotton Fabric Treated by Chitosan and Epoxy-silicon Micro-emulsion

Hao Wang[1,a], Chen Huang[1,b], Na Liu[1,c]

[1]College of Light-Textile Engineering and Art, Anhui Agricultural University,

Hefei 230036, Anhui, P.R.China

[a]haozijie2000@yahoo.com.cn, [b]silkhch@163.com, [c]freemyself1983@yahoo.com.cn

Keywords: Cotton, Wrinkle-resistance, Chitosan, Epoxy-silicon micro-emulsion, Treatment

Abstract. Cotton fabric was treated by chitosan and epoxy-silicone finishing agents to improve its wrinkle-resistant property. The study showed that mixed finish by two agents can provide higher wrinkle-resistance than single finish when applied to the cotton fabrics due to their synergistic effect. In the wrinkle-resistant finishing process, four main factors (chitosan mass concentration, organosilicon volume concentration, baking temperature and baking time) influencing finish effect were discussed and then process conditions were determined. After optimum process treatment, the wrinkle-recovery angle of mixed finished cotton fabric increased evidently while its whiteness and breaking strength dropped a little. In addition, the addition of organosilicon can improve fabric softness. After washed for 30 times, delay wrinkle-recovery angle of mixed finished fabric was 54° higher than that of native fabric, and the treated cotton exhibited good washing resistance.

Introduction

Chitosan is a non-toxic and chemically reactive, and biocompatible natural functional polymer, and has long been used as a biopolymer and natural material in many fields[1,2]. Recently, chitosan effects widely studied are antistatic, bacteriostatic, and biocompatibility properties conferred on various textiles[3,4,5]. According to some previous experiences, wrinkle-resistance finishing with chitosan for fabric can improve its wrinkle degree but its handle and mechanical property got worse to a certain extent. Besides that, good washing resistance of improved recoverability resulting from chitosan treatment is needed by adding crosslinkers[6]. Organosilicon has advantages such as excellent flexibility, elasticity and the easiness in film forming due to dual characteristic of both organic and inorganic materials and unique structure[7]. Reactive organosilicon can create a covalent binding with other molecules of textile fibre owing to its active groups on the side base of main chains, which makes the resulting textile product possess new features and good washing-resistance[8,9].

In this study, the mixture of reactive organosilicon micro-emulsion and chitosan were used for the wrinkle-resistance finishing of cotton fabric, which was expected to make full use of the advantages of two finishing agents and achieve their synergistic effect to get better results and good washing-resistance without addition of other reagents.

Experimental

Materials

Boiled and bleached cotton fabric(150g/m^2); Degrading commercial chitosan (the viscosity average molecular weight is 50,000, and degree of deacetylation is 85%); HA-920 epoxy-silicone micro-emulsion; Acetic acid was of analytical grade. Distilled water was used throughout the study.

Cotton fabric treatment

The fabric samples were immersed in chitosan and organosilicon mixed bath (1g fabric per 50mL) at 50°C for 30min, two soaked two rolled over. And then the samples were dried at 80°C for 5min and baked at a certain temperature for some time. Finally, the treated samples were thoroughly washed with distilled water and dried at room temperature and humidity.

Wrinkle-resistant properties test

The wrinkle-recovery angles of the cotton fabrics (before and after treatment) were evaluated according to crease perpendicularity recovery of GB/T 3819-1997 using YG541A wrinkle-recovery tester. The results were obtained by averaging 5 warp and 5 weft samples, respectively.

Mechanical properties test

Breaking strength of the cotton fabrics was determined using YG(B) 026D-250-type electronic fabric strength tester. The results were obtained by averaging 10 warp samples.

Whiteness and Stiffness test

The whiteness index was measured with a digital whiteness meter model SBD-1. The stiffness of the cotton fabrics were determined with automatic stiffness tester model YG(B) 022D. The results were all obtained by averaging 5 samples.

Wash-resisting properties test

The treated cotton fabrics were immersed in the washing liquor (5% washing powder) for 5min and rinsed for 2min as one washing process. The wrinkle-resistance properties of the treated fabrics separately after 5, 15 and 30 washing time were measured to test wash-resisting level.

Results and Discussion

In the wrinkle-resistance finishing, the influence of four main factors on the properties of cotton fabrics were discussed. And the properties of native cotton fabric were tested and listed in Table 1.

Table 1 The properties of native cotton fabric

Performance parameters	Whiteness index (%)	Warp breaking strength (N)	Stiffness (cm)	Wrinkle-recovery angle(°) (W+F)	
				Dry-immediate	Dry-delay
Native cotton	78.7	298	55	108	138

Influence of chitosan concentration on properties of cotton fabric

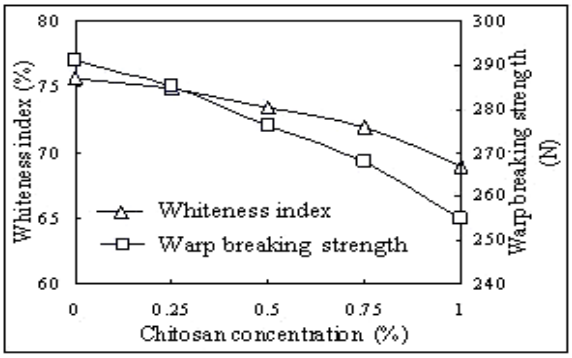


Fig.1 Whiteness and strength of samples treated with different concentration of chitosan

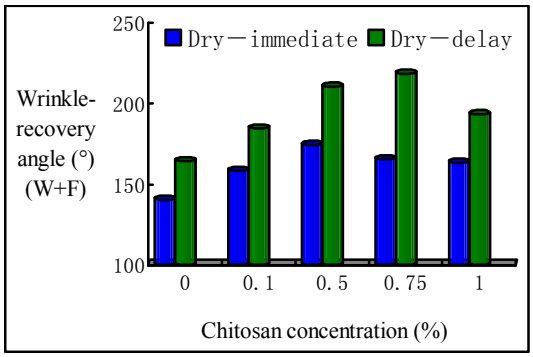


Fig.2 Wrinkle-resistance of samples treated with different concentration of chitosan

Fig.1 and Fig.2 show that the properties of cotton fabric samples treated with different concentration of chitosan solution. It can be seen from Figures that compared with native cotton fabric, whiteness and breaking strength of treated cotton declined slightly while immediate and delay wrinkle-recovery angles all increased when there was only reactive organosilicon agent without chitosan agent in finishing liquor. With the increase of added chitosan concentration, whiteness and breaking strength of cotton samples decreased obviously and wrinkle-resistance of fabrics fell after rising. The above results can be explained as that chitosan in acid liquid has positive charge due to the presence of NH_3^+ which can cause its molecule to adsorb strongly onto cotton fibre[3]. And chitosan bonded with cotton can form a thin film on its fibre surface in the treatment which can increase wrinkle-resistance of fabric. Meanwhile, inhomogeneous film causes the stress concentration easily leading to decrease in fabric strength. When the content of chitosan was greater, liquor viscosity increased which resulting in chitosan macromolecule spreading into the cotton fibers difficultly and so less chitosan was bound with cotton fibres. Comprehensive consideration to three performance parameters of treated cotton samples, the suitable mass concentration of chitosan was 0.5%.

Influence of organosilicon concentration on properties of cotton fabric

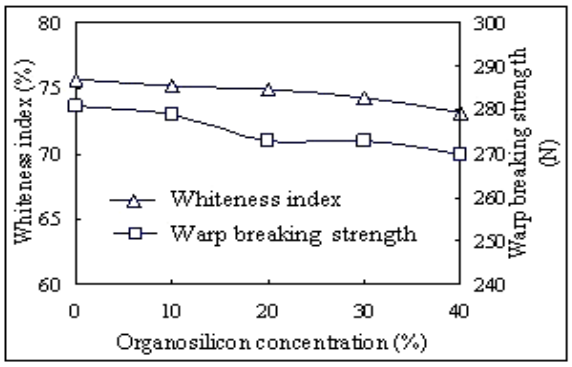


Fig.3 Whiteness and strength of samples treated with different concentration of silicon

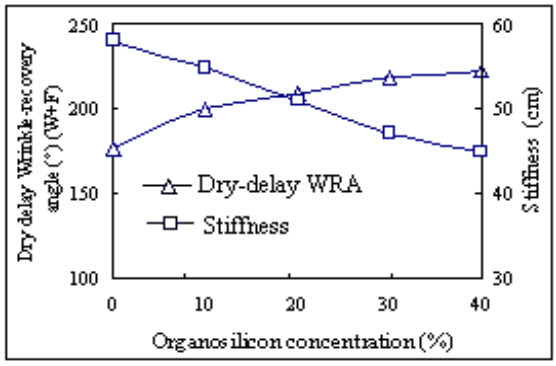


Fig.4 Wrinkle-resistance and stiffness of samples treated with different concentration of silicon

Fig.3 and Fig.4 show that the properties of cotton fabric samples treated with different concentration of organosilicon. Fig.3 shows that whiteness and breaking strength of treated fabrics dropped a little indicating that organosilicon agent has little effect on the two properties of fabric. Fig.4 shows that the addition of epoxy-silicone improved the recoverability of fabric further，and with increasing organosilicon volume concentration, wrinkle-resistance of samples increased. The result might be attributed to the following reasons: On one hand, epoxy-silicone micro-emulsion has unique structure and small particles so that it penetrated easily into microstructure of the cotton fibre and formed continuous thin film. On the other hand, Epoxy-organosilicon was introduced as adjuvant of chitosan crosslinking with cotton fibre due to the presence of its active groups[10], and the formed network crosslinking limited the movement of macromolecular chains in the amorphous field in the fibre. Besides, it can be seen that increment rate of wrinkle-recovery angle of treated fabric became low when the volume concentration of organosilicon surpassed 30%. Fig.4 shows that with increasing organosilicon concentration, softness of cotton fabrics improved markedly due to organosilicon having softing performance.

Influence of baking temperature on properties of cotton fabric

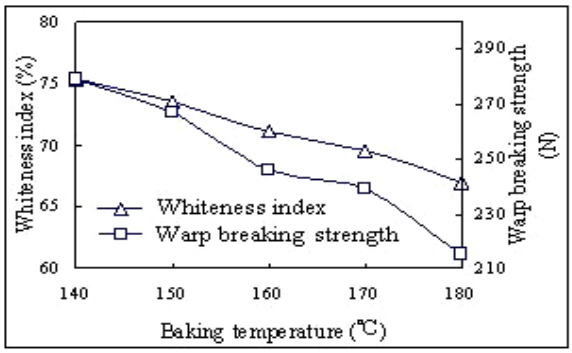


Fig.5 Whiteness and strength of treated samples under different baking temperature

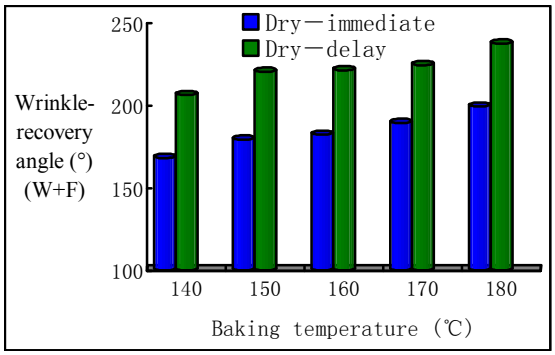


Fig.6 Wrinkle-resistance of treated samples under different baking temperature

Fig.5 and Fig.6 show that the properties of treated cotton samples under different baking temperature. It was found from Figures that high baking temperature led to the cotton becoming yellowish and decline in strength markedly. However, the recovery angles increased with increasing baking temperature because high-temperature baking is favor of improving the crosslinkage degree between the fibre and agents. Comprehensive consideration to three performance parameters of treated cotton samples, the suitable baking temperature was 150°C.

Influence of baking time on properties of cotton fabric

Fig.7 and Fig.8 show that the properties of treated cotton samples under different baking time. It can be seen that with increasing baking time, whiteness and breaking strength of treated cotton dropped gradually while that of wrinkle-resistance increased. Comprehensive consideration to three performance parameters of treated cotton samples, the suitable baking time was 120s.

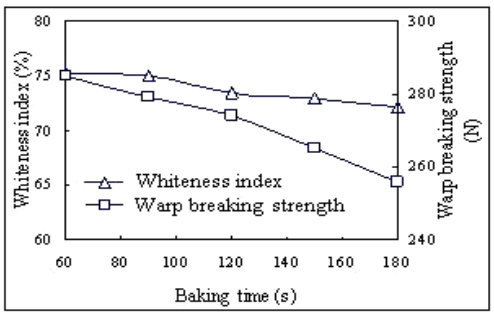


Fig.7 Whiteness and strength of treated samples under different baking time

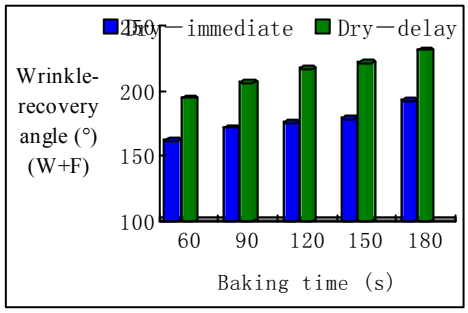


Fig.8 Wrinkle-resistance of treated samples under different baking time

Wash-resisting properties of treated cotton fabric

The contrast of the wrinkle-resisitance property of cotton fabrics treated by chitosan mixed with or without reactive organosilicon after different washing times is shown in Table 2. It was found that compared with fabrics single finishing by chitosan, wrinkle-resistance property of fabrics mixed finishing fell more slowly, indicating that mixed finishing agents have a better connecting fastness with cotton fibre. Besides that, after washed for 30 times, delay wrinkle-recovery angle of chitosan finished fabric was close to that of native fabric (138°) , and delay wrinkle-recovery angle of mixed finished fabric was 54°higher than that of native fabric resulting from higher crosslinking effect. Thus, cotton fabric mixed finishing by chitosan and organosilicon has a good washing fastness.

Table 2 The wrinkle-resistance property of treated cotton fabric after different washing times

Washing times / Delay WRA (°) (W+F)	0	5	15	30
Chitosan treated	176	168	156	144
Chitosan and organosilicon treated	220	214	205	192

Conclusions

Chitosan or reactive organosilicon can improve the wrinkle-resistance of cotton fabrics to a certain extent, however their synergistic effect can get higher recoverability. The optimum processing condition for cotton fabric wrinkle-resistance finishing by chitosan and organosilicon micro-emulsion is defined: chitosan 0.5 % (w/w), epoxy-organosilicon 30% (v/v), baking at 150°C for 120s. After treatment, whiteness and strength of cotton fabric dropped a little. Compared with fabrics single finished by chitosan, fabrics mixed finished by two finishing agents had better washing resistance. Moreover, the addition of organosilicon improved fabric softness.

References

[1] L.F. Qi, Z.R. Xu, X. Jiang, C.H. Hu and X.F. Zou: Carbohydrate Research Vol.339 (2004), p.2693
[2] K.N. Hong, H.K. Su, H.L. Shin and P. Witoon: Carbohydrate Polymers Vol.65 (2006), p.174
[3] X.L. Gao, Y.J. Liu, A.J. Liu, W. Song and Y.L. Fan: Modern Food Science and Technology Vol.21 (2007), p.25–30
[4] Z. Zhang, L. Chen, J. Ji, Y. Huang and D. Chen: Textile Research Journal Vol.73 (2003), p.1103
[5] Y.B. Chang, P.C. Tu, M.W. Wu, and S.H. Hsu: Fibers and Polymers Vol.9 (2008), p. 307
[6] F. Ferrero, M. Periolatto, S. Burelli and R.A. Carletto: Fibers and Polymers Vol.11 (2010), p.185-192
[7] W.W. Tian, X.P. Jia and Z.D. Liu: Fine and Specialty Chemicals Vol.13 (2005), p.4-8
[8] J. Yao, B.Y. Deng, N. Lu and W.D. Gao: Silk Vol.6 (2006), p.38-40
[9] H. Jiang, S.Y. Mei: Silk Vol.11 (1998), p.12-14
[10] C.F. Zang, H. Lin, Y.Y. Chen: China Textile Leader Vol.3 (2006), p.70-74

© (2011) Trans Tech Publications, Switzerland
doi:10.4028/www.scientific.net/AMR.331.386

Deepening Effect of Superfine Dyed Polyester by Escaping Electron-beam Atmospheric Pressure Glow Discharge Plasma

Tingting Liu[1,2,a], Yongqiang Li[1,2,b], Jinqiang Liu* [1,2,c], and Lingjie Meng[1,2,d]

[1]Key laboratory of Advanced Textile Materials and Manufacturing Technology (Zhejiang Sci-Tech University), Ministry of Education, Hangzhou 310018, P. R. China

[2]Engineering Research Center for Dyeing and Finishing of Textiles (Zhejiang Sci-Tech University), Ministry of Education, Hangzhou 310018, P. R. China

[a]liutinghome@163.com, [b]yqli@zstu.edu.cn, [c]jqliu@zstu.edu.cn (corresponding author), [d]loyd23@126.com

Keywords: Escaping Electron-beam APGDP, Dyed Fabrics, Deepening Effect, Surface Modification

Abstract. Surface modification of the dyed polyester was performed by the combination of escaping electron-beam atmospheric pressure glow discharge plasma (APGDP) and softener was studied. Apparent depth was tested and the morphological change along the fiber was observed and analyzed by scanning electron microscopy (SEM). Experimental results indicate that surfaces of the treated PET become rougher and have visible traces of etched, and the apparent depth are also significant increased. These results show that: deepening effect of PET is improved clearly and being a good durability.

Introduction

How to improve the deepening effect of the dyed polyester is a concerned issue in textile industry. Superfine PET fabrics hold a large surface area and it's different among each cross-section. Resulting in poor color of the dyeing fiber, it not only efficiently reflected the light, the surface diffusion also occurred [1]. According to this problem, deep-finishing process has good practical value. Already relevant literature has reported by Japanese scholars ARIMOTO sadao, what researched on agent for superfine denier polyester in deepen processing [2]. Besides, there are some physical methods used to change the fiber surface morphology to improve the fabrics performance of light reflectivity, such as roughness of the surface [3].

The adoption of green and dry chemical technology, atmospheric pressure glow discharge plasma, to handle the fiber surface is one of the popular technologies. As a result of being more ingredients and concentration of active particles than corona and filamentary discharge [4]. The method is well suited for fabric surface etching and activation, so as to achieve the purpose of dyed polyester modified. This article describes a kind of plasma generator, which is called escaping electron-beam atmospheric pressure glow discharge plasma device. The device joint silicone finishing agent apply to dyed fabric finishing. The surface morphology of treated and untreated samples were observed with scanning electron microsopy.

Experimental

Materials. polyester dyed fabric (golden goal Shaoxing Textile Co., Ltd.), high purity O_2, Ar gas (purity of 99.99%, Hangzhou Electrochemical Group), silicon softener agent TF-452 (Communication of Zhejiang Co., Ltd.).

Plasma Device. The principle of experimental device structure shown in Fig. 1. Escaping electron-beam APGDP generator is composed by many multi-needle array of negative high-voltage electrode and a plate electrode. There are many stainless steel needle uniformly distributed on the electrode, of which is spacing for 20 mm, 15 mm in length and 1 mm in diameter. The discharge gap between multi-needle electrode tip and the electrode plate is 25 mm. Around each end of needle

electrodes forms a conical shape glow discharge, and a large area of those distributed on the plate electrode [5]. Due to the rising time of discharge impulse is very short, with the high voltage, the fast escaping electron-beam was generated around the multi-needle electrons, and inspire ionization the surrounding air form glow discharge [6].

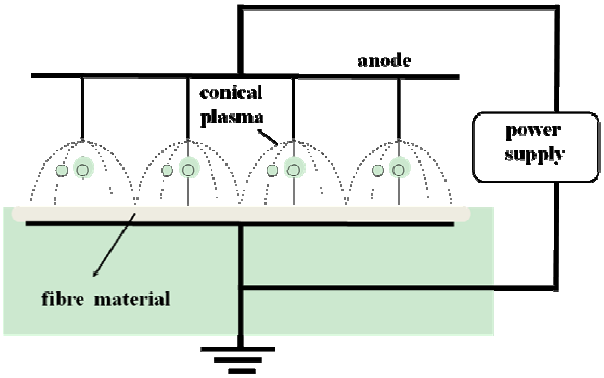


Fig. 1 The principle structure of experimental device

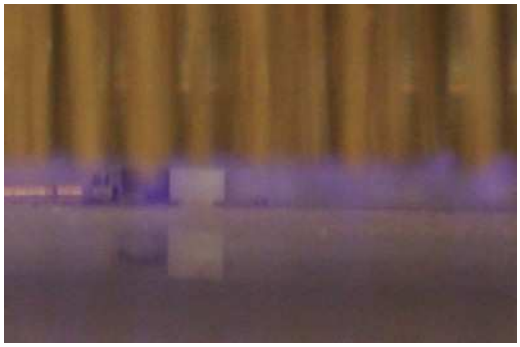


Fig. 2 Discharge plasma photo

Steps of Plasma Treated Fabrics. Fig. 2 was for the glow discharge photos. Regulating plasma device, the figure shows the blue glow launch from the cathode needle tip to the plate positive electrode. There were no arc and mercerizing phenomenon, which is full of uniform and stable glow. By adjusting the discharge impulse condition to regulate the effect of polyester dyed fabrics to achieve the purpose of surface modification. Fabric is put into the external electrode chamber of plasma equipment. Turn on the power switch then start the timer, turn off the power when required specified time and remove the sample.

The Deepening Finishing Process. Process A conditions: soaking and padding (mangle expression of 85%) → drying (80 ^{o}C, 3 min) → baking →washing →drying; process B conditions: soaking and padding (mangle expression of 85%) → drying (80 ^{o}C, 3 min) → plasma treatment→ baking→washing →drying. Otherwise, the pH of finishing agent is 4~5.

Experimental Results and Discussion

Apparent Depth Test. The finishing agent to the fabric surface layer of low refractive index films after treatent. Thereby reducing the light reflectivity of the fabric surface, making the vision in the depth is more darker than before [7]. On the other hand, the sample may reduces light reflection effect after treated by plasma. We are dealing with the apparent depth test of the samples before and after treatment. To measure K/S values of dyed fabric with Datacolor instrument, and judge the effect of increasing depth.

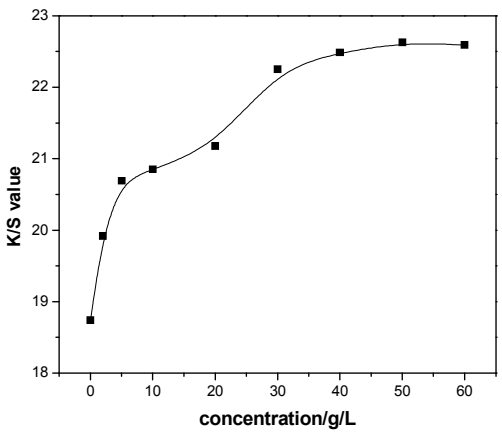


Fig. 3 The effet of agent concentration on deepening

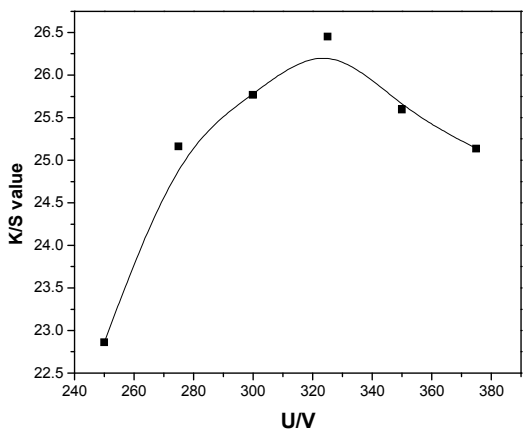


Fig. 4 The effet of plasma-treated voltage on deepening

Fig. 3 shows relationship between the increasing of depth effect and the concentration of finishing process A. It was found that, along with the increasing of finishing agent concentration the K/S is surging.But the K/S value growth trend leveled off when reach a certain concentration, and ultimataly the state of saturation.Taken together, this study selected finishing agent concentration 30 g/L.

Fig. 4 showes the relationship between K/S value of dyed sample and plasma voltage of the B treatment process. Here,all samples are treated for 3 min. The graph indicates that as the voltage increases, the fabric K/S value increases gradually. The K/S value reaches its highest at a voltage of 325 V and then decrease though voltage increase still. The reason may be that higher power induces to increase the concentration of more active plasma particles. Moreover, polymerization of part of silicon film and fabric could further reduce the refractive index of PET, causing a better modification. But if the power is too large, the plasma etching effect that damage on the fabric surface caused the K/S values gradually decrease.

Fastness test. Washing process based on JISL 0217-79 103, use household washing machine, condition as follow: bath ratio 1:30,detergent 2 g/L, 30 ^{o}C, 15 min. Water cleaning 2 times and each time 2 min, dehydration then dried at 100 ^{o}C for 3 min. Repeat the above steps, test the effect under 10 times washing.

Fixed the plasma treated voltage at 325 V. According to Fig. 5, along with plasma treatment time increasing, the K/S value increases linearly at begining. The growth rate of K/S value becomes balanced after more than 3 min. It means under certain conditions appropriate, time adjustments can improve deeping effect of the dyed polyester. In addition, by comparison and analysis of the four curves, we can easily get the conclution that K/S value has decreased compared with initial value after finishing, but the reduction degree is fairly small. In other words, durability effect of the deeping finishing holds a well standart.

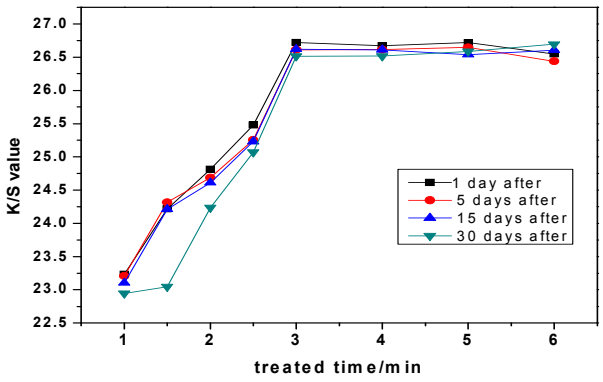


Fig. 5 Aging test of plasma-treated sample among different treatment time

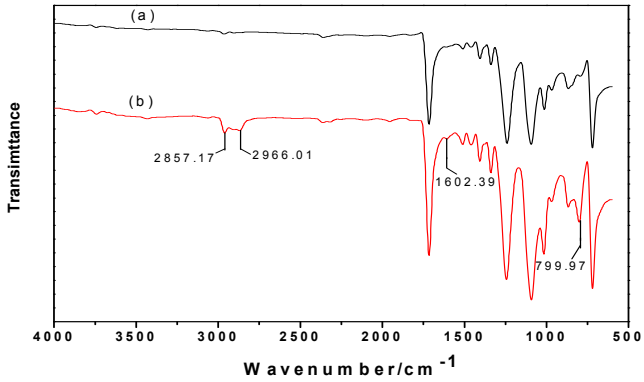


Fig. 6 Infrared analysis spectra of the sample, a: original dyed polyester; b: plasma-treated polyester

Infrared Analysis. Fig. 6 is infrared spectra that before and after modification of polyester fabric. compared with the intact polyester fabric, the line of treated one appeared the characteristic absorption peaks of silicone at 799 cm^{-1}. At 1602 cm^{-1} the absorption due to NH bending vibration, showes that the fabric structure contains amino groups. C-H asymmetric and symmetric bending vibration performance appears at the 2857 ~ 2966cm^{-1} absorption peak. And C-H is from silicone finishing agent, the above proof silicone finishing agent can initially be introduced in the polyester fabric surface.

Surface Morphology analysis. The SEM images of sample surfaces before and after the plasma treatment which is scaling up to 2000 times are shown in Fig. 7.

The SEM image shows that the untreated sample has a smooth, clean, and fine uniform surface. However, according to plasma treated sample from image b, the etching is so marked and polyester fiber surface is covered with a layer of thin polymer. Combined with the analysis results, this may indicates that plasma has reacted with the fiber and polymerized with solicone agent.

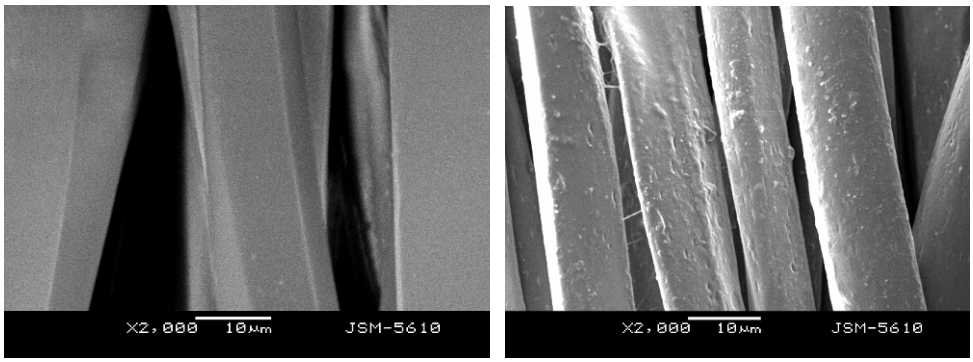


Fig. 7 SEM images of polyester fabric, A: original polyester (left); B: plasma-treated polyester (right)

Conclusions

(1) With atmospheric pressure plasma glow discharge device, surrounding the tip of multi-needle electrode forms a fast escaping electron-beam.It stimulates the surrounding ionized air to form the stable glow discharge interval. So as to meet the continuous surface treatment requirements of polyester fibers without damage.
(2) It is concluded from tests that the optimized conditions for deepening effect finishing with treatment are: agent concentration: 30 g/L, plasma treatment voltage: 325 V, time: 3 min.
(3) As a result of plasma treatment, the role of etching and polymerization could greatly improved performance of dyed fabric. The fiber surface becomes rougher and more solid link between silicone agent and fabric. The better deepening effect durability of the dyed polyester fabric can be obtained.

Acknowledgments

This research was funded by Zhejiang Provincial Top Academic Discipline of Applied Chemistry and Eco-Dyeing & Finishing Engineering (No.ZYG2010017) and Zhejiang Provincial Key Innovation Team (No.2010R50038).

References

[1] Xinyuan Song: Structural coloration and its application in dyeing and finishing(IV) (In Chinese). Dyeing and Finishing (2005).

[2] ARIMOTO Sadao: Color deepening agent and method for color deepening processing. JP 2002285475.

[3] Yanlan Zheng, Jianwei Xing, Juan Ding: Review of Mechanism about Fabrics Deep- Dyeing(In Chinese). Dyeing and Finishing Technology (2010).

[4] Hautojarvi Joni, Laaksonen Sanna: TextileRes Journal. Vol. 70 (2000), p. 391

[5] Jun Wan, Xianghong Jia: Nanosecond-pulsed Atmospheric Pressure Glow Discharge Plasma and Its Applications(In Chinese). High Power Laser and Particle beams (2010).

[6] Roth J R, Nourgostar S, Bonds T A: IEEE Trans on Plasma Science. Vol. 35(2007), p. 233.

[7] Xinyuan Song: New Fiber and Fabric Dyeing and Finsining (In Chinese). China Textile Press (2006).

© (2011) Trans Tech Publications, Switzerland
doi:10.4028/www.scientific.net/AMR.331.390

The Synthesis, Characterization and Application of Amino-modified polymethylhydrosiloxane softener

Xin Zhao[1, a], Wenying Zhu[1,b]

[1]The Light Industry and Textile Institute of Qiqihar University,Qiqihar,161006,China

[a]zx427213@sina.com, [b]zwy580231@126.com.

Keywords: Chloroplatinic Acid, Polymethylhydrosiloxane, Dimethylaminoethyl Acrylate, Amino Silicone Oil.

Abstract. Amino-silicone softener was synthesized by the hydrosilylation reaction, with dimethylaminoethyl acrylate, polymethylhydrosiloxane as the raw materials, and chlorioplatinic acid as the catalyst. The copolymer was analyzed using IR spectroscopy, then emulsified it and used in the linen fabric. The results showed that the amino group can be introducted to silicone side chains through hydrosilylation that dimethylaminoethyl acrylate grafted with polymethylhydrogensiloxane, obtained with the softness of the amino-modified silicone oil.

Introduction

Amino silicone oil is the product of hydrogen silicone oil that hydrogen replaced by an amino product, not only it has general silicone oil properties,for example,low surface tension, non-toxic, non-corrosion, but also possesses soft, hydrophobic, anti-foaming, lubrication, polishing and many other excellent properties because of its molecular chain of amino-polar and high reactivity [1], it can be widely used in many fields. The amino-modified polysiloxane as the main softener because the polarity of the amino can interact with hydroxyl, carboxyl of fiber surface, a very strong covering film will be formed among nodes through the surface of the fiber yarn and fabric The siloxane main chain can be directed attached to the surface of the fiber,so that the coefficient of friction among the fibers decreased, a small force can make the fibers began to slide, so as to achieve excellent soft, smooth results [2, 3].

In this experiment, amino silicone oil was synthesized by hydrosilylation reaction that polymethylhydrosiloxane and dimethylaminoethyl acrylate as raw materials in the presence of chloroplatinic acid catalyst,; then made it into emulsion, for linen fabric finishing.

Experimental

Raw Materials. Dimethylaminoethyl acrylate: industrial grade, ZiBo Wonderful Chemical Co., Ltd.; Polymethylhydrosiloxane: (active hydrogen content of 0.1%), industrial grade, dawn of Chengdu Institute of Chemical Industry; toluene, acetone, ethanol: AR, Tianjin Chemical Reagent Co., Ltd. Kay; phenothiazine: AR, Sinopharm Chemical Reagent Co., Ltd.; chloroplatinic acid: AR, Kodak Reagent Factory of Shenyang City.

The Main Instruments and Equipment. IR analyzer, NicoletAVATAR370, USA; Electronic scale, FA1004 Shanghai Shangping Instrument Co., Ltd.; hot air drying oven (101-3), Shanghai Feilong Instrument Electric Co., Ltd.; vacuum drying oven, A Shanghai permanent science and technology Co., Ltd.; high-speed centrifuge, TGL-16, Gongyi City Yuhua Instrument Co.,Ltd; Force electric mixer,JJ-2, Jintan Medical Instrument Factory, Jiangsu Province; Rotary Evaporator, KE-522AA, Shanghai JiaPeng technology Co., Ltd.; Water circulation pump, SHE-D, Gongyi City Yuhua Instrument Co.,Ltd.

Synthesis of Amino Silicone Oil. The hydrogen silicone oil, toluene, inhibitor, chloroplatinic acid catalyst at a certain ratio are put into 100mL flask of four with condenser and dropping funnel, after 5min through nitrogen, heating and mixing, when the temperature rise to 80 ˚C, dropping a certain amount of demethylaminoethyl acrylate and toluene mixture to control the dropping finished within 1-1.5h. The reaction continued 30h under the condition of 100-130˚C, then cooled it to room temperature, obtained yellow viscous oily

Application and Performance Testing.

Select two emulsifier with different proportions Span-80 and Tween-80, mixed at 40˚C, with traces of water, stir, mix in amino silicone oil, even stirring 10 mins at 40 ˚C, prepared emulsifier with different HLB Value, according to the Eq.1 calculate compound emulsifier HLB value.

$$HLB = (W_A HLB_A + W_B HLB_B) / (W_A + W_B) \text{ [4]} \quad (1)$$

To cut a linen soaked in silicone oil emulsion, and then rolled into the padder, then put it in the continuous setting of the dryer after padding, pre-baking 2 min at 80 ˚C , 170 ˚C baking 60s, its processing is as follows:

$$\text{A dip a rolling} \xrightarrow{\text{rate of rolling, room tempreture}} \text{pre-baking} \xrightarrow{80℃,2\text{min}} \text{baking} \xrightarrow{170℃,1\text{min}} \text{sample}$$

Performance Testing. The finished linen is placed on 24h under the conditions of temperature of 20 ˚C ± 2 ˚C, relative humidity was 65% ± 2%. Flexibility to the fabric is determined by elastic recovery angle, adopt yG541A tester to determine the elastic, whiteness with DSBD-1 Digital whiteness meter testing, according to the determination of GB 8425-1987. Water absorption is determined by Capillary effect with YG(B)871 tests. Fabric strength is determined by YG(B)026D-250 Electronic Fabric Strength Tester.

Results and discussion

Characterization of Amino Silicone Oil. The structure of amino silicone oil was characterized by infrared spectroscopy. The IR spectra of hydrogen silicone oil is shown in Fig 1,and the reaction product is shown in Fig 2. Comparison of silicone oil we can see that: in the IR spectra of hydrogen in the 2156cm^{-1} in the department has a strong absorption peak of Si-H, along with the hydrosilylation reaction, Si-H absorption peaks gradually weakened until disappeared , indicating that hydrosilylation reaction between hydrogen silicone oil and dimethylaminoethyl acrylate smoothly.

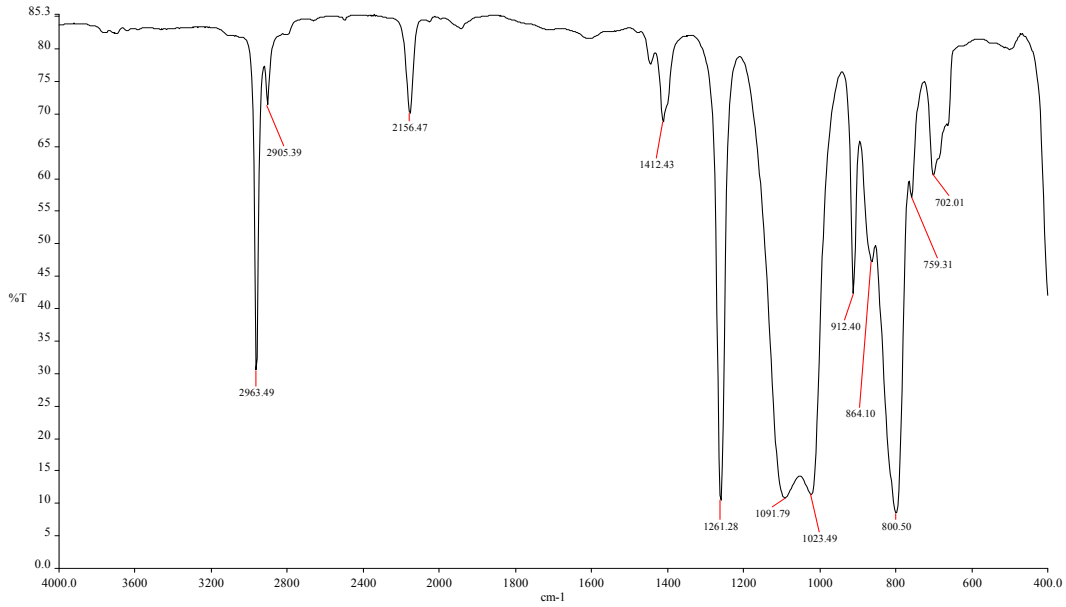


Fig.1 The IR spectrum of polymethylhydrosiloxane

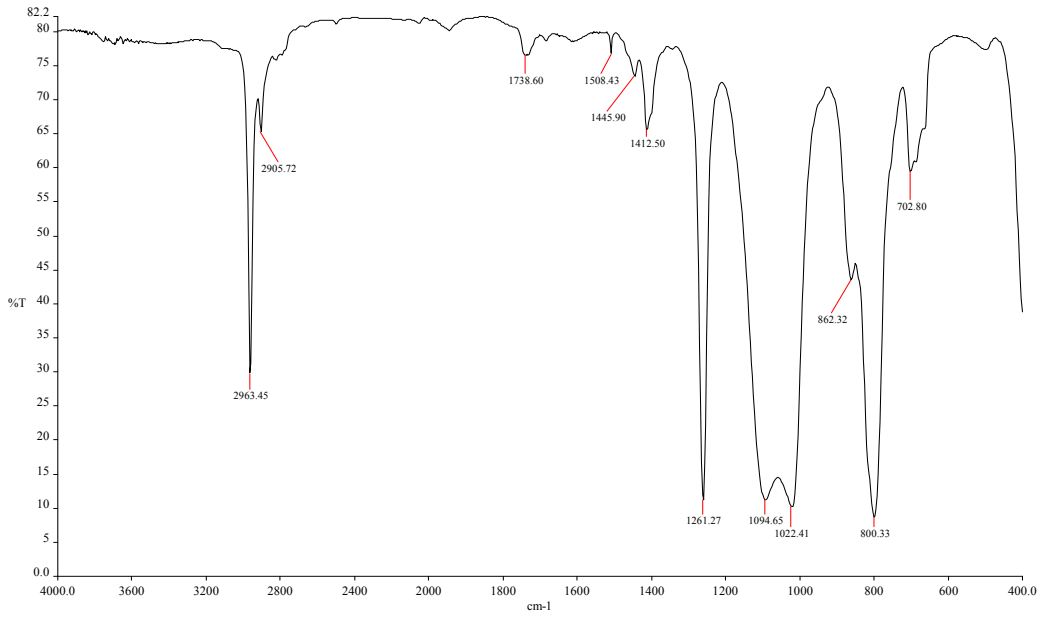


Fig 2 The IR spectrum of reaction product

Characterization of SEM on Linen Fabrics

Put the linen afer amino silicone treated into continuous stereotypes dryer, pre-baking 2min at 80 ˚C,then baking 60s at 170 ˚C, and then put them in a desiccator for 24 hours. After spraying with S-4300 Scanning Electron Microscope of HITACHI company (SEM, Scanning Electron Microscope) to observe, the SEM photographs are shown in Figure 3, Figure 4. SEM of Linen without amino-silicone are shown in Figure 3. Figure 3 is 1000 times magnification irradiation, From Figure 3 we can find, linen fiber surface is rough and uneven without finishing,and the fiber bongding closely,and the interval is uneven distributed.SEM of linen with amino-silicone finishing are shown in Figure 4, Figure 4 is1000 times magnification irradiation. It is clear that, flax fiber surface after finishing with the amino silicone oil is smooth, fiber bundles within the loose, the gap becomes uniform, so amino-silicone can increase smoothness of fiber surface. It makes the fabric has good fiber dispersion. This is the direct reason that silicone oil could produce good soft results.

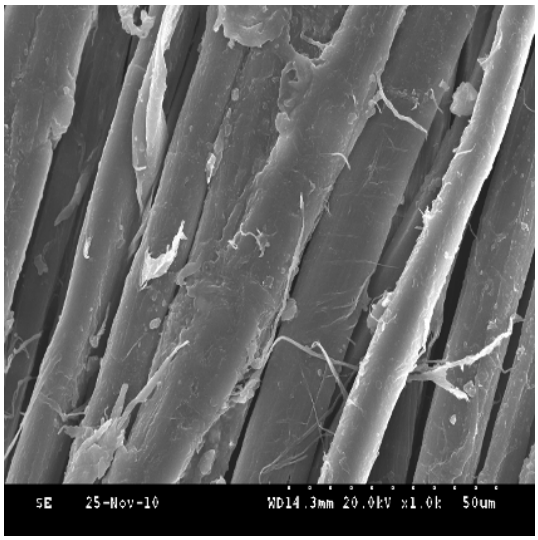


Fig 3

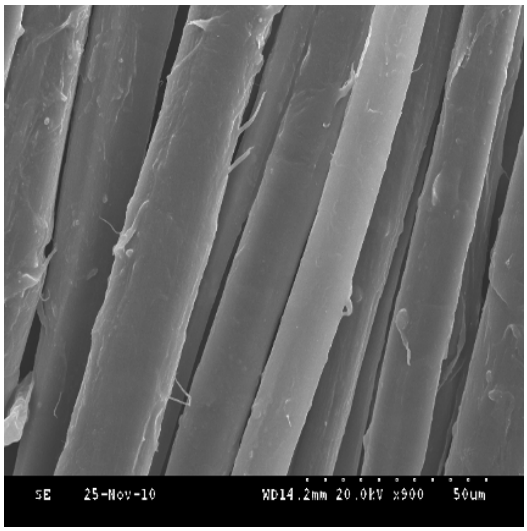


Fig 4

References

[1] Shaoyun Sun, Junfeng Li:China Textile Leader.Vol.12(2007),80-83.In Chinese.

[2] Zhenghong Luo, Xiaoli Zhan, Yongrong Yang: Fine Chemical intermediates.Vol.31 (2001).p.7-9.In Chinese.

[3] Guoqiang Chen, Xiangrong Wang, Zhanxiong Li: Textile finishing processing chemicals. Beijing: China Textile Press,2009.In Chinese..

[4] Zhong Zeng, Jihua Hu. The physics and chemistry of surfactant[. Guangzhou: South China University Press, 1995.In Chinese.

© (2011) Trans Tech Publications, Switzerland
doi:10.4028/www.scientific.net/AMR.331.394

Anti-hairfalling Finishing of Rabbit Hair Knitted Fabrics

Juan Liu [1,a], Ruoying Zhu [1,b], Yi Zhang [1]

[1]TianJin Polytechnic University, Department of Textile, 300160, TianJin

[a]823144358@qq.com, [b]ruoyingzhu@hotmail.com

Keywords: rabbit hair; knitted fabric; anti-hairfalling finishing; enzyme protein.

Abstract: The morphology of rabbit hair and wool were compared, results showed that rabbit hair was more fine and had more medulla component, imply easily to be damaged. Protease and two selfmade resins were used in order to reduce hair drops of rabbit hair knitted fabric in the study. Experiment results showed that the optimal concentration of protease was 1%(o.w.f) and the processing time was 40min. Treatment with two selfmade resins had evidently improve the anti-hairfalling with less damage to fiber, while the dosage of two selfmade resin finishes was 50g/l, the best effects of anti-hairfalling could been gain.

Introduction

Rabbit hair is a kind of precious animal fiber. It is used mainly for high-quality knitted fabrics with the performance of extremely smoothness, soft hand and excellent warmth retention.While part of this fibre drops away from the fabric in wearing process, restricting the development of rabbit hair products.

According to reports, the methods to improve anti-hairfalling properties of rabbit hair knitted fabric can be broadly divided into three categories, namely (1)Surface modification of rabbit hair by low temperature plasma; (2) Conferring fiber more curve through acid treatment; (3) Blending rabbit fibers with hot melt fibers. Although, method (1) and method (2) can increase cohesion force between fiber, usually damage the fiber and cause the fiber drop increase due to the strength loss of fiber after treatment , while method (3) was restricted for it could not been applied to pure rabbit hair fabric. In this paper, protease and two selfish made agents were employed to improve the anti-hairfalling properties of pure rabbit hair knitted fabric.

Experimental

1.1 Materials and Reagents

Fabrics used in the experiment are pure rabbit hair knitted fabrics(45tex×45tex), provided by PuNing JianFa rabbit fair knitting Co. Ltd; Esperase 8.0 L alkali protease, supplied by Novozymes Co. Ltd; Two selfmade Resins, namely resin A and resin B.

1.2 Protease treatment

Rabbit fair was pretreated by hydrogen peroxide before protease processing, the pretreatment formula:H_2O_2 (33%) 40ml/l; Sodium pyrophosphate 7.0g/l; Ammonium oxalate 3.5g/l; Temperature 60˚C; Bath ratio 1:30.

Heat the solution of hydrogen peroxide up to 60˚C→ immerse fabric into pretreated solution → kept it under constant temperature for 1h → fully wash it to remove residued liquid.

Protease processing formula: Enzyme x %; pH value 7.5; Temperature 50˚C; Processing time ymin; Bath ratio 1:25.

Rregulate enzyme solution to pH value 7.5 by Na_2CO_3 liquid, then heat up to 50˚C → immerse fabric into pretreatment solution → keep it under constant temperature according to given time → fully wash it to remove residual liquid from fabric → dry.

1.3 Resin finishing

We adopt resin A and resin B as finishes, then use silicon softener for soft finishing .Resin finishing prescription: Total liquid volume 100ml; pH value 7 ~ 8; The dosage of Resin agents (ml) according to Table 1.

Table 1 Dosages of resin finishing agent

Numbers	1#	2#	3#	4#	5#	6#	7#	8#	9#
Finishes(ml)	0	1	2	3	4	5	6	7	8

Use nonionic surfactant to wash fabrics → dip into finishing fluid (15min) → take off the liquid (20s) → dry (80˚C, 3min) → cure (175˚C, 1min).

Soft finishing process: dip into finishing solution for 15min(the volume ratio of silicon softener and total fluid is 1:20) → take off liquid (20s) → dry(80˚C, 3min) → cure(175˚C, 1min)

1.4 Dropping quantity testing

Use YG(B)401 fabric flat-ground apparatus to simulate hair-shedding environment. The testing results are given as follows:

$$W = (10 \times Wi) / (2 \times S) \quad (1)$$

W is the average hair loss of the specimen fabric per area(mg/100cm^2); Wi is the No.i specimen fabric's average hair loss(mg); S is the abraded area of the specimen(cm^2).

1.5 Test of stiffness

Stiffness is characterized by roll-out length. Add the sample(10 cm × 2.5 cm) on the top surface of slideway, then push the sample forward along the fence. Sample converges along the cantilever beam by gravity, then measure the slidding length L (accurate to mm) when the converged end contacts with inclined plane.

Results and Discussion

2.1 Analysis on the morphology of rabbit fiber

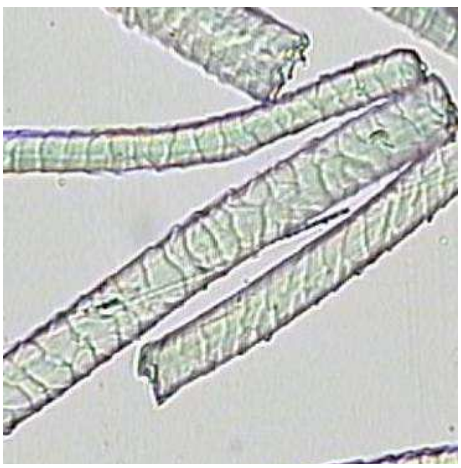


Fig. 1 The morpholory of rabbit hair

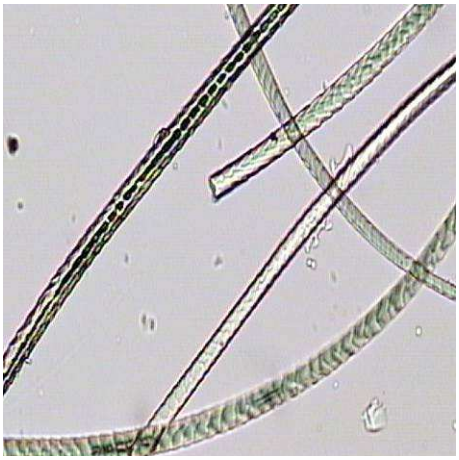


Fig. 2 The morpholory of wool hair



(a) (b)

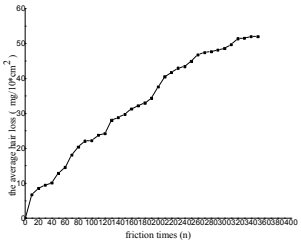
Fig. 3 The microscopic picture of rabbit fiber medulla layer

Fig.1 is the microscopic picture of rabbit hair. Compared with the wool(Fig.2), rabbit hair has lower high of scale, and the angle between the orientation of scales and fiber axial is small, most of them arrange as docking shape, this makes the surface of rabbit hair more smooth.

Fig.3(a)~(b) shows that the medulla layer of rabbit hair are composed by a rectangular cavity, and the chamber between each other isn't interlinked, causing rabbit hair has lower break force and more easier to break up during various treatment and wearing processing.

2.2 Dropping curve and Dropping rate curve

In this study we find that friction times has great influence on hair loss. From Fig.4 we can see that the hair loss increases with raising of friction times. When sanding 300 times, the slope of curve will change little and keep stable. Fig.5 shows that when fabric flat-grinded 50times, the dropping rate reaches first wave trough; Whlie flat-grinded 300 times, matching the simulation of daily wearing process, the dropping rate is very small and dropping quantity will no longer increase.



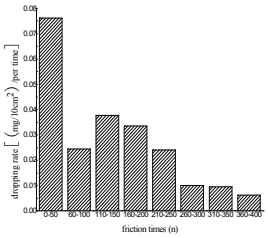
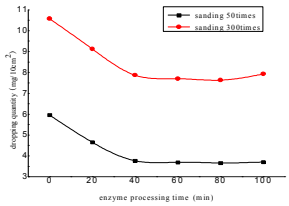


Fig. 4 Dropping curve **Fig. 5 The curve of dropping rate**

2.3Analysis on protease process

Fig.6 shows that the dropping quantity is least when the concentration is 1% (O.W.F). As the concentration increasing, the dropping quantity increase oppositely. Because etching actions make static frictional between fibers enhance, and damage the strength of fibers, lead to the dropping quantity increase. From Fig.7 we can see the effect of anti-falling reach best when treated by enzyme solution for 40min, more than that will be disadvantage to anti-hairfalling.



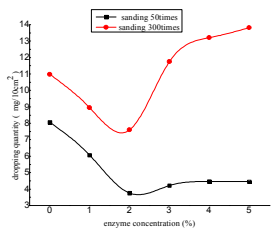


Fig. 6 The influence of enzyme on dropping quantity **Fig. 7 The influence of enzyme processing time on dropping quantity**

2.4 Analysis on the effect of resin finishing

From Fig.8 and Fig.9 we can see that when the volume of two agents are 5ml(dropping quantity decrease more than 60%), anti-hairfalling effect is the best. And over 5ml, hair loss will fluctuate because of cross-linking reactions occuring between excess fnishes. It enhances the stiffness as the latter can form soft membrane after crosslinking. In addition, the length will become small when finish agents reach a certain value, possibly due to cross-linkinged finishes over much, leding the weight increasing.

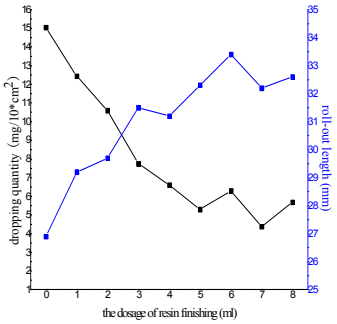


Fig. 8 The influence of resin A on dropping quantity and stiffness

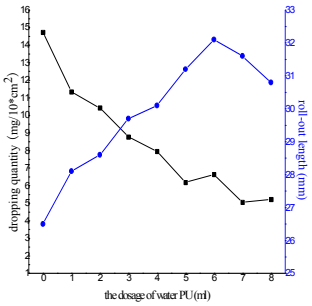


Fig.9 The influence of resin B dosage on dropping quantity and stiffness

Conclus0ions

(1) Using dropping curve and rate curve to analysis the reason why rabbit hair fabrics losing hair in different period and determine the standards of friction testing.

(2) When the concentration of enzyme is 1% (O.W.F) and processing time is 40min, dropping quantity of rabbit hair fabric is least. And the processing conditions should be controlled strictly to avoid the declining of fibers' strength.

(3) Treatment with two selfmade resins has evidently improve the anti-hairfalling properties of rabbit hair knitted. Compared with protease finishing process, this process is simple, less damage to fiber, as well as the characteristic of rabbit hair of soft, smooth and luster is well kept.

Acknowledgements

This work was financially supported by the National Rabbit Industry Technology System (nycytx-44-4-1).

References

[1] Dayin Hou, Liangfei Li, Qufu Wei. Rabbit hair low temperature plasma surface modification[J].Journal of Textile Research, 2007,28 (10) : 15-17. (In Chinese)

[2] Xiaolei Ji. Reduce rabbit hairfalling with blending technology of low melting hot melting fibers[J].Journal of Wool Textile, 1999 (4) : 17-20. (In Chinese)

[3] Shuying Sui, Ping Zhu. Studing on acid treatment to mprove the hair curly performance [J]. Journal of Textile Research, 1997, 18 (5) : 295-296. (In Chinese)

[4] Baijun Xi, Caiqian Zhang.Studying on the modification of rabbit fiber by enzyme[J]. Knitting Industry, 2005 (9) : 54-56. (In Chinese)

[5] Tsai PP Y,Roth J R: submitted to Surface Modification of Fabrics (1997)

[6] Suiju Wu: submitted to Dropping standards' determination (1997)（In Chinese）

© (2011) Trans Tech Publications, Switzerland
doi:10.4028/www.scientific.net/AMR.331.398

Effects of the Cotton Fabric Pretreatment on Application Properties of Digital Inkjet Printing with Reactive Dyes

Qian Zhu[1, a], Jianda Cao[1, b], Wang Wei[1,c], Jingcheng zhong[1,d], Jia Yao[1,e], Ying Ye[1,f] and Xinxin Yang[1,g]

[1] College of Materials and Textiles, Jiaxing University, Jiaxing Zhejiang, P.R.China 314000

[a] 371484571@qq.com,[b]dacao88@163.com, [c]zjxuwangwei@163.com, [d]782320162@qq.com, [e]yj279209319@163.com,[f]846608005@qq.com, [g]1056612606@qq.com

Keywords: pretreatment, digital inkjet printing, reactive dye inks, cotton fabric

Abstract. Cotton fabric was directly inkjet printed with reactive dye ink, the ink would appear on the permeability of the fabric, the depth of color yield is low, light fastness is poor. Pretreatment agents with different mass fractions had been used to do the pretreatment of the cotton fabric before ink-jet printing, the results showed that: when the concentration of alginate ester or seaweed was between 1.0% -1.5%, the fabrics had the high color yield and the fixation color rate of the dye was the highest. When the amount of $NaHCO_3$ was 3%, the inkjet printing effect of cotton fabrics was the best; color fastness of colors was all good. After Inkjet printing, the best effect can be achieved by steaming the cotton fabrics under the 100 ℃ saturated water vapor for 25min: the colors of black, red and yellow of the K / S value were of the maximum, color fastness was fine.

Introduction

Digital inkjet printing demonstrates the features of high accuracy, short process, small footprint, energy saving, less pollution and instantaneous response. It can meet the requirement of low-volume, multi-color and quick delivery and the style of the products can follow the fashion and meet the needs of personalization, and the fabric is suitable for the high-grade apparel and the special arts & crafts [1].Currently, one of the defects of the pigment ink inkjet printed cotton fabric is that the product has a serious bleeding, the vividness of the color is poor, and it has a poor performance of the rinsing, friction and fastness to light.

Through the modification of the hydrophilic polymer and the cation of the inkjet printing medium, the definition of inkjet printing, the vividness of the color of inkjet printing and the fastness of inkjet printing can be significantly improved [2][3].In this test, we do the pretreatment of the cotton fabric, analize the appropriate pretreatment process and its effect on the performance of anti bleed and the vividness of the color of the inkjet printing.

Test

Materials and Equipments.

Fabrics. Bleached cotton cloth

Dyestuff. Reactive inks(C,M,Y,K)

Chemical. Sodium alginate (ester),anhydrous sodium sulfate, sodium bicarbonate, sodium carbonate, carbamide (pure chemical),new alkali ESS, alkali penetrant CP105 (industrial)

Test Equipment. SPECIALCOLOE SCP1045 Digital inkjet printing machine, Q-SUN color fastness to light tester, SW-12A color fastness to washing tester, Y571Ldyeing fastness to friction tester.

Test Method. When the reactive dye inks used in digital printing, the fabric needs to be pretreated. The working liquid of pretreatment is consist of alkali, carbamide and sodium alginate. etc. The fabric undergo pretreatment can be inkjet printing only after drying, the inkjet printing fabric needs steaming to fix color.

Test Content Project

Test of the Bleed Performance

Inkjet Printing Spot. Make a picture contains 25（5×5）points which the diameter is 1cm,and print it on the no-bleeding paper by inkjet print machine, and print it on the cotton fabric full ground at the same time.

Scan. Scan the spot fabric under the 300 dpi resolution,-75 brightness and 60 contrast, obtain the image;

Image Process. Transform the spot image into gray using Image processing software Adobe Photoshop, analyse the Pixels of the blot (obtain from the histogram) and the outline of the spot sample at a certain allowance(set 20),calculate the area, warp(weft) radial length, get the average area value and the warp(weft) radial length of the blot of spot sample, treat them as the evaluation index.

The Performance of Bleeding Evaluation Index. The rate of increase of spot sample area (ΔS)and the rate of radial length of warp(weft)(ΔΦ) .

$$\Delta S=(Sf-Sp)/Sp\times 100\%, \quad (1)$$

$$\Delta \Phi=(Lf-Lp)/ Lp\times 100\% \quad (2)$$

where, Sf is the Pixels of fabric, Sp is the Pixels of paper, Lf is the length on the warp(weft), Lp is the length of paper sample.

The Admeasurement of K/S. K/S value, in criterion of the printing fabric has been steamed and washed, is determinated by Computer System in Measuring and Matching Colors, as a measure of the depth of ink-jet printed fabric dye indicators.

The Test of Color Fastness. Test rubbing color fastness, accord to GB/T 3920-1997"*Textile color fastness to rubbing and color fastness*".Test soap-washing color fastness, accord to GB/T 3921.1-1997"*Textile color fastness to washing: Test 1*".Test lighting fastness, accord to GB/T 8427-1998"*Textile color fastness to resistance to artificial light: Xenon arc*".

Results and Discussion

Fabric and Structure. Ink-jet printing technology to give full play to the color performance should be selected according to characteristics of ink-jet prints that match the fabric structure. To choose the 3 different specifications of the cotton fabric, accord to Table1, test the performance of bleeding respectively, and selected the appropriate pretreatment of cotton fabric. Fabric structure on the bleeding of the properties of the ink in Table 2.

As is apparent on the table 2, there are quite difference on three cotton fabrics, 1#, 2#, 3# significantly different from the bleeding of the situation. 3# thick compact area little loose than point-like sample 2 thin, because the thin gap between the fibers loose fabric large, Ink flow along the pores between the fibers, causing bleeding of, the phenomenon of bleeding obvious choice # 2 pretreatment of cotton fabric ink jet printing.

Table 1 Cotton Fabric Structure

Sample number	Warp density /R·10cm^{-1}	Weft density /R·10cm^{-1}	Quality /g·100^{-1}·cm^{-2}
1#（Twill）	421	285	283.5
2#（Satin）	324	265	175.6
3#（Plain）	523	325	385.3

Table 2 The ink of bleeding properties in different fabrics

Sample number	Point-like area of the increase rate/%	The increase rate of the length on the warp/%	The increase rate of the length on the weft/%
1#（twill）	22.5	16.7	14.6
2#（satin）	46.7	33.2	28.9
3#（plain）	13.5	5.8	3.7

The Amount Sodium Alginate and Cotton Fabric Quality of Inkjet Printing. In the *Test Content Project*, add sodium alginate (ester) (0.5%, 1%, 1.5%, 2%), pretreatment of the fabric, of sodium alginate (ester) was added to the cotton fabric inkjet printing quality, the results in Table 3.

Table 3 Sodium alginate (ester) on the quality of digital inkjet printing

Sodium alginate (ester) amount/%		0.5	1	1.5	2
Viscosity/Pa·s		1.121	1.224	1.278	1.331
K/S	Black	20.53	21.41	21.52	18.46
	Red	18.45	19.23	19.42	18.61
	Yellow	18.18	18.92	19.58	18.45
dry rubbing fastness/ degree		5	5	5	
fastness to wet rubbing/ degree		3~4	3~4	3~4	3~4
soaping fastness/ degree		5	5	5	5
light fastness/ degree		3	3	3	3

As can be seen from the Table.3 that paste viscosity will increase with more sodium alga acid (a kind of ester) has been used. That explain to a certain extent sodium alga acid can promote paste viscosity. Color yield is high when the concentration of Sodium alga acid or Algae acid ester varies from 1.0% to 1.5%. Solid color rate of dyestuff can reach the largest when K/S number is high, but when K/S number is too high or to low, solid color rate will be low.

The Dosage of Sodium Bicarbonate and Quality of Ink-jet Printing. Reach on the effect that the dosage of sodium bicarbonate have on the quality of ink-jet printing of cotton fabric when the dosage of sodium bicarbonate changed. Table 4 gives the result.

Table 4 The effect that sodium bicarbonate have on the quality of ink-jet printing

$NaHCO_3$/%		2	3	4	5	6
viscosity/Pa·s		1.137	1.213	1.221	1.227	1.213
K/S	Back	20.63	21.74	20.85	20.79	19.61
	Red	18.19	21.48	21.59	21.61	21.45
	Yellow	16.62	18.52	18.89	19.19	18.67
dry rubbing fastness/ degree		5	5	5	5	5
fastness to wet rubbing/ degree		3-4	3-4	3-4	3-4	3-4
soaping fastness/ degree		5	5	5	5	5
light fastness/ degree		3	3	3	3	3

As can be seen from the Table 4, with the dosage of sodium bicarbonate increasing the paste viscosity firstly increases and then decreases. And the paste viscosity reach the largest when the dosage of sodium bicarbonate is 5 percent. With the dosage of sodium bicarbonate increasing Black K/S number has a tendency of firstly increasing and then decreasing. The K/S number reach the largest when the dosage of sodium bicarbonate is 3 percent, but at the same time the red or yellow K/S number dosen't change a lot. To a certain extent, thechanging of dosage of sodium bicarbonate dosen't obviously influence the colour fastness.

Size can be partly dissolved by alkaline solutions leads to decreasing of its viscosity[4]. Because $NaHCO_3$ have a lower alkalinity than Na_2CO_3, size would be slightly dissolved by $NaHCO_3$ and viscosity has a low decrease. The dosage of sodium bicarbonate decided the PH number, and PH number is one of the crucial factors that affect the final color yield. The dosage of sodium bicarbonate is too low would lead to a low PH number, then very little cellulose anion would lead to a low solid

color rate and a low color yield. On the other hand the dosage of sodium bicarbonate is too high would lead to a high PH number, then a lot of cellulose anion would lead to hydrolysis of reactive dye. So when the dosage of sodium bicarbonate is 3%, the k/s number is appropriate, every kind of fastness is fine, at the same time it is also very economical.

The steaming time and cotton fabric inkjet printing. Pretreated cotton fabric according to *Test Content Project*, pretreatment program, after inkjet printing, we spend different steaming time (15,20,25,30min)to fix color and then study steaming times' influence on the quality of cotton fabric's inkjet printing. The result is as shown on the table 5.

Table 5 Steaming times' influence on the quality of cotton fabric's inkjet printing

Steaming time /min		15	20	25	30
K/S	Back	20.65	21.09	21.98	20.89
	Red	12.51	18.19	22.25	19.29
	Yellow	9.78	19.13	19.71	19.23
dry rubbing fastness/ degree		5	5	5	5
fastness to wet rubbing/ degree		3-4	3-4	3-4	3-4
soaping fastness/ degree		5	5	5	5
light fastness/ degree		3	3	3	3

Table 5 shows that when steaming time is 15 min, all colors get smallest K/S and the most shallow, As steaming time increased, K/S shows the tend that goes up first an then does down. When steaming time gets up to 25 min, all K/S get largest.

Steaming time is one of the main factors that influence the quality of printing [5]. When do steam, the reactive dyestuffs come fully into the fiber, and connect the fiber by the covalent key bond, finally fix on fibers under the effect of water and heat .If steaming time is too short, covalent bond reaction is not complete, and fix color reaction between cotton fibers and reactive dyestuffs is not complete, and color yield gets low. Along with the increase of steaming time, fix color reaction gradually be completed, the fabric color depth is improved significantly. But if steaming time is too long, part of the reactive dyestuffs hydrolyze, then carbamide will be decomposed into ammonia and biuret products. and then the reactive dyestuffs react with ammonia ,at the loss of alkali agent also lead to the decrease of the color yield. So, when steaming time is 25 minute, it not only can reach the appropriate K/S number but also has a batter color fastnesses.

Conclusions

The fixation rate can reach the highest when the concentration of Sodium alginate or algae acid vary from1.0% to 1.5% .When the dosage of NaHC03 is 3%, the effect of cotton fabric inkjet printing gets the best and the color fastness appears well. After the Ink jet printing, the best effect can be achieved by steaming the cotton fabrics under the 100 ℃saturated water vapor for 25min: the colors of black, red and yellow of the K / S value were of the maximum, color fastness was fine.

Acknowledgements:
This work was financially supported by the college students of Zhejiang province technological innovation activities project, item NO.851910128Z

References

[1]Kuanjun Fang:Printing and dyeing.Vol.18(2006)p.44(in Chinese)

[2]Kuanjun F,Shaohua W,Chaoxia W:Journal of Applied Polymer Science.Vol.107 (2008) , p.2 949

[3] Chunming Z, Kuanjun F, Shaohua W,edc: Printing and dyeing.Vol.13(2008),p.5(in Chinese)

[4] Jiaju W:Printing and dyeing.Vol.1(1993),p.46(in Chinese)

[5] Xiaofang L, Haiyu X: Printing and dyeing.Vol.3(1999),p.21(in Chinese)

© (2011) Trans Tech Publications, Switzerland
doi:10.4028/www.scientific.net/AMR.331.402

Preparation and Application of VE Microcapsules with Polyurethane Shell for Skin-care Textiles

Guoping Yao[1, a], Jinhuan Zheng[1, 2, b], Huifen Chen[1, c]

[1]Key Laboratory of Advanced Textile Material and Manufacturing Technology, Ministry of Education of China, Zhejiang Sci-Tech University, Hangzhou 310018, China

[2]Engineering Research Center for Eco-Dyeing & Finishing of Textiles, Ministry of Education, Hangzhou 310018, China

[a]yaogp2011@yahoo.cn, [b]hzzjh1968@163.com, [c]07131301@163.com

Keywords: Vitamin E, Polyurethane, Microcapsule, Skin-care finishing.

Abstract. Vitamin E (VE) microcapsules with polyurethane (PU) shell are successfully prepared via interfacial polymerization of polyurethane with toluene-2,4-diisocyanate (TDI) as the isocyanate, polyethylene glycol as the polyol, and 1,4-butanediol (BD) as the chain extender. In the preparation process, VE emulsion, prepolymer and microencapsulation of VE are studied using a particle size analyzer, butylamine titration, optical microscopy (OM), scanning electron microscopy (SEM), and transmission electron microscopy (TEM). Based on the present research, VE microcapsules prepared have smooth surfaces and spherical appearances, the mean particle size of about 550 nm. Vitamin E microcapsules have been glued effectively to textiles, and a kind of skin-care product has been developed.

Introduction

Vitamin E is a kind of staple medicine and dietary supplement, a majority of physiological functions of which have been well recognized, such as remarkable antioxidant efficacy, eliminating the internal free radicals [1]. The nature of VE is very unstable, when exposed to the air, the phenolic hydroxyl group of VE structure is oxidized susceptibly and has no longer biological activity. It causes the limitation of VE in practical application. It is necessary to remain the stability of VE in the skin-care finishing process of textiles and during wear. The effective way is to wrap up the sensitive part of VE molecule so as to keep it from contacting with air, for example, microencapsulation [2], transforming it into its derivatives by modifying its structure such as VE acetate [3] and VE linoleate [4].

The ways of microencapsulation include interfacial polymerization, in-situ polymerization, coacervation, spray drying, etc. The selection of the technique and shell material depends on the final application of the product, considering physical and chemical stability, concentration, desired particle size, release mechanism, and manufacturing costs.

This paper investigates microencapsulation of VE by interfacial polymerization of PU in an aqueous emulsion and application of VE microcapsules on textiles.

Experimental

Materials. VE acetate was offered by Zhejiang Xinhecheng CO., LTD. Toluene-2,4- diisocyanate (TDI) was purchased from Hangzhou Huipu Chemical Industry and Instruments CO., LTD. Polyethylene glycol with molecular weight of 400 (PEG-400) was obtained from Shanghai Pudong Gaonan Chemical Industry and dried at 80˚C under vacuous atmosphere for 2 hours . Dibuthyltindilaurate (DBTDL) was used as the catalyst, and 1,4-butanediol (BD) was used as the chain extender. Tween-20, Tween-80, A-980, OP-10 and SLS were employed as emulsifier. Silk fabrics and absolute alcohols (99.9%) were supplied by Zhejiang Sci-Tech University. The binder, Superprint 101, was obtained from Shanghai Yuhui Chemical Industry CO., LTD.

Preparation of Prepolymer and Microcapsules

Prepolymer Synthesis. The prepolymer of polyurethane is synthesized as a constituent material for the microcapsule shell. It is formed by the reaction of 1.96g PEG-400 and 1.79g TDI. The PEG-400 dissolved into acetone was mixed with TDI in a 250ml round-bottom flask. The mixture was then suspended in 50˚C oil bath for 2h and agitated using a mechanical stirrer. The prepolymer formed was next used for interfacial polymerization.

Microcapsules Preparation. At ambient temperature, the prepolymer was mixed uniformly with the acetone solution including 3.00g VE and 3.26g nonionic surfactant (Tween-80) in a flask with three necks. O/W emulsion was formed by pouring slowly 100ml deionized water into the flask and mixing well. After going up to 60˚C, BD as the chain extender was added dropwise to the aqueous phase. DBTDL as the catalyst was added into the O/W emulsion. Polyurethane microcapsules were fabricated containing VE after a reaction time of the subsequent 60 min. The suspension of microcapsules was centrifuged with the absolute alcohols as a deemulsifier and washed with 30% ethanol aqueous solution to remove unreacted TDI and free VE on their surfaces. The resultant microcapsules were air-dried for 24h.

Padding of Microcapsules on Textiles

The textiles were padded with the bath containing microcapsules and the binder. The conditions set for the procedure are presented in Table 1.

Table 1. Conditions of Textiles Padding Process

Finishing conditions	
Fabric	Silk
Mode of treatment	double-dip-double-nip
VE microcapsules	50~60 g/L
Superprint 101 (binder)	40 g/L
Preliminary drying conditions	80˚C, 5min
Baking conditions	120˚C, 2min
Pick-up	80-120%

Characterization Techniques

Particle Size Distribution and Mean Particle Size. The particle size distribution of VE emulsion and microcapsules dispersed in deionized water were analyzed by laser dispersion using a LB-550V instrument (Horiba Instruments Inc., Japan).

Scanning Electron Microscopy (SEM). Morphologies of the microcapsules and textiles padded with microcapsules were observed by SEM (ZEISS Ultra-55, Germany), operated at 1\2 KV.

Titration of NCO Content in the Prepolymer. 1.00 g of the synthesized prepolymer was added into a 250ml Erlenmeyer flask with a stopper. The prepolymer was dissolved in 10ml dry toluene. Di-*n*-butylamine solution (10ml, 0.1N) was added using a pipet. After swirling for 5 min, isopropyl alcohol (50 ml) and bromphenol blue indicator solution (4-6 drops) were added. The titration was performed with hydrochloride acid standard solution (0.1N) to a yellow end point. The blank test was done. The NCO content is calculated according to the Equation 1.

$$\mathrm{NCO}/\% = \frac{\left[\left(V_0 - V_1\right) \times N \times 0.042\right]}{W} \times 100 \qquad (1)$$

where V_0 and V_1 (both in ml) are the volumes of HCl for titration of the blank and the prepolymer, respectively, N normality of HCl, and W grams of prepolymer.

Results and Discussion

Emulsification of VE in the Aqueous Phase

Effects of Emulsifier Types on VE Emulsion. In the preparation of microcapsules via interfacial polymerization, the attainment of the desired size and distribution depends largely on the emulsifying process of core materials, including formation of oil drops, emulsification and stability. Tween-20, Tween-80, A-980, and OP-10 were used for preparation of VE emulsion in the dosage of 3% of total system at ambient temperature. As can be seen from Table 2, compared with the others, emulsification effect of Tween-80 is best and the mean particle size is 79.3nm.

Table 2. Mean particle size (D) of emulsion

Emulsifier type	Tween-20	Tween-80	A-980	OP-10
D/nm	157.2	79.3	131.6	141.9

Effects of Tween-80 Concentration in the Aqueous Phase on VE Emulsion. Emulsifier dosage has a remarkable impact on emulsification. That means it should be done to ascertain the optimal emulsifier dosage. In Figure 1, the mean particle size of emulsion decreases gradually with increasing of Tween-80 concentration and this change is not very obvious when up to 3%. So the optimal emulsifier dosage is 3% (in the system).

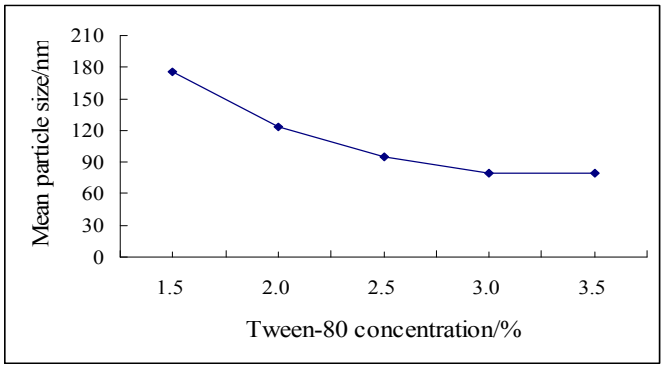
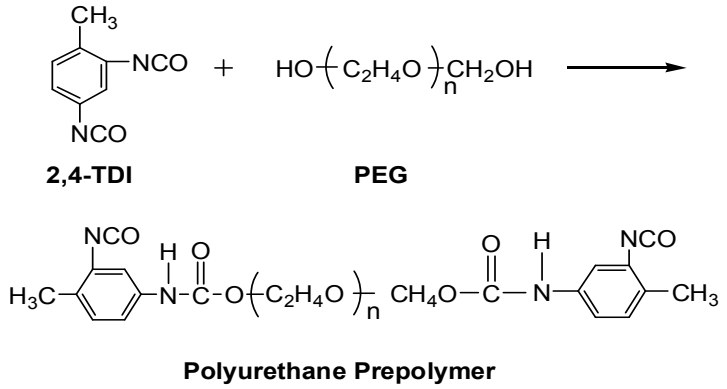


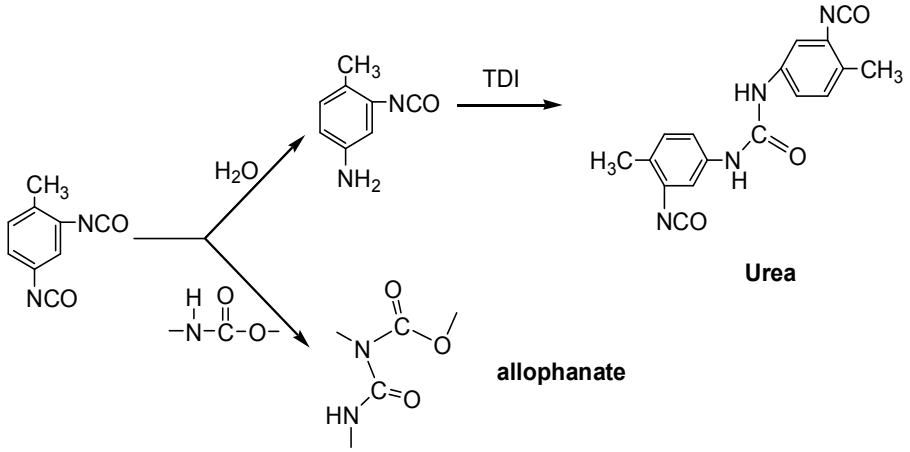
Figure 1. Mean particle size of VE emulsion.

Prepolymerization of Polyurethane

Influence of isocyanate structure on reaction activity is reflected in two aspects: inductive effect and steric effect. 2,4-TDI is an aromatic diisocyanate that includes two NCO groups, *ortho*- and *para*-NCO, which have an inducement with each other to make reaction activity of the isocyanate increase. Furthermore, the reactivity of the isocyanate group in the *ortho* position with active hydrogen is approximately 12% of the reactivity of the *para* position because of steric effect caused by the methyl group. In addition, after one of the isocyanate reacts, the reactivity of the other drops because of weakening of the inductive effect [5, 6]. The selective reaction of the diisocyanate is an essential condition for synthesis of polyurethane prepolymer. A representative synthesis route is shown in the supporting information (Scheme 1). However, side reactions of isocyanate with water and urethane may take place and form some crosslinking, byproduct including urea and allophanate (Scheme 2) [7]. In order to improve the utilization rate of isocyanates, in the case of 50˚Cand mechanical agitation, prepolymerization is carried out by TDI and PEG-400.



Scheme 1. Prepolymerization of polyurethane.



Scheme 2. Side reaction of isocyanate.

The NCO content in the prepolymer versus time was measured using butylamine titration and the result is presented in Figure 2. Along with the reaction time, the content of NCO decreases, when more than 2 hours, the reaction approaches the end of prepolymerization (10.08%) and is stopped for the purpose of preventing the occurrence of side reactions.

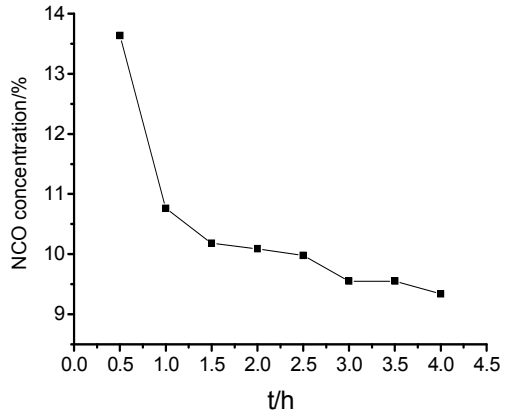


Figure 2. Titration of NCO content in the prepolymer.

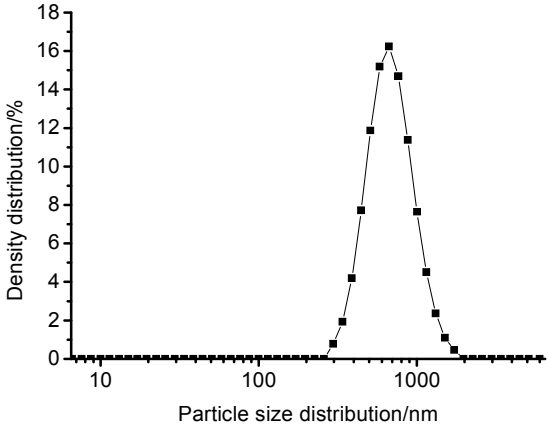


Figure 3. Particle size distribution of microcapsules solution.

Characterization of Microcapsules Performance

Particle Size Distribution. Figure 3 shows that the particle size distribution of microcapsules prepared in the study is in 0.26~2μm, the mean size 0.582μm, which meet the requirements of the textile finishing that is generally less than 5μm. Theoretically, for such a small mean particle size, the binders can more effectively affix them on fibers.

Microcapsules Morphology. The resultant samples have been observed using SEM, the results shown in Figure 4. Microcapsules have smooth surfaces and good spherical appearances, and the particle size is small and even. The result complies with laser dispersion analysis.

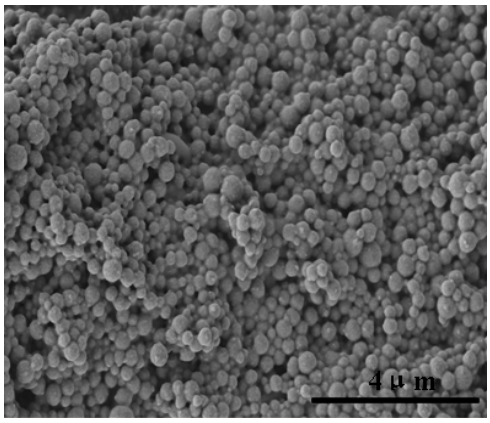


Figure 4. SEM micrograph of microcapsules.

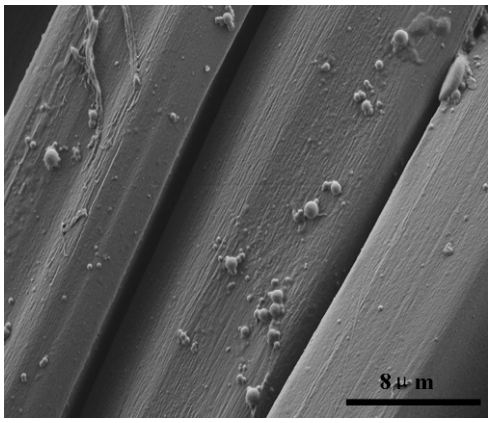


Figure 5. SEM photo of fibers finished with VE microcapsules solution.

State of Microcapsules on Textiles. Fabrics padded with microcapsules solution have been analyzed by FESEM. As shown in Figure 5, spherical microcapsules can be evenly distributed on the fibers, and they have a nano size so as to adhere effectively securely to the surface of the fibers.

Conclusions

VE have been successfully microencapsulated with polyurethane (PU) shell synthesized with TDI and PEG-400 as monomers via interfacial polymerization. Good performance of emulsion can be achieved when Tween-80 serves for the emulsifier and the dosage of which is 3%. Prepolymerization of polyurethane is finished at 50˚C for 2 hours. VE microcapsules have smooth surfaces and spherical appearances, the mean particle size of about 550 nm. Vitamin E microcapsules are glued successfully to textiles by the binder Superprint 101.

References

[1] Block G, Langseth L: Food Technology, No.7 (1994), p. 80-84

[2] H G Tang, W S Xia, in Chinese: Journal of Cereals and Oils, No.3 (2005), p. 7-9

[3] Bulychev E Y: Pharmaceutical Chemistry Journal, Vol. 32, No. 6 (1998), p. 331-332

[4] Horie M, Vitamin E Linoleate, JP 57,193,473. (1982)

[5] Aneja A, Wilkes GL, Rightor EG: J. Polym. Sci. Part B. Vol. 41(2003), p. 258-68

[6] Smith CH, Petersen CA: SPE. J. Vol. 18(4) (1962), p. 455-9

[7] S. Desilets, S. Villeneuve, M. laviolette, M. Auger: J. Polym. Sci. Part A. Vol. 35 (1997), p. 2991-8

© (2011) Trans Tech Publications, Switzerland
doi:10.4028/www.scientific.net/AMR.331.407

Preliminary study on the green anti-counterfeiting printing materials

Yan YANG[1,a] , Xiao-Hui ZHOU[2,b] , Ge ZHAO[3,] , Xiao-Ping LU*

[1]Gold Mantis School of Architecture and Urban Environment, Soochow University, Suzhou 215123, China

[2] Gold Mantis School of Architecture and Urban Environment, Soochow University, Suzhou 215123, China

[3]Gold Mantis School of Architecture and Urban Environment, Soochow University, Suzhou 215123, China

*(Corresponding author) Gold Mantis School of Architecture and Urban Environment, Soochow University, Suzhou 215123, China

[1]Email: yanyan8067@126.com [2]Email: zxhsjzgc@163.com [3]Email: xiaoge7908@163.com *Email: szlxp@yahoo.com.cn

Key Words Rhododendron simsii, fluorescence pigments, fluorescence ink.

Abstract By using DiaionHP-20 and SephadexLH-20 to isolated and purify the pigment of *Rhododendron simsii*, a high concentration of fluorescent substances from plant organs was obtained, and then study on the anti-counterfeit marking test was carried out. The result reveals that though extracting the pigment in the petals by SephadexLH-20, 5 different fluorescence regions can be clearly seen, of which the yellow-green region was the most obvious one. Fluorescent pigment from plant organs is plant secondary organic metabolites which have non-toxic, non-radiation matters to human. Thus the deeper research of the fluorochrome from plant organ could not only be used in the antibacterial activity of fresh food preservation aiming at preventing the abuse of chemical preservation substance, but also develop a new type of anti-counterfeit printing materials---natural water-based fluorescent ink, and the result brings business opportunities to the new industry of "green anti-counterfeit printing".

Introduction

Plant-derived fluorescent pigments refer to hetero-polycyclic compounds or flavonoids ones in plants. After being illuminated by ultraviolet ray, they can send out different wavelengths fluorescence. Being different from chemical synthesized fluorescent dyes or pigments, plant-derived fluorescent pigments are secondary metabolism organics, which have non-toxic, non-radiation matters to human. According to the difference of those organics in stimulating lights, they can be divided into spontaneous fluorescent ones and induced ones. The former such as chlorophylls et hetero-polycyclic compounds, will send out red fluorescence after being illumined by ultraviolet ray[1]; the fluorescent groups sent out from the latter, like flower pigments et flavonoids compounds, will send out blue or yellow fluorescence after being illumined by

ultraviolet ray. The petals of many ornamental plants is not only containing some pigments of different colors (cyanine, carotenoids, betains ect.), there still exists some kind of pigment precursors such as flavonoids compounds, most of which are colorless or flaxen under visible light circumstance, while these precursors will send out visible fluorescence when their electronics move from one layer to another with 254 nm ultraviolet ray lighting.

At present, there is no coverage about the techniques of extraction fluorescent materials from plant with high productivity and high purity. And environmental printing is adjusting and leading the development of global printing industry with strong influence. In recent years, environmental ink is being started to be applied for the printing of packing materials in food, drugs and other products. Generally speaking, its usage range is extremely limited, especially affected by the impact from more and more fierce competitions in printing market [2]. We extracted fluorescent pigments from petals leaching extract liquid of *rhododendron*, obtained high concentration of plant-derived fluorescent materials, and carried out preliminary experiments on anti-counterfeiting marking application by employing its environmental-production, concealment, security and other valuable merits. It is highly hoped that this study will bring new materials and initiated business opportunity for environmental anti-counterfeiting printing industry.

Materials and Mthods

1.1 Experimental Materials

Rhododendron simii petals were collected from Dushu lake campus, Soochow University, Suzhou City, Jiangsu Province, China. These fresh petals were firstly stoved in dryer with 35±1˚C temperature condition, then stored in drying-oven for further treatment and study.

1.2 Experimental Reagent and Equipments

Macroporous adsorption resin DianionHP-20(Japan), SephadexLH-20(Sweden), 10% formic acid solution, 95% ethanol, eluent Ⅰ (formic acid: ethanol=5:95), eluent Ⅱ (formic acid: ethanol: distilled water=5:50:45), ultraviolet analyzer (U-3000, HITACHI), WD-9403F ultraviolet instrument (Beijing, China).

1.3 Experimental Methods

1.3.1 Extraction of fluorescent pigments

Firstly, 150g rhododendron petals were taken out from previously preservation, then added 1000ml 10% formic acid. After 24 hours leaching and extracting under room temperature, the leaching extract liquid was filtered, then diluted with 1 time volume 10% formic acid solution. After being washed with 3000ml distilled water, the macroporous adsorption resin DianionHP-20 chromatography column was used to process the diluents, then eluted these pigments in chromatography with elution Ⅰ.

Secondly, the pigment liquid was collected, processed under reduced pressure concentration condition where the water temperature was controlled between 33˚Cand 37˚C and collected again. Then, the collected and concentration liquid was dissolved with 10% formic acid solution, chromatographyed with SephadexLH-20 column, and eluted with elution Ⅱ.

Finally, by observing the movement of pigments in chromatography column with 365nm wavelength ultraviolet ray lighting, we collected different kind of fluorescent pigments step-by-step till they moved to the cylinder exit, and at last gained plant-derived fluorescent pigments.

1.3.2 High efficient liquid chromatography test

Using 10ul the sample on separated liquid of fluorescent pigments carries out the HPLC analysis. Instrument: DGU-20-A3/LC-20AD; Condition for analysis: employing Cosmosil 5C18

column (length 250mm×diameter 4.6nm), mobile phase A: 10% formic acid solution; B: 10% formic acid + 40% acetonitrile + water; gradient eluention range: 0 ～40 min， from(80% A + 20% B) to(15%A＋85%B); 41～60 min; from(80%A＋20%B)to (80%A＋20%B).Test wavelength: 360nm, velocity is 1.0ml per minute.

1.3.3 Experiment on anti-counterfeiting mark

Taking out a slight of washing out liquid with yellowish green fluorescent pigments, dotting it on circular filter, observed the color of pigments on filter in visible light, and then observing the fluorescence effect when the filter was put in ultraviolet instrument.

Results and analysis

2.1 Spectral analysis of yellowish green fluorescent materials

After being processed by macroporous adsorption resin chromatography column, these pigments, in rhododendron petals leaching extract liquid, formed a clear pigments distribution zone in mobile phase. This zone was collected, concentrated and then separated by SephadexLH-20 chromatography column. Then flavonoids materials, which had different fluorescence effects, were collected step-by-step under ultraviolet ray condition. Using the high performance liquid chromatography column analyze the washing out liquid, which was processed by SephadexLH-20 chromatography column. The result shows that, there is one main peak and eight small peaks, each one's time of outflow and ratio are showed as Table1, Fig.3.

Table 1 HPLC analysis of yellowish green fluorescent pigment

	1	2	3	4	5	6	7	8	9
efflux time (min)	14.61	18.48	19.63	20.03	20.46	22.67	23.83	26.23	31.53
proportion(%)	6.59	14.90	8.45	3.30	2.35	2.08	49.39	8.63	4.29

The result shows that the yellowish green fluorescent materials in rhododendron are well being separated and purified after being processed by SephadexLH-20 chromatography column.

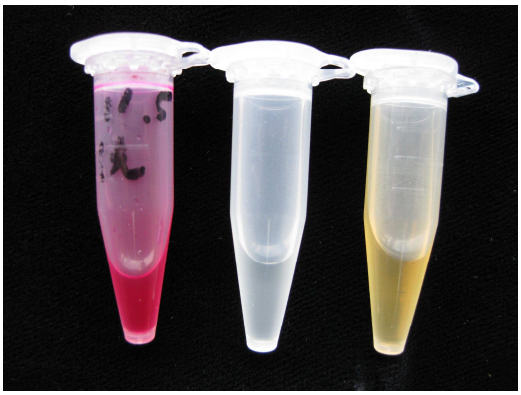


Fig.1. Fluorescent effect in visible light

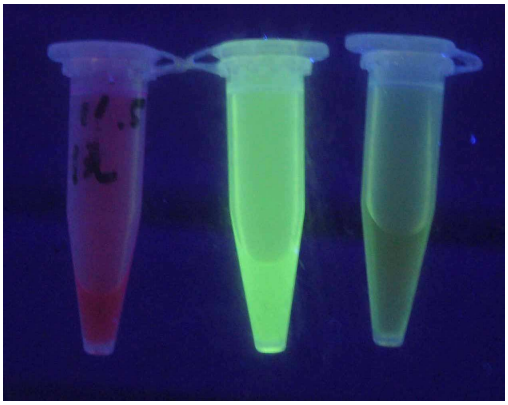


Fig.2. Fluorescent effect in ultraviolet ray

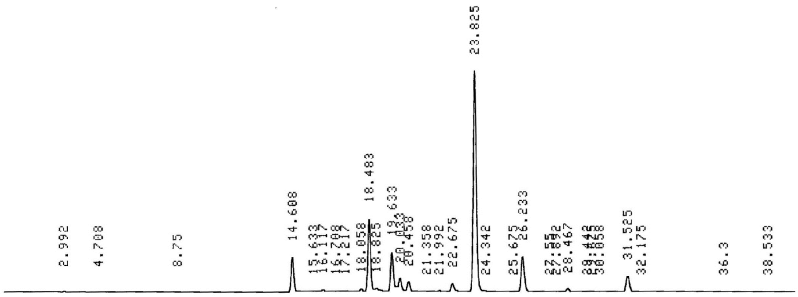


Fig.3. Pigment figures being processed by glucanLH-20

2.2 Anti-counterfeiting mark experiment

When yellowish green fluorescence pigments were dotted on paper-based materials, the spots were almost invisible in nature light. However, when presented under ultraviolet ray condition, a bright fluorescent spots was clearly revealed(Fig.4). Therefore, plant-derived fluorescent pigments can be tried and developed as a new kind of anti-counterfeiting mark printing materials.

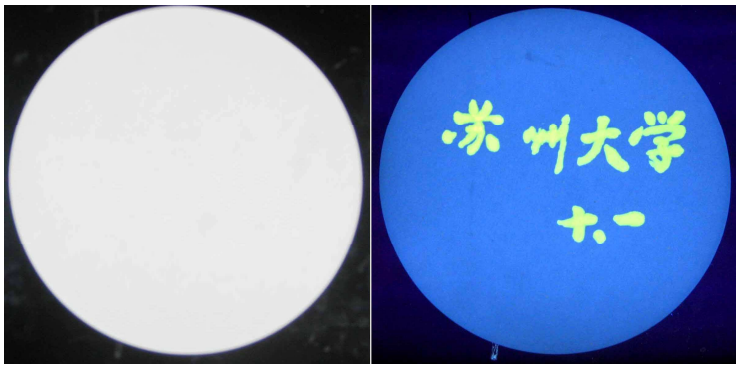


Fig.4. Fluorescence effect of yellowish green pigments in filter (left: in visible light; right: in ultraviolet ray)

3 Discussions

3.1 Extraction and appraisal of fluorescent pigments

There are many reports on rhododendron pigments studies to date. Li et al. (2008) did preliminary study on *alpine rhododendron* flower pigments species by means of flower pigments characteristic coming out reaction and ultraviolet absorption of light chromatography. Li et al. (2008) detected five kind of anthocyanin and eight kinds of flavones in *Yinghong rhododendron*. In their study, they used high efficient liquid chromatography—photoelectric diode array detection technology and high efficient liquid chromatography—electro spray ionization—mass spectrometry. However, they didn't analyze flavonoles class materials, which have the specialty of fluorescence. In our experiment, the method of extraction fluorescent pigments from *rhododendron* petals was improved. The result shows that, after using plant petals as the experiment object, leaching and extracting these pigments from the petals in 10% formic acid solution for 24 hours, and processing it by macroporous adsorption resin DianionHP-20, water-soluble distracters was removed (such as proteins, carbohydrates, organic acids ect.) in leach extract liquid. Then we chromatographied the liquid by glucanLH-20, these plant pigments were separated efficiently in chromatography column, especially those flavonids substances. In ultraviolet ray, there were different areas of which could be

seen clearly. We collected different color and luster fluorescent compounds step-by-step in order to get fluorescent pigments with quite high concentration and purity. By using the high efficient liquid chromatography method to analyze those petal leaching and carry liquid processed by macro porous adsorption resin chromatography column and yellowish green fluorescent substances, we make a conclusion that those pigments were separated and purified quite well. But that which kind of substance these kind of fluorescent pigments belonged to was still unknown. It remains to be further studied.

3.2 Concealment of fluorescent pigments and anti-counterfeiting ink

With the development of advanced printing technology and the impact of famous quality products coming from fake and inferior products, anti-counterfeiting technology has aroused more and more concern in printing and packaging industry. Therefore, it calls for a much higher requirement on the anti-counterfeiting technology of tickets. Anti-counterfeiting ink is being widely used as printing materials for it is the simplest printing material, good concealment, easy to be examined in anti-counterfeiting technology. Fluorescent ink is used in stamps, passports, the expo tickets, ID numbers, and tax marks of national unified bill and other anti-counterfeiting printings.

These kinds of ink printings are invisible when there is no light, so it won't affect the overall appearance of its picture. Besides, its concealment is perfectly well, when it is illuminated by ultraviolet ray, its fluorescent secret mark will then show up, so it can be used to identify whether the item is authentic or fake. Unfortunately, those anti-counterfeiting ink printings are mainly derived from chemical process synthesis, especially by in comporting heavy metals —Zinc (Zn)，copper (Cu), manganese (Mn), sulfide and rare earth oxides, which brings hidden danger for environmental protection. And this hidden danger cannot be underestimated. While, in our experiment, the obtained plant-derived fluorescent pigment belong to secondary metabolism organic materials. They contain non-toxic, and non-radiation matters to both human and the environment. What's more, in visible light they are colorless, while in ultraviolet ray they turn up evident fluorescence. If this pigment could be further studied, it is hoped that a new kind of "green" printing materials—which has those merits of low carbon, energy-saving, environmental and high efficiency—will turn up. Undoubtedly, it will bring a good development prospect for anti-counting printing industry.

Reference

[1] Li B T, Wang X, Li X J. The Applications of Macroporous resin in natural products separation [J]. The application Chinese Traditional and Herbal Drugs, 1990, 21(8) :42

[2] Liu L. leading the new trend in the green printing with environmental ink. China Printing Materials Business, 2008,12:34-36

[3] Li L, Xiao J Z, Li Z B et al . Preliminary studies on the components and stability of flower pigments of *Rhododehdron hybridum* [J], Journal of Agriculture University of Hebei, 2009，32（6）：47-51

[4] Li C H, Wang L S, Shu Q Y et al. Pigments Composition of Petals and Floral Color Change During the Blooming Period in Rhododendron mucronulatum [J], Acta Horticulturae Sinica, 2008,35(7):1023-1030

[5] Chen M, Yin S J, Anti-counterfeit Printing Technique and Chemistry. Journal of Chemical Education,2008,2:1-5

[6] Wang N Y. Screen Printing (2003)

[7] Bao X C. Printing Technology of Publishing and commercial printing （2003）

[8] Zhang W R, Z S S, Printing Technology of Publishing and commercial printing （2001）

[9] Ma J T, Screen Printing (2006)

© (2011) Trans Tech Publications, Switzerland
doi:10.4028/www.scientific.net/AMR.331.412

Morphology and Properties of PET Fabric Finished by β-Cyclodextrin and Citric Acid

Yunli Wang[1, a], Weilin Xu[1, 2, b, *], Ying Wang[2], Yuanming Wu[2], Shan Cheng[2]

[1]College of Textiles, Donghua University, Shanghai 201620, PR China

[2]Key Laboratory of Green Processing and Functional Textiles of New Textile Materials, Ministry of Education, Wuhan Textile University, Wuhan 430073, PR China

[a]wangyunli002@163.com, [b]weilin-xu@hotmail.com ([*]Corresponding Author)

Keywords: PET, β-Cyclodextrin, Citric Acid, Morphology, Hydrophilic Property, Antistatic Property.

Abstract. Polyethylene terephthalate (PET) fiber is a kind of widely used textile fiber due to its some desirable properties. However, it limited its application in clothing because of poor hydrophilic property and high static electric. In order to improve hydrophilic and antistatic properties of PET fabrics, β-cyclodextrin (β-CD) was finished onto them with citric acid (CA) as crosslinking agent. SEM showed that β-CD was finished successfully onto PET fibers. Moisture liberation curve indicated that the finished PET fabrics possessed favorable hydrophilic property. However, water vapor transport property of the finished PET fabrics slightly decreased. Antistatic property of PET fabrics finished by β-CD acquired improvement. In addition, tensile properties of PET fabric also were enhanced after finishing.

Introduction

PET fiber has been used in textile industry for several decades due to its outstanding properties such as high tenacity, elastic recovery, etc. However, PET fiber is lack of hydrophilic groups, resulting in the poor moisture adsorption and high static electric [1]. Thus, it affects the wearing comfortability of PET fabric. Therefore, it is necessary to exploit a new method to enhance the hydrophilic property of PET fabric. Researchers have made some fruits at this research field [2].

β-cyclodextrin (β-CD) is a kind of cyclic oligosaccharide containing seven glucopyranose units with twenty-one hydroxyl groups at the whole molecular [3]. It has been used in different domains such as cosmetics, foods, pesticides and drugs [4]. Szejtli [5] reviewed the application of CDs in the textile industry. Martel et al. [6-9] researched that cotton, wool and PET fabrics were finished with β-CD in the presence of polycarboxylic acid. The finished fabrics possessed some especial functions, such as sorption of metallic cations in water, and capture and controlled release of fragrances [8, 9]. Ghoul et al. [10] reported dyeability of polypropylene fabrics finished with β-CD-CA. However, they didn't pay earnestly attention to the variation of PET fabric hydrophilic property before and after treatment with β-CD, and the consequent wearing comfortability.

In this study, β-CD was finished on PET fabric through crosslinking action of CA based on literatures [7] and [8]. SEM images were taken to observe the morphological changes of PET fibers before and after treatment. Moisture liberation curve demonstrated that the finished PET fabrics had desirable hydrophilic property, however, water vapor transport property slightly decreased. Antistatic property of the finished PET fabrics acquired improvement. In addition, the tensile strength and elongation at break of PET fabric also were enhanced after finishing.

Experimental

Materials. PET woven fabric (surface weight = 65.1 g/m^2) was purchased from Hanzheng Street, Wuhan, China. β-CD, CA and sodium hypophosphite (SHP) were supplied by Shenshi Co. Ltd., Wuhan, China. Among them, SHP was used as catalyst.

Preparation of *β*-CD Finishing PET Fabrics. The finishing process of PET fabrics was based on the pad-dry-cure method reported in the literatures [7] and [8]. PET fabrics were immersed in aqueous solutions containing *β*-CD, CA and SHP and then passed through squeeze rolls to produce 80~90% wet pickup. Subsequently, they were dried at 80 ˚C and cured in oven at 150 ˚C for 30 minutes, and finally rinsed thoroughly in warm (50 ˚C) running water for 30 minutes and then gradually air dried under atmospheric conditions for the following characterization and experiment. The treatment with a mixture of *β*-CD, CA and SHP on PET fabrics caused a weight gain of them. The maximal weight gain ratio was obtained at about 150 g/L *β*-CD, 100 g/L CA, and 30 g/L SHP.

Measurements. SEM analysis was carried out using a scanning electron microscope (SIRION, FEI Corp., Netherlands). The samples were sputtered with gold, followed by observation and photography.

Moisture liberation curves of PET fabrics were tested according to Hu et al. method [11].

Water vapor transport property of samples was determined by using Huang's test method [12].

Antistatic property of PET fabrics was measured by using YG (B) 342D Fabric Electrostatic Tester (Wenzhou Darong Textile Instrument Co., China) according to GB/T 12703 (China) standard.

The tensile strength and breaking elongation of the samples were tested on an Instron tester, model 3410, at a 50 mm gauge length. Cross-head speed was 100 mm/min, and sample width was 15 mm.

Results and Discussion

Morphology of PET Fabrics. Fig. 1 (a) and (b) show morphology of PET fibers before and after treatment with *β*-CD, respectively. The original fibers possess a circular and smooth surface and void spaces between fibers on Fig. 1 (a). However, the adhesive film and particles are obvious on the surface of the treated PET fibers, and the void spaces between fibers are full of the irregular film on Fig. 1 (b). This clearly indicated that *β*-CD was finished successfully onto PET fabrics.

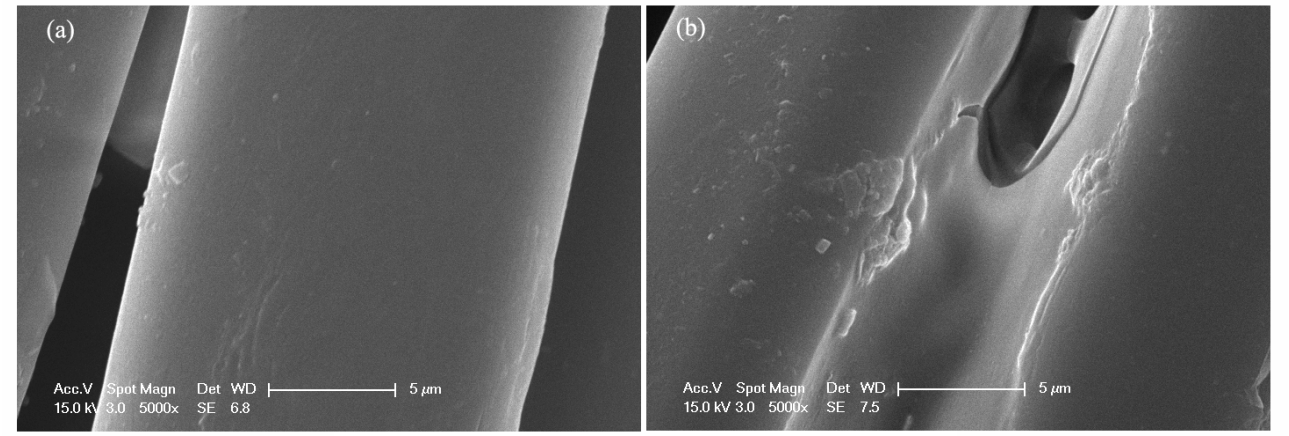


Fig. 1 SEM images of PET fibers before (a) and after (b) treatment with *β*-CD.

Moisture Liberation Curves of PET Fabrics. The liquid water content changes versus time of the samples are shown in Fig. 2. It obviously indicates the variation of moisture liberation of PET fabrics before and after treatment. From the curves, we found that the finished PET fabric contained more water than the control in initial stage. In the next stage, a large number of water vapor molecules on the surface of fabric evaporated quickly, leading to the sharp decline in water content with time. In the end, water content decreased to reach the equilibrium, and basically kept stable. In addition, the water content of the finished PET fabric is greater than that of the control at the equilibrium. This is because that the grafting *β*-CD increased the hydrophilic property of PET fabric.

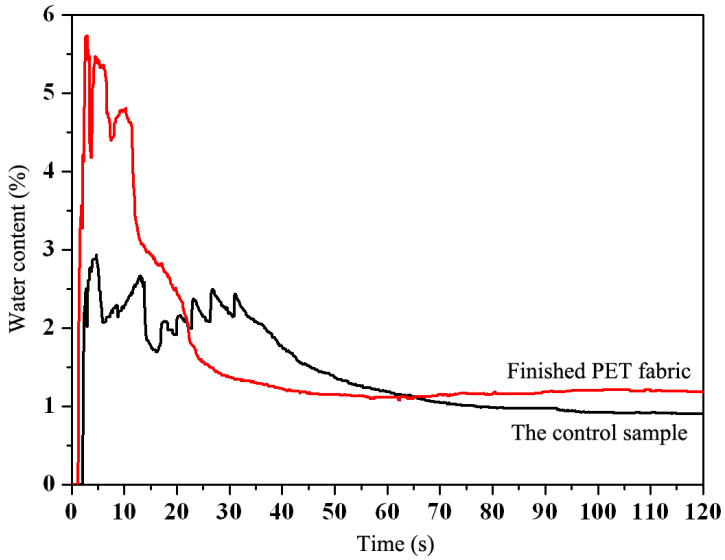


Fig. 2 Moisture liberation curves of PET fabrics before and after treatment.

Water Vapor Transport Property of PET Fabrics. Table 1 shows water vapor permeability of PET fabrics before and after treatment with *β*-CD. It is found that water vapor flux of finished PET fabric decreased about 6% than that of the control. Since the water vapor transport property is affected by the textile materials and tightness of fabrics, etc, however, as shown in SEM photos, the surface of the finished PET fibers was wrapped a layer of discontinuous film, restricting the water vapor transport path, and resulting in the decrease of water vapor flux.

Table 1 Water vapor transport property of the control sample and finished PET fabric.

Samples	The control sample	Finished PET fabric
Water vapor flux ($g/m^2/day$)	16046.03 (±84.35)	15102.15 (±218.15)

Antistatic Property of PET Fabrics. Results for the antistatic measurements are shown in Table 2. Electrostatic voltage and half-life period of the finished PET fabric all sharply descend than those of the control sample. Thus the *β*-CD finishing was highly effective to decrease the static electricity of PET fabrics. Antistatic property of the PET fabric finished with *β*-CD can be explained to be a function of the hydrophilic contribution of hydroxyl groups in *β*-CD.

Table 2 Electrostatic voltage and half-life period of the samples before and after treatment.

Samples	The control sample	Finished PET fabric
Electrostatic voltage (V)	349.8 (±11.6)	163.0 (±30.5)
Half-life period (s)	5.55 (±1.08)	0.50 (±0.06)

Mechanical Properties of PET Fabrics. Mechanical properties, especially the tensile strength and elongation at break, are significant for evaluating the properties of fabrics for appropriate application. As shown in Fig. 3, it depicts the tensile properties of PET fabrics before and after treatment with *β*-CD. The tensile strength and breaking elongation of the finished PET fabric increased when compared with the control sample. This is mainly because that the surface of the finished PET fibers formed a layer of compact film, which has been proved by SEM images, thus improved the mechanical properties of PET fabrics.

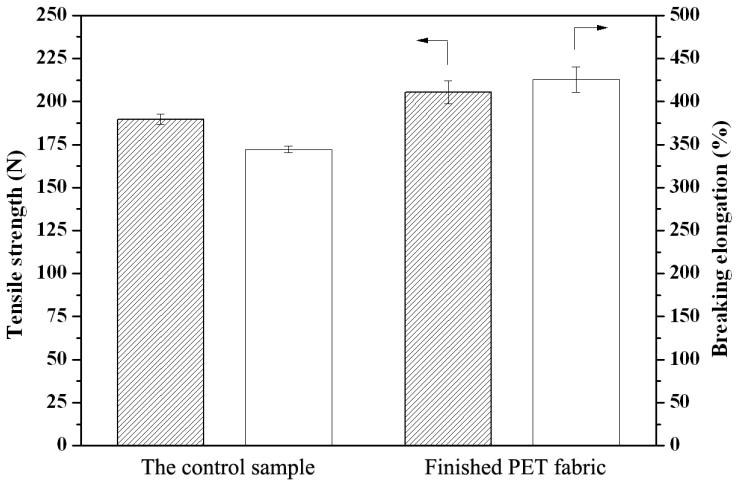


Fig. 3 Tensile property of the control sample and finished PET fabric.

Conclusions

β-CD was successfully finished onto PET fabrics by using CA as crosslinking agent through SEM observation. Moisture liberation curve showed that the finished PET fabrics improved hydrophilic property. However, water vapor permeability of PET fabric slightly decreased after finishing. Antistatic property of PET fabrics finished by *β*-CD had large improvement. In addition, tensile properties of the finished PET fabric also increased than those of the control.

Acknowledgements

This work was financially supported by Wuhan Textile University Foundation (2007).

References

[1] V. Singh, T. Singh, A. Chandra, S.K. Bandyopadhyay, P. Sen, K. Witte, U.W. Scherer and A. Srivastava: Nucl. Instrum. Meth. B Vol. 244 (2006), p. 243

[2] H. Wang, L. Pang, X. Jin, B. Yin and H. Wu: J. Eng. Fiber. Fabr. Vol. 5 (2010), p. 26

[3] M.L. Bender and M. Komiyama: *Cyclodextrin Chemistry* (Springer, Berlin 1978).

[4] J. Szejtli: *Cyclodextrin Technology* (Kluwer Academic Publisher, London 1988).

[5] J. Szejtli: Starch/Stärke Vol. 55 (2003), p. 191

[6] B. Martel, M. Weltrowski, D. Ruffin and M. Morcellet: J. Appl. Polym. Sci. Vol. 83 (2002), p. 1449

[7] B. Martel, M. Morcellet, D. Ruffin, L. Ducoroy and M. Weltrowski: J. Incl. Phenom. Macro. Vol. 44 (2002), p. 443

[8] L. Ducoroy, B. Martel, B. Bacquet and M. Morcellet: J. Incl. Phenom. Macro. Vol. 57 (2007), p. 271

[9] B. Martel, M. Morcellet, D. Ruffin, F. Vinet and M. Weltrowski: J. Incl. Phenom. Macro. Vol. 44 (2002), p. 439

[10] Y.E. Ghoul, B. Martel, A.E. Achari, C. Campagne, L. Razafimahefa and I. Vroman: Polym. J. Vol. 42 (2010), p. 804

[11] J. Hu, Y. Li, K.W. Yeung, A.S.W. Wong and W. Xu: Text. Res. J. Vol. 75 (2005), p. 57

[12] J. Huang: Polym. Test. Vol. 26 (2002), p. 685

© (2011) Trans Tech Publications, Switzerland
doi:10.4028/www.scientific.net/AMR.331.416

Study on Reuse of Dyes From Wastewater

Meizhen Li [1,a], Jin An[1]

[1]Institute of Light Industry and Textile, Inner Mongolia University of Technology, Hohhot 010051, Inner Mongolia, China

[a]lmz2909@126.com

Keywords: Cotton Fabric, Protein Additive, Dyes Wastewater, WLS Additives, Modification, Staining.

Abstract. Through putting protein additives in reactive dyes wastewater and decolorization, both of the additives and dye wastewater changed into a kind of complex compound. Protein additives with amorphous loose micelle structure which has $-NH_2$, -COOH, -OH and -CONH- produce electrostatic attraction, hydrogen bonding, van der Waals force and hydrophobic interaction between dye ions and dye molecules. Thereby, absorptive dye can embed dyes in micelles by adsorption, flocculation, coagulation to achieve the collecting of dye in dye wastewater. In this paper, we mainly discussed the performance and reuse of decolorized dyes. Further we studied on the reuse of the protein blends dye and the use of WLS for cotton fabrics pretreatment. By researching on the influence of WLS amount, optimal process conditions including pretreatment, dyeing, were both determined. The effect of WLS modification was also evaluated. It was found that the dyeing rate in decolorized dye increased after cotton was modified by WLS. Therefore, it is necessary to explore the decolorization of reactive dyes wastewater and the reuse in order to save dyes, chemicals and reduce emission.

Introduction

Reactive dye is widely used in cellulose fiber dyeing, because it has not very high appetency to cellulose fiber, and its hydrolyzed bonds easily break causing a lot of hydrolytic dyes remained in the bath. Dyes wastewater causes pollutants and more difficulties to sewage disposal. In this experiment, we mainly studied the performance of decolorized dyeing wastewater by protein additives and its reuse for dyeing, aiming at further reducing the secondary pollution problems and achieving zero pollution discharge. Results showed that the dyeing rate of bleaching dyes on cotton fabric was highest.

Experiment

Materials and Apparatus. Cotton fabrics (20 × 20, 60 × 60, 47 ") and reactive red M-2B were used in the experimental. Experimental reagents including sodium pyrophosphate, anhydrous sodium sulfate, anhydrous sodium carbonate, urea, sodium hydroxide, self-reactive cationic modifier WLS, ethanol, sodium bisulfite, sodium chloride , and experimental apparatus containing 722-type grating spectrophotometer, double-row four-hole electronic constant temperature water bath pan, BS110S electronic balance, SF-300 Siwei Shi computer color measurement instrument were also applied in experimental process.

Decolorization Prescription of Reactive Brilliant Red M-2B. According to Table1 prescription, dye wastewater was laying for 12 hours after decoloring. And then after filtering, the decolouring ratio was measured. Finally, the dosage of protein complex decolorizer was optimized.

Table 1 Decolorization Prescription

Dye wastewater (mg/L)	Protein additives (g/L)	Compound material (g/L)	PH value	Liquid volume (mL)	Decoloring temperature (℃)	Decoloring time (h)
50	0～0.8	0～0.4	5～9	50	25	12

The Solubility Performance of Decoloring Dye Wastewater. Experiment shows that the dye wastewater did not dissolve in water, so a good solvent should be selected at room temperature in the way of choosing from different solvents.

Decoloring Dye used for Dyeing of Non-modified Cotton Fabrics. Reactive Brilliant Red M-2B decoloring dye was gained by protein additive. And the process flow shows as follows: Dissolve 5g/l dye with additives → non-treatment cotton fabric→ salt addition →dyeing→ water washing →the dyeing rate measurement →K / S values measurement (%).Dyeing prescription and dyeing process curve are shown in Table 2 and Fig.1, respectively.

Table 2 Dyeing Prescription

Waste dye (o.w.f)	Na_2CO_3 (g / L)	NaCl (g / L)	Cotton fabric (g)	Liquor ratio
4%	5	0-40	1	1:25

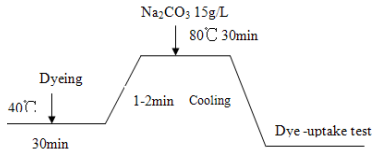


Fig.1 Dyeing Process Curve

Dyeing of Cotton Fabric Modified by Cationic Agent. Firstly, the cotton fabric was pretreated by WLS cross-linking cationic agent, and the modified process was shown in Table 3. Optimal dosage was determined on the basis of cationic modified cotton fabric dyeing. Then the process flow presents as follows: WLS cross-linking pretreated cotton fabric preparation →rinsing → bleaching alkali dyeing → salt adding→ rinsing →determination of the dye-uptake →K / S values measurement. And the dyeing of modified cotton fabric prescription is listed in Table 4.

Table 3 Cationic Modification Process of Cotton Fabric

Drugs	Dosage	Temperature / ℃	Time / min
Auxiliary WLS	10-50%（o.w.f.）	60	30
NaOH	6g/L	60	30

Note: cotton fabrics: 1g , bath ratio: 1: 25.

Table 4 Dyeing of Cotton Fabric Modified Prescription

Decolorization of Dye (o.w.f)	NaOH (g/L)	WLS (o.w.f)	Na_2CO_3 (g/L)	NaCl (g/L)	Cotton cloth (g)	Bath ratio
4%	6	0-0.4	15	0-40	1	1:25

Results and Analysis

Optimization of Protein Compound Bleaching Agent. In the case of other conditions fixed, the usages of chitosan and 16 alkyl benzyl trimethyl ammonium bromide were both changed. After magnetic stirrer mixing and filtering, absorbance value was measured. And then decolorization rate was calculated. The decolorization rate of chitosan and 16 alkyl benzyl trimethyl ammonium bromide are shown in Fig. 2 and Fig. 3, respectively.

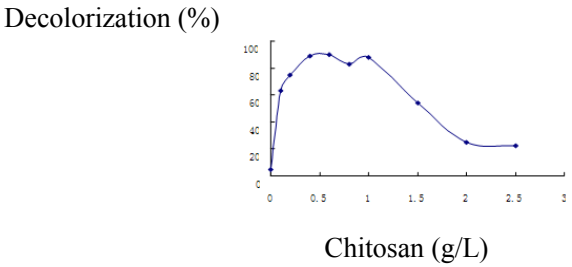


Fig. 2 Effect of Chitosan Concentration to Decolorization Flocculation (%)

Note: Decolorization conditions are pH= 6, 0.6g / L chicken-feather bleaching agent, 5 mg / L dye wastewater, bleaching time for12 hours and decolorization temperature at 25 ℃.

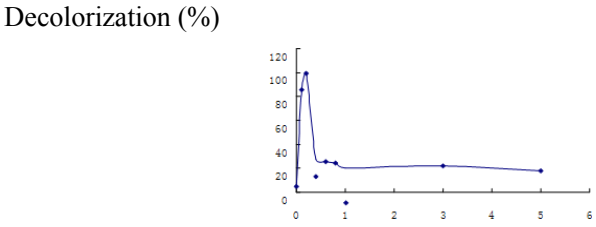


Fig.3 Effect of 16 alkyl-3-methyl Benzyl Bromide Dosage to Decolorization Flocculation (%)

The Dissolution of Waste Dyes. Waste dye by decolorization to wastewater does not basically dissolve in water and some organic solvents, but easily dissolves in the appropriate inorganic salt liquor, especially in sodium pyrophosphate liquor or sodium carbonate liquor. That is good for following dyeing.

Dyeing Conditions of the Waste Dyes in Different Solvents. Table 5 shows sodium pyrophosphate and anhydrous sodium carbonate solvents dyeing in normal dyeing conditions. It is found that using anhydrous sodium carbonate as solvent is better. Thus, it is necessary to select a good solvent for future experiments.

Table 5 Sodium Pyrophosphate and Anhydrous Sodium Carbonate Solvents Dyeing

Data	Sodium Pyrophosphate	Anhydrous Sodium Carbonate
Ai	0.225	0.227
A0	0.260	0.312
Dyeing rate(%)	13.6	27
K/S value	4.498	31.011

The Maximum Absorption Wavelength of Dye Decolorization with Anhydrous Sodium Carbonate Solvent. We measured optical density under the condition of 5g / L waste dye in15g / L anhydrous sodium carbonate solvent. The result shows in Table 6. It is shown that dyeing properties is not affected by anhydrous sodium carbonate solvent.

Table 6 Absorbance Values of Waste Dye

Wavelength (nm)	Absorbance	Wavelength (nm)	Absorbance
380	0.301	510	0.737
400	0.249	528	0.801
420	0.220	532	0.792
440	0.242	550	0.742
460	0.347	580	0.370
480	0.506	620	0.158
500	0.659	680	0.009

Dyeing of Fresh Waste Dye. Table 7 shows that NaCl is good to dyeing acceleration. However, excessive use is bad to dye dissolution and up-take.

Table 7 Dyeing of Waste Dye to Cotton Fabric

Data	Fresh Waste Dye				
NaCl（g/L）	0	10	20	30	40
Dye-uptake	5.6%	13%	44%	27.6%	31.5%
K/S value	22.498	23.062	37.208	31.565	32.964

Note: 4% waste dye (owf), 15g / L Na_2CO_3 solution, 0-40g / L NaCl solution

Dyeing of Waste Dye after Laying for 48h. Table 8 shows dyeing of waste dye after putting for 48h to cotton fabric. Comparing with Table 7, fresh waste dye is better. Relatively, waste dye after laying for 48h is worse.

Table 8 Dyeing of Waste Dye after Putting for 48h to Cotton Fabric

Data	Waste Dye (putting for 48h)				
NaCl (g/L)	0	10	20	30	40
Dye-uptake	3.5%	3.8%	21%	19.6%	15.6%
K/S value	19.972	20.021	28.149	27.143	25.314

Note: 4% waste dye (owf), 15g / L Na_2CO_3 solution, 0-40g / L NaCl solution.

Dyeing Effect of Cotton Fabric after Treatment with WLS Cationic Agent. Table 9 shows the dyeing effect of cotton fabric after treatment with WLS cationic agent. It is demonstrated that treatment with cationic agent WLS is good to improve up-take.

Table 9 Dyeing Effect of Cotton Fabric after Treatment with Cationic Agent WLS

Data	Fresh Waste Dye				
WLS (owf)	0	0.1	0.2	0.3	0.4
Dyeing rate（%）	47.3%	65.7%	66.9%	67.6%	61.8%
K/S value	38.603	47.683	48.500	48.683	45.894

Note: 4% waste dye (owf) , 15g / L Na_2CO_3 solution, 20g / L NaCl solution, 0-0.4% WLS (owf).

Conclusion

Protein additives used in bleaching of dyeing wastewater can gain higher dye up-take than the others in waste dye acquisition possessing. Chicken-feather bleaching agent used in the experiment is environment-friendly. And anhydrous sodium carbonate is a better solvent for dye wastewater. Waste dyes should be prepared freshly for higher dye up-take. And cotton fabric treated by cationic agent WLS is good to improve dye up-take.

References

[1] C. Zhang: Dyeing and Finishing Technology Vol. 24(2002), p. 42.
[2] J.X. Yan, Q.L. Cheng: Dyes and Dyeing Vol. 44 (2007), p. 48.
[3] J.Z. Li: *Dyestuff, Dyeing Industrial Wastewater Treatment* (Chemical Industry Press, Beijing 1997).
[4] Z.B. He: Dyeing Vol. 20(2007), p. 41.
[5] X.J. Feng, T.Y. Ge: China Resources Comprehensive Utilization Vol. 10(2005), p. 6.
[6] T.Q. Lu, X.R. Wang, Q.G. Yang: Dyeing and Printing Auxiliaries Vol. 8(2005), p. 31.
[7] W.Y. Li, Q. L. Deng: Dyeing and Printing Auxiliaries Vol. 24(2007), p. 5.

© (2011) Trans Tech Publications, Switzerland
doi:10.4028/www.scientific.net/AMR.331.420

The manufacture and dyeing of cationic dyes dyeable linen fibers

Shuzhen Gao[1,a], Qun Liu[2,b] and Qingjian Liu[3,c]

[1]The Light and Textile Institute of Qiqihar University,Heilongjiang Province China,161006.
[2]The Light and Textile Institute of Qiqihar University,Heilongjiang Province China,161006.
[3]The Light and Textile Institute of Qiqihar University,Heilongjiang Province China,161006.
[a]gaoshuzhen@126.com, [b]daweilai@yahoo.com, [c]sh1985113@163.com

Keywords: hydrogen sulfite sodium, oxidation, cationic dyes, sulphonation, linen fabric

Abstract. Sulphonated linen fabrics dyed with cationic dyes were prepared by chemically modifying linen fabrics oxidated by sodium periodate with hydrogen sulfite sodium. The effect on aldehyde group content and breaking strength of linen fabrics by oxidation conditions was investigated, the influencial effects of sulphonated by the concentration of hydrogen sulfite sodium, processing time,reaction temperature and so on were Analysised,the optimal oxidating and sulphonating process conditions of linen fabric were not only determined by means of infrared spectrum and the dyeable behevior of sulphonated linen fabrics with cationic dyes,but also the sulphonated linen fabrics dyed with cationic dyes have higher dye up-take, better colour fastness and levelness and more remarkable permeability.

Introduction

Uder persuiting the age topic of the harmony human with natrual, the green textile products manufactued by natural fibers are popular with more and more customers.Linen fibers have simple and noble qualities. Linen cloth has such good use of performance,for example worn with newness cool, a wet ventilate.But the linen cloth has the problems of low dye up-take, dark color, poor dyeing fastness and chromatic aberrations in dyeing processes,these constraints its development. To improve the dyeing properties of the linen fibers[1,2], people had been conducted in the modification research of linen fibers.In the paper,the linen fiber was selectively oxidated by sodium periodate, in the premise of the limited decline of the strength of linen fiber,the hydroxys of the linen fiber molecular become the active aldehyde groups[3], sulphonated linen fibers were prepared by carrying out nucleophilic additions with hydrogen sodium sulfite, they were then dyed with cationic dyes, furthermore the new dyeing technology of linen fibers was developed.

Experimental

Materials,Chemicals and instruments. Materials:Bleached linen fabric.Chemicals:sodium periodate,glycerol,hydrogen sulfite sodium,cationic red X-GRL,cationic blue GB.Instruments: SHA-C water bath oscillator,ISO-9001 Model Electronic scale,Y802K Model oven with eight basket,754pc Ultraviolet visible spectrophotometer,YQ-Z-48A Model whiteness Measurement Meter,Microscope.

Selective oxidation of linen fibers. The bleached linen fabrics were immersed in 0.5-10g/L sodium periodate solution,the time of oscillatory oxidation reaction at 45˚C range from 20 to 120 minutes, rinsing several times with deionized water,soaked in 1mol/L glycerol solution at amibent temperature for 30minutes, throughtly rinsing with deionized water.The aldehyde group content of treated linen fibers was quantitatively measured by means of the hydroxylamine-hydrochloride

solution[4]. The aldehyde groups quantitatively react with hydroxylamine-hydrochloride with pruducing schiff base,then accompanying hydrochloric acid was titrated with sodium hydroxide,the calculation equation of the aldehyde groups content was established as follows:

$$\text{the aldehyde groups content(g/mmol)} = \frac{30V}{W} \quad (1)$$

V (ml) means the consumption quantity of 0.03mol/L methyl alcohol solution of sodium hydroxide during titration, W (g)means the mass quantity of oxidated linen fibers.

Sulphonation of oxidated linen fibers. Linen fibers oxidated at the determined optimum oxidation condations were immersed in 0.01-0.6g/ml hydrogen sulfite sodium solution,the temperature of oscillatory sulphonation range from 20 to 50˚C,the time range from 10 to 180 minutes,then throughtly rinsing with deionized water.

Simultaneously,linen fanbics untreated,oxidated and sulphonated were analysed by the Infrared spectrums, and their strength were measured .

Dyeing of sulphonated linen fanbics. Linen fabrics sulphonated at the optimum conditions were dyed with cationic dye in liquor ratio of 1:50 containing 2%owf dyes at 60˚C for 30 minutes,then throughtly rinsing with 60˚C deionized water,natural dryed at ambient temperatu re.Then,the abrasion fastness,washing fastness,levelness and penetration[5] of dyed linen fabrics were tested.

Results and Discussion

Oxidation of linen fibers. Linen fibers were oxidated by sodium periodate at the different concentration for different time.The aldehyde groups content was measured by means of the method of hydroxylamine-hydrochloride, the breaking strength was measured with breaking strength apparatus.The aldehyde groups content and breaking strength of treated linen fibers were shown in Table 1 and Table 2.

Table 1 The aldehyde groups content of the oxidated linen fibers / mmol/g

Time[min]	the concentration of sodium periodate solution [$g \cdot L^{-1}$]			
	0.5	2	6	10
20	0.009	0.041	0.054	0.158
30	0.012	0.065	0.077	0.237
60	0.017	0.083	0.161	0.469
120	0.025	0.014	0.253	0.864

Table 2 The breaking strength of the linen fibers oxidated /N

Time[min]	the concentration of sodium periodate solution [$g \cdot L^{-1}$]			
	0.5	2	6	10
20	620	584	496	450
30	614	569	480	435
60	601	513	441	394
120	587	450	399	236

Note: the breaking strength of the unoxidated linen fibers is 625N.

Table 1 and Table 2 show the aldehyde groups content is low and the breaking strength decrease less at low concentration of sodium periodate solution for short time, the aldehyde groups content increased and the breaking strength decline significantly as well as with the increase of sodium periodate solution concentration and the reactive time. The optimum oxidation conditions were determined as sodium periodate solution concentration 2g/L, reactive time 60 minutes, In this case, though the aldehyde groups conten is 0.083mmol/g and the breaking strength decline 17.92 percent,linen fabrics don't lose the wearing value and can meet the need of sulphonation of linen fabrics.

Sulphonation of oxidated linen fabrics. The linen fabrics oxidated at the previous optimum process technology were sulphonated by hydrogen sulfite sodium solution at different conditions,the influencial factors on sulphonation were analysised by dye up-take.

Effects of concentration. The linen fabrics oxidated at the previous optimum process technology were sulphonated by hydrogen sulfite sodium solution at 30℃ for 90 minutes , the concentration of hydrogen sulfite sodium range from 0.01 to 0.6 g/mL,the treated linen fabrics were dyed with cationic dyes , simultaneously, the dye up-take was measured. The effects of the hydrogen sulfite sodium solution concentration on the dye up-take were presented in Fig. 1.

As seen from Fig. 1, the dye up-take gradually increased with increasing the amount of hydrogen sulfite sodium concentration, the highest dyeing up-take may win at the point of 0.35g/mL hydrogen sulfite sodium, then reduced. Of cause, the amount of sulfonic acid groups should be attributed to the amount of hydrogen sulfite sodium,the dye up-take was finally due to the amount of sulfonic acid groups, in the beginnning, the amount of sulfonic acid group increase with increasing the concentration of hydrogen sulfite sodium, after arriving at the highest point that the sulfonic acid group content is highest, reduced because of the degradation of cellulosic fibers under weak acid condition when the sulfonic acid groups are saturated. Therefore, 0.35g/mL concentration of hydrogen sulfite sodium should be best.

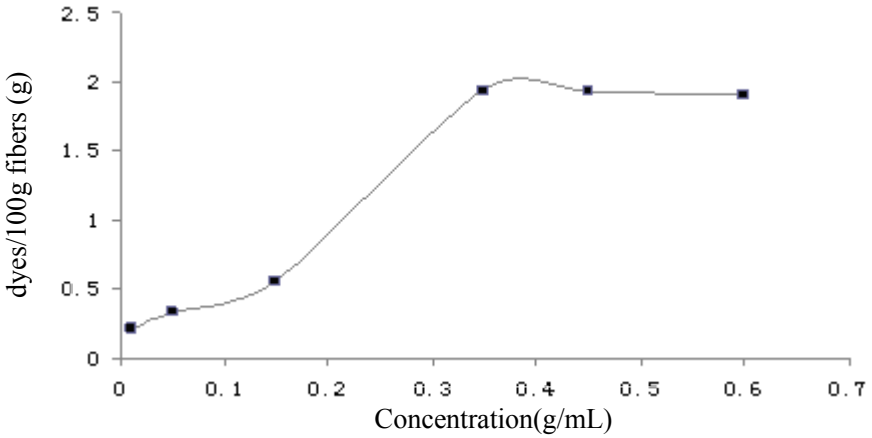


Fig. 1 The effects of hydrogen sulfite sodium solution concentration on dyestuff exhaustion quantity

Effects of time. The linen fabrics oxidated at the previous optimum process technology were sulphonated by hydrogen sulfite sodium solution containing hydrogen sulfite sodium 0.35g/mL at 30˚C,the time range from 10 to 180 minutes, the treated linen fabrics were dyed with cationic dyes, simultaneously,the dye up-take was measured[6]. The effects of time on dyestuff exhaustion quantity were presented in Fig. 2.

As shown in Fig. 2, the best sulfonation time should be 30 minutes.

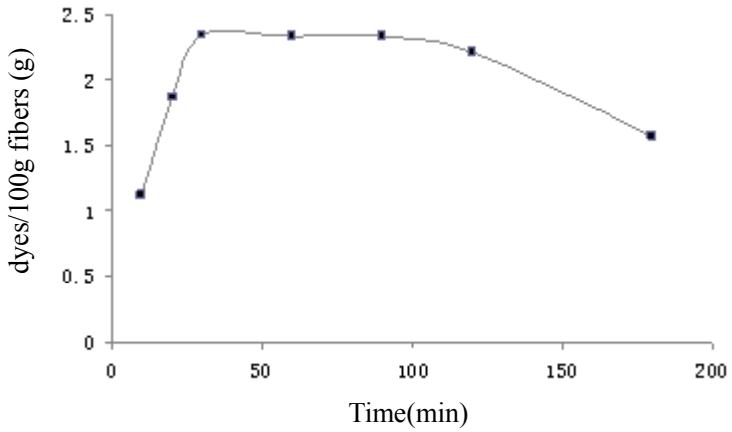


Fig.2 Effect of sulfonation time on dyestuff exhaustion quantity

Effects of temperature. The linen fabrics oxidated under the previous optimum process technology were sulphonated by hydrogen sulfite sodium solution containing hydrogen sulfite sodium 0.35g/mL for 30 minutes, the temperature range from 20 to 50˚C, the treated linen fabrics were dyed with cationic dyes, simultaneously the dye up-take was measured.The effects of temperature on dyestuff exhaustion quantity were presented in Fig. 3.

As shown in Fig. 3, the best sulfonation temperure should be 25˚C.

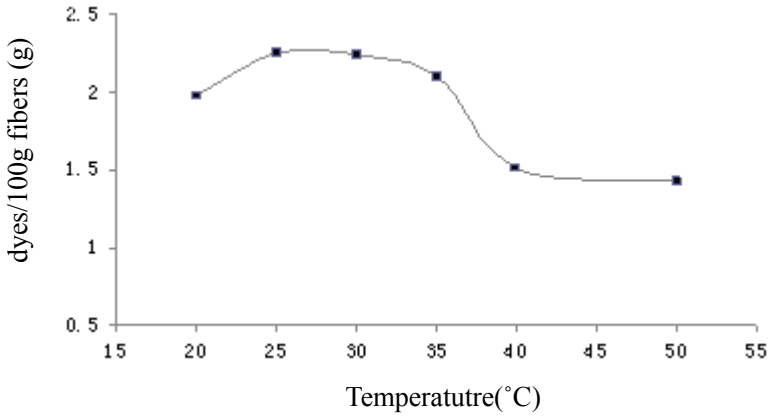
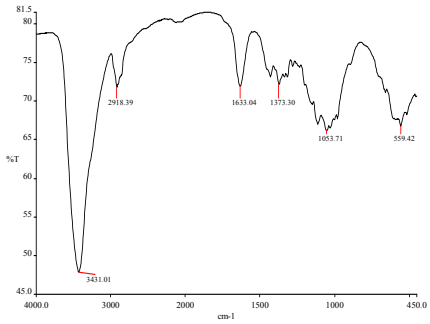


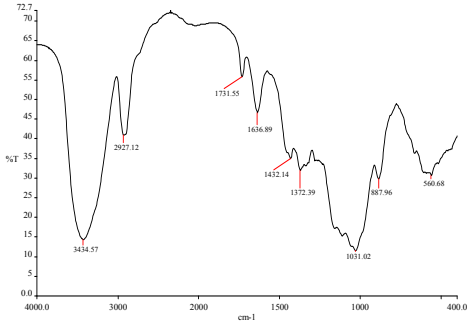
Fig.3 Effect of sulfonation temperature on dyestuff exhaustion quantity

Therefore the optimum sulfonation conditions are 0.35g/mL hydrogen sulfite sodium, 25˚C and 30 minutes.

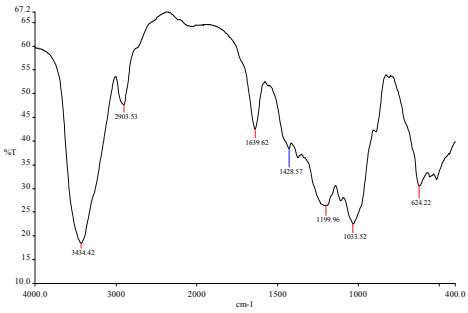
Infrared spectral analysis. Fig. 4 shows the Infrared spectrum of untreated linen fabrics (a), linen fabrics oxidated with sodium periodate at the optimum conditions(b), linen fabrics oxidated and sulfonated at the optimum conditions(c). Unlike the spectrum of the untreated linen fabrics,the spectrum of linen fabrics oxidated with sodium periodate under the optimum conditions shows a new weak signal at 1731.55 cm^{-1} derived from the aldehyde groups—CHO, while the spectrum of linen fabrics oxidated and sulfonated at the optimum conditions shows the disappearence of the weak signal at 1731.55 cm^{-1} derived from the aldehyde groups—CHO and the present of other new weak singal at 1199.96 cm^{-1} derived from sulfonic acid groups. The anylisis of the results of FTIR AIR spectrocopy confirmed the existent of the aldehyde groups and sulfonic acid groups and the nucleophilic addition reaction carrying out between aldehyde groups and hydrogen sulfite sodium.



(a) Infrared spectra of untreated linen fabrics



(b) Infrared spectra of linen fabrics oxidated with sodium periodate under the optimum conditions



(c) Infrared spectra of linen fabrics oxidated and sulfonated at the optimum conditions

Fig.4 Infrared spectra of untreated (a) and treated (b/c) linen fabrics

Quality analysis of dyeing products. The color fastness tests are with reference to GB/T 3920-97 standard of the measurement of fastness to abrasion of fabrics and GB/T 3921.1-97 standard of the measurement of fastness to washing of fabrics ,shown in Table 3.The properties of levelness were analysised by the tristimulus values (X,Y,Z)and total aberrations containing seven random Points on the fabric with chromameter ShadeEye,shown in Table 4.The dying penetration was assesed by the micrograph of cross section of dyed linen fibers.The magnification of the microscope used for indentation measurement is 400, presented in Fig.5.

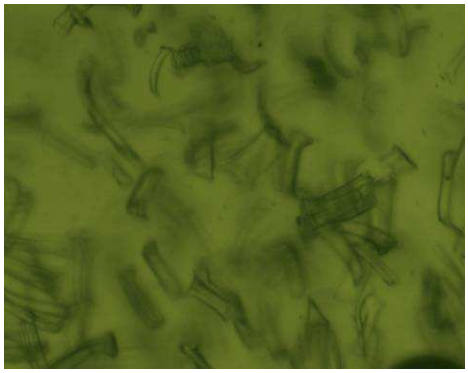
As seen from Table 3, Table 4 and Fig. 5, the linen fabrics oxidated and sulphonated under the above-mentioned optimum conditions can be well dyed with cationic dyes. The dyed fabrics had good color fastness, levelness and penetration. Theremore untreated linen fabrics cannot almost be dyed with cationic dyes.

Table 3 Color fastness

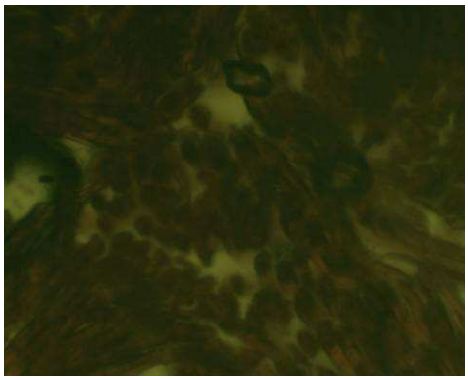
Dyestuffs	Fastness to abrasion		Fastness to washing	
	dry	wet	color fading	color staining
Cationic red X-GRL	3-4	3	3	3-4
Cationic blue GB	4	3	4	4

Table 4 Levelness

random Points	X value	Y value	Z value	total aberrations $\triangle E^*_{ab}$
1	52.06	26.97	21.36	0.00
2	50.61	25.71	20.13	0.2
3	51.67	26.49	20.94	0.2
4	51.28	26.83	21.61	0.3
5	52.23	28.8	23.88	0.00
6	51.98	26.58	21.25	0.1
7	50.29	24.31	20.06	0.4



（a）The microscops of undyed linen fabrics



（b）The microscops of dyed linen fabrics

Fig.5 The microscops of dyed and undyed linen fabrics

Conclusions

The optimal oxidation technology condition of linen fibers is concentration of sodium periodate 2g/L, temperature 45˚C,time 60 min; The optimal sulphonation technology condition of linen fibers is concentration of hydrogen sulfite sodium of 0.350g/ml,temperatue 25˚C,time 30 min; The infrared spectras confirm the existent of the aldehyde groups of linen fibers oxidated by sodium periodate and sulfonic acid groups of linen fibers sulphonated by hydrogen sulfite sodium;The fact that linen fibers cannot be dyed by cationic dyes is thoroughly altered;The modified linen fibers dyed with cationic dyes possess good dyeing fastness,levelness, penetration and wear properties.

References

[1] Xin Zhao,Shuzhen Gao,Jiang Chang:Textile and dyeing-finishing of flax.China's textile industry press.Beijing:(2007).p,2-9.

[2] Jiaqiang Shi:Biochemical process and dyeing-finishing of flax.China's textile industry press.Beijing(2005).p,4-16.

[3] Yunhui Xv,Hong Lin,Yu-yue Chen:The polymer structure of cotton fiber slectively oxidated.Textile journal.Vol,27(2006).p,1-5.

[4] Junmin Qian, Xvxiang Li:The research of oxidating linen fiber with sodium periodate.Modern chemical engineering.Vol,21(2001).p,28.

[5] Shujing Zhao:Experiment tutorial of textile material.China's textile industry press.Beijing (1989).p,7-10.

[6] Lvbing Yun:Organic chemistry.Higher education press.Beijing(2000).p,268-272.

© (2011) Trans Tech Publications, Switzerland
doi:10.4028/www.scientific.net/AMR.331.426

Structure and Properties of Modifier for Heat Transfer Printing on Cotton Fabric

Yi Mu[1, a], Lan Wang[1, b],Minghua Wu[1,c] and Junxiong Lin[2, d]

[1]Key Laboratory of Advanced Textile Materials and Manufacturing Technology, Ministry of Education, Zhejiang Sci-Tech University, Hangzhou Zhejiang 310018, China

[2]Engineering Research Center for Eco-Dyeing and Finishing of Textiles, Zhejiang Sci-Tech University, Ministry of Education Hangzhou, Zhejiang 310018, China

[a]myfdb219@yahoo.com.cn, [b]wlan_cn@yahoo.com.cn, [c]wumh001@126.com
[d]linjunxiong@zju.edu.cn

Keywords: modifier, semi-continuous emulsion polymerization, transfer printing, mononer, copolymer.

Abstract. Modifier for heat transfer printing on cotton fabrics was prepared by semi-continuous emulsion polymerization process with butyl acrylate (BA), styrene (St), acrylonitrile (AN) and cross-linking monomer. FT-IR characterization of modifier groups showed that individual monomer well carried out polymerization. Transmission electron microscopy (TEM) photos demonstrated that latex particles had regular spherical shape and uniform distribution. TGA curves indicated that thermal decomposition temperature of modifier was 439 ^{o}C. As for the transfer printing products had good colour fastness, high transfer rate and no formaldehyde.

Introduction

Transfer printing[1] has a lot advantages which are far superior than the normal. Patterns of transfer printing have fine, rich layers, realistic shape, high artistic quality and strong three-dimensional sense, what's more, transfer printing can print photography and painting style of design. Simple equipment and low investment are involved in this process. Since end product come out after the process, transfer printing has flexibility. These advantages meet individual consumer textile and clothing wear requirements. Properties that using no steaming, washing and other post-processing can save a lot of water resources and reduce pollution. This meets the new century green production requirements. Cotton fabric is popular because of its moisture permeability, comfortable wearing and appropriate personal characteristics. Therefore, applying transfer printing technology on cotton fabric combines their respective advantages and solves problems in the process of printing. Thus, textile and garment can satisfy people's safety, comfort and personalized pursuit and meet the national policy of energy saving and emission reduction which is significant to environmental protection. In this work, monomers were selected depending on high affinity with disperse dyes. Semi-continuous emulsion polymerization was used to develop a modifier to achieve the disperse dyes on cotton fabric and the successful transfer.

Experimental

Materials. Butyl acrylate(AR, Tianjin Kermel Chemical Reagent Co., Ltd.); Styrene(AR, Shanghai Lingfeng Chemical Reagent Co., Ltd.); Acrylonitrile(AR, Tianjin Yongda Chemical Reagent Co., Ltd.); 2-hydroxyethyl methacrylate (HEMA) was purchased from Shanghai Jingchun Chemical Co. Ltd.; Glycidyl methacrylate (GMA) were supplied by Guangzhou Shuangmao Co., Ltd; Aionic emulsifier A-6280, An-ionic emulsifier A-980 and plymerizable emulsifier V-10S were supplied Shanghai Honesty Fine Chemical Co., Ltd.; Persulfate(AR); Sodium bisulfite(CP); Sodium bicarbonate(AR).

Synthesis of Modifier. With pre-emulsified semi-continuous emulsion polymerization[2,3,4], part of the emulsifier was well dissolved with deionized water in a four-necked round-bottom flask, two third of the butyl acrylate(BA), styrene(St), acrylonitrile(AN)and crosslinking monomer were added and stirred rapidly. Thus 2/3 of pre-emulsion were prepared after emulsifying 30 minutes under 45^{o}C. 1/3 of pre-emulsion can be obtained in the same operation which is added the remaining emulsifier, monomer and deionized water to another four-necked round-bottom flask equipped with thermometer, stirrer bar, constant pressure funnel and condenser. And then heating while stirring to 65^{o}C, added into 1/3 of potassium persulfate and sodium bisulfite solution. The temperature shot up immediately after accession, when the temperature dropped to 80^{o}C, 2/3 of the pre-emulsion and 2/3 of the potassium persulfate and sodium bisulfite solution were dropping into and dropping time was 2h.The polymerization reactions were carried out at 80^{o}C. After that the temperature was heated to 85^{o}C and maintained 1 hour. Finally, the polymerization [5,6,7] was completed, the temperature was cooling to 60^{o}C, the emulsion pH values were adjusted to 7-8.

Test methods. The chemical structures of the products or copolymers were analyzed by Fourier-transform infrared spectroscopy (FT-IR, Bruker Vertex 70 FT-IR). Transimssion electron microscopy (TEM,JEM2100) was used to measure the morphology of latex particles. The diameter of latex particles and its distribution were characterized by the Dynamic Light Scattering Particle Size Analyzer(LB-550). The thermal decomposition temperature of the copolymers was measured with Thermogravimetric Analyzer (TGA, Pyris-1). Samples were scanned at a heating rate of 10^{o}C /min from room temperature up to 600^{o}C.

Washing color fastness of transfer printing products were measured according to GB/T3921.3~5 -1997. The determination of Perspiration color fastness was based on GB/T3922-1995. Rubbing fastness of samples were measured by employing the standard “Textiles-Tests for colour fastness-Colour fastness to rubbing” (GB/T3920-1997). By using Spectrophotometer (722s), the free formaldehyde content of fabric were tested according to GB/T2912.1-1998.

Transfer rate was the ratio that the modified cotton fabric K/S values divided by the pure polyester fabric K/S values. The samples were prepared by transfering 20s under 220^{o}C.

Results and Discussion

FT-IR analysis (Fig.1) was used to demonstrate the structure of modifier. As shown in Figure 1, the peak at 2239 cm^{-1} (-CN) indicated that AN monomer was polymerized successfully. The characteristic absorption peaks at 1602 cm^{-1}, 1494 cm^{-1} and 1453 cm^{-1} are attributed to C=C of benzene ring. The C=O stretching peak is at 1727 cm^{-1}. The strong absorption peaks at 1160cm^{-1} and 1028 cm^{-1} are attributed to C-O stretching peak. The characteristic absorption peaks at 961 cm^{-1} and 940cm^{-1} are assigned to the butyl acrylate. All these results demonstrated the successful synthesis of the individual monomer.

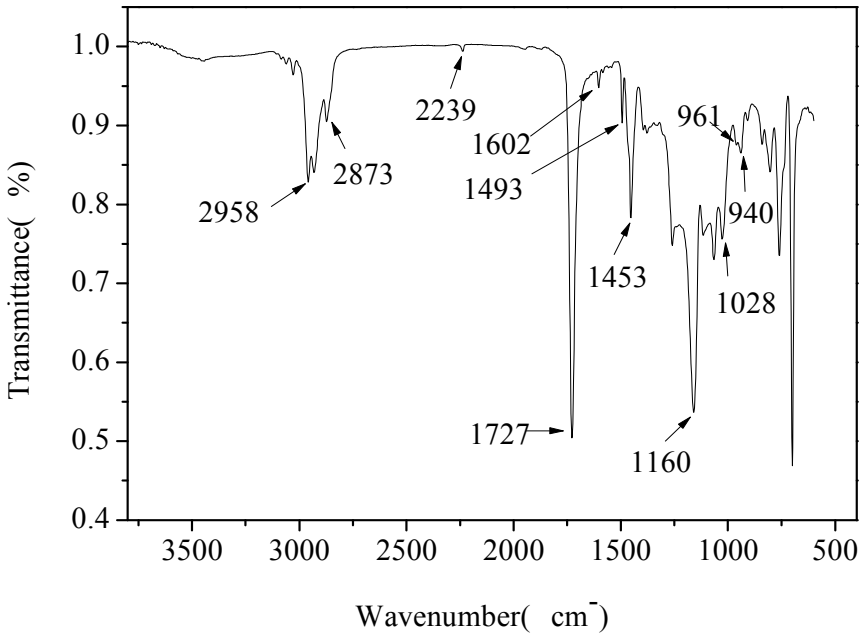


Fig.1 FT-IR spectra of copolymer

The relationship between the mass loss percentage and temperature can be observed from thermogravimetric analysis curves. As shown in Figure 2, the thermal decomposition temperature of modifier was 439 °C. It demonstrated that the modifier had good heat resistance. From the Figure 3 we can see that there only one thermal decomposition peak appeared on the curves and the maximum thermal weight loss rate appeared at the temperature around 490 °C.

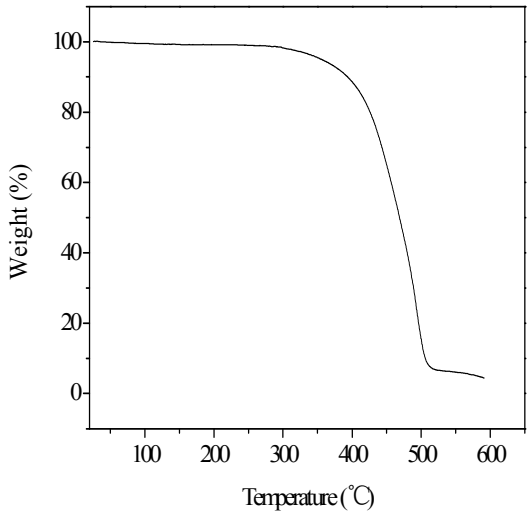


Fig.2 TGA curves of copolymer

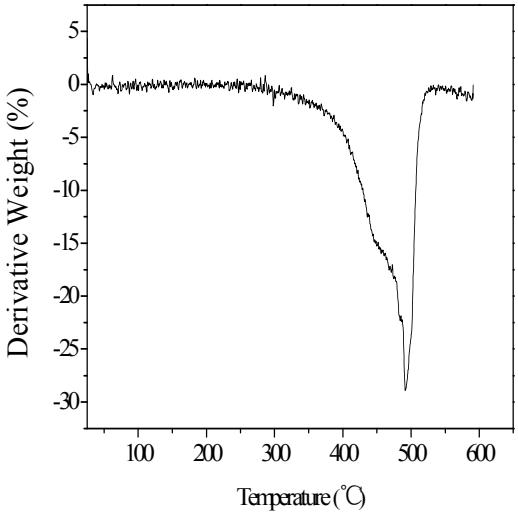


Fig.3 DGT curves of copolymer

In emulsion polymerization,the diameter of latex particles and their distribution was an important indicator of the polymer emulsion. The size of its value had a direct impact on the emulsion properties, such as emulsion color, gloss of film, the adhesive force of the polymer. As shown in Figure 3, the appearance of latex particles were observed by electron microscopy and it showed that they had regular spherical shape and uniform size. By using The Dynamic Light Scattering Particle Size Analyzer we measured that its diameter was about 65 nm and the distribution was less than 1. It was conducive to form a dense and transparent film. And the emulsion was translucent with strongly blue light.

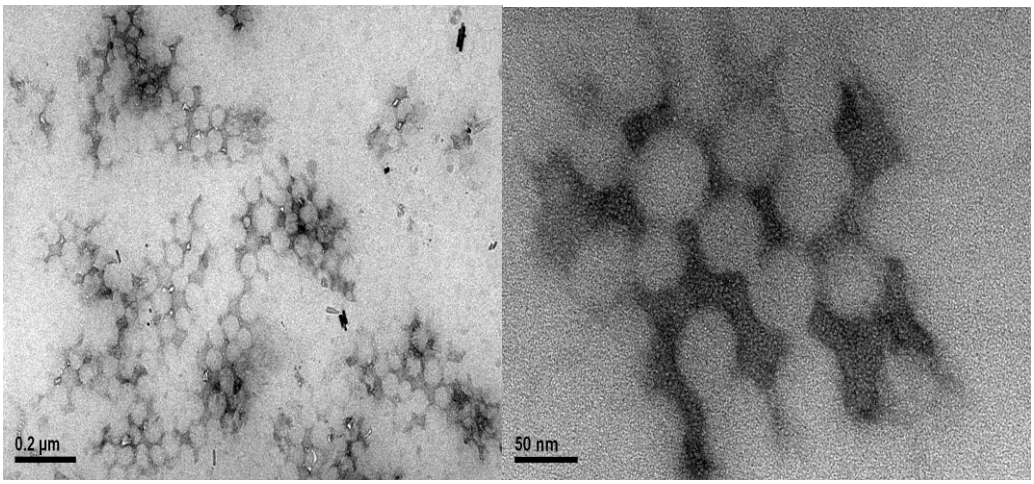


Fig.4 TEM images of latex particles

Modifier was prepared using the best conditions of synthesis process. Then the printing products was made by transfer printing with disperse red dye on modified cotton fabric. From Table 1 we can see that the transfer printing products have high transfer rate of 76%, no formaldehyde content and good color fastness.

Table.1 Effect of transfer printing of modified cotton fabric

Formaldehyde (mg/kg)	Transfer rate(%)	Rubbing (grade)		Washing (grade)		Perspiration (grade)	
		dry	wet	change	staining	change	staining
0.00	76	4-5	3	3	4-5	4	4-5

Conclusion

The results reported in this study showed that a new modifier for heat transfer printing on cotton fabric was successfully developed. FT-IR characterization of modifier groups showed that individual monomer well carried out polymerization. TEM photos demonstrated that the particle presented regular ball shape and its diameter was about 65 nm. TGA curves indicated that modifier had good thermal decomposition temperature of modifier was 439^{o}C. The printing products had good colour fastness and no formaldehyde. The transfer rate was 76%. Those can basically meet the requirements of people's daily dressing.

References

[1] A. A. El-Halwagy:Macromol. Mater. Eng. 286(2001), p330.

[2] Shahriar Sajjadi, Michael Yianneskis: Macromol. Symp. 206(2004), p201.

[3] C.S. Chern: Prog. Polym. Sci. 31(2006), p443.

[4] S. Oprea, T. Dodita:Progress in Organic Coatings. 42(2001),p194.

[5] Tongyu Cao, Qinpu Liu, Jinsheng Hu: Principles of Polymer Emulsion, Properties and Applications (Chemical Industry Publications,Beijing 1997).

[6] G S Corona, P J Castaneda, G A Martinez. Colloid and Polymer Science. 268(1990), p78.

[7] Valette L, Pascault J P, Magny B, et al.Journal of Applied Polymer Science, 86(2002), p753.

CHAPTER 3:

Textile Machinery and Equipment

© (2011) Trans Tech Publications, Switzerland
doi:10.4028/www.scientific.net/AMR.331.433

The Application of Motion Control Technology to Textile Production

Ming Han [1, a], Changyun Miao [2,b] and Jingmin Chang [3,c]
[1] School of Electronics and Information Engineering, Tianjin Polytechnic University , Tianjin
[2] School of Electronics and Information Engineering, Tianjin Polytechnic University , Tianjin
[3] School of Management, Tianjin Polytechnic University , Tianjin

[a]hanming.tjpu@163.com, [b]miaochangyun@tjpu.com, [c]changjinm@163.com

Keywords: Textile production, Motion Control, Textile machinery

Abstract. With the development of science and technology, Control Theory has been updating and progressing constantly. Motion Control Technology is continually going into all fields and in which it is pushed forward rapidly. It is playing a more and more important role and has found an increasingly wide utilization in the textile production. This paper expounds Motion Control Theory and its application, as well as some living examples of the application of Motion Control Technology to the textile production.

Introduction

The textile industry has made a tremendous contribution and pushing effect in the phylogeny of human society. Its rise and development are not only emancipating human beings from suffering hunger and cold, but also becoming a significant way to incarnate spiritual civilization for mankind. Meanwhile, the evolution and progress of the textile industry also play an irreplaceable role in the international economic boom as well as advanced science and technology. Nowadays, varieties of textile products are not only used for our apparel, but also for upholstery and interior decoration, which are influencing our daily life. In addition, textile materials can be widely used in computer, leisure, sports, automobiles, airplanes, civil construction, engineering and medicine when they are working as high-tech materials.

With the development of textile technology and social progress, textile enterprises' labor cost is gradually improving. Therefore, the past textile enterprises which only depended on handmade production can not adapt to the development of the times because their production cycle is short, production efficiency is low and the quality of products are difficult to guarantee. Textile mechanization came into being therefrom. The textile industry which is combined with mechanical electronics, developed from handcraft to mechanization and automation. Changing from the original manual operation to machine automatic control and mass production will not only reduce the cost of labor and production cycles, but also increase the quality and production of the product and facilitate management, which improved labor productivity and comprehensive competitiveness of enterprises.

Control Technology can be seen throughout the textile production process, which is almost used in all kinds of control products including Control, Motion Control, Transmission Control, Field Bus, Human-Machine Interface and Sensors.

Among these, technology such as motion controller, PLC,uniaxial independent drive, multi - unit synchro control and web - based data communications has been widely applied in the textile industry.

Extensive application of Motion Control Technology to the textile production makes textile machinery have faster respond speed, higher degree of flexibility and better quality .At the same time, it has greatly enhanced the quality of products, improved production efficiency as well as the working environment and conditions, which brought about a new leap in the development of the productive forces in textile.

Motion Control Overview

Principle of Motion Control. Motion Control which is based on mechanical movement as the main mode of production, and motor as the mainly controlled object is fast and high precision control. What makes Motion Control different from conventional automatic control is that it can fulfill certain

high precision speed control tasks, and can carry on repetitive motion. However, Motion Control also requires special components and technology whose performance is required higher than the conventional control systems. With the continuous development of science and technology, every component in motion control system has become component with control function or subsystem. Corresponding to the structure chart of automatic control system, we can draw a general form of motion control system as a block diagram, as shown in fig.1.

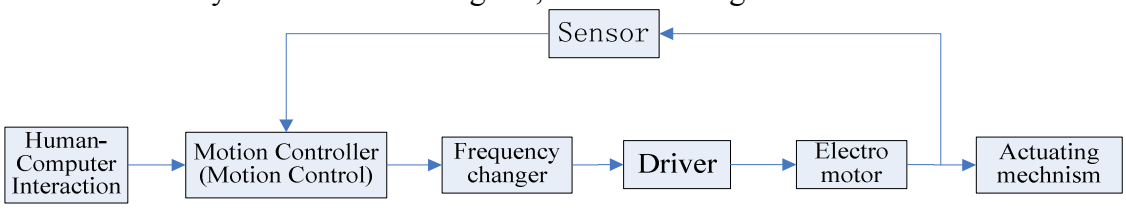


Fig.1 Motion Control System Block Diagram

Among them, preprocessor can be used in time of need and it can be a simulation component and can carry on digital processing as well. Actuator often refers to the combination of motor and its drive; components to enlarge and transform actuators in control system belong to driving amplifier units of the actuating mechanism. Motion controller is actually a motion control board which is used to control the output performance of control system after forming the entire control system. It often uses interpolation motion control card as the main control unit. Sensor is a kind of convertor which is used for measuring system output and transforming it into the needed form.

Applications of Motion Control. With the development of science and technology, Control Theory has been updating and progressing constantly. Motion Control Technology is playing a more and more important role and has found an increasingly wide utilization in the national economy and national defense construction. In industrial production, motion control system is used for improving the quality of products as well as raising the output of products. Motion Control Technology is constantly going into all fields and in which it is push forward rapidly. Its application has covered almost all industrial fields and mainly in the following areas: semiconductor manufacturing and testing, manufacturing industry and auto assembly line, materials handling equipment, processing machinery, aerospace, test and measurement, armarium, textile industry, robots and photoelectron encapsulation automation, etc. Among these, application in textile production is an important application of motion control system.

With the continuous development of science and technology in various fields, motion control technology is no longer a simple control of machinery with electronic devices, but a technology including cross-cutting integration of science and technology such as textile engineering, materials engineering, control engineering, mechanical engineering, electrical engineering and computer network, etc. As shown in fig.2 below.

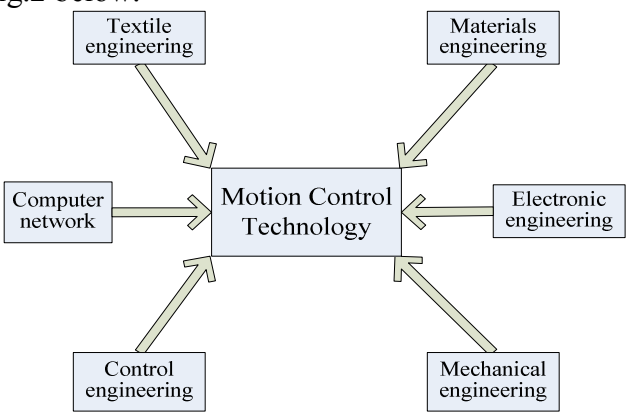


Fig. 2 Various Technologies involved in the Motion Control Technology

Motion Control Technology will get further progress along with the ongoing development and improvement of the hardware and software of motion control system. The developing trend of the future motion control system will be high performance, miniaturization, software, networking and

will be well adaptive to the environment. The content of open motion control technology research abroad mainly focus on three aspects: improving flexibility of motion controller, integration and standardization.

Motion controller is the core component of the motion control system, which refers to a control device with the central logic control unit at the core, sensor as signal sense components, motor or power plant and execution unit as control object. Its main tasks are to carry on logic or mathematical operations needed in accordance with the demand of tasks and the signals of sensor components, and thereby provide correct control signals for motors or other power plant and executive devices. According to the number of the independent motion axis it can control, motion controllers are called single-axis or multi-axis motion controller. Taking motion controller as an independent standard component can greatly shorten new product development cycle and help users to create their own brand products. At present, as the appearance of high-speed and high-performance professional microprocessors as represented by DSP and wide popularity of PC, the development tendency of open motion controller is based on DSP chip as motion control processor, with PC as the information processing platform. Motion controller embedded PC in the form of plug-in card, that is, " PC + motion controller " or " PC-based motion control " mode. Thus, the information processing capability and development style of PC combined together with the ability of motion locus control of motion controller, have the advantage of high information processing capability, high degree of opening, precise motion locus control and good versatility.

There are several design scheme of motion controller below: using single chip machine design, using DSP design, using complex logic device design, using special motion-controlling chip design and using finished products of motion control cards in the market directly in order to shorten development cycle. Nowadays, DSP and FPGA chip technology has developed at top speed, important features of DPS are the good compatibility and their good floating-point operation speed , and multi - axis motion control system concentrated in only one control card; FPGA chip technology has made it possible to update the hardware through software, which makes the traditional single-chip microcomputer-based motion control system changed a lot. If combining the DSP and FPGA with PC machine, we can make full use of the existing operating environment and resources to reduce system costs, further increase system versatility.

Application Examples of Motion Control Technology to Textile Production

In textile enterprises, characteristics of all kinds of textile production machineries are various in style and large in quantity. Due to the restrictions of the complex process, continuity of production is very poor, and it’s very difficult to achieve one-step production. Therefore, textile production occupies too much labor force, has too much manual operation and strong intensity of labor. It is the " light industry is not light " theory.On some problems like these, there’s a very urgent need of continuity and automation on the basis of technical innovation in textile industry, thus the application of motion control will be more important.

Application of motion control in textile production will not only improve working conditions, alleviate the heavy manual labor, but also improve the quality of products, reduce consumption so as to raise the efficiency of production and comprehensive competitiveness of enterprises. Applications of Motion Control Technology in the textile machinery are cropping up everywhere, such as spinning frame, roving frame, carding machine, and winding machine.

Spinning frame. The doffing aspect of the spinning frame used artificial tube change before and need manually connect when broken. Number of spindles in each spinning frame expands from the original a few hundreds to the current several thousand. If still using artificial change, the intensity of production personnel will be greater because of too much broken and low efficiency.

Roving frame. The function of roving frame is to stretch mature cotton and form roving so as to further increase the orientation and resolution and facilitate the processing of spinning frames after.Roving frame also mainly use motion control and man-machine interface use touch - screen or

text display while conventional roving frame use a motor to drive drawing roller, flyer, bobbins and lifting mechanism respectively through various transmission mechanism. Roller and the flyer use constant speed while bobbin and lifting mechanism use variable speed because of the enlargement of diameter of roving winding, which is achieved by cone-shaped pulley. Typical drive mode of the traditional roving frame adopt soft up, electromagnetic brake and mechanical sector, with the problem of complex structure, large amount of maintenance and the ineradicable thickness of the knot. New type of roving frame use the method of independent multi-motor variable frequency drive, electronic gear synchronization and cancel cone-shaped pulley, so that it can reduce the problem of thickness of the knot effectively.

Winding machine. Winding machine makes small spinning bobbins connect and wind so as to form large cylinders, and clear defects like thickness of the knot and the hairiness. It's a procedure before weaving. Tension control, spinning and forming are the keys of control in the winding process, which form a direct impact on processing efficiency and product quality. In addition, connecting and changing yarn is the key part of the winding process too. Current winding machine uses the automatic connector, manual or semi-automatic for yarn. Winding machine uses small PLC for motion control. The stator drive often adopts permanent magnetic DC motor, which usually needs tens of watts of power. The technology trend of winding machine is independent rotation of single spindle.

With people's increased aesthetic consciousness and the improvement of living standards, high-grade yarn-dyed products are even more loved. Not only silk, but also chemical fiber, rayon, blended yarn and cotton yarn can be woven with color silk, which prompt the dyeing process of bobbins to be widely applied in dyed industry. Generally, before yarn dyeing we need to wind the outsourcing of blanks into "pine-style bobbin" which is suitable for package dyeing using for the next procedure. Therefore pine-style precise winding machine is in increasingly demand.

Existing domestic pine-style winding machine's structure is generally focused on concentration of single spindle drive mode, which usually include several motion such as winding, yarn guide and over-feed, using mechanical gears and cam mechanism to complete. For winding yarn technology with a variety of yarn, equipment is difficult to adjust. Yarn body adopts grooved drum and rotary wing, which is easy to cause damage for some high-end yarn. Moreover, because the structure uses a mechanical drive, winding speed is not high. Currently, this pine-style winding has been completely using all digital winding structure abroad which based on electronic gear and electronic cam, that is, independent rotation of single spindle. Since the motor has no direct drive connection in the machinery, and combined with high-speed precision motion control software algorithms, it can easily achieve high-speed precision cross winding. The winding speed is greater than mechanical pine-style winding, which greatly improve the yarn efficiency.

Conclusion

Motion control technology is widely used in textile machinery nowadays and also in future trends. Extensive application of motion control technology not only saves the cost of textile enterprises and production time, but also improves product quality and production efficiency, and makes textile technology develop toward intelligent, large-scale, information technology and industrialization direction.

References

[1] Gao Xiaogang. Electromechanical Integration of Textile Machinery[J]. Electromechanical Integration Technology,2009(2):62-64

[2] Zhou Liping. Automatic Control Technology application in Textile Industry. Shandong Textile Economy,2007(5):100

[3] Petelin. D. P, Makarov, A. A. Control system for a winding machine[J] . Fibre Chemistry, 2006 (2) : 83-86.

[4] Wang Jiwei, Wu Zhenshun. Control Engineering Foundation[M]. Higher Education Press, 2010:77-81

[5] Chen Xingqiang. Modern Control Technology and Digital Textile Machinery. Textile Machinery, 2006(2):7-10

© (2011) Trans Tech Publications, Switzerland
doi:10.4028/www.scientific.net/AMR.331.437

Affect of Application of Hairiness Reduction Equipment on Winding Quality

Jianping Lin [1, a], Hongjun Cui [2,b]

[1] Zhejiang Textile & Fashion College,Ningbo Advanced Textile Technology & Fashion CAD Key Laboratory, Ningbo 315211

[2] Zhejiang Textile & Fashion College,Ningbo Advanced Textile Technology & Fashion CAD Key Laboratory, Ningbo 315211

[a]linjp6616@126.com, [b]ccl8325@yahoo.com.cn,

Keywords: Winding, Hairiness, HRE, Yarn Quality

Abstract. In order to reduce yarn hairiness of spooling procedure and improve the quality of knotless yarn, contrast experiments, under the given standard test conditions, is performed among several cheese with or without airflow hairiness reduction equipment (HRE); analyzing and discussing the application effect and affect of HRE on yarn quality indexs. It is found from the investigation that the application of airflow HRE can effectively reduce yarn hairiness and also reduce yarn's CV value of tenacity and improve its minimum tenacity, which can decrease ends' breakage and machine suspension during high speed warping and high speed weaving production and improve weaving efficiency and appearance quality of fabric. Through analytic comparison, the application of airflow HRE will slightly increase yarn neps, but it's still an effective method for reducing yarn hairiness and improve fabric appearance quality and weaving production efficiency.

Introduction

As the aesthetic requirements of fine count and high density for top grade fabric and technical requirements of new textile processing method for the yarn surface finish, for yarn quality, besides hairiness requirements, the users have proposed higher requirements for evenness of running thread, intensity, tenacity CV value, nep impurities and common yarn faults. Yarn hairiness refers to the fiber stretching out of yarn surface, which is one of the important factor affecting appearance, hand feel, style and application performance of final yarn products. Yarn hairiness will affect not only the surface finish and tenacity of yarn itself, but also the quality and production efficiency of the next production procedure. In particular, too much lengthy yarn hairiness will affect warping efficiency, create starch knots during starching to affect the leasing of yarn, as well as cause unclear opening of loom due to mutual tangling of yarn hairiness during weaving procedure and generate fabric defects of "three skips" and other defects as well. The situation will be even worse at the high speed of jet looms with high weft insertion speed, small warp opening and high opening frequency, the existence of yarn hairiness, especially loner than 3mm, will severely affect and block the flight of weft yarn, cause weft suspension fault and reduce weaving efficiency of jet loom. Therefore, yarn hairiness is listed as the important factor affecting fabric output and quality. Reduction of yarn hairiness has drew more and more attention in textile technology and increasingly been emphasized in textile industry.

The generation of yarn hairiness has many reasons. Charecteristics of raw materials, technical parameters of spinning processing, spinning equipment, machinery state, temperature and humidity are all the important factors which affect hairiness of yarn. Hairiness is originated in ring ingot and spun yarn procedure, and developed in spooling procedure. According to the experimental results, when yarn passes through processing of spooling procedure, the quantity of its hairiness will increase to 3.5-5.0 times as much as greige yarn [1]. During spooling procedure, due to high unwinding speed of yarn, severe collision and friction exists between yarn and machine, which caused some coiled fiber end exposed out of yarn body and form new hairiness, and some short hairiness turned out to be long after scrubbing. Therefore, to reduce winding hairiness become important. Measures like

keeping good equipment state of winding machine, controlling temperature and humidity of workshop, optimizing winding technology and adopting steel groove drum, non-contact electronic clearing equipment will lower yarn friction to certain extent and reduce winding hairiness as results, but they cannot control the increase of winding hairiness. For this reason, researchers explored many methods to effectively reduce winding hairiness, and techniques related to control of hairiness of resultant yarn [2-7] have emerged in endlessly. Among this techniques, the airflow HRE of Japanese Murata's N0.21C winding machine can effectively reduce winding hairiness [8][9], and improve yarn quality accordingly.

This paper experimentally discusses the results of applying of airflow HRE and its affect on yarn quality, which can provide theoretical reference for reducing winding hairiness, improving yarn quality and optimal usage parameters of the equipment.

Experimental equipment and set-up

Test equipment. All yarns in this experiment is produced on Murata N0.21C automatic winding machine, with or without HRE respectively. The mechanism is to tangle the long hairiness on yarn body when the yarn travelling through the channel under rotation of high speed airflow. It is therefore reduce and control the growth of hairiness. The structure of airflow yarn HRE is shown as Fig. 1.

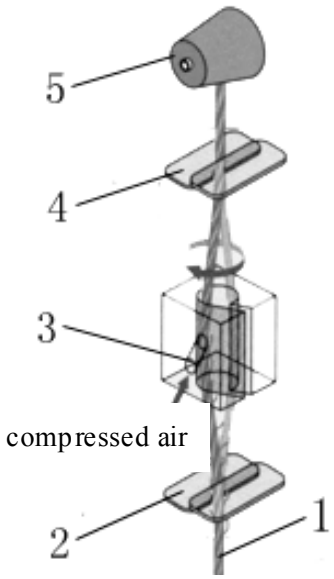


Fig. 1 Structural Drawing of Airflow HRE

1 - Yarn 2 - Lower yarn guide 3 - Jet nozzle 4 - Upper yarn guide 5 - Tube

HRE is installed on the top of tension part of unwinding channel of greige yarn, consisting of lower yarn guide 2, jet nozzle 3, upper yarn guide 4, solenoid valve, etc. When yarn passes through under high speed, compressed air switch is open and compressed air is erupted from jet nozzle 3. One small eddy area is formed for yarn to be rotated and twisted. Under the action of centripetal force, the wandering fiber of yarn surface is re-twisted on yarn trunk and wound in yarn, which lead yarn structure to be more compact and achieve bright, clean, smooth and glossy appearance, thus effectively reduce yarn hairiness and improve yarn appearance quality and performance.

Technical parameters. The technical parameters of winding is based on actual production experience, also considering production efficiency and output. Details are shown in Table 1.

Table 1 Technical parameters

Item		Parameters
Model of winding machine		Murata N0.21C
Winding speed($m \cdot min^{-1}$)		1000
Winding tension(cN)		10% of greige yarn breakage tenacity
Clearing parameters	Coarse nubs (%)	+50
	Fine nubs (%)	-50
	Neps (%)	+200
Tying form		Air splicing

Instruments and test methods. Test instruments are YG172A hairiness tester, YG061F electronic single yarn strength instrument and YG315G evenness of running thread tester, etc. 10 cheese of each yarn variety are tested, 5 sections per cheese at 10cm test length.

Yarn types for testing. Under standard test conditions, the test was performed for hairiness index, tenacity and tenacity CV value, evenness of running thread, fine nubs, coarse nubs and neps indexs of JC5.8tex, JC7.3tex, JC9.7tex, JC14. 6tex, JC18. 2tex, C19.6tex, C29tex yarn.

Experimental results and analysis

Comparative analysis of hairiness index. After analysis of the data achieved from the test, the winding hairiness before and after using airflow HRE are shown in Table 2.

Table 2 Test results of winding hairiness index

Type of Yarn (tex)	Yarn hairiness index a($pcs \cdot 10cm^{-1}$)			Application Effect Ya(%)
	a_0	a_1	a_2	
C29	71.6	112.0	89.8	19.8
C19.6	60.8	98.1	76.1	22.4
JC18.2	44.5	61. 0	52. 6	13.8
JC14.6	40. 7	46. 4	41.5	10.1
JC9.7	36. 7	43. 6	39. 8	8.7
JC7.3	31.1	37.8	35.2	6.9
JC5.8	24. 6	28.3	27.4	3.2

Note: in the table, a_0 is hairiness index of spun yarn; a_1 is hairiness index of cheese wound without using HRE; a_2 is hairiness index of cheese wound by using HRE;
Application effect $Ya = (a_1 - a_2) \div a_1 \times 100\%$.

It can be found from Table 2 that compared with spun yarn, spooling procedure will increase yarn hairiness. However, the test results before and after using airflow HRE through comparative analysis show that yarn hairiness index value decreased by 13.6% on average after using HRE,. Decreasing amplitude is within 6.9%-22.4%, C19.6tex yarn has maximum decrease while JC14.6tex yarn has the minimum decrease. Thus it's concluded that the application of airflow HRE can effectively reduce winding hairiness. But after applying airflow HRE, the hairiness reduction for extra fine yarn and combed yarn is not so obvious as medium extra yarn and combed yarn, it is because the cotton assorting quality of extra fine yarn and combed yarn is better than the medium one.

Comparative analysis of hairiness increment. After winding process, the variation of hairiness increment with different length on C19.6tex is shown in Table 3.

Table 3 C19.6tex yarn hairiness increment of different length after winding

Length of hairiness (mm)	Yarn hairiness indexs a(pcs·10cm^{-1})			Hairiness increment Rate ε(%)	
	a_0	a_1	a_2	ε_1	ε_2
0-1	35.16	48.87	46.06	39	31
1-2	17.15	31.21	20.92	82	22
2-3	5.28	8.50	4.80	61	-9
3-4	3.24	4.60	2.33	42	-28
4-5	2.10	2.67	1.15	25	-45
5-6	1.16	1.29	0.49	12	-57
6-7	0.72	0.73	0.23	2	-68
Above 7	0.31	0.30	0.08	-9	-75

Note: ε_1 in the table is hairiness increment rate of cheese wound without using HRE; ε_2 is hairiness increment rate of cheese wound by using airflow HRE.

It can be analyzed from Table 3 that, after using airflow HRE, increment of yarn hairiness less than 2mm in cheese is far less than that without using airflow HRE, and increment of hairiness over 3mm is negative value, which means airflow HRE is more effective for the hairiness reducing longer than 3mm. And hairiness over 3mm is just the leading factor affecting the efficiency of weaving production and fabric quality. Therefore, application of airflow HRE is beneficial for improving weaving efficiency and fabric quality.

Comparative analysis of yarn tenacity. Before and after using airflow HRE, the average tenacity, minimum tenacity and tenacity CV test results of cheese are shown in Table 4, Table 5 and Table 6, respectively.

Table 4 Average tenacity of yarn

Type of yarn (tex)	Average tenacity K_{cp} (CN)			Average Tenacity increment ε_{cp}(%)
	K_{cp1}	K_{cp2}	$\triangle K_{cp}$	
C29	413.9	414.7	+0.8	0.19
C19.6	291.3	295.3	+4	1.37
JC18.2	273.8	277.6	+3.8	1.39
JC14.6	201.2	205.2	+4	1.99
JC9.7	185.0	189.3	+4.3	2.32
JC7.3	128.0	131.8	+3.8	2.97
JC5.8	109.5	110.0	+0.5	0.46

Note: K_{cp1} in the table is average tenacity of cheese wound without using HRE; K_{cp2} is average tenacity of cheese wound by using airflow HRE.

Table 5 Minimum tenacity of yarn

Type of yarn (tex)	Minimum tenacity K_{min} (CN)			Minimum tenacity increment ε(%)
	K_{min1}	K_{min2}	$\triangle K_{min}$	
C29	314.0	328.7	+14.7	4.7
C19.6	205.2	211.5	+6.3	3.1
JC18.2	189.7	207.2	+17.5	9.2
JC14.6	120.2	138.9	+18.7	15.6

Type of yarn (tex)	Minimum tenacity K_{min} (CN)			Minimum tenacity increment ε(%)
	K_{min1}	K_{min2}	$\triangle K_{min}$	
JC9.7	117.2	121.4	+4.2	3.6
JC7.3	88.6	90.6	+2	2.3
JC5.8	55.4	65.3	+9.9	17.9

Note: K_{min1} in the table is minimum tenacity of cheese wound without using HRE; K_{min2} is minimum tenacity of cheese wound by using airflow HRE.

Table 6 Tenacity CV value of yarn

Type of yarn (tex)	Tenacity CV K_{cV} (%)		Decreasing amplitude of Tenacity CV Y_{CV}(%)
	K_{CV1}	K_{CV2}	
C29	7.9	7.7	2.5
C19.4	9.6	9.1	5.2
JC18.2	11.8	11.1	5.9
JC14.6	10.9	10.3	5.5
JC9.7	10.0	9.6	4.0
JC7.3	10.9	10.5	3.7
JC5.8	13.4	12.6	6.0

Note: K_{CV1} in the table is tenacity CV of cheese wound without using HRE; K_{CV2} is tenacity CV of cheese wound by using airflow HRE.

According to the analysis of the data in Table 4 and Table 5, after using airflow HRE, yarn average tenacity is increased, but the amplification is small. JC7.3tex yarn has only 2.97% increment, which is the maximum amplification. But the minimum tenacity of yarn increases obviously, JC5.8tex has maximum amplification at 17.9% In addition, according to the data in Table 6, tenacity CV value of single yarn reduces about 4.68% on average after using airflow HRE, decreasing amplitude is within 2.5%-6.0%. This shows that after using HRE, the tenacity and tenacity unevenness of yarn has been improved, which is beneficial for post production procedure.

Comparative analysis of yarn evenness CV value, coarse and fine nubs and neps. Before and after using airflow HRE, the test results of yarn evenness CV value, coarse and fine nubs and neps are shown in Table 7-10.

Table 7 Evenness CV value of yarn

Type of yarn (tex)	Yarn evenness CV(%)			Decreasing amplitude of evenness CV Y_{CV}(%)
	CV_0	CV_1	CV_2	
C29	17.72	18.38	18.03	1.9
C19.4	16.14	16.73	16.41	1.9
JC18.2	12.72	13.12	13.05	0.5
JC14.6	15.80	15. 98	15.72	1.6
JC9.7	14.25	14.63	14.52	0.8
JC7.3	13.76	14.49	14.04	3.1
JC5.8	15.92	16.60	16.42	1.1

Note: CV_0 in the table is spun yarn evenness CV; CV_1 is evenness CV value of cheese wound without using HRE; CV_2 is evenness CV value of cheese wound by using airflow HRE.

Table 8 Coarse nubs of yarn

Type of yarn (tex)	Coarse nubs S(pcs·km^{-1})			Decreasing amplitude of coarse nubs Y_S(%)
	S_0	S_1	S_2	
C29	472	566	537	5.1
C19.4	325	401	376	6.2
JC18.2	222	288	264	8.3
JC14.6	170	220	201	8.6
JC9.7	98	119	105	11.7
JC7.3	113	163	148	9.2
JC5.8	125	176	165	6.3

Note: S_0 in the table is number of coarse nubs of spun yarn; S_1 is number of coarse nubs of cheese wound without using HRE; S_2 is number of coarse nubs of cheese wound by using airflow HRE.

Table 9 Fine nubs of yarn

Type of yarn (tex)	Fine nubs T(pcs·km^{-1})			Decreasing amplitude of fine nubs Y_T(%)
	T_0	T_1	T_2	
C29	34	56	48	14.3
C19.4	30	51	45	11.8
JC18.2	22	31	25	19.3
JC14.6	20	23	21	8.7
JC9.7	31	37	34	8.1
JC7.3	54	63	59	6.3
JC5.8	86	112	93	17.0

Note: T_0 in the table is number of fine nubs of spun yarn; T_1 is number of fine nubs of cheese wound without using HRE; T_2 is number of fine nubs of cheese wound by using airflow HRE.

Table 10 Neps of yarn

Type of yarn (tex)	Neps J(pcs·km^{-1})			Amplification of neps Y_j(%)
	J_0	J_1	J_2	
C29	233	305	336	10.2
C19.4	209	247	284	14.9
JC18.2	243	253	260	2.8
JC14.6	433	412	441	7.0
JC9.7	189	211	232	9.9
JC7.3	167	235	268	14.0
JC5.8	176	258	274	6.2

Note: J_0 in the table is number of neps of spun yarn; J_1 is number of neps of cheese wound without using HRE; J_2 is number of neps of cheese wound by using airflow HRE.

According to the analysis of Table 7-10, spun yarn's evenness CV value and the total amount of coarse nubs, fine nubs and neps increases after spooling procedure into cheese, It's because collision and friction happened randomly between yarn and machine during unwinding and rewinding process, which lead some short fibers with loose combination dissociate from the yarn and form coarse and fine nubs, furthermore, the original inherent long hairiness has been rubbed into neps through high speed winding. But after using airflow HRE, cheese's evenness CV value, coarse and fine nubs will decrease, while neps will increase.

Conclusion

Yarn hairiness will increase to some extent after spooling, while the increase amplitude of yarn hairiness index falls after using HRE, The improvement is significant especially for hairiness over 3mm, which is even less than before winding with negative amplification value. It's concluded that airflow HRE is more effective for reducing the hairiness over 3mm.

During spooling procedure, the application of HRE has more significant effect on medium extra yarn and carded yarn than fine extra yarn and combed yarn. Therefore, based on economy and using effect consideration, HRE can be generally used during spooling process for medium extra yarn and carded yarn, while optionally used for fine extra yarn and combed yarn according to following production procedures which may have special requirement on yarn knotless quality.

HRE can improve average tenacity and minimum tenacity of cheese during spooling procedure and reduce tenacity CV value of single yarn, which is beneficial for high speed warping and weaving, and can reduce end breakage and machine suspension during high speed weaving production and improve weaving efficiency and appearance quality of fabric.

After spooling procedure, evenness CV value of cheese will increase slightly, coarse and fine nubs will increase too. After using HRE, coarse and fine nubs has significant improvement effect except evenness CV value.

As the short fiber with loose combination will be separated under the friction and rubbed into neps with part of original hairiness, therefore, application of HRE will increase yarn neps.

According to above analysis, airflow yarn HRE has notable effect on reducing yarn hairiness and improving yarn quality. But the effects are different due to yarn's type. But the disadvantage is higher production cost and more yarn neps Therefore, in the actual production, using the equipment or not should consider not only the quality and weaving production requirements of products but also the production cost, benefit and other factors, in order to get better economic benefits.

Acknowledgements

Fund Project: Project of Colleges and Universities Scientific Research Plan of Department of Education of Zhejiang Province, Project No.: Y201016951

References

[1] Bo Zhao. Discussion of Ways and Practice of Spooling Yarn Hairiness Reduction. Collected Papers of the 24th National Wool Spinning Annual Meeting 2004: 52 . In Chinese

[2] Boong Soo Jeon, Effect of an Air-Suction nozzle on Yarn Hairiness and Quality, TesJ, 2000, 70(11): 1019-1024

[3] Todo Yuji, Kimura Hideto, Takayasu Koji, Hairiness suppressing device for automatic winder, JP, EP1013803A2, 2000

[4] Mina Hiroshi, Nakaji, Furniaki Auto Winder, JP, EP0866014A2, 1998

[5] Wenxiang Ye, Fei Zhou, Zhihong Xiong, etc., Wool Textile Journal, 2006 (6): 47-51. In Chinese

[6] Yingqi Xu, Jun Lang, Lantian Lin, Shukang Zhu, Donghua University Journal (Natural Science Edition), 2004, 4: 5-8. In Chinese

[7] Liying Wang, Tianjin Textile Science and Technology, 1993, 3: 57-58. In Chinese

[8] Changbo Chen, Biying Liu. New Textile, 2005 (8) : 32-34. In Chinese

[9] Lijun Li, Hongjun Cui, Silk, 2006, 3: 43-45. In Chinese

© (2011) Trans Tech Publications, Switzerland
doi:10.4028/www.scientific.net/AMR.331.444

OPTIMAL GEOMETRY DESIGN OF THE COAT-HANGER DIE USED FOR MELT BLOWN NONWOVEN PROCESSING

Wanli Han[1, a], Xinhou Wang[1,2,b]

[1] College of Textiles, Donghua University, Shanghai 201620, China;

[2]Key Laboratory of Science and Technology of Eco-Textiles, Ministry of Education, Shanghai

[a]hanwanli@mail.dhu.edu.cn, [b]xhwang@dhu.edu.cn

Keywords: Genetic Algorithm, Numerical Simulation, the CV of Outlet Velocity, Residence Time, Coat-hanger Die

Abstract. In this article, a multi-objective optimization using genetic algorithms (GA) is proposed to optimize the coat-hanger die, combined with the finite element method. The manifold angle, the land height and the slot gap are chosen to be the optimized design parameters. The residence time and the coefficient of variation (CV) value of the flow velocity at the die outlet are regarded as the objective function. The optimal coat-hanger was chosen in the 30th generation among 20 individuals of each generation, which shows that the CV% value of the velocity at the die outlet is only 9.1% and residence time is 189s.

Introduction

Melt blowing is a one-step process and one of the most practical processes for producing microfiber nonwovens directly from thermoplastic polymers, in which hot/high velocity air blows the extruded filament from a die tip towards a moving conveyer belt or a cylinder. Nonwoven fibers having microfiber diameters are useful in a variety of field, such as biomedical, filter material, military and industry applications and so on. Most research on the melt blowing process are focused on the air drawing of the polymer[1,2], the performance of the jet slot dies[3,4,5], the fiber movement [6], and the prediction of the fiber diameter[7,8]. However, seldom research is conducted to deal with the coat-hanger distributor although its design is of significant importance [9]. In the melt blowing process, the polymer is passed through the coat-hanger die where the molten material is forced through a coat-hanger die. To produce meltblown nonwoven fabrics with a uniform microfiber structure, the coat-hanger die must be well designed to distribute the polymer melt uniformly across its width. In this paper, we focus on a uniform velocity distribution and minimal residence time. A multi-objective optimization using genetic algorithms (GA) is proposed to optimize velocity and residence time of coat-hanger die. Therefore, an optimal design method of the coat-hanger die geometry based on the combination of GA and numerical simulation is proposed in this article.

Numerical simulations

Figure 1 shows the coat-hanger die with linearly tapered manifolds used in the simulation.

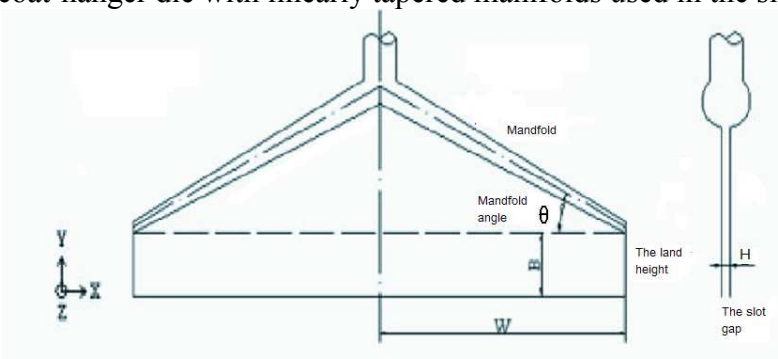


Figure1. Schematic diagram of a coat-hanger die

Assuming the polymer fluid flow in the coat-hanger die is an incompressible isothermal steady flow of Carreau fluid, the governing equations [10] are written as equation (1), (2), (3), and (4):

$$\nabla \cdot v = 0 . \tag{1}$$

$$-\nabla p + \nabla \cdot \tau = 0 . \tag{2}$$

$$\tau = \eta \dot{\gamma} . \tag{3}$$

$$\eta = \eta_0 \left[1 + \left(\lambda \dot{\gamma} \right)^2 \right]^{\frac{n-1}{2}} . \tag{4}$$

Where ∇ is nabla operator, $\boldsymbol{v}$ is velocity vector, p is pressure, τ is stress, $\dot{\gamma}$ is strain-rate tensor, η is viscosity, η_0 is the viscosity at zero shear rate, and λ is a time constant obtained from the viscosity curve of the material. η is not only related to the power-law index, but also is influenced by the temperature T. This paper adopted approximate Arrhenius law model for it as equation (5).

$$H(T) = \exp[-\alpha(T - T_\alpha)] \tag{5}$$

where α is the viscosity-temperature coefficient, and T_α is the reference temperature.

Equation (1) is the mass conservation equation with incompressible constraint. Equation (2) is the momentum balance equation, where the gravity and inertia terms are neglected. Equation (3) is the constitutive equation, in which the viscosity function is described with the Carreau model equation (4).

In the numerical simulation, because of the symmetry, only one-forth part of the coat-hanger die is simulated so that calculation time was saved much. The finite element meshes of the initial geometry are obtained and are shown in Figure 2. In the transition region, from the manifolds to the slot, the denser meshes are used to make the simulation accuracy because of the abrupt change of the geometry.

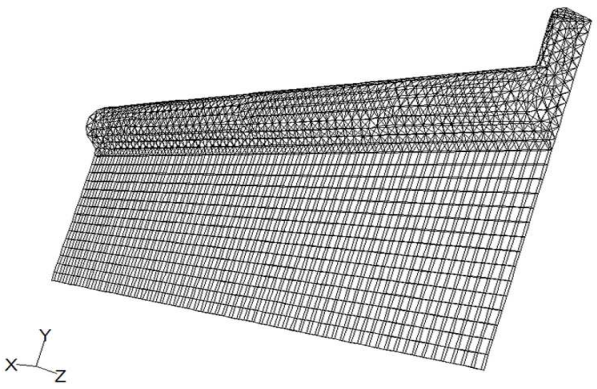


Figure2. Finite element meshes of the initial coat-hanger die

GA operation and settings

In melt blowing process, the continuous polymer stream is passed through the coat-hanger die for well-distribution. The uniform outlet velocity can produce high-quality meltblown nonwoven fabrics. At the same time, in the polymer flow channel, residence time also affects the quality of nonwoven fabrics. During the process, the residence time is the time taken by a polymer melt in passing along a specified flow stream through the coat-hanger die. Therefore, it is generally desirable to have the less

coefficient of variation (CV) value of outlet velocity as well as the short residence time. Both smaller CV of outlet velocity and residence time of the polymer flow are important for the design of coat-hanger die. Therefore, we focus on the CV of outlet velocity and residence time and want to get a polymer flow field with the smallest CV of outlet velocity and residence time for optimizing the coat-hanger die.

Genetic algorithms (GA) are search algorithms based on the mechanics of natural selection and natural genetics. It is categorized as global search heuristics which inspired by evolutionary biology such as inheritance, mutation, selection, and crossover. GA is a search technique used to find exact or approximate solutions to optimization and search problems. Nowadays this technique has been used in many research fields. In this paper, GA is aimed at finding the parameter values that the minimum CV value of outlet velocity and the minimum residence time simultaneously. So it turns out to be a multi-objective optimization using genetic algorithms (MOGA). The mathematical model of this problem can be described as equation (6):

$$Minimize \quad f(x) = \left(CV(x), RT(x)\right), \qquad where \ \ x \in X(feasible \ \ region) \tag{6}$$

In this research, the CV of outlet velocity and residence time are obtained from the simulation. In order to find the optimal values of the parameters in the feasible region X. Table 1 shows the domains of the three parameters.

Table1. Domains of slot die parameters.

	The manifold angle θ [°]	The land height[mm]	The slot gapH[mm]
a_i	5	50	2
b_i	30	150	5

Result and discussion

Figure3 shows the flowchart of the optimizing process. The first step in VEGA is to create an initial parent population consisting of random chromosomes in the problem domain, and then the parent population is randomly sorted into two sub-populations. After that these two sub-populations are carried out in the polymer flow field of coat-hanger die simulation procedure to calculate the CV of outlet velocity and residence time for each individual. According to the fitness, the genetic operations can be continued to produce the offspring. In every generation, the best individuals are left while the others are discarded. As a result, the generation will be better than the former ones during the iteration.

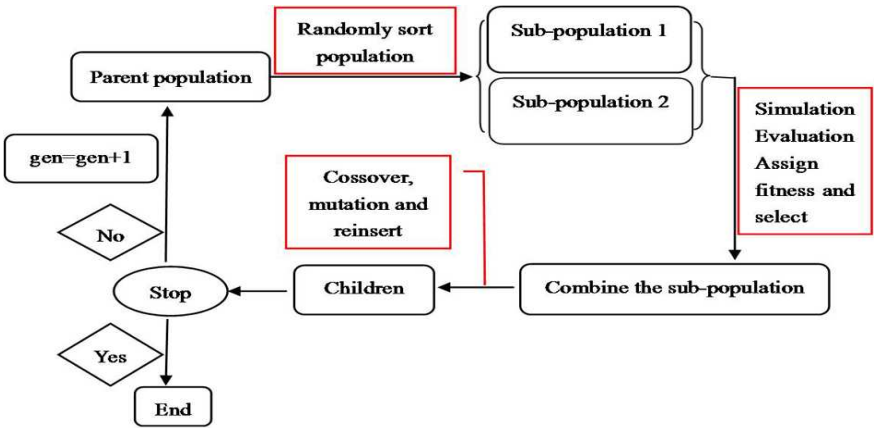


Figure3. Flow chart of optimizing process

Figure4 shows the evolution of the minimum objective function $f(x) = \left(CV(x), RT(x)\right)$. From the figure, it is clearly seen that the convergence is fast initially, and after 7 generations, the convergence slowed down and eventually led to the halting of the iteration process after 21 generations.

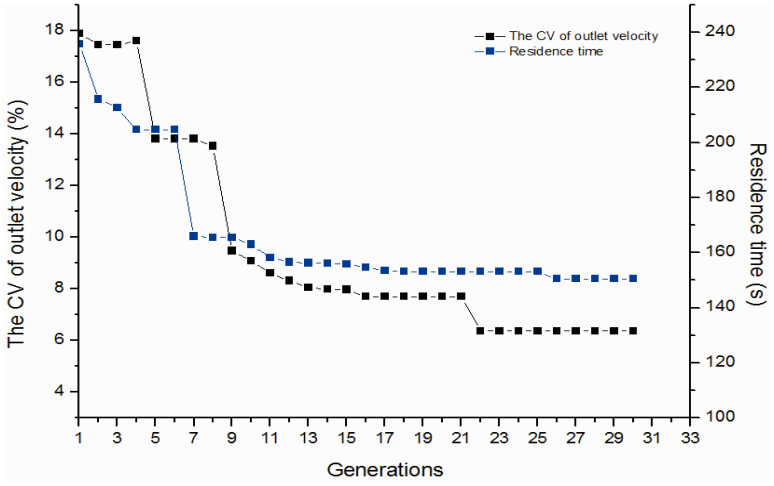


Figure4. Values of objective function versus GA iterations

Table 2 shows the optimal geometry of the coat-hanger die. It is clearly to find that the main different of the two geometries are the gap slot and manifold angle. Both of them are the prime significant factor for the distribution of velocity and residence time. The larger gap slot can achieve the uniform of velocity while a smaller one will cause the residence time decrease.

Table2. Optimal geometry of the coat-hanger dies

objectives	Manifold angle[°]	The land height[*mm*]	The gap slot[*mm*]
For CV of outlet velocity	5.1678	126.1267	4.0752
For residence time	8.7355	131.9205	2.0234
The optimal individual	5.1106	124.4184	2.6536

The geometry based on velocity has the distribution of velocity, with manifold angle of 5.1678°, the land height of 126.1267 and the gap slot of 4.0752 while the geometry based on residence time has the minimal residence time, with manifold angle of 8.7355°, the land height of 131.9205 and the gap slot of 2.0234. To meet the demands for the uniform outlet velocity and minimal residence time simultaneously, we use goal programming function among the last generation, equation (8), to calculate the optimal of coat-die.

$$f(x)=m\left[\frac{f_V(x)-f_{V\min}(x)}{f_{V\max}(x)-f_{V\min}(x)}\right]+n\left[\frac{f_T(x)-f_{T\min}(x)}{f_{T\max}(x)-f_{T\min}(x)}\right]. \tag{8}$$

where $f_V(x)$, $f_T(x)$ are the CV of velocity and residence time value respectively for every coat-hanger die, $f_{V\min}(x)$, $f_{T\min}(x)$ are the minimum CV of velocity and residence time value respectively. $f_{V\max}(x)$, $f_{T\max}(x)$ are the maximum CV of velocity and residence time value respectively. m= n=0.5.

Figure5 and Figure 6 compared the contour of the outlet velocity and residence time between the optimal coat-hanger die and the initial coat-hanger die. They showed that the velocity at the outlet optimal coat-hanger die, which is better than the initial die meanwhile residence time in the same coat-hanger die is also shorter than the initial coat-hanger die. Form the optimal coat-hanger die, the uniform of outlet velocity and short residence time can be gained.

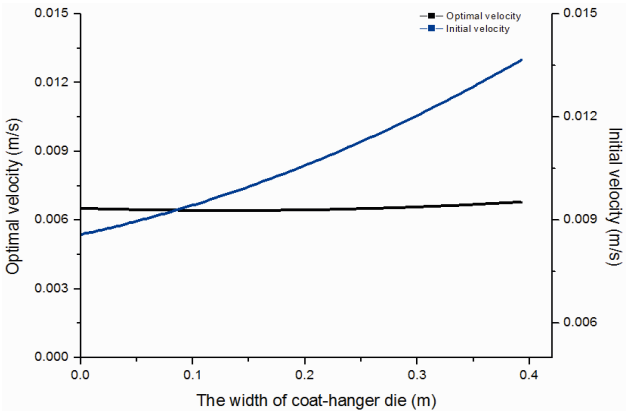


Figure5. Compared the velocity distributions at the coat-hanger die outlet

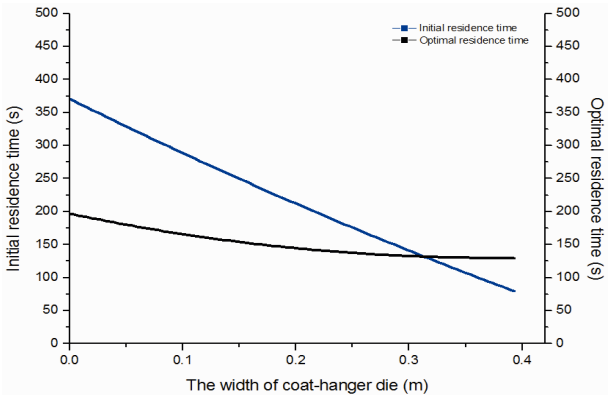


Figure6. Compared the residence time distributions at the coat-hanger die

Conclusion

The molten polymer flowing in the coat-hanger die is simulated by means of FME. The manifold angle (θ), the land height (B) and the slot gap (H) by using multi-objective optimization genetic algorithms, was proposed to optimize the CV of outlet velocity and the residence time in the coat-hanger die. It has proved that the systematic approach combining the application of numerical simulation and genetic algorithm is an effective way to optimize the geometry parameters of the coat-hanger die. With the goal programming function, the optimal geometry parameters of the coat-hanger die achieved in this study are: the manifold angle is 5.1106 degree, the height land is 124.4184mm, and the slot gap is 2.6536mm.

Acknowledgments

The authors are most grateful for the financial support provided by the Natural Science Foundation of China (50976091)

References

[1] V T Marla, R L Shambaugh: Industrial & Engineering Chemistry Research Vol. 42(2003), p. 6993.
[2] T Chen, X B Huang: Journal of Dong Hua University (English Edition) Vol. 19(2002), p. 1.
[3] B D Tate, R L Shambaugh: Industrial & Engineering Chemistry Research Vol. 43(2004), p. 5405.
[4] T Chen, X H Wang, X B Huang: Textile Research Journal Vol. 74(2004), p. 1018.
[5] Y F Sun, X B Wang: Journal of Applied Polymer Science Vol. 115(2010), p. 1540.
[6] Y C Zeng, Y F Sun, X H Wang: Journal of Applied Polymer Science Vol. 119(2011), p. 2112.
[7] T Chen, C Zhang, X Chen, et al: Journal of Applied Polymer Science Vol. 111(2009), p. 1775.
[8] T Chen, X H Wang, X B Huang: Textile Research Journal Vol. 75(2005), p. 76.
[9] Q Sun, D Zhang: Journal of Applied Polymer Science Vol. 67(1998), p. 193.
[10] X H Wang, T Chen, X B Huang: Journal of Applied Polymer Science Vol. 101(2006), p. 1570.

© (2011) Trans Tech Publications, Switzerland
doi:10.4028/www.scientific.net/AMR.331.449

Prediction of yarn quality based on BP neural network

Jing Yuan[1,2, a], Yinglin Li[1,2,b] and Suying Chen[3,c]

[1]School of Textiles, Tianjin Polytechnic University, Tianjin 300160, China

[2]Key Laboratory of Advanced Textile Composites, Ministry of Education of China, Tianjin 300160, China

[3]School of Textile and Clothing, Qingdao University, Qingdao, Shandong, 266071, China

[a]yuanjing2006@126.com, [b]tx8875@126.com, [c]chensyhk@163.com

Keywords: Textile, Yarn Quality, Prediction model, BP neural network.

Abstract. As the quality of yarn and the fiber indicators are nonlinear relationship, the traditional mathematical models or empirical formula has been unable to accurately resolve the problem. In view of artificial neural networks do not need to build accurate mathematical models, applicable to solving the problem of yarn quality prediction. In this paper, good nonlinear approximation ability of BP (Back Propagation) neural network be used, the use of neural network toolbox of MATLAB functions for modeling, good results was obtained. Prediction model set a hidden layer, using three-tier network architecture, and take the input layer 4 nodes, hidden layer 8 nodes and output layer 2 nodes. According to forecast results, can ensure the yarn quality effectively, use of raw materials rationally, to achieve optimal distribution of cotton. Meanwhile, the spinning process design can also be provided validation, for the development of new products to provide a theoretical basis.

Introduction

Essentially, Yarn quality prediction is to solve a large number of non-linear relationship between yarn quality indicators, performance indicators of raw materials and spinning parameters. In addition, in order to save costs with cotton, timely forecasts based on indicators of material quality and to adjust the distribution of cotton yarn is also very important.

At present, optimization of process parameters commonly used mathematical statistics in China. Uster statistics is widely used in textile industry of China, it contains a number of yarn indicators: evenness CV% breaking strength, breaking strength CV%, etc. Enterprises according to their own products and the results of Uster Statistics, identify gaps, analysis of the reasons, to adjust the production process of the future. However, Uster Statistics is very general, poor targeted, does not predict the quality of yarn.

In recent years, many researchers at home and abroad make the artificial neural network more and more used in textiles, Artificial neural networks have also gradually become the mainstream tool for prediction of yarn quality, many people have been studied it. Kuiyong Dong et al. studied on the use of BP neural network prediction of the quality of cotton yarn in 2001[1,2],YanxinWang et al. predicted raw material quality with BP neural network in distribution of wool[3]. Because of many factors affect the yarn quality,how to select key parameters of the model structure is also explored.

A lot of computer programming software can be used for Neural networks ,C language and C + + language is the two most common programming softwares. Currently, the U.S. company The MATHS WORKS launched neural network toolbox of MATLAB can also be used to easily implement various types of neural networks, applications can directly use the feature-rich functions to achieve the intended purpose, save a lot of programming time. In this study, constructed yarn quality prediction model with BP neural network, and used Matlab to Programme.

Neural network structure

About BP neural network. In the artificial neural network model, the most significant and wide range of applications is the BP neural network model. Characteristics of BP artificial neural network is, when dealing with issues, not accurate mathematical model, but its structure variability and strong

self-learning ability, gradually adapt to the various factors of the external environment, and constantly change their own behavior ,in order to achieve the purpose of the final solution. BP neural network formed by the input layer, output layer and several hidden layers, is a feed-forward multi-layer network model, the neurons in the same layer are not connected each other, the adjacent layers of neurons connected by weights, BP error back propagation training algorithm (gradient descent) is the commonly used algorithm.[5,6]

With a hidden layer BP network structure is shown in Figure 1, with M input nodes x_1, x_2, ..., x_M, L output nodes y_1, y_2, ..., y_L, there are q neurons in networks hidden layer.

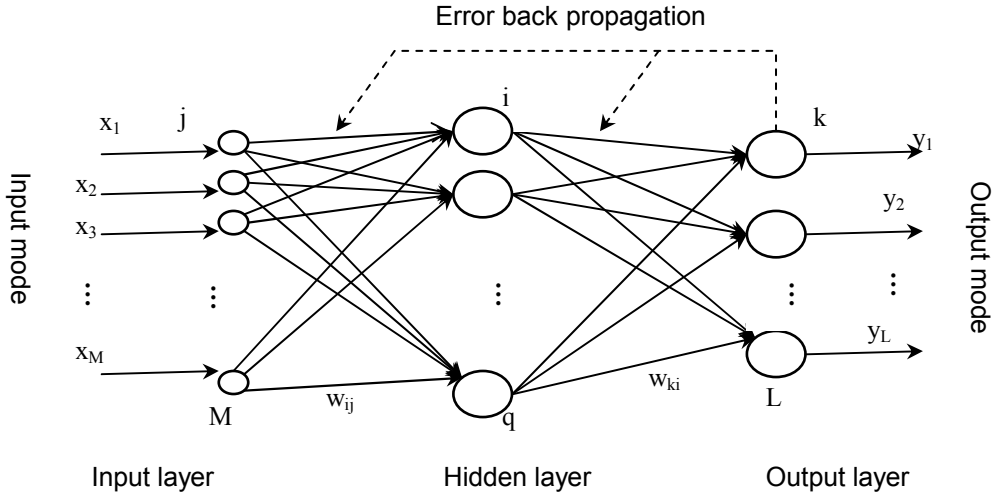


Fig.1 Schematic diagram of BP neural network

The basic principles of BP network model handling information is (The following is that to only one hidden layer BP network as an example, a number of hidden layer situation is similar): the input signal x through intermediate nodes (hidden points) on the output node, after a nonlinear transformation, produce an output signal y, each sample of network training consisted of input vector p and the expected output of T, the deviation between network output y and desired output value T, by adjusting the connection weights w_{ij} of the input nodes and hidden nodes, and the connection weights w_{ki} of the hidden nodes, output nodes and the threshold, the error decreased along the gradient direction, repeated learning and training, to determine the network parameters (weights and thresholds) corresponding to the minimum error, stop training. At this point, the trained BP neural network can handle the input information within the input range, then output the minimum output error after a non-linear transformation.

Yarn quality prediction model

Determination of neural network layers. In the spinning process, the raw cotton index, spinning parameters and yarn quality is not a simple linear relationship, therefore, the yarn quality prediction model can not simply use a layer structure, must be multi-layer network. In theory, a single hidden layer perceptron can be mapped all of the continuous function, when learning is not a continuous function, it requires two hidden layers, so BP network need a maximum two hidden layer. Therefore, in this paper, BP neural network yarn quality prediction model only set up a hidden layer, network structure has three layers, namely input layer, hidden layer and output layer.

Determination of input layer nodes. Analysis and researched the main factors affecting the quality of spinning, coupled with the expertise and practical investigations, finally, determined the close relationship with the yarn quality index value and parameters easy to quantify as a predictive model input data, the physical indicators of raw cotton: Length of the upper part (mm), Micronaire, specific breaking strength(gf/tex), fiber regularity(%).

The determination of output layer nodes. Since the main purpose of this research is to solve the problem of yarn quality prediction, the output value of the prediction model is the yarn quality index: yarn evenness CV(%), yarn breaking strength(cN/tex).

The determination of hidden layer nodes. This article uses three layers BP neural network network structure, the choice of hidden nodes is a relatively complex issue, which are directly related to how much input and output units, too much or too little hidden nodes can affect network performance. Too few hidden nodes, the capacity of network access to information is poor from the samples, not enough to summarize and reflect the law of the training set samples; too many hidden nodes, can cause learning time is too long, has a "transition agreement" issue, reduce the generalization.

Trial and error method used to determine the optimal number of hidden nodes, firstly,train the network with fewer hidden nodes, and then gradually increase the number of hidden nodes, trained with the same sample set, from which determine the corresponding hidden nodes when the network error is the smallest. In actual programming, you can refer to some empirical formula, as the initial value of trial and error method.

$$h = \sqrt{n+m} + a \tag{1}$$

Equation (1), h for the hidden nodes, n for the input layer nodes, m for the output layer nodes, α is a constant between 1 and 10.

Test

Taken the Raw cotton data and yarn quality data of a textile yarn C14.8tex variety under the period of time in a textile mill (shown in Table 1), using neural network toolbox of the MatLab finished the programming algorithm.

Table 1 The quality of raw cotton and yarn quality statistics

No.	quality of raw cotton				C14.8tex yarn quality	
	Length of the upper part [mm]	Micro naire	specific breaking strength[gf/tex]	fiber regularity[%]	yarn evenness CV[%]	yarn breaking strength[cN/tex]
01	29.22	4.49	27.80	83.45	15.80	14.10
02	29.31	4.46	27.6	83.40	15.97	13.90
03	29.23	4.50	27.78	85.50	16.00	14.70
04	29.33	4.45	27.75	83.60	15.83	14.60
05	29.49	4.42	28.36	83.66	16.13	14.20
06	29.51	4.49	28.50	83.60	15.95	13.90
07	29.45	4.46	28.46	83.58	16.00	13.70
08	29.40	4.47	28.51	83.52	16.28	14.00
09	29.25	4.41	28.28	83.27	15.86	13.70
10	29.28	4.39	28.37	83.31	16.17	13.70
11	29.06	4.25	28.20	82.80	16.28	13.40
12	28.93	4.20	28.10	82.60	15.93	14.40
13	28.85	4.30	28.10	82.50	15.80	14.30
14	29.1	4.40	28.34	82.88	16.00	13.90
15	28.88	4.30	28.10	82.50	15.90	14.00
16	27.15	4.70	28.60	80.80	16.11	15.80
17	27.70	4.60	28.84	81.10	15.60	15.20
18	27.06	4.55	29.20	81.00	15.80	14.90
19	27.62	4.50	29.70	81.20	15.60	14.70
20	27.10	4.45	29.40	81.40	15.70	14.60

The data is normalized. Normalized because of the value of sigmoid function is between 0 and 1,so the finally output of the network node is, the output of the sample is often normalized. Premnmx function and postmnmx function, which one is the normalized, one is against normalization, but the data of this function normalized is not good training effect.

Tansig, purelin, logsig is the transfer function of network structure, between itself and the normalized no direct relationship, normalization is a data preprocessing method. This data of all indicators have not magnitude difference, therefore, there is no singular samples, here all data multiplied by one per cent, all data are in [0,1] range, then you can begin operation.

Start training. After repeated verification, selecting the number of hidden nodes is 8 as an example.

```
>>P=p(1:4,1:15); T=p(5:6,1:15);  % Provide the input vector and target vector
>>threshold=[0 1;0 1;0 1;0 1];     % Set the range of input vector
>>net=newff(threshold,[8,2],{'tansig','logsig'},'trainlm');  % Networking
>>net.trainParam.epochs=10000;   % Training steps
>>net.trainParam.goal=0.0001;     % Error of training objectives
>>LP.lr=0.1;
>>net=train(net,P,T);
    TRAINLM, Epoch 0/10000, MSE 0.321269/1e-005, Gradient 2.89029/1e-010
    TRAINLM, Epoch 8/10000, MSE 4.77567e-006/1e-005, Gradient 0.0047794/1e-010
    TRAINLM, Performance goal met.
```

Seen from the above results , the network training speed quickly, and after a loop iteration achieved the required accuracy. Training error curve obtained is shown in Figure 2.

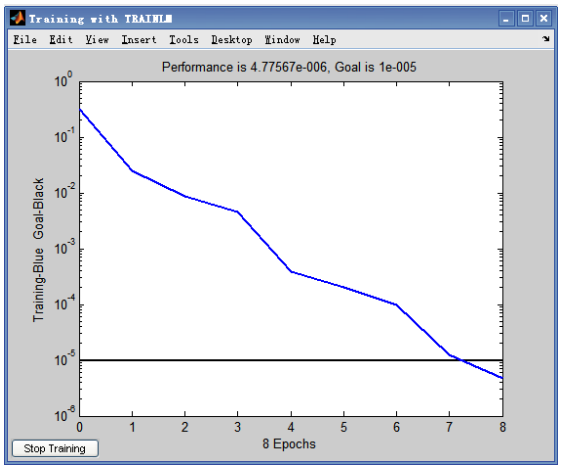


Fig. 2 Training error curve

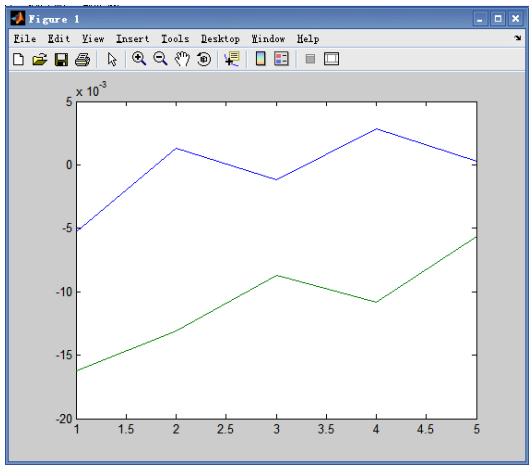


Fig.3 Prediction error curve

Results and Discussion

```
>> P_test=p(1:4,16:20); % Network test samples
>> a=sim(net,P_test) % Network prediction output in Table 2
>> plot(1:5,a-y) % Draw prediction error curve ,shown in Figure 3
```

As seen in Figure 3 and table 2, the error between the network prediction and the true value is very small, although the yarn breaking strength value are relatively large, which fully meet the application requirements.

Table 2 BP network prediction calibration data

yarn evenness CV[%]			yarn breaking strength[cN/tex]		
Predictive value [a]	Actual value [y]	Error[%]	Predictive value [a]	Actual value [y]	Error[%]
15.58	16.11	-0.53	14.18	15.80	-1.62
15.73	15.60	0.13	13.89	15.20	-1.31
15.68	15.80	-0.12	14.03	14.90	-0.87
15.88	15.60	0.28	13.62	14.70	-1.08
15.73	15.70	0.03	14.03	14.60	-0.57

From the above results shows that yarn quality prediction with BP neural network model is feasible, three-layer BP neural network achieved a better prediction performance and the accuracy prediction. And, during the prediction of yarn quality, it must be provided good training sample, so as to ensure that training results are meaningful.

Conclusions

(1)Test proved that the optimal prediction structure of the network is 3 layers BP neural network model, the input layer nodes is 4, hidden layer nodes is 8 and output layer nodes is 2. Maximum prediction error is 1.62%.

(2)The number of hidden layer nodes has a direct impact to the entire network performance and predicted results. The number of neurons obtained by the empirical formula in the hidden layer is feasible.

(3) The prediction of yarn quality using BP neural network is superior to use other methods in this experiment, can ensure the yarn quality effectively, use raw materials rationally, achieve to optimal distribution of cotton.

Artificial neural networks can solve the complex nonlinear relationship effectively in textile industry. Although the model presented here still have large errors for predicting yarn properties directly, but to some extent, it is more accurately when predict some yarn indicator. This model's performance can be further enhanced by improving the experimental conditions and expanded sample types, thus play a guiding role in the actual production.

References

[1] K.Y. Dong and W.D. Yu, in: Beijing Textile (2001),p. 53-56 (In Chinese)

[2] K.Y Dong and P.Yang, in: Jiangsu Textile (2002), p. 39-40 (In Chinese)

[3]Y.X. Wang and R.T. Liu, in: wool textile journal (2004), p. 12-14 (In Chinese)

[4] J.J.Chen,C.P.Xie and H.T.Hao, in：Beijing Textile (2004), p. 44-47 (In Chinese)

[5]Defeng,et al. MATLAB Neural Network Application Design[M]. Beijing: Mechanical Industry Press, (2009)(In Chinese)

[6] Guoyong Li. Intelligent Prediction Control and MATLAB implementation [M]. Beijing: Electronic Industry Press, (2010)(In Chinese)

© (2011) Trans Tech Publications, Switzerland
doi:10.4028/www.scientific.net/AMR.331.454

The Impact of Weft Quality on Air-jet Loom Weaving Efficiency

Cui Hongjun[1, a], Lin Jianping[1, b], Li Lijun[1, c]

[1]Zhejiang Textile & Fashion College, Ningbo Advanced Textile Technology & Fashion CAD Key Laboratory, Ningbo, P.R.China

[a]ccl8325@yahoo.com.cn, [b]linjp6616@126.com, [c]llj0924@yahoo.com.cn

Key Words: weft, quality, air-jet loom, fault shutdown, weaving efficiency

Abstract: The economic benefits of weaving production are mainly reflected in the yield of loom, whereas the loom weaving efficiency is the main decisive factor of high yield. In the production of air-jet loom weaving production, fault shutdown is the major factor impacting the weaving efficiency. Therefore, this paper carries out analysis on the quality of yarn of air-jet loom in actual production and discusses the impact of weft quality on fault shutdown of air-jet loom, so as to provide basis for the improvement of loom weaving efficiency, giving full play to the efficient weaving of air-jet loom and generating better economic benefits. The study shows that: yarn quality is the major factor influencing air-jet loom weaving efficiency, and the impact of weft quality is greater than that of warp; hence, weft quality improvement is the main way to improve air-jet loom weaving efficiency.

Air-jet loom enjoys rapid development because of its feature [1] of "four highs and one excellence", namely, high speed, high yield, high efficiency, high automation and excellent quality. However, compared with its high-performance characteristics, the weaving efficiency of air-jet loom is far short of the expected benefits. Thus, at the same time of air-jet loom development, the problem of how to improve its weaving efficiency and achieve the purpose of efficient weaving should be firstly addressed. As the economic benefits of weaving production is mainly reflected in the yield of loom, the loom weaving speed and efficiency are two main decisive factors of high yield. High-speed loom is the basis for enterprises to improve economic benefits, whereas it is not necessarily able to achieve high benefits, because benefits are also subject to the impact of weaving efficiency. The loom warp and weft fault shutdown is a key factor impacting weaving efficiency. For high-speed, highly automated air-jet looms, the impact of weft fault shutdown is particularly outstanding. Only through reducing the weft fault shutdown, the air-jet loom weaving efficiency can be improved, thereby truly achieve high production efficiency. Therefore, by the test method, this paper analyses the loom yarn quality, and discusses the impact of weft quality on fault shutdown of air-jet loom, so as to provide basis for giving full play to the efficient weaving of air-jet loom and generating better economic benefits.

Experimental Design

Fabric specification and yarn. The experimental fabric specifications are shown in Table 1.

Table 1 Experimental Species Fabric Specifications

No.	Items	Parameters
1	Name	Down-proof fabric
2	Organization	Plain
3	Side organization	Weft rib
4	Yarn fineness [tex]	CJ14.6

5	Weft fineness [tex]	CJ14.6
6	Warp density [piece/10cm]	524
7	Weft density [piece/10cm]	394
8	Fabric warp tightness [%]	74.1
9	Fabric weft tightness [%]	55.7
10	Fabric general warp [%]	88.5

The experiment design use A and B yarns in different quality for comparison. The selected two kinds of yarn are from the enterprise actual production. At the same time, to make all the experimental tests comparable, the two yarn varieties use the same sizing equipment and sizing process. According to the plant actual situation, the yarns are produced by the same Sucker sizing machine, and the size formula and sizing indicators are shown in Table 2.

Table 2 Size Formula and Sizing Indicators

No.	Items	Parameters
1	PVA－1799 [kg]	45
2	PVA－205MB [kg]	15
3	Modified starch [kg]	50
4	Propylene [kg]	3
5	Wax [kg]	2
6	Solid content [%]	14.2
7	Volume [L]	800
8	Sizing rate [%]	13
9	Rate of moisture regain [%]	6～7
10	Elongation rate [%]	<1

Experimental program design. This experiment designs four programs by using two kinds of yarn and applying different warp and weft combination methods. See Table 3 for the warp and weft combinations.

Table 3 Experiment Program

Items	Program 1	Program2	Program3	Program4
Warp variety	Yarn A	Yarn B	Yarn A	Yarn B
Weft variety	Yarn A	Yarn B	Yarn B	Yarn A

Experimental equipment and methods. The test of experimental yarn performance indicators uses YG172A hairiness tester, YG061F electronic yarn strength tester and YG315G evenness tester, etc [4]. Take 5 cones of yarn, select 5 sections for test from each cone, with the section length of 10m.

Experimental weaving equipment and main process. The fabric in this experiment is produced by Toyota JAT 710-190 air-jet loom with the working width of 190 cm; the loom is equipped with electronic warp feeding and electronic reeling mechanism, and uses cam opening device. The main experimental process parameters are determined based on the actual production experience, as shown in Table 4.

Table 4 Main Machine Process Parameters

Loom Type	Toyota JAT710-190
Speed [r/min]	650
Shed leveling time [°]	300±5
Rear girder height [grid]	3±1
Machine tension [CN/tex]	2.00±0.1
Main nozzle pressure [MP_a]	0.4
Auxiliary nozzle pressure [MP_a]	0.45
Main nozzle opening and closing time [°]	Open60 ～ Close170
Weft stop time	Open 60 ～Close 200

Experimental Results and Analysis

Yarn quality test. The quality indicators of the two yarns used by this experiment are tested under standard experimental conditions in terms of JC14. 6tex yarn hairiness index, strong and powerful CV value, evenness, snick, twit and nep. The results are shown in Table 5.

Table 5 Yarn Quality Indicators

Items	Yarn A	Yarn B
Yarn tex [Tex]	CJ14.6	CJ14.6
Strength VC[%]	8.79	11.66
Average strength[CN]	238.6	195.6
Minimum strength[CN]	199.6	145.9
Average intensity[CN / Tex]	16.34	13.40
Minimum intensity[CN / Tex]	13.67	9.99
Evenness CV[%]	15.05	16.55
Snick [PC/KM]	16	64
Twit	170	322
Nep [PC/KM]	150	253
Yarn fault [PC/10,000m]	6	23
Hairiness above 3mm	58.16	102.30

Weaving experiment results. According to experimental design, there are 4 looms in this experiments and the time is one week, so the statistical data basically reflect the actual production status of these experimental products, without chanciness. The weaving experimental results of the two different yarns are shown in Table 6. The statistical data in the table are the averages of 4 looms.

Table 6 Weaving Experimental Results

Items	Program 1	Program 2	Program 3	Program 4
Warp variety	Yarn A	Yarn B	Yarn A	Yarn B
Weft variety	Yarn A	Yarn B	Yarn B	Yarn A
Warp fault [time]	445	729	447	746
Weft fault [time]	968	2493	2398	1213
Manual shutdown [time]	84	113	87	77
Power supply OFF [time]	4	7	2	3
Waste selvedge fault [time]	9	9	10	8
Other fault[time]	16	19	18	16
Total fault [time]	1526	3370	2962	2063
Weft number [100 wefts]	59361	49271	55888	54905
Warp shutdown/100,000 wefts	7.5	14.8	8.0	13.6
Weft shutdown/100,000 wefts	16.3	50.6	42.9	22.1
Other/100,000 wefts	1.9	3.0	2.1	1.9
The ratio of wrap shutdown [%]	29.2	21.6	15.1	36.2
The ratio of weft shutdown [%]	63.4	74. 0	81.0	58.8
The ratio of others [%]	7.4	4.4	3.9	5.0
Weaving efficiency [%]	90.6	75.2	85.3	83.8

Note: others/100,000 wefts refer to the total amount of manual shutdown, waste selvedge fault, power supply OFF and other faults

Results discussion. In the production process, the shutdown times of various faults of 100,000 wefts of the 4 programs are shown in Fig. 1. It can be seen from Fig. 1 that there are fewest times of weft fault shutdown in program 1, while there are most times of weft fault shutdown in program 2. This is due to the quality indicators of yarn A are obviously better than these of yarn B; the warp fault shutdown and weft fault shutdown of using yarn A for both warp and weft are lower than these by using yarn B; therefore, the weaving efficiency of using yarn A is higher than that of using yarn B, see Fig. 2. Meanwhile, it can be seen from various fault shutdown ratio diagram of the 4 programs (see Fig. 3), the highest ratio of weft fault shutdown in loom shutdown percentage is program 3, which is 81.0%, the lowest is in program 4, which is 58.8%, but the average other fault shutdown ratio is less than 8%, so it can be concluded weft fault shutdown is the major reason for air-jet loom shutdown.

It can be seen from Table 6, Fig. 1 and Fig. 3, from the analysis of weft fault shutdown times in 100,000 wefts, program 2 has the highest weft shutdown times; while seen from the analysis of weft fault shutdown ratio in the percentage of loom shutdown, program 2 is the highest. The reason for this difference is despite both program 2 and program 3 use yarn B for the weft, they use different warps; in program 2, yarn B of low quality is used whereas yarn A of high quality is used in program 3; after sizing, the strength and hairiness of yarn A are much better than yarn B; as a result, program 3 has clear shed opening, fewer weft shutdowns, so the 100,000 weft shutdown times are fewer than that of program 2. Meanwhile, as the sizing yarn A has high strength, less hairiness, the warp fault shutdown times have been significantly reduced, only 59% of yarn B; consequently, due

to fewer warp fault shutdown times, the weft fault shutdown ratio of loom shutdown percentage increases, resulting in the weft shutdown times of 100,000 wefts in program 2 are higher than these in program 3, and the less weft fault shutdown ratio in loom shutdown percentage of program 2. Therefore, the ratio of weft fault shutdown in the percentage of loom shutdown can not fully reflect the impact degree of weft quality on air-jet loom fault shutdown. Only the weft fault shutdown times of 100,000 wefts can objectively reflect such impact degree.

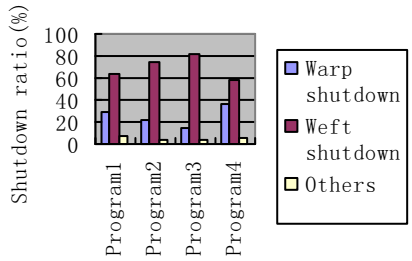


Fig. 1 Diagram of Various Fault Shutdown Ratios of the 4 Programs

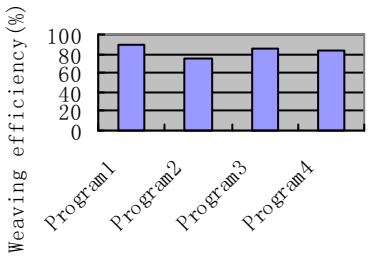


Fig. 2 Weaving Efficiency Comparison of the 4 Programs

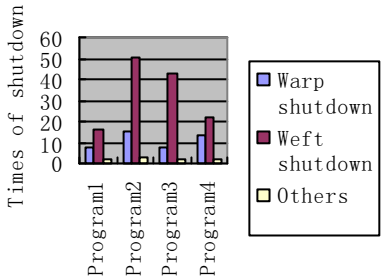


Fig. 3 Various Faults Shutdown Times of 100,000 Wefts of the 4 Programs

During the experiment, carry out experimental program comparison of the same warp and different wefts; compare program 1 and program 3, compare program 4 and program 2. Both program 1 and program 4 use high quality yarn A as the weft and program 3 and program 2 use low-quality yarn B as the weft; as yarn A has high strength, less hairiness, less broken weft, so there are fewer weft shutdown times of 100,000 times; whereas yarn B has lower strength, much hairiness, consequently, there are much broken weft and more shutdown times of 100,000 wefts; therefore, the fault shutdown times of 100,000 times in program 1 and program 4 are fewer than program 3 and program 2 respectively; but the difference of shutdown times of program 1 and program 2 is about 1,430 times, and that between program 4 and program 2 is about 1,285 times, which shows the impact of weft quality on weft fault shutdown is, the better the warp quality is, the more obvious the impact is; on the contrary, the worse the warp quality is, the less impact is.

In addition, it can be seen from the analysis of Table 5 and Table 6, compare the 100,000 weft warp faults of program 1 and program 2, these of program 2 are 1.97 times of these of program 1, whereas the weft fault shutdown of program 2 is 3.1 times of that of program 1, much higher than

warp fault. Therefore, in terms of yarn quality's impact on air-jet loom weaving efficiency, weft has higher impact than warp. This is because although warp yarn is in bad quality, after the process of warping and sizing, its strength and strength unevenness have been improved, and the hairiness are appressed; however, without preparation and process, the weft yarn performance has not been improved, so the impact of weft quality on air-jet loom is greater than that of warp.

Conclusions

Through the above analysis, the following conclusions can be obtained:

(1) As various quality indicators of yarn A are significantly better than these of yarn B, the weaving efficiency of using yarn A is better than that of yarn B; so yarn quality is a main factor impacting air-jet loom weaving efficiency. Yarn quality improvement is the main way of improving air-jet loom weaving efficiency.

(2) Through the processes such as warping and sizing, the warp yarn strength and strength unevenness have been improved, the hairiness is appressed, the weaving performance has been significantly improved and the loom shutdown caused by warp fault has reduced. However, without process, the weft weaving performance has not been improved; low strength, much hairiness make greater possibility of broken weft or weft blockage, thereby the times of loom shutdown caused by weft fault increase. Hence, in terms of yarn quality, the impact of weft on air-jet loom is greater than that of warp. Only by reasonably improve and control weft quality, including weft strength, hairiness and winding shape, etc, the weaving efficiency can be significantly improved.

(3) The ratio of weft fault shutdown in the loom shutdown percentage can not fully reflect the impact degree of weft quality on air-jet loom fault shut down; only the weft fault shutdown times of 100,000 wefts can objectively reflect such impact degree.

Acknowledgements

This work was financially supported by Ningbo Natural Science Foundation (2009A610091) and Ningbo Industrial Scientific Research Project (2007B10050).

References

[1] J. Zhang, Difficult Problems of Using Air-jet Loom, China Textile Press(2001), p. 113. (In Chinese)

[2] H.Yan, J. Dai, Air-jet Loom Principles and Use, China Textile Press(1996), p. 249. (In Chinese)

[3] Y. Li, J. Zheng, Production Practice and Analysis on Improving the Yield Quality of Shuttleless Loom, Proceedings of New Weaving and Preparatory Technology Seminar(2004), p. 20. (In Chinese)

[4] H. Zhu, Textile Materials, China Textile Press(1994),p. 190. (In Chinese)

© (2011) Trans Tech Publications, Switzerland
doi:10.4028/www.scientific.net/AMR.331.460

Comparative Study on Vibratory Stress Relief (VSR) and Thermal Stress Relief (TSR) of Cylinder Wallboard

Xuewu Dong [1, a], Xiping Zhao [2, b], Songqing Yu[2, b], Xiaowen Zhou[1, c], Dai Ren [1, d], Yafei Zhai [1,a]

[1] Zhongyuan University of Technology, Zhengzhou, P.R.China, 450007

[2] Zhengzhou Textile Machinery Company, Zhengzhou, P.R.China, 450007

[a]dxw@zzti.edu.cn, [b] foundryzfj@126.com, [c]xwzhou@zzti.edu.cn, [d]dianneren@zzti.edu.cn,

Keywords: Cylinder Wallboard; Vibratory Stress Relief (VSR); Thermal Stress Relief (TSR); Modal Analysis; Carding Machine

Abstract Dimensional stability of carding machine has a greater impact on the performance of the Cylinder wallboard. Compared with the thermal stress relief (TSR), the vibratory stress relief (VSR) is a new technology which may eliminate the residual stress in metal components with high efficiency, energy saving, environmental protection and low cost. We have 8 pieces of cylinder wallboard castings with every 4 pieces as a group. It takes 20 minutes to do VSR in one of the groups and 20 hours for TSR in another group. Three identical size accuracy indexes are measured, respectively at intervals of 1 month 2 months after aging treatment. The results show that: the dimensional stability of cylinder wallboard vibration by VSR is better than the one by TSR. Energy consumption and cost-saving is more than 90% without "three wastes" emissions.

Introduction

Cylinder wallboard (see fig. 1) is a key component in carding machine. The dimensional stability has a great influence on the performance of carding machine. At present, we usually use the traditional TSR to reduce the macroscopic residual stress of cylinder wallboard in order to ensure dimensional stability, with the shortages of limited effect, low efficiency, high energy consumption, exhaust and residue emissions. However the vibratory stress relief (VSR) possesses the advantages of high efficiency, energy saving, environmental protection, low cost and etc. compared with the thermal stress relief (TSR). So it is scientific and practical for the comparative study on cylinder wallboard by VSR and TSR. Let's take 8 pieces of cylinder wallboard castings and every 4 pieces as a group. One group is by VSR for 20 minutes. Another group is by TSR for 20 hours. Three identical size accuracy indexes are measured respectively at the intervals of 1 month and 2 months, after aging treatment.

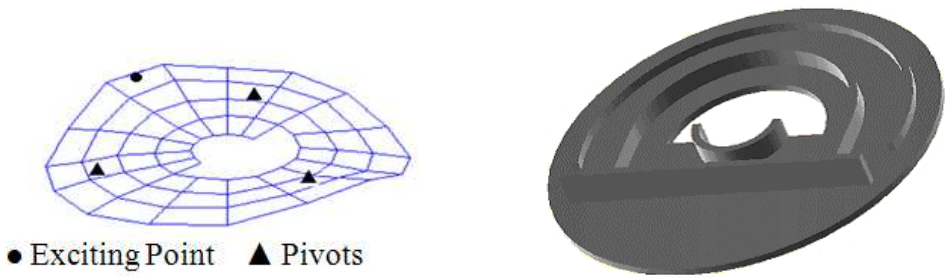


Fig.1 The 3D Drawing of Cylinder Wallboard

2.0 VSR Technical Parameters

VSR technical parameters cover exciting force, exciting frequency, exciting point, pivot and exciting time. By adopting modal analysis method to measure each order natural frequency and vibration mode of the cylinder wallboard, we can design the best VSR technical parameters.

2.1 Modal Analysis

The natural frequency, vibration mode and other natural parameters are measured for the cylinder wallboard by adopting experimental modal analysis system in Figure 2 as below:

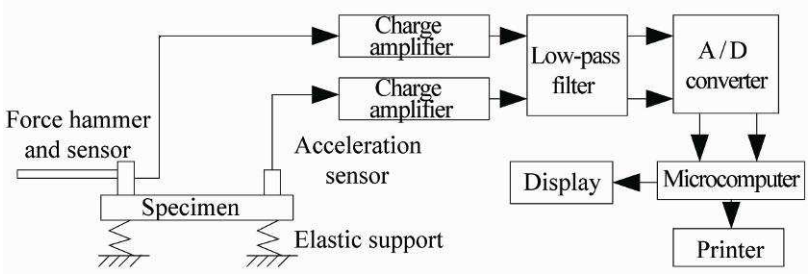
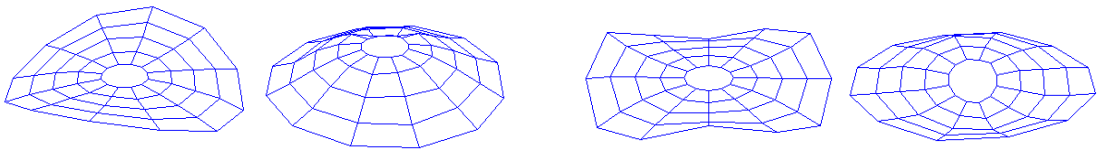


Fig.2 Principle of EMA system

There are many modes with some local modes between 0 ~ 1000HZ, due to the effect of the cylinder wallboard surface ribs. We obtain the basic natural vibration mode of disk parts and 4 low-order modes by modal analysis of cylinder wallboard, shown in Figure 3. Vibration mode (b) and (d) are called the drum shape vibration mode because it looks like a drum. The feature is that radius direction has uniform distributed bending vibration deformation.The vibration mode (a) and (c) are called the saddle shape mode because it looks like a saddle. The feature is the circumference direction has uniform distributed bending vibration deformation



(a) 1 order vibration mode (b) 2 order vibration mode (c) 3 order vibration mode (d) 4 order vibration mode

Fig.3 The first 4 modes of cylinder wallboard

2.2 Design of VSR Process Parameters

There are many ribs due to complex surface which causes residual stresses concentrating in these areas, in the casting molding process of the Cylinder wallboard. In addition, vibration displacement gets large by using low-order natural frequency to vibrate the cylinder wallboard and it is helpful to eliminate residual stress. So we choose 1 order mode as design basis of the VSR technical parameters. Figure 4 indicates parameters of exciting frequency, exciting point and pivot process. Since we select low-order natural frequency of the specimen as excitation, the smaller the excitation force is sufficient to excite the vibration. By experience, we generally take 1/10 specimens weight as excitation force amplitude [3]. Here we take 300N. Exciting time is 20 min. by experience,

Experiments

3.1 Experimental Program

We select 8 pieces of cast molding wallboards in the same condition. 4 of then are of VSR treatment. Another 4 are of TSR treatment. VSR treatment wallboards label V1, V2, V3, V4 and TSR treatment wallboards label T1, T2, T3, T4.

Methods for Experimental:

（1）Using experimental modal analysis technology to identify each order natural frequency values of cylinder wallboard and the corresponding modal shapes.

（2）We can develop the VSR process parameters of cylinder wallboard such as exciting frequency, exciting point, pivot etc. by considering the stress distribution of the components and experimental data of modal analysis, and use practical methods to determine vibration exciting force, exciting time and so on.

（3）We can do VSR treatment on the cylinder wallboard castings by assuming VSR process parameters.

（4）We measure workpiece deformation by detection of dimensional stability to verify validity of VSR design parameters and feasibility of the methods.

3.2 VSR Process Implementation

Place three rubber mats in the pivots of the cylinder wallboard and fix exciter on the excitation point of the cylinder wallboard, see Figure 4. Adjust vibrator eccentric and get exciting force as 300N. Start exciter. Adjust the speed to 5880r/min, and make it vibrate for 20min.

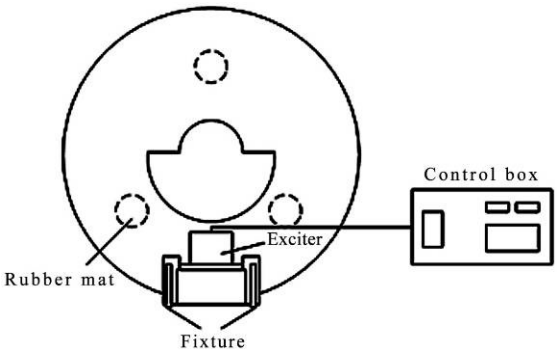


Fig.4 Sketch of VSR on Cylinder Wallboard

3.3 Detecting Effects

We measure the size deformation of cylinder wallboard by static dimensional stability detection, and then compare stress reduction effects of different treatment methods.

（1）Specimen processing: There are eight wallboards in the same group for processing, in the gantry machining centers and the processing parts diagram is shown in Figure 5.

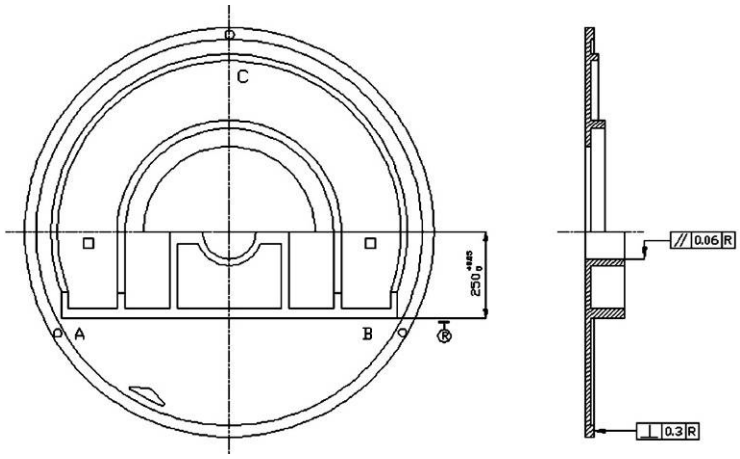


Fig.5 Drawing of Cylinder wallboard

（2）Measuring Item: Three items are to tested as flows.

$250_{0}^{+0.05}$: We use dial indicator for measurement because the distance between center line and reference plane cannot be measured directly. So measure the distance between the surface of the semicircle and R surface to determine its size tolerance. When measuring, measure a size value at each end of the hole and the average of the two dimensions is considered as measured size tolerance.

$\perp 0.3/R$: We do measurement with micrometer. It is as follow: first measure the distance between related point A of the two wallboards and then measure the distance between the related point B. Adjust the corresponding nut of A, B two points in the testing table so that pin push wallboard to an equal corresponding distance between wallboard A and B and set the size as a. Measure the distance between corresponding point C of the wallboard , note the measured size as b, then the measured vertical size is | b-a | / 2.

//0.06/*R*: The same measuring methods as $250_{0}^{+0.05}$ The measured size is the absolute of the difference between both ends measurements.

Based on the above methods, measure dimensions immediately after machining, as a benchmark, measure again at interval a month, conduct a total twice. We obtain the effect of VSR and TSR reducing residual stress and improve dimensional stability of the workpiece by comparing the measured size deformation.

Experimental data as shown in table 1.

Tab.1 Deformation of Cylinder Wallboard Unit: um

Measuring Item	Measuring time	TSR					VSR				
		T1	T2	T3	T4	Average	V1	V2	V3	V4	Average
$250_{0}^{+0.05}$	After cutting processing	50	30	10	5	23.8	50	50	40	10	37.5
	The deformation after one month	2	-8	12	27	8.3	12	12	2	12	9.5
	The deformation after two months	4	9	24	54	22.8	4	19	6	49	19.5
$\perp 0.3/R$	After cutting processing	100	80	80	100	90.0	100	30	50	100	70.0
	The deformation after one month	-30	-10	-10	-50	-25.0	-30	10	10	-50	-15.0
	The deformation after two months	-30	-5	-5	-30	-17.5	-30	-10	-10	-30	-20.0

//0.06/*R*	After cutting processing	20	20	20	20	20.0	20	10	10	15	13.8
	The deformation after one month	0	40	10	10	15.0	-20	0	10	15	1.3
	The deformation after two months	-20	-10	0	-10	-10.0	0	0	10	15	6.3

3.4 Analysis of Result

From Table 1, we can see that using VSR and TSR processing wall components can have effect of eliminating and smoothing residual stress. These eight wallboards are dealed by the two aging methods. Then the size deviation of its measured project is within the tolerance after two months of observation and measurement. However, the deformation vibration of the wallboards by VSR looks smaller than the ones by TSR, which indicates that the deformation resistance of the former is better than the latter**.**

Meanwhile, VSR of the cylinder wallboard is better than TSR in aspects of production efficiency, cost, energy consumption, environmental protection. TSR of a cylinder wallboard requires 20 hours or more while VSR of a cylinder wallboard only takes 20 minutes. TSR of a cylinder wallboard needs to use coal or oil and gas, and VSR of cylinder wall requires only about 3 degrees per hour energy consumption. Energy consumption is reduced by more than 95%. TSR produces waste and gas emissions while VSR does not produce gas, ash and other pollutants.

Conclusion

From the above test, we can draw a conclusion that deformation resistance of the cylinder wallboard by VSR is superior than the one by TSR and VSR treatment, with the advantages of high efficiency, low cost, energy saving, environmental protection.

Acknowledgements

I would like to give my sincere thanks to Natural Science Foundation of Henan Province, the technical staff in the Technology Service, Quality Department of Zhengzhou Textile Machinery Company and casting companies during our research job for their support and cooperation.

References

[1] Xuewu Dong, Xiaowen Zhou and so on. Study of plate casting VSR Process Parameters Design Method [J]. Zhongyuan Institute of Technology, 2006, 17(4):1-3.

[2] Dongjiang Wang, Xuewu Dong and so on. Study of the optimization of the Casting VSR Excitation Frequency Parameters [J]. Group Technology and Production Modernization, 2008, 25 (3):48-51.

[3] Zaiji Hu, Xuewu Dong. Discussion of VSR Process [J]. Casting Technology, 1995, (3):26-31.

© (2011) Trans Tech Publications, Switzerland
doi:10.4028/www.scientific.net/AMR.331.465

Study on New Drafting Form of Comber

Xin Rong LI [1, 2, a], Xiu Ming JIANG [1], Jian Cheng YANG [1]

[1]School of Mechanical Engineering, Tianjin Polytechnic University, Tianjin, 300160

[2] JingWei Textile Machinery Co Ltd YuCi Branch,Shanxi,030601

[a] lixinrong7507@hotmail.com

Keywords: comber, curvilinear draft, three over three drafting form under pressure bar, drawing frame, high-speed

Abstract. With analysis of development tendency of domestic and abroad high-speed combers, in this paper we proposed a new drafting form to comber--three over three curvilinear draft under pressure bar combining with development and successful experience for high-speed drawing frame. Moreover, combing experiment in this new drafting form was performed on basis of theoretical analysis and calculation. The results showed that this new type of drafting form satisfied the users' demand for high-speed as well as the comber's qualification.

Introduction

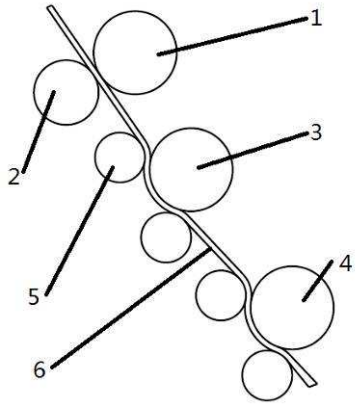
Combing machinery, as textile machinery equipment of collecting comprehensive application with advanced technology such as machine, electricity, gas, light etc, plays an important role in enhancement of textile products' grade and quality. Currently, comber develops toward the direction of high-speed, high-quality and automation, so advanced drafting form needs to be put forward. And a proper drafting form of comber has a significant impact on combed silver and yarn evenness [1]. At present, comber mainly applies in three-over-five drafting form consisting of two draft zones--prozone (main drafting area) and backzone (preliminary drafting area) as shown in Fig.1 where are composed of five rollers and three leather-rollers. But this type of drafting form has some problems as follows:

(a) Its drafting ratio cannot meet the requirement for high-speed of comber. Blow effect of cylinder to cotton fiber is enhanced with increase of comber speed, namely cylinder revolving speed. Thus, comber laps need to be raised quantitatively. That is, cotton silver on the surface of comber is increased quantitatively. Therefore, drafting ratio is required to be higher.

(b) Its drafting quality cannot satisfy the demand for high-quality of comber. When comber develops toward the direct of high-speed, we pay more attention to the improvement of products' quality. In old drafting form, curve surrounded arc which is produced by web on roller surface in main drafting area is used to enhance friction bounded strength at middle-back of main drafting area; thus the control to floating fiber is strengthened, and the shift point is put forward; and finally combed sliver evenness is improved. But the curve surrounded arc produced by this drafting type is short, making controlling ability of fiber movement relatively weak; and anti surrounded arc produced by cotton web on surface of front leather roller has a negative influence on combed silver evenness.

(c) Its spinnability cannot meet the demand to current comber. The drafting range of current comber is adjusted narrowly, i.e unadjustable backzone spacing, leading to bad spinnability to different lengths of fibers.

As mentioned above, it is necessary to improve the drafting form of comber, with development of current comber. And the improvement of drafting form is a basic requirement for high-speed, high-quality and better spinnability.



1—front leather roller; 2—front roller; 3—middle leather roller; 4—back leather roller; 5—middle-back roller; 6—cotton web

Fig.1 Three over Five Drafting Form Schematic Diagram

New Drafting Form

By analysis of the developing tendency of domestic and abroad comber, and on basis of the, we conclude the requirements of comber drafting form as follows [2-3] based on technological superiority for present comber:

(a) New drafting form makes use of curvilinear draft to improve the control for fiber movement by means of increasing additional friction bound and to shorten the length of floating area, making shift point of fiber forward and concentrated.

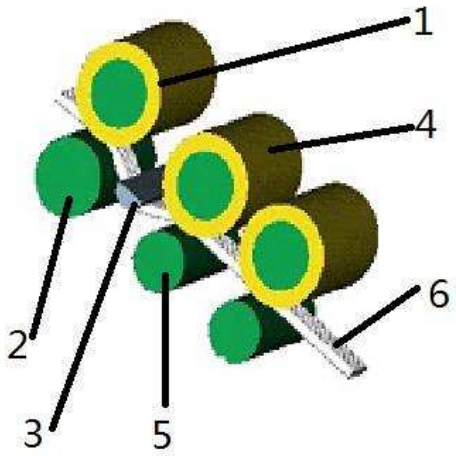
(b)New drafting form makes cotton web fed into front nip directly along tangent direction in order to avoid anti surrounded arc that is produced at the front of first pair of rollers destroying sliver evenness.

(c)New drafting form is beneficial to enhance degree of fiber's extension and parallelism, thus drawing ratio is larger and fiber spinnability is better.

(d) New drafting form develops toward to direction of simple construction and convenient process adjustment.

Comparing with drafting form to combers and drawing frame at abroad, we found that, drafting form of the above two machines tends to be consistent, thus the development and success of drafting form to high-speed drawing frame establish a fine basis for that of comber. In conclusion, we proposed a new type of drafting form to comber-- three over three under pressure bar with adjustable distance (shown in Fig.2). The new type of drafting form contains two drafting zones, where are composed of three rollers and three leather rollers. In the main drafting zone, a pressure bar is installed, and front roller in larger diameter and boosting middle-back roller are also applied. The former is used to reduce the speed of front roller, as well as to maintain high-speed silver; the latter is to avoid roller center distance and gripping distance increasing too excessive, and meanwhile, to make the pressure bar position proper. Prozone, the main drafting area, adopts curvilinear draft under pressure bar. Pressing effect of pressure bar makes silver produce surrounded arc on the surface of roller and pressure bars when by draft, so strong friction filed is produced, the control of floating fiber is enhanced in main drafting zone and the combed silver quality is

improved. On the other hand, increase of friction filed of silver on pressure bar surface satisfies the demand of fiber stretching force, and larger roller gripping distance is in favor of prolonging the stretching time of fibers and further improving the extending and parallel degree of fibers. But because of backzone, the preliminary drafting area with adjustable drafting spacing, the spinnability of comber is increased to different lengths of fibers.



1—front leather roller; 2—front roller;3—pressure bar; 4—middle-back leather roller; 5—middle-back roller; 6—cotton web

Fig.2 Three over Three Drafting Form Three-dimensional Diagram

Pressure Bar Position in New Drafting Form. Curvilinear draft with additional pressure bar aims at enhancing control of slower fiber to floating fiber. If the number of slower fiber is less than that of floating fiber, most of floating fibers would not be contacted with the slower fiber in planktonic instability state. In order to increase the contact probability of slower and faster fibers, the amount of slower fibers in the adherent point of pressure bar and cotton web needs to be no less than that of the floating fibers [4].By calculation of fiber numbers held and non-held by rollers in the drafting area, the reasonable spot of pressure bar can be known based on draft theory [5].

Firstly, set holding distance as R and draft rate as D, fiber heads of output silver per unit length is $\frac{n(X)}{D}$. If the feeding strand is regarded as fundamentally uniform, to make the output strand uniform as well, the controlling point position of slower fiber to floating fiber should be properly planed. Supposing that $f(l)$ is ratio of number of fibers in the feeding web whose length is between l and $l+d(l)$ to the total amount of fibers in different lengths (namely frequency), the number of fibers from bundles is $n(X)dX$ in the length of $d(X)$. And X is the gauge between pressure bar controlling point to back-roller nip as shown in Fig.3. Therefore, the total number of fibers is $\int_X^{X+l} n(X)dX$ from feeding place X to $X+l$.If fibers from the bundles are in the same length, each fiber in above equation also has equal length. But in fact, the length of fiber that forms fiber bundles has a difference among each other. Set the shortest fiber length as S and the maximal length as W, the length distribution frequency of fibers is $f(l)dl$.

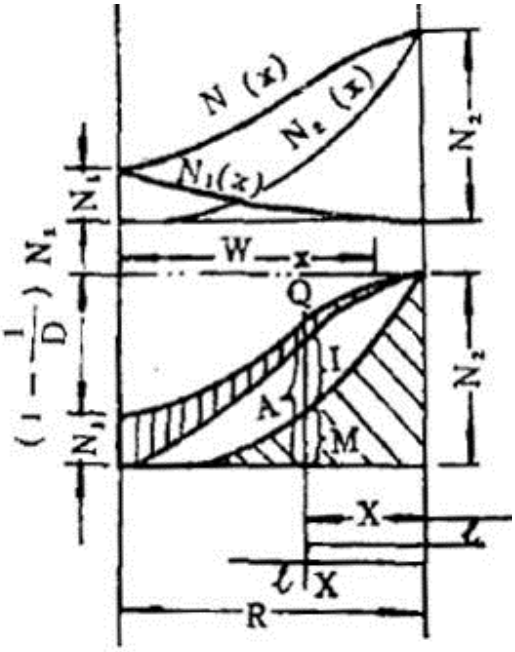


Fig.3 Fiber Number Distribution in Front Drafting Area

In Fig.3, total number of fibers through X section we require, subtracting the amount of slow fiber M held by back roller and then deducting the number of fast fiber Q that is held by front roller after drawing, is the quantity of floating fiber I that is fed into back-roller at X section. The number of these floating fibers should be inferior or nearly equal to that of the slow fibers held by back-roller at X section, so that slow fibers well control the floating fiber. And also because of $I = A - M - Q$, it is expressed as:

$$A - M - Q \le M$$
$$A - Q \le 2M \tag{1}$$

At ideal condition fiber head changes speed when reaching to front nip, so the amount of fibers drawn by front nip approximately is $\frac{W-(R-X)}{W}(1-\frac{1}{D})n(X)$. And at X point the average number of total fiber heads is $\left[1-\frac{W-(R-X)}{W}\left(1-\frac{1}{D}\right)\right]n(X)$, thus

$$A = \int_S^W \left\{\int_X^{X+1}\left[1-\frac{W-(R-X)}{W}(1-\frac{1}{D})\right]n(X)dX\right\}f(l)dl$$
$$= \left[1-\frac{W-(R-X)}{W}\left(1-\frac{1}{D}\right)\right]n(X)\int_S^W lf(l)dl \tag{2}$$

Because the space between acting arc back-end of pressure bar and surrounded arc front-end of the second roller is less than the shortest fiber length, the integral of slow fiber number M from S to W is:

$$M = \int_S^W \left[\int_R^{R-X+1} n(X)dX \right] f(l)dl$$
$$= \int_S^W \left[\int_S^l n(X)dX \right] f(l)dl \quad (3)$$

But distance between frontier point of pressure bar and front nip is greater than the shortest fiber length, so fast fibers in less than $R-X$ length cannot be controlled by pressure bar. Thus, the integral of fast fiber number Q from $R-X$ to W is:

$$Q = \int_{R-x}^W \left[\int_R^{x+1} \frac{1}{D} n(x)dx \right] f(l)dl \quad (4)$$

Substituting Eq. 2, Eq. 3 and Eq. 4 in Eq. 1, it is obtained:

$$\left[1 - \frac{W-(R-x)}{W} \left(1 - \frac{1}{D} \right) \right] n(x) \int_S^W lf(l)dl$$
$$- \int_{R-X}^W \left[\int_R^{X+1} \frac{1}{D} n(X)dX \right] f(l)dl \quad (5)$$
$$\le 2 \int_S^W \left[\int_S^l n(x)dx \right] f(l)dl$$

Eq. 5 represents fiber accumulative length frequency in the range of fiber length at X section divided by the number of heads per length. And when length is multiplied by weight linear density per length, the weight in the range of unit length is gained. By Rukov length analysis of feeding cotton silver, from Eq. 5 distance between pressure bar frontier spot and front nip X value can be calculated by accounted weight percentage from floating region space between frontier pressure spot of pressure bar to front nip to longest fiber on basis of weight percentage multiplied by each fiber length and accumulative length percentage.

Distance between frontier pressure point position of pressure bar and front nip needs to consider two factors--the processed fiber length or their length distribution, and drawing ratio. In summary, the pressure bar gripping spacing X is closely related to processed fiber length.

Leather-roller and Roller Position. Fig.4 shows the pressure bar drafting form. It is presented that the first roller is 35mm diameter, and the second and third roller are both 27mm diameter. In order to directly feed cotton web into the front roller nip along with tangential direction, and to avoid forming anti surrounded arc at the front first pair of rollers, the second and third pairs are raised up by 4mm.

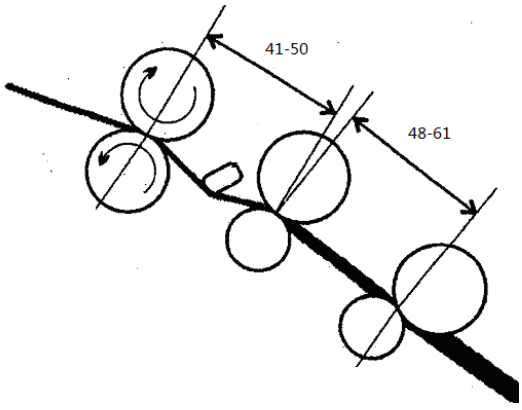


Fig.4 Three over Three under Pressure Bar Drafting Form Schematic Diagram

In pressure bar holding space, in order to extend anti surrounded arc of the two rollers and strengthen the control of silver, the two rollers holding point should be in the same vertical center line, so that, surrounded arc in the prozone is enlarged and anti surrounded arc in the backzone is eliminated or decreased. For sake of lessening the floating time and the number of floating fibers between front and middle rollers, free length in prozone should be as short as possible under license of controlling force and holding force. That is, the rollers gripping distance should be narrowed, simultaneously the frontier point of pressure bar is arranged as maximal as possible.

Experimental and analysis

New Drafting Form Experimental. According to theoretical analysis and combed experimental, the test datas for new drafting form are shown in Table1 and Fig.5.

Table 1 Experimental Data in New Drafting Form

No.	U (%)	CVm (%)	CVm1m (%)	Rel.Cnt (±%)
1	2.23	2.86	0.85	0.4
2	2.29	2.87	1.07	-0.4
3	2.38	2.99	1.43	-0.6
4	2.17	2.73	0.78	0.6
Mean	2.265	2.865	1.035	0

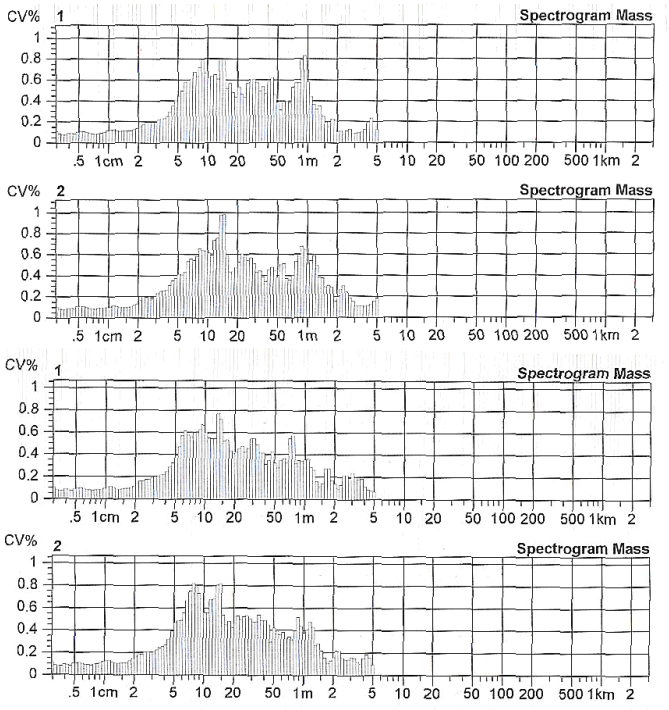


Fig.5 Experimental Wave Spectrogram

Comparative Experimental. Table 2 shows the experimental results for new and old types of drafting forms.

Table 2 Experimental Data for New and Old Drafting Form at Different Speeds

	Three-over-three				Three-over-five			
Speed(nips /min)	250	300	350	400	250	300	350	400
Evenness CV (%)	3.4	3.14	3.07	2.78	3.2	3.4	3.53	3.82
Nep (grain /g)	25	24	22	20	22	24	25	28
Impurity (grain /g)	18	18	19	18	19	17	19	18

Table 3 Experimental Data to 31mm Long Fibers in Old and New Drafting Form

	Combed silver eveness CV (%)			Combed cotton nep (grain/g)		
	1	2	3	1	2	3
Three-over-three pressure bar	2.77	2.84	2.78	18	19	18
Three-over-five	3.55	3.45	3.52	24	23	25

As indicated in Table 2 and Table 3, we find that, the technical qualification of three-over-five drafting form is better than that of three-over-three at low speed of 300 nip/min. On contrary, at a speed of 350 nip/min, three-over- three drafting form is better than three-over-five drafting form in technical characterization. And drafting in three-over-three form makes spinnability of long fibers better than three-over-five form. That is, new drafting form is more proper to spin different lengths of fibers.

Conclusion and Prospect

When using new drafting form system, it makes the institution simple and transmission reasonable. By contrast of two drafting forms, the experimental results showed that, technical qualification of three-over-three drafting form at high-speed was better than that of three-over-five old drafting form; but at 300 nip/min, three-over-five drafting form was better than three-over-three drafting form; and for the spinnability of long fiber, three-over-three form was superior to three-over-five form. New type of drafting form satisfies the demand for users' high-speed, as well, it meets requirement for technical specifications of combed products. And owing to decrease of rollers number, the center spacing among rollers is also narrowed, which is beneficial to process staple fibers and thus enhance the spinnability of combed fibers. Furthermore, combed silver directly is span by roving frame and air spinning, both of which shorten the process flow. That is because three-over-three under pressure bar curvedly-drafting form increases friction field and enhances the drawing ratio, and also, the technical qualification of combed silver corresponds to the first drawn silver.

References

[1] J.Y.Reng, Y.G.Yang: Cotton Textile Technology Vol.35(2007),p.25

[2] H.Z.Lv: Cotton Textile Technology Vol.23(1995),p.11

[3] J.Z.Ren: China Textile Leader Vol. 1(2003),p.30

[4] G.R.Wang, W.M.He: Cotton Textile Technology Vol.1(1986),p.12

[5] H.Z.Lv: China Textile Leader Vol.5(1995),p.55

© (2011) Trans Tech Publications, Switzerland
doi:10.4028/www.scientific.net/AMR.331.472

Research on Mechanism of Magnetic Suspended Knitting Needles

Xiaoguang Wu[1, a], Wenbin Zhu[1,b], Chi Zhang[1,c] and Chengjun Zhang [1,d]
[1]School of Electrical and Mechanical Engineering，Wuhan Textile University, Wuhan, Hubei,430073,China
[a]2008wuxiaoguang@wtu.edu.cn,[b]alson1012@yahoo.com.cn, [c]betazhang13@sina.com,
[d] zchengj_wuse@163.com

Keywords: Magnetic Suspension Needles, Jacquard Circular Knitting Machine, Driving Theory, Ansys Simulation.

Abstract. This paper has proposed a drive theory for magnetic suspended knitting needles based on the magnetic suspension theory. The feasibility of the principles for suspended-driven needle selection of circular knitting machine has been discussed. The mechanical characteristics of needles under different drive conditions, and the stress analysis of electromagnetic force have been simulated with ANSYS software.

Introduction

At present, there are two kinds of electronic needle selectors generally used in the world: piezoelectric type and electromagnetic type[1]. According to data, two measures are being taken to improve knitting efficiency：one is to improve the abrasion resistance, heating processing technology and the shape about needle; the other is to use the converse piezoelectric effect of piezoelectric ceramics[2].But their drive mode are also rigid contact. So it will be limited by the drive mode and principle while improving the efficiency of jacquard base on existing foundation.

Research on suspended knitting needle and its structure

The suspended needle is suspended in axis by the magnetic suspension technology, they are all make fro beeline movement to the cylinder by the action of magnetic push and magnetic attraction, and maks continuously knitting possible after load continuously drive current.

The suspended needle selector integrates the needle selector, pattern bit, needle jack and triangular part of the electronic needle selector device into a sole part. According to the characteristic of suspended needle, the best shape of selector device is cylindrical as shown in Fig.1. There are three types of the suspended needles: inside needles, middle needles, outside needles, as shown in Fig.2.

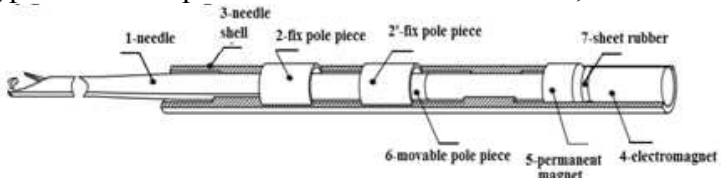


Fig.1 The structure of suspended knitting needles

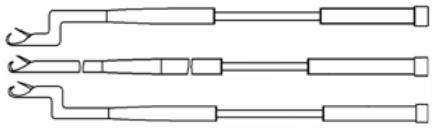


Fig.2 Three kinds of needles

Research on driven principle of needle

With the traditional needle selector device, the track of needle is decided by triangular part track, and the track form of needle will not change. And the suspended needle doesn't rely on the triangular part, and its characteristics of motion are controlled by electromagnetic device.

Analysis of motion patterns of needle. The movement of suspended needle is controlled by the current value and direction of electromagnetic device, so it can change the acting force of permanent magnet below the needle. The relation between the needle movement and driving current is as follows.

According to analysis, the electromagnetic force, while adopting electromagnetic-permanent magnet suspended mode, between electromagnet and permanent magnet is[3]:

$$F = \int_0^{d_1} dx_1 \int_{d_1+h}^{d_1+h+d_2} \frac{3\pi NB_r r_2^{\,2} r^2{}_1 n(x_2 - x_1)}{2d_1[(x_2 - x_1)^2 + r_2^2]^{2.5}} dx_2 I = C_e I \tag{1}$$

Where: n is the coil turns, N is the magnetic induction magnification factors which is produced by iron core, B_r is remanence rate of permanent magnet, I is the current in coil, h is gap, d_1 and r_1 is the thickness and radius of electromagnet, d_2 and r_2 is the thickness and radius of permanent magnet, C_e is the power coefficient.

Analysis of motion in the ascent stage of needle. According to the ascent stage of needle by theory of motion, we can get the follow relations:

$$F - F_2 = Ma \tag{2}$$

Where: F_1 is the electromagnetic force, F_2 is the force that includes the needle gravity and frictional force, M is the needle mass, a is the needle acceleration.

The needle uses five-ordered polynomial curve during the ascent stage of needle, and the needle acceleration is cubic polynomial, it can be recorded as $a = f(t)$, so we can get the follow relations:

$$I = I(t) = \frac{M}{C_e} f(t) + \frac{F_2}{C_e} \tag{3}$$

According to drive current expression, we can load corresponding current to the electromagnetic device, so it can realize the designed needle motion.

Analysis of motion in the descent stage of needle. There are two forms during the needle descent stage, so it must be discussed separately.

(1) the needle motion controlled by the attraction between electromagnetic and permanent magnet

The needle uses cycloid motion during the ascent stage of needle, and the needle acceleration can be recorded as $a = f[\sin(t)]$, so we can get the follow relations:

$$I = I(t) = \frac{M}{C_e} f[\sin(t)] + \frac{F_3}{C_e} \tag{4}$$

Where: F_1 is the electromagnetic force, F_3 is the force that includes the needle gravity, yarn tension and frictional force, M is the needle mass, a is the needle acceleration.

(2) the needle motion controlled by the attraction between permanent magnet and iron core.

Because no current exists in the device, the needle motion is decided by the essential performance of permanent magnet and iron core. And we can get the follow realtion:

$$F_4 - F_3 = Ma \tag{5}$$

The motive power is the attraction F_4 between permanent magnet and iron core, its value is:

$$F_4 = \frac{\mu_0 S H_c^{\,2} d^2}{[h(t) + d/\mu_r]^2} \tag{6}$$

Where: μ_0, μ_r is the magnetic permeability of air and permanent magnet, S is the sectional area of gap, H_c is the coactivity, d is the thickness of permanent magnet, h (t) is the value of the gap.

So we can get the follow relations:

$$a = \frac{F_4}{M} - \frac{F_3}{M} = \frac{\mu_0 S H_c^{\,2} d^2}{M} \bullet \frac{1}{[h(t) + d/\mu_r]^2} - \frac{F_3}{M} \tag{7}$$

And we can know that some parameter is constant, so we can assume that: $\frac{\mu_0 S H_c^{\,2} d^2}{M} = K_1$, $\frac{F_3}{M} = K_2$, $d/\mu_r = K_3$. The speed is equal to the acceleration integral, so we can get the instantaneous displacement value, and we can get the follow relations:

$$2h^3(t) + (4K_3 + K_2 t^2)h^2(t) + (2K_3^2 + 2K_2 K_3 t^2)h(t) + (K_2 K_3^2 - K_1)t^2 = 0 \tag{8}$$

Research on kinematics analysis of needle.

Analysis of motion frequency of needle. At present, the efficiency is measured by the action frequency of needle selector blade. And the calculation formula is:

$$f = \frac{N \bullet v}{60n} \tag{9}$$

Where: f is the action frequency of needle, N is the amount of group, n is the segment number of needle selectors, v is the cylinder angular velocity.

For the sake of comparison, we convert the action frequency of needle selector blade into the action frequency of fro beeline movement of needle, so there is the follow relations:

$$f_{\mathrm{N}} = \frac{N_1 \bullet v}{60} \tag{10}$$

Where: f_N is the action frequency of fro beeline movement of needle，N_1 is the way number of knit circular knitting machine，v is the cylinder angular velocity.

While the highest action frequency of needle selector blade amount to the action frequency of fro beeline movement of needle is 24Hz. The highest action frequency of fro beeline movement of suspended needle can reach 160Hz, it is six times higher than the action frequency of traditional needle.

Force analysis of the needle. The force of needle is different during the descent stage and ascent stage, and the force analysis as follows.

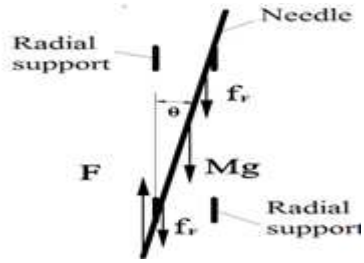


Fig.3 The stress analysis while needle rising

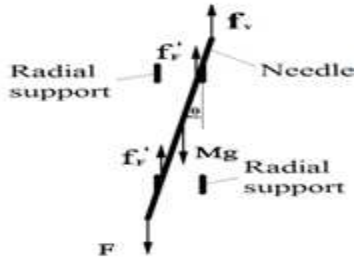


Fig.4 The stress analysis while needle dropping

As shown in Fig.3, during the rising stage of needle, the needle will bias, so there will produce friction between the needle and radial support.

There assume the angle of inclination is θ, the friction factor is μ, the electromagnetic force F, the friction force of needle f_F as follows:

$$f_{\mathrm{F}} = \mu \bullet F \tan\theta \tag{11}$$

There assume the acceleration is a, so the force of needle is:

$$F - M\mathrm{g} - f_{\mathrm{F}} = Ma \tag{12}$$

So we can get the the expression of electromagnetic force:

$$F = M\mathrm{g} + \mu \bullet F \tan\theta + Ma \tag{13}$$

As shown in Fig.4, during the dropping stage of needle, the friction force of needle f_{F}' as follows:

$$f_{\mathrm{F}}' = \mu \bullet (F + Mg) \bullet \tan\theta \tag{14}$$

There assume the tension is f_{Y}, so there we have the following relational expression:

$$F + M\mathrm{g} - f_{\mathrm{Y}} - f_{\mathrm{F}}' = Ma \tag{15}$$

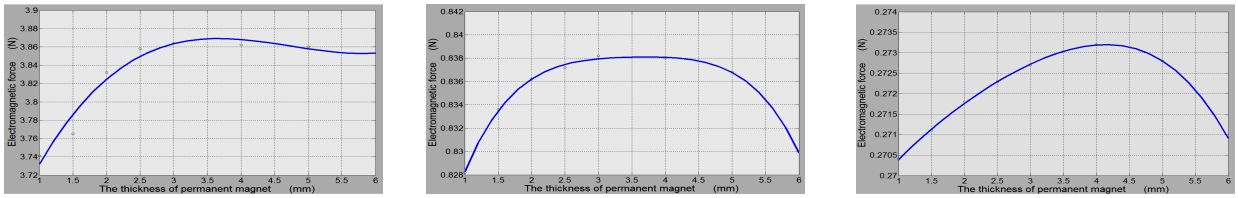
So we can get the expression of electromagnetic force:

$$F = \frac{f_{\mathrm{Y}} + \mu M\mathrm{g}\tan\theta + M(a - \mathrm{g})}{1 - \mu\tan\theta} \tag{16}$$

We can get the information about the different stages of needle motion through analyzing the needle motion. And the value of θ is 0.5°-1°， the f_{Y} is 3CN-5CN, the friction factor is 0.1.

Simulation experiment

This paper analyses the electromagnetic force by finite element method.The relationship among the force about permanent magnet with different thickness and gap is as shown in Fig.5.

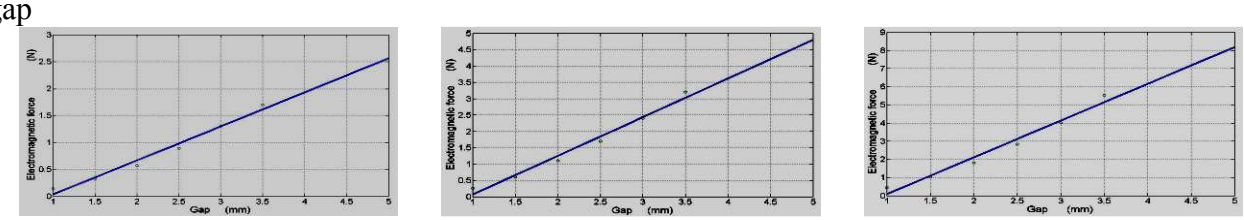


（a）While the gap is 3mm （b）While the gap is 6mm （c）While the gap is 9mm

Fig.5 The force permanent magnet at different gap

As shown in Fig.5, the force of permanent magnet is increasing as it gets increasingly thicker in a certain range, but when thickness adds up to a certain value, the force increases slowly or won't increase any more.

As shown in Fig.6, it is the relationship between current and electromagnetic force at different gap



（a）While the gap is 1mm （b）While the gap is 2.5mm （c）While the gap is 4mm

Fig.6 The relationship between current and electromagnetic force at different gap

As shown in Fig.6, the relation is a linear function, and the slope is decreasing while the gap increases. This is because the reluctance and magnetic flux leakage also increase as the gap increases, so the electromagnetic force is decreasing correspondingly.

Conclusion

This paper has analyzed the mechanical features and operating principle of circular knitting machine and researched its needle selection features, and proposed a suspended-driven needle selection theory combining to magnetic suspension technology. The core of this theory is to impose the electromagnetic force directly on the knitting needles, and to enable the drive principles of "zero transmission" from conventional "multi-level transmission" for knitting needles. And the proposed theory of electromagnetic-permanent magnetic suspension can provide reference and theoretical support for the magnetic suspension technology applications in other fields.

Acknowledgements: Project supported by the Ended Foundation of Hubei Digital Textile Equipment Key Laboratory, DTL 200904.

References

[1] Wu Xiaoguang, Zhang Jian’ gang, et al.Force analysis of the piezoelectric ceramic and of the needle selector design[J]，Knitting Industries，2008.2:19-21.

[2] H.Behr．New weft knitting machine peripheral equipment developments[J]．Melliand Textil berichte Volume：82，Issue:9，Sept 9，2008，pp.698-699.

[3] Hu Jie, Niu Hong-pan，et al.The Experimental Study on Vibration Control of Viscoelasticity Electromagnetic Active Dynamic Absorber [J]，Journal of Experimental Mechanics，2006. 21 (6):735-740.

© (2011) Trans Tech Publications, Switzerland
doi:10.4028/www.scientific.net/AMR.331.476

Circular nets printing machine synchronicity system based on intelligent PI controller

Xiaoding Gao[1.a],Gang Wang[1.b]and Zhaoming Nie[1.c]

[1] Xi'an Polytechnic University mechanical and electrical Engineering college Shaanxi Xi'an 710048 China

[a]gaopengpeng119@ytahoo.com.cn, [b]ganggang7n@126.com, [c]niezhaoming1@163.com

Keywords: Circular nets printing machine, Motors synchronous transmission system, Intelligent control, PI controller

Abstracts. The Circular nets printing machine synchronicity system based on intelligent PI controller has been designed. The intelligent PI controller can adjust its structure and parameters online, which can remarkably improve dynamic performance of the system. Comparing with common PI control system, it successfully solves the contradiction between quickness and smoothness. The synchronous operation system operation testing results indicate that the biggest error of synchronicity is less than δ =5r / min. It can completely meet the technological requirements of circular nets printing machine.

Preface

Circular nets printing machine, which is electric drive system with many parts coordinately moving, now is widely used in printing and dyeing industry. The technology of circular nets printing require that the space of the printing circular nets as well as the space between circular nets and transmission belt should strictly keep synchronous movement, which affect the quality of the printing. Therefore, the advanced designation of the circular nets printing machine synchronicity system is the key to produce the circular nets printing machine. The function of the synchronous controller is that it provide synchronous control signal for each of the printing system's four driving motors(close feed, printing belt, oven, drop cloth), it makes the analog output of the indicated panel (speed panel) as the main given input, and according to the feedback of every controlled units, uses the closed loop control to achieve the requirement that the speed of every unit's work speed is coordinate.

The circular nets printing machine synchronicity system based on intelligent PI controller has been designed in this passage. The intelligent control is a new control method, which has strong adaptive ability .The intelligent PI controller can adjust its structure and parameters online, which can remarkably improve dynamic performance of the system. Comparing with common PI control system, it successfully solves the contradiction between quickness and smoothness.

Structure of the system

The circular nets printing machine synchronicity system is consist of four units(close feed, printing belt, oven, drop cloth). The control part uses the Samsung's ARM9 S3C2440 as the core CPU. The whole system's main control unit use the ALTERA company's EC2C5Q208CN,which finish the data processing, human-computer interaction, control, message storage, sending, and communication. At the same time, FPGA is used to set the whole system's subordinate control part. The whole system use S3C2440 as the main control CPU to control the whole system, including the data's input, electrical control, work management, and so on. S3C2440 can also communicate with PC through serial port. The subordinate control CPU EC2C5Q208CN finish the whole system's distribution of resource, as well as the action of the synchronous controller. When the system is running, EC2C5Q208CN FPGA synchronously collect the code signal of the incremental photoelectrical encoder on the axes of servo motors, get the speed signal and position signal of each axe. The processor ARM9 S3C2440 deal with incremental photoelectrical encoder signal which is

synchronously get by FPGA on the all motors' axes, and make PI control calculation of the set requirement of the four servo motor's speed and position. Then the control instruction is converted by D/A convertor, and sent to all servo motor driver by FPGA to realize the four motor's synchronous performance. The system's structure is shown as Fig. 1.

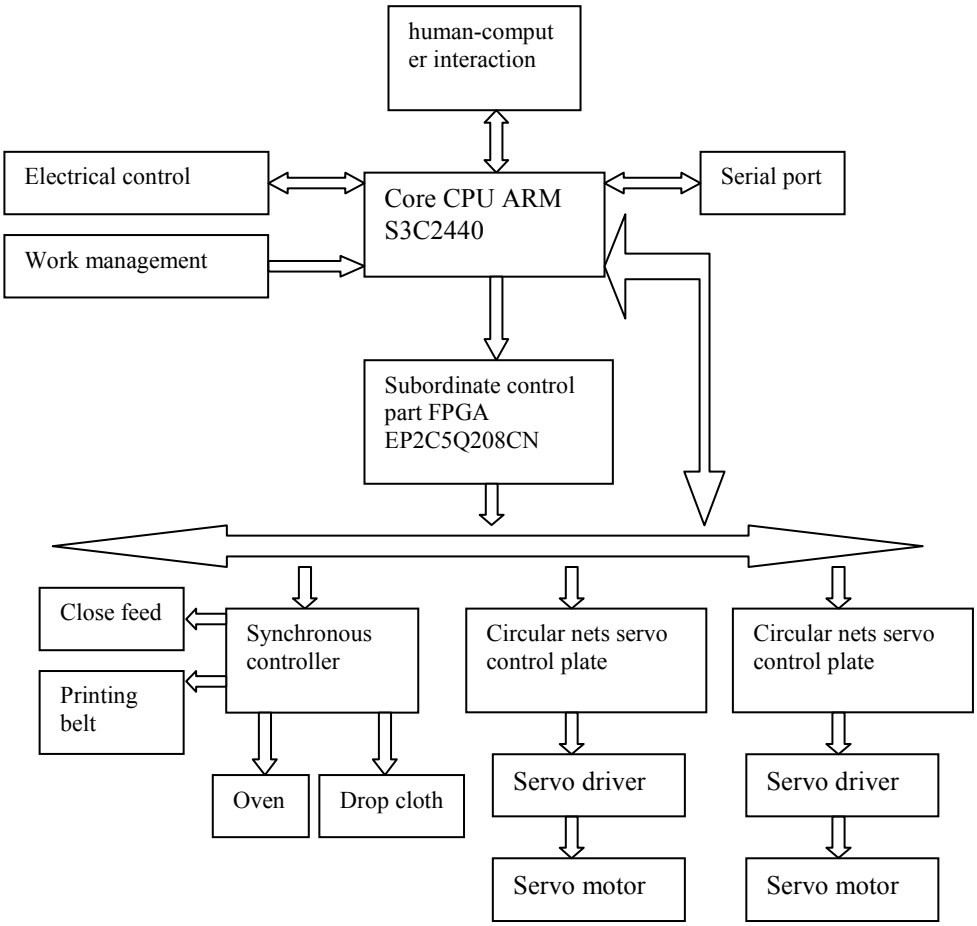


Fig. 1. System's structure

The intelligent PI control algorithm of the circular nets printing machine synchronous operation system

There are two ways to control the motors synchronization operation control system. One is the master-slave control, the other is the equivalence control. According to the technical requirements of the circular nets printing machine，the circular nets printing machine synchronous operation system choose the master-slave control which use the conduction band printing motor as the master motor，the rotational speed is n_1，the rotational speed of the cloth feed, oven, and drop cloth is n_i（i=2,3,4）, the rotational speed of the conduction band printing motor is Controlled by the controller.

The proportionate part of the Intelligent PI controller is used to quickly eliminate the current bias, the integral part of the Intelligent PI controller is used to eliminate the steady state deviation. Actually, in order to avoid the frequent control action of the system, the oscillation caused by the frequent control is eliminated,the dead zone e_o is set,inorder to suppress overshoot effectively, integration and output limiting umax is set.

The error $e_i(k)= n_1(k)- n_i(k)$, the integration and differentiation of the error represent three states that are the current, the past and the future of the system. The set of the controller's dead zone and the output limiting represents the ability to eliminate bias of the system. The algorithm of the Intelligent PI controller is shown as follows:

when $e_i(k)<e0$ $U_i(k)=o.$ (1)

when $e_0 \leqslant e_{ei}(k)< \delta$ $U_i(k)=k_{Pi}e_i(k-1) +k_{Ii} \sum e_i(j).$ (2)

when $e_i(k) \geqslant \delta$ $_{Ui}(k)=Sign[e_i(k)]* umax .$ (3)

In the formula: k is the sample number; Ui(k) is the control variable output of No.i motor on the first k times sampling by controller; $e_i(k)$ is offset value of the No.i motor's rotational speed on the first k times sampling; k_{pi} is the scale factor ; k_{Ii} is the integral factor; δ is the upper limit of deviation (δ, umax, and e_o can be set according to the technical requirements of the circular nets printing machine).

When the deviation is large, that is $e_i(k) \geqslant \delta$, the controller directly output the limit amplitude which is the same as the deviation symbol $Sign[e_i(k)]*$ umax, which is equal to the proportion regulator that has large enough scale factor, the system eliminate the deviation of No.i motor's speed as fast as possible. When the error is in a little range($e_0 \leqslant e_i(k)< \delta$), the system uses PI regulation, gradually adjusts the proportion factor k_{pi} and integral factor k_{Ii}, It eliminates the bias of No.i motor's speed. In order to have no ambiguity, k_{pi} and kIi should be larger than zero.

Intelligent PI controller k_{pi} and k_{Ii} regulation rules

Intelligent PI controller k_{pi} and k_{Ii} regulation principles are that when the deviation is large or the deviation tend to increase, the bias should be eliminated as soon as possible. When the deviation is small or the deviation tend to decrease, the system should run smoothly, reduce or avoid the negative super-tone. In order to analyze conveniently, define as follows:

$f_{1i}=n_1(k)- n_i(k)=e_i(k).$ (4)

$f_{2i}=\sum e_i(k).$ (5)

$f_{3i}=[e_i(k)- e_i(k-1)]/ \Delta t.$ (6)

The regulation rules of scale factor k_{pi}

When $|f_{1i}|$ gradually decreases and tends to e_o, the No.i motor tend to synchronize with the main motor, in order to avoid reverse overshoot, the k_{pi} should decrease gradually. The rate of scale factor's decrease is relevant to f_{1i} and f_{3i}. $|f_{3i}|$ is greater, the rate that $|f_{1i}|$ tends to eo is faster, k_{pi} will decrease faster:

k_{pi}（m+1）$=k_{pi}$ (m) $- H_P*|f_{3i}/f_{1i}|.$ (7)

In which m is the number of adjustment times; H_P is adjustment factor of k_{pi}.

When$|f_{1i}|$ gradually increase, the NO.i motor's speed deflect the speed of the main motor. At this point, proportional regulation is useful to eliminate bias, but the integral regulation is not conducive to reduce the deviation. Therefore, at the time of reducing the integral factor k_{Ii} (in k_{Ii} regulation), the scale factor k_{pi} should be increased to offset the role of the integral. The rate that the scale factor increase relate with f1i and f_{3i}, $|f_{3i}|$ is greater, the rate that the faster, $| f_{1i}|$ increase is the faster k_{pi} increase:

k_{pi}（m+1）$=k_{pi}$ (m) $+ H_P*|f_{3i}*f_{1i}|.$ (8)

The regulation rules of Integral factor k_{Ii}

When it is $f_{1i}*f_{2i}>0$, the role of integral regulation is to decrease or increase the speed of the NO.i motor, and make the actual speed of the NO.i motor in to tend to the speed n_1 of main motor. At this point, integral regulation help to eliminate bias, k_{Ii} should be turned up.

When it is $f_{1i}*f_{2}i<0$, the integral regulation make $|f_{1i}|$ to increase, the k_{Ii} should be reduced. Consider two points above and the sign of f_{1i} and f_{2i} ,it can be get:

$$K_{Ii}（m+1）=k_{Ii}(m) + H_I*f_{2i}*f_{1i}. \quad (9)$$

In which H_I is the adjustment factor of k_{Ii}

The regulation rules of special point

When it is $f_{3i}*f_{1i}=0$, the system is at a special point. When $f_{1i}=0$ and $f_{3i}=0$, the system is perform at a stable synchronous state. k_{pi} and K_{Ii} should not be regulated.

If there are $f_{1i} = 0$ and $f_{3i} \neq 0$ or $f_{1i} \neq 0$ and $f_{3i} = 0$, the system is in a special limit state,that is a transition state, and keep k_{pi} and K_{Ii} unchanged. The system will divorce the limit state under the role of the original control. Once the system is out of the limited state, it will re-enter the adjustment state.

The design of the intelligent PI controller and the test of synchronous operation system of the circular nets printing machine

The structure of the synchronous operation Intelligent PI controller of circular nets printing machine is shown in Fig. 2.

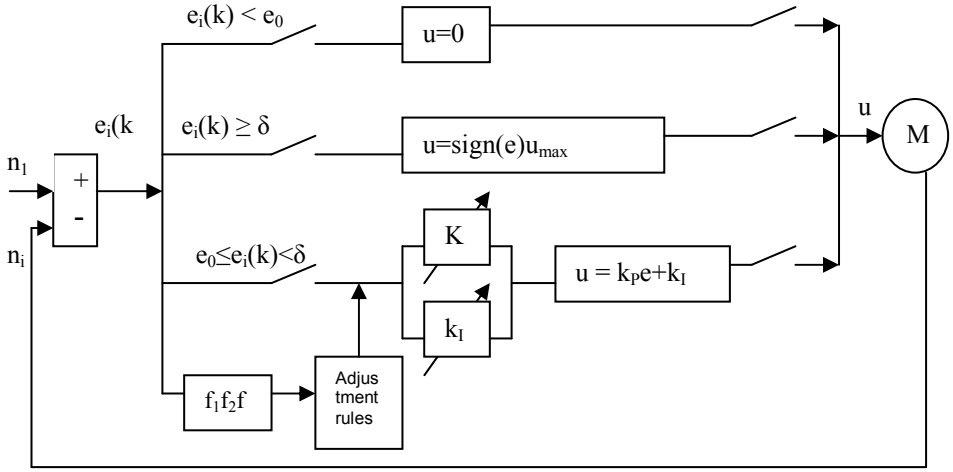


Fig. 2. The structure of Intelligent PI controller

The test of synchronous operation system of circular nets printing machine select four permanent magnet synchronous motor, whose parameters are that electrical power P=500W, phase voltage U=220V, stator resistance R=4.495Ω, d, q two-phase inductance Ld=0.027H, Lq = O. 067H, moment of inertia J = 0.00579kg • m2, speed n = 1500-3000r/min. Four motors' synchronous operation test data is shown in Table 1, the waveform that two oscilloscope detect of the four motors' synchronous operation is shown in Fig. 3, Fig. 4.

Table 1 The test of motor sync signal (frequency units: Hz)

NO.1 motor	NO.2 motor	NO.3 motor	NO.4 motor	Maximum deviation $\|\triangle f\|$
31.25	31.25	31.22	31.27	0.03
32.92	32.90	32.91	32.94	0.02
34.72	34.72	34.72	34.72	0.00
36.76	36.77	36.76	36.75	0.01
38.51	38.50	38.51	38.52	0.01
41.72	41.74	41.71	41.73	0.02
44.16	44.09	44.11	44.15	0.07
47.24	47.24	47.23	47.25	0.01
52.55	52.54	52.55	52.56	0.01
55.76	55.71	55.70	55.73	0.06

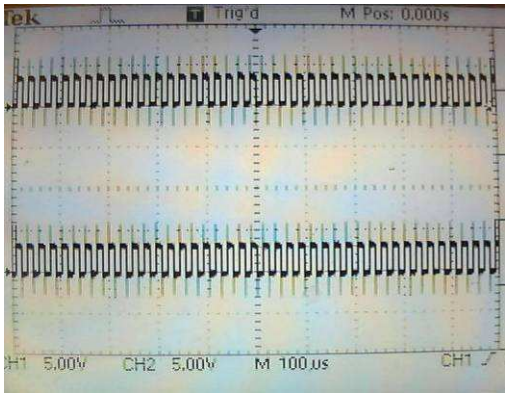


Fig. 3. Waveform of motor 1,2

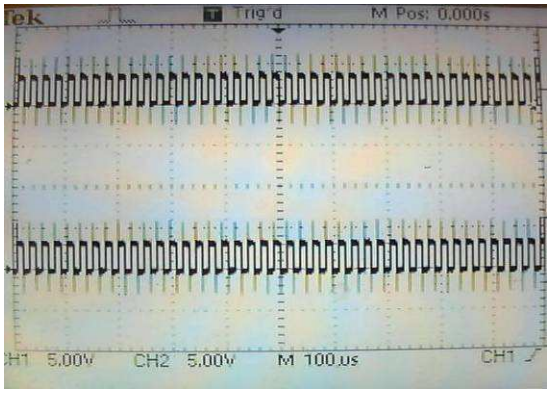


Fig. 4. Waveform of motor 3,4

Conclusions

(1) The result of the control system's test indicate that the minimum error is less than 5r/min when the four motors work synchronously, and completely meet the circular nets printing machine's technical requirements.

(2) The intelligent PI controller automatically change the controller's structure and parameters according to the system's speed offset, the offset's proportion and integration, that effectively ease the contradictions of the common PI system's quickness and stability, and improve the speed changer's dynamic performance.

(3) The optimization of the intelligent PI controller's speed change, such as the selection of the proportion and integration parameters, needs more analysis and research.

Preference

[1] Wenhuan Sun and so on: The Development of Multi-motor Coordinated Control(Electrical Transmission In Chinese ， China 1999).

[2] Ribao Liu and so on: The Research of the Servo System of the Permanent Magnet Synchronous Motor(Electrical Transmission In Chinese, China 2005).

[3] Yongdong Li: Digital Control System of AC Motor(China Machine Press,China,2002.21-26,306-360).

[4] Yonghua Tao: New PID Control and Application(China Machine Press,China,2002.14-96).

[5] Weixiang Shi and so on: The Electrical Control Project at Modern times(China Machine Press,China,1998.16-70).

[6] Xiaoyan Wang, Lilin Zang: The Research of Distributed Multi-Motors synchronous transmission control system based on PCC(Electrical Transmission Automation In Chinese, China 2005).

[7] Tuanshan Zhang, Yuan Liu, Chaokui Chen: The design of Independent Transmission Control System of Circular Nets Printing Machine based on FPGA(Textile Mechanic In Chinese,China,2006)

© (2011) Trans Tech Publications, Switzerland
doi:10.4028/www.scientific.net/AMR.331.481

Fabric Defects Detection Using Multi-scale Wavelet and Locating

Junfeng Jing[1,2, a], Hang Li[1,b] and Pengfei Li[1,c]

[1] School of Electronic and Information, Xi'an Polytechnic University, Xi'an, Shaanxi, 710048, China

[2] School of Electronical and Mechanical Engineering, Xidian University, Xi'an, Shaanxi, 710126, China

[a] jingjunfeng0718@sina.com, [b]lihangmail@126.com, [c]li6208@163.com

Keywords: Multi-scale Wavelet, Quadtree, Encoding, Locating, GUI.

Abstract. In this paper, multi-scale wavelet edge detection approach is investigated for real time inspection of diversified fabric texture. Multi-scale edge detectors smooth the signal at various scales and detect sharp variations points from their first or second order derivative. The extreme values of the first derivative correspond to the zero crossings of the second derivative and to the inflection points of the smoothed signal. Quadtree decomposition of segmented defects shows pinpoint location of specific web flaw. Further, preliminary graphical user interface (GUI) was designed so as to facilitate operation. After integrate GUI with procedure, parameters material can be acquired, which is vital to applying the inspection system on industrial PC.

Introduction

Machine vision based fabric defect detection provides high speed, high efficiency and low cost defects detection method for textile production departments. In the actual production of textile industry, the texture of fabric is one of the important influences of defect detection [1]. The main fabric texture structure has the three following features: the first is cycle; the second is direction; the third is homogeneity [2]. In fabric texture structure, the emergence of defects is meaning that normal fabric texture's structure is damaged. Generally, the issue of woven fabric defects detection can be categorized into three classes: spectral, statistical and model based. Among these methods, spectral approach, wavelet analysis, is comparatively successful on fabric defects detection[3,4].

Multi-Scale Wavelet Method

The objective of using multi-scale wavelet representation is to attenuate the background texture and accentuate the defects. Multi-scale wavelet image processing method using smooth filter functions S(x) with different scales is applied to the image. Differential effect determines the catastrophe point, maximum of first order differential is corresponds to the zero intersection and signal inflection point of quadratic differential[5]. When selected wavelets function $\Psi(x)$ and smooth functions S(x) satisfy $\Psi(x)=\frac{dS(x)}{dx}$, edge detection can be proceeded on the ground of extreme value of wavelet coefficients. Here, two two-dimensional wavelet functions defined and satisfy wavelet allowable condition. As Eq. 1 shown below:

$$\Psi^1(x,y)=\frac{\partial S(x,y)}{\partial x},\Psi^2(x,y)=\frac{\partial S(x,y)}{\partial y} \tag{1}$$

S(x,y) is the smooth function. After $\Psi(x)$ transform by scale factor d, the wavelets function shown as Eq.2 :

$$\Psi_d^1(x,y)=d\frac{\partial S_d(x,y)}{\partial x};\quad \Psi_d^2(x,y)=d\frac{\partial S_d(x,y)}{\partial y} \tag{2}$$

where $S_d(x,y)=\frac{1}{d^2}S\left(\frac{x}{d},\frac{y}{d}\right)$. For any two dimension function, there are two directions component of wavelet transform, respectively are x direction y direction, as Eq.3 shows:

$$WT_d^1 f(x,y)=f(x,y)*\Psi_d^1(x,y),\ WT_d^2 f(x,y)=f(x,y)*\Psi_d^2(x,y) \tag{3}$$

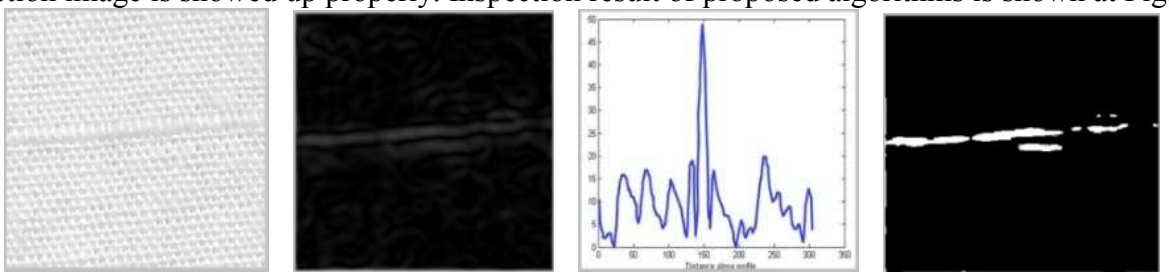
normally, the fabric image, which represented by pixels, are digital image. Hence, continuous wavelet transformed into binary form as we detect the edge. That is to say $d=2^j(j\in z)$. The vector form is Eq.4.

$$\begin{bmatrix} WT_{2^j}^1 f(x,y) \\ WT_{2^j}^2 f(x,y) \end{bmatrix} = 2^j \vec{\nabla}\left[f(x,y)*S_{2^j}(x,y)\right] \tag{4}$$

where $WT_{2^j}^1 f(x,y)$ is partial derivative at x direction of f(x,y), $WT_{2^j}^2 f(x,y)$ is partial derivative at y direction of f(x,y). The two dimension transform vector is gradient. From equation (4), the length of gradient vector with scale $d=2^j$ is defined as Eq.5:

$$M_{2^j} f(x,y)=j\sqrt{\left|WT_{2^j}^1 f(x,y)\right|^2+\left|WT_{2^j}^2 f(x,y)\right|^2} \tag{5}$$

As a result, the inflection point of smoothed image $f(x,y)*S_{2^j}(x,y)$ is maximum value of local modulus. Edge point can be acquired by detecting modulus $M_{2^j} f(x,y)$ along the gradient $A_{2^j} f(x,y)$ direction, and the amplitude of modulus value is edge intensity. Then, connecting the point with approximate edge amplitude gets the chain of edge detection. Some point in the chain is made by noise signal, if amplitude point is less certain threshold value, it should be removed. Thus, the edge detection image is showed up properly. Inspection result of proposed algorithms is shown at Fig.1.



(a) (b) (c) (d)

Fig. 1 Result of yarn evenness defects detection using multi-scale wavelet approach. (a) fabric gray-scale image, (b) multi-scale wavelet transformed image, (c) longitudinal section gray level amplitude figure, (d) corresponding segmentation of defects.

Comprehensive Analysis and Locating Quadtree Decomposition

Due to various fabric material texture and illumination condition, identical arithmetic may has diverse outcome of detection. In this research, six different textured fabrics are considered. These images are of size 512×512 pixels. The single yarn diameter in these fabrics is 1/2/3/4 pixels. Provided warp and weft have same diameter, take woven fabric for example, fabric of size 512×512 pixels approximately have 256/128/85/64 yarns both in x direction and y direction. If single yarn diameter is two pixels long, one period of warp and weft cell is of size 4×4 pixels. So, there are only 512/ (2×2) = 128 cells/yarns in each direction. Locating of every cell only need seven times ($2^7=128$) quadtree decomposition.



(a) (b)

Fig. 2 Process of quadtree decomposition on defects locating. (a) is principle of image cell encoding, (b) is upper left point encoding position in slubby yarn defect fabric.

Every image block is divided equally into four quadrants, each subregion is labeled respectively as (0,0), (0,1), (1,0), (1,1). For any cell, lets' say (0,1), have defects information, quadtree decomposition applied in this cell, and new four children are (01,00), (01,01), (01,10), (01,11), the rest may be deduced by analogy, principle description as shown at Fig.2 (a). Take slubby yarn defects for example, locating and labeling the non-subdivided cell in the original image is only need seven pairs coordinate number. Tab.1 shows relevant position encoding of slubby yarn defect.

Tab. 1 Position and encoding of main geometry point of slubby yarn defect.

Position	Encoding
Upper left	(00,10,11,01,10,00,10)
Upper right	(00,11,11,01,11,00,01)
Lower left	(00,11,10,10,01,01,10)
Lower right	(00,11,11,10,00,00,11)

Similarly approach applied to some other fabric defects, test results are shown as Fig.3. The encoding of defects area is helpful for pinpointing relevant position on web.



(a) (b) (c) (d)

Fig. 3 (a) Images of defective fabrics, the upper is evenness defect, the lower is slubby yarn defect, (b) inspection results of multi-scale wavelet method, (c) the corresponding segmented defects, (d) results of quadtree decomposition

Graphical User Interface (GUI) Design

In order to facilitate the experiment of fabric defect image inspection as well as design independent operation fabric image capture and inspection software. This paper, basis on the Matlab2010b version, has design interface of ordinary textile image monitoring and detection GUI, which accommodated with this paper. Main interface shown at Fig.4.

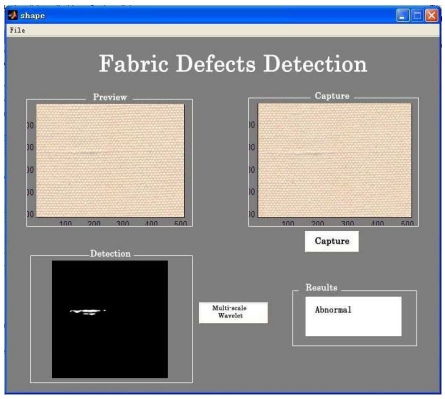


Fig. 4 Main interface of defects detection.

This GUI has two practical features. First item is the defect detection operation process can be disintegrated, and when necessary, use parameter modification to obtain best test conditions of relevant texture, which is very helpful for study. The second is the on-line monitoring function. The window at the upper left is real-time preview video window; upper right window is manual acquisition and display window of single frame image; the lower left window is classification detection window.

Conclusion

In this paper, multi-scale wavelet analysis method are proposed to conduct combined inspection of fabric textures, which aim at enhancing algorithm advantage in machine vision inspection. The experiment results have been proved the testing measure is appropriate. Quadtree decomposition encoding locates specific position of defects segmentation. Through conversion of programming language, this paper obtained relevant parameter information, which of great value for applying combined detection approach to small industrial computer that inspect multi-looms online.

Acknowledgement

The author is grateful to Graduate Innovation Fund (Project support NO.chx110926) support from Xi'an Polytechnic University, Xi'an, Shaanxi, PRC; Scientific Research Program Funded by Shaanxi Provincial Education Department (Program No. 11JK0910), Shaanxi, PRC; Research and Development Project of science and technology(Project NO. 2010K09-17), Shaanxi, PRC.

References

[1] Ajay Kumar, Grantham K.H.Pang: IEEE Transactions on Industry Applications, (2002),p.425

[2] Li-Wei Han, De Xu: International Journal of Automation and Computing, (2010),p.86

[3] Jiri Kula, Maros Tunak, Ales Linka: 7th International Conference, Liberec, Czech Republic (2010).

[4] Zhang Yu: *Automatic Fabric Defect Detection and Classification Using Machine Learning Technology* (Xi'an,China,2010).

[5] P. Hornby, F. Boschetti and F.G. Horowitz.: *Analysis of Potential Field Data in The Wavelet Domain* (Australia)

© (2011) Trans Tech Publications, Switzerland
doi:10.4028/www.scientific.net/AMR.331.485

Curve Matching Algorithm Applied to Fabric Automatic Register Detection

Junfeng Jing[1,2,a], Guangyan Li[1,b] and Pengfei Li[1,c]

[1] Xi'an Polytechnic University, Xi'an, Shaanxi,710048,China

[2] Xi'an University of Electronic Science and Technology,Xi'an,Shaanxi,710126,China

[a]413066458@qq.com, [b]1327256889@qq.com, [c]li6208@163.com

Keywords: Rotary Screen Printing, Register Error, Curve Matching, Fourier-Mellin Transform.

Abstract. With the register detection problems in the rotary screen printing process, the curve matching strategy was proposed to get the position vector of off-pattern-topping, on the basis of the proposed rotary screen printing machine automatic register detection system based on machine vision. In order to ensure the capture positions of the target edge image and the standard edge image is the same, Fourier-Mellin curve matching was used to match them to eliminate the shooting error;then the curve matching method, based on the Fourier transform shift theorem,was used to match the well-tuned target edge image and the standard edge image to detect the register error. The matching strategy eliminated the error, and the computation is small.The experiments show that its detection accuracy and the computing speed can meet the requirements of the fabric register detection on line.

Introduction

In the printing process, the register accuracy is an important indicator, which directly affects the quality of printing products and also limits the machine running speed and other economic and technical parameters. With this problem, in the current industrial production it also depends on the human eye to detect, and the detection accuracy is limited. Under the trend that machine vision technology is widely used in the textile industry, this paper uses image processing techniques[1,2] to detect register error, on the basis of the proposed rotary screen printing machine automatic detection system based on smart camera[3,4-6]. Therefore, selecting high-precision and high-efficiency image matching method is particularly important.

This paper selects the edge as characteristic quantity to match. Its advantage is that: the polygonal approximation of curves and other related processing are not needed, but the frequency-domain characteristics of the whole curve was directly used to achieve the two curves matching. In the current literature about machine vision, the shooting errors are not taken into account. For example, in the literature[7], the block matching is taken directly before eliminating the error. In this paper, fristly the Fourier-Mellin curve matching algorithm was used to eliminate shooting errors. secondly, considering the characteristics of broken pattern image, the curve matching algorithm based on Fourier transform shift theorem was used to only detect the curve shift. Although matching algorithm was used twice, there was not much computation, which ensured the operation speed of the matching strategy.

Curve Matching Algorithm

Curve matching based on Fourier transform displacement theory. For the two-dimensional real functions $f(x,y)$ and $g(x,y)$,their related operation is defined as:

$$c(\alpha,\beta) = f(x,y) \otimes g(x,y) = \int_{-\infty}^{+\infty}\int_{-\infty}^{+\infty} f(x,y)g(x+\alpha, y+\beta)dxdy \quad . \tag{1}$$

From the Eq. 1,it can be seen that the higher the similarity between the functions $f(x,y)$ and $g(x,y)$ is, the greater the correlation peak is. And the peak position (α,β) is the relative displacement of the similar composition between $f(x,y)$ and $g(x,y)$.

$f_2(x,y)$ are assumed to be the image $f_1(x,y)$ changed into after translation of x_0 and y_0 in the x and y directions, that is:

$$f_2(x,y) = f_1(x - x_0, y - y_0) \quad . \tag{2}$$

$F_1(u,v)$ and $F_2(u,v)$ are the corresponding Fourier transform of f_1 and f_2, so the Fourier transform displacement theory as follows is workable:

$$F_2(u,v) = F_1(u,v)e^{j(ux_0+vy_0)} \quad . \tag{3}$$

And the cross-power spectrum of $f_1(x,y)$ and $f_2(x,y)$ is:

$$\frac{F_1(u,v)F_2^*(u,v)}{\left|F_1(u,v)F_2^*(u,v)\right|} = e^{j(ux_0+vy_0)} \quad . \tag{4}$$

In the Eq. 4, F_2^* represents the complex conjugate of F_2.

Inverse Fourier transform is applied to the formula above, and a pulse function is obtained at (x_0, y_0). x_0 and y_0 are the relative displacement between the two images.

Fourier-Mellin curve matching. Fourier-Mellin curve matching algorithm was put forward by Chen[8] and others in 1994. The algorithm is pure phase correlation method[9] based on Fourier transform displacement theory. When there are translation,rotation and scaling transformation between two images, we can use the Fourier-Mellin transform[10].

Assuming the two images $s(x,y)$ and $r(x,y)$ to be matched, $s(x,y)$ is the image which $r(x,y)$ changed into after translation (x_0, y_0), rotation α ,and consistent scale transform σ , that is:

$$s(x,y) = r[\sigma(x\cos\alpha + y\sin\beta) - x_0, \sigma(x\cos\alpha + y\sin\beta) - y_0] \quad . \tag{5}$$

The relationship between the corresponding Fourier transform of $s(x,y)$ and $r(x,y)$ is

$$s(u,v) = e^{-j(u,v)}\sigma^{-2}R[\sigma^{-1}(u\cos\alpha + v\sin\alpha), \sigma^{-1}(-u\sin\alpha + v\cos\alpha)] \quad . \tag{6}$$

In the Eq. 6, the phase $e^{-j(u,v)}$ depends on translation, rotation and zoom scale, but the amplitude has nothing to do with the translation.The amplitude spectrum is:

$$\left|s(u,v)\right| = \sigma^{-2}\left|R[\sigma^{-1}(u\cos\alpha + v\sin\alpha), \sigma^{-1}(-u\sin\alpha + v\cos\alpha)]\right| \quad . \tag{7}$$

Define:

$$r_{p1}(\theta, \log^{\rho}) = r_p(\theta, \rho) \quad , \tag{8}$$

$$s_{p1}(\theta, \log^{\rho}) = s_p(\theta, \rho) \quad . \tag{9}$$

In the Eq. 8 and Eq. 9, r_p and s_p are the amplitude spectrums of r and s in the polar coordinates (θ, ρ) .Then it is easy to draw:

$$s_{p1}(\theta, \log^{\rho}) = r_{p1}(\theta - \alpha, \log^{\rho} - \log^{\sigma}) \quad , \tag{10}$$

$$s_{p1}(\theta, \lambda) = r_{p1}(\theta - \alpha, \lambda - \kappa) \quad . \tag{11}$$

The equations $\lambda = \log^{\rho}$, $\kappa = \log^{\sigma}$ is called Fourier-Mellin transform.It can be seen that through the transformation above , α and κ can be obtained applying the Fourier transform theory in the transform space.If the base of logarithms is e ,so

$$\sigma = e^x \quad . \tag{12}$$

So the rotation α and the consistent scale σ can be obtained.When α and σ are obtained, use the two parameters to amend $s(x, y)$; The only difference between $s(x, y)$ amended and $r(x, y)$ is a translation transform,and the amount of translation can be got,after using Fourier transform displacement theory again.

The Curve Matching Used in the Register Error Positioning

As shown in Fig. 1: figure (a) is a standard textile image and figure (b) is a broken figure textile image.Both of them are 228× 176 pixels,and are taken by the CANCam.



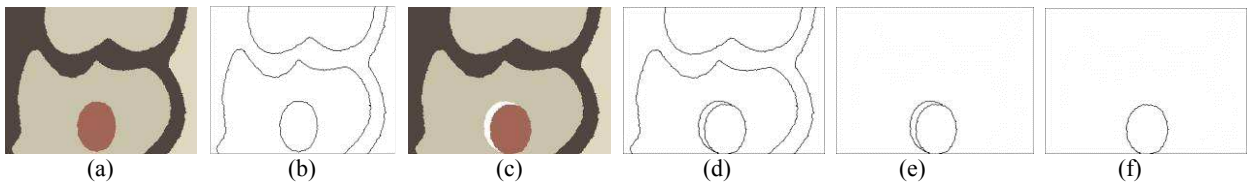
(a) (b)

Fig. 1. The textile image (a) standard image; (b) broken figure image

Frist the figure (a) and figure (b) in Fig. 1 were segmented, then the edge of them were extracted and matched.The closed operation was done on the extracted edge images, with the rectangular template with 4 pixels side length, and then the thinning operation was done with 3 pixels width, finally the needed edge of printing and dyeing image was got. As shown in Fig. 2: obtained by the above method,(b)and (d) were the the edge images of (a)and (c).

In Fig. 2, (b)and (d) was matched by the Fourier-Mellin curve matching algorithm and through calculation: the offset of (d) is 0 pixels in all the directions;that is no rotation and no scaling.And there is no need to adjust the shooting errors. The left upper corner of (b) was set as the coordinate point (0,0), and then move the upper left corner of (d) at the above point (0,0). Apply for an image ,whose size is the same with (b). Compare the gray value of the same point of (b)and (d),and if they are the same, set the gray value of the corresponding point of the applied image as 255;and if different,set the gray value as 0.After treatment,the edge of the off pattern can be obtained, As shown in (e) of Fig. 2. Apply for an image ,whose size is the same with (e), and make its left upper corner coincide with the upper left corner (0,0) of (e) and (b). Clear away the same part of the edge in (e) and (b),and put the different edge between them in the above applied image,with the result shown in (f) .

The figure (f) and (b) were matched by the curve matching method based on Fourier transform shift-theorem,and the result was shown in the Table 1: the edge of (f) shifted to the right by 20 pixels and to the downside by 10 pixels, relative to the corresponding part of the standard image. That is to say ,the red region shifted to the right by 20 pixels and to the downside by 10 pixels. In accordance with the calibration, each pixel represents the distance of 0.0928125mm.Finally,through calculating,the red region shifted to the right by 0.6496875mm and to the downside by1.0209375mm.



(a) (b) (c) (d) (e) (f)

Fig. 2. the edge matching of fabric image (a) standard segmented image; (b)edge image; (c)segmented broken figures image; (d)broken figures edge image; (e)different edge between (b) and (d); (f) broken figures topping edge

Table 1 The final detect result

translation direction	the number of translation pixels	off-pattern error [mm]
to the right	20	0.6496875
to the downside	10	1.0209375

Conclusions

In this paper, the curve matching methods based on Fourier transform shift theory and based on Fourier-Mellin transform were used to detect register errors.The two curve matching methods based on phase relevance have strong robustness to the differences of two images and the additive noise.Besides this matching strategy is not sensitive to the partially sheltered caused by threadbare and colour overlapping in the image,and it is suitable for the detection of register errors.In addition, Fourier-Mellin curve matching can eliminate the shooting errors, and the final output of register errors is more accurate.The matching strategy lays the foundation for the rotary printing closed-loop control system.

Acknowledgements

The authors would like to thank for the support of Scientific Research Program Funded by Shaanxi Provincial Education Department (Program No. 11JK0910)； Research and Development Project of science and technology(Project NO. 2010K09-17), Shaanxi, PRC.

References

[1] Binjie Xin,Jinlian Hu,and George Baciu:Textile Research Journal,Vol.80,2(2010),p.166-176.

[2] Jeanette M. Cardamone,William C. Damert,John G.Phillips,andWilliam N. Marmer:Textile Research Journal,Vol.72,10(2002),p.906-916.

[3] Gang Wang,Junfeng Jing:Progress in Textile Science & Technology,Vol.(4)(2009), p.43-44. In Chinese.

[4] Juntang Tang:Textile Machinery ,Vol. (1)(2006),p.44-47. In Chinese.

[5] Hyung J. Kim,Jong S. Kim,Jung H. Lim,and You Huh:Textile Research Journal,Vol.79,17 (2009),p.1616-1624.

[6] Chaoli Huang,Jianxi Qiu:Progress in Textile Science & Technology,Vol.3(2006),p.48-50. In Chinese.

[7] Peng Li,Kuangrong Hao,Yongsheng Ding: Journal of Textile Research,Vol.29(7)(2009), p.112-116. In Chinese.

[8] Chen Q S,Defrise M,Deconinck F:IEEE Transactions on Pattern Analysis and Machine Intelligence,Vol.16(12)(1994),p.1156-1168.

[9] Zhibin Zheng,Zhongfu Ye:Journal of Data Acquisition&Processing, Vol.21(4)(2006), p.444-449. In Chinese.

[10] Reddy B S, Chatterjib N:IEEE Transactions on Image Processing, Vol.5(8)(1996),p.1266-1271.

© (2011) Trans Tech Publications, Switzerland
doi:10.4028/www.scientific.net/AMR.331.489

The Research of Two-For-One Twisting Spinning Frame

Xueqin Ren[1,a], Wenya Li [2,b] and Xiaofei Shen[3,c]

[1]Xi'an Polotechnical University, Shaanxi Xi'an

[2] Xi'an Polotechnical University, Shaanxi Xi'an

[3]Suzhou Huafei Textile Co.Ltd, Suzhou

[a]xueqinren@pub.xaonline.com, [b]liwenya200608@126.com, [c]szhfsxf@sina.com

Keywords: New machine, Two-for-one twisting spinning frame, New two-for-one twisting spindle, Ring spinning frame, Doubling and twisting machine

Abstract. Now many enterprises have used the two-for-one twister to replace the ring spinning frames, in accordance with the same principle, the enterprises will use two-for-one twisting spinning frames instead of ring spinning frames in the future.Compared with the ring spinning frame, the obvious advangtages of the two-for-one twisting spinning frame are as follows: the production efficiency is improved,which can reach the aim to get the higher single spindle production with the lower speed; The two-for-one twisting spinning frame is a machine that can spin and wind to cheese with larger capacity.The package form in this new machine is the cheese instead of the ring cop, so the automatic winding frame is saved, which not only improve the production efficiency and make the spinning process easier,but also improve the single yarn quality[1]. Additionally this machine can be used in this way: the output from the front roller would be introduced from the side of the spindle, the filaments /the rovings /the strands can be introduced through the bottom of the spindle at the same time, then they are twisted for two different effects and spun for special fancy yarn.

Two-for-one Twisting Spinning Frame

The new spinning frame is invented based on the principle of two-for-one twisting spindle which would twist and wind the output from the front roller directly.It is a new spinning frame, and the technical patent have been applied.It would be used instead of ring spinning frames in future. The most important and biggest difference between two-for-one twisting spinning frames and ring spinning spindle frames is the spindle. One twist will be produced when the commen spindle turn a round, but the two-for-one twisting spindle can produce two twists[2-3]. For this reason, with the same spindle speed and same standards of products, the production of single spindle would be doubled. Using the two-for-one twisting technology in spinning frame is the biggest breakthrough and the best innovation in the way of spinning.

The function of winding is achieved by a two-way screw instead of the ring bar lifting in this new spinnig frame. The cheese is designed motionless, but the two-way screw is opposite, so there is relative rotation between cheese and the two-way screw, the two-way screw drive the yarn carrier winding smoothly. This design is realized by adding the reverse polarity magnets on a certain place of frame. Relying on the influence of magnets, the cheese can be fixed motionless. And the magnetic force can be adjusted properly according to the concrete requirements. When we want to change a new cheese after the cheese is full, we only need to take off the upper twisting dish, pull out the full cheese from the yarn plate and put on a new cheese. It is convenient for the operation. The design of static cheese can reduce the power consumption and because of the center of gravity the shake of spindle is reduced. As mentioned above, the two-for-one twisting spinning frame can meet the requirements of improving the speed of spindle and enlarging the package and improving the production of the single spindle, also the power consumption can be saved.

This new spinning frame conbines the assembly winder with the twister together. The concrete operation is as follows: two strands of single yarn are controlled by the front roller individually, their tension will be consistent with each other after passing a tension regulator, then they will be converge into a plied yarn to twist together by the new two-for-one twisting spindle. In this new spinning frame the single yarns will be processed into plied yarns and winded to cheese package directly. In this way the automatic coning machine have been saved, and the labor as well as space have been reduced. Additionly,the machine be used for spinning fancy yarns. We can get a conclusion that the machine with so wide application range can be used in many aspects in texile industry from all mentioned above.

But now the new spinning frame still has some problems: We have installed the two-way screw just on one side of spindle, which drives the yarn guide winding.As a result, the direction of twist is limited, so the yarn guide should have a reverse installation if it need a opposite twist; another is that the cheese diameter can be made more larger and the height of cheese can be made some higher on the basis of now. The rising speed and the falling speed of two-way screw we choosed are the same,so the yarn capacity of cheese need to be improved. It means that the speed of rising and falling of the yarn carrier should be choosed according to a reasonable method.

The Design For The New Two-for-one Twisting Spindle

The new two-for-one twisting spindle can be called as direct twisting type spindle. It has been researched and designed all by ourselves. Its design is so complex that it is different from comment spindle.There are so many different parts which are unique for the new spingning spindle such as transmission devices/the magnets/ a two-way screw and a weight blance device and so on. Fig.1 shows the front view of the new spindle.



Fig.1 The Front View of Spindle

What we can see from Fig.1 is that the direction of yarns on the direct twisting type spindle is opposite to the ordinary two-for-one twisting spindle. As for the new spindle the yarn is introduced positively through the front roller, then be twisted together and winded to cheese. Oppositely the yarn is pulled out from cheese, then be twisted and winded on ordinary two-for-one twister.So a difficulty question of the new spindle is how to solve the main problem about winding power. Based on theoretical analysis and many experiments, we solve the main problem successfully about the winding power in a close space between yarn guide and cheese. All transmission devices are installed in the enclosed space of upper twisting dish inside, so the dust and fly of raw materials can not fall in when this new machine is used. This can prolong the life of spindle and make it more convenient for maintainness.

Another problem we have met in the research process is how to blance the weight of spindle. As mentioned above, in order to winding smoothly and have a good shape, we have installed the two-way screw on one side of spindle which drive the yarn guide to finish winding the yarn. The problem is how to blance the weight of two-way screw and its transmission device.Through experiments we find a way to solve this problem by adding a blancer on the other side,so that the weight of blancer is equal to the whole weight of the two-way scerw device,thus making the new spindle steady in running.

One special design for the new spindle is that two different materials can be introduced into machine through different passageways. Fig 2 illustrates the concrete operation.

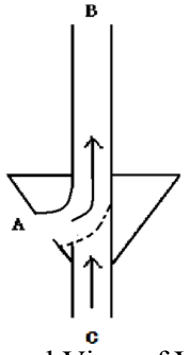


Fig 2 General View of Yarn Feeding

The output from the front roller can be introduced from the spindle side through Point A to Point B, and the filaments /the rovings /the strands can be introduced from the bottom of spindle through Point C to Point B at the same time.Then they are twisted individually for two different effects.The twist of the bottom yarn is a half of the side yarn,so the two-for-one twisting spinning frame can make two different twisting effects, which is a new creation in spinning. Just for this reason the new spinning frame can be used for spinning several special kinds of fancy yarns.

Conclusion

We have designed and processed a two-for-one twisting spinning frame already, and proved this new machine can spingning successfully by using certain technological parameters.This frame is the only one in textile feild.The basic technology and theory has initially matured. Through testing the yarns various performances and compared it with the ring spun yarns we have known that the new spun yarn properties such as yarn line evenness/yarn twist /yarn hairness/yarn strength/yarn breaking strength and so on, all these can meet the basic requirements. Two-for-one twisting spinning frame as a new frame can spin smoothly with its unique and obvious advantages. The new frame has a variety of functions so that it can be used widely in many aspects.

Due to the experimental conditions and factors such as research funding restrictions, there exists some problems to be resolved. To realize the industrial application, it needs further research and development.

Application Perspective

The creation of two-for-one twisting spinning frame is not only a great breakthrough but an important innovation. The development trends of modern spinning technologies which require a higher speed and a larger package can be met with the new machine. Not only a novel spinning thought and a new research orientation are presented for new innovations of spinning technology, but also a new creation and a new breakthrough are shown. A blank of spinning technology is filled with our innovation of two-for-one twisting spinning frame.

The direct twisting type of two-for-one twisting spindle can be used for spinning frame/for the doubling and twisting machine/for spinning fancy yarns.Many obvious advantages and advanced technologies are presented with the two-for-one twisting spinning frame.It would bring more economic benefits and social values if a successful industrialized application is made. Also the development of productivity and the technological process would be vigorously promoted in textile industry[4].

At present, although this technology has matured and we have spun yarns on the two-for-one twisting spinning frame successfully.But in order to meet the high demands for industrial usage, we have some problems to be solved in subsequent research. We hope we can cooperate with the demestic or abroad corporations who are so powful and willing to do the research on two-for-one twisting spinning frame to do the production and processing, and put the new spinning frame into a successful industrialized application.

Acknowledgement

This research is supported by special foundation item of the key academic subjects development of shaanxi province[Shaanxi education Supporting(2008)169].So it is gratefully ackonwledged.

References

[1] P Artzt, prospectus of the ring spinning process, Melliand International (1998)

[2] Gustav Franzen, Neersen, two-for-one twisting spindle, U.S. Patent 3,368,336. (1968)

[3] Hermann,Gronnau-Epe,Fed.Rep.of Germany, two-for-one twisting spindle, U.S. Patent 5,155,988. (1992)

[4] Owen P, A vision of spinning's future, Textile Horizons (1999)

© (2011) Trans Tech Publications, Switzerland
doi:10.4028/www.scientific.net/AMR.331.493

Reducing Yarn Hairiness in a Modified Ring Spinning Yarn path by Various Offsets

Xuzhong Su[1, a], Weidong Gao[1,b], Tingting Wu[1,c], Xinjin Liu[1,d] and Yun Zhang [1,e]

[1] Key Laboratory of Eco-Textile, Ministry of Education, Jiangnan University, Wuxi 214122, P. R. China

[a]mfgucv@163.com, [b]gaowd3@163.com, [c]wtt330327@163.com, [d]liuxinjin2006@163.com, [e]997299140@qq.com

Keywords: Ring spinning, Spinning angle, Yarn hairiness, Offsets

Abstract. Spinning triangle is a critical region in the spinning process of yarn. Its geometry influences the distribution of fiber tension in the spinning triangle and the properties of spun yarns, such as the yarn breakage and hairiness. In this paper, the relationships between the spinning angle and yarn properties especially the yarn hairiness were investigated under various horizontal offsets. The properties of spun yarns produced by the modified system were evaluated and analyzed. Both left diagonal and right diagonal yarn arrangements were examined. The results indicate that the right diagonal yarn path leads to reduce yarn hairiness but the left diagonal yarn path leads to increase yarn hairiness; the breaking force of yarn changes little; yarn evenness deteriorates slightly with the changes of offset.

Introduction

In spite of modernization and rapid technological development in the field of ring spinning, the mechanism ring-traveler spindle has remained almost the same until now [1]. In the ring spinning process, the drafted roving leaves the front roller at the nip with a width, and then the fibers enter the twisting zone and are tied into a yarn by twisting the strand. The twisting area between the front roller nip and the yarn twist point is known as the spinning triangle or twisting triangle [2-5]. It is in this zone that individuals or bundles of fibers are twisted and consolidated to form a yarn structure. Therefore, the spinning triangle and spinning angle affect the yarn breakage and influence the yarn structure [6]. The long and narrow width spinning triangle implies a long weak point and hence causes more end breakages. However, a resultant advantage of this small width triangle is that the edge fibers are better bound in the yarn, which gives a smoother yarn and hence less fly generation [3,7].

The spinning geometry of a ring spinning frame plays an important role, and the spinning triangle is a critical region in ring spinning. Changes in the spinning geometry may affect yarn properties [8,9]. Stalder [11] has confirmed that when the spinning triangle gets smaller with increasing spinning tension, the hairiness is reduced. According to Klein [10], when the spinning triangle is short, the fibers from the edges must be strongly deflected to get bounded into the yarn structure [7]. In the study of reducing yarn hairiness with a modified yarn path in worsted ring spinning conducted by Wang and Chang [12], it was pointed out that the twist triangle is a critical region in ring spinning and changes of its geometry affect yarn properties. G Thilagavathi pointed out that there is up to 40% reduction in hairiness at 60mm offset left diagonal path with slight increase in the strength for all the counts produced except 100s [7].

The present research approach is similar to that presented by G Thilagavathi and Wang [7,12], while some important modifications were made. First, an offset d was introduced for describing the skew level of the geometry of spinning angle. Second, a new approach was used to modify the yarn path. Our experiment work in this paper evaluates the performance of these diagonal yarn path arrangements in terms of yarn quality.

Experimental

Materials and methods

100% cotton yarns of the counts Ne 20s, 30s, 40s, 50s, 60s were spun in the modified ring spinning system invented by our group under various offsets in a modified EJM 128k ring spinning frame with the diagonal devices. In order to compare with the modified yarns, homologous conventional yarns without diagonal offset were also spun. And all yarns were spun with Z twist. The fiber specifications and process parameters are given in Table 1 and Table 2.

Table 1 Fiber specifications for various yarns

Count Ne	Fiber Length mm	Fiber Strength g/tex	Micronaire Value
20s	28.1	22.6	4.5
30s	28.1	22.6	4.5
40s	28.1	22.6	4.5
50s	32.0	24.5	4.1
60s	33.5	25.5	4.0

Table 2 Process parameters for various yarns

Count Ne	Roving Count tex	Total Draft	TM	Traveller Type
20s	483	16.567	3.9	C1UL 2/0
30s	483	24.850	3.9	C1UL 4/0
40	483	33.030	4.0	C1UL 5/0
50s	425	36.443	4.0	C1UL 7/0
60s	350	36.374	4.3	C1EL 14/0

Wang confirmed that right diagonal path produces yarn of lower hairiness in worsted spinning in his study [12]. According to G Thilagavathi [7], left diagonal path reduces hairiness in coarser counts than straight path and right diagonal path. But both of their research methods were implemented by threading the yarn in adjacent spindle. Hence, as shown in Fig. 1, the yarns were spun with a modified yarn path by various offsets (left, conventional or right) in our work.

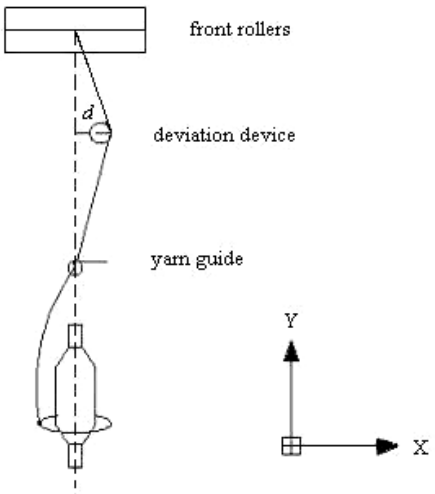


Fig. 1 A schematic diagram of the modified ring spinning system

Yarn test

Table 3 Number of 3-9mm length hairiness per 100m for various yarn counts

Offset length mm	Numbers of 3-9mm hairiness per 100m				
	20s	30s	40s	50s	60s
L6	1275	1342	712	1034	1112
L12	1732	1449	866	954	1163
L18	1710	1182	813	1035	1015
0	1211	997	713	889	628
R6	1011	743	548	680	625
R12	695	573	510	640	494
R18	733	707	571	688	566

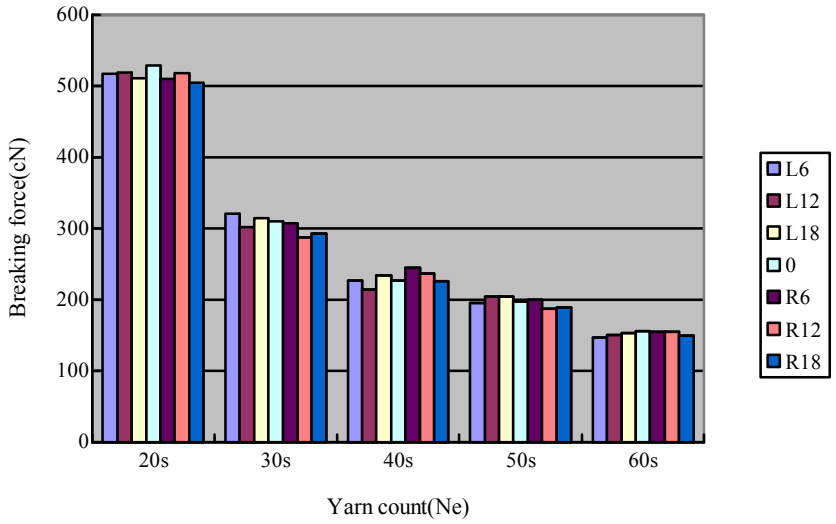


Fig. 2 Breaking force of various yarn counts with different offsets

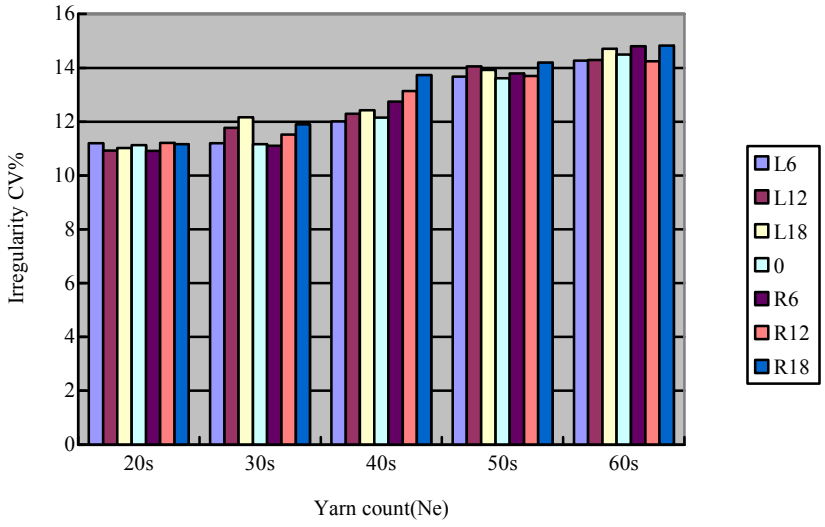
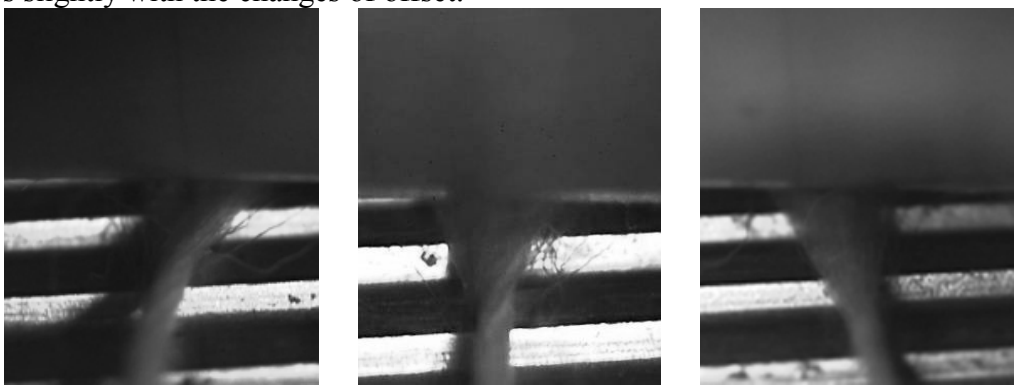


Fig. 3 Irregularity of various yarn counts with different offsets

In order to study the effects on yarn harmful hairiness of spinning for different offsets, number of 3-9mm hairiness per 100m for various yarn counts were tested. In addition, the breaking force and irregularity of yarns were also measured. All the samples were conditioned for at least 48 hours under standard conditions (65±2% RH and 20±2℃). The hairiness was tested using Changling YG172A hairiness tester under 100 m/min speed and 5g pretention. The number of hairiness for all the classes was observed. The breaking forces of yarns were tested on YG063 fully automatic single yarn strength tester at a speed of 500mm/min and at a pretension 1.8cN/tex. The irregularity was done by YG135G evenness tester at a speed of 400m/min. The results of yarn hairiness for all samples are given in Table 3 (L—left diagonal, 0—without diagonal, R—right diagonal). And the results of breaking force and irregularity are shown in Fig. 2 and Fig. 3.

Results and discussions

Based on the comparison of yarn hairiness in the three states, it was observed that spinning with the different right offsets has different effects on reducing harmful yarn hairiness. And it is obviously shown that the number of 3-9mm length hairiness reduced largest with 12mm right offset. Meanwhile, from Table 3, the results indicate that the harmful hairiness readings for yarns spun with the different left offsets arrangement are more than the hairiness readings of conventional and right diagonal ring spun yarns. As shown in Fig. 2 and Fig. 3, breaking force of various yarn counts with left or right offsets changes little comparing with the conventional yarns. However, yarn evenness deteriorates slightly with the changes of offset.



(a) Left diagonal (b) Without diagonal (c) Right diagonal

Fig. 4 Spinning triangle with different offsets

To illustrate the effects on yarn hairiness during spinning for different offsets, a high speed camera system (OLYMPUS i-speed3) was used to capture the geometry of the spinning triangle. As shown in Fig. 4(b), for a conventional Z-twist yarn without diagonal arrangement, fibers on the right hand side of the triangle often undergo a pre-twisting process that effectively binds the fibers, while fibers on the left hand side are less controlled. It can be seen from Fig. 4(a) that left diagonal aggravates the pre-twisting process of the fibers on the right hand side of the triangle, while fibers on the left hand side are less controlled and shows a state of relaxation. Fig. 4(c) shows the pre-twisting effect at the right-hand side of the spinning triangle is reduced when the right offsets are used. So it is stated that hairiness reduction may be due to right diagonal balance the pre-twisting effect in our experiment. While the definite relationships between hairiness and right offset need for further research, and it will be discussed in our next study.

Conclusions

In this study, the simple idea of ring spinning with a diagonal yarn path by changing various offsets and how this modified yarn path affects yarn quality and spinning efficiency have been examined. Both left diagonal and right diagonal yarn arrangements have been examined and the results from yarn

hairiness tests indicate that the right diagonal yarn path leads to reduce yarn hairiness but the left diagonal yarn path leads to increase yarn hairiness; breaking force of various yarn counts with left or right offsets change little comparing with the conventional yarns; yarn evenness deteriorates slightly with the changes of offset. In a word, taking appropriate right offset of the spinning triangle can help to improve the spun yarn quality with 'Z' twist. However, the yarn quality is not always improved with the increasing of the offset. Hence, the optimal offset will be investigated in our further study.

Acknowledgements

This paper is sponsored by Science and Technology Agency of Xinjiang Uygur Autonomous Region (Technology Support Project in Xinjiang in 2011, 201191112) and State of College Students Innovative Experiment (101029517).

References

[1] M. Nikolić, Z. Stjepanovič, F. Lesjak, A. Štritof: Fibers & Textiles in Eastern Europe Vol. 4 (2003), P. 30.

[2] W. G. Zhang, M. Y. Chen, S. J. Ding, W. L. Peng: *The basic theory of the twisting process* (Textile Engineering Publishers, Beijing 1983).

[3] T. Hua, X. M. Tao, K. P. S. Cheng and B. G. Xu: Textile Research Journal Vol. 11 (2007), P.853.

[4] T. Hua Tao, X. M. Tao, K. P. S. Cheng and B. G. Xu: Textile Research Journal Vol. 2 (2010) , P.116.

[5] J. Feng, B. G. Xu, X. M. Tao et al: Textile Research Journal Vol. 14 (2010), P.1456.

[6] X. G. Wang: Research Journal of Textile and Apparel Vol. 1 (1998), P.1.

[7] G. Thilagavathi, D. Udayakumar, L. Sasikala: Indian Journal of Fiber and Textile Research Vol. 34 (2009) , P.328.

[8] L. Ren: Shang Hai Textile Science &Technology Vol. 3 (2009), P.16.

[9] L. Ren，J. K. Chen，G. C. Fan，Q. J. Song，G. Q. Liu: Progress in Textile Science & Technology Vol. 2 (2009), P.39.

[10] W. Klein: International Textile Bulletin: Yarn Fabric Forming Vol.139 (1993), P.22.

[11] H.Stalder: Textile Asia Vol.3 (2000), P.43.

[12] X. G. Wang, L. L. Chang: Textile Research Journal Vol. 14 (2003), P. 327.

© (2011) Trans Tech Publications, Switzerland
doi:10.4028/www.scientific.net/AMR.331.498

Quasistatic model for the symmetrical Ring Spinning Triangle

Xinjin Liu[1,a], Xuzhong Su[1,b] and Tingting Wu[1,c]

[1] Key Laboratory of Eco-Textile, Ministry of Education, Jiangnan University, Wuxi 214122, P. R. China

[a]liuxinjin2006@163.com, [b]mfgucv@163.com, [c]wtt330327@163.com

Keywords: Symmetrical Spinning triangle, Quasistatic model, Force balance.

Abstract. In this paper, theoretical model of the distribution of fiber tension in the symmetrical spinning triangle was given firstly. Then, based on the force balance of the twisting point, the quasistatic model for the symmetrical ring spinning triangle was present. It is shown that the convergence point can be determined with ease for different spinning tension, torsion moment, the numbers of fibers at the roller nip, the fiber tensile Young's modulus and cross-section, and the width of the spinning triangle.

Introduction

In the ring spinning process, first, the fiber strand comes from the draft zone, almost of which are flat and parallel to the twisting axis of the strand in this time. Second, when the twisting inserted into the fibers by the rotation of the traveler, the strands at the jaw rotate around the axis and the width begin to decrease. The fibers on both sides of the axis fold gradually and roll into the centre of the spun yarn, and the spinning triangle formed consequently [1]. Therefore, the spinning triangle is a critical region in the spinning process of yarn. Its geometry influences the distribution of fiber tension in the spinning triangle and, thus, affects the properties of spun yarns [2]. Taking appropriate measures to influence the spinning triangle geometry and thus improve the quality of yarn has attracted great interesting in the spinning of yarn recently [3,4]. All the existing spinning technologies are achieved by changing the ring spinning triangle in a sense, such as the Sirospun [5], Solospun [6], and Compact spinning [7] and so on.

Over the past decades, the subject of spinning triangle has been one of the most important research topics and attracted more and more attentions [2,3,8]. A theoretical model was firstly developed in order to predict the distribution of tension forces of the fibers in the spinning triangle by using the principle of stationary total potential energy [8]. In this model, only a symmetric geometry of the spinning triangle was considered. Then, this model was further extended to the asymmetric spinning triangle by introducing a shape parameter for describing the skew level of the geometry of spinning triangle [2]. Finally, a more general theoretical model for the distribution of tension forces of the fibers in the spinning triangle with offset was proposed by considering the inclination angle of the spinning tension based on the analysis above [3].

Motivated by all these research works above, this paper attempts to investigate the quasistatic model for the ring spinning triangle deeply. For simplicity to discuss, we only analyze the symmetrical spinning triangle in this paper, and the case for spinning triangle with offset will be discussed in our future study. First, theoretical model of the distribution of fiber tension in the symmetrical spinning triangle was given. Then, based on the force balance of the twisting point, the quasistatic model for the symmetrical ring spinning triangle was present.

Theoretical model of the distribution of fiber tension in the symmetrical spinning triangle

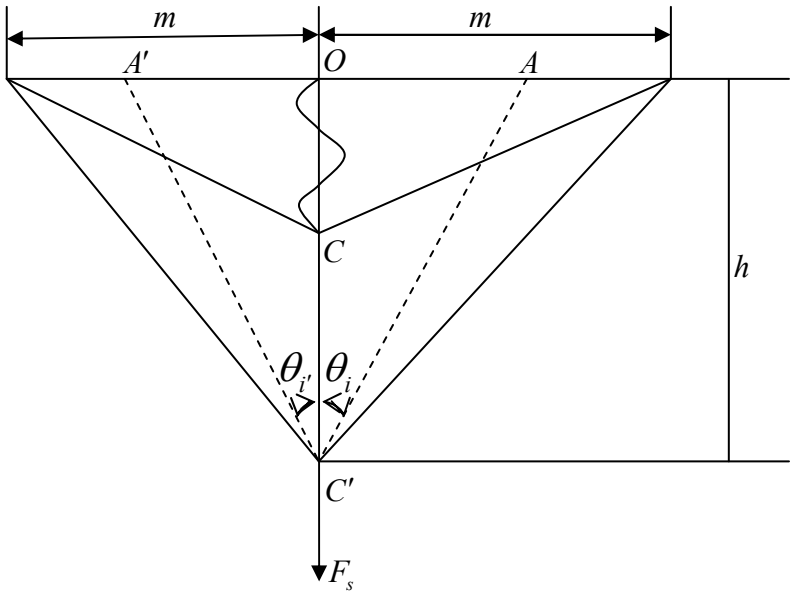


Fig.1 Symmetrical spinning triangle

The symmetrical spinning triangle model is shown in Fig.1. Here, the point C is an initial convergence point without any force. O is the middle point of the nip line, C' is the twisting point with the constant force F_s. m is the half width of the spinning triangle. h is the height of the spinning triangle. θ_i is the angle between the right i-th fiber and the central fiber, $\theta_{i'}$ is the angle between the left i'-th fiber and the central fiber correspondingly. Suppose that the number of each side of the central fiber is n, i.e. there are $2n+1$ fibers in the spinning triangle.

Using the principle of minimum potential energy and based on the analysis in [3], the distribution of the fiber tension in the symmetrical spinning triangle can be given as:

$$\begin{aligned} F_{i=0,1,\cdots,n} &= \frac{F_s - AE\left(\sum_{i=0}^{n} M_i\left(M_i-1\right)+\sum_{i'=0}^{n} M_{i'}\left(M_{i'}-1\right)\right)}{\sum_{i=0}^{n} {M_i}^2+\sum_{i'=0}^{n} {M_{i'}}^2-1} M_i + AE\left(M_i-1\right) \\ F_{i'=0,1,\cdots,n} &= \frac{F_s - AE\left(\sum_{i=0}^{n} M_i\left(M_i-1\right)+\sum_{i'=0}^{n} M_{i'}\left(M_{i'}-1\right)\right)}{\sum_{i=0}^{n} {M_i}^2+\sum_{i'=0}^{n} {M_{i'}}^2-1} M_{i'} + AE\left(M_{i'}-1\right) \end{aligned} \tag{1}$$

Here, A is the cross-section of fiber, E is the fiber tensile Young's modulus. $M_i = \dfrac{1}{\cos\theta_i}$, $M_{i'} = \dfrac{1}{\cos\theta_{i'}}$.

We further assume that the ends of all fibers gripped in the front roller nip distribute evenly, i.e. $m_i = m_{i'} = i\frac{m}{n}$, where m_i is the distance between the end of the i-th fiber in the right side and the point O, and $m_{i'}$ is the distance of i'-th fiber in the left side correspondingly. Then, from the Fig.1, we have

$$\begin{aligned}
&\tan(\theta_i) = \tan(\theta_{i'}) = \frac{m_{i'}}{h} = \frac{m_i}{h} = \frac{im}{nh} \\
&\sin\theta_i = \sin\theta_{i'} = \frac{i\frac{m}{n}}{\sqrt{\left(i\frac{m}{n}\right)^2 + h^2}} \\
&\cos\theta_i = \cos\theta_{i'} = \frac{h}{\sqrt{\left(i\frac{m}{n}\right)^2 + h^2}}
\end{aligned} \tag{2}$$

for $i = 1, 2, \cdots, n$.

The quasistatic model for the symmetrical ring spinning triangle

For the symmetrical spinning triangle model as shown in Fig.1, taking the twisting point C' as the research object, and according to the force decomposition as shown in Fig.2, we can get the equations for the force balance of the C' as follows.

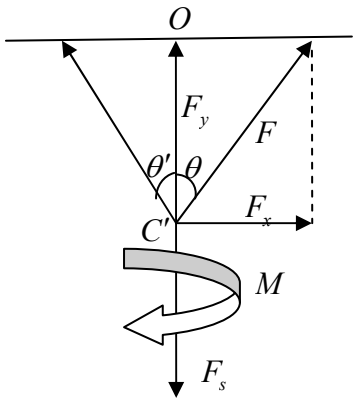


Fig.2 The force decomposition of the twisting point

$$M + R\sum_{i=0}^{n} F_i \sin\theta_i = 0 \tag{3}$$

$$F_s = 2\sum_{i=0}^{n} F_i \cos\theta_i \tag{4}$$

Here, M is the twisting torsion moment produced by the rotating action of traveler, R is the diameter of the yarn, F_i is the fiber tension in the symmetrical spinning triangle as present in Equation (1).

From the four equation (1)-(4), h and R can be solved. However, the explicit analytical relation is difficult to get, thus the numerical calculation is advisable. The numerical calculation will be discussed in our future study for specific ring spinning process.

Conclusions

In this paper, the quasistatic model for the symmetrical ring spinning triangle has been given based on the force balance of the twisting point and the theoretical model of the distribution of fiber tension in the symmetrical spinning triangle. This model can describe the static coverage point of the symmetrical ring spinning triangle completely from the theory. However, it is shown that the explicit analytical relation is difficult to get. Therefore, the numerical calculation will be discussed in our future study for specific ring spinning process. It should be noted that only symmetrical spinning triangle has been investigated in this paper, the general spinning triangle with offset remain to be challenging subjects for future research.

Acknowledgments

This paper is sponsored by Northern Jiangsu Science and Technology Development Plan (SBC201060102), State of College Students Innovative Experiment (101029517) and Technology Yuanjiang Project 2011 (201191112).

References

[1] W. G. Zhang, M. Y. Chen, S. J. Ding, W. L. Peng: *The basic theory of the twisting process* (Textile Engineering Publishers, Beijing 1983).

[2] T. Hua, X. M. Tao, K. P. S. Cheng and B. G. Xu: Textile Research Journal Vol. 11 (2007), P.853.

[3] J. Feng, B. G. Xu, X. M. Tao et al: Textile Research Journal Vol. 14 (2010), P.1456.

[4] G. Thilagavathi, D. Udayakumar, L. Sasikala.: Indian Journal of Fiber and Textile Research Vol.34 (2009), P.328.

[5] X. L. An, C. W. Yu: Journal of the Textile Institute Vol. 9 (2010), P.805.

[6] L. D. Cheng, P. H. Fu, X. Y. Yu: Textile Research Journal Vol. 9 (2004), P.763.

[7] N. Momir, S. Zoran, L. Franc, S. Andrej: Fibers & Textiles in Eastern Europe Vol. 4 (2003), P.30.

[8] N. S.Shaikhzadeh: *An Analysis of the Twist Triangle in Ring Spinning* (PhD Thesis, University of New South Wales, Australia 1996).

© (2011) Trans Tech Publications, Switzerland
doi:10.4028/www.scientific.net/AMR.331.502

Effect of Siro-spun Processing Parameters on Properties of 55/45 Flax/Cotton Blended Yarn

Shuqiang Liu[1, a], Jinming Dai[1,b], Husheng Jia[2,3,c,*], Xuguang Liu [2,3,d] and Bingshe Xu[2,3,e]

[1]College of Textile & Arts, Taiyuan University of Technology, YingBin Road 113#, Yuci, Shanxi, 030600, China

[2]Key Lab of Interface Science and Engineering in Advanced Materials (Taiyuan University of Technology), Ministry of Education, West YingZe Road 79#,Taiyuan, Shanxi, 030024, China

[3]Taiyuan University of Technology Research Center of Advanced Materials Science and Technology, Taiyuan, Shanxi, 030024, China

[a]liushuqiang8866@126.com.cn, [b]tgmydjm@163.com.cn, [c]jia_husheng@126.com.cn, [d]liuxuguang@tyut.edu.cn, [e]xubs@tyut.edu.cn

[*]Corresponding author

Keywords: Flax fiber, Siro-spun, Spinning process, Hairiness, CV of count.

Abstract: Limited studies exist related to the siro-spun spinning of flax (Linum usitatissimum L.) and cotton (Gossypium hirsutum) blends. The purpose of this study was to determine the influence of various siro-spun processing parameters, including twist factor, space between two rovings and specification of traveler, on yarn qualities, such as yarn hairiness, tenacity and evenness. Results show that both specification of traveler and space between two rovings significantly influenced yarn hairiness and evenness, and heavier traveler and greater space led to decreased hairiness, but bad evenness. Twist factor influenced yarn evenness highly significantly, and smaller twist factor led to worse yarn evenness. Results also indicate the optimum levels of siro-spun process parameters as follows: twist factor α_m = 150, space between two rovings 8 mm, traveler Fo 5/0. In relation to the general ring-spinning yarn, the siro-spun spinning yarns had decreased hairiness, little increased tenacity and similar evenness.

Introduction

Flax, as one kind of bast fiber, is preferred by consumers and used widely in clothing and garment because its fabric has many virtues, such as fast moisture absorption and carry-off, antibacterial property, UV resistance, antistatic property, bland color and unique style. Meanwhile, flax fiber meets all known environmental regulations with regard to processing and use [1-3].

However, flax fiber has some characteristics unfavorable to spinning, such as more nep and high rigidity, which could lead to the more hairiness, low strength, and bad evenness of flax ring-yarn [4,5]. The physical properties of flax fiber are given in Tab. 1.

In order to diminish the above mentioned yarn's unfavorable characteristics, there is an urgent need for the investigation of the behavior of flax during processing in textile mill. Although some literatures has reported that the flax fiber could blend with other fibers, such as cotton, Lyocell, PP, etc. for spinning and could be adaptable to some spinning technologies, such as rotor, compact, core-spun etc. [6-10], there is still need for more research on the spinning of flax fiber, especially on the new spinning system like siro-spun spinning applied by few literatures to spinning flax yarn. Siro-spun spinning technology is a spinning method which could provide blended yarn with decreased hairiness, high strength, and good evenness [11-13]. The process of the siro-spun spinning is shown in Fig. 1, in which the double-hole cone with different distances between two holes' centers determines the space between two rovings. This study was aimed at optimizing the siro-spun processing of 18.2 tex flax/cotton blended yarn and studying the relation between various processing parameters and qualities of yarns.

Tab. 1. Physical properties of flax fiber

Fiber Property	Value
Technical fiber fineness for spinning, nominal (dtex)	12-25
Technical fiber length for spinning, nominal (mm)	400-800
Density (g/cm3)	1.49
Tenacity at break, nominal (cN/dtex)	4.4
Elongation at break, nominal (%)	2.5-3.3
Moisture regain (%),20℃, 65% RH	8-11
Antibacterial rate (%),20℃,12h	Staphylococcus aureus 94 Colon bacillus 92

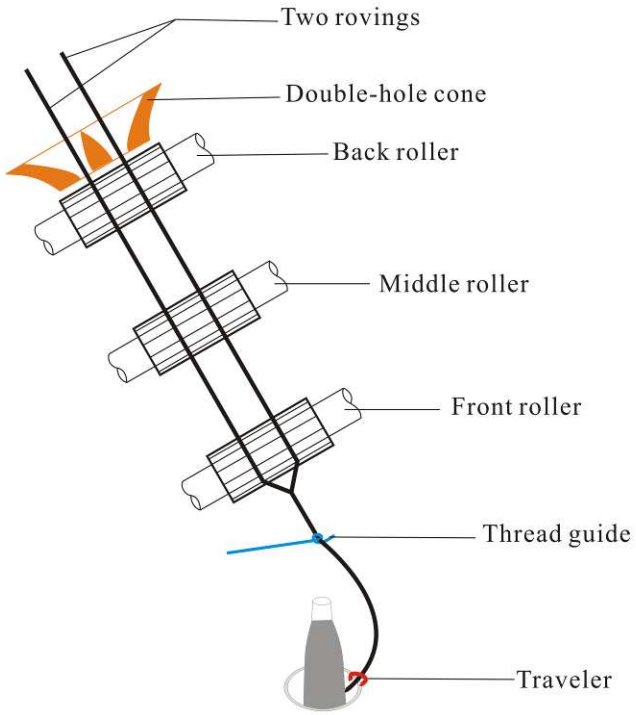


Fig. 1. Illustration of siro-spun spinning

Experimental

Materials

The roving used to spin the yarn samples was obtained from the material made at Taiyuan University of Technology. Flax/Cotton blend of 55/45 blend ratio was selected for the purpose of studying the variation of yarn indices with changing processing parameters. The specifications of the fibers used are given in Tab. 2. Flock blending was used to blend the fibers. The roving count was 5.5 g/10 m×2.

Tab. 2. Properties of fibers used in experiment

Fiber Property	Fiber Type	
	Cotton	Flax
Fiber fineness (dtex)	1.6	15
Staple length (mm)	32.6	37.5
Weighted average Length (mm)	28.8	33.6
CV of length (%)	25.5	30.6
Short fiber content (%)	6.4	14.23
Tenacity (cN/dtex)	3.7	4.147

The yarn samples were spun using a laboratory model siro-spun spinning machine, type FA 001 with the following machine parameters:

Total drafting ratio	60.4
Back zone drafting ratio	1.15
Center distance between back and middle rollers	63 mm
Center distance between front and middle rollers	43 mm
Spindle speed	5000 r/min
Yarn count	18.2 tex

The siro-spun yarn samples of count 18.2 tex were spun according to the experimental design discussed later. And the ring spinning yarn of 18.2 tex was also spun to be compared with siro-spun yarn, which need some adjustment of machine parameters (i.e. two rivings adjusted as one, total drafting ratio reduced by half, and double-hole cone changed as one hole cone).

Experimental design

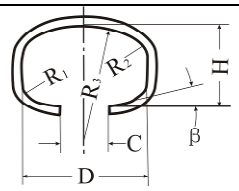
While many factors affect the performance and quality characteristics of siro-spun yarns [14,15], in this research work three parameters, twist factor α_m (A), space between two rovings (B) and specification of traveler (C) were selected and designated as the variables. The actual values for the factors used are given in Tab.3. The travelers used in experiment have the same shape but different weights. The specifications of travelers are given in Tab. 4. The effect caused by changes in the variables was studied by monitoring changes in the yarn quality indices.

Tab. 3.[a)] Actual factor levels

Factor Level	Factors		
	A Twist factor α_m	B Space between two rovings (mm)	C Specification of traveler
1	130	6	Fo 7/0
2	140	8	Fo 5/0
3	150	10	Fo 3/0

[a)] The levels of factors were obtained by spinning trials and some references [16,17].

Tab. 4. The specification of traveler

Shape	Specification of traveler	Size (mm)							Weight (g/100)
		D	H	C	R1	R2	R3	β	
	Fo 7/0	4.5	2.95	1.55	0.7	0.90	4.15	13°	3.56
	Fo 5/0	4.6	3.00	1.55	0.8	1.00	4.25	13°	4.21
	Fo 3/0	4.6	3.00	1.55	0.8	1.00	4.25	13°	4.86

These quality indices were designated as responses. To study the relationship between the variables and the responses, orthogonal experimental design was used, where the variables were twist factor, space between two rovings and specification of traveler.

An experimental design (Tab. 5) was set up and the changes in the three variables were monitored through changes in six yarn quality indices, which are hairiness, tenacity, CV of count, neps, thick places and thin places. The data obtained from the experimental design was used to design optimum conditions for the three spin-processing variables. The effects of the three spin-processing variables on the main three quality indices, hairiness, tenacity, and CV of count, were studied.

Tab. 5. Experimental design

Experimental Design No.	Variable		
	A	B	C
1#	130	6	Fo 7/0
2#	130	8	Fo 5/0
3#	130	10	Fo 3/0
4#	140	8	Fo 7/0
5#	140	10	Fo 5/0
6#	140	6	Fo 3/0
7#	150	10	Fo 7/0
8#	150	6	Fo 5/0
9#	150	8	Fo 3/0

Yarn testing

The initial yarn samples obtained from the experimental designs were subjected to yarn testing as per the six yarn quality indices. All the six indices were measured under standard testing conditions, using evenness tester (YG135G, China), yarn tensile strength tester (YG061, China) and yarn hairiness tester (YG172,China). The optimum yarn samples were also subjected to the same yarn testing conditions as the samples from the experimental design conditions.

Statistical analysis

Analysis of variance (ANOVA) was used to compare the significance of the three variables, twist factor, space between two rovings and specification of traveler, on the quality of siro-spun yarn samples. If one factor's F-value was higher than the critical F-value of level 0.05 (i.e. 95% confidence limit) or 0.01 (i.e. 99% confidence limit), the factor was regarded as significant or highly significant, and as the main objective.

Analysis of surface morphology

The KH-1000 Digital Three-dimensional Fiber Measurement System (DTFMS) made in China, was employed to analyze the surface morphology of the ring spinning or siro-spun spinning yarns and corresponding fabrics. The magnification of the image was set in the range of 50-100×. The yarn or fabric was placed directly on the microscope stage for observation.

Results and Discussion

Results of yarn testing

Tab. 6. Results of yarn testing

Experimental Design No.	≧3 mm Hairiness (m^{-1})	Tenacity (cN/tex)	CV of Count (%)	Thin Places -50% (km^{-1})	Thick Places +50% (km^{-1})	Neps +200% (km^{-1})
1#	18.01	13.369	28.56	1715	3605	2505
2#	10.38	14.084	29.39	1900	3470	2330
3#	10.46	13.794	30.36	1860	3675	3050
4#	17.09	13.022	28.23	1525	3380	2760
5#	9.19	13.841	29.57	1865	3530	3190
6#	15.02	13.587	28.44	1275	3590	3115
7#	14.32	12.499	28.26	1595	3515	2815
8#	14.09	13.054	27.81	1235	3640	2900
9#	11.39	14.373	28.27	1495	3630	3335

The yarn testing results are given in Tab. 6. Based on the principle of variance analysis, the data obtained from the yarn samples using the experimental designs were analyzed; hence the effects of the variables on the yarn quality characteristics were studied and the best fitting factor levels of variables, as best fitting siro-spun processing of flax/cotton blended yarn, were optimized.

Effect of variables on yarn hairiness

Tab. 7 shows the calculation procedure of variance analysis of yarn hairiness. Tab. 8 shows the result of variance analysis.

Tab. 7. [b] The calculation procedure of variance analysis of yarns' hairiness

Experimental Level	Factors A	B	C	Error	≧3 mm Hairiness (m^{-1})
K1	38.85	47.12	49.42	38.59	
K2	41.3	38.86	33.66	39.72	K=119.95
K3	39.8	33.97	36.87	41.64	
U	1599.68	1628.12	1644.91	1600.25	P=1598.67
Q	1.01	29.45	46.24	1.6	

[b] In 1#-9# order, if the data of one yarn quality were named as "Y_1-Y_9" , Ki means sum of data at level i ($i = 1,2,3$), $K = \sum_{i=1}^{9} Y_i$, $P = \frac{1}{9} K^2$, $U_j = \frac{1}{3} \sum_{i=1}^{3} (K_i^j)^2$ (j = A , B , C), $Q_j = U_j - P$ (j = A , B, C).

Tab. 8. The result of variance analysis of yarns' hairiness

Source	Sum of Squares	Degree of Freedom	Mean Square	F-value	Critical F-value	Optimum Processing
A	1.01	2	-	-		
B	29.45	2	14.725	22.6 **[c]	F0.10 (2,4)=4.32	10 mm
C	46.24	2	23.12	35.4 **	F0.05 (2,4)=6.94	Fo 5/0
Error	1.6	2	-	-	F0.01 (2,4)=18	
Correct error	2.61	4	0.65	-		
Sum	78.3	8	-	-		

[c] "**"means high significance.

Tab. 8 gives the comparison of three factors' sum of squares. Factor C, specification of traveler, whose sum of squares was biggest, had the most apparent influence on yarn hairiness; factor B, space between two rovings, was the second and factor A, twist factor, was the smallest. And the error' sum of square was larger than factor A', which mean that effect of error on hairiness was bigger than factor A that would be caused by narrow level range selected. So the effect of factor A on hairiness could be ignored and added factor A with error as correct error. The comparison of the calculated F-values and critical F-values shows that the calculated F-value, of factor B and factor C, were larger than the critical F-value, of the level 0.05 even level 0.01, indicating that the influence of factor C and factor B on the yarn hairiness was highly significant, but the factor A was not significant.

The effect of the specification of traveler on hairiness is given in Fig. 2, which shows the yarn at level 2 had the least hairiness. Different specifications of traveler had different weights that affected the trigonal twist zone of siro-spun spinning formed by lines joining points ABO in Fig. 3. The traveler having lighter weight could lead to larger balloon, lower spinning tension, and could also reduce the twist of the spinning yarn's section between the front nip of front roller and the guide wire, which could cause more hairiness easily. A heavier traveler could lead to smaller balloon and higher spinning tension, which could cause longer twist zone or longer "H" in Fig. 3. In this case the trigonal twist zone could become very instable even shaking violently, leading to the instability of twisting fibers, hence more hairiness. Therefore, only the traveler with appropriate type and weight could slide on the ring stably, and lead to suitable-size balloon, and reduced hairiness.

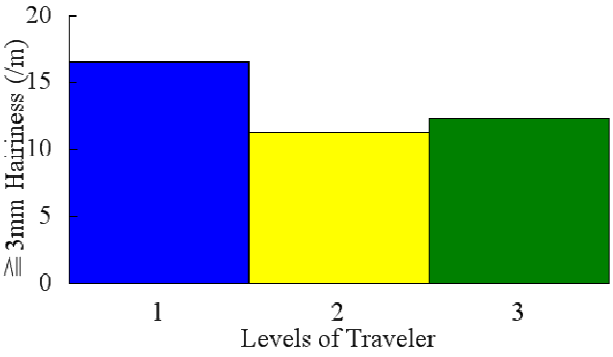


Fig. 2. Effect of the specification of traveler on hairiness

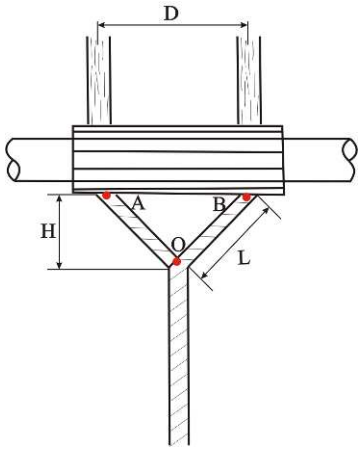


Fig. 3. Illustration of trigonal twist zone in siro-spun spinning

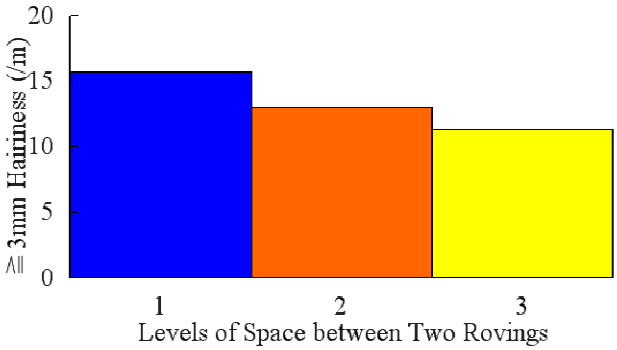


Fig. 4. Effect of the space between two rovings on hairiness

Fig. 4 presents the effect of the space between two rovings on hairiness. It is shown that the yarn hairiness decreased as space between two rovings increased and the yarn at level 3 had the least hairiness. Siro-spun spinning has its own unique twist form and the yarn's structure is similar to ply yarn's (two single yarns twist to form a resultant yarn). In the processing of siro-spun spinning, the resultant yarn and two single yarns all had twist. As the space between two rovings ("D" in Fig. 3) increased, owing to the constant spinning tension, the point "O" in Fig.3 moved down, the height of trigonal twist zone ("H" in Fig.3) and the length of single yarn ("L" in Fig. 3) both increased, so that each single yarn twisted more adequately, and less fiber head-end extended from yarn's surface, leading to less hairiness.

Just for decreasing yarn hairiness, the optimal processing parameters were B3C2, i.e. 10 mm space between two rovings and Fo 5/0 specification of traveler.

Effect of variables on yarn tenacity

Tab. 9 shows the calculation procedure of variance analysis of yarns' tenacity. Tab. 10 shows the result of variance analysis.

Tab. 10 shows that both A and B factors' sum of squares were smaller than error's, which mean that effect of error on tenacity was bigger than factor A and B that would be caused by narrow level range selected. So the effect of factor A and B on tenacity could be ignored and added factor A and B with error as correct error. Tab. 10 also shows that the calculated F-value of factor C, were smaller than the critical F-value, of the level 0.05 even level 0.10, indicating that the influence of factor C on the yarn tenacity was not significant.

Tab. 9. The calculation procedure of variance analysis of yarns' tenacity

Experimental Level	Factors				Tenacity (cN/tex)
	A	B	C	Error	
K1	41.247	40.01	38.89	41.583	
K2	40.45	41.479	40.979	40.17	K=121.623
K3	39.926	40.134	41.754	39.87	
U	1643.868	1644.015	1645.036	1644.131	P=1643.573
Q	0.295	0.442	1.463	0.558	

Tab. 10. The result of variance analysis of yarns' tenacity

Source	Sum of Squares	Degree of Freedom	Mean Square	F-value	Critical F-value
A	0.295	2	-	-	
B	0.442	2	-	-	F0.10 (2,6)=3.46
C	1.463	2	0.731	3.387[d)]	F0.05 (2,6)=5.14
Error	0.558	2	0.279	-	F0.01 (2,6)=10.9
Correct error	1.295	6	0.216	-	
Sum	2.758	8	-	-	

[d)] Having no "*" and "**"means the factor is not significant.

Effect of variables on CV of count

Tab. 11 shows the calculation procedure of variance analysis of CV of count. Tab. 12 shows the result of variance analysis.

Tab. 11. The calculation procedure of variance analysis of CV of count

Experimental level	Factors				CV of count (%)
	A	B	C	Error	
K1	88.31	84.81	85.05	86.4	
K2	86.24	85.89	86.77	86.09	K=258.89
K3	84.34	88.19	87.07	86.4	
U	7449.743	7449.101	7447.907	7447.136	P=7447.115
Q	2.628	1.987	0.792	0.0263	

Tab. 12. The result of variance analysis of CV of count

Source	Sum of Squares	Degree of Freedom	Mean Square	F-value	Critical F-value	Optimum Processing
A	2.628	2	1.314	123.079 **		150
B	1.987	2	0.993	93.032 * [e)]	F0.05 (2,2)=19	6 mm
C	0.792	2	0.396	37.091 *	F0.01 (2,2)=99	Fo 7/0
Error	0.026	2	0.013	-		
Sum	5.433	8	-	-		

[e)] "*"means significance.

Tab. 12 shows that the factor A, with the biggest mean square, affected the CV of count the most, then factor B the second, factor C the least. Furthermore, the comparison of F-value with critical F-value reveals that the effect of factor A on the CV of count was highly significant, the effects of factor B and C were significant. The effects of three factors on CV of count are given in Fig. 5, Fig. 6 and Fig. 7, respectively.

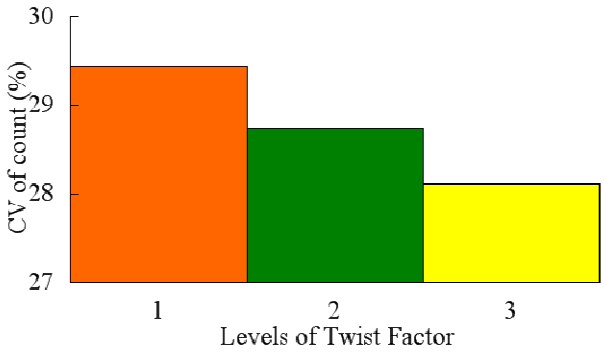


Fig. 5. Effect of twist factor on the CV of count

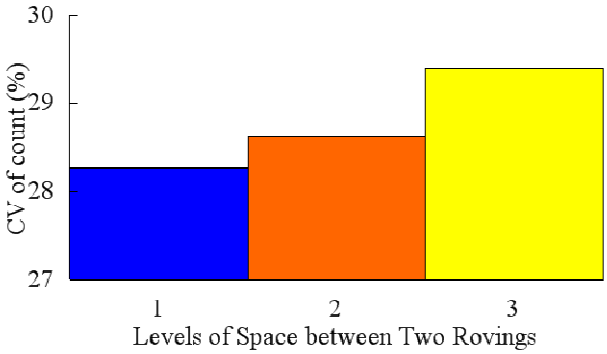


Fig. 6. Effect of space between two rovings on the CV of count

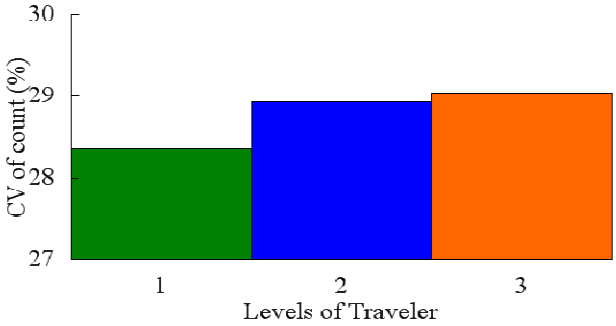


Fig. 7. Effect of traveler on the CV of count

The best levels for lest hairiness are as follows: factor A at level 3, factor B at level 1, and factor C at level 1. With decreasing twist, increasing space between two rovings and heaving traveler, the length and width of trigonal twist zone became larger and more instable, which could lead to more weak-link on the yarn and lower CV of count of the yarn.

Just for increasing the CV of count, the optimal processing parameters were A3B1C1, i.e. twist factor $\alpha_m = 150$, 6 mm space between two rovings and Fo 7/0 specification of traveler.

The optimum yarn

According to the above analysis, all factors that influence the yarn's quality and the optimum levels are given in Tab. 13.

Tab. 13. The order of factors' effect on the yarn's quality

Yarn Quality	Order of Factors' Effects
Hairiness	C2** → B3**
Tenacity	Ignored
CV of count	A3** → B1* → C1*

Factor A affected the CV of count most significantly, so factor A selected level 3 based on the evenness index, i.e. twist factor $\alpha_m = 150$.

The effects of factor B on the hairiness and CV of count were second significant, and the optimum level of factor B was level 3 based on hairiness or level 1 based on CV of count. The hairiness in Tab. 6 and the CV of count in Tab. 10 at B2 were close to optimal qualities. So the factor B chose level 2, i.e. 8 mm space between two rovings.

The effect of factor C on the hairiness was highly significant, and that on the CV of count was significant. So the emphasis was selected on decreasing the hairiness, then the factor C chose level 2, i.e. Fo 5 / 0 specification of traveler.

To sum up the above arguments, the optimum processing of spinning 18.2 tex flax/cotton blended yarn was A3B2C2.

Verification of optimum yarn in mill

In order to verify the optimum processing in mill, the yarn spun by optimum siro-spun spinning was compared with the yarn spun by general ring spinning. The qualities of the yarns are given in Tab. 14.

Tab. 14. Quality of the optimum yarn

Yarn Quality	Optimum Siro-spun Spinning Yarn	General Ring Spinning Yarn
	A3B2C2	
≧3 mm Hairiness (m^{-1})	10.58	23.01
Tenacity (cN/tex)	14.75	13.98
CV of tenacity (%)	9.47	10.31
Elongation at break (%)	4.76	4.62
CV of count (%)	28.38	28.40
Thin places -50% (km^{-1})	2295	2215
Thick places +50% (km^{-1})	4020	3935
Neps +200% (km^{-1})	3850	3700

The comparison of the two siro-spun spinning yarns with the general ring spinning yarn reveals that the siro-spun spinning yarns had decreased hairiness, little increased tenacity and similar CV of count. Between the two optimum siro-spun spinning yarns, the yarn of A3B2C2 had less hairiness and lower CV of count.

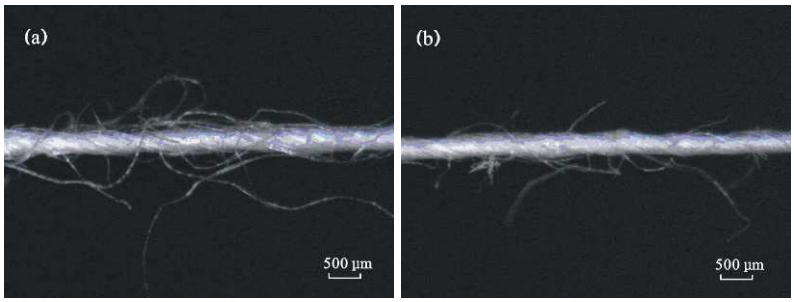


Fig. 8. The DTFMS photographs of yarn surface: (a) ring yarn, (b) siro-spun yarn at A3B2C2

The DTFMS photographs of yarns are shown in Fig. 8. The siro-spun yarn (Fig. 8 (b)) seem cleaner than the ring yarn (Fig. 8 (a)).

Conclusions

For a 18.2 tex 55/ 45 flax/cotton blended yarn, the effect of twist factor on yarn evenness was highly significant, and smaller twist factor led to worse yarn evenness. The effects of space between two rovings on yarn hairiness and evenness were significant, and the greater space between two rovings led to less hairiness, but worse evenness. The effects of specification of traveler on the yarn hairiness and evenness was significant, and the heavier traveler led to less yarn hairiness, but worse evenness.

The optimum process of siro-spun spinning was A3B2C2, i.e. twist factor α_m = 150, 8 mm space between two rovings, Fo 5/0 traveler.

In relation to the general ring-spinning yarn, the siro-spun spinning yarns had decreased hairiness, little increased tenacity and similar evenness.

Acknowledgements

This work was financially supported by the National Natural Science Foundation of China (50943027); the Program for Changjiang Scholar and Innovative Research Team in University (IRT0972); and the Young Scientist Project of Taiyuan University of Technology (K201029).

References

[1] Kimmel L. B., Boylstom E.K., Goynes W.R., et al. Nontraditionally Retted Flax for Dry Cotton Blend Spinning. Textile Res. J. 5 (2001) 375- 380.
[2] Zhang Yuan-ming, Yu Wei-dong. Study on the Physical and Chemical Properties of Flax Fibers. Plant Fiber Sciences in China. 25 (2003) 130-134.
[3] Zhang Y, Lin H, Chen YY. Structure and Properties of Oxidized Flax Fiber Treated with Sericin Solution. Textile Bioengineering and Informatics Symposium Proceedings. Vols 1 and 2 (2008) 126-130.
[4] Danny E. Akin, David S. Himmelsbach and W. Herbert Morrison Ⅲ. Biobased Fiber Production: Enzyme Retting for Flax/Linen Fibers. Journal of Polymers and the Environment. 8 (2000) 103-109.
[5] Foulk JA, Akin DE, Dodd RB. Miniature spinning enzyme-retted flax fibers. Journal of Natural Fibers. 6 (2009) 1-13.
[6] Gamble G, Foulk J. Effect of Overspray Treatments on the Processing Efficiency of A 50/50 Flax/Cotton Blend. Textile Res. J. 80 (2010) 754-759.
[7] Sun Y, Zhang JF. Processing Superfine Flax/Lyocell Fiber Blended Knitting Yarn with Rotor Spinning. Proceedings of the Fiber Society 2009 Spring Conference. Vols I and II, (2009) 290-293.
[8] Jiang JH, Chen NL, Xu HH, et al. Effect of Process Parameters on the Mechanical Properties of Co-wrapped PP/Flax Yarn. Proceedings of 2009 International Textile Science and Technology Forum. (2010) 241-247.
[9] Xu BJ, Ma J. Radial Distribution of Fibres in Compact-spun Flax-Cotton Blended Yarns. Fibres & Textiles in Eastern Europe. 18 (2010) 24-27.
[10] Wang SR, Yan TH, Jiang JH, et al. Evaluation of Mechanical Properties of Thermoplastic Composites Based on Flax/Polypropylene Core-spun Yarns. Proceedings of 2009 International Textile Science and Technology Forum. (2010) 556-561.
[11] Ghasemi R, Mozafari-Dana R, Etrati SM, et al. Comparing the Physical Properties of Produced Sirospun and New Hybrid Solo-Siro spun Blend Wool/Polyester Worsted Yarns. Fibres & Textiles in Eastern Europe. 16 (2008) 24-27.
[12] Zhang LN, He JH. Geometry Condition for Optimal Two-strand Yarn Spinning part I: Sirospun. Textile Res. J. 79 (2009) 243-246.
[13] Icoglu HI, Kirecci A. Investigation of the Fastness Properties and Color Values of Cotton Fabrics Knitted from Ring Spun and Sirospun (R) Yarns. Journal of the Textile Institute. 102 (2011) 114-119.
[14] Temel E, Celik P. A Research on Spinnability of 100% Polyester and Polyester-Cotton Blend Sirospun yarns. Tekstil Ve Konfeksiyon. 20 (2010) 23-29.
[15] He JH, Zhang LN. On convergence point of the two-strand yarn spinning. Textile Res. J. 78 (2008) 1022-1024.
[16] Shen Junliang, Bian Cheng, Guo Dadong, et al. Cotton spinning manual, 2th ed., China textile & apparel press, Beijing, 2001.
[17] Yao Mu, Zhou Jinfang, Huang Shuzhen, et al. Textile Materials Science, 2th ed., China textile & apparel press, Beijing, 2001.

© (2011) Trans Tech Publications, Switzerland
doi:10.4028/www.scientific.net/AMR.331.512

Research on the manufacture of tapered artificial vascular

Dong Xueqing [1,a] , Li Yuling [2,b] , Ding Xin [3,c] and Wang Lu [4,d]

[1,2,3,4] Key Lab. of Textile Science & Technology, Donghua University, Shanghai,201620, China

[a]xue0631@mail.dhu.edu.cn, [b]lylu@dhu.edu.cn,

[c]xding@dhu.edu.cn, [d]wanglu@dhu.edu.cn

Keywords: Tapered artificial vascular, Manufacture, Special fan-shaped reed, Warp density changed weaving, Rigid rapier sampling weaving machine, Modification.

Abstract. The design principle and manufacture of the new tapered artificial vascular was introduced. The idea of combining of special fan-shaped reed and lifting devices of front rest was proposed. The hardware of rigid rapier sampling weaving machine was modified to meet the request of the tapered artificial vascular weaving. It was verified through weaving a tapered artificial vascular and confirmed that the modificated equipment is successful and effective.

Introduction

Vascular diseases, with their high rates of morbidity and mortality in patients, are one of the most challenging research domains in medical science[1]. So the reserch on artificial vascular is very necessary. The most importanct thing what should be done now is to develop one artificial vascular which is the same with the host vascular.But there is one problem here.

The host blood vessel is tapered, and the taper angle of blood vessel is very small, only 1°, so many researchers believe that the effect of it on the blood flow can be neglected[2]. So far, the blood vessel have always been taken as cylindrical in most studies. But in the recent years, the simulated experiments have proved that the straight artificial vasculars are considerably different from the tapered ones in the axail velocity profile. And the straight artificial vascular can't be used to replace the tapered blood vessel in simulated experiments. So the research on tapered artificial vascular must be very necessary and important.

In the ordinary loom, tapered tubular fabric can be got at the now by adding or reducing warp yarns to change ends in warp[3], as shown in Figure 1(a). However, the shortcomings of this method are: (1) burr left at the edges of the tube, affecting the integrity and stability of the tubular fabric. (2) failure to achieve continuous variation of the diameter. (3) should not be applied to weaving tapered fabrics of wider taper angle,which is for some special purpose, such as endovascular graft exclusion(EVGE). To this end, we proposed a new tapered artificial blood vessel which can solve the problems above, and the design principles and fabrication techniques of it were studied in follows.

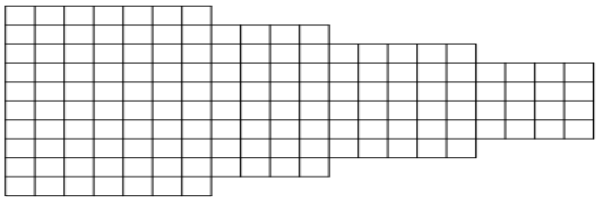
Design principle of a new tapered artificial blood vessels

The essence of weaving tapered tubular fabric is changing fabric width in the weaving process.

$$M = P_j \times W \quad (1)$$

M is the ends in warp of the tubular fabric; P_j is the warp density; W is the fabric width

According to Eq.1,we can see that there are two ways to changing fabric width to get tapered tubular fabric: (1) To maintain warp density unchanged, change ends in warp in the weaving process(Fig.1(a)); (2) to keep the same ends in warp, vary warp density in the weaving process (Fig.1(b)).



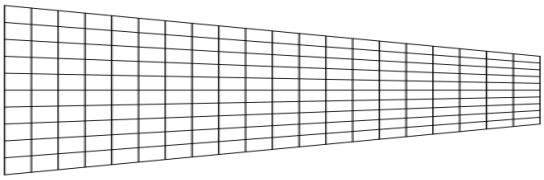


Fig. 1(a) Method of ends in warp changed Fig. 1(b) Method of warp density changed

Fig. 1 Schematic diagram of tapered artificial vessels weaving

Using method one, ends in warp changed method, in the weaving process, yarns should be added or reduced in correspondence with the increase or decrease of the fabric diameter. The disadvantages of this method has been described above.

Based on method 2, this paper proposeed a new tapered artificial blood vessel, its design principle is: in the weaving process, maintain the same ends in warp and vary warp density to achieve changing the diameter of fabric (Fig.1(b)). In the weaving process, the ends in warp keeps the same, and don't need to reduce or add yarns. Increasing the warp density can decreasing the diameter of tube; Decreasing the warp density can increasing the diameter of tube. The tapered artificial blood vessel woven got by using this method, is perfect and no burr at the edges. This method ensure the integrity and continuity of the tube.

Modification of the equipment

The key design principle of the new tapered artificial blood vessel is how to change warp density in the weaving process. The role of traditional reed on the conventional weaving loom is to fight the weft to the cloth fell and to determine the density and width of the fabric. The space between dents of conventional reed is fixed. In the weaving process, dents per inch is fixed, so the warp density remain the same. Therefore, to chang warp density in the weaving process, the conventional reed must be replaced by a special reed which can change dent spacing in the weaving process. The essence of weaving tapered tubular fabric is changing fabric width in the weaving process.

Design of a special fan-shaped reed. The subject design a special fan-shaped reed(Fig.2), which can satisfy the demand above. The more upper of the reed, the more lower count of reed. The more lower of the reed, the more greater count of reed. The middle reed count is linear change. When the reed fight to the cloth fell, the relative position of the special fan-shaped reed and the cloth fell determines the weaving warp density. In case of the same ends per dent, the different relative position of the special fan-shaped reed and the cloth fell lead to different density. The contact of reed and the cloth fell at the more upper of the reed, the more greater reed count, the more lower fabric width, the more lower diameter of the artificial blood vessels; contact at the more lower of the reed, the more lower reed count, the more greater fabric width, the more greater diameter of the artificial blood vessels.

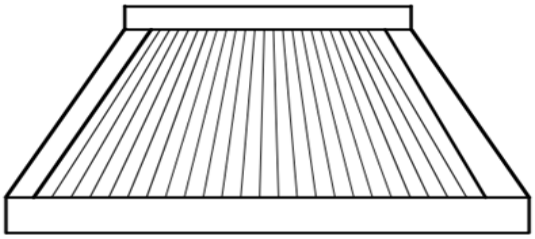


Fig. 2 Appearance of the specialc fan-shaped reed

Front rest lifting device. Changing warp density can be achieved by using a special fan-shaped reeds. But to vary the relative position of the special fan-shaped reed and the cloth fell, the project has designed a special fan-shaped reeds and the matching front rest lifting device. During the weaving process, cloth fell can be left by the front rest lifting device, and the special reed keep still at the same time, then the relative position of reed and the cloth fell change.

Fig.3 is the diagram of the special fan-shaped reed compatible with matching front rest lifting devices to change warp density. With lifting front rest (D→E), the location of the cloth fell is up. So when the reed beat up, the relative height of the special fan and cloth fell are different (F→G). When the contact is at the top of the reed(G), the density is greater. When the contact is at the bottom of the reed(F), the density is lower. So as to achieve changing the warp density in the weaving process.

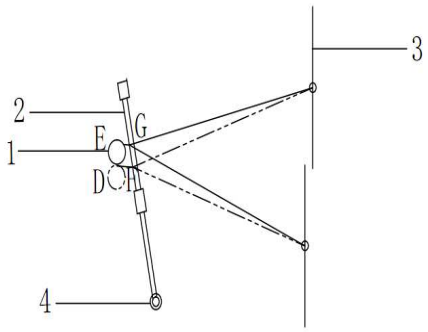


Fig. 3 Schematic diagram of warp density-changed weaving

1 is the front rest of the loom; 2 is the special fan-shaped reed; 3 is the heddle; 4 is the laid.

Institutional rationality validation

The subject had completed the hardware modification of the loom, and the test weaving of the tapered artificial blood vessels was followed. The project designed parameters of tapered artificial blood vessel on the machine, and carried out the weaving on the rigid rapier sampling weaving machine, and the sample had gotton as showed in Fig.4. From the weaving process and the sample obtained, we can achieve the following results:

1) the edges of the tapered tubular fabric is smooth, no burr.
2) the diameter variation of the tapered tubular fabric is continuous.
3) The system can weave tapered tubular fabric with larger taper angle and can achieve dramatic variation in diameter of tubular fabric so as to expand the application.

The conclusions above and samples obtained demonstrate that the research on tapered artificial blood vessel is successful.



Fig. 4 Sample graph of tapered artificial blood vessels

Conclusion

Because the traditional shuttle looms and the rigid rapier sampling weaving machine before modification are unable to meet the request of tapered artificial blood vessels. The paper design a special fan-shaped reed and matching front rest lifting device to change the warp density. After modification in the loom, tapered artificial blood vessels was test weaved on the machine. The experimental process and the results show that the improved rigid rapier sampling looms meet to the requirements of tapered vascular products, and the modification is effective and successful.

References

[1] Halima Kerdjoudj, PHD,* Nicolas Berthelemy, PHD,* Simon Rinckenbach, MD, PHD. Small Vessel Replacement by Human Umbilical Arteries With Polyelectrolyte Film-Treated Arteries. Applied Mathematics and Mechanics, Vol. 52, No. 19, 2008.

[2] Renjing Cen, Zhedong Tan, Zhengzong Chen. the coupled motion of wall and blood flow in the entrance region of the variable diameter blood vessel. Applied Mathematics and Mechanics, Vol. 16, No. 15, 1995. In Chinese.

[3] Chan Qin, Zhirun Yuan, Xiaoming Wu, Fuxiang Wu, Changqu Ru, Rock. The measuring of simulating the fluctuation speed in variable diameter blood vessels. Jinan University (Natural Science), Vol. 12, No. 9, 1997. Green: High Efficiency Silicon Solar Cells (Trans Tech Publications, Switzerland 1987). In Chinese.

© (2011) Trans Tech Publications, Switzerland
doi:10.4028/www.scientific.net/AMR.331.516

Test Reliability of Impurity Parameters of Uster AFIS

Pengzi Sun[a], Jipeng Cao

Eastern Liaoning University, No.325, Wenhua Road,Yuanbao District, Dandong, 118003, China

[a]kyc3@163.com

Keywords: Uster AFIS, total impurity, impurity size, dust; trash, VFM, reliable test time

Abstract. This paper presents test reliablity of Uster AFIS for impurity test by calculating the Reliable Test Time (hereinafter referred to as RTT) and CV% of test results. The CV% value of test results of impurity-related parameters in card sliver obtained in 8 experiments totally with 313 different plans were calculated. By statistical analysis method, the reliable test time of AFIS for some impurity-related parameters was estimated. It is concluded that the impurity result obtained by 10-time tests with AFIS was inaccurate. The reasons for this are that the sample weight is too small, the impurity is unevenly distributed and the impurity in card sliver may have some loss in the manually-sampling process.

Introduction

Advanced Fiber Information System (AFIS) single fiber tester of USTER Company is an instrument to test length, neps and impurities of raw cotton and semi-finished products. Because it can make fast and all-round test on the quality of raw cotton and semi-finished products, it is widely used in quality control and related theoretical study [1, 2]. Townes et al. [3] studied the test correlation between AFIS and Shirley Analyzer and High Volume Inspection (HVI) Video Trash Meter. They thought that AFIS had good correlation with other instruments. Schenek [4] described the basic test principle of AFIS impurity module and studied the change of impurities in the spinning process with it. Williams [5] compared the test principle, sample size and test speed of HVI, MDTA-3 and AFIS-T and analyzed the advantages and disadvantages of these instruments. They proposed that AFIS impurity module could not measure impurities in the waste. Yankey et al. [6] introduced test time of different items of AFIS, of which 3 times for neps and 5 times for impurities. The test times for different items recommended by USTER Company to Chinese users are listed in Table 1. Schlichter et al. [7] tested neps and impurities of raw materials with AFIS under the conditions stipulated by Uster when they studied the adaptability between high performance cleaner and card and different impurity-containing raw materials. Schenek [1] mentioned that the variability was higher in testing impurities of cotton fiber with HVI, and he did not discuss the issue of AFIS impurity test. By experiments, Xu Jie [8] systematically studied the change of neps and impurities in raw cotton and semi-finished spinning products with AFIS. He considered that the number of dust and trash would usually be reduced with blowing-carding process. But sometimes their number could be increased. The reason for this he thought was due to the uneven distribution of impurities in raw cotton and the inadequate weight of test sample. He suggested that the test times should be increased when using AFIS to test impurities, but he did not give appropriate test times. Farber [9] studied the relationship between neps and impurities in semi-finished product and the faults in ring yarns with AFIS and Uster Tester UT-3. Reference [10] indicated that trash and dust in cotton could be measured objectively with AFIS. Peters et al. [11] thought that the number of trash and dust in yarns could be compared with the results of AFIS. He also gave the change curve of total impurities in the spinning process (tested with AFIS). With a microscope and AFIS, Karin et al. [12] studied the change of neps, seed coat fragments and non-seed impurities in cotton processing. He thought that combing process could effectively remove non-seed impurities. Anthony et al. [13] studied the influence of cotton varieties and gin machinery on trash particles and evaluated the particle sizes of the foreign matter in the ginned and cleaned lint

with AFIS. Frydrych et al. [2] made comments on the application of AFIS to the comparison of cotton characteristics from different areas, the change of the number and size in the process of spinning, the relationship between neps of card sliver and that of yarn, as well as the variety in testing impurity number, but they did not discuss impurity test times of AFIS. Siddaiah et al. [14] studied impurity test of different kinds of cotton with Camera and Scanner and AFIS, and made comments on their correlation degree. Noticeably, 3-time tests were adopted for impurity test with AFIS. Lewandowski et al. [15] indicated the performance of the opening and cleaning line, of cards, and combers can be substantially enhanced by analyzing the input/output relationship of fiber length and short fiber content, neps, and trash with AFIS.

From above description we can see that all of the references did not involve the Reliable Test Times (hereinafter referred to as RTT) of AFIS for impurity test. Therefore, we ananlyzed the test results of impurity-related parameters of 8 experiments totally with 313 different plans, and calculated the RTT of these parameters under different fluctuation degree by statistical analysis.

Table 1 Sample test times recommended by AFIS

Test item	Sample number	Sample quality or number of fibers
Nep, etc.	Raw cotton, cotton lap: 5; cotton sliver:6	0.5g
Fiber length and maturity, etc.	5	0.5g，3000
Trash and dust, etc.	10	0.5g
Integrated test	10	0.5g，3000

Materials and Methods

Seven kinds of raw cotton were used in the experiments. Details of each experiment are listed in Table 2. The AFIS test results of raw material used in each experiment are shown in Table 3.

Table 2 Details of each experiment and occurrence frequency of “0 Trash”

Experiment	Materials	Plans of each experiment	Plan sequence number and corresponding figures	Test times of each plan (total test times)	Time of “0 Trash”	Percentage of “0 Trash”
1	Liaoning Heishan cotton	64	1-64 (Figures1-5)	8 (512)	55	10.7
2	Xinjiang cotton Grade 2	54	1-54 (Figures 6-10)	10 (540)	92	17.0
3	Xinjiang cotton 229	57	55-111 (Figures 6-10)	10 (570)	88	15.4
4	Xinjiang cotton 129	35	112-146 (Figures 6-10)	10 (350)	100	28.6
5	Xinjiang cotton 129B	50	147-196 (Figures 6-10)	10 (500)	38	7.6
6	Xinjiang cotton (of which Grade 129 is 90% and Grade 229 is 10%)	15	197-211 (Figures 6-10)	10 (150)	0	0
7	Xinjiang cotton and Shandong cotton	14	212-225 (Figures 6-10)	10 (140)	16	11.4
8	The same with the sixth experiment	24	1-24 (Figures 11-15)	30 (720)	1	0.1

Table 3 Test results of raw cotton in each experiment with AFIS

Experiment	L(n) (mm)	SFC(n) %<12.7	5% (mm)	Nep (cnt/g)	SCN (cnt/g)	Total (cnt/g)	Mean size	Dust (cnt/g)	Trash (cnt/g)	VFM (%)
1	23.8	14.0	35.8	146	28	237	305	201	36	0.83
2	22.0	20.3	35.9	279	32	221	300	193	29	0.72
3	20.9	19.9	33.6	265	23	211	292	188	23	0.58
4	20.0	25.3	34.2	237	29	238	282	206	31	0.51
5	21.8	20.6	36.0	192	22	193	340	158	34	0.80
6	20.9	21.7	35.3	299	12	204	332	170	34	0.89
7	21.5	20.4	35.3	277	21	146	337	119	28	0.57

The experimental process flow was that, A002 bale plucker→A006B mixer→A034 step opener→A036 porcupine opener→A092 tandem feeder→A076A single beater lap machine→A186F carding machine

Eight experiments were done under following conditions. The first experiment was carried out to study the effect of pin taker-in and saw-tooth taker-in, the suction volume of web cleaner and the forms of pre-carding, etc. on the quality of card slivers; the second experiment was done mainly to comparatively study for the carding performance of pin taker-in and saw-tooth taker-in, pin carding plate and saw-tooth carding plate; the third experiment was done mainly to compare the effect of card back stationary flat gauge, web cleaner mote knife gauge on the card sliver quality; the fourth experiment was done to study the effect of pin taker-in and saw-tooth taker-in, feed plate gauge on the quality of card slivers; the fifth experiment was to study the different effect of web cleaner, web cleaner mote knife gauge, pin carding plate and saw-tooth carding plate on card sliver quality; the sixth experiment studied the effect of card taker-in speed and the number of back stationary flat on the quality of card sliver; the seventh experiment was to compare the function of pin carding plate and saw-tooth carding plate; and the eighth experiment was conducted to study the effect of different heel-toe difference of movable flat on the quality of card sliver.

The above AFIS testing on the card slivers were all carried on under the stipulated conditions in the laboratory.

Results and Discussion

Table 4 shows the range and mean of CV% value of five impurity-related parameters in Experiment 2-7. Table 5 shows the range and mean of CV% value of five impurity-related parameters in Experiment 1 and Experiment 8.

Table 4 The statistics of CV% value range and mean value of five impurity-related parameters in Experiment 2-7

Experiment	Total	Mean size	Dust	Trash	VFM (%)
2	20.8-60.3 (35.6)	13.3-68.8 (26.4)	19.6-71.1 (38.3)	40.5-141 (74.0)	21.3-111.0 (61.4)
3	16.1-73.5 (39.5)	12.1-48.1 (29.2)	14.0-79.9 (42.9)	33.9-135.5 (77.8)	34.6-113.4 (67.7)
4	22.3-74.7 (43.0)	16.1-52.6 (27.8)	22.1-83.9 (45.8)	51.9-140.5 (89.4)	38.2-123.6 (67.3)
5	18.8-71.9 (34.0)	11.5-39.8 (20.6)	14.4-77.1 (36.6)	32.1-90.8 (60.8)	28.4-103.5 (54.4)
6	17.6-50.0 (29.8)	9.9-24.0 (17.4)	17.4-58.9 (34.3)	26.9-73.6 (43.3)	28.5-48.2 (37.8)
7	24.0-59.1 (39.4)	18.5-44.3 (28.5)	24.5-68.5 (44.0)	35.1-111.0 (71.6)	41.1-92.6 (65.0)
Total mean value	36.9	25.0	40.3	69.5	58.9

Table 5 The statistics of CV% value range and mean value of five impurity-related parameters in Experiment 1 and Experiment 8

Experiment	Total	Mean size	Dust	Trash	VFM
1	18.9-73.7 (38.8)	11.6-49.7 (28.7)	15.5-81.3 (42.4)	31.4-120.6 (69.4)	29.3-108.2 (68.2)
8	19.3-39.5 （28.9）	10.5-23.3 （16.4）	21.2-42.6 （31.4）	28-60.2 （44.8）	26.5-67.2 （44.3）

The distributions of CV% value of impurity-related parameters in 8 experiments were shown on Figures 1-15. The CV% value fluctuation of impurity-related parameters test results of the first experiment was shown in Figures 1-5; that of the second to the seventh experiments was shown on Figures 6-10; that of the eighth experiment was shown on Figures 11-15.

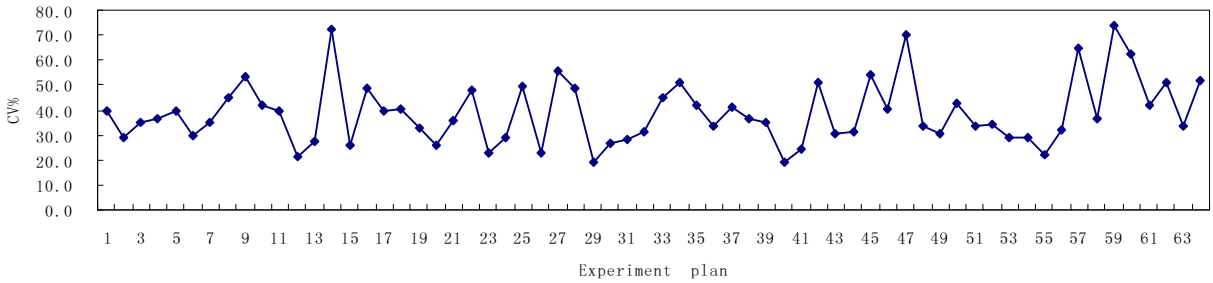


Fig.1 CV% value distribution of total dust and trash test results in the first experiment

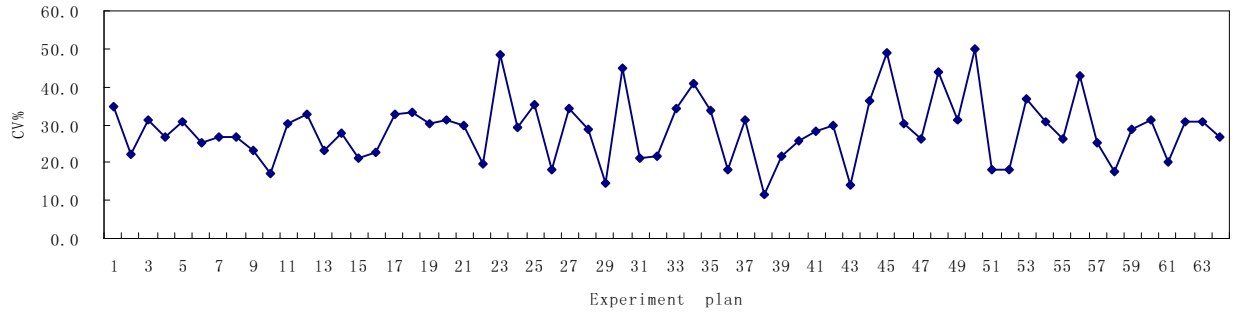


Fig.2 CV% value distribution of mean size of impurity test results in the first experiment

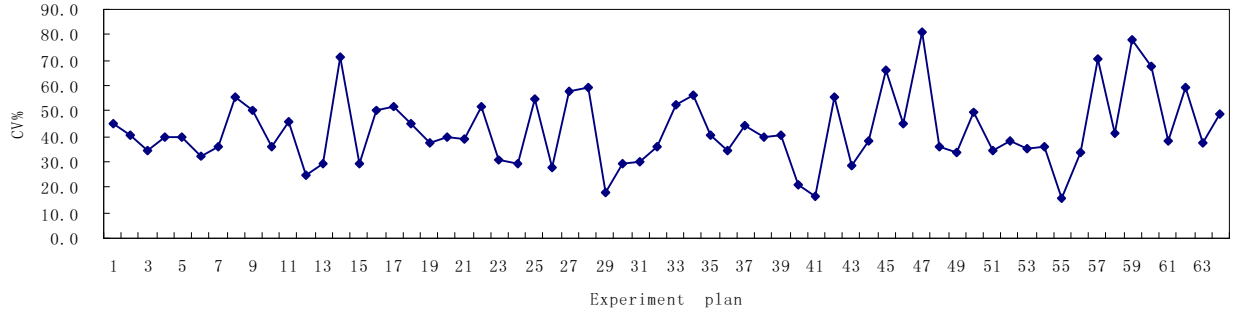


Fig.3 CV% value distribution of dust content test results in the first experiment

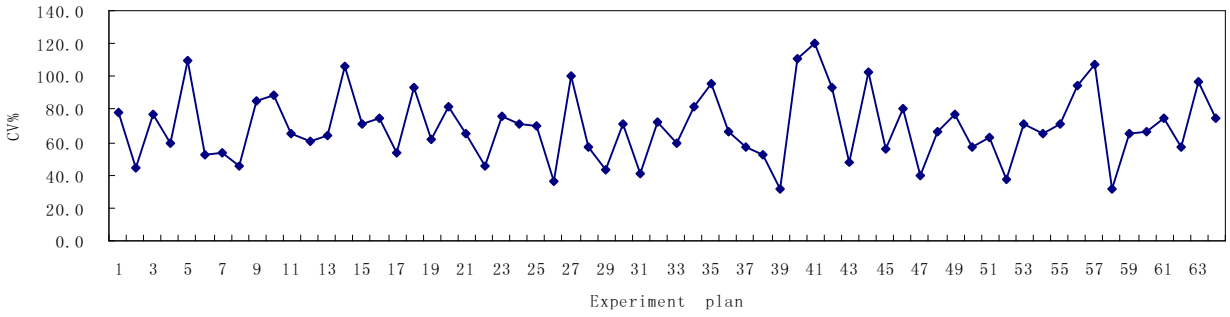


Fig.4 CV% value distribution of trash content test results in the first experiment

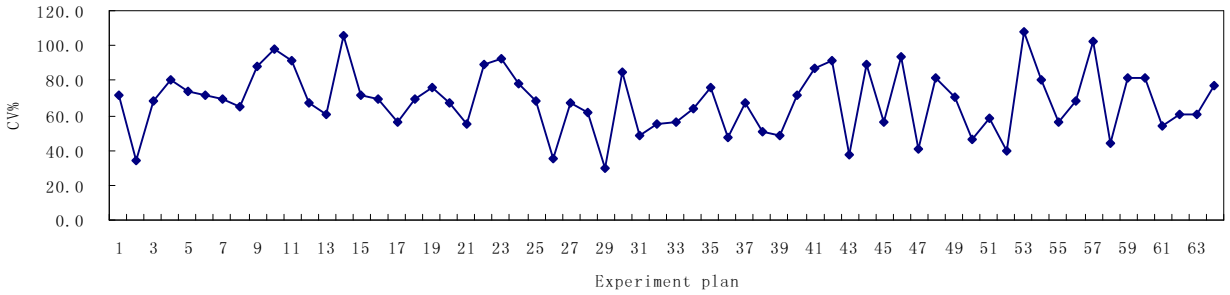


Fig.5 CV% value distribution of VFM content test results in the first experiment

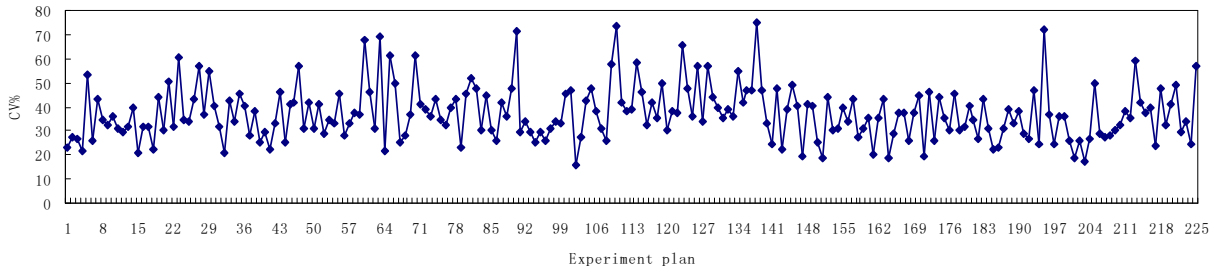


Fig.6 CV% value distribution of total of dust and trash test results in the second to the seventh experiments

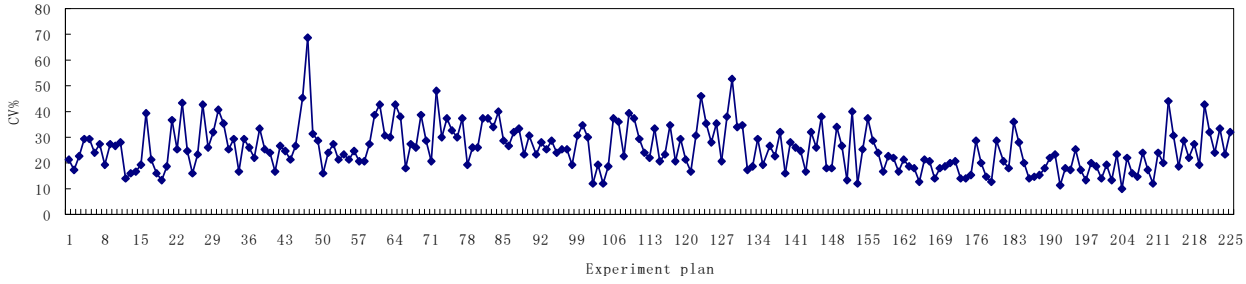


Fig.7 CV% value distribution of mean size of impurity test results in the second to the seventh experiments

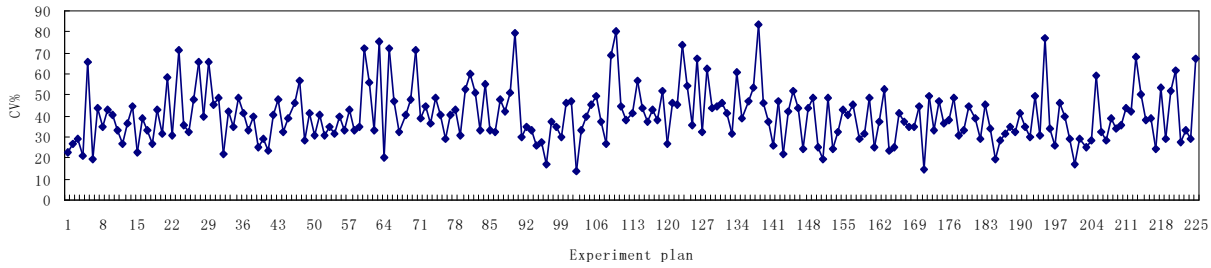


Fig.8 CV% value distribution of dust content test results in the second to the seventh experiments

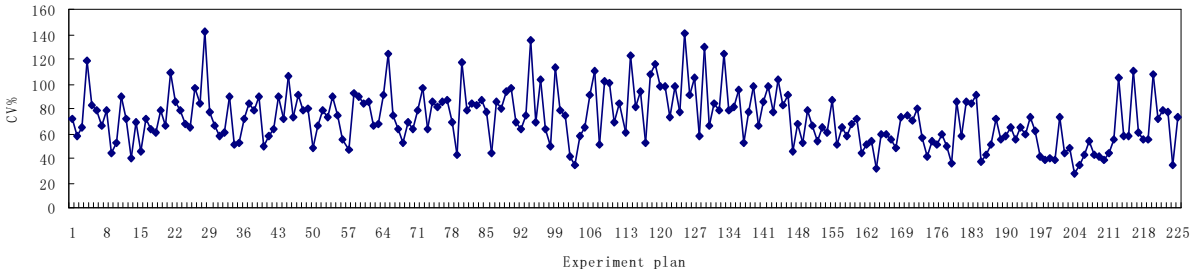


Fig.9 CV% value distribution of trash content test results in the second to the seventh experiments

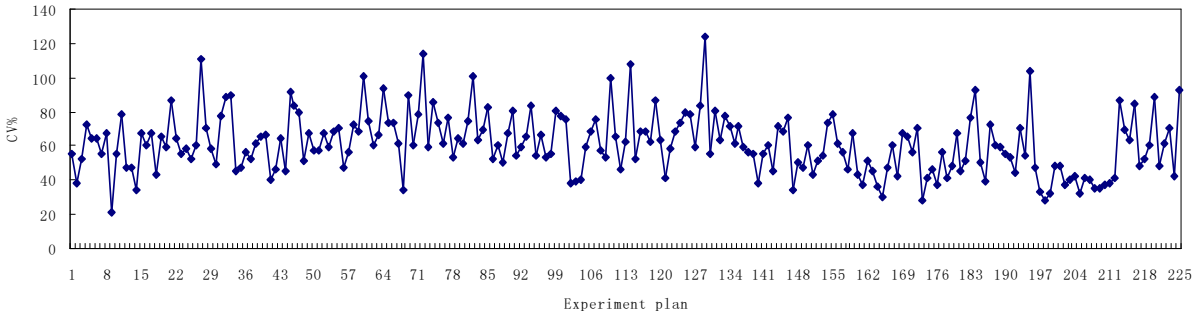


Fig.10 CV% value distribution of VFM content test results in the second to the seventh experiments

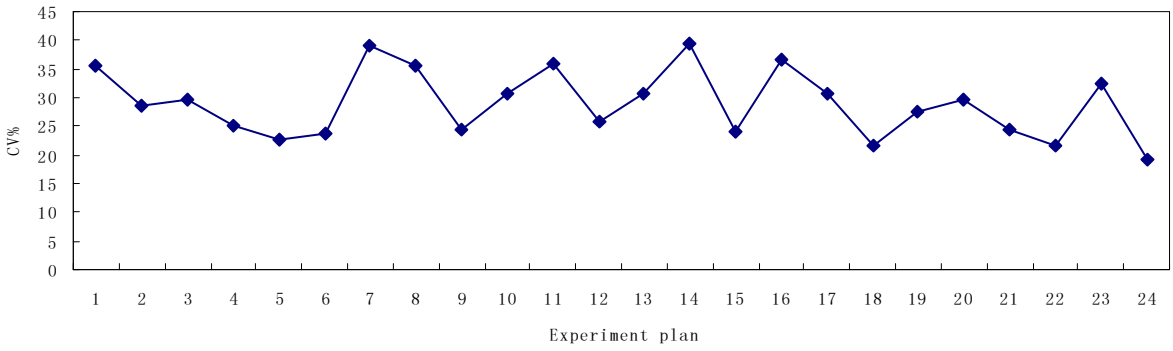


Fig.11 CV% value distribution of total of dust and trash test results in the eighth experiment

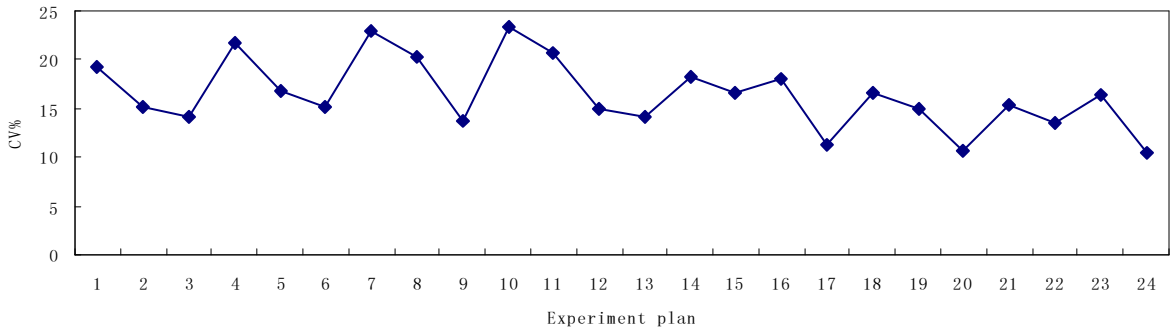


Fig.12 CV% value distribution of mean size of impurity test results in the eighth experiment

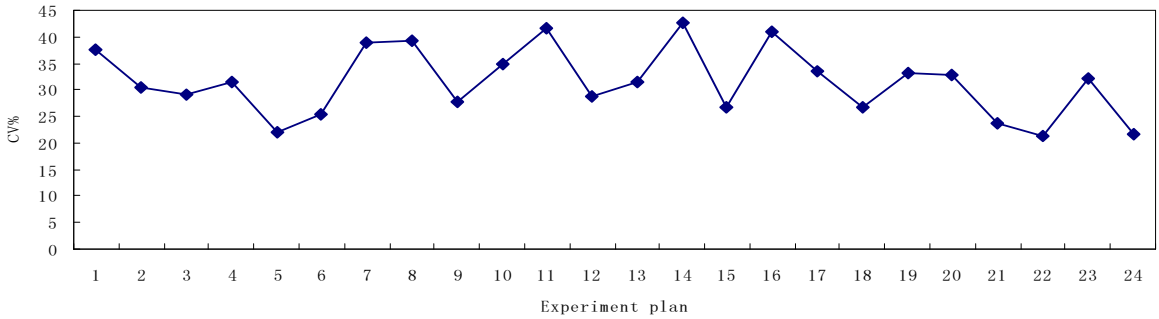


Fig.13 CV% value distribution of dust content test results in the eighth experiment

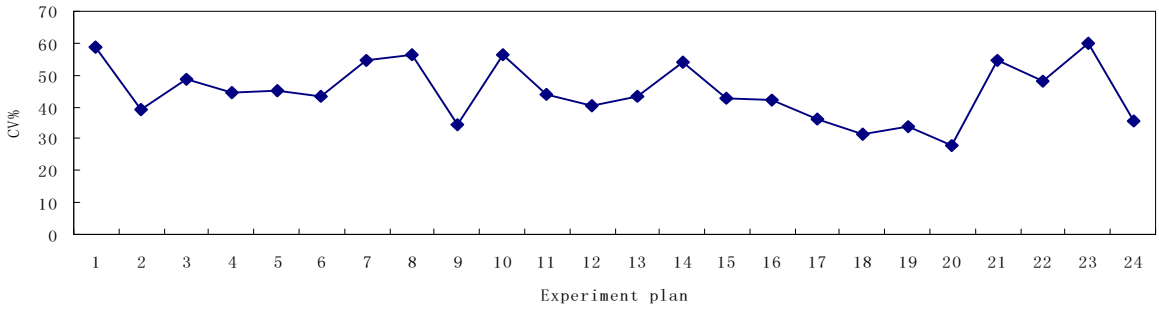


Fig.14 CV% value distribution of trash content test results in the eighth experiment

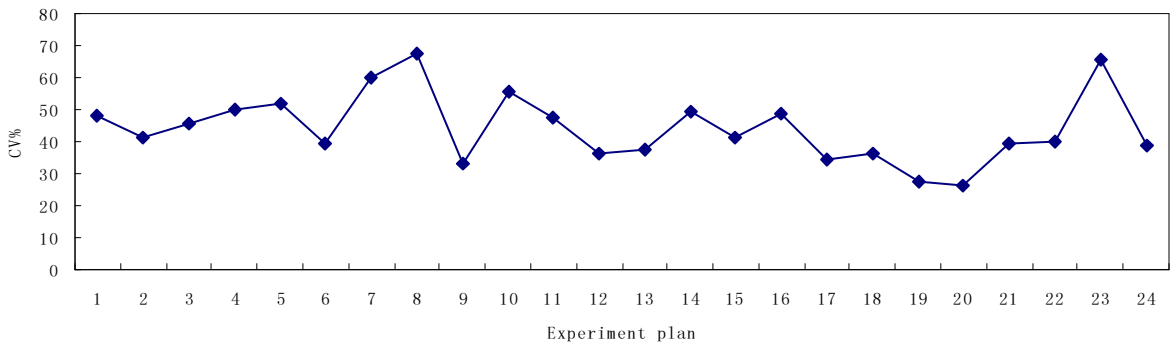


Fig.15 CV% value distribution of VFM content test results in the eighth experiment

Analysis on CV% value. As shown in Tables 4-5, in the first experiment (8 sampls were tested in each plan), the CV% value of total dust and trash is between 18.9 and 73.7 and the mean value is 38.8. In the second to the seventh experiments (different materials and carding conditions were adopted), the CV% value of total dust and trash (10 sampls were tested in each plan) is between 16.1 and 74.7 and the mean value is 36.9. In the eighth experiment, the CV% value of that (30 sampls were tested in each plan) is between 19.3 and 39.5 and the mean value is 28.9. It indicates that CV% value tend to decrease with the increase of test times, and we can almost draw the same conclusion by analyzing other impurity-related parameters.

From Tables 4-5, we can observe that, (1) the range and mean of CV% value varies in different experiments, which show that experiment materials (especially uneven distribution of imurity) and process conditions have some effect on test results. Thus, to evaluate the change of impurities in card sliver with unchangeable and fewer test times may be improper. Therefore, we suggest that, if a user finds that the CV% value is too big in testing, the test times should correspondingly increased so as to ensure that test results are more accurate; (2) the CV% values of impurity-related parameters are also different, and the order of these values from big to small is trash, VFM, dust, total and mean size with obvious regularity; (3) when testing for 30 times, the mean CV% values of the trash and VFM parameters are still more than 40%, while the mean CV% value of the dust parameter is also more than 30%, which shows that adopting 30-time test on these parameters with AFIS is quite inaccurate.

By comparing the CV% values between impurity-related parameters, length-related parameters (Table 6) and nep-related parameters (Table 7) of each experiment, we can see that CV% values of impurity-related parameters are much bigger than those of the length-related parameters and nep-related parameters (the CV% value of SCN is also bigger, which shows that the fluctuation degree of test results on SCN is also big), which also indicates that the fluctuation is bigger in testing impurity-related parameters.

Table 6 CV% value range and mean of length parameters, etc. test results in 8 experiments

Experiment	L(w)	UQL(w)	SFC(w)	L(n)	SFC(n)	5.0%	IFC
1	0.3-1.3 (0.8)	0.2-1.0 (0.6)	2.3-14.2 (8.4)	0.5-2.1 (1.3)	3.1-12.0 (7.2)	0.3-1.1 (0.7)	3.4-23.4 (8.4)
2	0.9-2.6 (1.5)	0.6-1.9 (1.2)	4.6-21.5 (10.4)	1.1-4.6 (2.3)	4.2-19.6 (9.3)	0.5-5.0 (1.3)	2.5-13.2 (7.2)
3	0.9-2.8 (1.7)	0.7-2.1 (1.4)	4.0-19.0 (10.2)	1.4-4.9 (2.5)	4.3-16.4 (8.9)	0.8-2.5 (1.4)	3.2-12.1 (7.3)
4	0.9-2.3 (1.7)	0.6-1.8 (1.3)	4.9-14.3 (9.6)	1.4-3.3 (2.5)	4.3-11.8 (7.9)	0.8-1.8 (1.3)	3.6-11.4 (6.9)
5	1.1-2.4 (1.7)	0.6-2.0 (1.3)	6.1-14.2 (9.9)	1.8-3.5 (2.6)	4.8-12.0 (7.9)	0.6-1.8 (1.3)	4.6-11.5 (8.1)
6	0.7-2.1 (1.3)	0.6-1.1 (0.9)	4.3-15.4 (8.4)	0.9-3.8 (2.0)	3.1-12.3 (6.6)	0.8-1.3 (1.1)	4.8-13.9 (8.1)
7	1.0-2.0 (1.5)	0.7-2.1 (1.3)	5.8-15.4 (9.9)	1.4-3.4 (2.3)	5.4-13.5 (8.7)	0.5-1.8 (1.2)	4.7-11.5 (7.5)
8	1.2-2.1 (1.5)	0.9-1.4 (1.1)	5.8-18.4 (9.0)	1.9-4.3 (2.5)	4.4-14.3 (7.0)	0.8-1.4 (1.1)	5.5-25.1 (8.4)

Table 7 CV% value range and mean of nep and SCN content test results in 8 experiments

Experiment	Nep content	SCN content
1	8.4-31.8 (15.7)	11.6-65.3 (40.4)
2	9.1-27.0 (16.1)	15.8-50.8 (30.6)
3	7.4-39.3 (19.2)	9.4-68.5 (37.8)
4	8.5-24.6 (16.9)	27.5-76.8 (49.9)
5	10.8-53.9 (22.8)	25.2-73.5 (46.2)
6	8.1-21.9 (14.9)	17.0-49.4 (34.2)
7	7.1-21.9 (16.4)	21.9-56.9 (39.9)
8	11.0-25.2 (15.9)	25.7-50.9 (38.2)

Analyses of the RTT. First of all, a 3σ principle verification was done on the 24-group test results of the eighth experiment and the verification results show that test results conform to the normal distribution.

On this basis, the statistic value $\bar{x} = \sum_{i=1}^{n} x_i$ is introduced, by which the value of RTT, n, can be estimated by fluctuation scope of given permission measurement value in two steps according to $\bar{x} \sim N\left(\mu, \frac{\sigma^2}{n}\right)$.

(1) Estimating the value of σ^2

Since the statistic $S^2 = \frac{1}{n-1}\sum_{i=1}^{n}(x_i - \bar{x})^2$ is the unbiased estimation of random variable x variance , we can use S^2 to estimate σ^2.

(2) Using $\bar{x} \sim N\left(\mu, \frac{\sigma^2}{n}\right)$, for our given permission fluctuation degree ε and given level α, we can calculate the minimum value n according to

$$P\left(|\bar{x} - \mu| > \varepsilon\right) = P\left(\left|\frac{\bar{x} - \mu}{\sigma/\sqrt{n}}\right| > \frac{\varepsilon}{\sigma}\sqrt{n}\right) = 2\left(1 - \phi\left(\frac{\varepsilon}{\sigma}\sqrt{n}\right)\right) = \alpha \tag{1}$$

If $\alpha = 0.05$, then $\frac{\varepsilon}{\sigma}\sqrt{n} = 1.96$, that is:

$$n = \left[\frac{\sigma^2}{\varepsilon^2} \cdot 1.96^2\right] + 1 \tag{2}$$

Above formulas mean that, if we measure an object, the measurement value that is gotten by the average value of n times will certainly fluctuate for different experiment. Then for given ε, which is the permissible fluctuation scope, the value of n can be determined by calculation. The above equation has given the calculating formula of n, and with such an n, the probability that the difference between $\bar{x}$ and the true μ is bigger than ε will be smaller than the given level a.

This shows that the smaller is the ε, the bigger is the n, which means the test results approach more closely to the true value; and contrariwise, it means the precision of test results is lower. In this paper, we take $\mu/5$, $\mu/10$ and $\mu/15$, respectively for ε to calculate the RTT of the eighth experiment, and calculate μ and σ^2 with the average value and variance of 30-time test data per plan, respectively. Concrete calculation results are shown in tables 8-10.

Table 8 Calculated results of RTT of the 8th experiment ($\varepsilon = \mu/5$)

Plan	Total	Mean Size	Dust	Trash	VFM	Plan	Total	Mean Size	Dust	Trash	VFM
1	13	4	14	33	23	13	10	2	10	18	14
2	8	3	9	15	17	14	16	4	18	29	24
3	9	2	9	23	20	15	6	3	7	18	17
4	7	5	10	19	25	16	13	4	16	17	23
5	5	3	5	20	26	17	10	2	11	13	12
6	6	3	7	19	15	18	5	3	7	10	13
7	15	6	15	29	35	19	8	3	11	12	8
8	13	4	15	31	44	20	9	2	11	8	7
9	6	2	8	12	11	21	6	3	6	29	16
10	10	6	12	31	31	22	5	2	5	23	16
11	13	5	17	19	22	23	11	3	10	35	42
12	7	3	8	16	13	24	4	2	5	13	15

Table 9 Calculated results of RTT of the 8th experiment ($\varepsilon = \mu/10$)

Plan	Total	Mean Size	Dust	Trash	VFM	Plan	Total	Mean Size	Dust	Trash	VFM
1	49	15	55	132	90	13	37	8	38	72	55
2	32	9	36	60	67	14	61	13	70	113	93
3	35	8	33	91	80	15	22	11	28	71	66
4	25	19	38	76	97	16	52	13	64	68	92
5	20	11	19	29	104	17	37	5	44	51	47
6	22	9	25	73	60	18	18	11	28	38	50
7	59	21	59	115	138	19	29	9	43	45	30
8	49	16	59	123	174	20	34	5	42	31	28
9	23	8	30	46	43	21	23	10	22	115	61
10	37	21	47	122	121	22	18	8	18	89	62
11	50	17	67	75	88	23	41	11	40	140	166
12	26	9	32	63	52	24	15	5	18	49	59

Table 10 Calculated results of RTT of the 8th experiment ($\varepsilon = \mu/15$)

Plan	Total	Mean Size	Dust	Trash	VFM	Plan	Total	Mean Size	Dust	Trash	VFM
1	113	37	150	168	196	13	83	18	86	161	123
2	71	21	80	134	150	14	136	29	157	254	209
3	77	18	73	204	180	15	50	24	62	160	147
4	56	41	86	170	218	16	117	29	144	153	205
5	45	25	43	178	234	17	82	11	97	114	104
6	49	20	57	164	134	18	41	24	62	84	112
7	132	46	132	258	309	19	65	20	96	101	66
8	109	36	133	276	391	20	76	10	94	68	61
9	52	17	67	103	95	21	52	21	49	258	136
10	82	47	104	274	271	22	41	17	39	200	139
11	113	37	150	168	196	23	91	23	89	314	373
12	58	20	72	140	116	24	33	10	41	111	131

According to the calculated RTT shown in Tables 8-10 under different ε values, when the permitted fluctuation degree ε is taken to be μ / 5 which means a lower test precision is required, for five parameters of total, mean size, dust, trash and VFM, the values of RTT range from 4 to 16, 2 to 6, 5 to 18, 8 to 35 and 7 to 44 respectively, and the averages of 24-group data are 9, 3, 10, 21 and 20 respectively; when the permitted fluctuation degree ε is taken to be μ / 10, for five parameters of total, mean size, dust, trash and VFM, the values of RTT range from 15 to 61, 5 to 21, 18 to 70, 29 to 140 and 28 to 174 respectively, and the averages of 24-group data are 34, 11, 40, 79 and 80 respectively; when the permitted fluctuation degree ε is taken to be μ / 15, for five parameters of total, mean size, dust, trash and VFM, the values of RTT range from 33 to 136, 10 to 47, 39 to 157, 68 to 314 and 61 to 391 respectively, and the averages of 24-group data are 76, 25, 90, 176 and 179 respectively.

According to the above results, it can be seen that (1) in the impurity-related parameters, the order of the RTT from big to small is VFM, trash, dust, total and mean size, which is almost consistent with the CV% value arrangement of them in the eighth experiment; (2) the RTT for trash test parameter is bigger, which has relation to uneven distribution of trash in card slivers. The statistical results show that in eight experiments, the highest percentage of "0 trash" is 28.6%, the lowest is 0, and the average is 11.4%, thereby indicating the quite uneven distribution of trash in card sliver. This is a very important reason to increase the sample weight and test times for testing impurity of card sliver.

Reasons for big fluctuation on impurity-related parameters. Based on the above analysis we can see that, when AFIS is used to test impurity-related parameters, the results of 10-time test are inaccurate. The reasons for the big fluctuation of test results in impurity-related parameters may be (1) the impurity distribution in raw cotton from different cotton-producing regions is uneven [16]; (2) process technology also has certain effect on impurity distribution; (3) the distribution of trash is uneven, which can be proved by the fact that the average percentage of "0 trash" is 11.4%; (4) some impurities are likely to be lost when samples are selected and tidied manually; (5)in comparison with nep test results by aQura and AFIS [17], we can see that the small sample weight is a basic reason resulting in bigger variability of nep test results (the sample weight of AFIS is 0.5g and that of aQura is 10g). Therefore, we can conclude that the reason resulting in inaccurate test results on impurity with AFIS has relation to the small sample weight. Similarly, it can be thought that 10-time for AFIS impurity test is also one of the reasons for inaccurate test results.

Conclusions

When testing impurities in card sliver with AFIS, the results of a 10-time test are quite inaccurate.

The factors lead to unstable test results of impurities with AFIS are (1) the effect of materials and process technology; (2) uneven distribution of trash; (3) the loss of impurities caused by manual sampling in AFIS test; (4) too small sample weight and insufficient test times.

References

[1] Anton Schenek: International Textile Bulletin (Yarn and Fabric), Vol. 36 (1994), p. 19

[2] I. Frydrych, M. Matusiak: FIBRES & TEXTILES in Eastern Europe. Vol. 7/9(2002), p. 35

[3] M.G. Towners, J. C. Baldwin, F. M. Shofner, "*Comparison of AFIS-T counting and sizing of trash and dust particles with other methods,"* in the Beltwide Cotton Production Conference, 1992.

[4] A. Schenek, A. Schleth, M.G. Townes, et al.: Textil Praxis International, Vol. 48 (1993), p. 379

[5] G. F. Williams: Textile World, Vol. 143 (1993), p. 66

[6] J. M. Yankey, P. C. Jones, "*Multidata Advanced Fiber Information System (AFIS),"* in the Beltwide Cotton Production Conference, 1993.

[7] Stefan Schlichter, Andreas Kuschel: International Textile Bulletin (Yarn and Fabric Forming), Vol. 37 (1995), p.74

[8] Xu Jie: Cotton Textile Technology, Vol. 23 (1995), p. 16 (In Chinese)

[9] C. Farber: Melliand Textilberichte, Vol. 77 (1996), p. 652

[10] U. E. Kechagia, F. P. Xanthopoulos, "*Factors affecting neps, dust, trash and total impurities in cotton,"* in the International Committee on Cotton Testing Methods, 1999.

[11] G. Peters, W. sÖll: Melliand International, Vol. 6(2000), p. 36

[12] R. Karin Jacobsen, Yaffal Grossman, You-Lo Hsieh, et al.: The Journal of Cotton Science, Vol. 5 (2001), p. 53

[13] Anthony, W. Stanley: Applied Engineering in Agriculture, Vol. 18 (2002), p. 183

[14] Siddaiah, Murali Park, Mesilla Hughs, et al., "*Comparison of Small Trash Measurements between Imagine Techbiques and AFIS,"* in the Beltwide Cotton Conferences: Cotton Quality Measurements Conference, 2005.

[15] Lewandowski, Stanislaw: Przeglad Wlokienniczy, Vol. 60 (2006), p. 21

[16] S.schlichter: *Textile Month*, Vol. 30 (1997), p. 25

[17] V.Srimnivason, M.Anbarasan: International Textile Bulletin, Vol. 45 (2003), p. 34

© (2011) Trans Tech Publications, Switzerland
doi:10.4028/www.scientific.net/AMR.331.528

Heart Move With Color--- Color Psychology and Textile Color Aesthetic

Xiao Yi

Academy of Fine Arts, Hunan First Normal University, Changsha, Hunan, 410002, China

imxiaoyiyi@yahoo.com.cn.

Keywords: Color Psychology, textiles, Color Aesthetic.

Abstract: Color psychology impacts on the textile color aesthetic. This article starts from the relations between the color psychology and the textile aesthetic to explore people's color psychology and analyze the effects of people's color psychology on the process of appreciating textile and color aesthetic. Thus, it will provide more references for textile color designing to cater for people's color psychological demands and enhance color aesthetic connotation.

Introduction

Textile products surface art beauty aesthetic features include beautiful models, colors and decorations. People will have different physical and psychological feelings facing with colors of different wavelengths, frequency and brightness. Textile color effects, that is, the direct aesthetic feeling hidden in indirect or inspiring aesthetic feelings, make textile arts are not only has a common aesthetic feeling of art but also have a unique color aesthetic appeal. This aesthetic appeal arouses people's inspiration and produces better expectations on the textile. Then in consuming the textile products, people develop an aesthetic pleasure. Look from textile consumption, material consumption patterns and spiritual consumption patterns coexist in the textile consumption. With the economy and textile technology development, people have more choices of the textiles and have more personalized pursues. Therefore, the impact of spiritual consumption patterns in the textiles seems particularly outstanding. This article starts from the relations between the color psychology and the textile aesthetic to analyze the effects of people's color psychology on the process of appreciating textile and color aesthetic. Thus, it will provide more references for textile color designing to cater for people's color psychological demands and enhance color aesthetic connotation.

Organization of the Text

2.1. Color Psychology Analysis

Color psychology mainly explores how the colors lead to a range of changes in people's consciousness, emotions, memory, thought, will and symbols through the visual stimulation of the human brain, and explores how people's accumulated color experience is changed into color psychology standard. Color psychology is one branch of modern color study, which mainly studies people's subjective color perception such as emotional color performance, color symbol, color imagine, etc. The color psychology has become one of the theories of analyze the textile vision factors.

2.1.1 The Characteristics of the Color Vision and its Particularity.

Color is a feeling which caused by objects reflect light that stimulate the human eye and then reflected in the visual center of brain. Color represents the factors of colors impact on vision through its wavelength, frequency, brightness and movement. Color is not purely has physical quantity, it also has the characteristics of psychological physical quantities and the characteristics of the color vision and particularity. The essential difference between color study and physics lies in, from the point of

view of the color study, people's physiological reaction is proportional to the wavelength of the light stimulation, rather than in proportional to the strength of light wave energy. Human eyes have different reactions toward light stimulation with the same light wave energy but different wavelengths. This light stimulation influences people's thought and the emotion. We need to test color effect presented in textile fabrics and understand the effects of specific textile color on people.

2.1.2 **Psychological Induction Caused by Color.**

Direct color physical induction develops into some kind of psychological experience is called direct psychological induction. Color has no specific emotion in essence, it is color identity that people's accumulated experience is given emotional symbolism meaning, and then forms people's mental feeling toward colors. According to the analysis of the color psychology, each color has some kind of heterogeneous relationship between some concrete object, abstract vocabulary and some scenes. In understanding colors, people will produce some associations, especially the associations toward social experience and personal experience. These associations have direct impact on psychology, thus making colors develop a psychological effect on the basis of "property".

2.1.3 The Color Psychological Standards

People will transform their accumulation of living and cultural experience into a group- consented color psychology standard. Color psychological standards change and redefined along with the time of conception update.

Such as Chinese and western culture lead to China honors yellow while the western culture honors blue because of the different natural background. Chinese culture mainly originated in the middle and lower Yellow River basin, which life and cultural production is closely linked with the land. In ancient five temples, five lines and five colors, the central is the yellow land. The yellow represents the central government, homeland. And yellow has been the royal color for textile products since the Han dynasty. While the western culture originated in the blue Aegean sea. Thus the blue is given the meaning of life and culture. The westerners view color blue as a symbol of noble. However, yellow in western culture has a derogatory sense. This cultural experienced color psychological standard becomes the social level standard for textile color for people to comply with. And with the diverse modern social cultural exchanges, the color view transforms from regional culture to human cultural exchange, and it generates more inclusiveness in culture and the meaning of color is more abundant. In people's daily life, yellow and blue no longer has the typical symbolic significance of the cultural birthplace of the Chinese and western. For example, yellow has now been widely used in children's textile for its highest, strongest lightness and its characteristics of easy to notice in the visible spectrum of light.

The study of color's mental and emotional value from the angle of psychology can express the positive role of color in psychology, thus making textile color brings more pleasant aesthetic appreciation to us.

Color Psychology and Textiles Color Aesthetic.

3.1Color Psychology Impacts on Textile Color Aesthetic Psychological Process.

All things in color consciousness would become the content of color mental activity. Color psychology activities affect the choices of color emotional experience activities, and the psychology color choices directly impact on the entire textile color aesthetic psychological process. Color aesthetic psychological process can be divided into three stages, namely color aesthetic expectation, color aesthetic spread and color aesthetic diffusion. In color aesthetic expectation stage, the key is to finish the transformation from daily color psychology to color aesthetic psychology. Color aesthetic

motivation needs emotion to mobilize color experience and then toward the stage of appreciation preparation. After having the aesthetic attention, the aesthetic experience and aesthetic emotional need intent to acquire the some of the object, and then change the daily colors into aesthetic attitude. The color aesthetic spread stage is the stage of aesthetic realization. The whole process of aesthetic spread consists of main psychological factors including the color perception, the color understanding and the color imagination. Color aesthetic dispersion refers to after finishing the color appreciation, the aesthetic psychology obtains certain meet and create an aesthetic accumulation and precipitation of experience, enhance aesthetic taste and improve situation aesthetic ideal. Three phases of the psychological activity together constitute the color aesthetic psychological dynamic and complex integrated process, and produces the basic characteristics of color aesthetic psychology. People's individuality and freedom of aesthetic features decide that develop the color aesthetic by the individual subject manner, and has the distinct individual psychology color characteristics.

3.2 The Color Psychology Participation in the Construction of Textile Color Aesthetic Relations.

Color aesthetic relations refer to the special relationship established between the aesthetic person and the color aesthetic object. The relations have with perceptual characteristics, away from the limit, and then realize the free spiritual communication with the color object. Through the feeling, empathetic, intentionality projection psychological activity, the color psychology participates in the construction of textile color aesthetic relations.

Color feelings need color psychology to improve and through the color psychology can perfect color feelings.

Empathy is the outward projection of ego thought and emotion. It is the unity of the personification of the object's aesthetic characteristics and the objection of objective emotions. Textile colors have no thoughts and feelings, but with people's perception it has a shot of the connotation of these properties. Empathy will drive the migration of the experience of the color, and forming emotional self-leading feelings for the color aesthetic space.

The construction of self awareness in color experience is the formed space of limitless thoughts. Thus it gets rid of the limits and lays foundation for construction of aesthetic. This self-awareness projection in color psychology realize the combination between the expansion of visual experience and self awareness, thus construction the colorful aesthetic relations.

3. 3.The application of Color psychology and textile color aesthetic in textile color design.

Textile color design gives color more widely life space. We usually use design behavior to help people to form a certain emotional experience about specific color or color combination, and then produce aesthetic pleasure. In our work by using scientific attitude and methods of color psychology and textiles color aesthetic knowledge; we make the research and application and give consumers color vision effect and cause them positive psychology color reflection.

3.3.1 Color designing with the consideration of both individual experience and social common sense.

The color which consumers choose is an important embodiment of color psychology and color aesthetic. Because of people's particularity as an individual and the regional and cultural commonness as a member of the society are manifesting interchangeable. Different consumers have different reactions toward colors, even the same individual's color preference staged phenomenon is outstanding. So you can't get the colors of the psychological reaction hard-core. For example consumer groups of physiology sex age in the different levels may also appear the same type of color preferences. It is generally thought that children and teenagers like tall lightness of high purity color, while the middle-aged like partial implicative color. And domestic clothing brand "seven Wolf men's

clothing" which mainly toward middle-aged men for the market roll out "the green label" series dress stressed color collocation, the use of the lightness and high purity of color. Color effect in relatively single color of men's clothing market is particularly outstanding, and sales also got good market benefit. We need to keep interaction design and color sensitivity with times, find times "general character", also careful analysis of each segment market group "personality," planning the reasonable color range so as to better meet consumers' psychological color need.

3.3.2 Strengthening the Color Management.

In this paper, in understanding Chinese textile and clothing colorific standard-CNCS on the basis of color psychology, and with China's life and cultural conditions color system. Through the comparison and the analysis of the MUNSELL system, OSTWALD system, CIE table color system, Japan's Japanese color research P.C.C.S) (table with color, market analysis, this paper systematically explores the enterprise textile color design color is. Using 3-d color theory, color matrix, color calibration, pixel, the microscopic color is applied, and a series of standard management combining scientific color management method to color management, we can from color psychology and color of aesthetic sensibility and abstract analysis to design out specific textile color.

3.3.3 USES color marketing theory.

Marketing theory presents two major characteristics: "color" for media and performance means in order to realize the goal of enterprise marketing. Color marketing has gradually developed into an integrated marketing strategy system that covers brand planning, product design, packaging color, display advertising. Color designers fully understand the consumer color psychology and behavior, comprehensive understanding reaction color marketing theory connotation from textile brand building, the color system overall situation, color of color design aesthetic guide textiles, it will enhance textile market competitiveness of color.

References

[1] Arnheim: the art visual perception ", Beijing: China social science press (1984).

[2] John, Eaton, within. Color art [M]. Du DingYu, al. Shanghai: Shanghai people's art publishing house,(1993).

[3] HaoBaoYuan etc: "the psychology of experiment, Beijing: Peking University press, (1983).

[4] LiGuangYuan. Color art [M]. Harbin: Heilongjiang art publishing house, (2000).

[5] ZhangYaoXiang: the feeling, emotions and other ", Shanghai: Shanghai people's publishing house, (1986).

[6] (Japan) Xiao Lin heavy the color psychology. Analysis [M]. Beijing: people's fine arts press,

© (2011) Trans Tech Publications, Switzerland
doi:10.4028/www.scientific.net/AMR.331.532

Effects of Enzyme and Softener Treatment on Properties of Ramie Fabrics

Lihong Bai[1,a] , Hongqin Yu[2,b]

[1]Henan Institute of Engineering,TongbaiRoad,Zhengzhou, 450007 PRC

[2]College of Textile,Zhongyuan University of Technology, Zhengzhou 450007 PRC

[a]email: biaozhun201000@163.com,[b]email:nyyuhq@126.com

Keywords: ramie fabric, enzyme, softener, treatment, property

Abstract. The purpose of this paper was to compare the effects of enzyme and softener treatment on properties of ramie fabrics. Performances before and after treatment on bursting, tensile, drape, abrasion resistance, fuzz and pills resistance, bending and scratchiness were tested and compared to find the optimal modification method. The results show that the strength of fabrics descend after the two modification treatments while the softness and elongation were improved . The effect of enzyme treatment is more satisfactory since it can make the ramie fabrics show better drape, better bending, lower propensity to surface fuzzing and to pilling and weak scratchiness .

Introduction

Ramie fibers and its fabirc have many unique virtues such as cool, excellent resistance to sunlight, static, and high temperature. Ramie fabrics have a vast potential for future development. But ramie fibers are the bast fibers which have the characteristics of higher young modulus, higher degree of polymerization and higher strength than cotton fibers[1,2]. These determine the ramie fibers are stiff, rigid and difficult to cohere in the process of spinning. There are too many hairinesses in the yarn. The fabric has poor hand , easy to wrinkle and feel scratchiness .Therefore, the study on modification of ramie was begun in 1950s in China to try to lower the scratchiness and improve the softness to make the wearabilities of ramie fabric better. The main modification methods are enzyme and softener treatment[3]. This paper was to test the physical properties and scratchiness of the ramie fabric before and after these two treatments to compare which modification effect was better.

Experimental Materials and Instruments

Materials. The materials include pure ramie fabric whose specification is 14×14/54×54 and the yarn twist is 138 twists/10cm, NaOH(liquid), alkali resistant penetrating agent, solid degreaser, HAC, cellulose enzyme, amino silicone oil.

Instruments. The instruments include HD026N bursting tester, YG026D tensile tester, YG811 drape tester, YG502 fuzzing and pilling tester, YG522 disc-type fabric abrasion tester, LLY-01B bending tester, HHS21-6 thermostatic water bath, 101A-1 Electric constant temperature drying oven, laboratory mangle.

Properties Test Methods

Test the fabric properties of bursting, tensile,drape, propensity to surface fuzzing and to pilling, abrasion resistance, and bending separately according to GB/T7742.1，GB/T3923.1，FZ/T01045, GB/T4802, GB/T13775, GB/T18318.

Modification technology

Scouring. Treat the grey ramie fabrics at 100℃ for 40 minutes with NaOH solution of 2g/L and alkali resistant penetrating agent of 1g/L according to liquor ratio of 1:30.

Enzyme Treatment. First, the grey ramie fabrics were pretreated at 100℃ for 60 minutes with NaOH solution of 4% and alkali resistant penetrating agent of 1.0% according to liquor ratio of 1:17, then treated with HAC of 0.5g/L, finally treated with cellulose enzyme of 0.5g/L at 60℃ for 45 minutes.

Softener Treatment. Treat the scoured fabrics at normal temperature with amino silicone oil of 30g/L and alkali resistant penetrating agent of 1g/L according to liquor ratio of 1:30.

Scratchiness Evaluation

Using forearm touch test method, scratchiness are divide into ratings of 0～5, the greater the rating the stronger the scratchiness[4]. Five boys and five girls were selected to evaluate the scratchiness of fabrics, each person evaluate each fabric for three times at 9, 12 and 18 o'clock. The rating were obtained according to the formula 1:

$$A = \frac{\left(a_1 + a_2 + \ldots + a_n + \ldots + \ldots + a_{10}\right)}{10} \quad , \tag{1}$$

A---- The rating of scratchiness,

a_n---- The arithmetic mean of the ratings which the critic(n) estimated,

n = 1, 2, 3…10.

Results and Discussion

For convenience's sake, the fabrics treated by different technologies are represented with corresponding codes shown in table 1.

Table 1 The fabrics treated by different technologies and their corresponding code

Sample code	Fabrics treated by different technologies
0	Scouring
1	Enzyme treatment
2	Softener treatment

The tested data of sample 0, sample 1and sample 2 on bursting, tensile, drape, propensity to surface fuzzing and to pilling, abrasion resistance, and bending were shown in table 2.

Table 2 The tested data

Sample code	Bursting properties		Breaking force [N]		Elongation [%]		Drape coefficient [%]	Fuzzing and pilling [grade]	Abrasion resistance [turns]	Bending length [mm]
	Strength [N]	Distension [mm]	Warp-wise	Weft-wise	Warp-wise	Weft-wise				
0	257	15.42	568.6	476.1	6.1	7.8	58	3	38	6.39
1	212	16.38	478.3	456.8	6.4	8.1	42	3.5	41	5.89
2	232	16.12	498.6	443.5	6.7	8.9	49	2.5	40	6.08

The grade of sample 0, sample 1 and sample 2 on scratchiness were shown in table 3.

Table 3 The ratings on scratchiness

Sample Code	0	1	2
grade	4	2.6	2

Bursting properties. We can see from the table 2 that there is a decrease in the bursting strength of sample 1 and 2, this is because amino silicone oil in the softener lower the friction coefficient of the fibers , which can lower cohesive force between fibers, so the strength of yarns is reduced. The strength loss of sample 1 is greater than that of sample 2, The reason lies in the fact that with the treatment of cellulose enzyme the fiber crystallinity decreased, resulted in lower strength and greater softness which could reduce the interweave drag. There is a increase in the distension of sample 1 and sample 2 which indicates the extensibility has been improved by the two treatments.

Tensile properties. The data in the table 2 show that there is a good consistency between bursting properties and tensile properties for the same reason as above.

Drape. The results show that the drape coefficients of modified samples are all lower. The drape coefficient of sample 2 is higher than that of sample 1. Because lower fiber crystallinity can make lower fabric stiffness. The hairinesses on the fabric surface are softened, fallen up to come off, which results in the softer yarn and looser fabric structure which could lead to better drape.

Propensity to Surface Fuzzing and to Pilling. It can be seen in table 2 the propensity to surface fuzzing and to pilling of sample 1 is the minimum. It is mainly because some hairinesses on the fabric surface are removed by enzyme treatment, a clean fabric has fewer fuzzes and is not easy to generate fills. While the fuzz and pill resistance of sample 2 is worse than that of sample 0 . Because the softened fiber ends is easier to foul, the strength of the fibers is so high that the pills are not easy to be rubbed off. While the hairinesses of sample 0 is stiff , they are difficult to form pills.

Abrasion Resistance. Abrasion resistance of the modified samples is a little better than that of sample 0, it is mainly because the friction coefficient between the yarns is reduced by which the fabric stress is decreased.

Bending Behaviour. Because the surface tension of cellulose is decreased by softener, the fibers are getting easy to bend. The data in the table 2 show that there is a good consistency between drape and bending for the same reason as drape.

Scratchiness. It can be seen in table 3 that the scratchiness of sample 0 is rating 4, which is the strongest scratchy sensation in the three samples. The scratchiness of sample 2 is improved to rating 2. Softener treatment could not only lower the stiffness of fibers but also increase their free degree to make fibers back when they are given a force[5]. The scratchiness of sample 1 is a little stronger than that of sample 2. The pointed tips of hairinesses could be passivated by enzyme treatment and the reduction of fibers crystallinity could lead to a decrease in fibers rigidity [6] .The data show the two modification methods have obvious influence on scratchiness.

Conclusions

Using enzyme treatment and softener treatment, the wearabilities of ramie can be improved obviously. The modified fabrics show better bending, drape, scratchiness and elongation property, but their bursting strength and breaking force are worse.

The bending, drape, abrasion resistance, especially fuzz and pill resistance of fabrics treated by enzyme are better than that of fabrics treated by softener, while the scratchiness, abrasion resistance, bursting strength and breaking force show little difference between them.

Based on an overall consideration of various effcts, we draw a conculsion that the enzyme treatment is the better finishing for improving the wearablities of ramie fabrics.

References

[1] A.Ansari et a1:Sructre—Property Relationships in Natrual Cellulosic Fibres，Part 1：Characterisation．J．Text．1nst，No．4 (1999), p.469—480．

[2] R Thakur．C R Sarkar & Sarmah:Chemical Composition of Some Varieties of Ramie and Their Fiber Characteristics．Indian Journal of Fibre & Research．No．12 (1999),p.276—278．

[3]Q.M.Ling,L.Tan Journal of Textile ResearchVo1．31，No．7 Ju1．(2010), p.92.

[4] L.Han, W.D.Yu, Y.M.Zhang: Journal of Donghua University Vo1．28．No．2 Apr. (2002), p.134.

[5] D.M.Cheng: Ramie textile science and technology．Vo1．21(1992),.p.9—22.

[6] X.Q.Ye, L.M.Ao, C.W.Yu: Plant Fibers and Products. Vo1．26，No．2 (2006), p.84.

© (2011) Trans Tech Publications, Switzerland
doi:10.4028/www.scientific.net/AMR.331.536

The Study on 3D Weaving Method for Tubular Fabric

Zhihong Sun[a], Shenhua Zhou[b], Feifei Tang[c], Cheng Liu[d], Dan Ran[e], Jianrun Yuan[f], Zhiyao Li

Donghua University, Engineering Research Center of Advanced Textile Machinery, Ministry of Education, Shanghai 201620, China

zhsun@dhu.edu.cn, shenhua_zhou@163.com, tff616@gmail.com, snowbluemaple@mail.dhu.edu.cn, randanma@163.com, yuanjr070800823@163.com, zhiyao_li@yahoo.cn

Keywords: weaving method; 3D tubular fabric, circular weaving; binding yarn; weft binder

Abstract. A 3D weaving method for tubular fabric was advanced in this paper. Warp yarns are input axially, weft yarns and binding yarns are inserted into the fabric circumferentially by shuttles which connecting warp yarns not only within weaving plane but also through thickness of the fabric. Due to the specially designed shedding order and under the pull force of shuttles, warp yarns could be bound without beating.

Introduction

Tubular structure is the basic element which is widely used in engineering. Resin-based 3D tubular composite has the advantages of lightness, high stiffness, high strength, good fatigue resistance and corrosion resistance, etc. it has become an important structural material. This kind of 3D tubular composites can be made into products such as scaffolds, pipelines, bushings, casing, ultra high-temperature resistant and thermal-insulating pipes, they have an extensive and promising application prospect in energy transportation, environmental protection, chemical engineering, aerospace, bio-chemical industry, medicine and so on [1].

In this paper, we will advance a 3D circular weaving method which can produce 3D tubular fabric. The size and thickness of the tubular fabric could be changed easily.

Existing forming methods for 3D fabric

Till now, there are many kinds of methods to make 3D fabric, for example 3D braiding, 3D weaving, 3D stitches and so on [2].

As for the 3D braiding, spindles run regularly in the tracks to produce 3D fabric. Some mechanisms and equipments related to 3D braiding were advanced in USA Patent 5,337,647, 4,719,837 and 6,439,096 [3-5] respectively. The main drawback of these approaches is that, each yarn needs to be carried by a spindle during the braiding process, a large number of spindles are needed while braiding large-sized structures, so the machine will be energy consuming and the motion control system is very complicated. If the amount of yarn carried by spindles is reduced in order to decrease the load and prolong the running speed, then the continuous weaving period will be short and the machine has to shut down to change yarn tubes when anyone of them is run out of yarn. This leads to huge workload of changing yarn cops and piecing yarns, the waste of raw materials is also very serious, and what's more, the piecing quality could not be guaranteed. [6]

3D weaving method has been used to produce various 3D fabrics of rectangular section, such as L-shaped, T-shaped, etc [7]. It also can produce tubular fabric while adopting specific shedding pattern[8]. However, tubular fabric produced this way has obvious creases at two sides, the property of weft yarns at the crease is damaged and therefore the performance of the composite is influenced.

3D stitched fabrics are formed by overlaying flat fabrics to a required thickness, and then sewing them up into a whole. The process is simple without special equipment, and what's more, the shapes of the fabrics are optional. However, the fibers are likely to be damaged and the fabrics be distorted when the needles penetrate the fabrics, this will decrease the composites' property.

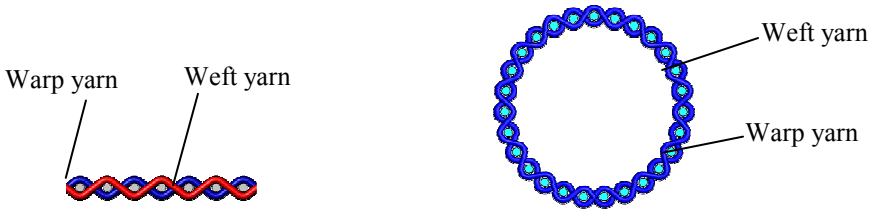
In conclusion, there are various kinds of 3D forming techniques which can produce 3D tubular fabrics. However, the fabrics produced by these methods have one or another shortcoming, and due to their general disadvantages of high cost and low production rate, so they are not suitable for mass production.

3D circular weaving method

Just like planar weaving, circular weaving also interweaves warp yarns and weft yarns to form a fabric. But the very difference is that, the warp yarns of circular weaving are arranged circumferentially and inserted along the axial direction other than placed horizontally in the usual planar weaving, and the weft yarns are inserted into the fell continuously by shuttles which running clockwise or counterclockwise other than to and fro in the planar weaving. Therefore, the weft yarns in the fabric have the form of a helix [9]. The helix angle of the weft yarns, which mainly affects density of weft, is determined by the velocity ratio of the weft insertion to the take-up speed. Fig.1 shows the different yarn status within one layer of the planar weaved fabric and circular weaved fabric.

The 3D fabrics formed by circular weaving are significantly different from the 2D fabrics in that 3D tubular fabrics are connected and enhanced by yarns in the thickness direction. This type of yarns is named binding yarn, tied yarn or consolidation yarn [10] according to their different organizations. In this paper, it is called binding yarn.

In 3D tubular fabric, warp yarns and weft yarns are arranged in axial and circumferential direction respectively, while the binding yarns are arranged along radial direction. Just like warp yarns and weft yarns, binding yarns also need to be inserted into the fabric, and either warp yarn or weft yarn could act as the binding yarn, the structures of these two kinds of fabrics are shown in Fig.2.



(a) Planar weave (b) Circular weave

Fig.1 Yarn statues of planar weaving fabric and circular weaving fabric

For the circular fabric with some warp yarns act as binding yarn, the common warp yarns form a fell and only interweave with the corresponding weft yarn to form one layer of fabric, while the warp yarn which act as binding yarn interweaves with all layers and form 3D fabric. The advantage of this method is the binding yarn can be continuously supplied just as warp yarn. However, in the process of weaving, the binding yarn needs to be controlled by a special designed insertion mechanism which is relative complicated. On the contrary, if weft yarns are used as binding yarns, they are inserted into the fell by the same devices as weft yarn, namely shuttles. Then no special mechanism is need. This makes it flexible to develop new kinds of 3D tubular fabric. This paper mainly introduces the circular weaving method with weft yarns work as binding yarn.

In weft binding circular weaving, the binding yarns are pulled and inserted into the fell by shuttles. The shedding pattern is controlled by computer program according to the fabric structure to be weaved, several layers of fabric are weaved at the same time and they are bound together by the binding yarns to achieve a 3D tubular structure. 3D circular loom is the equipment to produce 3D tubular fabric. Fig.3 is a sketch of one kind of 3D circular loom. The shedding devices and shuttle

pushers are carried by the main shaft. The shuttles which are pushed by shuttle pushers pass through the fells and insert weft yarns or binding yarns into them to form fabric, and the fabric is then reeled on axially from the middle of the loom by a roll-up mechanism[11]. Because the weft yarns and binding

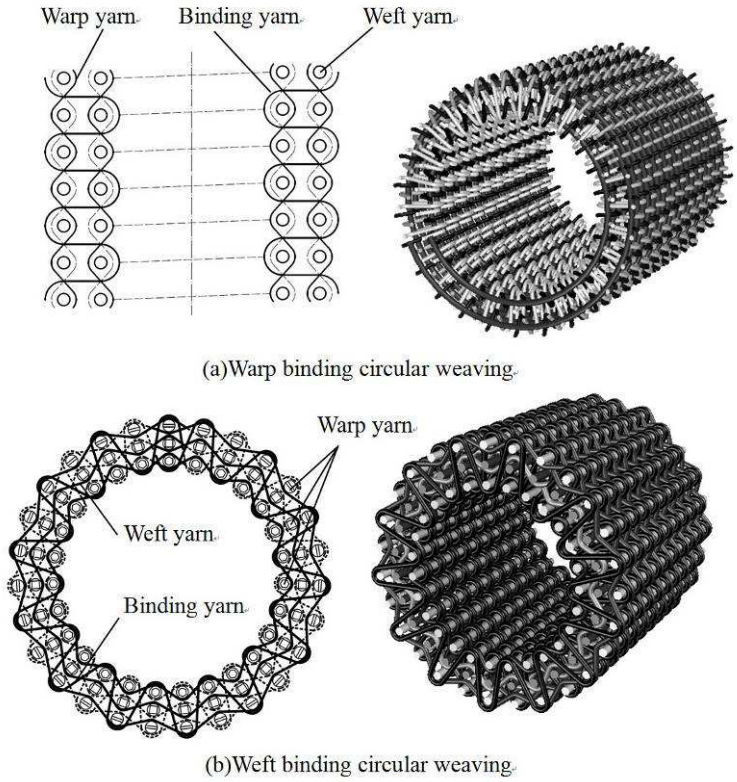


Fig.2 Structure of the two kind 3D tubular fabrics

yarns are clockwise or counterclockwise inserted into the tubular fabric whose diameter is much smaller than the diameter where the fell locates, under the tension of weft yarns and binding yarn, a tubular fabric of 3D structure will be formed spontaneously, beating-up mechanism is unnecessary.

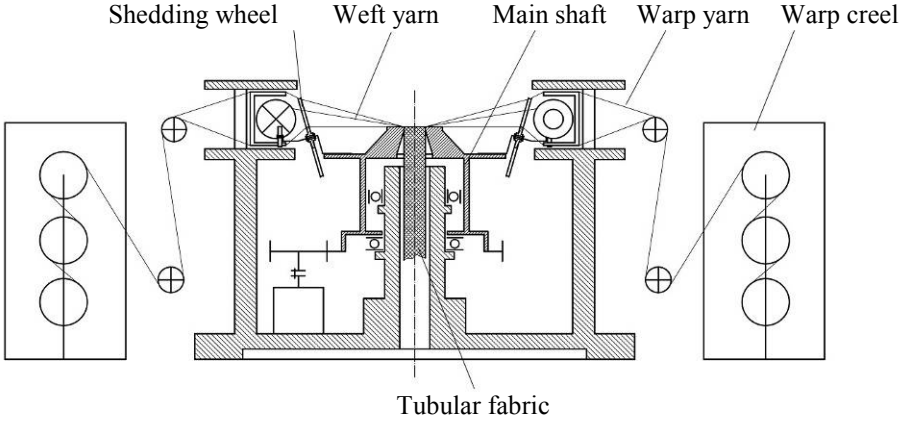


Fig.3 Sketch of 3D circular loom

Fig.4 is the top view of 3D tubular fabric forming process with 3 layers, three shuttles draw weft yarns to interweave with corresponding warp yarns respectively and form three layers fabric, while one shuttle which carries binding yarn goes from the outmost to the innermost of the fabric and bind the three layers together. For example, the shuttle 2 makes the weft yarn interweave with the warp yarns in the second layer only, and the warp yarns which belong to the inner layer will pass this shuttle from its top while the warp yarns belong to the outer layer will pass this shuttle from its bottom to avoid interweaving with this weft yarn. For the binding yarn, every three adjoining warp yarns work as a group to form a fell with the next three warp yarns, the binding yarn go through the fell and

integrate three layers fabric together. Binding yarns distributed helically in the fabric structure, just like weft yarns. However, weft yarns only interweave within one layer while binding yarns interweave with all layers. At last, warp yarns belong to different layers will separate and move in the radial direction while weft yarns are tightened. Fig.4 reveals the section view of the final fabric.

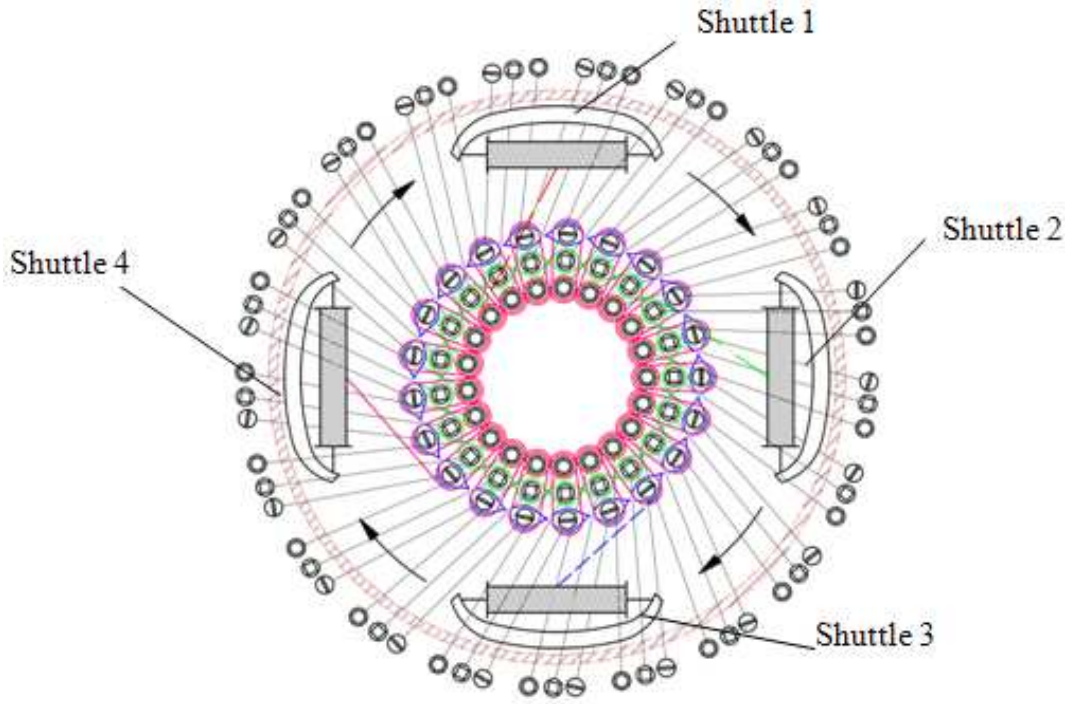


Fig.4 The principle for circular weaving method

Fig.5 shows the looming draft corresponding to the 3 layer tubular fabric. Line 1A and 1B means the pattern grid corresponding to shuttle 1, Line 2A and 2B means the pattern grid corresponding to shuttle 2, Line 3A and 3B means the pattern grid corresponding to shuttle 3 and Line 4A and 4B means the pattern grid corresponding to shuttle 4. Here, every six warp yarns group into a cycle (there are 3 cycles in Fig.5), and in order to avoiding warp-skipping phenomenon, the warp yarns of adjoining two cycles must have a half-cycle difference with each other, that means stagger 3 warp yarns in this case.

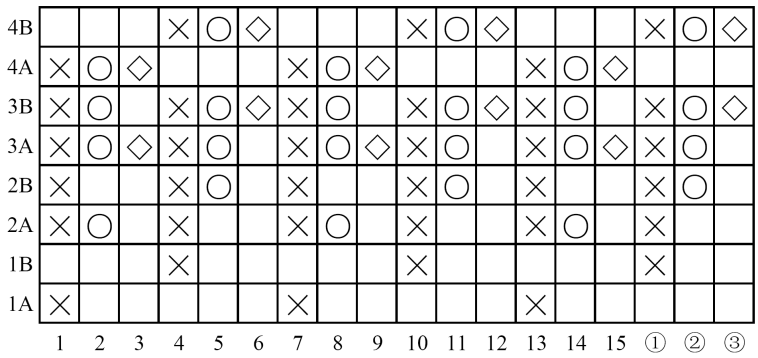


Fig.5 Looming draft for weaving 3 layers tubular fabric

Conclusion

A new weaving method for 3D tubular fabric advanced in this paper was developed based on traditional circular weaving. It has the following advantages:

1) Due to the structure of this kind 3D tubular fabric is close to orthogonal structure, the fabric mechanical properties along the warp direction, weft direction and through-thickness direction are reliable.

2) Since the warp yarns are supplied from the warping creels which are not move, so their volume could be big enough, this means there is no need to change warp yarn cops frequently. Meanwhile, shuttles insert weft yarns by moving in a circle pattern without reversing of direction like traditional looms. As a result, this method has the advantage of low workload, high speed, high efficiency and good continuity.

3) The diameter and fabric density of this kind 3D tubular fabric are mainly determined by the ends in warp, the size of the control ring and the speed ratio of let-off to take-up, each one of these factors is convenient to adjust, so the range of the fabric diameter could be very wide. The thickness of the fabric is decided by the number of the shuttles, and a circular loom with N shuttles can weave N-1 layer tubular fabric at most. Therefore, the adaptability of the product is outstanding.

3D circular weaving method can continuously produce 3D tubular fabric which could push the development of tubular textile composites. This is convenient for designers to consult and select. They may also become a kind of basic structural parts just like metal and engineering plastics and are utilized widely.

References

[1] Dj.M. Maric, P.F. Meier and S.K. Estreicher: Mater. Sci. Forum Vol. 83-87 (1992), p. 119

[2] M.A. Green: High Efficiency Silicon Solar Cells (Trans Tech Publications, Switzerland 1987).

[3] Y. Mishing, in: Diffusion Processes in Advanced Technological Materials, edtied by D. Gupta Noyes Publications/William Andrew Publising, Norwich, NY (2004), in press.

[4] G. Henkelman, G.Johannesson and H. Jónsson, in: Theoretical Methods in Condencsed Phase Chemistry, edited by S.D. Schwartz, volume 5 of Progress in Theoretical Chemistry and Physics, chapter, 10, Kluwer Academic Publishers (2000).

[5] R.J. Ong, J.T. Dawley and P.G. Clem: submitted to Journal of Materials Research (2003)

[6] P.G. Clem, M. Rodriguez, J.A. Voigt and C.S. Ashley, U.S. Patent 6,231,666. (2001)

[7] Information on http://www.weld.labs.gov.cn

[8] HUANG Xiaomei. The texture design and weaving of tubular 3D fabric[J]. Journal of Textile Research, 2002,23(4): 51-52+3.

[9] DU Fangchao, HUANG Xiangqiu, WANG Dagang. Plastic Fabric and Products[M]. Beijing: China Petrochemical Press. 1998:129-152.

[10] HUANG Xiaomei. Design and weaving for some three-dimensional tubular preforms[J]. Cotton Textile Technology, 2002 (12): 44-46

[11] SUN Zhihong, ZHOU Shenhua, SHAN Hongbo et al. A circular weaving equipment and method for 3D textile tubular fiber composites. CN Patent 201010260981.5[P], 2010-08-24

[12] MA Chongqi. Research of a new three-dimensional circular loom, Composite Materials--Life, Environment and Advanced Technology [C], Tianjin:[s.n.]2002

CHAPTER 4:

Apparel Design and Merchandising

© (2011) Trans Tech Publications, Switzerland
doi:10.4028/www.scientific.net/AMR.331.543

The Researchment of Knitted Antifouling Fabrics and the Splicing Design on Leather Garment

Hongtao Deng[1,a]

[1]Design College of Jiaxing University, Jiaxing Zhejiang, P.R.China 314000

[a] hzgdht@126.com

Keywords: knitted fabrics, antifouling, leather garments, splicing design.

Abstract. The garments splicing together the knitted and leather are main products in leather garment market in recent years. In view of the reflection of terminal market, the contradiction between washing and maintainance method of knitted and leather fabrics and undesirability of splicing design are the main factor that influence promotion of products. Through the antifouling treatment of the knitted fabrics, it make them have the function of waterproofness, oilproofness and antifouling;Splicing knitted fabrics on the parts that are easy to wearn out and easy to be restained, and other parts that impact comfort and produce esthetic fatigue on the leather garments, it meet the multivarient need of consumers' comfort and fashion more. On this basis, Taking integrative consideration of combinative match, stitching technics splicing design, splicing reasonablity of fabrics and garments style, it initially form theoretical basis of splicing design of antifouling knitted fabric on leather garment.

Introduction

In the leather garments, knitted fabrics are the fashion trend, are the need that consumers pursuit individuation and emphasize co-existence of fashion and taste, are the need that enterprise seek survival and capture the market[1]. But in view of current marketing situation, on the one hand, because of the difference between washing and maintenance method of knitted and leather fabrics, it lower the practical performance of this splicing design, on the other hand, because of the undesirability of splicing design, it affect the depth and breadth of such products' promotion. It adopt fluorinated compounds to make antifouling organization to knitted fabrics, make them not easy to stick dirt, and make sticking dirt easy to clean and not easy to stick again[2]. Then in accordance with the principle of combination of practicality and esthetic, it slice together antifouling knitted fabrics and leather fabrics, it will be widely loved by consumers after the products are launched on the market.

Knitted Fabrics are Easy to Make Antifouling Organization

Fabric. 3% spandex, 9% polyester, 23% wool,65% acrylic;9 stitch; 2*1 ribbing.

Technics Process. fabric pre-treatment →water washing →drying →dipping organization liquid →drying → baking.

Pre-treatment Technics Prescription. Deoiling liquid 4g/l; penetrating liquid 2g/l; Na_2Co_3 1g/l washing time 30 min; washing temperature 100˚C.

Technics Prescription of Antifouling Treatment.PM-492 organization liquid: 60g/l; catalyst: 8g/l; baking temperature: 150˚C; baking time:60min; Ph:5.5～6.5.

Performance testing of products

Test Method of Washing. Washing equipment: household washing machines; washing powder: 2g / L; bath ratio: 1:30; washing temperature: 30 ˚C; pH <9; washing time: 10min.

Drainage, clear, dehydration, drying are one time of washing, until 10 times of Washing.

Test result as table1

Table 1 The test result of waterproofness, oilproofness and antifouling of knitted fabrics

Test item	Minimum	Test result
Waterproof grade	1	3
Oilproof grade	1	3
Test result of three protection	Non-accordance/ accordance	Accordance

The Splicing Design of Knitted Antifouling Fabrics on the Leather Garments. Leather fabrics have good shaping, they are not easy to distort, the shape is erect, it can mould and beautify the body, however, the wearer will feel heavy and the body is restrained, the stress surface of garments is easy to wear out, traditional full-leather clothing still make people feel esthetic fatigue of the mould, etc [3]. Knitted fabrics are soft and close to skin, they have excellent flexibility and extensibility, along with a rich texture changes. Following practical and aesthetic principles, splicing together knitted fabrics and leather fabrics, it can solve these problems better.

The Choose of Splicing Part

The Part Easy to Wear out on the Leather Garments. The edges of collar, lap, cuff and pocket and so on are the focus of the design of leather garments, but movements the human's head, neck, body and so on are easy to produce repeated friction with the edges of garments, damage the appearance of garments; In aaddition, the tension of leather fabrics is comparatively large, they feel comparatively cold, they are easy to produce a uncomfortable feeling when they touch the human body directly. The knitted fabrics with soft texture and fine flexibility that are spliced on the edge part . as shown in Fig.1, not only can increase the comfort of skin of neck, wrist and other touch part and reduce the wearing out of edge parts of leather garments, but also make the fitness degree between garments and body higher, make wearer more comfortable. In addition, as to the leather garments of autumn and winter style, it also can enhance the windproof effect.

Restraining Parts of Garment Body. Because of the problems about flexibility and extensibility strength of leather fabrics, Traditional full-leather garments often adopt comparatively loose outline style to meet the needs of human exercise amount. With the development trends of young and individualized design of leather garments, especially the popularity of Gothic style in recent years, the style of leather garments is getting more and more tend to thinness and fitness, however, this kind of style is easy to produce restraint for dressed human body, it is not beneficial to body activity. As the design shown in Fig.2, splicing knitted fabrics at the bottom of sleeves , the side of garments and other parts, it can meet the needs of modern leather garments, can also solve the problem of body restraint well.

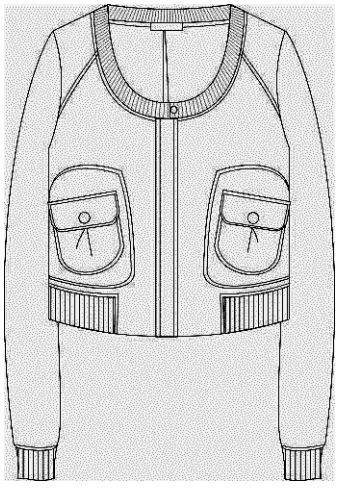


Fig.1. Knitted fabrics on the edge of leather garments



Fig.2. Knitted fabrics on the bottom of sleeves and the side of clothing body of leather garments

Other Parts. Traditional, especially full-leather garments of autumn and winter style still have two problems, one is heavy wearing, it impact comfort; another is comparatively simple style and pattern, it makes people produce esthetic fatigue. Splicing knitted fabrics on the edge , at the bottom of sleeves and armpit can solve these problems at certain extent, but after all, visual impulsive force of the appearance it produce is relatively weak, as shown in Fig.3, Fig.4, if we splice the knitted fabrics on the garment body , sleeves body and other parts that have larger area , use the method of ready-made clothes to make the knitted fabrics reduce the edge joint maximumly and reduce the weight of garments, changeful organization texture of knitted fabrics make the leather garments produce special texture and details, it can display performance feature of respective fabrics , can also produce tactile and visual contrast between softness and hardness, smoothness and acerbity. Different materials between thickness and thinness, transparentness and denseness, concaveness and convexness interweave the elegant charm of leather garments, make up the monotony in style, enhance the personality and fashion of leather garments [4].

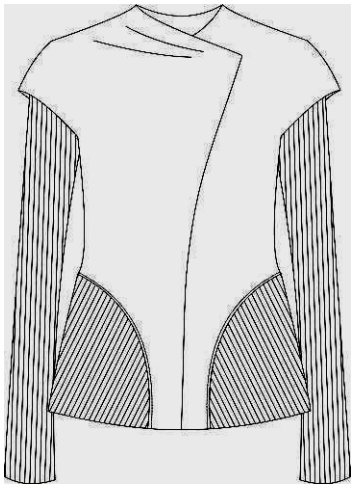


Fig.3. Knitted fabrics make leather garments more ethereal

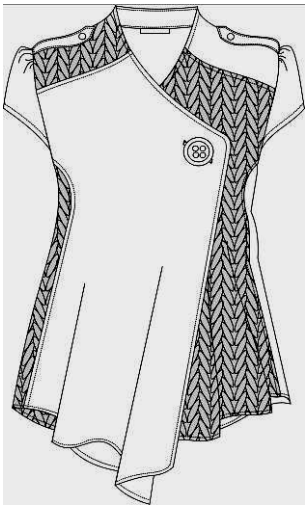


Fig.4. Knitted fabrics make leather garments produce rich texture

Combinative Match of Fabrics and Garments Style. Nowadays, the most advanced leather processing technology, special technics processing[5], especially the design of leather garments more and more in accordance with other fashion garments, they make appearance style of the modern leather fabrics and garments increasingly tend to diversification, or nobleness and elegancy, or simplicity, or smoothness, or roughness ... ... as shown in Fig.5 and Fig.6. Likewise, the style of knitted fabrics and garments are also rich and varied, so when splicing design, we should take full account of combinative match of fabrics and garments styles.

When combining, we should treat leather garments style as keynote, and take integrative consideration of the texture, quality feeling, color, pattern and so on. In general, there are two combinative ways.

Similar Style. Choosing similar style of fabrics to splice is comparatively easy to hold the holistic style of garments. The garments that combine knitted fabrics of wide needle distance with wild leather fabrics can keep warm, can also give people wild, leisure and free feeling, they are suitable for men to wear. The garments that combine knitted fabrics of thin needle distance with light leather fabrics are ethereal and free, they are suitable for women to wear and use.

Different Style. Choosing different style of fabric to combine can build fashionable and avant-garde feeling. If combining exquisite or openwork knitted fabrics and leather fabrics, it will make the details of leather garments more vivid, and distribute elegant and fashionable charm.

Splicing Reasonablity. The splicing design between knitted fabrics and leather fabrics need considerate ergonomic accordance and esthetic factors, the used parts and size also need pay attention to reasonability on design, reasonably using it to appropriate parts can ensure the functionality of leather garments away from damage.

Stitching Technics. The usage of antifouling knitted fabrics on leather garments also need consider stitching technics. In this respect, we need to consider the feasibility of respective stitching technics on knitted and leather fabrics, we also must consider the feasibility of stitching technics on their mutual stitching place.

Splicing Line Design. Common dividing methods of leather garments are vertical, horizontal, diagonal and free division [6], different dividing methods constitute different spicing lines, we need take full advantage of the function that splicing lines can replace structure lines and can save seam to enhance the holistic sense of garments.



Fig.6. The match between knitted and leather fabrics with different style



Fig.5. The match between knitted and leather fabrics with similar style

Conclusions

Through the antifouling organization of the knitted fabrics, it make them have the function of waterproof, oilproof and anti-fouling, and solve the contradiction between washing and maintainance method of knitted and leather fabrics maximumly.

Complying the principle that combine practicality and esthetic together, splicing knitted fabrics at the edge, the bottom of sleeves , body side, garment body, sleeves body and other parts of leather garments, it can make leather garments more comfortable, also can meet pursuit of consumers' individuation and fashion.

Taking integrative consideration of combinative match, splicing reasonablity of fabrics and garments style, it will make the splicing design of knitted and leather fabrics more feasible.

References

[1] Hongluan Liu, Yiyou Li: Textiles Science Progress.(1)(2008),p.80-82(In Chinese).

[2] ZhenWan,Wei Wang, Jun Xie: Knitting Industry. (3)(2005), p.45-47. (In Chinese).

[3] Shaohua Zhou, Jing Wu: Leather Science and Engineering. (4)(2007), p.60-62(In Chinese).

[4] Canzhi Huang: Western Leather.(7)(2008), p.16-18(In Chinese).

[5] Canzhi Huang: China Leather. (12)(2006), p.22-24(In Chinese).

[6] Zhongqi Zhang: Western Leather. (18)(2010), p.36-39(In Chinese).

© (2011) Trans Tech Publications, Switzerland
doi:10.4028/www.scientific.net/AMR.331.547

Research on Children's Functional Clothing of Keeping Safety in the Car

Lei Shen [1, a], Xuehuan Jiang[1, b] and Yunyin Chen [1, c]

[1]College of Textile and Clothing, Jiangnan University, Wuxi 214122, China

[a]sl999@sina.com, [b]xuehuan6298@126.com, [c]achiun@126.com

Keywords: Apparel Design and Manufacturing, Functional Clothing, Car Safety for Children

Abstract. A new type of design, which combines clothing with the seat cover of automobile are from the perspective of children's functional clothing for protecting children safely in the car according to ergonomic principles. This design is based on the analysis of structure design and fabric design, using the software of MADYMO to simulate the collision on child dummy in car and analyze the dynamic response to get damage parameters of the head and chest. By comparing with regulation value we get conclusion that this design has good function on protecting children in the car.

Introduction

With the development of technology and social progress, great changes are happening in all walks of life, and a variety of innovation is emerging. Apparel industry is no exception; especially the functional clothing. With the continuous development of various industries, the research field continues to expand; the intersection between different disciplines is also increasing. For the apparel industry, currently has the interdisciplinary of with the space industry, electronic industry, medical, and each reap rich fruits continuously, such as the invention and development of spacesuit; clothing used the GPS navigation; functional clothing using the clothing pressure to treat cerebral thrombosis [1].

Currently, functional clothing in the clothing market has played an important role, but the main target is used for adult group, functional apparel products designed for children is relatively less. And with the growth of economic, the vital issues on road safety, the increase in number of family of single child, the urgent requirements of safety, emphasizing the beauty, comfort and safety of functional clothing products become more and more demanded. Thus, product aim at car safety for children, with concept from the functional clothing design process, this design as a combination of children's clothing with car seat is of high value, and is reasonable and feasible a novel design ideas to increase children's safety in car.

This design of functional clothing is combined with the application of ergonomic principles and a detailed analysis of children's characteristic figure, guided by the aesthetics of car seat design eventually fit children's clothing on the car seat, which is both beautiful and functional, so as to achieve the purposes to secure children in car, to lessen tragedy and injuries caused by traffic accident, and to promote the harmonious development of society.

Design principles

The design principle of the program has the following two aspects:

In accordance with ergonomic principles, when the force is invariable, increase the contact area of upper body with the clothing can spread out the pressure in the clothing in contact with body parts, reducing the clothing pressure that caused by the external to the different parts of body [2]. Children's bones are more fragile and cannot withstand too much external pressure. When child wearing this functional clothing subject to strong external pressure, this device will spread the pressure which may act on the seat belt to the waist, shoulders, chest and other part, avoid injury to neck thanks to the equipment.

The functional clothing of children's clothing and car seats form a hollow closed body as a whole, protecting the body of a child in all directions to avoid life-threatening that children are thrown away in car accidents.

Structure Design. The design includes design of a car seat and a matching children's vest combined with the car seat.

The matching children's vest combined with the car seat consists of the circumference adjustable belt, the adjustable shoulder belt, the belt at bust and waist reinforcement, the reinforced thigh fixed component. The circumference adjustable belt is conducive to adults according children's figure of fat or thin, the number of clothes they worn, different season to make different choices for children to achieve the proper fit and spread a sudden force to the different body parts scattered to reduce risk and in case of accidents; designed shoulder belt can adjust with the height of a growing child with the length adjustment shoulder belt, to ensure children gain comfort in long-term growth process, no need for re-purchase and replacement; the two belt at bust and waist reinforcement guarantee the safety of child by firmly fixed in the car seat; the thigh fixed component designed to fix a child on the seat, prevent child's body sliding down at a long ride.

Children's vest design. The design select children aged 6-12 as target; it is according to the tasks of these stage and the physical characteristics of children. Children of this age become primary school students from kindergarten or nursery. Primary schools are also far away from the residential area than kindergarten; hence most of the parents are often use the vehicles to take their children every day, especially for the student on first grade. Children in childhood are actively, curious about the outside world, fond of entertainment after-school, and beg their parents to take them out. Therefore automobile become a necessary to meet the needs of children. The growth and development of children in this period is in a relatively stable velocity, about 4 to 5 cm in height, 1.5 to 2 kg in weight per annum. The difference of figure, taste between boys and girls is not large[3]. This selection on children of this age will make the design object has a higher application value, and applicability to a wider range.

Considering the vest is adjustable, we choose children that the height is 130 cm as a figure sample to guarantee the design can have extensive use. The children's clothing prototype structure is drawn in B = 67 cm, back length = 30 cm, and then, based on the prototype draw the final structure of children vest (see Fig. 1) [4].

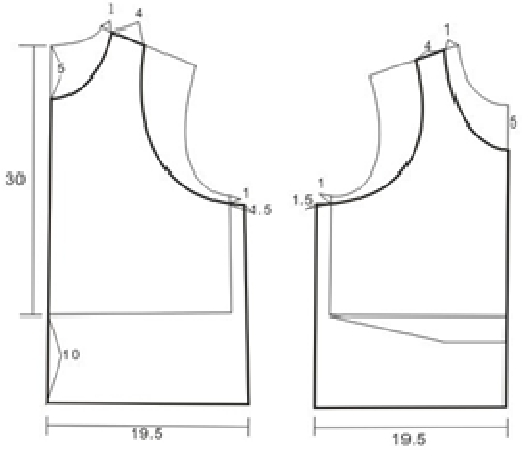


Fig 1. Structure of children's vest

In order to make this device have a wider use, the thigh fixed component should be designed based on the principles of garment processing ease, and to consider the amount of overlap of buckles, portray the structure (see Fig. 2).

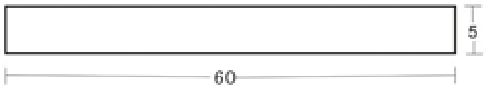


Fig 2. Structure of the thigh fixed component

Choice of Fabric. Choice of fabric for this vest should be a balanced consideration of comfort and firmness. As to comfort, we should pay more attention on use in hot summer, and needs of warmth in winter can be met the child's own wearing clothing and car's air-conditioning. Therefore the fabric should be chosen to meet the needs in summer, allowing the sweat rapidly transmit from the inside to the outer of fabric to maintain clear and clean on skin, so that children have physical comfort.

Simulation

Simulation analysis of children's vest with car seats is based on knowledge of automobile field, and the simulation model is established using the Multi-body dynamics software MADYMO6.2.1 developed by TNO to simulate the collision of car with child dummy dressed in it. Then child dummy's simulation injury parameters are obtained and compared with the regulation values, and have the conclusion finally.

Introduction of MADYMO Software. MADYMO (Mathematical Dynamic Model) multi-body dynamics analysis software originally developed by Road Vehicle Research Institute of Netherlands Organization for Applied Science Research (TNO) (National Technical Research Institute) in 1975, it has become a industrial standards of restraint system for the vehicle occupant's safety. Currently, MADYMO has developed to edition 6.3 and has successfully integrated the finite element analysis with multi-body system to become more than a combination of rigid body and finite element mathematical modeling software, which widely used in area of automotive, aerospace, heavy industry, military, accident reconstruction and injury biomechanics research and other fields.

MADYMO can predict the kinematics and dynamics response on structure of a vehicle and victims through the collision. MADYMO program has a good interface with the finite element program DYNA3D, PAM-CRASH, LS-DYNA3D, MSC \ DYTAAN; besides calculating the large deformation of the car body it can calculate the dynamic response of the vehicle occupant. A MADYMO model is consisted of one or more multi-rigid body systems and finite element model, in which the multi-rigid body model used to simulate the motion of the system, such as the crash dummy, vehicle suspension, mechanical systems; finite element model used to simulate large deformation of the structure, such as airbags, seat belts, auto body parts and so on. These systems are located in a reference space, rigid body are represented by connected plane or ellipsoid, and then using hinge to connect the rigid for simulation, MADYMO according to the multi-rigid body kinetic theoretic output equation of motion of 2D or 3D of multi-rigid body systems, and educed from the Lagrange theorem[5, 6].

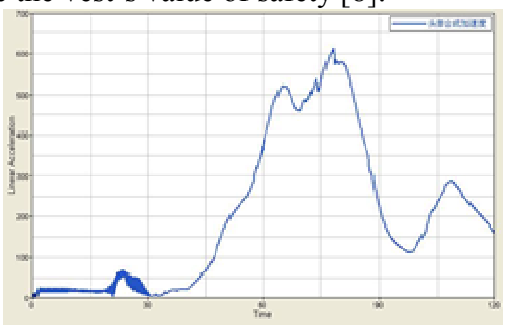
The dummy. The program used the 6-year-old child dummy of P series developed by TNO for multi-body simulation. The model is developed by Netherlands Organization for Applied Science Research.

The figure and weight of the dummy is based on the 6-year-old children. Its quality is 22kg, 116.6cm height. The model is composed of 15 ellipsoids, each ellipsoid's inertia is got by measuring the corresponding physical properties of P6 dummy, the less important inertial parameters is from the corresponding scaling parameter on P3 / 4 (9 months) dummy, the ellipsoids connected by kinematic hinge, the P6 dummy model in the location of reference. The initial position of the dummy has a significant impact on simulation results. Dummy's sitting position is adjusted by intuitive visual, so that dummy of children fit the seat surface integrated to reach static equilibrium in the gravity field to obtain the initial sitting position consistent with the dummy in test (see Fig. 3) [7].

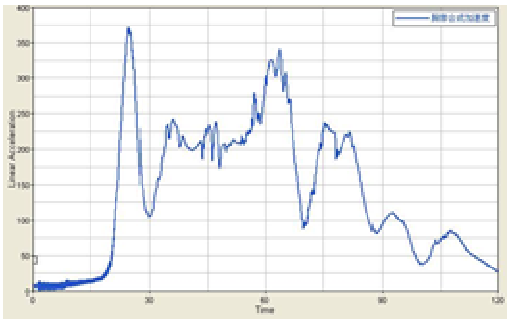


Fig 3. Children dummy wearing the vest at the initial sitting position

Since the development of children's physical and psychological is not mature, in a traffic accident the most vulnerable parts of children body are the head and chest, as shown in the following, we selected the head and chest as parts for analysis to get dynamic response during the collision, to evaluate the vest's value of safety [8].



a) Synthesis of the head acceleration



b) Synthesis of the chest acceleration

Fig 4. Dynamic response of the child dummy in frontal crash simulation

The synthesis curves of the head and chest acceleration show the injury parameters that are summarized in Table 1, there are head HIC36, HIC15, synthetic acceleration of head (3ms) aH3ms, synthetic acceleration of chest (3ms) aT3ms and acceleration of the chest in z direction aTZ(3ms). Table 1 shows that synthetic acceleration of head 3ms is 573m/s2. The acceleration of chest in z direction 3ms is 126.1m/s2, synthesized acceleration of chest 3ms is 302.4m/s2. The injury values of dummy are within the range of the regulations.

Table 1 Children's frontal crash dummy injury parameters simulation

Name	HIC36	HIC15	a_{H3ms} (m/s^2)	a_{T3ms} (m/s^2)	a_{TZ} (m/s^2)
Regulation values	1000	570	784	539	294
Reference		IARV	FMVSS213	ECE R44	ECE R44
Simulation values	519.9	332.7	573.0	302.4	126.1

Conclusions

From the curve we chalk up the data in the table 1 above, compare it to the regulation we draw the conclusion that the simulation experiment data are within the scope of the regulations, which proves that the design meets the provisions and has the function to protect children.

References

[1] H. Jiang: *History of Western Costume* (Donghua University Press, Shanghai 2007), In Chinese.
[2] W.B. Zhang, F. Fang: *Clothing Ergonomics* (Donghua University Press, Shanghai 2008), In Chinese.
[3] F. Liu: Journal of Nantong Textile Vocational Technology College, Vol. 9 (2005), p.48, In Chinese.
[4] W.B. Zhang. *Pattern Making For Fashion Design*. (China Textile and Apparel Press, Shanghai 2006), In Chinese.
[5]*MADYMO Version Institute 6.2.1. Theory Manual*. TNO Road-vehicles Research Institute (2002)
[6]*MADYMO Version 6.2.1. Database Manual*. TNO Road-vehicles Research Institute (2004)
[7] W.L. Ren, X.M. Li, W.M. Gao: Shanghai Automobile, Vol. 5 (1999), p.18-21, In Chinese.
[8] *Side Impact System Integration and Development Method of a BASIS + sled test simulation with MADYMO PSM*. TNO Road-vehicles Research Institute (2005)

© (2011) Trans Tech Publications, Switzerland
doi:10.4028/www.scientific.net/AMR.331.551

The Functional Requirements Analysis of A/W High Altitude Cleaning Overall Materials

Weiwei Huang[1,a] , Bei Guo[1,b]

[1] Fashion·Art Design Institute, Donghua University, 1882 West Yanan Avenue, Shanghai, China, 200051

[a]feelshoushou@yahoo.com.cn, [b]h-beibei@163.com

Keywords: overall, air permeability, moisture penetrability, antistatic property

Abstract. The high altitude cleaning work is usually carried out far away from the ground; the special environment and work content make the special demands on overall materials. This paper chooses 8 kinds of materials, measure their air permeability, moisture penetrability, waterproofness, abrasive performance and antistatic property. Based on the comprehensive consideration, select the Vinyl chloride-acrylonitrile copolymer with antistatic property and waterproofness as the primary material, use other materials at local areas according to the specific requirements as to optimize the function.

Introduction

As the increase of high altitude cleaning workers and extension of working content, the demands of the overalls are becoming diversified gradually. There are many overalls flooding the market which not only affects the market's standardability, but also cannot provide solid safety ensure. For the sake of avoiding risk from the radiation, static electricity, chemical liquid, consider the functions when choosing the overall materials. This paper chooses 8 kinds of materials, measure their air permeability, moisture penetrability, waterproofness, abrasive performance and antistatic property, finally selects the Vinyl chloride-acrylonitrile copolymer as the primary material, use other material at local areas according to the specific requirements as to optimize the function.

The Samples

Table 1 includes 8 kinds of materials. 1# has been treated with acid and alkali resistant finish. 2# and 3# are taken from the existing overalls. 4# is P/C with acid and alkali resistant finish. 5# is the Vinyl chloride-acrylonitrile copolymer with antistatic property and waterproofness finish, 6# is P/C with fire retardant treatment, 7# is 100%C with waterproofness, 8# is cotton with antistatic property and grease proofing.

Table 1. The Basic Information of Materials

Number	*Gram Weight [g/m^2]*	*Thickness[mm]*	*Number*	*Gram Weight [g/m^2]*	*Thickness [mm]*
1#	2.649	0.439	*5#*	3.445	0.926
2#	1.941	0.435	*6#*	2.114	0.411
3#	2.222	0.440	*7#*	3.061	0.633
4#	2.561	0.428	*8#*	1.560	0.412

The Physical Performance of Materials

Air Permeability. Air permeability means the capacity of air to pass through the material vertically when there is pressure difference at the both side [1]. It can exchange the CO_2 accumulated inside with the fresh air outside. The material should be able to drive out the gas quickly in order not to cause the discomfort. Use YG461E Computerized permeability tester to measure it.

Fig.1 indicates 6# and 8# are better than the existing overalls' materials. 5# and 7#'s air permeability are good along while 1# and 4# perform inversely.

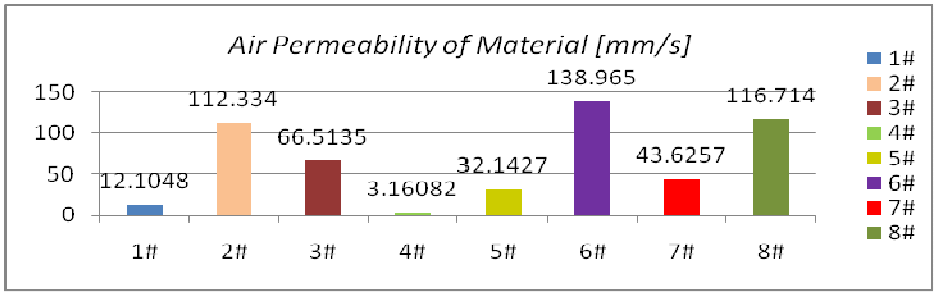


Fig. 1 The bar graph of material air permeability

Moisture Penetrability. The high altitude is characterized by both high working strength and long working time. It will produce a lot of sweat during the work. The material ought to be good at moisture penetrability so that it can absorb the sweat quickly and release it outward to create a dry microclimate on the skin, preventing cooling and chilling after physical activity [2]. This paper uses Dish method and gets result in Fig.2 through Equation (1). Both of the existing overalls' materials are very thin, so the water can easily pass through them. The other samples are good at moisture penetrability except 4#.

$$WVP=\frac{24(M2-M1)}{A*t}. \quad (1)$$

A=0.0054113m^2. T=the time between two record times (5 hours).

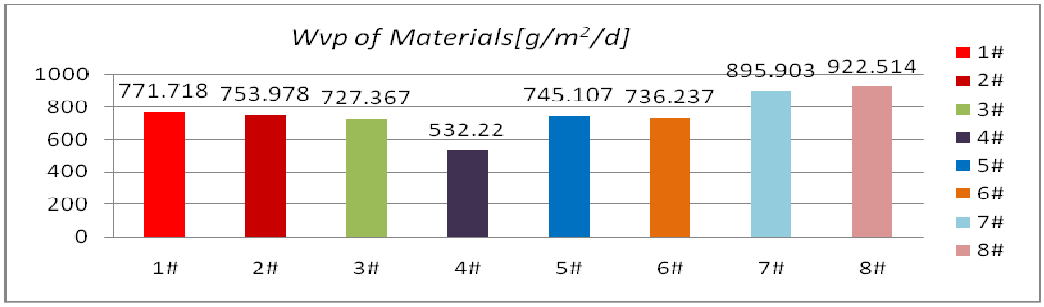


Fig.2 The Bar Graph of Materials' Moisture Penetrability

Waterproofness. Waterproofness is the capacity of material to avoid water passing though the cloth surface from the outside. The workers need use pistol to spray water which dabbles the overall onto the walls to clean the dirty. The existing overalls are made of P/C or 100% C, they are easily wetted and hard to dry. The cloth will stick to the skin, take away much heat and chill the body, even cause fever. So the waterproofness is critical for the overalls. This paper uses YG813 Fabric touch water locator to measure this performance. There are five levels (1, 2, 3, 4, 5). As the levels increase, the waterproofness advances.

Table 2 shows that all kinds of materials' performance are different. 1#, 4#, 5#, 7# and 8# perform well, reaching to lever 3~4. But the existing overalls have very poor performance, easily wetted with only level 1. This is a big drawback of existing overalls.

Table 2. The Waterproofness Level of Material Surface

	1#	*2#*	*3#*	*4#*	*5#*	*6#*	*7#*	*8#*
Level	4	1	1	4	3	1	4	4

Abrasive Resistance. The overall will wear as the cloth rub with the wool and walls. The tools are very heavy on the shoulder, causing the material on the shoulder damaged if the abrasive resistance is not good enough. Therefore, add the material with good abrasive resistance to the proper section is feasible. This paper uses Y522 Dise-type wearable instrument to record the rotational frequency.

Fig.3 shows that 4# performs extraordinary well, the yarn is not broken even it reaches 10,000 (use 10,000 as its number to make the bar graph). It can be added to local area of overall as to enhance total abrasive resistance.

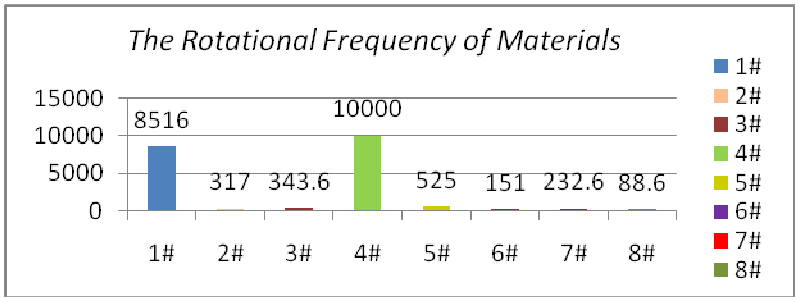


Fig.3 The Bar Graph of Abrasive Resistance

Antistatic Property. The static electricity will occur when material rub which results in dust absorption, sticking to skin, sizzling, bringing the discomfort and inelegance even the hurt [3]. It is common that the overall produces static electricity when the humidity is low. This paper uses YG(B)342E Fabric inductive static tester to get the dates.

The antistatic property depends on two factors—the static voltage and half-life period. Fig.4 and Fig.5 shows that 5# performs best with 0 s half-life period, and low static voltages. 7# is also a good choice.

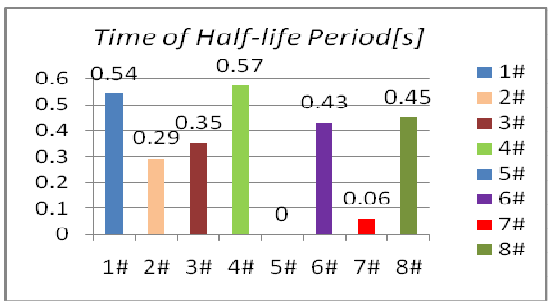


Fig.4 The Bar Graph of *Time of Half-life Period*

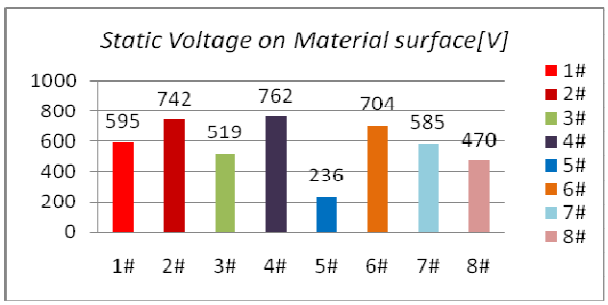


Fig. 5 The Bar Graph of Static Voltage on Material Surface

Discussion

(1) 6# and 8#'s air permeability are better than existing overalls materials. 5# and 7# are medium, 1# and 4# are worst; 7# and 8#'s moisture penetrability are best among all the alternative materials followed by 1#, 5# and 6#. 4# performs a little badly. But there is not obvious gap between each other; Waterproofness is one of the critical performances for overalls. 1#, 4# and 8# are best, 5# and 7# belong to second level. 6# follows; In terms of abrasive performance, 4# performs extraordinary well, reaching over 10,000. 1# reaches 8516, 5# follows; Observing the bar graph of half-life period and static voltage, 5# can be found best with 0s and 236 V.

(2) Other properties should be considered as the cleaning situation requires like warm ensure and smoothness. As Fig.1 shows that 1#'s air permeability is very bad, feeling stiff when touching it, being bad at antistatic property. 4#'s air permeability is bad too as well as its moisture penetrability. 6# is poor at waterproofness, can't provide basic warm in A/W with its small thickness. 7# performs badly on abrasive performance and very easily produces wrinkles which cannot disappear in short time, bringing very bad appearance. 8# will chill body if worn under cold environment. In conclusion, 5# can be a relatively good choice for the overall with its good comprehensive performances.

(3) On some special local areas, other materials can be used to meet a certain demand. For example, knees and elbows often rub during working, 1# and 4# can prevent its worn with their good abrasive performance. 6# and 8# can be added to oxter and back area to rapidly discharge unnecessary heat from body.

Conclusion

The particularity of the high altitude cleaning work requires the material to possess specific functions to meet the practical demands. Apart from the primary functions, analyze other performance is also necessary. The dates show that among all the alternative materials, Vinyl chloride-acrylonitrile copolymer with antistatic property and waterproofness finish has a good comprehensive performance. It can be chosen as the main material of overall, others can be used according to local areas' requirements in order to maximize functionality, finally to achieve a comfortable, safe and appropriate result.

Reference

[1] H.Y Lin and J. Zhang: Quality and Technical Supervision Research. (2010), p. 28.

[2] O. PAMUK, M. J. ABREU and Z.ÖNDOGAN: TEKST_L ve KONFEKS_YON. Vol. 3 (2008), p. 236.

[3] L. Zhang, G.Y Xie and H Zhang: Progress in Textile Science & Technology. (2010), p. 70.

© (2011) Trans Tech Publications, Switzerland
doi:10.4028/www.scientific.net/AMR.331.555

Study on Improvement of Manufacturing Cycle Effectiveness of Apparel Vendor——Case Study of Order Scheduling and Batch Feeding manegement and Control

Cheng Yang[1, a], Yixiong Yang[2,b] and Wennan Qi [3,c]

[1]Fashion Design and Engineering, Dong Hua University, Shanghai, 200051, China

[2] Fashion Design and Engineering, Dong Hua University, Shanghai, 200051, China

[3] Fashion Design and Engineering, Dong Hua University, Shanghai, 200051, China

[a]christine249@126.com, [b]yyx@dhu.edu.cn, [c]qwn@mail.dhu.edu.cn

Keywords: Manufacturing Cycle Effectiveness, Order Scheduling, Batch Feeding Control, Apparel Vendor, On Time Delivery.

Abstract. With the structural adjustment and industry transformation of the domestic apparel enterprises, as well as the rise of fast fashion, apparel manufacturing cycle time reduction and on time delivery rate have become performance indicators for brand enterprises to choose apparel vendors. In this paper, jeans processing factory is taken as a case study of apparel vendor. The improvement of production order scheduling and reasonable batch feeding process is analyzed to provide feasible programs for apparel vendors to achieve shorter manufacturing cycle, on time delivery and throughput increase.

Introduction

In recent years, the global market competition of apparel industry is being further intensified by the economic integration, cost increase of raw material and labor force, RMB appreciation, etc. [1]. To realize the quick response to the market, on one hand apparel enterprises, especially those operating fast fashion brands, set forth stricter requirements to the vendors on manufacturing cycle shortening and on time delivery. On the other hand, apparel vendors should meet the demand of brand buyers. Meanwhile in the post-financial-crisis era, they would face quite a lot of problems such as how to improve operation effectiveness, release the pressure of cost increase, raise the throughput and speed up the turnover rate to enhance the core competitiveness [2]. Therefore, the idea of quick response in supply chain is set up. It is the key point of raising the economic efficiency of apparel vendors to replace the idea of local, cost and experience with system, throughput and logic [3], so as to realize the manufacturing cycle time reduction, on-time-delivery rate rise and cash flow turnover increase.

Theory of MCE

MCE (Manufacturing Cycle Effectiveness) [4] is one of the key indicators of evaluating the production process operation performance.

The equation is as follows:

$MCE = P / Q$.

P (Process Time) = actual operational time; Q (Throughput Time) = process time (including quality control time) + moving time + queuing time or inventory time; $MCE \leqslant 1$.

The improvement of production operation performance can be implemented through rational resource planning and order scheduling to shorten the manufacturing cycle and decrease the number of WIP (work-in-process), so as to reduce inventory, release cash, increase throughput and build competitive advantage of vendors [5].

Case Study of the Jeans Processing Factory

Present Situations of the Factory. The research implementation object is a jeans processing factory (Factory Z), an apparel vendor mainly engaged in quick response OEM orders of women's wear for domestic sale. There are nearly 100 workers in the factory with 3 production lines, 20 workers in every line which can produce a capacity of 400 per day, in total about 30 000 per month of the factory. The order manufacturing cycle is 40 days (including rest days) when it refers to CMT order, while 60 days if it is FOB order. Due to the quick-response (QR) orders and additional orders, the on-time-delivery (OTD) rate in the factory was 35% before it takes the improvement implementation.

Reasons for the Low Efficiency. The main reasons for the late delivery reckoned by the factory's administrators are: fabrics and accessories late for FOB orders, with too much QR orders and additional orders of the best sellers which leads to the frequently changing production schedule; high order rework rate, workers' absence from work and low skill rate of new workers. It is found in the spot survey and data analysis that the administrators in factory Z make the production schedule and batch feeding plan mainly according to their experiences, ignoring the key constraints of throughput. Although the factory is always on the run, the situations of order manufacturing cycle out of control or delivery delay frequently occurs.

MCE Analysis of Factory Z. According to the capacity of every department in factory Z, take order K (2 000 pieces of five-pocket jean trousers) as a case, conduct a calculation of P_i, the processing time of every link (8 hours a week day):

Order placing/pattern making (P_1=240min) → Cutting (P_2=480min) → Fell seam / embroidery (P_3=480min) → Sewing (P_4=1 200min) → Bar-tack (P_5=480min) → Washing (P_6=480min) → Button sewing (P_7=480min) → Ironing (P_8=480min) → check / packaging (P_9=240min).

The production process and time-consuming of each link of order K is shown in Figure 1.

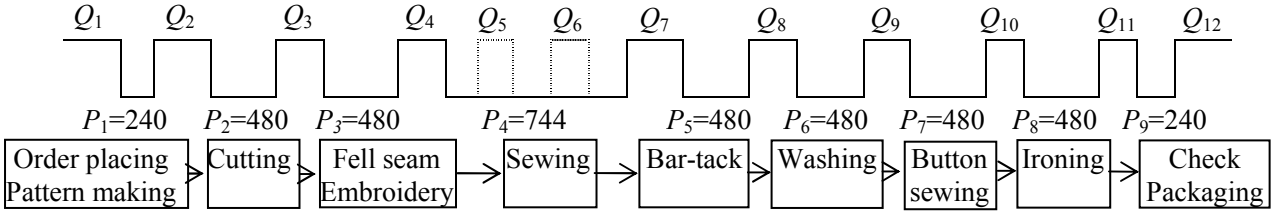


Figure 1 Order K production process and time-consuming of each link (unit: min)

Inner multiplication method is used to calculate the Floating Ratio of the production lines in the factory[6].

$$\text{Floating Ratio} = \text{Floating Time} / \text{Working Time} \times 100\%$$
$$= (1\text{-Processing Time}) / \text{Working Time} \times 100\%$$

The floating ratio in the factory is 38%, that is, the processing time of order K is (1-38%)×1 200mim(P_3) = 744min. Q_i represents the waiting, inventory and moving time. In addition, the average manufacturing cycle of CMT orders in the factory is 40 days (19 200min), so that MCE = (240+480+480+744+480+480+480+480+240) / 19 200 = 0.214.

Improvement Goal and Implementation Proposal

To raise the MCE of factory Z and to carry out the real-time control of order production, orders are scheduled according to the OTD, and buffer time is properly set. Order control is realized through color board management to shorten the manufacturing cycle, raise the OTD rate, increase the throughput, and improve the economic benefit (the technology route of MCE improvement is shown in Figure 2).

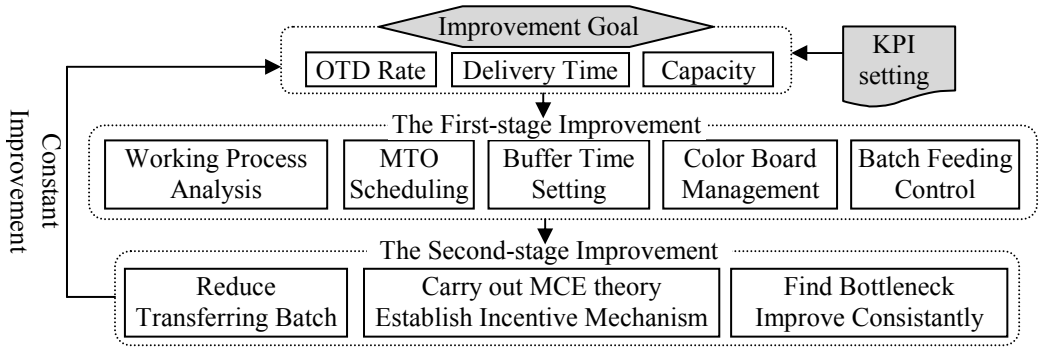


Figure 2 Technology route of MCE improvement

The goals of improvement implementation are as follows:

① OTD rate raised from 35% to 90% and above;

② Output increased by 10%;

③ Average manufacturing cycle shoterned by 20%.

Order Scheduling Based on Fast Fashion Brand Vendory Deliver Time. To raise the MCE and rationalize the production batch feeding, the orders in factory Z are organized on the premise of ensuring the on-time delivery of each order. According to the fast fashion brand vendor delivery time, orders are arranged with the asistance of computer to make the production lines smooth. Generally, due to the delivery time sequence, order insertion is not allowed. But under the condition of not affecting other orders's OTD, QR or resupply orders can be moved up. An improvement case of factory Z is shown in Table 1.

Table 1 Order scheduling case of factory Z based on delivery time (part)

Order No.	Category	Order Quantity	Agreed Delivery Date
100323142 dark	*Women's trousers*	*4 000*	*10-12-30*
100323142 light	*Women's trousers*	*4 000*	*10-12-30*
RTWK12163	Women's trousers	1 500	10-12-19
RTWK04D77	Women's trousers	1 300	**10-12-19**
RTWK12405	Women's trousers	1 190	**10-12-21**
TKCK12063	/	1 240	10-12-21
100320000 black	Knitted pants	3 774	10-12-24
100320000 dark blue	Knitted pants	3 764	10-12-24
110323010	*Women's trousers*	*4 035*	*11-01-08*
MAWQ12274	/	1 220	10-12-29
110223011	*Women's trousers*	*4 700*	*11-01-18*
100323071	Women's trousers	4 408	11-01-15

Note: a. tabulation date is December 15th in 2010;
b. the italic scripts with shadow represent the resupply or QR order.

In theory, the schedule in Table 1 can ensure the OTD of the orders, while in practice, buffer time, color board and WIP control should be considered as management means to gradually realize the OTD, manufacturing cycle shortened so as to enhance the vendor's ability to achieve orders, manufacture and negotiate the price.

Buffer Time Setting. Due to the uncertain factors such as stops and waiting caused by unbalanced pitch time, production loss brought by assortment change, workers' different degrees of proficiency in skill, workers' absence, breakdown of machinery etc., the manufacturing cycle time often exceeds the sum of standard hours of every working procedure. Therefore, buffer time is necessary to set to ensure the smooth of the manufacturing process and the OTD [7]. Buffer time should be set proper to avoid the process chaos caused by too long or too short buffer time (shown in Figure 3).

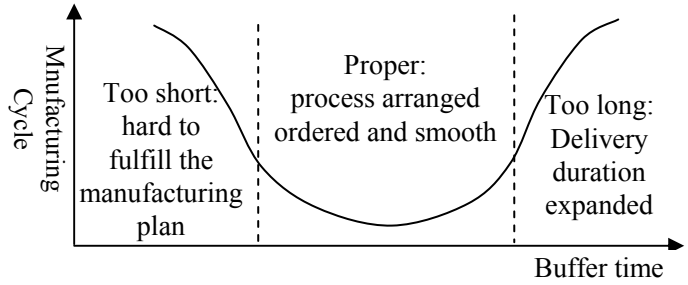


Figure 4 Effect of the buffer time setting on the manufacturing cycle
Source: Zhiping Zhao, Mingzhe Chen. Guidebook for Lean TOC Practice. Haitian Publishing House, 2009:58.

The buffer time determination accordance at the first stage of improvement implementation for factory Z is as follows:

The orders listed in Table 1 can be accomplished within 10 days (only processing time) according to the sum of the standard hours of each working procedure (take batch transferring into consideration). Buffer time is set twice of the sum of standard hours and had better be the multiple of 3(considering the 3 buffer state demonstrated below), that is, 21 days (without break days). The MCE on this occasion is 10÷21=0.476. As the improvement proceeds, buffer time could be shortened gradually in the production schedule control to raise the MCE.

Order schedule based on the buffer state. Buffer state demonstrates the proceeding of an order, which can be calculated as buffer occupation rate (B): B = {1 – [(Agreed Delivery Date (D_j) – The Present Date (D_i) – Break Days (d) + 1) / Buffer Time (T_B)]} ×100%.

The implementation state of orders can be monitored by the color code system composed of green, yellow, red and black through which orders are scheduled by the delivery urgency intuitively [8]. Orders with B ≤ 33% are turned to be green, while with 33% <B ≤ 66% yellow, with 66%<B ≤ 100% red and B>100% black (shown in Figure 5).

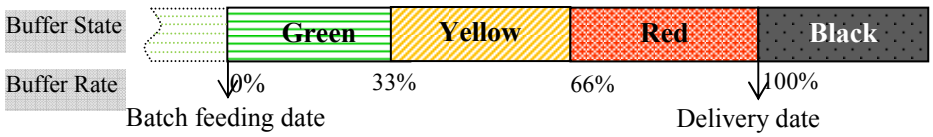


Figure 5 Relationship between the buffer occupation and the buffer state

To implement the order scheduling through color code system, factory Z sets buffer management boards in the workroom of headquarter and workshops to inform the workers of the proceeding of orders and enable them to arrange and adjust orders to realize the goal of decreasing the rate of red and black orders to below 10%.

As shown in Table 2, according to the 21 days' buffer time (break days excluded), the batch feeding date of CMT orders is set to be 21 days ahead of the delivery date[1]. After calculating the buffer occupation rate and marking the colors of orders, the order buffer occupation rate is compared with the proceeding rate of working procedure. ① If the buffer occupation is in the red section, the order might be delayed and should be adjusted to ensure the OTD. If the buffer occupation is in the yellow or green section, the order might be accomplished in time. ② If the working procedure proceeding rate is less than the buffer occupation rate, the proceeding is slower than it should be. If the working procedure proceeding rate is more than the buffer occupation rate, proceeding is faster than it should be so that the order might be accomplished in advance.

[1] Note: a. 6 workdays in factory Z; b. Batches of resupply and QR orders are fed 10~20% in advance.

Table 2 Buffer management table of factory Z (example)

Order No.	Order Quantity	Batch Feeding Date	Agreed Delivery Time	Working Procedure Proceeding Rate	Present Working Procedure	Buffer Occupation Rate
100323142 dark	*4 000*	*10-11-25*	*10-12-30*	*100%*	*Finished*	***58%***
100323142 light	*4 000*	*10-11-25*	*10-12-30*	*100%*	*Finished*	***58%***
RTWK12163	1 500	10-11-26	10-12-19	64%	Washing	**81%**
RTWK04D77	1 300	10-11-26	10-12-19	64%	Washing	**81%**
RTWK12405	1 190	10-11-27	10-12-21	57%	Loosing Thread 1	**76%**
TKCK12063	1 240	10-11-27	10-12-21	57%	Bar-tack	**76%**
100320000 black	3 774	10-12-01	10-12-24	85%	Flat Ironing	**62%**
100320000 dark blue	3 764	10-12-01	10-12-24	64%	Washing	**62%**
110323010	*4 035*	*10-12-05*	*11-01-08*	*31%*	*Sewing Group 3*	***30%***
MAWQ12274	1 220	10-12-05	10-12-29	57%	Loosing Thread 1	**43%**
110223011	*4 700*	*10-12-14*	*11-01-18*	*30%*	*Sewing Group 2*	***6%***
100323071	4 408	10-12-21	11-01-15	0%	Precommissioning	**-26%**

Note: a. Tabulation date: 2010/12/15.
b. Italic and shaded parts are resupply and QR orders.

Batch feeding management and control. Before improvement implementation, batch feeding size is determined by experience and instinct, which always leads to over size of batch feeding that causes the overstock of IP, congestion in production line and delivery time delay, etc.. To drive the production line to be smooth, improvement and control of batch feeding is conducted in factory Z. Reasonable batch feeding control can ensure that the workers in the field of production focus on what they should do or what is effective, so that to unobstruct the material flow, decrease the stock of WIP, increase the cash flow and eventually shortern the MCE [9]. Besides computer tools and production boards, improvement solution of transforming the 3 graded management and control to 1 graded one is put forth according to the present situation of factory Z (shown in Fig.6).

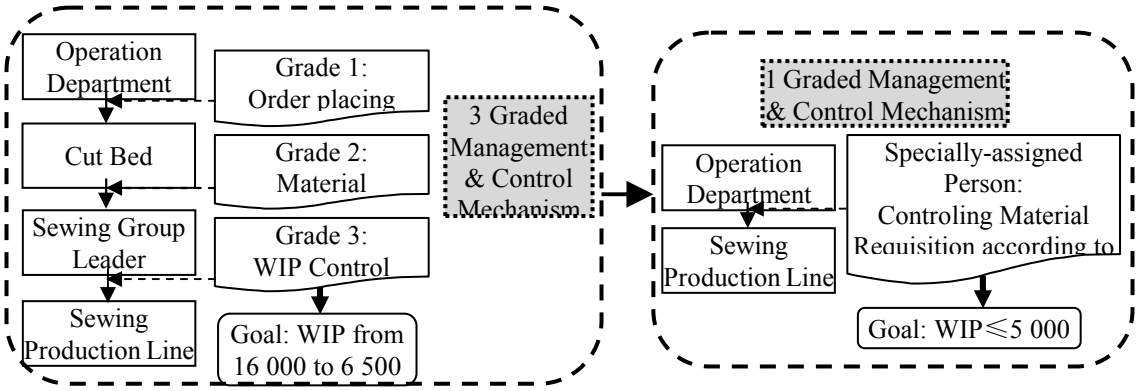


Figure 6 The improvement solution of batch feeding management & control in factory Z

As shown in Fig. 6, the core of batch feeding management and control is to limit the quantity of WIP. The daily output of the factory reaches 1 300. Therefore, the first step of 3 graded management and control is to reduce the WIP quantity from 16 000 to 6 500, that is to say, to set a 5-day buffer. After the preliminary goal being achieved, 1 graded management and control mechanism is to be implement to further reduce the quantity of WIP to 5 000.

Achievement of improvement. After 2 months' improvement implementation, the OTD rate of factory Z is raised from 35% to 95%. Monthly output increases from 30 000 to 40 000 by 33%. The average manufacturing cycle of CMT orders decreased to 26 days by 35%, that the MCE is 0.385 (10/26) which is 0.171 higher. The WIP in sewing line is reduced from 16 000 to 6 300 (shown in Fig.7 and Fig.8). In conclusion, factory Z's ability of accomplishing the QR orders and achieving overall profitability is enhanced.

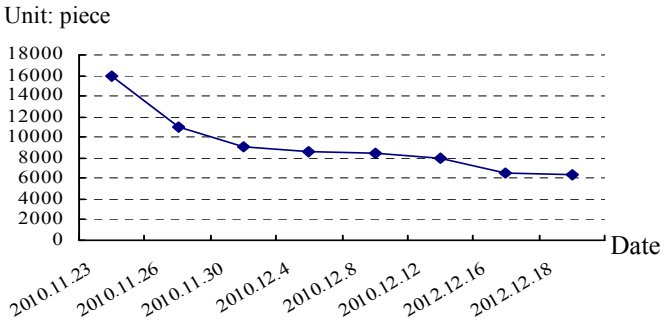


Figure 7 Quantity change of WIP in the sewing line of factory Z



Figure 8 The contrast of WIP state in the workshop before and after improvement

Summary

In the processing cycle, queuing and waiting time take a larger part. In the apparel manufacturing process, reasonable buffer time setting, batch feeding management and WIP control are vital methods of raising MCE.

According to the MCE theory, through the improvement implementation in factory Z, the buffer management and batch feeding management and control mechanism are established to realize the goal of raising OTD rate, reducing WIP quantity and increasing throughput.

MCE should be improved constantly. Based on the preliminary implementation, measures such as reducing the batch size, analyzing the reason of red and black orders and releasing the bottleneck will further enhance the competitive advantage of the factory among apparel vendors, in the meanwhile, to satisfy the OTD and resupply requirement of apparel buyer, finally achieving the win-win situation of the buyers and vendors.

References

[1] 2009-2010 China Garment Industry Development Report. Beijing: China Textile & Apparel Press, 2010.4:115.

[2] Zhongfan Shui. Post-crisi-era: new trend • new strategy • new opportunity (Edition 1). Beijing: China Commercial Press, 2010.1.

[3] Lihua Xiao, Nicheng Tong, Yongsheng Han. Scientific Operations: build brand-centric quick-responsed supply chain. Beijing: China Economics Publishing House, 2008.11.

[4] Zhiping Zhao, Mingzhe Chen. Lean TOC. Shenzhen: Haitian Press, 2009:23,58.

[5] Murakami Sato. Make Your Company Run: TOC management operation manual. Beijing University Press, 2004.

[6] Yixiong Yang. Apparel Production Management. Shanghai: Donghua University Press, 2005:186.

[7] Eli Goldratt. Critical Chain. Beijing: Publishing House of Electronics Industry, 2009:122-138.

[8] Jun-Huei Lee, Jia-Ging Chang, Chih-Hung Tsai, Rong-Kwei Li.Research on enhancement of TOC Simplified Drum-Buffer-Rope system using novel generic procedures[J]. Expert Systems with Applications, 2010(37): 3747- 3754.

[9] Tao Tao, Shilong Xiang. The application of TOC in furniture production[J]. China Forest Products Industry, 2010(1):46-50.

© (2011) Trans Tech Publications, Switzerland
doi:10.4028/www.scientific.net/AMR.331.561

Application of Pattern Recognition System in the Automatic Generation Pattern Technology

Qiu Li [1,a],Chen Xiaodong[2,b]

[1]College of Textile and Light Industry, Inner Mongolia University of Technology, Hohhot, China

[2]College of Textile and Light Industry, Inner Mongolia University of Technology, Hohhot,China

[a] 540601336@qq.com,[b] 178031664@qq.com

Key words: pattern recognition, expert model, pattern, apparel CAD

Abstract: The apparel CAD intelligence is one development direction for apparel CAD technology. Automatic generation of apparel pattern technology is the embodiment of apparel CAD intelligence. This study applied pattern recognition system into the automatic generation pattern technology for the purpose that the according apparel structure chart will be generated directly under the premise of being given the apparel pattern pictures. That is to say, to achieve automatic generation of sample plates. Sophisticated application of this technology will improve the design efficiency which can adapt to the needs of modern apparel industry development.

Introduction

The apparel CAD system at present is aided design system, which designs in a manner of man-machine interaction. The fair or foul of the pattern depends entirely on the experience and proficiency of designers.

With the development of new generation of computers and artificial intelligence technology, knowledge engineering and expert system gradually penetrate into the apparel CAD system. Apparel CAD intelligence becomes a development direction for apparel CAD Technology[1]. Automatic generation of apparel pattern technology is the embodiment of apparel CAD intelligence, whose purpose is to realize the input of individual parameters and directly generate two-dimensional patterns, and thus improve the design efficiency and rapid response capabilities of apparel enterprises in order to meet the development needs of modern apparel industry.

This paper studies how to directly generate the according apparel structure chart under the premise of being given the apparel pattern chart, which is to complete automatic patterns. The pattern system of apparel CAD should give full play to its advantage in the apparel industry. To achieve automatic generation of patterns, you first need to classify and screen the apparel patterns, and then choose the corresponding apparel structure chart according to categories after screening. The screening process of the apparel pattern is the pattern recognition system.



Figure 1
Shirt collar

The Application of Pattern Recognition System

the information identification hindrance of computers leads to its intelligence hindrance in the application of apparel CAD. For example, for the collar model in Figure 1-1, we can judge that it is a collar model for shirts by naked eyes, while computers can not complete the screening process initiatively. Because of this intelligence hindrance, the current apparel CAD doesn't have the recognition function for apparel patterns, as a result, it can not

conduct the corresponding pattern design generation, making the apparel CAD depend on a lot of manual operations. It can not reduce production time or improve production efficiency, which limits the application and popularization of apparel CAD.

The pattern recognition theory is applied to the apparel CAD; apparel pattern recognition can be conducted through the analysis and the establishment of the pattern models. See the pattern recognition system shown in Figure 1-2; the pattern acquisition completes the acquisition of patterns. The combination of feature extraction realizes the transformation from pattern space to feature space, and the dimension has been compressed effectively [2].

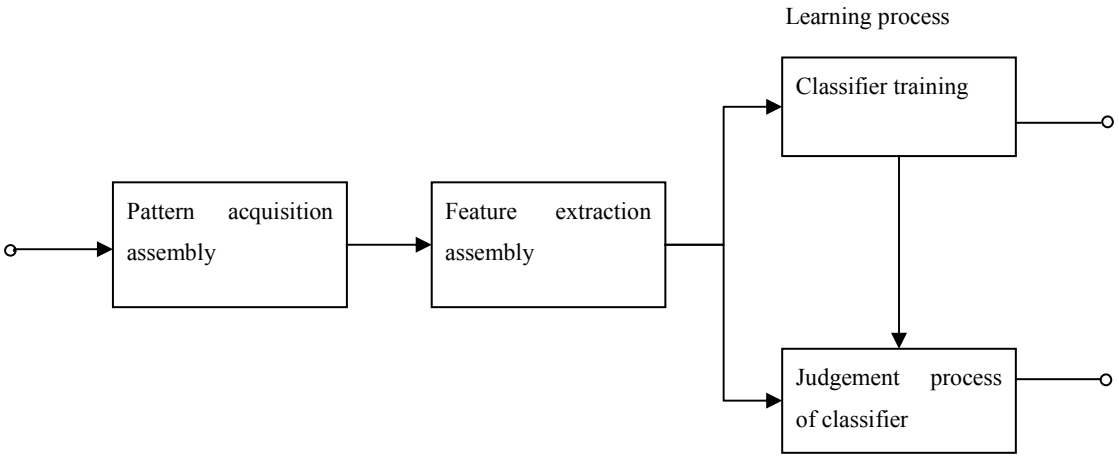


Figure 1-2 Pattern recognition system

The classifier should realize the classification and judgment to patterns of unknown types and attributes. In the pattern recognition system, the classifier is designed to aggregate and stock the feature model that is to be established; classifier is used to establish feature pattern to a particular pattern [3]. On this basis, conduct feature extraction to the collected pattern assembly, and the category of the pattern assembly can be judged through classifier. The systematic procedure can be applied to the automatic generation pattern system. The main method is to conduct feature modeling to the apparel components that can characterize the category of apparel patterns in order to extract the feature information of patterns (classifier training), and combine the pattern types to form the classifier. In this way, the given apparel pattern can be formed, which means a systematic process to judge the pattern types. Conduct the pattern type judgment, and compare it with the expert pattern that has been designed, then the structure chart of this pattern type can be used.

At the same time, expert pattern can be formed through the analysis and establishment of structural model, then form the expert pattern library. This combination is the core of automatic generation technology of apparel patterns, and automatically generated apparel pattern technology is one of the future developmental directions of CAD [5]. That is to say, the application of pattern recognition technology in apparel CAD intelligentizes the apparel, and thus testifies that pattern recognition technology can intelligentize apparel CAD.

Establish the expert pattern library

the expert system can store prior summarized expert knowledge which has been represented by a certain format (to form a knowledge base), and it also has a inference mechanism that experts solve practical problems (to form an inference system) [4].

At present, the expert system mainly adopts the rule-based deduct technology. The system has the reasoning ability. It can deduct the needed answers according to the stored formula and knowledge. In the apparel CAD system, we can learn from outstanding fashion designers to constitute a system of automatic pattern design and layout. The automatic generation of apparel

pattern is to make use of the reasoning technology of artificial intelligence and design garment pieces through the creation of knowledge base and the means of logical reasoning mechanism. According to the universality and individuality of apparel, the experience of pattern experts can be summarized rule base, database and method base as the knowledge base, users can choose and determine the pattern and structure of apparel by the means of man-machine interaction. The computer can search in the knowledge base according to the structural features that users select, then conduct a series of calculation, using the pattern rules, methods and data, and ultimately generate a reasonable pattern.

The technical route of the application of Pattern Recognition System in the automatically generated pattern technology

Expert database and pattern recognition system are combined to form a system which can screen the apparel patterns. Besides that, the system could also invoke the corresponding patterns to achieve the effects of various changes of one pattern as well as automatic generation of patterns, which is the technical core of automatically generated pattern system.

The technical route to be taken

Take the pattern recognition as the core, the parameterized patter design as the assistance, combined with other technologies, and ultimately realize the automatic generation of apparel pattern. This idea of automatically generated pattern system in this paper is as follows Figure 2-1:

Process decomposition and implementation

Process 1: Scan the profile of the image--contour extraction. Using the image contour extraction in apparel pattern recognition technology the fashion drawing graphic contour which can be applied in the apparel pattern recognition will be obtained.

Process 2: Select the key point -apparel components decomposition (be shown in the figure 2-1).

Process 3: extract feature data. Obtain the pattern graphs with key points from process 2. Extract feature data according to the arranged feature data extraction means and transmit the extracted data to the feature database to conduct further judgment on the features, and then distinguish the concrete type of apparel components.

Process 4: Match the feature data obtained in the process 3 with the established feature database.

Process 5: Set the expert pattern data which matches the pattern information determined in process 4, each set or several sets of expert pattern data correspond to the only determined pattern. When a certain pattern is determined, the expert pattern data should be called correspondingly.

Process 6: from pattern selection to pattern data output. Combine the type data and the pattern categories, search and call in the established type database to determine the corresponding type data of pattern categories.

Process 7: generate the conversion ratio. All data output after type selection are all type data, which outputs in two directions: one is to combine with expert pattern data and pattern graphic data; the other is to compare with the shared dimensional data in the obtained type data and form the conversion ratio.

Process 8: Transform pattern graphic data into pattern data through conversion ratio. Since the pattern graph data comes from the pattern graphs, we do not know its scaling, so the pattern graph data can not be used directly. In the previous process, the conversion ratio has been formed, which is to transform all data in the pattern graphs into viable pattern data.

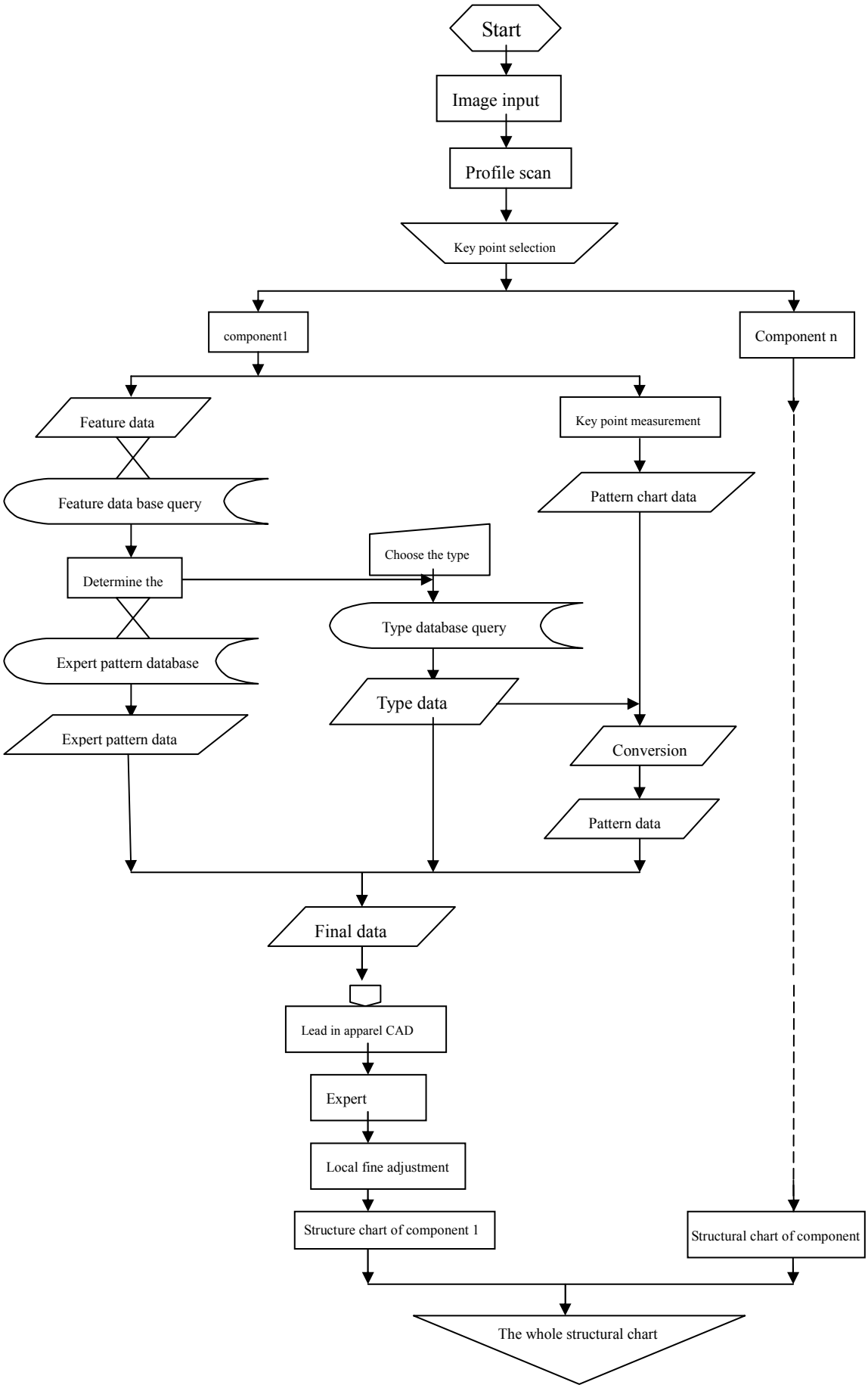


Figure 2-1 Flow chart of automatically generated pattern system

Process 9: generate the final data and import the apparel CAD. Aggregate the style data, shape data and pattern data to produce the final data. And then import the data into a certain apparel CAD pattern drawing system. The previously mentioned final data is the key point coordinates of expert patterns. After the import of apparel CAD, link the key points and generate the apparel components structural graphs that correspond to pattern types, which are expert patterns. Process 10: manually conduct fine tuning to the generated expert pattern to increase the reasonability of the pattern. After manual fine tuning, we can get the final pattern of apparel components, and then it will be aggregated to generate the whole structural graphs. Henceforth, the whole processes of automatically generated pattern system have been completed.

Conclusion

The technology of automatically generated apparel pattern is an embodiment of apparel CAD intelligence, and it is also an inevitable product of apparel CAD development. This is a new field of technology, but there are already more and more scholars beginning to set foot in this field. This paper proposes to apply the pattern recognition system in the automatically generated pattern technology. As a result, under the premise of being given the apparel pattern graphs, the corresponding apparel structural graphs can be generated directly, that is to say, to achieve the purpose of automatic generation of patterns, designing the flow path of automatically generated patterns and explaining the adopted technical route. The mature application of this technology will improve the design efficiency to meet the requirements of the development of modern apparel industry; as a result, it has good prospects for future development

References

[1] Zou Ping .On Application of CAD Technology in Modern Garment Field and its Developing Tendency. Journal of Zhejiang textile & fashion college. 2007 6(1)

[2] Liu rei-qi. Clothing pattern design principle and technology(Ladies article) . Beijing. China textile press.2005(9)

[3] Wang xiu-zhi. Xu jing. The ideas about development pattern computer generated garment expert system automatically. science &technology information. 2007 (8)

[4] Yang Xue-mei Xu Xiao .Parameterized design of block pattern parts of garment industry. Knitting industries.

[5] Huang Yan-hua. sun wen-lei. A new method of 2D view feature automatic recognizing. Manufacturing automation. 2003.25(z1)

[6] He Yan CAD/CAM diffusion and infusion in the US apparel industry,Department of Family and Consumer Sciences, California State University, Long Beach, California, USA, and Susan S. Florio Accepted May.2006.

© (2011) Trans Tech Publications, Switzerland
doi:10.4028/www.scientific.net/AMR.331.566

Research on bra constitute and performance evaluation

Hui Shi[1, 2, a], Jianping Wang[1, b], Zhiyun Wu[2, c] and Xiaona Chen [1, d]

[1]Fashion institute of Donghua University, No.1882yan'an west road, Shanghai, Changning District, 200051, China

[2]College of Textile and Light Industry of Inner Mongolia University of Technology, No.49 Ai'min street, Hohhot, Xincheng District, 010051, China

[a]shihui180206@126.com,[b]wangjp@dhu.edu.cn,[c]willie323@163.com, [d]chen_xn@yahoo.cn

Keywords：bra,structure,performance, 3D virtual technology

Abstract. The study reviewed the research of the structure and performance test on bra product and made an outlook for further research .It concluded the main research direction for further exploration should be to study digital and functional of bra product.

Introduction

Exactly when the modern-day bra came to be is up for debate, but it's generally agreed that the first mention of the word "brassiere" appeared in a Vogue magazine ad in October 1907.

Danish Fashion historian Rudolf Kristian Albert Broby-Johansen predicted in an article in May 1969 titled "Obituary for the Bra" that bras would soon go out of fashion. Approximately 90% of women in North American wear a bra as of 2006. Brassieres are worn by the great majority of women in modern society. There are now unprecedented array of styles and models, including those that barely cover the breasts, barely provide support, and the various sports bras which often function as outerwear. Women, fashion and health professionals, feminists appear to be increasingly questioning its place and function.

Many researches and bra manufactures have engaged their efforts in the studies on women's torso involving the analyses on basic physical structure, biomechanics of breast, dynamical mechanical behavior of breasts, dynamic simulation of breasts displacement and bra deformation, pressure and stress distributions to explore perfect functional products with multiple actions.

This paper made an overview on the current researches and achievements on bra's structure and performance test, the methodologies and innovation in the exploration were introduced such as 3d body scan, 3D dynamic simulation, and the innovation of pattern structure and performance test method and experimental apparatus.

Bra structure study

3D body measurements and human body modeling study

Outlined of 3D body measurement methods. There are many methods in 3d body measuring such as Triangle measuring, Moll-fringe method, Penetrate type principle equipment, Reflection ranging measurement, TC^2Layered profilometry imaging etc. The imaging theory: lights projected onto body surface is captured through the application of photosensitive equipment,such as laser, white and infrared ray,form images on body surface,using computer image processing to describe the human body three-dimensional characteristics. The studies include establish standard Mannequin, model of the human body and garment size designations, 3D garment CAD and super dimension garment CAD, virtual garment and virtual garment show, MTM, bodily form, garment data card etc.

Research on dynamic posture anthropometric. 3D body scanning can provide higher for standard static posture measurement of human body, but it can't provide faster and higher precision results for dynamic posture measurement.

liuchi [1]said：Although the 3D body scanner collects data almost instantaneously and without physical contact with the target surface, the readings taken in respect of dynamic poses showed significant variations from manually-taken measurements, with discrepancies as large as 6.8 cm over a 16cm distance. The scanning techniques and the associated analytical software have been optimized for specific, conventional body postures. When scanners are used to take measurements of unusual anthropometric configurations, such as when a body assumes a dynamic posture, which might be required to assist in the design of clothing used in particular sporting activities, and then the measurements taken using a scanner are not necessarily from optimal locations.

Elizabeth Bye [2] found all seam line alignment scores were significantly lower with 3D scan models than live models. Judges had significantly lower ability to score dart placement with 3D scan models than with live models. When analyzing seam and dart alignment with body landmarks is an important part of the fit analysis, judges may have difficulty with assessment.

Research on the relationship between moving body and chest deformation. Chang Li-xia[3]studied the female breast forms based on the dynamic analysis. She said in back, sensors are placed under the straps to measure how much pressure they exert on the shoulders, and electrodes are placed on the upper torso and the neck to monitor the bra's effects on muscle activity. Small, light-emitting diodes are placed in front of the sternum, nipples and bra cups to measure the subject's breast and torso movements (Figure1).

X. Zhang and Y. Li, from the Hong Kong Polytechnic University, made an investigate on the breasts and sports bra by using mechanical mechanisms theory involved in the dynamic contact between breast and bra experimentally and theoretically (Figure2).



Figure 1 Human movement measuring method

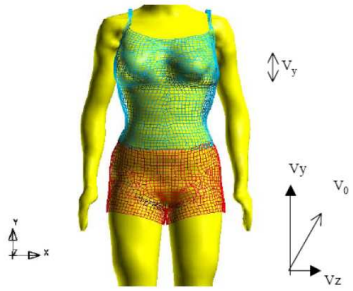


Figure 2 Dynamic 3D body simulations

Jian-Ping Wang [4] used a suitable deformation method Free-form deformation (FFD) in her study to enable the object deformation by deforming the space around them which method was an important and a powerful modeling tool in both computer animation and geometric modeling (Figure3).

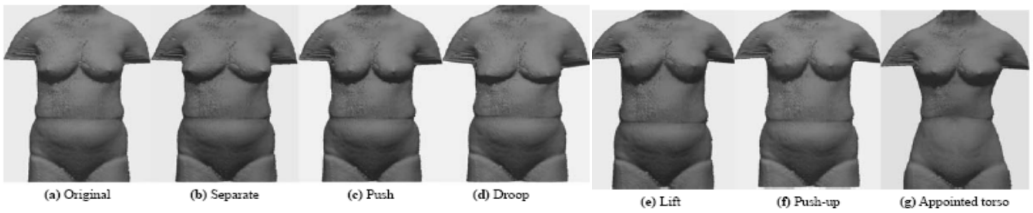


Figure 3 Chest virtual deformations

Static anthropometric which used traditional contact anthropometric develops non-contact anthropometric with fast and accurate data. The theories such as 3D dynamic simulation, electronic sensor and dynamics, mechanical kinematics, biomedical mechanical and so on were widely introduced in the field.

Bra pattern method research

Plane prototype model. Plane prototype model is the foundation of parameterized and modeling technology. Flat pattern studied on technology development and solve practical problems in production factory. So the study should solve the actual problem in industrial production. Research direction should be Comprehensive factors on structure design as structure and fabrics, function etc. or providing easy operation method, rapid, efficient and accurate industrialization model.

Application of 3d virtual technology and math diagram analysis methods. K. L. Yick's paper [5] proposed on an example-based method for designing molded bra cups. Using an example-based method, virtual master moulds were constructed based on the 3D surfaces of the investigated bra cups after eliminating the style lines and size differences. Then a new bra cup design can be developed from the master moulds, either by drawing the style lines in the virtual environment or using scissors to cut the moulded plastic shot along the desired style lines. Different sizes can also be made by grading the wire frame model in 3D manner (Figure4).

Xiao gang Chen [6] presents a mathematical model to determine the pattern geometry for the front panel of female body armor. The raised bust area was divided into seven different parts for the modeling, using the simplest surfaces possible. This mathematical model takes the body size and bra size as the input, and the output is the profile of the front pattern of the female body armor. Angle-interlock woven fabric off the potential to make female body armor as it can form integrally the required dome shape without cutting or molding because of its extraordinary mold ability (Figure5).

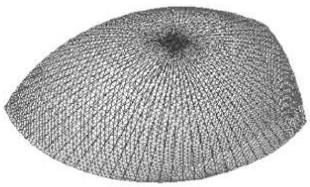


Figure 4 A wire frame presentation of a bra cup

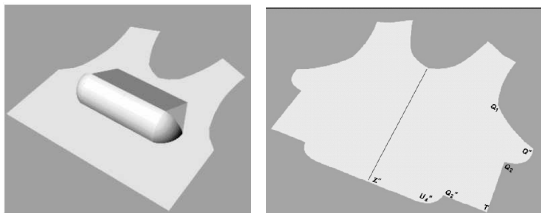


Figure 5 3D forming process of Angle-interlock woven fabric female body armor

Three-dimensional computer technology, mathematical modeling geometry method and graphics technology etc. are widely used and expanded field of garment structure design research greatly. The purpose of most research is to provide technical foundation the realization of MTM.

Research of Bra performance evaluation

The current study focused on the index test of dress on and material performance. The research should focus on the equipment changes and the reasons, and the test conditions, the condition of experiments, instruments, plan, test items and evaluation methods.

RongZheng [7, 8] studied knitted bra tension and pressure. Seamless knitting is a new technology; aim at identifying the key knitting parameter sand experimentally investigating their relationships with the knitted bra tension provides the new knowledge of seamless knitted bra fitting and the resulted bra pressure, as well as some guidelines for seamless knitted product design and manufacturing as shown in Figure 6.

C. H. M. Hardaker [9] thought garment fit was further assessed through wearer trials where the performance of a garment was evaluated over a set period of time. K-A Bowles [10] aimed to quantify the breast support wearing and purchasing habits of young women and to assess factors that affect their sports bra usage during physical activity. Kit-lun Yick [11] studied thermal–mechanical properties of polyurethane foam and the three-dimensional shape of molded bra cups (Figure 7).



Figure 6 Wire mould cup bra and seamless knitting bra

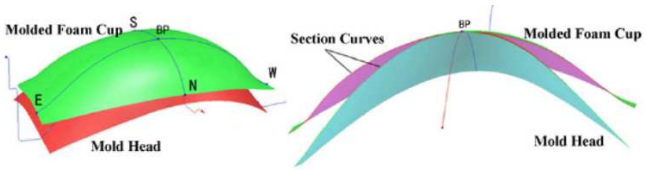


Figure 7 3D cover cup model

In order to develop the structure and properties of the bra, researchers need to make further study on flowing aspects.

Based on ergonomics. Including effects of skins stretch to dynamic modeling, effects of torso's distortion to dynamic modeling, human psychological feeling besides the biochemical and biomechanics analyses, Special bodily form feature research (obesity, larger chest).

Based on 3d virtual technology and digital garment. Including bra's dynamic balance properties and the interactive factors, combining size and style and fabric and functional factors of 3-d virtual research, bra specification design and grading.

Based on the comfort evaluation. Including evaluation method and testing equipment complete or innovation, relevant comfort indicators test and research on dress dynamic state, study on mold cup bras and sports bra.

References

[1] Liu Chi, Richard Kennon. International Journal of Clothing Science and Technology, 2006, 18（3）: 166-178.

[2] Elizabeth Bye,Ellen McKinney. International Journal of Clothing Science and Technology, 2010, 22（2/3）: 88-100.

[3] Chang Li-xia, Gao Wei-dong. Bioinformatics and Biomedical Engineering, ICBBE 2009. 3rd International Conference on page(s): 1 – 4.

[4] Jian Ping Wang and Wei Yuan Zhang. International Journal of Clothing Science and Technology Vol. 19 No. 5, 2007 pp. 361-373.

[5] K. L. Yick*, S. P. Ng, X. J. Zhou, W. Yu, D. Chan. Fibers and Polymers 2008, Vol.9, No.5, 653-658.

[6] Xiaogang Chen, Dan Yang. Textile Research Journal 2010Vol 80(15): 1589–1601.

[7] Rong Zheng, Winnie Yu*, Jintu Fan. Fibers and Polymers. 2008, Vol.9, No.6, 785-792.

[8] Rong Zheng, Winnie Yu*, Jintu Fan. Fibers and Polymers 2009, Vol.10, No.1, 124-131.

[9] C. H. M. Hardaker and G.J.W. Fozzard. International Journal of Clothing Science and Technology, Vol. 9 No. 4, 1997, pp. 311-325.

[10] K-A Bowles, J R Steele, B Munro. British Journal of Sports Medicine. 2008 42: 670-673

[11] Kit-lun Yick, Long Wu, Joanne Yip, Sun-pui Ng, Winnie Yu. Journal of Materials Processing Technology 210 (2010) :116–121

© (2011) Trans Tech Publications, Switzerland
doi:10.4028/www.scientific.net/AMR.331.570

Research on Consumer Motivation for Luxury Products in China

Zhe Zheng[1,2,a]

[1] School of Textile and Fashion Engineering, Soochow University, Suzhou, Jiangsu, 215021, China

[2] College of Fashion, Zhejiang Sci-Tech University, Hangzhou, Zhejiang, 310018, China

[a]aggiezz@163.com

Keywords: Luxury Product, Consumption, Motivation, Chinese Consumer.

Abstract. Chinese people who have become well off are experiencing a shift of consumption concept from traditional and practical style to luxurious style. It is time to understand the Chinese consumption demand and behavior in luxury products. Based on the previous researches and by way of intensive talks and questionnaire survey, this article takes advantage of Statistical Product and Service Solutions (SPSS) to conduct factor analysis, then to conclude the consumer motivation for luxury products in China as four main factors: "active social motivation", "passive social motivation", "desirable personal motivation", and "hedonistic personal motivation".

Introduction

According to the latest report released by the World Luxury Association, the consumption of luxury products in 2008 has amounted to 8.6 billion dollars in China, taking up 25% of the world market. It overtakes America for the first time, and after Japan, becomes the second largest country in consumption of luxury products in the world. It is estimated that by the year of 2015, China will have shared 32% of the world market of luxury products, dwarfing Japan and ranking first. [1] It is crucial time to understand and master Chinese consumer's demands and motivation on luxury products.

Research Review

Western Research on Purchase Motivation of Luxury Products. In terms of purchase motivation of luxury products, Western scholars mainly focus their researches on social motivation and personal motivation.

Veblen (1899) for the first time put forward the conspicuous motivation of luxury consumption, after investigating the consumption patterns of leisure class. It was his opinion that consumers bought luxury products mainly for making a show, and show of wealth and leisure can win a better social position. [2] He considered it in view of social motivation.

Leibenstein(1950) raised three motivations as conformity, uniqueness and conspicuousness, thus expanded the longitude of social motivation. [3] He said conformity is to gain the social value of a group by identity of most people; uniqueness is to achieve a unique value by feel different; and conspicuousness is to obtain a vain value by making a show of wealth and social position.

In the way of personal motivation, Dubois and Laurent (1994) developed a scale with 34 items, which targeted French students to carry on empirical study on luxury attitude. For the first time, they pointed out that apart from social motivation; there is personal motivation in the luxury consumption, which is hedonism and perfectism. They advanced that hedonist is for one kind of self-realization and emotional happiness, while perfectism is for a high-quality grantee and value. [4]

Vigneron and Johnson (1999) adopted a concept related to self-orientation, and after subdividing the purchase motivation of consumers, they classified consumers into public self-conscious and private self-conscious, and put forward five purchase motivation: conspicuousness, uniqueness, bandwagon, hedonism and perfectism. They also combined social motivation and personal motivation, and thought that five motivations were involved in the consumption of luxury products. [5]

Research on Chinese purchase motivation of luxury products. Nancy Y Wong and Aaron C Ahuvia (1998) shifted their focus to the luxury market in East Asia. They compared the difference of oriental and western cultures from the angle of trans-culture. By analysis of self-caring, social status, bandwagon pressure and meaning of products, they advanced preliminarily the purchase motivation of luxury products in the oriental culture.

Zhu Xiaohui (2006) brought forward on the basis of western motivation structure, the revising model of the purchase motivation with empirical study. He classified the motivation of Chinese consumers into social purchase motivation and personal purchase motivation. The social purchase motivation includes conspicuousness, bandwagon, social life, status representation, while the personal purchase motivation includes exquisite quality, self-pleasing and self-presenting. During his research, he found that there is no leading and internal representation in Chinese motivation, which has status symbol instead. [6]

Research Method

Interview. Based on the previous researches, the author talked with some consumers who have had the experience of buying luxury products or have luxury products of his/her own. By way of intensive talks, we made the options in the questionnaire.

Questionnaire.

- **Design of the questionnaire.** The survey is carried on with a self-ordained questionnaire named "Research on Consumer motivation for Luxury Products in China". The questionnaire is a sum scale (Likert Scale) using 5 points in each item, namely from "strongly agree" (marked 1) to "strongly disagree" (marked 5). The lower scores questioners register in the questionnaire, the stronger motivation they have for luxury products. This article takes advantage of Statistical Product and Service Solutions (SPSS) to conduct factor analysis, then to conclude the consumer motivation for luxury products in China.
- **Sampling.** According to the latest rankings of luxury cities in China, Beijing, Shanghai, and Hangzhou were the top three [7], so the location of this survey for the three cities. The object sampled in the questionnaire includes people from show business, successful businessmen, white-collar elite, teachers, public servants and EMBA students. 12 people from show business, 24 businessmen, 24 white-collar elites, 17 teachers, 15 public servants and 8 EMBA students). 95 pieces of questionnaire paper were taken back from 100 with a rate of 95%, and the 95 pieces of questionnaire paper are 100% effective.
- **Validity and reliability test.** (1)Validity test T-test with SPSS reveals that the t values of the 20 items have all reached the level of significance, which means each t value can be used to identify the reflection from different testees, which proves in a way the high effectiveness of the questionnaire. Meanwhile, the questionnaire involves multiple choices, and the construct validity should be taken into consideration. Because the questions are discriminative, factor analysis can be applied here to test the construct validity. Conventionally, 4 factors with eigenvalue greater than 1 are chosen from the 20 items. Their contribution rate is 0.74184, which mean these 4 factors can explain 74.184% of the total variance of the 20 items. Factor analysis can simplify the pointer to data, and express the original pointer to data. It finds out the potential structure according to the relations among them. So, it can be assumed that the construct validity is 0.74184, which is sociologically acceptable. (2) Reliability test. Coefficient alpha is used to test the inner reliability of the questionnaire. The total Cronbach's coefficient alpha in the test is 0.80, therefore the general inner reliability of the questionnaire is good enough to meet the demand of metrology.

Statistical Method. SPSS for Windows 12.0 and Excel are both applied to handle the statistics obtained in the questionnaire.

Results and Analysis

With SPSS 12.0 to deal with the result from the questionnaire survey, we get 20 variables. The KMO value is 0.774, and X2 Value Bartlett globular test is 1487.123, and is significant, which shows that it is suitable to conduct factor analysis.

By principal component analysis involved in the factor analysis, and the rule that the eigenvalue is internally decided to be greater than 1, we get 4 main factors with eigenvalue greater than 1. Their contribution rate reaches 74.184%, and has met the basic demand of covering the overall information (see Table 1).

Table 1 Rotated Component Matrix(a)

	Component			
	1	2	3	4
x1（taste pursuit）			0.903	
x2（bandwagon）		0.739		
x3（superiority）	0.934			
x4（status embodiment）	0.733			
x5（quality pursuit）			0.897	
x6（design favor）			0.818	
x7（technology identity）			0.841	
x8（designer adoration）			0.822	
x9（brand favor）			0.702	
x10（social integration）		0.848		
x11（conspicuousness）	0.789			
x12（taste embodiment）	0.719			
x13（respect acquisition）	0.827			
x14（self-image exhibition）	0.751			
x15（giving gift）		0.767		
x16（scorn free）		0.861		
x17（pleasure from luxury product）				0.738
x18（self-gift）				0.922
x19（symbol）	0.803			
x20（self worth embodiment）				0.918

Extraction Method: Principal Component Analysis. Rotation Method: Varimax with Kaiser Normalization.
a Rotation converged in 4 iterations.

We deal with the loads of 20 original variables by way of Varimax Rotation, and decide 4 main factors whose loads are over 0.5.

Factor F1: Active social motivation. Factor 3,4,11,12,13,14 and 19 can be classified as one main factor named active social motivation as one main motivation with loads of all factors greater than 0.5.From the result of the statistics, part of the consumers of luxury products in China think that it is kind of superiority to purchase luxury products, which makes others feel he is capable of consumption of luxury product. Meanwhile, the act of purchase and consumption is to embody his status and personal taste. During our interview, some interviewees said that their status and tastes become different become of the clothes they wear and the bags they carry, and selection of different brands of luxury products can embody their personalities. Conspicuousness and self-image exhibition is one of the main motivation factors, and is classified “active social motivation” in this study.

Factor F2: Passive social motivation. Factor 2, 10, 12, 15 and 16 can be classified as another main factor named passive social motivation as one main motivation. With the rapid development of economy, there are more and more people buying luxury products in China. Through the interview, some people said that it is a shame if I don’t have a PRADA when everyone gets their LVs and

GUCCIs, from which we can see that the social circle has greatly affected consumer motivation of luxury products. Equal-level brands can win others' recognition and respect. Therefore, "Wherever you go, LV bags can prove your class or taste", "I should also have one since everyone has LV", these opinions obviously tell the factor of bandwagon in the motivation. The four variables above are classified as "passive social motivation".

Factor 3 Desirable personal motivation. Factor 1, 5, 6, 7, 8 and 9 are classified as another main motivation named desirable personal motivation. Compared with common products, Luxury products are relatively perfect and delicate, so, those who are in pursuit of beautiful design and delicate quality will choose luxury products. One teacher from a university said when she is asked about luxury product "I may not buy luxury product, but I love its design and technology". So we conclude the passion toward quality, design, technology, designer and brand as "desirable personal motivation".

Factor F4: Hedonistic personal motivation. We name factor 17, 18 and 20 "hedonistic personal motivation". The consumers of luxury products in China include bank clerks, teachers, public servants, doctor and lawyers whose incomes are 3000 to 10000 RMB per month and senior managers in enterprises, securities company, bank, etc who earn 10000-15000 RMB per month. These people are characterized by high education and high income, and they tend to treat themselves fairly and dare to spend what they have earned. Another group is from show business. They earn money fast, but not stably. "Go merry and be kind to myself since I have taken efforts." This kind of motivation can be classified as hedonistic personal motivation.

Conclusions.

(a) Chinese luxury consumers have twenty motivation in consuming luxury products: conspicuousness, taste embodiment, superiority, status embodiment, respect acquisition, Self-image, exhibition, symbol, bandwagon, social integration, giving gift, scorn free, taste pursuit, quality pursuit, design favor, technology identity, designer adoration, brand favor, pleasure from luxury product, self-gift, and self-worth embodiment.

(b) Chinese consumers' motivation for luxury consumption can be grouped into four main factors: active social motivation, passive social motivation, desirable personal motivation and hedonistic personal motivation.

References

[1] Information on http://space.tv.cctv.com/video/VIDE1248595389811884
[2] Veblen, T.B. The Theory of the Leisure Class. New York: Mentor Books, 1899.
[3] Leibenstein, H.. Bandwagon, snob, and veblen effects in the theory of consumer's demand. Quarterly Journal of Economics, 1950, 64: 183-207.
[4] Dubois, B., Laurent, G.. Attitudes toward the concept luxury: An exploratory analysis. Asia-Pacific Advances in Consumer Research, Siew Meng Leong and Joseph A. Cote, Singapore, 1994, (1): 273-278.
[5] Vigneron Franck， Lester W Johnson. A Review and a Conceptual Framework of Prestige-Seeking Consumer Behavior. Academy of Marketing Science Review, 1999,(3): 237-261.
[6] Zhu Xiaohui, Empirical Study of Chinese Purchase Motivation of Luxury Products. Commercial Economy and Management, 2006 (7).
[7] Information on http://www.lux007.com/html/2009/03/lux007_21091712.html

© (2011) Trans Tech Publications, Switzerland
doi:10.4028/www.scientific.net/AMR.331.574

Comparative Analyses between Consumers' Actual and Targeted Transaction of Menswear Based on Taobao E-Business

Xueqin WANG[1a] , Minghui CHEN[2b*], Aidan ZHANG[3c]

[1,2,3]Key Laboratory of Advanced Textile Materials and Manufacturing Technology of MOE，Zhejiang Sci-Technology University, Hangzhou, Zhejiang, China.

[a]WXQ780@163.COM,[b] 249653424@qq.com[*], [c]zad.andan@163.COM

Keywords: menswear; e-business; targeted transaction; actual transaction; deviation.

Abstract. This paper introduces two aspects of menswear B2C e-business, i.e. the consumers' actual-transaction and targeted-transaction. Circumstances of both aspects were researched by online questionnaires and data from Taobao, in order to check if there are some deviations between them and further analyze the detailed difference, reasons, and potential impacts which caused the deviations. Aiming at improving the circumstances of the deviations between target market and real market based on Taobao menswear, the paper gives some practical suggestions, such as online 3D garment system, establishing a database of products and features, improving the credit rating system, and increasing efforts of network marketing.

Introduction

For a healthy market, consumers should be the most dominant reason. It is better that the consumers' intentions [1] are parallel to the ones of actual market. However, for online buying as a type of virtual shopping, consumers can not actually touch products and sellers. They might feel higher perceived risks [2] than by the traditional shopping, because of lack of tangible and overall experience to actual products and their real evaluation about the purchase procedure. Besides, some misleading information from webs would influence and seduce some impulsive consumers who are actually not appropriate users of certain products to buy "wrong" things or quantity, and then bad purchase experiences might be committed. All the above problems have shown that there are sorts of deviations between supply of virtual markets and actual intentions of consumers, and the problems might be solved by finding more accurate consumers' inherent intentions. About where the deviations are and how to reduce the deviations, this research discloses the consumers' profile of present Taobao menswear, and presents the detailed comparative analyses on the brand, style, price, and evaluation system.

Research method

In this research, "targeted transaction or market" refers to online consumers' inherent or intentional shopping preferences, and is not some realized transaction. "Actual transaction or market" means the real online transaction, and it is provided by real e-market. This study covers three parts, namely consumers' profile of online menswear shopping, targeted market, and actual market (see Fig. 1).

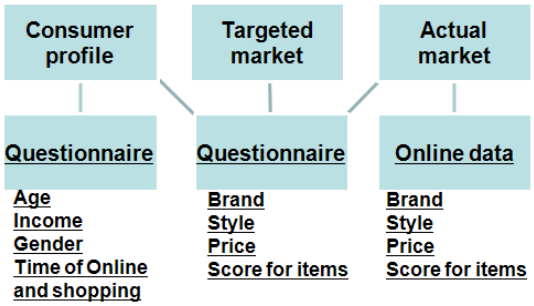


Fig1. Research method

Basically, consumers' profile, including age, income, gender, time of online and shopping, was confirmed through our online survey (http://www.sojump.com/jq/700312.aspx, 300 effective replies from China nationwide), as following: (1) For menswear, the ratio of male to female consumers was 59.5% to 40.5%; (2) For the ratio of consumers with different ages, over 40 years old was only about 4%, 30-39 years old was about 10.3%, less than 30 years old accounted for about 85.7%, of which consumers ages between 20-29 accounted for 73.7%. (3) Consumers' income less than 5000 RMB accounted for 83.7%, less than 2000 RMB accounted for 41%. The main consumers have middle or low income. (4) 59.4% consumers spent about 3-8 hours in internet, and only 6% consumers took less than 1 hour in internet. From 20:00 to 22:00 each day, transaction quantity reached a peak. For the present online consumers of menswear, it is obvious that both young men and young women (less than 30) may be the main potential consumer，and they usually have no high income, and the shopping time is usually at night.

Based on the above consumer profile of menswear, "targeted market" expected by them were studied also through the above questionnaire, including "brand", "style", and "price" of products for the 2011s/s season, as well as "forecast evaluation for e-shopping based on past shopping experience". In comparison with "targeted market", "actual market" refers to the present and this season menswear e-market. In this study, we researched Taobao official data cube to collect the equal information on "brand", "style", "price" and "goods credit" for the present products recorded from top 45 brands in April. The detailed comparative analyses are shown as follows.

Analysis on the derivation of actual brands and target brands

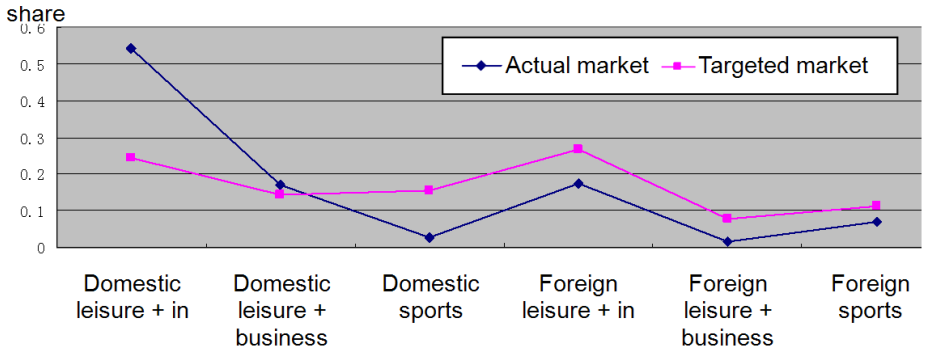


Fig.2 Comparison between actual brands and target brands

For brands on the Taobao menswear market, a primary consideration of consumers is if the products are real products from the brands. Consumers firstly want to select the Taobao malls from the brand owners to buy goods. Direct sale platforms from the brand are preferred.

Based on selling data from Taobao mall the comparison result to the survey data are illustrated in Fig.2. It is obvious that share of shopping intention for foreign brand is much higher than the actual market. Perhaps, most of foreign leisure fashionable brands do not launch their Chinese Taobao malls because of geographical and lingual constraints, and concerns on the security of Chinese e-shop as well as their neglect for the Chinese mass market may be the other causes. The relative higher actual purchase of domestic brands may indicate the consumers selected some local substitutes and caused certain transfer of consumers.

Analysis on the derivation of actual styles and target styles

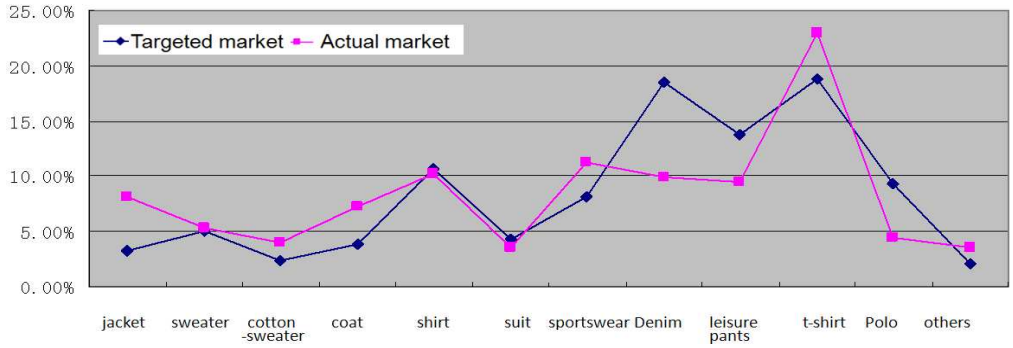


Fig. 3 Comparison between actual styles and target styles in April

Data from Taobao has shown that there is a wider category of menswear online than the traditional market. Life cycle of product is longer, and seasonal changes of each product are slower than before. This phenomenon might be caused by bigger and cheaper storage system for online shopping, and the open online market has bigger consumer group from different regions of the whole country with diverse climates.

Fig.3 has shown that the share of jacket, cotton-sweater, coat, sportswear, T-shirt and other products of actual market are significantly higher than the targeted style of consumers. As T-shirts and other off-season items are generally relatively low price, the regarded consumers' perceived risks are lower than buying other things, and they are easily deviated from the actual shopping intentions.

Analysis on the derivation of actual prices and target prices

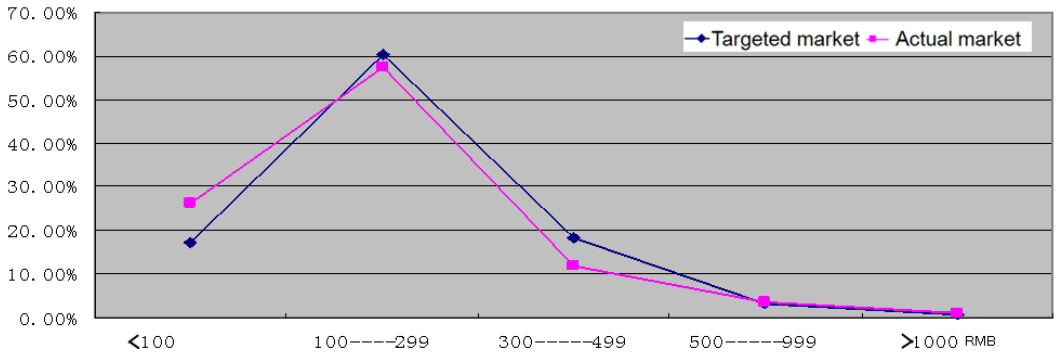


Fig. 4 Comparison between actual prices and target prices in April

For perceived risk, financial determinant is one of biggest factors [2-3]. The online consumers are sensitive to price, being compared to the consumers with high income. That means the higher the price, the higher the perceived risk of consumers, and vice versa.

Two aspects can be seen in Fig.4. In the 300-1000 RMB price segment, the successful purchases are lower than the 100-299 RMB price, even when most of purchase intentions are relatively higher than the actual transactions. The reason is that consumer choice based on perceived risk is too high for the price above 300 RMB. Most of online consumers accept the 100-300 prices. The present actual prices are mostly coincidental with the consumers' hopes.

Analysis on the derivation of actual evaluation and forecast evaluation

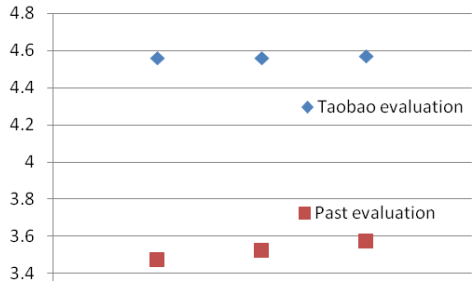


Fig. 5 Actual evaluation and forecast evaluation

Fig. 5 shows that the recorded evaluation of online shopping is much higher than the actual consumers' experience and forecast evaluation for future shopping. The online evaluation, to some extent, would mislead online consumer behavior. The main reason might be that Taobao's mechanism for evaluation is too simple and limited, which breeds a confusing reputation.

Summary

Through the analyses above, it is obvious that the derivations are distinct for brands, styles, and evaluations, but not for the prices. The E-market may be improved in how to develop more oversea popular brands and increase the network of direct sales, update proper styles according to requirements of some VIP consumers, and setup a more transparent and convenient evaluation system for shopping experience.

Acknowledgements: This work was financially supported by Science Foundation of Zhejiang Sci-Tech University（ZSTU）.

References

[1] F. Wang, *Research on Factors that Effect on Consumer s Intentions about Online Clothes Shopping under the B2C Model*. Dissertation of Beijing Clothing University, 2010

[2] A. Li, *Empirical Research on Clothing E-Commerce in China*, Dissertation of Tianjin Polytechnic University, 2004

[3] B. Shao, Z. Yan, Y. Yan. *Utility of Perceived Risk Reduction Strategies in B2C E-commerce*, Soft Science, 10(04) (2006), p.131-135.

© (2011) Trans Tech Publications, Switzerland
doi:10.4028/www.scientific.net/AMR.331.578

Women's suit Pattern Parameterized Intelligent Design

Yanzhen Wang [1,2,a], JianPing Wang [1,b], Sun Sun [2,c] and Yanmei Li[2,d]

[1] College of Fashion, DongHua University,1882 Yan'an Road, Shanghai,200051, China

[2] College of Fashion ,Shanghai University of Engineering Science, 333 Longteng Road, Shanghai,201620,China

[a]wangyanzhen1227@126.com, [b]wangjp@dhu.edu.cn, [c]sunsun2006_1@126.com, [d]lym0350@126.com

Keywords: Suit, Parameterization, Intelligent.

Abstract. To study the parameterized intelligent generation of women's suit pattern, it is proposed a concept about rapid generation of individualize pattern. Focused on research principal parts (Body modular, Sleeve modular and lapel modular) of lady's suit automatic generation system and built up the curve mathematics parameters model, it obtained the data base of system structure. Realization of suit showed how to establish the parametric model of body, sleeve and collar. It began to set up a automatic system about interactive pattern tentatively on the base of VC++ and Arcobjects.

Introduction

Currently, there are some bottlenecks on the development of Computer-Aided design, which was used in the garment's industry [1]. Pattern making system is not only isolated from design system, but also not completely intelligent realization, which have influenced and restricted efficiency and quality of garment's production [2]. Meanwhile, garment structure design is one of the bottlenecks in the process of industrial production, and its techniques directly affect the quality of garments.

Foreign companies have harvested many fruits, such as AG-CUMARK System of GERBER Company in UK, ASSYST System in Germany, MODARIS FITNET System of LEC-TRA in French, which can select the most appropriate pattern according to the selected style and convert 2D pattern to 3D display [3]. Domestic CAD systems such as NACPRO, Richforever and Arissa in intelligent pattern were still in its infancy. Their pattern and data base is too small to play the role of expert systems, it didn't find the most similar prototype model and bodies, collars, sleeves, etc., and adjust the corresponding pattern [4,5].

This paper research the mathematical model structure of parametric suit pattern, establish pattern parametric design of prototype body, sleeves and lapels. It possessed the base of lady's suit by means of its patterns. Take the advantage of pattern automatic generation and interactive technology, combined with garments and the user' needs to complete theories analyze of body module, sleeve module and lapel module, built the corresponding mathematical base and realized the intelligent operation for women's suit.

Parametric Mathematic Models

Body, no matter how complex they may be, have similar appearance outlines, the given numerical value could making connections with geometrical dimension of garments. Pattern is ordinarily signified by point, straight line and curve. The curve is the key as well as the difficulty of the system. It is important that the curve, displayed in computer, consistent with its in realistic pattern for the realization and modification of pattern's automatic generation.

Points. Point A was defined as A (x, y). Fig. 1 shows the coordinates of A_1 and A_2.

Line. Fig.1 shows that A_1 and A_2 are given in the two dimensional space. Introducing to parameter μ, the equation of line can be represented as:

$$x = x_1 + (x_2 - x_1)\,\mu. \quad (1)$$

$$y = y_1 + (y_2 - y_1)\,\mu. \quad (2)$$

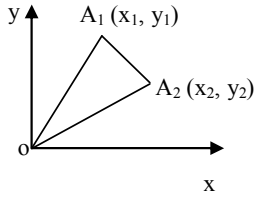


Fig.1. Point and Line

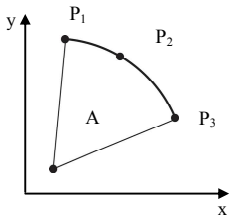


Fig.2.Curve

Curve. There are many ways of establishing parametric mathematical model by Curve, such as Spline Curve, Bezier Curve, B-Spline Curve and Gamma Curve, Bezier curve are the better way in curve fitting, but not ensure the line round shape when pattern was revised. It was built the curvilinear equation by taking advantage of new method in the paper. The curve can be drawing for three known points.

Fig.2 shows that the known $P_1(x_1,y_1)$, $P_2(x_2,y_2)$ and $P_3(x_3,y_3)$ form the curve. By using the following formula derived dot coordinate A(x, y) and radius r.

If $y_2=y_1$, then $x=(x_1+x_2)/2$. (3)

If $y_2=y_3$, then $x=(x_2+x_3)/2$. (4)

Other
$$x=\frac{(x_2^2+y_2^2-x_1^2-y_1^2)/2(y_2-y_1)-(x_2^2+y_2^2-x_3^2-y_3^2)/2(y_2-y_3)}{(x_2-x_1)/(y_2-y_1)-(x_2-x_3)/(y_2-y_3)}\quad . \tag{5}$$

So similarly, it can calculate y values. A parameter r was defined as:

$$r=\sqrt{(x_1-x)^2+(y_1-y)^2}\quad . \tag{6}$$

Design and Algorithm of Suits' Pattern Modules

Women's pattern system was mainly divided into four modules (the whole module, body module, sleeve module and lapel module). Three modules (body, sleeve and lapel modules) were relatively independent, but also intricate. For example, the generation of lapel module was dependent on neckline's structural shapes and dimensions of body modules. Fig. 3 shows Skeleton Module of women suit pattern.

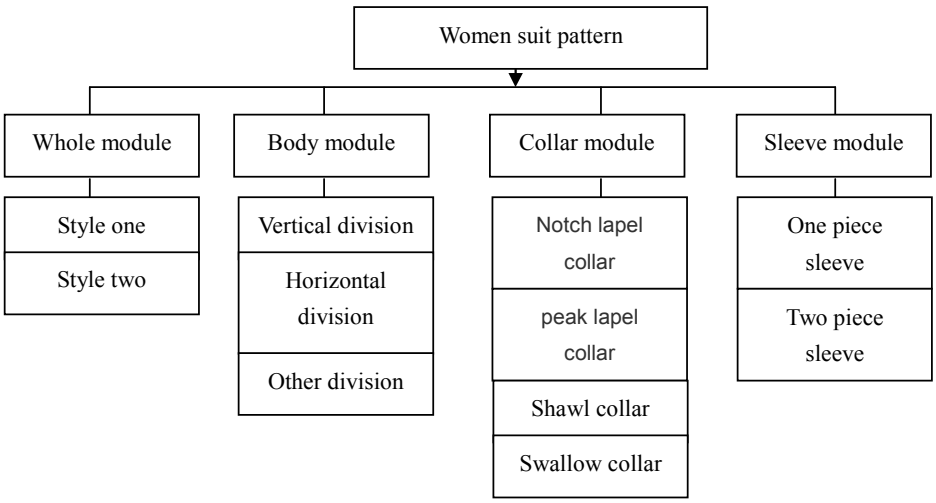


Fig. 3.Women suit module framework

Body Module Design and the Principal Curve Algorithm. Body module is mainly the part that can be sorted by ways of garment division, such as vertical division, horizontal division and other division. There are three main types of the construction lines-the staight lime, slow curves and sharply curves. The straight line in the pattern should be identified by two known points, the slow curves in the picture could be achieved, but the sharply curves must be split into two parts for drawing it.

As shown in Fig. 4, it was ensure that neckline arc is perpendicular to the center back line, two specific points were determined 1(x, y), 2 (x+2.9, y+0.3). Point 4-5 in the armhole was be located for the same reason. The following calculation can get the coordinate of point 3-4.

Assuming the coordinate of point 3 and 4 is (x_1,y_1) and (x_2,y_2), determine the coordinate of point 3-4. If $y_1=y_2$, then $y=y\pm0.2$, $x=x_2$. If $x_1=x_2$, then $x=x\pm0.2$, $y=y_2$. In addition, the slope of line 3-4 was defined as $k= (y_2-y_1)/(x_2-x_1)$. Assuming $a=-1/k$, the line equation is $y=ax+c$, then $c=y_2-ax_2$. Likewise, assuming $Ea=1+a_2$, $E_b=2a(c-y_2)-2x_2$, $E_c=x_2^2-(c-y_2)^2-0.2^2$, then $x=(-E_b+\sqrt{E^2-4E_aE_c})/2E_a$, $y=ax+c$.

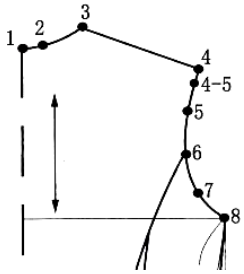
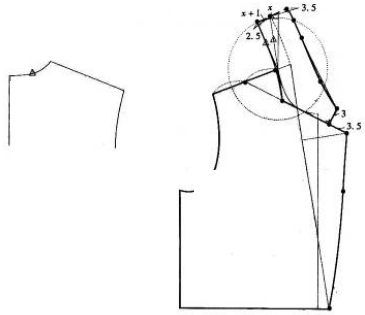


Fig.4. The Arc of Neckline and Armhole


Fig.5. The Lapel

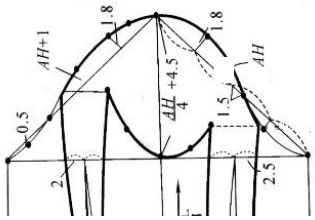


Fig.6. The Sleeve

Lapel Module Design and the Principal Curve Algorithm. The gradient data of lapel is the most critical factors in the lapel's structural design. The difference in height between the collar stand and the upper collar is one of the main factors affecting the design of gradient data of lapel. In general, the difference between the upper collar and collar stand is usually 0.8~1cm, the location of the break point collar lies between bust line and waist line. The gradient data will be changed with the relevant structures and materials of tailor collar. Typically, when the break point positions increase, gradient data will increase; when the difference between collar stand and upper collar increase, it will increase. However, in order to facilitate the study, it neglect the fabric's influence, only consider the clothing structure's influence.

As shows in Fig.5, the first button of the notch lapel lies in the waist line, the collar stand is n (2cm), the upper collar is m (2.5cm). The picture shows the process of the gradient data of collar.

Sleeves Module Design and the Principal Curve Algorithm. This module can be divided into two piece sleeve and one piece sleeve, two piece sleeve is fitted style, one piece sleeve is better fitted style. In the sleeves module, it is important how to decide the easing of sleeve cap (the easing of sleeve cap is the length difference between sleeve cap and armhole), its dimensions directly affects the shoulder shape of women suits. The potential impact factors of the easing of sleeve cap are elastic of fabric, the thickness of fabric and style characteristics. Fig.6 shows the method of drawing the sleeve cap curve.

Automatic Generation of Women Suits System

Process of System Framework. Automatic generation of garment pattern design system is based on understanding the mechanism of the expression of thinking, intelligent human-machine interface technology, knowledge base and intelligent model. The whole system is divided into three layers, Fig.7 shows that the first layer is input layer, the second layer is the implementation layer, the third layer is output layer.

Basing on the data from a non-contact three-dimensional body scanner, in accordance with the principles of drawing by hand, by setting related variables, the pattern can be produced in this system.

By changing the value of the parameter data, we can obtain the corresponding size of the human body model. And we use coordinate variables x, y to describe the map center line, curve and point.

Automatic Generation System of Women Suits Pattern. The automatic generation system used 160/84A (the size of end-product garment), can be variable according to customer's actual size variation within a certain range. Fig.8 shows the interface of the women's suit pattern intelligent system.

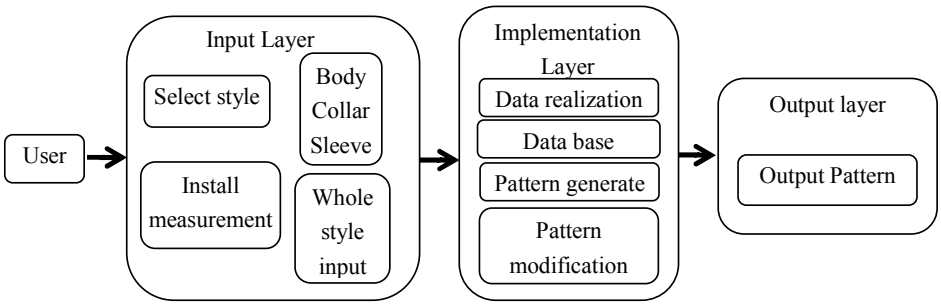


Fig.7. Frame Diagram of Women Suit System

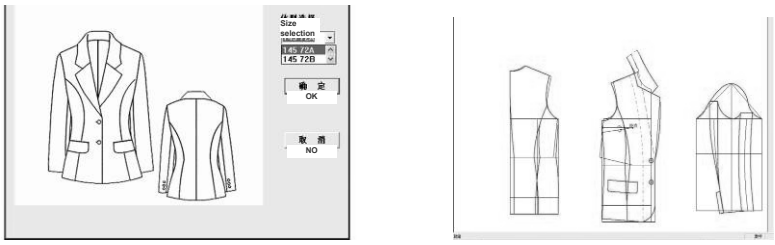


Fig.8. Women suits style and pattern

Conclusion

Baseing on apparel pattern in the parameter of the mathematical model, we proposed the concept of Parametric clothing, established the parameters of design patterns, and realized the garment pattern digitization. In short, automatic generation system is a new problem, there is no ready-made model to follow，we should make in-depth study. As can be seen from the application, automatic generation system can automatically generate. With the rapid development of the CAD and computer technology, it will improve and develop continuely, and it has broad application prospects.

Acknowledgements

This work was financially supported by the Shanghai Education Committee Foundation (09YS381) and (10YZ170).

References

[1] Juhong Xu, Wenbin Zhang. Study of MTM and the Optimal Cutting-plan for Uniform Custom-making. Journal of Yangzhou Polytechnic College(2003)12:28-30.

[2] Lei Xia. 3 dimensional body measurement technology in apparel industry. Shanghai Textile Science & Technology(2006)5:76-77.

[3] Ying He, Fengyuan Zou. Research on The Garment Measurements for MTM. Journal of Zhejiang Institute of Science and Technology(2004)12:328-332.

[4] Ming Xia. Research on the Made to Made To Measure System of the Men's Individual Pattern Based on MTM. Donghua University(2004)1.

[5] Lindi Wu, Jianwei Wang. Intelligent technology of garment. Shanghai Textile Science & Technology(2005)4:7-9.

© (2011) Trans Tech Publications, Switzerland
doi:10.4028/www.scientific.net/AMR.331.582

The Application of Chinese Element in Fashion Design

Gai-Hang Li[1,2,a], Rui Shi[1,2,b], Guo-Lian Liu [1,2,c]

[1]National Engineering Laboratory for Modern Silk, 199 Ren Ai Road, suzhou 215123, P.R. China

[2]College of Textile and Clothing Engineering, Soochow University 178 East Ganjiang Road, Suzhou 215021, P.R. China

[a]gaihangabc@163.com, [b]xiurui8888@126.com, [c]liuguolian@suda.edu.cn

Keywords: Chinese Element, Fashion Design, Innovative Application

Abstract. As a combination of materiality and spirituality, costume is not just a practical thing to protect us but also the identification tag of social roles and the carrier of culture transmission. In fashion design, we should integrate with the international trend and pay more attention to the national culture.In order to inherit and propagate the local culture, this article analyzes the innovative application of traditional Chinese element in fashion design, try to promote the development of Chinese costume enterprises.

Introduction

The concept of "Chinese element" was proposed in 2007. The concept points out that: all the images, signs and national customs which condense the traditional cultural spirit, embody the dignity and interest of Chinese Nation, and was accepted by the majority of Chinese people (including Overseas Chinese) can be regarded as "Chinese element"[1].It not only includes traditional utensils, characters and marks, manual skills, color and patterns, but also includes Chinese culture and spirit.

Costume has a unique cultural attributes. French fashion designer Christian Dior [2] has stressed in his speech at Paris University that, “Costume will exist forever accompanied with history and culture.” Chinese culture is recognized as broad and profound, the five thousand years of historical accumulation in culture is inexhaustible. Since the late 20th century, with the launching of a variety of cultural movements, Chinese people began to take a rational perspective on Western culture, and re-examine the cultural value and design value of the traditional Chinese element. The design elite`s consciousness of culture also contributed to the applications range of traditional elements spread to various industries rapidly.

Throughout the domestic major fashion design matches, it is not difficult to find out that the award-winning works which all were based on the deep and unique Chinese culture and blended the traditional feature and modern together. The research point of this paper is how to create the fashion design with unique aesthetic value and culture connotation which combine traditional Chinese elements and modern design method together.

The Application Of Chinese Element in Fashion Design

China has always been known as "A nation with highly developed culture ".With the development, more and more people realize the importance of "cultural identity " among different nationalities, and began to re-understanding their national history and culture.Chinese traditional element supply creation material and inspiration source to the designers *continuously*. This paper explores the use of traditional elements in fashion design from four aspects.

The Realistic Significance of Traditional Aesthetic Philosophy. The evolution history of costume also is the development history of social civilization. The core foundation of Chinese culture is philosophy, as early as the Qin Dynasty the costume system had a certain specification including costume color, pattern, shape, etc, the system of philosophy contained by which has been formed at the same time. Therefore, if we want to understand the traditional costume and culture, we must understand the system of traditional humane and aesthetic philosophy at first [3].

As the central gist of traditional aesthetic philosophy *"R*ite" is the root of the traditional costume system. It emphasizes that everything in the universe should comply with a certain order to finally reach the ultimate of "Harmony of Human with Nature". It mainly reflects in Costume by dress and personal adornment institution to show the difference of display hierarchy, young and old, intimacy, to create the content space of relationship.

Traditional Chinese culture focuses on interdependence and the unity of opposites between creature and human being, nature and existence of all thing, it emphasizes spatial awareness and the "Harmony of Human with Nature ".

Therefore, traditional costume advocates natural and simple, rational but facile, pursues of the "invisible form " and artistic conception of Metaphysics.It has conveyed the Chinese Style Philosophy of implicit and simple realm of life virtually

The Application of Traditional Silhouette and Style. The different natural environment and economic background of Eastern and Western civilizations creating the different ideology, aesthetic philosophy and universal consciousness.The difference is also reflected in the three-dimensional shape of traditional utensils and the clothing styles.

Traditional Chinese utensils including pottery, porcelain, bronzes, etc, some of the utensils are concise and simple, some of them are tender and round. But if we research on their outline form, we will find most of the traditional Chinese utensils take curve and circle shape as the main element but not straight line or square, which is consistent with the aesthetic philosophy, such as "The Harmony between Human Being and Nature"and "The Harmony between Yin and Yang", at the same time, the using of circle and curve also reflects the humanistic spirit of auspice seeking and equalization.

Traditional aesthetic philosophy focuses on the creation of artistic conception. Such ideology prompt to formed the distinct culture of loose-fitting costume which is different from the body size costume of West. The structure of traditional Chinese costume is Two-dimensional, loose-fitting, less supporting points, no darts, the inner space of it changes with human motion, and it emphasizes the beauty of trends and harmony between human and space. On the contrary, the Western costume is Three-dimensional, close-fitting, using darts, focus on the performance of the human body, and it emphasizes the static beauty.

At present more and more domestic designers try to integrate "Chinese element" into their costume design, but most of the integration ignore the traditional culture and are just the using of surface elements which are too superficial. Japanese traditional costume is similar with traditional Chinese costume, the exploration of national costume design of Japanese designer can give us some inspiration. The fashion design of Issey Miyake is shown in Fig. 1 Their success in modern fashion design is because of taking root in traditional Japanese customs and values to design the fashionable costume which is rich in eastern characteristic at the same time, it is easy to distinguish with the Western costume.

The Application of Traditional Color and Patterns. China has always attached great importance to color, the color preferences are different in different periods. Traditional color system based on



Fig. 1 The fashion design of Issey Miyake



Fig. 2 Tai Chi Diagram

Yin-yang and the Five Elements and take the overcome of WuXing as a criterion, “Five Colors”contact with “Five-Virtue” and “Five Elements” to form the color system which is rich of Chinese traditional culture. “Five Colors” refers to black, white, blue, red and yellow, different colors have different meaning. In fashion design we should take full account of the Chinese nation of using color.

As the key elements of fashion design, pattern together with color form the visual effects of clothing. China has a wide variety of traditional pattern, the traditional pattern is not only beautiful but also carries a certain meaning and significance. For example “Tai Chi Diagram” uses a simple lines and two-color of black and white to show the relationship of color and space, and express the Chinese aesthetic philosophy of “The Harmony between Human Being and Nature”. The “Tai Chi Diagram”is shown in Fig. 2.The traditional Chinese pattern emphasizes balance and coordination, so most of the composition is symmetrical. In addition, the folk art is an integral part of the traditional pattern such as New Year pictures, paper-cut, Shadow play and woodcarving.

Mostly traditional patterns take homophony, empathy and allusion as the expression means. Using of traditional pattern in fashion design not only increasing the formal beauty of clothing, but also added its own culture. But we should note that the using of traditional designs, should match the clothing style and material, we can use the modern design methods such as deconstruction and recombination to reconstruct the pattern.

The Application of Traditional Fabric. As the carrier of garment, fabric directly determines the style of clothing, so the selection and design of fabric is exceptionally important in fashion design. Reference to traditional Chinese fabric we will think of silk at first. As the first country rearing silkworm and Reeling, the type and quality of silk is the leading of the world. For the smooth texture, good drape and flowing characteristics of silk, that it coincides with the traditional aesthetic philosophy which emphasizes artistic conception. At the same time as natural fiber, the characteristic of silk is draping, breathable and clammy, that is fully in line with the mind of returning to nature

The innovative using of traditional fabric is not just fabric itself but also including traditional technology, such as embroidery, tie-dyeing and wax printing. In fashion design, we can consider using traditional fabric, or using traditional technology to reconstruct the modern fabric.

Conclusion

This paper explores the use of “Chinese element” in the fashion design from the following four aspects: traditional aesthetic philosophy, traditional silhouette and style, traditional color and patterns and traditional fabric. Costume design is embodied in the humanistic care of people, so the designers should focus on digging into the depth of traditional culture, and take costume as the carrier to convey a deep humanistic concern to consumers.

But we should note that the inheritance of the traditional culture is not the application of surface elements, only by combining costume itself, taking root in traditional culture, mining the humanism of the traditional philosophy and re-using the traditional elements could we find the development way of local fashion design.

Acknowledgements

This paper is funded by the First Phase of Jiangsu Universities’ Distinctive Discipline Development Program for Textile Science and Engineering of Soochow University.

References

[1] He HL, He HQ, The application strategy of Chinese element in the advertisement, Writer Magazine, 2009.
[2] Liu YF, Hu Y, Fashion Art Design, China Textile &Apparel Press, Bei Jing ,2006.
[3] Ye LC, Aesthetics of Costume, China Textile &Apparel Press, Bei Jing , 2001.
[4] Zhou J,A study of the usage of traditional elements in Chinese modern packing design. Master's thesis. Soochow University (2006).
[5] Xu LL,The Research of Demonstration Design of Chinese Costume by Using the Chinese Element, Master's thesis. Jiangnan University (2008).
[6] Li YT, The Application of Traditional Costume Elements in Fashion Design, Master's thesis. Tsinghua University (2007).

© (2011) Trans Tech Publications, Switzerland
doi:10.4028/www.scientific.net/AMR.331.586

Study on the Innovative Design of Fur Clothing

Tong Xu[1,a], Min Fang[1,b] and Guangde Li [*1,a]

[1]College of Quartermaster Technology, Jilin University, Changchun, 130062, China

[a]732589826@qq.com,[b]mfangdesign@hotmail.com,*corresponding author

Key words: Fur, Design, Fashion

Abstract. In recent years, with the trend of young, fashion, variety, fur has become one part of fashion clothing. The aim of this article is to study the innovation design of fur clothing with the combination of the status of fur's development home and abroad and the international fashion trend. For this study the author has designed series furry clothing from the color, technology, style and material.

Introduction

Fur industry plays an important part in the history of human civilization. With the change of the social conception and the innovation of processing technique, fur material enriches and develops by constant self-denial and fur garments have been endowed with new connotation. With the trend of young, fashion, diversity, fur has been a part of fashion. Today, fur has not only been used to cover ancestors' bodies and keep modest on their waists. Fur and leather industry will take sustainable development as its strategies and take environmental protection, exquisite fashion as its main melody of development [1].

Development Status of Furs

Foreign status. International fur market is quite active. From the point of fur market discipline, the low-end and middle-end of market are more active. Although the amount of mink production in American is large, because of its high consumption, it still needs to import a great quantity of fur garments from Korea, Hong Kong, Canada, Greece and other countries and districts. The style primarily is long coat, the natural color is more popular than coloration. The fox skin trade in Nordic (Denmark, Norway, Finland, Sweden) occupies nearly 90% of the total trade in the world, only in Finland the trade has occupied 67%. Helsinki has become the largest international fur auction centre.

Domestic status. After the baptism of market economy, Chinese fur industry's general trend has formed which is international, fashion, branding. Specifically, Chinese fur industry has several obvious trends as followed:

Industry development tends to be mature. Fur clothing is getting fashionable. Domestic market expands rapidly. Market upgrade has become the order of the day. Effect of industry support is prominent. Brand operation is beginning. Application fields escalate. Except traditional fur garments, fur accessories has also been used in various kinds of fashion garments with large quantity of demand.

Problems of Fur Industry in China. However, facing the relatively good fur development tendency, we should realize that China is just a big fur production country not a powerful country. China has been facing a quantity of problems.

Industrial regional brand and enterprise brand have developed unbalanced, brand operation is not perfect. Domestic consumers advocate high-end fur garments, however, except for Pearl River Delta most of fur enterprises take the middle-and-lower grade fur machining as their principal business and rarely build their own brands. Now Hang Kong brands have taken the position of leading fashion in mainland market; other European top brands, Japanese and Korean Brands, they are basically the supplement for the high-end market whose market share less than 1%. Brands in other districts inland such as Beijing, Xinji of Hebei, Tong Erbao of Liaoning, Haining of Zhejiang and Tongxiang, basically do the business of wholesale and OEM(original equipment manufacturer) accounting for 30% [2].

Design and technology are not mature and perfect enough. The Asian market principals of NAFA said that: "from the point of quality and price, the fur garments made in China could contend against all the other districts in the world, but they are not mature enough at design and technology." Especially in the middle-and-lower grade market, the styles lack innovative and autonomous design spirit and enterprises mostly rely on mode of knockoff production. The market value of fur garment depends on the quality of design, so if the mainland enterprises should develop with this model, their product would hardly have competitive power and their brands would have been emptiness.

The Innovative Design of Fur Garment

Objective and meaning of design. In the old days, the major consumer group of fur garment was over 35 middle-aged women with economic capability. But now with the trend that the young and fashionable character of fur garments are getting more and more obvious, fur garments increasingly attract attention of younger women. Therefore this design pick out urban white-collar female between 25~35 as the target consumption group who pay attention to represent their charm and style by clothing and have great market consumption potential. The objective of this design is to create fur garments which are concise and comfortable and has sense of times and decorative style through research from aesthetic appreciation, fashionable front information fashion trends tracking technology and materials etc. It will make the wearer feel the quality and fashion, and meanwhile highlight character further and make the intrinsic value of fur design get more extension and expansion in aspects of time and space.

Analysis of fashion trend. Button, paillette and other details are important parts of fashion inner structure, this year metal material and shiny metallic paillette are extensively used in the design of fur garment. Although these compositions take quite small area and proportion in the whole fur garment, they are the important influenced factors for the whole silhouette and style character which can't be neglected. In recent years, rhinestone, stereoscopic embroider slice, lace, even the metal materials such as rivet and air hole usually used in suitcase design are widely used in fur garments to embellish the monotonous color. Especially now carbon green has been advocated, many big brands have given up the staining method which is not environmental and chosen the natural wild fur with more natural color. But this choice brought big challenges to design, designers placed emphasis on the use of details design and special materials, which made the finishing point, designers made the detail structures which looked like fashion accessories and auxiliary materials become the main part of modeling fashion style.

Fabric reconstruction for fur has become one of the important innovation means in current fur garment design. Designers combine new techniques with modern design concepts to concentrate on how to change the texture of fur garments and how to not only save the raw materials but also reflect the plump effects. Fur can be used by the means of shearing, pulling guard hair, sculpture,

printing, punching, stretching, laser, embroidery to create bran-new perception effect. The staining technique cooperating with the new ways of monochrome, polychrome bleaching and dying, gradual change bleaching and dying, spray-painting, printing etc has brought more abundant change of details to fur materials.

Multiple materials mix and match and crossover. Fur garments design that combines fur with leather, knitted fabric, woven is the popular focus all this time. The materials usually used for match include silk, lace, wool fabric, chiffon, jean, the main combinations are the splice of fur rags and whole fur; the splice of woven fabric and a part of fur; fur knit and dual materials of leather and fur.

Accessories become popular items: fox fur has been widely used on the design of bags to make bags more stereo and have contrastive effect of materials. The design of bag, gloves, hat with partial fur is this year's mainstream fashion.

Analysis of "purple dream" fur design. Traditional fur design is a little more conservative, the color is usually nature, the silhouette is always bloated and massive. To the questions of what is said above, from the color, design, match, this design walks fashionable and popular route to make the modest luxury of design show one's noble temperament and at the same time show the sense of graciousness. This series decomposed the clothing structure of traditional fur design to compose the new clothing structure that is different from the type before. The series combine the latest adornment language with special texture and manufacturing process to let the fashion design element and the fur garment design perfectly hold together. Crossover of material mix and match was used in terms of the style, broke the limitation of traditional ideas and design approach. The main textures of mix and match are knit fabric, leather fabric. The color of this design is violet matched with brick red daringly to embody elegant and noble and personalized. Hairy surface process used gradient dyeing to emphasize the layer effect. On the choice of texture, mink, fox, rabbit hair mainly were used in the design.

Design1. Although fur is getting more and more light-minded, wrapping by fur warmly is still a kind of fashion trend in millennium. So in design1 the designer chose H line long coat silhouette. The treatment of hat and shoulder chose the splice technology of in direction hair and against direction hair and matched two interphase color to create rolling effect in part of garment. Light-minded mink used in front was cut into small rectangle sheets to splice, every strip's color is gradual change. The technology of pulling guard hair was used on the both sides and back of the coat with the fur cutting into 1cm wide trips to splice keeping the stitch to show the layer effect. Fox fur was put on the hem of the coat and accumulated to add massive effect and sense of security wrapped by fur. Loose-bodied fur coat matched with chunky knits on the shoulder and placket to avoid bloated effect and bring leisure fashion. Fig. 1 shows the fashion drawing of design1.



Fig. 1 Design 1

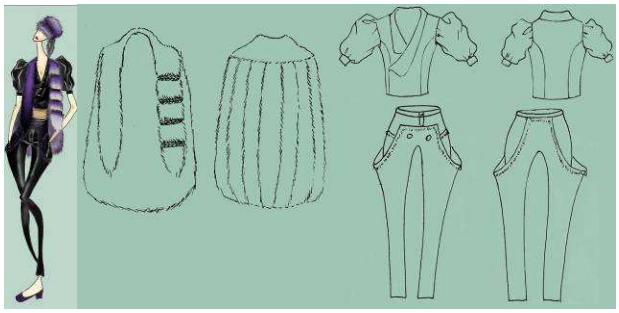


Fig. 2 Design2

Design2. Fox fur and mink are the frequently-used materials of fur garment. Because fur design was getting fashionable and light-minded around the world, light-minded mink has been leading fashion trend in these years. Under this fashion fad, fox fur was obviously massive and far away

from the centre of fashion gradually. However latest fur garment fashion trend also required activity and dynamic. Fox fur is designed as pithy mantle by thinning, reducing hair and separating them by the knit of thick wool. Thus the design can create graceful effect and avoid its massive appearance. Fig. 2 shows the fashion drawing of design2.

Design3. In design3, fur was mixed and matched with knit fabric to implement crossover mix and match and show unusual visual effect. It is taboo that fur collocation looks old. So, large area brick-red chunky knits were mainly used in this design, there was a little lilac rabbit hair on the brim, waist and cuff as the trimming. Though the area is small, it has existed as a kind of fashion decoration language to highlight entire concept and make the design fashionable, good-looking and warm. Fig. 3 shows the fashion drawing of design3.

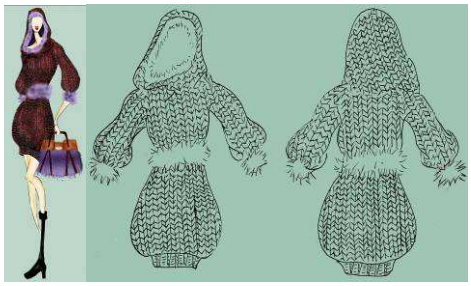


Fig. 3 Design3

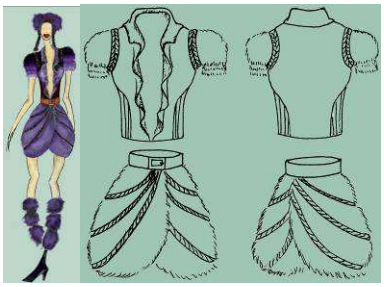


Fig. 4 Design4

Design4. Separation line is indispensable for fur garment. The area of every fur sheet is different because of fur species. So fur garment should base on the character of materials to combine structure line of clothing with separation line of fur so that the materials can be made best use of. The details design of structure line is the emphasis of fur garment design. Fig. 4 shows the fashion drawing of design4.

Knit fabric was used on the waist not only to show the special texture that was created by the mix and match of materials but also to show the trim waistline perfectly and overcome the effect that mink hardly achieved. Fox fur was put on the shoulder to pile up and enhance the linear quality and dimension of shoulder.

Conclusions

Now, Chinese fur industry is facing with problems such as international trade barriers and anti fur movement. China has been a fur production country but still not a fur power. Innovation design is the important link of fur industry development. With the help of the variety of fur, pay close attention to international fashion trend, combine fur clothing manufacturing, innovation of designers with new technology are what we should do now. Only if the enterprises persistently create new concepts and styles of fur clothing, their brands can have a place on the international market. Thus they can grab the opportunity of the industry by the means of strengthening science innovation and extending fur industry chain to make the transition from a fur production country to a fur power and to make the industry brands keep pace with enterprises.

References

[1] Yan Zheng: Leather and Fur (Zhejiang Science and Technology Press,2008,12) in Chinese
[2] Yi Zhou: Leather Science and Engineering (2005) in Chinese

© (2011) Trans Tech Publications, Switzerland
doi:10.4028/www.scientific.net/AMR.331.590

Application of Typology Method in Chinese- Style clothing Pattern Design

Shigang Wu

School of Fashion and Textile, Eastern Liaoning University,

Dandong Liaoning, China 118000

wshg138@163.com

Keywords: typological method, structural design, clothing pattern, traditional culture, shaping memory

Abstract. In order to make clothing style sculpts to embody inherent culture and memory of clothing, and realize element design of pattern, here introduce typology method. This way use type extracting, type transforming, type innovating, and apply new idea and means. Through applying pattern example analyze process of clothing pattern design. It will provide new method for clothing structure design and reference for pattern design.

Introduction

It not only depend on elements application of traditional culture, but also lie on proper pattern design of clothing structure for designing clothing which have historical culture memory and embody inherent form and style.

Clothing pattern is the key link in garment production process, and provide precondition for operation modes and production division in ready-made clothing and mass production. It also is the technology resources of sustainable development of enterprise. Its action finally corresponds to the design requirements of style, and accurately reflects the structural form and hold three-dimension shape. Furthermore it reflects the inherent style and clothing cultural connotation. It is necessary to search for a pattern design method with cultural memory.

Analysis of clothing pattern design

The pattern is 2D expression which constructs body 3D shape according clothing style and figure size. It uses geometry principle to transform 3D shape to a number of 2D plans with definite shape [1].

The current pattern designs methods are mainly contain proportionate allocation method and prototype method. These two methods reveal the relationship between figure and garment from different angles.

The proportionate allocation method is a further direct way base on clothing shape with its circumstance requirement and individual. This way mainly utilize major part measurement and use formula of body scale to calculate other details, then draw clothing patterns. It is suitable for those garments whose structure is not complicated; style is fixed and less changed. The relation of scale depends on body parts proportion, but it may lead to different style on different body shape. So in this method, a appropriate proportionate allocation is a hard problem to grasp, and it need a large amount of practice and rich experience, otherwise it is difficult to control garment style [2].

Prototype method is conforming to body first principle. It firstly draw basic type correspond with body shape and then adjust it according to style requirement on basic type, finally obtain pattern structure. The methods which fit body before varying clothing style make the structure not complicated and simplify the complex design procedure. At end clothing shape change following body variation, result in not adverse to control type shape. It is easy for deviate garment shape by adjusting partial lines. So here introduce typological method to study on garment pattern design procedure.

Typological method

The content of typological method is mainly consciousness of human classification and behavior activities. Typology usually classify with function, shape, structure, region and culture etc. It try to find general principle from history variation and combination, then through extract prototype and peel object which awake collective memory off, and utilize these principles to turn into specific design practice and adapt to new shape accommodating new circumstance [3].

Typology base on biology and psychology which regard as systemized theory be introduced in many different fields, such as architecture, art, linguistics, sociology and economics etc. This method really is cycling way of variations that regard essence as prototype and comply with logic thinking following model-type-new form. It has obvious revelation meaning [4].

Appearance and evolution of clothing undergo lengthy period, form many clothing type that have collective memory. No matter which style clothing develop and change, the elements containing in clothing will activate people to recall its culture and symbol. Just right the method can abstract from specific shape of clothing, and express deep structure, namely collective memory, from clothing. Therefore new method for garment pattern require a kind of process of identification and classification to restore and classify similar character of structure from traditional clothing and then integrate and reappear clothing culture and style. Using typological method to study on pattern design is conducive to keep continuity of style and type of clothing, and maintain tradition and culture memory of clothing.

Application of typological method

The emphasis on pattern design of typology is of elements extrication and type transformation. Here clothing type is not a sort of specific fashion style, but in the same classical style of clothing extract regular shape principle. It should have concrete relation of proportion and space structural model.

Typological method includes 3 phases: type extract, type regression and form innovation. The first two stages are analysis process of objects; also eliminate variation and reducing prototype process. Designers need to analyze its internal form and structure for the regression of certain universality and primordial nature "original form", i.e., "a regular modeling principle" [5]. The final stage is the process of creating and design, is on the basis of the prototype to research variability and transitional forms, and through a new form to present particular image that existing in people brain, ultimately make a similar new forms but not same as past form. This not only keeps visual consistency from form cognition, also made psychological emotional resonance and identity.

Selection of Chinese-type clothing and prototype extraction. Through studying Chinese-type clothing, can fine out new fashion form derivation from historical type, all the same there exist many differences in appearance, structure, process, material and decoration etc. Clothing type and shape directly effect ultimate design consequence. So according to typological method, the type of clothing assuredly is a procedure of selection, refinery and abstraction. As shown in Fig. 1: First collect classical samples from significant clothing shape, and objectively carry on analysis to obtain inductive information from these clothing sample, such as basic type, modeling and size etc. Secondly, perceptual information is refined which exclude the unstructured and additional elements, and simplify it into geometric figure, gradually confirm fixed elements from variation in the refined process. Such as connection mode and structural type, typical components, etc. Finally the fixed elements are further abstract to get and capture the most universal significance original element, namely can keep a continuous prototype, such as scale relation, space structure model, etc.

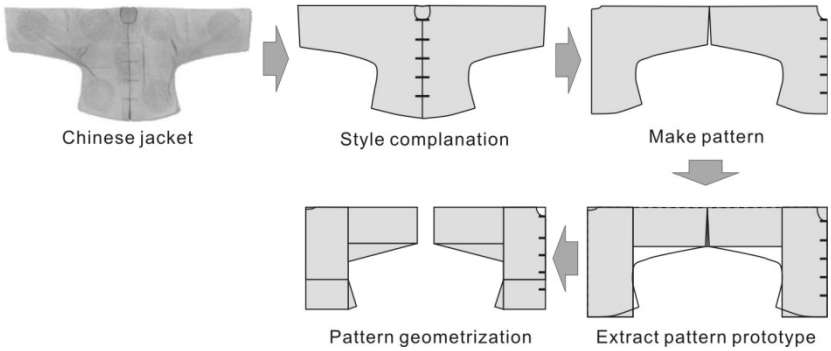


Fig.1: The selection and abstraction of Chinese-style clothing prototype

Typical transformation of Chinese-type clothing. Transformation is the procedure of restructure and regression on type, furthermore integrate with life and aesthetics and find out a new variant which can reform.

In this process the original type must keep fixed and similar on deep layer structure, meanwhile perform different combination, change and extension in surface structure. Therefore it can obtain innovational shape along essential continuity, i.e. form an integrated effect between new and old shapes, and then generate a fresh shape with new elements.

Typical transforming usually starts with form combination, topological switch with structural model, adjusts with proportion scale and adds and deletes elements of entity. It is very important that such transformation must be on typology, but directly change clothing shapes itself, both are different in the way: the former not change original type and the later directly imitate. Hence the two ways have essential different in ultimate result. As follow in figure 2, it shows that procedure of prototype transformation.

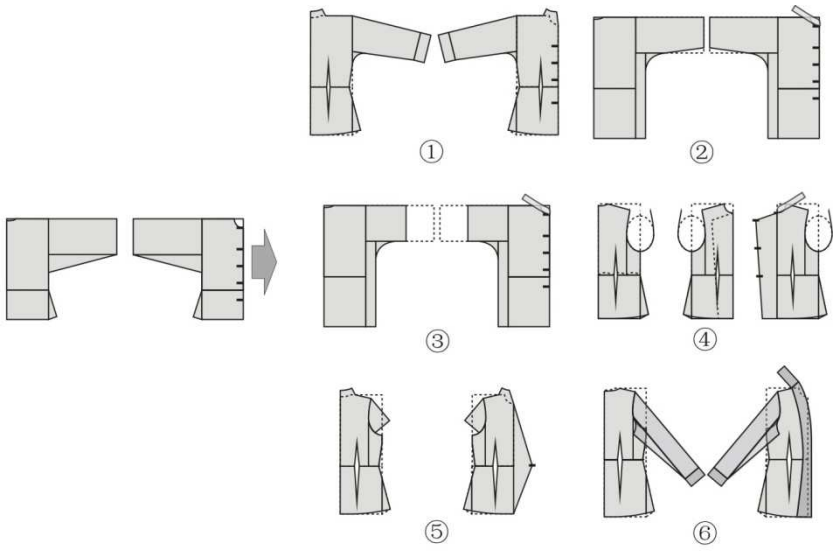


Fig.2: The style changing process of Chinese-style clothing prototype

Shape innovation of clothing pattern. Through selecting and transforming type and style, a modeling group is formed base on prototype (see Fig. 2). This group provides necessary reference and basic skeleton for garment pattern innovation in the aspects of replacement, combination and restructure. Innovation process is put in modern circumstance and applied in place, is given specific appearance, such as material, technique and decoration etc. Namely it has similarity in spirit and difference in shape. The innovation way can use reverse design, replace design and judge design etc. For instance, be sure of keeping function and structure, according body shape to reform pattern shape, recombine pattern and multipurpose use new materials, and refresh decorated style and theme, blend with modern symbol and fashion element etc. [6]. In addition, expressing form should not be

restricted to clothing itself, furthermore should mix other regions in culture art and scientific technique, make the garment pattern really inherit traditional culture and at the same time be suited for modern life and ideology. Following figure3, they are the results of fashion style who are using typological pattern design method.



Fig.3: The new Chinese style fashion design by typological pattern method:

Conclusions

Introduction of typological method in clothing pattern design is a valuable means and approach for studying Chinese-type clothing style and selecting and abstracting prototype to creative design. Simultaneously, it is beneficial to critically inherit Chinese-type clothing style, and arouse people memory and perceiving of traditional culture. It also will avoid unquestioning imitation and duplication in modern design, or blindly restore ancient ways.

References

[1] R.Q. Wang, F.Q. Wang, J.Q. Wen: Shanghai Textile Science & Technology （in Chinese） Vol. 7(2009), P. 23-25.

[2] W.L. Cao, Y. Xiu: Journal of Beijing Institute of Clothing Technology (Natural Science Edition) （in Chinese） Vol. 1(2008), P. 13-17.

[3] N.LI, L.LI, Y.Yang: City Development Study （in Chinese） Vol. 15 (2008), P. 33-34.

[4] L.J. Wang: *Architectural Typology* (Tianjin university press, China 2005).

[5] M.G. Wang: Packaging Engineering Vol. 28 (2007), P. 174-176.

[6] G.C. Feng: *Contemporary Design of Chinese Style* (Chongqing press, China 2007).

© (2011) Trans Tech Publications, Switzerland
doi:10.4028/www.scientific.net/AMR.331.594

Regression Analysis on Influences of Hem Parameters On Flare Sagging of Semi-Circular Skirt

Hong NI

Jiangyin Polytechnic College, Jiangyin Jiangsu, 214405，P.R of China

jynh0608@126.com

Key words: Semi-Circular Skirt; Fabrics; Flare Sagging; Parameters of Skirt Hem; Relationship; Linear Regression

Abstract: Select 45 pieces of silk, cotton and wool fabrics in total, with semi-circular skirt modeling as object of study, investigate the relationship between flare sagging in straight & inclined grains of skirt pieces and fabric types, analyze the influence of hem parameters on flare sagging of semi-circular skirt and obtain multiple linear regression equation by disposing the measured data with SPSS statistical analysis software. The study result shows that the skirt hem of silk fabric is sagging more significantly than that of cotton and wool fabrics and there is a multi-linear relationship between semi-circular flare sagging and parameters. The research of this subject has both theoretical value and practical value.

Introduction

In cloth molding design, in order to achieve the desired tiered effect, the designer always likes taking straight and inclined grains at 45 degrees angle as the center line of garment pieces. The tiered show best in shape in this way and its ripples are distributed evenly with symmetrical trough and good effect in pleat and large amount in ruffles[1] . But in this case, we will face a problem, after this kind of garment is dressed, the tiered sagging of garment pieces differs in length so as to make the skirts rugged and reduces the dressing effect. [2]

Since the tiered modeling is widely applied in skirts, in order to quantitatively study the sagging of garment pieces, this paper intends to adopt semi-circular skirt modeling as object of study, selecting three such fabrics as silk, cotton and wool to tailor them into skirt pieces with the same pattern and measures sagging and related parameters of skirt hem so as to look into the quantitative relation between sagging and parameters of skirt hem.

Experimental Materials and Method

Experimental Materials. For the experiment, totally select 45 pieces of fabrics in three types, owing to the tiered modeling mostly made of silk fabric, pick out silk fabric for 30 pieces, cotton fabric for 12 pieces and wool fabric for 3 pieces and the fabrics differ in style. In Table 1, are basic specifications and parameters of fabric samples.

Table 1 Specifications of Fabrics

Fabric Sample	Raw Materials	Density/g·m^{-2}	Fabric Texture
Silk Fabric	Silk and Polyester Filament	22.4-201.4	Plain, Twill, Satin, and Jacquard
Cotton Fabric	Cotton and Polyester Staple Fiber	84.3-299.7	Plain, Twill, Satin, and Jacquard
Wool Fabric	Wool and Staple Fiber	152.8-169.6	Diversified Twill and Backed Weave

Experimental Methods. Select the front semi-circular skirt pieces as the object of study, taking length of skirt L=40cm，half waist W=32.1cm，and draw out the pattern of front skirt pieces, shown as Fig.1.

Lay the patterns on the 45 pieces of fabrics above-mentioned, align the side seam of a side of skirt pieces with the radial straight thread of fabric, after cutting along the pattern, 45 pieces of skirt samples can be obtained and the center line of skirt pieces just is the straight and inclined grain. Pin the hipline of each piece of sample on the same dummy, gently turn the dummy, enabling the skirt pieces in the natural sagging state, after the skirt pieces stand still, measure the vertical distance from the front center of skirt hem to the ground. And meanwhile, put camera lens parallel to the skirt hem, fixing the relative distance from lens to skirt hem and shoot the still effect picture of skirt hem, shown as Fig.2.

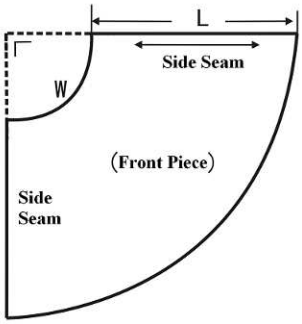


Fig. 1 Skirt Piece Sample Drawing

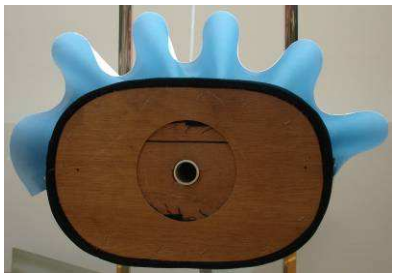


Fig. 2 Picture of Skirt Hem

Data Acquisition for Skirt Hem Parameters. The skirt hem differs in shape and size with the different draping property. [3] in the shot 45 pictures of skirt hem, respectively obtain hem area, tiered peak number, tiered peak length a, tiered peak length b, the angle between adjacent peaks x_5, angle between adjacent tiered valley x_6 and the standard deviation of these parameters. These parameters may fully reflect the shape and size of skirt hem. [4] See Fig.3 for the specific indicators, among which standard deviation is used to judge dispersion of indicator data. In order to acquire area of skirt hem x_1， cut along its profile after printing the picture of skirt hem and obtain the area picture of skirt piece hem, weigh it on the electronic balance and calculate the picture area S_2 by Formula (1)

$$S_2 = \frac{G_2}{G_1} \times S_1 \tag{1}$$

In this formula, S_2 refers to the picture area（cm^2）of skirt hem;G_1 refers to the weight (g) of regular square pattern weighed by electronic balance ;G_2 refers to the mass (g) of skirt hem picture pattern weighed by electronic balance ;S_1 refers to the area of regular square pattern. The area is 100 cm^2.

Since the scale between the real skirt hem and its picture comes to 1:4.33, the actual area x_1 of skirt hem shall be calculated by Formula (2).

$$x_1 = 4.33^2 \times S_2 \tag{2}$$

Tiered peak length x_3 and tiered valley length x_4 resulted from the measured data a and b respectively multiplied by 4.33; tiered number, angel between adjacent tiered peak and angle between tiered valley are subject to the measured data; the standard deviation of tiered peak length, tiered valley length, angle between adjacent tiered peaks and angle between tiered valleys are calculated by STDEV function of EXCLE software.

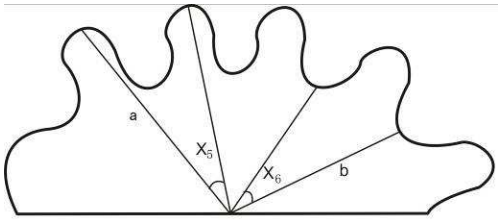


Fig.3 Skirt Hem Parameters

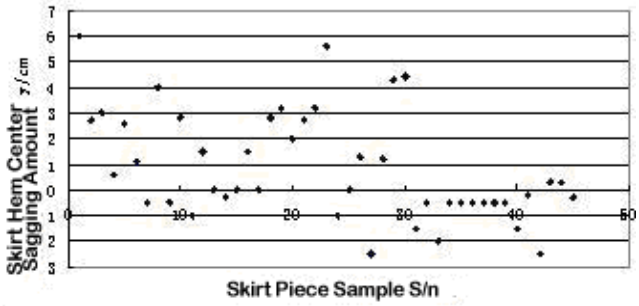


Fig.4 Flare Sagging Distribution Graph

Result and Analysis

Skirt Piece Sagging Result and Analysis . The dead center sagging distribution of skirt hem is shown as Fig.4. In the figure, No. 1 to No.30 are silk fabric skirt pieces, No.31 to No.42 are cotton fabric skirt pieces and No. 43 to No.45 are wool fabric skirt pieces.

Seen from the figure, the hem center of silk fabric skirt pieces sags significantly, in contrast, skirt hem made of cotton and wool fabric doesn't sag obviously, most hem sagging of skirt pieces appear to be negative value, indicating skirt hem doesn't sag but lift. Therefore, when making semi-circular skirt with different fabrics, the skirt piece sample must be revised accordingly. Generally, the hem center of silk fabric skirt piece sample should be taken in and the hem center of cotton and wool fabric skirt piece sample is not changed or taken outward slightly. Shown as Fig.5 and 6, the dotted line in the figure represents the revision line of sample hem.

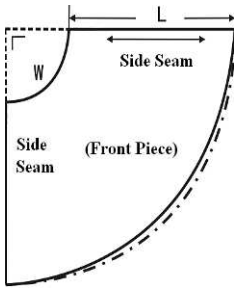


Fig.5 Revision Plan of Front Piece Sample of Silk Fabric Semi-Circular Skirt

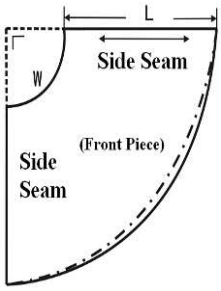


Fig.6 Revision Plan of Front Piece Sample of Cotton and Wool Fabric Semi-Circular Skirt

Multiple Linear Regression Analysis On Front Center Sagging and Parameters of Skirt Hem. In order to research the quantitative relation between front center sagging and parameters of skirt hem, multiple linear regression method [5] in SPSS statistical analysis software is adopted to make stepwise regression analysis on the experimental measured result of front center sagging and relative parameters of skirt hem, achieving the results output from Table 2, Table3, Table 4 and Table 5.

Table 2 Variables Introduction or Elimination

Fit process step number of regression model	Independent variable introduced for regression equation	Independent variable eliminated from regression equation	Criterion of independent variable introduced for or eliminated from regression equation
1	x_1	.	Stepwise regression (judgment：introduction probability≤0.050，elimination probability≥0.100)
2	x_7	.	stepwise regression (judgment：introduction probability≤0.050，elimination probability≥0.100)
3	x_{10}	.	stepwise regression (judgment：introduction probability≤0.050, elimination probability≥0.100)

It can be seen from Table 2, the variables x_1, x_7 and x_{10} are introduced in model, the relative indicator parameters are respectively skirt hem area, standard deviation of tiered peak length and standard deviation of angles between adjacent tiered valleys and the other variables are eliminated. Seen from the analysis on fit result in Table 3 and mean variance in Table4, multiple correlation coefficient in Model 3 is 0.745, the adjusted coefficient of determination R^2 is 0.523 and F value is 17.062,indicating the regression equation and goodness of fit are in general.

Table3. Fitting Result

Model No.	Multiple Correlation Coefficient R	Coefficient of Determination R^2	Adjusted R^2	Standard Error of Estimated Value
1	0.641	0.411	0.398	1.6185
2	0.704	0.495	0.471	1.5164
3	0.745	0.555	0.523	1.4408

Table 4. Analysis of Variance

Model No. l		Sum of Squares	Freedom Degree	Mean Square Deviation	F Value	Significance
1	Regression	78.721	1	78.721	30.052	0.000
	Residual	112.638	43	2.619		
	Sum	191.359	44			
2	Regression	94.786	2	47.393	20.611	0.000
	Residual	96.573	42	2.299		
	Sum	191.359	44			
3	Regression	106.251	3	35.417	17.062	0.000
	Residual	85.108	41	2.076		
	Sum	191.359	44			

Table 5 refers to the partial regression coefficient and the significance test value of each factor in the model, so the multiple linear regression equation of experimental sample can be achieved, shown as Formula (3). Seen from Formula (3), the greater the standard deviation of skirt hem area and tiered peak length is, the smaller the angle between adjacent tiered valleys is and the smaller sagging of skirt hem $\hat{y}$ is; and vise versa.

$$\hat{y} = 18.848 - 0.028\,x_1 - 1.377\,x_7 + 0.123\,x_{10} \quad (3)$$

It is of great practical value to predict the sagging of skirt hem. The garment company can conduct cost accounting according to the sagging of skirt hem and have a clear idea of quotation and production, reducing the manufacturing cost effectively.

Table 5 Equation Coefficient Table During Regression Calculation

Model		Non-standard Equation Coefficient		Standardized Regression Coefficient	t Value	Significance
		Partial Regression Coefficient	Standard Deviation			
1	Constant	15.784	2.729		5.785	0.000
	x_1	-0.025	0.005	-0.641	-5.482	0.000
2	Constant	17.461	2.634		6.629	0.000
	x_1	-0.025	0.004	-0.644	-5.874	0.000
	x_7	-1.068	0.404	-0.290	-2.643	0.011
3	Constant	18.848	2.571		7.330	0.000
	x_1	-0.028	0.004	-0.720	-6.601	0.000
	x_7	-1.377	0.406	-0.374	-3.393	0.002
	x_{10}	0.123	0.052	0.269	2.350	0.024

Conclusion

In view of semi- circular skirt modeling, this paper studies the relationship between the sagging at straight and inclined grains of skirt hem, concluding that the sagging of silk fabric skirt hem is greatest and that of cotton and wool fabric skirt hem is relatively smaller, most of which doesn't sag but lift; It sets up the multiple linear regression equation based on the data of 45 pieces of fabric samples and obtains the quantitative relationship between sagging and relative parameters of skirt hem. This is an entirely new attempt. With the establishment of regression model, it takes the research work in this paper a step forward and lays a certain foundation to deepen the study of this subject in future.

Acknowledgements

Financial support for this work was provided by the Science and Technology Project of Jiangyin Municipality (2009-26).

References

[1] H.Wen and X.Q.Ding: Shanghai Textile Science & Technology .Vol.37(2009),p.36

[2] H.Ni:Silk. 12 (2003), p.44

[3] H. Ni and C.S. Zhang:Journal of Suzhou Institute of Silk Textile Technology.Vol.24(2004),p.86

[4] J. Li，Y. Ke，X.Y. Lin，Y.Y. Wang and X.H.Zhang: Journal of Textile Research .Vol.31(2010),p98

[5] J.Y. Yu and X.H. He: Data Statistics Analysis and SPSS [M].Beijing：Posts & Telecom Press，2003：204-214.

© (2011) Trans Tech Publications, Switzerland
doi:10.4028/www.scientific.net/AMR.331.599

The analysis of structural mathematical model of suitable female jacket design based on waist and hip

Ping Zou[1, a], Shigang Wu[1,b]

[1] School of Fashion and Textile, Eastern Liaoning University,

Dandong Liaoning, China 118000

[a] pingping1968321@yahoo.com.cn, [b] wshg138@163.com

Keywords: waist girth, hip girth, mathematical model, stepwise regression, influence, mathematical model

Abstract. Computer application technology which is changing with each passing day has shown strong vitality, and garment CAD technology has become the inevitable trend in garment industry and it is accelerating economic development. The relation between control parts and details for female jacket structure was established by applying stepwise regression and using C++ language. By comparing between different mathematical models, it was discovered the waist and hip had more influence to the small bust female jacket structural design. The conclusion will provide the garment pattern making experience for clothing enterprises, and it will provide data basis for garment CAD technology.

Introduction

If we want to make China's garment industry be in an invincible position in the international market, we must vigorously promote garment CAD technology and application development, and gradually raise domestic CAD system software and hardware commercialized and practicality level. It should improve the degree of modern enterprise and competitiveness, which has become an urgent task[1]. As is known to all, in the female jacket structure design, the effect of transverse parts of bust to clothing structure is extreme, such as Japanese culture prototype which use bust size to calculate the other detail size, and so as proportion method in China[2]. The effect of waist and hip on female jacket is very great through comparing to structure design mathematical model of each part stepwise regression, which will break the previous principle that bust is the main effect on female jacket. In this paper, the relationship between main control parts and the details specifications was established by using c + + language, This conclusion will provides experience for clothing enterprise, and it also will provide basic of technology research for garment CAD three-dimensional, automation, integration, network, digital technology applying to pattern design [3].

Body measurement and somatotype

Anthropomitric measuring. According to state principle of garment series size GB/T1335.2—1997, we measured 500 female graduates whose age was between 18 to 24 years old. Requirement includes dressing sexy suits and natural status. Totally contain 25 parts, control parts such as neck, breast, waist, hip, shoulder and height etc., and detail parts were shown in Tab.2.

somatotype. Body somatotype will break the current standard of garment series size and propose more detail about somatotype. This method is redistricting body type by height-breast and waist-breast ratio, so it can clearly and precisely describes body characteristics [4].The height-breast ratio is a direct ratio. In the mathematic model of structure, select 40 people as model objects: A0 standard small breast body, A1 less small breast body, A2 standard middle body, Y2 less small waist body, Y3 large breast and small waist body, as shown in tab.1.

Tab.1 Chart of body type category

breast /waist	height / breast					
	0 (2.1)	1(2.0)	2(1.9)	3(1.8)	4(1.7)	5(1.6)
	slender	thin	moderate	Slight fat	fat	corpulent
X(≥1.4)over thin	X0	X1	X2	X3	X4	X5
Y(1.3)slender	Y0	Y1	Y2（94P）	Y3（74P）	Y4（40P）	Y5
A(1.2)standard	A0（65P）	A1（137P）	A2（46P）	A3	A4	A5
B(1.1)slight fat	B0	B1	B2	B3	B4	B5
C(1.0)corpulent	C0	C1	C2	C3	C4	C5
D(≤0.9)over fat	D0	D1	D2	D3	D4	D5

Stepwise regression

Generally, jacket structure design mathematical model of clothing is linear equations, less use the binary linear equation, and it can't meet development request of future garment CAD system because of the complexity of the human body. In this study, the calculation method of mathematical model will break the original traditional structure by using stepwise regression.［5］.

Establishment of structure mathematics model

In the mathematical model of female jacket structure, by utilizing C + + language to calculate the stepwise regression, control parts and the detail of the relationship between parts specifications calculation was established. Variable parameters were 1.5, 3.0, and 4.5，the larger parameter the less variable. The significance setting was 0.9, if larger than 0.9 than regard as significance, or regard as no significance. Then compare to the results of regression, firstly judge relationship of linear was significant, secondly find out model with smallest residual, if with the same residual, to find model with less variable. The results in the analysis are all significant, such as body type A0, A1, A2, Y2 and Y3, as shown in Tab.2 to Tab. 4.

Tab.2 Mathematic model of body type A0,A

The stepwise regression mathematic model of Body type A0 with standard small breast	A0 residual standard deviation	The stepwise regression mathematic model of Body type A1 with standard slight small breast	A1 residual standard deviation
Neck root = 0.88N+ 7.1	1.1	Neck root = 0.78N+ 0.04H+ 6.1	1.4
Across Front = 0.33B + 5.4	1.9	Front bust width = 0.21 B + 15.1	1.9
under bust= 0.95W + 6.1	1.8	Under bust= 0.95W + 7.2	2.0
abdomen = 0.52W+ 0.69H -16.9	2.7	abdomen = 0.44W + 0.52H + 4.8	2.8
Breast distance = 0.1 W + 8.5	1.4	Breast distance = 0.08W-0.05B + 0.13S+8.3	1.0
Breast high = 0.19W + 0.06H + 5.4	1.3	Breast high = 0.13W+0.11H+0.13S-0.17	1.2
Front arm hole = 0.07H+ 0.24S + 0.69	1.0	Front arm hole =0.15N+0.04H+0.22S-0.93	1.0
Front waist line = 0.2W + 24.8	1.8	Front waist line =0.06G+0.1B+0.2W+5.6	1.7
Across back =0.16W-0.13G + 0.63S+17.6	2.1	Across back = 0.22W + 0.5S -2.7	2.0
Back AH depth = 0.18S + 13.6	1.2	Back AH depth = 0.08G + 0.08H -1.7	1.5
Back waist line=0.14G-0.17B+0.12W+20.3	1.6	Back waist line = 0.16G + 0.09W + 6.7	1.5
Front shoulder high = 0.07H + 5.8	1.2	Front shoulder high = 0.05H + 7	0.9
Back shoulder high = 0.05G + 0.05H + 1.3	1.3	Back shoulder high = 0.1H -0.11S + 9.6	1.2
Arm root = 0.12W + 0.3H + 0.33	1.5	Arm root = 0.09G + 0.35W -1.9	1.6
Up arm = 0.19W + 0.3H - 14.3	1.5	Up arm = 0.31W+0.1 H-3.8	1.3
elbow = 0.08W + 0.16H + 1.5	1.1	elbow =0.1W+0.11H+0.11S-0.17	0.7
wrist = 0.04W + 0.07H + 5.1	0.8	wrist =0.04W+0.06H+0.11S+1.8	0.6
Elbow high = 0.19G + 0.08W -10.2	1.5	Elbow high = 0.17G + 0.08W-0.06H	1.3
Arm length = 0.34G+ 0.19S -12.5	1.6	Arm length = 0.34G -4.9	1.6

note：neck(N),bust(B),waist(W),hip(H),should(S),height(G)

Tab. 3 Mathematic model of body type A2,Y2

he stepwise regression mathematic model of Body type A2 with standard middle body	A2 residual standard deviation	he stepwise regression mathematic model of Body type Y1 with standard slight small waist	Y2 residual standard deviation
Neck root = 0.73N+ 11.7	1.5	Neck root	1.2
Across Front =0.06G + 22.5	1.8	Across Front = 0.2B + 16.3	2.2
under bust = 0.94W + 8.5	1.9	under bust = 0.14G + 0.13B +1.03W -31.2	1.7
abdomen =1.09N+0.38W +0.61H+0.61S-57.9	3.6	abdomen = 0.42W + 0.57H + 1.3	2.8
Breast distance = 0.15W + 5.7	1.0	Breast distance = 0.18W -0.12S + 8.3	1.0
Breast high = 0.22H + 5	1.2	Breast high = 0.06G + 0.2W + 1.1	1.1
Front arm hole depth=0.34S + 3	1.1	Front arm hole depth =0.05G-0.1B+0.04H+0.13S+7.6	0.9
Front waist line = 0.13G + 17.5	1.7	Front waist line =0.17G-0.13B+0.13W + 13.5	1.5
Across back = 0.3W + 0.37S -2.8	2.1	Across back = 0.32 W-0.06G + 0.39S + 5.4	1.8
Back AH depth = 0.1H + 11.1	1.5	Back AH depth =0.1G-0.1W+0.15H+0.13S-8.7	1.2
Back waist line =0.11G+0.24B+0.3S-11.5	1.8	Back waist line = 0.11G+0.15W+10.8179	1.6
Front shoulder high = 0.1B + 0.09G -11.1	1.0	Front shoulder high =0.04G -0.06 B+0.04H+7.3	1.0
Back shoulder high =0.04G-0.22N + 0.07W+9.1	1.2	Back shoulder high = 0.11H + 5	1.1
Arm root = 0.13G + 0.37W -9.8	1.6	Arm root = 0.07G + 0.24W + 0.15H -5	1.4
Up arm =0.23W+0.27H-0.07G-0.21N+6	1.2	Up arm = 0.3W + 0.16H -7.7	1.6
elbow = 0.14W + 0.1H + 3.7	0.8	elbow = 0.14W + 0.11H + 2.5	0.7
wrist = 0.1H + 5.2	0.6	wrist = 0.02G + 0.06W + 0.05H + 2.3	0.5
Elbow high = 0.15G + 0.11H -7.1	1.0	Elbow high =0.15G+0.08B+0.21S-12.8	1.1
Arm length =0.27G+ 0.44N-0.2B+0.37S-4.7	1.5	Arm length =0.3G +0.05H +0.16S-10.7	1.7

Tab.4 Mathematic model of body type Y3

Body type A2 with standard large breast and small waist body	Residual standard deviation
Neck root = 0.93 N-0.14S + 11.3	1.2
Across front = 0.08H + 26.2	1.8
Under bust= 1.15W -3.5	2.3
abdomen = 0.51W + 0.65H -9.8	3.2
Breast distance = 0.04B + 0.16W + 0.8	0.9
Breast hight= 0.06G + 0.15W + 0.13H -6.4	1.2
Front AH depth = 0.06G + 0.16N + 0.12H -10	0.9
Front waist line = 0.09G+ 0.13B + 0.16W + 0.16H+ 12.8	1.8
Across back = 0.24W+ 0.38S+ 1.5	2.1
Back AH depth =0.1G + 0.06H -1.2	1.5
Back waist line = 0.19G + 0.15W -0.8	1.6
Front should height = 0.06G + 0.15N+ 0.07H -10	0.7
Back should height = 0.04G + 0.1W + 1.1	1.0
Arm root = 0.07G +0.4 W -1.3	1.6
Up arm =0.36W+ 0.11H -6.2	1.2
elbow =0.14N -0.04B + 0.12W +0.1H + 3.8	0.7
wrist = 0.02G + 0.1N + 0.06W+ 0.05H -0.6	0.5
Elbow height = 0.13G + 0.09H -2.9	1.2
Arm length = 0.28G + 3.9	1.5

Result of mathematic model

The linear relation analysis of residual standard deviation and regression. The total body type of residual standard deviation is 95 models. In Tab.5, it is shown that the more residuals from 0 to 2 , it has 85 models, occupying proportion 89.5%; it has 8 models between 2 and 3, and proportion is 8.4%; it has only less residuals between 3 and 4, and proportion is 2.1%. Above results show that the mathematic models are meaningful.

As shown in tab.5, the relation of regression including 95 models, all models have significance. Overall the relation of regression is more steady and meaningful. So the female jacket structure mathematic model is sound.

Tab.5 The compare result of regressing residual standard deviation and linear relation

Body type	residual standard deviation			linear relation	
	0～2	2～3	3～4	Sig.	Non sig.
Body type A0	17	2	0	19	0
Body type A1	18	1	0	19	0
Body type A2	17	1	1	19	0
Body type Y2	17	2	0	19	0
Body type Y3	16	2	1	19	0
total	85/（89.5%）	8/（8.4%）	2/（2.1%）	95（100%）	0（0%）

Tab.6 Occurrence number of control parts in regression model

part	waist（W）	hip(H)	bust(B)	height(G)	shoulder(S)	neck(N)	tatol
Body type A0	12	9	1	5	4	1	32
Body type A1	12	11	3	8	9	2	45
Body type A2	9	6	3	9	5	5	37
Body type Y2	13	9	6	12	6	1	47
Body type Y3	11	12	3	11	2	5	44
total	57 /27.8%	47/23%	16/7.8%	45/22%	26/12.7%	14/6.8%	205/100%

Conclusions

Establishing mathematic model of female jacket structure make the relation of regression and residual satisfy the demand of model, and the model is successful. From the aspect of relation of effect between parts, the most effect factors are waist and hip, the waist significance is 3.6 times than breast, the hip significance is 2.9 times than breast. The result will break the principle which the breast is the main control part in female jacket structure design. It will provide experience of making pattern for garment enterprises and provide optimal data and reference for garment CAD system.

Acknowledgements

This work was financially supported by the Foundation of Education Department of Liaoning (2009B183).

References

[1] Z. Liu, X.C. Wang: Shanghai Textile Science & Technology（in Chinese） Vol. 32 (2004), P. 53-54.

[2] P. Zou: Journal of Southwest China Normal University (Natural Science Edition) （in Chinese） Vol., 33(2008), P. 127-131.

[3] J. Wu; W. Tuo: Shanghai Textile Science & Technology（in Chinese） Vol. 32(2004) , P. 45-46.

[4] R.P. Liu: design principle and technique of female clothing pattern (china textile &apparel press, China 2005).

[5] X.K. Yu, J.P. Wang: Journal of Donghua University, Natural Science（in Chinese）Vol. 29(2003) , P. 43-47.

[6] K.T.Fang: practical regressing analysis (science press, China 1988).

© (2011) Trans Tech Publications, Switzerland
doi:10.4028/www.scientific.net/AMR.331.603

Redesigning the Apparel Product Development Process Based on the No-Interval Coherently Phased Product Development Model

Chun-Sheng Wu [1, a], Qiao-Ying Wu [2, b]

[1] School of Fashion Design, Zhejiang University of Science and Technology

Hangzhou, Zhejing, P.R.China

[2] School of Fashion, Zhejiang Sci-Tech University, Hangzhou, Zhejiang, P.R.China

[a]artdesign2002@126.com, [b]bettywu2000@126.com

Keywords: Apparel product development, Product development process, Merchandising, Model

Abstract. The objective of the research was to redesign generic process of the apparel product development adopted in Chinese apparel enterprises currently by comparing and analyzing several important models. The revised apparel retail product development model by Wickett, Gaskill and Damhorst, Kunz's taxonomy of the apparel merchandising system, and the no-interval coherently phased product development model for apparel (NICPPD) by May-Plumlee and Little were analyzed. The key factors of product development process that need to be improved were anylized according to the NICPPD model. The end result was the redesigned process of apparel product development.

Introduction

The apparel industry has been changing greatly in recent years. Growing economic globalization, new technological developments, increasingly sophisticated consumers, and heavy retail competition are causing apparel enterprises to reevaluate their strategy and tactics of product development. New product development is one of the riskiest, but more critical strategies in any competitive industry [1]. In general, apparel product development includes all of the processes needed to take a garment from design inception to delivery to the final customer [2]. As the strategic, creative, technical, production and distribution planning of goods that are designed to reach the marketrplace when that group is ready to buy, product development has a perceived value for a well-defined consumer group. Apparel product development process varies depending on the type and size of company, product type, and business plan etc. Since there are more styles for each company, more merchandise assortments, larger target markets, the level of activity in apparel product development has been steadily increasing [3]. For instance, more and more apparel enterprises have taken the store brands concept one step further by offering complete merchandise assortments to better meet the needs of their target customer.

Since apparel product development is becoming increasingly important in apparel industry, it has become a research hotspot. The number of publications devoted to apparel product development has increased significantly. For instance, many product development models for apparel were proposed by researchers. In this research, one of these models will be used to redesign the product development process adopted in Chinese apparel enterprises.

Comparison of models for apparel product development

Several apparel product development models that depict the process used in developing seasonal apparel lines can be found in the literature. Each product development model consists of the different process arrangements and has its own characteristics. Nevertheless, all apparel product development models have similarities in the key activities and functions [4].

The Revised Apparel Retail Product Development Model by Wickett, Gaskill and Damhorst

Wickett, Gaskill and Damhorst's apparel retail product development model was based on the Gaskill's model depending on an investigation carried out across a broader range of specialty stores. Since the model is of a sequential type, it describes the sequencing of events that occur in the product development process. The product development processes include four phases: research, line conceptualization, product visualization and evaluation, and technical development. This model includes the post adoption of product development process. Internal and external factors as a unique feature compared to other models are considered in this model, which include business/sales trends, target customer base, employee input and marketplace research as internal factors and global market trends, competition, media, government regulations and producer capabilities as external factors. However the model does not effectively show the responsibility of different divisions and coordination between them for each of the defined stages. The line conceptualization phase of the process shows backward and forward movement, but the decision points are not clearly defined and thus it is difficult to assess how and when the process moves forward.

Kunz's Taxonomy of the Apparel Merchandising System (TAMS)

Kunz's Taxonomy of the apparel merchandising system depicts the activities involved in creating apparel from the manufacturer's perspective. This model has integrated the product development more into the mainstream business decision structure of the firm. The development process is divided into three stages: pre-adoption, line adoption, and post-adoption [5]. Line concept, pre-adoption product development, line adoption, and post adoption product development outline the process needed to determine what merchandise will be developed. The pre-adoption phase in product development focuses on the analysis, creativity, and formation of product groups that are unique and that reflect the line concept. In the line adoption stage, merchandisers and other members of the design team decide which styles and which merchandise groups meet the criteria of the product lines. During the post-adoption stage of product development, production styles are prepared. This stage requires that members of the product development team perform several tasks to develop prototypes. After visualizing the seasonal line, the prototype construction to develope samples of the proposed line is prepared. The system consists of four basic components that are line planning, line development, line presentation, and garment production.

The NICPPD Model for Apparel by May-Plumlee and Little

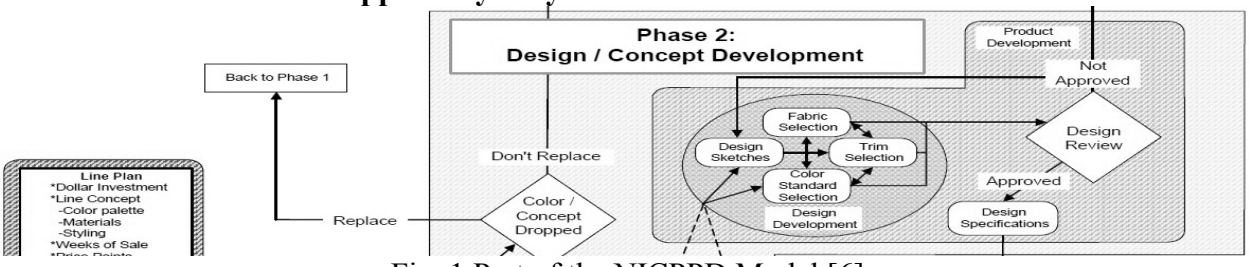


Fig. 1 Part of the NICPPD Model [6]

The no-interval coherently phased product development (NICPPD) model for apparel consists of six phases: line planning and research, design/concept development, design development and style selection, marketing the line, pre-production, line optimization [6]. The further description of each phase with detailed explanations has been presentation by using six figures. Marketing, product development, merchandising, and production planning and control as different functional divisions are involved in the product development process corresponding to different stages. There are fuzzy gates and multiple functional units in the model, which are helpful to integrate sources. The fuzzy gates, also known as soft gates, imply that teams involved in the product development must collectively make decisions on the progression. For instance, marketing, merchandising, and product development are involved in color and concept meeting. This model also indicates some alternative processes, for instance concept tests as an alternative activity in phase 2. Therefore, the adaptability of the model is improved. In addition, decision points which were surrounded by diamond were set to strengthen the control of the entire process. One case is Design Review as shown in Fig. 1 [6]. There

were also some special items such as Back to Previous Phrases and Archive for Future Reference. This model provides for developing both product lines and individual products, developing seasonal lines and multiple seasons annually, and use of alternative development strategies including original design development, knock-offs or take-offs, and modification of existing products[6].

Redesigned procedure of apparel product development

The NICPPD model is generic representation of the stages involved in all types of firms and is helpful to look at in detail the stages and activities in the product development process. The system constraints that may vary depending on the type of product line and firms are included in the NICPPD model. So this model will be used to redesign the product development process adopted in Chinese garment enterprises. Redesigning the apparel product development process involves division collaboration, resource integration, and post set and so on.

Changes in coordination among various divisions

The synergy of different divisions that share the responsibility and risk for producing a quality product is necessary to successfully meet and interpret the ever-changing demands of the consumer [7]. In practice many activities of the product development process are carried out simultaneously and interaction will be common.Compared to the sequential process, simultaneous phases of development reduce time to market and smooth the transition between phases. Therefore, it is critical to be aware that the product development process is a multicross-functional program, where all functions work together to accomplish the required task [4]. According to the NICPPD model, the steps or activities in the product development are carried out by the members who come from the four areas of marketing, product development, merchandising, and production. The incorporation of the four functional divisions of the product development is important. For example, a comment made by 28.5% of the respondents was that one of sources of trend inspiration for fashion can be internal sources, including sales tracking information [8]. Information from marketers allows developer to get an idea of general marketplace trends and to pick up on influences that might dominate fashion design for the upcoming season. Different divisions incorporate according to fuzzy gates. Decision points depict critical convergent points of each function in the development process. The major decision points include color and concept selection, design review, material tests, fit and style evaluation, preliminary costing, sales and merchandising meeting, review retail orders etc.

Changes in staffing and decision point

Apparel product development team members who participate in the product development process include designers, technical designers, and marketing/sales personnel. According to the NICPPD model, the functions of the division of product development include color research, trend research, Fabric research, conception development, design development, raw materials development, garment development, style selection, and order fabrics for sales samples, order duplicates, production patterns, final garment specifications, and size specification sheets. Ideas for products come from a variety of sources and involve a number of employees. Creative design has long been biased in Chinese apparel companies, but merchandising and technical design neglected. The product developer or merchandiser and technical designers are not in proper position in product design and development division. Merchandising as the central coordinating point for the product line is the process of planning, developing, and presenting product lines for identified target market with regard to prices, assortments, styling, and timing [9]. Merchandiser should be the core staff in product development team throughout the whole process. Technical designers evaluate prototype garments and ensure that a style has been perfected before it is approved for production. Therefore technical designer should also be treated as a key member of product development team. Then decision points should be set carefully based on staffing changes. For instance, there are color and concept meeting, design review, and preliminary costing and so on in the NICPPD model.

Redesigned product development process

Product development process varies depending on whether the products being developed are wholesale brands, private label or store brands, licensed brands, or customized [2]. Product developers of store brands offer a complete assortment of privately developed products. The NICPPD model indicates specific activities, but too complex. In addition, the model also requires a combination of the actual situation of Chinese apparel enterprises. Therefore, the process of apparel product development is redesigned based on NICPPD and the new model is shown in Fig. 2. The model effectively shows the responsibility of different divisions and coordination between them for each of the defined five stages. In addition, the model also identifies the actual product or file at each stage and the responsible departments.

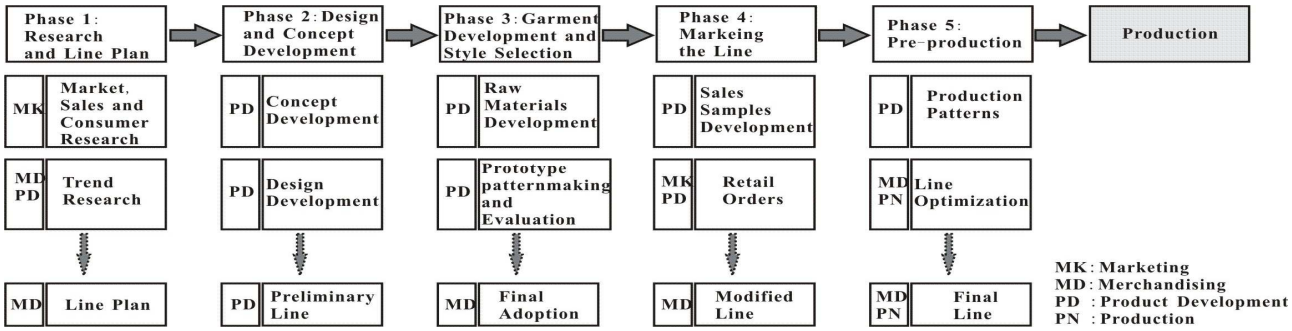


Fig. 2 The model of redesigned product development process

Conclusions

Refinement of the product development process is conducive to the success of product development. The redesigned process of apparel product development is divided into five phases which define the specific functional requirements. Meanwhile, specific product and responsible person at each stage is explicitly proposed. The New model is relatively clear and has better applicability. Finally, this research result will benefit future researchers with theory development pertaining to the apparel product development process.

References

[1] R. G. Cooper, Winning at New Products, 3rd edition. New York: Addison-Wesley, 2001, pp.8.

[2] S. J. Keiser and M. B. Garner, Beyond Design: the Synergy of Apparel Product Development, 2nd edition. New York: Fairchild, 2008, pp.86–87.

[3] M. M. Senanayake and T. J. Little: Journal of Textile and Apparel, Technology and Management, vol. 1, Spring 2001, Issue 3, pp. 1-14

[4] W. Choi, N. B. Powell and N. L. Cassill: Journal of Textile and Apparel, Technology and Management, vol. 4, summer 2005, Issue 4, pp. 1-28

[5] G. I. Kunz, Merchandising: Theory, principles, and practice, 2nd edition New York: Fairchild, 2005, pp.86–87.

[6] T. May-Plumlee and T. J. Little: International Journal of Clothing, Science and Technology, vol. 10, Agu. 1998, pp. 342-364.

[7] L. Ren and W. M. Zhu: In Chinese Journal of Zhejiang Sci-Tech University, vol. 26, No. 3, May 2009, pp. 354-358

[8] J. L. Wickett, L. R. Gaskill and M. L. Damhorst: Clothing and Textiles Research Journal, vol. 17, 1999, No. 1, pp. 21-35

[9] R. E. Glock and G. I. Kunz, Apparel Manufacturing: Sewn Product Analysis, 3rd edition. New Jersey: Prentice Hall, 2000, pp.61–89.

© (2011) Trans Tech Publications, Switzerland
doi:10.4028/www.scientific.net/AMR.331.607

An analysis of marketing function of fashion show

Yi Xu[1,a], Mei Zhang[*1,b]

[1]College of Quartermaster Technology, Jilin University, Changchun, 130062, China

[a] xuyi0307@sina.com , [b] zhangmeisdh@sina.com, * corresponding author

Keywords: fashion show, marketing, 4p, transmitting promotion

Abstract. The fashion show was come into being with the appearance of retail of costumes in the middle of the 19th century. Up to now, it has become an indispensable media, added with a lot of artistic elements which strengthen its value of appreciation, in the fashion field. However, what could not be overlooked is that the ultimate goal of the fashion show is still the commercial value in the costume market and still to emphasize the significance and function in the costume marketing. By summarizing the practical experience of fashion show of hers and referring to all kinds of information at home and abroad, the author divides the fashion show into five categorizes and explains one by one. At the same time, the author analysis the marketing function of fashion show in practice by connecting marketing theory.

Introduction

The fashion show has been in existence in China for more than 20 years as a newly developed profession. With the development of costume industry in society and in China, the fashion show in China is developing drastically when the costume retail, advertisement and publishing are developing rapidly. On the December 5, 1982, during the time when the Soviet Union Trade delegation visited China, Shanghai fashion show team gave the delegation a special performance, which successfully increased the volume of trade. Hence, this is the first time that our fashion show has the function of sales and promotion in the costume market. [1]

The origin and development of fashion show

The fashion show is the performance of showing costumes. It is a way of promoting the costumes to the market and adopts the method of making the models dress clothing samples according to the designers' creation and intention to show (perform) the costumes to the audience in a certain place. [2]

At the very beginning, the fashion show originates from the promotion of products and its purpose is to strive for more recognition from the customers so as to promote the sales of products or to get more orders from the manufactures and the retailers as well as to raise the designers' and enterprises' prestige and fame in order to enlarge their social influence and build the social image of the designers and the enterprises and so forth.[3]

In the fashion, the costumes and the models are both the main parts of the performance and they all serve to show people the costumes to let them feel the beauty and value of costumes totally and directly. The costumes are the core parts that the fashion shows intent to display. Although the performance level of the performers of costumes-----the models has immense influence on the effect of costume showing, the models are not the ultimate purpose of the fashion show. In term of this, the fashion show is different from other arts of performance, because the final goal and essence of the fashion show is to promote the sales of the products.

The category of fashion show

After hundreds of years of development, today, the form of fashion show is more abundant and the means is more various. From the man model of 'doll' type to the professional model performance in the commercial activity, and to the international costume designing and model communicative

competition as well as the artist program which aims to satisfy people's appreciation of beauty, it has formed a rich and colorful performance type. [4] According to the difference of its purpose and character, the author divides the type of fashion show into five categories by collecting information and connecting her own experience in the fashion show:

Fashion show of commercial promotion. The fashion show of commercial promotion is a performance of promoting the products of certain industries or trademarks and designers to the retailers and the consumers. It is a performance directly serving for exchange of merchandise trade. This is the most important, the most original and the most fundamental method of fashion show.

According to the purpose of the performance, we can categorize this kind of performance into performance of promoting trademark, the show of exhibition of ordering and performance of promoting retailing and so on.

Performance of promoting trademark**.** In order to introduce their products to the retailers and the ultimate consumers and to enlarge the fame of their brand, the clothing enterprises and the tailoring industries always hold the fashion show in the fashion week, the fashion expo and the commodities fair. Meanwhile, by the propagation of the media and the clothing reviewer, they strengthen their effect of the representation and set up their image.The purpose of this kind of performance is to set up image and show their power, which reveal their potential commercial purpose.

The show of exhibition of ordering**.** People who benefit from this show are mainly the retailers and the sales person. The audience and the employees who want to order will choose to buy the products while appreciating the fashion show with the indents. This form is flexible and the whole atmosphere is joyful which help the audiences get the knowledge of the characters and style features of the clothes and have a feeling of beauty. This enhances the rate of ordering greatly.

Performance of promoting retailing**.** This performance is the fashion show organized by the retailers or the markets regularly or irregularly in order to attract consumers enhance their popularity and enlarge sale.

The target audience of the fashion show is the consumers. Most of the form of the show is very easy. The retailers give a direct image of the clothes to the consumers by the exhibition of the models so as to guild consumption and stimulate it.

The fashion show of design and release. The major fashion center of the world would hold the high-quality clothing collection and popular information conference (Fig.1) in every January and July. Some fashion intelligence research institutes sometimes introduce their idea toward the latest style of clothes by way of fashion show and they take the market fashion trend into consideration to reveal their prediction of the next season's trend, in this way, they can also stimulate and direct consumption. These 'collection of fashion trend' is the professional guide of ready-made clothes production and clothing consumption.



Fig.1. Chanel fall-winter 2011/1012 in the Paris Fashion Week

Fashion show of competition. Every model agency and clothing manufacture find new models and clothing-design talents through clothing model contest and designing work contest in and out of home. This contest, at the same time, improves their ability through the communication.

Model Contest**.** The characteristics of this performance is this form of contest helps propagate the clothing enterprises. For example, the clothes in the national final contest of the China Model Star Contest were sponsored by the Asahi Kasei Corporation (Fig.2: the author attending the Model Star Contest). And every champion would be the spokesperson of the corporation.

Designing Work Contest**.** The clothing designing work contest is held for the purpose of seeking for new star of clothing designing and collecting designing ideas. And the contest focuses on the designs --- the clothes. (Fig.3: the fashion show of the author attending the Northern Fur Cup Design Competition)



Fig.2



Fig.3



Fig.4



Fig.5

Academic fashion show. This kind of performance sometimes is the process of learning among different universities and sometimes the organizers would invite many manufacturers, designers and retailers to attend. In this way, they not only show their teaching achievement, but also make their students show the professional standards, what's more, they even build a bridge between the students and the enterprises as well as the institutions. The Institution of Clothing Design and Engineering in Jilin University held the first graduate works conference in June, 2010 (Fig.4), which had an achievement.

Fashion show of recreation. With the widespread of art of fashion show and the development of public fashion show, fashion show becomes more and more the public recreation. For example, the fashion show organized by the Fashion Model Association in Jilin University is highly praised by people in and out of school. (Fig. 5)

The marketing function of fashion show

The fashion show is not only an art, but also a planned marketing method. Especially for the relative professions and enterprises, the expense of fashion show is a part of the cost of marketing. Hence, they pay more attention to the profits and effects. In other words, the meaning and effect of fashion show in the marketing cannot be neglected.

The brand promotion function of fashion show. Different from other performance, behind every fashion show, there is the purpose of promotion. From this point of view, we can divide the five fashion shows above into commercial transmission and non-commercial transmission.

The commercial transmission is launched by the enterprises, trademarks, designers and retailers, which aim at transmitting commercial information, setting up the images and promoting the spread of products in the markets and it is the performance for marketing effect. The commercial promotion performance is the typical representative of this kind.

Non-commercial transmission, such as the fashion shows for design publication, competition, academic communication, and entertainment are mainly held by artists, Relevant government departments and various associations and universities. These shows aim at exhibiting art works, disseminating cultural values, promoting culture communication and so on, but these shows can also promote the images of clothing enterprises, Enhance brand awareness of the public and benefit the later operation of the brand.

To promote the sales of textile, clothing and accessories directly. In the countries where garment industry is well developed, the final purpose of a fashion show is to maximize its business function. Fashion shows have been given an unavoidable purpose—sale promotion since the middle 19th century when Voss, the founder of High Fashion, put the shawl on Mary. Though later fashion shows have experienced a series of ups and downs, Sale promotion is always the most direct purpose and naturally, it becomes the main mission. According to the performance of models, fashion shows win not only the identity from consumers to the largest extent, but large profits for manufacturers. With the development of garment industry, fashion shows make textile and accessories into their coverage, so now the shows undertake not only the sale promotion of clothing but also the popularization of textile and accessories.

Marketing function of fashion show in the 4P theory. We should always mention the theory of 4P by John McCarthy when talking about marketing.

Product**:** From the aspect of marketing, product means the thing which can be provided to the market and can be used and consumed and can meet people's need. Product includes tangible product, service, personnel, associations, ideas or the combinations of them.

A fashion show exhibits products to the audience in the most direct way and provide service at the same time to make the process enjoyable.

Price**:** It refers to the price when the consumer buys the product which includes discount, time of payment and so on. Price or price decision relates to profit, cost compensation and whether it would benefit the sales and sale promotion.

The audience of fashion shows are mainly consumers, media, reviewers and other industry insiders. Garment manufacturers or designers gain reliable and timely information from the audience's feedback and then design and purchase and produce and fix the price and prepare for sale

Place**:** Place means that the links in the process of goods move from manufacturers to consumers. A fashion show is the sale activity which can be organized in different levels of sales channels. For example, product ordering exhibition can be organized by the direct sales channels of manufacturers and distributors.

Promotion**:** Promotion is any communication ways a corporation or association uses to show the product, service, image and idea to target market. Promotion is used to persuade and notice the market the reputation and the products of a corporation. The four sales elements are advertisement, Publicity, personal selling and sales promotion

Summary

Fashion shows are the combination of advertisement, Publicity, personal selling and sales promotion. In different situations, the shows emphasize on different aspects: some shows stress sales promotion, such as retail sales performance; some stress personal selling, such as design release performance; some are personal selling, such as product ordering exhibition. Some other promoting ways are added into fashion shows such as making brochures for a show, pasting posts and so on. These way belong to advertisement.So we say that fashion shows can be the integrated marketing way which make 4P marketing theory to practical application

References

[1]Xianzhuang Li: A Study of the Basic Development of Fashion Marketing in China. Donghua University (Master's paper)
[2]Dangqi Li: Guide to fashion. Higher Education Press
[3]Jie Guan:Directing and Organizing of Fashion Show. China Textile& Apparel Press(2008)
[4]Guorui Hu: The Fashion Show Art Beginning. Journal of Donghua University, Social Science(2003)
[5]Jieying Yuan: Fashion Model Performance Art. China Light Industry Press

© (2011) Trans Tech Publications, Switzerland
doi:10.4028/www.scientific.net/AMR.331.611

Mathematical Model of Attaching Sleeve Based on the Change of Underarm Point

YongMei Liu[1, a], Lu Zhang[1,b] and GanHong Feng [1,c]

[1] Fashion Institute, Donghua University, Shanghai, 200051, China

[a]maggie_liu@sohu.com, [b]benzzgf@yahoo.com.cn, [c]chouganzi@126.com

Keywords: Sleeve, Armhole, Construction, Shape of sleeve, The placement of underarm point.

Abstract. Armhole is a base part of the sleeve. The sleeve morphological characteristics affect the construction and shape of sleeve. The underarm point is one of key restraining factors affecting armhole's three-dimensional configuration. The experiments of armhole's three-dimensional configuration and attaching sleeve experiments were designed according to the changes of the vertical and horizontal displacement of underarm point. The regression equation is established through the method of correlation analysis and regression analysis.

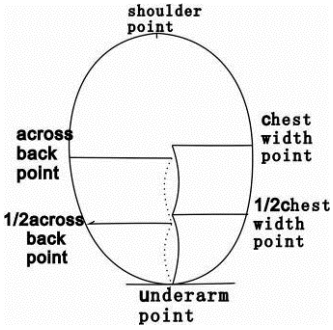
Introduction

In all researches about sleeve construction, the number of studies of match problem between sleeve crown and armhole is quite large. These researches analyse the correlation between sleeve crown and armhole from two-dimensional methods. Although the construction of sleeve and armhole is perfected though this kind of papers, this method of study can't meet designers and customers's requirement. A good three-dimensional shape of armhole is not only a proving of a better body structure but also a guarantee of perfect sleeve. The three-dimensional shape of armhole is a key part of sleeve. And the underarm point is the most important point of armhole. When it moves at vertical or horizontal direction, the height and the angle of armhole will change. The experiments are designed according to the vertical and horizontal change of underarm point. The samples are made and fit on the dummy to adjust the three-dimensional shape of armhole and collect the data of the armholes. The attaching sleeve experiments were done and worked out the relevance of the three-dimensional shape of armhole and sleeve.

The factors of armhole's three-dimensional configuration.

This paper defines three-dimensional configuration of the armhole as Table.1.

Table.1 Definitions of armhole's three-dimensional configuration.



Definition	Position
Armhole width	From chest width point to across back point
Armhole height	From shoulder point to underarm point
Armhole angle	Angle between armhole height line and vertical line
L1	Arc from shoulder point to chest width point
L2	Arc from shoulder point to across back point
L3	Arc from chest width point to 1/2 chest width point
L4	Arc from across back point to 1/2 across point
L5	Arc from 1/2 chest width point to underarm point
L6	Arc from 1/2 across back point to underarm point

The experiment based on underarm point vertical change.

Experiment Design. When underarm point changes at vertical direction, length, curvature and height of armhole will change. According to fashion and different styles, underarm point changes vertically from -2cm to 3cm. **(**1)Made samples. Grade is 0.5cm in this experiment. 11 sample will be made and

named successively A1, A2, A3 …A11. Measure every arc of armhole and analyse data with SPSS. (2)Attach Sleeves. Attaching sleeve experiment based on the armhole already known. The sleeve construction is one-piece sleeve, and sleeve width is 16cm. Use the same method to attach sleeve, and make sure seam shrinkage is 2.5cm. The sleeve top height is dependent variable.

Data of Experiment. Measure every arc of armhole as Table.2.

Table.2 Data of armholes three-dimensional configuration when underarm point changes vertically.

No.	Vertical change	L1	L3	L5	FAH	L2	L4	L6	BAH	AH	Armhole height
A1	-2	9.00	4.40	5.40	18.8	10.2	5	3.8	19	37.7	12.5
A2	-1.5	9.00	4.40	5.80	19.2	10.2	5	4.3	19.5	38.7	13
A3	-1	9.10	4.40	6.30	19.8	10.2	4.9	4.9	20	39.8	13.5
A4	-0.5	9.10	4.50	6.80	20.4	10.4	4.6	5.4	20.4	40.8	14
A5	0	9.20	4.20	7.20	20.6	10.4	4.8	6	21.2	41.8	14.5
A6	0.5	9.10	4.30	7.60	21	10.3	4.8	6.6	21.7	42.6	15
A7	1	9.10	4.30	8.00	21.4	10.4	4.8	6.9	22.1	43.5	15.5
A8	1.5	9.10	4.30	8.50	21.9	10.3	4.7	7.6	22.6	44.5	16
A9	2	9.00	4.20	9.20	22.4	10.2	4.7	8.2	23.1	45.5	16.5
A10	2.5	9.10	4.20	9.70	23	10.3	4.6	8.8	23.7	46.7	17
A11	3	9.10	4.30	10.10	23.5	10.3	4.7	9.4	24.4	47.9	17.5

When the attaching sleeve experiment is done, fit dummy with samples and take pictures of sleeves. The angles of sleeve should be measured with Corledraw. The data is collected and showed in Table.3 .Pictures of three samples are showed in Fig.2.



a) b) c)

Fig.2 a) Vertical change:3cm . b) Vertical change:1cm. c) Vertical change:-2cm.

Table.3 The data of sleeve based on underarm point vertical change.

No.	Vertical change	Armhole height	Sleeve width	Sleeve top height	Seam shrinkage	Angle of sleeve
A1	-2	12.5	16	10.6	2.5	27.2°
A2	-1.5	13	16	11.2	2.5	26.78°
A3	-1	13.5	16	12	2.5	25.85°
A4	-0.5	14	16	12.7	2.5	25.03°
A5	0	14.5	16	13.4	2.5	24.24°
A6	0.5	15	16	14	2.5	23.2°
A7	1	15.5	16	14.7	2.5	22.41°
A8	1.5	16	16	15.5	2.5	21.52°
A9	2	16.5	16	16	2.5	20.88°
A10	2.5	17	16	16.8	2.5	19.87°
A11	3	17.5	16	17.5	2.5	18.56°

Analysis of underarm point vertical change and armhole's three-dimensional morphological characteristics. (1) Analysis of underarm point vertical change and armhole's morphological characteristics. According to Table.2, armhole height will become greater if the vertical change of underarm point is increased. Use the data of armhole height and the vertical change of underarm point to do regression analysis and curve-fitting. In linear regression equation (Eq.1), y is armhole height, and x is the vertical change of underarm point.

$$y=14.5+x. \quad (1)$$

(2) Analysis of underarm point vertical change and every arc of armhole. 1) Correlation analysis. Use data analysis tool SPSS to do correlation analysis between vertical change of underarm point and each arc of armhole. The consequence shows that the correlation coefficients of underarm point vertical change and different arcs are different. The correlation coefficient is L6>L5>L4>L3, L1 and L2 are independent to underarm point vertical change.

2) Establish mathematics model. Use SPSS to do linear regression analysis and curve-fitting to L3, L4, L5 and L6. The consequence is showed in Table.4.

Table.4 Regression function of underarm point vertical changes and every armhole arc.

dependent variable（y）	Linear equation	Curve equation
L3	y=4.3382-0.04x	Non-significant
L5	y=7.1973+0.8782x	$y=7.1438+0.8454x+0.0238x^2$
L4	y=4.8136-0.0636x	$y=5.9443+1.0969x+0.0229x^2$
L6	y=5.98+1.1127x	Non-significant

Analysis of underarm point vertical change and attaching sleeve. According to Table.3, underarm point vertical change determines armhole height. It is a major factor to sleeve top height and angle of sleeve. Use SPSS to do regression analysis. In Eq.2, y is sleeve top height，x is underarm point vertical change. In Eq.3, y is angle of sleeve， x is underarm point vertical change.

$$y=13.347+1.378x \quad (2)$$

$$y=24.091-1.72x \quad (3)$$

The experiment based on underarm point horizontal change

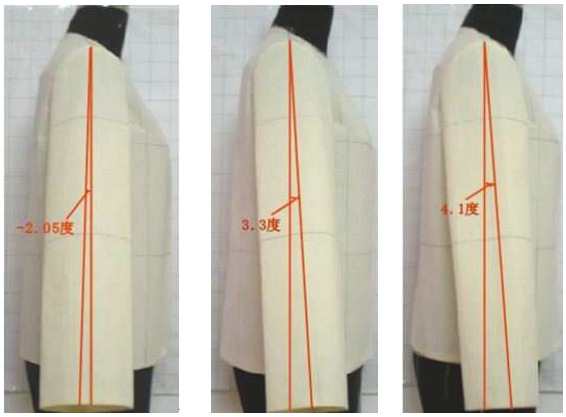
Experiment design. Arm is tilted forward, when it naturally droops. Arm is accustomed to move forward, and it more likely moves forward than backward. Underarm point horizontal changes from -1cm to 2cm. (1) Made samples. Grade is 0.5cm in this experiment. 7 samples will be made and named successively C1, C2, C3 … C7. Measure every arc of armhole and analyse data with SPSS. (2) Attach sleeves. Attaching sleeve experiment is based on armhole already known. The sleeve construction is one-piece sleeve, and the sleeve width is 16cm. Use the same method to attach sleeve, and make sure seam shrinkage is 2.5cm.

Data of experiment. Measure every arc of armhole as Table.5

Table.5 Data of armholes three-dimensional configuration when underarm point changes horizontally

No.	Horizontal change	L1	L3	L5	L2	L4	L6	Armhole width	Armhole angle	Chest width	Across back
C1	-1	9.1	4.2	8	10.2	4.9	5.3	11	0	15.8	17.4
C2	-0.5	9.1	4.2	7.6	10.3	4.8	5.7	10.9	3.1	15.7	17.6
C3	0	9.2	4.2	7.2	10.4	4.8	6	10.8	6.3	15.6	17.8
C4	0.5	9.1	4.2	6.9	10.3	4.8	6.3	10.7	9.4	15.5	18
C5	1	9.1	4.3	6.6	10.3	4.7	6.5	10.6	12.5	15.4	18.2
C6	1.5	9.1	4.3	6.4	10.2	4.7	6.8	10.4	15.6	15.3	18.4
C7	2	9.1	4.3	6.2	10.2	4.7	7.1	10.3	18.7	15.2	18.6

When the attaching sleeve experiment is done, fit dummy with samples and take pictures of sleeves. The angles of sleeve should be measured with Corledraw. The data is collected and showed in Table.6 .Pictures of three samples are showed in Fig.3.



a) b) c)

Fig.3 a) Horizontal change:-1cm. b) Horizontal change:1.5cm. c) Horizontal change:2cm.

Table.6 The data of sleeve based on underarm point horizontal changes.

No.	Horizontal change	Armhole angle	Sleeve top height	Sleeve width	Seam shrinkage	Sleeve angle
C1	-1	0°	13.5	16	2.5	-2°
C2	-0.5	3.1°	13.5	16	2.5	0°
C3	0	6.3°	13.5	16	2.5	1°
C4	0.5	9.4°	13.5	16	2.5	2.1°
C5	1	12.5°	13.5	16	2.5	2.8°
C6	1.5	15.6°	13.5	16	2.5	3.3°
C7	2	18.7°	13.5	16	2.5	4.1°

Analysis of underarm point horizontal change and armhole's three-dimensional morphological characteristics. (1) Analysis of underarm point horizontal change and armhole's morphological characteristics. According to Table.5, chest width, across back, armhole width and armhole angle change, if underarm point changes horizontally. Do regression analysis. The horizontal change is independent variable. The consequence is shown in Table.7.

Table.7 Regression equation of underarm point horizontal change and armhole's morphological characteristics

Dependent variable(y)	Linear equation	Curve equation
Armhole width	y＝10.75-0.32x	$y=10.79-0.26x+0.06x^2$
Armhole angle	y＝6.25+6.24x	$y=6.27+6.26x-0.02x^2$
Chest width	y＝15.62-0.16x	$y=-0.17x+0.01x^2$
Across back	y＝17.8+0.4x	Non-significant

(2) Analysis of underarm point horizontally changes and every arc of armhole. 1）Correlation analysis. According to Table.5, when the underarm point changes horizontally, AH has tiny change. L5 and L6 take maximal change. Use SPSS to do the correlation analysis of underarm point and every arc of armhole. The consequence shows that the related coefficient of L3, L5, L4 and L6 is larger than L1 and L2. 2) Establish mathematics model. Use SPSS to do linear regression analysis and curve-fitting to L3, L4, L5 and L6. The horizontal change is independent variable, and arc length is dependent variable. The consequence is showed in Table.8.

Table.8 Regression function of underarm point horizontal changes and every armhole arc.

dependent variable（y）	Linear equation	Curve equation
L3	y=4.2214+0.0429x	Non-significant
L5	y=7.2857-0.6x	$y=-0.6952x+0.0952x^2$
L4	y=4.8036-0.0643x	Non-significant
L6	y=5.9536+0.5786x	$y=-0.6119x-0.3333x^2$

Analysis of underarm point horizontal change and attaching sleeve. Although the length of AH takes tiny change, underarm point horizontal change will influence the FAH and BAH. When the sleeve width is fixed, underarm point horizontal change will influence armhole width distribution and the angle of fixed sleeve. (1)Equation of armhole angle and sleeve width. In Eq.4, y is front sleeve width，x is armhole angle. In Eq.5, y is back sleeve width, x is armhole angle.

$$y=16.379-0.141x. \quad (4)$$

$$y=15.689+0.131x. \quad (5)$$

(2) Equation of armhole angle and sleeve angle. Use SPSS to do linear regression analysis. Regression equation is shown below. In Eq.6, y is sleeve angle，and x is armhole angle.

$$y=-1.397+0.487x. \quad (6)$$

Conclusions

This research analyses the regression relation of every arc of armhole and change of underarm point, and establish relational model of every arc of armhole and armhole three-dimensional configuration. At the same time this research also analyses mathematic relation of underarm point change with armhole architectural feature, sleeve top height and sleeve angle, and establish regression equation. These regression equations have a certain reference function to armhole three-dimensional configuration and shape of attaching sleeve. The sleeve pattern design can be done according to these regression equations. This research provides the basis for armhole three-dimensional configuration. And more importantly, this research provides theoretical basis and technical support for sleeve pattern automatic generation.

References

[1] Shi Chunle, Liu Guanbin, Zhang Wenbin. The theoretic research and practice on using angle in sleeve structure design. Journal of Xi'an University of Engineering Science and Technology Vol.3 (2006), p284-287.

[2] Liu Chengfang. Study-based pattern structure design research of sleeve. DongHua University(2008).

[3] Zhang Wenbin. *Costume techniques* (China Textile & Apparel Press 2000).

[4] Gan Yingjin, Liu Hui, Jiang Yan. On design of armhole prototype. Journal of Textile Research.

[5] Guo Yang. Sleeves rotating theoretical research based on the compatibility relations between sleeves and body. DongHua University(2008).

[6] Zhang Zhibin. On the relationship among sleeve head height, sleeve style and armhole. Journal of Xingtai Vocational and Technical College Vol.5 (2005),p27-29.

[7] TOMOKO Miyoshi. *Clothing Model Theory: Theoretical Articles*(China Textile & Apparel Press 2006).

[8] Liu Dong. Sleeve curve easy and means of fitting sleeve and panel together. Melliand-china, Vol.10(2005),p75-79.

© (2011) Trans Tech Publications, Switzerland
doi:10.4028/www.scientific.net/AMR.331.616

Research on Clothing Styles Classification Model Based on the MDS and K-means Method

Huijuan Xu[1, a], Fengyuan Zou[*2,b], Jing Wei[1,c] and Ying Zhang [2,d]

[1] College of Fine Arts and Design, Wenzhou University, Wenzhou, Zhejiang, 325035, China
[2] School of Fashion, Zhejiang Sci-Tech University, Hangzhou, Zhejiang, 310018, China

[a]xhj_jin@163.com, [b]zfy166@hotmail.com, [c]weijing@wzu.edu.cn, [d]zhangying1221@hotmail.com

Keywords: Clothing Styles, MDS, K-means, Classification Model.

Abstract. In this paper, the classification model of clothing styles is established based on the MDS (Multi-dimensional Scaling) and K-means method. MDS is adopted to make the quantitative analysis of the clothing styles and the similar perceptual mapping of the clothing styles is set up. In addition, according to the intuitional visual effects of similar perceptual mapping, the groups of clothing classification are preliminarily determined, coordinate values of the multidimensional space are achieved, and through cluster analysis of coordinate values, the categories of the clothing styles are finally determined. Then, this model is adopted to conduct the research on Ladie's Wear for testifying the operability of the model.

Introduction

Clothing styles refers to the comprehensive expression of clothing appearance and styles as well as its spiritual connotations, which conveys the contents and feelings of clothes [1]. As an abstract concept, clothing styles lacks accurate measurement method. There are rich and colorful clothing styles, which provide many choices to people in modern society. The selection of clothing styles is accomplished by designers in the process of design, and the styles relies on various aspects in the form of personality, life attitudes, aesthetic tendency as well as cultural accomplishment, as a result, the types of clothing styles are various.

Judged from the researches of literature, there are several representative clothing types as follows: Y.Q. Wang and J.C. Ma started with the study on the trend colors and combine with fashion trends of each year, in this way, four styles of fashion clothing were concluded, namely, classical, light, romantic and national [2]. Based on the quantification of clothing styles, L. Feng and X.G. Liu divided the female clothing styles currently in domestic market into eight categories that were, neutral, avant-garde, leisure, sports, classic, elegant, light, and national [3]. H.L. Xu and Z.K. Guan started with the essence of the clothing styles and therefore eight clothing styles were concluded [4].

In this paper, with use of the research result of other people as reference, the classification model of clothing styles is established based on the MDS and K-means method.

Building Clothing Styles Classification Model

Principle of MDS. MDS is often used to establish a reasonable multidimensional cognitive space from a group of similarity data by things or sensory.

Low dimensional space is adopted in MDS to reveal the relations among several research objects and make use of the plane distance to reflect the degree of similarity among research objects. Since the MDS method is generally conducted based on the similarity among research objects, as long as the distance matrix of two research objects is obtained, corresponding similar perceptual mapping can be made through relevant statistical software, such as SPSS.

Other multivariate analysis methods can also be used to find out the features concealed behind the observed data, however, in the process of collecting material and establishing perceptual mapping, the MDS method does not need the subjects make judgments according to certain standard, the usable criterion of subjects is their own feelings on the objects. This shows the convenience of the MDS method in collecting materials when compared to factor analysis and discrimination analysis.

Supposed that there are *m* pieces of clothes, through the comparison between every two pieces of clothes by subjects, the judgment of the degrees of similarity can be made; hence, a matrix expressing the degree of similarity in clothing styles can be obtained. Too many clothes will create the difficulty for the mutual comparison. In this sense, classification method is adopted to classify clothing, which requires the subjects to freely divide clothes into several categories with mutual repulsion, the tested times of objects in the same category refer to the accessibility index among clothes.

E.g. supposed that there are *m* pieces of clothes, each serial number represents an article of clothe, number these clothes from 1 to *m* respectively, presume that the K-th subjects divide the *m* articles of clothing into X_k groups, if the i-th clothes is classified to the group s, the value of i-th clothes will be recorded as F_i=s, at last, the corresponding form of clothing groups is show as Table 1.

Table 1 The Corresponding form of Clothing Groups

Clothing Number	1	2	3	…	i	…	m
Group Results (F)	F_1	F_2	F_3	…	s	…	F_m

As to two arbitrary evaluation objects “i” and “j”:

If F_i=F_j， that is, two objects are in the same group, the K-th subjects regards them as the similar objects, then their distance is recorded as D_{ijk}=0； if $F_i \neq F_j$, the K-th subjects regards them as the dissimilar objects, then their distance is recorded as D_{ijk}=1； in this way, the similarity evaluation among research objects conducted by the K-th subjects can be achieved, which is recorded as D_k=(D_{ijk}). As to all *n* subjects, using Eq.1, addition of all distance matrixes of all tested experiments can bring out overall distance matrix [5]:

$$D = (D_{ij}) = (\sum_{k=1}^{n} D_{ijk}) \tag{1}$$

According to the ways of matrix formation, it is easy to find out the matrix is symmetric and it meets D_{ii}=0, and in this way, the overall matrix is obtained, the MDS software is adopted to conduct an analysis on this matrix in order to figure out an overall similar perception figure of research objects.

K-means Method. The basic thought of K-means is: first, select a batch of cohesive points according to certain methods. Second, enable samples close to the nearest cohesive point to form the initiation classification. And then, modify unreasonable classification according to the nearest distance principle to make it reasonable. When utilizing K-means method, the amount of categories should be determined in advance.

The concrete process of K-means calculation is as follows [6]:

Step1: Select K objects as initial cluster center;

Step2: According to the cluster center value, give each object with the most similar cluster;

Step3: Recalculate the average value of objects in every cluster, and regard the new average value as the new cluster center;

Step4: Repeat steps2 and 3 until the cluster center takes no changes.

The cluster results of K-means arithmetic is largely influenced by the choices of initial cluster centers, if the choice of initial cluster centers is inappropriate, the results of cluster may possibly be lost in local optimum solutions and relatively good cluster effects cannot be achieved.

Classification Model Based on the MDS and K-means Method. Combining the features of clothing styles, MDS and K-means, classification model of clothing styles based on the MDS and K-means is established, show as Fig.1.

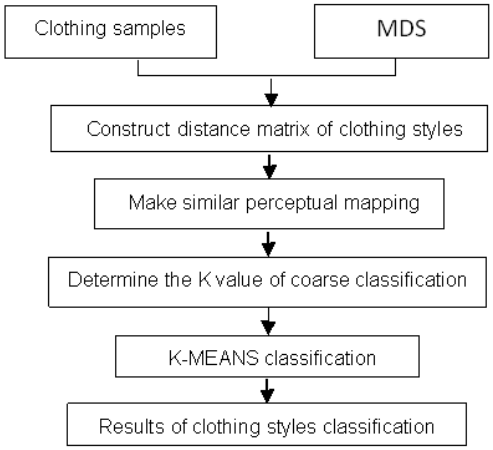


Fig.1 Classification model of clothing styles

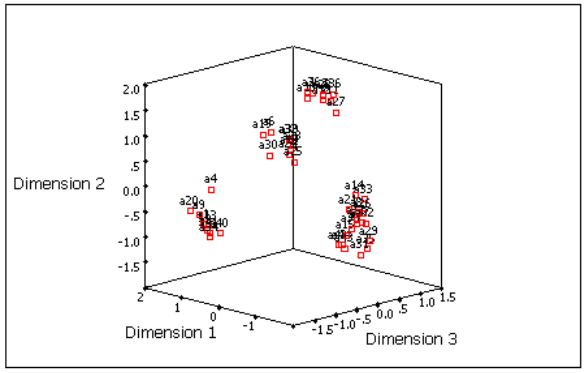


Fig.2 Cognitive space perceptual mapping of 44 samples

Ladie's Style Classification Experiment

Select Samples. CHANEL Ladie's Wear pictures in recent ten years were collected from domestic and foreign fashion websites with more than 300 in total. Combining with experimental requirement, screening was carried out on these pictures, only retaining ready-to-wear pictures with over 100 pictures in total. In order to ensure the complete information of each article of clothes, the pictures selected were front clothing pictures as far as possible, and then 44 styles of clothes were selected as the experimental samples finally.

Since these clothing pictures were model show photos, which require unified treatment. Photoshop was adopted to make gray as the background color for these 44 styles of clothes, wipe out head portraits, arms and legs as well as the lower clothes and clothing decoration, only the upper clothes were remained, and finally, gray scale treatment was carried out on pictures.

Design Questionnaire. 44 samples will be numbered, so that the subjects on the basis of subjective feeling to classified the 44 samples according to style. In order to understand the possible problems encountering in the sample classification process in advance, four fashion design teachers were invited to carry out pre-experiment, and then, tests find that the number of clusters of 6 to 7 groups, the subjects in the cluster will be determined more easily. As a result, in a formal cluster experiment, cluster 6 and 7 are regarded as the cluster standard, and after the subjects carefully observe all samples, fill the serial numbers of comparatively similar samples in the same column, and the quantity of each cluster can be different, which was based on the difference degrees among samples.

Construct Distance Matrix. The experiment was clustered based on Ladie's style sense, the experimental subjects must have a certain degree of understanding of clothing, so the 35 senior students majoring in fashion design were invited to conduct the grouping experiments including 15 males and 20 females. The experimental data was adopted to establish the 44 × 44 distance matrix based on the method of building the distance matrix.

Make Similar Perceptual Mapping. Put the data of 44 × 44 distance matrix into software SPSS, and two-dimensional DMS to six-dimensional DMS was adopted to conduct analysis.

After the concept and index of stress coefficient was proposed in 1964 by the J.B.Kruskal, the DMS was established as a standard combining the conformation resulted from assessment and the goodness of fit of input data. Kruskal divides stress into five levels. Each grade represents different goodness of fit in order to regard them as the selection standard [7].

Therefore, in the MDS analysis, kruskal stress coefficient of 0.100 was treated as common, less than 0.050 was good or very good. In this experiment, the output of 0.0672 (RSQ = 0.9525) in the software system was adopted to conduct on in the six-dimensional analysis, the distribution of each sample in one three-dimensional cognitive space show as Fig.2, and research on the distance matrix among samples was shifted to the spatial value in one cognitive space, which was conducive to the further cluster analysis.

K-means Classification. From the tree diagram, the most suitable number of cluster was selected based on the cluster situation, the selection principle was to try to get rid of the single cluster. Based on the tree analysis diagram of cluster, it was best to divide into 5 groups. And then, K-means was conducted analysis, set 5groups cluster as the cluster condition to make cluster, calculate the distance of each sample to cluster focus. Based on the distance as the judgment, the object which was nearest to the center can be regarded as the representative sample in this group. Finally, representative samples in 5 groups were got: namely, Group1 was No.28, Group2 was No.2, Group3 was No.23, Group4 was No.44, Group5 was No.8, sample classification as well as the analysis results of K-means were shown as Fig.3. In the Fig.3 S means sample, C means classification, D means distance. And 5 representative clothing samples which were ultimately determined show as Fig.4.

S	C	D
6	1	0.905
18	1	0.600
19	1	0.913
24	1	0.972
25	1	1.026
28	1	0.526
30	1	0.979
32	1	0.724
39	1	0.616

S	C	D
1	2	0.457
2	2	0.308
4	2	0.988
9	2	0.498
13	2	0.473
20	2	2.066
34	2	0.826
40	2	1.285
41	2	1.058

S	C	D
3	3	0.915
7	3	0.327
10	3	0.609
11	3	0.656
12	3	0.974
16	3	0.416
23	3	0.256
27	3	1.839
36	3	1.374

S	C	D
14	4	1.704
15	4	0.639
29	4	0.927
31	4	1.016
33	4	1.217
35	4	1.273
42	4	0.760
43	4	0.686
44	4	0.569

S	C	D
5	5	0.412
8	5	0.394
17	5	0.452
21	5	2.352
22	5	0.550
26	5	1.074
37	5	0.412
38	5	0.792

Fig.3 Classification of the sample



Fig.4 Representative clothing samples

Conclusions

Aiming at the abstract features of clothing styles and combining with the advantages of MDS, the classification model of clothing styles is established based on MDS and K-means methods.

The classification experiment of CHANEL Ladie's Wear styles is conducted according to MDS and K-means classification model. The experiment result indicates that these 44 styles are divided into 5 categories, and the representative clothing of each category as well as key distance of each category are achieved.

In this thesis, new methods are provided for the research on the categories of clothing styles, through the classification experiment of Ladie's Wear styles, this model is tested and verified with strong feasibility, it also can provide reference for subsequent relevant researches.

References

[1] Y.F. Liu: *Fashion Design* (Higher Education Press, China 1997)

[2] Y.Q. Wang, J.C. Ma: *Color Clothing and Beauty* (China Light Industry Press, China 1996)

[3] L.Feng, X.G. Liu: Journal of Donghua University. Vol.30 (2004), p.57

[4] H.L. Xu, Z.S. Guan: *Clothing Aesthetics Tutorial* (ChinaTextile&Apparel Press, China 2007)

[6] D.L. T. Rohde. Neutral Composition. Vol.14 (2002), p.1195

[7] T. Kanungo, D.M. Mount, N.S. Netanyahu: IEEE Transactions on Pattern Analysis and Machine Intelligence. Vol.24 (2002), p.881

[8] J.B. Kruskal: Psychometrical. Vol 29(1964), p. 1

© (2011) Trans Tech Publications, Switzerland
doi:10.4028/www.scientific.net/AMR.331.620

Research on the Development Situation of Transmutability Clothing

Hui'e Liang, Lanming Jin

The College of Textiles and Clothing, Jiangnan University, Wuxi, 214122, China

Email: lanminger@hotmail.com

Keywords: Transmutability clothing; Multi-useful clothing; Low Carbon; Humanistic Spirit

Abstract. Transmutability clothing arises from traditional aesthetic demands and needs of modern life. It coordinated with the development and the concept of environmental protection. It meets the diverse needs of people and personality of consumer psychology. This article analyses the Transmutability clothing causes of the rapid rise, lists of current global fashion market Transmutability clothing phenomenon, and then comes to a conclusion after summarizing its importance: Transmutability clothing is imperative to in-depth research and development, this kind of clothing has immeasurable development trend.

Introduction

Transmutability clothing means a / sets of clothing, by simply changing its form, materials, or the way they wear, derived from a variety of style of the original single-style clothing. We also explain this kind of clothing like this, one clothing with several ways to wear. People have become increasingly demanding everyday dress with Enrichment and development of social life ,not only to meet the common TPO principle, but also requires a more practical adaptability and variability. Clothing brand SISLY 2009 promotes a model of one-piece dress receives the attention in the summer , the bottom of the skirt upside down, remove or tape can be folded clothes, a garment worn and 5 different styles. It is possible to put on the skirt through turning upside down or folding any part of it. There are 5 kinds of styles in just one dress and they are totally different. Meters • Bowne's both sides to wear jacket make people feel compelling. Black side looks very simple, green side is full of bright colors. And variety ways to wear dress by designer Osman Yousefzada is also impressive. This kind of clothing is popular and welcome gradually in people's daily life. Therefore, starts from the designer to the consumer pay attention to Transmutability clothing.

The development of Transmutability clothing in modern times

In modern times, clothing has gone through about three stages. Past clothes, were generally design themselves to produce, or tell your tailor what the requirement is. This is decorative design stage, it is to select and copy the old style. With development of garment industry, the way to produce clothing brought changes on design. Therefore, we entered the stage of production design. In particular, the birth and development of modern Haute Couture is important to fashion design obviously. Before the mid-60s, designers take the popular center, named designer fashion trend. Along with time progress, people pursue the freedom and individuality. Diverse style of life has brought clothing's diversity. The popular of clothing is no longer comes by the designer, but consumer creates. Each designer hopes that his consumers choose clothing by themselves. With continuous development of the industrial revolution, mechanized production design stage have encouraged people to pursue individuation and differentiation. And in the degradation of the ecological environment, green living ideas make people pay more attention to the quality of life. Single product's performance has been insufficient to meetthe needs of people. They need something like *Swiss Army knife*, including clothing (Fig.1). Simple changes mean *get more than before*. Transmutability clothing meets our needs. It enters our lives gradually and plays an important role. The *detachable sleeves jacket*, *removable hat coat*, *additional fur collar coat* and so on. Transmutability clothing gradually gets into our hearts deeply (Fig.1). Especially in our country, such a large population and energy crisis-affected country,

Transmutability clothing has a broad market and development potential. Under the guidelines of the humanism, Transmutability clothing fully reflects the personality of people. And advocating respects the rights of people to choose clothing patterns. It turns popular from the "swarm" to diversify



Fig.1 Transmutability clothing gradually gets into our hearts deeply

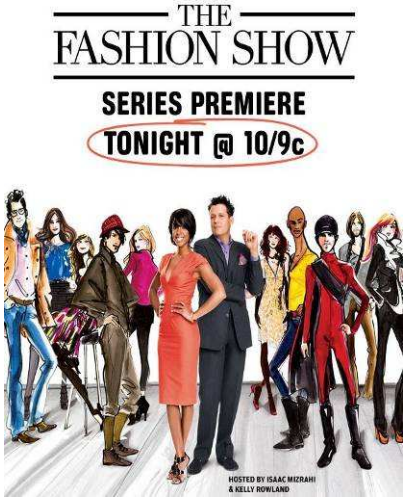


Fig.2 Fashion TV program-- The Fashion Show

.

The main reason for the rise of Transmutability clothing

The main reason which helps Transmutability clothing have a place in the clothing market with greet speed includes three aspects: social aspect, medium aspect and personality aspect.

Social aspect: In the 20 century the tailoring develop quietly. Because of quickened pace of life and upturn living standards, people increasingly emphasis on the rationality and functional quality of clothing, especially since the Second World War. Fashion industries are obviously carrying on tailoralization process ,with a wide range of consumption strata for object. As other design fields, functional quality attracts more and more attention in construction, automobile, plane or other artificial objects.*Functional quality is a kind of beauty itself* , this new aesthetic concept is enjoying more and more support by people with the development of modern life. With the young consumer group and the tailoring rising sharply, suit-dress is changing to simplification.People's dress consciousness is altering with the development of society. Nowadays diversified way of life is also enriching people's dress. Transmutability clothing gets the functional quality of clothing, which is different from Haute Couture; it is not only the sample but its peculiarity of optional changes make Transmutability clothing charming. The enhancing of social consciousness and the coming of personality age provide suitable platform for the rising of Transmutability clothing.

Medium aspect: Along with the science and technology maturing, people acquire their knowledge more widely. Especially the development of internet, TV and other medium make consumer close to the center of fashion. Advertisement for various kinds of websites and variety shows make people have a face-to-face communication with the fashion, even create their own fashion. Fashion TV program,such as *The Fashion Show(Fig.2),Pretty Woman,I am a great beauty*, combining with advanced technology, help people to learn more experience personally , and then they becoming keen on clothing as well. Transmutability clothing ---one clothing with several ways to wear, has become the hot topic on the net. *Style Hive, Trend Spot, Refinery* and other fashion website also add new column for it specially. The homepage of designers also have plenty of related video tutorial on YouTube, which have a highlight. In fact, these high-tech communication medium give full play to their characteristics of wide coverage, high penetration rate and short production cycle, making the rise of Transmutability clothing possible.



Fig. 3Donna Karan launched an infinity elastic dress fabric skirt



Fig. 4 Albert Elbaz for Lanvin designed a series Transmutability clothing of holiday last summer

Personality aspect: The fun of Transmutability clothing is changing, through the dresser's own effort making the clothing change. It incarnates the dresser's attitude to the fashion, not just a product from mechanical process, without vitality. People increase their confidence and personal charming through dressing this kind of clothing. Accordingly, fulfilling their life with confidence. It is the most valuable meaning of clothing at the present stage, which is also the most attractive characteristic of Transmutability clothing. Clothing has rise from the basic function of warming and covering bodies to become the symbol of the fashion, brand and the quality of life. The consumer would rather deliver their emotion and the understanding of fashion through clothing. The clothing in a rut can't satisfy the demand of people. It reflects everyone's character, and they longing for be sure and not simulating others.

Analysis of situation of Transmutability clothing

The current Transmutability clothing market analysis: In the pursuit of economic environment for maximizing the value, relevance and value for money is just a part of the reason for Transmutability clothing's successful. Customers on a garment to wear in hot pursuit are not completely derived from economic considerations. Now, everyone wants to be their stylist. Wear clothing with a mentality of play, and aroused the people unlimited imagination. Transmutability clothing appears in the different grades and different styles of shops.

Fashion TV programs stimulate the creative inspiration of ordinary people. Celebrity Stylist Rachel Zoes showed her *five in one* dress with 80 dollars by Rachel Pally in the program. If you make just a little change, you could turn it to be a small party dress; Alexander Wang's jacket—it's sleeves detachable locomotive for many fashion people relish; Norma Kamali designs a kind of sleeve shawl can be turned into a wool coat; Donna Karan launched an *infinity elastic dress* fabric skirt (Fig. 3), the skirt a little play with can become a cover sleeve on the back of skirt or no shoulder dress. Brand spokesman revealed that despite the price up to 1000 dollars, but this skirt on the company's Web site, once published, it sold more than 100 pieces in just a few days. Aloha Rag's Transmutability clothing about coat and dress is also very popular; Victoria's Secret launched the put method for knitted dress successfully, continuing launched a multi-wearing disco-style Horn joined pants recently.

In addition to American Apparel, Target and Victoria ' s Secret such parity trend brands in addition to many world brand and also have a strong interest on Transmutability clothing. Albert Elbaz for Lanvin designed a series of holiday last summer . We can find Transmutability clothing in it(Fig. 4). Fickle fashion is not all just innovation, transformational fashion appeared already in the international stage. Many years ago, Junya Watanabe designed a upside to wear Jersey. Hussein Chalayan has created a folding table side skirt.

Transmutability clothing also appear in the popular novel more than once. In William Gibson's science fiction in the pattern recognition, female protagonist Cayce Pollard is a fashion consultant who has a keen sense of smell, there is a basic dress in her handbag. She could change this dress

according to the different needs quickly. Although Transmutability clothing attracted a lot of people, some people do not want to attempt to wear complexity clothing . As Amber Garrett said from shopping blog *We Covet*,I'm reserved my opinion about this kind of specifically wear method clothes.

Importance of Transmutability clothing's development

Introducing *low-carbon* to fashion clothing. In recent years, the development of low-carbon economy will gradually become the mainstream ideology in the world and international values. Low-carbon economy, with its unique advantages and enormous market, has become a hotspot of world economic development. One of the industrial revolution based on the low-carbon economy has emerged, developing low-carbon economy is also a kind of innovation of world economic development model of the future. It is an important way to achieve sustainable economic development in China. As a whole new model of economic development, Low-carbon economy reduce energy consumption rate. *Low-carbon dress idea*: reduce purchase frequency, select environmentally friendly fabrics for clothing, buy green style, reduce the frequency of washing, select environmentally friendly washing, hand-washing place of washing machines, use secondhand clothing, renew, transfer others' clothes to wear, etc. Transmutability clothing can reduce the carbon emissions of a garment at least. It's fit the requirement of *low-carbon dress idea*. Every one who bought this kind of clothing could join the ranks of the environmental protection easily. It's an important reason about people buy Transmutability clothing.

Humanism instructs the practical significance of Transmutability clothing. Changing times and technological advances enable people to pursue freedom and the pursuit of individuality. The variety life styles brought clothing diversity. Under the guidance of the Humanism, Transmutability clothing shows some characteristics like differing from persons, varying with the time changed, according to local conditions, human oriented. This is an opportunity for Transmutability clothing's development. It also makes Transmutability clothing have more practical significance than ordinary single function of clothing. The fun of Transmutability clothing is changes of clothing through the wearer's own efforts. It is intelligence. It bears more weight of wearers' for attitude about fashion, rather than a lifeless clothing which stylized from the factory of mechanical process. People wear such clothing will enhance their self-confidence, and then full of confidence in life. During clothing developed to this stage, this is one of the most valuable meanings.

Conclusions

Modern clothing more focus on the process of *meeting the psychological*, which is a deeper level and inheritance flags of clothing at humanistic spirit. Transmutability clothing arises from traditional aesthetic demands and needs of modern life. It coordinated with the development and the concept of environmental protection. It meets the diverse needs of people and personality of consumer psychology. As a product of technology development and crystallization of human wisdom, this kind of human oriented will say goodbye to the simple style of clothing, breaking the material constraints, enters more specialization, marketing, a wide range of age. Transmutability clothing will continue to bring more convenient and pleasant surprise to people's lives and the culture of clothing with immeasurable development trends. To sum up, it is imperative to in-depth research and develop on Transmutability clothing.

References

[1] Dangqi Li: History of Western Costume. Higher education Publications.1995.2(In Chinese)

[2] Dangqi Li: Introduction to Clothing. Higher education Publications.1990.4(In Chinese)

[3] Lorain Blanken. DIY Clothing[EB / OL]. (2010-03-16). [2010-05-02].

© (2011) Trans Tech Publications, Switzerland
doi:10.4028/www.scientific.net/AMR.331.624

BWH Reshaped Made Use of Reshape Underwear Based on the Model of Female Physical Beauty

Wei Jiang[1,3], Xiaoming Qian[2,3,*], Lili Zhai[2]

[1] School of Art and Clothing, Tianjin Polytechnic University, Tianjin 300387, China.

[2]School of textile, Tianjin Polytechnic University, Tianjin 300160, China

[3]Key Laboratory of Advanced Textile Composites (Tianjin Polytechnic University), Ministry of Education

* Corresponding Author ： qianxiaoming@tjpu.edu.cn

Keywords: female physical beauty, reshape underwear, proportion, cluster analysis

Abstract. The common evaluating indicators of female physical beauty aren't able to point out which parts and how many sizes need to be reshaped. So, other indicators must be introduced, which are present proportions of the perfect body, some critical parts are selected. Unmarried female college students, 18-25, are chosen in the experiment and their sizes of BWH are collected by non-contact 3D body scanning apparatus. Compared with the best proportions, some need breast implants and waist diminution; others need hip implants and waist diminution. Then, the relevant data is analyzed in SPSS software, refer to the national shape standard of reshape underwear and two kinds of females are separately classified to four categories. It may be helpful to provide adjusted sizes of reshape underwear in industrial production.

Introduction

Reshape underwear is made in high elastic fabrics, integrating different structures and cutting technology to support and constrict the body, essentially to make up women's figure disadvantages. The undergarment is mainly divided into corset, slimming underwear, shape pants and bellyband. According to the fitness strength, it also can be divided into light, medium and heavy.

The research is point at light reshape effect.

There are no accepted standards in the world [1]. WHR (waist-to-hip ratio), BMI (body mass index) and VHI (volume height index) are three main evaluating indicators.

WHR is the ratio of the waistline and hipline. WHR is divided into three categories as thinner, normal and fatter. The value of most body beauty is 0.7 [1].

BMI can be expressed by Eq. 1:

$$BMI = Weight / Height^2 \quad Kg/m^2 \tag{1}$$

The ideal BMI range is 18-20kg/m^2 [2].

VHI can be expressed by Eq. 2:

$$VHI = Volume / Height^2 \quad L/m^2 \tag{2}$$

The VHI value of most attractive female is 14.2L/m^2 [3].

The above three indicators are used to calculate the rank of female physical beauty simply and easily, but can not accurately determine the existence of the body beauty and disadvantages. BMI and VHI predict the body beauty overall. Sometimes, female have the same BMI and VHI, are evident different in body beauty rank, due to the difference in characteristics of the body. Therefore, the three of appraisal indicators have respective limitations.

Data Collection and Analysis

Female physical beauty is dominated by the proportions of representative parts of human body. So, on the basis of WHR, BMI and VHI, a prediction model of female physical beauty can be established. It should not only predict the level of female physical beauty, but also demonstrate the body parts which are short of beauty. It is used to offer a theoretical basis for increasing beauty in reshape underwear.

The model of female physical beauty established by Lili Zhai, graduated from Tianjin Polytechnic University, summarizes the proportions of perfect body parts [4]. It is showed in Table 1.

Table 1. Proportions of Perfect Body Parts

proportion	value	proportion	value	proportion	value	proportion	value
head height/ body height	7.046	hip girth / body height	0.552	breast width / shoulder width	0.766	waist depth / breast depth	0.745
breast height/ body height	0.714	breast girth / thigh girth	1.26	hip width / shoulder width	0.932	breast depth/ hip depth	1.113
waist height/ body height	0.622	breast girth / hip girth	0.949	BP width / shoulder width	0.469	hip width / hip depth	1.627
hip height/ body height	0.494	waist width / hip width	0.692	BP width / hip width	0.507	breast width/ breast depth	1.205
crotch height/ body height	0.441	waist width / breast width	0.859	BP width / breast width	0.614	waist width / waist depth	1.26
waist girth / body height	0.382	waist width / shoulder width	0.621	BP width / waist width	0.748	WHR	0.703
breast girth / body height	0.529	breast width / hip width	0.819	waist depth / hip depth	0.751	WCR	0.745

Sample Selection. Unmarried female college students, 18-25, stand for Chinese young women are chose in the experiment. Their secondary sex characteristic and body curve are visible. They are full of energy and beauty.

Sample Size. Sample size can be expressed by Eq. 3:

$$N = (1.96 \times \sigma)^2 / E^2 \quad (3)$$

Where, N is sample size, 1.96 is critical value when significant level is 0.05 in normal distribution, σ is overall standard deviation and E is largest error allowed.

According to the results of the relevant research in The Hong Kong Polytechnic University, the standard deviation is 2.2 in female physical beauty ratings. The largest error allowed is 0.5 [5].

Female physical beauty is a subjective evaluation, which is uncertain and affected by valuators' own factors. To make the samples represent as general information of Chinese young women as possible, the overall standard deviation is defined as 2.5. Then, N is 96 according to Eq. 3. Actually, N is 120 in the research.

3D body scanning. The surface of body is complicated, soft and elastic. It will be changed and different from natural conditions under external force in contact measurement. Therefore, to make the measurement correct, non-contact measurement is able to solve the problem better [6].

The body data is collected by non-contact 3D body scanning apparatus made by a corporation named Lectra in France. The apparatus include 3D body scanning hardware named VitusSmart and automatic digitized analysis software named ScanWorX. The data of cross section of body is collected and analyzed in the way of interactive measure, which is used for depth analysis about body [7-8]. It can measure 86 indicators, including the sizes of all parts of the body. But, not all the

indicators are a need for subsequent research. Only the parts which influence on the type of female body significantly are selected. The parts are reshaped by reshape underwear, such as waist girth, breast girth and hip girth.

The scanning experiment is carried out in a special lab, where the temperature is 28 ± 2℃ and relative humidity is 60% ± 5%.

Data Analysis. The proportions of perfect body have limited the sizes of women of different body heights. Under ideal conditions, corresponding parts need to be adjusted to meet the proportions. In fact, not all the components can be adjusted, for example, body height and shoulder width. While the height and width of breast and hip and so on, are relatively easy to be adjusted. In dressing, bra cups have effect on support and gather round breast. Similarly, shape pants will push fat in waist, abdomen and thigh to hip cup, then make the hip up and curve plump. So, the sizes of breast girth and hip girth aren't considered decreased. Therefore, the only mean is to change the sizes of waist girth or thigh girth to meet the perfect proportion roughly, under the premise of keeping hip girth or waist girth.

The best ratio of breast girth / hip girth is 0.949. So, if hip girth × 0.949 > model's actual breast girth, stating that the best breast girth exceeds actual girth when hip girth is sustained, then preserving hip girth is chosen. Otherwise, stating that the best breast girth is less then actual girth when hip girth is sustained, then preserving breast girth and increasing hip girth are chosen.

The above principles determine the breast girth, hip girth and waist girth, which are the target sizes in reshape underwear.

Before the analysis, the national shape standard GB/T1335, in Table 2 and Table 3, must be consulted and help to make sure reference frame.

Table 2. Shape Pants

shape	64(S)	70(M)	76(L)	82(XL)	90(XXL)
waist girth(CM)	61-67	67-73	73-79	79-85	85-91
hip girth(CM)	80-88	85-93	90-98	95-103	100-108

Table 3. Slimming Underwear

shape	70(S)	75(M)	80(L)	85(XL)	90(XXL)
under breast girth(CM)	68-72	73-77	78-82	83-87	88-92
breast girth(CM)	80-90	88-98	90-103	95-108	103-113

This research objects, are basically in the normal range. And the example of breast girth is greater than 103cm or hip girth surpasses than 100cm did not occur. Cluster analysis of Original and target sizes are taken in SPSS software, and the data is only divided into four categories.

In 120 samples, the number of samples whose BWH need to be reshaped takes 75.8% of the total, is 91. The number of breast implants and waist diminution is 41, while the number of hip implants and waist diminution is 50.

The final results are in Table 4 and Table 5.

Table 4. Breast Implants and Waist Diminution

index	category			
	1	2	3	4
quantity	6	15	4	16
body height	154.75	163.81	151.17	161.68
breast girth	78.23	83.85	86.03	86.72
waist girth	61.45	66.11	67.07	70.25
hip girth	83.73	90.06	91.93	95.06
target breast girth	79.45	85.47	87.27	90.21
target waist girth	58.85	63.30	64.60	66.84
target hip girth	83.73	90.06	91.93	95.06

Table 5. Hip Implants and Waist Diminution

index	category			
	1	2	3	4
quantity	9	22	6	13
body height	153.00	160.33	152.05	158.36
breast girth	79.13	88.82	86.25	94.17
waist girth	61.48	69.05	65.95	76.01
hip girth	82.22	90.97	86.80	93.89
target breast girth	79.13	88.82	86.25	94.17
target waist girth	58.97	66.17	64.25	70.16
target hip girth	83.38	93.60	90.90	99.24

Conclusions

In the cluster analysis of breast implants and waist diminution, the quantity of category 2 and 4 comes up to 75.6%. The sizes of breast adjusted are respectively 1.62 and 3.49. The sizes of waist adjusted are respectively 2.81 and 3.41. Obviously, the sizes of waist adjusted are close. So, these two types of women are considered similar in body height and waist type, while more different in breast type.
Equally, in the cluster analysis of hip implants and waist diminution, the quantity of category 2 is obviously more than the other three categories. Category 2 and 4 take up 70%. The sizes of hip adjusted are respectively 2.63 and 5.35. The sizes of waist adjusted are respectively 2.88 and 5.85. The sizes of waist and hip adjusted are not close. These two types of women are similar in body height, while more different in breast type and waist type.
In data processing, an interesting phenomenon is found that only 46% unmarried young women who are above164cm need to adjust their BWH while the proportion of the women who are shorter than 164cm is 88%. This verifies that beauty is proportional to body height.

Outlook

Due to various reasons, each age group of women is different in perfect proportions, and the models of female physical beauty can be settled respectively. If more samples will be selected in the experiment, then the data of body and the conclusions will be convincing and accurate. Especially, women from 30 to 40, who are after childbirth or lack enough exercise, are the mainstay in consumption. They have certain social and economic status, and have a relatively high aesthetic consciousness.

References

[1] Singn D: Human Nature Vol. 4 (1993), p. 297-321

[2] Tovée M J, Maisey D S, et al: Proceedings of Royal Society of London Series B- Biological Sciences Vol. 266 (1999), p. 211-218

[3] Fan J, Dai W, Qian X M: Perceptual and Motor Skills Vol. 105 (2007), p. 117-132

[4] Lili Zhai: Doctoral Dissertation of Tianjin Polytechnic University (2011), p. 71

[5] Lim Ngai Ying: Hong Kong polytechnic university institute of textiles and clothing (Hong Kong 2007)

[6] Chunmei Fu: Foreign Silk Vol. 3 (1998), p. 32-35

[7] Application Manual about Lectra Non-contact 3D Body Scanning Apparatus, p. 3

© (2011) Trans Tech Publications, Switzerland
doi:10.4028/www.scientific.net/AMR.331.628

Aerobics Clothing Consumption Behavior of College Students in Hangzhou

Yuxiu Yan[1,a], Wenjuan He[1,b], Lijuan Lou[1,c], Jianwei Tao[2,d] and Minbo Lin[2,e]

[1]Zhejiang Sci-Tech University, Hangzhou, China

[2]Zhejiang Bangjie Digital Knitting Co., Ltd, Yiwu, China

[a]yanyuxiu777@163.com, [b]527127842@qq.com, [c]louli10001@163.com, [d]bangjie@vip.sina.com, [e]777abc@163.com

Keywords: College Students, Aerobics Clothing, Consumption Behavior

Abstract. Paper studies the aerobics clothing consumption behavior of college students in Hangzhou. By the way of detailed questionnaire and statistics analysis, the survey gets the conclusions about the preferred shopping site, factors influencing consumers` shopping decision, price choices, sources of information, color preference and decorative elements. So the research can help the enterprise fully understand college students` consumption behavior of aerobics clothing and meet their demands.

Introduction

With the increasing development of sports, Aerobics as the backbone of physical courses gets the welcome of many college students. In all kinds of sportswear, their favorite is aerobics clothing [1]. Recently, a lot of famous international sportswear companies are sweeping into the domestic market, resulting in intense competition [2]. Domestic sportswear bands can carve out a strong specific market by developing a new product, establishing a reasonable price and making corresponding market strategies, which can help increase the market share.

By means of the literature research, we founded that the researches about the aerobics clothing are little, only a few articles focused on the dress aesthetics, comfort and function, and few studied on the consumer psychology and behavior. From the angle of design, literature [3] analyzes the color of aerobics clothing. From the fit perspective, literature [4] uses the basic law to design the style of aerobics clothing.

From the angle of the aerobics clothing consumption psychology and behavior of college students, this article mainly analyzes the factors which affect the purchase decision.

Research method

Survey method. This paper adopts the subjective evaluation and takes a questionnaire survey analysis of 150 college students in Hangzhou, totally 135 effective recalled.

Respondents.72 females and 63 males account for 53.3% and 46.7% respectively. The survey covers the 29 liberal arts, 35 engineering, 38 science and 33 arts, accounting for 21.5%, 25.9%, 28.1% and 24.4% respectively. Statistics show that the surveyed college students not only are evenly distributed in the sex and subject, but also has a widespread scope. So, the results can truly reflect the basic information of the college students.

Analysis method. The gained data is processed by frequency statistics, mean and standard deviations. The consumption psychology and behavior of college student are assessed by five rating scale, “strongly dislike” (1 score), “dislike” (2 score), “general” (3 score), “like” (4 score), “really like” (5 score). Then calculating the mean and standard deviation, the higher mean represents the higher degree of liking the choice. And the standard deviation reflects whether the surveyed students share the same view of the choice [5].The more different views show the smaller standard deviation.

Results and analysis

Consumption motivation is an important part of the consumer psychology and behavior [6].

The basic information about the surveyed college students. The college students haven`t got the economic independence, so monthly expense can influence their choice. The article uses the method of single variable frequency to analyze the surveyed students [7] (see Table1). We get the information that most students` month amount of consumption is between 500RMB and 1000RMB.

Table1. College students` information

Items	Contents	No.	Percent
Monthly expense /RMB	Less than 500	17	12.6%
	500-1000	96	71.1%
	1000-1500	19	14.1%
	above 1500	3	2.2%

Table2. Preferred shopping sites

Shopping Sites	Mean	Standard Deviation	No.
franchise house	3.81	1.36	1
department store	3.68	1.17	2
general clothing store	3.14	0.85	3
on-line store	2.73	0.94	4
supermarket	2.68	0.98	5
wholesale market	2.55	1.12	6

College students` preferre d shopping sites. In table2, we find out college students who have a certain source of income prefer the franchise house and department store [8].

In randomly interviews, this part of surveyed students think that aerobics clothing in franchise house has a reliable quality and a fashionable pattern. Though the on-line store, supermarket and wholesale market have advantages in low prices and variety, students seldom purchase there because of the irregular quality and poor shopping environment. Analyzing the standard deviation, we get that students` views on the franchise house are not in accord compared with other shopping sites.

**Factors impacting customers` decision.** According to products` characteristics, factors are sorted into appearance factors including style, aesthetics, color, material, technology, patterns and packing, internal factors including comfort, moisture vapor transmission and elasticity, and the other factors including price, after-sale services, shopping environment, brand image and discount [9].

Table3. Factors impacting customers` decision

Factors	Mean	Standard Deviation	No.	Factors	Mean	Standard Deviation	No.
comfort	3.93	0.55	1	technology	3.46	0.69	9
style	3.81	0.69	2	pattern	3.43	0.72	10
aesthetics	3.78	0.52	3	shopping environment	3.39	0.84	11
moisture transmission	3.68	0.57	4				
elasticity	3.53	0.51	5	after-sale services	3.32	0.91	12
price	3.50	0.61	6	brand image	3.27	0.86	13
color	3.48	0.57	7	discount	3.16	0.92	14
material	3.46	0.65	8	packing	2.90	0.92	15

As shown in Table3, the 5 major factors are comfort, style, aesthetics, moisture vapor transmission and elasticity. It`s found that all the internal factors are ranking in the top five. College students care more about the clothes` function, which fits in with students` choice of franchise house and department store having high quality products. And because the aerobics has dual characteristics of motion and artistry, many students pay more attention to the style and aesthetics.

In the bottom five are shopping environment, after-sale services, brand imagine, discount and packing. It shows that these factors have smaller effect to students` purchase decision.

Watch the standard deviations, the minimum is the elasticity. It shows that students care about the elasticity and have the same opinion on it. The following relatively consistent views are aesthetics, moisture vapor transmission and color. Packing has a maximum standard deviation. It shows that students have different views on it, the discreteness is very great. The following are discount, after-sale services and brand imagine.

College students and preferred prices. As shown on Fig1, the preferred prices conclude as follows: 65.9% students the prices between 200～300, 16.3% preferred 300～400. All the findings correspond with their choice of franchise house and department store. Through the interview, 75.6% of the students think that aerobics clothing can be used in performance and competitions. They are willing to pay a high for a high quality and more aesthetics clothing.

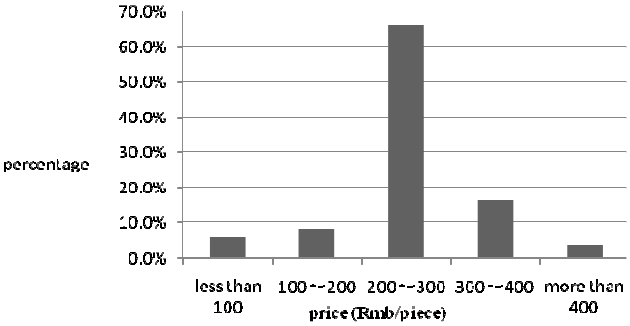


Fig.1 Preferred prices

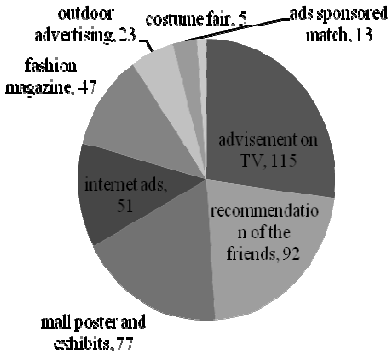


Fig.2 Purchasing source

College students and purchasing source of information. The primary source of information includes 8 pathway（see Fig.2）. The surveyed students should take a multiple-choice, selecting out the main way of getting information. We get the frequency distribution, as shown on Fig.2.

115 students think they mainly get the information from the advertisement on TV. 92 students mainly get the information on the recommendation of their friends. And 77 students exact the information from mall poster and exhibits, 51 students obtain their information from internet ads. Those students think that it`s convenient for them to compare different clothes. However, only few students give attention to costume fair and ads sponsored match. To improve the purse rate, the domestic sportswear brands can make full use of this result and choose the ideal from of advertising.

College students and color preference. In the process of visual perception, the color of the clothing not only conveys the feelings strongly, but also has the deepest visual impact.

As shown on Fig.3, 68.1% female and 52.9% male believe that brighter colors sufficiently express the ideological sentiment and spirit of athlete, represent dual characteristics of motion and artistry, show invigoration and youth.

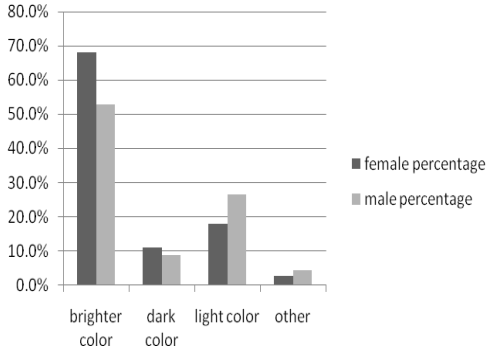


Fig.3 Color preference

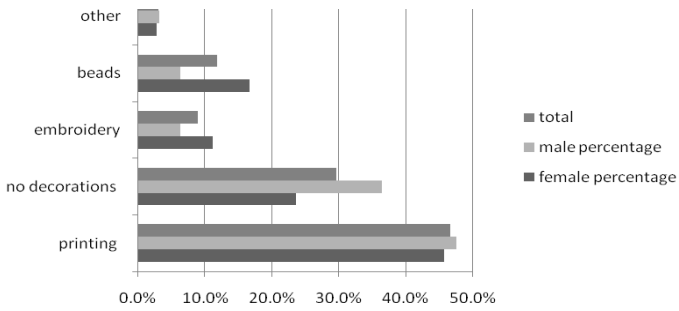


Fig.4 Ornamentation preference

College student and ornamentation preference. Table3 shows the college students care the most about comfort, style and aesthetics when they buy the aerobics clothing. And the ornamentation has a great influence on the above factors.

As shown on Fig.4, both the female and male like the printed decoration most, the following is no decorations. Through interviewing probe, the athletes think that printing has the advantage of various patterns, novel fashion, gorgeous color and lightweight. The most important is that printing has no side-effect on the comfort. Embroidery and breads looks very beautiful, but they feel hard, easy to produce scratchiness. The worst is that they are bad for athletes` performance.

Conclusions and suggestions

Conclusions

1)Franchise house and department stores are the main shopping sites for the college students.

2)The main factors affecting college students` shopping decision are comfort, style and aesthetics. And college students have the same opinion on them.

3)College students prefer the clothing whose price is between 200RMB and 300RMB.

4)College students mainly get the information from advertisements on TV, recommendations of their friends and mall poster and exhibits.

5)College students preferred the brighter colors and printed clothing.

Suggetions

1)College students care about the comfort and style of the clothing, so the sportswear brands should take into account these two core factors when they develop the new products.

2)The sportswear brands should pay more attention to the clothing`s dual characteristics of motion and artistry. When they design the new product, they should select the reasonable color and decoration to meet the needs of the comfort and aesthetics.

3)The sportswear brands should establish a reasonable price, select the suitable mall and make strategy for advertisement rationally.

References

[1] Jun Hao, “Investigation and study on learning interest on sports.aerobics of female undergraduate”[J]. Journal ofShenyang Institute ofEngineering(SocialSciences), Vol·6 No·1,Jan.2010.In Chinese.

[2] Hui Zhang, Qihui Qi, “The excellence of the domestic sportswear brands and foreign brands”[J]. Journal Of Market.2003(8). In Chinese.

[3] Wei Deng, Pei Xie, “The color of the aerobics clothing”[J]. Journal Of Physical World, 2009(09):88-89. In Chinese.

[4] Liu Geng,“design and apply the underwear based on the basiclaw ”[D].Tianjin Poly-echnic University,2008. In Chinese.

[5] Yuxiu Yan,Zimin Jin, “Zhejiang Female College Students Consumption Behavior of Clothing”[J].Journal of Donghua University (Social Science), Vol.8, No.4,Dec. 2008. In Chinese.

[6] Solomon M R,Hong-Tai Lu,“Consumer Behavior: Buying, Havingand Being”[M].Beijing Electron Industry Press, 2006: 173.

[7] Jianying Yu, Xuhong He,“Data statistics and the usage of SPSS ”[M]. Beijing Ren Min You Dian Press. 2003:81-82. In Chinese.

[8] Ji Hye Park,Sharron JLennon,Leslie Stoel. On Line Product Presentation: Effects on Mood, Perceived Risk, and Purchase Intention[J]. Psychology & Marketing, 2005,22(2): 695-719.

[9] Yuan Kong, Xiuli Zhu, “Research on the College Students Perceived Quality of CasualWea,” [J].Journal of Zhejiang Sci-TechUniversity, Vo.l 23, No. 3, Sep.t 2006. In Chinese.

© (2011) Trans Tech Publications, Switzerland
doi:10.4028/www.scientific.net/AMR.331.632

Research on dynamic clothing show of virtual character during the online shopping

Zhiyun Wu[1, a], Yao Zhang[1,b]

[1] College of Textile and Light Industry, Inner Mongolia University of Technology, Huhhot, Inner Mongolia, 010080, China

[a]willie323@163.com, [b]xingqing.sky@163.com

Keywords: online shopping, 3d technology, fabric simulation.

Abstract. The research presented in this paper is to develop a technique of virtual clothing show during the online shopping. At present, the online shopping commodity demonstrated is the simple picture showed, individual sites using the fitting room show the stereo clothing, nevertheless, these ways can't reflect the dress sense of reality. So the dynamic clothing show is needed. This paper introduces the production process of dynamic clothing show. 3D models were designed with 3ds Max 2009, then be added bones. When bones meet the model, the fabric was simulated. The simulated fabric reflected the state of clothing with movement. Dynamic clothing show during the online shopping should provide consumers with more real clothing purchase experience.

Introduction

The popularity of the network and the number of internet users growth, enabling the network shopping in recent years to rapid development, online shopping become a new trend. At present the main network business platform have a lot of online sales of clothing shop. These online clothing store only provide the 2d images of clothing and briefly some text, customers when choosing dress online can only refer to these pictures to imagine themselves putting on clothes look like, can't see their practical effect intuitively .When the carefully selected clothing mailed in actual, the consumer know that is not appropriate, he have to return of. This often causes the loss of buyers and sellers. So customers want to observe a 3D effect and see the dynamic effect during purchasing on internet.

Technical support

3D digital technology is based on computer, network, and digital platform of modern technology based share tool. As in recent years the rapid development of computer technology, the research and development of 3D technology application has been through the decades of previous groping stage of maturity, perfect technology degree, usability, human nature, economy and so on, all have made huge breakthroughs. Along with the rapid spread of the application of computer network, 3D application is concerned, it is to become more common college students easily control the basic computer tools, like computer typing the same; 3D consumption and use, such as through 3D technology to make the games, movies, building, car, mobile phone, clothing, etc., the more has become the general public work and a part of life. In this topic, 3D software is mainly used for 3D model of the human body modifications, the model of the human body bone construction, clothing production and fabric of the model simulation.

Model establishment

The model can be made by 3ds Max software production, or derived from poser software, also can download from the internet. The models are shown in Fig. 1. The model with simple underwear is the best choice, because the designer can make the cloth they want, and do simulation.



Fig. 1 The model of the human body

Bone structure

The main bones are the Biped bone of 3ds Max software. Bones are shown in Fig. 2. The bones were band completed to human body and clothes, and then bone move can make human body do any action. The bones of bind completed are shown in Fig. 3. Binding bones is a complicated state; every point of the model has to be added to the proper bone, otherwise the muscle and cloth of model may be stretched. Fig. 4 shows the state of model movement with bones.

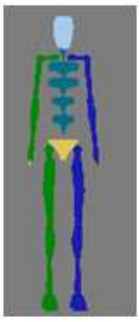


Fig. 2 Biped bone

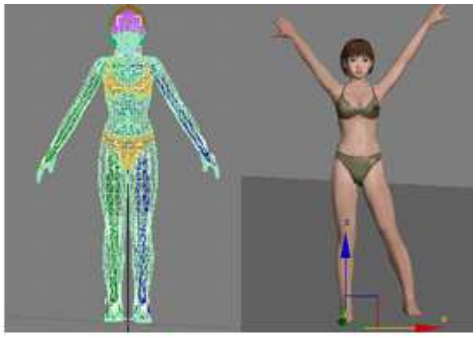


Fig. 3 Binding model



Fig. 4 The state of model movement with bones

Clothing manufacture

First of all, 2 patterns are made; Fig. 5 shows the 2 patterns. Then the patterns sutured by the garment maker of 3ds Max. Then the cloth modifier is added, it is used for fabric simulation. The body is added object; the material of fabric simulation is cotton. Fig. 6 is the set box of objects properties. The state of static simulation is shown in Fig. 7. The dynamic simulation is going when

the static state is finished. Fig. 8 is the dynamic simulation state; the upper left corner is automatic analog box, the cloth with motion model simulation in this image. Fig. 9 is the complete state of fabric dynamic simulation. Cloth moving with model moving, and drape，floating are reflected in Fig. 9.

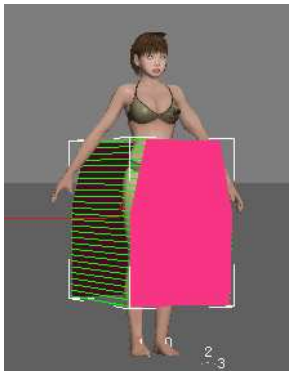


Fig. 5 Two pattern

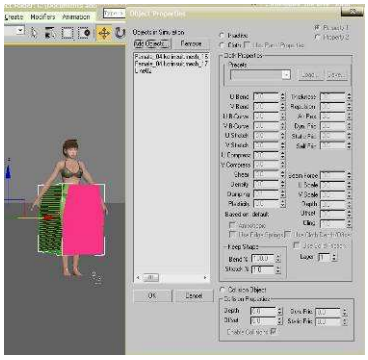


Fig. 6 The set box of objects properties

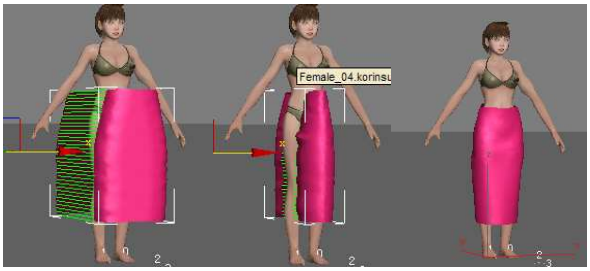


Fig. 7 The state of suturing static clothing

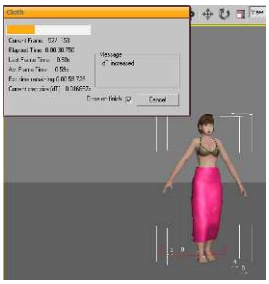


Fig.8 Dynamic simulation state



Fig. 9 Clothing motion state

Conclusion

This paper makes a detailed introduction on dynamic display. Dynamic clothing show is realized tentatively. Items show is no longer limited to 2D images. Clothing simulation technique can reflect the material of the clothing easily. Luster, drape, flap of clothing movement are also reflected. Clothing dynamic display builds a strong visual impact and appeal. It can make people feel more real during online shopping.

The network shopping will become the subject of future shopping, and 3D garment dynamic display will meet the shortcomings of the clothing reality during purchasing, provide consumers with more real shopping experience. Clothing simulation is the difficulty of subject. Making the clothing which is the most reality is necessary. This will help consumers save a lot of trouble during online shopping. However, virtual technique is still in its research process, dynamic clothing show has many shortcomings. The most prominent problem is that the clothing simulation is not real enough. Moreover, there are some difficulties in process of making dynamic clothing show. So powerful hardware, good technology of making 3D and sufficient imagination are needed.

References

[1] L.L. Li, Arts In China, (2010), p. 03

[2] M.Li, Public Art, (2010),p.07

[3] G.Y.Jing, R.L.Luo, Silk,(2007),p.04

[4] D.Cao,W.G.Ma, Heilongjiang Science and Technology Information,(2007),p.20

[5] L.Fan, IT Managers World,(2008),p.19

[6] X.Q.Chen,China Fashion,(2009),p.06

[7] Information on http://www. zf3d.com

[8] Information on http://www.baidu.com

© (2011) Trans Tech Publications, Switzerland
doi:10.4028/www.scientific.net/AMR.331.636

Simulation of Efficiency of Liquid Cooling Garments

Mingwei Tian[1, a], Sukang Zhu[1,b] and Ning Pan [2,c]

[1] Institute of Physics of Porous Soft Matters, Donghua University, Shanghai, Shanghai, 200051, China

[2] Biological and Agricultural Engineering Department, University of California, Davis, California, 95616, USA

[a]tmw0303@mail.dhu.edu.cn, [b]zusukang@dhu.edu.cn, [c] npan@ucdavis.edu

Keywords: Liquid Cooling Garment, Thermal Manikin, Effective Cooling Temperature, Finite Element Method, Heat transfer, Heat-flux Coupling.

Abstract. Liquid cooling garment (LCG) is treated as one kind of effective form-fitting garment applied to remove and release extra heat efficiently from human body whose internal temperature can be easily maintained at a safe dynamic equilibrium level under the severe boundary conditions. In this paper, firstly, two specialized types of liquid cooling garments, wrapped around thermal manikin, are designed as the three-dimensional heat-flux coupling models that are solved numerically using a finite element method, and then the effective cooling temperatures of the thermal manikin skin are proposed as the characteristic parameter to evaluate the cooling effects of these garments. Finally, A comparison of thus effective cooling temperature with the experiment data from the existing reference are shown that this simulation model develops very reliable results for the heat transfer between liquid cooling garments and thermal manikin.

Introduction

Water cooled garments have found a variety of applications in aerospace and industrial settings since 1962 [1], they have an important role in the individual protection field which can alleviate the heat attacked from the external environment, such as aerospace, military (in cockpits, etc.) and in some industrial situations (in mines, etc.), and also they can be applied in some special individual healing who have certain illness such as multiple sclerosis and hypohidrotic ectodermal dysplasia [2]. Several works has been done on this attractive issue and acquired some practicable designs and results from different experimental approaches, such as Kayacan [2] designed two different types of liquid cooling garments (LCG) with different compositions and placed them alternatively on thermal manikin then compared the different cooling effect of two cases. Cao [3] created eight fabrics with different fiber content, fabric structure and thickness as the inner layer of LCGs and then their thermophysical properties are measured, compared and analyzed. Here, these experimental methods were used as the common ways to investigate the thermal response and performance of LCGs, but explained very little physical essence of the heat transfer of thus system, moreover, the testing process inevitablely contained some uncertainties and usually held a bored long period. Stimulation methods, owing to the high accuracy and convenient operation, were extensively used in engineering area including the textile heat transfer scope, such as thermophysical properties measurement [4] and the heat and mass transfer [5,6]. To the best of my knowledge, there is little stimulation work concerning the cooling effect of liquid cooling garments.

In this paper, a finite element method is employed to investigate the efficiency of LCG and the model of this system is built considering the heat-flux coupling effect, including the flow flux in the tubing and the heat transfer through the system composed of thermal manikin, LCG and external conditions. The effective cooling temperatures are deemed as the characteristic parameters of LCG that covers on the thermal manikin, the obtained curves of this parameter compare with the corresponding experimental data from the reference under different inlet temperature.

Experimental method

In this section, experimental details in [2] is briefly reintroduced and this will be treated as the original evidence of the following model section. System design and test conditions are depict as follow.

System Design. The whole system was basically composed of three pieces, thermal manikin, chiller and liquid cooling garment as shown in Fig. 1. Thermal manikin was a dry style and embedded plenty of thermocouples which could record its local temperature, control panel and water tank were two attachments of manikin body, the function of control panel was to set up, adjust and record thermal manikin thermal response while water tank was the container of the water used to heat the manikin body from the panel command. The chiller was designed to cool the water injecting into the LCGs. Two kinds of LCGs were designed and their structural properties could be found in this reference. Their inner layers, tubes and outer layers were both configured with the same structures, the sponge was filled in the interspace between out layer and inner layer of Type 1 but without in Type 2.

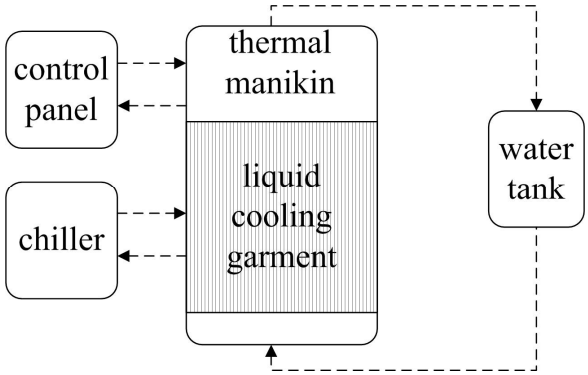


Fig. 1 Sketch diagram of the system design

Test conditions. There were definitely two steps of the experimental process; the first step was the "reference step" means that the temperature of thermal manikin and the external condition stabilize at corresponding adjusted temperature, 40 degree and 23 degree, respectively. While the manikin body reached the reference state, water tank stopped heating but the water was continuously pumped through the manikin body during the remaining process to simulate the influence of human metabolism. At the second step, chiller adjusted its internal water to inlet temperature and injected the cool water into the LCG from the inlet, then the garment started its cooling process and the temperatures were recorded by the thermocouples located at different skin positions, three different inlet temperatures, 7, 10 and 13 degree, and flow rate, 250,375 and 500 ml/min, were set up for three comparison tests respectively. The effective cooling temperatures were used to describe the cool effect of LCG for each adjusted inlet temperature and flow rate, their values could be facility determined by the average temperature recorded from the thermocouples subtracting the reference values.

The authors found that the effective cooling temperature slightly decreased when the inlet temperature decreased, and at lower flow rates, effective cooling function increased slightly while this effect disappeared for higher flow rates.

Modeling

In this section, constitutive equations of heat-flux coupling are first given and the model of LCG is then built and calculated.

Constitutive Equations. In the above case, the flux flow can be assumed as single, Newtown and incompressible flow, so the constitutive equations as follow,

Continuity: $\nabla V = 0$ (1) Momentum: $\rho(\frac{\partial V}{\partial t} + V\nabla V) = -\nabla P + \mu\nabla^2 V + F$ (2)

Energy: $\rho C_p \frac{\partial T}{\partial t} + \rho C_p V \bullet \nabla T = \nabla(k\nabla T) + Q$ (3)

Where V, ρ, C_p, μ and k are the velocity vector, density, heat capacity, shear viscosity and thermal conductivity of water flow, P is pressure, F is body forces (gravity, etc) and Q is the heat source.

From Eqs.1-3, the heat transfer of fluid and solid system can be obtained and specified once the initial and boundary conditions are both given in each special case.

Modeling of Liquid Cool Garment. Some assumptions and simplifications are applied for each piece of this cooling system. COMSOL is used to develop the LCG model for FEM analyses and the models of system are shown in Figs.2(a-d).

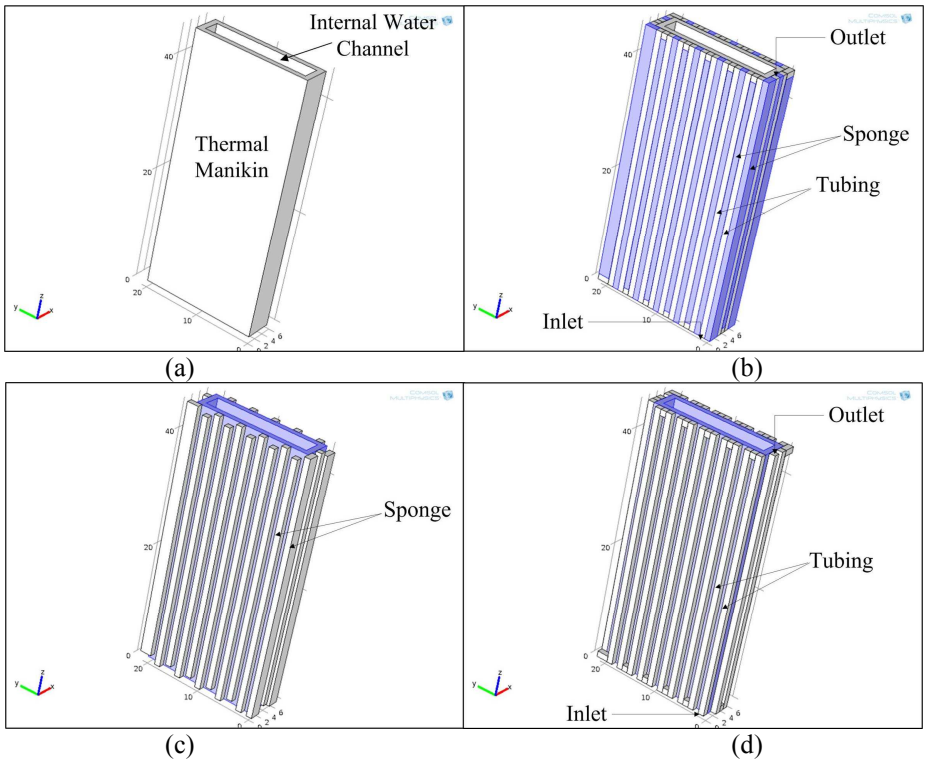


Fig. 2 The models of CLG system: (a) thermal manikin, (b) Type 1, (c) sponge and (d) Type 2

Thermal manikin shown in Fig.2(a) can be treated as a solid block with a internal water channel which can recycle the hot water from the water tank to preserve the constant core temperature of body. In our model, the inner face is of this block is installed at the constant temperature 40 degree.

Liquid cooling garment is placed on the thermal manikin, two models named as type 1 and type 2 are shown in Figs. 2(b) and (d) respectively, their inner and out layers, used to fix the tubing, are ignored for their marginal contribution on the heat transfer, S-shaped tubing of them parallel around the skin to cool body evenly and its inlet temperature and initial flow rate are both indicated at the inlet. Type 1 is composed by the S-shaped tubing and sponge shown in Fig.2(c) while Type 2 is the case removing the sponge. The outside surfaces of two models transfer heat to the external situation by convection and heat convection coefficient is 10 W/m^{2}K. The properties and structure details of our model are list in Table 1.

Table 1 Calculation properties of models

	Geometry [cm]	k [W/mK]	ρ [kg/m^3]	C_p [J/kgK]	Initial temperature [K]
thermal manikin	block 5×20×45 internal channel 3×18×45	0.97	1877	1205	40 23 (external condition)
tubing water	cross section 1×1 total length 1150	0.63	1000	4200	40
sponge	cross section 1×1 total length 1100	0.053	30	1080	40

These two models are then meshed and solved; the results can finally reach convergence once the mesh size is decreased to 0.00005m. The temperature distribution of this system can be obtained facility and the average temperature of manikin surface is deemed as the effect cooling temperature once subtracting the reference temperature (40 degree).

Results and Discussion

In this section, the simulated results are compared with the experimental data in the reference and interpret the physical essence of this phenomenon.

The comparisons of two types under different inlet temperature levels (7, 10 and 13 degree) are shown in Figs.3(a-c) respectively and their flow rate are all fixed at 250ml/min. Definitely, their effective cooling temperature curves with time coincide with each other very well under these three levels.

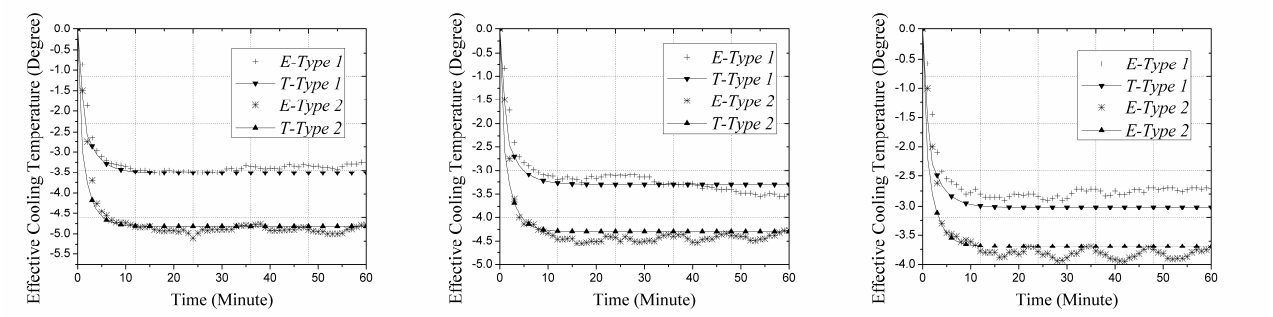


Fig. 3 The comparison between simulated results (T-Type) and experimental data (E-Type) of two types, water inlet temperature: (a) 7 degree, (b) 10 degree and (c) 13 degree

Form the Figures, we also can find some special information. Firstly, the cool function of type 1 are always lower than type 2, this inefficiency mainly caused from the configuration discrepancy of two models, the sponge of type 1 function as the insulation layer can block the heat released from tubing and manikin to the outside, imaginably, this design may play an important roll in the high temperature case which can slower down the body temperature rise than type 2. Secondly, with the increasing of inlet temperature, effective cooling temperatures of both types become smaller because the water of high temperature plunders smaller energy from manikin.

Conclusion

The models to simulate liquid cooling garments were particularly investigated in this paper, two kinds of LCG were built and good agreements were made with the existing experimental data. This model can be facility extended to research other LCG design and boundary conditions.

References

[1] S.A. Nunneley: Orig. Life Evol. Biosph. Vol. 2 (1970), p. 335

[2] O. Kayacan, and A. Kurbak: Text. Res. J. Vol. 80 (2010), p. 1442

[3] H. Cao, D.H. Branson, S. Peksoz, J. Nam and C.A. Farr: Text. Res. J. Vol. 76 (2006), p. 587

[4] S. Cimilli, F.B.U. Nergis and C. Candan: Text. Res. J. Vol. 78 (2008), p. 53

[5] F.L. Zhu and K.J. Li: J. Fire Sci. Vol. 29 (2011), p. 3

[6] F.L. Zhu and K.J. Li: Fire Technol. Vol. 47 (2011), p. 801

© (2011) Trans Tech Publications, Switzerland
doi:10.4028/www.scientific.net/AMR.331.640

Evolution Law of TheTraditional Baina Textile and Its Application Style in The Clothing

Huie Liang, Le Xing

School of Textile and Garment; Jiangnan University; Wuxi 214122; China

xingle5945@163.com

Keywords: The traditional Baina textile, Patchwork, Inheritance, Fashion applications

Abstract. The traditional Baina textile, a kind of traditional Chinese patchwork has a long history with thousands of years. It has not only quite high practical value but also profound artistic aesthetic, which demonstrating human's plain yearning for beauty. Based on the document and literature collection, this article summarized its main style and law under the evolution. Meanwhile the paper analyzed the current application of the traditional Baina textile in the fashion industry, in order to expand the concept of modern design.

Introduction

The traditional Baina textile, a kind of traditional Chinese patchwork comes from "the art of Mother's". As its inheritance from generation to generation and surpassing beyond the time and space, it has formed a series of characteristics: simple and plain, mysterious and singular, elegance and conventional. And now it is similar with the "all-match style" from the collision of nationality and fashion. The Baina elements are integrated in every season's fashion shows. More and more designers combine this traditional expression with modern design idea intentionally or unintentionally. For example: they will make a recombination after the whole unit's separation, or integrate the separate parts into a whole unit, which have formed many familiar but innovative fashion images. So it is quite necessary to have a deep understanding and an innovative application of traditional Chinese patchwork- Baina textile.

The main style and Evolution law of the traditional Baina Textile

The Chinese expression "Baina", "Bai" is a classifier, referring to "a large number", and "Na" meaning "patches". [1] Just as its name implies, "Baina" meaning many patches and single pieces are integrated into a complete unit, which is practical and appreciating. The styles of the traditional Baina textile in history are as follows: " Shabby Clothes" , " Kasaya", "Paddy Clothing", "The Beggar's Gown", "Baijia Clothes", "Baina Clothes" and so on.

In China, there is a variety of claims on the origin of the Baina textile, but till now no final conclusion has reached yet. According to the records of literature, the traditional Chinese patchwork perhaps originated from the Spring and Autumn period (770B. C- 476B. C).and it was mainly worn by the children and beggars . *Clad in Colorful Clothes to Please His Parents*, the seventh story in *The Twenty-four Filial Exemplars* told a story about Lao Laizi supported his parents , "Lao Laizi, came from the Zhou Dynasty in the Spring-Autumn period, was extremely filial. He supported his parents extraordinarily well by offering them with delicious food. Though he was seventy years old, he never said that he was old, and he often wear colorful clothes and played like a child at the side of his parents. "

Although "Baina Clothes" was not mentioned in this story, the offspring always called "Colorful Clothes" as "Baina Clothes". During the Western Jin Dynasty period (265-316), there was a record in *Jin Shu* written by Wang Yin, it said, "Dong Weinian, who was not known to others. One day, he turned up in Luo Yang, Henan province. In the evening, he had nowhere to go, so he slept in Baishe. Having no clothes to wear, he found some rags and pieced them together into a garment named 'Baijia clothes'." However, "Baijia clothes" means "clothes made of patches" [2], which is another statement of "Baina Clothes". The definite description of "Baina" was written in *"Bian Wen" of Dunhuang • Vimalakitinirdesasutra*, which was stemmed from the Tang and The Five Dynasties periods（618—

960）, and unearthed at Thousand Buddha Caves in Dunhuang Grotto. It was described that, “A skillful tailor embroidered the phoenix, where there was raining, there the phoenix would alive and all of them can be made to ‘Baina Clothes’, once the senior apprentice wore the ‘Baina Clothes’, the fairy maidens would love him in no time.” It is easy to find the complicated relation between “Bai Na” and Buddhism from the later documentary evidence. Another name of “Baina Clothes” is “monk's ragged robe”. With the dissemination of Buddhism, the traditional Baina textile has become standardized and expanded. According to the folk records, influenced by Buddhism , a special form of costume named “Paddy clothes”, was loved by people in the Tang dynasty (618-907).It was quite popular during the Tang, Ming and Qing dynasties, and always worn by women. Wang Wei, a famous poet in Tang dynasty said, “tailors should learn from the ‘Paddy clothes’ when making clothes.”The characteristic of “Paddy clothing” is exactly that rich texture characteristics and unique art form of the traditional Baina textile. In the late Ming Dynasty, because of people valued the skin texture of the garment very much and wished wasteful life enjoys, the “Paddy clothing” became fashionable for a time. “Paddy clothes” has absorbed characteristics of the rich skin texture and unique art form of the traditional Baina textile. In the later period of Ming Dynasty, because of people valued the texture of the garment very much and wished wasteful life enjoys, the “Paddy clothes” became a fashion style for a time.

After the monarch in Qing Dynasty occupied ShanHaiGuan, they carried out a series of policies such as "Shaving the hair and exchanging the clothes". This policy had changed some customs of the Han culture in a certain degree, but a lot of fashion apparel made in the Ming dynasty was retained. There were many records about the “Paddy Clothes” of women’s garments in Kangxi and Qianlong period of the Qing dynasty (As shown in Figure 1).In the post-period of Republic of China (1911-1949), “Paddy Clothes” were worn occasionally in the southern region of China. However, it was not applied in women's clothing, but specially made for children to pray for auspiciousness. Having had undergone the clothing system reform and the infiltration coming from the Chinese and Western culture, the adult's garment took on enormous changes, but children's clothing had kept more traditional elements after the 1911 Revolution. So the most common form of Baina is children's clothing such as “Baijia Clothes”, “Baina Clothes” in modern times.



Fig.1 “Paddy Clothes” [3]

With the constant cultural communication from home and abroad, the traditional Baina textile has surpassed its original form, and mutually penetrated through the western patchwork technology. Western patchwork technology, with a long history, has developed into an artistic form both in technical art and artistic beauty. Since the world first patchwork art race has started in 1930, the patchwork has become popular in American in 1970.And soon it has promoted in Japan in 1976. In 2007 the “Patchwork Art” had been held in four cities in China for the first time. In March, 2010, “Shanghai International Patchwork Festival” has been successfully held at Shanghai International Fashion Trade Fair. On 29th March, 2011, “China Quilts Color and Art Committee” has been founded, aiming to encourage the protection of traditional patchwork culture and the international non-governmental communication, and promote the combination of art and industry. In the eastern region of China, such as Shanghai, and Hangzhou, a Specific Patchwork Culture-Life Museum has been founded spontaneously by those who love the patchwork. They are folk organizations, using for communication and learning. Compared with the eastern region, the traditional Baina textile which is

widely used in people's daily life there has preserved well in the central and western parts, such as Shaanxi, Shanxi, Henan, etc. What's more, in Xi'an, Shanxi province and other places, "Baina Clothes" and "Baina Quilt" have become a representative signal with local characteristic, welcomed by tourists from home and aboard.

Table1: Evolutionary styles of The Traditional Baina Textile in Different Periods

Original Time	Title	Source & Forms
the Spring and Autumn period (770B. C-476B. C)	"Colorful Clothes"	*Clad in Colourful Clothes to Please His Parents*, the seventh story in *The Twenty-four Filial Exemplars*, "Lao Laizi often wear colorful clothes and played like a child at the side of his parents."
the Western Jin Dynasty (265-316)	"Baijia Clothes"	Wang Yin said in *Jin Shu*, "Dong Weinian, who was not known to others. One day, he turned up in Luo Yang, Henan province. In the evening, he had nowhere to go, so he slept in Baishe. Having no clothes to wear, he found some rags and pieced them together into a garment named 'Baijia clothes'."
Tang and The Five Dynasties （618—960）	"Monk's Ragged Robe", "Kasaya", "Shabby Clothes"	*"Bian Wen" of Dunhuang • Vimalakitinirdesasutra,* "A skillful tailor embroidered the phoenix, where there was raining, there the phoenix would alive and all of them can be made to 'Baina Clothes', once the senior apprentice wore the 'Baina Clothes', the fairy maidens would love him in no time."
Tang, Ming and Qing Dynasties （618—1911）	"Paddy Clothes", "The Beggar's Gown"	Wang Wei, a famous poet in Tang dynasty said, "tailors should learn from the 'Paddy clothes' when making clothes."
Post-Period of Republic of China （After 1911）	"Children's Baijia Clothes", "Monk's Ragged Robe"	It is mainly used as the Baijia Clothing for Children, or and some daily necessities, like: door curtain, cushion.etc.
Today （1949~）	"Children's BaiJia clothes" "Monk's Ragged Robe", handicrafts	The morable articraft and handicrafts

It can be seen from table1, the traditional Chinese patchwork has transform into a part of the new fashion as time passing by. Seen from the evolution of traditional Baina textile, we can reach conclusions as follows: (1) Different from other clothing's evolution law, which meaning from top to bottom, the traditional Baina textile is originated from the non-governmental traditions. Affected by the strict religious demanding on clothing of Buddhism, it returns to the folk through "displacement", a traditional Chinese design method. The characteristic of this process: "being of, by and for the people". (2)The form of the traditional Baina textile has developed from plane to space, the material from homogenous to diversity, the application scope from singularity to fertility. (3)The traditional Baina textile, whose practical connotation is raised to the aesthetic standard from the pure practicality, and even the multicultural heritage and artistic fashion are mixed, has become "a kind of life artwork" with aesthetic value.

The outstanding evolution law of traditional Baina textile has manifested its Wide range of applications in the modern life. It has high practicability, applicability and deep cultural connotation, is used in the modern clothing and household textiles, and also multi element multi personalities and eco-friendliness theories mixed.

The Application Style of The Traditional Baina textile in The Modern Clothing

The traditional Baina textile is widely used in all aspects of modern people's life. And it is divided into three types: home textiles, art decoration, and clothing. According to its application in the clothing, three different styles can be classified depending on the different ways it supported and the vision impression: the amorous national style, the modern optical style, the natural hippie style, etc.

The Amorous National Style. The national style, vaguely referring to the forms and characteristics of a certain nation's traditional color, pattern and so on used in the modern clothing design. Of many different national style designs, the traditional Baina textile is one of them. What's the most distinct difference is on the shell fabric choosing, the color matching, and the cloth joining. For example, the patchwork chosen in Russian clothing often has an abundant hue and sharp comparison, so it takes on a rich color when some tiny fragments are pieced together to geometric patterns, then combined with a piece of bigger cloth, or embedded in some parts of the clothing as a decoration. While the purity of color is low but the lightness is high of the patchwork used in Japan clothing, which gives off a flesh feeling. The African patchwork, with complementary and high purity color, takes on a sharp visual impact, so the wilder style as well. Although no specific official restrict on the color and material of the patchwork clothing in China, the standard convention is made. For instance, Children's Baijia Clothing, blue and purple shell fabric should be included. In Chinese, the pronounce of blue, purple is the same of what lanzi pronounced.The Chinese expression lanzi, which meaning to protect children, is a way to pray for safe and sound. What's more, there is much differences in the color and material choose between the south and the north. The color in the north is bright while in the south is flesh.







Fig.2 2011KENZO spring/summer [4] Fig.3 2011HERMES fall/winter [5]Fig.4 Baina Clothes with National Style [5]

In the fashion stage nowadays, it is easy to notice the fashion of the patchwork style. For example, the figure2 above is the clothes showed in the 2011 spring/summer fashion show of KENZO, and figure3 is in the 2011 fall/winter fashion show of HERMES. With the traditional Chinese Baina textile decorated in the clothes, a rich national style is taken on. Figure4, manifesting the unique national characteristic with the patchwork style largely used is the work designed by students coming from the International Garment Universities in 2011.

The Modern Optical Style. "OPART" means the visual art of the "OPTICAL ART". It is a kind of visual art in the works of two-dimensional (Drawing) or three-dimensional (carving) with the comparison of black and white or strong color of abstract geometrical shape, which stimulates observer's vision, such illusions as the shape transformed and others would appear. OPTICAL ART has been accepted and applied by the fashion industry the time it appeared in the 1960s. There is a

natural combination between the clothes of OPART style and the traditional Baina textile in vision, i.e. both of them have tried to create a kind of transformation amid the order, so the illusion can be made. Particularly speaking, it is a sense of visual rhythm formed through using the geometrical shape such as stripe, grid, etc. under permutation and combination, then adding a strong comparison of color. Besides, it is easier for the combination of the planar graph and human body at the integrated of the traditional Baina textile and OPART style (As shown in Figure 5).



Fig.5.The Optical Style Clothes Using the Baina Textile Design Form [4]

The Baina textile with OPART style mainly makes use of the optic theorem, by means of the repetition of geometrical shape (which can be a pure color unit or geometrical patterns unit) and color contrast, an impression of visual disorder will be created. Cloth of simple patterns and shapes can be arranged according to the visual movement under the application of the traditional Baina textile. The skin texture of the cloth itself can strengthen the feeling of visual disorder, which enhances the visual impact with vibration. Therefore, the one who is in op-style Baina textile would in a dynamic cinditon, meanwhile gazing at him, one would feel dizzy, and even have an illusion, just like visual games.

The Natural Hippie Style. The Hippie Style originated from the subculture- The Hippie Movement, started in the 1960s.This style has a close relation with the Hippie's wearing. After 1970s, though The Hippie Movement has declined day by day, its influence to the modern society is larger and larger. This fashion style is often adopted by the fashion designers for its reflection on the affirmation of the youth, the admiration for the peace, nature and love, the protection of the environment and the objection of the routine style. The rich color, taking the national themes with the handicraft style as a reference and manifesting a natural sense of the skin texture with the clothing matched, are the designers' favorite. Sometimes, clothes are made old or broken on purpose, in order to fight against the maturity and elegance in the mainstream society, but focus on the personal style. Through various materials and rich color, especially the combination of the heavy material and creative structure, the designers change the graphic sense of the old-fashioned patchwork, so a vigorous and unrestrained style, which the trend-setter deeply love is taken on (As shown in Figure 6).



Fig.6.2011 MACARONIC fall/winter [5]

There are huge differences among these three styles mentioned above when referring to the background of their age, the aesthetic image, the regions of various culture and so on, however, they are adopted and loved by people under different cultural backgrounds at the same time. The reasons can be generalized as blow: A: the multi-cultural information and strong national charming is connoted in the traditional Chinese patchwork, so the strong independence and uniqueness can be found in very piece of work. It can not only meet people's enthusiasm on the inheriting of the national Symbolic language, but cater to modern people's pursuing of personality and creativity. B: the traditional Chinese patchwork, linking up with the modern fashion theory, can break up the tediousness added by the rigidness and standardization, as the visual impact emerging, the equilibrium point is found between the mess and monotonousness. C: Because of its abundant color and grain, the traditional Chinese patchwork gives off a sense of peculiar and challenging, meanwhile, during the creation process, designers will get a feeling of infinite achievement from breakdown, rearrangement, and recreation.

Conclusions

As mentioned above, the traditional Baina textile has changed together with the times, and the evolution law gone through from simple to complex, concrete to abstract, and practical to aesthetic. It takes on inheritance, diversity, and uniqueness, what's more, the amorous national style, the modern optical style, and the natural hippie style have been showed in modern fashion application. Today, with the merging of patchwork industry, the traditional Chinese patchwork is like the nirvana of the phoenix, filling with glory and infinite hope. It will be bestowed upon new meanings in the future fashion stage. Moreover, the patchwork fabric has been discovered in many places of the world, and distinct features are appeared in different nations and regions. Thus we should not ignore this national symbolic language, but distinguish it from others and inherit it well.

Acknowledgements

This work was financially supported by Humanities and Social Science Research Project of the Education Department: *Traditional Costume Preservation and Application in Modern Fashion Design Industry （08JA760010）； Research on Chinese Folk Weaving Art (09YJA760015).*

The Author: Huie Liang (1967-), female, is a professor and Master tutor. She mainly engaged in the clothing culture research, and the modern theory of fashion design teaching and research.

Le Xing(1987-), Female, Master of School of Textile and Garment; Jiangnan University. Her research interests include the culture of costume and fashion design.

References

[1] China Social Sciences Institute of Linguistics Dictionary Editing Room. The Contemporary Chinese Dictionary [M]. (Beijing: The Commercial Press,1993.812. In Chinese)

[2] Yuzhou Du, Liangyun Miao: The Chinese Clothing [M], (Shanghai Culture Press, Shanghai, 2000, In Chinese)

[3] http://image.baidu.com

[4] http://www.haibao.cn/

[5] http://www.renren.com/home

© (2011) Trans Tech Publications, Switzerland
doi:10.4028/www.scientific.net/AMR.331.646

Research on the influence of the Fabric organization to wind-resistant property of sportswear

Yuxiu Yan[1,a], Xiu Yi[1,b], Jianwei Tao[2,c], Minbo Lin[2,d] and Rongqi Li[3,e]

[1]Zhejiang Sci-Tech University, Hangzhou, China

[2] Zhejiang Bangjie Digital Knitting Co., Ltd, Yiwu, China

[3]Hefei Gas Group Co. , Ltd, Hefei, China

[a]yanyuxiu777@163. com, [b]ruheshow@163. com, [c]bangjie@vip.sina.com, [d]777abc@163.com, [e]sky_0120123@163.com

Key Words: sportswear, wind-resistant property, organization

Abstract. Selected four organizations in those are most frequently-used in sportswear, then weaved a common sports-vest by the seamless knitting machines. Used the methods of wind tunnel test and data analysis, reached a conclusion about the influence of the organizations to wind-resistant property of sportswear: in the winding speed scope of the experiments, when the winding speed are between 3.3 m/s and 11.55 m/s, the wind-resistant property of the four organizations are almost the same; when the winding speed are between 11.55 m/s and 18.70 m/s, the wind-resistant property are different, the order from bad to good is 1×2 false rib organization, one road off staggered 1×1 false rib organization, mesh organization, plain weave, and reached the fitting curve equation. The study provides theoretical and practical reference for the research and development of sportswear.

Introduction

The athletics sports of sports activities are usually full of competitive, what make full use of every minute. Though 0.001 second in competitions is a key time to distinguish success or failure[1]. The performances are subject to many subjective and objective factors[2], such as the athletes' own abilities, the sites and the facilities, the equipments of athletes, etc. The first deals to the personal capabilities; the second is objective to all the athletes who take part in; but the third is different and decisived by the level of science and technology[3]. To improve the performance by improving the equipments is a main direction of science study.

In athletics sports, the athletes overcome all kinds of resistance, such as wind-resistance[4], water resistance, continually to reach a good score by quicker speed. Designing scientific sportswear is an effective way to reduce resistance. Jack R[3], American atmosphere dynamics expert, said that it could reduce 6% air resistance if the race athletes dress scientific tights. Visibly, it is an valuable research to design the sportswear with good wind-resistance property. The study has a great value and research space because it is found a vacancy when reading refrences of domestic and overseas.

This issue is researched on the wind-resistance of the sportswear those are weaved by different organizations through the experiments in the wind tunnel which usually be used in the car and helicopter design[5]. The study makes a preliminary study on how to achieve a good wind-resistance property of sportswear for reducing wing-resistance and enhancing the performance of athletes, even offer a guide for enterprises and designers.

Wind tunnel test

Experimental principle. The principle of using the wind tunnel test[6] is: through measured the differential pressure values when the wind blowing over the vests, to analyze the odds of the wind-resistance property. The so-called the differential pressure value, is the difference of the pressure value that formed before and after the wind blew over the experimental model in the wind

tunnel, it represents the wind-resistance of the experimental model. Thus, according to the differential pressure values measured by the experiment, the comparison of experimental model for the resistance caused by wind can be more intuitive, also the wind-resistance property of the experimental model can be characterized. The greater the value, the greater the resistance of experimental clothing, the worse the wind-resistance property is; the smaller the value, the smaller the resistance of experimental clothing, the better the wind-resistance property is.

Experimental equipments and preparation

Experimental equipments. Testo 510 differential pressure meter(0-100 hpa) and Pitot tube , reflux-type low speed wind tunnel.

Experiment clothing. After the market research of sportswear, selected the most common material and style used in sportswear weaving. Weaved them by the common material:40s combed cotton + coolmax modified polyester. Four organizations are:plain weave, mesh organization, one road off staggered 1×1 false rib organization, 1×2 false rib organization. The size designation is 160/84A.

Experimental program

Speed calibration. Sealed the wind tunnel and made it operated normally. Measured the steady-state of speed in experimental area[7]. Selected 36 points uniformly in each rectangular experiments region, connected the differential pressure meter and Pitot tube with rubber hose pipe, measured the speed of each point at every certain rotate speed. Knowing that, in the speed of 0-40 m/s , the wind speed is uniform and stable. The rotate speed and the wind speed in this study is basical meet the relationship:v = 0. 055r +0. 55. (1)

Pressure measurement. Used the standard mannequin to simulate the human body. Putting the model which wearing the tests' vest on into the wind tunnel. To maintain the model still[8] , then the wind speed can be used to simulate model's movement speed .The two joints of the differential pressure meter are connected with the front contact and back-end contact of test model by rubber hose pipe. Adjust the differential pressure meter to the function of measuring pressure with the units pa. Measured the pressure changes at different wind speeds. Obtained the experimental statistic data. The rotate speed is 50-330 rpm in the test, the corresponding wind speed was 3.3-18.7 m/s.

Data analysis

Statistical analysis. By statistical analysis[9], obtained the relationship of wind speed and differential pressure diagram what is shown in Fig. 1.

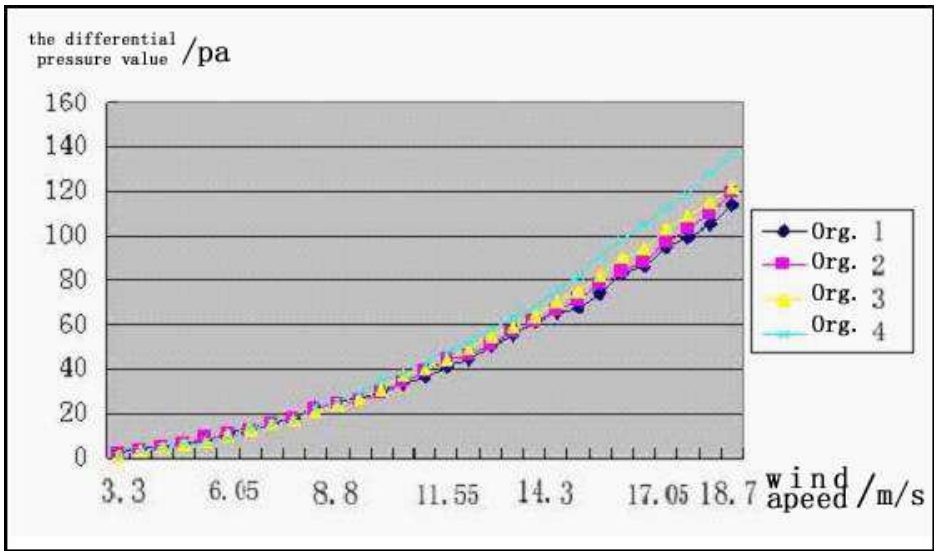


Fig. 1 Wind speed - differential pressure diagram

Fig. 1 shows that when the wind speed are between 3.3 m/s and 11.55 m/s, the corresponds rotate speed among 50-200 rpm, the differential pressure curves of the four organizations are basic coincide, the differential pressure are nearly the same, the wind-resistant property of the four vest in

four organizations are almost the same;when the winding speed are between 11.55 m/s and 18.70m/s, that corresponds rotate speed among 200-330 rpm, the differential pressure curves of the four organizations are basic coincide, the differential pressure have certain dispersion, the wind-resistant property are different, the order from bad to good is 1×2 false rib organization, one road off staggered 1×1 false rib organization, mesh organization, plain weave.

Regression analysis fitting calculation[10] by using SPSS

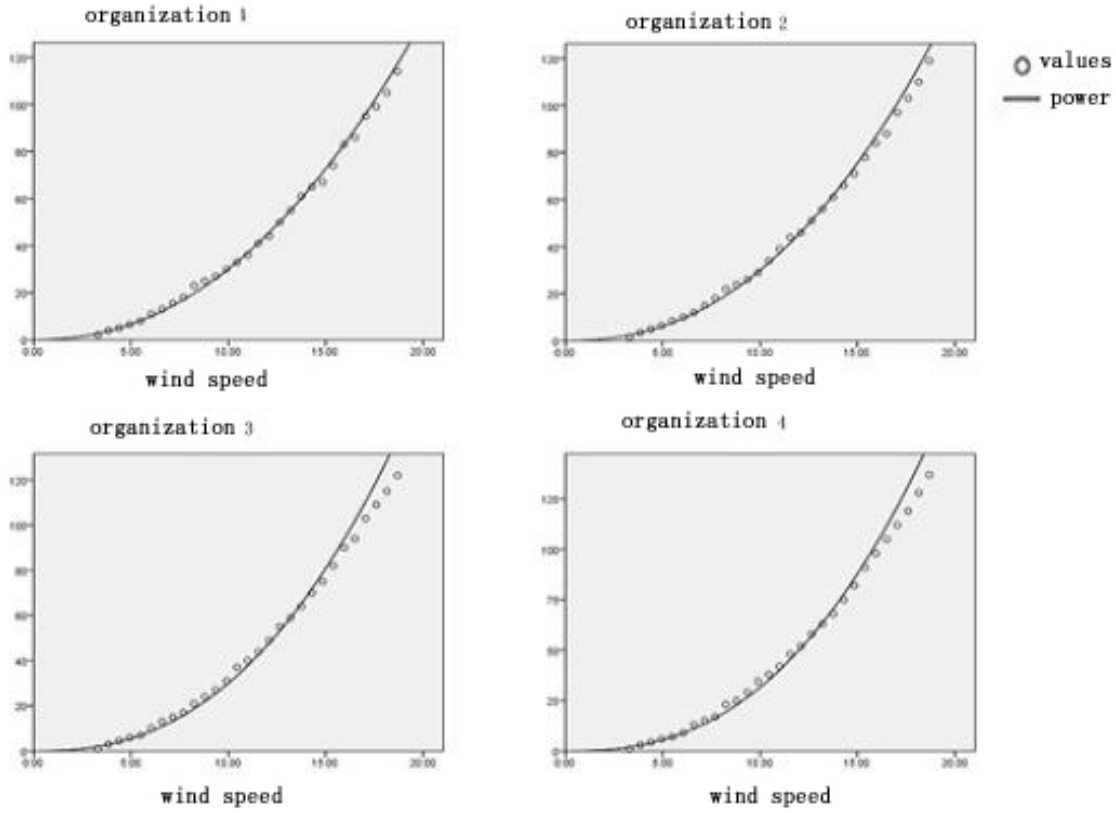


Fig. 2 Power function fitting curve of the experimental data

It can be seen from Fig. 1, the change of the differential pressure value of the organization following with the wind speed are non-linear process. Through observation, found that the curve is similar with power function curve. Regression analysis[5] by using SPSS software, reached the power function fitting curve of the four differential pressure values, that shows in Fig. 2.

From the fitted curve, the power model fits the data with good results. By using SPSS analysis to the data, knowing that:for the organization 1, R^2 is 0.995, F-test is 5555.064; for the organization 2, R^2 is 0.991, F-test is 3186.036; for the organization 3, R^2 is 0.983, F-test is 1656.723; for the Organization 4, R^2 is 0.986, F-test is 1928.275. Confirmed the four fitting curves have very high goodness of fit. Obtained a result that the curve fitting equations are:

$Y_1=0.200*v^{2.176}$ (2); $Y_2=0.158*v^{2.279}$ (3); $Y_3=0.108*v^{2.444}$ (4); $Y_4=0.094*v^{2.524}$ (5)

(Y_1, Y_2, Y_3 and Y_4 stands for the differential pressure value of organization 1, organization 2, organization 3 and organization 4; v stands for the speed of the experiment.)

The regression equation shows that, as the wind speed increases, the differential pressure values of four kinds of vest gradually increases, and the difference among the four organizations gradually increase, the wind-resistant property from bad to good is 1×2 false rib organization, one road off staggered 1×1 false rib organization, mesh organization, plain weave, and we reached the fitting curve equation. So for the athletic sportswear, it is better to use plain weave at high speeds.

Conclusions

1) In the wind speed scope of the experiments，when the winding speed are between 3.3 m/s and 11.55 m/s, the four vest in four organizations are almost the same.
2) When the winding speed is between 11.55 m/s and 18.70 m/s, the order of the wind-resistant property from bad to good is 1×2 false rib organization, one road off staggered 1×1 false rib organization, mesh organization, plain weave.

3）Analyzing and calculating through SPSS software we obtain a result that the Curve fitting equations is：$Y_1=0.200*v^{2.176}$；$Y_2=0.158*v^{2.279}$；$Y_3=0.108*v^{2.444}$；$Y_4=0.094*v^{2.524}$.（Y_1, Y_2, Y_3 and Y_4 stands for the differential pressure value of organization 1, organization 2, organization 3 and organization 4；v stands for the speed of the experiment. ）

4）For athletic sports，it is better to use plain weave at high speeds.

References

[1] Debao Zhang, “Modern science and technology and the development of competitive sport”[J]. sports world. 2008 (12), 106-107. In Chinese.

[2] Ming Zhou, “Technological progress and the evolution of sportswear”[J]. Friends of Science. 2010 (3), 91-92. In Chinese.

[3] Fuxiu Li, “Wear on the high-tech sports clothes”[J]. Encyclopedic knowledge, 2006 (5):41.

[4] Yun Bai, “Magical air magic - air resistance”[J]. Modern Car, 2007 (6), 84-85. In Chinese.

[5] Mike Dale, (translation) Jianbao Han, Xiaojiang Luo. “Pickup truck tailgate air resistance simulation and wind tunnel experiment”[J]. Automotive repair and maintenance of . 2005, (1):38-40. In Chinese.

[6] Jianying Yu, Xuhong He, “SPSS statistical analysis and application”[M]. Beijing Posts and Telecom Press, 2003: 81-82. In Chinese.

[7] Weiping Ma, Keli Yan, “Sports and high-tech sports clothing”[J]. Journal of people's liberation army (PLA) physical education college, 2004, 23 (3):126-128. In Chinese.

[8] Lu Xi, Cheng, Yun Zhang, "Physical Modeling of Atmospheric Boundary Layer Wind Tunnel Experiment”[J]. Journal of changde normal university (natural science edition), 2002, 14(3):76-77. In Chinese.

[9] Diyi Yin, Xiaozhong Yang, Quyv Guo etc., “The data collection and processing of the force measurement in wind tunnel experiments”[J]. J pneumatics experiment and measurement control, 1950, (2):66-70. In Chinese.

[10] Yaqing Zheng, “The force measurement test of WDPSS shrinkage model in low speed wind tunnel”[J]. Journal of overseas Chinese university (natural science edition), 2009, 30(2):119-122. In Chinese.

© (2011) Trans Tech Publications, Switzerland
doi:10.4028/www.scientific.net/AMR.331.650

Establishment and Application of Evaluation Model for college students' perceived quality of clothing

Zhe Li[1, a]

[1] College of Design, Jiaxing University, Jiaxing, Zhejiang, China

[a] zjjxlz@163.com

Keywords: Perceived quality of clothing, College students, Evaluation Model.

Abstract. Perceived quality occupy an increasingly important position in the factors that affect consuming. Perceived quality is the subjective judgment by consumers which is different from the actual objective quality, and it is an overall evaluation to the product performance. College students, as a special consumer groups， have higher cultural level and are in pursuit of individuality. Through this research, it can be known which perceived quality have an impact on buying behavior when students buy clothing, thus provide a reference to the clothing enterprises. In the process of production or distribution, they can pay attention to these perceived qualities to meet the needs of college students, so as to reach a win-win situation.

Introduction

With the improvement of Chinese market economy system, consumer-centric philosophy has became more common. At the same time, "perceived quality" is gradually accepted. Perceived quality is the subjective judgment by consumers which is different from the actual objective quality, and it is an overall evaluation to the product performance. Perceived quality of apparel is a value recognized by customers which may be brought to by purchasing it. There are many factors which affect the perceived quality of clothing. In all quality factors, customers can not conduct a comprehensive comparison to choose the best, customers only measure those factors that they consider more important, and evaluate the overall quality of the product only based on these indicators.

Although the model of perceived quality is widely concerned abroad, research about this aspect is still insufficient in China and few people carried out research on evaluation model for perceived quality of clothing. Product consumption behavior patterns of different types are different. Effect weight and correlation significance on the perceived quality of various factors have a big difference in different product categories. Evaluation model for perceived quality of other products can not be applied to clothing. In addition, there are necessarily different emphases and preferences when different types of consumers perceive quality of clothing [1].

College students' market is a noteworthy huge market, containing the unlimited business opportunities. Grasping this consumer market of college students has important significance for businesses. Perceived quality of clothing has a very important impact on college students' clothing consumption behavior. To expand the clothing consumption of college students depends not only on improving the quality of clothing itself, but also on the quality of clothing perceived by college students [2]. This paper studies the evaluation model for college students' perceived quality of clothing and provides reference for designing clothing. It can provide the necessary basic material for selling marketable clothing and establishing the correct market strategy.

Questionnaire Survey

Questionnaire Design. Questionnaire should be made scientifically and rationally. Based on the measurement of perceived quality research, combined with the characteristics of college students and clothing, conducting increase and screen through interviews, ultimately 25 measurements were produced. The questionnaire uses the Likert scales of 5 grade (1 - strongly disagree, 5 - strongly agree).

Questionnaire Survey. Questionnaire survey was conducted in Jiaxing University. The questionnaires were issued one by one in girls' and boys' dormitory. 200 copies were actually recovered and recovery rate is 100%, 200 questionnaires are all valid. The distribution of the survey sample consists of 100 boys and 100 girls, each account for 50 percent of the total number of samples. It corresponds with quantitative requirements for large sample in mathematical statistics.

Establishment and Application of Evaluation Model for college students' perceived quality of clothing

Evaluation Model for college students' perceived quality of clothing. Factor analysis is a method which can reduce multiple variables to a small number of potential factors on the condition of information being lost as little as possible. These factors can highly summarize the information in a large amounts of data, so that not only can the number of variables be reduced, but also the intrinsic link between the variables can be equally reproduced.

In this paper, 25 measurement items of college students' perceived quality of clothing were analyzed using SPSS statistical software with factor analysis method, thereby a factor model of college students' perceived quality of clothing is constructed.

Table 1 Rotated component matrix

Measurement item	factor1	factor 2	factor 3	factor 4	factor 5	factor 6
style	0.696	0.100	-0.069	-0.014	-0.116	0.147
color	0.591	0.002	0.170	0.078	0.174	-0.227
snagging	0.572	0.181	-0.054	0.145	0.193	0.051
fabric type	0.547	-0.008	0.205	-0.079	0.082	0.233
fade	0.503	0.112	-0.190	0.282	0.437	0.239
price	0.469	0.001	0.064	0.086	0.188	-0.254
shop reputation	0.069	0.712	-0.103	0.096	0.038	0.186
after service	0.032	0.683	0.035	0.346	0.093	0.055
service attitude	0.125	0.680	0.173	0.317	0.067	-0.001
shopping guide	0.078	0.565	0.502	-0.072	0.063	-0.014
display	0.188	0.311	0.692	0.035	0.038	0.037
production place	-0.011	-0.142	0.610	0.211	0.042	0.068
package	-0.014	-0.034	0.584	0.093	-0.020	0.122
shopping environment	0.063	0.388	0.570	0.104	0.167	0.003
promotion	0.337	-0.156	0.423	0.173	-0.359	0.013
seam security	-0.017	0.159	0.156	0.768	0.190	-0.036
fine degree	0.109	0.224	0.025	0.641	-0.044	0.067
thread end	0.057	0.210	0.197	0.624	0.105	0.069
comfort	0.120	-0.064	0.165	0.116	0.750	-0.019
fabric handle	0.329	-0.095	0.176	-0.102	0.594	0.045
shrinkage	0.336	-0.090	-0.207	0.220	0.476	0.250
label information	0.020	0.191	0.038	0.054	0.068	0.791
certification	-0.013	0.161	0.088	0.176	0.274	0.743
brand	0.094	-0.082	0.132	-0.111	-0.232	0.455
content label	0.010	-0.058	0.319	0.106	0.313	0.365

The result of the factor loading matrix being varimax orthogonal rotated is shown in Table 1. Factor analysis produced six factors, which mean college students perceive quality of clothing from six dimensions. The meaning of common factor is decided by the variables of larger loads, and we named factors according to the original meaning of the variables contained in various factors. Eventually evaluation model for college students' perceived quality of clothing containing total twenty-five variables of six dimensions was established, as shown in Fig. 1 below.

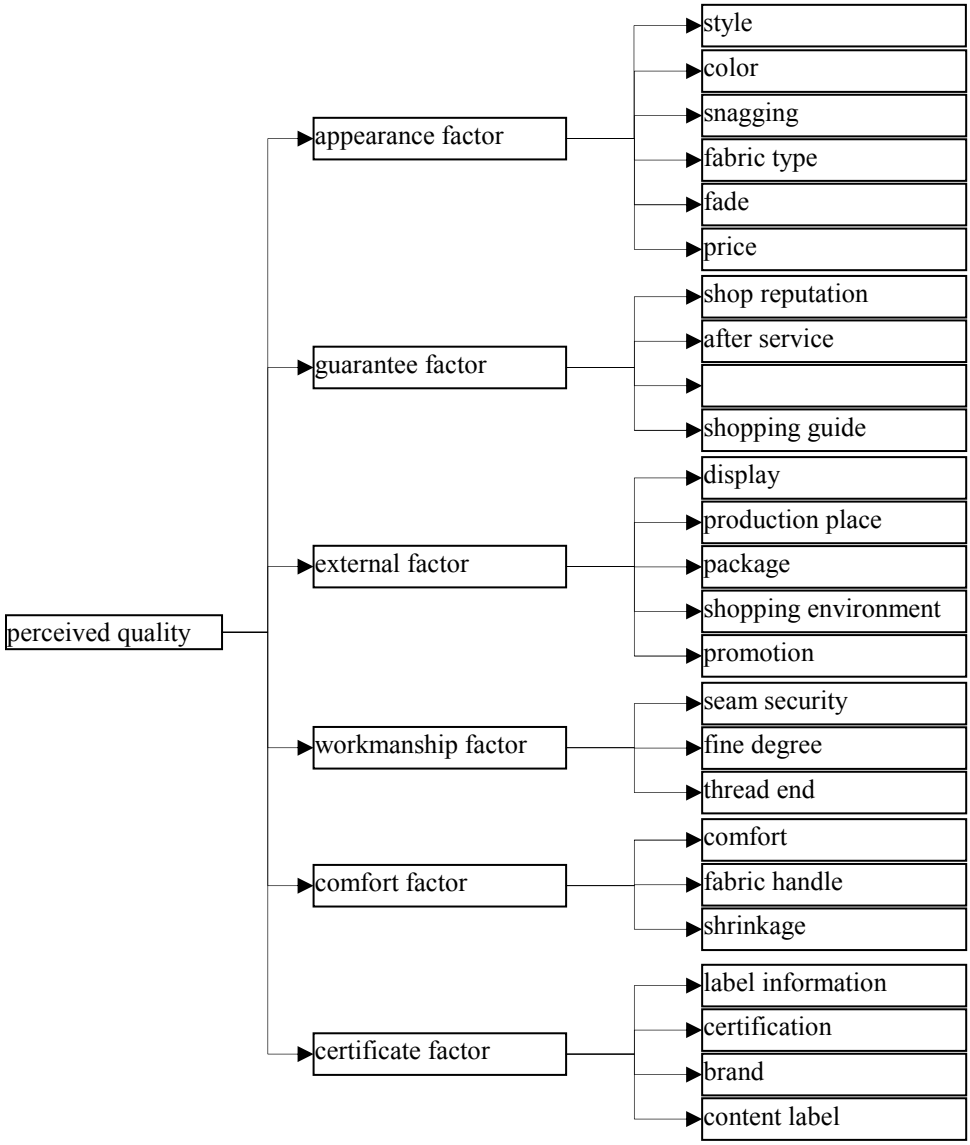


Fig. 1 Evaluation Model for College Students' Perceived Quality of Clothing

In all measurement items, five measurements which have the highest average score are comfort, fade, style, fabric handle and snagging; the lowest are production place, package, content label, brand and promotion. Thus, in the six factors, the perceived quality of clothing which college students pay most attention to is comfort factor (comfort, fabric handle), appearance factor(style, fade), workmanship factor(snagging), while the perceived quality which college students pay least attention to is certificate factor(production place, package, content label, brand) and external factor (promotion).

Cluster analysis of college students. Cluster analysis is a multivariate statistical method which classifies individuals in accordance with certain criteria. Cluster analysis can be divided into hierarchical clustering method and dynamic clustering method according to their classification system. The dynamic clustering method, also known as quick clustering method, or K-means clustering method, is a method for classifying samples and very effective to large sample. The method is as follows: first, divide n observation units into K classes, and determine the K initial class center, then samples are classified with an iterative method under the principle of minimum Euclidean distance away from the center.

If quick clustering is processed directly with 25 measurements, then the result of classification is difficult to see practical significance. Therefore, factor scores for each observed value are calculated in factor analysis, and then cluster analysis is processed according to factor scores of the various factors. Based on the previous factor analysis which classifies 25 variables into six main factors, in cluster analysis, the college students are classified into four categories according to the value degree of students to the six factors.

Table 2 Cluster Analysis of College Students

factor	cluster1	cluster2	cluster3	cluster4
appearance factor	-0.2451	-0.2422	0.4264	0.2876
comfort factor	0.9733	-0.1630	0.5831	-1.2337
workmanship factor	-0.8071	0.7121	0.0490	-0.7717
external factor	0.2386	0.1365	-0.4138	-0.0720
certificate factor	0.4305	-0.0296	-0.5165	0.2034
guarantee factor	-0.3701	-0.3157	0.9241	0.0252

The final cluster centers of the cluster analysis are shown in Table 2. The results indicate that: the first category of college students attach importance to comfort factor, certificate factor and external factor, but do not attach importance to workmanship factor and guarantee factor, so they can be defined as “casual type”. The second category of college students pay most attention to workmanship factor and external factor, but do not attach importance to the appearance factor and certificate factor, thus they can be named as “economical type”. The third category attach most importance to guarantee factor, also attach importance to comfort factor and appearance factor, but do not attach importance to certificate factor and external factor, therefore the type of students can be classified as “mature intellectual type”. The fourth category of university students attach great importance to the appearance factor and certificate factor in selecting clothing, but pay less attention to workmanship and comfort factors, thus they can be named as “ fashionable type”.

Conclusions

The perceived quality of clothing affecting the buying behavior of college students include a variety of factors, thereinto college students pay most attention to appearance and comfort factors, while pay least attention to certificate factor. Enterprises or vendors should give top priority to appearance and comfort factors of clothing, improve the garment's comfort and diversify style and color, etc., in order to meet the needs of college students. College students do not attach much importance to the brand, the enterprise or a vendor which wants to occupy more market of college students need to fully enhance the perceived quality of their brand.

College students can be clustered into four classes according to different characteristics of clothing perceived quality, the degree of concern about the six perceived quality factors of different college students are different. Enterprises or vendors should aim at the different characteristics of college students’ apparel consuming behavior and design or sell different clothing to meet the needs of college students for clothing.

References

[1] Liping Qian，Yi Liu，Chao Cheng: Modern Economic Science. (3)(2005), p.73-78(In Chinese).

[2] Xiaofang Liu，Xiaofen Ji, Jie Wang，et al. Silk Monthly. (12)(2007), p.49-52(In Chinese)

© (2011) Trans Tech Publications, Switzerland
doi:10.4028/www.scientific.net/AMR.331.654

Relationship between Special Body Variable and Figure of Women's Trousers Pattern

Lu Xin

College of Garment and Textile, Eastern Liaoning University, Dandong, Liaoning, 118000, China

email: luxin66cn@yahoo.com.cn

Keywords: special body shape, pattern design, women's trousers, figure

Abstract. The special body shapes of women, such as convex belly and convex hip are chosen to sum up its body shape change law and set up the relationship between variable of four types of body shapes and pattern figure to complete the initial research of body feature corresponding to the digitalization of women's trousers pattern in this paper. This is the basic research directing at women's trousers pattern auto-design system of special body shape, setting up the correlative relationship between women' body shape feature and structure feature of trousers to guarantee the consistency between body shape and pattern design in the process of garment PCAD system intelligent design, which provides the possibility for the research of intelligent women's trousers pattern design system based on the body shape and plays a positive role in changing the traditional pattern design concept and design means.

Introduction

Pattern design is the important necessary link in the process of garment production, but the application of this link in the garment CAD system is rare. Besides the large equipment investment, the other important reason is that the intellectualized degree of the garment pattern design system is not high. That is, the system itself lacks in flexible capacity of judgement, reasoning and analyses, making the operators only limited to the garment professional with higher professional knowledge and rich experiences, which hinders the spreading and popularizing of garment pattern design system in the garment enterprises [1]. As a result, improving the intellectualization of pattern design system can help to improve this problem.

This research chooses four kinds of body shapes, such as convex belly, convex hip, X style legs and O style legs, to study the division of special body shape and change law and complete the relationship between body change parameter and women's trousers pattern figure [2], which provides the basic research for the development of intelligent women's trousers pattern design system.

Somatotype factors affecting women's trousers pattern design

Human body figures can be divided into standard body and special body. Directing at the pattern design of special body shape, most experienced plate makers complete it based on the empirical value, but many inexperienced plate makers is difficult to make it. As a result, the setting up of intelligent pattern design system needs to find out the parameter change relation between special body shape and standard body shape, and then complete the digitalization of human body feature through mathmatics function simulating human body curve, which can classify systemically the change parts of human body controlling the pattern [3, 4].

Abdominal line. The abdomen of standard body is flat, but the abdomen of women is easy to accumulate fat, which can lead to the phenomenon of abodomen hill [5]. According to the different degree of abdominal convex, the abdominal convex body can be divided into light, mezzo and heavy abdominal convex body. The judgement of abdominal convex degree can be determined by the angle of abdominal convex. The abdominal convex angle of the standard body is 8°, and the angle is more than 8° can be considered as abdominal convex body. The reference figure of the different degree abdominal convex body is shown in Fig. 1.

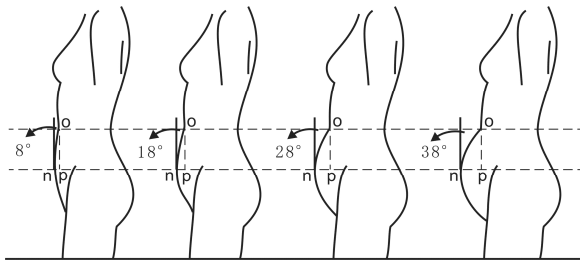


Fig.1 Different degree abdominal convex body

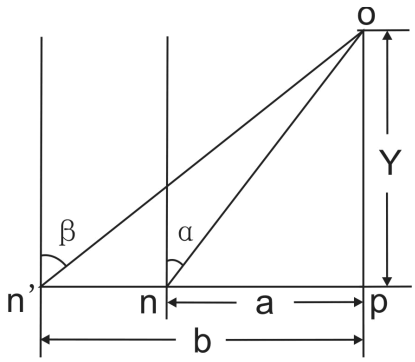


Fig. 2 Plane geometry of abdominal convex

Transform approximately the change condition of human body abdominal line in Fig.1 into abdominal convex plane overlapped geometry diagram of abdominal convex body and standard body in Fig. 2. Combining Fig. 2, “a” stands for the abdominal convex value of standard body; “b” stands for the abdominal convex value of abdominal convex body; “α”stands for the abdominal angle of the standard body; “β” stands for the abdominal angle of the abdominal convex body; “Y” stands for the distance between abdominal convex point and waist circumference. The following relation can be got through the application of triangle function:

$$\begin{cases} \Delta x = b - a \\ \tan\alpha = a/y \\ \tan\beta = b/y \end{cases}$$

By the combination of three equations, the relation of abdominal convex heightened value and abdominal convex angle change can be got:

$$\Delta x = y(\tan\beta - \tan\alpha) \qquad (1)$$

Hip line. The common special change of women hip curve is convex hip. The convex hip body can be divided into light, mezzo and heavy convex hip body according to the different degree of convex hip degree. The judgement of convex hip degree can be determined by the angle of convex hip. The convex hip angle of the standard body is 20°, and the angle is more than 20° can be considered as convex hip body. The reference figure of the different degree convex hip body is shown in Fig.3.

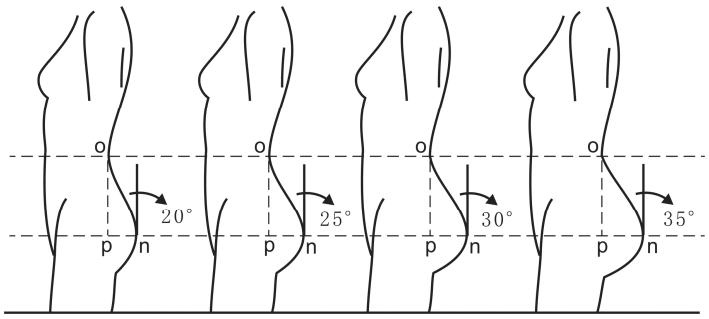


Fig.3 Different degree convex hip body

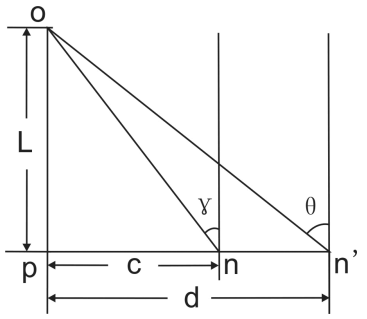


Fig. 4 Plane geometry of convex hip

Transform approximately the change condition of human body hip line in Fig. 3 into hip convex plane overlapped geometry diagram of convex hip body and standard body in Fig. 4. Combining Fig. 4, “c” stands for the convex hip value of standard body ; “d” stands for the convex hip value of convex hip body ; “y” stands for the convex hip angle of the standard body ; “θ” stands for the abdominal

angle of the abdominal convex body; “L” stands for the distance between convex hip point and waist circumference. The following relation can be got through the analyses of figure property and application of triangle function:

$$\begin{cases} \Delta x = d - c \\ \tan\gamma = c/L \\ \tan\theta = d/L \end{cases}$$

By the combination of three equations, the relation of convex hip heightened value and convex hip angle change can be got:

$$\Delta x = L(\tan\theta - \tan\gamma) \qquad (2)$$

Women’s trousers pattern design of special body figure

Pattern design of abdominal convex. The change of abdomen has an effect on the value of hip circumference. The relative research shows that the increased value of hip circumference is 1.2cm when the abdominal convex is heightened 2cm each time. As a result, the back piece fatness remains the same when the front piece fatness of the trousers changes [5, 6]. The structure of the front trousers pieces under the different abdominal convex state shows in Fig. 5.

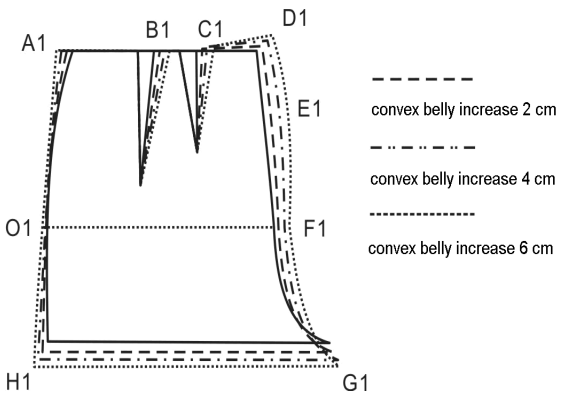


Fig.5 Overlapped figure of different abdominal convex body pattern

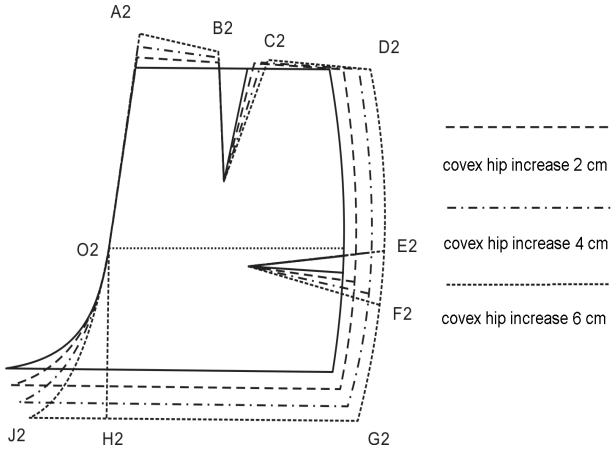


Fig.6 Overlapped figure of different convex hip body pattern

The heightened value of the abdominal convex and the dispersion between transverse and longitudinal of front trousers piece parts can be shown respectively in the following mathmatics relations:

A_1 transverse a_n=0.1n longitudinal b_n=0;
D transverse a_n=0.4n, longitudinal b_n=0.25n;
E_1 transverse a_n=0.45n, longitudinal b_n=0;
F_1 transverse a_n=0.3n， longitudinal b_n=0;
G_1 transverse a_n=0.05n, longitudinal b_n=0.4n;
H_1 transverse a_n=0.15n longitudinal b_n=0.4n. (3)

Among the formula (3), a_n stands for the transverse change value of its parts when the abdominal convex is heightened n; b_n stands for the longitudinal change value of its parts when the abdominal convex is heightened n; n stands for the heightened value of the abdominal convex.

Pattern design of convex hip. The change of hip has an effect on the value of hip circumference. The relative research shows that the increased value of hip circumference is 3.2cm when the convex hip is heightened 2cm each time. The increased value of hip circumference is all provided by the heightened value of the convex hip. As a result, the back piece fatness changes when the front piece fatness of the trousers remains the same. The back trousers pieces structure under the different convex hip state shows in Fig. 6:

The heightened value of the convex hip and the dispersion between transverse and longitudinal of back trousers piece parts can be shown respectively in the following mathmatics relations:

A transverse a_n=0, longitudinal b_n=0.5n; B_2 transverse a_n=0, longitudinal b_n=0.25n;
C_2 transverse a_n=0.75n, longitudinal b_n=0.25n; D_2 transverse a_n=0.9n, longitudinal b_n=0;
E_2 transverse a_n=0.8n, longitudinal b_n=0; F transverse a_n=0.8n，longitudinal b_n=0.4n;
G_2 transverse a_n=0.75n, longitudinal b_n=0.9n; H_2 transverse a_n=0，longitudinal b_n=0.9n;
J_2 transverse a_n=0.2n，longitudinal b_n=0.9n. （4）

Among the formula (4), a_n stands for the transverse change value of its parts when the convex hip is heightened n; b_n stands for the longitudinal change value of its parts when the convex hip is heightened n; n stands for the heightened value of the convex hip.

Conclusion

This paper comes up with the women's trousers pattern design methods based on the body figure directing at the common special body figure. The women body figures of convex belly, convex hip are chosen as the study objects and sum up its body shape change law and set up the relationship between women body figure feature and trousers structure feature and study the relationship between the variable of body shapes and women trousers pattern .

This paper also studies the difference and the judgement standard between convex belly, convex hip and standard body figure to complete the digitalization of the human body feature. The digitalization of special body women trousers pattern figure is completed through summarization of the women trousers pattern correction law of convex belly and convex hip.

The study of the relationship between the variable of special body figure and women trousers pattern figure provides a good start for the garment PCAD intelligent design system based on the body shape. Its advantage lies in the quick acquisition of the association between body figure and the digitalization of pattern, which provides the technical possibility for the collaborative design and manufacture in allopatry.

Acknowledgements

Financial support for this work was provided by the Education Department Funds of Liaoning Province P. R. China (2009A808).

References

[1] X. M. Yang, J. H. Yu. China Text Lead Vol. 4 (2004), p. 94. In Chinese

[2] X Lu. J Text Res Vol. 12 (2006), p. 62. In Chinese

[3] M. Santos, F. Rebelo. Lect Notes Comput Sci Vol. 8 (2007), p.284

[4] G. Farin. Curves and surface for computer aided geometric design: A practical guide. Academic press, (1998), 6:24-28

[5] T. J. Kang, S. M. Kim. Int Cloth Sci Technol J Vol. 1 (2000), p. 39-19

[6] X. Lu, Y. F. Gu. J Text Res Vol. 2 (2009), p. 89-94. In Chinese

© (2011) Trans Tech Publications, Switzerland
doi:10.4028/www.scientific.net/AMR.331.658

Study on The Fashionable and Preferable Emotion of Men's T-shirt Between Males and Females

Xiaoxia Zhang[1, a], Shanshan Wang[1,b] and Guolian Liu [1,2,c]

[1]College of Textile and Clothing Engineering, Soochow University, Suzhou, Jiangsu, 215000, China

[2]National Engineering Laboratory for Modern Silk, Soochow University, Suzhou, Jiangsu, China

[a]summer-hades@163.com, [b]249297697@163.com, [c]liuguolian@suda.edu.cn

Keywords: Visual cognition, Fashionable Emotion, Preferable Emotion, Men's T-shirt.

Abstract. T-shirt attracts a crowd of various consumers and endures worldwide popularity for both ever-changing style and colour-rich. In this article, it takes 42 men's T-shirts as the objects, "fashionable" and "preferable" as emotional stimuli words were used from the point of view visual cognition. The aim of this paper is to provide concrete basis for the design of more fashionable and preferable emotion of men's T-shirts to meet the needs of young consumers.

Introduction

For a hundred years, T-shirt has been playing a very special role in the history of human clothing, it becomes a vital type of clothing in our modern life. With the developing of society and the materials, when choosing a T-shirt, people pay much more attention to highlighting their personal characteristics except the psychological contented. How to attract consumers and encourage the desire to buy at the first glance, becomes the focus of designers and clothing companies.

Now, the clothing companies have to analyse the consumer psychology in order to design more fashionable T-shirts. At present, Kansei Engineering in Japan is very representative among many product theories which take consumer as research object. Kansei Engineering widly used in clothing design collects informations by questionnaire which contains variety range of issue. Besides, there is no time limit for the participants, so that we can gain dependable results and their true ideas, which finally result in the accurate data[1].

Everyone knows the importance of consumer psychology, but the cognitive psychology applied in clothing is still an elementary stage. The cognitive psychology is the areas of psychology, which is being taken in other subjects gradually, such as linguistic, medicine, music, market economy and brands development. The Influence of Colour Brightness on the Perception of Clothes Gorgeousness and Influences of Collar Types towards Women's T-shirt Fashionable Design whether the clothing fullness is tight, fit and loose based on visual cognition have studied before[2,3]. Both them have been agreed by researchers working in this filed at home and abroad.

This article targeting on the youth researches the fashionable and preferable emotion of clothing from the view of visual perception with the men's T-shirts as research object. It will provides certain references for Clothing enterprises to design more fashionable and preferable men's T-shirt.

Experiment

Participants. The 36 master students at Soochow University in China(18 males, 18 females, aged between 22-25) participated in the experiment, who major in other subjects. All participants had normal or corrected-to-normal vision and were unaware of the purpose of experiment.

Samples. As the visual stimulus samples, the 42 men's T-shirts sold in S/S 2010 are different in style, pattern and colour. All the samples are shown by photoes of material object which is shown below in Fig.1 and Fig.2 .



Fig.1 Part of The Samples



Fig.2 Part α of The Samples

Equipments and Stimuli. The stimuli were presented by a computer with a 17 inches monitor with a refresh rate of 85HZ in a darkroom, the distance between participant and monitor is about 60cm, and the visual angle was 12.3°×4.9°. Using E-Prime 2.0 (Psychology Software Tools, Inc.)

Procedure Design. The experiment was consisted of two phases. One is evaluation of the stimulation words and another is the image of 42 men's T-shirts. Each trial had only one word and sample image, and it began with a fixed cross on the screen for 100ms. After 400ms, a word "fashionable" or "preferable" was displayed for 300ms followed by a sample image which appeared randomly. Then the responses of the participants were collected via keyword. The participants pressed "Z" or "/" according to whether the emotion in line with the word. Before the experiment, 4 images were provided to make sure the participants acquainted with the experiment. The stimuli and procedure in phase 2 were the same with phase 1. To ensure the precision of the results, the opposite way of confirmation was applied by the second half of the participants. That is, the subject pressed "/" in keyword if he thought the sample emotion was in accordance with the word and "Z" if not.

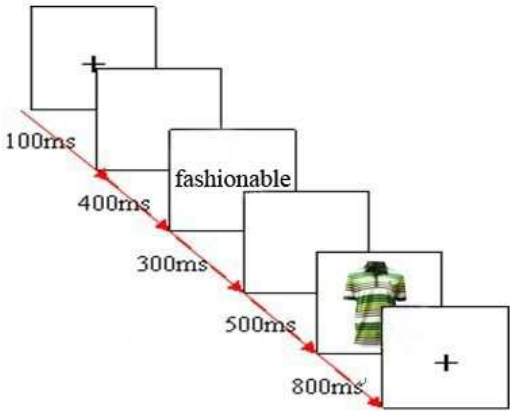


Fig.3 Sequence of stimulus presentation

Results and Discussion

The data were processed by Microsoft Excel and SPSS 16.0.

Ⅰ.The Variance Analysis on Fashionable Emotion. Fig.4 presents the mean cognitive accuracy of fashiongable emotions of ever single amples.

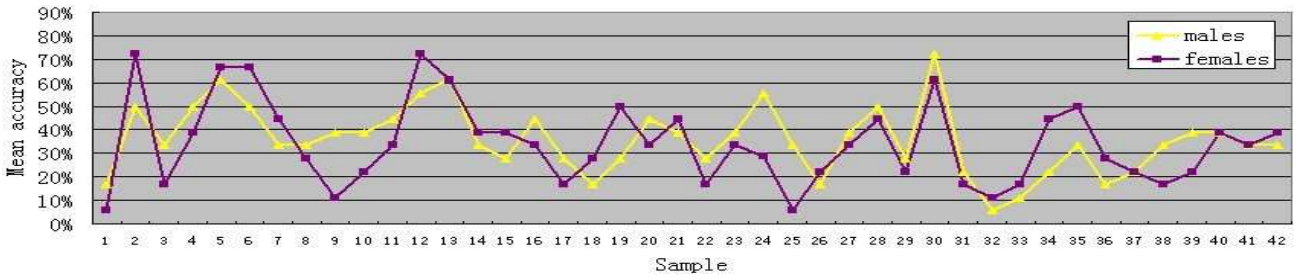


Fig. 4 The difference between males and females on the fashionable sense

ⅰ.Analysis on Young Male's Fashionable Emotion. From Fig.4, we can see that there are 9 T-shirts' mean accuracy is above 50%, 5 samples below 20% and others between them. That is to say, these 9 samples are more fashionable than others.

ⅱ.Analysis on Young Females' Fashionable Emotion. As shown in Fig.4, we can see that there are 8 T-shirts' mean accracy are above 50%, 10 samples below 20% , and others between them. It indicates that women have higher fashionable identity in these 8 samples than others.

ⅲ.The Comparison of The Fashionable Emotion Between Males and Females. Besides the similarity between males and females with the evaluation of fashionable emotion of 42 men's T-shirts, there are many differences. Tab.1 shows an independent sample T test by the SPSS. For S13, S37, S40, S41, their F=0, Sig.=1, it shows that people have the same emotion in the 4 samples. The identity of S1, S2, S3, S9, S10, S19, S25, S34, S38, S39, all their Sig. < 0.05, which shows that there's significant difference between males and females. From Fig.4, we can see that the difference is especially significant in S9 and S25. The female tend to middling, and the males' attitude is completely negative. S1, S3, S10, S38, S39 have the similar situation as above. We can find that the 5 samples have the same characteristics with single pattern and regular color. It seems that young women prefer mature men dress style. On the contrary, the characteristics of S2, S19, S34 are more active in pattern and color, it reports that young males want to be more lively and looks like "the man child". The results above prove that the fashionable evaluation of men's T-shirts between males and females are completely different in angle of view and psychological demand.

Sample	F	Sig.	Sample	F	Sig.	Sample	F	Sig.
1	4.922	0.033	15	1.816	0.187	29	0.564	0.458
2	4.185	0.049	16	1.495	0.230	30	1.816	0.187
3	5.464	0.025	17	2.556	0.119	31	0.681	0.415
4	0.883	0.354	18	2.556	0.119	32	1.440	0.238
5	0.445	0.509	19	4.185	0.049	33	0.901	0.349
6	2.125	0.154	20	1.495	0.230	34	6.616	0.015
7	1.495	0.230	21	0.394	0.534	35	2.125	0.154
8	0.493	0.487	22	2.556	0.119	36	2.556	0.119
9	18.35	0.000	23	0.445	0.509	37	0.000	1.000
10	4.389	0.044	24	0.394	0.534	38	5.464	0.025
11	1.495	0.230	25	29.623	0.000	39	4.389	0.044
12	3.415	0.073	26	0.681	0.415	40	0.000	1.000
13	0.000	1.000	27	0.445	0.509	41	0.000	1.000
14	0.445	0.509	28	0.212	0.648	42	0.445	0.509

Tab. Ⅰ The Data of fashionable emotion

Sample	F	Sig.	Sample	F	Sig.	Sample	F	Sig.
1	0.681	0.415	15	1.816	0.187	29	3.299	0.078
2	0.000	1.000	16	1.816	0.187	30	1.495	0.230
3	1.816	0.187	17	18.35	0.000	31	3.299	0.078
4	0.000	1.000	18	0.901	0.349	32	0.901	0.349
5	0.883	0.354	19	0.394	0.534	33	0.000	1.000
6	7.589	0.009	20	0.000	1.000	34	29.623	0.000
7	0.000	1.000	21	0.394	0.534	35	2.125	0.154
8	7.099	0.012	22	10.393	0.003	36	0.901	0.349
9	43.84	0.000	23	0.000	1.000	37	0.681	0.415
10	0.681	0.415	24	4.185	0.049	38	6.616	0.015
11	2.125	0.154	25	0.901	0.349	39	4.389	0.044
12	1.495	0.230	26	0.681	0.415	40	0.883	0.354
13	3.415	0.073	27	0.883	0.354	41	0.564	0.458
14	0.564	0.458	28	0.213	0.648	42	9.029	0.005

Tab. Ⅱ The Data of preferable emotion

Ⅱ.The Variance Analysis on Preferable Emotion. Fig.5 presents the mean cognitive accuracy of preferable emotions of 42 samples, including the influence of single sample.

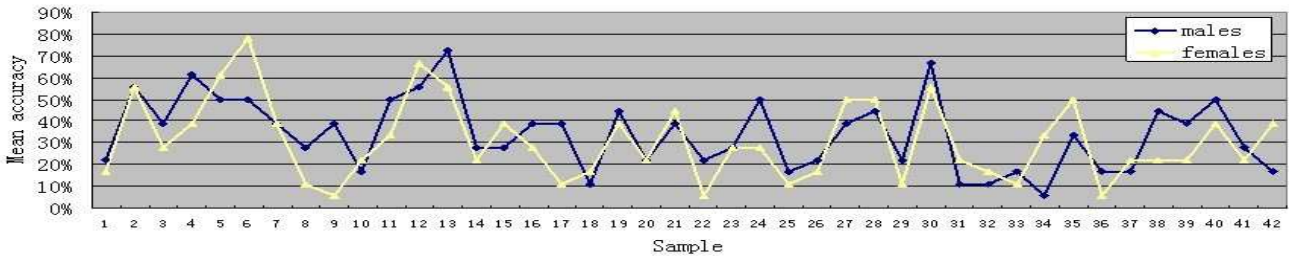


Fig.5 The difference between males and females on the preferable sense

ⅰ.Analysis on Young Males' Preferable Emotion. From Fig.5, we can easily find that there are 10 T-shirts' mean accuracy is above 50%, and 10 samples below 20%. It's concluded that young males prefer the 10 samples above 50% much more than others, especially the 10 below 20%.

ⅱ.Analysis on Young Females' Preferable Emotion. Fig.4 shows that there are 9 T-shirts' mean accuracy is above 50%, 12 samples below 20% and others between them. Young females seem prefer a lot in the 9 samples than others.

ⅲ.The Comparison of The Preferable Emotion Between Males and Females. The evaluation between males and females are general similar, besides some little differences. Tab.2 shows the independent samples T test by SPSS. the preferable identity of S2, S4, S7, S20, S23, S33, which

F=0.00, Sig.=1.00, shows that people have the same emotion in the 6 samples. At the meaning time, the Sig. of S6, S8, S9, S17, S22, S24, S34, S38, S39, S42 is less than 0.05. It shows that there is significant difference about the recognition of preferable emotion for males and females. It can be seen in Fig.5, the difference of preferable emotion is especially significant in S9 and S17, the evaluation of melas' preferable emotion is fair to middling, but the females' attitude is completely negative. S8, S22, S24, S38 have the same condition, males' preferable evaluation of the 4 samples are much higher than the females'. Looking at the style of them, we can find that the 4 samples have the same characteristics which has single pattern and regular colour, it shows us that young men prefer to the T-shirts that is more conservative and common. The results of S6, S34, S42 are just contrary, females' fashionable evaluation is obviously higher than the males'. The characteristics of the three are more active in pattern and colour, it report that young females expect young men's appearance can be more sunshine and frankness. The result all above prove that the preferable evaluation of men's T-shirts between males and females are completely different in angle of view and psychological demand.

Conclusion

Several significant findings have been revealed from the experiments. First, The evaluation of fashionable and preferable emotion of 42 men's T-shirts between males and females have general similarity. From the data of fashionable and preferable emotion evluation, both males and females consider that the men's T-shirt with brightly colour, which looks activity and powerful are more fashionable and preferable. Second, after comparison of males and females, we can find out there are many differences between men and women in the same sample. Young famales mostly pay their attention to the colour, lots of young women feel like the T-shirts in brightly colour and the stripe in strongly contract. But young men are very insensitive in colour. At the same time, for one T-shirt, there are also many divergences, for example, the fashionable evaluation of young males is higher than the famales', but the preferable evaluation of young men is much lower. Third, it can be found that the number of samples which catch young females higher fashionable and preferable evaluation is far from the males', it shows that women are much pickier than men when they choose or evaluate a men's T-shirt.

The results obtained from this study can not only be a guide for the fashion disigner, but also provide advices to consumers for more proper selection of men's T-shirts during purchasing. Clothing enterprises should be based on the fashionable and preferable needs of the youth and to design unique, neoteric and extremely fashionable and preferable men's T-shirts.

References

[1] Yuan TZ. Kansei Engineering research strategy. Arts and Sciences Research Center of Tsinghua University for: Expert Essays In Tsinghua International Design Management Forum. 2002; 2:186-187.

[2] Jiang XF, Liu GL. The Influence of Color Brightness on the Perception of Clothes Gorgeousness. Proceeding 2009 IEEE 10th international conference. 2009; 2: 1273-1276.

[3] Qin F, Liu GL. Study on Influences of Collar Types towards Women's T-shirt Fashionable Design Based on Visual Cognition. Proceeding 2009 IEEE 10th international conference. 2009; 2:1579-1583.

© (2011) Trans Tech Publications, Switzerland
doi:10.4028/www.scientific.net/AMR.331.662

Research on the Relationship between Special Dart and Fabric of Women's Wear

Li Wang

School of Fashion.Dalian Polytechnic University.

#1 Qinggongyuan Dalian Liaoning China 116034

wangli48000230@126.com

Keywords: special dart, fabric, clothing design

Abstract. As a relatively new concept in terms of theoretical research, special dart is the dart that not only fits the curves of human body, but also satisfies the demands of clothing design. By studying the inherent characters and designing methods of special dart as well as by summarizing innovative designing concepts and methods, this thesis attempts to serve as a beneficial complement to the modern design of fit women's wear. It begins with an elaboration on the concept of special dart. Then, through a study of fit women's wear and fabric, the author summarizes the relationship between special dart and fabric. Finally, the author comes to conclude several designing methods of special dart adopted in women's wear.

Overview of Special Dart

Special Dart. Human body presents an irregular stereoscopic shape. Therefore, how to wrap up the body with a garment in a reasonable and nice way becomes an important issue in the field of clothing design. An effective approach to fit a plane piece of fabric to the stereoscopic body is to use special dart. In order to achieve an artful and innovative design, common dart is transformed into another form, which is referred to as special dart.

As a derivative of dart, special dart aims to show the natural body of human beings and to highlight the beauty of body shape. A garment is made according to the human body. The relationship between those two can be summarized into two closely interrelated aspects, that is, the shape of human body or the internal shape and the style of the garment or the external shape. Special dart shows the internal shape of a female by fashioning a "fit" external shape and helps a garment to better display the body through tailoring or gathering the fabric from the perspective of style design.

Distinguishing Special Dart from Common Dart. Special dart is the transformation and extension of common dart. They are different from each other in terms of intended use as well as stylistic characters. For details see Table 1.

Table 1 Comparison between Common Dart and Special Dart

Category		Intended Use	Stylistic Characters
Special Dart	Tailoring	Not only to fit the curves of human body, but to satisfy the demands of style design as well	Mostly open darts without ends; concealing or exposing fabric surplus
	Gathering		Presenting an effect of stereo relief; transferring fabric surplus into gathers
Common Dart		To fit the curves of human body	Mostly closed darts with ends directed at the highest heaving point of the body; concealing fabric surplus

Relationship between Special Dart Design and Fabric

Throughout history, a great variety of fabrics have been used to produce garments. The selection of fabric counts a great deal in the artistic expression of clothing design. The so-called fabric refers to the cloth garments are made of. Different fabrics possess different physical properties such as flexibility, elasticity, rigidity, air permeability and so forth, which have a great influence on clothing design, especially on the design of fit women's wear. Therefore, those properties should all be taken into consideration in the designing process.

Fabric is the material carrier of garments as well as the physical basis embodying the designer's ideas. Hence a fine selection of fabric predetermines whether or not a nice garment can be made. Only with suitable fabric can a garment give full expression to the artistic style of its designer. The selection of fabric, as a result, plays a vital role at the initial designing stage.

The design and use of special dart in fit women's wear is affected by the question of whether one or more fabrics are used. While designing special dart for a single fabric, there is no need to think of the elasticity or rigidity of the fabric. However, when two or more fabrics are pieced together, different tensility and shrinkage of every fabric should be taken into account. Therefore, the relationship between special dart design and fabric will be elaborated from two aspects, that is, special dart design of single fabric and that of two or more fabrics.

Single Fabric. Special dart design of single fabric refers to clothing design with a single kind of fabric as the object. In this case, only one kind of fabric is used to produce the integral garment. Every fabric has its intrinsic and unique physical properties, requiring corresponding manners of special dart design. According to two basic properties, single fabric can be divided into two categories: light & soft fabric and stiff & smooth fabric.

Light & soft fabric includes silk, nainsook and certain chemical fiber fabrics. Such fabrics as silk, charmeuse and pongee are most frequently used in special dart design, for they are comparatively light and soft and easy for tailoring and gathering. Complicated designs should be avoided when tailoring light & soft fabric, as most soft fabrics have such loose structure that over-complicated cuts would be bad for the overall effect. Straight cut and large area of arc cut are frequently used in special dart design.

A relatively common technique of special dart used against soft fabric is multi-tucking. It adds a strong sense of layers and volume to light fabrics. As light fabric lets through rays of light, tucking not only concentrates the fabric, but also brings about rich textural effects through the overlaying shadow.

As the name suggests, fabrics in this category are all stiff and smooth. They are also easy to fashion and shape, with a certain sense of volume. Khaki fabric, denim and various kinds of medium thick worsted all fall into this category. The thickness of stiff & smooth fabric enables the designer to use complicated cutting techniques in special dart. Denim is tailored many a time according to the curve of human breast so as to transform fabric surplus into the cut. The selvage is also made rough to reflect the style of the garment. In this case, selecting fabric, designing and processing are combined well to bring about a wild and glamorous quality in the garment. The use of stiff and thick worsted, together with the use of concise arc lines for special dart, brings the overall style of the garment in line with the properties of the fabric.

Two or More Fabrics. Piecing two or more fabrics together means that a garment is divided into several sections of fabrics through special dart cutting and every section has its own physical properties. In this way, the garment comes to display rich artistic effects and also produces a strong visual impact by highlighting the style of special dart.

Fabric piecing discussed in this thesis can be divided into two categories. One deals with piecing fabrics of different feels and shapes, that is, fabrics of different textures. The other refers to piecing fabrics of the same feel and shape but of different patterns and colors, that is, fabrics of the same texture.

Piecing together fabrics of different feels and shapes creates a contrasting effect. Fit women's wear aims to display the graceful curves of women. To this end, the use of special dart strengthens structural designs by magnifying differences in shape between two fabrics. As shown in Fig.1, piecing reflective fabric with matte fabric produces a visual effect of conflict. The shuttle-shaped bottom half of the garment is emphasized both through the contrast between different fabrics and through the style of special dart. Asymmetric cuts strengthen the contrast of glossiness between different fabrics and further emphasize different fabric textures. Furthermore, cuts can also be highlighted by contrasting transparent fabric with opaque fabric. Crystals are inserted in the transparent fabric to mitigate visual conflicts with their gloss, so that the garment attains visual balance.

Piecing together fabrics of different textures lays great emphasis on special dart, where combination of reflective fabric with matte fabric and that of transparent fabric with opaque fabric are commonly put to use. Special dart puts together fabrics of different textures organically so as to fulfill the ultimate goal of design.



Fig. 1 Special Dart in Pieced Fabrics of Different Textures

Fabrics of the same texture here refer to fabrics that share the same basic physical properties, such as the same feel, shape and so forth, yet their patterns and colors differ from one another. Piecing, in this sense, does not brings about the contrasting effect through the texture, but by making use of the visual conflict of different colors and patterns as well as by piecing together fabrics of different colors. Generally speaking, if several grey-toned fabrics possess the same brightness but differ in their hues, the color contrast they produce would be rather weak. Piecing such fabrics together brings about a mild overall effect. Special dart also adopts smooth lines to coordinate the style with the color in order to fit into the expression of such a theme. However, if several fabrics differing greatly in colors are pieced together, then special dart has to employ broken lines which are rich in the sense of conflict so as to give full expression to the contrasting effect of the garment.

Conclusions

The use of special dart has been taking up greater significance in the design of modern women's wear. Designers have always pay close attention to the use of fabric. How to make a perfect combination of special dart design with fabric has become an unavoidable issue. Through its study on the relationship between special dart and fabric, this thesis attempts to summarize regular patterns of clothing design so as to provide guidelines for further practice. Special dart is not only able to shape the body, but also improves the design with respect to the color and fabric of the garment. While dealing with special dart, different colors and fabrics should be combined and matched with one another effectively in order to underline the design and style. In terms of structure, special dart produces a fitting effect with

its unique design. In a word, special dart and fabric are closely related to each other. Modern fit women's wear is the entirety of special dart and fashion designing elements, which are coordinated with each other through the designer's ingenious work.

References

[1] Susan B. Kaiser. The Social Psychology of Clothing. Trans. Hongwei Li. Beijing: China Textile & Apparel Press, 2000. (In Chinese)

[2] Asakura Naomi. Art: The Plane Constitution of Design. Trans. Zheng Lin and Hua Lin. Beijing: China Plan Publishing Company, 2000. (In Chinese)

[3] Nakaya Noriko and Miyoshi Mithiko. Clothing Modeling Design: Techniques. Trans. Meihua Liu, Xianying Jin and Yushun Jin. Beijing: China Textile & Apparel Press, 2006. (In Chinese)

[4] Bunka Fashion College. Lecture on Cultural Clothing (7): Clothing Design. Trans. Xumin Feng and Cunyi Ma. Beijing: China Light Industry Press, 2001. (In Chinese)

[5] Dangqi Li. An Introduction to Clothing. Beijing: Higher Education Press, 1998. (In Chinese)

[6] Jianqun Lin. Fundamentals of Modeling. Beijing: Higher Education Press, 2000. (In Chinese)

[7] Liya Zhou and Jun Liang. Clothing Constitution Foundation. Beijing: China Textile & Apparel Press, 1996. (In Chinese)

[8] Yuming Zhu. The Stereo Constitution of Fashion Clothing. Hangzhou: Zhejiang University Press, 2005. (In Chinese)

[9] Weigang Wu. Costume Aesthetics. Beijing: China Textile & Apparel Press, 2000. (In Chinese)

[10] Marilyn J. Horn. The Second Skin: An Interdisciplinary Study of Clothing. Trans. Jinghong Yue and Zhiliang Yang. Shanghai: Shanghai People's Publishing House, 1991. (In Chinese)

© (2011) Trans Tech Publications, Switzerland
doi:10.4028/www.scientific.net/AMR.331.666

Zen View of Nature in the Performance of Modern Fashion Design

Nan Qiao[1,a], Lijun Liu[1,b], Yuanyuan Lv[1,c]

1 School of Textile and Garment, Hebei University of Science & Technology, Shijiazhuang, China

[a]email: wm9606@yahoo.com.cn, [b]email: liulijun20082002@yahoo.com.cn

[c]email: 519910777@qq.com

Keywords: zen; nature; clothing; design; principles

Abstract. The view of nature is an important character of Zen aesthetic. At present, the Zen view of nature and cause of design was widely used in architecture, interior, furniture, household goods and clothing designs, giving a modern design with new field and angle. Zen view of nature through the exposition, analysis of its role in modern fashion design style and influence, and the concrete embodiment of the design elements. Intended to demonstrate - not only the material culture of clothing bearing, it is "yardsticks", concerned about the soul of the "refined." Pointed out that the essence of traditional culture, to learn from the design of nutrition will have a more mellow and spiritual implication of precipitation, so the design will have a long-term vitality.

Zen view of nature

As a representative of Buddhism in China crystallization of the human spirit, Zen and the art of China has been closely related. At present, the Zen view of nature and cause of design was widely used in architecture, interior design, furniture, household goods and clothing designs to give a new field of design and perspective.

Zen in China long ago proposed the harmonious coexistence between man and nature aesthetic philosophy, the view of nature is an important character of Zen aesthetic. From the Zen point of view of natural, on the one hand skillfully retained all its details,still seems to Zhuang Zi, Confucius and the Metaphysicians' view of nature;

on the other hand, It makes the same nature hollowly. Thus, nature is given a new meaning, which contribute to the Chinese people is an extremely sophisticated and detailed, flexible and functional space to enjoy the spirit subtly and infinitely, the aesthetic experience of the Chinese people to the mind of the extreme, the so-called "Best sound stream Is widely tongues, mountains no more than pure in body "[1]. Buddhist monk never want to conquer the natural objects as, not from nature, he is equivalent to the natural. Natural starting place for people, but also people to return to the place. Zen view of nature against man carving and decoration, emphasizing the use of purely natural, simple materials, through a very succinct way to create a foreign object, the performance of pure and beautiful nature, and then reaction inside the ethereal, quiet and meditation, which also constitute The most attractive part of the Zen aesthetic one.

Zen view of nature on the impact of modern clothing design

Concise and simple

Zen aesthetics, to light as yet, to simply as an elegant, thin with weak to wonderland. Zen and the people advocating all things are one with roots in the most pure natural, the largest show of its simple factors in reaching the ultimate beauty. Of the deep is free and easy, change bold to soft, washed anger, manic gas, Turbulent of anger into a deeper or more fundamental level, rhythm in the nothingness to show the intrinsic nature and the rhythm of life and nature its characteristics must be

serene and pure, lays down non-essential things close to nature. Unorganized and confusing it can be said to deny the infinite, like a clear sky without clouds. Simple pursuit of a smooth fashion design, easy, simple, low-key, high-quality state, showing a simple, peaceful, warm, simple, subtle and quiet of the realm, as far as possible the appearance of a pile of discarded materials and the easy way out gorgeous exquisite decoration, requirements Will all return to the body in order to "reduce", "no", "purification"to abandon the trivial and unorganized, which shows the most essential elements of clothing, access to clean and clear results,embodies the Zen spirit "one that is much more that one".

Natural and free

The essence of Zen is to ask the environment to maintain harmony with nature, not to any object as a confrontation and division, in the search for differences in the symbiotic relationship and unity. This "follow nature","one with everything"attitude from the art of performance is the need to follow the natural state of things, the natural instinct and emotion, as well as complementary harmony. Renowned Japanese designer Issey Miyake clothing works have a profound interpretation of this exchange of man and nature, Zen philosophy. He will be the relationship between fabric and body, with the ancient Zen Oriental its re-definition. Breaking the structure of traditional Western clothing (that is, mainly to reflect the curves of the main female costumes), a non-structure model used by the body's shape for the cut. Issey Miyake view that clothing should not cause any stress on the body or tied, so he Kimono tailoring technology background, to restore a piece of cloth clothing concept, once removed from the body's support, it could fall down and become soft pile of "paper Constituted. "Overall there is little open-cut clothing, convergence is not a provincial highway, clothing, and only a slight contact with the body, stretching the body while in a free, able to subtly pulling clothes to movements, thus the structure of the wearer from the shackles of clothing freed.

Vacant and filling

The ultimate goal of Zen is to "meditation",in the realize "no"or"empty " state. Pay attention to clear your mind of Zen enlightenment, clarity of mind to seek freedom and lead people in a calm indifferent attitude to see the world in search of nothing in the concept of mind, the myriad things all empty in life consciousness expresses one kind comfortable, but for life pursue,to see Seems indifferent exterior hides a very broad idea of space, Zen revel adaptive approach to life and the ethereal realm of quiet fashion design industry into a new direction and creative pursuit of the source. In fashion design art, Zen design has always shown a natural foreign objects in the deserted, it "as things like, unexpected meaning " painted showing a very quiet ethereal mood.

Famous fashion designer Yohji Yamamoto's line of departure from the two-dimensional, forming an asymmetrical appearance, with little regard to the body curve, some places do not even stitch, to retain a smooth and elegant, these irregular forms of less The correction kneading and pretentious, look natural and smooth.

Deconstruction and vitality

Incomplete means not complete, incomplete, and easy disappear. Zen wanted to go beyond the object and focus the phenomenon of the spirit of the law in the spirit of discovery and change the world, so as to achieve the unity of spirit and imagination, as insufficient, so only enhance the space. Zen pursuit of "incomplete and fragmentary objects in the state," where people feel broken and fragile impermanence of life, which raised a self-reflection and emotional value, and then the pain people are free from sorrow into the leisurely, be an indifferent beauty. Rei Kawakubo's "broken style" clothing perfect interpretation of this incomplete sense of beauty, and manifests the uncertainty and the fuzzy expression in the design, with the deconstruction techniques, upset the nature of the clothing between the already perfect, measure of damage to the original laws of the United States in the form [3]. Broken mesh-style fabric that strange style, dull color, or intended to retain the rough sewing stitches, it is felt in a powerful offensive force,and enables the design contain rich, subtle and diverse, so that people found the tattered piece of cloth in the back , and contains part of the Zen and Eastern thought.

Zen view of nature in modern clothing design principles

Modeling principle

Because Zen fashion designer who inspired the most associated with nature, it put the clothes in the shape of the performance of the freedom of body and mind on the first consideration - loose. Zen with simple lines, simple shapes, and the omission of extra material to achieve the internal needs and physical comfort, stress free and casual wear with ease; in the overall profile shape, the trend of H-type, trapezoidal, more income no Traces the waist, chest, waist, buttocks, "siege difference between" deliberately not emphasized, so that cutting one's intentions, and attention to the wearing state of the design, the clothing with the body to produce natural changes; with pleating, layering, draping, wrapping, etc. Means the formation of a non-fixed structure, without rules and unbalanced design, but also to show a casual clothing creativity. Sometimes in the details of the selvage does not deal with, nor cut off the extra fabric, natural drape a garment formed unexpectedly when the fluid space and movement; in tailoring the structure of, and often do not use provinces for non-Structure, non-binding freely to maximize publicity.

Meanwhile, the extensive use of asymmetric means. That: is to give law to change, thereby causing the rich enjoy the beauty. Asymmetric emphasized that "words are intended to do infinite" realm, in order to enrich the viewer's imagination.

Color Principles

Because of Zen thinking, designers formed a respect for nature and simple atmosphere, most in color with black multi-purpose, while the color of the material itself makes use of treatment to simple factors for the United States, so obscure is full of rich colors Eastern affair. Zen clothing color to use more black, white, gray, brown, brown, mixed color and other low-key color. Quiet, clean, restrained, not play, so calm personality, first with the color related. Zen designers to use black and white and contains a large number of gray colors, and use the natural color fabric itself, in the mottled, fuzzy, and conveyed a simple peace and quiet.

Zen pursuit of a pure color extreme beauty, fresh and subtle brightness changes, including changes in gray and the purity of food for thought, as if all hearts embodies the corresponding "the smiling. " More use of color on the white rice, brown, black, simple and elegant natural color. Black and white is the "Zen" one of the main use of color, the color is faded in popularity of the eternal. A variety of gray in the "Zen" is also much loved color, such as drunk brown, mustard yellow, rusty red, brown bird, this simple meaning conveyed by color, implies its ecology and nature color mood.

Material principle

In the material selection and re-creation, the Zen design is very prominent. About this, the performance of Chinese and foreign designers are stunning in these designer Issey Miyake to the most. He traditional fabrics combined with modern technology to his own Zen position, creating a convex surface of natural materials and fine loose texture effect, creating unprecedented material and garments, known as "the fabric of the magician. " He designed the material is always a surprise, more choice of matte and coarse texture, such as the Japanese rice paper, white cotton, knitted cotton, linen, etc., create a variety of special effects, the beauty of the material to create texture, and defeated the West Rule the fashion industry for many years the beauty of the decoration, forming a unique calm and texture effects.

In addition, the manifestation of natural materials is the basic language of Zen design. Zen designers to use more cotton, hemp and other materials, and apply them to the extreme, but also with the woven fabric used in the above ornamental engraving showing a superposition of three-dimensional bump effect, and by the same color to create a heterogeneous mix of rich visual Perception. Fiber using natural materials viable, show a restrained, elegant and subtle means.

Decorative principle

Zen design is the emphasis on clothing in general, simple, so it is even more exquisite detail and refined decoration, and focus manually. Follow the "one is more" principle, does not emphasize decorative, pattern and decorative patterns of use are subject to very little. In the decoration, not respected and luxurious, magnificent, the elegant restraint, Zen for the state of deep silence. Zen design in a complex rare decorating, color piling. The decoration may be a sideline, a button, a knot or a little color, even go beyond that by also, do not let it be too bold and prominent.

In short, the "naturalistic " costume design is a hot spot in today's international fashion trends, although the countries in the design community has its own point of view, ideas and content, but the Zen "view of nature, " convey the soul of the nourishment and survival of the realm of praise, and the unique vision of things and simple, elegant consistent form, has been increasingly more and more the concern of the world's designers. Habitat is the human pursuit of the most settled and ownership of life, information society, busy, rush, congestion and fatigue, so that people in the rest of the body, more attention and restoration of mind to be settled. Basic necessities of life is most closely associated with the daily life of the part, so the fashion designers who advocate Zen think that "dress is edifying refined", and the Zen of all perfusion to the design of everyday life, reflecting the state of the simple life, eau, quiet and aloof. Therefore, China must focus on the traditional essence of the designer's in-depth study and master its true meaning, and then fused with modern fashion, and then from a pure element used to convey meaning and create the transformation.

Note: This paper is subsidized by "scientific planning of arts and culture in Hebei province key project"-"Zen and the naturalistic design of clothing" paper series, issues No. - 09AE006

References:

[1] Jiemo Zhang: *Zen Aesthetic*(Peking University Press, Beijing, 2006).

[2] Laixiang Zhou: *Zen view of nature*(Peking University Press, Beijing, 2003).

[3] Xinming Bao: *Foreign post-modern dress*(Jiangsu Art Press, Nanjing, China, 2001).

© (2011) Trans Tech Publications, Switzerland
doi:10.4028/www.scientific.net/AMR.331.670

The Application of Geometric Form in Clothing Design

Chin-Mei Lin[1,a], Ching-Hui Lin[1,b],Pei-Chen Hsiao[1,c],Yi-Chang Yang[2,d]

[1]Department of Fashion Design, Asia University, Taichung 41354, Taiwan, R.O.C

[2]Department of Fashion Styling and Design Communication Shih Chien University, Kaohsiung 845, Taiwan, R.O.C

Email: [a] cheri6688@hotmail.com, [b] chinghui@asia.edu.tw, [c]at5678h@yahoo.com.tw, [d]yang.yichang@gmail.com

Keywords： Geometric Form，Fashion Design，New bunka prototype

Abstract. The design of geometric form is widely used in daily life, such as Product Design, Communication Design and Digital Animation. In fact, it is an indispensable element of artistic creation. However, there is still a large possibility to explore for clothing design. This study discusses the relationship between the features of geometric form and clothing patterns. Through the works of fashion designers analyse the techniques used and the possibility of development. In order to break the traditional concepts of pattern making and to dismantle the patterns, the geometric form was used as the basic structure to create a three-dimensional silhouette. As a result, the clothing would produce visual effects with the movement of body. The overall design process and creative outcomes contribute researchers different design thinking for further study and development.

Introduction

The first step of formation of knowledge is usually through the senses, then the level of rational thing. In the twentieth century, the rise of constructivism has made geometric form widely used in furniture, architecture or mechanical design[1]. In the early twentieth century, most of items were constructed by geometric form. From point, line and surface to the era of digital image design, geometric form plays a very important role in both Eastern and Western Art and Design. The geometric form is indispensable in the Art creation, especially has a significant influence on Architectural design, modern design and clothing design.There are three elements of clothing design shapes, colors and materials. The structure has an influence on the shape of garment. This study discusses the relationship between the features of geometric form and clothing patterns. Through the works of fashion designers analyse the techniques adopted and the possibility of transformation and application. Furthermore, using geometric form as basic structure of pattern to go beyond the traditional thinking, deconstruct the pattern and to form a three-dimensional silhouette.

Theory

2.1. Geometric form

Geometric form is the application of the concept of geometry, creates graphic pattern or shape. It presents in the two-dimension is painting and in the three-dimension is sculpture. Geometric form includes: straight line, curve, parabola, segments, triangles, quadrilaterals, polygon, round and oval [2]. Round was the earliest found form of geometry[3]. Round is the limit of polygon and Sphere is the limit of polyhedron. Oval can be considered as the angle projection of round. From the point of view of aesthetics, Round means a "complete form. According to the philosophical point of view, round has a signification of perfection. Triangle is the most stable form. This form has a higher frequency of usage in architecture and rarely adopted in product design. In geometry, the triangle has the strongest direction, with a keen sense of direction, therefore, usually used as the mark of direction. Square has the characteristics of stability and simplicity. It is consider as the most economic effect and applied in the product design such as wardrobe, refrigerator, TV. According to

the cognitive psychology researches, simple graphic catch more attention than complex one. Simple geometric form such as circles, triangles and squares are easier to be noted than complex ones including oval, dodecagon and trapezoidal[4].

2.2. Clothing prototype

Clothing covers a person's body, therefore, it is important to know the shape of body before clothing design.Human body is composed of divers shapes. It can be devised into several parts including head, neck, chest, abdomen, upper and lower legs. The bone, muscle, fat create human body silhouette. The pattern was made according to the structure of human body and drawing down refers to the measured size. Through the pattern to create different types of clothing, as a result, the preciseness and reliability of pattern has an influence on the silhouette of clothing.

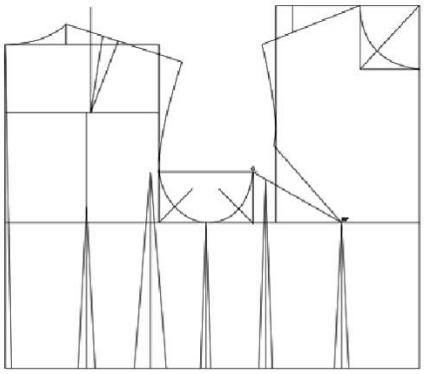


Fig.1. New bunka prototype

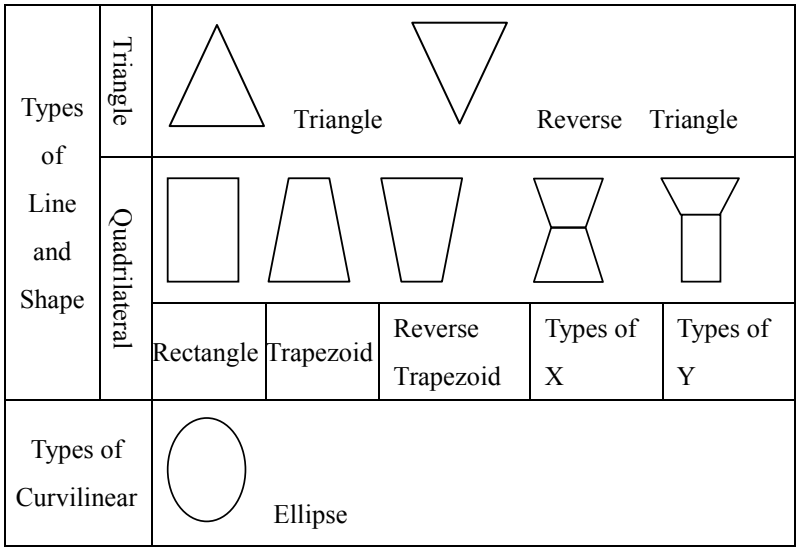


Fig.2. Sketch map of cloth style

2.3. The relationship between geometric form and pattern

The basic geometric form of a triangle, four Square and round can be extended to the complex form such as polygon, oval and diamond. The transformation from 2D to 3D including the cube, cylinder and vertebrae, etc. Impressionist painter Paul Cezanne devised the nature into the cone, sphere and cylinder. Human body is constituted by the concave and convex surfaces to express the beauty of clothing. The Greeks wore light, loose clothes, usually just made from a single piece of rectangular material, which is the earliest application of geometric form in the construction of clothing. With the enhancement of sewing skill and the needs of different clothing shape, the pattern drawing technique was developed to decompose human body into plane, which is the basic principle of geometric form for clothing construction. The shape of clothing attracts the most of attention. The contour of clothing is the silhouette, usually described as triangular, trapezoidal, rectangular, square and oval. The geometric shape could be classified into single or multiple geometric plane contour shape composed by straight lines and curves lines.

2.4. The expression of international fashion designers

Beside the material, Special structure and production methods are used to make the dialogue between the body and clothing. Technique and innovative form can change not only the lines of body, but also express the features of garment. The following discussion concerns the creation of international fashion designers. The study intends to contribute the knowledge of how to combine the geometrical structure of contemporary design concepts to create a unique design.

2.4.1 Rei Kawakubo：Rei Kawakubo upholds the anti-fashion design philosophy, fuses both Eastern and Western concepts, joins elegant and restrain characteristics of Japanese tradition, overlaps, asymmetric kimono cutting, innovates geometry model with neat lines and colors, to present an independent, strong conceptual sense of beauty. In the collection of spring and summer 1997, she experimented asymmetry, unfit and the cutting edge line（Fig.3）.

2.4.2. Issey Miyake：Issey Miyake uses of material and re-interprets contour line, make a perfect combination of clothing and art. He is not only designer, but also modern sculpture artist. He upholds a piece of cloth is a piece of clothing, uses polyester fabric to make clothing without sewing. The crimping fabric can be storage without dry cleaning and ironing. Clothing is fit but not tight. Crimping fabric is decorative, easy for storage and for body movement. Using machine to crimp the fabric and adjust cut pieces and fold according to the curve or shape of human body. The garment is like a sculpture, showing a three-dimensional geometric pattern when it is fold flat （Fig.4）. His clothing is consistent with the rhythm of movement and the body curves. The combination of the shape of human body and clothing make unlimited fantasy.



Fig.3. Rei Kawa -kubo by 1997



Fig.4. Issey Miyake's fashion design



Fig.5. Hussein Chalayan's fashion design



Fig.6 Pierre Cardin's fashion design

2.4.3. Hussein Chalayan：Hussein Chalayan is one of the most innovative, experimental and conceptual fashion designers. He takes his inspiration from a wide range of different disciplines such as nature and science, culture and anthropology. For example: the wood made skirts, a combination of geometric shapes, the simple plastic dress, are all the Ingenious application of geometric structure in clothing design（Fig.5）.

2.4.4.Pierre Cardin：Pierre Cardin started his business in 1950. With a unique creative vision and smart business notion and innovative design made him an influential figure in fashion industry. In 50's, the lunar trend had an important influence on geometric form for various design. Pierre Cardin collaborated with DU PONT to create nylon fabric and adopted geometric form and primary colors to subvert the Fashion Industry and built an unconventional image（Fig.6）.

3. Application And Creation In Clothing Design

3.1 Creative concepts

Using functional textile, combined divers material, geometric shape to build the clothing with rich grade and complex structure. This allowed remodeling the materials and creating numerous visual effects.

3.2 Process Of Creation

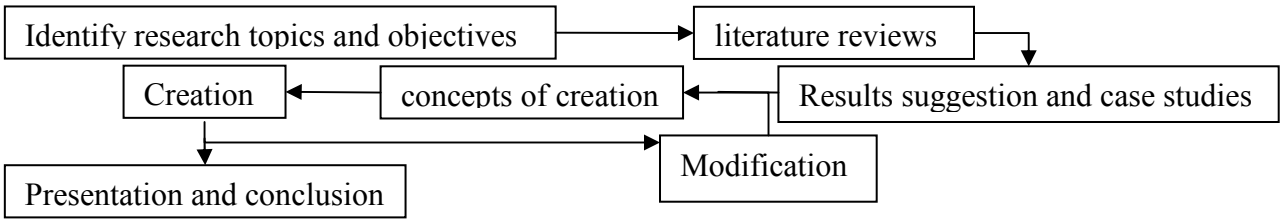


Fig.7 Process of creation

3.3 Types of creation

The outline of clothing gives an impression and a particular style. For example: Rectangular, square and triangle shapes, the straight lines give people the tough, decisive, and the masculine feelings. Round, oval and curved body gives smooth, soft and female feelings. All the geometric surfaces are formed by straight or curve lines. The geometric surfaces deliver a simple, crisp, clean feeling. In geometry, the circle is the most complete and uniform shape, oval, long round, wave shaped, parabolic all can be included in a perfect circle. Both lines and forms can exhibit graceful and soft feelings. The creations show both the lines and natural rhythm by using circular geometric

elements as the main form of contour. To combine opposite feature such as Upper and lower, more and less, long and short, big and small, light and weight in the pattern design. Concise lines give the combination of rhythm, proportion and configuration, to achieve the strength and beauty of visual display.

3.4 Creation techniques

In this study, the circular shape was used as the basis of creation. To break the traditional concepts and thinking deconstructed the pattern, used geometric shapes as the main structures of clothing. The two collections are presented as follow: Series I: compositing two sizes of circular pieces to create the pattern and gain the main structural line. Starting from a single point, extending to the line, and then break the plane, through and beyond the third dimension, rendering quality, create the flowing cutting aesthetic. To coordinate the exterior structure and the internal structure of line design, using a circular geometric modeling, the upper circular surface was used as the sleeve, and The lower circular surface was decorated with the stitch-line. Reasonable compositions of internal and external structure create rhythm, balance, contrast, harmony beauty. Through the use of a regular combination of point, line and plane to create a relationship between densities and scattered in a composition. Series II: Patterns were designed with semi-circular form. The clothing was formed with a narrow upper part and width lower part contour lines. The pressure lines to spiral seam were used for the internal structure with smooth homogeneous hem waves and simple natural outline.

4. Analysis and explication of creation

In this collection, different materials and design methods were used to create rich layers and three-dimensional and change the structure. The ccreation of this research tried to break through the traditional version of dress, adopted simple geometric shape as patterns, interpreted vitality and movement of clothing. The clothing was grouped into two collections. Using the pattern of Series I, the two circles were superimposed on the waist to create the natural beauty of female body. For the fit of waist, the size of congruence of two circles needs to be considered wearing convenience, style and characteristics of fabric. The material selected was flexible and resistance of sun radiation knitted fabric. Soft transparent tube was used for the internal structure to strengthen the sense of spatial dynamics of irregular shape, flowing curves structural characteristics, therefore create a sculpture-like structure shape and free-spirited multi-line.



Fig.8 Fashion design 1



Fig.9 Fashion design 2



Fig.10 Fashion design 3



Fig.11 Fashion design 4



Fig.12 Fashion design 5



Fig.13 Fashion design 6



Fig.14 Same structure with different material designs

Fig.9 show the pattern of Series I was used and the material selected was flexible and resistance of sun radiation knitted fabric. The elasticity was lower than the first work, thus, the internal structure lines was made with wrinkles pumping method. These two works were made from the same pattern, however, the different characteristics of fabrics and techniques used, the overall appearance and style were complete different. Fig.10 show the volume has an influence on visual effects of clothing, for example: cute, mini, generous or the free and easy feeling. The structure has been changed for this work. The bottom round down to the Knee and the width of transverse was larger than vertical. The pattern was oval version. Knitting fabric was used and t external structure was formed with different material to create a solid contour line. Fig.11 show the pattern of Series I was used. The lower half circle was adjusted to become the arc lines with wider top part and narrower lower part. Right and left external lines were set around edges. Two sleeves lines were drawn for the front pattern. A slight change of sleeves direction was made to create different visual

effect. Concerning the color, pink and pastel colours were used to interpret sweet and elegant style. Fig.12 show the structure has an impact on the outlook of clothing. Clothing structure line can be grouped into the internal and external structure line. The pattern was designed with semi-circular form. With this form to create narrow top part and wide lower part clothing contour lines. The internal structure was made with decorative spiral-line and soft transparent tube to enhance the overall three-dimensional effect of clothing. Oblique collar with homogeneous fluid wave hem form the natural and simple contours. In the sewing process, the pressure decorative spiral seam lines have took a lot of time. For sewing, the lower the bias strips have a certain degree of difficulty. Therefore, it is suggested to change the size of inner layer of bias strips to consistent with the surface fabric, place soft transparent tube after sewing the surface and inner layer. Fig.13 show using of three-dimensional geometric surface to structure clothing line, with different materials, internal structure arose the change of spiral shape. Shorten the length of the fifth model, use knitting fabric and combine the features of different materials to sculpture clothing contour, irregular hem make the rhythm when walking. Using double-stitched fabrics reduce the difficulty of sewing. Different color or fabrics were used for the inner to create various effects.

Conclusion

Fashion design focus on style and structure of the overall aesthetic. The creation combined both techniques and aesthetic, by changing the form of fabric and using geometric shape to construct the patterns. This research reveals the relationship between fabric and structure. With the change of fabric or structure can make various silhouette of clothing (Fig.14). The traditional pattern making demands lot of consideration of human body size and functional features, with complicated formula and plate making process. The change of geometric system leads to the pattern making easier and simplify the composition process. Geometric forms are widely used and there remain great possibility to explore in clothing design. The application of geometric forms would bring unexpected surprise in design. The finding of this research offers a different thinking of pattern making process and contributes to the state of knowledge for further study.

The top female pattern of new bunka prototype takes only the amount of body size of the bust and back length. Set the size of bust into the formula to calculate the size of other parts, which corresponds the prototype of human body. It was innovated in 1936 and successive modification according to the evolution of the human body. New bunka prototype was created in 1999 and widely used in the fashion industry.

References

[1] G.S YE, M.H ZHANG, Graphic Design Basics, Yi-Feng-Tang Press, Taipei (1991).

[2] M.S SU, Y.Y WANG, Y.X ZHOU, Design Basics, East Great Books, Taipei (2001).

[3] P.Z LIN, Principles of Shaping, Quan Hua Science and Technology Library, Taipei (2000).

[4] Nicholas Roukes, Design forms, Kuni Publishing, Taipei (1995）.

[5]S.R CHEN, Fashion & costume designing, visual communication culture co.,ltd, Taipei (2003).

© (2011) Trans Tech Publications, Switzerland
doi:10.4028/www.scientific.net/AMR.331.675

The Drapability Effects Test Method of Lining and Shell Fabric

Fang Yu[1, a]

[1] Yuan Pei college, Shaoxing University, Shaoxing, Zhejiang, China

[a]39584424@qq.com

Keywords: multi-layer fabric; drapability; image processing; test equipment

Abstract: The fabric drapability is the peformation due to fabric weight to sagging, reflecting the drape degree and drape shape of fabric. This paper design a new method to measure the drapability of mulit-layer fabric by computer image processing technology. It can evaluate the drapability performance and the interaction of fabrics and lining. A test equipment was made. Photos were took in planfprm and side elevation in warp and weft by a digital camera while the sample fabric was overhanging naturally. The datas, like drape coefficient and drape degree, were processed and analysized by AUTO CAD. The paper's results are that: The drape coefficient and the drape degree of the mulit-layer fabric are between the single-layer fabric's and single-layer lining's, and they are closer to the target fabrics.

Introduction

With the growing demand for beauty of clothing, and the constantly update new type of fiber fabrics,there are more and more researchs on all kinds of fabrics, while the fabric drapability is an important factor. The drapability is the performance due to fabric weight to sagging, reflecting the drape degree and drape shape of fabric.It is an important aspect to evaluate the visual style and aesthetic comfort. Fabric drape Degree measures the sagging degree under its own weight [1]. It has better drapability while the degree of sagging is greater. fabric Drape shape is related to the graceful curving surface sculpt and good fitting while actual use. Good arrange in paris of fabrics and lining can improve the quality and grades of costume, to improve its wearability.

There are two evaluation methods of the fabric drapability——Subjective evaluation method and objective evaluation method.Subjective evaluation method, with the advantages which is simple and fast, has vary results because of different persons.It has limitations. Objective evaluation method can evaluate fabric drapability completely and objectively. This paper use objective method to evaluate the drapability of double-layer fabric. The test equipment is completed based on the design principle of Guo Yongping umbrella drapability test device. In order to evaluate interaction result between lining and fabric better, The test selects 6 kinds of single-layer fabrics, 9 groups multi-layer fabrics which are combined by lining and fabric, gains the images of natural drapability through a digital video camera, then the paper uses AUTOCAD to obtain each evaluation index data by image processing and analysis.

Experiment

2.1 Materials

The paper chooses 6 kinds of single-layer fabrics from the mainstream market, which have different drapability, including cotton, polyester, nylon, viscose fabrics.Then they are numbered respectively from No. 1 # to No. 6 #. The sample specification are shown in Table 1. The sample size is 24cm diameter round fabric. In order to obtain more accurate data, the data in this experiment calculates average by taking three tests. Eirst, the drapabilities of six single-layer samples are tested. Second, the mulit-layer samples are experimented which are combined one by one of these 6 kinds of fabrics.

Table 1 Sample Specification

No.	Raw materials	Warp density [radix/ 10cm]	Weft density [radix/ 10cm]
1 #	20% wool 80% mixed fibers	210	190
2 #	100% Cotton	250	170
3 #	100% viscose	450	220
4 #	100% Nylon	720	540
5 #	100% Polyester	520	275
6 #	100% Polyester	520	350

2.2 Method

2.2.1 Image Acquisition

Put the circle sample fabric on a round table and buckle tip in to fix.Because the data obtained through AUTO CAD image processing is non-actual value, it should be translated into the actual value reference the object length. So, it is covered a diameter of 12cm circle disk on the sample fabric in ord to facilitate image processing and data conversion, (Figure 1). Then the digital camera fixes the same focal length in the environment of the non-wind and natural light, and takes photoes above the sample fabric, in the wrap side and in the weft side at a distance of 30cm(the photo ensure vertical direction in weft, the level direction in wrap).The experiment obtains the original images while the sample fabrics overhang.

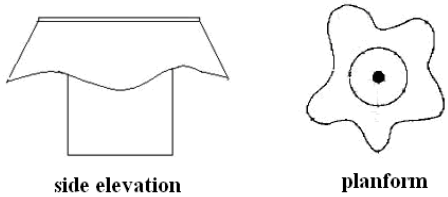


Fig.1 Sample overhang

2.2.2 Image Processing

It obtains the sample fabric area in the planform view image with AUTO CAD software processing, as shown in Figure 2.

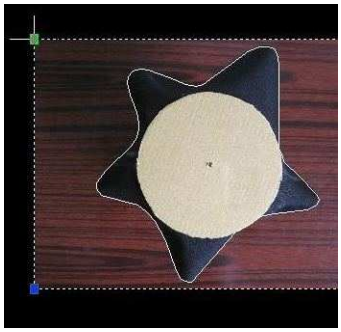


Fig.2 The area image in the planform

The drape range of the sample fabric in wrap and weft are obtained by image processing in the side elevation view. The image processing methods and processes of area measurement in warp and

weft side view are the same, so this paper selects the wrap side elevation view as an example to illustrate the method using of AUTO CAD image processing in wrap and weft Side,to measure the range of fabric drapability indicators, as shown in Figure 3.

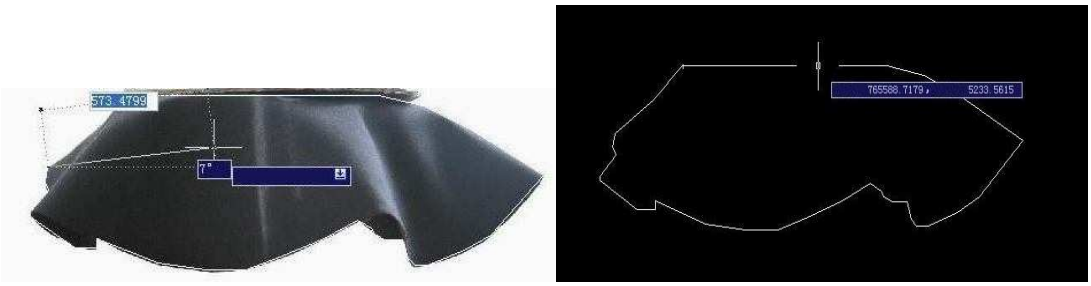


Fig. 3 Image processing in the side elevation view

Results and discussion

As being combined sample 2 with sample 3 to the multi-layer fabirc,it is prepared for the experimental group numbered No.1. The experiment was divided into 9 groups respectively, 3 and 2, 3 and 5, 3 and 4, 1 and 5, 1 and 2, 1 and 4, 6 and 4, 6 and 5, 6 and 2 combined. It liquidates and analyzes all the data.Then it calculates and compares the drape coefficient of the single-layer and the mulit-layer fabrics according to the formula $F_T = (S-A_{d)} / (A_D - A_d)$, in Figure 4. F_T represents drape coefficient which measured by image processing , S represents the actual sample area after calculating form the drape images, A_D represents the actual area of the sample and A_d represents the actual area of disk.

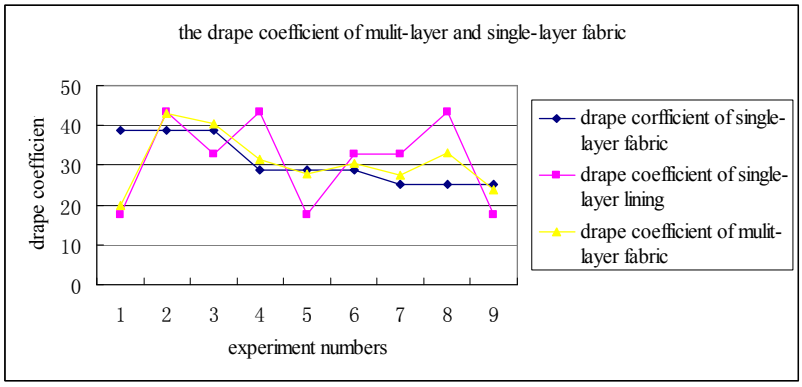


Fig. 4 Drape coefficient experiment on mulit-layer and single-layer fabric (planform view)

It can be obtained from Figure 4 that the drape coefficient of mulit-layer fabric is between the single-layer fabric's and the single-layer lining's. And it is near the data of single-layer fabric.So this study results that the mulit-layer fabric is closer to the target fabric.

Compared the drape degree of the single-layer and multi-layers fabric,the curves are shown in Figure 5 and Figure 6:

It can be obtained from Figure 5 and Figure 6 that the drape degree of mulit-layer fabric is between the single-layer fabric's and the single-layer lining's. And it is near the data of single-layer fabric.So this study results that the mulit-layer fabric is closer to the target fabric.

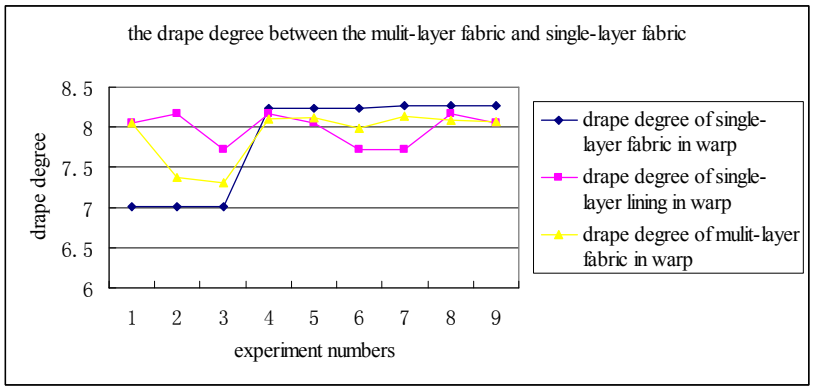


Fig. 5 Drape degree experiment on mulit-layer and single-layer fabric in warp(side elevation view)

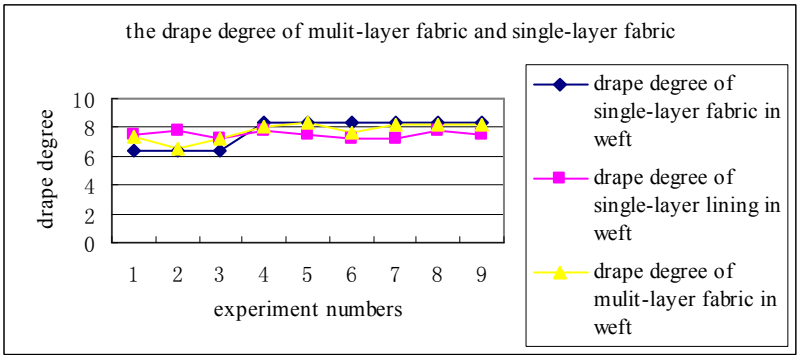


Fig. 6 Drape degree experiment on mulit-layer and single-layer fabric in weft(side elevation view)

Conclusion

It is comprehensive that test the drapability performance of lining and fabric influence each other with the image method. With the rapid development of computer technology, the new image processing technology could be applied better to the fabric drapability performance measurement. It can establish a set of image processing system, to measure the fabric drapability performance quickly, easily and effectively. It can improve the quality and grade of clothing and improve its wearability while lining and fabric mixed reasonably.

References

[1] Xinlin Huang, Ruqin Li. Image testing method on fabric drapability [J]. Textile Research, 2006,27 (11) :14-19

[2] Youmin Zhang, Dunmin Yin . Fabric drapability evaluation [J]. Dyeing Translations, 1990 (4) :98-99

[3] K．T．Aswani. The research of cotton drape [J]. Int.Text.Bull, 1986 (2) :39-45

[4] Lixi Chen, Xiuru Zeng, Wenxian Zhao. Research on the fabric drapability evaluation method and index [J]. Northwest of Textile Institute, 1991 (1) :15-24

[5] Xiaohong Wang, Jun Xu, Mu Yao. Objective evaluation to the fabric drapability using image processing techniques [J]. China Textile University, 1999.25 (3) :38-41

© (2011) Trans Tech Publications, Switzerland
doi:10.4028/www.scientific.net/AMR.331.679

Design and Development of Chinese Primary and Secondary New Type School Uniform

Miao Yu [1, a], Xin He [2, b]

[1] College of Fashion, Dalian Polytechnic University, Dalian, China

[2] College of Arts and Information Engineering, Dalian Polytechnic University, Dalian, China

[a] watercolorskirt@126.com, [b] hexin0905@126.com

Keywords: Primary and Secondary School Uniform, style, color, material, structure, practicability

Abstract. As a unique form of culture, school uniform play an important role in the performance of a country or region's economic, educational, cultural level and religious beliefs. This article also put forward new design ideas in school uniform style, color, fabric and clothing accessories, which could better demonstrate the need of the implementation of new school uniform. And hope this article could provide beneficial ideas for China's school uniform development.

Introduction

1. Status and problem of Chinese primary and secondary school uniform

Since 1993, the the State Education Commission issued a "city students wear uniform ", it has been 15 year for the development of our country's school uniform. In those 15 years, school uniform as an important concept of school culture, its growth and changes obtained great attention from students, parents, and education experts. However, there are still lots of problems exposed during the development of school uniform, which should arouse our deep thinking and research.

1.1 Monotone in style and indefinite for shape

Our country's primary and secondary school uniform mostly are sports clothing, dominated with T-shirts, and knitted sweaters. Only a few schools adopt western style suits, which are determined by our country's economic and education level. There are other problems in china's school uniform, for example, no distinctive gender difference; most of school uniform only in three sizes (large, medium and small), which is not accordance with national standard. Many schools adopt sportswear as school uniform directly, which could not demonstrate the vibrant vitality of youth and is not conductive to the formation of youth aesthetics.

1.2 Serious problem for uniform' material

(1) Poor in airy and permeability

The material's airy and permeability is very important for summer clothing. At present, probably for cost reason, school Uniform companies usually adopt pure polyester or pure acrylic fabric material, which is small in moisture regain rate and slightly large in density. The chosen material caused the uniform in poor ventilation, and incapable of sweat absorption. It is negative to student's health.

(2) Negative performance in anti-static, anti-pilling and abrasion

General ingredients for school uniform fabric and structure are: pure polyester knitted fabric, knitted fabrics of pure acrylic, polyester and other synthetic blended knitted fabrics and cotton knitted fabrics (polyester and cotton), etc. without finishing treatment after fabric dyeing, it's easy to generate static electricity, which both severely influence the beauty of the uniform and could be harmful to student's health. And nylon, polyester knitted fabric are most likely to cause pilling. Once it pilling at the surface and difficult to fall off severely affects the performance of the uniform.

(3) Dad dyeing

Dyeing is supposed to be taken physical, chemical processing, and this will cause chemical remains in textiles. Many companies use low-grade dyes containing pathogenic material in order to save cost, for example, phenol aromatic dyes prohibited by national laws. The dyed textile form fat-soluble compounds, which could enter student's body through skin and cause damage to student's

health. The symptom is skin allergies, itching, severe harm to nervous system and liver. The main function of school uniform is to protect student's health and make them comfortable. So for this reason, it is regulated school uniform material should be natural fiber or mixed textiles which meet the requirement for airy and water permeability test. The dyeing safety standard should also be followed to guarantee students health.

1.3 Rough processing

There are even without bag sewing process during production caused jump sewing in lining or pocket. There are clear standards for uniform manufacture, but they are ignored by the school uniform company, which is the reason for the low quality of uniform.

2. Design focus on new type Chinese primary and secondary school uniform

2.1 Definition of the uniform style

The current domestic school uniform which are widely used are mainly sportswear, though sportswear can show unity and the relaxed style allows students to exercise in a great range of activities but the bloated style obscures the personality of young students. Comparatively, the standard school uniform can better reflect the vigorous spirit of students. However, the promotion of standard uniform has always been unsuccessful due to firstly the discrepancy between price and quality: that is at the affordable price for the students, the materials' quality is not good enough, not stiff enough, and the uniform are easily to become out of shapes; secondly, it is the time and space constraints. Unlike the students in foreign schools, the Chinese students don't have their own lockers and dressing room in school. During physical activity time, there is no enough space for the students to change their clothes.

Therefore, the design of new models need to coordinate school uniform' price, quality, service life of the uniform before the next replacement, space and a series of contradictions. Although these problems can not be fully resolved in a short time, but we can combine the advantages of both sportswear and uniform, positioning the style in formal wear with leisure element. As shown in Fig. 1 and Fig. 2, in the design of the primary school uniform for male and female students in spring and autumn,(the design comes from a project called the design and research of new school uniform for primary and secondary school), I used the brightly colored leisure knitting cardigan as uniform jacket, with white shirt inside just like the formal wear. It is comfortable to wear, easy to take off, good to keep warm and suitable for larger movement. As shown in Fig. 1, the lower clothing design is inspired by uniform design of the foreign school uniform: the Blended plaid skirts for the girls. As shown in Fig. 2, boy's trousers in the same color with the knitwear. In the overall unity of uniform style, the uniform for girls and boys has their own traits. It is formal wear but with leisure style, highlighting the healthy, lively and staid image of the Chinese students.





Fig. 1. Dalian primary school girl's new type uniform in spring and autumu

Fig. 2. Dalian primary school boy's new type uniform in spring and autumu

2.2 Basic outline of school uniform

In the whole school uniform design process, the waist part plays a decisive role, and especially the waist tightness and level are the key point. China's current uniform is generally no waist line and dominated in H or O type, and the loose structure could not reflect the vibrant the students should have. To solve above problems, in "new school uniform Dalian R & D" project, refer to Fig.3, I raise the summer primary school girls' uniform to an appropriate level and add princess line with shaped design. The whole profile shows X type. Besides that, my design is girls' school uniform in skirts

culottes style for safety sake, which is both beautiful and suitable for student movement. As shown in Fig. 4, boy's uniform is with hem above the knee shorts and a crisp outline to enhance student's overall image. In the overall proportion of partitions, the size of upper and lower parts should be proper. The gold split is the best choice, and middle division should be avoided. The whole shape should be simple and decent.





Fig. 3. Dalian primary school girl's new type uniform in summer

Fig. 4. Dalian primary school boy's new type uniform in summer

2.3 School uniform inner structure design

After the overall profile is defined, the internal structure is also very important, which consist of structure line, collar type, sleeve type and component design. The structure line is used to shape clothing appearance, including provincial lines, pleating and editing lines and decorative lines. To sum up, there are three types of structure line in total: straight lines, arcs and curves. During internal structure design process, take students' each stage physiological characteristics into consideration, adopt simple, smooth line. In the Fig. 5, "Dalian primary and secondary school students new type school uniform R&D" the design idea of boys'uniform draw military uniform characteristics. Use military insignia shoulder shape to decorate the school uniform skirt shoulder, and visually segment the monotonous white shirt with add decorative line at the edge of placket and cuffs. The above internal structure lines could raise boys' temperament.





Fig. 5. Shirt style of Dalian primary school boy's new type uniform

Fig. 6. Shirt style of Dalian primary school girl's new type uniform

Clothing's structure design also includes collar and sleeve. Collar is a vital component of clothing. Uniform's collar design should coordinate with uniform overall style. If the school uniform is in simple and concise style, the collar should also in the same style correspondently. The rotator cuff and sleeve design include armhole, and sleeve tow parts. The design of collar and sleeve are supposed to match with uniform's overall style and the students' temperament. Refer to Fig. 6, in order to highlight the lovely little princess style, girls' uniform internal structure mainly adopt curves. That the waist shaped coast with round neck, and uplift lilac shaped princess sleeves design is more convenient for student to move. Made with the skirt fabric and mounted with wood ear shaped wave edges, the collar and cuffs like petals add elegant for the simple style school uniform.

2.4 The comfort and functionality of uniform

In considering the profile of the aesthetics and structure, we must also emphasize the function and comfort of school uniform .The design of the uniform must have certain functionality because of the basis of physical development between Primary students and secondary students. Function is the most important part of costume design. Costumes in the deployment of each language need not only

of aesthetic composition, but also to focus on the human body function, form, convenience, adaptability, physiological and psychological needs coincide in order to maximize the performance apparel. Because students are energetic and lively and their lives are colorful after classes, which requires uniform design must take into account the activities of comfort.

Clothing fabrics can be interpreted not only the style and features, but also directly influences the color of clothing and the shape of the performance results. Ingredients should be used in washing uniform, anti-wrinkle, shrink-proof, anti-static natural or blended fabrics: wool suits fabrics should be used the appearance of flat and smooth, plump and elastic; Casual style of uniform must be use of cotton Lycra mix fabric, with the characteristics of natural fibers and the necessary resilience and good moisture permeability. And it is not easy deformation and comfortable. Uniform is different from any other clothes and it's target consumers are students ,so we should first consider comfort at the same time we must consider the price ,regional differences and individual economic differences .we must combine the uniform positioning with the spending power of students . In short, the choice of fabrics must be reflect the safe, practical and health topics, combined with the specific spending power of students to enable students to dress in uniform to develop students' healthy body and mind.

Conclusion

Based on the recognition of the history and status of school uniform at home and abroad, this thesis conducts some explorations on our new design and development of primary and secondary school uniform and further elaborates the ways of the new uniform design which are attempting to solve a series of problems existing in our current school uniform. The below conclusions follow the above analysis:

On the use and promotion of school uniform, we should fully consider the students' psychological states and attitudes, understand the students' specific circumstances and the environment around and then develop a comprehensive system for uniform use, such as for different regions, different economic levels, and different grades etc. The uniform style should be chosen based on the season, time and occasion for appropriate wear. A clear distinction between sportswear and school uniform should be acknowledged as well.

To select the most suitable color for the school uniform, consideration should be given to school environment, learning atmosphere, satisfaction of psychological needs, the trends and other factors. The materials for school uniform are yet to be improved. Healthier and safer clothing materials should be highly advocated to ensure the healthy growth for the youngsters.

With full consideration about the students' needs, the school uniform matching design requires complete and necessary matching forms, such as the matching shoes, socks and hats to the clothing, and multiple types of clothing which can adapt to the climate change in different seasons. On the design of uniform style, processing design and material configuration, consideration should be grounded on the special characteristics the youngsters have such as being vigorous and active, so that the goal can be achieved as to reduce breakage and prolong the service life for school uniform.

References

[1] Ying Xie: Fujian commercial school paper, Vol. 6 (2010), p.45-48 (In Chinese)

[2] Hong Liu: Arts fond, Education Edition, Vol. 1,(2009), p.12-14 (In Chinese)

[3] Xiaoming Ren and Hui Tao: Wu Han technology school paper, Vol. 9 (2006), p.19-22 (In Chinese)

CHAPTER 5:

New Trends in Textile Industry

© (2011) Trans Tech Publications, Switzerland
doi:10.4028/www.scientific.net/AMR.331.685

Predictive Modeling and Empirical Analyses of Regional Silk Fabrics Price Index Based on BP Neural Network

Hai Liu[1,2,a],Bingdi Liu[1,2,b] and Cen Feng[1,2,c*]

[1]National Engineering Laboratory for Modern Silk, Suzhou, Jiangsu, 215021,China

[2]College of Textile and Clothing Engineering, Soochow University, Suzhou, Jiangsu 215021,China

[a]595369354@qq.com,[b]634109924@qq.com,[c*]fengcen@suda.edu.cn

Keywords: The BP Neural Network, Silk Fabrics, Price Index, Prediction Model

Abstract. The article is based on the actual collection of silk fabrics price in oriental silk market and surrounding areas for data support, using related theory and experiment analysis method of artificial neural network to analyze and predict regional silk fabrics price index, second class silk fabrics price index and single variety silk fabrics price index. Compare the accuracy and applicability by related index, applied the accumulative total of instant statistics to analysis the silk market fluctuations through the reasonable modeling prediction method. This article confirms that the neural network is a kind of good method used in Analysising and forecasting of regional silk fabrics price index.

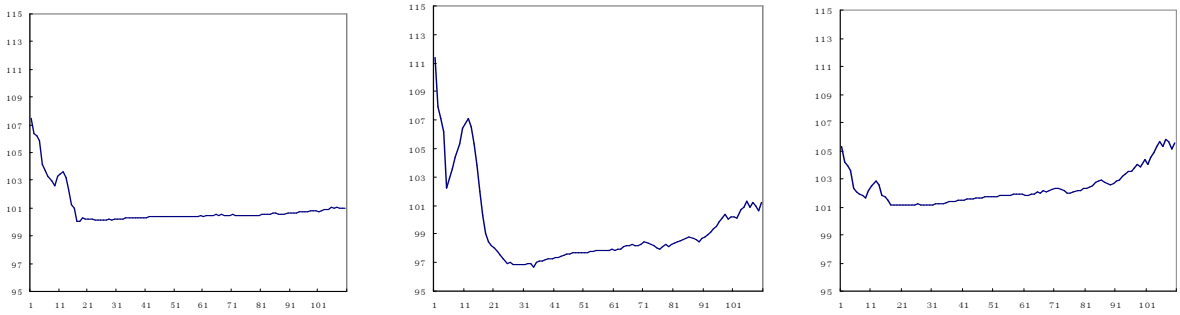
Introduction

In previous years, the statistics and data acquisition process of silk industry,afterwards judgement and qualitative judgement in the market management and policy have the defect of lag and lack of quantification. As built not long, region silk fabric price index system has not been carried on the systematic economic analysis. In recent years, the artificial neural network is widely used in time series analysis and market forecasts, but it has not been applied to the area of silk fabrics index analysis and prediction. Compared with methods that have been applied to this area, it has great advantage in fault tolerance and prediction. This paper based on the actual market operation data sampling and network system, discusses the show features in BP artificial neural network modeling the prediction process of regional silk fabrics price index, second class silk fabrics price index and single variety silk fabrics price index. Analysis and forecast regional silk fabrics price index.

The BP neural network model establishment of regional silk fabrics price index

Regional silk fabrics price index is an economic indicator of product price changes direction, the trend and degree in Oriental silk market and circumjacent area silk fabric market. Silk fabrics price index system is in a single variety price index basis and becomes silk fabrics secondary price index based on volume weight filtering and eventually forms the silk fabrics level price index [1].

The paper uses regional silk fabrics weekly price index data which from Chinese silk nets website [2], namely the Oriental silk market, from August 1, 2008 to 2010 October 22, for a total of 110 set of data. Regional silk fabrics price index curve, grain sewn damask fabrics price index curve and 14654 grain crepe damask fabrics price index curve are shown in Figure.1.



(a) (b) (c)

Figure.1 (a) Curve variation of regional silk fabrics price index (b) Curve variation of grain crepe damask fabrics price index (c) Curve variation of 14654 grain crepe damask fabrics price index.

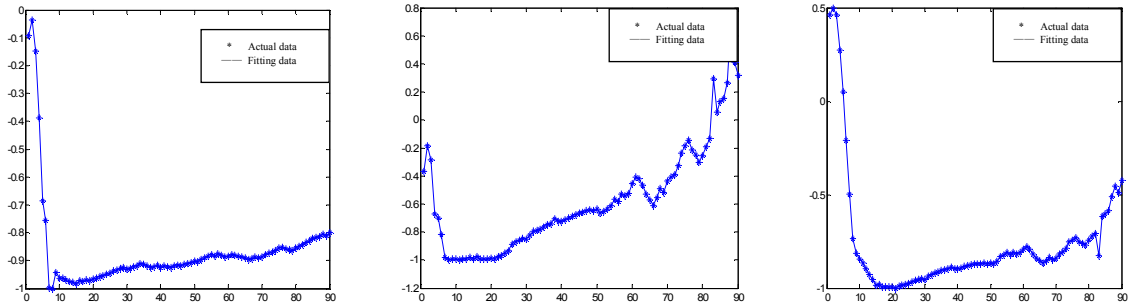
The establishment of grain sewn damask fabrics price index BP artificial neural network model

Take 14654 grain crepe damask fabrics price index for example, the paper uses 100 sets of data as the training sample and10 sets of data as a test sample to analyze. It uses MATLAB software and analyze according to BP artificial neural network modeling steps [3]. Similarly, it uses the data of an order of 10 sets of data as an input data, and then the following 10 sets of data as network output namely the target data, along the way, it forms the arrangement of roll-out of the neural network training samples. Using Levenberg-Marquardt method, increase the number of neurons in hidden layer according to trail-and-err, determine the number of neurons in hidden layer when Network error smallest and training fastest [4]. The results of different hidden layer neurons are shown in Table.1.

Table.1 The results of different model

Hidden neurons	Times	Iterative-number	Hidden neurons	Times	Iterative-number
1	15	0.00116	15	9	7.81×10^{-6}
2	66	1.33×10^{-5}	16	6	7.34×10^{-6}
3	2000	1.21×10^{-5}	17	32	9.52×10^{-6}
4	49	9.89×10^{-6}	18	5	3.72×10^{-6}
5	63	9.86×10^{-6}	19	38	9.28×10^{-6}
6	70	9.94×10^{-6}	20	43	9.33×10^{-6}
7	53	9.81×10^{-6}	21	7	2.06×10^{-6}
8	24	9.84×10^{-6}	22	24	9.12×10^{-6}
9	44	9.77×10^{-6}	23	27	9.61×10^{-6}
10	25	8.82×10^{-6}	24	5	4.97×10^{-10}
11	7	8.64×10^{-6}	25	36	8.16×10^{-6}
12	19	7.97×10^{-6}	26	5	8.30×10^{-6}
13	6	5.34×10^{-9}	27	10	9.45×10^{-6}
14	18	8.48×10^{-6}	28	9	7.59×10^{-6}

In the same way, set up BP artificial neural network model for second class silk fabrics price index and 14654 grain crepe damask fabrics price index. Corresponding the number of hidden layer neurons were selected16, 25 and 24. Finally it obtains three prediction results of those three levels, just as Figure.2.



(a) (b) (c)

Figure.2 (a) Fitting map of Regional Silk Fabrics Price Index Based on BP Neural Network (b) Fitting map of grain crepe damask fabrics price index (c) Fitting map of 14654 grain crepe damask fabrics price index

The analysis of BP artificial neural network to grain sewn damask fabrics price index

According to the different-level price index, use each network to predict the following 10 sets of data and compare the forecast results and actual results. Results of comparison are shown in table.2.

Table.2 Result comparison of forecasting and actual

Number	14654		grain crepe damask		Regional Silk	
	Actual	Predictive	Actual	Predictive	Actual	Predictive
101	93.27	93.2818	104.35	104.0329	100.69	100.6926
102	93.46	95.0967	104.01	103.6039	100.78	100.8769
103	93.86	92.4015	104.52	105.0534	100.86	100.9658
104	94.16	97.5422	104.86	104.7814	100.93	100.9364
105	94.52	97.238	105.33	105.3153	101.05	101.1375
106	94.03	98.1772	105.27	105.8938	100.98	100.9684
107	94.07	98.8075	105.83	104.805	101.07	101.1068
108	94.14	98.4088	105.64	106.8662	101.02	101.2217
109	93.82	98.5331	105.14	105.2123	100.95	101.1369
110	94.06	98.7847	105.53	104.3337	101.02	101.0656

Compared the prediction results with Actual results, the mean absolute error, the average relative error and precision among the three are show as table.3. And the comparison of their actual data and forecast data are shown in Figure.3.

Table.3 Prediction results evaluation of forecasting and actual of variety price index at all levels

Name	MAE	MAPE (%)	A (%)
Regional Silk Fabrics Price	0.0782	0.0774	99.9226
grain crepe damask fabrics	0.5144	0.4884	99.5116
14654 grain crepe damask	3.1799	3.3813	96.6187

Empirical analysis shows that a single variety fabric price index, silk fabrics secondary price index, regional silk fabrics price index become better and better prediction effect. The generation of this kind of phenomenon is because in price index build process middle-upper level price index comes from weighted average of lower level price index. That is to say regional silk fabrics price index comes from secondary price index weighted average, silk fabrics secondary price index

comes from a single variety of silk fabrics price index weighted average, namely the more information each point of the information in the curve carries, the smoother the curve will be and the peak will not obvious. The accuracy will be higher when modeling.

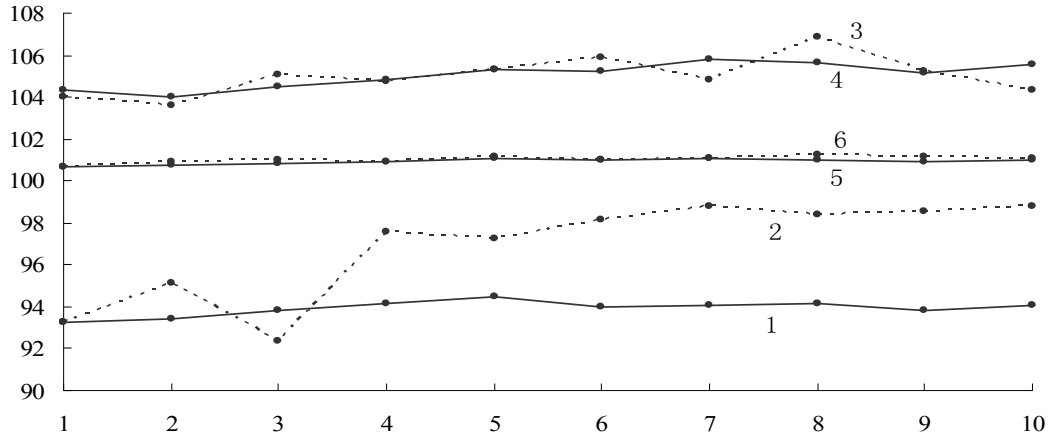


Figure.3 Result comparison about Variety price index at all levels

1--Actual data of14654 grain crepe damask fabrics price index; 2-Forecast data of 14654 grain crepe damask fabrics price index; 3--Actual data of grain crepe damask fabrics price index; 4-Forecast data of grain crepe damask fabrics price index; 5-Actual data of Regional Silk Fabrics Price Index; 6-Forecast data of Regional Silk Fabrics Price Index

Conclusions

(1) The paper uses BP neural network to analysis and predict the first class regional silk fabrics price index, second class silk fabrics price index and single variety fabrics price index, shows that it can be used for the short-term forecast and the effect is good.

(2) The forecasting accuracy of single variety fabrics price is 96.6187%, second class silk fabrics price index is 99.5116%, and first class regional silk fabrics price index is 99.9226%. So the more information each point of the information in the curve carries, the smoother the curve will be and the peak will not obvious. The accuracy will be higher when modeling.

Acknowledgements

Research Project for Silk Association of China (K4115902) and Creative Research Project for Graduate Students of Jiangsu Province (CX10B_037Z) and A Project Funded by the Priority Academic Program Development of Jiangsu Higher Education Institutions.

References

[1] Bo Nie, Li Fang, Bing-Di Liu, Cen Feng*: Textile Bioengineering and Informatics Symposium Proceedings.2010:1113-1118,in Chinese;

[2] China silk nets: http://www.silkcapital.com/;

[3] Fengfa Hu, Bing Liu, Xiaoli Ma: CD technology.2009 (2) : 25-26;

[4] Xiaotong Zhang: *A Guide to Using Eviews* [M].China Machine Press.(2007) , in Chinese.

© (2011) Trans Tech Publications, Switzerland
doi:10.4028/www.scientific.net/AMR.331.689

Influence of Color and Style on Clothing Identification

Xiaofeng Jiang[1,2,a], Xiaoxia zhang[2,b], Guolian Liu[1,2,C]

[1] National Engineering Laboratory for Modern Silk, Soochow University, 215023, China

[2] College of Textile and Clothing Engineering, Soochow University, Suzhou, 215021, China

[a]xfjiangsz@163.com, [b]summer-hades@163.com, [c]liuguolian@suda.edu.cn

Keywords: clothing; color; style; identification; behavioral

Abstract. This study is aimed to investigate how color and style influence clothing identification. 60 undergraduate students participated in this study, and a behavioral experiment was carried out to identify colored / achromatic Formal Dress (FD), Casual Wear (CW) , Sports Wear (SW) and Business Wear (BW). The findings were as follows: (1) while color had no significant influence on clothing identification, the style had an obvious influence on it, which showed that the accuracy of identifying FD was the highest and the accuracy of identifying BW was the lowest; (2) color had little influence on identification speed, but the style had a great influence on it; (3) women performed better in clothing identification than men did.

Introduction

The type of clothing is a kind of visual effect generated by our eyes, brains as well as life experiences, and color and style are regarded as important visual information to identify clothing types [1]. Previous researches have demonstrated that the identification of objects is realized by means of telling the difference of their colors and shapes and looking for the internal relations among them.

Some researches were carried out in different ways to investigate influences of color and shape on object identification. Ke et al. did a study on global precedence of unconscious visual perception on local geometric characteristic processing, and it was found that visual perception had a shape precedence effect on unconsciously occurred image processing [2]. Ou-yang et al. conducted a psychophysical experiment designed with the aid of computers to investigate the identification responses of color channel and shape channel, and it was found that the color channel and shape channel worked independently and parallelly in the human visual system [3]. Hanna et al. used memory tasks to investigate characteristics of color and shape, and it was that color and shape were characterized separately, and the human visual system could integrate the information from color channel and shape channel, which was a conscious and strategic response [4]. S. Shi et al. declared that the beauty reflected by color and shape was a kind of interdependent and incorporated comprehensive phenomenon, and the rational combination of them could strengthen the meaning of beauty experience in visual perception [5].

Some scientists did lots of researches to figure out whether the identification of an object was determined by its color or its shape, and it was finally found that shape mainly determined people's identification of an object, and color could only partly assist in identification process. In addition, previous studies also demonstrated that it would speed up identification process and increase identification accuracy if the color of the object being identified coincided with the real object's color, otherwise, the identification speed and accuracy would be delayed[6].

All researches above showed that color and shape did affect the identification process of objects. As an important part of our life, that how color and shape influence clothing identification really deserves our special attention. Consequently, an investigation on effects of color and style on clothing identification was carried out in this study, and the following problems were generally probed into:

(1) How color and style influence clothing identification;

(2) How color and style affect response speed of clothing identification;

(3) Whether there are any differences between male and female subjects in clothing identification.

Experiment

Equipments and Stimuli. The stimuli were presented by E-Prime 2.0 on a computer with a 17-inch screen at a refresh rate of 85Hz in a dimmed room. The distance between a participant and the monitor was about 60cm, and the height of each stimulus was 15cm.

In this study, pictures of 4 types of colored / achromatic clothes were used as stimuli, which were Colored Casual Wear (CCW), Colored Sports Wear (CSW), Colored Business Suit (CBS), Colored Formal Dress (CFD), Achromatic Casual Wear (ACW), Achromatic Sports Wear (ASW), Achromatic Business Suit (ABW) and Achromatic Formal Dress (AFD) respectively. In the behavioral experiment, each kind of picture displayed 30 times, and 240 pictures in all were presented in through the whole process. All pictures used in this study were downloaded from the Internet, and processed with a software called Photoshop 7.0, in order to make their backgrounds uniformly white (as shown in Fig. 1).



Fig. 1 Colored clothes and achromatic clothes samples

Participants. 60 undergraduate students from Soochow University in China (25 males and 35 females, aged between 19 and 25) participated in this study. All of them had normal or corrected-to-normal vision, and were absolutely unaware of the purpose of this study.

Procedure Design. The experiment consisted of two blocks. In one block the colored clothes were evaluated and in the other block the achromatic clothes were evaluated. Each trial had only one image, and the detailed procedure was as follows: at the beginning, a fixed cross was presented in the center of the computer screen for 100ms; after 400ms, 1 of the 120 pictures was randomly presented on the screen for 500ms in each block, and subjects had to identify the type of clothes shown in the picture during this period, and press “A” / “D”/ “J” / “L” (“A” represented Casual Wear (CW); “D” represented Sports Wear (SW); “J” represented Business Suit (BS); “L” represented Formal Dress (FD)) on the keyboard to input their identification results.

To ensure the precision of the results, subjects were divided randomly into two groups, and the sequence of the two blocks was arranged randomly[7].

Results and Discussion

Influence of Color and Style on Clothing Identification. Fig. 2 showed the influence of color and style on clothing identification accuracy. Through a two-way ANOVA of Type (colored, achromatic) × Style (CW, SW, BS and FD), it was indicated that color had no significant main effect on clothing identification ($F(1, 59) = 2.012$; $p=0.161>0.05$). That was to say, compared with achromatic clothes, colored clothes had no advantages in clothing identification at all. However, the identification accuracy of achromatic clothes was a little higher than that of colored clothes. It was likely because that during the identification of colored clothes, both color and style were important visual factors, so that subjects' attention might be slightly interfered with by color, but during the identification of achromatic clothes, style was the only visual factor, so that subjects just had to identify clothes' type based on the style, as a result, the higher identification accuracy was brought about.

The statistical result showed that style had a significant main effect on clothing identification ($F(1, 59) = 28.001$, $p=0.000$). The accuracy of identifying FD was the highest($M=0.959$, $MSE=0.008$), while the accuracy of identifying BW was the lowest($M=0.809$, $MSE=0.011$). It was indicated that subjects participated in this study might have some difficulties in identifying BW, which could be attributed to their lack of access and attention to it. As shown in Fig. 2, the standard deviation of CW identification was the largest while the standard deviation of FD identification was the smallest, which meant that the identification difference of FD among different subjects was the smallest while that of CW was much larger. This identification difference among clothes of different styles was likely caused by stimuli as well as definitions of CW and FD. CW is a kind of clothes which is commonly worn in our leisure lives, and all kinds of clothes different from formal wear are usually thought to be CW; FD is a kind of dress which is usually worn in ceremonial occasions, so that it has very distinct characteristics to be recognized. The definition of FD is narrow and detailed while the definition of CW is wide and unspecific, therefore, there was a great identification accuracy difference between them.

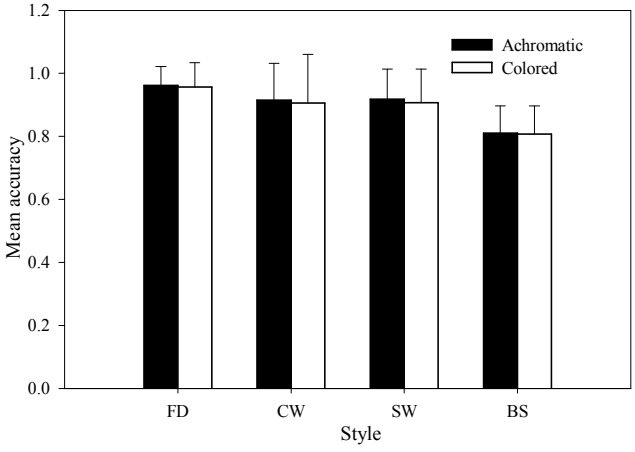


Fig. 2 Mean accuracy of indentifying 4 types of clothes

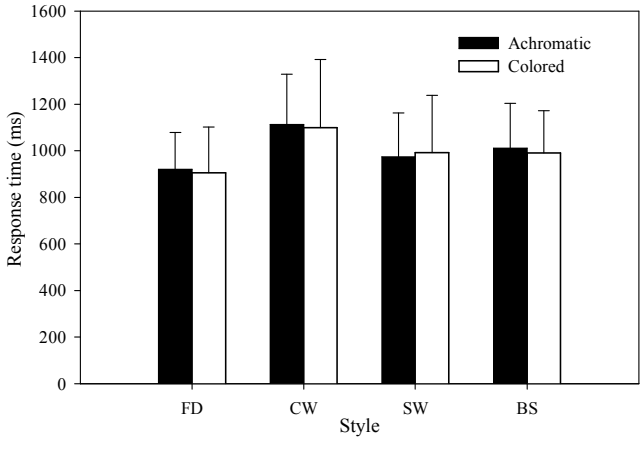


Fig. 3 Response time difference in clothing identification

Influence on Response Time of Clothing Identification. Fig. 3 showed the response time difference between identifications of colored and achromatic clothes. The statistical result indicated that color had no significant main effect on response time ($F(1, 59) = 0.051$,

p=0.822＞0.05). As shown in Fig. 3, for FD, CW and BS, color didn't make any contributions to promoting identification speed, but for SW, the identification speed of colored clothes was a little higher than that of achromatic clothes, therefore, color seemed to partly facilitate clothing identification.

The statistical result also indicated that style had a significant main effect on response time (F (1, 59) = 36.341, p=0.000). The response time to identify FD was the shortest while the response time to identify CW was the longest. This result suggested that it was much more difficult to define sportswear than to define formal dress, and it confirmed the previous conclusions.

Influence of Gender on Clothing Identification. In this article, behaviors of male and female subjects in clothing identification were compared. Fig. 4 showed the identification accuracy difference between female and male subjects. Generally, for both colored and achromatic FD, SW and BW, the accuracy of identification made by female subjects was higher than that of identification made by male subjects, but for CW, there seemed to be no difference in identification accuracy between female and male subjects.

Fig.5 showed the response time difference between female and male subjects in clothing identification. It was obvious that for each type of clothes, no matter it was colored or achromatic, female subjects responded more quickly than male subjects. That was probably due to two reasons: on the one hand, male subjects paid less attention to clothes; on the other hand, male subjects' experience in clothing color and style was relatively less than female subjects, and the absence of experience made it hard for male subjects to indentify clothing types accurately.

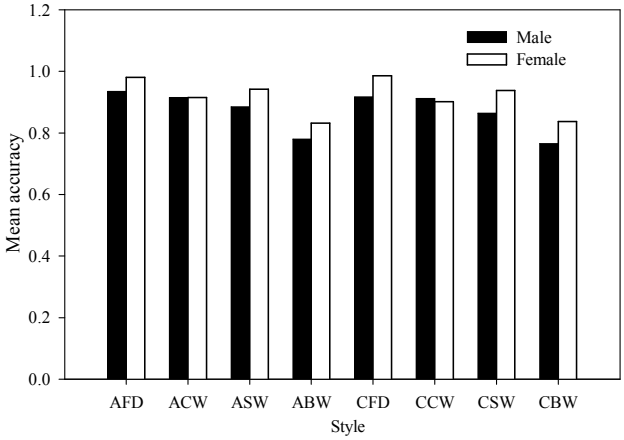


Fig. 4 Accuracy difference between men and women

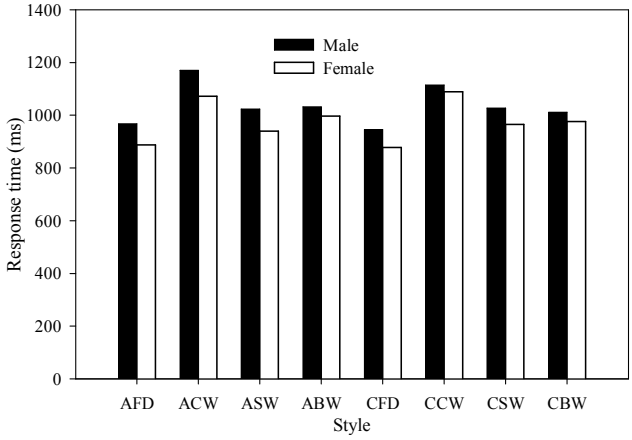


Fig. 5 Response time difference between men and women

In this study, all results above showed that color had no significant influence on clothing identification, while style had a great influence on it. It was indicated that style played a decisive role in clothing identification, and this finding was in accordance with the previous research results.

In fact, in Liu et al.'s study, it was discovered that an individual responded more accurately and quickly when he identified an object with similarly inherent color[8]. It was indicated that the inherent color existing in human's consciousness affected human's identification of an object. However, in present study, color was found to have little influence on clothing identification accuracy and response time. It was probably because clothes didn't have any inherent colors in

human's consciousness, and clothes with any kind of color were easy to be accepted by people. Additionally, that style had a significant influence on clothing identification accuracy and response time indicated that style played an important role in clothing identification.

Conclusions

(1) Style played a decisive role in clothing identification, while color seemed to make little contributions to it;

(2) Style had a great influence on response time in clothing identification, while color had slight influence on it;

(3) There was a were great differences in both identification accuracy and response time between men and women, and that women responded more accurately and quickly than men indicated that women were more experienced in clothing identification than men.

Acknowledgements

This work was funded by the First Phase of Jiangsu Universities' Distinctive Discipline Development Program for Textile Science and Engineering of Soochow University.

References

[1] Information on http://wenku.baidu.com.

[2] X. Ke, X.J. Bai and N. Sui: Psychological Science, Vol.31 (2008), p.336

[3] X.T.Ou-yang, D.G. Li, Q.Y.Hong, and S.X.Gao: Acta Biophysica Sinica, Vol.7 (1991), p.571

[4] A. Hanna and R. Remington: Memory & Cognition, Vol.24 (1996), p.322

[5] S. Shi: Journal of Donghua University (Social sciences), Vol.3 (2003), p.45

[6] L.H.Wurm, G.E. Legge and L.M. Lesenberg: Human Perception and Performance, Vol.19 (1993), p.899

[7] X.F. Jiang, G.L. Liu, F. Qin and S.S. Wang: 2010 Sixth International Conference on Natural Computation, (2010), p.1979

[8] A.T. Liu, et al.: Neuroscience Letters, Vol.469 (2010), p.405

© (2011) Trans Tech Publications, Switzerland
doi:10.4028/www.scientific.net/AMR.331.694

Rising labor cost and the comparative advantage of Chinese textile industry analysis

Jin WANG[1, a]

[1] School of Business & Management, Shaoxing University, Shaoxing, Zhejiang, 312000, China

[a] wj2800@163.com

Keywords: comparative advantage, Textile Industry, labor cost, Competitive Advantage

Abstract: The textile industry is a typical labor-intensive industry, which is also one of the most comparative advantage industries of China. However, with rising labor cost in recent years, the comparative advantage of Chinese textile industry is facing challenges. Based on the theory of comparative advantage analysis, this article analyzes of the comparative advantages of Chinese textile industry based on the background of rising labor cost while propose that Chinese textile industry shall transfer the Comparative Advantage to Competitive Advantage.

Comparative Advantage Analysis and Its Development

1.1 Summary of comparative advantage theory

1817, British economist David Ricardo in his <<Principles of Political Economy and Taxation>> propose the comparative advantage theory, of which international trade is based on the relative differences in production technology and the result of Differences in the relative costs of production; whatever development state of a country or region be, Each country should act according to the principle that "take the heaver of the two advantage and take lighter of the two disadvantage". They shall participate in international division combined with their advantage, focusing on produce and export their comparative advantage products, and import their comparative disadvantage products. So that international resources can be effectively used, thus both can gain from trade. Comparative advantage theory develops from the absolute advantage, which based on a more general speaking explains the basis of trade and how trade profits generated.

But what causes the comparative cost is different when different countries produce different production? Comparative cost theory does not offer answer. Heckscher and Ohlin create the theory of factor endowments, from which perspective explains the comparative cost difference. They believe that differences in factor productivity between countries determined by the relative stock of factors. These different elements supply will affect production cost of specified commodities. Therefore, countries should produce and export relatively abundant element intensive products, while importing relatively scarce elements goods. For example, if a country or region is relatively rich in labor, lack in capital, it should develop labor-intensive industries and produce or export relatively labor-intensive products; conversely, if relatively abundant in capital, labor relatively scarce, then it should develop capital-intensive industry and produce or export of capital-intensive products. The comparative advantage theory explain the most important reason for international trade, the theory also has been developed among the following days.

1.2 The development of comparative advantage theory

Since 1990s, economists represented by XiaokaiYang has been rethinking traditional trade theory and breaking though the traditional framework of the comparative advantage theory, emphasizing both the inner and dynamic nature of comparative advantages, at the same time, based on the different productivity between before and after, they divide the comparative advantage into endogenous and exogenous comparative advantage. Endogenous comparative advantage can be acquired through learning or professional experience through technological innovation and the accumulation of human created, and endogenous comparative advantage is selected by the professional level after generation.

The specialized division led to the accumulation of human capital and knowledge, thus creating endogenous comparative advantage; that endogenous comparative advantage may be the same in the natural conditions of production completely equal between countries. A given difference in technology and endowments of comparative advantage is exogenous comparative advantage, which caused by differences in natural conditions, producing a special trade benefits. The difference is led by the advance. Endogenous Comparative Advantage emphasizes the dynamics of comparative advantage, on the other words, as the division of labor rising, the level of endogenous comparative advantage being developing. Therefore, this based on division of labor development and continuous creating comparative advantage is significant. It has become a source to a country's trade development and sustained economic growth.

2. The comparative advantages of Chinese textile industry analysis

2.1 The status of the Chinese textile industry

China is the world's largest textile producer and exporter. And its textile industry is also one of the comparative advantage industries. As the pillar industry of national economy and an important livelihood industry for a long time, the textile industry plays an active role on meeting the people's need of living, absorbing labor and capital accumulation. Meanwhile, Chinese textile in China's foreign trade and international textile market also occupies an important position. The data from the table is evident.

Table 2-1: 2004-2009 Chinese textile import and export trade situation (billion U.S. dollars)

project	2004	2005	2006	2007	2008	2009
	Textile of nation account for%	Textile of nation account for%	Textile of nation account for%	Textile of nation account for%	Textile of nation account for%	Textile of nation account for%
Import & export	9.89	9.47	9.38	8.94	8.13	8.3
export	16.41	15.42	15.18	14.42	13.27	13.43
import	2.99	2.59	2.28	1.96	1.65	2.16

Data sources: China Statistical Yearbook 2008, 2009 arrange

Concluded from Table 2-1, textile exports account for about 15% of the Chinese export trade from 2004 to 2009. Thus to say, the textile industry is the main force of China's foreign trade. And it's one of the important forces on driving China's foreign trade export. Textile export is not only accounting for a large proportion in China's exports but also plays an important role on the global textile trade. Its export volume rank first in the world for many years.

Table 2-2: The status of China's textile exports among the global textile trade in 2004-2009 (unit: billion U.S. dollars)

year	Global textile trade	Chinese textile exports	China accounted for%
2004	4545.3	952.9	21
2005	4786.1	1152.1	24.1
2006	5300	1440.7	27.2
2007	5834.3	1712.1	29.3
2008	5538.5	1602.1	28.9
2009	5637.7	1691.3	30

Data sources: According to the China Textile Industry Development Report 2008/2009, WTO site arranging

Concluded from Table 2-2, Chinese textile almost takes up 30%.of the world textile market share. Thus, China is a big country of manufacturing and exporting the world's textiles. Seen from the current share of Chinese textiles in global textile market, China's textile industry has a strong competitive power.

2.2 The comparative advantage of China's textile industry

For a long time, comparative advantage theory has been an important theoretical basis of national industrial development strategy. Three decades from reform and opening up, the reason for China's textile industry has been able to rapidly develop is that it followed the strategy of comparative advantage. According to the traditional trade view of comparative advantage theory, all parties to participate in international trade, should take its comparative advantages to participate different industry division production and trade different types of products with partners to gain trade interests. Labor is the most abundant production factor of china, meanwhile it’s generally believed that exporting labor-intensive products is comparative advantage of China. This is true. So far, net exports of China are mainly labor-intensive products, of which textile and apparel is net main exports of China.

Textile industry is a typical labor-intensive industry. China owns a huge labor resource of which has a large population. At the same time, compared with developed countries and many developing countries, Chinese labor price is very low. Given 2007 for example, average wage of workers in the textile industry of China is $ 0.785 / h, not only lower than the U.S., Japan and other developed countries, but also much lower than South Korea, Hong Kong, Taiwan and other regions. Therefore Chinese textile has obvious comparative advantage on labor cost. The competitiveness of Chinese textile industry is mainly presented on use of abundant cheap labor and strict control of labor costs. We ca say that the rapid development of the textile industry in China is the natural selection of factor endowments composition. Depending on exogenous comparative advantage in resource endowment is the main source of Chinese textile industry competitiveness at present stage.

Although China has already become the world's largest textile producer and exporter, but hidden behind the rapid growth is that textile industry of china has been relying on low-cost expansion of the extensive model of development style. Growth of trade in textiles led only in the number of industries development, however, lack of technology, brand and effect of management. On the same side, it also lacks in technology, knowledge elements to drive the formation of endogenous comparative advantage. Among the global textile industry chain, Chinese textile is still in the low end of value chain. The United States, European Union, Japan and other developed countries occupy the high end of the world textile market and maintain an overwhelming competitive advantage. Among the low-end market, while textile and garment industry of well-developed national transferred to developing countries, China has been from the strong competition of developing countries with similar comparative advantage.

3. The challenge to the textile industry’s comparative advantage by the rising cost of labors

As the development of economy in China, the labor cost at home is also rising per year, so the traditional comparative advantage depended on by textile industry for a long time is upon decreasing. First of all, the structure of labors in china also shows the dynamic changing feature. Since The 1980s, farmers have come into the cities for working in large amount. As the Chinese textile industry contains plenty of labors from the countryside, this part of “migrant workers” have become the source of labor cost’s advantage in Chinese textile industry. But after more than 30 years of reform and opening up, the symptoms of labor shortages will become more and more serious from the view of structure. Lacking for workers in the textile industry has already made the operations turn into difficult conditions, especially in recent years. So the enterprises may face the problem of the shortages of workers, if the salary is not improved.

Secondly, the improvement of consumption level of citizens. With the quick development of Chinese economy, people's living levels has also raised up continuously. And as the demand of materials among people is growing, the consumer price index has shown a increasing trend in every year. Especially in recent years, with the faster rising price, the laborers' consuming spending may increase significantly and the labor wage level also must improve in order to maintain his basic life. Therefore, higher labor costs are an inevitable trend.

Thirdly, the "Labor law" has been implemented. On January 1, 2008, the new "Labor Law" came into implementation. And on some sides such as protection of the laborers' interests ,the free flows among laborers, the balance of interests in capitals etc, it maintains the interests of the workers better, and also enhance the harmony degree between the social goals and economic target, but to a certain extent in the short terms, it will bring about the pressure of labor cost to enterprises, which mainly embodied in the labor contract signed by the enterprises and the employees, the health insurance bought for the staff, the standardized working hours and the multiplied growing of overtime payments. Obviously, if textile enterprises technical level is not improved in the short term,the production efficiency can't get promoted, it will face pressure of higher labor costs. Table 3-1 reflects the textile industry salary change in the years of 2002-2008.

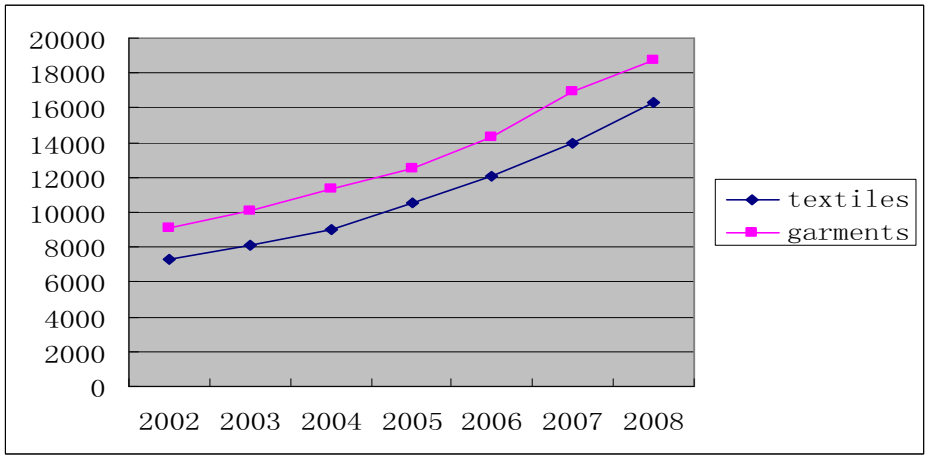


Fig1-1 The average wage of the whole textile and apparel industry
Data sources: http://www.bls.gov/fls/china.htm

Fig1-1 shows that the average wage of whole industry is increasing year by year, about 16% per year increasing since 2002， especially after 2005.

4. The transformation from comparative advantage to competitive advantages

At present, though China's textile industry has the comparative advantage of labor resources, the comparative advantages in the international competition do not have a competitive advantage. For there is a fact that labor costs in textile industry is rising, it will affect the play of comparative advantage in China's textile industry. Therefore, to maintain the comparative advantage of Chinese textile industry and make textile industry to sustainable development, it needs to achieve the transformation from comparative advantage to competitive advantage.

4.1 Adjust the trade orient

The difference between comparative advantage and competitive advantage is that products having comparative advantage do not necessarily have the competitive advantage. China now has comparative advantage in abundant labor resources, but this doesn't mean the competitive advantage of foreign trade in China is labor-intensive products. For a long time, China's textile industry participates in the international competition, and its' trade structure is based on its own supply conditions, such as abundant supply of labor, with resources endowment (such as cheap labor) as the guidance. This kind of comparative profits structure may made national textile industry get some trade interests in a time, but it strengthened the low level industrial structure of textile industry, let the

trade structure not stable and in a disadvantageous position of the international division, which finally entered the "comparative advantage trap" . Therefore, China textile industry must adjust guidance, namely to international trade market direction, improve the structure of products, improve the level of product quality, provide ones having competitive advantage in international market and make the Chinese textile competitive advantage .

4.2 Create endogenous comparative advantage

Endogenous comparative advantage is that the comparative advantage can be acquired through professional learning or through technology innovation and accumulated experience. If China's textile industry always makes the congenital productivity differences (such as the comparative advantage of labor costs) as the conditions of division, it will lead trade products, trade direction and trade pattern to be static, which is also the basic reason existing comparative advantage trap in a certain degree. If you want to jump out of the trap of the comparative advantage trap, we must make the textile industrial comparative advantage dynamic evolved, so the China's textile industry will develop quickly. Based on the biochemical theory in the comparative advantage of YangXiaoKai, China's textile industry should strengthen the inputs on human capitals and technology, improve the intensity of textile industry technology, make it transform from simple labor-intensive into intelligence labor-intensive one; strengthen the independent innovation, introduce advanced and new technology, combine the high and new technology with China's abundant and cheap labor, create the endogenous comparative advantages, which may improve continuously with the development of division, and become the source of the textile industry development and trade growth. At the same time, this kinds of endogenous comparative advantages in the continuous evolution also can push the upgrading of China's textile industry value chain, making the textile no longer a simple labor-intensive products, which is that not only has the advantages of labor costs, but also has the advantages of technology and brand, turning itself to the high technical labor-intensive products, so as to realize the transformation from the comparative advantages to competitive advantages.

References

[1] Kun Wang LI. International economics [M].Beijing: higher education press,2009.6(In chinese).

[2] Yin Xing Hong. From comparative advantage to competitive advantage—With theory of comparative advantage's defect of international trade [J]. Economic research, 1997(6),(In chinese).

[3] Xiao Kai Yang, Yong Sheng Zhang. The new trade theory, the theory of comparative advantage and new findings of experience research: literature review. Economics quarterly, http//www.ccer.edu.cn (In chinese).

[4] Jia Liu, FeiXiang Chen. The path selection of dynamic conversion on achieving comparative advantage in China [J]. Finance and trade research 2006(1),(In chinese).

[5] Shu Bo Zhao, JiangYunHu. The analysis of Chinese textile industry security situation[J]. International economic cooperation. 2009(6) (In chinese).

[6] QingDu. Analysis of the international competitiveness and the influence factors of China' textile [J]. Chinese economy and trade, 2010(2) (In chinese)

[7] MingLi Li. The current export situation of textile industry in China and the enterprises' countermeasures [J].New finance (theory version), 2010, (5) (In chinese).

[8] Meng Nian. China's textile industry status and analysis [J]. Commercial economy, 2009 (In chinese).

© (2011) Trans Tech Publications, Switzerland
doi:10.4028/www.scientific.net/AMR.331.699

The Molding Technology Of Manufacturing Waste Blend fiber Composites By Mixed Hotpressing

Lihua Lv[1, a], Guangjian Wan[1,b] and Yongling Yu [1,c]

[1]Green fiber applied technology institute, Dalian Polytechnic University, Dalian 116034, China

[a]dllvlh1978@163.com, [b]wgj-357@163.com, [c]dlyyling@163.com

Keywords: Waste blend fibers; polyester/cotton/hemp; polypropylene; mixed hotpressing; mechanical properties

Abstract. For the waste polyester/cotton/hemp blend fiber of largest abandoned number,this paper designed and optimized the molding technology of manufacturing waste blend waste composites by mixed hotpressing,and analyzed the mechanical properties of composites. Through the orthogonality experiment,the optimum conditions were given as follows:the ratio of waste blend fabrics 1:1,the Concentration of PP 60%,the temperature of hotpressing 185˚C，the hotpressing pressure 12Mpa, the hotpressing time 5min. Under above conditions,the composites had the density 0.9326g/cm2,the tensile strength 45.37Mpa, the bending strength 48.31Mpa and the energy absorption of impact 15.32 KJ/m2.

Introduction

As a big production and consumption country of fiber, China not only produce considerable quantity of various fiber on their own, and still need a large number of imports every year. As people living standard rise,the lifecycles of textile becomes shorter and shorter,producing a large number of old clothes and cutting corners from textile factory.This causes a striking waste,and not only prodcues more and more serious pollution[1-4],but also hides danger of fire disaster. So how recycling these waste to manufacture the products of high value-added is a urgent task to the researchers.

Commonly three methods are used to treat the textile waste in domestic and international: combustion method, degradation method and regeneration method[5-7]. Combustion method is burning the textile waste in the incinerator,recycling the heat.The special combustion equipment of this method need a huge one-time investment,and has high technical difficulty; Degradation method is developping and manufacturing degradable fiber in the source of production of textlie,then then process into various kinds of textiles,in order to treat such waste.This method with high technological content is expensive and hard to popularize; Regeneration[8] method is process some textile waste in a certain way,reworking to available products,it is a better way to recycle the textile waste.In this paper,waste polyester,cotton,hemp and polypropylene fiber as raw material used to manufacture blend fire composites by mixed hotpressing is the best way to slove above problems.In this way,it avoids separation problem,and can make use of mixing effect to improve the mechanical properties.

In this work,waste polyester,cotton,hemp and polypropylene fiber composites are manufactured by mixed hotpressing method and its mechanical properties are studied.On the one hand,it utilizes the resourse rationally,solving the contamination of textile waste to the environment, with good social benefits.On the other hand,the new materials with goog performance can satisfy the needs of many areas such as ships, the electromechanical, building materials, furniture, automobile,getting good economic benefit.This reaserch conforms to the strategic requirements of the circular economy, low cost processing and sustainable development of our country.

Experimental

Experiment materials

(1) Polyester/cotton/hemp reinforced materials:selected from Dalian Xindi texile factory's abandoned fiber,and the ratio of Polyester/cotton is 65/35,the ratio of cotton/hemp is 55/45.

(2)PP matrix material:selected from Dalian Jinlun chemical fiber hi-tech Co.Ltd's abandoned PP fiber.

Experiment equipments

Digital sample spinning system (DS series)，Fast spinning system(Y015F/F102B), Plate vulcanizing press(QLB-50D/Q), Universal sample maker(RGT-5), Cantilever impact test enginery(UJ-40), Computer controlled electronic universal testing machine (GT-5).

The molding technology Of composites

Waste blend→Loosening→Mixed into a bar→Vertical cross to spread Fiber net→Hotpresssing→ Preparation→Pressing composites in the Thermal press→Cooling and solidification→Sample preparation and testing

Detection index and method

Test mechanical properties of samples maked by universal sample maker. Tensile strength test according to GB/T 1040-1992, bending strength test according to GB/T 1449-2005, impact energy absorption test according to GB/T 1451-2005.

Results

Orthogonal test

To optimize the molding process of mixed hotpressing method to manufacture the waste fiber composites,a orthogonal test table(L9(34)) was made, it took the ratio of waste blending fabric(the ratio of polyester-cotton fabric and polyester-hemp fabric),concentration of PP fiber,hotpressing temperature,hotpressing pressure as factor,and took tensile strength,bending strength,impact energy absorption as detection index,as showen in the Table1.

Table1 Results and analysis of orthogonal experiment

NO.	Ratio of waste blending fabric	Concentration of PP fiber(%)	hotpressing temperature (˚C)	hotpressing pressure (Mpa)	tensile strength (Mpa)	bending strength (Mpa)	impact energy absorption ($KJ \cdot m^{-2}$)
1	1:0.5	55	180	10	21.25	25.13	4.62
2	1:0.5	60	185	12	32.47	36.42	7.21
3	1:0.5	65	190	14	23.55	27.21	4.93
4	1:1	55	185	14	46.27	50.18	8.54
5	1:1	60	190	10	42.03	46.36	8.27
6	1:1	65	180	12	35.94	39.74	7.85
7	1:2	55	190	12	30.26	34.11	6.64
8	1:2	60	180	14	25.68	29.27	5.83
9	1:2	65	185	10	24.15	28.34	5.49
Mean 1 impact energy absorption	5.587	6.600	6.100	6.127			

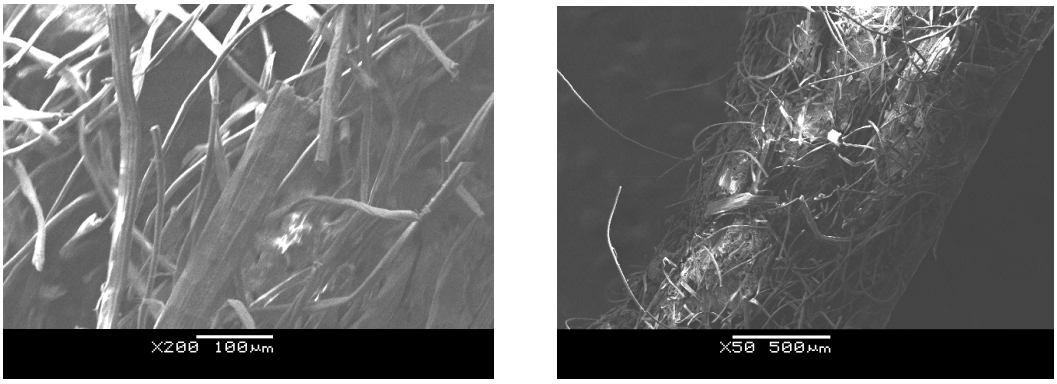
Mean 2 impact energy absorption	8.220	7.103	7.080	7.233
Mean 3 impact energy absorption	5.987	6.090	6.613	6.433
Range	2.633	1.013	0.980	1.106
Optimum level	A_2	B_2	C_2	D_2
Important order	*A>D>B>C*			
Mean 1 tensile strength	25.847	32.683	27.713	29.233
Mean 2 tensile strength	41.413	33.393	34.297	32.890
Mean 3 tensile strength	26.697	27.880	31.947	31.833
Range	15.566	5.513	6.584	3.657
Optimum level	A_2	B_2	C_2	D_2
Important order	*A>C >B>D*			
Mean 1 bending strength	29.587	36.473	31.380	33.277
Mean 1 bending strength	45.427	37.350	38.313	36.757
Mean 1 bending strength	30.573	31.763	35.893	35.553
Range	15.840	5.587	6.933	3.480
Optimum level	A_2	B_2	C_2	D_2
Important order	*A>C>B>D*			

★Hotpressing time 5 min。

From the orthogonal experiment and range analysis we learned that the order of effect of each factor on impact energy absorption of composite was A>D>B>C, on tensile strength was A>C>B>D, and on bending strength was A>C>B>D. After comprehensive consideration,we selected the better processing conditions of waste polyester,cotton,hemp,PP fiber composite:the ratio of waste blending fabric 1:1,hotpressing temperature185˚C， the concentration of PP fiber 60%,hotpressing pressure 12Mpa,hotpressing time 5 min.The density of composite made by this condition was 0.9326 g/cm2.

Interface analysis

In order to observe the interface(the composite made by best molding technology) between matrix material(PP) and reinforcements(polyester,cotton,hemp),SEM observation was used,the result is shown in figure1.



Low power High power

Figure1 SEM grahics to the tensile section of composite

Conclusion

1. This paper design the technics process of manufacturing of waste polyester, cotton,hemp/PP composite rationally:

Waste blend→Loosening→Mixed into a bar→Vertical cross to spread Fiber net→Hotpresssing→ Preparation→Pressing composites in the Thermal press→Cooling and solidification→Sample preparation and testing

2. Through orthogonal experiment,the technological condition of manufacturing waste polyester,cotton,hemp/PP composite by mixed hotpressing was optimized: :the ratio of waste blending fabric 1:1,hotpressing temperature185˚C，the concentration of PP fiber 60%,hotpressing pressure 12Mpa,hotpressing time 5 min.In this condition,the density of composite made was 0.9326 g/cm2,tensile strength was 45.37Mpa,bending strength was 48.31Mpa,impact energy absorption was 15.32 KJ/m2.

Acknowledgements

The authors of this paper gratefully acknowledge financial supports from the Education Department of the Government of Liaoning Province (LT2010011).

References

[1] Yufa Qiu.Jiangsu Textile.2007:68-69.(In Chinese)

[2] Xuemin Hu, Haiyan Zhang. China Textile Leader,2006,7:52-53. (In Chinese)

[3] Xiaoqing Wu, Guanxiong Qiu, Jialu Li etc. New Building Materials,2002,5:44-46. (In Chinese)

[4] Yongjiang Wang.Recycling in textiles[M].Woodhead Publishing Limited,2008,1-5. (In Chinese)

[5] Gowayde Y A,Vaidyanathan R,El-Halwagi M.Elastomers and Plastics,1995,2:79-90.

[6] Kotliar A,Michielsen S.Utilization of waste fibers in laminates,US Patent 5912062,1999.

[7] Yanmin Gao,Wang Shaoming,Chen Lizhuang. Industrial Textile,2005,8:10-14. (In Chinese)

[8] Qiuwen Feng, Guanxiong Qiu.Reaserchs of molding process and properties of waste textile fiberboard[D].Tianjin: Tianjin Polytechnic University，2002. (In Chinese)

© (2011) Trans Tech Publications, Switzerland
doi:10.4028/www.scientific.net/AMR.331.703

Study on Water-based High Reflectivity Insulation Coating

Ya-fen Luo[1, b], Zhao-qun Du[1, a] and Wei-dong Yu[1, c]

[1]College of Textiles, Donghua University, Shanghai 201620, China

[a] duzq@dhu.edu.cn,[b]luoyafen1021@163.com,[c]wdyu@dhu.edu.cn

Keywords: Flake aluminum powder, silane coupling agent, titanium dioxide, reflectivity, thermal insulation.

Abstract. A solar heat-reflective insulation coating method was investigated based on coating morphology, membrane material and the type of insulation pigments as well as pigment to binder ratio affecting the performance of thermal insulation. It used solar heat reflectivity and infrared spectroscopy to characterize the coating thermal insulation performance. The results showed that the average reflectance of visible light and the UV reflectance and the infrared reflectivity are 56%, 53% and 58% with the silane coupling agent for the bonded dispersant, the flake aluminum powder and titanium dioxide for the thermal insulation filler, together with water and additives.

Introduction

Solar energy is essential for human living, but the intense radiation also brings many problems to industrial production and daily lives. To meet with the rapid development of construction industry, a related insulation coating researches have been investigated for wide application [1, 2].

Thermal insulation coating can be divided into thermal barrier coatings, reflective coatings and radiation-based heat insulation coatings so as to reduce the accumulation of internal heat and to save energy [3]. The reflective insulation coating is the most practical value coating method among the three types [4]. However, there are still many problems on the reflective insulation coatings. Reflective insulation coating is still basically solvent application system, water need to be developed into the reflective insulation coating with high cost. Moreover, there is no standard method for the light and heat reflective performance on the reflective coatings.

Therefore, the paper aims to develop a water-based heat-reflective coating method to improve its insulating properties with low price. This coating can meet insulation, climate and decorative functions, so as to achieve energy saving effect.

Experiment

Materials and Equipment. Materials include silane Coupling Agent KH-560; flake aluminum powder; Titanium dioxide; Ethylene glycol; sopropanol; Triethanolamine (TEA); Ethanol; Thickener; demonized water. Equipments include dispersion machine; DDS-307A conductivity meter; JSM-5600LV SEM; Hitachi U4100 spectrophotometer; FA2004A Electronics Balance.

Structure and Performance of Aluminum. It can be seen from SEM images of aluminum powder in Fig. 1 that the sample particle size distributes in the 2μm-20μm, the flake aluminum powder is the micron particles. The aluminum powder distributes overlapped into a sheet, covering the surface completely, and particles rarely reunion.

Coating Preparation and Testing. The coating formula was listed in Table 1. The preparation firstly added pigment into dispersant with high stirring speed; then, added the diluted silane coupling agent and other additives to mix with a slow stirring speed. Reflectivity of coating was measured based on infrared light irradiation and UV-visible-infrared spectrophotometer.

Table 1 Formulation of the coatings

Reagents / materials	Amount w/%	Conductivity（μm/cm）
Silane Coupling Agent KH-560	2%~25%	0.01
flake aluminum powder	5%~20%	
Titanium dioxide	1%~5%	
Ethylene glycol	15%~30%	
Ethanol	appropriate amount	1.41
Thickener	appropriate amount	
Deionized water	appropriate amount	0.4

Results and Discussion

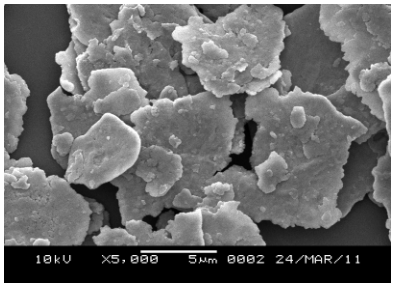
Base Material. Silane coupling agent (SA) is an improving type of additive which can combine two different materials with physical and chemical effects on improving coating surface performance and corrosion performance [5], accompanying the hydrolysis and condensation reactions [6]:

$$R\text{-}Si(OR)_3 + \text{excess } H_2O \Leftrightarrow R\text{-}Si(OH)_3 + 3ROH \quad (1)$$

$$R\text{-}Si(OR)_3 + R\text{-}Si(OR)_3 \Leftrightarrow R\text{-}Si(OH)_2OSi(OH)_2R\text{-} + H_2O \quad (2)$$

The condensation between silanols reduces the number of silanol and decreases the conductive of silanol and pigment. So, it should minimize the condensation reaction the dispersion process [7].

Detection of Hydrolysis Degree of Silane Agent Coupling. Fig. 2 shows hydrolysis of different ratios of silane coupling agent KH560 in neutral conditions by the conductivities of deionized water and silane coupling agent KH-560 and Ethanol listed in Table 1. When KH560: water: ethanol = 1:1:1, the system conductivity gradually increases with the hydrolysis, and reaches the maximum on 27 h, indicating that silane coupling agent has been hydrolyzed completely. Then, the conductivity decreased rapidly by condensation. When the concentration of KH560 reduced to 10%, the conductivity increased gradually with time. The system conductivity reduced slightly 30 h later, indicating that silanlol has a condensation reaction, then the reaction reached equilibrium and the system is stable. As the silane concentration increased, the conductivity increased slowly. While diluted, after 100 h hydrolysis, the solution doesn't appear muddy. So coupling agent can disperse particles after 3 h hydrolysis process and generate enough alcohols to combine with particles.



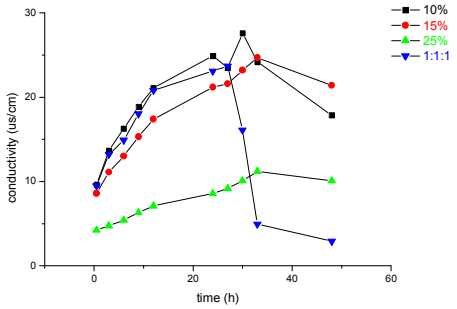


Fig. 1 SEM image of Aluminum sheet Fig. 2 Effects of silane coupling agent KH560 hydrolysis

Aluminum Powder Infrared Spectra (FT-IR) Analysis. Fig. 3 and Fig. 4 respectively show the aluminum coating in the infrared spectrum. It can be seen from Fig. 3 that an absorption peak appears in the 2500~3600cm^{-1}, indicating the existence of –COOH on aluminum powder surface for being lubricated by fatty acids. From the infrared spectrum in Fig. 4, there is a –NH vibration peak

in the 1650~1550cm^{-1}, indicating the existence of KH-560; in 1100~1200cm^{-1}, it appears Si-O-Si absorption peaks; in1600~1700cm^{-1}, it occurs the Si-O-Al absorption peaks. The above groups mentioned show that the silane coupling agent coated on the aluminum surface.

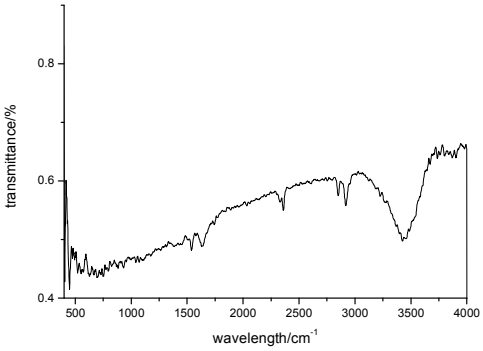


Fig.3 Aluminum powder infrared spectrum

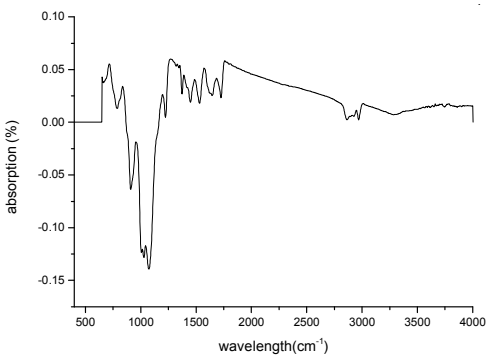


Fig.4 Aluminum powder infrared spectrum

Detection of Reflection Properties

Effects of Flake Aluminum Powder on Reflection Properties. Fig. 3 shows different ratio of aluminum in coating. With the appropriate increase of the aluminum content, they can overlap to form a better surface. We use the silane coupling agent as a dispersant and binder in this topic, keeping the other experiment conditions in a stable state, changing quality of pigments and the ratio of coupling agent, and then changing the pigment in the share of the dry film, as shown in Fig. 4. It can be seen from Fig.4 that coating reflectivity decreased with concentration of silane coupling agent increasing. Generally when the amount of the pigment is little, with the increasing amount, the thermal insulation performance is gradually increasing. This is because the pigments and fillers have a reaction with the silane coupling, and form a silicon-oxygen metal bond, generating a film on the surface. While the silane hydrolysis product silanol can condense with each other, generating a network structure covered on the substrate surface. While increase the concentration of silane coupling agent, it may be because the silane hydrolyzed a small number of silanol and aluminum produce less metal bonds with the silanol. It may be the aluminum surface wrapped by a layer of coupling agent and affects the reflection of aluminum. It can be the silanol molecules condensation rather than to play the role of pigment dispersion and binding, so the coating appears voids and defects. These make the insulation performance decreased.

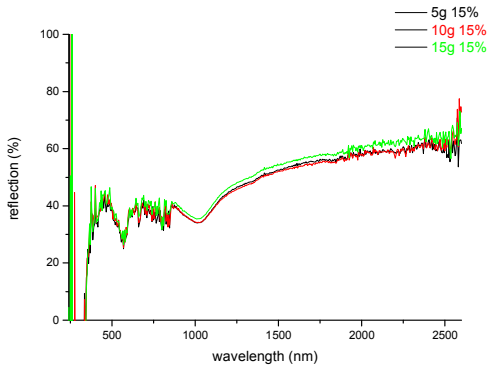


Fig. 3 Reflection of different Al ratio

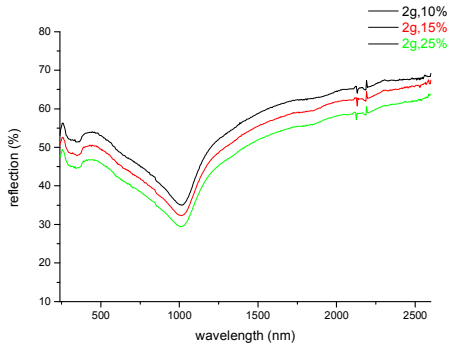


Fig. 4 Reflection of different silane coupling agent ratio

Titanium Dioxide on the Reflection Properties. The titanium dioxide has the most stable thermodynamic in coating system and has a higher refractive index for visible light. Obtained from the experimental, titanium dioxide is one of the necessary pigments in heat-reflective coating. For

practical application, we initially selected the titanium dioxide as one of the pigments, used the polyol TEA as bridge, and modified the surface of titanium dioxide and increased the surface hydroxyl groups to nano particles. It will improve dispersion in aqueous media. Then, we added silane coupling agent with different ratio of titanium dioxide to make high-concentration aqueous and coat it on the specimen and the insulation was tested after dried. It can be seen from Fig. 5 that with the titanium dioxide content increasing, the coating insulation gradually increased. Compared with reflectance spectra of aluminum flake, titanium dioxide has a high reflectivity in the visible range 400 ~ 800nm, the average reflection rate was 59%.

Effects of Ratio of Titanium Dioxide and Flake Aluminum Powder on Reflection Properties. As it shows in Fig. 6, the reflectance increased compared with titanium dioxide, while decreased slightly compared with aluminum power in the near infrared part. When titanium dioxide and flake aluminum used together, the reflection spectra are complementary. In the visible range, titanium dioxide plays a major role; the reflection has an increase rate. So we can conclude titanium dioxide content increasing will contribute to visible and near infrared reflectance. The flake aluminum powder content is less; the titanium dioxide can effectively cover the gray color. Flake aluminum powder can be formed as overlapping structure on the coating layer to form an effective thermal barrier so as to play better insulation effect. However, when the flake aluminum powder content continues to increase, the absorption increases and coating insulation performance degraded again.

Summarized experimentally, initially identified the thermal insulation coating composition of pigments and fillers as: the ratio of titanium dioxide and aluminum flake is 5:2~3:1. In addition, accounting for 20% ~40% of the total paint coating of silane coupling agent will increase the coating adhesion and outdoor durability.

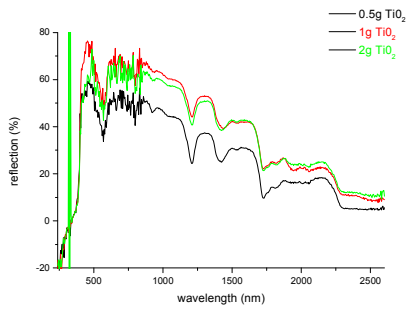


Fig. 5 Reflection of different titanium dioxide ratio

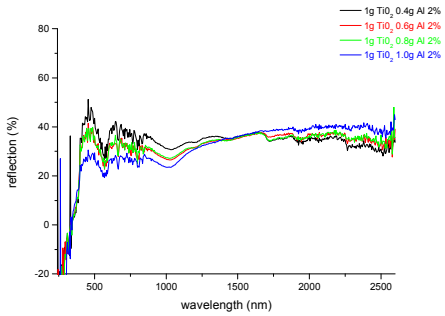


Fig. 6 Reflection of two kinds of fillers

Conclusions

(1) Different types of film forming have less influence on the coating insulation properties; the water-based silane coupling agent has a good transparency as well as low refractive index, so the coating thermal insulation is very good. (2) Flake aluminum power used in this study was silver, but mixed with titanium dioxide, it can achieve a good insulation effect and a low product cost. (3) When the content of pigments and fillers in the paint is less, the coating thermal insulation gradually increased with the increasing amount of its accession. When the content of pigment is more than 40%, particles can not be completely dispersed and exist voids and defects in the coatings. So the heat insulation performance decreased.

References

[1] Santamouris M, Pavlou K, Synnefa A: Energy and Buildings Vol.39(2007),p.859
[2] Synnefa A, Santamouris M, Apostolakis K: Solar Energy Vol.81(2007),p.488
[3] Hongbin Lu, Jianhua Chen: Materials Review Vol.19 (2005), p.71, In Chinese.
[4] Synnefa A, Santamouris M, Livada I: Solar Energy Vol.80(2006),p.968
[5] Deming Xie, Mei Hong, Xiaochun Ma: Corrosion Science and Protection Technology Vol.17 (2005), p.237, In Chinese.
[6] A. Franquet, C.Le Pen, H.Terryn: Electrochemical Acta.Vol.48(2003),p.1245
[7] C.M.Bertelsen, F.J.Boerio: Progress in Organic Coatings Vol.41(2001)p.239

© (2011) Trans Tech Publications, Switzerland
doi:10.4028/www.scientific.net/AMR.331.708

The Influence on Hydrophilic after the Surface Treatment Of the Singed Gray Fabric by the Low Temperature Plasma

Peng Li[1, a], Shenjun Zhang[1, b] and Shouguo Wang[2, c]

[1] Jiaxing Research and Institute for Technology, Chinese Academy of Sciences, Jiaxing, Zhejiang, 3339 Linggongtang Road, 314000, China;

[2] Institute of Microelectronics of Chinese Academy of Sciences, Beijing, 100029, china

[a]airrob@163.com, [b]zsj.313@163.com, [c]wangshouguo@ime.ac.cn

Keywords: Low Temperature Plasma; Gray Fabric; Surface Treatment; Singed; Desizing;

Abstract. We carried on the surface treatments to the cotton fabric (singed and hadn't been singed) with the low temperature plasma device. We studied the desizing performances, compared the capillaries. The results showed that after the same plasma treatment, the intensity of the singed hydrophilic was similar to those that hadn't been singed yet. We also explained the influence on hydrophilic, the results provide a scientific basis for the using of the pretreatment plasma technique in the future.

Introduction

People usually use strong base in the process of the desizing, and the heat vapor steams to boil off; the pollution is serious [1]. After being treated by the low temperature plasma, the sizing can be removed effectively. This technique may take the place of the traditional methods or shorten the dosage of the srong base and the heat vapor steam. The technique helps to achieve the aim for reducing greenhouse gas emissions by conserving energy [2, 3]. The using of the plasma technique in the pretreatment of the dyeing has attracted a lot of academic attention [4]. However, up to new, no systematic research has been made about when to take the technique. We conducted experiments for the singed cotton fabric and those hadn't been singed yet, using the low temperature plasma device developed by the Institute of Microelectronics of Chinese Academy of Sciences. We also studied the influence on hydrophilic in different conditions.

Experimental set-up

Device. The gray fabric for experiment provided by the Zhejiang BAIRUI Textiles Printing and Dyeing Co., Ltd. Fig.1 shows that the plasma device includes two electrodes, the dielectric layer and the high frequency power supply. Fig.2 shows the Current and Voltage versus time wave forms. The aluminum electrode's diameter is 40 mm, the thickness of silica glass is 2 mm, the thickness of the silicon rubber is 2 mm, the silica glass's diameter is 50 mm, etc.

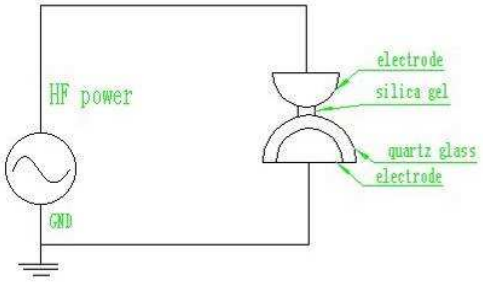


Fig.1 Schematic sketch of the low temperature plasma treatment system

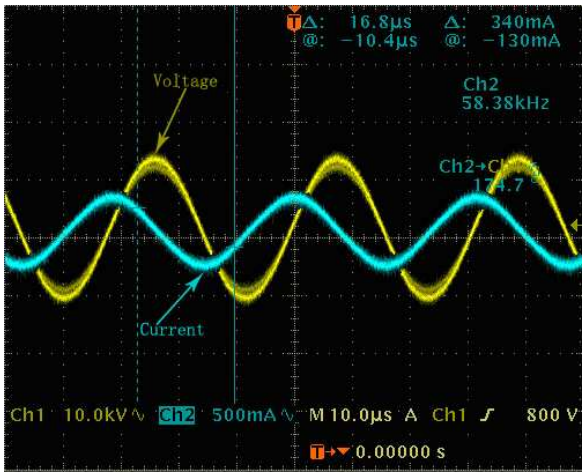


Fig.2 Current and Voltage versus time wave forms

Experimental methods. Treating: We conduct experiments for gray fabric with the low temperature plasma treatment system. Washing: We wash samples three times with 80℃ hot water and three times with cold water.

Measurement. Capillary: We dispose 250 ml solutions with 0.4% fuchsine and carry on the test according to the FZ/T01071 standard. Time: 30 min, Temperature: 20℃. We measure the last lift of the fuchsin solutions, following the shape testing sample. If the liquid surface isn't even, take low. Wet affinity: Dropping the water (0.02 ml), measure the time for complete absorption.

Results and discussion. We conduct experiments for gray fabric with the low temperature plasma treatment system. Differ from traditional methods, our method clean and environmental. We don't need hot water for pretreated, and don't remain osmosis agent. So when measure the wet affinity, we don't need to combine to back a slurry rate, pectin to clean rate and cotton wax and clean and lead synthesis assessment.

Capillary

Experimental methods. Select examinations at the power of 200 W, 400 W, 600 W and 800 W, the transaction has been singed and once hadn't yet. The transaction after completing 80 ℃ washes three times, cool water washes three times and dries gradually in shade and recording a different power, dissimilarity transaction condition, the red climbs lift after the 30 minutes. The results are shown in Tab.1 and Tab.2.

Tab.1 Experimental results for gray fabric

	200W	400W	600W	800W
Treating times/per	20	20	20	20
Height/cm	2.8	4.2	5.6	6.2
Treating times/per	40	40	40	40
Height/cm	3.2	5.8	7.5	8.3
Treating times/per	60	60	60	60
Height/cm	7.5	9.8	13.2	15
Treating times/per	80	80	80	80
Height/cm	7.8	10.2	14.5	15.2

Tab.2 Experimental results for singed gray fabric

	200W	400W	600W	800W
Treating times/per	20	20	20	20
Height/cm	2.8	4.2	5.6	6.2
Treating times/per	40	40	40	40
Height/cm	3.2	5.1	7.1	8.3
Treating times/per	60	60	60	60
Height/cm	7.2	9.8	13	13.8
Treating times/per	80	80	80	80
Height/cm	7.4	10.2	13.5	14.5

The simulation results are shown in Fig3**.**

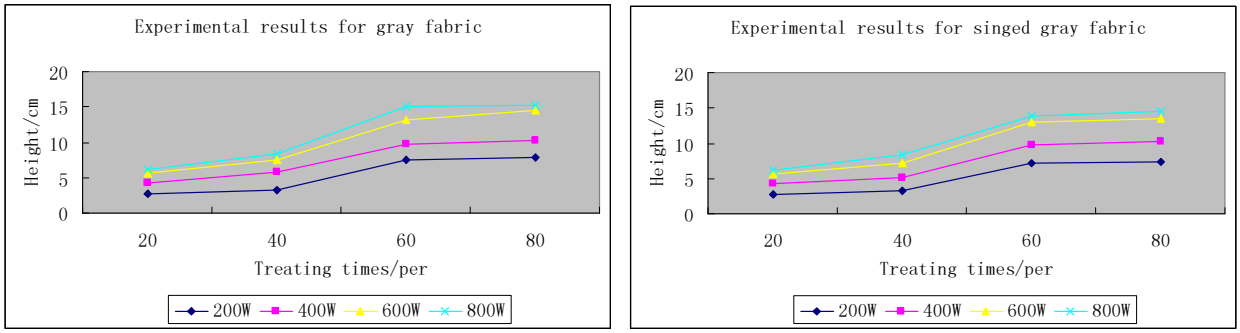


Fig.3 a) Simulation results for gray fabric b) Simulation results for singed gray fabric

The results show that the capillary is improved because of the increasing of the micro pits, slots and projection on the surface, which helps to increase the area, improves the capillary.

Drying. Select examinations at the power of 600 W and handle 60 times. We measure the red climbs lift after 30 minutes and dry our gray fabric gradually in shade or use the heat. The results are shown in Tab.3.

Tab.3 Experimental results

	Singed gray fabric	Gray fabric
Height(drying in shade)/cm	13.5	14.5
Height(heating dry)/cm	1.8	1.9

Results and discussion. The results show that heating dry destroy the capillary of the gray fabric. The dry heat air makes the wax guilder and the fat flood to the surface and forms new water-repellent layers[7].

Washing. After treating the gray fabric, we wash them 3 times with 80 ℃ hot water and another 3 times with cold water, then dry gradually in shade. In order to learn the impact of the washes, we wash the gray fabric before treating, and treat before washing. Select examinations at the power of 600 W and handle 60 times. We measured the red climbs lift after 30 minutes. The results are shown in Tab.4.

Tab.4 Experimental results of different conditions

Height/cm	Singed gray fabric	Gary fabric
Washing before treating	11.8	12
Treating before washing	11	11
Only washing	0.4	0.5
Only treating	2.5	2.7

Results and discussion. The results show that washing the gray fabric before treating with plasma device helps to improve the capillary appreciably. It's because that the hot water makes the surface swells, which helps the moisture osmosis and diffusion. The capillary is badly when only being treated. It's because that after treating there are also remain many residue consist of the slurry, the cotton seed, the fat and so on. The residue obstructs the osmosis of moisture.





Fig.4 Capillarity photographes for different conditions

Wet affinity

Experimental methods. Select examinations at different powers and different times. We drop the water (0.02 ml) and measure the time for complete absorption. The results are shown in Tab.5 and Tab.6.

Tab.5 Experimental results for singed gray farbic

	200W	400W	600W	800W
Treating times/per	20	20	20	20
Absorb Time/sec	2.5	2	2	2
Treating times/per	40	40	40	40
Absorb Time/sec	2.5	2	1.5	1.5
Treating times/per	60	60	60	60
Absorb Time/sec	2	1.5	1	0.5
Treating times/per	80	80	80	80
Absorb Time/sec	2	1	0.4	0.2

Tab.6 Experimental results for gray fabric

	200W	400W	600W	800W
Treating times/per	20	20	20	20
Absorb Time/sec	2.5	2.5	2	2
Treating times/per	40	40	40	40
Absorb Time/sec	2.5	2	2	2
Treating times/per	60	60	60	60
Absorb Time/sec	2	1.5	1	1
Treating times/per	80	80	80	80
Absorb Time/sec	2	1	1	0.5

The simulation results are shown in Fig.5**.**

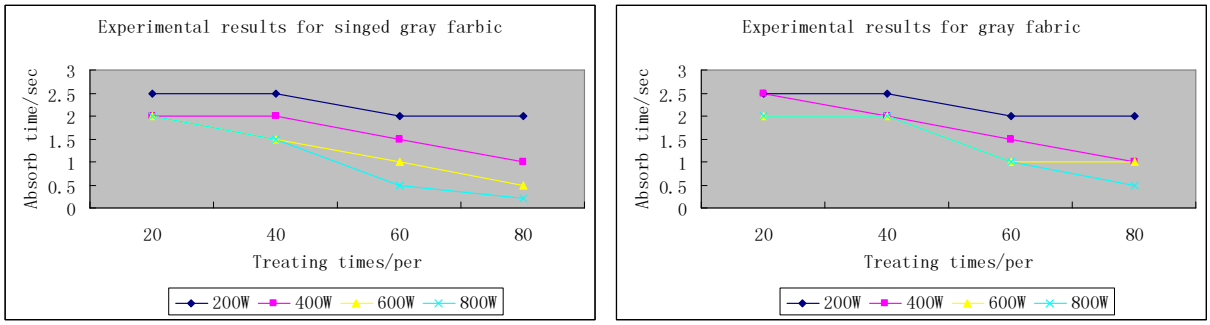


Fig.5 a) Simulation results for singed gray fabric b) Simulation results for gray fabric

Results and discussion. The results show that the wet affinity is greatly improved, and wet affinity is improved appreciably when treating the singed gray fabric. It's because that the gray fabric needs to be extinguished with water and dried. The hot water makes the surface swells, which helps the moisture osmosis and diffusion.

Conclusions

The results of the examinations to treat the singed gray fabric with atmosphere plasma show that:

a. The wet affinity and capillary are greatly improved for singed gray fabric also. Treating singed gray fabric can improve the treating process.

b. The heat dry the gray fabric, also destroy the wet affinity and capillary. We can only dry the gray fabric gradually in the shade.

c. Washing helps to wipe off the drain impurity, also improve the wet affinity.

d. The wet affinity has certain relation with the capillary. The capillary is well and the wet affinity is well too.

f. The examinations are conducted at the atmosphere press and the low temperature, the technique is easy to be converted into production.

References

[1] Weidong Gao: *The re-baking craft of the cotton blend fabric*, (ChinaTextile&ApparelPress, Forum Vol. 17-18, Beijing 2001).

[2] Jierong Chen: *Low temperature plasma chemistry and its application*, (Science Publications, Forum Vol. 21-22, Beijing 2001).

[3] Haibo Zhang: *Plasma electron engineering*, (Science Publications, Forum Vol. 25-27, Beijing 2002).

[4] Gucang Xu: *The shortened pretreatment of the fabric*, (China textile Publications, Beijing 1999).

[5] Ping Wang: Evaluation of Wetting Property of Cotton Fabrics after Enzyme Pretreatment, Dyeing and Finishing, Forum Vol.28~31, 12(2002).

[6] Xianying Wang: Theory and application effect of Cotton Fabrics after Enzyme Pretreatment, Dyeing and Finishing, Forum Vol.5~9, 23(1997).

[7] Jian Wang, Rong Zhou: Mechanism and application of the water-repellent and oil-repellent finishing, [J], Henan Chemical Technology, Forum Vol.38~39, 10 (1999).

© (2011) Trans Tech Publications, Switzerland
doi:10.4028/www.scientific.net/AMR.331.713

Comparison of plasma-aided desizing with conventional desizing of polyacrylate on PET fabrics

Xuming Li[1,2,a] Yiping Qiu[1,b]

[1] Key Laboratory of Textile Science and Technology, Ministry of Education, China, College of Textiles, Donghua University, Shanghai 201620, China

[2] College of Textile and Clothing, Shaoxing University, Shaoxing 312000, China

[a] lixm@mail.dhu.edu.cn [b] ypqiu@dhu.edu.cn

Key words: Atmospheric pressure plasma jet, Polyacrylate, Desizing, PET fabrics, AFM, XPS, SEM

Abstract: The influence of He/O2 atmospheric pressure plasma jet (APPJ) treatment on subsequent wet desizing of polyarylate on PET fabrics was studied in present paper. Atomic force microscopy (AFM) and Scanning electron microscopy (SEM) showed an increased surface roughness after the plasma treatment. SEM also showed that the fiber surfaces were as clean as unsized fibers after 35 s treatment followed by $NaHCO_3$ desizing. X-ray photoelectron spectroscopy (XPS) analysis indicated that oxygen-based functional groups increased for the plasma treated polyacrylate sized fabrics. Compared to conventional wet desizing, plasma treatment could significantly reduce desizing time.

Introduction

Warp sizes are the polymeric substances that are applied to warp yarns for the improvement of their weavability [1-2]. Polyacrylate sizes are one of the most important and useful ingredients in warp sizing [3]. But in order to ensure the qualities of further processes, such as dyeing and finishing, the applied sizes must be removed. However, polyacrylate sized fabrics must be subjected to hot water washing with NaOH agents in order to effectively remove the size in conventional desizing process. From the chemical processing point of view the NaOH treatment requires a more careful process technics than that of $NaHCO_3$, as it is an alkalis that easily to bring about alkaline hydrolysis of PET fiber. Plasma treatment is an environmentally friendly technique which introduces polar groups or increases surface roughness to improve surface properties, as well as finishing properties without affecting the bulk properties [4-8]. Therefore, more and more researchers[9-12] have paid close attentions to plasma aided desizing.

However, until now, little has been reported about atmospheric plasma aided desizing of polyacrylate sizes on PET fabric. Thus, the present study investigated the influence of atmospheric plasma jet (APPJ) treatment on sodium bicarbonate ($NaHCO_3$) desizing of polyacrylate on PET fabric. The desizing effect of polyacrylate on fabrics was characterized by scanning electron microscope (SEM) and the percent desizing ratio (PDR). X-ray photoelectron spectroscopy (XPS) was applied to study the changes of chemical composition of the fabric treated by APPJ.

Experimental

2.1. Materials

The fabric used was a 100% PET filament with 75 denier warp and weft yarns composed of 36 filaments and the polyacrylate size agents was 35% solution supplied by Zhejiang Tiansheng Holding Group Co., Ltd, Shaoxing, China.

2.2. Preparation of polyacrylate film

Polyacrylate solution (15ml) was put onto a glass plate (2×10cm), then the plate was placed into an oven at 80°C for 3h. A polyacrylate film was peeled off from the surface of glass plate. The film thickness was about 45 μm measured by a thickness gauge (within an accuracy of ±1μm).

2.3. Plasma treatment

The samples were plasma treated on an atmospheric pressure plasma jet (APPJ) machine (Atomflo-R, Surfx Company, USA) with 30 L/min of pure helium+0.3 L/min of oxygen (He/O_2) gas. The distance between the nozzle and the substrate was 2mm and output power was 60 W. The gas discharge was ignited by applying a low 13.56 MHz radio frequency power.

2.4. Wet desizing

The plasma treated fabrics and the untreated fabrics were subjected to wet desizing with different temperature and stirred time. The concentration of $NaHCO_3$ and the liquor: fabric ratio were 3g/L and 50:1, respectively.

The percent desizing ratio (PDR) was calculated as mass reduction of the desized fabric divided by the total original mass of the size on the fabric.

2.5. Surface morphology analysis (SEM)

The PET fabric surface morphology was examined using a SEM machine (JSM-5600LV model. Japan). The samples were inspected at 5000× magnification to reveal the surface morphological changes before and after plasma treatment.

2.6. Surface chemical composition analysis (XPS)

The X-ray photoelectron spectroscopy (XPS) experiment was performed using ESCALAB 250 photoelectron spectrometer (Thermo Electron VG Scientific, USA) equipped with a Mg Ka (1253.6 eV) X-ray source. The deconvolution analysis of C1s peaks was carried out using the XPS Peak analysis software.

2.7. Surface roughness analysis

Atomic force microscopy (AFM) (Multimode Nanoscope IIIa, Digital Instrument, USA) was used to examine the surface morphology of the polyacrylate film before and after the plasma treatments.

Results and discussion

3.1 AFM analysis

The surface morphology change of polyacrylate films was measured using AFM (as shown in Fig. 1(a)-(c)). It shows that the untreated film had a relatively smooth and uniform surface, however, the surfaces became progressively rougher after the plasma treatment. The average roughness (Ra) and root mean square roughness (Rrms) of the control and the plasma-treated polyacrylate film are shown in Table 1. The Ra values are 2.9, 12.1 and 20.9 nm for control, the plasma treated for 35 and 50s, respectively. This indicates that the surface roughness increased with an increase of plasma exposure time.

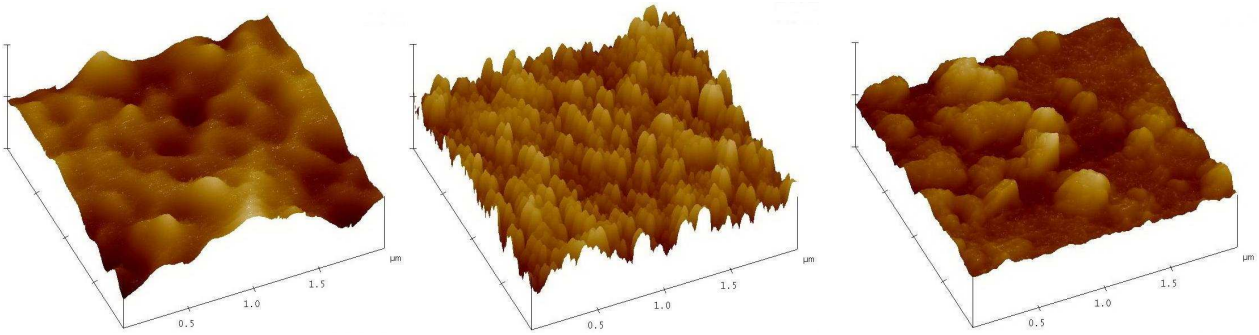


Fig. 1. AFM images of polyacrylate film surfaces (a: control; b: 35s; c: 50s)

Table 1 Surface roughness of polyacrylate films before and after plasma treatment.

Sample	Roughness(nm)	
	Ra	Rrms
Control	2.9	4.1
He/O2, 35s	12.1	14.7
He/O2, 50s	20.9	26.9

3.2. XPS analysis

Relative chemical composition for sized PET fabrics untreated and treated with APPJ is shown in Table 2. The results show that the O/C ratios were 38%, 66% and 70% respectively for the control, the samples with plasma treatment time of 20s and 50s. Compared to the control, the O/C ratios for all two plasma-treated fabrics increased dramatically with an increase of treated time suggesting that oxidation occurred and a higher level of oxygen-based functional groups were formed on the treated surface as reported in the literature [13-14]. But further increase exposure time let to a slow and steady buildup of functional groups, because the relative oxygen content on the surface will not further increase after a certain treatment time [15-17].

Table 3 presents the results of C1s peak deconvolution analysis showing a distinctive change of functional groups on the polyacylate film surface after the plasma treatment. A decrease of C-C/C-H signal was observed which is typical for plasma treated polymers due to the chain scission caused by the bombardment of the active species in the plasma [18-19]. Meanwhile, the C=O and O=C-O bonds had remarkable increase. This means He/O_2 plasma attacks mainly resulted in the chain scission and oxidation of C-C/C-H groups rather than ester groups [14]. The increase of these polar O=C-O and C=O groups is responsible for the higher hydrophibility of the polyarylate sizes.

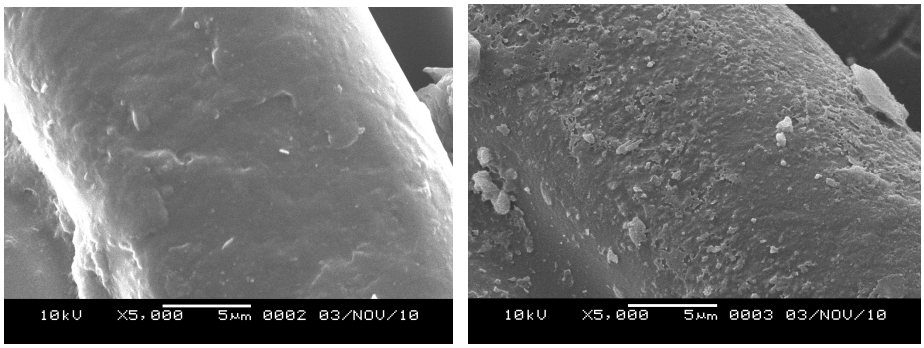
Table 2 Relative chemical composition for sized PET fabrics untreated and treated with APPJ.

Sample	Chemical composition (%)			Atomic ratio O/C
	C1s	O1s	N1s	
Control	71.5	27.5	1.0	0.38
Plasma treated, 20s	59.4	39.2	1.5	0.66
Plasma treated, 50s	57.8	40.6	1.6	0.7

Table 3 Results of deconvolution of C1s peak of sized PET fabrics untreated and treated with APPJ.

Sample	Relative area of different chemical bonds (%)			
	C-C/C-H	C-O-H/C-O-C	C=O/O-C-O	RO-C=O/HO-C=O
Control	72.9	12.0	5.9	9.2
Plasma treated, 20s	58.4	16.5	9.5	15.6
Plasma treated, 50s	56.5	17.3	10.2	16.0

3.3. SEM analysis



(a) (b)

Fig.2. SEM of control and treated sized fabrics under 5000× magnification: (a) control, (b) plasma 35s.

Fig.2. shows the SEM imagines of control and plasma treated sized PET fabrics at 5000× magnification. The results of SEM show that a rougher surface can be observed for plasma treated sample compared with the control covered with intact size coating. Surface etching by plasmas could be due to oxidation hence chain scission by oxygen during and after the plasma treatments. After 35s plasma treatment, the sizes were broken into fragments, revealing some sizes removal by plasma etching.

3.4. Influence of plasma treatment on polyacrylate desizing

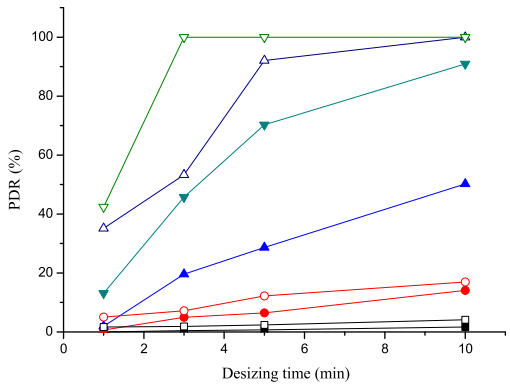


Fig.3. Effect of plasma treatment on wet desizing of polyacrylate. Solid symbols represent the results of wet desizing without plasma treatment at different temperatures of 25˚C (■), 50˚C (●), 75˚C (▲) and 100˚C (▼). Open symbols represent the results of 35s plasma treatment followed by wet desizing at different temperatures of 25˚C (□), 50˚C (○), 75˚C (△) and 100˚C (▽).

Fig.3 shows the influence of temperature and desizing time on the PDR of control and APPJ treated samples. From the result, we can see that the PDR of both two groups increased with the increase of wet desizing temperature and time, and the desizing effect of treated samples was obviously better than that of control samples. Plasma treatment did not enhance desizing efficiency at 25˚C and 50˚C. However, at 75˚C, desizing efficiency of treated samples was higher, and the 100% of PDR was reached after 10 min wet desizing. This difference was further increased at a desizing temperature of 100˚C, so that near 100% of sizing agents was removed within 20 s plasma treatment and subsequent 3 min wet desizing. But for untreated samples, only about 91% of polyacrylate was removed after wet desizing at 100˚C for 10 min. So, plasma was an effectively pre-treatment method for subsequent wet desizing. Meanwhile plasma treatment could not observably decrease desizing temperature but dramaticlly reduce desizing time.

Conclusions

The potential of using He/O_2 APPJ as a treatment prior to $NaHCO_3$ desizing of polyacrylate on PET fabrics has been studied. Plasma treatment could directly remove some of polyacrylate size on PET fabrics because of plasma etching. The plasma treatment resulted in changes of size agents surface chemistry and morphology as well as polyacrylate accessibility. Compare to conventional wet desizing, plasma pre-treatment could dramaticlly reduce desizing time.

Acknowledgements

This work was supported by the National High Technology Research and Development Program of China (No. 2007AA03Z101).

References

[1] C.D. Livengood, C. Tomasion, Text. Chem. Col. 12 (1980) 67–70.

[2] J.P. Moreau, Text. Chem. Col. 13 (1981) 22–27.

[3] Zhifeng Zhu, Zhiyong Qiao, Cuizhen Kang, Yuehua Li. Journal of Applied Polymer Science 91(2004) 3016–3022

[4] J.R. Chen, X.Y. Wang, W. Tomiji, J. Appl. Polym. Sci. 72 (1999) 1327–1333.

[5] P.H. Bae, Y.J. Hwang, H.J. Jo, H.J. Kim, Y. Lee, Chemosphere 63 (2006) 1041–1047.

[6] H. Zhuang, J.P. Wightman, J. Adhes. Sci. Technol. 62 (1997) 213–245.

[7] Z.S. Cai, Y.P. Qiu, J. Appl. Polym. Sci. 109 (2008) 1257–1261.

[8] J. Rahel, M. Simor, M. Cernak, Surf. Coat. Technol. 169 (2003) 604–608.

[9] Cai, Z. Qiu, Y. J. Appl. Polym. Sci. 99 (2006) 2233-2237.

[10] Cai, Z. Qiu, Y. Zhang, C. Hwang, Y. Mcord, M. Text. Res. J. 73 (2003) 670-674.

[11] Cai, Z.; Hwang, Y. Park, Y. Zhang, C. Mccord, M. Qiu, Y. AATCC Rev. 2 (2002) 18.

[12] Cai, Z. Qiu, Y. Hwang, Y. Zhang, C. Mccord, M. J. Ind. Text. 32 (2003) 223-229.

[13] U. Kogelschatz, Plasma Chem. Plasma Process. 23 (2003).

[14] N. De Geyter, R. Morent, C. Leys. Surf. Coat. Technol. 201 (2006) 2460–2466.

[15] B. Gupta, J. Hilborn, CH. Hollenstein, C. J. G. Plummer, R. Houriet, N. Xanthopoulos. Journal of Applied Polymer Science 78 (2000) 1083–1091.

[16] Z. Fang, Y. Qiu, Y. Luo, J. Phys. D: Appl. Phys. 36 (2003) 2980.

[17] X.J. Dai, L. Kviz, Proc. Textile Institute 81st World Conference, Melbourne-Australia, 2001, p. 1.

[18] D. Pappas, A. Bujanda, J. Demaree, J. Appl. Polym. Sci. 201 (2006) 4384–4388.

[19] V. Svorcik, V. Kotal, J. Siegel, P. Sajdl, A. Mackova, V. Hnatowicz, Polym. Degrad. Stabil. 92 (2007) 1645–1649.

© (2011) Trans Tech Publications, Switzerland
doi:10.4028/www.scientific.net/AMR.331.718

Influence of atmospheric pressure plasma pre-treatment on sodium bicarbonate desizing of polyacrylate on PET fabrics

Xuming Li[1,2,a], Yiping Qiu[1,b]

[1] Key Laboratory of Textile Science and Technology, Ministry of Education, China, College of Textiles, Donghua University, Shanghai 201620, China

[2] College of Textile and Clothing, Shaoxing University, Shaoxing 312000, China

[a] lixm@mail.dhu.edu.cn [b] ypqiu@dhu.edu.cn

Key words: Atmospheric pressure plasma jet, Polyacrylate, Desizing, PET fabrics, AFM, XPS, SEM

Abstract: The influence of He/O_2 atmospheric pressure plasma jet (APPJ) treatment on subsequent wet desizing of polyarylate from PET fabrics was studied in present paper. Scanning electron microscopy (SEM) analysis showed an increased surface roughness after the plasma treatment. And SEM results also showed that the fiber surfaces were as clean as unsized fibers surfaces after 35s treatment followed by $NaHCO_3$ desizing. X-ray photoelectron spectroscopy (XPS) analysis indicated that oxygen-based functional groups increased for the plasma treated polyacrylate sized fabrics. The percent desizing ratio (PDR) results showed that more than 99% PDR was achieved after 65s plasma treatment followed by a 5min $NaHCO_3$ desizing.

Introduction

Warp sizes are the polymeric substances that are applied to warp yarns for the improvement of their weavability [1-2]. Polyacrylate size is the one of the most important and useful ingredients in warp sizing[3]. But in order to ensure the qualities of further processes, such as dyeing and finishing, the applied sizes must be removed. However, polyacrylate sized fabrics must be subjected to hot water washing with NaOH agents in order to effectively remove the size in conventional desizing process. From the chemical processing point of view the NaOH treatment requires a more careful process technics than that of $NaHCO_3$, as it is an alkalis that easily to bring about alkaline hydrolysis of PET fiber. It has been a major contributor to water pollution of textile industry. Plasma treatment is an environmentally friendly technique which introduces polar groups or increases surface roughness to improve surface properties without affecting the bulk properties [4-6]. Therefore, more and more researchers [7-10] have paid close attention to plasma aided desizing.

However, most studies are limited to PVA desizing by plasma treatment. Until now, little has been reported about atmospheric plasma aided desizing of polyacrylate sizes on PET fabric. Thus, the present study investigated the influence of atmospheric plasma jet (APPJ) treatment on sodium bicarbonate ($NaHCO_3$) desizing of polyacrylate on PET fabric.

Experimental

Materials

The fabric used was a 100% PET filament with 75 denier warp and weft yarns composed of 36 filaments. (bleached for print cloth) and the polyacrylate size agents was 35% supplied by Zhejiang Tiansheng Holding Group Co., Ltd, Shaoxing, China.

Plasma treatment

The samples were plasma treated on an atmospheric pressure plasma jet (APPJ) machine (Atomflo-R, Surfx Company, USA) with 30 L/min of pure helium+0.3 L/min of oxygen (He/O_2) gas. The distance between the nozzle and the substrate was 2mm and output power was 60 W. The gas discharge was ignited by applying a low 13.56 MHz radio frequency power.

Wet desizing

The PET fabrics treated by plasma were subjected to wet desizing at 75℃ and stirred for 5 min. The concentration of $NaHCO_3$ and the liquor:fabric ratio used throughout the experiment were 3g/L and 50:1, respectively.

The percent desizing ratio (PDR) was calculated as mass reduction of the desized fabric divided by the total original mass of the size on the fabric.

Surface morphology analysis (SEM)

The PET fabric surface morphology was examined using a SEM machine (JSM-5600LV model. Japan). The samples were inspected at 1000× and 5000× magnification to reveal desizing effect under different conditions and the surface morphological changes before and after plasma treatment.

Surface chemical composition analysis (XPS)

The X-ray photoelectron spectroscopy (XPS) experiment was performed using ESCALAB 250 photoelectron spectrometer (Thermo Electron VG Scientific, USA) equipped with a Mg Ka (1253.6 eV) X-ray source.

Results and discussion

3.1. XPS analysis

Relative chemical composition for sized PET fabrics untreated and treated with APPJ are shown in Table1. The result shows that the O/C ratios were 38%, 66% and 70% respectively for the control, the samples with plasma treatment time of 20s and 50s. Compared to the control, the O/C ratios for all two plasma-treated fabrics increased dramatically with an increase of treated time suggesting that oxidation occurred and a higher level of oxygen-based functional groups were formed on the surface exposed to He/O_2 APPJ as reported in the literature [11-12].

Table 1 Relative chemical composition for sized PET fabrics untreated and treated with APPJ.

Sample	Chemical composition (%)			Atomic ratio O/C
	C1s	O1s	N1s	
Control	71.5	27.5	1.0	0.38
Plasma treated, 20s	59.4	39.2	1.5	0.66
Plasma treated, 50s	57.8	40.6	1.6	0.7

C1s deconvolution analyses were performed using XPSPEAK software as shown in Fig. 1(a)-(c). The C1s spectra of the control and plasma-treated samples mainly contain four sub-peaks corresponding to C-C/C-H (285 eV), C-O-C/C-OH (286.6 eV), C=O/O-C-O (288 eV) and O=C-OR/ O=C-OH (289 eV). Table 2 presents the results of C1s peak deconvolution analysis

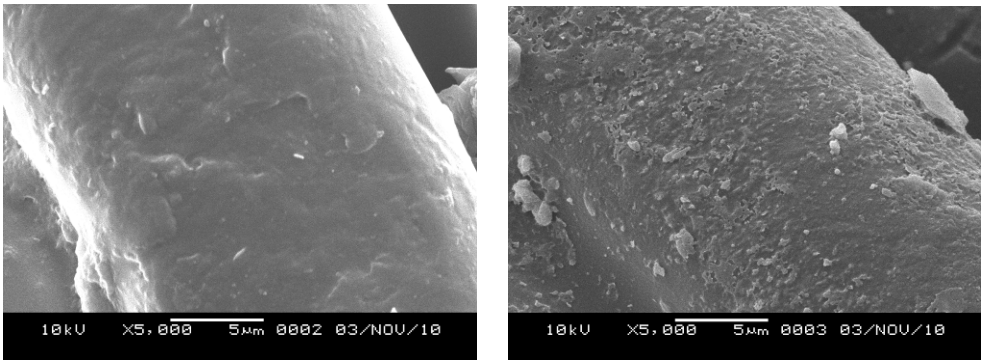
showing a distinctive change of functional groups on the polyacylate film surface after the plasma treatment. A decrease of C-C/C-H signal was observed which is typical for plasma treated polymers due to the chain scission caused by the bombardment of the active species in the plasma [13]. Meanwhile, the C=O and O=C-O bonds had remarkable increase. The increase of these polar O=C-O and C=O groups is responsible for the higher hydrophibility of the polyarylate sized PET fabrics after plasma treatment.

Table 2 Results of deconvolution of C1s peak of sized PET fabrics untreated and treated with APPJ.

Sample	Relative area of different chemical bonds (%)			
	C-C/C-H	C-O-H/C-O-C	C=O/O-C-O	RO-C=O/HO-C=O
Control	72.9	12.0	5.9	9.2
Plasma treated, 20s	58.4	16.5	9.5	15.6
Plasma treated, 50s	56.5	17.3	10.2	16.0

3.2. SEM analysis

Fig.1. shows the SEM imagines of control and plasma treated sized PET fabrics at 5000× magnification. The results of SEM show that a rougher surface can be observed for plasma treated sample compared with the control covered with intact size coating. Surface etching by plasmas could be due to oxidation hence chain scission by oxygen during and after the plasma treatments. After 35s plasma treatment, the sizes were broken into fragments, revealing some sizes removal by plasma etching.



(a) (b)

Fig.1. SEM of control and treated sized fabrics under 5000× magnification: (a) control, (b) plasma treated 35s.

3.3. Influence of plasma treatment on polyacrylate desizing

The percent desizing ratio (PDR) for the control and plasma treated PET fabrics with different exposure time is given in Fig.2. The result shows that as the helium/oxygen plasma treatment time increased, the PDR had a significant increase after wet desizing. More than 99% PDR was achieved after 65s plasma treatment followed by a 5min wet desizing, whereas only about 28% PDR could be reached for the untreated fabrics. The main reasons could be that the plasma treatment increases the accessibility of the polyacrylate surface would be increased, so the penetration and reaction of $NaHCO_3$ with the polyacrylate were increased, resulting in speeding up three desizing stages of physical action-swelling, dissolving and dispersing.

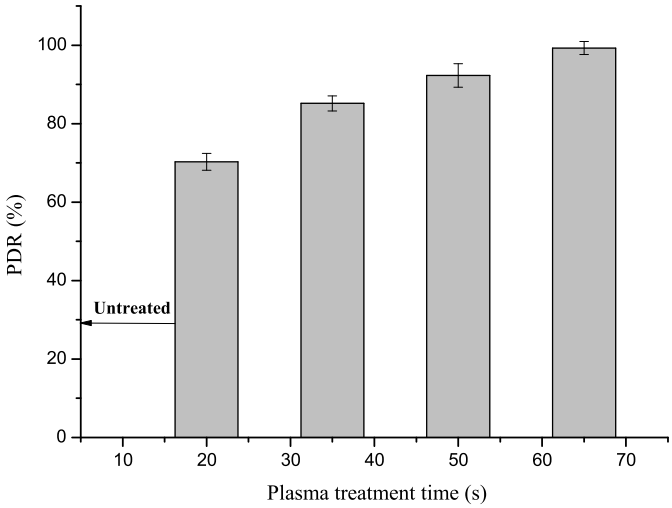


Fig.2. The PDR of the control and treated fabrics followed by wet desizing($NaHCO_3$: 3g/L; 5min; 75℃).

Conclusions

The potential of using He/O_2 APPJ treatment as a treatment prior to $NaHCO_3$ desizing of polyacrylate on PET fabrics has been studied. The plasma treatment resulted in changes of size agents surface chemistry and morphology as well as polyacrylate accessibility. And with the increase of plasma treatment time, this difference further increased resulted in significant improvement of polyacrylate removal in subsequent wet disizing.

Acknowledgements

This work was supported by the Natural Science Foundation for the Youth (Nos. 50803010 and 60904056).

References

[1] C.D. Livengood, C. Tomasion, Text. Chem. Col. 12 (1980) 67–70.
[2] J.P. Moreau, Text. Chem. Col. 13 (1981) 22–27.
[3] Zhifeng Zhu, Zhiyong Qiao, Cuizhen Kang, Yuehua Li. Journal of Applied Polymer Science 91(2004) 3016–3022
[4] J.R. Chen, X.Y. Wang, W. Tomiji, J. Appl. Polym. Sci. 72 (1999) 1327–1333.
[5] P.H. Bae, Y.J. Hwang, H.J. Jo, H.J. Kim, Y. Lee, Chemosphere 63 (2006) 1041–1047.
[6] H. Zhuang, J.P. Wightman, J. Adhes. Sci. Technol. 62 (1997) 213–245.
[7] Cai, Z. Qiu, Y. J. Appl. Polym. Sci. 99 (2006) 2233-2237.
[8] Cai, Z. Qiu, Y. Zhang, C. Hwang, Y. Mcord, M. Text. Res. J. 73 (2003) 670-674.
[9] Cai, Z.; Hwang, Y. Park, Y. Zhang, C. Mccord, M. Qiu, Y. AATCC Rev. 2 (2002) 18.
[10] Cai, Z. Qiu, Y. Hwang, Y. Zhang, C. Mccord, M. J. Ind. Text. 32 (2003) 223-229.
[11] U. Kogelschatz, Plasma Chem. Plasma Process. 23 (2003).
[12] N. De Geyter, R. Morent, C. Leys. Surf. Coat. Technol. 201 (2006) 2460–2466.
[13] D. Pappas, A. Bujanda, J. Demaree, J. Appl. Polym. Sci. 201 (2006) 4384–4388.

© (2011) Trans Tech Publications, Switzerland
doi:10.4028/www.scientific.net/AMR.331.722

An analysis of Shaoxing textile industry's international competitiveness: the perspective of the export evaluation indexes

Aiqing Jiang[1, a], Rong Zhang[2,b]

[1]School of Business & Management, Shaoxing University, Shaoxing, Zhejiang, 312000, China

[2]Yuanpei College of Shaoxing University, Shaoxing, Zhejiang, 312000, China

[a]joyce312000@yahoo.com.cn, [b]zhangr61@21cn.com

Keywords: Shaoxing textile industry; international competitiveness; international market share; trade competitiveness index; revealed comparative advantage index

Abstract. First the thesis analyzes the development situation of Shaoxing textile industry. Then three export evaluation indexes (international market share, trade competitiveness index, revealed comparative advantage index) were selected to analyze and prove the international competitiveness of Shaoxing textile and clothing. At last, it proves that Shaoxing textile and clothing has very strong competitive advantage and also puts forward several suggestions to strengthen this competitiveness.

Introduction

Shaoxing is famous for its textile, which has the biggest textile market in China- Chinese Light Textile Center. The textile industry's grown-up causes Shaoxing to fully exert its comparative advantage of the cheap labor force, take advantage of abundant labor resource, accumulate the capital and then develop to the direction of industrialization. Now at the background of globalization, the urgent thing for Shaoxing textile industry is to think how to cope with the problems of the industry structure's upgrading and fiercer international competition, further improve its international competitiveness.

The development present of Shaoxing textile industry

1.1 The textile industry displays the distribution of nubby cluster

Owning to the development for many years, Shaoxing textile industry has formed the integrate industry chain at present, which includes chemical fiber's raw materials, textiles, dying, dyeing and finishing, clothing and machine of spinning and weaving. It also has the corresponding professional market and marketing networks. The textile industry displays the distribution of nubby cluster. The details are shown in table 1.

Table1: Textile industry's nubby cluster details in Shaoxing

Line of Business	Centralized District	Main Products	Representative Companies	Scale
chemical fiber's raw materials	downtown, Shaoxing county, Shangyu	terylene long-silk, polyester	Yuandong, Cifu	The total output of polyester in Shaoxing could arrive 3,500,000 tons, which is equal to Zhejiang's 50% total outputs, China's 20%.
weaving business	downtown, Shaoxing county	Chemical fiber's weaving	Zongheng, Nanfang	Different weavings achieve yearly 7 billion meters, which is equal to Zhejiang's 1/2, China's 1/6.
dyeing and finishing	downtown, Shaoxing county	dyeing clothes	Yatau group, Tianma dyeing	The dyeing clothes output from the above-scale companies is equal to Zhejiang's 70%, China's 35%.
dyes	Shangyu	active leveling agent, textile auxiliary agent	Runtu group,Longsheng group	The dyes output of these two companies is equal to China's 47.1%.
clothing	Shaoxing county, downtown, Zhuji, Shengzho, Xingchang	western-style clothes, tie, sock	Hengbai, Busen	The clothing output is equal to Zhejiang's 13%, China's 2%; The tie output is equal to China's 90%, world's 40%, the sock output is equal to China's 33%.
machine of spinning and weaving.	Shaoxing county, Xingchang	double twister, rapier loom	Shaoxing machine of spinning and weaving group, Jinggong, Rifa, Taitan	The output of double twister Arrive at 5000 pieces, the output of rapier loom are 4500 pieces, whose market share is NO.1 in this business.

However, there are also a lot of problems: the cluster cooperation is asynchronous, the products' quality is jagged, the brand's construction is weak, the innovation ability is far behind to the international level, and the products' added value is needed to further promote.

1.2 Shaoxing textile's exporting

In order to interpret Shaoxing textile's exporting, the author draws one figure to describe the textile's exporting tendency through looking into Shaoxing annual from 2003 to 2010.From the figure 1, it could be inferred that Shaoxing textile's exporting rises year by year and the yearly increase rate is highly to 34%. This result suggests that Shaoxing textile occupies bigger market share in international market and has stronger competitiveness.

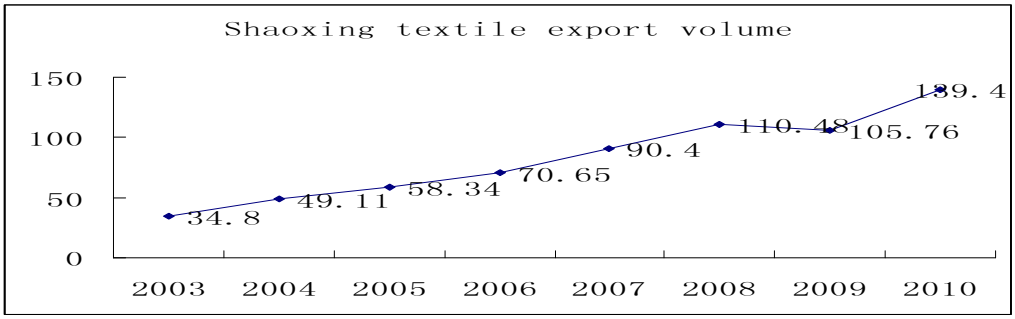


Figure 1 Shaoxing textile and clothing exports' volume from 2003 to 2009 (unit: hundred million U.S. dollar), **Resource:** Shaoxing annual (2003-2009)

An analysis of Shaoxing textile industry's international competitiveness

In this part, the thesis will further discuss Shaoxing textile industry's international competitiveness from the perspective of some export-evaluation indexes.

2.1 International market share (IMS)

International market share refers to the rate of certain product's export volume in one country and this product's export volume in the world. The fomula is IMSij= Xij/Xwj (IMsij is the international market share, Xij is the product j's export volume in i country, Xwj is the product j's export volume in the world). This index could indicate certain industry or product's ineternational competitiveness or the competitive position's change. The high rate could declare that the international competitiveness is strong, and versus.

In this thesis, in order to mearuse Shaoxing textile industry's international competitiveness, the author makes a little change. The molecule in the above formular is displaced by Shaoxing textile and clothing export volume, and the denominatoris kept the same.The result is shown in table 2.

Table 2: Shaoxing textile and clothing's international market share

year	Shaoxing textile and clothing export volume (hundred million U.S. dollar)	The world textile and clothing export volume (hundred million U.S. dollar)	International market share（%）
2003	34.80	1737.30	2.00
2004	49.11	1953.80	2.51
2005	58.34	2029.70	2.87
2006	70.65	2185.90	3.23
2007	90.40	2381.30	3.80
2008	110.48	2501.98	4.42

Resource: www.wto.org; Shaoxing annual (2003~2008) (The data after 2008 is not found in the internet of WTO.)

From the table 2, it shows that the international market share of Shaoxing textile and clothing is raised year by year and kept the stead development tendency. It also indicates that Shaoxing textile's international competitiveness is comparatively high from the perspective of IMS.

2.2 Trade competitiveness index (TSI)

Trade competitiveness index is the important index to measure the industry strong or weak in one country. Its formula is TCij= (Xij- Mij)/(Xij+ Mij), (TCij is the product j's trade competitiveness index in i country; Xij is the product j's export volume in i country, correspondingly, Mij is import volume). TCij fluctuates the rage -1~1. If TC>0, it indicates that the product has the competitive advantage; versus, if TC<0, the product has the competitive inferiority.In this thesis, Shaoxing textile and clothing's export volume and import volume are selected as the evaluating indexes.So Shaoxing textile and clothing's trade competitiveness index is shown in table 3.

Table 3: Shaoxing textile and clothing's trade competitiveness index (2003~2010)

year	Shaoxing textile and clothing export volume (hundred million U.S. dollar)	Shaoxing textile and clothing import volume (hundred million U.S. dollar)	trade difference (hundred million U.S. dollar)	trade total amount (hundred million U.S. dollar)	trade competitiveness index
2003	34.80	4.52	30.28	39.32	0.77
2004	49.11	4.30	44.81	53.41	0.84
2005	58.34	2.52	55.82	60.86	0.92
2006	70.65	2.83	67.82	73.48	0.92
2007	90.40	3.67	86.73	94.07	0.92
2008	110.48	3.31	107.17	113.79	0.94
2009	105.76	2.33	103.43	108.09	0.95
2010	139.4	3.30	136.1	142.7	0.95

Resource: Shaoxing nation economic performance report (2003-2010), Shaoxing customs

From the table 3, it could be inferred that Shaoxing textile and clothing's competitiveness index is above 0, which indicates that Shaoxing textile industry has obvious competitive advantage, and the competitiveness is improved year by year.

2.3 Revealed comparative advantage index (RCA)

Revealed comparative advantage index refers to a quotient of two rates. The formula is RCAij= (Xij/Xit)/(Xwj/Xwt). In the formula, Xij is the product j's export volume in i country; Xit is all product's export volume in i country; Xwj is the product j's export volume in the world; Xwt is all product's export volume in the world. RCA is usually used to measure the international competitiveness intensity of one country industry. If RCA>1, it says that the product or the industry lies in the comparative inferiority, versus, if RCA<1, it lies in the comparative advantage, what's more, the bigger the RCA is, the more the comparative advantage is. In this thesis, the molecule in the above formular is displaced by Shaoxing textile and clothing's export volume and the total products' export volume, and the denominator is kept the same. So the table 4 could be counted.

Tabele 4: Shaoxing textile and clothing's revealed comparative advantage index (2003~2008)

year	The rate of textile and clothing's export volume to the total products' export volume in Shaoxing (%)	The rate of textile and clothing's export volume to the total products' export volume in the world (%)	RCA
2003	76.80	2.38	32.27
2004	74.31	2.19	33.93
2005	71.70	2.00	35.85
2006	67.30	1.90	35.42
2007	65.50	1.70	38.53
2008	63.20	1.60	39.50

Resource: www.wto.org; Shaoxing annual (2003~2008)

From the table 4, RCA of Shaoxing textile and clothing is far above 1 from 2003 to 2008, which indicates that Shaoxing textile and clothing's export competitiveness is very strong. In general, RCA rises year by year, which says that Shaoxing textile industry's competitiveness is constantly improved in the fiercer competitive international market.

Conclusion and suggestions

From the above analysis, it could be inferred that Shaoxing textile and clothing has very strong competitiveness in the international markets. According to the result from 2003 to 2008 or 2010, it also indicates that the competitiveness keeps rising year by year and the competitive advantage of Shaoxing textile and clothing is very obvious.

In order to further strengthen this competitive advantage, here the author puts forward several suggestions.First, in the new background, Shaoxing textile industry and product structures should be adjusted and developed to the high-efficient and friendly environmental economic growth.Second, brand construction should be submitted to the agenda. Because brand could add much more value to the product and help to stretch the bigger markets.Third, the above two points' realization will rely on the talents. So the textile company should train all kinds of talents who could help strengthen that comparative advantage.

References

[1] Liping Wang, A study on the evaluation index system of Chinese textile's international competitiveness I, Chemical fiber and textile technology, Vol.2 (2006),p15~18(In Chinese).

[2] Ruqing Yao, A research of Shaoxing textile industry, Zhejiang Economy, Vol. 4 (2003), p49~51(In Chinese).

[3] Chunheng Fu, A study on the international competitiveness of Zhejiang textile and clothing, Sichou, Vol. 3 (2004), P1~4 (In Chinese).

[4] Xiaoli Ren, Analysis on international competiveness of China textile industry, Wool textile technology, Vol. 11 (2008), p59~63 (In Chinese).

© (2011) Trans Tech Publications, Switzerland
doi:10.4028/www.scientific.net/AMR.331.726

Strategies for Textiles and Apparel Enterprises in Jilin Province "Going global"

Yan Liu [1, a], Feiyue Wang [1, b]

[1]College of Quartermaster Technology, Jilin University, Changchun, 130062, China

[a]Liuyan19680906@126.com, [b]wangfeiyue133@163.com

Keywords: the textile and apparel enterprises, "Going global", export trade, external investment

Abstract. The textile and apparel enterprises in Jilin province should go out under the new international economic situation, explore international market and develop the textile export trade. In this paper, several problems in textile and apparel industry of Jilin province have been discussed, the measures of improving brand consciousness, accelerateing adjusting upgrading the industrial structure and improving the industrial chain have been studied.

Introduction

"Going global" strategy is that government upholds competitive enterprises external investment, to stimulate exports of goods and services and make more powerful transnational corporations and brand companies. It means that Chinese enterprises should go out to reconstruct the resources externally when transnational corporations are structuring the resources of China.

In recent years, the textile and apparel industry had a great development, at the same time the R&D (research and development) also had a great progress. While, the new round of inbound investment boom leads to overcapacity and aggravation of domestic competition; RMB appreciation and raw materials price appreciation will make export risk aggravating and will reduce profits; for a long time the amount of export license has failed to meet the export requirement of domestic enterprises; excessive growth of exports will intensify trade protectionism and technical barriers[1]; at the same time lowering the rates of tax refund for export makes the textile and apparel industry face a huge potential crisis. To fix this situation the textile and apparel enterprises and the industry should take precautions to meet the new challenge. In order to adapt the international trend, enhance the international competitiveness, resolve trade disputes current, solve capital surplus and overcapacity and accelerate the textile and apparel industrial restructuring, "going global" is an inevitable choice. International industry resources are distributed in these links of design, development, production, marketing, management and promotion, including human, financial, material and intangible assets in many areas. Domestic enterprises go out to use the resources externally, set up factories abroad by outbound investment and established multinational model to optimize and reorganize the industry links global, which is the source of profit of enterprises' and the industry and the key to get into international markets.

Analysis on existing condition of the textile and apparel industry of Jilin

Government helps the textile and apparel enterprises to choose appropriate developing countries and regions to set up factories and industrial parks, plans cluster investment, which can reduce the risk and blindness of enterprises' and gradually make a complete industry chain. Industrial parks can exert the superiority that has strong supporting and industrial cluster effect to help enterprises to go global especially small and medium enterprises.

While industry conditions in different province are quite different. Enterprises in different region how to avoid weaknesses and play to its advantages which needs further study and discussion.

According to incomplete statistics, there are about 300 garment manufacturers in Jilin province, mainly small and medium. Most of them are manufacturing, including clothing foreign trade and OEM (Original Equipment Manufactures), wholesale business processing. Only a small part of them have involved in apparel sales [2]. In conclusion, the industry in Jilin province is very immature and little enterprise does very well.

Problems of the textile and apparel industry of Jilin

There are many problems that exist in the textile and apparel enterprises in Jilin province.

Most apparel business in Jilin province is mainly involved in processing industry. However, processing is a low link of the industry. Insufficient the R & D results low-tech products, which have no competitive power, then little profit.

The textile and apparel industry chain is incomplete and lack of professional techniques which impact the developing of industry. Though there are many high level clothing colleges in Jilin province, most students graduated will go to southern provinces. The lack of Sales professionals and professional designers hinder the development of fashion design and branding. To make things worse, the fabric market in Jilin is disturbing, only Beifang market and Sanmalu which are into the scale in Changchun, where the lack of variety and the low quality of fabrics become a barrier of choosing. This situation even compels college students to purchase fabric in neighboring provinces. In addition, the lack of cooperation between colleges and enterprises badly impacts the Industry restructuring.

There is also a shortage of market awareness, and there are few excellent domestic brands. 80% of sales in Jilin province of garments are manufactured by enterprises in others provinces currently, which indicates that the garments industry in Jilin is weak, yet has potentials to develop.

In 2010, the total value of exports was $4476000000 in Jilin province. Garment and accessories was the first in the ranking, about $523000000, sharing 11.7% of the whole value. Then comes to the fabric and products, which was the third, accounting for 3.8% share for $170000000, increasing 20.7% compared with other year. Textile and apparel goods are main commodities in trade goods, which show that textile and apparel goods of Jilin have several advantages, while it has downward trend under the impact of trade protectionism.

The import and export trade is unbalanced among the regions of Jilin. In 2010 the main export cities are Changchun, Yanbian and Jilin (city), accounted for 85.6% share; the other six cities' exports total value was accounted for 14.4% share (Fig. 1). The import is mainly in Changchun, accounted for 90.7% share; the other else was accounted for 9.3% share (Fig. 2) [3]. This situation is adverse to the development of external trade.

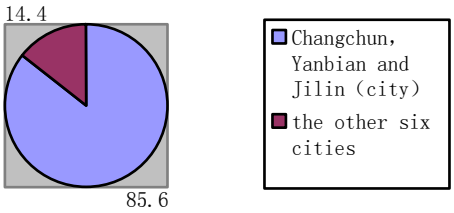


Fig. 1 2010 Distribution of export trade in Jilin

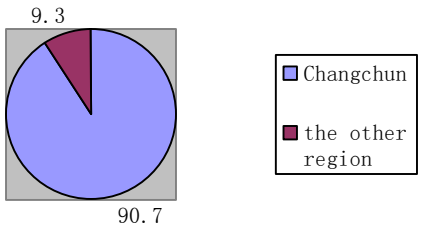


Fig. 2 2010 Distribution of import in Jilin

Only four enterprises have done “go global” in Jilin province limiting to Japan and North Korea, a small number and narrow coverage.

The modes of “going global”

To go global enterprises need deep understanding of national policy and industrial development direction to grasp the market, and make right strategy. There are some starting points for enterprises to go global, such as marketing, R & D, brand management, diversity of origin, control of raw material, global strategy, and so on.

“Go global” mainly includes four modes:

Outbound foreign direct investment. Domestic enterprises outbound foreign direct investment can build foreign plant or establish subsidiary. This mode needs large investment, long period so it has to face high risk.

Border Mergers and Acquisitions & Trade Cooperation. Through financing initiatives like mergers and acquisitions, holding, equity participation or long-term trade cooperation, etc., enterprises obtain the resources to take part in the international market international competition. This mode can reduce investment costs and risks, shorten the construction period, achieve strong joint and complement each other's advantages.

Contracting and leasing. Enterprises can make contractual joint venture through technological superiority and brand effect. This mode needs small investment and a short period, and it gets quick returns.

Establishing Sales map and R&D centre Overseas. Enterprises can proceed from product sales, market research and customer service. Then, enterprises can establish their own sales map, promoting the brands and enhance the brand image.

The measures of “going global” of Jilin

First of all, “going global” needs to choose deliberatively where to build plants. It needs the assessments of target nation’s political situation, security, climate, foreign policy, labor conditions, capacity of the market and preferential trade policy. Enterprises should look into the policy environment and market information in the host country by setting office, timely developing new product and new technique, enhancing the ability of independent innovation by using local professional design and sales staffs, then gradually built unique brands and establish sales map, improve the international competitiveness and market occupancy[4]. There are many fields can invest outbound, e.g. equipment, raw materials, technology, production lines these physical capital; and patents, intellectual property, management those intangible assets. Enterprises should be adept in restructuring the resources in the host country, be open and enhance drive ability to form a pattern of multi-directional, multi-level and wide-ranging opening to the outside world, and increase the total exports.

Most enterprises in Jilin are processing, the point of "go global" is transferring the overcapacity to the developing countries, which are neighboring, to achieve diverse origin and control of raw material market. Domestic enterprises should focus their work on Research and developing designs, to achieve industry upgrading and lower production cost. Most of the developing countries whose textile industry is the pillar expect China to invest and set up plants, even provide confessional terms.

Consultations and suggestions

Plans cluster investment, set up factories and industrial parks. Government helps enterprises to choose appropriate developing countries and regions to set up factories and industrial parks, organize enterprises to joint developing. Advisory organs and legal advisers should be set in factories and industrial parks. There also should be corresponding supporting agencies in the country. There should be bilateral trade accord between the governments, in order to reduce the risk and blindness of enterprises and gradually make a complete industry chain. Industrial parks can exert the superiority that has strong supporting and industrial cluster effect to help enterprises to go global especially small and medium enterprises.

The cooperation should be strengthened between enterprises. Small and medium enterprises should conglomerate companies in other provinces, cooperate with transnational corporations when going global. Enterprises should bring in new technology, enhance brand awareness, and accelerate industrial restructuring. Products should be upgraded to increase value-added and enhance the international competitiveness.

The main business of most enterprises in Jilin is processing of business wear, which makes the formation of business wear processing industrial park is feasible. The mode of the Northeast Socks Textile Industrial Park can be behaved. Enterprises can joint colleges to establish business wear industrial park, draw talent to develop cultural and creative industry, and establish unique brands.

Build or rebuild old spin fabrics terminal markets to make the largest and most sound spin fabrics terminal market, which can improve material supplying and accelerate the industrial chain's completeness.

References

[1] Shouming Chen, Yaohui Gao: Manager' Journal Vol. 180, (2009), p.192 (In Chinese)

[2] Information on http://honghan.blog.sohu.com/24688264.html

[3] Information on http://tjj.jl.gov.cn/tjfx/2008/201104/t20110406_973001.html

[4] Lei Zhang: Foreign Business Vol. 181. (2010), p.10 (In Chinese)

© (2011) Trans Tech Publications, Switzerland
doi:10.4028/www.scientific.net/AMR.331.730

Design Driven Innovation for Textile Industry

Anna Lottersberger

Fashion and Textile Unit – INDACO Department – Politecnico di Milano

Via Durando 38/A – 20158 Milano - ITALY

annalottersberger@hotmail.com

Keywords: Textile Design, Design Driven Innovation, Network, Trends

Abstract. This paper outlines a different perspective to look at research and product development in textile design. The aim is to provide a strategic model and specific tools for starting a Design Driven Innovation process into a textile company, in order to achieve radical meaning innovations.
This studio is typically exploratory, because of the contemporary of the issue and the fewness of references connecting Design-oriented theories, and specifically Design Driven Innovation, to textile manufacturing field. The objective of the work is to suggest prepositions and tools for the textile sector to be consequently validated with the collaborating industrial partners.

Introduction

Nowadays, consumers are paying increasing attention towards the sociocultural aspects of products: what consumers are looking for in products are new forms of psychological satisfaction that go beyond normal and simple consumption.
Design Driven Innovation (from now on: DDI) is so defined as an innovation where novelty of meaning and design language, pushed by design, is significant and prevalent compared with novelty of functionality, pushed by technology. The DDI strategy aims at radically transformation of the emotional and symbolic content of products, i.e. their meanings and languages, through a deep understanding of broader changes in society, culture and technology. Rather than being pulled by user requirements, design driven innovation is pushed by a firm's vision about possible new product meanings and languages that could diffuse in society [1].
The DDI has been firstly recognized and formalized in specific industries, such as furniture and food (see projects by Alessi [2], Artemide [3] and Barilla), in a specific context: the Italian one. Subsequently the strategy has been tested and validated in other industries (information technology, entertainment, automotive, etc.) beyond a precise country environment.
Therefore the first field of investigation referrers to 'Made in Italy' manufacturing, which usually includes: Food, Furniture and Fashion. These industrial sectors share peculiar characteristics: strong brand identity, high quality, design orientation, low-tech, tacit knowledge and export prominence [4].
While Furniture and Food are widely described in DDI cases, Fashion (including Textile, Apparel and Shoes) is hardly represented. Textile sector is a traditional industrial field and deeply rooted into Italian production environment, with 15.000 companies and 10.200 mil. Euro in export revenues, which represent the second position in worldwide ranking. Now it is facing the challenging contemporary global market, and need to find trajectories to be always competitive [5].
Even if yarns and fabrics are intermediate products, they are strictly connected to the final products: apparel garments. To remain cutting-edge and competitive in the global arena, they have to think and get in contact with final products and final consumers. Textile companies need to anticipate future trends and invent meaningful and recognizable products. The same visions and products promoted by the DDI approach. The outcome of the paper is a proper framework to promote a DDI strategy into the Textile market.

The textile product development

The textile design practice classically intends to define physical and chemical structure (i.e. composition, material structure and coatings), technical characteristics in order to achieve specific functions (wash-ability, comfort, breathability, waterproofing, etc.) and sensory perception (sheen, feeling, warmth, etc.). Because textile products are in-between products, and sold into a B2B market, the characteristics of the fabrics are often directly pulled by apparel clients' requirements. The functionalities attend to satisfy the operative needs of the business clients first and just secondly of final customers [6]. The company risks to be far from the end-user market and to forget that products define their own presence not only through their attributes but also through the meanings that they assume and also through the symbolic nature that they emanate. The semantic dimension of a fabric –also before becoming a dress – could reflect one or more linguistic functions [7]: expressive (e.g. hand-painted taffetas of Brian Froud for Prada), conative (e.g. Lycra for bathing suits), aesthetic, phatic (e.g. Mugello fabric for Dainese D-System), meta-linguistic (e.g. Goretex for active-wear), referential (e.g. Thermosensitive fabric for Stone Island Ice Jacket).

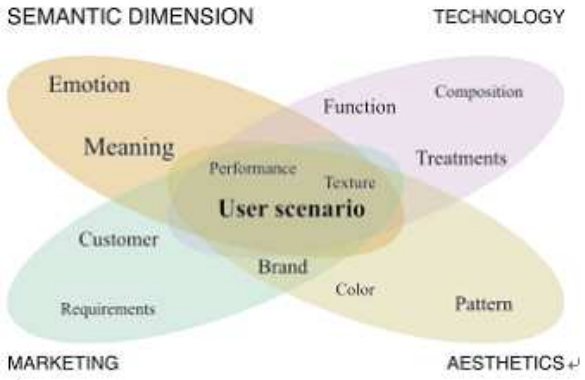


Fig.1. Product-development of textile.

Unlike a classical market-pull product development process, based on in-depth analysis of user needs, a DDI strategy is suitably centred on the capacity of understanding, anticipating and influencing the diffusion of new products languages and meanings, that are what end-users are actually waiting for [8]. In this sense the concept/product development of a radical new fabric has to manage marketing strategies, technology innovations, aesthetic characteristics and the semantic dimension in order to spread new scenario (see Fig.1). Textile companies and designers must use product signs and languages, such as fibres' composition, colours, surface treatments, etc., to embody symbolic and emotional values in one product [9].

The DDI Strategy

A textile company striving a breakthrough meaning has to manage two sets of knowledge: one about technologies and the other one about socio cultural trends. There is no centralized repository where it is possible to retrieve all information about future scenarios or technological innovations. When Verganti describes the DDI strategy, claims "the knowledge is diffused within our environment in a sort of *Design Discourse*" (cf. [8]). For what regards socio-cultural trends, the introduction of radical design driven innovations requires the development of several channels to access a typically tacit and distributed knowledge. It is necessary to be a part of a network in which several stakeholders interact and share their knowledge. In the same time, the literature underline how the so called fifth generation of R&D proposes to manage the innovation process as a network, in which all those people who could bring useful know-how have to participate: suppliers, clients, distributors and even competitors [10]. The necessity to share the huge technological investments and to separate the research from the development, spontaneously suggests cooperation cross-firms with other subjects. The research

department becomes totally devoted to the exploration of new technological solutions while the product development should focalize in the exploitation of this accumulated knowledge [11].
DDI strategy needs three crucial capabilities:
- Internal resources: company knowledge, seductive brand identity, charisma of top management;
- External resources: key interpreters of the Design Discourse, referring both to the technological world and to socio-cultural sphere, converging in an elite circle called Design Driven Laboratory
- Interpretation asset: a broker able to integrate the suggestions coming from external resources with the internal knowledge in one right scenario, one concept, one product/product family.

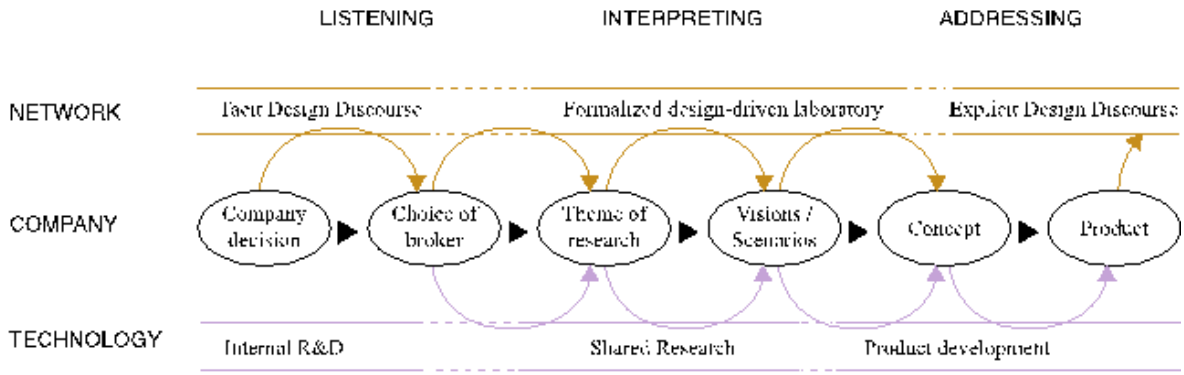


Fig.2. DDI Process for a textile company.

The process of design-driven innovation entails a suitable interaction with the selected interpreters and consists of three actions: listening, interpreting and addressing (see Fig.2) [12].
Listening means to gain access to knowledge about possible new product meanings by developing privileged relationships with a distinguished circle of key interpreters, formalizing the Design Discourse into a Design Driven Laboratory. A cutting-edge firm has to search, detect, attract those researchers who are developing, often for their own purposes and outside the usual network, unique visions about how meanings could evolve in the life context the company is investigating.
Interpreting consists in the assessment, recombination and integration of the knowledge gained during the first interaction with visions, technologies and assets settled inside the company. This process is conducted by the Broker and reflects the profound and precise dynamics of research activity. The outcome is the development of a breakthrough meaning/scenario.
Addressing is the critical phase of the process. On one side the new scenario is internally cultivated in a concept first, and finally in a product. Contemporarily companies should leverage the seductive power of interpreters, who have discussed and internalized the ground-breaking meaning and the firms' novel vision. They work as opinion makers influencing their environment through the inputs developed during the DDI process.
The next paragraphs describe the exploratory investigation of organizational specificities of *Design Discourse*, *Brokers* and *Design Driven Laboratories* for a textile firm.

Design Discourse: Exploration

Every company is surrounded by several agents who could share its interests. Consider, for example, a technical textile company that, instead of closely looking with a magnifying lens at how the fabric protect a climber, asks, "What meanings could a boulder team searches for when they are planning an expedition on Cordillera Blanca?" Other actors are investigating this same question: active-wear brands, safety equipment manufacturer, sunglasses manufacturer, travel agencies, insurance agencies, mountaineering journalists, producer of video and photo cameras, manufacturer of freeze-dried food, local policy makers, Andean Geographic Institution, a psychologist expert in risky situations. All are looking at the same people in the same life context: hard trekking for a long period with companions in a foreigner and extreme environment. And all are conducting research on how those people could give meaning to things. They could be the interpreters of this Design Discourse.

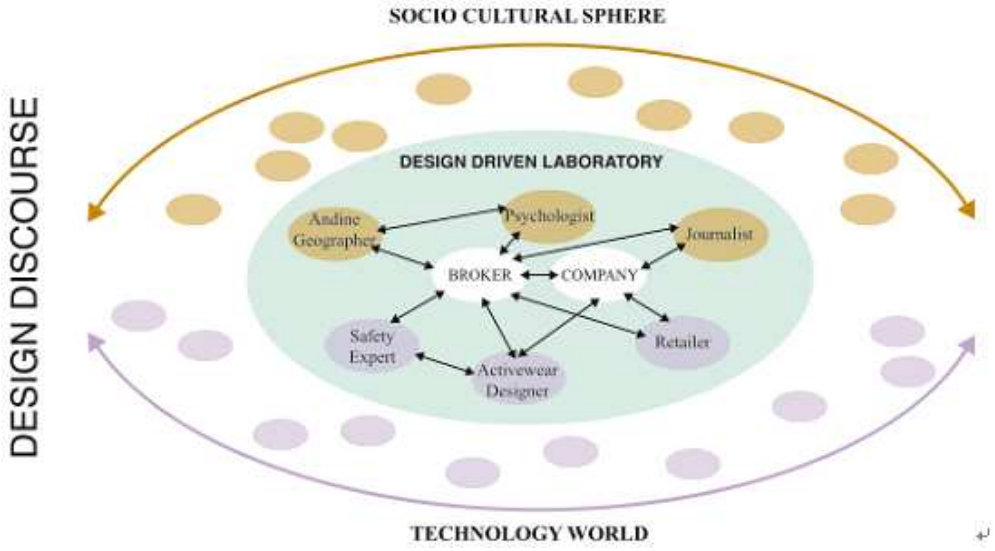


Fig.3. Design Discorse: adapting general map by Verganti to the mentioned example of Design Driven Laboratory.

Interpreters could belong both to the technological world (research centres, technology advisors, manufacturers in other areas, design agencies, retailers, trade-shows etc.) and to socio-cultural sphere (academy, artists, cultural associations, sociologists, anthropologists, marketers, media, etc.).
Companies that produce design-driven innovations highly value their interactions with these actors. With them they exchange information on scenarios, test the robustness of their assumptions, and discuss their own visions (See Fig.3).
The fact is that once the company has defined the possible products' ranges, general competences and roles, it is fundamental to carefully identify the exact firms, associations, institutions and professionals. It's highly dispersing and quite impossible to involve all the possible stakeholders.
The formalization of the Design Driven Laboratory consists in cultivating privileged relationships among individuals, even if they represent a big company or a research centre.
A firm, which intends to promote Design Driven Innovations, is aware that there is not just one network right for similar textile companies, nor just one network for all its Design Discourses.

Brokers: Entrusting

The top management is the first responsible in charge to decide if design and design-driven processes are core elements into the innovation strategy of the company.
In the DDI strategy the firm is always the promoter and centre of the design discourse. In the case of a textile company, in particular for what regards Italian small and medium enterprises (from now on SMEs), there are not the right internal competences and roles to manage a similar process. In R&D units hold highly technological knowledge and competences, while Sales departments manage market ones. Very often the launching of new products is in charge of the management (frequently in Italian SMEs the management is family run), which collects external inputs and requires to R&D unit specific researches through empirical tests.
So, companies need a support in the exploration of the Design Discourse, in detecting the key actors, in interpreting and integrating technological suggestions and socio-cultural scenarios, in the creation of product meanings acting on the semantic dimension of a product. Designers can interpret this role: they capture, recombine and integrate knowledge about different socio-cultural contexts proposing new aesthetical solutions that can become paradigmatic [13].
As brokers, designers have to be entrusted by the company and the Design Discourse. In some cases they can be employed in the firm activity, in order to share the internal knowledge. In other cases they collaborate as freelancers, to be recognized more autonomous by the other interpreters of the Design Driven Laboratory.

Design Driven Laboratories: Team Building

When the Design Discourse is activated, the critical phase consists in detecting the *Names*.
The Design Discourse can include individuals and/or collective entities like companies or academic units. On the other side, if the formalization of a Design Driven Laboratory consists in cultivating privileged relationships, the elite circle requires individuals, even if they represent a firm or a research centre. This research process can last a significant period of time: the selection of the Names pass through an interview phase and one or more meetings. The Laboratory must also enrol some strategic company members, such as the R&D manager and/or Marketing manager, in order to face internal and external knowledge. All the interpreters involved in the Design Driven Laboratory must trust the others. They must feel comfortable in sharing visions, studies, suggestions, etc. In some occasions the presentation and the discussion of the different contributions must be hold in one-to-one meetings, in some others they deserve collective reunions. The broker and the management divide the responsibility of properly selecting the right interpreters (in order to avoid useless competition and personal distastes) and of organizing agendas and objectives.

Conclusion

The framework, suggested to promote Design Driven Innovation and to validate DDI strategy into the apparel-textile manufacturing system, now needs to be effectively tested into selected case studies. The research activity is developing with three textile-related and design-oriented Italian companies, responding to the criteria established by famous furniture cases like Alessi and Artemide. They have been the first interlocutors of this platform, making a critical review of the model. I have been asked by these firms to be the broker of their first attempts to develop a DDI strategy. This participatory research represents the preliminary test of the proposed framework.

Acknowledgements

This work is supervised by prof. Iannilli, into the Fashion and Textile Unit of INDACO Department in Politecnico di Milano.

References

[1] R. Verganti: Design, meanings and radical innovation: a meta-model and a research agenda. Journal of Product Innovation Management, 25, 5 (2008), 436-456.

[2] A. Mendini: Tea and Coffee Towers. Edited by Electa, Milano, Italy (2003)

[3] F. Zurlo, R. Cagliano, G. Simonelli, R. Verganti: Innovare con il design. Il caso del settore illuminazione in Italia. Edited by Il Sole 24 Ore, Milano, Italy (2002)

[4] M. Fortis: Il Made in Italy. Edited by Il Mulino, Bologna, Italy (1998)

[5] P. Bertola in: Design del prodotto moda. Edited by Franco Angeli, Milano, Italy (2009)

[6] C. Gale, J. Kaur: The Textile Book, Edited by Berg, Oxford, UK (2002)

[7] S. Zingale: Gioco Dialogo, Design. Edited by Atì, Milano, Italy (2009)

[8] C. Dell'Era, R.Verganti: Design driven laboratories: organization and strategy of laboratories specialized in development of radical design-driven innovations. R&D Management 39 (2009)

[9] A. Van Onck: Semiotics in design practice. Design plus research. Proceedings of the Politecnico di Milano Conference, May 18-20 (2000)

[10] D. Nobelius: Towards the sixth generation of R&D. International Journal of Product Management, 22 (2004).

[11] H.W. Chesbrough: Open Innovation: The New Imperative for creating and Profiting from Technology. Edited by Harvard Business School Press, Boston, (2003).

[12] R. Verganti: DesignDrivenInnovation Edited by Harvard Business School Press,Boston,(2009)

[13] J.F. Durgee: Freedom of superstar designers? Design Management Review, 17, 3 (2006)

© (2011) Trans Tech Publications, Switzerland
doi:10.4028/www.scientific.net/AMR.331.735

The Analysis of Fashion Buyers' Development in Clothing Industry of China

Lijun Liu[1,a], Nan Qiao[1,b], Xiaopeng Li[2,c], Min Feng[3,d]

[1] School of Textile and Garment, Hebei University of Science &Technology, Shijiazhuang, China

[2] School of Foreign Languages, Hebei University of Science & Technology, Shijiazhuang, China

[3] Journal of Hebei University of Science & Technology, Shijiazhuang, China

[a]email: liulijun20082002@yahoo.com.cn, [b]email: wm9606@yahoo.com.cn

[c]email: lxp1022@163.com , [d]email: f1121m@163.com

Keywords: clothing; buyers; brand; abilities; improvement

Abstract. Buyer-based clothing brand is a new type of brand operating mode. Fashion buyers as the core of the new mode influence the circulation of products. This paper aims to find the role of fashion buyers in helping the brand development for the enterprise. This paper reveals the evolution rules of clothing fashion buyers and discusses its basis characteristics, compares the development of fashion buyers at home and abroad. It suggests the basic knowledge for fashion buyers and ways to improve their comprehensive abilities. Finally it puts forward measures to promote the sound development of brands by making the buyers system perfect.

With the pluralistic development of clothing industry and its subdivisions from product designing to terminal selling, some new professions related to the industry have emerged, such as people who deal with dress matching, clothing display, color diagnosis. Fashion-buyers are just among them. Though fashion buying is a new profession in China, it's still in great demand because of China's many production bases and big market. Fashion buyers are those who can play their roles in visual merchandising, product decisions, brands establishment and brand sustaining in the retailing of costumes [1]. In this sense, it's important to explore the growth and development of fashion buyers, and to find measures to improve the comprehensive abilities of fashion buyers.

The basics of fashion buyers

Basic definition

Following the international rules, fashion-buyers refer to those who travel around the world, pay attention to the latest fashion information, have a large number of orders in command, contact frequently with suppliers, provide different markets with different products and guide the market, thus, bridging the designers and the consumers[2]. The concept of buyers firstly refers to be a purchasing agent for supermarkets from large department stores in America. It shows the basic meaning of buyers, namely purchasing for the brands and being responsible for what are purchased. Because buyers are always keeping up with the latest fashion, they are also called fashion buyers.

In China, buyers are subdivided into buyers of clothing enterprises and business buyers， which are gradually accepted by the brand enterprises and the commercial terminals. Buyer-system usually refers to an enterprise or commerce operating system in which buyers are taken as the core of brand development. Buyer-system prevails in foreign countries, especially in the industries of clothing, shoes and hats. A buyer is not a professional designer but a skilled talent who is needed in clothing industry for his/her great management capability.

Basic characteristics

Fashion buyers' work is very professional. It calls for the integration of product design, originality and marketing to meet the consumers' needs. And the fashion buyers should also have the comprehensive ability of designing, marketing, consumer studying and so on.

Being sensitive to fashions is the basic characteristic of the buyers. That means buyers must have a better understanding of fashions and consumers. Based on the analysis of fashion trends, they can predict the coming style, plus materials, colors etc. Then they communicate with designers to work out the latest design. With the designed sample, buyers contact the suppliers, together with the designers, to decide what kind of goods should be in stock and discuss more details of the product such as style, color etc. After that the buyers discuss more details such as price with the suppliers [3].

Fashion buyers should not only be concerned about and sensitive to the latest trend, but also have a good knowledge of design, plus material, technology and process to catch the fashion information as quickly and accurately as possible. However, this kind of profession requires fashion buyers to have analytical ability and clear thinking so as to find the potential products and predict the perfect matching and its effect of the product. They should also communicate and negotiate skillfully with suppliers to lower the cost and make profits. What's important again to buyers is that they have a good command of language and cross-cultural knowledge to be international buyers [4]. Therefore, fashion buyers must have the strength to travel around the world without feeling tired.

Professional characteristics

The biggest characteristic of buyers operating mode is the buyers' coordination ability of information and decision. The buyers coordinate with different objects and manage to achieve the fastest operating effect. In the buyer-system, the buyers are responsible for marketing and learning about the market and the consumers accurately enough. During the two fashionable clothing seasons of spring-summer and autumn-winter, a buyer must stock at least one fashion brand for some specific clients, for instance, the clothing brands, boutique, shopping mall, etc.

Fashion buyers look like a bridge. To clients, buyers are essential for their influence on local trend and fashion culture. For some areas where fashion is not so important, a buyer could lead the fashion by introducing fashionable products. For some areas where people are fashionable, the buyer's task is to provide abundant and more fashionable products. In practice, buyers should be flexible to deal with the real situations. From the point of brand operation, the buyers are in the middle of products development and terminal clients, linking the two sides effectively. Especially for those companies emphasizing on developing brands, the buyers make the marketing procedure simpler and time-saving because the buyers serve as a bridge between the manufactures and the specialty stores. As a result, the buyer's hard work leads to the inventory reduction.

The buyers' working procedure is full of effectiveness. They often first contact with a business strategic planner to confirm the style and amounts of products to be purchased based on the general situation of the enterprise. Then, they go to find the suppliers and check up their samples. After that, the business strategic planner ensures the arrival of goods and the successful stocking. Subsequently, the buyer contacts marketing department to print brochures and to carry out marketing activities etc. Meanwhile, a buyer should help training the employees, so that the product concept and consuming guidance etc. can be conveyed to consumers. During selling season, buyers should review sales figures of former style, and compare them with other shops of the same trade. After selling season, buyers should sum up the experience and make arrangements for the next selling season.

Development of fashion buyers and skills requirements

Development in foreign countries

The first professional buyers appeared in the 1960s in Europe. Originally, a buyer is a person who stocks for a department store. The buyer orders various kinds of products and stocks them. During the Second World War, the concept of buyers was accepted by Europeans and Americans, and was widely used in chain stores and other fields. The 1980s to 1990s is the rapid development period of buyers. Because of the increasing labor costs, local textile manufacturing in England shrink drastically and most clothing manufacturing enterprises turn to service industry to avoid the fierce competition [5]. The demand for quick product circulation, high quality designing service and high value-added products promotes the development of buyers' profession.

The history of buyers is nearly 50 years in western countries, and a relatively perfect buyer mode also has become mature. It is the buyer mode that makes many brands become successful, such as ZARA, H&M, MANGO and GAP. Those brands are well-known at home and abroad and many chain stores have been opened in other countries. Among them, the Spanish brand ZARA and the American brand GAP relied on their respective buyers to lead fashion and become the chief retailing enterprises in the world. Swedish brand H&M positioned itself as fashionable with reasonable prices and developed fast with the help of buyers mode. The adaption of "rapidness" of buyers mode improved H&M's development and management. Its particular buyer mode had been formed with the establishment of a stable and powerful buyer team with lots of training. In this way, H&M has become one of the 50 fast developing retailing companies.

As a popular marketing operation mode in international clothing terminals, buyers also find their ways in Japan. Especially when the traditional business terminals such as department stores and specialty stores showed their declining tendency,while the daily sales of buyer-integrated stores had been increasing. The Japanese mode is worth using for reference due to its advantage in merchandising and skills. For example, the brand "UNIQLO"successfully gains a larger share of the market in commodity construction, profitability and retailing performance.

Based on the analysis of some foreign brands, the development of buyers mode has its own features. First, itslong history ensures its perfect quality; second, the quick response to market of buyer-based brands makes it lead fashion; third, the mature and suitable developing environment for buyers in foreign countries guarantees their comprehensive roles by learning about the product source and the terminal market; last, the training and education of buyers in brands industries are kept up with time, which ensured their maximum performance.

Current situation of Chinese fashion buyers and its difference from the western countries

In China, the manufacturing, the agent and the designer brands are the main clothing brands. In recent years brands based on buyer-system are gradually accepted, and are implemented by some enterprises in the area of Yangtze River Delta, Pearl River Delta and Beijing-Tianjin region. Yet the unsatisfactory situation and the slow development lead to a big difference from the western countries.

First, the later development of Chinese buyers causes the lack of talented buyers. Chinese buyers team grows with the blossom of retail market, on the basis of abundant products and subdivided markets. However, high-quality buyers are still in great demand in China.

Second, the insufficient education and training causes buyers' low professional degree. The study of buyers has not become an independent subject in Chinese clothing education. Buyers are still in great demand though some universities and training institutions have set up buyer courses. Besides, the concept of buyers is not clear to some brand companies and little attention has been paid to its importance by the industry. Therefore, the theory and practice can't be combined together, which hinder the development of buyers.

Third, the buyers are inexperienced and not good at whole controlling. The work of buyers is systematic and closely related to market. In China, some enterprises in Beijing, Shanghai, Guangzhou, Jiangsu and Zhejiang have gathered much experience. But on a whole, buyers' control ability is still weak. Thus, they can't have an effective command of goods. As a result, personal preference and marketing orientation deviation become the main problems. There are some other shortcomings such as the insufficiency in cost budgeting and controlling.

Developing trend and qualifications for the profession

The developing road for future buyers will focus on specialization, independence and diversification. It requires the buyers to keep up with the market and improve their comprehensive abilities so as to provide better service for brands development and improvement.

The development of clothing industry becomes more and more specialized because of its subdivisions and elaborations. Therefore, a buyer should have a good knowledge of the profession. Some Chinese enterprises have gathered experience through implementing buyer-system in practice, added by foreign buyers' experience. In this way, buyers will become an independent profession in China. The fact should be noticed is that the development of buyers is pluralistic, namely it's not the

continuity of one simple existing mode, it will be continuously adjusted and supplemented. In a word, fashion buyers must follow the marketing rules and obtain more professional knowledge to improve their own comprehensive abilities.

The analysis of improving fashion buyers' comprehensive abilities

A qualified buyer should not only have the basic abilities of clothing design, fashion sensitivity, art and aesthetics but also the basic knowledge of finance and statistics analysis. In addition, methods and measures for related professional knowledge and abilities are also important to a qualified buyer.

Knowledge points of improving fashion buyers' comprehensive abilities

First, fashion buyers must be familiar with all aspects from fashion information to manufacturing. They should also have systematic knowledge about the expression of trend and design concept, technique and features of plus materials in the designing process characteristic, and clothing matching skills and so on. Besides, they should have a good understanding of the rules of each procedure. Buyers should also have the imagination to understand product style, character evolution and various needs of customers, and decide what kind of product is more fashionable, suitable and practical for the target population [6].

Second, fashion buyers must have knowledge of a comprehensive course from products to goods. A buyer is like a bridge between manufacturing and marketing enterprises. Because there are many complex procedures in the course of products to goods, the buyers' responsibilities are great. First, a buyer should make each procedure clear, flowing and efficient. The knowledge structure of fashion marketing includes not only the understanding of the subdivided markets, market positioning, price strategies, the consumers' behaviors, and marketing information of rivals, but the knowledge about running cost, logistics, purchase, information, expenses and selling. So the knowledge of marketing is vital. And the knowledge of public relations and the communication among industries are important.

Last, fashion buyers must have the knowledge of marketing procedure from goods to consumers. The ultimate aim of goods is to obtain maximum profit. So the buyers should make correct decision at the beginning, ensure the efficiency in the middle, and monitor and analyze the selling process at the end. If necessary, buyers provide the terminal stores and shops with proper promotional suggestions. The sales figures should be clear for the buyers to offer advices. This will directly reflect the marketing of product style, the sales analysis ability of shops and the buyers' coordinating ability with enterprises. Based on the selling data of shops, the buyers analyzes the data of product style, and decide the supplementary styles and balance the stock of different shops. Besides, clothing product displaying and marketing displaying are important promotion means. Buyers will create and lead fashion by the clever use of color with specific displaying requirements, better displaying methods [7].

A buyer needs to possess the professional knowledge of product precognition andorder, marketing, sales analysis, planning, etc. From this viewpoint, a buyer is a versatile person.

Basic forms of improving fashion buyers' comprehensive abilities

A buyer should be both perceptual and rational. That means a buyer should have both the creativity and sensitivity to new things and the rationality of obeying marketing laws to promote sales. At the same time, a buyer is also an organizer, knowing how to balance the income and expenses, conduct quantitative statistics and decide the proper purchasing date. Therefore, a buyer is like a bridge linking products, retailers and consumers. The improvement of comprehensive abilities is to treat the market rationally and to enter the market based on the needs analysis of different parts of market.

Firstly, fashion buyers are wholesale buyers. Commonly they work for trade companies. They don't have their own brands, but stock and sell goods, mainly by wholesale and retailing. This kind of buyers take part in training courses to improve their comprehensive ability. Professional training institute is the best choice for those buyers.

Secondly, fashion buyers are brands buyers. Companies own their own brands, and buyers are as the supplement of insufficient design. Thus, the buyers are not so important to the companies and they can't enjoy the leading position of brand selling. For this reason, buyers still need to improve their aesthetic , management and analysis abilities, paying attention to international fashion and target market, and to communicate with the designer timely and effectively.

Thirdly, fashion buyers are marketplace buyers. There are very few of buyers of this kind in China. Their job is mainly to import brands that are suitable for marketplace. This practice is different from the common practice in China, which is the complete entry of a brand name for a shopping centre. The task for a buyer is to carefully choose the goods of that brand which the shopping centre needs. This kind of buyers can go to western or European countries to learn about the advanced operating mode of fashion buyers to improve themselves. In addition, they can enjoy a higher status within the circle by introducing potential brand names with the information exchange inside the trade.

Measures of improving of fashion buyers' comprehensive abilities

First, the information channel of fashion buyers should be free-flowing and be widened. The information channel is vital for the brand management and it determines the working direction of a buyer. The information channel from raw material manufacturers, clothing processing enterprises at the beginning to the joining agents, the practice of selling and its feedback at the end must be free-flowing to ensure the buyer's scientific decisions. Due to the changeable clothing market, the channel should be extended. Buyers' sensitivity and quick response to information, especially about new science, new development and research, and featured products, will lay a solid foundation for the elevation of a brand's competitive force, thus, playing a leading role in the market.

Second, the training mechanism for fashion buyers should be perfect and continuous. Buyers are in the core of brands operation and development, so their continuous training must be guaranteed. By establishing the effective training mechanism, a reasonable team with the old and the young would be formed, which helps the stability of buyer-system based brands and avoids excessive individual influence. The continuous and perfect training program will make the buyers more energetic and provide continuous power for the operation and development of brands.

Third, systemic supervision and evaluation for buyers are needed. Different aspects will be managed and controlled with different effective methods to ensure the good development of brands. The systematic supervision is particularly important for buyer-system based brand. The order plan, allocation arrangement, marketing plan and the related feedback and analysis from the buyers should be supervised. At the same time, the effectiveness of the buyer's work should be evaluated. During the evaluation process, first, the evaluation standard should be worked out; second, the buyers' achievement fluctuation and lasting efficient management should be quantified; third, the evaluation focusing on sales achievement and plans implementation should be strengthened.

Buyer modes are needed in Chinese commerce. With the subdivision of the industry and the skills specialization, the profession of fashion buyers has been concerned by many people. Courses about fashion buyers have been introduced into universities and some official training institutions. The profession of fashion buyers will be paid more attention to in the clothing industry that will lead to the increasing number of fashion buyers and the improvement of their skills at various levels.

References

[1] H. Goworek: *Careers in Fashion and Textiles* (Blackwell publishing Ltd, UK 2006).

[2] H. Goworek: *Fashion Buying* (Blackwell publishing Ltd, UK 2007).

[3] Z. Y. Wang: *Garment sourcing guide* (In Chinese, Chemical Industry Press, Shanghai, 2008).

[4] S. R. Wang: *Consultative store based on fashion buying* (In Chinese, China Machinery Press, Shanghai, China 2007).

[5] G. Pintel & J Diamond: *Retail buying*(Prentice Hall, UK 2004).

[6] Y. L. Wu: *Clerk manual of clothes shop* (In Chinese, Chinese Astronaut Press, Beijing, 2006).

[7] J. J. Sun: *Terminal operation and management of retail of costumes* (In Chinese, Donghua University Press, Shanghai, China 2009).

[8] S. R. Wang: *Buyer mode of apparel industry* (In Chinese, China Textile Press, Beijing, 2005).

© (2011) Trans Tech Publications, Switzerland
doi:10.4028/www.scientific.net/AMR.331.740

The apparel industry as an example of industry development trend of China –

Segmentation module within the industry, strengthening of cooperation between industry

Aiying Yun[1,a], Min Fang[1,b],Dongming Wang[1,a,*]

[1,]College of Quartermaster Technology, Jilin University, Changchun, 130062, China

[a]yunaiying301@163.com, [b]mfdesign7@hotmail.com, *corresponding author

Keywords: Fashion industry, Supply chain, Module, Fractionize, Cooperate, Telemedicine clothes

Abstract. Based on the operating mode of the domestic apparel industry chain statistics and research on new integrated industry-in-depth study of telemedicine, summarizes the development of the domestic industry chain status and future trends-supply relationships within the industry more and more sub-modules of different gradual strengthening of cooperation between industries, integrated across multiple disciplines the rise of new industries, analyze the problems encountered in the development process and make recommendations accordingly to solve.

Introduction

"Clothing" is very important to us as the first of the four categories "basic necessities"of human life, we can say is closely related to the higher level of economic development in particular. The rapid development of increased demands on our industry, not as long as human understanding of the structure, fabric performance understanding, sense of control over color, clothing grasp of the structure, clothing details of the deal, clothing technology can become proficient in the apparel industry The winners of the costume-depth understanding of the whole industry chain, including its composition from the initial raw materials, processing methods, level of development of industrial machinery, auxiliary materials to intermediate products, including its weaving method, performance, printing and dyeing, post-processing methods, and then methods of operation to include clothing brand including brand positioning, brand culture, brand image to maintain and enhance the other, but also related to the terminal plate clothing sales store VI design, displays, service concept, as well as clothing from the role of psychological control science, social background on the impact of clothing, clothing trends in the development and, finally, as the soul of the fashion design modules, such as the present, many garment enterprises to adopt the new SPA information chain,as the fig. 1[1].

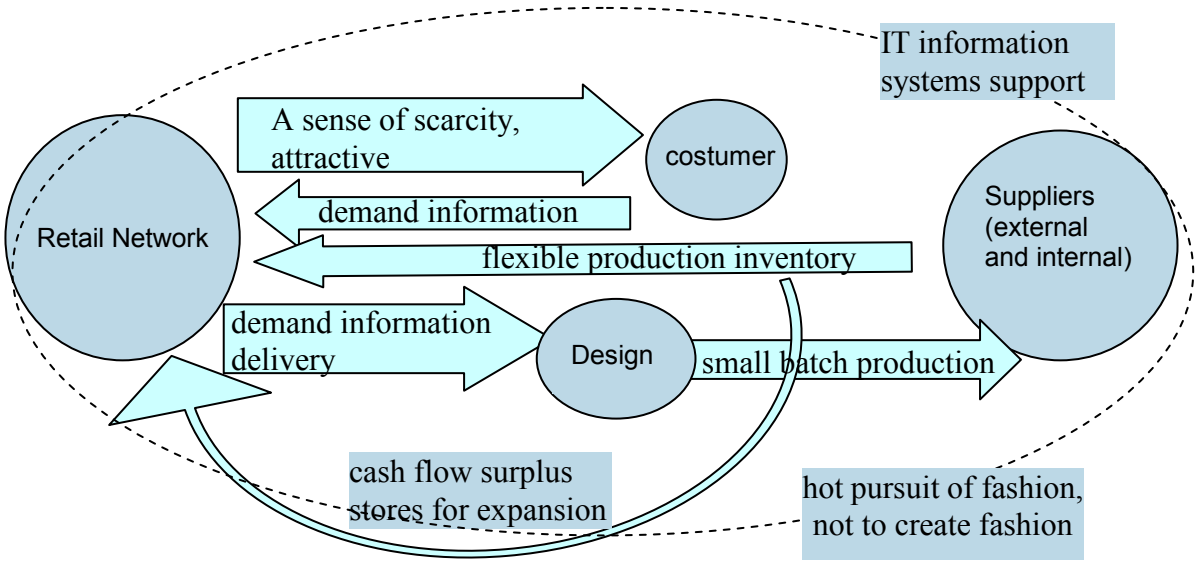


Fig. 1. The new SPA information chain

The garment industry as an example of the composition of the industrial chain segmentation module

China's garment industry chain development and trend. Course of development of garment industry**.** Industry is the development of social productive forces, the inevitable result of industrial development in the social development of productive forces and achieve social division of labor and form. Social productive forces, including the producers, the production of material and social conditions, industry is materialized in the social productive forces, or the emotional reality of the social productive forces, industry that is the way to achieve social production.Garment industry is often a national industry leader in the development process industries, because clothing is a necessity of people's lives, the vast market for the development of the industry provided the impetus. Meanwhile, the garment industry is activity-intensive industries, early stage of development in the industry, turnover is quick, and technology low, you can quickly achieve profitability, the development of garment industry but also other sectors of the national economy has a strong leading role. Throughout the history of textile and garment industry, the world textile and garment industry development process can be divided into the following phases: Phase handmade textiles and clothing (agricultural society - before the industrial revolution in the 18th century), mechanical textile and garment stage (the 18th century industrial revolution - half of the 19th century), the power stage of textiles and clothing (19 th century - 20 century), modern textile and garment stage (20th century) the early century - 20 century, 70 years), the new stage of economic textiles and clothing (20 Century 70 - 21 century), ecological and economic textile and garment stage (December 2009-present). [2]

Of the mid-90s in the 20th century had the world's largest apparel producer, but also the world's largest apparel exporter. However, the overall development of China's garment industry is very uneven. Is most concentrated in eastern coastal areas, the most active region, which focused on the Yangtze River Delta and the Pearl River Delta region of China's textile and garment industry nearly 2 / 3 of capacity, is the most important industrial base, and has formed a relatively complete industrial chain. Bohai Bay with a good basis for industrial development, excellent investment conditions, the market environment increasingly smooth, as textile and garment industry from eastern north to the Middle East focused on the transfer gradient transition zone, has become the Yangtze River Delta and PRD textile and garment industry, the third largest economic zone. Central and western region has abundant natural and human resources, but its textile and garment industry chain is not complete and matching lack of coordination, development is highly unbalanced, need to be improved in the country under the policies of developing the west, but also as the Yangtze River and Pearl River Delta, the direction of transfer of textile and garment industry[3].

At present, China's garment industry is basically in perfect competition, many small and medium companies within the industry, few companies have the whole chain of industrial products, pricing, relative to the size of the existing companies are mostly textiles and clothing for their own array, multiple operations, instability. China's textile and garment industry's ups and downs, or can not be sustained and efficient development, under certain circumstances because of its industrial chain is caused by fragmentation, in the raw materials, design, processing, logistics, sales, service, brand (product) chain, most of often has only one branch to both nodes. Single raw material or intermediate production and processing enterprises can not be good in the economic crisis continues to survive, these are caused by a lack of core resources and core business competitiveness.

Efficient integration of garment industry chain. Integration of garment industry chain structure. Industry chain, many different types can be divided into different types of industrial chain. But the basic structure shown in Fig. 2.

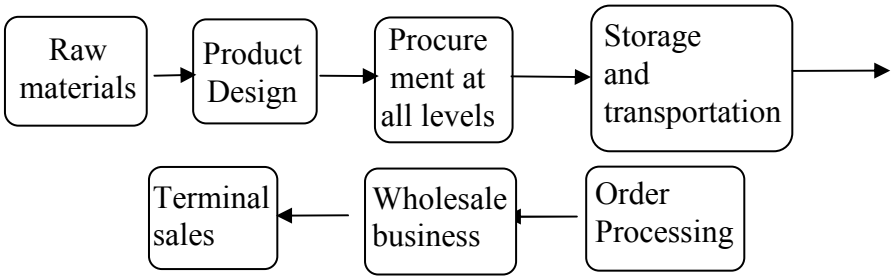


Fig. 2. Manufacturing production chain

Garment industry chain from one or several resources through a number of industries, such as the upper level to keep the spinning, weaving, dyeing and finishing one-stop integration, but also to the downstream logistics, channel, store, service integration. Do in-depth supply chain of textile industry, garment industry association to strengthen cooperation (industry association is stronger, the more closely the chain, the higher the efficiency of resource allocation), to strengthen the penetration depth of processing resources. The longer the chain, the deeper the degree of processing, can adapt to consumer demand[4].

First, the garment industry chain is a form of upper, middle and lower reaches of the various branches of industry, the relationship between the formation of interconnected chain, the chain of the product is different, the specific form, complexity and so different, but the chain should be broken down as much as possible and extended, so that a complete industrial chain and increase the depth of processing products so as to promote value-added chain.

Second, the clothing chain is essentially embodied in industry chain and between the various nodes within the branch of industry relevance, the relevance of the industrial chain, including physical form of the products, technology, value, supply and demand, including inputs and outputs relationship. Garment industry's competitiveness depends on the industry chain in the chain of Industrial Relations, Industrial Relations, the stronger, the greater promotion of the industry, between industries and enterprises become more relationship between the competing balance, industry chain development The greater the force, the more competitive and attractive.

Finally, the apparel industry chain structure plan itself is a strategy that under the conditions of modern economic background of the performance of the cluster as a strategy to attract enterprises to gather nuclear chain to drive the overall development of the industrial chain. Chain competitiveness of nuclear and other industries, companies clustering together determine the competitiveness of garment industry chain, to determine industrial competitiveness. Garment industry chain structure through the implementation of the integration will improve the industry in varying degrees, the status quo[5].

According to industry chain theory, the garment industry chain is the upper, middle and lower reaches of the various branches of industry, the relationship between the formation of interconnected chain of clothing products from the start the whole process until it reaches the consumer. Apparel industry chain structure, shown in Figure 3[6].

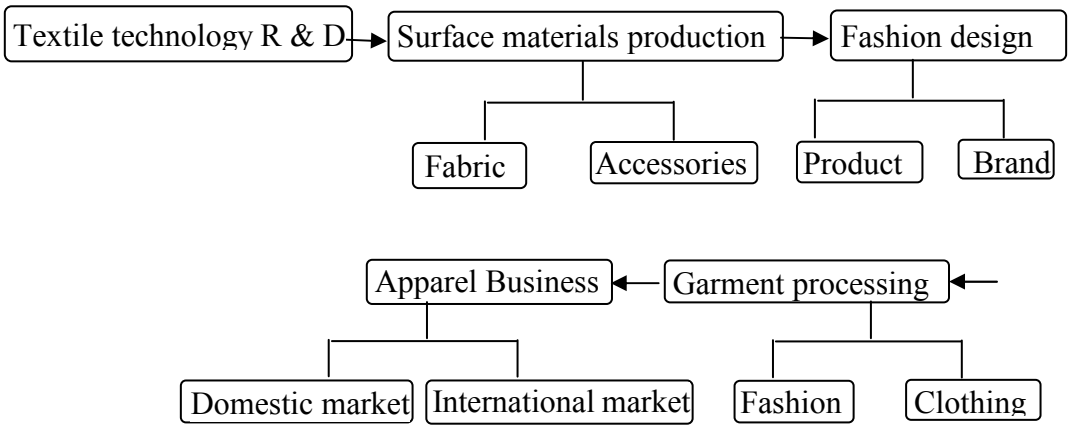


Fig. 3. Garment industry chain structure

Garment industry chain integration strategy. Under the barrel theory, the capacity of the water bucket by bucket number of the shortest piece of wood determined the probability of a successful business enterprise is by this decision the weakest link, the so-called "short-board effect." Of course, can not avoid the "short board" situation[7]. Bucket can be tilted, so that the shortest living on board water capacity to increase the bucket, the so-called "coordination of balance." Garment industry chain development of the basic strategy is harmonious and balanced development strategies, harmonious and balanced development strategies, including all sectors of the industry chain systems integration strategy.

The coordinated development of garment industry chain integration strategy, one must first of all sectors of the apparel industry chain systems integration, to achieve the match between the various sectors to ensure coordination of all aspects of development. System integration strategy is part of the industrial chain ratio between the number, structure, quality and the rationalization of three integrated positioning. First, the overall planning and garment industry with a reasonable proportion of chain links. Related links within the clothing industry in the number, size should maintain a certain ratio between the production of products such as the number of surface materials and clothing should be designed to match the demand for processing, too much will cause product backlog, caused by insufficient supply varies over . Second, a reasonable part of the development of garment industry chain hierarchy. Income level of residents of different regions of the hierarchy determines the garment trade, processing, design, surface materials production, textile technology, R & D hierarchy, therefore, should note that the links are high, medium and low rational allocation of product or technology. Finally, to rationalize the development of garment industry chain links the quality of structures. Provided by all sectors of the brand, products, services, technology, the minimum level of quality to determine the degree of quality to meet customer demand, so the quality level between the various links should match. In short, the garment industry, the coordinated development of chain links, can improve their overall level of service and collaboration between all sectors[8].

In short, a successful apparel industry chain can effectively promote industrial development and regional economic growth. Construction and garment industry chain refinement and clarity of content, help to promote the coordinated development of garment industry and the optimization of industrial structure. For all aspects of garment industry chain, some things to Industrial Relations to drive the entire apparel industry.

For an example of telemedicine strengthening of cooperation between industry

The issue of cooperation between the domestic industry and cause analysis. When can the Chinese people thoroughly understand the real co-operation, and China has truly become a world power, the remark is precisely the lack of Chinese people has always been, but is facing a more serious problem - cooperation. Segmentation of the current industrial structure module, give full play to the good advantage, to become the main trend of the industry, so that each sub-module only needs to concentrate to do their part of responsibility, can do fine to do it the best, and then each module mutual cooperation between, this will give full play to all areas of personnel, so the issue of cooperation between industry, our generation of Chinese one of the main problems to be solved.

Reform from 1978 to 2011, 33 years rapid development, China has heavy industry, light industry, aerospace, communications, science and technology have made miraculous leap, without that there is, from weak to strong, from being divided up into Let the world's attention, but always with the European and American developed countries there is a big gap in many areas, The main reason, not the Chinese people's heads stupid, nor is our technical equipment is not advanced, more than lack of resources in China, but we lack the concept of cooperation , or that is not good at cooperation, the Chinese people is characterized by scattered, fragmented, difficult to harmonious cooperation with others, of course, by the composition of China and historical background, and many other factors, summarized two main reasons : 1, Chinese people do not believe the Western countries most people have common beliefs, even as the racial characteristics of religious belief, a common faith when there

will be a common point of view, the principle of cooperation will be much easier, such as Jewish , their common envelope Judaism, has experienced so much even after the external destructive elements coming together very quickly; 2, China is not a nationality state, but multi-ethnic coexistence, ethnic differences and alert to a large extent on the industry play a role in the cooperation between the resistance, there is always a conflict between nations, the Government has to spend a lot of experience dealing with national problems of peaceful coexistence, to avoid conflicts arising from its approach is to minimize the inter-ethnic co-operation between the interests of; 2 China is a one-party dictatorship, such a system is double-edged sword, both national stability can reduce a lot of strife, but will also suppress the many free market, many industries there is no opportunities for cooperation[9].

The rise of cross-disciplinary industry. Now emerging industries in areas - telemedicine, for example, this is a representative of the industry, because it is a lot of modern technology in one product. With the basic components industry matures, the rapid development of the industry, one innovation of new products with its impact on the function of almost magical world of the eye. Originally appeared only in science fiction into the real life of equipment ever. For example, one of the new product R & D is the ECG, blood pressure monitors and other equipment condensed into a coin-sized chip, installed in the clothing, the player wearing the first application of R & D in the U.S., mainly in two areas: 1 , sports athletes in the body during exercise indicator data collection, athletes in motion to do every action or speed of the body in a blood pressure, heart rate, breathing and other indicators of data collection, 2, safety and security of elderly people living alone , the elderly body functions have been degraded, it is prone to sudden onset of the accident, children are not around, so it may not get held up in time the disease was found, so they need to carry around such a medical products, anytime, anywhere to detect their physical condition, they accidentally slipped in their own homes, the rapid acceleration of the heart beat, shortness of breath, these signals are quickly collected by the instrument, through the amplification system via the 3G network after the form of a signal transmitted to the hospital to accept the system, Doctors will soon know the old man had an accident, to take relief measures, the entire process may be a minute, however, the operation shown in Fig 4.

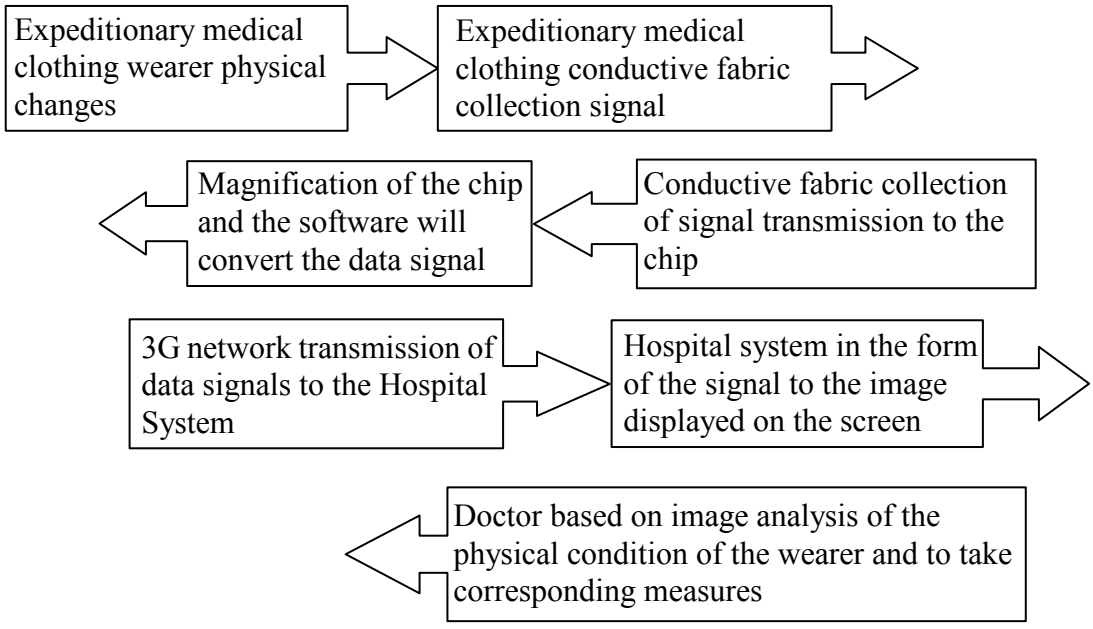


Fig 4 Workflow remote medical clothing

This product conveys to us the power of the strongest signal is the "cooperation", the product media - the structure of clothing do with people caring heterozygosity is higher, the more complete collection of physical data, apparatus, software program designed to more closely, the most signals collected the higher the rate, 3G networks more powerful the signal, the signal transmission faster and more complete ... ... the perfect all aspects of joint cooperation to complete the power of this product.

The industrial cooperation between the problems and solutions. How can be the perfect co-operation? First, to understand what cooperation is, how we need to do, what rules is shared between people, between the groups, business to business, business to business or even region to region, mutual trust between countries, communication and mutual understanding through the exchange of each other's features, choose something mutually beneficial to each other and humbly accept, tolerate shortcomings of the process.

So do the prerequisite for cooperation is a cooperative two or more parties must have a consistent philosophy of cooperation, close cooperation and reasonable process, the precise division of labor cooperation, specific responsibilities and authority, the most important thing is mutual trust, integrity guarantee, in place through a thorough communication to ensure co-operation will be disputes in the conflict to a minimum, the successful completion of the work, all efforts to make sets, set the industry results in an integrated results.

References

[1] Fujun Fan, Jianying Zhong, Lunde Hua, Discussion on Adjustment of Apparel Industry Chain, China Textile Leader, 2010(4):23-25;

[2] Weixia Wu, Yougan Zhu, Beijing to explore the integration of apparel industry chain[J], Beijing Institute of Clothing Technology, 2006(6):2-3;

[3] Jun Ning, Garment Industry Economics [M]. China Textile Press, 2004:112-137;

[4] Junzi, Fashion Entrepreneurship: studio wave upon us[J], Venture, 2003(2):33-34;

[5] Desong Jiang, Deconstruction SPS model ZARA, UNIQLO tips, entrepreneurs:96-97;

[6] Jan Johanson, Jan-Erik Vahlne, Commitment and Opportunity Development in the Internationalization Process: A Note on the Uppsala Internationalization Process Model [J]. Management Int ernational Review, 2006,46(2);

[7] Qinlin Gong, On the extension of industrial chain and overall regional development [J]. Economists, 2004(3) :3-5;

[8] Fashion supply chain organization and management between the UK and China, Zhimin Chen, Richard Murray and Richard M. Jones Manchester Metropolitan University, Manchester, UK ,Journal of Fashion Marketing and Management Vol. 11 No. 3, 2007: 380-397;

[7] Creating agile supply chains in the fashion industry Martin Christopher Robert Lowson and Helen Peck , International Journal of Retail & Distribution Management Volume 32 Number 8, 2004 : 367-376;

[8] Qin Liu ,Service one step ahead of the industry chain - Interview with Tian Hao, general manager of Shanghai Mart, textile and clothing magazine, 2010(11):71;

[9] A Brief Analysis on the Adjustment and Development of Chinese Garment Industry under Globalization, LI Di, Article&Design:238-240.

Keywords Index

"" Shaped Cross Section 202
2 D Braided 52
2-D Braiding 210
3 D Geometric Textile Modelling 44
30°/-60° Carbon Fiber Plain Woven Fabric/Epoxy Resin Composites 175
3D Technology 632
3D Tubular Fabric 536
3D Virtual Technology 566
3D Woven Composite 171
3D Woven Fabrics 202
4P 607

A

Abilities 735
Absorption 19
Acacia 160
Accelerating Agent 253
Acid Treatment 347
Actual Transaction 574
Adsorption 291, 372
Aerobics Clothing 628
AFM 713, 718
Air-Jet Loom 190, 454
Air Permeability 551
Alkali Deweighting 310
Amino Silicone Oil 390
Analysis 298
Analytic Hierarchy Process (AHP) 40
Annealing 194
Annular Shaped Woven Fabrics 198
ANSYS Simulation 472
Anti-Bacterial Property 330
Anti-Hairfalling Finishing 394
Anti-Shrinkage 283
Anti-Static 318
Antibacterial 115, 165, 265
Antifouling 543
Antistatic Finishing 270
Antistatic Property 412, 551
Apparel Cad 561
Apparel Design and Manufacturing 547
Apparel Product Development 603
Apparel Vendor 555
Application 214, 241
Armhole 611
Aroma Finishing 306
Artistic Creativity 214
Atmospheric Pressure Plasma Jet 356, 713, 718
Attenuation Curve of Acceleration 175
Auxiliary Devices 261
Azoic Dyeing 279

B

β-Cyclodextrin 412
Bacterial 179
Baicalin 287
Bamboo Fiber 89
Batch Feeding Control 555
Behavioral 689
Biaxial Tension 65
Biaxial Weft Knitted Fabrics 89
Binding Yarn 536
Biodegradation 148
Body Armor 73
Body Surface Area 27
BP Network 23
BP Neural Network (BPNN) 449, 685
Bra 566
Brand 735
Brassiere 101
Breast Root Girth 101
Butyl Acrylate 105
Buyers 735

C

Calcination Tempreture 14
Car Safety for Children 547
Carbon Fiber 110
Carding Machine 460
Carrier 19
Cashmere 40
Cationic Dyes 420
Cationic Graft Starch 144
Cell Immobilization 19
Chelating Surfactant 245
Chemistry Method Dye 364
Chinese Consumer 570
Chinese Element 582

Chitosan (CS) 160, 165, 283, 326, 330, 377, 382
Chloride 194
Chloroplatinic Acid 390
Chrome Shavings 61
Circular Nets Printing Machine 476
Circular Weaving 536
Citric Acid (CA) 412
Classification Model 616
Clothing 666, 689, 735
Clothing Area Factor 27
Clothing Design 662
Clothing Pattern 590
Clothing Styles 616
Cluster Analysis 624
Clustering Analysis (CA) 77
Coat-Hanger Die 444
Coating 165
Collagen 61
College Students 628, 650
Color 679, 689
Color Aesthetic 528
Color Psychology 528
Color Rubbing Fastness 225
Color Separation 77
Color Symbology 156
Comber 465
Combination Dyeing 352
Combination Technology 241
Comparative Advantage 694
Competitive Advantage 694
Complex Coacervation 160
Composite 89
Composite Fiber 61
Composite Material 83
Composite Yarn 129
Computer Simulation 23
Conductivity 36
Construction 611
Consumption 570
Consumption Behavior 628
Cooperate 740
Copolymer 426
Cored Rope 210
Cost Performance Ratio 40
Costume 97
Costume Color 156
Costume Geography 156
Cotton 279, 382
Cotton Combing 31
Cotton Fabric 237, 249, 261, 265, 306, 322, 398, 416
Cotton Textiles 93
Cultural Code 156
Curve Matching 485
Curvilinear Draft 465
CV of Count 502
CV of Outlet Velocity 444
CV Value 219
Cylinder Wallboard 460

D

D5 334
Decorative Screen 69
Deepening Effect 386
Degumming 245
Deposition 165
Design 69, 586, 666
Design Driven Innovation 730
Desizing 708, 713, 718
Desizing Enzyme 261
Deviation 574
Digital Inkjet Printing 398
Digital Spackle Correlation Method 65
Dimethylaminoethyl Acrylate 390
Disperse Dye 334
Double-Faced Jacquard 69
Doubling and Twisting Machine 489
Drapability 675
Drawing Frame 465
Drive Theory 472
Drying Efficiency 9
Dust 516
Dye 372
Dyeability 347
Dyed Fabrics 386
Dyeing 253, 257, 287, 291, 298, 302, 364, 377
Dyeing Performance 253
Dyeing Property 275, 338, 352
Dyes Wastewater 416

E

E-Business 574
Effect 347
Effective Cooling Temperature 636

Electric Conduction 93
Electrospinning 206
Electrospraying 165
Encase 133
Encoding 481
Energy Storage 83
Environmental Protection 97
Enzyme 532
Enzyme Protein 394
Epoxy-Silicon Micro-Emulsion 382
Escaping Electron-Beam Apgdp 386
Ethanediyl-n-hexadecyl-tri(*Sodium α-glycinate*) 245
Ethnic Brocade Style 69
Evaluation Model 650
Evolutionary Engineering 148
Experimental Mode Analysis 175
Expert Model 561
Exploration 97
Export Trade 726
External Investment 726

F

Fabric 19, 77, 594, 662
Fabric Reconstruction 214
Fabric Simulation 632
Fabric Styles 56
Fabric Tightness 48
Fabric Treating 318
Far-Infrared 179
Fashion 586
Fashion Applications 640
Fashion Design 582, 670
Fashion Industry 740
Fashion Show 607
Fashionable Emotion 658
Fastness 275
Fault Shutdown 454
Fe^{3+} La^{3+} Co-Doped 14
Female Physical Beauty 624
Fenton Reagent 368
Fiber Length Distribution 31
Figure 654
Finishing 265, 283
Finite Element Model (FEM) 636
Flake Aluminum Powder 703
Flame Retardant Agent 249
Flare Sagging 594
Flax Fiber 502
Flocculation 368
Fluorescence Ink 407
Fluorescence Pigments 407
Fluoride-Containing Acrylate 229
Folkloric Decoration 3
Force Balance 498
Fourier-Mellin Transform 485
Fractionize 740
FT-IR 249
Functional Clothing 547
Fur 586

G

G7 Technology 314
Genetic Algorithm (GA) 444
Genetic-Fuzzy Algorithm 77
Geometric Form 670
Going Global 726
Graft 133
Grafted Copolymerization 105
Grafting 342
Grafting Modification 61
Graphene 93
Gravure Printing 314
Gray Fabric 708
Green Tea 279
GUI 481

H

Hairiness 437, 502
Handfeel 225
Heat-Flux Coupling 636
Heat Transfer 636
Heat Transfer Coefficient 9
Heat Transfer Printing 314
Henna 302
High Performance Fiber 73
High-Speed 465
High-Speed Camera 190
Hip Girth 599
Home Laundry 9
Home Textile Design 214
Hotel Interior Space 3
HRE 437
Humanistic Spirit 620
Hybrid 110
Hydrogen Sulfite Sodium 420
Hydrophilic Polyurethane 139

Hydrophilic Property 412

I

Ideal Drafting 123
Identification 689
Image Processing 675
Improved BP 219
Improvement 735
Impurity Size 516
Indigo Naturalis 352
Influence 599
Inheritance 640
Innovative Application 582
Intelligent 578
Intelligent Control 476
International Competitiveness 722
International Market Share 722
Ionic Liquid (IL) 253, 326

J

Jacquard Circular Knitting Machine 472
Jade Polyester Fiber 298
Jasmine Microcapsules 306
Jute Fiber 110

K

K-Means 616
KES Fabric Style Testing Instrument 56
Kevlar-49 210
Key Control Point 171
Kinetics 291
Knitted Fabric 184, 394, 543
Knots 219

L

Labor Cost 694
Leather Garments 543
Lightweight Silk Fabric 119
Linear Regression 594
Linen Fabric 420
Liquid Cooling Garment 636
Locating 481
Low Carbon 620
Low-Temperature Plasma 338, 342, 708
Luxury Product 570

M

Magnetic Suspension Needles 472
Main Factor Analysis 56
Manufacture 512
Manufacturing Cycle Effectiveness 555
Marketing 607
Material 679
Mathematical Modal 129
Mathematical Model 599
MDS 616
Mechanical Property 119
Meltblown 206
Men's T-Shirt 658
Menswear 574
Merchandising 603
Method Comparison 27
Micro-Wave 105
Microcapsule 402
Mixed Hotpressing 699
Mmt 237
Modal Analysis 460
Model 603
Modification 416, 512
Modified 93
Modifier 426
Module 740
Moisture Absorption and Permeability 23
Moisture Management 237
Moisture Penetrability 551
Mononer 426
Mordant Dyeing 257, 302
Morphology 412
Motion Control 433
Motivation 570
Motors Synchronous Transmission System 476
Multi-Function 179
Multi-Layer Fabric 675
Multi-Scale Wavelet 481
Multi-Useful Clothing 620
Multinomial Regression 129

N

Nano-Fiber 206
Nano-Titanium Dioxide 330
Nanometer Titanium Dioxide 160

Natural Dye 279, 287, 352
Natural Dyestuff 302
Natural Extract 257
Natural Fiber Fabric Composite 65
Nature 97, 666
Needled Mat 110
Negative Oxygen Ions 179
NEPS 219
Network 730
New Bunka Prototype 670
New Machine 489
New Two-for-One Twisting Spindle 489
Nomex 364
Non-Aqueous Dyeing 334
Nonwoven 241
Numerical Simulation 444
Numetrical Representation 171
Nylon 6 287
Nylon 6 Fabric 347

O

Offsets 493
On Time Delivery 555
One-Way Moisture Transport 237
Online Shopping 632
Optimal Technological Parameters 23
Order Scheduling 555
Organization 646
Orthogonal Experiment 261
Overall 551
Oxidation 420

P

Pan 318
Parameterization 578
Parameters of Skirt Hem 594
Patchwork 640
Pattern 561
Pattern Design 654
Pattern Recognition 561
PCA 23
Penetration 356
Perceived Quality of Clothing 650
Performance 566
PET 206, 412
Pet Fabric 342, 713, 718
Photo-Catalytic Degradation 160
Photocatalysis Activity 14
Physiological Comfort 184
PI Controller 476
Placement of Underarm Point 611
Poly(lactic acid) (PLA) 89
Poly(*N*-isopropylacrylamide) 342
Poly(Vinyl Alcohol) (PVA) 61
Polyacrylate 713, 718
Polyamide Fibers 179
Polyaniline 318
Polyester 52, 133, 310
Polyester Fabric 270, 318
Polyester/Cotton/Hemp 699
Polyether 139
Polymethylhydrosiloxane 390
Polypropylene (PP) 699
Polypropylene Nonwovens 160
Polyurethane 402
Practicability 679
Practice 360
Pre-Treatment 398
Prediction 110
Prediction Model 449, 685
Preferable Emotion 658
Preparation 322
Price Index 685
Primary and Secondary School Uniform 679
Principles 666
Printing and Dyeing Wastewater 360, 368
Printofix Pigment 225
Product Development Process 603
Production 115
Property Analysis 139, 532
Proportion 624
Protective Clothing 184
Protein 133
Protein Additive 416
PVAc/TiO_2 Nanofiber 14

Q

Q-Model 156
Quadtree 481
Quality 454
Quasistatic Model 498

R

Rabbit Hair 40, 394
Ramie 65
Ramie Fabric 532

Random Distribution 31
Reactive 265
Reactive Dye 291
Reactive Dye Inks 398
Reflectivity 703
Regionalism 3
Register Error 485
Relationship 594
Reliable Test Time 516
Research Progress 229
Reshape Underwear 624
Residence Time 444
Resistivity 194
Revealed Comparative Advantage Index 722
Rhododendron Simsii 407
Rigid Rapier Sampling Weaving Machine 512
Ring Spinning 493
Ring Spinning Frame 489
Ring-Spun Yarn 40
Ropes 52
Rotary Screen Printing 485

S

Salvia Miltiorrhiza Bge 257
Seam Pucker 119
Seam Shrinkage 119
Sector 27
SEM 713, 718
SEM/EDS 249
Semi-Circular Skirt 594
Semi-Continuous Emulsion Polymerization 426
Sensitivity 36
Shaoxing Textile Industry 722
Shape 654
Shape of Sleeve 611
Shaping Memory 590
Shear Deformation 198
Shrinkage 326
Silane Coupling Agent 377, 703
Silk 245, 253, 257, 287, 291
Silk Fabric 302, 685
Silver-Plated Fiber 36
Simulation 123
Singed 708
Single-Printing Finishing 237
Siro-Spun 502
Siro-Spun Yarn 40
Sizing Agent 144
Sizing Performance 144
Skin-Care Finishing 402
Sleeve 611
Sliver 123
Sodium Alginate 310
Sodium Polyacrylate 372
Soft Segment 139
Softener 532
Softening Agent 9
Sol-Gel 83, 194
Sorghum Red Pigment 275
Special Body 654
Special Dart 662
Special Fan-Shaped Reed 512
Spinning Angle 493
Spinning Process 502
Splicing Design 543
Sportswear 646
Spunbond 241
Spunlace 241
Spunlaced Nonwoven Fabric 23
Stab-Resistant 73
Staining 416
Starch 105
Statistical Property 123
Status 73
Steel Ring 101
Steel Ring Girth of Breast 101
Stepwise Regression 599
Stochastic Simulation 31
Strain Filed 65
Structural Design 590
Structure 139, 566, 679
Structure Parameter 356
Style 679, 689
Suit 578
Sulfamic Acid 377
Sulphonation 420
Supply Chain 740
Surface Activity 245
Surface Evolution 14
Surface Modification 338, 386
Surface Treatment 708
Symmetrical Spinning Triangle 498
Synthesis 229

T

Tapered Artificial Vascular 512
Targeted Transaction 574
Technical Process 360
Technological Parameter 356
Telemedicine Clothes 740
Temperature-Sensitivity 342
Tencel Loose Fibre 275
Tensile Properties 129, 210
Terephthalic Acid (TA) 148
Test Equipment 675
Texgen Software 44
Textile 3, 115, 144, 314, 449, 528
Textile and Apparel Enterprises 726
Textile Design 730
Textile Industry 694
Textile Machinery 433
Textile Materials 356
Textile Production 433
Textile Weave 48
Thermal Insulation 703
Thermal Manikin 636
Thermal Stress Relief (TSR) 460
Thermochomic 83
Three over Three Drafting Form under Pressure Bar 465
TiO_2 270, 703
Titania Nano-Sol 322
Total Impurity 516
Trade Competitiveness Index 722
Traditional Baina Textile 640
Traditional Culture 590
Transfer Curves 175
Transfer Printing 426
Transmittance 194
Transmitting Promotion 607
Transmutability Clothing 620
Trash 516
Treatment 382, 532
Trend 730
Turmeric 352
Tussah Silk 330
Twist 48
Two-for-One Twisting Spinning Frame 489
Typological Method 590

U

Ultrasonication 261
Ultraviolet Protection 279, 322
Ultraviolet Protective Property 257
Uniformity 356
Uster Afis 516
UV-Curing 306

V

VFM 516
Vibratory Stress Relief (VSR) 460
Visual Cognition 658
Visualization Technology 152
Vitamin E 402
Volume Cutting 152

W

Waist Girth 599
Warp Density Changed Weaving 512
Washing Fastness 270
Waste Blend Fibers 699
Water Permeability Rate 48
Water Sol 270
Wearable Sensor 36
Wearing Resistance 40
Weave Structure 19, 198
Weaving Efficiency 454
Weaving Method 202, 536
Weft 454
Weft-Backed Structure 69
Weft Binder 536
Weft Insertion 190
Weft Knitted Fabric 36
Weft Tension 190
Wicking 9
Wind-Resistant Property 646
Winding 437
WLS Additives 416
Women's Trousers 654
Wool 165, 283, 326, 377
Wool Fiber 338
Wool Knitted Fabric 56
Wool-Like 310
Woven Fabric 152
Wrinkle-Resistance 382

X

XPS 713, 718

Y

Yarn Cross-Section Shape 152
Yarn Evenness 40
Yarn Hairiness 40, 493
Yarn Quality 437, 449
Yarn Strength 40
Yarn Structure 171

Z

ZEN 666
ZnO 270

Authors Index

A

An, J. 416
Arnold, L. 165

B

Bai, L.H. 532
Bai, Y.J. 249
Brown, L.P. 44

C

Cai, J.H. 229
Cao, J.D. 398
Cao, J.L. 287
Cao, J.P. 516
Chang, J.M. 433
Chang, Y.T. 202
Chen, F.M. 65
Chen, G.Q. 229
Chen, H.C. 198
Chen, H.F. 402
Chen, K.N. 19
Chen, L. 14
Chen, M.H. 574
Chen, S.Y. 237, 449
Chen, X.D. 561
Chen, X.M. 65
Chen, X.N. 566
Chen, Y. 322
Chen, Y.F. 3
Chen, Y.Y. 547
Chen, Y.Z. 368
Cheng, D.H. 253
Cheng, H.T. 65
Cheng, L. 52, 56
Cheng, S. 412
Cheng, Y. 225
Chu, Y.Y. 270
Cui, H.J. 437, 454
Cui, R.R. 156
Cui, S.Z. 270

D

Dai, J.M. 502
Deng, H.T. 543
Ding, G.Q. 19
Ding, X. 512
Ding, Z.Z. 73
Dong, X.Q. 512
Dong, X.W. 460
Du, E.D. 368
Du, M. 129, 356
Du, Z.Q. 703

F

Fan, X.P. 144
Fan, X.R. 156
Fang, J. 165
Fang, M. 586, 740
Feng, G.H. 611
Feng, M. 735

G

Gao, S.H. 133
Gao, S.Z. 420
Gao, W.D. 493
Gao, X.D. 476
Ge, H.Y. 9
Gong, J.X. 19, 148
Gu, W.L. 93
Gu, Z.Y. 139
Guan, L.P. 318
Guo, B. 551
Guo, L.H. 314
Guo, S.S. 206
Guo, X.F. 198
Guo, X.H. 314
Guo, Y.C. 368

H

Han, M. 433
Han, W.L. 444
Hao, X. 352
He, T.H. 237
He, W.J. 628
He, X. 679
He, X.M. 377
He, Z.P. 275
Hsiao, P.C. 670

Hu, H.X. 298
Huang, C. 382
Huang, W.W. 551

I

Islam, S. 165

J

Jadhav, A. 165
Jia, H.S. 502
Jiang, A.Q. 722
Jiang, W. 624
Jiang, X.F. 689
Jiang, X.H. 547
Jiang, X.M. 465
Jiang, Z.H. 65
Jiao, X.N. 23
Jiao, Y.N. 14, 210
Jin, L.M. 620
Jin, X.Y. 206
Jing, J.F. 481, 485

K

Ke, Q.F. 206
Kong, D.J. 265

L

Lei, Z.W. 360
Leng, L.X. 190
Li, G.D. 586
Li, G.H. 582
Li, G.Y. 485
Li, H. 302, 481
Li, H.J. 219
Li, H.Q. 19
Li, J. 27
Li, J.L. 175
Li, L.J. 454
Li, L.M. 334
Li, M.Z. 225, 416
Li, P. 708
Li, P.F. 481, 485
Li, P.L. 56
Li, Q. 27
Li, Q.J. 19, 148
Li, R.Q. 646
Li, S.Z. 334
Li, W.Y. 489
Li, X.C. 287
Li, X.M. 713, 718
Li, X.P. 735
Li, X.R. 465
Li, Y.L. 265, 449, 512
Li, Y.M. 578
Li, Y.Q. 334, 342, 386
Li, Z. 19, 148, 650
Li, Z.X. 229
Li, Z.Y. 536
Liang, H.E. 620, 640
Liang, S.Z. 101
Liang, Y.X. 14
Lin, C.H. 670
Lin, C.M. 670
Lin, H. 44
Lin, J.P. 437, 454
Lin, J.X. 426
Lin, M.B. 628, 646
Lin, S.Y. 19
Lin, T. 165
Liu, B.D. 685
Liu, C. 536
Liu, G.L. 582, 658, 689
Liu, H. 685
Liu, H.W. 89, 202, 202
Liu, J. 394
Liu, J.Q. 9, 334, 342, 386
Liu, L.J. 666, 735
Liu, M.Y. 310
Liu, N. 382
Liu, Q. 420
Liu, Q.J. 420
Liu, R. 302
Liu, S.Q. 502
Liu, T.T. 342, 386
Liu, W.X. 152
Liu, X.G. 502
Liu, X.J. 493, 498
Liu, Y. 726
Liu, Y.L. 40
Liu, Y.M. 611
Liu, Z.D. 265
Liu, Z.M. 330
Long, A.C. 44
Long, H.U. 36
Lottersberger, A. 730
Lou, L.J. 628
Lu, X. 654

Lu, X.P. 407
Lu, Y.H. 330, 352
Lu, Z.M. 241
Luo, B.J. 77
Luo, Y.F. 703
Lv, H.N. 326
Lv, J.C. 23
Lv, L.B. 129
Lv, L.H. 699
Lv, Y.Y. 666

M

Ma, H.L. 190
Ma, X.G. 83
Mao, C.D. 48
Mao, Y.J. 368
Meng, L.J. 386
Miao, C.Y. 433
Min, L. 310
Mu, Y. 426

N

Nawaz, N. 184
Ni, H. 594
Nie, Z.M. 476

P

Padhye, R.J. 165
Pan, N. 636
Pan, Z.J. 372
Pei, X.Y. 175
Punrattanasin, N. 279

Q

Qi, W.N. 555
Qi, Y. 156
Qian, C.J. 9, 342
Qian, X.M. 73, 202, 241, 624
Qiang, T.T. 347
Qiao, N. 666, 735
Qiao, Y.L. 283, 338
Qin, X. 110
Qiu, L. 561
Qiu, Y.P. 356, 713, 718
Quan, H. 139

R

Ran, D. 536
Ren, D. 460
Ren, L.F. 347
Ren, X.Q. 489

S

Shen, L. 547
Shen, X.F. 489
Shen, X.X. 283, 338
Shen, Y.Q. 105
Shi, H. 566
Shi, R. 582
Shi, X.L. 372
Song, G.L. 89
Song, H. 372
Su, M. 214
Su, X.Z. 493, 498
Su, Y.H. 31, 123
Sui, Z.H. 61
Sun, B.K. 40
Sun, P.Z. 516
Sun, S. 578
Sun, S.S. 257
Sun, W.W. 179
Sun, X.T. 245
Sun, Z.H. 536

T

Tan, Y.J. 364
Tang, F.F. 536
Tang, R.C. 257
Tang, Z.X. 19
Tao, J.W. 628, 646
Tian, J.Y. 310
Tian, M.W. 636
Troynikov, O. 184
Tu, J.L. 9

W

Wan, G.J. 699
Wang, C.X. 356
Wang, D.M. 740
Wang, F.Y. 726
Wang, G. 65, 476
Wang, H. 206, 382
Wang, H.F. 326

Wang, J. 322, 694
Wang, J.F. 36
Wang, J.J. 257
Wang, J.K. 144
Wang, J.M. 110
Wang, J.P. 566, 578
Wang, L. 426, 512, 662
Wang, L.J. 165
Wang, L.P. 368
Wang, M. 27
Wang, P.Y. 347
Wang, Q. 156, 270
Wang, R. 144, 194, 249, 322
Wang, S.G. 708
Wang, S.L. 171
Wang, S.S. 658
Wang, W. 306
Wang, X.C. 249, 347
Wang, X.G. 165
Wang, X.H. 219, 444
Wang, X.M. 160
Wang, X.Q. 69, 574
Wang, X.R. 245
Wang, Y. 412
Wang, Y.L. 412
Wang, Y.Q. 249
Wang, Y.Z. 578
Watson, C. 184
Wei, J. 616
Wei, W. 398
Wei, Y.J. 61
Weng, Y. 115
Wu, C.S. 603
Wu, H.L. 105
Wu, M.H. 426
Wu, N. 14
Wu, Q.Y. 119, 603
Wu, S.G. 590, 599
Wu, T.T. 493, 498
Wu, X.G. 472
Wu, X.H. 23
Wu, Y.M. 412
Wu, Z.L. 83
Wu, Z.M. 275
Wu, Z.Y. 566, 632

X

Xi, C.L. 360
Xiao, Q. 194
Xie, K.L. 377
Xing, L. 640
Xu, B.S. 502
Xu, H.J. 616
Xu, L. 194
Xu, N. 306
Xu, T. 586
Xu, W.L. 412
Xu, Y. 607
Xue, X.T. 291

Y

Yan, G.S. 31, 123
Yan, Y.X. 628, 646
Yang, C. 555
Yang, G.Y. 360
Yang, J.C. 465
Yang, L.H. 152, 171
Yang, W.F. 283, 338
Yang, X. 685
Yang, X.X. 398
Yang, Y. 322, 407
Yang, Y.C. 670
Yang, Y.X. 555
Yao, G.P. 402
Yao, J. 398
Yao, J.B. 237
Ye, H.H. 229
Ye, Y. 398
Yi, X. 528, 646
Yin, H. 225
Yu, C.W. 31
Yu, D. 306
Yu, F. 675
Yu, H.Q. 532
Yu, M. 679
Yu, S.Q. 460
Yu, W.D. 703
Yu, Y.E. 364
Yu, Y.J. 152
Yu, Y.L. 699
Yu, Z.X. 65
Yuan, J. 449
Yuan, J.R. 536
Yuan, Z.Q. 14
Yun, A.Y. 740

Z

Zhai, L.L. 624
Zhai, Y.F. 460
Zhang, A.D. 69, 574
Zhang, C. 472
Zhang, C.J. 472
Zhang, C.R. 160
Zhang, F.X. 133, 291
Zhang, G.X. 133, 291
Zhang, H. 144, 179
Zhang, J.F. 19, 148
Zhang, J.Q. 52
Zhang, L. 611
Zhang, M. 607
Zhang, M.Y. 314
Zhang, Q.F. 283, 338
Zhang, R. 722
Zhang, S.J. 708
Zhang, S.Y. 261
Zhang, W.B. 119
Zhang, W.F. 65
Zhang, X.L. 326
Zhang, X.X. 658, 689
Zhang, Y. 245, 394, 493, 616, 632
Zhang, Y.Q. 73
Zhao, C. 89
Zhao, D.F. 302
Zhao, G. 407
Zhao, J. 97
Zhao, L. 110
Zhao, Q.J. 210
Zhao, Q.M. 261
Zhao, X. 61, 390
Zhao, X.P. 460
Zhao, Y.N. 93
Zheng, J.H. 402
Zheng, Z. 570
Zheng, Z.Y. 190
Zhong, J.C. 398
Zhong, L. 291
Zhou, S.H. 536
Zhou, S.Q. 229
Zhou, X.H. 190, 407
Zhou, X.L. 275
Zhou, X.W. 460
Zhou, Y.K. 179
Zhu, J. 3
Zhu, Q. 398
Zhu, R.Y. 394
Zhu, S.K. 636
Zhu, W.B. 472
Zhu, W.Y. 390
Zhu, X.S. 372
Zou, F.Y. 616
Zou, P. 599
Zou, W.L. 123